



Effect of Different Levels of Spacing on Growth, Yield and Quality of *Asparagus densiflorus* 'Sprengeri' L

P.Sowmiya¹ and P. Karuppaiah^{2*}

¹Research Scholar, Department of Horticulture, Annamalai University, Tamil Nadu, India.

²Professor, Department of Horticulture, Annamalai University, Tamil Nadu, India.

Received: 06 Dec 2021

Revised: 22 Dec 2021

Accepted: 13 Jan 2022

*Address for Correspondence

P. Karuppaiah

Professor,

Department of Horticulture,

Annamalai University,

Tamil Nadu, India.

Email: vpkhortic@yahoo.com



This is an Open Access Journal / article distributed under the terms of the **Creative Commons Attribution License** (CC BY-NC-ND 3.0) which permits unrestricted use, distribution, and reproduction in any medium, provided the original work is properly cited. All rights reserved.

ABSTRACT

A study was conducted during the year 2020-2021 at Annamalai University, Annamalai nagar to find out the response of spacing on growth, yield and quality of *Asparagus densiflorus* 'sprengeri' L. cut foliage. The experiment was laid out in randomized block design with 8 treatments and 3 replications. Among the different treatments, the spacing treatment T₆ (45×45 cm) was found to be the best in respect of all growth, yield and quality attributes such as foliage stalk length (36.13 cm), number of primary branches per foliage stalk (30.16), length of primary branches in foliage stalk (7.80 cm), number of cladodes per foliage stalk (753.59), plant spread – East-West (49.63 cm²), plant spread – North-South (35.92 cm²), chlorophyll content (0.303 mg g⁻¹), fresh weight of foliage stalk per plant (163.38 g), dry weight of foliage stalk per plant (19.04 g), fresh weight of roots and tubers per plant (231.01 g), dry weight of roots and tubers per plant (53.77 g), dry matter production (105.55 g), number of tubers per plant (56.03), number of foliage stalks per plant (23.13), visual scoring (8.44), vase life of foliage stalk without pulsing (8.14 days) and with pulsing (11.92 days), followed by T₇ (45×50 cm). The closest spacing of 30×30 cm (T₁) recorded the minimum growth, yield and quality attributes of asparagus.

Keywords: Asparagus, Cut foliage, Plant spread, Spacing and Vase life of cut foliage

INTRODUCTION

Floriculture is a fast emerging, highly competitive and the most profitable business sector all over the world. Science based techniques in flower cultivation have given an impetus to the growth of this industry and rapidly expanding all over the world, including India (Datta., 2019). Cut foliage is the vegetation used in large quantities as a source of



**Sowmiya and Karuppaiah**

decoration on its own or on association with flowers in bouquets. This trend is set to increase further because of the green healthy image presented by such products and predicted increase in consumption of floral products. Cut foliage is used as a filler, lining and background material in various flower arrangements. They are also used for bringing life to the bouquets, wreaths and garlands, which would otherwise look dull. In recent decades, there has been increasing interest in floriculture and its products with great potential in the domestic as well as in export market. *Asparagus densiflorus 'sprengeri'* L. is an important cut foliage which is being cultivated on small area in tropical, subtropical and temperate parts of the world (Asma et al., 2018). The ornamental *Asparagus* are grown for their fine, feathery foliage, often used in bouquets and floral arrangements. Cultivated species are *A. asparagoides*, *A. plumosus*, *A. sprengeri* and *A. officinale* – edible asparagus. *A. densiflorus* is suitable for mass planting, cascading down a wall, container or above ground planter, border, ground cover and suitable for growing indoor. These are propagated either by seeds or divisions (Edward, 2014). There is a very little reliable information available on production technology and how best to grow *Asparagus* in the tropics. Among various cultivation aspects, planting density plays an important role in achieving the maximum productivity per unit area and also an important practice for providing good open position for sunlight, nutrients and moisture availability for quality crop production (Singh and Dubey, 2014). At wider planting the individual plant may get sufficient distance for its growth and development. Due to wide spacing, per unit production is less. On the other hand, in closer spacing the plants do not get sufficient distance for their development and consequently drastic reduction occurs at close planting. Hence, planting distance should be regarded for massing sufficient production and quality (Singh et al., 2018). The optimum spacing level helps not only in obtaining increased production of better quality but also in proper utilization of land and other inputs (Sudhagar et al., 2019). So, keeping the importance and potential of cut foliage in international and national scenario and scarcity of information regarding scientific cultivation of ornamental foliage filler plants like *Asparagus* in the tropics, the present investigation on "Effect of different levels of spacing on growth, yield and quality of *Asparagus densiflorus 'Sprengeri'* L." was carried out.

MATERIALS AND METHODS

The study was carried out in the Department of Horticulture, Annamalai University, Annamalai Nagar, Tamil Nadu during 2020-2021. The experiment was laid out in randomized block design with 8 treatments and 3 replications. The treatments of different spacing levels used in the study were T₁ (30×30 cm), T₂ (30×35 cm), T₃ (35×35 cm), T₄ (35×40 cm), T₅ (40×45 cm), T₆ (45×45 cm), T₇ (45×50 cm) and T₈ (50×50 cm). The raised beds are formed in uniform size by the mixture of 1:1:1 ratio of sand, red earth and FYM. The well maintained, uniform size seedlings having 3 – 4 foliage stalks per plant were transplanted. Life irrigation was given immediately and two subsequent irrigations were given at two days interval through rose can. Subsequent irrigations were done as per the requirements. Uniform culture practices were maintained for all the treatments. The biometric observations on growth and physiological parameters like foliage stalk length, primary branches per foliage stalk, length of primary branches in foliage stalk, cladodes per foliage stalk, plant spread, chlorophyll content, fresh weight of foliage stalks per plant, dry weight of foliage stalks per plant, fresh weight of roots and tubers per plant, dry weight of roots and tubers per plant, dry matter production per plant, number of tubers per plant, yield and quality parameters such as number of foliage stalks per plant, visual scoring and vase life of foliage stalks with and without pulsing were observed at 180 days after planting. The visual scoring of the cut foliage was recorded as per the Hedonic sensory evaluation method. Vase life without pulsing (days) and vase life with pulsing (days) of the cut foliage in each treatment replications were noted under room temperature. Third foliage stalk from the top was used to measure the biometric observations. The data on various parameters were analysed statistically as per the procedure suggested by Panse and Sukhatme (1997).

RESULTS AND DISCUSSION**Growth and physiological parameters**

The data indicated that there was a significant difference on growth of asparagus due to different levels of spacing (Table 1). Among the growth attributes, foliage stalk length, number of primary branches per foliage stalk, length of



**Sowmiya and Karuppaiah**

primary branches in foliage stalk and number of cladodes per foliage stalk were observed to be the maximum in T₆ (45×45 cm) with the values of 36.13 cm, 30.16, 7.80 cm and 753.59 respectively, followed by T₇(45×50 cm)with the values of 35.11 cm, 29.33, 7.52 cm and 730.32 respectively. The minimum values on foliage stalk length (29.07 cm), number of primary branches per foliage stalk (24.26), length of primary branches in foliage stalk (5.13 cm) and number of cladodes per foliage stalk (605.52) were recorded in T₁ of 30×30 cm spacing. There was slight increase in the average foliage stalk length with the decreasing planting density and the production of branches was also increased in line with the decrease of plant density (Table 1).The increase in growth attributes at the optimum spacing of 45×45 cm might be due to the uptake of sufficient nutrients, water and utilization of more sunlight which ultimately favoured the plant to grow more rapidly in the optimum spacing, while the factors which may have restricted the plants in closer spacings. The optimum spacing allows the plants to synthesize more carbohydrates and hormones like GA₃ that enhanced longitudinal growth as internodal length and resulted in longer plants (Kumar et al., 2016).This is in accordance with findings of Malam et al. (2010) in tuberose cv. Double, Sympli et al. (2019) in tuberose Cv.Single and Poornima et al. (2021) in gypsophylla.

The plants irrespective of their treatments had more spread on East-West direction than the North-South direction which may be due to sunlight availability and solar movement in the tropics. Among the different spacing levels, T₆ (45×45 cm) recorded the maximum plant spread on both the direction with the values of 49.63 cm² (East-West) and 35.92 cm² (North-South) than the other treatments. The minimum values of plant spread were 38.49 cm² (East-West) and 29.82 cm² (North-South) in 30×30 cm spacing (Table 1). It may be due to the fact that under optimum spacing there was an approximate usage of moisture, nutrients and light which leads the plants to synthesize more photosynthates, better growth and development and increased the number of primary branches, number of cladodes per plant which resulted in significantly increased the spread of plants. The results are supported by Jena and Mohanty (2021) in chrysanthemum. The chlorophyll content of *Asparagus* have a significant variation with spacing levels. The maximum content of chlorophyll (0.303 mg g⁻¹) was registered in the treatment with spacing level of 45×45 cm (T₆),followed by 45×50 cm (T₇) with the value of 0.297 mg g⁻¹. The minimum chlorophyll content (0.260 mg g⁻¹) was recorded in a spacing of 30×30 cm (T₁).The increase in chlorophyll content due to wider spacing gives more space to plant to derive more nutrients from the soil and reduced competition between the plants for nutrients, moisture and light might have helped in production of more number of cladodes for photosynthetic activities. The low shading effect with high light intensity was absorbed under low planting density regime which ultimately increased the net photosynthesis and chlorophyll content. Similar results were suggested by Singh and Dubey (2014) in boston fern ,Kumar et al. (2016) in gladiolus and Sudhagar et al. (2019) in tuberose.

The treatmentT₆(45×45 cm)was found to be the best in respect of fresh and dry weight of foliage stalks per plant (163.38 g and 19.04 g), fresh and dry weight of roots and tubers per plant (231.01 g and 53.77 g) and dry matter production of *Asparagus* (105.55 g), followed by T₇ (45×50 cm). The minimum values of these attributes were recorded in the spacing of 30×30 cm(125.04 g, 15.61 g, 177.75 g, 32.71 g and 85.24 g respectively).This can be attributed to the fact that dry matter production of crop depends on the amount of incident solar radiation and the conversion of solar energy to chemical energy. The low and optimum plant density might have high efficiency of crop in intercepting and converting solar energy, also the proper canopy distribution and good posture of cladodes in the canopy converts the solar energy into chemical energy effectively, which resulted in the maximum fresh and dry weight of foliage stalks per plant and dry matter production Concomitant observations were made by Poornima et al. (2021) in gypsophylla. As roots and tubers are in direct contact with soil and any changes in their surrounding spatial arrangement can greatly affect its growth. The healthy growth of shoots, roots, storage of foods in the tubers in wider spacing might be due to availability of more area per plant for absorption of nutrients and moisture that ultimately resulted in the maximum fresh and dry weight of foliage stalks per plant and also fresh and dry weight of roots and tubers per plant. The treatmentT₆ (45×45 cm) gave the maximum number of tubers per plant with the value of 56.03, followed by T₇ (45×50 cm) with the value of 54.23. This may be due to the reason that the number of cladodes was the highest in optimum spacing and resulted in production of more photosynthates in the plant which help translocation of carbohydrates from the source to sink and produce more tubers. The present findings are in agreement with the findings of Khalaj and Edrisi (2012) and Fatmi and Singh (2020) in tuberose.



**Sowmiya and Karuppaiah****Yield and quality parameters**

The treatment T₆(45×45 cm) recorded the maximum number of foliage stalks per plant (23.13), followed by T₇ (45×50 cm) with the value of 22.18. The minimum value of 16.13 was recorded in the spacing of 30 x 30 (Table.3). The increase in number of foliage stalk may be due to the availability of more stored food materials in large number of tubers per plant in optimum spacing, which also helped in early and rapid vegetative growth of cut foliage. This was also noticed by Marino et al. (2003) in *Asparagus plumosus*. In view of quality aspects as visual scoring and vase life of foliage stalk both under without and with pulsing, the treatment T₆(45×45 cm) was found to be the excellent spacing level with the values of 8.44, 8.14 and 11.92 days, followed by T₇(45×50 cm) with the values of 8.24, 7.88 days and 11.56 days respectively. The closer spacing of 30×30 cm was reported to have the minimum visual score and vase life of foliage stalk both under without and with pulsing, 7.36, 6.41 days and 9.72 days respectively (Table 3). The increase in cut foliage quality with optimum plant spacing might be due to less intra plant competition for light, moisture, space, nutrients and aeration which ultimately favoured more synthesis of photosynthates. The higher level of carbohydrates in the tissues due to higher photosynthesis in turn facilitated better appearance and vase life of the cut foliage. These results are in line with the findings of Singh and Dubey (2014) in boston fern and Malik et al. (2019) in snapdragon. From the results, it may be concluded that the spacing level of 45×45 cm (T₆) was found to be optimum and significantly beneficial with respect to growth, physiological, yield and quality parameters for the effective cultivation of *Asparagus* cut foliage under field cultivation.

REFERENCES

1. Asma, A., F. Summiya and M. Wajid. 2018. Impact of different environmental temperature on chemical composition of *Asparagus densiflorus sprengeri* L. collected from different areas of Punjab, Pakistan. Journal of Biochemical and Microbial Toxicology 1(1):1-4.
2. Datta, S.K. 2019. Present status of research on floriculture in India. LS-An International Journal of Life Sciences 8(2):71-93.
3. Edward, G. F. 2014. *Asparagus densiflorus sprengeri*, Sprengeri asparagus fern. Institute of Food and Agricultural Science (IFAS) Extension. University of Florida.
4. Fatmi, U. and D. Singh. 2020. Flower quality, yield and bulb production of different varieties of tuberose as affected by different planting time and geometry under Prayagrajagro-climatic conditions. Journal of Pharmacognosy and Phytochemistry 9(2):74-77.
5. Jena, S. and C.R. Mohanty. 2021. Effect of spacing on growth and flowering of annual chrysanthemum (*Chrysanthemum coronarium* L.). The Pharma Innovation 10(2):495-498.
6. Khalaj, M.A. and B. Edrisi. 2012. Effect of plant spacing and nitrogen levels on quantity and quality characteristics of tuberose (*Polianthes tuberosa* L.) under field experiment. International Journal of Agri Science 2(3):244-255.
7. Kumar, K., C.N. Singh, V.S. Beniwal and R. Pinder. 2016. Effect of spacing on growth, flowering and corm production of gladiolus (*Gladiolus* sp.) cv. American Beauty. International Journal of Environment, Agriculture and Biotechnology 1(3):550-554.
8. Malam, V.R., S.P. Singh, T.R. Ahlawat, R.K. Mathukia and Giriraj Jat. 2010. Effect of spacing and crop duration on growth, flowering and bulb production in tuberose (*Polianthes tuberosa* L.) cv. Double. J.Hortl.Sci5(2):134-137.
9. Malik, S.A., Z.A. Neelofar, I.T. Quadri, S.A. Nazki, Mir, F.A. Khan and M.S. Puktha. 2019. Effect of gibberellic acid, spacing and nutrient sprays on growth and flowering in snapdragon (*Antirrhinum majus* L.) cv. Rocket Pink. Journal Bank 28(1):1-6.
10. Panse, V.G. and P.V. Sukhatme. 1978. Statistical methods for agricultural workers, ICAR, New Delhi, pp.141-151.
11. Poornima, S., P.M. Munikrishnappa, G.K. Seetharamu, Rajeev Kumar, Amreen Taj, Anil Kumar and Mohan Kumar. 2021. Effect of spacing and growing conditions on growth and quality of Gypsophila (*Gypsophila paniculata* L.) cut flower. The Pharma Innovation Journal 10(8):1255-1258.





Sowmiya and Karuppaiah

12. Singh, H., J. Singh and J.K. Ahirwar. 2018. Effect of spacing and pinching on growth and flowering in African Marigold (*Tagetes erecta* L.) cv. PusaNarangiGainda. Journal of Pharmacognosy and Phytochemistry 7(2):1764-1766.
13. Singh, P. and R.K. Dubey. 2014. Effect of planting distance on growth and frond production in boston fern (*Nephrolepis exaltata* L. Schott). Hort Flora Research Spectrum 3(4):323-328.
14. Sudhagar, R., I. Karthikeyan, S. Kamalakannan, S. Kumar and S. Venkatesan. 2019. Effect of spacing and zinc application on growth parameters of tuberose (*Pollianthes tuberosa* L.) cv. single. Plant Archives 19(2):3620-3622.
15. Sympli, H., U. Fatmi and D. Singh. 2019. Effect of plant spacing on growth, flower quality and yield of four different varieties of tuberose (*Pollianthes tuberosa*). International Journal of Agriculture Sciences 11(13):8706-8708.

Table 1: Effect of different levels of spacing on growth parameters in *Asparagus densiflorus* 'sprengeri' L.

Treatments	Foliage stalk length (cm)	Primary branches per foliage stalk	Length of primary branches (cm)	Cladodes per foliage stalk	Plant spread (East-West) (cm ²)	Plant spread (North-South) (cm ²)
T ₁	29.07	24.26	5.13	605.52	38.49	29.82
T ₂	30.18	25.02	5.40	628.82	39.97	30.22
T ₃	31.28	25.86	5.68	640.40	41.45	30.62
T ₄	32.36	26.69	5.97	663.66	42.93	31.03
T ₅	33.70	28.10	6.71	685.34	45.68	33.42
T ₆	36.13	30.16	7.80	753.59	49.63	35.92
T ₇	35.11	29.33	7.52	730.32	47.93	34.04
T ₈	34.80	28.92	7.39	708.67	47.19	33.90
S.Ed	0.43	0.35	0.11	9.14	0.65	0.29
CD (P=0.05)	0.86	0.71	0.23	18.29	1.30	0.58

Table 2: Effect of different levels of spacing on growth and physiological parameters in *Asparagus densiflorus* 'sprengeri' L.

Treatments	Chlorophyll content (mg g ⁻¹)	Fresh weight of foliage stalks per plant (g)	Dry weight of foliage stalks per plant (g)	Fresh weight of roots and tubers per plant (g)	Dry weight of roots and tubers per plant (g)	Dry matter production per plant (g)	Tubers per plant
T ₁	0.260	125.04	15.61	177.75	32.71	85.24	36.46
T ₂	0.265	127.79	15.88	179.46	35.02	86.51	38.59
T ₃	0.270	130.54	16.33	183.59	36.54	87.77	40.71
T ₄	0.276	133.26	16.57	188.67	37.58	89.02	42.84
T ₅	0.289	155.99	17.74	203.77	44.61	97.27	49.98
T ₆	0.303	163.38	19.04	231.01	53.77	105.55	56.03
T ₇	0.297	161.95	18.25	225.44	47.77	101.79	54.23
T ₈	0.294	157.84	17.93	218.85	46.65	98.52	52.10
S.Ed	0.002	1.31	0.17	2.23	1.14	0.95	1.04
CD (P=0.05)	0.004	2.62	0.34	4.46	2.29	1.90	2.08





Sowmiya and Karuppaiah

Table 3: Effect of different levels of spacing on yield and quality parameters in *Asparagus densiflorus* 'sprengeri' L.

Treatments	Foliage stalks per plant	Visual scoring	Vase life (days)	
			Without pulsing	With pulsing
T ₁	16.13	7.36	6.41	9.72
T ₂	16.92	7.38	6.69	10.07
T ₃	17.72	7.60	6.96	10.40
T ₄	18.54	7.66	7.22	10.72
T ₅	20.94	7.74	7.47	11.04
T ₆	23.13	8.44	8.14	11.92
T ₇	22.18	8.24	7.88	11.56
T ₈	21.77	8.08	7.62	11.21
S.Ed	0.35	0.07	0.12	0.15
CD (P=0.05)	0.71	0.15	0.24	0.31





Seasonal Variation in the Proximate Composition of Flatfishes (Order: Pleuronectiformes) Collected from Cuddalore, Southeast Coast of Tamil Nadu

Manikandan Ramasamy¹, Rajakumar Ramachandran^{2*}, Emmanuel Charles Partheeban³ Vinothkannan Anbazhagan³, Rajaram Rajendran⁴, and Aruljothiselvi Subramanyan²

¹Research Scholar, PG & Research Department of Zoology, Periyar Govt. Arts College, Cuddalore, Tamil Nadu, India – 607 001.

²Assistant Professor, PG & Research Department of Zoology, Periyar Govt. Arts College, Cuddalore, Tamil Nadu, India – 607 001

³Research Scholar, DNA Barcoding and Marine, Genomics Laboratory, Department of Marine Science, Bharathidasan University, Tiruchirappalli, Tamil Nadu, India – 620 024.

⁴Associate Professor, DNA Barcoding and Marine Genomics Laboratory, Department of Marine Science, Bharathidasan University, Tiruchirappalli, Tamil Nadu, India – 620 024.

Received: 18 Nov 2021

Revised: 28 Dec 2021

Accepted: 11 Jan 2022

*Address for Correspondence

Rajakumar Ramachandran

Assistant Professor,

PG & Research Department of Zoology,

Periyar Govt. Arts College, Cuddalore,

Tamil Nadu, India – 607 001

Email: rajakumar@pacc.in



This is an Open Access Journal / article distributed under the terms of the **Creative Commons Attribution License** (CC BY-NC-ND 3.0) which permits unrestricted use, distribution, and reproduction in any medium, provided the original work is properly cited. All rights reserved.

ABSTRACT

Seasonal variation in the proximate composition of 30 flatfish species collected from Cuddalore and Puducherry fish landing centers during 2020–2021 across two seasons was evaluated with a view to provide nutritional data for dietary planning. The obtained results revealed that protein was the most important component found in flatfishes comprising towering percentages. The overall protein content fell in the range of 6.09–54.62%, with the lowest value observed during the monsoon season ($6.09 \pm 0.19\%$) and the highest in the summer season ($54.62 \pm 0.76\%$). The carbohydrate level was between 1.13 and 15.05%, with the lowest value observed during the monsoon season ($1.13 \pm 0.39\%$) and the highest in the summer season ($15.05 \pm 0.08\%$). Overall, lipid percent was in the range of 0.44–2.79%, with the lowest ($0.44 \pm 0.28\%$) and the highest values both observed in the in the monsoon season. The proximate composition of flatfishes during the summer season was richer compared to the monsoon season. Flatfish may not be available through all seasons and look unappealing to eat because of their body shape and size, but they are equally rich in nutritional value to the other marine fishes. With the dwindling marine resources, flatfishes can be a viable replacement for lean protein dietary foods. The flatfishes can be also





Manikandan Ramasamy et al.,

suggested to be used as supplements to increase the nutritional value of commercially available snacks and food products.

Key words: Proximate Composition, Flatfish, Protein, Lipid, Carbohydrate and Seasonal Variation

INTRODUCTION

Fish that come under the families of Bothidae (fumbles), Cynoglossidae (tongue soles), Psettoodidae (Indian halibut), and Soleidae (soles) are prevalently known as flatfishes. Flatfishes (flounder, sole, halibut, turbot, plaice, and tonguefish) are among the most effectively identifiable of all fish groups, characterized by particular side packed body morphology with both eyes located on the same side of the head [1]. Flatfishes are a monophyletic group (order Pleuronectiforms inside the Percomorph) comprising of more than 700 species distributed worldwide in the marine and estuarine waters, including species that inhabit remote ocean warm vents and new waterways [2]. Adults can range in size from 2 cm to more than 2 m in length. They spend a big portion of their lives as benthic (bottom dwelling) animals that lay on one side in the ocean floor. Flatfish are the most accounted vertebrates to ever exist with left-right unevenly formed body with typical lateralization [3]. Flatfish are benthic fishes whose body is amazingly smoothed. Coasts and estuarine environment are considered most favourable for civilization on the planet and house half of the world population [4]. These coastal ecosystems are enriched with ichthyofaunal resources as these ecosystems play the critical job of nursery for many marine species [5].

Well, known commercial fish, including flounder, halibut, sole, and turbot, are flatfish. Flatfish range in colour from a speckled brown, black, and beige, like a black sea turbot; or spotted, like the blue-and-yellow peacock flounder. Most species live in highly diverse tropical and subtropical oceans [6]. The composition of fish is fundamentally composed of lipid, protein, and carbohydrates which form the nutritional value, purpose aspects, and sensory characteristics of the flesh [7]. Data on proximate composition of fishes are not only useful to the nutritionist, but also to the fishery technologist. Such data are not available for many species of Indian fishes, and when they are usually do not provide the necessary information concerning taxonomic status, size of the specimen, seasonal variation, degree of freshness, method of sampling, and body part analysed [8]. These details are necessary for defining the variation in the proximate composition in different species as obtainable in different landing centres across different seasons.

Fish production landings in India are expected to total 3.56 million tonnes in 2019, with flatfish accounting for only 50,013 tonnes (1.4%) [9]. the demersal fishery has grown in recent years, with 50–70% of shrimp trawler harvest being by catch of which flatfish occupy the major portion [10]. Regular fishery has been extant for the Malabar sole and this fish is valued for table use in the fresh and dried state. The four-lined tongue sole and Indian halibut are acknowledged as important fish varieties. Proximate composition of the Malabar sole and Indian halibut is published [10]. The main aim of this study was to record the flatfish species available along the Cuddalore and Puducherry coastal waters and assess their proximate composition for nutritional value.

MATERIALS AND METHODS

Study area

Flatfish were collected from three fish landing centres along Puducherry and Tamil Nadu coastal waters. The sampling locations shown in Figure 1 are as follows: (1) Cuddalore fish landing centre (11°42'58.5"N, 79°46'30.6"E); (2) Modasalodai fish landing centre (11°29'07.7"N, 79°46'28.3"E); and (3) Puducherry Thengaitthittu fish landing centre (11°54'32.3"N, 79°49'25.0"E). The selected three regions are influenced by anthropogenic activities including chemical industries, factories, and power plants. Cuddalore is the city which harbours a major port, SIPCOT (State Industries Promotion Corporation of Tamil Nadu) industrial hub, heavy water plant (HWP), thermal power plants, many chemical industries, chains of the salt pans, and influenced by pollution from untreated sewage [11]. The flatfishes were collected from the fishing boats that operate only in the coast of Tamil Nadu and Puducherry.



**Manikandan Ramasamy et al.,****Collection of flatfishes**

To cover the Puducherry and Cuddalore coast, flatfish samples were collected from the three stations (Cuddalore, Modasalodai, and Puducherry) along the southeast coast during the monsoon (June–August 2020) and summer seasons (March–May 2021). It is to be noted that the sampling locations were geographically equidistant for consistently collecting the fishes along the coastline. The collected samples were transferred to the laboratory in cold storage. Until further analysis, the samples were kept in a frozen state (-20°C) to avoid denaturing. Prior to experimentation in the laboratory, the specimens were defrosting and thawed to room temperature. Collected samples were photographed and the morphometrics of the flatfishes were noted. Species identification was conducted using monographs, FAO description sheets, and FISHBASE — database for fishes. Totally, 30 different species of flatfishes were collected for analysis.

Flatfish tissue sample processing

All specimens were rinsed using distilled water before dissection. For analysing the protein, lipid, and carbohydrates, the muscle parts of the fish were taken. Tiny pieces of muscle tissue (~ 20 g) were dried at 70°C in a hot-air oven. Once the tissue was fully dried, pestle and mortar were used to grind it into a fine powder and stored in air-tight polyethylene covers for further analysis [12].

Estimation of Protein

The protein content in flatfish was estimated according to the method [13]. In brief, flatfish sample 1 g of sample was taken individually and homogenized in distilled water to precipitate the protein. The samples were then centrifuged at 4000 RPM (revolutions per minute) for 10 min and the precipitate was collected, redissolved with 4 ml of 1N NaOH solution. About 5 ml of freshly prepared alkaline copper solution containing 1 ml of 0.5% copper sulphate in 1% potassium tartrate (W/V) and 50 ml of 20% sodium carbonate in 0.1N sodium hydroxide was added to the redissolved precipitate and allowed to stand for 20 min. 1N NaOH solution and 0.1% bovine serum albumin (W/V) served as blank and standard solutions, respectively. The colour developed was subjected to absorbance at 650 nm with a UV–visible spectrophotometer. Standard curve was plotted using the known standards and based on the optical density (OD) value the total protein concentration in the sample was estimated with reference to the standard curve.

Lipid estimation

Lipid was estimated by using the chloroform–methanol method as described [14]. In brief, 10 mg of finely ground dried flatfish sample was taken in a test tube; 5 ml of chloroform–methanol (2:1) mixture was added. The mixture sample was incubated at room temperature for 24 h after sealing the mouth of the test tube with aluminium foil. After incubation, the sample was purified and collected in a pre-weighed beaker, which was kept in a hot-air oven for drying. The solvent (chloroform–methanol) mixture was vaporized leaving a remaining lipid layer at the bottom of the beaker. Then, the weight of empty beaker was subtracted from the weight of beaker with lipid to estimate the total quantity of lipid present in the flatfish sample using the following formula:

$$\text{Lipid \%} = \frac{\text{Amount of lipid in the sample}}{\text{Total weight of sample taken}} \times 100$$

Carbohydrate estimation

Carbohydrate was estimated according to the method [15]. A weight of 5 mg of flatfish powdered sample was taken and homogenized with double-distilled water. Then, the homogenized sample was centrifuged for 10 min at 3000 RPM. Later, to the supernatant, about 1 ml of 5% phenol solution and 5 ml of Con. H_2SO_4 were added, and it was allowed to stand for 30 min. The OD was measured at 490 nm using a UV–visible spectrophotometer. D-glucose was used as the known standard to plot the standard curve. The quantity of carbohydrate present in the flatfish sample was determined by referring to the obtained OD values against the standard curve.





Manikandan Ramasamy et al.,

RESULTS AND DISCUSSION

The family classification, common names, depth ranges inhabited by the particular species of fish, and their body lengths observed for the 30 species of flatfish in the current study are reported in Table 1. The percentages of protein, carbohydrate, and lipids in the flatfish are presented as mean and standard deviation (SD) in Table 2. The protein levels in the muscle of flatfishes are represented as a bar diagram in Figure 2. The highest value for protein was observed in *Pseudorhombus arsius* (54.62%) during the summer season and the lowest was in *Zebrias quagga* (6.09%) during the monsoon season. The protein values ranged from 6.09–46.31% with a mean of 28.05% during the monsoon season. During the summer season, the values ranged from 14.18–54.62% with an average value of 39.15%. The protein content in flatfishes during the monsoon season was in the order of *Brachirus oriemails* (46.30%) > *Zebrias synaptruroides* (45.41%) > *Pardachirus pavoninus* (44.42%) > *Pseudorhombus arsius* (42.33%) > *Synaptura commersonnii* (42.28%) > *Citharoides macrolepis* (42.23%) > *Cynoglossus arel* (40.06%) > *Heteromycteris hartfeldii* (36.64%) > *Psettodes erumei* (36.60%) > *Bothus guibei* (36.32%) > *Cynoglossus itinus* (35.70%) > *Paraplagusia bilineata* (35.37%) > *Crossorhombus azureus* (31.36%) > *Pseudorhombus triocellatus* (30.68%) > *Zebrias craticulus* (29.22%) > *Aesopia cornuta* (28.83%) > *Synaptura lusitanica* (26.92%) > *Pseudorhombus elevatuss* (26.76%) > *Cynoglossus semifasciatus* (25.82%) > *Zebrias cochinchensis* (25.77%) > *Pseudorhombus diplospilus* (25.28%) > *Laeops macrophthalmus* (18.77%) > *Laeops guentheri* (17.34%), *Crossorhombus valderostratus* (15.60%) > *Grammatobothus polyophthalmus* (12.52%) > *Cynoglossus carpenter* (11.27%) > *Pseudorhombus javanicus* (10.01%) > *Samaris cristatus* Gray (8.15%) > *Synaptura albomaculata* (7.52%) > *Zebrias quagga* (6.09%). The protein composition observed in flatfish our study was comparatively higher than the values observed [16]. Our results more or less coincide with the findings of Nobi and Hossain who reported the protein content in *M. aculeatus* and with the findings [17] and who analysed the protein levels in *P.gononiotus*. In a similar study, the chemical composition in different edible portions of the fish including the central body and the edge of the muscles of flatfish was assessed and reported [18] in *Lepidorhombus whiffiagonis*. The protein content in the different flatfish species during the summer season was in the decreasing order as follows: *Pseudorhombus arsius* (54.62%) > *Pseudorhombus diplospilus* (53.95%) > *Heteromycteris hartfeldii* (51.41%) > *Laeops macrophthalmus* (49.52%) > *Pardachirus pavoninus* (48.30%) > *Citharoides macrolepis* (48.22%) > *Synaptura albomaculata* (47.44%) > *Cynoglossus arel* (47.32%) > *Paraplagusia bilineata* (47.25%) > *Grammatobothus polyophthalmus* (44.13%) > *Crossorhombus valderostratus* (43.37%) > *Bothus guibei* (43.21%) > *Brachirus oriemails* (42.38%) > *Zebrias synaptruroides* (41.39%) > *Psettodes erumei* (40.99%) > *Crossorhombus azureus* (40.84%) > *Synaptura commersonnii* (40.77%) > *Synaptura lusitanica* (40.68%) > *Cynoglossus carpenteri* (40.55%) > *Zebrias cochinchensis* (39.61%) > *Zebrias craticulus* (32.89%) > *Zebrias quagga* (31.56%) > *Aesopia cornuta* (30.77%) > *Cynoglossus semifasciatus* (29.33%) > *Pseudorhombus javanicus* (29.31%) > *Pseudorhombus triocellatus* (27.75%) > *Samaris cristatus* (27.65%) > *Cynoglossus itinus* (26.38%) > *Laeops guentheri* (18.64%) > *Pseudorhombus elevatuss* (14.18%). On an average, the composition of proteins in the muscles of the flatfish was found to be higher in the summer season compared to the monsoon season among the 30 species studied. The protein and biochemical composition vary from one species to another depending on a range of factors, viz., feeding, breeding, fishing season, and migration [19, 20]. The main reason of variation in the proximate composition may be due to the quantity of feed intake, season, size, and habitat of fishes [21, 22, 23]. The variation in the protein levels in flatfish species across the seasons might be influenced by their feeding and breeding habits [20]. Similar observations were reported [24] in agreement with our results that analysed the potential of flatfish frame in preparation of snack products. Our results were slightly similar to previous study [25].

The carbohydrate levels of flatfishes are presented as a bar diagram in Figure 3. The highest value for carbohydrate was observed for *Pardachirus pavoninus* (15.05%) during the summer season and the lowest was in *Pseudorhombus elevatuss* (1.13%) during the monsoon season. The carbohydrate values ranged from 1.13–11.19% with a mean of 4.79% during the monsoon season. In the summer season, the values ranged from 4.64–15.05% with an average value of 9.45%. The carbohydrate content in flatfish during the monsoon was in the descending order as follows: *Zebrias quagga* (11.19%) > *Cynoglossus arel* (10.65%) > *Zebrias cochinchensis* (10.34%) > *Pseudorhombus diplospilus* (10.30%) > *Citharoides macrolepis* (9.34%) > *Cynoglossus carpenter* (8.13%) > *Pseudorhombus javanicus* (6.22%) > *Synaptura lusitanica* (6.20%) > *Crossorhombus valderostratus* (6.11%) > *Cynoglossus itinus* (5.99%) > *Brachirus oriemails* (4.37%) > *Aesopia cornuta* (4.35%) > *Crossorhombus azureus* (4.17%) > *Grammatobothus polyophthalmus* (4.12%) > *Laeops guentheri* (4.08%)

38596





Manikandan Ramasamy et al.,

>*Pardachirus pavoninus* (3.79%) >*Pseudorhombus triocellatus* (3.75%) >*Psettodes erumei* (3.38%) >*Pseudorhombus arsius* (3.18%) >*Heteromycteris hartfeldii* (3.13%) >*Paraplagusia bilineata* (2.73%) >*Zebrias synaptruroides* (2.57%) >*Cynoglossus semifasciatus* (2.50%) >*Bothus guibei* (2.41%) >*Zebrias craticulus* (2.23%) >*Laeops macrophthalmus* (1.97%) >*Synaptura commersonii* (1.77%) >*Synaptura albomaculata* (1.74%) >*Samaris cristatus* (1.73%) >*Pseudorhombus elevatuss* (1.13%). In the summer season, the carbohydrate content in the fish was in the order: *Pardachirus pavoninus* (15.05%) >*Laeops macrophthalmus* (13.51%) >*Zebrias craticulus* (13.42%) >*Synaptura lusitanica* (13.08%) >*Zebrias synaptruroides* (13.2%) >*Synaptura commersonii* (11.65%) >*Pseudorhombus diplospilus* (11.41%) >*Brachirus oriemails* (11.01%) >*Cynoglossus arel* (10.84%) >*Crossorhombus azureus* (10.45%) >*Laeops guentheri* (10.43%) >*Citharoides macrolepis* (9.87%) >*Bothus guibei* (9.69%) >*Pseudorhombus arsius* (9.50%) >*Cynoglossus carpenter* (9.41%) >*Synaptura albomaculata* (9.33%) >*Pseudorhombus triocellatus* (9.07%) >*Pseudorhombus elevatuss* (8.53%) >*Aesopia cornuta* (8.40%) >*Crossorhombus valderostratus* (7.87%) >*Samaris cristatus* (7.53%) >*Cynoglossus itinus* (7.48%) >*Psettodes erumei* (7.25%) >*Zebrias cochinchensis* (7.09%) >*Pseudorhombus javanicus* (7.07%) >*Zebrias quagga* (6.96%) >*Heteromycteris hartfeldii* (6.83%) >*Grammatobothus polyophthalmus* (6.87%) >*Cynoglossus semifasciatus* (6.18%) >*Paraplagusia bilineata* (4.64%). The carbohydrate content of the experimented flatfish in summer seasonal most of the fish level increased *Pardachirus pavoninus*, *Laeops guentheri*, *Synaptura commersonii*, *Samaris cristatus*, *Pseudorhombus arsius*, *Brachirus oriemails*, *Synaptura lusitanica*, *Zebrias synaptruroides* and *Psettodes erumei*, respectively. Carbohydrate content of fish gets affected by environmental and physiological factors like seasons and feed intake. Seasonally, differences in the availability of food and changes in the reproduction cycle have considerable effect on the tissue biochemistry of the fish, particularly fat [26] and also analysed the variation of carbohydrate content with feed and found that intensive feeding in *Gangetic sillago* and *Sillaginopsis panijus*. The levels of carbohydrates observed in their study correlates well with our finding of the occurrence of high carbohydrate content in the fish muscle. These findings were slightly similar with previous report [27].

The levels of lipids in the muscle of flatfishes are presented as a bar diagram in Figure 4. The lipid values ranged from 0.44–2.79% with a mean of 1.49% during the monsoon season. The highest value for lipid was observed in *Laeops guentheri* (2.79%) and the lowest was in *Synaptura lusitanica* (0.44%) both during the monsoon season. In the summer season, the values ranged from 0.67–2.19% with an average value of 1.35%. During the summer season, lipid content was highest in *Samaris cristatus* (2.19%) and lowest in *Zebrias quagga* (0.67%). Converse to the protein and carbohydrate contents, lipid percentages in flatfish were slightly higher in the monsoon season than in the summer [28] and reported the range of fat content of different commercial marine fishes collected from Bay of Bengal from 0.99% in *Dasyatis pastinica* to 2.01% in *Dasyatis americana* which agree well with the ranges of lipid profiles reported in this study. The study revealed that the nutritive values of sharks, skates, and rays caught from the Proto-Nova coast, and they reported that the proximate composition varied from species to species and across the different seasons [29]. The present study results are in good agreement with the study of with respect to the variations in the fat content among different fish species [29]. Higher lipid content was observed in the monsoon season, while the values gradually decreased in the flatfishes reaching lower levels of lipids in the summer season. The flatfish showed minimum level lipid before spawning. These data coincide with that in the literature as reported [30].

Fish is a highly proteinaceous food consumed by the people. A larger percentage of people do eat fish because of its availability, taste, and palatability, while fewer percentages do so because of its nutritional value. The proximate composition of fish varies greatly from one species or one individual to another based on the starvation and intensive food intake periods [31] and external factors such as a salinity and temperature [32]. The present study demonstrated the proximate composition (protein, carbohydrate, and lipid) of the flatfish species collected from the southeast coast of Tamil Nadu in the Cuddalore and Puducherry coastal waters. As the name implies, flatfish have an unusually flat body shape which make them well suited for life close to the ocean floor. With the results obtained in our current study, we can validate that flatfish from the southeast coast water have a good protein content, low carbohydrate and lipid levels. The proximate composition analysis of the flatfishes in two seasons (monsoon and summer) demonstrates that the proximate composition of flatfish has seasonal variations. Protein levels fluctuate with no regular seasonal trend; however, a slight increase was detected in the summer of 2021 in flatfish from all the study area in both male and female. This may be related to the increasing accumulation in gametes, of which





Manikandan Ramasamy et al.,

proteins constitute the major organic component [33]. The flatfish may not look appealing to eat because of their body shape and size, but they are equally rich in nutritional value to the other marine fishes. With the dwindling marine resources, flatfishes can be a viable source of protein to the humans. The flatfishes can be also suggested to be used as supplements to increase the nutritional value of commercially available snacks and food products.

CONCLUSION

The flatfishes are a less studied group of fishes and are ignored by many researchers due to the sampling difficulties and their unavailability throughout the year. The flatfishes are considered as food fish only in the western cuisine and a few parts of India like Kerala and Karnataka. The fact that they accumulate toxins excessively compared with the pelagic fishes has made them to be considered as trash fish and unsuitable for consumption. The proximate composition data across two seasons for 30 species of flatfish of the order Pleuronectiformes have shown that the protein content of these fishes is considerably high, and these fishes have low-to-moderate lipid accumulation in them. Also, the carbohydrate content is considerably lower. Thus, with reference to the above points the flatfish's high protein content and low lipids can be considered as a replacement for lean protein dietary foods. The other fishes with higher carbohydrates and lipids can be used as an ingredient in the aquaculture feed formulations. The declining fish in the oceans demands a lookout for the alternate fishes that can be considered as food fish. Flatfish with stringent quality controls in seafood processing can be opted for the human diet.

ACKNOWLEDGEMENT

The authors would like to express their gratitude to the Department of Marine Science, Bharathidasan University, Tiruchirappalli, India, for providing the necessary facilities, as well as the Periyar Govt. Arts College, Cuddalore, for providing extended facilities.

REFERENCES

1. Munroe TA. Systematic diversity of the Pleuronectiformes. Flatfishes: biology exploitation. 2005:10-41.
2. Friedman M. Osteology of *Heteronectes chaneti* (Acanthomorpha, Pleuronectiformes), an Eocene stem flatfish, with a discussion of flatfish sister-group relationships. *Journal of Vertebrate Paleontology*. 2012;32:735-56.
3. Schreiber AM. Asymmetric craniofacial remodeling and lateralized behavior in larval flatfish. *Journal of Experimental Biology*. 2006;209:610-21. Epub 2006/02/02.
4. Costanza R, d'Arge R, deGroot R, Farber S, Grasso M, Hannon B, Limburg K, Naeem S, O'Neill RV, Paruelo J, Raskin RG, Sutton P, vandenBelt M. The value of the world's ecosystem services and natural capital. *Nature*. 1997;387:253-60.
5. Vanderveer H, Berghahn R, Miller J, Rijnsdorp A. Recruitment in flatfish, with special emphasis on North Atlantic species: Progress made by the Flatfish Symposia. *ICES Journal of Marine Science*. 2000;57:202-15.
6. Partheeban EC, Anbazhagan V, Arumugam G, Seshasayanan B, Rajendran R, Paray BA, Al-Sadoon MK, Al-Mfarjij AR. Evaluation of toxic metal contaminants in the demersal flatfishes (Order: Pleuronectiformes) collected from a marine biosphere reserve. *Regional Studies in Marine Science*. 2021;42.
7. Mary LCL, Sujatha MR, Santhanam P, Periyarayaki MT. Nutritional profiling of some commercially important seagrass associated edible marine fin fishes collected from Mimisal, southeast coast of India. *International Journal for Innovative Research in Science Technology*. 2015;1:2349-6010.
8. Nair RJ, Gopalakrishnan A. A Review on the Fisheries, Taxonomy, and Status of the Flatfishes in Tropical Waters. *Reviews in Fisheries Science & Aquaculture*. 2014;22:175-83.
9. CMFRI F. Marine Fish Landings in India-2019. 2020.
10. Keshava N, Sen D. Proximate composition of five species of flat fishes. *Fishery Technology*. 1983;20:24-8.
11. Mathivanan K, Rajaram R. Anthropogenic influences on toxic metals in water and sediment samples collected from industrially polluted Cuddalore coast, Southeast coast of India. *Environmental Earth Sciences*. 2013;72:997-1010.



**Manikandan Ramasamy et al.,**

12. Arumugam G, Rajendran R, Shanmugam V, Sethu R, Krishnamurthi M. Flow of toxic metals in food-web components of tropical mangrove ecosystem, Southern India. *Human and Ecological Risk Assessment: An International Journal* 2018;24:1367-87.
13. Lowry OH, Rosebrough NJ, Farr AL, Randall RJ. Protein measurement with the Folin phenol reagent. *Journal of biological chemistry*. 1951;193:265-75.
14. Folch J, Lees M, Sloane Stanley GH. A simple method for the isolation and purification of total lipides from animal tissues. *Journal of Biological Chemistry*. 1957;226:497-509. Epub 1957/05/01.
15. Dubois M, Gilles KA, Hamilton JK, Rebers Pt, Smith F. Colorimetric method for determination of sugars and related substances. *Analytical chemistry*. 1956;28:350-6.
16. Zhang H, Zhu HJ, Wang SP, Wang WH. Investigation of hydrolysis conditions and properties on protein hydrolysates from flatfish skin. *Frontiers of Chemical Science and Engineering*. 2013;7:303-11.
17. Salam M. Seasonal changes in the biochemical composition of body muscles of a freshwater catfish, *Heteropneustes fossilis* Bangladesh Journal of Life Science. 2002;14:47-54.
18. Barbosa RG, Trigo M, Prego R, Fett R, Aubourg SP. The chemical composition of different edible locations (central and edge muscles) of flat fish (*Lepidorhombus whiffiagonis*). *International Journal Food Science & Technology*. 2018;53:271-81.
19. Lall S, Parazo M. Vitamins in fish and shellfish. *Fish fishery product: composition, nutritive properties stability*. 1995:157-86.
20. Islam MN, Joadder MAR. Seasonal variation of the proximate composition of freshwater gobi. *Glossogobius giurus* (Hamilton) from the river Padma. 2005.
21. Binoy KD, MAHANTA R, GOSWAMI UC. Seasonal variation of Protein and essential amino acid contents in *Labeo gonius* from lotic and lentic water bodies. *World Journal of Life Sciences Medical Research*. 2012;2:71.
22. Begum M, Akter T, Minar M. Analysis of the proximate composition of domesticated stock of pangas (*Pangasianodon hypophthalmus*) in laboratory condition. *Journal of Environmental Science Natural Resources*. 2012;5:69-74.
23. Begum M, Minar MH. Comparative study about body composition of different SIS, shell fish and ilish; commonly available in Bangladesh. *Trends in Fisheries research*. 2012;1:38-42.
24. Kang KT, Heu MS, Kim JS. Preparation and food component characteristics of snack using flatfish-frame. *Journal of the Korean Society of Food Science Nutrition*. 2007;36:651-6.
25. Kim JD, Lall SP. Amino acid composition of whole body tissue of Atlantic halibut (*Hippoglossus hippoglossus*), yellowtail flounder (*Pleuronectes ferruginea*) and Japanese flounder (*Paralichthys olivaceus*). *Aquaculture*. 2000;187:367-73.
26. Azim M, Islam M, Hossain MB, Minar M. Seasonal variations in the proximate composition of Gangetic Sillago, *Sillaginopsis panijus* (Perciformes: Sillaginidae). *Middle-East Journal of Scientific Research*. 2012;11:559-62.
27. Drazen JC. Depth related trends in proximate composition of demersal fishes in the eastern North Pacific. *Deep-Sea Res Pt I*. 2007;54:203-19.
28. Barua P, Pervez M, Sarkar D, Sarker S. Proximate biochemical composition of some commercial marine fishes from Bay of Bengal, Bangladesh. *Mesopot Journal of Marine Science*. 2012;27:59-66.
29. Deradoss P. Nutritive values of sharks, skates and rays caught from Protonova coast. *Indian Journal of Fisheries*. 1983;30:156-61.
30. Hardy R, Keay JN. Seasonal variations in the chemical composition of Cornish mackerel, *Scomber scombrus* (L), with detailed reference to the lipids. *International Journal of Food Science Technology*. 1972;7:125-37.
31. Huss HH. Quality and quality changes in fresh fish: FAO Rome; 1995.
32. Zlatanov S, Laskaridis K. Seasonal variation in the fatty acid composition of three Mediterranean fish – sardine (*Sardina pilchardus*), anchovy (*Engraulis encrasicolus*) and picarel (*Spicara smaris*). *Food Chemistry*. 2007;103:725-8.
33. Beninger PG, Lucas A. Seasonal variations in condition, reproductive activity, and gross biochemical composition of two species of adult clam reared in a common habitat: *Tapes decussatus* L. (Jeffreys) and *Tapes philippinarum* (Adams & Reeve). *Journal of Experimental Marine Biology and Ecology*. 1984;79:19-37.





Table 1. Representation of depth range inhabited by the flat fish and their body lengths observed in the current study.

S.No	Family	Scientific name	Common name	Depth range ^a (m)	Length as per current study ^b (cm)
1	Bothidae	<i>Bothusguibei</i>	Guinean flounder	15–40	21.30 ± 3.90
2		<i>Crossarhombusvalderostratus</i>	Broad brow flounder	35–146	11.50 ± 1.70
3		<i>Laeopsmacrophthalmus</i>	Left eye flounder	183	8.30 ± 3.90
4		<i>Laeopsguentheri</i>	Gunther flounder	15–329	7.50 ± 6.10
5		<i>Crossorhombusazureus</i>	Blue flounder	13–60	11.50 ± 1.20
6		<i>Grammatobothus polyophthalmus</i>	Three spot flounder	0–90	10.00 ± 3.70
7	Cynoglossidae	<i>Cynoglossuscarpenteri</i>	Hooked tongue sole	27–420	14.00 ± 5.80
8		<i>Cynoglossusitinus</i>	Speckled tongue sole	-	13.00 ± 1.20
9		<i>Cynoglossusarel</i>	Largescale tongue sole	-	21.10 ± 3.40
10		<i>Cynoglossus semifasciatus</i>	Bengal tongue sole	12–18	37.00 ± 2.40
11		<i>paraplagusiabilineata</i>	Double lined tongue sole	1–25	48.20 ± 2.90
12	Citharida	<i>Citharoides macrolepis</i>	Two spot largescale flounder	182–200	11.50 ± 1.60
13	Paralichthyidae	<i>Pseudorhombusarsius</i>	Large tooth flounder	0–200	17.50 ± 4.50
14		<i>Pseudorhombusdiplospilus</i>	Four twin spot flounder	10–75	18.50 ± 1.90
15		<i>Pseudorhombuselevatus</i>	Deep flounder	7–200	13.50 ± 4.10
16		<i>Pseudorhombusjavanicus</i>	Javan flounder	22–38	6.00 ± 3.10
17		<i>Pseudorhombustriocellatus</i>	Three spotted flounder	17	5.00 ± 2.50
18	Psettodidae	<i>Psettodeserumei</i>	Indian halibut	1–100	25.00 ± 2.10
19	Samaridae	<i>Samariscristatus</i>	Cockatoo righteye flounder	20–114	19.00 ± 3.20
20	Soleidae	<i>Aesopiacornuta</i>	Unicorn sole	8–100	18.00 ± 1.60
21		<i>Brachirusorienails</i>	Oriental sole	15–20	20.00 ± 2.50
22		<i>Heteromycterishartfeldii</i>	Hook nosed sole	-	12.00 ± 3.10
23		<i>Pardachiruspavoninus</i>	Peacock sole	2–40	14.50 ± 2.50
24		<i>Synapturaalbomaculata</i>	Kaups sole	-	13.80 ± 1.60
25		<i>Synapturacommersonnii</i>	Commersons sole	-	17.50 ± 4.30
26		<i>Synapturalusitanica</i>	Portuguese sole	0–125	29.00 ± 1.00
27		<i>Zebriascochinensis</i>	-	-	17.00 ± 2.10
28		<i>Zebrias craticulus</i>	Wicker work sole	-	6.00 ± 5.30
29		<i>Zebriassynaptruroides</i>	Indian zebra sole	43–125	16.00 ± 1.20
30		<i>Zebrias quagga</i>	Fringefin zebra sole	-	8.00 ± 2.50

^aData as per FISHBASE data

^bData represent as mean ± standard deviation

Table 2. Protein, carbohydrate, and lipid profiles in the flatfishes

Name of the fish species	Protein %		Carbohydrate %		Lipid%	
	Monsoon	Summer	Monsoon	Summer	Monsoon	Summer
<i>Samariscristatus Gray</i>	8.15 ± 0.27	27.65 ± 1.91	1.73 ± 0.47	7.53 ± 0.52	1.12 ± 0.14	2.19 ± 0.33
<i>Pseudorhombusarsius</i>	42.33 ± 1.00	54.62 ± 0.76	3.18 ± 0.37	9.50 ± 0.60	1.21 ± 0.32	2.07 ± 0.58
<i>Pseudorhombusdiplospilus</i>	25.28 ± 0.75	53.95 ± 1.66	10.30 ± 0.70	11.41 ± 1.09	1.32 ± 0.31	1.59 ± 0.38
<i>Aesopiacornuta</i>	28.83 ± 0.23	30.77 ± 0.75	4.35 ± 0.78	8.40 ± 0.78	1.53 ± 0.95	1.43 ± 0.45
<i>Zebriascochinensis</i>	25.77 ± 0.28	39.61 ± 0.84	10.34 ± 0.99	7.09 ± 0.59	1.77 ± 0.57	1.47 ± 0.37
<i>Synapturaalbomaculata</i>	7.58 ± 0.36	47.44 ± 0.68	1.74 ± 0.56	9.33 ± 0.67	2.13 ± 0.49	1.88 ± 0.40
<i>Cynoglossuscarpenteri</i>	11.27 ± 0.28	40.55 ± 0.52	8.13 ± 0.28	9.41 ± 0.84	1.62 ± 0.24	1.33 ± 0.20





Manikandan Ramasamy et al.,

<i>Pseudorhombustriocellatus</i>	30.68 ± 0.63	27.75 ± 0.87	3.75 ± 0.85	9.07 ± 0.33	2.54 ± 0.28	1.12 ± 0.51
<i>Pseudorhombusjavanicus</i>	10.01 ± 0.35	29.31 ± 0.58	6.22 ± 0.24	7.07 ± 0.51	1.10 ± 0.21	1.12 ± 0.60
<i>Zebrias quagga</i>	6.09 ± 0.19	31.56 ± 0.93	11.19 ± 0.65	6.96 ± 0.17	1.93 ± 0.67	0.67 ± 0.35
<i>Synapturacommersonii</i>	42.28 ± 0.29	40.77 ± 1.01	1.77 ± 0.76	11.65 ± 0.92	1.13 ± 0.37	1.51 ± 0.27
<i>Cynoglossusitinus</i>	35.70 ± 0.66	26.38 ± 0.44	5.99 ± 0.55	7.48 ± 0.80	1.24 ± 0.29	0.84 ± 0.30
<i>Heteromycterishartfeldii</i>	36.64 ± 0.34	51.41 ± 0.54	3.13 ± 0.76	6.83 ± 0.33	0.61 ± 0.30	0.98 ± 0.41
<i>Psettodeserumei</i>	36.60 ± 0.49	40.99 ± 1.05	3.38 ± 0.64	7.25 ± 0.72	2.16 ± 0.31	1.26 ± 0.55
<i>Brachirusoriemails</i>	46.30 ± 0.31	42.38 ± 0.47	4.37 ± 0.72	11.01 ± 1.64	2.35 ± 0.71	0.80 ± 0.27
<i>Synapturalusitanica</i>	26.92 ± 0.17	40.68 ± 1.06	6.20 ± 0.76	13.08 ± 0.47	0.44 ± 0.28	1.41 ± 0.14
<i>Cynoglossusarel</i>	40.06 ± 0.11	47.32 ± 0.67	10.65 ± 1.02	10.84 ± 0.64	2.29 ± 0.30	1.51 ± 0.34
<i>Pardachiruspavoninus</i>	44.42 ± 0.82	48.3 ± 0.46	3.79 ± 0.27	15.05 ± 0.08	0.45 ± 0.39	1.76 ± 0.67
<i>Crossorhombus valdeostratus</i>	15.6 ± 0.48	43.37 ± 0.56	6.11 ± 0.73	7.87 ± 0.67	1.44 ± 0.48	1.15 ± 0.15
<i>Paraplagusia bilineata</i>	35.37 ± 0.69	47.25 ± 0.67	2.73 ± 0.68	4.64 ± 1.08	1.28 ± 0.28	0.95 ± 0.07
<i>Zebriassynaptururoides</i>	45.41 ± 1.01	41.39 ± 0.44	2.57 ± 0.78	13.02 ± 0.06	0.77 ± 0.12	1.90 ± 0.30
<i>Cynoglossus semifasciatus</i>	25.82 ± 0.69	29.33 ± 0.51	2.50 ± 0.45	6.18 ± 0.58	1.58 ± 0.31	1.33 ± 0.31
<i>Pseudorhombuselevatuss</i>	26.76 ± 0.44	14.18 ± 1.04	1.13 ± 0.39	8.53 ± 0.56	2.73 ± 0.30	1.44 ± 0.38
<i>Bothusguibei</i>	36.32 ± 0.93	43.21 ± 0.58	2.41 ± 0.52	9.69 ± 0.52	0.50 ± 0.05	0.77 ± 0.58
<i>Crossorhombusazureus</i>	31.36 ± 0.32	40.84 ± 0.82	4.17 ± 0.61	10.45 ± 0.77	1.56 ± 0.47	1.59 ± 0.39
<i>Laeops macrophthalmus</i>	18.77 ± 0.53	49.52 ± 0.75	1.97 ± 0.39	13.51 ± 0.62	1.36 ± 0.29	1.04 ± 0.56
<i>Zebrias craticulus</i>	29.22 ± 0.88	32.89 ± 0.51	2.23 ± 0.58	13.42 ± 1.00	1.58 ± 0.49	1.13 ± 0.86
<i>Grammatobothus polyophthalmus</i>	12.52 ± 0.75	44.13 ± 0.67	4.12 ± 0.59	6.87 ± 0.65	0.49 ± 0.36	1.80 ± 0.21
<i>Citharoides macrolepis</i>	42.23 ± 0.96	65.49 ± 0.53	9.34 ± 0.79	9.87 ± 0.99	1.67 ± 0.42	1.49 ± 0.50
<i>Laeops guentheri</i>	17.34 ± 0.72	18.64 ± 1.06	4.08 ± 0.67	10.43 ± 0.45	2.79 ± 0.27	0.97 ± 0.78

All data are computed from triplicate readings of the sample and represented as mean ± standard deviation

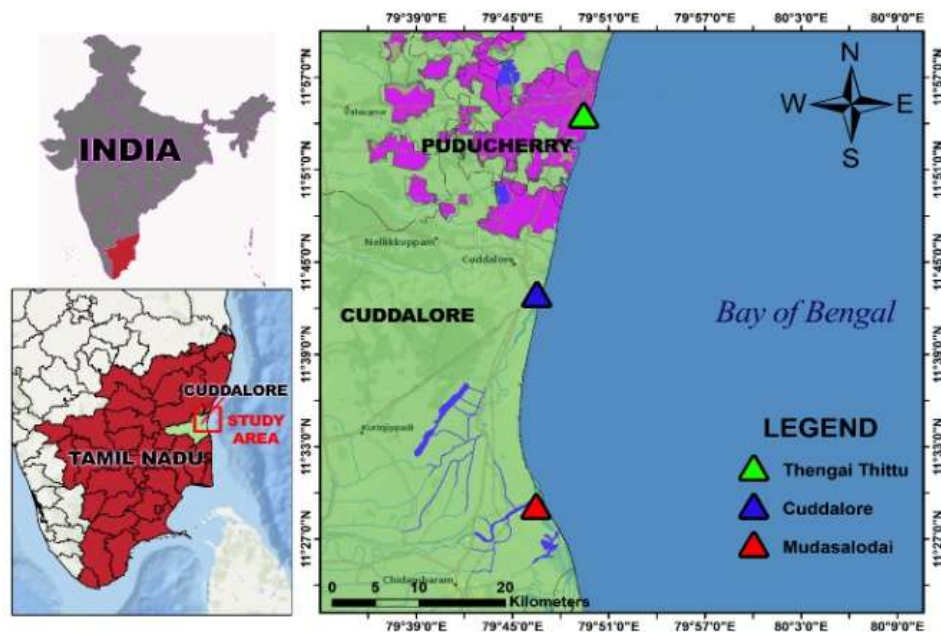


Figure 1. Map of the study area





Manikandan Ramasamy et al.,

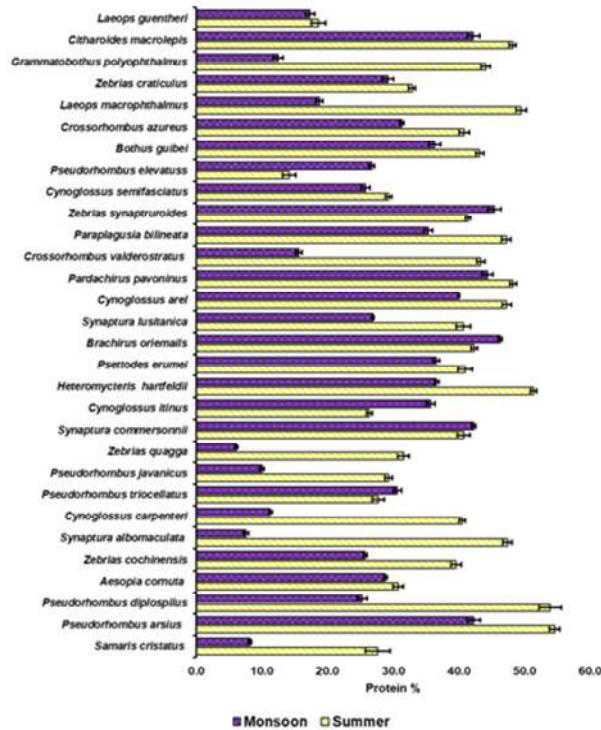


Figure 2. Bar diagram showing the seasonal variation in protein levels in the muscle of flatfishes

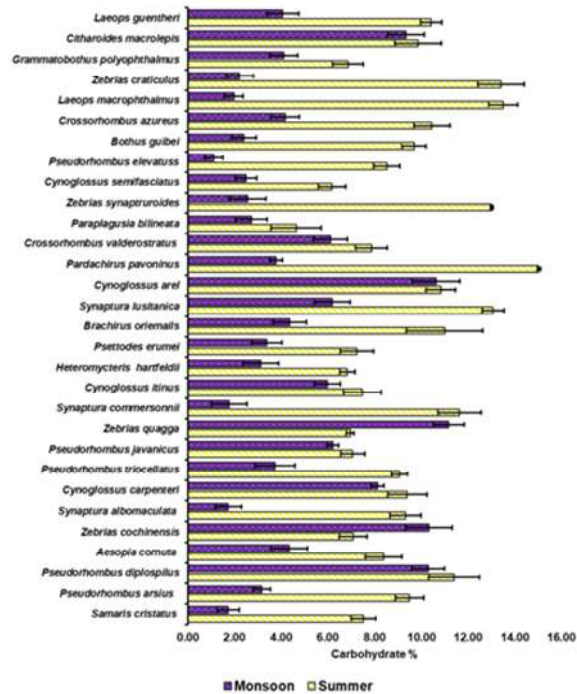


Figure 3. Bar diagram showing the seasonal variation in carbohydrate levels in the muscle of flatfishes





Manikandan Ramasamy et al.,

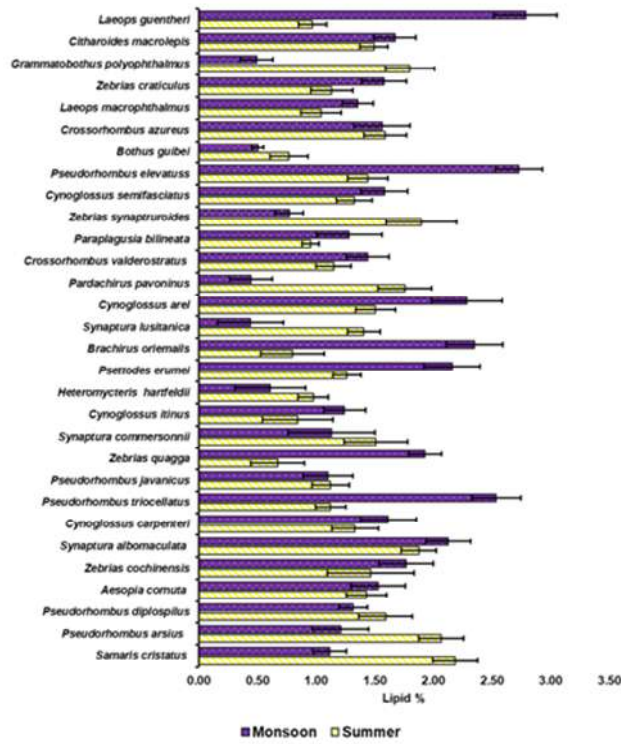


Figure 4. Bar diagram showing the seasonal variation in lipid levels in the muscle of flatfishes





Development of Customised Genomic DNA Isolation Protocol for Crop Wild Relatives of *Cymbopogons* Sourced Out from Karnataka – A Secondary Metabolite Rich Genus

Sree Latha K¹ and K J Thara Saraswathi^{2*}

¹Research Scholar, Department of Microbiology and Biotechnology, Jnanabharathi Campus, Bangalore University, Bangalore, Karnataka, India.

²Professor, Department of Microbiology and Biotechnology, Jnanabharathi Campus, Bangalore University, Bangalore, Karnataka, India.

Received: 25 Dec 2021

Revised: 03 Jan 2022

Accepted: 18 Jan 2022

*Address for Correspondence

K J Thara Saraswathi

Professor,

Department of Microbiology and Biotechnology,

Jnanabharathi Campus,

Bangalore University,

Bangalore, Karnataka, India.

Email: dr.thrabiotech@gmail.com



This is an Open Access Journal / article distributed under the terms of the **Creative Commons Attribution License** (CC BY-NC-ND 3.0) which permits unrestricted use, distribution, and reproduction in any medium, provided the original work is properly cited. All rights reserved.

ABSTRACT

Cymbopogon primarily is one amongst the most important Genera of the family Poaceae due to its essential oil yielding properties. Isolation of good quality DNA is an important pre-requisite of various molecular and biotechnological studies. Extraction of DNA from medicinal and aromatic plants is often problematic; since these plants contain high levels of secondary metabolites which interfere with the isolation process. The present study was taken up to optimize an efficient DNA isolation protocol for *Cymbopogon* species growing naturally in different regions of Karnataka. The quantity and quality of DNA was assessed by using Nanospectrophotometer as well as by performing Agarose Gel Electrophoresis. The quality of the results obtained indicate the efficacy of the protocol developed. The efficacy of this protocol in terms of cost effectiveness, quantitative and qualitative retrieval of Genomic DNA makes the present method a noticeable alternative for total genomic DNA extraction from wild *Cymbopogon* species growing in Karnataka.

Keywords: Crop Wild Relatives, *Cymbopogon* species, Genomic DNA Isolation, CTAB method, Agarose Gel Electrophoresis



**Sree Latha and Thara Saraswathi**

INTRODUCTION

The Genus *Cymbopogon* is one amongst the major aromatic plant genera belonging to the tribe Andropogoneae of the family Poaceae, comprising about 180 species, subspecies, varieties, and sub varieties [1,2,3]. They occupy an important place in the socio-cultural, spiritual and perfumery aspects all over the world [4]. Global *essential oil market* for *Cymbopogons* is segmented by type (aldehyde, alcohol, and intermediate types) [5]. Due to their vast economic potential, they continue to play a central role in flavour and fragrance industries [6]. The basis for this use is that these plants contain so called ethereal or active ingredients. These plants grow in tufts where long, narrow leaves and multiple stems arise directly from rhizomatous root (root like subterranean stem that sends out roots and shoots from its nodes). Classification of this Genus based upon their morphological parameters is preposterous as these members of Poaceae are morphologically indiscernible [7]. The variation in essential oil components can serve as taxonomical classification markers to find the diversity present in *Cymbopogon* [8]. But, all the various morphological and chemo-taxonomical markers (essential oil composition) are variable parameters for classification as they can be strongly influenced by environmental factors and show slight difference at inter and subtle difference at intra-specific level [9].

Correspondingly, it requires better understanding of genetic diversity in the view of increasing global demand of *Cymbopogon* essential oils and their individual components[10].Consequently, in order to understand the genetic composition, diversity and phylogeny of *Cymbopogon*, different DNA molecular markers play an important role[11]. With the advancement in plant molecular and genomic studies, one can observe numerous advents of techniques and analyses involving sequencing of whole genomes, manipulation of plant genomes for producing superior cultivars aimed for better yield of essential oil, molecular breeding, identifying different genes responsible for key traits and their management, establishing phylogeny and creating genetic maps[12]. For all these diverse downstream genome applications to be followed, the very crucial step is to obtain contaminant free DNA in high concentration [13]. All the phenotypic traits observed whether being morphological or chemotactic are the selective expression of the genotype of an organism [14]. Therefore, DNA markers can provide conclusive results for the genetic variation among these species as the results would not be affected by environmental factors, age and processing of the sample [15]. These are solely based upon the genetic composition of a species and will help in accessing these variations appropriately aiding in distinguishing different taxa [16].

There are various protocols developed for extraction of genomic DNA from different plant sources. But no single protocol can be applied ubiquitously to all plants due to the complexity of metabolites present in plant tissues [17]. Many modifications and standardization steps in the established protocols are needed based upon the purpose of isolation and the source of isolation. In literature, some of the most frequently used protocols for isolation of plant chromosomal DNA are given [18,19,20,21].The best and most commonly used protocol for extraction of total genomic DNA from plant tissues is Cetyl Trimethyl Ammonium Bromide (CTAB) method [19].Several efficient protocols developed for isolation of genomic DNA from plant tissues is majorly a modification of this procedure. In *Cymbopogon* species, retrieval of quality DNA gets hampered due to the interference of biomolecules such as polysaccharides, polyphenols and secondary metabolites such as essential oils [22] which demand complex and time-consuming DNA isolation procedures in the species. To encounter these issues, an efficient protocol for isolation of DNA from different *Cymbopogon* species is described vividly [17], which is a modification of the CTAB method. They described a rapid DNA isolation protocol that could be commonly used for diverse medical and aromatic plants and specifically for cultivated species of *Cymbopogons* using dry and fresh plant tissue. This was further modified [23]. This protocol did not work for the samples that were collected from wild locations of Karnataka. Crop Wild Relatives (CWR) are rich in broad spectrum secondary metabolites for their survival in natural environment [24]. Hence, the present study was to develop competent protocol that precisely worked for *Cymbopogon* species indigenously growing across Karnataka.





Sree Latha and Thara Saraswathi

MATERIALS AND METHODS

Source: Three different species of *Cymbopogon* were selected for the study – *C.citratus*, *C.flexuosus* and *C.martinii* that predominantly grow across wild locations of Karnataka. The study consisted of six samples which included two accessions from each *Cymbopogon* species. (Table 1). Fresh and young leaves were collected, labelled, and stored at -20°C till further use. Samples were stored at that temperature to upsurge their longevity. 100 mg of tender leaves were used for the isolation of genomic DNA. The procedure developed here is a modification of the protocol established [23]. The experiment was conducted in triplicates.

Reagents and Chemicals Required

Genomic DNA Isolation: Tris-Cl (0.2M) pH 8.0, EDTA (0.05M) pH 8.0, NaCl (2M), 10% SDS (w/v), 4% CTAB (w/v), 10% PolyVinylPyrolidone (PVP) (w/v), 0.2% β -Mercaptoethanol (v/v), Chloroform: Isoamyl Alcohol (24:1) (v/v), 75% Ethanol (v/v), Sodium Acetate (3M) (w/v)

DNA Extraction buffer (pH 8.0): Tris-Cl (0.2M) pH 8.0, EDTA (0.05M) pH 8.0, NaCl 2M, 10% SDS (w/v), 4% CTAB (w/v), 10% PolyVinylPyrolidone (PVP) (w/v) (added immediately before use), β -Mercaptoethanol (v/v) (added immediately before use)

TE Buffer for preservation of isolated DNA (pH 8.0): Tris-Cl 10 mM (pH8.0), EDTA 1mM (pH 8.0), 1MNaCl

Agarose Gel Electrophoresis (AGE): Agarose 0.8% (w/v), DNA marker (100 bp DNA ladder), Bromophenol blue-loading dye (8 μ l for each 2 μ l of DNA sample), Ethidium Bromide (2-5 μ l in 100 ml of Agarose solution)

1X TAE Buffer (pH 8.5) for preparation of Agarose solution: Tris Base (0.04M), Disodium EDTA (0.002M), Acetic acid (0.02M).

Procedure

Genomic DNA Isolation

- i. Extraction buffer was pre-heated in a water bath at 65°C (to allow the activation of all compounds in the buffer).
- ii. 100 mg of leaf sample was finely chopped and stored at -20°C for an hour before grinding.
- iii. Sample transferred to the mortar. 1 ml of 4% CTAB extraction buffer (1:10) added and the plant sample was grinded to obtain a homogenised mixture. Extra buffer was added if required during grinding.
- iv. The mixture was filtered in sterile muslin cloth to eliminate fibrous and tough debris, filtrate was transferred to 2 ml centrifuge vial.
- v. Vial was kept for incubation at 65°C for 40 min. in water bath.
- vi. After incubation, the sample was subjected to centrifugation at 6000 r.p.m. for 15 min. at RoomTemp. (RT).
- vii. The supernatant was collected in fresh vial. 2.5 μ l of RNase A enzyme added and incubated at 37°C for 30 min.
- viii. After incubation, Chloroform: Isoamyl Alcohol (24:1) mixture was added in equal proportion to the supernatant and mixed by gentle inversion of the vial.
- ix. The vial was then subjected to second round of centrifugation at 6000 r.p.m. for 10 min.
- x. Steps viii and ix were repeated.
- xi. The supernatant was transferred to fresh vial, two-thirds volume of chilled Isopropanol was added. The vial was vortexed thoroughly.
- xii. The vial was then incubated overnight at -20°C.
- xiii. After incubation, sample was centrifuged at 6000 r.p.m. for 15min. DNA pellet was observed.
- xiv. Supernatant discarded. 75% chilled ethanol was added to wash out any remaining chemical associated with the pelleted DNA. The vial was kept open in a non-dusty place overnight for the evaporation of residual 75% ethanol from the pellet.
- xv. The pellet was re-suspended in TE Buffer (30 μ L) for preservation of the isolated DNA. The vial containing isolated DNA was stored at -20°C (remains stable and intact for longer duration) for further downstream application processes.



**Sree Latha and Thara Saraswathi****Treatment for secondary metabolites associated with DNA**

The vials which appeared to be contaminated due to the association of secondary metabolites (brown coloured DNA pellets) were further treated with the reagents. This was performed after the third centrifugation. 80µL of 3M sodium acetate and 80µL of Isopropanol were added to the DNA pellet. These vials were subjected to centrifugation at 5000 r.p.m. for 10 min. The colourless pelleted DNA saved, and supernatant discarded. Pelleted DNA was further subjected to wash with 75% ethanol (Step xiv).

Quantitative and Qualitative assessment of isolated DNA

The quality and quantity DNA samples were assessed using Nanodrop Spectrophotometer. The quality of DNA samples was also assessed by AGE. The gel concentration used was 0.8%. AGE was performed by standard technique [23].

RESULTS AND DISCUSSION

Genomic DNA Isolation through CTAB method for plant samples was established by [19] for the first time. The species of *Cymbopogon* are known to synthesize a wide spectrum of terpenoid compounds, functional polysaccharides, polyphenols, and other secondary metabolites [11]. These components interfere extensively while extracting genomic DNA. As a result, securing pure and intact DNA will get compromised. To prevail pure, intact, and high-quality genomic DNA, [23] established a modified version of CTAB protocol to suit extraction of DNA from *Cymbopogon* species. It has worked well for cultivated varieties of *Cymbopogons* as the hindrance from secondary metabolites is not beyond manageable levels in them. This protocol was initially followed for the Crop Wild Relatives (CWR) of *Cymbopogon* species sourced out from Karnataka. Due to the presence of diverse complex metabolites in wild accessions, high concentration of pure DNA could not be obtained from the regular protocol. Owing to unsatisfactory results even after multiple attempts, authors have brought in few modifications in the protocol developed by [23] to suit each of the samples taken for the study.

The use of pre-chilled mortar and pestle along with liquid nitrogen for the leaf samples helped in good maceration without needing much physical pressure which avoided any mechanical damage that could be caused during homogenization. Due to excessive cell debris, distinct layer of cellular components and the debris could not be distinguished in the initial stages. Here, filtration post homogenisation played a very crucial role wherein the cell debris was eliminated immediately after homogenization process. Hence, appropriate amount of extraction buffer could be added for easy movement of cellular components within the vial to expel the active cellular components from inside the cell while vortexing. This led to precise contact and action of buffer on cellular components and not the debris. Using concentrated β-Mercaptoethanol successfully removed the polyphenols making it easier for extraction of high-quality DNA. The superior quality of DNA obtained could also be attributed to the addition of a pinch of PVP that is added as part of usual CTAB protocol which acts effectively on polyphenols [23]. PVP with low molecular weight has less tendency of precipitating polyphenols that are associated with nucleic acids as compared to PVP with high molecular weight thus separating DNA by omitting significant amount of polyphenols [25]. The addition of NaCl at concentrations higher than 0.5 M in the extraction buffer is known to remove polysaccharides and also, participates in precipitating DNA during extraction [26]. In the present work, using higher concentration of NaCl (2M) in the extraction buffer eased the removal of high levels of polysaccharides which is plant specific and therefore, leading the way to obtain improved quality of DNA. Beyond this control measure taken in the initial steps, few polysaccharides escaped this step and their occurrence associated with DNA sample was characterized by formation of a highly viscous solution. Further alterations needed to be made to yield high-quality and quantity genomic DNA. Additional incubation of the samples in Isopropanol played a key role in pooling and precipitation of higher amount of DNA present in samples.

Role of Isopropanol along with salt solution (NaCl) is to precipitate DNA from the solution. The salt neutralizes the negative charge of the phosphate in DNA and Isopropanol removes hydration shell of water molecules around the phosphate [27]. Consequently, DNA gets precipitated along with salt solution. Further washing with 75% ethanol



**Sree Latha and Thara Saraswathi**

removes all organic impurities (salt, phenols, chloroform etc.) associated with genomic DNA. As part of additional modification, the samples after washing with 75% ethanol was further incubated in Isopropanol at -20°C for 5-6 days. Subsequently, visual discrimination indicated the procurement of whitish, pure and intact DNA in the vials. TE buffer was used to preserve the extracted DNA until further use. Quantity and quality of the isolated DNA from all the samples were assessed by regular methods- Nano spectrophotometer (Fig. 1), (Table 2) and AGE (Fig. 2). The present study stipulated customised additional modifications to be made in the protocol for the accessions collected from natural sites of Karnataka. The slight modifications brought in this study made a prominent remark in obtaining high quality DNA in reasonably good amounts. Addressing physical, chemical, and mechanical parameters adds value to obtain high throughput DNA. Hence, DNA isolation is both an art and science. The protocol established in this work is recommended for the wild species of *Cymbopogon* which produce complex secondary metabolites to withstand diverse biotic and abiotic stresses they encounter in natural environments.

REFERENCES

1. Bor, N. L. (1960). The grasses of Burma. *Ceylon, India and Pakistan*, 1.
2. Chase, A., & Niles, C. D. (1962). Index to grass species.
3. Soenarko, S. (1977). The genus *Cymbopogon Sprengel* (Gramineae). *Reinwardtia*, 9(3), 225-375.
4. Oladeji, O. S., Adelowo, F. E., Ayodele, D. T., & Odelade, K. A. (2019). Phytochemistry and pharmacological activities of *Cymbopogon citratus*: A review. *Scientific African*, 6, e00137.
5. Meena, S., Kumar, S. R., Venkata Rao, D. K., Dwivedi, V., Shilpashree, H. B., Rastogi, S., ... & Nagegowda, D. A. (2016). De novo sequencing and analysis of lemongrass transcriptome provide first insights into the essential oil biosynthesis of aromatic grasses. *Frontiers in plant science*, 7, 1129.
6. Yakubu, M. T., Mostafa, M., Ashafa, A. O. T., & Afolayan, A. J. (2012). Antimicrobial activity of the solvent fractions from *Bulbinenatalensis* tuber. *African Journal of Traditional, Complementary and Alternative Medicines*, 9(4), 459-464.
7. Shah, G., Shri, R., Panchal, V., Sharma, N., Singh, B., & Mann, A. S. (2011). Scientific basis for the therapeutic use of *Cymbopogon citratus*, stapf (Lemon grass). *Journal of advanced pharmaceutical technology & research*, 2(1), 3.
8. Bhatnagar, A. (2018). Composition variation of essential oil of *cymbopogon* spp. Growing in Garhwal region of Uttarakhand, India. *Journal of Applied and Natural science*, 10(1), 363-366.
9. Labra, M., Miele, M., Ledda, B., Grassi, F., Mazzei, M., & Sala, F. (2004). Morphological characterization, essential oil composition and DNA genotyping of *Ocimum basilicum* L. cultivars. *Plant science*, 167(4), 725-731.
10. Kumar, J., Verma, V., Goyal, A., Shahi, A. K., Sparoo, R., Sangwan, R. S., & Qazi, G. N. (2009). Genetic diversity analysis in *Cymbopogon* species using DNA markers. *Plant Omics*, 2(1), 20.
11. Adhikari, S., Bandopadhyay, T. K., & Ghosh, P. D. (2013). Assessment of genetic diversity of certain Indian elite clones of *Cymbopogon* species through RAPD analysis.
12. Jackson, S. A., Iwata, A., Lee, S. H., Schmutz, J., & Shoemaker, R. (2011). Sequencing crop genomes: approaches and applications. *New Phytologist*, 191(4), 915-925.
13. Martignano, F. (2019). Cell-free DNA: an overview of sample types and isolation procedures. *Cell-free DNA as Diagnostic Markers*, 13-27.
14. Te Pas, M. F., Madsen, O., Calus, M. P., & Smits, M. A. (2017). The importance of endophenotypes to evaluate the relationship between genotype and external phenotype. *International journal of molecular sciences*, 18(2), 472.
15. Russell, J. R., Fuller, J. D., Macaulay, M., Hatz, B. G., Jahoor, A., Powell, W., & Waugh, R. (1997). Direct comparison of levels of genetic variation among barley accessions detected by RFLPs, AFLPs, SSRs and RAPDs. *Theoretical and Applied genetics*, 95(4), 714-722.
16. Soliveres, S., Van Der Plas, F., Manning, P., Prati, D., Gossner, M. M., Renner, S. C., ... & Allan, E. (2016). Biodiversity at multiple trophic levels is needed for ecosystem multifunctionality. *Nature*, 536(7617), 456-459.
17. Khanuja, S. P., Shasany, A. K., Darokar, M. P., & Kumar, S. (1999). Rapid isolation of DNA from dry and fresh samples of plants producing large amounts of secondary metabolites and essential oils. *Plant molecular biology Reporter*, 17(1), 74-74.





Sree Latha and Thara Saraswathi

18. Murray, M. G., & Thompson, W. F. (1980). Rapid isolation of high molecular weight plant DNA. *Nucleic acids research*, 8(19), 4321-4326.
19. Doyle, J. J., & Doyle, J. L. (1987). A rapid DNA isolation procedure for small quantities of fresh leaf tissue (No. RESEARCH).
20. Rogers, S. O., & Bendich, A. J. (1994). Extraction of total cellular DNA from plants, algae and fungi. In *Plant molecular biology manual* (pp. 183-190). Springer, Dordrecht.
21. Lodhi, M. A., Ye, G. N., Weeden, N. F., & Reisch, B. I. (1994). A simple and efficient method for DNA extraction from grapevine cultivars and Vitis species. *Plant Molecular Biology Reporter*, 12(1), 6-13.
22. Porebski, S., Bailey, L. G., & Baum, B. R. (1997). Modification of a CTAB DNA extraction protocol for plants containing high polysaccharide and polyphenol components. *Plant molecular biology reporter*, 15(1), 8-15.
23. Bishoyi, A. K., Kavane, A., Sharma, A., & Geetha, K. A. (2016). An efficient DNA isolation protocol for *Cymbopogon* species suitable for diverse downstream applications. *Journal of Applied Horticulture*, 18(2), 164-168.
24. Monteiro, F., Frese, L., Castro, S., Duarte, M. C., Paulo, O. S., Loureiro, J., & Romeiras, M. M. (2018). Genetic and genomic tools to assist sugar beet improvement: the value of the crop wild relatives. *Frontiers in plant science*, 9, 74.
25. Puchooa, D. (2004). A simple, rapid and efficient method for the extraction of genomic DNA from Lychee (*Litchi chinensis* Sonn.). *African Journal of Biotechnology*, 3(4), 253-255.
26. Sahu, S. K., Thangaraj, M., & Kathiresan, K. (2012). DNA extraction protocol for plants with high levels of secondary metabolites and polysaccharides without using liquid nitrogen and phenol. *International Scholarly Research Notices*, 2012.
27. Zhang, M., Cao, P., Dai, Q. Y., Wang, Y. Q., Feng, X. T., Wang, H. R., ... & Fu, Q. M. (2021). Comparative analysis of DNA extraction protocols for ancient soft tissue museum samples. *Zoological research*, 42(3), 280.

Table 1: Details of CWR of *Cymbopogon* Species collected from six districts of Karnataka used in the study

CWR of <i>Cymbopogon</i> Species	Abbreviation	Collection Site
<i>C. citratus</i>	C1a	Thonnur Lake, Mandya District
	C1b	Nandi hills, Doddaballapur district
<i>C. flexuosus</i>	C2a	Rocky hills, Bannerghatta Forest
	C2b	Sakaleshapura, Dakshina Kannada District
<i>C. martinii</i>	C3a	Bilikal betta, Ramanagara District
	C3b	Savandurga hills, Tumkur District

Table 2: Mathematical assessment of total genomic DNA intensity as revealed by Nanodrop Spectrophotometer in *Cymbopogon* spp.

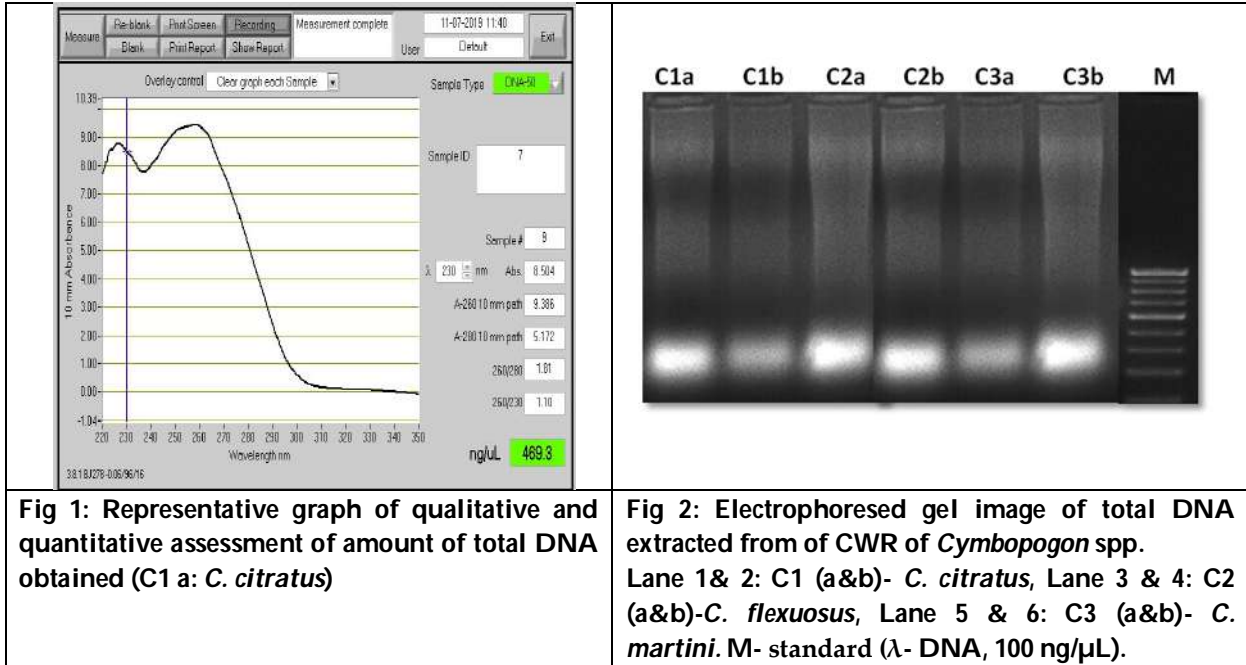
CWR of <i>Cymbopogon</i> Species	Abbreviation	Absorbance (nm)	Amount of DNA (ng/uL)
<i>C. citratus</i>	C1a	8.504	469.3
	C1b	8.603	470.9
<i>C. flexuosus</i>	C2a	5.620	391.9
	C2b	5.323	357.2
<i>C. martinii</i>	C3a	8.419	465.0
	C3b	7.474	429.8

*Experiments were conducted in triplicates





Sree Latha and Thara Saraswathi





Effect of Organic and Inorganic Fertilizer on Seed Germination of Some Millets in Chitradurga District, Karnataka, India

Shaila M^{1*} and Nafeesa Begum²

¹Research Scholar, Department of Botany, Sahyadri Science College, Kuvempu University, Shivamogga – 577203, Karnataka, India.

²Associate Professor, Department of Botany, Sahyadri Science College, Kuvempu University, Shivamogga – 577203, Karnataka, India.

Received: 22 Dec 2021

Revised: 29 Dec 2021

Accepted: 17 Jan 2022

*Address for Correspondence

Shaila M

Research Scholar,
Department of Botany,
Sahyadri Science College,
Kuvempu University,
Shivamogga – 577203, Karnataka, India.
Email: shailamresearchscholar95@gmail.com



This is an Open Access Journal / article distributed under the terms of the **Creative Commons Attribution License** (CC BY-NC-ND 3.0) which permits unrestricted use, distribution, and reproduction in any medium, provided the original work is properly cited. All rights reserved.

ABSTRACT

Millets are small seeded grasses that are hardy and grow well in dry zones as rain fed crops under marginal conditions of soil fertility and moisture. Our investigation was conducted to assess the effect of Organic (Vermicompost) and inorganic fertilizers (DAP) and different types of soils on seed germination of selected Millets are Foxtail millet, little millet, Proso millet and Kodo millet were germinated by Nursery plate and the evaluation of germination by petri-dishes lined with blotting paper. The seeds were germinated in 15 days intervals for the seed germination percentage was significant and the process is affected by the application of DAP, Vermicomposting, Loamy soil and Black Soil. Vermicompost was more effective than other fertilizers and soil types of all the selected millets. The germination percentage and the growth parameters were observed in up to 7 days. The obtained results showed that the germination rate of the germination percentage, root length, shoot length of the Millets were gradually decreased with increases. The highest germination and morphological parameters observed in foxtail millet and the results are graphically interpreted. Moreover, Vermicompost is found to be the good source of nutrients for selected Millets growth. Hence the application of Vermicompost can be recommended as an effective organic source. Organic farming minimizes environmental pollution and maintains the sustainability of soil by maintaining high soil organic matter.

Keywords: Foxtail Millet, Kodo Millet, Little Millet, Proso Millet, Vermicompost



**Shaila and Nafeesa Begum****INTRODUCTION**

Millets are group of coarse cereals that produce a small seeds and used mainly as food, feed and forage grown in arid and semi-arid regions in the world. The millets of sorghum (*Sorghum bicolor* L.) and pearl millet (*Pennisetum glaucum* L.) are known as major millets. Small millets are cultivated by resource-poor farmers in subsistence cropping system with an acreage of around 7.0 lakh ha with a productivity of 633 kg/ha (Maitra and Shankar, 2019). In India, small millets are grown in 6.8 lakh ha and the country ranks the first with 80% of the production of Asia (Maitra, 2020). Out of different small millets cultivated in India, finger millet (*Eleusine coracana* L. Gaertn) shares about 80% of production and it is followed by kodo millet (*Paspalum scrobiculatum* L.) Little millet (*Panicum sumatrense* L.) and foxtail millet (*Setaria italica* L.) Foxtail millet and Little millets and small millets, belongs to the family Poaceae the plants are grown in highly drought tolerant crop grown in dry lands under rain fed conditions (Brahmachari *et al.*, 2018). In India, the cultivation of foxtail millet is confined mainly to Andhra Pradesh, Karnataka and Tamil Nadu. Small millets are considered as functional foods containing bioactive ingredients useful to combat against chronic diseases (Banerjee and Maitra, 2020).

In the present context of adverse climatic conditions due to global warming, dry land agriculture became more risky and growing of hardy crops is one of the solutions to combat climate change. Foxtail millet and Little Millets are low input demanding and ecologically crop which can automatically be chosen for agricultural sustainability in dry lands. The average productivity of foxtail millet in India is 780 kg ha⁻¹ (Monisha *et al.*, 2019). Synthetic fertilizers are sometimes referred to as being artificial or chemical Fertilizers, Implying that, these are inferior to those termed natural (mainly organic) products. However, fertilizers are neither unnatural nor inferior products. Many fertilizers are finished products derived from natural deposits, either made more useful for plants (Eg: Phosphate) or separated harmful components (Eg: Potassium fertilizers). The current practice in agriculture is basically chemical based farming that makes a considerable contribution to the degradation of our natural resource especially soil. In Karnataka small millets are occupy 26 thousand hectares with the production of 12.3 thousand tonnes (Anon 2012). The Millets are occupies in marginal area but is a truthful crop under situations of very late onset of monsoon or prevalence of intermittent drought. Its cultivation is majorly seen in dry belts of Chitradurga, Shivamogga, Haveri and Davanagere districts of the state. It is considered as a coarse grain and is used as food in situations where other food grains generally cannot be raised (Divyashree U *et al.*, 2018).

A traditional agricultural practice of applying nutrients was through organic manures such as green manure, Farm Yard Manure (FYM). Organic manure application improved soil physical properties through increased soil aggregation, improved aggregate stability, decreased in the volume of microphones while increasing while microphones, increased saturated hydraulic conductivity and water infiltration rate and improved solid water holding capacity i.e., field capacity. The Organic, Inorganic fertilizer and soil nutrients help plants to establish strong roots, defend against pests and grow into vibrant and productive plants, using organic fertilizer (Vermicompost) is safe and effective for all garden & landscape plant. Now, the agricultural research is focused on evolving ecologically sound, biologically sustainable and socio-economically viable technologies. The organic farming approaches using the local manorial and bio-pesticide sources for growing organic crops. The Organic farming minimizes the environmental pollution and it maintains the sustainability of soil by maintaining the high soil organic matter. For that reason this research was undertaken to find out an optimum level of chemical fertilizer Di-Ammonium Phosphate (DAP) & Organic fertilizer Vermicompost that can maximize the growth, production and much more importantly, yields of brown top millet under climatic and soil conditions of Chitradurga district, Karnataka.

Study Area

Chitradurga district is located on the valley of the Vedavati River and in the heart of the Deccan Plateau. Geographically the district is situated between 13°34' to 15°02' latitude and 75°37' to 77°02' longitude. The district is surrounded by Ananthapur district of Andhra Pradesh by east, Davanagere district by west, Chikkamagalur and Tumkur by south east and Bellary district by north. Chitradurga district falls in Agro-climatic Zone-4 i.e. **Central**





Shaila and Nafeesa Begum

Dry Zone. The district receives scanty and unevenly distributed rainfall and having shallow and poor soils. Chitradurga district enjoys moderate climate throughout the year. It consists of hot humid monsoon type of climate; the annual rainfall is 592.5mm and the temperatures ranges from 21°C – 31.8° C, depending upon the climatic season. We have chosen **Chitradurga** taluk for the Effect of organic inorganic fertilizer on Seed germination of millets.

MATERIALS AND METHODS

Collection of Seed Sample: Seed sample of Foxtail millet, little millet, Proso millet and Kodo millet were collected from the farmers in APMC market of Chitradurga. The collected seed samples were stored in polythene bags at room temperature.

Collection of Soil Samples: The soil sample collected from Chennyanahatti, Sibara, Madanayakanahalli village near Chitradurga. The collected soil samples are red soil, black soil & loam soil.

Fertilizer Used

Inorganic fertilizer: Di ammonium phosphate (DAP)

Organic fertilizer: Vermicompost

DAP were purchased from the APMC market of Chitradurga. Vermicompost was obtained from department of agriculture and also from the preserve Vermicompost manure. To study seed germination some selected fertilizer solutions were prepared such as DAP, Vermicompost in a range of 1gm/100m¹ of distilled water. Soil were collected from the agricultural land was sieved the fine soil particles after sieving were collected in a container for further use. Although there are several methods to study the effect of organic & inorganic fertilizers on seed germination but in the current study, the nursery plate method was followed. This method is more appropriate for germination study of millets. Before the seeds were immersed in different fertilizer solutions of known concentration.

To know the effect of organic & in organic fertilizer on seed germination and growth % of germination it has been calculated by using below mentioned formula.

$$\% \text{ of germination} = \frac{\text{Number of seeds germinated}}{\text{Total number of seeds plated}} \times 100$$

Evaluation of Seed Germination by Standard Blotter Method

Two blotter discs are taken and marked with details like date of experiment result Expected date etc. It is dipped into a tray containing distilled water, the dipped blotter beets allowed for 1-2 minutes to remove the chemicals present in the paper further the beets are lifted with the help of forceps and pulled against the tray to remove excess of water. The moistened blotter are placed on the lower side of plastic petriplate and to this foxtail millet and little millet seeds were placed, 100 seeds at rate of 25 each plated on the blotter so that the 4 replicate were maintained while sting the seeds much care were taken to maintain the uniform distance side and incubated in incubation chamber by maintaining for 8 days. To measure the root length shoot length of selected millets and the percentage of germination was calculated by using the formula.

$$\text{Vigour index} = \frac{\text{Shoot length} + \text{Root Length in cm}}{\text{Time (in hrs)}} \times 100$$

Or
Morphological Vigour

RESULTS AND DISCUSSION

The germinability of stored seeds of foxtail millet and little millet is affected by the certain abiotic factors like light, temperature, salinity etc. Seed germination has been tested by application of both organic and inorganic fertilizer solution. Nursery plate method has been followed to study the germ inability of seeds of Millets. Present work was



**Shaila and Nafeesa Begum**

carried out to assay the effect of inorganic and organic such as DAP and vermicomposting also used in the black soil and loam soil are represented in Table-1.

Percentage of Germination

Seed germination is one of the major aspects of physiology of plants. Germination is an important phenomenon which will be affected by different conditions. When the conditions are appropriate the seed will renew its growth and germinates. That the percentage of germination in two fertilizers system increased and the % of survival is greater than that of % of germination. Seeds were germinated after 3 days. The seed germination percentage was significant and the process is affected by the application of DAP, Vermicompost, Loamy soil and Black Soil Table-1 & graphically represented in fig.1. Seed germination of foxtail millet was ranged highest between 40-92% with treatment of Vermicompost. Due to treatment of DAP, Vermicompost, loam soil and Black soil the germination percentage were 70%, 92%, 40% and 80% respectively (Table:1). The seed germination of little millet is ranged highest of 84% with the application of Vermicompost, followed by 64%, 30% and 60% for the application of DAP in loam and Black soil respectively. The seed germination percentage of Kodo millet is ranged highest of 80% with application of Vermicompost followed by 70%, 58% and 26% respectively (Table -1). According to overall observation of **Table-1** Vermicompost was more effective than other fertilizers and soil types.

Root Length

Seedling height is significantly influenced by root length. The seeds are germinating by the standard blotter method. The root length is measured by the soaking seeds on germination blotter sheet. The root length is measured soaking day and after 3 day, 5 day and 7 day recorded the root length. The root length is increased in the range of 2.3-3.5 cm and 3.5 - 4.2 cm of foxtail millet. In Little millet the root length is increased in the range of 2- 3 cm and 3 - 3.7 cm. In Proso millet the root length is increased in the range of 2-2.3 cm and 2.3-3.0 cm. In Kodo millet the root length is increased in the range of 0.6-0.9 cm and 0.9 -1.2 cm respectively. According to our investigation foxtail millet shows the highest root length as compared to little millet, Proso millet and Kodo millet Table-2.

Shoot Length

The seed germination that grows upward in a shoot where leaves will develop. The shoot length was measured after soaking of the seed and after 3 day, 5 day and 7 day recorded the shoot length. In foxtail millet, the length of shoot was increased between 2.6-4.6 cm and 4.6-5.2 cm. In Little millet, the length of shoot was increased between 2.4-3.9 cm and 4.4cm. In proso millet, the length of shoot was increased between 0.9-1.5 cm and 1.5-2.3cm. In Kodo millet, the length of shoot was increased between 1.1-2.8 cm and 2.8-3.2cm respectively. Finally, it is concluded that foxtail millet is significantly increased the shoot length in 168 hours Table 2. On % of seed germination root length, shoot length of plants. Root/Shoot ratio on crop plants in terms of most important technique to study the above said parameters. Results indicated that the significant differences in germination parameters amongst treatments. The germination of seeds was observed after 3 days and survival was noted after 5 days and after 7 days intervals. The observed results were interpreted in **Table-2** and recorded values are graphically represented in fig: 2.

Root/Shoot Ratio

According to Table-2 it is concluded that the highest root ratio is 4.2 cm observed in foxtail millet and lowest ratio is 1.2 cm observed in Kodo millet. Similarly the highest shoot ratio is 5.2 cm observed in foxtail millet and lowest shoot ratio is 2.3 cm observed in Proso millet.

CONCLUSION

Milletts are cultivated in low fertility soils of dry lands with improper management practices; fertilization plays a pivotal role for increasing the crop yield. Organic fertilizer is considered as one of the best approaches for production sustainability of milletts. The application of inorganic fertilizer DAP and Loamy soil which reduces the percentage of seed germination but in Vermicompost and Black soil seed germination is high as compared to inorganic fertilizer





Shaila and Nafeesa Begum

(DAP) and Loamy soil. Among the various organic sources, Vermicompost is found to be the good source of nutrients for Millets growth. Hence, it is concluded that application of Vermicompost can be recommended as an effective organic source for Millets production under irrigated condition. Organic farming minimizes environmental pollution and maintains sustainability of soil by maintaining high soil organic matter.

REFERENCES

1. Anil Kumar BH (2000) "Integrated use of organic and inorganic manures on growth and yield of finger millet, *Eleusine coracana* (L) Gaertn under rainfed conditions. MSc (Agric) thesis, University of Agricultural Sciences, Bengaluru, Karnataka, India.
2. Barad H.L. Patel C.K. Patel D.K. Sharma Seema and Joshi J.R. (2017) "Effect of Organic Manures and levels of Inorganic Fertilizers with and without Banana sap on yield, quality and Economics of Summer Pearl millet (*Pennisetum glaucum* L.) Under South Gujarat Condition", International Journal of Science, Environment ISSN 2278-3687 (O) and Technology, Vol. 6, No 4, 2224 – 2231.
3. Divyashree U, M Dinesh Kumar, S Sridhara and T Basavaraj Naik (2018) "Effect of different levels of fertilizers on growth and yield of little millet (*Panicum sumatrense* Roth ex Roem and Schult)", International Journal of Farm Sciences 8(2): 104-108
4. Govindappa, M., (2003), Efficacy of different organic manures and inorganic fertilizer on growth and yield of rainfed finger millet (*Eleusine coracana*), M.Sc.(Agri.) Thesis, Univ. Agric. Sci., Banagalore.
5. Jadhav, P. B., Singh, A., Mangave, B. D., Patil, N. B., Patel, D. J., Dekhane S. S. and Kireeti, A. (2014). Effect of organic and inorganic fertilizers on growth and yield of African marigold (*Tagete serecta* L.). Annals of Biological Res., 5(9): 10-14.
6. G Priya and K Sathyamoorthi (2019) "Influence of Organic Manures on the Growth and Yield of Foxtail Millet [*Setaria Italica* (L.) Beauv]", 8(29), 114-117
7. Maitra, S. (2020). Potential horizon of brown-top millet cultivation in drylands: A review. Crop Res. 55(1 & 2): 57-63. doi: 10.31830/2454-1761.2020.012
8. Maitra, S., Reddy, M. D. and Nanda, S.P. (2020). Nutrient Management in Finger Millet (*Eleusine coracana* L. Gaertn) in India. International Journal of Agriculture, Environment and Biotechnology. 13(1):13-21. doi: 10.30954/0974-1712.1.2020.2
9. Mubeena, P., Halepyati, A. S. and Chittapur, B.M. (2019). Effect of Date of Sowing and Nutrient Management on Nutrient Uptake and Yield of Foxtail Millet (*Setaria italica* L.). International Journal of Bio-resource and Stress Management. 10(1):092-095; doi: 10.23910/IJBMS/2019.10.1.1891
10. Nandini, K.M., Sridhara, S. and Kumar, K. (2018). Effect of different levels of nitrogen on yield, yield components and quality parameters of foxtail millet (*Setaria italica* L.) genotypes in southern transition zone of Karnataka. International Journal of Chemical Studies. 6(6): 2025-2029.
11. Nouri Maman and Stephen Mason (2013) "Poultry manure and inorganic fertilizer to improve pearl millet yield in Niger" African Journal of Plant Science, Vol. 7(5), pp. 162-169.
12. Shanti, N. and Vijayakumari, B. (2005). Influence of NPK with different organic manures on yield attributes of bhendi (*Abelmoschus esculentus*). J. of Ecobiology, 17(1): 49-54.
13. Sharma, D.P., Prajapat, J. and Tiwari, A. (2014). Effect of NPK, Vermicompost and vermin wash on growth and yield of okra. Int. J. of Basic and App. Agric. Res. 12(1): 5-8.
14. Suruthi S, K Sujatha and C Menaka (2019) Effect of organic and inorganic foliar nutrition on growth and yield attributes of barnyard millet (*Echinochloa frumentacea* L.) var. MDU1, International Journal of Chemical Studies, 7(3): 851-853.
15. Upendra Naik, P., Rao, S., Desai, B. K., Krishnamurthy, D. and Yadahalli V.G. (2018). Effect of Different Sources of Organic Manures on Growth and Yield of Foxtail Millet (*Setaria italica* L.) under Integrated Organic Farming System. Advances in Research, 13(2): 1-6, doi: 10.9734/AIR/2018/38541.
16. Wagh, S.S., Laharia, G.S., Iratakhar, A.G. and Gajare, A.S. (2014). "Effect of INM on nutrient uptake, yield and quality of okra (*Abelmoschus esculentus* L. Moench". An Asian J. of Soil Sci. 9(1): 21-24.





Shaila and Nafeesa Begum

Table-1: Effect of Inorganic and Organic fertilizers on Germination of Selected Millets

Sl. No	Seed Name	Inorganic Fertilizer (DAP)			Organic Fertilizer (Vermicompost)			Loamy Soil			Black Soil		
		Total	Germinated	% germinated	Total	Germinated	% germinated	Total	Germinated	% germinated	Total	Germinated	% germinated
1.	Foxtail Millet	50	35	70	50	46	92	50	20	40	50	40	80
2.	Little Millet	50	32	64	50	42	84	50	15	30	50	30	60
3.	Kodo Millet	50	29	58	50	40	80	50	13	26	50	35	70
4.	Proso Millet	50	37	74	50	48	96	50	25	50	50	45	90

Table-2: Root Length and Shoot Length Measurement

Sl. No	Name of the Seeds	Root Length (cms)			Shoot Length (cms)		
		3 rd day	5 th day	7 th day	3 rd day	5 th day	7 th day
1.	Foxtail Millet	2.3	3.5	4.2	2.6	4.6	5.2
2.	Little Millet	2	3	3.7	2.4	3.9	4.4
3.	Kodo Millet	0.6	0.9	1.2	1.1	1.5	3.2
4.	Proso Millet	2	2.3	3.0	0.9	2.8	2.3

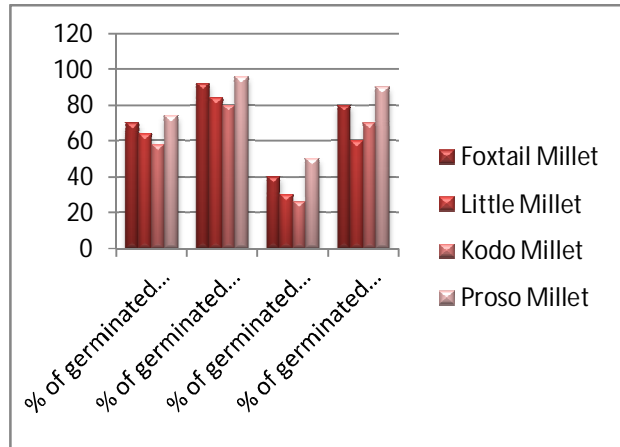


Fig 1: Effect of Inorganic and Organic fertilizers on Germination of Selected Millets

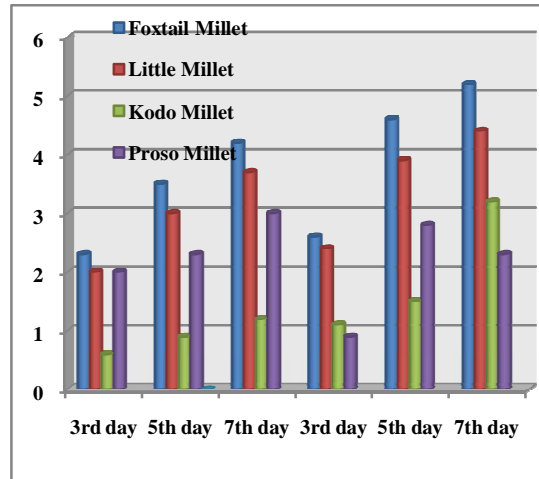


Fig 2: Root Length and Shoot Length measurement of Selected Millets





Pyramidal Attractive Color Texture Shape Patterns for Medicinal Plant Image Retrieval

K.Uma^{1*}, B.Sathya Bama², A.Siva Prasanth³ and T. Aravindh Kumar³

¹Research Scholar, Department of ECE, Thiagarajar college of Engineering, Madurai, Tamil Nadu, India.

²Associate Professor, Department of ECE, Thiagarajar College of Engineering, Madurai, Tamil Nadu, India.

³UG Student, Department of ECE, Thiagarajar college of Engineering, Madurai, Tamil Nadu, India.

Received: 10 Dec 2021

Revised: 22 Dec 2021

Accepted: 21 Jan 2022

*Address for Correspondence

K.Uma

Research Scholar, Department of ECE,

Thiagarajar college of Engineering,

Madurai, Tamil Nadu, India.

Email: umak@tce.edu



This is an Open Access Journal / article distributed under the terms of the **Creative Commons Attribution License** (CC BY-NC-ND 3.0) which permits unrestricted use, distribution, and reproduction in any medium, provided the original work is properly cited. All rights reserved.

ABSTRACT

Many medicinal plants are available but not many people can identify them and know about their rich medicinal values. Preservation knowledge of these herbal plants is important because it allows the general public to obtain valuable information that they can apply wherever they are needed. Plant identification is based on leaf and flower, since they are visible and easy to obtain. This paper investigates the color, shape, and texture features of the leaf and flower using Histogram of Gradients (HOG), Local Tetra Pattern (LTrP), and Color Histogram (CH) to identify the medicinal plants. Initially, segmentation has been done for the input image to remove the unwanted information. To minimize the computations, a novel attractiveness-based feature descriptor has been proposed. Attractiveness tells about the spatial dependence with the neighboring pixels. Instead of calculating features for all the pixels, features are calculated only for the spatial dependent attractive pixel. Finally, a standard BOW model has been used to identify the plant by the collective flower and leaf information. A comparative study has been conducted between HOG and Pyramidal Attractive Histogram of Gradients (PAHOG), LTrP and Pyramidal Attractive Local Tetra Pattern (PALTrP), Color Histogram (CH) and Pyramidal Attractive Color Histogram (PACH). A new dataset has been constructed from different medicinal plants of south India. Experimental results using the new constructed dataset indicate that the proposed attractiveness based texture extraction has been produced better recognition performance.

Keywords: Pyramidal Attractive Histogram of Gradients, Pyramidal Attractive Local Tetra Pattern, Pyramidal Attractive Color Histogram, Attractiveness.





Uma et al.,

INTRODUCTION

Plants play a key role in Earth's ecology by providing sustenance, shelter, and maintaining a healthy breathable atmosphere. The role of plants is most important in the natural circle of life. According to World Health Organization 80% of people depend on plants for their primary health care. So it is very much essential to have a plants database and also to access the data using graphical user interface. In particular, five Indian Medicine Systems, namely Ayurveda, Siddha, Unani, Homeopathy and Folk, use plants as a source for the treatment of minor to major diseases [1]. Ayurveda and Siddha medicines are in the form of decoctions, pills, or powders made from medicinal plant extracts. Drugs are usually used in three ways in the Unani method of medicine: solid, liquid, and gaseous. Only the specific practitioners and some rural experts have the rich knowledge of identification and use of medicinal plants. The experts maintain confidential about their knowledge of the plants and it will vanishes with the experts. Hence it is essential to develop a technique that will automate the identification of the medicinal plants. A detailed survey on computer vision based plant species recognition has been done for the flowering plant species (aka angiosperms). It includes detailed view of benchmark plant datasets; various feature extraction methods for plant recognition including shape, color, texture [12]. Recently, Convolutional Neural Networks (CNNs) have also been applied towards this goal with significant results [2][10][11]. In case of leaf based retrieval, the CNN based methods work well. But on inclusion of flower and leaf, the expected training rate has not been obtained. A machine vision system for identification, collection and domestication of medicinal plants has been developed in India [3]. But, they have concentrated text based medicinal plants retrieval alone. Medicinal plant image retrieval for the android system determines the identity of the plant based on text query and leaf based retrieval [9]. A mobile application has been proposed for identifying Indonesian medicinal plant using the combination of leaf features including leaf texture, leaf shape, and leaf color distribution. But they have not concentrated on flower information [6].

A Further variation is added to the images through the acquisition process itself resulting in potentially large differences in shape and appearance, depending on the perspective from which the image is taken.

Fig.1(a) Periwinkle white (*Vinca rosea*), is a type of drug that blocks cell growth by stopping mitosis and used to treat cancer, leukemia in children. (b) Periwinkle pink (*Catharanthus roseus*), used to treat diabetes, malaria, Hodgkin's lymphoma and leukemia (c) Bhringraj white (*Wedelia calendulacea*), is used as a tonic to treat coughs, cephalalgia, skin diseases, and alopecia. (d) Bhringraj Yellow (*Sphagneticola calendulacea*), the plant is mainly used for the treatment of inflammations, including abscesses and sore throat; it is also used to treat coughs. Fig.2 (a)Hoary Basil (*Ocimum americanum*) used to treat coughs, respiratory problems, rheumatism, renal colic calcifications and cancer. (b) Holy Basil (*Ocimum sanctum*) used to treat cough, cold, fever, Mouth ulcer and Diabetes. (c) Holy Basil (*Ocimum tenuiflorum*) used to treat headache and **eye disorders.**(d) **Camphor** Basil (*Ocimum canum*) used in lowering blood glucose and to treat cold, fever, parasitic infestation on the body and inflammation of joints and headaches.

Furthermore, images should be captured with limited external conditions, such as lighting condition, focus, zoom, resolution, and the image sensor. Fig 3(a) shows the original image and Fig 3(b), (c) and (d) have been taken in illumination, rotation and scaling conditions. These variations made a great challenge for an automated approach in contrast to human perception. Therefore, it is important for considering flower as well as leaf features in identifying the medicinal plants. It is necessary to develop an automatic method that identifies the medicinal plants from the images. The organization of the paper is as follows: Section II outlines the proposed approach with discussions on feature computations. Section III provides details of the dataset and experimental results obtained. Section IV brings up the overall conclusion and scopes for future research.

METHODOLOGY

Plants play the major role in emerging the nature. Because of the side effects of the allopathic method of medicine's rapid healing, medicinal plants now play a significant role. In the current situation, medicinal plants are being investigated as possible curing agents to aid people in fighting COVID-19 by strengthening their immune systems. Hence, identification of plants using their leaf and flower with high accuracy is essential. The proposed methodology





Uma et al.,

for the medicinal plant image retrieval is shown in Fig 4 and are explained below: Initially, segmentation has been done to remove the background of the flower/ leaf and Histogram of Gradient (HOG) has been done for the segmented image to find the shape of the flower and leaf [4][7].

A threshold (T) has been set based on the average value of the pixels. In order to reduce the computation, Attractiveness (A), a newly designed parameter is calculated to find the spatial distribution with the pixels. If $A < T$, the image has been split into 4 quadrants and for each quadrant, the texture and color information were extracted using LTrP and CH. If $A > T$, the features are extracted and all the features are concatenated and stored in a database. The database images along with its botanical name and medicinal values of the plants has been stored in a Bag of Words (BoW) model. In the testing stage, when the query image has been given, its features are extracted and similarity matching takes place between the features in the database and BoW containing its relevant information are also retrieved with the help of GUI for the user to access the data.

The overall proposed algorithm is described below:

Algorithm

Given:

Input Image (I_{ij}) with $i*j$ pixels

$Size_{max}=4$

Step 1: Find HOG features for the segmented image (I_{ij})

Step 2: Find the center pixel C_{ij}

Step 3: Calculate Attractiveness A_{ij} and threshold for the patch/image (T_i)

Step 4: If $(A > T) \parallel patch\ size > Size_{max}$

Find LTrP, CH

Else

Partition patch into 4 quadrants [P_1, P_2, P_3, P_4]

Step 4: Repeat step 1 to 3 until all patches are processed

End

Proposed Attractiveness

The color and texture patterns computed at pyramidal level will increase the computational complexity. To make these combined features more efficient, an attractive feature description is proposed. Instead of calculating the texture and color feature values for all pixels, it is efficient to calculate only for the proposed attractive pixels. For each color and texture feature instead of calculating feature values for all pixels, the values are computed only for the attracted pixels.

Attractiveness calculation

Attractiveness is a value which tells about the spatial correlation between neighboring pixels. First, the attractiveness A_i has been calculated for every 'i' pixel and is predicted as a distance weighted function of its neighbours $j=1, 2, \dots, n$.

$$\text{Attractiveness } A_i = \sum_{j=1}^n \lambda_{ij} \cdot Z(x_j) \quad (1)$$

Where,

n= Number of neighbors

λ_{ij} =Weight Predicted

$Z(x_j)$ =Value of the class based on the threshold.





Uma et al.,

The threshold is considered as a $\frac{3}{4}$ th value of the given image (I_m) with $i*j$ pixels which represent a same class for the same distance. For each patch, the threshold value is calculated to find the attractiveness of the pixel.

λ_{ij} is a distance-dependent weight predicted as:

$$\lambda_{ij} = \exp\left(\frac{-h_{ij}}{\alpha}\right) \quad (2)$$

' h_{ij} ' is the distance between the location x_i of pixel i for which the attractiveness is desired, the location x_j of a neighboring pixel j , and α is the non-linear parameter of the exponential model. The advantage of this algorithm is that, it is computationally efficient. For each pixel, the attractiveness is calculated as a distance-weighted function of its neighbors based on threshold, and the total attractiveness of a pixel is summed. The spatial dependency is calculated based on Euclidean distance.

$$h_{ij} = \sqrt{(x_i - x_j)^2 + (y_i - y_j)^2} \quad (3)$$

h_{ij} = lag between a pixel and its neighbors

As shown in Fig 5, attractiveness is calculated for the centre pixel. If the attractiveness is lesser than the threshold, the given image is partitioned into four quadrants and for each quadrant, attractiveness and threshold is calculated. This approach is called Pyramidal Attractive Color and Texture based feature extraction. In the texture extraction, leaf and flower features are dominant one and the remaining features are considered as the secondary. Attractiveness is calculated only for the primary features and the secondary features are eliminated. Similarly, for the color extraction, the pigmentation details are seen only in the primary colors. So, attractiveness is calculated only for the primary color components.

Texture Feature Extraction

The shape features are extracted by using the HoG method whereas the texture features are extracted by using Local Tetra Pattern (LTrP). LTrP is one of the most effective methods for texture identification. It encrypts the connection between the referenced pixel and their neighbours based on their horizontal and vertical directions. The image is loaded and converted into grey scale; the first order derivatives in horizontal and vertical axis are applied. Based on the direction of center pixel, the pattern is divided into four parts. The patterns are divided into four parts. The tetra patterns are calculated and separated into three binary patterns and are used to predict texture patterns in an image [5].

Color Feature Extraction

Color histogram has been calculated for all the class of images to find the color distribution of pixels in a plant image. Since color is not uniform over the images, the image from RGB space has been transformed to HSV color spaces, so that variance in color becomes observable well [1].

Bag of Words Model

In the BOW model, each plant can be treated as a document. The features of the flower and leaf are to be defined and documented as shown in Fig.6. To achieve this, it usually includes following two steps: Feature Extraction and clustering. Here, shape, texture and color feature extraction and Vector quantization are involved. Finally, the concatenated feature vector is given as input to the vector quantizer. Forming Visual words by quantization process and generating centroid values. Based on the centroid values the flower and leaf is retrieved from the database.

Experiment and Analysis

Datasets

Experimentations to demonstrate the efficacy of the proposed approach is performed on a dataset of 1000 medicinal plants acquired from many botanical websites targeting the specified medicinal plant varieties. All the images are

38620





Uma et al.,

taken in the size of 100*100 pixels. Furthermore, we have increased the variation of the images by augmenting the data by rotation, illumination and scaling under different photometric and geometric variations. The scientific name, common name, usable parts of the plant and its medicinal values are stored in the Bag of Words Model. In the testing phase, features are extracted and histogram matching is done for the testing image and its medicinal values are displayed using the GUI interface model. The sample dataset images taken for our considerations are shown in Fig.7.

Segmentation

Segmentation has been applied on the images to extract the particular Region of Interest (RoI). The descriptor mismatch will occur if the entire image is considered to extract the shape and texture features. So, the images of medicinal plants are initially segmented to extract the features using Graph Cut Segmentation. Graph cut segmentation is the most efficient method to detect the boundaries [8]. For a given input image, the targeted leaf and flower are chosen using bounding box and the graph cut segmentation is done separately to extract the features. The segmentation results for the flower and leaf are shown in Fig.8

Feature Extraction

From the segmented image, HOG features are extracted to find the shape of the leaf and flower. Then, attractiveness is calculated to find the spatial distribution with the pixels. Later, color and texture features are calculated using PALTrP and PACH. The concatenated feature histogram is shown in Fig 9.

Graphical User Interface (GUI)

A GUI allows the users to perform tasks interactively through controls such as buttons and sliders. Within MATLAB, GUI tools enable to perform tasks such as creating and customizing plots (plot tools), fitting curves and surfaces (cf tool), and analyzing and filtering signals (sp tool). The feature histogram of the input query image is then compared with the histograms of all the leaf and flower images in the database. If the histogram matches with one of the database images then the plant is recognized and its botanical name, uses are displayed as shown in Fig.10.

Performance Analysis

Performance of the proposed system can be evaluated using precision and recall. Our database consists of different flower and its corresponding leaf samples. Many groups of relevant images are stored in the data base. The efficiency of the proposed work is measured by Precision and Recall values.

$$\text{Precision} = \frac{\text{No.of Relevant Images Retrieved}}{\text{Total No.of Images Retrieved}} \quad (4)$$

$$\text{Recall} = \frac{\text{No.of Relevant Images Retrieved}}{\text{Total No.of Relevant Images in the database}} \quad (5)$$

$$\text{Error Rate} = \frac{\text{No.of Non-Relevant Images Retrieved}}{\text{Total No.of Relevant Images Retrieved}} \quad (6)$$

The Retrieval Efficiency(RE) is calculated by

$$R = \frac{\text{No. of Relevant Images Retrieved}}{\text{Total No. of Images Retrieved}} N \leq R$$

$$\frac{\text{No. of Relevant Images Retrieved}}{\text{Total No. of Relevant Images}} \quad \text{Otherwise} \quad (7)$$

Fig 11 (a) shows the comparative result of the proposed method with the existing HOG and PLTrP feature extraction methods. It clearly shows that the proposed system has retrieved more number of images than the existing method. In Fig.11(b), Fig. 11(c) and Fig.11 (d) shows that the proposed method has the high recall, precision value and lowest error rate. With the combination of PHOG, PALTrP and PACH, the retrieval efficiency has better results than the existing method as shown in Fig.11 (e). The Experimental Results for the existing and proposed methods are tabulated in Table 1 and Table 2.





Uma et al.,

CONCLUSION AND FUTURE WORK

This paper evaluated two new texture features for leaf and flower based medicinal plant recognition, namely PALTrP and PACH. One of the important characteristic for scene images such as medicinal herb plants is tolerant to illumination changes and geometric changes. Experimental results on these features extracted from leaf and flower images in a new constructed data set shows that PALTrP and PACH are better than PLTrP and PCH. Attractiveness is insensitive to rotation, illumination and geometric changes, hence the methods uphold invariance to geometric and photometric transformations. Thus, they are very suitable for recognizing medicinal herb plants. The work is further extended with creating more number of medicinal plants and to perform with neural networks.

REFERENCES

1. Anami, Basavaraj S., Suvarna S. Nandyal, and A. Govardha. "A combined color, texture and edge features based approach for identification and classification of Indian medicinal plants." *International Journal of Computer Applications* 6.12 (2010): 45-51.
2. Gonçalves, Filipe Marcel Fernandes, Ivan Rizzo Guilherme, and Daniel Carlos Guimarães Pedronette. "Semantic guided interactive image retrieval for plant identification." *Expert Systems with Applications* 91 (2018): 12-26.
3. <http://hdl.handle.net/10603/20929>
4. Jamshed, Muhammed, Shahnaj Parvin, and Subrina Akter. "Significant HOG-Histogram of Oriented Gradient Feature Selection for Human Detection [J]." *International Journal of Computer Applications* 132.17 (2015): 20-24.
5. Murala, Subrahmanyam, R. P. Maheshwari, and R. Balasubramanian. "Local tetra patterns: a new feature descriptor for content-based image retrieval." *IEEE transactions on image processing* 21.5 (2012): 2874-2886.
6. Nguyen, Quang-Khue, Thi-Lan Le, and Ngoc-Hai Pham. "Leaf based plant identification system for android using surf features in combination with bag of words model and supervised learning." *2013 International Conference on Advanced Technologies for Communications (ATC 2013)*. IEEE, 2013.
7. Navneet Dalal and Bill Triggs "Histograms of Oriented Gradients for Human Detection", *International Conference on Computer Vision & Pattern Recognition*, vol. 2, June 2005, pp. 886–893.
8. Peng, Bo, and Olga Veksler. "Parameter selection for graph cutbased image segmentation." *BMVC*. Vol. 32. 2008.
9. Prasvita, DestaSandya, and YeniHerdiyeni. "Medleaf: mobile application for medicinal plant identification based on leaf image." *International Journal on Advanced Science, Engineering and Information Technology* 3.2 (2013): 103-106.
10. Sharif Razavian, Ali, et al. "CNN features off-the-shelf: an astounding baseline for recognition." *Proceedings of the IEEE conference on computer vision and pattern recognition workshops*. 2014.
11. Vilasini, M. "The CNN Approaches For Classification Of Indian Leaf Species Using Smartphones." *Computers, Materials & Continua* 62.3 (2020): 1445-1472.
12. Wäldchen, Jana, and Patrick Mäder. "Plant species identification using computer vision techniques: A systematic literature review." *Archives of Computational Methods in Engineering* 25.2 (2018): 507-543.

Table 1. Experimental Results for Proposed Attractiveness based Plant retrieval

Retrieval	Holy Basil	<i>Aloe vera</i>	Indian Tulip	Peri Wrinkle	<i>Solanum Trilobatum</i>
Precision	0.8	0.7	0.75	0.83	1
Recall	0.08	0.07	0.05	0.05	0.03
Error Rate	0.25	0.428	0	0	0
Retrieval Efficiency	0.8	0.7	0.7	0.83	1





Uma et al.,

Table 2. Experimental Results for Plant Retrieval without Attractiveness

Retrieval	Holy Basil	<i>Aloe vera</i>	Indian Tulip	Peri Wrinkle	<i>Solanum trilobatum</i>
Precision	0.714	0.66	0.2	0.2	0.66
Recall	0.05	0.04	0.01	0.01	0.02
Error Rate	0.8	0.5	0.7	0.55	0.41
Retrieval Efficiency	0.71	0.66	0.2	0.2	0.66



Fig. 1. Plants with the same vernacular name, structure, and same types of leaves but with different colored flowers and medicinal values



Fig.2. Plants with same structure and with different vernacular name and different medicinal values



Fig.3 Periwinkle (*Catharanthus roseus*) with Photometric and Geometric variations

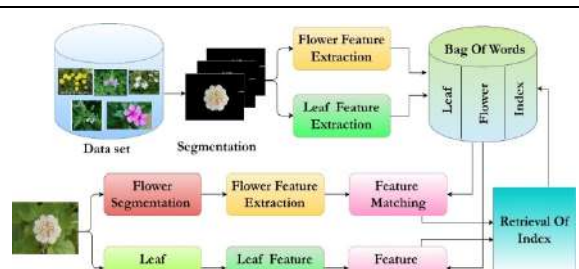


Fig.4 Proposed Methodology for Plant Recognition

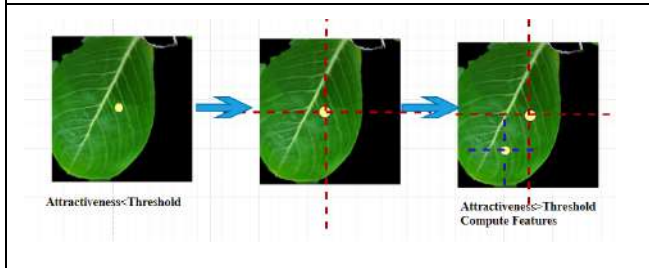


Fig.5 Attractiveness for 4-directions

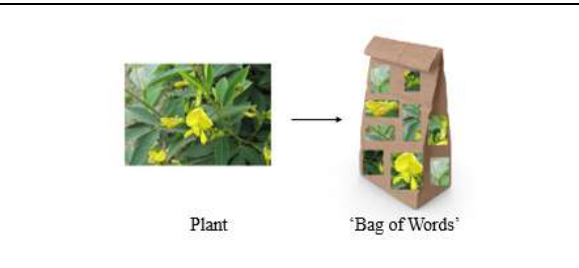


Fig.6.Bag of Words model



Fig.7 Dataset used for the proposed work

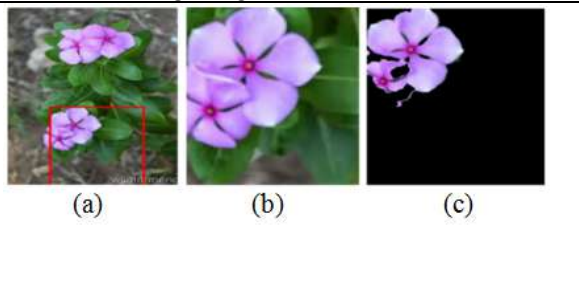


Fig.8 (a) Input Image with ROI (b) Targeted flower (c) Single Segmented Flower





Uma et al.,

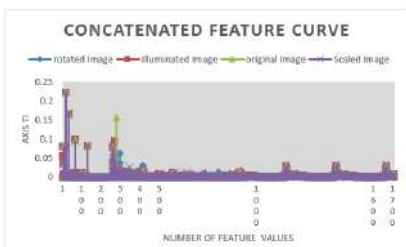


Fig.9. Concatenated Feature Curve

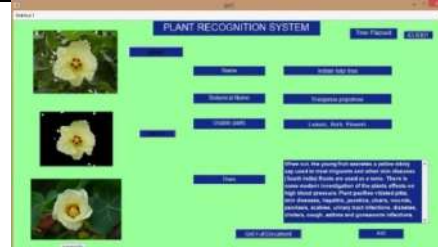


Fig.10 GUI Results

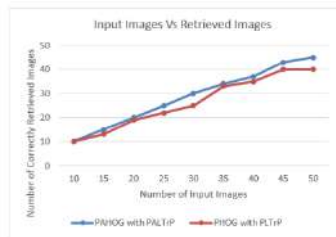


Fig 11(a) Comparative Results

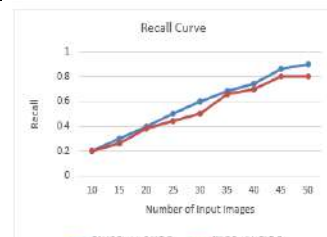


Fig 11 (b) Recall curve

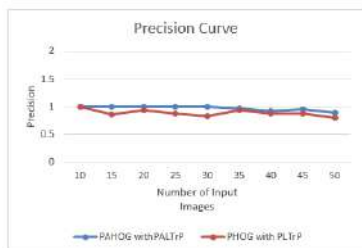


Fig 11 (c) Precision curve

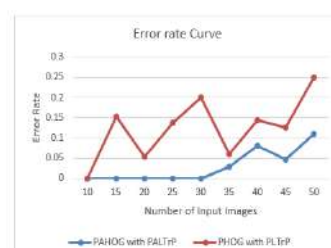


Fig 11 (d) Error Rate curve

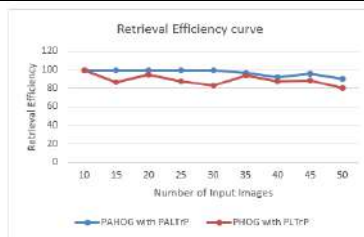


Fig 11 (e) Retrieval Efficiency curve





Spiritual, Socio-Cultural and Political Consciousness in S. K. Sharma's *the Door is Half Open*

Rabindra Kumar Verma*

Assistant Professor (English), Department of Languages, Manipal University Jaipur, Rajasthan, India.

Received: 20 Nov 2021

Revised: 25 Dec 2021

Accepted: 12 Jan 2022

*Address for Correspondence

Rabindra Kumar Verma

Assistant Professor (English),

Department of Languages,

Manipal University Jaipur,

Rajasthan, India.

Email: rkverma1984@gamil.com.



This is an Open Access Journal / article distributed under the terms of the **Creative Commons Attribution License** (CC BY-NC-ND 3.0) which permits unrestricted use, distribution, and reproduction in any medium, provided the original work is properly cited. All rights reserved.

ABSTRACT

Susheel Kumar Sharma's *The Door Is Half Open* has been studied by critics from different viewpoints by the critics. For example, Savitri Tripathi opines that the poet chooses to write poetry because he wants to express his philosophical and social concerns. G. Damodar states that symbolism, imagery, and native fervour are the remarkable qualities of Sharma's poetry. K. G. Srivastava points out about poet's use of poetic devices, poetic charm, unique poetic style, lexical dexterities and language used in *The Door Is Half Open*. N. N. Monachari views *The Door Is Half Open* a collection of narrative poetry. S. C. Dubey compares the poet Susheel Kumar Sharma with the Hindi poet Ramdhari Singh Dinkar. In his opinion, Dinkar aims at the throne while Sharma at entering the Kingdom of God for making India a better republic with no economic and social disparities. Patricia Prime sates that the poet is engaged in the presentation of human life, family and expression of his individual feelings and emotions throughout the collection of poems. Sandeep Gupta opines that the poet reflects upon the serious human and social issues like grief, poverty, and struggle for welfare of humans. However, it appears that the literary critics and scholars of the poet have not deliberated on the spiritual, social, cultural, and the political consciousness depicted in the poet in *The Door Is Half Open*. Therefore, the article is an attempt to explore out spiritual, social, cultural, and political consciousness in *The Door Is Half Open*.

Keywords: Consciousness, Political, Religion, Social, Spiritual.





Rabindra Kumar Verma

In his book, *Modern English Poetry: Its Characteristics and Tendencies* James Cousins writes, “. . . it is impossible for great poetry to escape thought and philosophical utterance, not because these things are in themselves poetical, but because greatness in poetry can only spring from greatness of consciousness, and greatness of consciousness inevitably embraces the contemplation of the fundamental relationships of humanity with itself and the universe, and express them” (67). It is true to the poetic art of Susheel Kumar Sharma, who without escaping the poetic thoughts and philosophical utterances, raises the consciousness of the human beings. Like John Milton’s *Paradise Lost*, Susheel Kumar Sharma’s *The Door Is Half Open* begins with a prayer to the goddess “Ganga Mata”, the symbol of fertility and source of livelihood for people residing in the rural as well as urban spaces of India. *The Door Is Half Open* is a collection of poems about human consciousness. The consciousness that ties humanity with spirituality, religion, socio-cultural and political values. The poet has touched upon almost every aspect of human life as a theme as there are poems on spirituality, and rituals reflecting on the Indian society, religion, social awareness, grief, poverty, education, and democracy. In his interview with T. S. Chandra Mouli, the poet acknowledges that his poems are fulcrum of the social consciousness. He says, “Social consciousness is concerned with the broader issues of a society . . . A poet has to ponder over the issues that concern individuals and also the social groups and I am no exception to it. . . I feel good literature cannot be produced in absence of a social consciousness but can be produced even in absence of ideological stand” (105).

The poems in *The Door Is Half Open* can be divided into three categories of human consciousness: spiritual, socio-cultural, and political. The theme of poverty, education, and grief fall within the second category i. e. socio-cultural consciousness while democracy falls within the purview of the political consciousness. All these categories of poems dealing with the consciousness are intertwined with one another. Hence, sometimes, it is very difficult for readers to separate them from one another. It is so, perhaps, because the poet spots places where the essence of spirituality, religion, socio-cultural and democratic values is subsumed under temples, slums, and battlefields. Consequently, readers cannot easily categorize or differentiate poems from one another only by considering their titles. The unique quality of Sharma’s poetic art is his artistic presentation of spirituality in the poems of this collection. The title of the collection suggests that *The Door Is Half Open* but the threshold of the half open door explicitly symbolizes spiritualism indicating towards the holy river Ganga. Such presentation of spirituality is rare in the poems of the modern Indian English poets. Reflecting upon the significance of spirituality, James Cousins states, “This spiritual achievement, the highest within the limits of the human consciousness and of its expression in literature, comes not wholly by prayer and fasting, but by grace and race. It cannot be found by searching, or circumvented by argument” (84). The poet’s faith in spirituality and its manifestation in his poetry echoes in the auditory images used in different poems. For example, in the poem “Ganga Mata—A Prayer” the poet’s use of spirituality can be traced from auditory images attuned with the followers of the mother Ganga that resonates: “Har har Gange”, “Har har Mahadev” and “Jai Bhole Ki” (9). The utterances of these devotional slogans reveal that the poet wants to immerse in spirituality. Abha Iyengerrightly points out, “Some poems hanker after a past. Others soak in spirituality; there is a desire to be one with God, to find peace”. (http://thebrowncritique.blogspot.in/).

The half open gate is portrayed symbolically as a pathway to the spiritual fulfilment. The first as well as the longest poem in the collection titled “Ganga Mata—A Prayer”, details the spiritual importance of the sacred river in India. The poet uses forty-three synonymous names for the word ‘Ganga’. Each name conveys some spiritual story, myth, and characteristics of the sacred river. He worships Ganga as “*Mokshadayini*” who liberates people from time, place and the cycle of birth and rebirth. Apparently, the poem is about the ‘Water Body’ alluded to the river as Ganga, but it highlights the conflict between the ancient and the modern socio-cultural values in general, and spiritual values in particular. In her review of *The Door Is Half Open*, Reena Sanasam writes, “The poem “Ganga Mata: A Prayer” by S. K. Sharma harps on the spirituality associated with the sacredness of the river Ganga. The spiritualism is so strong that he wants to totally commune his soul with the praise and beauty of Ganga” (217).

In the collection, almost all the poems are attuned to spirituality. Expressing his views on the poet’s faith in spirituality and religion, N. S. Sahu identifies the poems which deal with such themes: “The poems like “Ganga Mata: A Prayer”, “Yama”, “Liberation at Varanasi” and so on attest Sharma’s religious fervour in which he has very





Rabindra Kumar Verma

skilfully blended the secular values with the spiritual" (244). Besides, in the collection of poems, the poet names those who are considered as radiators of hope and spirituality among people, particularly 'sadhus' and 'nagas'. The poet's utmost faith in religion as well as the Almighty can be understood when he reiterates faith in God and propagates presence of God everywhere in the universe, in the poem titled "Hope is the Last Thing to be Lost":

Hope radiates from the monk
Who sits patiently on the Ganga Ghat
For salvation to descend on him and his disciple.
The world does not move
If he does not get peace within. (89)

Jyotsna Prabhakar points out mood of the poet in the different poems of the collection but she lurks in the themes of disgust, distress and spiritual faith. It may be due to her efforts to perceive the poems merely based on their titles. She writes, "The overall mood of the poems is that of disgust and distress but the silver lining spiritual faith shines through dark clouds of "Grief", "Vanity", "Poverty: Some Scenes", "A Racist Attack", "Agony", "Nithari and Beyond", and the likes" (152). Similarly, Shamenaz Bano seems to tune with the same ideology and interpretation of poems. She considers the poem "From Left to Right" as a transition of the town Allahabad into a city with its spiritual and historical details while the poet is perhaps raising the political consciousness of people. She writes, "The poem "From Left to Right" expresses poet's feelings towards his city Allahabad. He has tried to describe its spiritual and historical aspects" (409). Shamenaz Bano's consideration of the poem does not seem to be an offshoot either of the poem or of the poet's viewpoint, hence; her statement seems to be untenable.

The poet's consciousness about poverty not only attracts attention of the readers but it envisions humanistic aspects of poverty irrespective of caste, class, and religion. Shubha Dwivedi points out, "The poet's vision is humanistic and his writings confirm his faith in the spiritual unity of the world demolishing all barriers caste, class, colour, gender and nationality" (2-3). In his review of *The Door Is Half Open*, M. R.Joshi writes, "In some of the poems of this collection, the poet seems to have a social consciousness about the people who live in utter poverty" (180). "Poverty: Some Scenes", a poem in eight sections, presents an authentic picture of poverty affecting lifestyle of the people in the slums of the Indian states. The poet adroitly visualizes poverty suppressed by the officials at important places like the Hanuman Temple where the narrator wanted to share the grief of the poor by distributing fruits to them. In "Ganga Mata—A Prayer" the poet also expresses his grief about squalor and dirt arising due to poverty:

Poverty, squalor, dirt, sloth and melancholy
Everyone is weeping bitterly
Everyone is crying hoarsely
Everyone is worried knowingly. (9)

The poverty, expressed in these lines, is the only cause of grief, and pitiable situation of people. It is depicted as a socio-cultural phenomenon. The use of the negative adjectives like "squalor", "sloth", "melancholy", "weeping bitterly", and "crying hoarsely" leave a message to humanity and help us to raise human consciousness for the betterment of those people who struggle for their livelihood and sometimes also die of starvation. Further, the poet also envisions poverty observed at the different places especially where a few poor people live to carry-out their livelihood. Such glimpses of poverty can be seen in the poem "Gopalpur on Sea" where the poet satirizes poverty by depicting a woman who struggles for her livelihood:

The fisherwomen whine and fight
The crow, the cat, and their poverty
It is difficult to cover the body
Before the uncovering eye-sight
That penetrates from all sides

(65)





Rabindra Kumar Verma

It is clear from the above lines that the poet is not merely raising the consciousness of human beings about poverty, but he also makes an appeal to the humanity to preserve life of other creatures on earth, hence; he gives examples of poverty associated with the life of the birds. Moreover, the familiar scenes of poverty find manifestation in the poem titled "Poverty: Some Scenes" in which the poet expresses his plight on poverty and depicts realistic picture of the poor at the railway platforms:

The encounter with poverty
Is most disturbing
At the railway platforms
When somebody opens the tiffin-box
And someone else just stares at it
With a hope of one morsel in one's mouth. (35)

Roy Robert De Vos highlights the tragic views and the beauty in S.K.Sharma's poems. In his opinion, the poet has depicted human misery emerging from the various scenes of poverty in India and other countries of the world as well. Although he has not delved into all the poems, he adroitly extracts the crux of the collection of poems by the poet. However, in the poem "A Poem for My Country" the poet expresses his plight on human misery caused by poverty in India. The different scenes of poverty are presented satirically by the poet: "A weeping child, destitute mother, naked faqir/hungry farmer, homeless engineer" (63). Similarly, in the sixth section of the poem "Poverty: Some Scenes" the poet expands his vision and depicts the plight of the poor from different nooks and corners of the world:

And have seen the images
Flashed on U-Tube
Of the people dying of
Hunger and malaria—
Bony and skinny people
Black people
Brown people
Yellow people --men unable to stand
--women unable to walk
--children unable to raise their hand
Who can say 'Amen'? (39)

The poet seems to be conscious about his culture and civilization. He criticizes people who have moved to the cities from village and have forgotten their cultural values, hence; he deplores them for the unexpected habits of shirking responsibilities for preserving the culture. Apart from his poems, his passion about spiritual and cultural consciousness can be identified from one of his interviews with Sayed Ahmad Raza Abidi, where he says, "Most of the people particularly those who have settled in cities, have taken to western education system and have no time to look at and ponder over their culture from their own perspective are oblivious of this aspect of religion and culture. They just have one notion that religion and cultures are meant for the uneducated and backward-looking people. The poem 'Ganga Mata - A Prayer' deals with some of these issues'" (47). However, in the poem 'Ganga Mata - A Prayer' the poet not only depicts the utmost belief of people in the river Ganga but he propagates about the Hindu culture, "Hinduism at its best can be understood on the banks of the river" (4). The poet's intervention in the cultural happenings of the Indian society finds reflection in many of his poems of the collection. Poverty is one of them through which the poet attracts attention of the readers. In the poem "Poverty: Some Scenes" he unmasks poverty prevailing not only in the country like India but in the African country, Uganda where poor people suffered and they were on the verge of starvation. In the poem "Agony" the poet visualizes socio-cultural evil of gang rape: "Like a helpless woman/Gang raped unconcernedly again and again/Loses her natural vision"(46). In the poem "Crisis", the poet reveals the struggle for socio-cultural identity in the modern society. He desires to be part of a society where





Rabindra Kumar Verma

“There are no boundaries/Of colour, caste, creed, age, sex, likes and dislikes, culture, -isms and –ages” (12). Stuti Khare rightly comments about the cultural consciousness of the poet. She writes “Prof. Sharma makes extensive use of culture-specific Hindi and Sanskrit, mythological allusions, and topical references which may prove a deterrent to the reader who is unfamiliar with the cultural ethos of the country-it is quite difficult to grasp the semantic and tonal nuances of such references” (117). Further, Carol Abrahams writes, “The last poem of the book is entitled ‘Liberation at Varanasi’ -- this is again a poem rooted in Indian culture for Varanasi has a special significance for the Hindus, Buddhists and Jains . . . it is not only located on the banks of the Ganges but is one of the oldest living cities of an ancient civilization” (<http://www.cartyspoetryjournal.com/index.php/the-door-is-half-open-susheel-kumar-sharma/>).

Arbind Kumar Choudhary compares the poet S. K Sharma with other Indian English poets for depicting cultural prosperity of the Indian society. He writes, “Like Charu Sheel Singh, Syed Ameeruddin and K. N. Daruwalla, Susheel Sharma glorifies the cultural prosperity, the most precious wealth of India for which Indians are proud of themselves” (83). However, the sentiments of the poet on cultural aspects of the Indian society are not only lofty in nature but they are realistic their approach. His loftiness finds manifestation in the poem “For a Bride Who Thinks of Suicide” where he reveals socio-cultural and traditional vice of suicide of brides that happens due to dowry:

Brides are the carriers of tradition
Brides are the need of the civilization
Brides are the solace of bleeding hearts
Not to be trampled and kicked
But to be embalmed with care. (61)

Jyotsna Prabhakar rightly asserts, “His [the poet’s] consciousness is deeply embedded into the Hindu way of life” (154). Many poems of the collection deal with the Hindu ways of living. In the poem, “Liberation at Varanasi”, the poet not only depicts the cultural heritage of India, but he also shares his cultural ecstasy and religious happiness with the people indulged in the preservation of the social, religious and cultural values of the Indian society:

To have my fill with
Idlis, kachauri, halwa and puri,
Shiva’s call from every corner
To have my fill with Smoke,
ganja, bhang and thandai
Saraswati’s call from the pathashalas
To have my fill with
Jñāna, karma, bhakti and moksha
Brings me to thy lap O Varanasi!
I ponder, I stare, I wait
I hold my breath, I look within
When I see lit pyres
I chant
Om Namah Shivaya. (92)

This collection of Sharma’s poems has come out thirteen years after his first one entitled *From the Core Within* (1999). The poet’s agony for his dormant creativity during the intervening period also finds a satirical expression in the poem “Agony” where he equates his agony with that of Draupadi who screams for help:

Like Dharmaraja and Dhananjaya
Remained unbudged
When Draupadi cried for help





Rabindra Kumar Verma

On her modesty being violated by Duhshasan
 The poet is crying for words
 Clad in unblemished white Saraswati does not oblige
 She is busy riding a golden peacock (47)

As a poet, S. K. Sharma signifies role of images in poetry. It is apparent from his interview titled "T. S. Chandra Mouli in Conversation with Susheel Kumar Sharma" where he acknowledges: "Poetry basically deals with ideas that are abstract. In order to communicate an abstract idea to another mind a poet has to use certain images and symbols that are derived out of the one's personal and collective repository/experiences. While some of them would be traditional others might be personal as well." (www.cartyspoetryjournal.com, Issue IX 2012, 37). He puts this idea into practice as well when he uses different types of images to express his view. It is noteworthy that the poet's religious consciousness is rooted in the use of auditory images. For instance, in the poem "Liberation at Varanasi" he evokes them:

The enthralling shouts, *Har har Gange'*
 The exuberant dance, *Har har Mahadev'*
 The melodious violin, *'Jai Bhole Ki'* (91)

The sound emanating from the auditory images "Har har Gange", "Harhar Mahadev" and "Jai Bhole Ki" raises religious consciousness of the followers of Hindu religion. It is a celebration in the worship of the Hindu deity. The poet also signifies the religious importance of Nature and fruits in his life, hence; he depicts the significance of the favorite fruit, mango. The poem titled "Mangoes" is one of them where he emphasizes the religious importance of mango leaf: "A mango leaf is need to pour water/On every sacred occasion./Even death and the dead/Cann't ignore a mango" (44). For Carol Abrahms' "Mangoes" reminds about India's civilized past and present. However, mango stones have been used for curing stomach diseases of the people in the Indian societies while mango leaves are used for pouring water on sacred occasions and the dead in the Hindu religion.

The poet ji be simplicity at the secondary position of women who are treated as commodity and compared with the different objects. For instance, in the poem "Ganga Mata-A Prayer", the poet compares womankind with different objects. He compares wives and daughters to objects like refrigerator, television and car. Similarly, in another poem titled as "For a Bride Who Thinks of Suicide", the poet makes ironical presentation of brides as carriers of the tradition because they conform to the expectations of the male dominated society and submit themselves to the fulfillment of male desires. But, by depicting women as carriers of tradition, the poet raises consciousness of people about the subordinate position of women and their struggle for independence, freedom, and equality with their counterparts. Like other poems, in this poem, the poet portrays realistic picture of women as objects to be played with. He compares a bride to a flute and a harmonium which produces rhythm and harmony:

A bride belongs to a groom.
 She is a flute to be played on
 She is a harmonium to produce a rhythm.
 She is a synthesizer to modulate a discordant note.
 She is the tune of a young heart,
 Full of music and meaning
 Signifying harmony
 Brides are the need of the civilization (60-61)

The poet's utterances on socio-cultural, and political or democratic consciousness find reflection in the poem "Democracy: Old and New". He makes comparison between the "New" and "Old Democracy" by naming or conflating them with the various countries of the world and the role of democracy among people. He depicts





Rabindra Kumar Verma

democracy as a system of fraudulent that merely shows dreams to the public which do not fructify the depiction. The poem "Liberation at Varanasi", apparently religious in nature, is a beautiful gods, goddesses, and the followers.. The poem also deals with the political understandings as the poet sketches the real picture of sham democracy in London and Washington, the two proclaimed seats of modern democracy: "In the streets of London/ And democracy has been strangled/ On the pavements of Washington" (91). Further, the other aspect of the river Ganga is that it symbolises celebration of democratic spirit with self-discipline. The Hinduism at its best can be understood on the banks of the river. The Ganges celebrates the democratic, pluralistic and philanthropic character of the Hindu society; she does not discriminate on the basis of one's class, social, political and economic status, caste, creed, educational background etc." (4).

Besides the above discussion on the different aspects of consciousness, the language of the poems cannot be ignored as it is equally important for the readers to understand different themes and the poetic flavours of the poet. It is interesting that poet has used English language with felicity though it is not his mother tongue; his poetry conveys the message to the readers clearly. He uses words from Sanskrit (the language of religious and cultural activities in India) and Hindi (his mother tongue) profusely to convey his Indian sensibility. In a way he justifies his diction (particularly proper nouns used in his culture) when he writes, "Words convey ideas imbued with cultural significance which is mostly lost in translation. It is all the more difficult to translate proper nouns. In India, for example, there exists a tradition of *Sahasranama* (one thousand names of the object of one's reverence) where every word connotes a meaning embellished with physical or other characteristics such as history, geography, culture, myth, literary reference etc." ("Glossary" 93). In this way, the poet intervenes in the intellectual debate on the use of words from one's own tongue and culture to communicate his sensibility and not to make a show of his pedantry. It is, perhaps for the first time that an Indian poet has appended such an exhaustive glossary (running into 16 pages) to his poems to explain the lexical items from his mother tongue and culture throughout the collection of poems. Without this some of the poems would have remained obscure not only to the foreign readers but also to some of the Indians. In the "After words" of *The Door Is Half Open*, Ann Rogers very aptly justifies the relevance of the poet's use of words and phrases from his mother tongue to his poetry in English. In her opinion, if an author writes in a foreign language, the author may lose originality of the writing and consequently, there may be a gap of understanding between the writer's viewpoint and the reader's perception. Ann, therefore, finds the glossary meaningful source. She writes, "For those of the readers unfamiliar with the Indian language, Sanskrit, a poem that includes words unknown to them, may lose some of its glory. Equally, in translation it may lose something vital . . . there fore a detailed 'Glossary' is justified" (111). Further, Rogers appreciates the poetic art of the author by expressing her views on the use of imagery, similes, diction, and style. In the "After words" of *The Door Is Half Open*, Kenneth Lumpkin's opinion reveals his deep understanding of the different social issues in Sharma's work. He rates S. K. Sharma a better poet than Ezra Pound because Sharma uses allusions from his culture: "Mr. Sharma's Hindi did not interfere with the sensibility of the poem, but enhanced it as Pound's Atic Greek never really could for me" (133). However, Kenneth Lumpkin appears to be lost in the poetic art of the poet when he points out the "lyrical spirit of the poet" pervading throughout the collection. Being an anthropologist, a poet and a musician, Kenneth Lumpkin displays deep appreciation of writing poetry when he writes, "It is hard to find any fault with this remarkable collection, since he, like Candide, has managed to have the best of both worlds and been able to present them as one, intact universe" (135). Thus, the critics, scholars and the authors from the different nooks and corners of the world applaud with the poetic art of S. K. Sharma as a modern Indian English poet.

The Door Is Half Open is certainly an important contribution to the Indian Poetry in English. The collection of the poems touches heart of the readers. It deals with every aspect of human life depicting spiritual, socio-cultural, and political consciousness that can also be understood with the help of the 'Glossary' and the 'After words' facilitated at the end of the collection. Moreover, the book invites a fresh debate on reverberations of Indian sensibility in the twenty-first century Indian Poetry in English and it compels the critics to rethink their claims to have found Indian sensibility in S. K. Sharma's predecessors as poets.





Rabindra Kumar Verma

REFERENCES

1. Abidi, S. A. R. (2013). "An Interview with Susheel Kumar Sharma". *The Criterion: An International Journal in English*. Vol. 4.3:1-7.
2. ---"Tete-a-tete with Prof S K Sharma: 'Poetry Appeals to Sensitive Soul'". *The Expression: A Refereed Journal of English Literature*. Vol 5.1 (2012-13): 46-51.
3. Abrahams, C. <http://www.cartyspoetryjournal.com/index.php/the-door-is-half-open-susheel-kumar-sharma/>
4. Bano, S. (2012). "Susheel Kumar Sharma: *The Door Is Half Open*". *Ruminations* Vol. 2.2 (June:): 408-10.
5. Choudhary, A.K. (2012). "Susheel Kumar Sharma: *The Door Is Half Open*". *Kohinoor: An International Literary Journal of Creative and Critical Writing in English*. Vol. 12.2: 84-87.
6. Cousins, J. H. (1921). *Modern English Poetry: Its Characteristics and Tendencies*. Madras: Ganesh.
7. Damodar G. (2014). "Journey from Tradition to Modernity: A Study of Sharma's Poetry". *Kakatiya Journal of English Studies*. Vol. 33. Warangal: Kakatiya University, pp. 8-18.
8. De Vos, R. R. (2012). "Afterwords." *The Door Is Half Open*. New Delhi: Adhyan Publishers.
9. Dwivedi, S. (2021). "Susheel Kumar Sharma: *The Door Is Half Open*". *The Criterion: An International Journal in English* Vol. 3.4: 2-4.
10. Dubey, S. C. (2012). "Susheel Kumar Sharma: *The Door Is Half Open*". *The International Journal of Culture, Literature and Criticism*. Vol. 6. India: Allahabad, pp. 81-84.
11. Gupta, S. "A Review of Susheel Kumar Sharma's *The Door Is Half Open*". *Sublime Tradition* Vol. 5: 4-6.
12. Joshi, M. R. "Susheel Kumar Sharma: *The Door Is Half Open*". *Litscape: Journal of Vuetc* Vol. 8.1:179-181.
13. Khare, S. (2012). "Susheel Kumar Sharma: *The Door Is Half Open*". *Dialogue: A Journal Devoted to Literary Appreciation*. Vol. 3.1:115-17.
14. Monachari, N. N. (2013). "Susheel Kumar Sharma: *The Door Is Half Open*". *Journal of Literatures in English*. Vol. 6.11&12. Gulbarga: Chaitayna Offset Printers,150-51.
15. Mouli, T. S.C. (2013). "T. S. Chandra Mouli in Conversation with Susheel Kumar Sharma". *Spectrum* Vol 1.2: 103-109.
16. Prabhakar, J. (2013). "Susheel Kumar Sharma: *The Door Is Half Open*". *Indian Ethos: A Peer Reviewed Inter-disciplinary International Journal*. Vol. 3.1:152-155.
17. Prime, P. (2012). "Susheel Kumar Sharma: *The Door Is Half Open*". *Points of View*. Vol. 19.1. India: Ghaziabad, pp. 124-25.
18. Sahu, N. S. (2014). "Susheel Kumar Sharma: *The Door Is Half Open*". *Ars Artium: An International Peer Reviewed-cum-Refereed Research Journal of Humanities and Social Sciences*. Vol. 2: 244-45.
19. Sanasam, R. (2013). "Tradition, Nostalgia and Spiritualism in S K Sharma's Poems Entitled "*The Door Is Half Open*". *Spectrum: An International Journal of Humanities and Social Sciences*. Vol. 1.1: 217-23.
20. Sharma, S. K. (2012). *The Door Is Half Open*. New Delhi: Adhyan Publishers.
21. Srivastava, K. G. (2013). "*The Door Is Half Open: A Critique*". *Litcrit: An Indian Response to Literature*. Vol. 39.1. Thiruvananthapuram: Joyace Ranjan, pp. 227-29.
22. Tripathi, S. (2014). "Susheel Kumar Sharma: A Poet of Philosophical and Social Concern". *The Cocktail Book of English Literature*. Jaipur: Yking Books, pp. 19-36.





Boundary Weight Domination on S-Valued Graphs

A.Arul Devi¹ and V.Thiruveni^{2*}

¹Assistant Professor, Department of Mathematics, Sri Ramanas College of Arts and Science for Women, Chidhambarapuram 626 134, Tamil Nadu, India.

²Assistant Professor, PG and Research Department of Mathematics, Saiva Bhanu Kshatriya College, Aruppukottai, Tamil Nadu, India.

Received: 10 Dec 2021

Revised: 26 Dec 2021

Accepted: 13 Jan 2022

*Address for Correspondence

V.Thiruveni

Assistant Professor,
PG and Research Department of Mathematics,
Saiva Bhanu Kshatriya College,
Aruppukottai, Tamil Nadu, India.
Email: thiriveni2009@gmail.com



This is an Open Access Journal / article distributed under the terms of the **Creative Commons Attribution License** (CC BY-NC-ND 3.0) which permits unrestricted use, distribution, and reproduction in any medium, provided the original work is properly cited. All rights reserved.

ABSTRACT

The study of domination in Graph Theory is growing fast as it has variety of applications in the fields such as communications, social networks, etc., In 1958, Berge gave the formal definition of domination in Graph. In 2010, K.M. Kathiresan, G. Marimuthu and M. Sivanantha Saraswathi, introduced the boundary domination in graphs. In the year 2015, Chandramouleeswaran and others introduced the notion of semiring valued graphs (briefly called S-valued graphs). In the same year, Jeyalakshmi and Chandramouleeswaran introduced the concept of vertex domination in S-valued graphs. Motivated by this, in this paper we introduce the notion of Boundary Weight Domination on S-Valued Graphs.

2010 AMS Classification: 16Y60, 05C25, 05C76

Keywords: S – Valued graphs, Weight dominating vertex set, Boundary neighbourhood, Boundary degree of a vertex, Boundary Weight domination number.

INTRODUCTION

In graph theory, the concept of domination plays a vital role. Recently a new parameter of domination called boundary domination in graphs is introduced by Kathiresan and others [6]. A subset S of $V(G)$ is called a boundary dominating set if every vertex of $V - S$ is boundary dominated by some vertex of S . The minimum taken over all boundary dominating sets of a graph G is called the boundary domination number on G and is denoted by $\gamma_b(G)$. Puttaswamy and Mohammed Alatif introduced the concept of boundary edge domination in graphs [8]. In 2015, Chandramouleeswaran and others introduced the concept of S-valued graphs [9]. Jeyalakshmi and Chandramouleeswaran introduced the concept of vertex domination in S-valued graphs [2]. Consider the S-valued graph $G^S = (V_S, E_S)$. A vertex $v_i(s_i)$ in G^S is said to be a weight dominating vertex if $v_j(s_j) \leq v_i(s_i)$ for all $v_j(s_j) \in$





Arul Devi and Thiruvani

$N_S[v_i(s_i)]$. A subset $D_S \subseteq V_S$ is said to be a weight dominating vertex set of G^S if for all $v_i(s_i) \in D, v_j(s_j) \preceq v_i(s_i)$ for all $v_j(s_j) \in N_S[v_i(s_i)]$.

In this paper we introduce the concept of boundary weight domination on S-valued graphs and discuss some of its properties.

PRELIMINARIES

Definition 2.1. [6]

Let G be a simple graph $G=(V, E)$ with vertex set $V(G) = \{v_1, v_2, \dots, v_n\}$. For $i \neq j$, a vertex v_i is a boundary vertex of v_j if $d(v_i, v_i) \leq d(v_j, v_i)$ for all $v_i \in N(v_i)$. A vertex v is called a boundary neighbour of u if v is a nearest boundary of u . If $u \in V$, then the boundary neighbourhood of u denoted by $N_b(u)$ is defined as $N_b(u) = \{v \in V : d(u, w) \leq d(u, v) \text{ for all } w \in N(u)\}$

Definition 2.2.[5]

$deg_b(u)$ in G is defined to be the number of boundary neighbours of $u \in G$. The maximum and minimum boundary degree of a vertex in G are denoted respectively by $\Delta_b(G)$ and $\delta_b(G)$.

Definition 2.3 [4]

A subset S of $V(G)$ is called a boundary dominating set if every vertex of $V-S$ is boundary dominated by some vertex of S . The minimum taken over all boundary dominating sets of a graph G is called the boundary domination number on G and is denoted by $\gamma_b(G)$.

Definition 2.4 [4]

Let $G^S = (V, E, \sigma, \psi)$ be a S-valued graph. By V_S mean the set $V \times S$ and E_S mean the set $E \times S$ any element of V_S will be denoted by $v_i(s_i)$ where $v_i \in V$ and $s_i \in S$ for all $i = 1, 2, \dots, n$. Similarly, any element of E_S will be denoted by $e_i^j(s_i, s_j)$ where $e_i^j = (v_i, v_j) \in E$ and $s_{ij} = \min\{s_i, s_j\}$.

Definition 2.5 [2]

Consider the S-valued graph $G^S = (V_S, E_S)$. where $V_S = \{v_i(s_i) / v_i \in V \text{ and } s_i \in S\}$ and $E_S = \{e_i^j(s_i, s_j)\}$

- The order of G^S is defined as $p_S = (|V_S|, |V|)$
- The size of G^S is defined as $q_S = (|E_S|, |E|)$
- The open neighbourhood of v_i in G^S is defined as $N_S(v_i) = \{(v_j, \sigma(v_j)) | (v_i, v_j) \in E, \psi(v_i, v_j) \in S\}$.
- The closed neighbourhood of v_i in G^S is defined as $N_S[v_i] = N_S(v_i) \cup \{(v_i, \sigma(v_i))\}$.

Analogously, we can define the open(closed) neighbourhood of an edge in G^S .

Definition 2.6 [2]

Consider the S-valued graph $G^S = (V_S, E_S)$. where $V_S = \{v_1(s_1), v_2(s_2), \dots, v_n(s_n)\}$. A S-path between $v_i(s_i)$ and $v_k(s_k)$ is defined as the sequence $P^S(v_i v_k) = v_i(s_i), e_i^j(s_i, s_j), v_j(s_j), \dots, v_k(s_{k-1, k})$

The weight of the S-path $P^S(uv)$ is defined as $wt(P^S(uv)) = \sum_{e_i^j \in P^S(uv)} \psi(e_i^j)$.

Let $P_i^S(uv)$ be the i^{th} path that connects u and v , $i = 1, 2, \dots$. The length of the path $P_i^S(uv)$,

denoted by $l(P_i^S)$ is defined to be the number of edges along the path $P_i^S(uv)$. The set of all paths $P_i^S(uv)$ that connects u and v together with their weights and lengths be denoted by P_{uv}^S .

Definition 2.7 [3]

Consider the S-valued graph $G^S = (V_S, E_S)$. where $V_S = \{v_1(s_1), v_2(s_2), \dots, v_n(s_n)\}$. The distance between the vertices u and v of a S-valued graph G^S is defined by $dist_S(u, v) = \min(P_{uv}^S) = \min \{(wt(P_i^S), l(P_i^S)) / P_i^S \in P_{uv}^S, i = 1, 2, \dots, k\}$. where the minimum runs over all S-path between u and v .

Definition 2.8 [2]

Consider the S-valued graph $G^S = (V_S, E_S)$. A vertex $v_i(s_i)$ in G^S is said to be a weight dominating vertex if $v_j(s_j) \preceq v_i(s_i)$ for all $v_j(s_j) \in N_S[v_i(s_i)]$. A subset $D_S \subseteq V_S$ is said to be a weight dominating vertex set of G^S if for all $v_i(s_i) \in D, v_j(s_j) \preceq v_i(s_i)$ for all $v_j(s_j) \in N_S[v_i(s_i)]$.





Arul Devi and Thiruvani

Definition 2.9 [2]

Consider the S-valued graph $G^S = (V_S, E_S)$. A subset $D_S \subseteq V_S$

- The dominating set D_S is said to be a minimal weight dominating vertex set if no proper subset of D_S is a weight dominating vertex set.
- The cardinality of a minimal weight dominating vertex set is called the weight dominating vertex number of G^S and is denoted by $\gamma_{wv}^S(G^S)$.
- D_S is said to be a connected weight dominating vertex set if the subgraph $\langle D \rangle_S$ is a connected subgraph.
- The cardinality of a minimal connected weight dominating vertex set $\gamma_{wv}^S(G^S)$, denoted by is called the connected weight dominating vertex number of G^S .

BOUNDARY WEIGHT DOMINATION ON S-VALUED GRAPHS

In this section we introduce the notion of boundary weight domination in S-valued graphs.

Definition 3.1

Consider the S-valued graph $G^S = (V_S, E_S)$ where $V_S = \{v_1(s_1), v_2(s_2), \dots, v_n(s_n)\}$. For $i \neq j$, a vertex $v_i(s_i)$ is said to be a boundary vertex of $v_j(s_j)$ if $dist_S(v_i(s_i), v_t(s_t)) \leq dist_S(v_i(s_i), v_j(s_j))$ for all $v_t(s_t) \in N_S(v_i(s_i))$

Definition 3.2

Consider the S-valued graph $G^S = (V_S, E_S)$ where $V_S = \{v_1(s_1), v_2(s_2), \dots, v_n(s_n)\}$. A vertex $v_i(s_i) \in V_S$ is called boundary neighbour of a vertex $v_j(s_j) \in V_S$ if $v_i(s_i)$ is a nearest boundary of $v_j(s_j)$. If $v_j(s_j) \in V_S$, then the boundary neighbourhood of $v_j(s_j)$, denoted by $bN_S(v_j(s_j))$, is defined to be the set $bN_S(v_j(s_j)) = \{v_i(s_i) \in V_S / dist_S(v_i(s_i), v_t(s_t)) \leq dist_S(v_j(s_j), v_t(s_t)) \text{ for all } v_t(s_t) \in N_S(v_j(s_j))\}$.

Definition 3.3

The boundary degree of a vertex $v_j(s_j) \in V_S$, is denoted by $bdeg_S(v_j(s_j)) = (|bN_S(v_j(s_j))|_S, |bN(S)|)$. The maximum and minimum boundary degree of the graph G^S are denoted respectively be,

$$\Delta_S^b(G^S) = \max_{v_j(s_j) \in V_S} (|bN_S(v_j(s_j))|_S, |bN_S(v_j(s_j))|)$$

$$\delta_S^b(G^S) = \min_{v_j(s_j) \in V_S} (|bN_S(v_j(s_j))|_S, |bN_S(v_j(s_j))|)$$

Definition 3.4

A vertex $v_j(s_j)$ is said to be a boundary weight dominating vertex of a vertex $v_i(s_i)$ if $v_i(s_i)$ is a boundary neighbour of $v_j(s_j)$. A subset $D_S \subseteq V_S$ is called boundary weight dominating set if every vertex $V_S - D_S$ is boundary weight dominated by some vertex of D_S

The minimum cardinality of all boundary weight dominating set of a graph G^S is called boundary weight domination number of G^S and is denoted by $\gamma_b^S(G^S)$.

Example 3.5 Consider the semiring $S = (\{0, a, b, c, d, e\}, +, \cdot, \preceq)$ with the following Cayley tables.

+	0	a	b	c	d	e	·	0	a	b	c	d	e	⪯	Elements of S
0	0	a	b	c	d	e	0	0	0	0	0	0	0	0	0, a, b, c, d, e
a	a	a	b	c	d	e	a	0	0	0	a	a	e	a	a, b, c, d, e
b	b	b	b	d	d	e	b	0	a	b	a	b	b	b	b, d, e
c	c	c	d	c	d	e	c	0	0	0	c	c	e	c	c, d, e
d	d	d	d	d	d	e	d	0	a	b	c	d	e	d	d, e
e	e	e	e	e	e	e	e	0	c	e	c	e	e	e	e

Consider the S-valued graph $G^S = (V_S, E_S)$. (Refer Graph at the end: Example 3.5)





Arul Devi and Thiruvani

One can easily verify that the boundary degree of the vertex of G^S as follows:

$$bdeg_S(v_1(e)) = (e, 2), bdeg_S(v_2(d)) = (d, 2), bdeg_S(v_3(e)) = (e, 2),$$

$$bdeg_S(v_4(a)) = (e, 3), bdeg_S(v_5(d)) = (e, 3), bdeg_S(v_6(d)) = (d, 2)$$

A subset $D_S = \{v_1(e), v_5(d), v_4(a)\}$ is a boundary weight dominating vertex set if every vertex $V_S - D_S = \{v_3(e), v_2(d), v_6(d)\}$ is boundary weight dominated by D_S .

The minimum cardinality of a boundary weight dominating set of $\gamma_b^S(G^S) = (e, 3)$

The maximum degree of G^S is $\Delta_S^b(G^S) = (e, 3)$ and minimum degree of G^S is $\gamma_b^S(G^S) = (d, 2)$

Theorem 3.6

For any path $P_n^S, n \geq 3$, the boundary weight dominating vertex number is

$$\gamma_b^S(P_n^S) = (|D_S|_S, n - 2).$$

Proof

Consider the S- path P_3^S is given by, $v_1(s_1), e_1^2(s_{12}), v_2(s_2), e_2^3(s_{23}), v_3(s_3)$.

$$P_{v_1v_2}^S = \{v_1(s_1), e_1^2(s_{12}), v_2(s_2)\}. w(P_{v_1v_2}^S) = \sum \psi(e_i^2) = \psi(e_1^2) \text{ and } l(P_{v_1v_2}^S) = 1.$$

$$P_{v_1v_3}^S = \{v_1(s_1), e_1^2(s_{12}), v_2(s_2), e_2^3(s_{23}), v_3(s_3)\}. w(P_{v_1v_3}^S) = \sum \psi(e_i^2) + \psi(e_2^3) \text{ and } l(P_{v_1v_3}^S) = 2.$$

$$dist_S(v_1(s_1), v_2(s_2)) = \min\{w(P_{v_1v_2}^S), l(P_{v_1v_2}^S)\} = (\psi(e_1^2), 1);$$

$$dist_S(v_1(s_1), v_3(s_3)) = \min\{w(P_{v_1v_3}^S), l(P_{v_1v_3}^S)\} = (\psi(e_1^2) + \psi(e_2^3), 2);$$

$$P_{v_2v_3}^S = \{v_2(s_2), e_2^3(s_{23}), v_3(s_3)\}. w(P_{v_2v_3}^S) = \sum \psi(e_i^3) = \psi(e_2^3) \text{ and } l(P_{v_2v_3}^S) = 1.$$

$$dist_S(v_2(s_2), v_3(s_3)) = \min\{w(P_{v_2v_3}^S), l(P_{v_2v_3}^S)\} = (\psi(e_2^3), 1)$$

Let $D_S = \{v_2(s_2)\}$. Then $V_S - D_S = \{v_1(s_1), v_2(s_2), v_3(s_3)\}$ is a boundary weight dominating vertex set if every vertex D_S is a boundary weight dominating vertex set.

provided $\sigma(v_2) = s_1, s_2, s_3 \leq s_2$

Therefore $\gamma_b^S(P_n^S) = (|D_S|_S, |D_S|) = (\sigma(v_2), 1) = (|D_S|_S, n - 1)$. where $n = 3$.

We know that, a vertex $v_i(s_i)$ will dominate $v_{i-1}(s_{i-1})$ and $v_{i+1}(s_{i+1})$ in any path P_n^S

Proceeding as in the case of $n = 3$, we conclude that $\gamma_b^S(P_n^S) = (|D_S|_S, n - 2)$.

Where D_S is a boundary weight dominating vertex set.

Theorem 3.7

For any complete S-valued graph, $K_n^S, n \geq 4$, the boundary weight dominating vertex number is

$$\gamma_b^S(K_n^S) = (|D_S|_S, 1).$$

Proof: Consider the complete graph K_n^S , is given by the path,

$$v_1(s_1), e_1^2(s_{12}), v_2(s_2), e_2^3(s_{23}), v_3(s_3), e_3^4(s_{34}), v_4(s_4), e_4^2(s_{42}), v_2(s_2), e_1^2(s_{12}), v_1(s_1), e_1^3(s_{13}), v_3(s_3)$$

$$P_{v_1v_2}^S = \{v_1(s_1), e_1^2(s_{12}), v_2(s_2), v_1(s_1), e_1^3(s_{13}), v_3(s_3), e_2^3(s_{23}), e_3^4(s_{34}), v_2(s_2),$$

$$v_1(s_1), e_1^4(s_{14}), v_4(s_4), e_3^4(s_{34}), v_3(s_3), e_2^3(s_{23}), v_4(s_4), v_2(s_2)\}$$

$$w(P_{v_1v_2}^S) = \{\psi(e_1^2) + \psi(e_1^3) + \psi(e_1^4) + \psi(e_2^3) + \psi(e_3^4)\} \text{ and } l(P_{v_1v_2}^S) = \min(1, 2, 3) = 1$$

$$P_{v_1v_3}^S = \{v_1(s_1), e_1^3(s_{13}), v_3(s_3), v_1(s_1), e_1^4(s_{14}), v_4(s_4), e_3^4(s_{34}), v_3(s_3),$$

$$v_1(s_1), e_1^2(s_{12}), v_2(s_2), e_2^3(s_{23}), v_3(s_3)\}$$

$$w(P_{v_1v_3}^S) = \{\psi(e_1^3) + \psi(e_1^4) + \psi(e_2^3) + \psi(e_3^4)\} \text{ and } l(P_{v_1v_3}^S) = \min(1, 2, 3) = 1$$

$$P_{v_1v_4}^S = \{v_1(s_1), e_1^4(s_{14}), v_4(s_4), v_1(s_1), e_1^3(s_{13}), v_3(s_3), e_3^4(s_{34}), v_4(s_4),$$

$$v_1(s_1), e_1^2(s_{12}), v_2(s_2), e_2^3(s_{23}), v_3(s_3), e_3^4(s_{34}), v_4(s_4)\}$$

$$w(P_{v_1v_4}^S) = \{\psi(e_1^4) + \psi(e_1^3) + \psi(e_2^3) + \psi(e_3^4)\} \text{ and } l(P_{v_1v_4}^S) = \min(1, 2, 3) = 1$$

$$dist_S(v_1(s_1), v_2(s_2)) = \min(\psi(e_1^2) + \psi(e_1^3) + \psi(e_1^4) + \psi(e_2^3) + \psi(e_3^4), 1);$$

$$dist_S(v_1(s_1), v_3(s_3)) = \min(\psi(e_1^3) + \psi(e_1^4) + \psi(e_2^3) + \psi(e_3^4), 1);$$





Arul Devi and Thiruvani

$$dist_S(v_1(s_1), v_4(s_4)) = \min(\psi(e_1^4) + \psi(e_1^3) + \psi(e_3^4) + \psi(e_2^2) + \psi(e_2^3), 1).$$

$$bN_S(v_1(s_1)) = \{v_2(s_2), v_3(s_3), v_4(s_4)\}; bdegN_S(v_1(s_1)) = \{s_2 + s_3 + s_4, 3\}$$

Let $D_{1S} = \{v_1(s_1)\}, V_S - D_{1S} = \{v_2(s_2), v_3(s_3), v_4(s_4)\}$. Every vertex in $V_S - D_{1S}$ is dominated by D_{1S} , D_{1S} is a boundary weight dominating vertex set provided $\sigma(s_1) = s_1, s_2, s_3, s_4 \leq s_1, \gamma_b^S(D_{1S}) = (|D_{1S}|_S, 1)$.

Proceeding like this, we can find the other vertices of the bounded neighbourhood is,

$$bN_S(v_2(s_2)) = \{v_1(s_1), v_3(s_3), v_4(s_4)\}; bdegN_S(v_2(s_2)) = \{s_1 + s_3 + s_4, 3\}$$

Let $D_{2S} = \{v_2(s_2)\}, V_S - D_{2S} = \{v_1(s_1), v_3(s_3), v_4(s_4)\}$. Every vertex in $V_S - D_{2S}$ is dominated by D_{2S} , D_{2S} is a boundary weight dominating vertex set provided $\sigma(s_2) = s_1, s_2, s_3, s_4 \leq s_2, \gamma_b^S(D_{2S}) = (|D_{2S}|_S, 1)$.

$$bN_S(v_3(s_3)) = \{v_2(s_2), v_1(s_1), v_4(s_4)\}; bdegN_S(v_3(s_3)) = \{s_1 + s_2 + s_4, 3\}$$

Let $D_{3S} = \{v_3(s_3)\}, V_S - D_{3S} = \{v_1(s_1), v_2(s_2), v_4(s_4)\}$. Every vertex in $V_S - D_{3S}$ is dominated by D_{3S} , D_{3S} is a boundary weight dominating vertex set provided $\sigma(s_3) = s_1, s_2, s_3, s_4 \leq s_3, \gamma_b^S(D_{3S}) = (|D_{3S}|_S, 1)$.

$$bN_S(v_4(s_4)) = \{v_2(s_2), v_1(s_1), v_3(s_3)\}; bdegN_S(v_4(s_4)) = \{s_1 + s_2 + s_3, 3\}$$

Let $D_{4S} = \{v_4(s_4)\}, V_S - D_{4S} = \{v_1(s_1), v_2(s_2), v_3(s_3)\}$. Every vertex in $V_S - D_{4S}$ is dominated by D_{4S} , D_{4S} is a boundary weight dominating vertex set provided $\sigma(s_4) = s_1, s_2, s_3, s_4 \leq s_4, \gamma_b^S(D_{4S}) = (|D_{4S}|_S, 1)$.

$$bN_S(v_4(s_4)) = \{v_2(s_2), v_1(s_1), v_3(s_3)\}; bdegN_S(v_4(s_4)) = \{s_1 + s_2 + s_3, 3\}$$

Let $D_{4S} = \{v_4(s_4)\}, V_S - D_{4S} = \{v_1(s_1), v_2(s_2), v_3(s_3)\}$. Every vertex in $V_S - D_{4S}$ is dominated by D_{4S} , D_{4S} is a boundary weight dominating vertex set provided $\sigma(s_4) = s_1, s_2, s_3, s_4 \leq s_4, \gamma_b^S(D_{4S}) = (|D_{4S}|_S, 1)$.

Thus we conclude that for K_n^S , then the set $D_S = \{v_i(s_i)\}$ will be a boundary weight dominating vertex set if $s_j \leq s_i$, for all $i \neq j$.

Since any vertex in a complete graph K_n^S will be dominated all vertices preceding as above we conclude that $\gamma_b^S(K_n^S) = (|D_S|_S, 1)$ for some $s_i \in S$ such that $s_j \leq s_i$, for all $i \neq j$

Theorem 3.8

For any complete bipartite S-valued graph, then the boundary weight dominating vertex number $\gamma_b^S(K_{mn}^S) = (|D_S|_S, 2)$

Proof

Let V_{1S} and V_{2S} be partition of the vertex set of K_{mn}^S . Let Then $v_1(s_1) \in V_{1S}$. Then $dist_S(v_1(s_1), v_2(s_2)) = (\psi(e_1^2) + \psi(e_2^3), 2)$ for all $v_2(s_2) \in V_{1S} - \{v_1(s_1)\}$ and every vertex $v_2(s_2)$ in V_{1S} is a boundary vertex $v_1(s_1)$ of except $v_1(s_1)$. Similarly if $u_1(s_1) \in V_{2S}$, then every vertex of $v_2(s_2)$ is a boundary neighbour of $u_1(s_1)$ except $u_1(s_1)$. Thus $\gamma_b^S(K_{mn}^S) = (|D_S|_S, 2)$.

Theorem 3.9

Let T^S be a S-valued tree of order $(|V|_S, n)$ with $(|V_1|_S, n_1)$ pendent vertices. Then the boundary weight dominating vertex number is $\gamma_b^S(T^S) = (|D_S|_S, n - n_1)$.

Proof

Let V_{1S} be the set of all pendent vertices of the tree T^S of order $(|V|_S, n_1)$. Then every vertex in $V_S - V_{1S}$ has a maximum weight and boundary neighbour in V_{1S} . Then the boundary weight dominating vertex number is $\gamma_b^S(T^S) = (|D_S|_S, n - n_1)$.

Theorem 3.10

For each pair of integers m and n , there exists a connected S-valued graph G^S having a vertex $v(s)$ such that $deg_S(V(s)) = (|N_S(v(s))|_S, m)$ and $bdeg_S(V(s)) = (|bN_S(v(s))|_S, n)$.

Proof

Let m and n be two positive integers.





Arul Devi and Thiruvani

Case(i): $m = 1, n$.

Consider the S-star $K_{1,n+1}^S$ has a vertex $v(s)$ such that $deg_S(V(s)) = (|N_S(v(s))|_S, 1)$ and for the vertex $N_S(v(s))$ only the pole whereas all other n-pendent vertices will be in the bounded neighbours of $v(s)$. Hence $bN_S(v(s))$ will have a n-vertices and therefore $bdeg_S(V(s)) = (|bN_S(v(s))|_S, n)$. Thus the result is true for $m = 1$ and any integer n.

Case(ii): $m = n = 2$

Consider the S-cycle C_5^S For any vertex $v_1(s_1)$ the vertices $v_3(s_3)$ and $v_4(s_4)$ are in the bounded neighbours. Hence we conclude the, for C_5^S , $deg_S(v_1(s_1)) = (|N_S(v_1(s_1))|_S, 2)$. and $bdeg_S(v_1(s_1)) = (|N_S(v_1(s_1))|_S, 2)$

Case(iii)

Consider the cycle C_5^S with verices $v_1(s_1), v_2(s_2), v_3(s_3), v_4(s_4)$ and, $v_5(s_5)$ now the $deg_S(v_1(s_1)) = (|N_S(v_1(s_1))|_S, 2)$ Now consider n-2 copies p_3^S of with vertices $v_{1i}(s_{1i}), v_{2i}(s_{2i}) \dots \dots v_{(n-2)i}(s_{(n-2)i}), i = 1, 2, 3$ respectively. merge the vertices $v_{j1}(s_{j1}), j = 1, 2, 3, \dots, (n - 2)$ with the vertex. Let the resulting graph denoted by H^S (Refer Graph at the end: Theorem 3.10: Case(iii))

One can easily verified that,

$$deg_S(v_1(s_1)) = (|N_S(v_1(s_1))|_S, |N_S(v_1(s_1))|) = (|N_S(v_1(s_1))|_S, 5)$$

$$bdeg_S(v_1(s_1)) = (|bN_S(v_1(s_1))|_S, |bN_S(v_1(s_1))|) = (|bN_S(v_1(s_1))|_S, 5)$$

Case(iv): $m < n$

Consider the graph H^S in the above case odd $n - m = k$ vertices $u(s)$ and $w(t)$ join $u(s)$ and $w(t)$ with any one of the vertices $v_{j2}(s_{j2})$ where $j = 1, 2, 3, \dots, m - 2$.

Let the resulting graph denoted by H_1^S (Refer Graph at the end: Theorem 3.10: Case (iv): $m < n$). For example, let us add two vertices $u(s)$ and $v(s)$ to the graph H^S , above. Let this graph be denoted by H_1^S the bounded neighbours of $v_1(s_1)$ will increase by k and while the will be $bdeg_S(v_1(s_1))$ given by,

$$deg_S(v_1(s_1)) = (|N_S(v_1(s_1))|_S, m)$$

$$bdeg_S(v_1(s_1)) = (|bN_S(v_1(s_1))|_S, n)$$

Case(v): $m > n$.

Consider the graph H^S constructed as in the case(i) now introduce $k(s)$ -new vertices as in the case(ii) such that $a = b + k$. Then the proof as follows case(ii).

CONCLUSION

In this paper, we have studied the notions of boundary weight dominating vertex sets and boundary weight dominating vertex number of S-valued graphs. Further, we have introduced the notion of boundary weight dominating polynomials of a given S-valued graphs and determined the same for certain class of S-valued graphs. In future, we have proposed to study the boundary edge weight domination on S-valued graphs and boundary edge weight domination number on S-valued graphs.

ACKNOWLEDGEMENT

The research is supported by the PG and Research Department of Mathematics of Saiva Bhanu Kshatriya College, Aruppukottai. The authors would like to thank the department.

REFERENCES

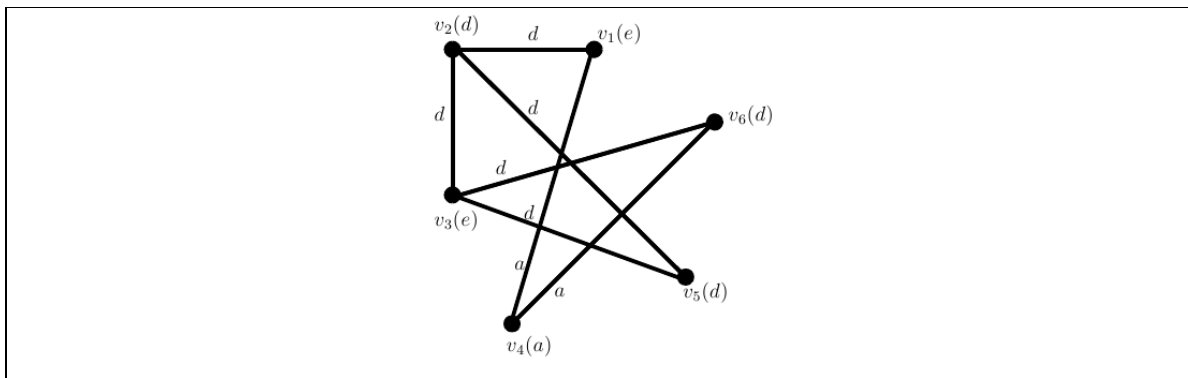
1. C. Godsil and G. Royle, Algebraic Graph Theory , Springer-Verlag, Newyork, 2001.
2. Jeyalakshmi. S. and Chandramouleeswaran. M Vertex Domination on S-Valued graphs, IOSR Journal of Mathematics., Vol 12, 2016, PP 08-12.



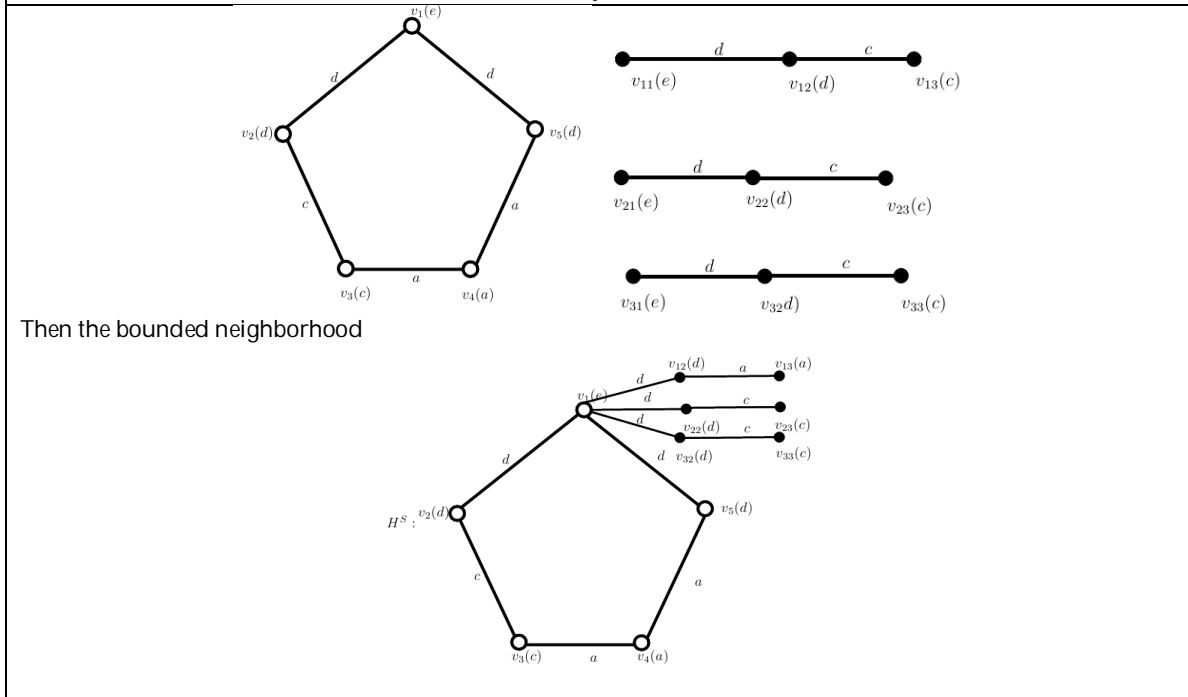


Arul Devi and Thiruvani

3. Jeyalakshmi. S. and Chandramouleeswaran. M Diameter on S-Valued graphs, Mathematical Sciences International Research Journal, 2017, 6, 121-123.
4. Jeyalakshmi. S. and Chandramouleeswaran. M Degree regular on S-Valued graphs, Mathematical Sciences Engineering Applications 2015, 4, 326-328.
5. Jonathan Golan Semiring and their Applications, Kluwer Academic Publishers, London.
6. K.M.Kathiresan, G. Marimuthu and M. Sivanantha Saraswathi, Boundary Domination in Graphs, Kragujevac j. Math. 33(2010) 63-70.
7. Mohammad Alatif, Puttaswamy and Nayaka Connected boundary edge domination in graphs, International Journal of Mathematics and its application, Volume 4, Issue 1-A (2016) 33-38. ISSN: 2347-1557.
8. Puttaswamy and Mohammad Alatif, Boundary edge domination in graphs, Bullets of the International Mathematical Virtual Institute, ISSN (P) 2303-4874, ISSN (o) 2303 – 4955, Vol 5(2015), 197-204.
9. Rajkumar.M, Jeyalakshmi. S. and Chandramouleeswaran. Semiring Valued graphs, Mathematical Sciences and Engg. Appls. Vol. 9(III), 2015, 326-328.



Example 3.5

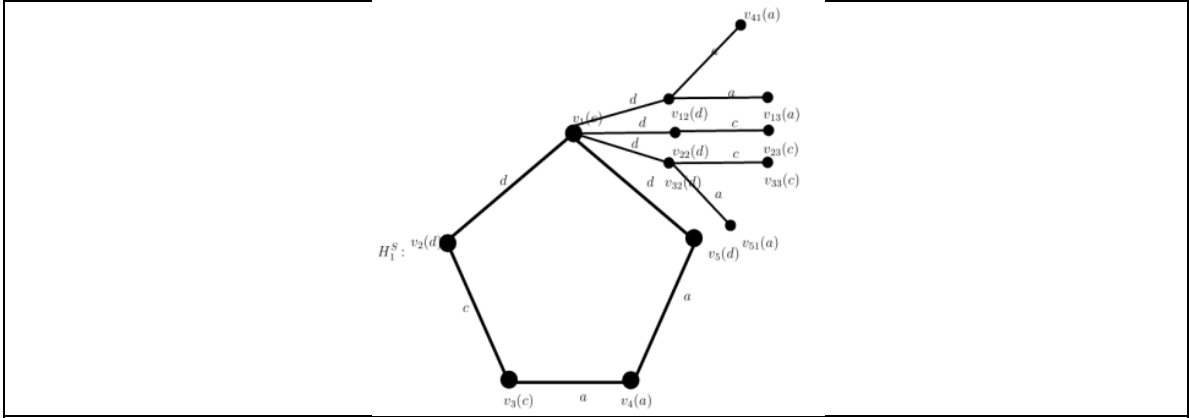


Theorem 3.10: Case (iii)





Arul Devi and Thiruvani



Theorem 3.10: Case (iv): $m < n$





Identification of Heavy Metal Source and Seasonal Variation in Flatfish from Cuddalore Coastal Waters in Southern India

Manikandan Ramasamy¹, Rajakumar Ramachandran^{2*}, Emmanuel Charles Partheeban³, Vinothkannan Anbazhagan³, Rajaram Rajendran⁴, and Aruljothiselvi Subramanyan²

¹Research Scholar, PG & Research Department of Zoology, Periyar Govt. Arts College, Cuddalore, Tamil Nadu, India – 607 001.

²Assistant Professor, PG & Research Department of Zoology, Periyar Govt. Arts College, Cuddalore, Tamil Nadu, India – 607 001

³Research Scholar, DNA Barcoding and Marine, Genomics Laboratory, Department of Marine Science, Bharathidasan University, Tiruchirappalli, Tamil Nadu, India – 620 024.

⁴Associate Professor, DNA Barcoding and Marine Genomics Laboratory, Department of Marine Science, Bharathidasan University, Tiruchirappalli, Tamil Nadu, India – 620 024.

Received: 25 Nov 2021

Revised: 29 Dec 2021

Accepted: 17 Jan 2022

*Address for Correspondence

Rajakumar Ramachandran

Assistant Professor,

PG & Research Department of Zoology,

Periyar Govt. Arts College, Cuddalore,

Tamil Nadu, India – 607 001

Email: rajakumar@pacc.in



This is an Open Access Journal / article distributed under the terms of the **Creative Commons Attribution License** (CC BY-NC-ND 3.0) which permits unrestricted use, distribution, and reproduction in any medium, provided the original work is properly cited. All rights reserved.

ABSTRACT

In this study, we have evaluated the concentrations of four heavy metals (Cd, Cu, Pb, and Zn) across the monsoon and summer seasons in 30 flatfish species collected from the Cuddalore coastal waters in Tamil Nadu, India. Out of the four metals, Cd and Cu were below detection limits in both seasons in all 30 flatfish. Pb was reported in the monsoon season in 27 species of flatfish. However, in the summer season, Pb was detected only in three species. Zn was detected in all flatfish in both seasons. The order of metal concentration in the flatfish was Zn > Pb > Cu & Cd. Principal component analysis (PCA), and hierarchical cluster analysis (HCA) were carried out revealing the interrelationships between metal and species for two seasons. Beneficial Zn was present in all the collected species of flatfish in both dry and wet seasons. Flatfish with their nutritional value, seasonal availability, and absence of harmful heavy metals may be considered for human consumption. However, continued surveillance of metal concentration in environment and flatfish are recommended to monitor the metal pollution in an effective manner to mitigate environmental pollution and health of humans who consume fish.

Key words: Metal pollution, trophic transfer, seasonal variation, toxic metals, ecotoxicology.



**Manikandan Ramasamy et al.,**

INTRODUCTION

In the aquatic system, sediments serve as a significant sink for trace metals. Metal concentrations in sediment can be many orders of magnitude higher than in surface water. Several pollutants, including harmful metals and organic compounds, have been emitted along India's southeast coast by various industries dependent on heavy metals [1, 2]. Heavy metals are persistent in the environment and can be sourced from a variety of industries such as mining, pesticides, paints, photographic papers, home appliances, dental amalgams, photo-chemicals, vehicles, and so on [3]. Metals enter the marine and coastal environments through a variety of anthropogenic and lithogenic sources. The runoff of untreated industrial and domestic effluents, harbors activities, litter dumping, spilling of cargo material, chemicals and metal ores, fishing and related activities, etc., being the main sources of pollution along the Tamil Nadu coast [4]. In recent decades, more cases of anthropogenic metal contamination affecting the inshore and coastal sediments are reported. These harmful pollutants are not only distributed in the water column, but also in the sediments where they may persist for decades, being ultimately absorbed by marine organisms [5]. The marine sediments play a substantial role in the pollution of coastal ecosystems, as they are less susceptible to movement compared to the water column. Depending on the physiochemical conditions of the environment, a major portion of the pollutants drops to the seabed or is absorbed by the oceanic sediments. When harmful heavy metals are discharged into the environment, they are transferred to marine sediments via adsorption onto suspended materials and subsequently exposed to consecutive sediments, which function as an ultimate sink for the toxic heavy metals introduced into the aquatic ecosystem [6]. Several studies have been conducted in recent years to validate the safety of seafood, including fresh and frozen flatfish fillets including European Plaice and Common Sole. Demersal fishes are those that live on the bottom, and flatfish (Order — Pleuronectiformes) are a significant group among them. Flatfish are divided into 14 families, totaling 822 species [7].

Flatfish have thin, oval, or diamondshaped bodies that enable them lie flat on the bottom, as their name suggests. Many small sized flatfish that are caught in the commercial fisheries belong to various families. Bothidae, Cynoglossidae, Citharida, Paralichthyidae, Psettodidae, Samaridae, and Soleidae are usually bycatch species in industrial fisheries where they are either discarded at sea after capture or are processed into fish meal or other products [8]. Flatfish also possess a remarkable ability to match the color and pattern of their background and bury themselves in the sediments. Flatfish interact more with marine sediments than other marine pelagic fishes, and as a result, metal bioaccumulation and its consequences are more visible in flatfish [9]. The predicted marine fish landings in mainland India for 2019 are 3.56 million tonnes, with flatfish accounting for just 50,013 tonnes i.e., about 1.4% of the total landings [10]. Fish from tropical fish landing areas are taxonomically distinct and significantly more varied than those landed in temperate regions, which is common for tropical demersal fish [11]. Many global reports on the bioaccumulation of heavy metals in the pelagic fish are available, but only scarce studies are undertaken on demersal flatfish. The aim of this study was to determine the level of heavy metals (Cd, Pb, Cu, and Zn) in the tissue of 30 flatfish species collected from the Cuddalore and Pondicherry coastal waters. Cd and Pb were assessed for their toxicity. Cu and Zn were selected as they are vital for the growth of fish. Thirty flatfish species including groups of flounders, soles, halibuts, turbot, plaices, and tonguefish were analysed. Flatfish may be particularly vulnerable to pollution and other forms of deterioration because they live in bottom sediments, which collect chemical contaminants over time. Flatfish use nearshore environments as nursery grounds, where environmental deterioration is most likely to occur. Hence, the study assesses the heavy metal concentrations in the bottom dwelling flatfish from the polluted coastal waters of Cuddalore.

MATERIALS AND METHODS

Study area

Cuddalore is a coastal city in the state of Tamil Nadu in South India that hosts a number of large-scale industries and the SIPCOT industrial complex (State Industrial Promotion Corporation of Tamil Nadu). The Cuddalore district's total geographical area is 3678 square kilometres, with a 68-kilometer-long coastline. This area is traversed by five



**Manikandan Ramasamy et al.,**

rivers. The area has some minor lignite sources that help in the generating electricity. The region is one of the most profitable fishing areas in Tamil Nadu, with a considerable fisher community. Farming and industries are other prominent sectors in this region. This fish landing centres are in close proximity to untreated and partially treated industrial effluents including hazardous waste from the SIPCOT industrial complex's 55 enterprises [12]. The Uppanar river flows parallel to Cuddalore's southern shore, and it connects the coast after crossing the urban settlements. Treated and untreated effluents from industry are also drained into the Uppanar River. Chemicals, beverage manufacturing, tanneries, oil, soap, paint production, paper and metal processing plants are among the main industries along the western bank of the Uppanar river. Cuddalore harbour, located in the estuarine region of the Uppanar river, is home to a fleet of mechanised fishing boats that operate in the coastal zone. The northern shore of Cuddalore is bordered by Pondicherry Thengaithittu fish landing centre. We selected three sampling locations in the coast where the local catch of fish was landed. The three stations in Fig.1, where the flatfish samples were collected are as follows: (1) Cuddalore fish landing centre; (2) Modasalodai fish landing centre; and (3) Thengaithittu fish landing centre.

Collection of flatfish

To cover the whole Cuddalore coast, the flatfish sample were collected from three location, namely Cuddalore fish landing centre, Mudasalodai fish landing centre, and Pondicherry Thengaithittu fish landing centre across the monsoon and summer seasons (October 2020–June 2021). It is to be noted that the sampling locations were geographically equidistant for consistently collecting the fishes from the entire Cuddalore coast. The collected samples were transfer to the laboratory in iceboxes. Untill further analysis, the samples were kept in a frozen state (-20°C) to avoid denaturing. Before any experimentation, the specimens were thawed and brought to room temperature. The morphometrics of the flatfish were measured and recorded for each species. Monographs, FAO description sheets, and the FISHBASE database for fishes were used to identify the collected samples [13, 14]. The identification and the average length of the 30 species of flatfish is tabulated in Table 1. Across all sample stations, 30 distinct flatfish species belonging to 7 different families (Bothidae, Cynoglossidae, Citharidae, Paralichthyidae, Psettodidae, Samaridae, and Soleidae) of the Order Pleuronectiforms were identified. The species identified for each sampling station are as follows: Cuddalore fish landing centre — *Samaris cristatus*, *Pseudorhombus arsius*, *Pseudorhombus diplospilus*, *Aesopiacornuta*, *Zebrias cochinchensis*, *Synaptura albomaculata*, *Cynoglossus carpenteri*, *Pseudorhombus triocellatus*, *Pseudorhombus javanicus*, *Zebrias quagga*, *Synaptura commersonii*, *Cynoglossus sitinus*, *Heteromycteris hartfeldii*, *Psettodes erumei*, and *Brachirus oriemails*; Modasalodai fish landing centre — *Synaptura lusitanica*, *Cynoglossus arel*, *Pardachirus pavoninus*, *Crossorhombus valderostratus*, *Paraplagusia bilineata*, *Zebriassynaptruroides*, *Cynoglossus semifasciatus*, *Pseudorhombus elevatus*, and *Bothus guibeii*; Thengaithittu fish landing centre — *Crossorhombus azureus*, *Laeops macrophthalmus*, *Zebrias craticulus*, *Grammatobothus polyophthalmus*, *Citharoides macrolepis*, and *Laeops guentheri*.

Sample processing for AAS analysis

All specimens were washed using distilled water before dissection. For the study of heavy metals analysis, the muscle parts of the flatfish were taken. The concentration levels of metals were analysed as per the European standards. Tiny pieces of tissue (20g) were processed at 70°C in a hot air oven. After the tissue had dried completely, it was ground into a fine powder with a pestle and mortar for further acid digestion. Acid digestion was carried out in 1g of the dry ground sample at 60°C on a hot plate using a 5:2:1 proportion of HNO₃ (70% strength), HClO₄ (70% strength), and H₂SO₄ (98% strength) until only 2–3 mL of the extract remained. In order to accomplish thorough digestion, 5mL of 2NHCl was added to the remaining residue and heated further. Once the samples were completely digested in the acid and only about 1mL of the final extract remained, the samples were diluted with double-distilled water and made up to 25 mL by volume. After cooling, the extract was filtered with Whatman filter paper (Grade 1) and transferred into a metal-free container for AAS analysis [15, 16].

Heavy metals analysis and quality control and assurance (QC/QA)

An atomic absorption spectrophotometer (AAS) (Shimadzu AA7000, Japan) was used to determine the concentration of heavy metals (Cd, Pb, Zn, and Cu) in the samples. The working wavelengths for heavy metals were 213.85 nm for





Manikandan Ramasamy et al.,

Zn, 324.75 nm for Cu, 228.80 nm for Cd, and 217.00 nm for Pb. The AAS instrument (Shimadzu AA-7000 with flame furnace) had a lower detection limit of 0.01 µg/g for all four metals analysed here. The entire metal analyses were carried out in a clean and metal-free environment to guarantee that no external contaminants were present, assuring quality assurance. Furthermore, all chemical reagents, such as deionized water and all acids reagents, were freshly prepared. For quality assurance, standard metal solutions of industrial grade were used to draw the calibration curve for the instrument. For checking the accuracy of the readings, control blank was run for every ten samples [17].

Statistical approach

The mean and standard deviation (mean SD) were used to represent the concentration of all metals. Two-way ANOVA was utilized to test the significance (alpha: 0.05) of the metals in the 30 flatfish across the two seasons. To explore the relationships between metal levels amongst the fishes, we have used principal component analysis (PCA) and hierarchical cluster analysis (HCA). Both work under the principle of correlation coefficients with the help of PAST Ver.3.0 (Windows 10). In HCA, metals with similar kinds of properties/sources will fall within a cluster followed by others [18, 19].

RESULTS

Heavy metal distribution across different species

Among the four metals analyzed across two seasons, Zn was detected in all 30 species of flatfish. Cu and Cd were not detected in any of the flatfish across both seasons. However, Pb concentrations were reported in 27 species of flatfish during the monsoon season. Pb was not detected in *Pseudorhombus arsius*, *Pseudorhombus diplospilus*, and *Samaris cristatus* during the monsoon season. During the summer season, Pb was reported only in three species (*Pseudorhombus arsius*, *Samaris cristatus*, and *Zebrias cochinensis*) and were below detection limits in the remaining 27 species. The metal concentration observed in the flatfish are presented as mean and standard deviation (mean ± SD) in Table 2. The mean concentrations of metals for all species of flatfish in the monsoon season ranged as follows: Zn (0.37–53.17 µg/g) and Pb (0–1.57 µg/g). In the summer season, metals ranged as follows: Zn (9.75–40.23 µg/g) and Pb (0–1.48 µg/g). The other two metals (Cu and Cd) were not detected in the muscle of any flatfish. The concentration of Pb observed in the flatfish across the seasons was statically significant ($p < 0.0001$; $f = 27.11$) at 0.05 level, and Zn was statistically insignificant ($p = 0.25$; $f = 1.40$) at 0.05 level. The maximum concentration of Zn during the monsoon (53.59 ± 0.17 µg/g) was recorded in *Cynoglossus carpenterii*, and the minimum concentration of Zn (0.37 ± 0.02 µg/g) was recorded in *Brachirus oriemailis*. In the summer season, highest concentration of Zn (40.23 ± 1.83 µg/g) was recorded in *Pseudorhombus diplospilus*, and the minimum concentration (9.75 ± 0.95 µg/g) was recorded in *Paraplagusia bilineata*. During the monsoon season, highest concentration of Pb (1.76 ± 0.24 µg/g) was observed in *Grammatobothus polyophthalmus*, whereas the concentration for Pb was not detected (ND) in *Pseudorhombus arsius*, *Pseudorhombus diplospilus*, and *Samaris cristatus*. Coming to the summer season, the highest concentration of Pb was observed in *Pseudorhombus arsius* (1.48 ± 0.14 µg/g), followed by *Zebrias cochinensis* (0.95 ± 0.05 µg/g), and *Samaris cristatus* (0.85 ± 0.09 µg/g). Pb concentrations were observed to be lower than the detection limits or not detected in the remaining 27 species of flatfish. The mean metal concentrations in all flatfish species were in the following order: Zn > Pb > Cd = Cu. Table 3 shows a comparison of the mean metal levels reported in our study for flatfish compared with the permissible concentration limits for fishes set forth by several international organizations. The family-wise mean concentrations of the four metals and two seasons for the seven flatfish families studied are listed below in descending order: monsoon season: Zn (Citharidae > Bothidae > Samaridae > Psettodidae > Paralichthyidae > Cynoglossidae > Soleidae); and Pb (Bothidae > Cynoglossidae > Paralichthyidae > Soleidae > Psettodidae > Citharidae > samaridae). For summer season: Zn (Samaridae > Paralichthyidae > Bothidae > Citharidae > Soleidae > Cynoglossidae > Psettodidae); and Pb (Paralichthyidae > Soleidae > Samaridae > remaining four families had no Pb). Flatfish collected in our study area varied in length from 5 ± 2.5 cm to 48.2 ± 2.9 cm on average. *Paraplagusia bilineata* was the largest flatfish species collected in our study area, with an average length of 48.2 ± 2.9 cm, while *Pseudorhombus triocellatus* was the smallest, with an average length of 5 ± 2.5 cm (Table 1).



**Manikandan Ramasamy et al.,****Principal component analysis (PCA)**

PCA was used to find the association of metal concentration in the tissue of flatfish among the different species separately for each season. The results of PCA for the summer and monsoon seasons are presented in Table 4. The monsoon dataset of metal distribution in flatfish generated four different. Out of the four PCs, only PC1 and PC2 were considered for discussion owing to their eigenvalues, 1.05 and 0.95, respectively. PC1 accounted for 26.15% followed by PC2 accounting for 26.15% of variance. The summer data of metal distribution in flatfish generated four different PCs. Out of the four PCs, only PC1 and PC2 were considered for discussion with regard to their eigenvalues, 1.27 and 0.73, respectively. PC1 accounted for 31.63% followed by PC2, accounting for 18.37% of variance, respectively (Table 4; Figs. 3 and 4). Hence, in both seasons, only two PCs are considered for discussion. Furthermore, in both PC1 and PC2, there was a strong positive loading of Zn (0.71) in both the seasons. Likely, loading values of Pb showed positive loading (0.71) values in PC1 for both seasons. However, in PC2, Pb was negatively loaded (-0.71) for both seasons. In support of PCA, HCA for both seasons produced three different clusters for the dataset where Pb was Cluster 1, Cd and Cu formed Cluster 2, and Zn was in Cluster 3 (Figs. 6 and 7). The distance however was higher for Zn due to the higher concentration values in the HCA for both the seasons.

DISCUSSION

The study of heavy metals concentration in fishes is important with respect to the human utilization of fish as a food source. Some of the earlier studies state that heavy metal concentrations in the muscle of fishes from the coastal ecosystem may vary greatly among the different species. This may be perhaps due to differences in metabolism and feeding patterns of the fishes. Fish is among the leading bioindicator species used for acute toxicity assay of pollutants such as heavy metals. since much attention has been drawn due to the wide phenomenon of metal pollution in aquatic system. The rapid development of industries and agricultures have promoted the increase of environment pollution, although heavy metals in aquatic system can be naturally produced by slow leaching from rocks and soil into water system which usually present at significant level in water system and may pose high toxicities to the aquatic organisms [20]. Fish are considered as one of the most susceptible aquatic organisms to toxic substance present in water [21]. Metals can accumulate in marine creatures, including fish, through direct absorption or through the food chain, and then be absorbed by humans, causing chronic or acute illness. Metal residues in wild fish from maritime species have been reported in a number of studies [22, 23].

Flatfish are particularly vulnerable to pollution because they thrive in the bottom sediments, which trap chemical contaminants. Flatfish use near-shore environments as nursery grounds, where environmental deterioration is most likely to occur. Because *Crossorhombus azureus* lives in the benthic zone, this might explain the substantial accumulation of metals found in the current research. In the study area, the median concentrations of the essential metal Zn observed in the muscle of flatfish during both the monsoon and summer seasons are well below the permissible limits described by various organizations. The essential element Cu was not observed in the flatfish in both seasons which may be a due to the fact that Cu in coastal ecosystem may be in lower concentrations and get accumulated in the livers of the fishes and not being reflected in the muscle tissue. However, the mean concentration of Pb (non-essential metal) observed during the monsoon (0.69 µg/g) season was marginally higher than the permissible limits of FAO/WHO (Table 3). Nevertheless, during the summer season, the mean concentration of Pb was only 0.11 µg/g, which was below the permissible limits set forth by global agencies. The concentration of Pb in the tissue of *Pseudorhombus arsius* was observed to be higher in summer season, while being lower in monsoon season. A similar finding was also reported by Ebrahimpour et al. [24]. The increase of Pb levels in the summer could be due to an increase of the physiological activity of flatfish during summer caused primarily by the increasing water temperature and decrease in the wastewater input from industrial activities during the summer months [25]. During the monsoon season, Pb was well below the permissible limits described by various organization like MAF and USEPA. The other non-essential metal Cd analyzed in our study was not detected in either season. Pb has natural sources that occur as lead compounds in combination with two or more elements. In the current study, the largest cumulative amount of Pb was detected in *Grammatobothus polyophthalmus* (1.57 ±0.11 µg/g) during the monsoon



**Manikandan Ramasamy et al.,**

season. The lead metal is sourced from soldering, coal combustion, mining, smelting, non-ferrous metal production, iron and steel production, battery manufacture, etc. Oil and gasoline combustion, fertilizer manufacture, waste incineration, water pipes made of metal, boring of wastes, paint, and petrol, and SIPCOT chemical company waste material, fishing boat production, and some of the anthropogenic sources, which discharge metals to the environment provide a steady but generally diffuse source of metals to the sediments [26, 27, 28]. When swallowed or breathed in excessive levels, Pb is a non-essential hazardous element that may harm people. It can cause deficiencies, reduce survival rate, growth rate, and metabolism in fish, as well as increased mucus production [29].

Zinc which is an essential micronutrient for both animals and humans has been a cofactor for about 300 enzymes in all marine organisms [30, 31]. Zn is a component of many enzymes and is important for a number of biological activities that require a reasonably high amount of Zn to sustain [32]. The daily limit for growing youngsters is 10 mg, while for adults it is 15 mg [33]. Zinc deficiency causes stunted development, loss of taste, and hypogonadism, which leads to diminished fertility [34]. Zinc poisoning is uncommon, although a quantity of up to 40 mg/kg in water can cause symptoms such as agitation, muscle stiffness and soreness, lack of appetite, and nausea [33]. Zn content was greater in *Cynoglossus carpenteri* ($53.17 \pm 2.65 \mu\text{g/g}$) during the monsoon season in this research. We can consider consumption of these flatfishes as a Zn supplement to enhance the human health. In the marine system, Cd and Cu usually occurs in trace levels in the open oceans [35]. The migratory nature of the flatfishes from the coastal to deep waters in certain seasons may be a reason they have lower accumulation of these toxic metals. Higher concentration Cd are recorded in coastal and estuarine environment because of the severe industrial discharge and harbor and mining activities in the river [36, 37, 38]. Though flatfish are of lower commercial value in India and are not sought as prominent seafoods, many southern states of India use a few species flatfish such as the Malabar sole as food fishes in small quantities or as dried or salt-dried products [39, 40, 41].

Among the 30 flatfish collected from three fish landing centers (Cuddalore, Modasalodai, and Pondicherry), four metals were analyzed across two seasons (monsoon and summer). Zn and Pb were present in the flatfish. In addition to the industrial activities, anthropogenic introduction of metals pollution also resulted from urbanization. This study has enlightened the fact that persistent pollutants like metals should be regularly monitored, and any variation from the normal distributional pattern can furnish an idea about the proper management of the coastal area [42]. A competent monitoring program is an essential adjunct to any attempt of managing the coastal areas in an ecologically sound and sustainable manner. Cd and Cu were not detected in any season highlighting the fact that the flatfish may be devoid of some toxic metals [43]. There are a few published data on Pb and Cd concentrations in deep-water fish collected using analytical methods sensitive enough to identify concentrations in muscle tissue [44, 45]. This study aimed to bridge the knowledge gap about heavy metal toxicities in flatfish species, which are a neglected group.

CONCLUSION

In this study, we have measured the accumulation of heavy metals (Cu, Cd, Pb, and Zn) in the selected flatfish from the Cuddalore and Pondicherry coastal waters during the wet and dry seasons. From this, Pb and Zn were present in both seasons, but Cu and Cd were not detected. When compared to Pb, Zn was present in all the collected species with permissible limit. However, Pb concentration was very lower than the limit because of the depth which they prefer to live. Only limited studies have assessed the flatfish because of the sampling and collection difficulties. We suggest that flatfish may be consumed by humans in the future where the marine resources are dwindling fast. The flatfish may also be considered as nutritional supplements in other commercial food. Flatfish may be captured well with advanced methods of fishing gear and lures such as casting or spinning gear, fly tackle, and trolling. The seasonal availability of the flatfish can be utilized and they can be considered for human consumption with implementation of more guidelines for seafood safety. Regular monitoring of metals in the bottom sediments and the flatfish must be made in the future to control metal pollution more effectively. Further, flatfish can be used as excellent bioindicators to assess the benthic ecosystem, especially to assess the metal pollution.



**Manikandan Ramasamy et al.,****ACKNOWLEDGEMENT**

The authors wish to thank the Department of Marine Science at Bharathidasan University in Tiruchirappalli, India, for providing the needed facilities, as well as the Periyar Govt. Arts College in Cuddalore for providing facilities.

REFERENCES

1. Arulkumar A, Paramasivam S, Rajaram R. Toxic heavy metals in commercially important food fishes collected from Palk Bay, Southeastern India. *Mar Pollut Bull.* 2017;119:454-9. Epub 2017/04/08.
2. Rajaram R, Ganeshkumar A, Vinothkannan A. Health risk assessment and bioaccumulation of toxic metals in commercially important finfish and shellfish resources collected from Tuticorin coast of Gulf of Mannar, Southeastern India. *Mar Pollut Bull.* 2020;159:111469. Epub 2020/07/22.
3. Lohani MB, Singh A, Rupainwar DC, Dhar DN. Seasonal variations of heavy metal contamination in river Gomti of Lucknow city region. *Environ Monit Assess.* 2008;147:253-63. Epub 2008/01/23.
4. Mathivanan K, Rajaram R. Anthropogenic influences on toxic metals in water and sediment samples collected from industrially polluted Cuddalore coast, Southeast coast of India. *Environmental Earth Sciences.* 2013;72:997-1010.
5. Rabaoui L, Balti R, Zrelli R, Tlig-Zouari S. Assessment of heavy metals pollution in the gulf of Gabes (Tunisia) using four mollusk species. *Mediterranean Marine Science.* 2013;15.
6. Pekey H. Heavy metal pollution assessment in sediments of the Izmit Bay, Turkey. *Environ Monit Assess.* 2006;123:219-31. Epub 2006/06/10.
7. Munroe TA. Flatfishes: Biology and Exploitation. In: Robin N. Gibson RDMN, Audrey J. Geffen, Henk W. Van der Veer editor. *Fish and Aquatic Resources.* hoboken: Wiley; 2015. p. 576.
8. Munroe TA. Systematic diversity of the Pleuronectiformes. In: Robin N. Gibson RDMN, Audrey J. Geffen, Henk W. Van der Veer, editor. *Flatfishes: biology exploitation.* UK: Wiley Blackwell; 2005. p. 10-41.
9. Ghribi R, Correia AT, Elleuch B, Nunes B. Testing the impact of contaminated sediments from the southeast marine coast of Tunisia on biota: a multibiomarker approach using the flatfish *Solea senegalensis*. *Environ Sci Pollut Res Int.* 2019;26:29704-21. Epub 2019/08/14.
10. CMFRI F. Marine Fish Landings in India-2019. 2020.
11. Nair PM, Chung IM. Impact of copper oxide nanoparticles exposure on *Arabidopsis thaliana* growth, root system development, root lignification, and molecular level changes. *Environ Sci Pollut Res Int.* 2014;21:12709-22. Epub 2014/06/27.
12. Soundarapandian P, Premkumar T, Dinakaran GK. Studies on the physico-chemical characteristic and nutrients in the Uppanar estuary of Cuddalore, South east coast of India. *Curr Res J Biol Sci.* 2009;1:102-5.
13. Fischer W, Bianchi G. FAO species identification sheets for fishery purposes: Western Indian Ocean (Fishing Area 51). v. 1: Introductory material. Bony fishes, families: Acanthuridae to Clupeidae.-v. 2: Bony fishes, families: Congiopodidae to Lophotidae.-v. 3:... families: Lutjanidae to Scaridae.-v. 4:... families: Scatophagidae to Trichiuridae.-v. 5: Bony fishes, families: Triglidae to Zeidae. Chimaeras. Sharks. Lobsters. Shrimps and prawns. Sea turtles. v. 6: Alphabetical index of scientific names and vernacular names 1984.
14. Nair RJ. Studies on the flatfish diversity of India: Mahatma Gandhi University; 2011.
15. Arumugam G, Rajendran R, Shanmugam V, Sethu R, Krishnamurthi M. Flow of toxic metals in food-web components of tropical mangrove ecosystem, Southern India. *Hum Ecol Risk Assess.* 2018;24:1367-87.
16. Karunanidhi K, Rajendran R, Pandurangan D, Arumugam G. First report on distribution of heavy metals and proximate analysis in marine edible puffer fishes collected from Gulf of Mannar Marine Biosphere Reserve, South India. *Toxicol Rep.* 2017;4:319-27. Epub 2017/09/30.
17. Rajaram R, Ganeshkumar A, Vinothkumar S, Rameshkumar S. Multivariate statistical and GIS-based approaches for toxic metals in tropical mangrove ecosystem, southeast coast of India. *Environ Monit Assess.* 2017;189:288. Epub 2017/05/26.
18. Yang Z, Wang Y, Shen Z, Niu J, Tang Z. Distribution and speciation of heavy metals in sediments from the mainstream, tributaries, and lakes of the Yangtze River catchment of Wuhan, China. *J Hazard Mater.* 2009;166:1186-94. Epub 2009/01/31.



**Manikandan Ramasamy et al.,**

19. Ahmed ASS, Rahman M, Sultana S, Babu S, Sarker MSI. Bioaccumulation and heavy metal concentration in tissues of some commercial fishes from the Meghna River Estuary in Bangladesh and human health implications. *Mar Pollut Bull.* 2019;145:436-47. Epub 2019/10/09.
20. Zhou Q, Zhang J, Fu J, Shi J, Jiang G. Biomonitoring: an appealing tool for assessment of metal pollution in the aquatic ecosystem. *Anal Chim Acta.* 2008;606:135-50. Epub 2007/12/18.
21. Alibabic V, Vahcic N, Bajramovic M. Bioaccumulation of metals in fish of Salmonidae family and the impact on fish meat quality. *Environ Monit Assess.* 2007;131:349-64. Epub 2006/12/16.
22. Storelli MM, Barone G, Storelli A, Marcotrigiano GO. Trace metals in tissues of mugilids (*Mugil auratus*, *Mugil capito*, and *Mugil labrosus*) from the Mediterranean Sea. *Bull Environ Contam Toxicol.* 2006;77:43-50. Epub 2006/07/13.
23. Dhaneesh KV, Gopi M, Ganeshamurthy R, Kumar TTA, Balasubramanian T. Bio-accumulation of metals on reef associated organisms of Lakshadweep Archipelago. *Food Chem.* 2012;131:985-91.
24. Ebrahimpour M, Mushrifah I. Seasonal variation of cadmium, copper, and lead concentrations in fish from a freshwater lake. *Biol Trace Elem Res.* 2010;138:190-201. Epub 2010/01/21.
25. Tekin-Ozan S, Kir I. Seasonal variations of heavy metals in some organs of carp (*Cyprinus carpio* L., 1758) from Beysehir Lake (Turkey). *Environ Monit Assess.* 2008;138:201-6. Epub 2007/05/16.
26. Russell Flegal A. Lead in tropical marine systems: A review. *Sci Total Environ.* 1986;58:1-8.
27. Romic M, Romic D. Heavy metals distribution in agricultural topsoils in urban area. *Environmental Geology.* 2003;43:795-805.
28. Panel EC. Scientific Opinion on lead in food. *EFSA Journal* 2010; 8 (4): 1570, 151 pp. 2010.
29. Burger J, Gaines KF, Boring CS, Stephens WL, Snodgrass J, Dixon C, McMahon M, Shukla S, Shukla T, Gochfeld M. Metal levels in fish from the Savannah River: potential hazards to fish and other receptors. *Environ Res.* 2002;89:85-97. Epub 2002/06/08.
30. Sharma A, Patni B, Shankhdhar D, Shankhdhar SC. Zinc - an indispensable micronutrient. *Physiol Mol Biol Plants.* 2013;19:11-20. Epub 2014/01/02.
31. Koske D, Goldenstein NI, Rosenberger T, Machulik U, Hanel R, Kammann U. Dumped munitions: New insights into the metabolization of 2,4,6-trinitrotoluene in Baltic flatfish. *Mar Environ Res.* 2020;160:104992. Epub 2020/09/11.
32. Heath AG. *Water Pollution and Fish Physiology.* England: Taylor & Francis; 2018.
33. Committee on Dietary Allowances F, Nutrition Board NRC. Recommended dietary allowances. National Academy of Sciences Washington, DC; 1980.
34. Abdel-Naser MB, Zouboulis CC. Male fertility and skin-diseases. *Rev Endocr Metab Disord.* 2016;17:353-65. Epub 2016/06/28.
35. Dick AL. Concentrations and Sources of Metals in the Antarctic Peninsula Aerosol. *Geochim Cosmochim Acta.* 1991;55:1827-36.
36. Hamed MA, Emara AM. Marine molluscs as biomonitors for heavy metal levels in the Gulf of Suez, Red Sea. *J Marine Syst.* 2006;60:220-34.
37. Soliman ZI. A study of heavy metals pollution in some aquatic organisms in Suez Canal in Port-Said Harbour. *Journal of Applied Sciences Research.* 2006;2:657-63.
38. Haynes D, Johnson JE. Organochlorine, heavy metal and polyaromatic hydrocarbon pollutant concentrations in the Great Barrier Reef (Australia) environment: a review. *Mar Pollut Bull.* 2000;41:267-78.
39. Pappalardo AM, Ferrito V. DNA barcoding species identification unveils mislabeling of processed flatfish products in southern Italy markets. *Fish Res.* 2015;164:153-8.
40. Partheeban EC, Anbazhagan V, Arumugam G, Seshasayanan B, Rajendran R, Paray BA, Al-Sadoon MK, Al-Mfarrij AR. Evaluation of toxic metal contaminants in the demersal flatfishes (Order: Pleuronectiformes) collected from a marine biosphere reserve. *Regional Studies in Marine Science.* 2021;42.
41. Coulson PG, Poad JA. Biological characteristics of the primitive flatfish Indian halibut (*Psettodes erumei*) from the tropical northeastern Indian Ocean, including implications of the use of incorrect aging methods on mortality estimates. *Fish B-Noaa.* 2021;119:168-83.





Manikandan Ramasamy et al.,

42. Thiyagarajan D, Dhaneesh KV, Ajith Kumar TT, Kumaresan S, Balasubramanian T. Metals in fish along the southeast coast of India. Bull Environ Contam Toxicol. 2012;88:582-8. Epub 2012/02/09.
43. Carvalho ML, Santiago S, Nunes ML. Assessment of the essential element and heavy metal content of edible fish muscle. Anal Bioanal Chem. 2005;382:426-32. Epub 2005/04/15.
44. Cronin M, Davies IM, Newton A, Pirie JM, Topping G, Swan S. Trace metal concentrations in deep sea fish from the North Atlantic. Mar Environ Res. 1998;45:225-38.
45. Hornung H, Krom MD, Cohen Y, Bernhard M. Trace-Metal Content in Deep-Water Sharks from the Eastern Mediterranean-Sea. Mar Biol. 1993;115:331-8.

Table 1. Representation of depth range inhabited by the flat fish and their length

S. No.	Family	Scientific name	Common name	Depth range in m	Length reported in cm (Present study)
1	Bothidae	<i>Bothus guibeii</i>	Guinean flounder	15–40	21.3 ± 3.9
2		<i>Crossorhombus valderostratus</i>	Broad brow flounder	35–146	11.5 ± 1.7
3		<i>Laeops macrophthalmus</i>	Left eye flounder	183	8.3 ± 3.9
4		<i>Laeops guentheri</i>	Gunther flounder	15–329	7.5 ± 6.1
5		<i>Crossorhombus azureus</i>	Blue flounder	13–60	11.5 ± 1.2
6		<i>Grammatobothus polyophthalmus</i>	Three spot flounder	0–90	10 ± 3.7
7	Cynoglossidae	<i>Cynoglossus carpenteri</i>	Hooked tongue sole	27–420	14 ± 5.8
8		<i>Cynoglossus itinus</i>	Speckled tongue sole		13 ± 1.2
9		<i>Cynoglossus arel</i>	Largescale tongue sole		21.1 ± 3.4
10		<i>Cynoglossus semifasciatus</i>	Bengal tongue sole	12–18	37 ± 2.4
11		<i>Paraplagusia bilineata</i>	Double lined tongue sole	1–25	48.2 ± 2.9
12	Citharida	<i>Citharoides macrolepis</i>	Twospot largescale flounder	182–200	11.5 ± 1.6
13	Paralichthyidae	<i>Pseudorhombus arsius</i>	Largetooth flounder	0–200	17.5 ± 4.5
14		<i>Pseudorhombus diplospilus</i>	Four twin spot flounder	10–75	18.5 ± 1.9
15		<i>Pseudorhombus elevatus</i>	Deep flounder	7–200	13.5 ± 4.1
16		<i>Pseudorhombus javanicus</i>	Javan flounder	22–38	6 ± 3.1
17		<i>Pseudorhombus triocellatus</i>	Three spotted flounder	17	5 ± 2.5
18	Psettodidae	<i>Psettodes erumei</i>	Indian halibut	1–100	25 ± 2.1
19	Samaridae	<i>Samaris cristatus</i>	Cockatoo righteye flounder	20–114	19 ± 3.2
20	Soleidae	<i>Aesopia cornuta</i>	Unicorn sole	8–100	18 ± 1.6
21		<i>Brachirus orientalis</i>	Oriental sole	15–20	20 ± 2.5
22		<i>Heteromycteris hartfeldii</i>	Hook nosed sole		12 ± 3.1
23		<i>Pardachirus pavoninus</i>	Peacock sole	2–40	14.5 ± 2.5
24		<i>Synaptura albomaculata</i>	kaups sole		13.8 ± 1.6
25		<i>Synaptura commersonnii</i>	Commersons sole		17.5 ± 4.3
26		<i>Synaptura lusitanica</i>	Portuguese sole	0–125	29 ± 1.0
27		<i>Zebrias cochinensis</i>			17 ± 2.1
28		<i>Zebrias craticulus</i>	Wicker work sole		6 ± 5.3
29		<i>Zebrias synaptruroides</i>	Indian zebra sole	43–125	16 ± 1.2
30		<i>Zebrias quagga</i>	Fringefin zebra sole		8 ± 2.5
ªData as per FISHBASE data					
*Data represent as (mean ± standard division)					





Manikandan Ramasamy et al.,

Table 2. Heavy metal concentration (µg/g dry weight) in flatfish from the Cuddalore–Pondicherry coast.

S. No.	Species	Monsoon				Summer			
		Cd	Cu	Pb	Zn	Cd	Cu	Pb	Zn
1	<i>Aesopia cornuta</i>	ND	ND	1.35 ± 0.08	23.5 ± 1.48	ND	ND	ND	20.89 ± 1.67
2	<i>Bothus guibeii</i>	ND	ND	0.5 ± 0.02	29.07 ± 2.58	ND	ND	ND	18.39 ± 1.35
3	<i>Brachirus orientalis</i>	ND	ND	0.4 ± 0.02	0.37 ± 0.02	ND	ND	ND	25.11 ± 1.56
4	<i>Citharoides macrolepis</i>	ND	ND	0.42 ± 0.02	40.96 ± 3.75	ND	ND	ND	25.79 ± 1.99
5	<i>Crossorhombus valdeirostratus</i>	ND	ND	1.16 ± 0.04	33.43 ± 2.48	ND	ND	ND	38.24 ± 2.11
6	<i>Crossorhombus azureus</i>	ND	ND	0.54 ± 0.04	37.46 ± 2.97	ND	ND	ND	22.55 ± 1.03
7	<i>Cynoglossus arel</i>	ND	ND	0.66 ± 0.05	24.79 ± 1.22	ND	ND	ND	14.08 ± 1.19
8	<i>Cynoglossus carpenteri</i>	ND	ND	0.89 ± 0.07	53.17 ± 2.65	ND	ND	ND	22.27 ± 1.63
9	<i>Cynoglossus itinus</i>	ND	ND	0.31 ± 0.01	28.01 ± 1.90	ND	ND	ND	15.85 ± 1.63
10	<i>Cynoglossus semifasciatus</i>	ND	ND	1.25 ± 0.10	7.99 ± 0.65	ND	ND	ND	23.74 ± 2.13
11	<i>Grammatobothus polyophthalmus</i>	ND	ND	1.57 ± 0.11	44.52 ± 2.16	ND	ND	ND	38.44 ± 1.95
12	<i>Heteromycteris hartfeldii</i>	ND	ND	0.54 ± 0.02	31.32 ± 1.64	ND	ND	ND	28.80 ± 1.67
13	<i>Laeops guentheri</i>	ND	ND	1.45 ± 0.10	19.09 ± 1.91	ND	ND	ND	28.74 ± 1.88
14	<i>Laeops macrophthalmus</i>	ND	ND	0.51 ± 0.05	24.64 ± 1.77	ND	ND	ND	23.45 ± 2.39
15	<i>paraplagusia bilineata</i>	ND	ND	0.24 ± 0.01	11.8 ± 1.25	ND	ND	ND	9.75 ± 0.95
16	<i>Pardachirus pavoninus</i>	ND	ND	0.82 ± 0.07	8.67 ± 0.51	ND	ND	ND	18.75 ± 1.01
17	<i>Psettodes erumei</i>	ND	ND	0.62 ± 0.03	33.21 ± 2.45	ND	ND	ND	13.34 ± 0.83
18	<i>Pseudorhombus arsius</i>	ND	ND	ND	27.86 ± 2.04	ND	ND	1.48 ± 0.14	34.17 ± 2.23
19	<i>Pseudorhombus diplospilus</i>	ND	ND	ND	20.12 ± 1.63	ND	ND	ND	40.23 ± 1.83
20	<i>Pseudorhombus elevatus</i>	ND	ND	0.38 ± 0.03	25.85 ± 1.95	ND	ND	ND	16.95 ± 1.02
21	<i>Pseudorhombus javanicus</i>	ND	ND	1.07 ± 0.09	32.08 ± 2.55	ND	ND	ND	31.88 ± 1.46
22	<i>Pseudorhombus triocellatus</i>	ND	ND	0.97 ± 0.04	35.17 ± 2.65	ND	ND	ND	26.17 ± 1.62
23	<i>Samaris cristatus</i>	ND	ND	ND	34.03 ± 1.74	ND	ND	0.85 ± 0.09	36.06 ± 1.59
24	<i>Synaptura albomaculata</i>	ND	ND	1.03 ± 0.08	32.19 ± 1.54	ND	ND	ND	36.07 ± 1.89
25	<i>Synaptura commersonnii</i>	ND	ND	0.25 ± 0.02	31.04 ± 2.16	ND	ND	ND	22.82 ± 2.04
26	<i>Synaptura lusitanica</i>	ND	ND	0.5 ± 0.02	30.46 ± 2.16	ND	ND	ND	26.75 ± 1.89
27	<i>Zebrias cochinchensis</i>	ND	ND	1.32 ± 0.09	21.07 ± 1.68	ND	ND	0.9 ± 0.05	23.31 ± 1.05
28	<i>Zebrias quagga</i>	ND	ND	0.6 ± 0.05	45.30 ± 2.58	ND	ND	ND	23.38 ± 2.29
29	<i>Zebrias synaptruroides</i>	ND	ND	0.61 ± 0.03	17.38 ± 1.03	ND	ND	ND	23.79 ± 1.39
30	<i>Zebrias craticulus</i>	ND	ND	0.85 ± 0.05	30.03 ± 1.93	ND	ND	ND	25.34 ± 1.32

Data are represented as mean ± standard deviation (µg/g dry weight)

ND – not detected/ below detection limits

Table 3. Comparison of metal concentration in flatfish reported in the present study with global permissible limits.

Seasons	Element	Present study (µg/g)	Permissible limits (µg/g)					
			FSSAI (2015)	FAO (1983)	FAO/WHO	MAFF (2000)	USEPA (2000)	EC (2014)
Monsoon	Cd	-	0.3	-	0.5	0.2	2	0.5
	Cu	-	-	-	30	20	120	-
	Pb	0.69	-	-	0.5	2	4	0.3
	Zn	27.82	0.3	30	100	50	120	30
Summer	Cd	-	0.3	-	0.5	0.2	2	0.5
	Cu	-	-	-	30	20	120	-
	Pb	1.07	-	-	0.5	2	4	0.3
	Zn	25.17	0.3	30	100	50	102	30





Manikandan Ramasamy et al.,

Table 4. Eigen values and percentage of variance of two principal components for the monsoon and summer seasons

Season		PC1	PC2
Monsoon	Cd	0	0
	Cu	0	0
	Pb	0.71	0.71
	Zn	0.71	-0.71
	Eigenvalue	1.05	0.95
	Percentage variance	26.15%	26.15%
	Cumulative	26.15%	50%
Summer	Cd	0	0
	Cu	0	0
	Pb	0.71	0.71
	Zn	0.71	-0.71
	Eigenvalue	1.27	0.73
	Percentage variance	31.63%	18.37%
	Cumulative	31.63%	50%

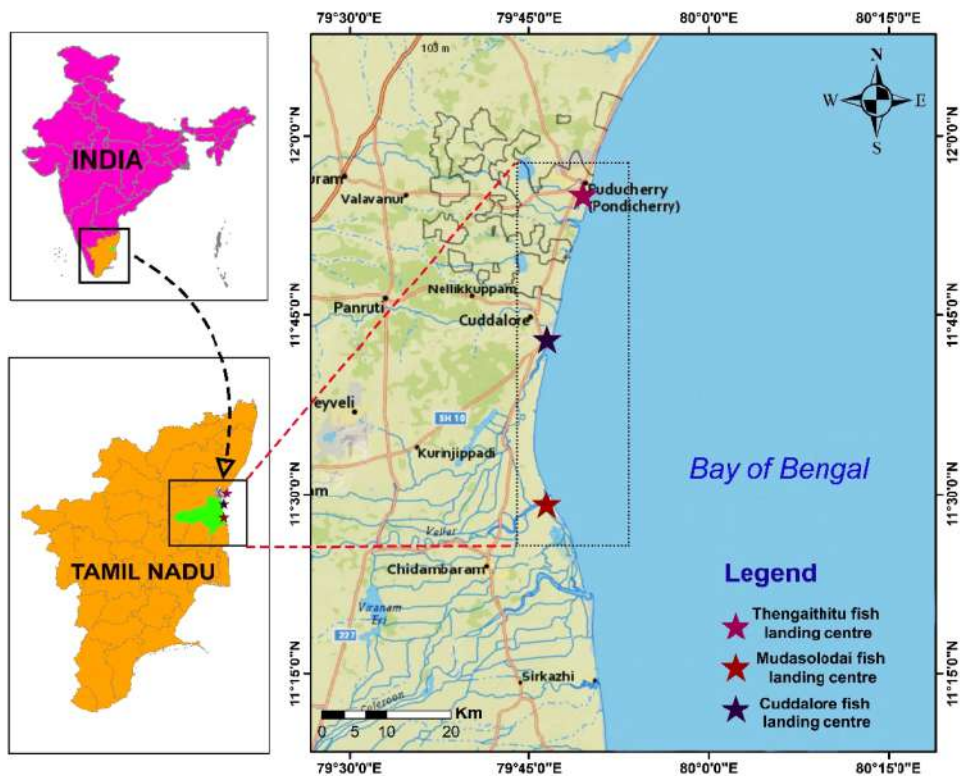


Fig. 1. Map of sampling locations along the Cuddalore coast in Tamil Nadu.





Manikandan Ramasamy et al.,

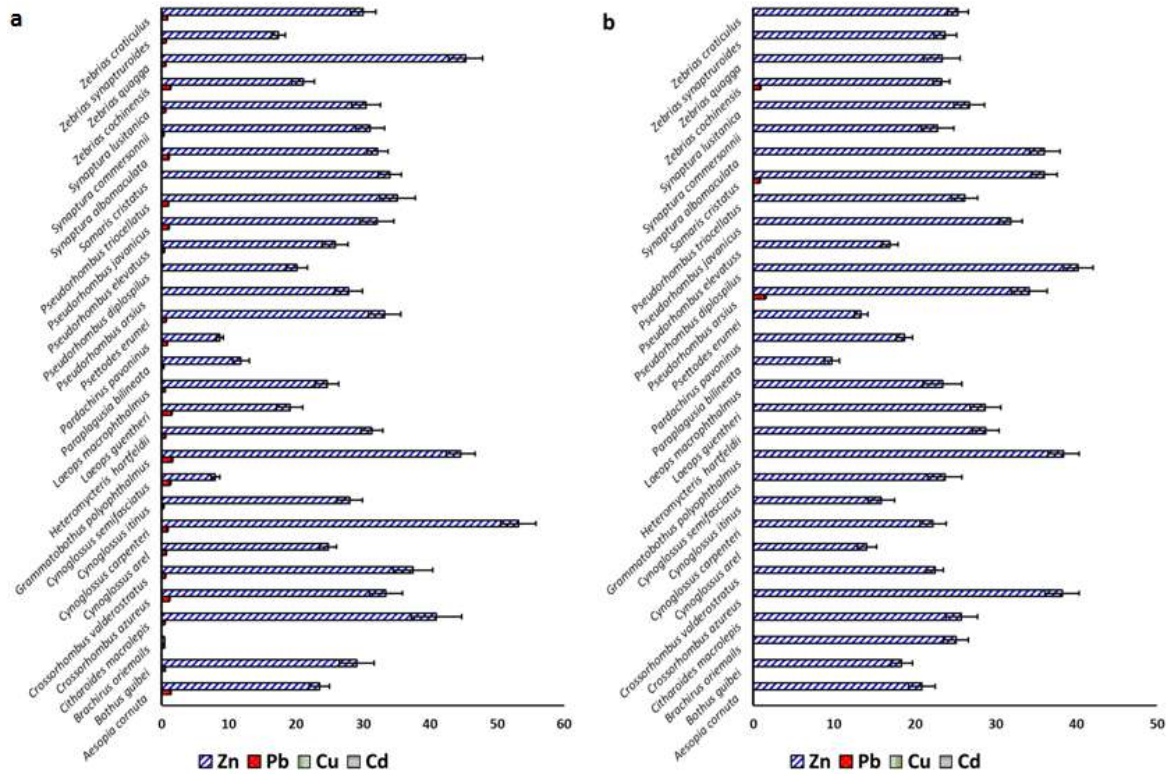


Figure 2. Distribution of heavy metals in the flatfish species during the (a) monsoon season and (b) summer season

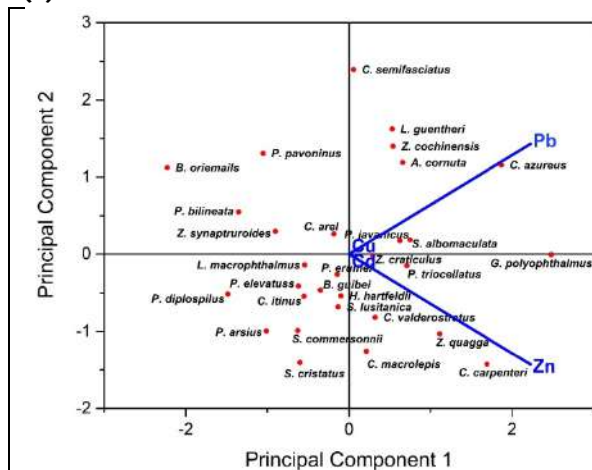


Fig. 3. Biplot showing the relationship between metals and flatfish species during the monsoon season

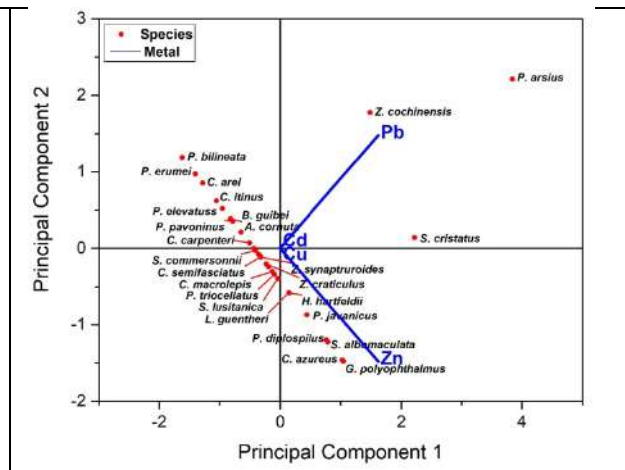


Fig. 4. Biplot showing the relationship between metals and flatfish species during the summer season





Manikandan Ramasamy et al.,

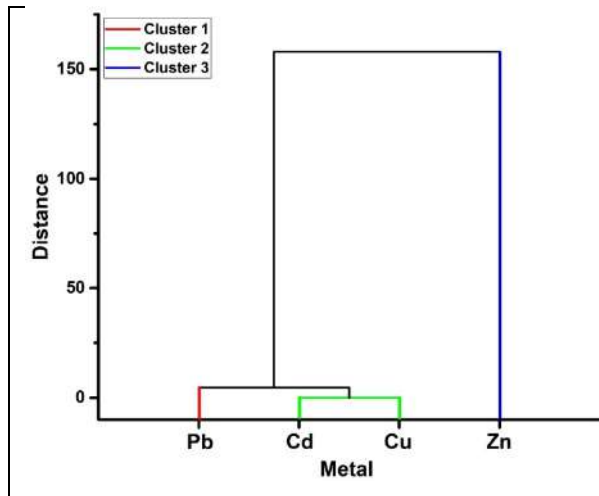


Fig. 5. Hierarchical cluster analysis of metal concentration in flatfish during the monsoon season

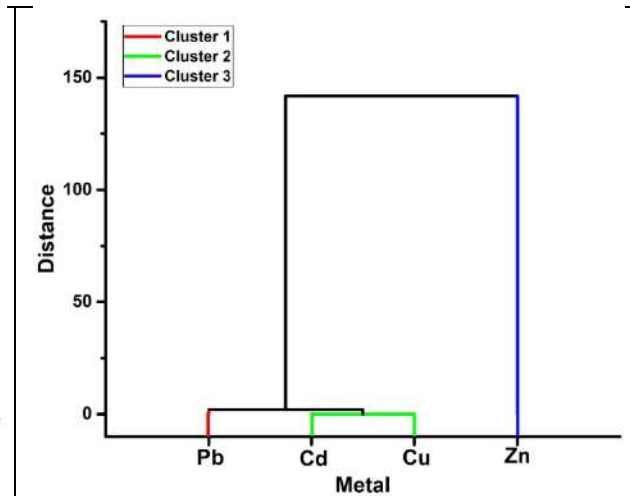


Fig. 6. Hierarchical cluster analysis of metal concentration in flatfish during the summer season





Image Processing and Machine Learning Techniques for Detection of Mosaic Disease in Banana

Murali B^{1*} and Nagaraju C²

¹Research Scholar, Yogi Vemana University, Kadapa, Andhra Pradesh, India.

²Professor, Yogi Vemana University, Kadapa, Andhra Pradesh, India.

Received: 22 Dec 2021

Revised: 03 Jan 2022

Accepted: 18 Jan 2022

*Address for Correspondence

Murali B

Research Scholar,

Yogi Vemana University,

Kadapa, Andhra Pradesh, India

Email: bmuralicse@gmail.com



This is an Open Access Journal / article distributed under the terms of the **Creative Commons Attribution License** (CC BY-NC-ND 3.0) which permits unrestricted use, distribution, and reproduction in any medium, provided the original work is properly cited. All rights reserved.

ABSTRACT

Plant diseases are the major constraints to the crops and account for significant yield and economic loss. Plant pathogens including fungi, bacteria and viruses infect their host plants and cause various diseases. Accurate and timely detection of disease(s) in plants is one of the major challenging steps in crop protection. There are several laboratory based diagnostic methods are available for accurate disease detection in plants, however, which are labour intensive, expensive, time consuming and required scientific experts. To overcome these limitations recently computer-based machine learning approaches are being used to detect plant diseases. In this study we have used Image processing and Machine learning techniques like Image acquisition, Pre-processing, K- means clustering segmentation, Gabor features, Random Forest Classifier (RFC) and Support Vector Machine (SVM) classifier in Python platform to detect mosaic disease of banana caused by *Cucumber mosaic virus* (CMV) from training dataset. The RFC and SVM classifiers have shown an accuracy of 98.94% and 98.07% for detection of mosaic disease of banana, respectively.

Keywords: Image processing, *Cucumber mosaic virus*, K-means clustering, Gabor features, RFC and SVM classifier.

INTRODUCTION

Disease detection is one of the important steps in crop protection. Plants are susceptible for many pathogens such as bacteria, fungi and viruses. Their infections have significant impact on sustainable agriculture production. Banana is one of the most economically important fruit crops in tropical and subtropical countries and India is occupied world first place at production as well as export of banana. Its fruit is relatively in expensive, rich in calories and every part of the plant is made use of in various ways (Dadzie, 1998). However, the crop is susceptible to various plant pathogens and account for significant yield loss. *Cucumber mosaic virus* (a member of the genus *Cucumovirus*, family

38654



**Murali and Nagaraju**

Bromoviridae) is one of the viruses of banana widely reported for mosaic disease in banana. The characteristic symptoms of the viruses are chlorotic mosaic symptoms or interveinal continuous or discontinuous chlorotic streaks or stripes on the leaves (Aglave *et al.*, 2007). An early detection of pathogen for the disease would allow to take effective control measures for crop protection. Laboratory techniques like PCR (Polymerase chain reaction), ELISA (Enzyme linked immunoassay) and tissue-blot immunoassay can be used to detect the CMV, nevertheless, these are expensive, time taking, labour intensive and required skilled ones. The diseased banana plants show characteristic symptoms for CMV on leaves, however, at an early stages of disease progression, symptoms are not prominent and, hence, detection by visual inspection is somehow difficult. In order to overcome such limitations, in recent years, image processing was introduced in agriculture as a substitute for lab-based disease detection. Image processing-based plant disease detection is a rapid, inexpensive, automatic, field compatible and sensitive method. In Image processing, a series of steps including image acquisition, pre-processing, segmentation, feature extraction and classification are followed to enhance the attributes of the image for accurate detection of the disease (Hatuwal *et al.*, 2020; Sullca *et al.*, 2019). In the present work we have focussed to detect mosaic disease in banana by using image processing and machine learning.

Literature Survey

In recent year's there have been many reports noticed on classify the plant diseases by using Image processing and machine learning techniques. In a study image processing techniques like L*a*b* color space, K-means segmentation, Euclidean Distance have applied to detect Brown Spot and leaf scald diseases in rice plants with an effected area of 15.4302% and 15.013%, respectively (Sethy *et al.*, 2017). Padol and Yadav have applied K-means clustering segmentation and SVM Classification and detected Downy mildew and Powdery mildew in Grape Leaves with an average accuracy of 88.89%. (Padol and Yadav, 2016). The diseases Chimaera and Anthracnose are very common in oil palm leaf in nursery stage, which are detected by SVM with 97% and 95% accuracy, respectively (Kamal *et al.*, 2018). In some of the studies Gabor filters have used for feature extraction and SVM to detect diseases in tomato, for example, both Gabor and SVM are used, detected and annotated powdery mildew or early blight in tomato leaves with an accuracy 99.5 % (Mokhtar *et al.*, 2015a). Similarly, SVM with different kernel functions are used for detection of tomato leaf diseases caused by *Tomato spot wilt virus* (TSWV) and *Tomato yellow leaf curl virus* (TYLCV), in this study SVM alone has given an average accuracy of 90% whereas with the quadratic kernel function obtained 92%. (Mokhtar *et al.*, 2015b). Haralick feature extraction technique and machine learning models like SVM, KNN, Random Forest and CNN are applied for detection of various plant leaf diseases in apple, cherry, grape, peach, bell pepper and strawberry, and found 87.43%, 78.61% accuracy with RFC and SVM, respectively. In view of these studies RFC and SVM classifiers are reliable to detect plant diseases in various agricultural crops (Hatuwal *et al.*, 2020). Support Vector Machine (SVM), Artificial Neural Networks (ANN) and Random Forest Classifier (RFC) and Convolutional Neural Network (CNN) are used to detect diseases and pests like *Alternaria* sp, Whitefly, Fruit borer (*Heliothis virescens*), Trips (*Thrips tabaci*) and Fumagina in Blueberry Leaves where SVM and RFC using with LBP have shown with an accuracy of 83% and 68%, respectively (Sullca *et al.*, 2019).

Proposed Methodology

In the present study we have applied various steps including Image Acquisition, Image Pre-processing, Image Segmentation (K-means clustering), Feature extraction (Gabor features) and Classification (Random Forest Classifier and Support Vector Machine) for detection of mosaic disease in banana leaves.

Image Acquisition: The banana infected leaf image database of this study has taken from the Shodhganga (ID:10603/93037). The author has taken these pictures by canon digital camera in day light at a distance of 1 feet from the object. The database with 15 JPG images of different viral diseases of banana including banana bract mosaic, cucumber mosaic and banana streak are used as a training dataset. The main criteria in this study is to detect the *Cucumber mosaic virus* mediated leaf disease of banana accurately from the other diseases of banana.

Image Pre-processing: Pre-processing is a method, apply on raw image to avoid the non-essential distortions or improve certain image features which are necessary for subsequent processing. In this study input image is





Murali and Nagaraju

converted into LAB image and then splits into L, A and B channel (Sethy *et al.*,2017).Further histogram, Histogram equalization and Contrast Limited Adaptive Histogram Equalization (CLAHE) have applied to L channel. (Jeon and Lee, 2013)

Image Segmentation: Image segmentation is a technique to split digital image into multiple segments (sets of pixels or image objects). In this process, image is assigned with label such that pixels with the same label share similar characteristics such as colour, intensity or texture. Hence, these labels specify boundaries and lines, which separate the most required objects from the image. This is one meticulous step in image processing to discriminate the affected area from the healthy part of the plant, for example leaf symptoms like necrotic lesions, chlorotic spots, mosaic on infected leaf. In this study image segmentation was done by using K-means clustering algorithm (Warne and Ganokar,2015; Jadhav and Patil, 2015; Kamal *et al.*,2018; Sethy *et al.*,2017).

K-Means Clustering Algorithm.

In this algorithm Euclidean distance metric was used to divide k number of clusters based on the objects of the image features as follows

1. In k-means algorithm randomly selected objects are considered as centroids of the active image.
2. The objects which are closed to the centroids are divide into groups and these groups are considered as clusters in such a way the complete image have number of clusters.
3. The mean value of clusters considers again as a centroid from the objects and this process repeat until getting the mean convergence value.

Feature Extraction

For feature extraction Gabor features are used. Gabor is a convolution filter representing a combination of Gaussian component and the Sine component. Gaussian component provides the weights and the sine component provides directionality. Gabor can be used to generate features that represent texture and edges. The following equation is used for feature extraction by Gabor features.

$$g(x, y', \lambda, \theta, \varphi, \sigma, \Upsilon) = \exp\left(-\frac{x'^2 + \Upsilon^2 y'^2}{2\sigma^2}\right) \exp\left(i\left(2\pi\frac{x'}{\lambda} + \varphi\right)\right)$$

λ = Wavelength of the sine component

θ = Orientation of the filter

φ = Phase offset

σ = Standard deviation of the gaussian envelope

Υ = Spatial aspect ratio

$x' = x\cos\theta + y\sin\theta$

$y' = -x\sin\theta + y\cos\theta$

Classification

RFC and SVM are the popular algorithmic methods for image classification in machine learning (Vapnik,1998; Alexandros *et al.*, 2006; Hatuwal *et al.*, 2020). In this study we have used RFC and SVM as a classifiers for the detection of banana leaf disease (Singh *et al.*, 2021; Mokhtar *et al.*, 2015(b); Weizheng *et al.*,2008).The dataset which is taken for the study having the infected leaf images of bract mosaic (5), banana streak(6) and mosaic symptoms (4), caused by *Banana bract mosaic virus (BBRMV)*, banana streak virus(BSV) and *Cucumber mosaic virus(CMV)* respectively. From the training data set an image of mosaic disease (CMV infected leaf) has taken as a test image after applying mask and then used it for comparison with the training dataset for detection.





RESULTS AND DISCUSSION

Disease detection is one of the critical steps in crop protection. Banana is a widely cultivating horticulture crop in India and it is frequently infected by many pests and pathogens. Among the plant pathogens, viruses and their infections have negative impact on crop production. The major economically important viruses of banana are *Banana bract mosaic virus* (BBrMV), Banana bunchy top (BBTV), Banana streak virus (BSV) and *Cucumber mosaic virus* (CMV). All these viruses cause and express more or similar symptoms on infected plant leaves, hence, misleads their accurate detection in banana. Image processing and Machine learning based approaches have been introduced in agriculture to detected diseases accurately. In this study, training dataset is having infected banana images by BSV, BBrMV and CMV. In order to detect CMV infected image (mosaic disease) from the training dataset followed image processing and Machine learning techniques like pre-processing, segmentation, feature extraction and classification. The input image (fig1) is initially converted into LAB colour image (fig2) and subsequently split into three channels L, A and B. Further histogram was applied to L (luminosity) channel which (L histogram) shows overall brightness of the image (graph1). Later to obtain improvements in image brightness and contrast, applied Histogram equalization to L (fig3, graph2). In order to improve the local contrast and enhancing the definitions of edges in each region of the image applied Contrast Limited Adaptive Histogram Equalization (CLAHE) to L (fig4, graph3). Then the active image is subjected for segmentation by K-means cluster algorithm. Of the results, the cluster4 (k=5) has discriminated the diseased region (yellow region) from the other part of the leaf area (fig5). Similar methods have applied in many studies to detect different diseases in various crop lands. For example, Downy mildew and Powdery mildew in grape leaves (Padol and Yadav, 2016); black Spot, anthracnose and rust in rose (Ambatkar et al., 2017); Bacterial blight and Cercospora leaf spot, powdery mildew and rust in chilli, grape, rice, soya bean, wheat, rose, cotton, apple, mango etc (Oo and Htun, 2018); Powdery Mildew disease in cherry leaves (Gupta et al., 2017). Later mask was applied to the segmented image (cluster4, k=5) and it was taken as a test image in both RFC and SVM classifier for classification. In this classification the test image was compared with the training dataset of this study to detect the same or similar diseased leaf image. The comparative studies revealed that the test image was detected CMV infected banana leaf. In order to classify the disease applied the Gabor features and it revealed that the RFC and SVM have shown accuracy and execution time values of 98.94% & 98.07% and 0:00:01.575645 (seconds=1, microseconds=575645) & 0:00:02.148242 (seconds=2, microseconds=148242) for disease detection, respectively. These results suggest that RFC has superior values to SVM at both accuracy and execution time for CMV disease detection in banana leaf. In a similar study RFC has shown more accuracy than to the SVM in detection of various plant leaf diseases in apple, cherry, grape, peach, bell pepper and strawberry (Hatuwal et al., 2020)

Experimental Output

Gabor1 : theta= 0.0 : sigma= 1 : lamda= 0.0 : gamma= 0.05
 Gabor2 : theta= 0.0 : sigma= 1 : lamda= 0.0 : gamma= 0.5
 Gabor3 : theta= 0.0 : sigma= 1 : lamda= 0.7853981633974483 : gamma= 0.05
 Gabor4 : theta= 0.0 : sigma= 1 : lamda= 0.7853981633974483 : gamma= 0.5
 Gabor5 : theta= 0.0 : sigma= 1 : lamda= 1.5707963267948966 : gamma= 0.05
 Gabor6 : theta= 0.0 : sigma= 1 : lamda= 1.5707963267948966 : gamma= 0.5
 Gabor7 : theta= 0.0 : sigma= 1 : lamda= 2.356194490192345 : gamma= 0.05
 Gabor8 : theta= 0.0 : sigma= 1 : lamda= 2.356194490192345 : gamma= 0.5
 Gabor9 : theta= 0.0 : sigma= 3 : lamda= 0.0 : gamma= 0.05
 Gabor10 : theta= 0.0 : sigma= 3 : lamda= 0.0 : gamma= 0.5
 Gabor11 : theta= 0.0 : sigma= 3 : lamda= 0.7853981633974483 : gamma= 0.05
 Gabor12 : theta= 0.0 : sigma= 3 : lamda= 0.7853981633974483 : gamma= 0.5
 Gabor13 : theta= 0.0 : sigma= 3 : lamda= 1.5707963267948966 : gamma= 0.05
 Gabor14 : theta= 0.0 : sigma= 3 : lamda= 1.5707963267948966 : gamma= 0.5
 Gabor15 : theta= 0.0 : sigma= 3 : lamda= 2.356194490192345 : gamma= 0.05
 Gabor16 : theta= 0.0 : sigma= 3 : lamda= 2.356194490192345 : gamma= 0.5





Murali and Nagaraju

Gabor17 : theta= 0.7853981633974483 : sigma= 1 : lamda= 0.0 : gamma= 0.05
 Gabor18 : theta= 0.7853981633974483 : sigma= 1 : lamda= 0.0 : gamma= 0.5
 Gabor19 : theta= 0.7853981633974483 : sigma= 1 : lamda= 0.7853981633974483 : gamma= 0.05
 Gabor20 : theta= 0.7853981633974483 : sigma= 1 : lamda= 0.7853981633974483 : gamma= 0.5
 Gabor21 : theta= 0.7853981633974483 : sigma= 1 : lamda= 1.5707963267948966 : gamma= 0.05
 Gabor22 : theta= 0.7853981633974483 : sigma= 1 : lamda= 1.5707963267948966 : gamma= 0.5
 Gabor23 : theta= 0.7853981633974483 : sigma= 1 : lamda= 2.356194490192345 : gamma= 0.05
 Gabor24 : theta= 0.7853981633974483 : sigma= 1 : lamda= 2.356194490192345 : gamma= 0.5
 Gabor25 : theta= 0.7853981633974483 : sigma= 3 : lamda= 0.0 : gamma= 0.05
 Gabor26 : theta= 0.7853981633974483 : sigma= 3 : lamda= 0.0 : gamma= 0.5
 Gabor27 : theta= 0.7853981633974483 : sigma= 3 : lamda= 0.7853981633974483 : gamma= 0.05
 Gabor28 : theta= 0.7853981633974483 : sigma= 3 : lamda= 0.7853981633974483 : gamma= 0.5
 Gabor29 : theta= 0.7853981633974483 : sigma= 3 : lamda= 1.5707963267948966 : gamma= 0.05
 Gabor30 : theta= 0.7853981633974483 : sigma= 3 : lamda= 1.5707963267948966 : gamma= 0.5
 Gabor31 : theta= 0.7853981633974483 : sigma= 3 : lamda= 2.356194490192345 : gamma= 0.05
 Gabor32 : theta= 0.7853981633974483 : sigma= 3 : lamda= 2.356194490192345 : gamma= 0.5

CONCLUSION

In this study we have applied image processing and machine learning techniques to detect mosaic disease of banana from the training dataset by K-means clustering algorithm, Gabor features, RFC and SVM. The results of the study revealed that RFC classifier has shown better accuracy and execution time than SVM for detection of mosaic disease of banana.

REFERENCES

1. Dadzie BK. International Plant Genetic Resources Institute (An INIBAP Technical guideline): post-harvest characteristics of black Sigatoka resistant banana, cooking banana and plantain hybrids in Rome, Italy .1998.
2. Aglave BA, Krishnareddy M, Patil FS, Andhale MS. International Journal of Biotechnology & Biochemistry: Molecular identification of a virus causing banana chlorosis disease from Marathwada region.2007; vol. 3, no. 1, pp-13–23.
3. Hatuwal BK, Shakya A, and Joshi B. POLIBITS: Plant Leaf Disease Recognition Using Random Forest, KNN, SVM and CNN. 2020; vol. 62, pp. 13–19.
4. Sathy PK, Negi B and Nilamani. International Journal of Computer Applications: Detection of healthy and defected diseased leaf of rice crop using K-means clustering technique.2017; Vol.157, Issue.1.
5. Padol PB and Yadav AA. Conference on Advances in Signal Processing (CASP) IEEE: SVM Classifier based grape leaf disease detection.2016.
6. MokhtarU, Ali MAS, Hassenian AE, and Hefny H. International Computer Engineering Conference: Tomato leaves diseases detection approach based on support vector machine.2015a; pp-246-250.
7. Mokhtar U, Ali M A, Hassanien A E, and Hefny H. Information Systems Design and Intelligent Applications: Identifying two of tomatoes leaf viruses using support vector machine.2015b; 771-782.
8. Kamal MM, MasazharANI, Rahman FA. Indonesian Journal of Electrical Engineering and Computer Science: Classification of Leaf Disease from Image Processing Technique.2018; pp.191~200.
9. Ambatkar A, Bhandekar A, Tawale A, Vairagade C, Kotamkar K. International Conference on Recent Trends in Engineering Science and Technology (ICRTEST): Leaf disease detection using image processing.2017; Vol.5, Issue.1, pp-333-336.
10. Jadhav SB and Patil SB. International Journal of Advanced Research in Electronics and Communication Engineering (IJARECE): Grading of soybean leaf disease based on segmented image using K-means clustering.2015; Vol.4, Issue.6, pp-1816- 1822.

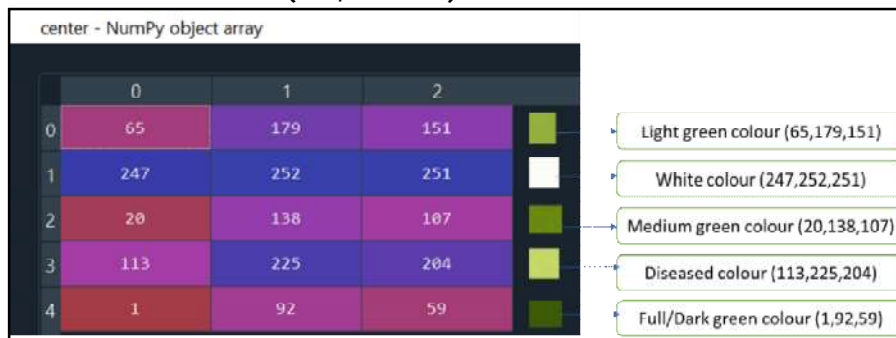




Murali and Nagaraju

11. Warne PP and Ganokar SR. International Journal of Engineering and Technology (IJET): Detection of diseases of cotton leaves using k-mean clustering method.2015; Vol.2, Issue. 4.
12. <http://hdl.handle.net/10603/93037>
13. Gupta V, Sengar N, Dutta MK, Travieso CM, Alonso JB. IEEE: Automated segmentation of powdery mildew disease from cherry leaves using image processing.2017.
14. Sullca C, Molina C, Rodríguez C, and Fernández T. International Journal of Machine Learning and Computing: Diseases Detection in Blueberry Leaves using Computer Vision and Machine Learning Techniques.2019; Vol. 9, No. 5.
15. Oo YM and Htun NC. International Journal of Research and Engineering: Plant Leaf Disease Detection and Classification using Image Processing.2018; Vol. 5 No. 9 | PP. 516-523.
16. Weizheng S, Yachun W, Zhanliang C and Hongda W. international Conference on Computer Science and Software Engineering: Grading Method of Leaf Spot Disease Based on Image Processing.2008.
17. Vapnik V. Wiley: Statistical Learning Theory, New York.1998.
18. Alexandros K *et al.*, Journal of Statistical Software: Vector Machines in R.2006; vol/issue: 15(9).
19. Jeon G and Lee YS. Advanced Science and Technology Letters: Histogram Equalization-Based Color Image Processing in Different Color Model.2013; Vol.28, pp.54-57.

Table 1: Pixel values of (k=5, cluster 4)



In the implemented K-means clustering algorithm the output of the image (k=5, cluster4) centroids are (65,247,20,113,1) and ret value = 26253013.487576008

Table 2: Feature importance's and their values

Features_ Importance	Values
Gabor21	0.141043
Gabor31	0.101165
Gabor29	0.092816
Original Image	0.091713
Gabor23	0.079256
Gabor32	0.073554
Gabor5	0.072152
Gabor4	0.064596
Gabor6	0.062765
Gabor24	0.045695
Gabor30	0.043937
Gabor7	0.035808
Gabor8	0.023926
Gabor3	0.023626
Gabor12	0.018462



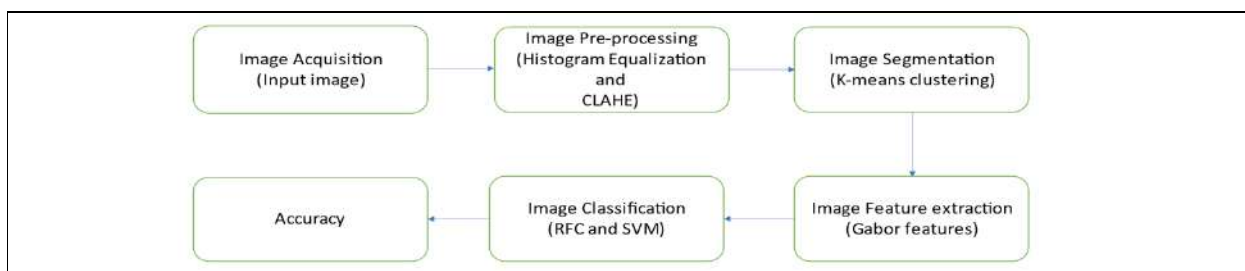


Murali and Nagaraju

Gabor11	0.017741
Gabor22	0.010490
Gabor20	0.000878
Gabor28	0.000334
Gabor27	0.000043

Table 3: Accuracy of classifiers

Classifiers	Accuracy
SVM	98.07%
RFC	98.94%



Flow Chart: Work plan of proposed methodology

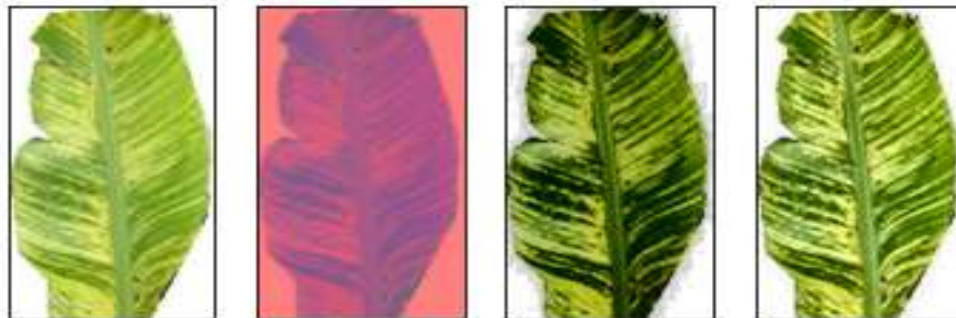


fig 1

fig 2

fig 3

fig 4

Fig 1: Input Test image of the Banana Leaf affected by *Cucumber mosaic virus* (Cmv), Fig 2: Lab Colour Image, Fig 3: Histogram Equalized Image, Fig 4: Clahe Image



k=1, cluster 0

k=2, cluster 1

k=3, cluster 2

k=4, cluster 3

k=5, cluster 4

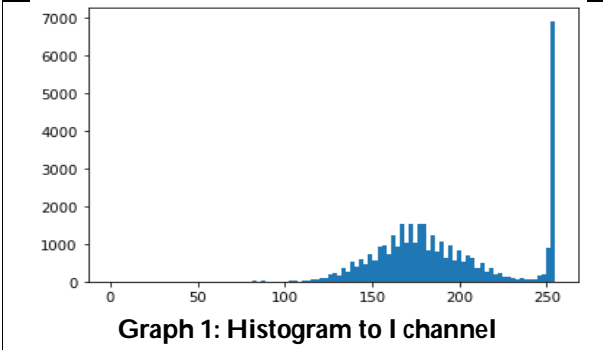
Fig 5: Clusters of segmented image of CMV infected banana leaf

In the K-means clustering algorithm, a total of five clusters (0 to 4) are used. The cluster4 (k=5) is given the good output of the diseased area. The segmented images are used in the feature extraction and classification.

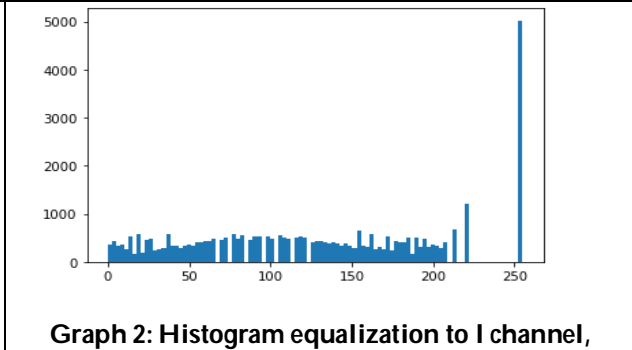




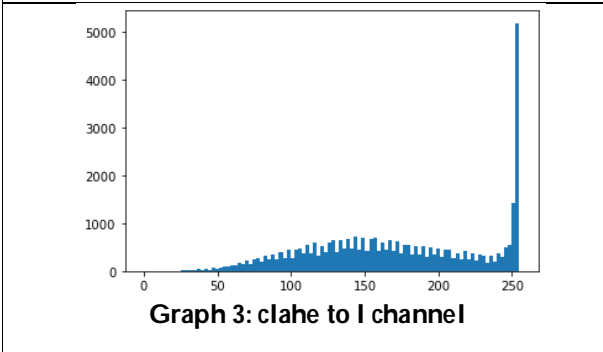
Murali and Nagaraju



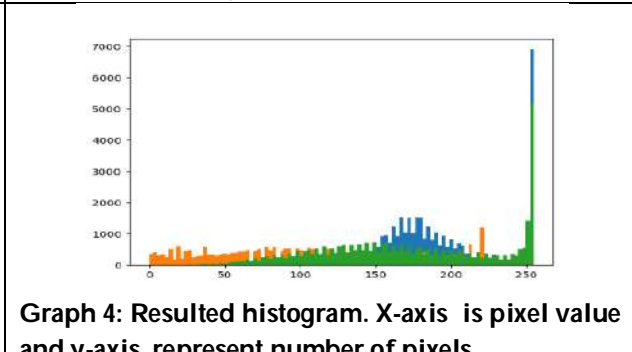
Graph 1: Histogram to I channel



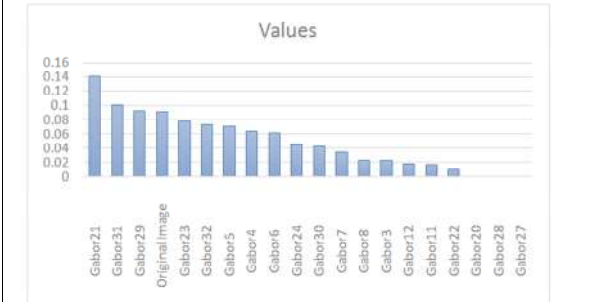
Graph 2: Histogram equalization to I channel,



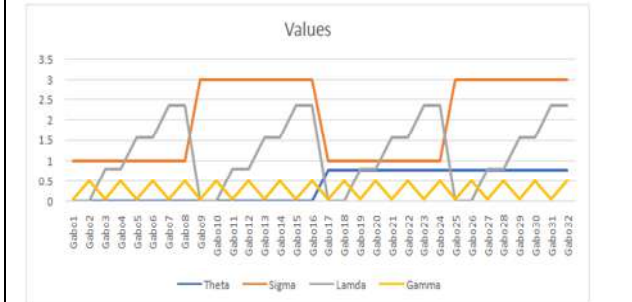
Graph 3: clahe to I channel



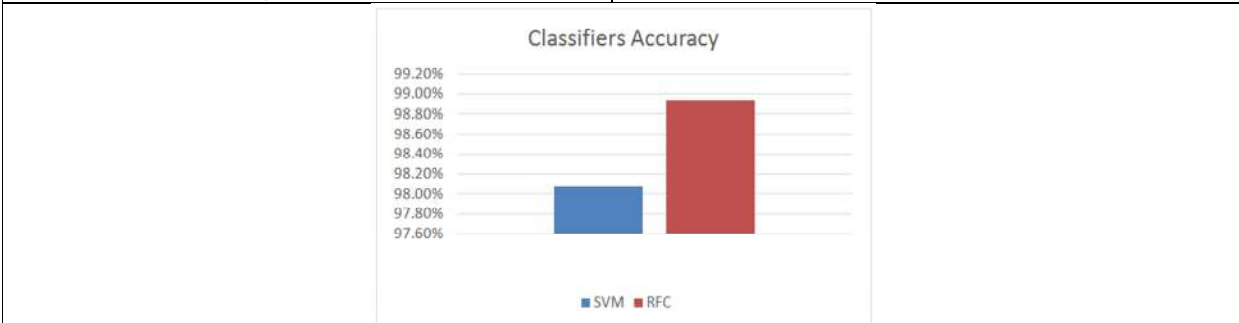
Graph 4: Resulted histogram. X-axis is pixel value and y-axis represent number of pixels.



Graph 5: the significant features (x-axis) and their respective values (y-axis) for feature extraction of the image;



Graph 6: the experimental output values of gabor features



Graph 7: The overall accuracy of RFC and SVM classifier for CMV disease detection in banana





Corrosion Inhibition of Mild Steel in Acid Medium using *Madhuca longifolia* Plants Aqueous Extract - A Comparative Study

P R Sivakumar*

Assistant Professor, Department of Chemistry, Adithya Institute of Technology, Coimbatore - 641107, Tamil Nadu, India.

Received: 08 Nov 2021

Revised: 17 Dec 2021

Accepted: 17 Jan 2022

*Address for Correspondence

P R Sivakumar

Assistant Professor,
Department of Chemistry,
Adithya Institute of Technology,
Coimbatore - 641107, Tamil Nadu, India.
Email: shivarashee@gmail.com



This is an Open Access Journal / article distributed under the terms of the **Creative Commons Attribution License** (CC BY-NC-ND 3.0) which permits unrestricted use, distribution, and reproduction in any medium, provided the original work is properly cited. All rights reserved.

ABSTRACT

The weight-loss method, potentiodynamic polarization, and electrochemical impedance spectroscopy techniques were used to evaluate the inhibitory impact of various components of the plant *Madhuca longifolia* extract (leaves, barks, fruits, and seed peels) on mild steel corrosion in 1 N HCl medium. The plant extract acts as a mixed-type inhibitor, according to polarisation experiments. The weight-loss method revealed that the inhibitory efficacy of *Madhuca longifolia* extracts increases in a concentration-dependent way, which was backed up by electrochemical data. In comparison, *Madhuca longifolia* stem extracts had the highest inhibitory effectiveness, at 97.14 percent at 20 v/v concentration. The remarkable performance of the plant extract's inhibitive activity was validated by the SEM morphology of the adsorbed protective coating on the mild steel surface. Surface coverage levels were graphed to see if they were acceptable for adsorption.

Keywords: Metals; Corrosion test; EIS; SEM.

INTRODUCTION

Mild steel is a structural material that is commonly utilized in autos, pipelines, and the chemical industry in general. Mild steel corrodes rapidly in acidic environments and during the pickling process. Pickling, descaling, and chemical cleaning of mild steel are all done using hydrochloric acid. Acid solutions such as HCl and H₂SO₄ are extensively employed in industrial processes such as cleaning, pickling, descaling, and etching of metals, but they also contribute to metal surface corrosion [1-8]. Organic compounds with heteroatoms such as N, O, S, P, and aromatic rings in their structure have been observed to be the most efficient inhibitors. Chelating compounds with transition series metals are recognized to be good complexes. The creation of a supporting layer on the metal surface explains their adsorption in general. Organic chemicals have been shown to have better inhibitory efficacy than inorganic



**Sivakumar**

inhibitors, which are utilized in their detrimental effects on humans and the environment (especially those containing phosphate, chromate, and other heavy metals). Synthetic organic inhibitors have also been widely used, but their toxicity and high manufacturing costs are now limiting their usage. This has motivated scientists to look into other areas in order to develop green corrosion inhibitors that are environmentally benign, inexpensive, and biodegradable to replace inorganic and synthetic organic inhibitors. Plant extracts, amino acids, proteins, and biopolymers, among other natural products, have been shown to be effective corrosion inhibitors. Plant extracts are thought to be a rich source of chemical components that have been generated naturally and may be extracted. Several researchers [9-24] have been drawn to environmentally friendly inhibitors. Plant extracts have been investigated as corrosion inhibitors in recent years due to their biodegradability, non-toxicity, and environmental friendliness, as well as their easy availability, low cost, and straightforward technique. Our chosen plant names (leaves, barks, fruits, and seed peels) in this study included *Madhuca longifolia* (ML), which had no record in the Literature Review.

EXPERIMENTAL PROCEDURE

Preparation of mild steel specimen

Mild steel strips were mechanically cut into strips of size 4 cm x 2 cm x 0.1 cm containing the composition of C- 0.030 %, Mn- 0.169 %, Si- 0.015 %, P- 0.031 %, S - 0.029 %, Cr- 0.029 %, Ni- 0.030 %, Mb- 0.016 %, Cu- 0.017 % and the remainder Fe and provided with a hole of uniform diameter to facilitate suspension of the strips in the test solution for weight loss method. Mild steel strips with the same composition but a 1cm² exposed area were employed for electrochemical tests. Four digital electronic balances were used to accurately weigh the metal (shimadzu ay 220 model).

Preparation of the plant extract

The medicinal plants *Madhuca longifolia*'s leaves, barks, fruits, and seed skins were chopped into small pieces, dried at room temperature, and powdered into powder. 10g of each powder was refluxed in 150 mL of distilled water overnight. The refluxed solution was then thoroughly filtered, and the filtrate volume was increased to 250 ml using double distilled water as the stock solution, with the stock solution's concentration stated in terms of v/v [25].

RESULTS AND DISCUSSION

Weight loss methods: One of the basic, easy and frequently used methods of determining corrosion in metal by mass loss analysis. The polished mild steel rectangular (4 x 2 x 0.1) were precisely weighed and submerged in the test solution in a beaker. The presence of phytochemical constituents in the plant extract is discovered to be larger molecules in order to cover a wider surface area on adsorption. The majority of corrosion inhibitors work by adsorbing their molecules onto metal surfaces. As a result, the influence of temperature on the green inhibitor's inhibitory efficacy on mild steel in 1N HCl medium becomes more critical. Table 1 shows the corrosion rate and inhibition efficacy of plant extract on mild steel at various immersion times and temperatures. However, the inhibition effectiveness decreases with increasing temperature, while the difference is not substantial. These findings clearly demonstrate that the ML plants extract the greatest amount of putative anticorrosive characteristics. The results showed that ML leaves > seed peels > fruits > barks at the optimal concentration (aqueous extract 15 v/v) of all four inhibitors.

FTIR Measurement: Earlier researchers have confirmed that FTIR spectrometer is a powerful instrument that can be used to determine the type of bonding for organic inhibitor adsorbed on the metal surface [26-29]. Although various compounds present in the ML extract which contributed in effective working in the inhibitor, it is very difficult to identify each compound separately to know the group present in the ML plants extracts. FTIR spectra of the *Madhuca longifolia* plants of various parts like leaves, barks, fruits, and seeds peels extract was shown in Fig. 1. For *Madhuca longifolia*, which contain bands (leaves, barks fruits and seed peels) corresponding 3301, 3272, 3396, 3170



**Sivakumar**

cm^{-1} can be assigned to (hydroxyl group) respectively. The Tafel parameters for mild steel in the absence and presence of an inhibitor concentration of ML plants aqueous extract in 1N HCl are presented in Table 2 and its polarization curve is shown in Fig.2. The addition of ML has no effect on the values of E_{corr} , but it does impact both the anodic dissolution of mild steel and the cathodic reduction reaction, suggesting that the composite might be categorized as a mixed type inhibitor, as shown in Fig.2. The corrosion current density (i_{corr}) decreases with increasing inhibitor concentrations, as seen in the table. The greatest inhibition efficacy seen at higher inhibitor concentrations indicates that more inhibitor molecules are deposited on the metal surface, providing more surface coverage for the MS active regions where the direct attack occurs and the corrosion attack migrates [30].

Electrochemical impedance studies: Impedance spectroscopy is one of the most simple and consistent techniques and is also used to study the characterization of electrode (surface) behavior in 1N HCl solution in the absence and presence of the plants extracts. Figure 3 depicts Nyquist plots of several sections of *Madhuca longifolia* plants at varying concentrations, including leaves, fruits, barks, and seed peels. Table 3 shows the various corrosion parameters generated from EIS measurements. The impedance spectra show a single semicircle, with the diameter of the semicircle increasing as the inhibitor concentration increases, indicating that the charge-transfer process primarily controls mild steel surface corrosion by delaying the electron transfer reaction and forming a strong protective film. The results reveal that when the inhibitor concentration rises (forming a protective layer), the R_{ct} rises as well, and as the C_{dl} values fall, the inhibitor efficiency rises [31-33].

Surface analysis: The observation of the mild steel specimen was carried out using scanning electron microscope. Figure 4 shows the SEM image of mild steel surface after immersed in 1NHCl in the absence and presence of selected ML plant extract for 24 hours. Closely observed very strong corroded (pits and crack) and uneven (heavy damage) metal surface obtained when the metal was kept immersed in 1N HCl for absence of inhibitor. In presence of inhibitor the metal surface shows smoother layer with clearly different morphology (surface covered means no pits and cracks). The protective film formed on the mild steel surface confirmed by SEM also supported the optimum inhibition efficiency.

Bode measurement: The bode plots figure 5 shows resistive region at high frequencies and capacitive region at intermediate frequencies but do not show a clear resistive region (horizontal line and a phase angle = 0) at low frequencies. These plots show two overlapped phase maxima at low frequencies. In the bode plot, the impedance is plotted with log frequencies on the X axis and both the log of absolute value of the impedance and the phase shift on the Y-axis. Unlike the nyquist plot, the phase angle does not reach 90° as it would for pure capacitive impedance. In the bode plot at the highest frequencies, $\log(R_{\text{s}}+R_{\text{ct}})$ appears as a horizontal plateau.

Phytochemical screening method: Table 4 summarises the results of a preliminary examination of phytochemical constituents in plant extract. The chemical structure of these phytochemical constituents reveals that they are easily hydrolysable, and that they can be adsorbed on metal surfaces via the lone pair of electrons present in their oxygen atoms (i.e. they contain multifunctional group), creating a barrier for charge and mass transfer, reducing the metal's interaction with the corrosive environment. The metal's corrosion rate was reduced as a result of this. The creation of a film layer prevents H^+ discharge and metal ion dissolution. The protonated constituent's molecules are adsorbed (physisorption) due to electrostatic contact, resulting in a high level of inhibition.

Effect of immersion time: The variation of inhibition efficiency for different concentration of plant aqueous and alcoholic extract of ML was listed in the Table 5. Maximum inhibition efficiency of aqueous extract for 1N HCl was found to be 96.91% at 12 h with 20 v/v concentration of the inhibitor (barks) respectively. This behaviour may be attributed to the increase of the surface coverage by the extract, which retards the corrosion of mild steel.

Effect of temperature: The effect of temperature on the corrosion inhibition properties of ML leaves extract was studied by exposing the mild steel to 1 N HCl containing 5, 10, 15, 20 v/v of the leaves extract in the temperature range of 303-323K. The data in Table 6 indicate that the leaves extract is effective as inhibitor for mild steel in 1N HCl



**Sivakumar**

upto 303K and increase thereafter. The inhibition showed a maximum of 80.41 % at 303K for aqueous extract of ML seed peels extract in 1N HCl.

Adsorption isotherm: Adsorption isotherms can offer information on the partnership between inhibitor molecules (organic adsorbate) and mild steel surfaces. Temkin, Langmuir, and Frumkin were used to identify the optimal isotherm for evaluating the adsorption process of chosen ML plant extract on the metal surface, which is described in this work [Fig.6-8]. This isotherm is connected to the amount of surface covering and the concentration of inhibitors. According to the isotherm, metal surfaces have a set number of adsorption sites, each of which holds one adsorbate. Because the linear regression coefficient or correction factor (R^2) is nearly one. According to the literature, heterocyclic (Organic) adsorptions generally have a polar function with heteroatoms such as N, S, O, and P, as well as a double or triple bond or aromatic ring. Which of these groups is the most electron donor, and is there a potential of an adsorption centre. This isomerism is crucial in establishing the mechanism of Organo-electrochemical reactions, since they reveal the nature of the metal-inhibitor relationship. The establishment of either electrostatic or covalent bonding between the adsorbates and the metal surface atom results in the creation of the metal / solution interface. A good association was found between plant water soluble constituents and a possible physical adsorption process.

Mechanism of inhibition: The centre of adsorption method and the structure of the components present in the ML plant extracts can be used to describe the possible mechanism of inhibition. The most important component of ML plant extract is [Fig. 9], which has multiple bonds through which it is adsorbed on the metal surface. The compounds must block the aggressive corrosion sites on the MS surface, and therefore adsorption happens through the bonding of the inhibitor's free electron with the metal. Glycosides, flavonoids, saponins, steroids, tannins, and alkaloids were found in phytochemical analysis. Above Organic fragments grow adsorbed on the metal surface, forming a protective coating, and the variation in inhibitory characteristics is directly connected to molecular structural differences. The structure of the following component comprises electron-rich oxygen and nitrogen, which might be useful active components for plant corrosion inhibition. Through van der Waals force, these complexes may adsorb onto the steel surface, giving further corrosion protection [34].

CONCLUSION

In 1N HCl acid medium, a selected ML plant aqueous extract acted as a possible benign inhibitor for mild steel corrosion. The inhibitor acts as a mixed type inhibitor, according to tafel and impedance experiments. The production of the Fe complex has been confirmed by FTIR tests on corrosion products. SEM investigations show that specific ML plant extracts adsorb to the mild steel surface. The creation of a smooth, thick protective layer is shown by FT-IR and SEM in the presence of effective inhibitors.

REFERENCES

1. Vinothkumar K, Nivetha M, Sethuraman MG (2020) Robust composite coating with superior corrosion inhibitory performance on surgical grade 316L stainless steel in Ringer solution. *Iran Polym J* 29:919–931
2. Hamidi Z, Mosavian SY, Sabbaghi N (2020) Cross-linked poly(*N*-alkyl-4-vinylpyridinium) iodides as new eco-friendly inhibitors for corrosion study of St-37 steel in 1 M H₂SO₄. *Iran Polym J* 29:225–239
3. Pekdemir ME, Öner E, Kök M (2021) Thermal behavior and shape memory properties of PCL blends film with PVC and PMMA polymers. *Iran Polym J* 30: 633–641
4. Dagdag O, El Harfi A, El Gana L, Hlimi Z, Erramli H, Hamed O, Jodeh S (2019) The role of zinc phosphate pigment in the anticorrosion properties of bisphenol a diglycidyl ether-polyaminoamide coating for aluminum alloy AA2024-T3. *J Bio-Tribo-Corros* 5(1):7-16
5. Huang R, Guo X, Ma S, Xie J, Xu J, Ma J (2020) Novel phosphorus-nitrogen-containing ionic liquid modified metal-organic framework as an effective flame retardant for epoxy resin. *Polymers* 12(1):108-120





Sivakumar

6. Dagdag O, Hsissou R, Berisha A, Erramli H, Hamed O, Jodeh S, El Harfi A (2019) Polymeric-based epoxy cured with a polyaminoamide as an anticorrosive coating for aluminum 2024–T3 surface: experimental studies supported by computational modeling. *J Bio-Tribo-Corros* 5:58-64
7. Li L, Cai Z (2020) Flame-retardant performance of transparent and tensile-strength-enhanced epoxy resins. *Polymers* 12:317-324
8. Song K, Wang Y, Ruan F, Liu J, Li N, Li X (2020) Effects of a macromolecule spirocyclic inflatable flame retardant on the thermal and flame retardant properties of epoxy resin. *Polymers* 12:132-140
9. Rane AV, Abitha V, Jadhava S (2020) Non-isocyanate polyurethane systems: a review. *Moroc J Chem* 8:8–4
10. Kanojia R, Singh G (2005) An interesting and efficient organic corrosion inhibitor for mild steel in acidic medium. *Surface Eng* 21(3):180–186
11. Li W, He Q, Zhang S, Pei C, Hou BJ (2008) Some new triazole derivatives as inhibitors for mild steel corrosion in acidic medium. *Appl Electrochem* 38:289-295
12. Sivakumar PR, Srikanth AP (2016) Anticorrosive activity of Santalum Album leaves extract against the corrosion of mild steel in acidic medium. *IntJ PhyAppli Sci* 3 (1):10-20
13. Sivakumar PR, Karuppusamy M, Perumal S, Elangovan A, Srikanth AP (2015) Corrosion Inhibitive effects of Madhuca Longifolia on mild steel in 1N HCl solution. *J Envi Nanotech* 4(2):31-36
14. Karuppusamy M, Sivakumar PR, Perumal S, Elangovan A, Srikanth AP (2015) *Mimusops elengi* Linn plant extract as an efficient green corrosion inhibitor for mild steel in acidic environment. *J Envi Nanotech* 4(2):09-15
15. Sivakumar PR, Karuppusamy M, Vishalakshi K, Srikanth AP (2016). The inhibition of mild steel corrosion in 1N HCl solution by *Melia azedarach* leaves extract. *Der Pharma Chem* 8(12): 74-83.
16. Sivakumar PR, Srikanth AP (2016) Inhibiting effect of seeds extract of *Pithecellobium dulce* on corrosion of mild steel in 1N HCl medium. *Int J Eng Sci and Comp* 6(8): 2744-2748
17. Sivakumar PR, Vishalakshi K, Srikanth AP (2016) Inhibitive action of *Bombax malabricum* leaves extract on the corrosion of mild steel in 1N HCl Medium. *J AppliChemi* 5(5):1080-1088
18. Vishalakshi K, Sivakumar PR, Srikanth AP (2016) *Tetrameles nudiflora* Leaves Extract as Green Corrosion Inhibitor for Mild steel in Hydrochloric Acid Solution. *Int Org Sci Res J Appl Chemi* 9(9):50-55
19. Sivakumar PR Srikanth AP (2016) Inhibiting effect of fruits extract of Santalum Album on corrosion of mild steel in Hydrochloric acid solution. *Int Org Sci Res J Appl Chemis* 369(10): 29-37
20. Sivakumar PR, Srikanth AP (2016) Inhibitive action of aqueous extract of *Holoptelea integrifolia* leaves for the corrosion of mild steel in 1N HCl solution. *Der Phar Chemi* 8(19):433-440
21. Sivakumar PR, Karuppusamy M, Vishalakshi K, Srikanth AP (2017) Inhibitory effect of *Michelia Champaca* leaves extracts on the corrosion of mild steel in 1N HCl acid: A Green Approach. *IOSRD Int J Chemi* 4(1):14-18
22. Sivakumar PR, Srikanth AP (2017) Anticorrosive Activity of *Schereaberasweietenoids* Leaves as Green Inhibitor for Mild Steel in Acidic Solution. *Asian J Chemi* 29(2):274-278
23. Vishalakshi K, Sivakumar PR, Srikanth AP (2016) Analysis of Corrosion Resistance behavior of green inhibitors on mild steel in 1N HCl medium using electrochemical techniques. *Der Pharma Chemica*, 8(19), 548-553
24. Akilkhajuria, Modassir Akhtar, Raman Bedi, Rajneesh Kumar, Mainak Ghosh, Das CR, Shaju K Albert (2020) Microstructural investigation on simulated intercritical heat-affected zone of boron modified P91-steel. *Material Science and Tech* <http://doi.org/10.1080/02670836.2020.1784543>
25. Akilkhajuria, Modassir Akhtar, Raman Bedi, Rajneesh Kumar, Mainak Ghosh, Das CR, Shaju K Albert (2020) Influence of boron microstructure and mechanical properties of gleeble simulated heat-affected zone in P91-steel. *Int.J. Pressure vess pip* <http://doi.org/10.1016/j.ijpvp.2020.104246>
26. Akilkhajuria, Modassir Akhtar, Raman Bedi, Rajneesh Kumar, Mainak Ghosh, Das CR, Shaju K Albert (2018) Phase transformations and numerical modelling in simulated HAZ of nanostructured P91B steel for high temperature applications. *App. Nanoscience* <http://doi.org/10.1007/s13204-018-0854-1>
27. Sivakumar PR, Srikanth AP (2017) *Ziziphus jujube* leaves extract as green corrosion inhibitor for mild steel in 1N hydrochloric acid Medium. *J AppliChemis* 6(4):476-483
28. Sivakumar PR, Srikanth AP (2018) Eco friendly green inhibitor for corrosion of mild steel in 1N hydrochloric acid Medium. *J AppliChemis* 7(1):239-249





Sivakumar

29. Sivakumar PR, Srikanth AP (2018) *Gloriosa superba* linn extract as eco friendly inhibitor for mild steel in acid medium: A comparative study. Asi J Chemis 30(3):513-519
30. Sivakumar PR, Srikanth AP, Muthumanikam S (2017) The corrosion inhibition and adsorption properties of ecofriendly green inhibitor - A comparative study. Int J Chemtech Res 10(12):386-398
31. Sivakumar PR, Karuppusamy M, Srikanth AP (2017) Corrosion inhibition of mild steel in 1N HCl media using *Millingtonia hortensis* leaves extract. Int Org Sci Res J Appl Chemi 10:65-70
32. Sivakumar PR, Karuppusamy M, Srikanth AP (2018) *Pithecellobium dulce* extracts as corrosion inhibitor for mild steel in acid medium. Der Pharma Chemi 10:22-28
33. Sivakumar PR and Srikanth AP (2020) Green corrosion inhibitor: A comparative study. Sadhana 45:45-56

Table 1 Percentage of inhibition efficiency (IE %) and corrosion rate (CR) at different concentration of inhibitor in 1N HCl medium

Aqueous extract				
Parts of (ML) plant	Conc. of the extract (v/v)	Weight loss (g)	Corrosion rate (mmpy)	IE (%)
<i>Madhuca longifolia</i> Leaves	Blank	0.1007	37.218	-
	5	0.0011	4.678	40.23
	10	0.0017	0.486	57.55
	15	0.0013	0.454	73.20
	20	0.0015	0.070	97.14
<i>Madhuca longifolia</i> Barks	Blank	0.0445	20.830	-
	5	0.0046	5.117	42.07
	10	0.0040	1.018	58.18
	15	0.0001	0.106	79.76
	20	0.0035	0.091	82.98
<i>Madhuca longifolia</i> Fruits	Blank	0.0350	19.110	-
	5	0.0083	3.181	48.18
	10	0.0002	0.136	63.13
	15	0.0005	0.119	71.39
	20	0.0040	0.045	88.07
<i>Madhuca longifolia</i> seeds peel	Blank	0.0849	10.281	-
	5	0.0089	2.063	49.41
	10	0.0003	0.970	62.04
	15	0.0120	0.450	78.76
	20	0.0110	0.278	89.04

Table 2 Electrochemical parameters from polarization measurement and calculated values of inhibition efficiency.

Aqueous extract						
Parts of MLplant	Conc. (v/v)	E_{corr} (mV/ SCE)	I_{corr} (mA/cm ²)	b_c	b_a	IE (%)
leaves	Blank	-0.471	4.7×10^{-3}	208	153	*
	5	-0.468	3.3×10^{-3}	184	133	99.77
	10	-0.469	1.3×10^{-3}	166	101	84.58
	15	-0.483	8.5×10^{-4}	162	115	93.12
	20	-0.476	4.4×10^{-4}	132	093	87.08
barks	Blank	-0.471	5.2×10^{-3}	199	140	*
	5	-0.469	3.2×10^{-3}	180	127	76.00
	10	-0.466	3.3×10^{-3}	203	136	99.63
	15	-0.469	1.7×10^{-3}	174	104	99.59





Sivakumar

	20	-0.474	1.8×10^{-3}	172	125	85.29
Fruits	Blank	-0.471	4.0×10^{-3}	208	153	*
	5	-0.469	1.5×10^{-3}	171	118	86.00
	10	-0.486	2.6×10^{-4}	141	088	99.79
	15	-0.475	5.4×10^{-4}	152	098	99.80
	20	-0.491	2.3×10^{-4}	137	098	91.01
Seed peels	Blank	-0.471	4.0×10^{-3}	208	153	*
	5	-0.479	1.5×10^{-3}	167	122	90.44
	10	-0.479	6.7×10^{-4}	146	097	99.21
	15	-0.482	1.1×10^{-3}	157	118	84.50
	20	-0.485	9.7×10^{-3}	148	110	97.00

Table 3 Impedance parameter for mild steel in 1 N HCl acid solution in the absence and presence of varied concentration of inhibitor.

Aqueous extract				
Parts of <i>Madhuca longifolia</i> plant	Concentration(v/v)	R_{ct} (ohm cm ²)	C_{dl} (μ F/cm ²)	IE (%)
<i>Madhuca longifolia</i> leaves	Blank	9.221	6.79×10^{-4}	*
	5	8.182	6.66×10^{-4}	55.96
	10	19.202	1.20×10^{-4}	59.99
	15	31.031	4.49×10^{-4}	84.78
	20	51.008	1.74×10^{-4}	68.43
<i>Madhuca longifolia</i> barks	Blank	6.581	1.193×10^{-2}	*
	5	10.936	5.10×10^{-3}	70.36
	10	10.266	4.290×10^{-3}	62.30
	15	13.969	2.298×10^{-3}	42.29
	20	15.452	2.081×10^{-3}	77.75
<i>Madhuca longifolia</i> fruits	Blank	9.436	6.893×10^{-3}	*
	5	18.225	1.650×10^{-3}	63.88
	10	83.448	7.285×10^{-5}	74.79
	15	42.037	2.904×10^{-4}	77.00
	20	103.26	4.257×10^{-5}	84.01
<i>Madhuca longifolia</i> seed peels	Blank	9.633	6.439×10^{-3}	*
	5	16.560	1.665×10^{-3}	78.63
	10	32.420	4.440×10^{-4}	40.51
	15	24.093	8.602×10^{-4}	62.52
	20	22.126	8.477×10^{-4}	58.50

Table 4. Phytochemical screening test for extract of ML plants

Phytochemical test	leaves	fruits	Barks	Seeds peel
Alkaloids	+	+	+	+
Carbohydrates	+	+	-	+
Proteins	+	+	+	-
Saponins	-	-	+	+
Thiols	-	-	-	-
Tannins	-	-	+	-
Flavanoids	-	+	+	+
Phenol	-	+	+	-
Glycosides	+	+	+	+





Sivakumar

Table 5. Inhibition efficiency as a various immersion time.

Parts of <i>Madhuca longifolia</i> plant	Conc. of the extract (v/v)	Inhibition efficiency (%)					
		1h	3h	5h	7h	9h	12h
<i>Madhuca longifolia</i> leaves	Blank	*	*	*	*	*	*
	5	68.10	71.53	66.76	64.39	54.32	45.56
	10	78.10	80.25	78.54	76.76	60.12	68.72
	15	87.50	89.99	86.16	87.96	82.49	86.95
	20	90.21	92.16	93.15	90.37	91.30	97.10
<i>Madhuca longifolia</i> barks	5	70.31	74.90	80.33	86.16	85.78	90.12
	10	75.08	86.59	87.88	87.72	86.88	94.78
	15	78.85	88.90	89.19	89.15	87.22	95.92
	20	84.93	92.03	93.05	94.09	90.78	96.91
<i>Madhuca longifolia</i> fruits	5	72.81	78.90	76.14	74.21	83.89	78.90
	10	75.95	80.16	85.33	76.78	87.28	89.13
	15	78.84	84.56	87.60	82.59	87.99	92.98
	20	93.21	91.89	92.69	90.17	93.89	94.16
<i>Madhuca longifolia</i> seed peels	5	78.90	74.93	80.23	83.78	86.87	89.21
	10	86.98	80.54	85.33	84.98	88.96	90.56
	15	87.98	83.44	86.59	88.98	89.18	92.21
	20	92.62	90.34	94.25	92.09	91.54	94.60

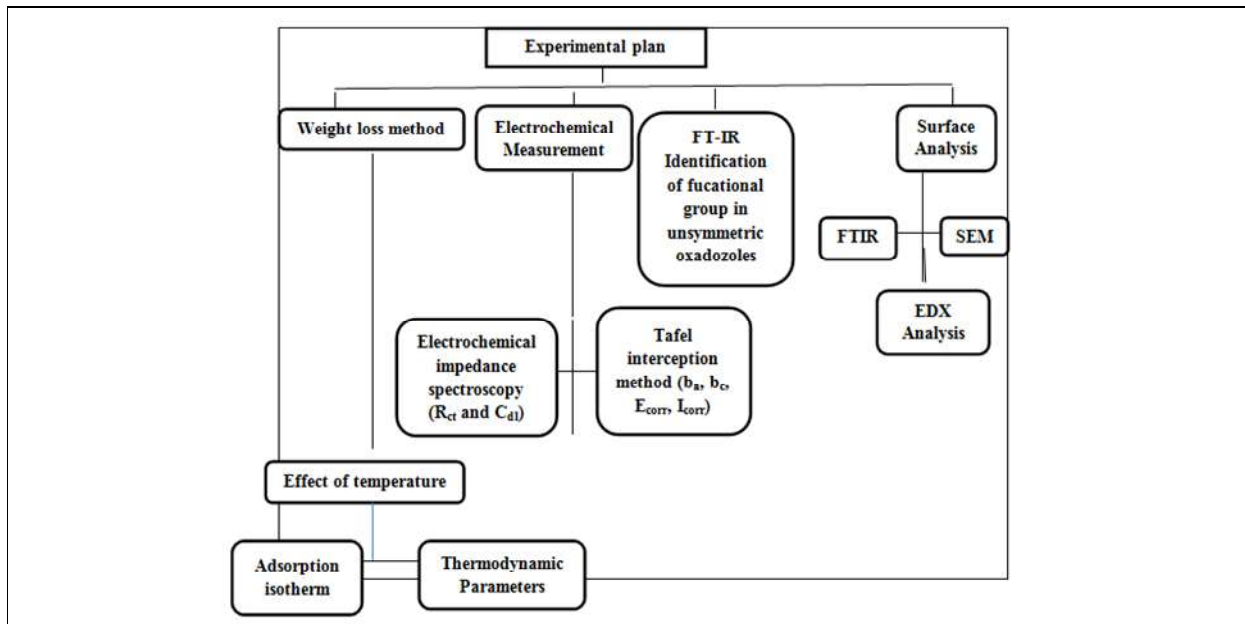
Table 6. IE at various temperatures

Aqueous extract				
Parts of <i>Madhuca longifolia</i> plant	Conc. of the extract (v/v)	IE (%)		
		303K	313K	323K
<i>Madhuca longifolia</i> leaves	Blank	*	*	*
	5	44.10	46.20	60.70
	10	57.60	58.60	74.80
	15	62.20	62.80	82.20
	20	71.10	77.30	86.10
<i>Madhuca longifolia</i> barks	5	47.40	53.10	58.61
	10	51.50	59.40	65.71
	15	56.20	61.60	70.15
	20	64.30	69.15	76.18
<i>Madhuca longifolia</i> fruits	5	44.35	49.85	51.00
	10	48.69	53.97	59.59
	15	54.55	57.60	64.84
	20	59.10	62.10	70.50
<i>Madhuca longifolia</i> seed peels	5	53.84	43.47	34.59
	10	66.43	59.56	46.76
	15	74.40	69.56	57.42
	20	80.41	73.69	60.12





Sivakumar



Work plan

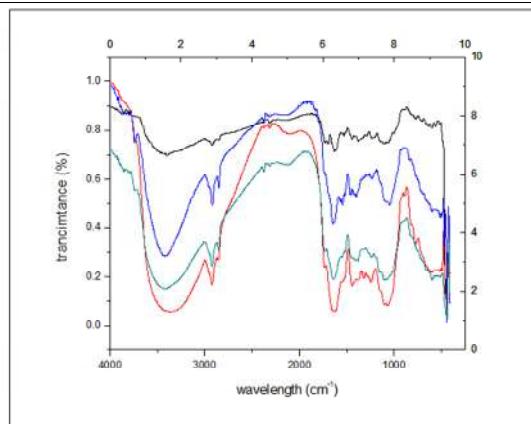
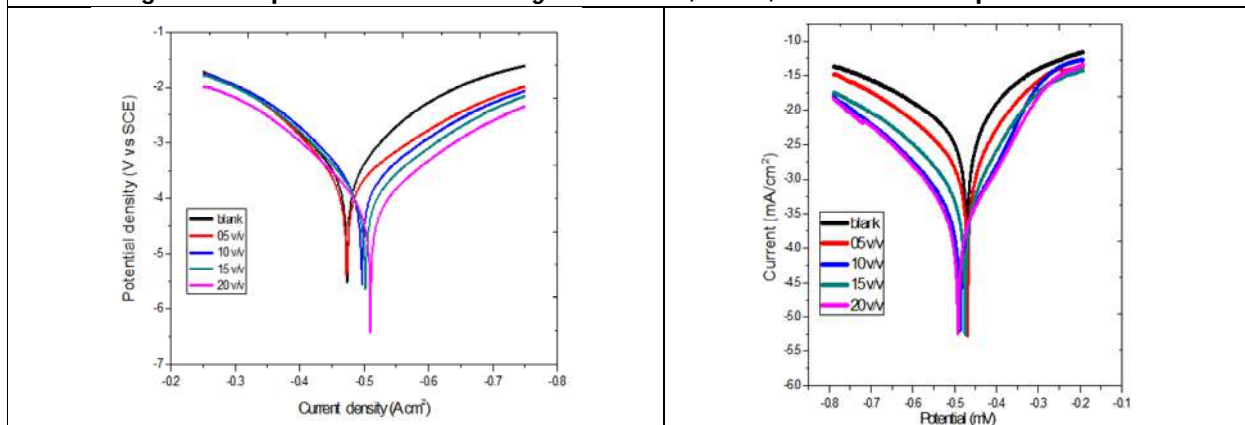


Fig 1. FTIR Spectra of *Madhuca longifolia* leaves, barks, fruits and seeds peels Extracts





Sivakumar

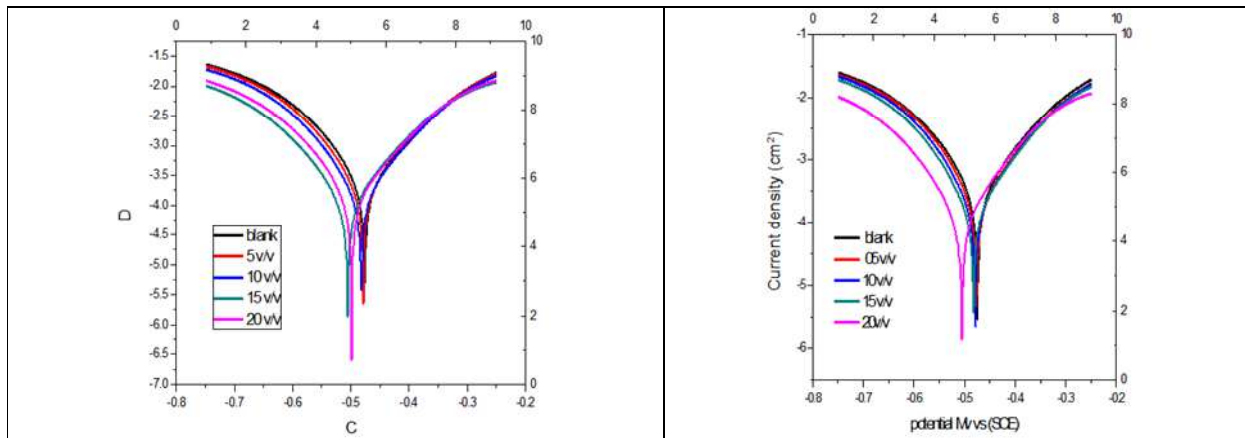


Fig 2. Potentiodynamic polarization (Tafel) curves for mild steel in 1N HCl solution in the absence and presence of different concentration of *Madhuca longifolia* extracts of (a) leaves (b) barks (c) fruits (d) seeds peels

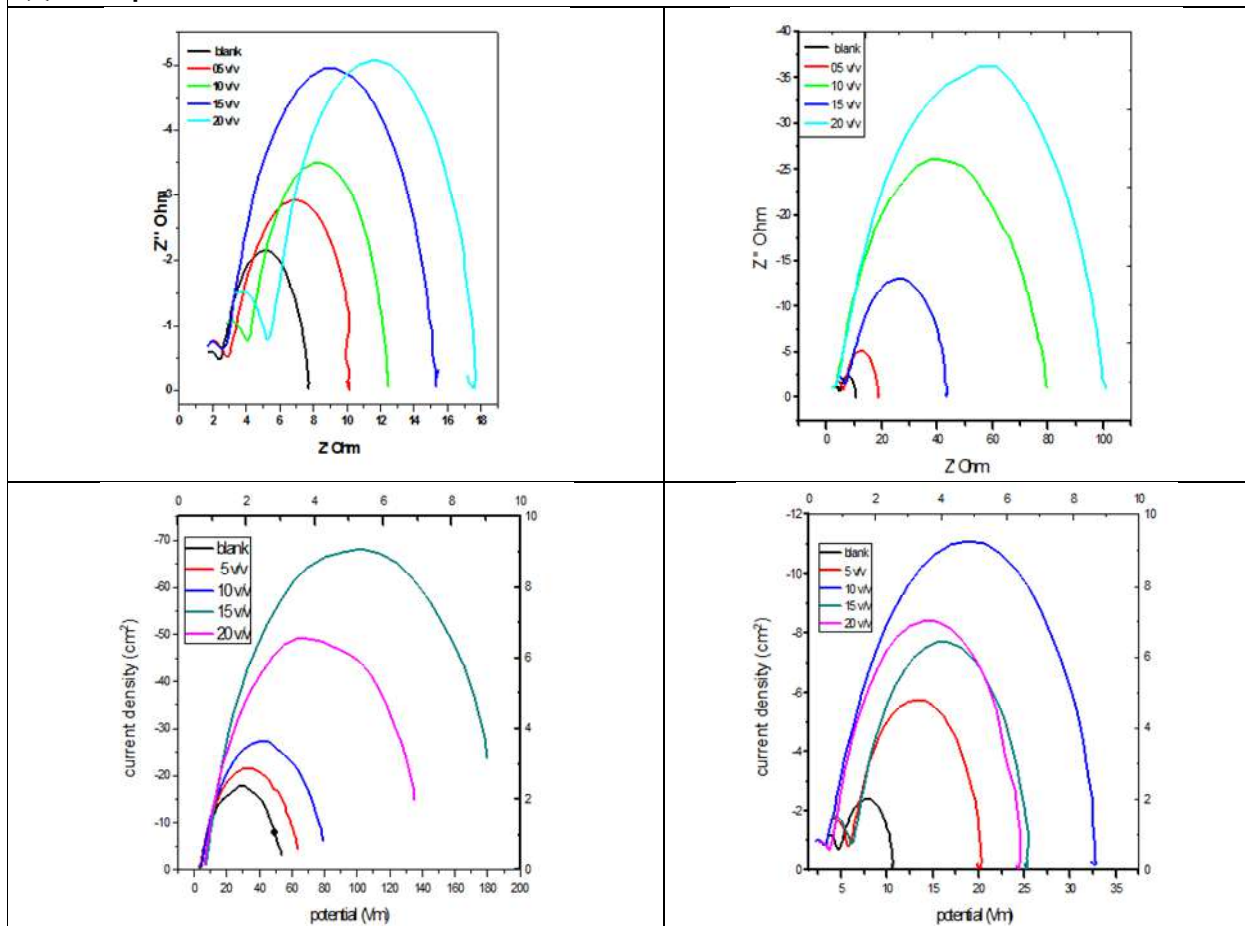


Fig 3. Nyquist plots for mild steel in 1N HCl acid solution without and with presence of different concentration of *Madhuca longifolia* extract of (a) leaves (b) bark (c) fruits (d) seeds.





Sivakumar

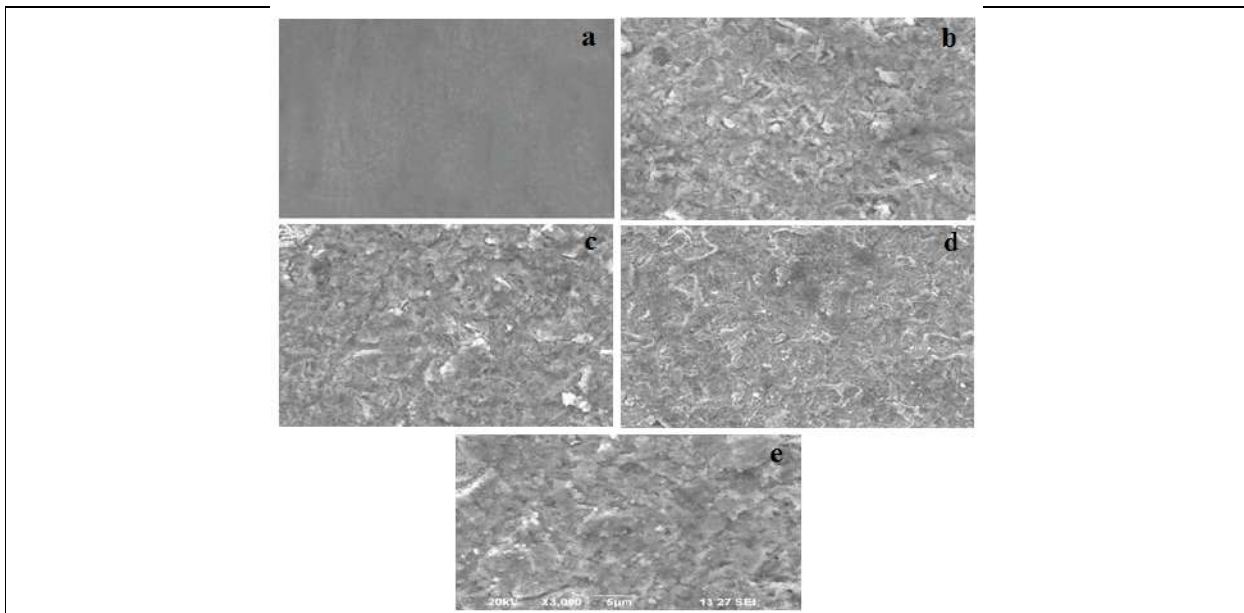


Fig 4. SEM image of the surface of mild steel after immersion for 24 hours in 1N HCl solution (a) blank and in the presence of optimum concentration of the plant extracts from (b) Seeds peels, (c) Leaves, (d) Barks and (e) Fruits.

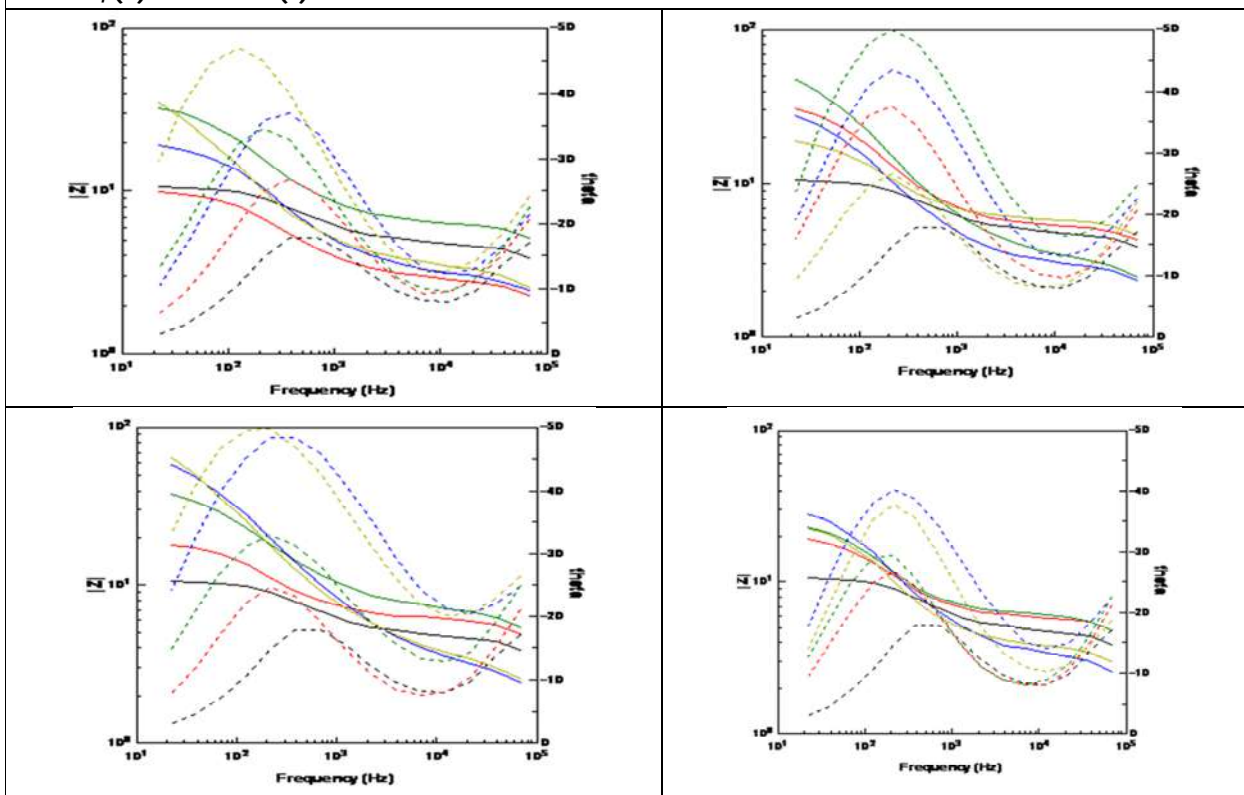


Figure 5 bode plots of mild steel in aqueous solution.





Sivakumar

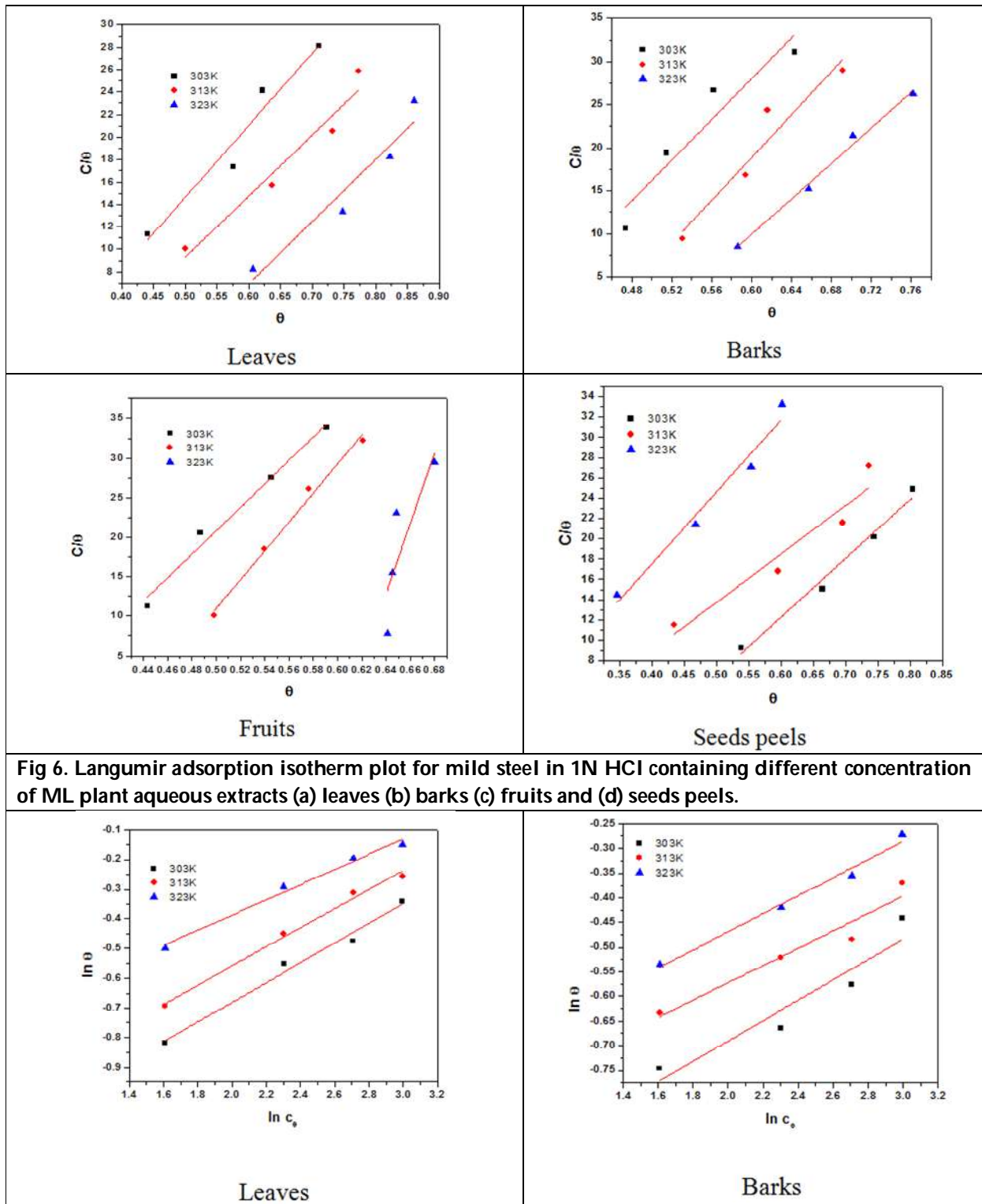


Fig 6. Langumir adsorption isotherm plot for mild steel in 1N HCl containing different concentration of ML plant aqueous extracts (a) leaves (b) barks (c) fruits and (d) seeds peels.





Sivakumar

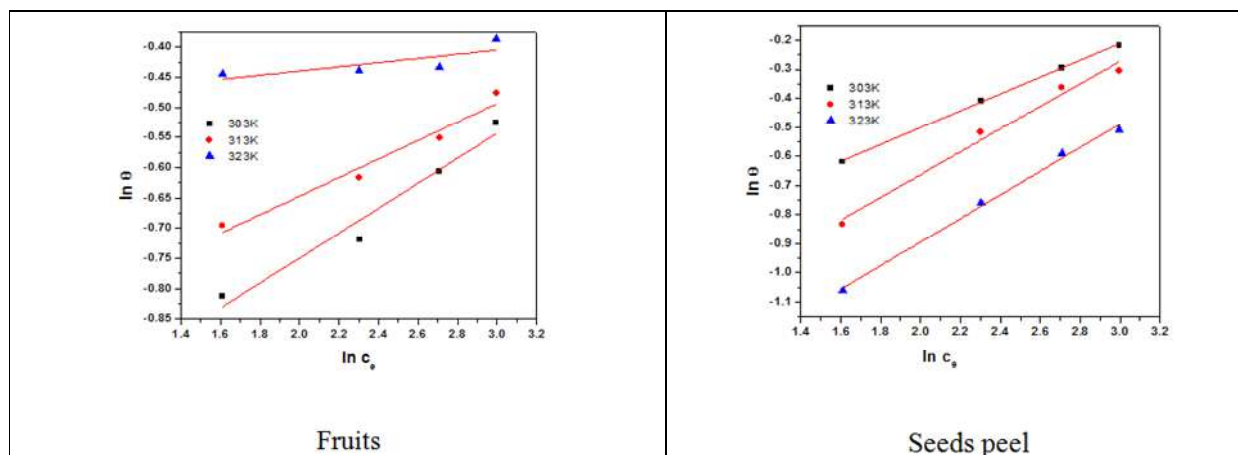


Fig 7. Hasley adsorption isotherm plot for mild steel in 1N HCl containing different concentration of ML plant aqueous extracts (a) leaves (b) barks (c) fruits and (d) seeds peels.

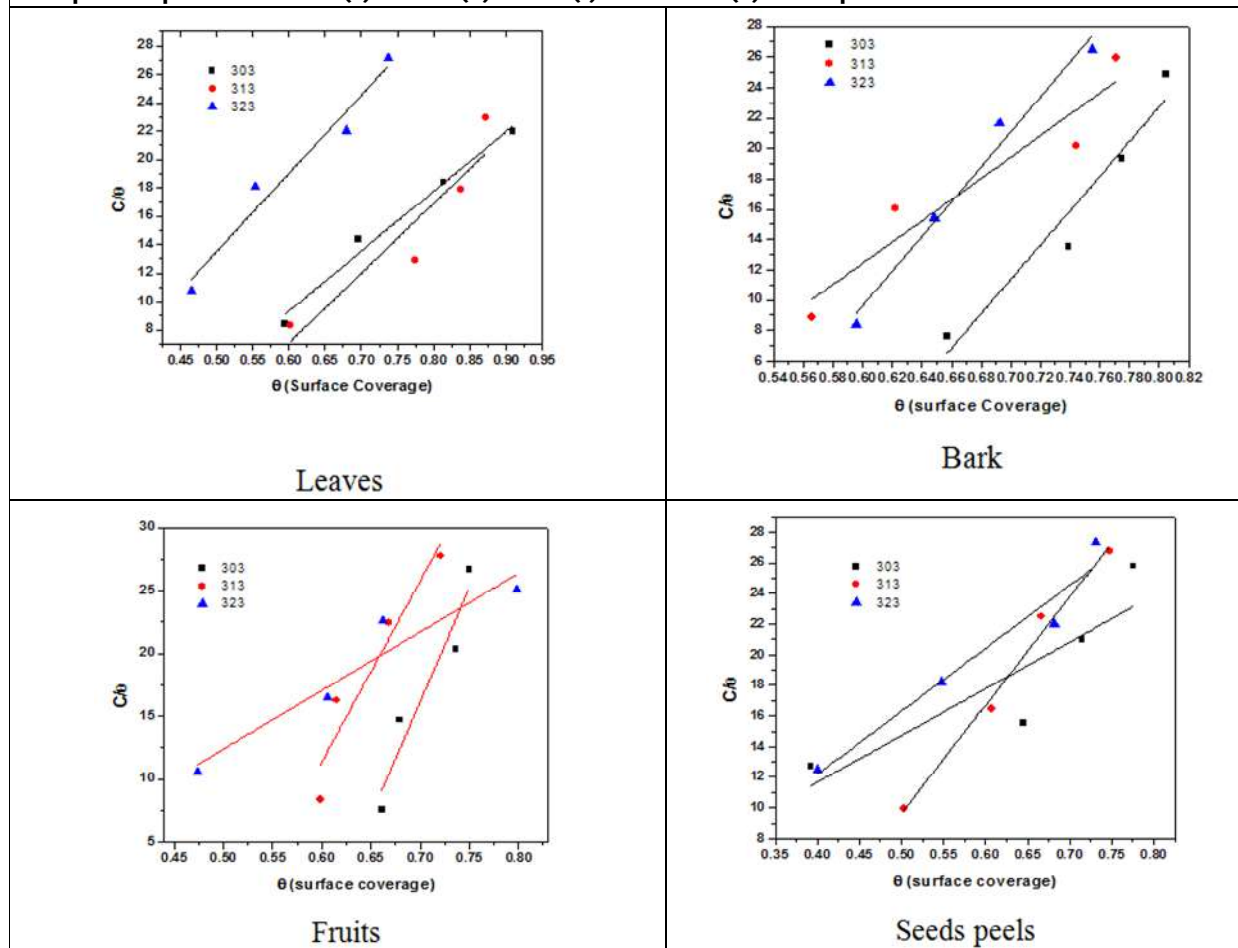


Fig 8. Temkin adsorption isotherm plot for mild steel in 1N HCl containing different concentration of ML plant aqueous extracts (a) leaves (b) barks (c) fruits and (d) seeds peels.



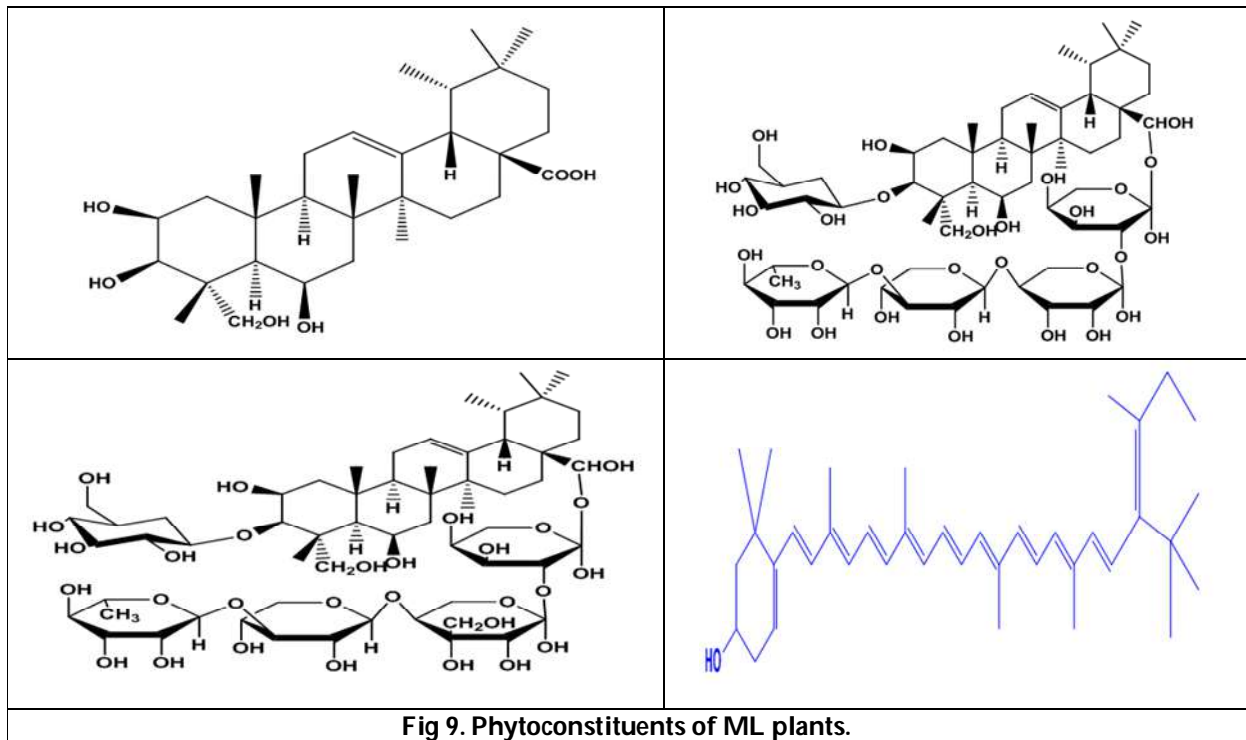


Sivakumar





Sivakumar





An Overview of Scientific Paper Recommendation System

Sivasankari.R¹ and J.Dhilipan^{2*}

¹Research Scholar, Department of Computer Science, SRM Institute of Science and Technology, Ramapuram Campus, Chennai, Tamil Nadu, India.

²Professor and Head, Department of Computer Applications (MCA), SRM Institute of Science and Technology, Ramapuram Campus, Chennai, Tamil Nadu, India.

Received: 10 Nov 2021

Revised: 15 Dec 2021

Accepted: 11 Jan 2022

*Address for Correspondence

J.Dhilipan

Professor and Head,
Department of Computer Applications (MCA),
SRM Institute of Science and Technology,
Ramapuram Campus, Chennai, Tamil Nadu, India.



This is an Open Access Journal / article distributed under the terms of the **Creative Commons Attribution License** (CC BY-NC-ND 3.0) which permits unrestricted use, distribution, and reproduction in any medium, provided the original work is properly cited. All rights reserved.

ABSTRACT

Recommendation systems are gaining attention for their best performance in different areas like research, e-commerce, medical, industry, education and other related fields. The focus of this recommendation system is to suggest items that are more relevant and accurate to the search key. All these methods aim to provide accuracy in retrieving papers that are very similar to the search term. The accuracy of the results are measured based on metrics like PRECISION, RECALL, F- MEASURE, MAP, MRR. The challenges that are related to this recommendation system are also summarized in this survey.

Keywords: Citation graph, bibliography, scientific paper recommendation, information retrieval

INTRODUCTION

Today, the increased activity on the Internet gradually increases the volume of data flooded over the internet. Due to this massive increase in data, it is difficult to search and find the data that is required. To make it possible, there are a number of widely used techniques. One such technique is the Recommendation system, which fetches the data for the needs of the user depending on the input search term. These recommendation systems are now used in a variety of applications, like recommending movies, songs, e-commerce sites, education, medicine, and so on. The main aim of these systems is to provide the user with highly acceptable data. There are four major techniques used by recommendation systems, based on which the system recommends the results for the query. They are content-based systems, collaborative systems, graph-based and hybrid systems. The major task of the recommendation system is to suggest the relevant papers for the users' query. The result should be very accurate in recommending the papers that match the query of the user. The content based system usually retrieves the relevant paper for the user by considering the activity of the user. Here the suggestions for the papers will be





Sivasankari and Dhillipan

based only on the user's activity for a period of time. But in the case of collaborative filtering methods, the recommendation list of papers is generated by comparing the activity of one user with another. The graph-based models compute the recommendation of the paper by constructing the graph network of the citation data. The hybrid system combines two or more of the above methods to recommend the relevant paper for the user query.

The following is the paper's content

It goes over some of the most common approaches utilized in the scientific paper recommendation system. The most often used datasets and metrics in the scientific paper recommendation system. Finally, there are the difficulties that must be overcome when creating these systems. The remaining sections of this work are organized as follows: Section II examines related works. Section III examines the various datasets that are used in the paper recommendation system. The metrics utilized for evaluation are presented in Section IV. The challenges in building the paper recommendation system are listed in Section V, and the conclusion is presented in Section VI.

Related Work

This section covers the most common methods for developing recommendation systems. The four types of methodologies include content-based systems, collaborative filtering, graph-based systems, and hybrid systems. The review papers are grouped and reviewed based on these four types.

Content-based filtering

In content-based filtering techniques, the system tries to choose and recommend items based on features that are of interest to the user. It uses a few similarity metrics to choose the features. The CBF using MN algorithm considers the different features of items along with the importance of calculating the similarity of items to construct a score and recommends the item depending on the score [1]. The Cb-GRS recommendation system is built using three different techniques, where the first technique used in Cb-GRS is CB-GRS Rank, where the ranking of an individual is merged with the group ranking using aggregating techniques [3]. The second technique used is CB-GRS-Match, which matches the individual item with the recommendation of the group to produce the result [4]. The neural probabilistic model is used to build a semantic model for words along with the documents that are cited in them for recommending the citation [6]. This method suffers from a cold start where all the features of the item used for recommendation should be known clearly. This makes it difficult to identify all the features of an item. Bhagavatula et al. proposed a neural model that embeds all the candidate documents into the vector space and computes the score of the K nearest document, then rearranges the score to recommend the top-k documents that match the query document [18].

Collaborative Filtering (CF)

The collaborative filtering system uses similarity measures to recommend an item. The similarity measures can be either based on the user similarity or based on the item similarity. In MATU user model evaluates the large dataset by decomposing it into small units depending on the single rating and multiple ratings, then evaluates the metrics based on coverage or mean absolute error [5]. CCF compares pair wise paper representations obtained from citation context to compute similarities between citing publications. The reasoning behind this similarity estimate is that citing articles are considered comparable if they co-occur with other citing papers [7]. SemCiR evaluates the paper by considering six different types of features and constructing the similarity [8]. For measuring the similarity measure, a genetic algorithm is used to compute the weights [8]. The 2-level paper-citation relation matrix attempts to find papers that have the same citing and cited papers, then it computes the link between them to evaluate the similarities and suggest papers depending on the results [9].

Graph-based Systems

The creation of the graph is the fundamental objective of graph-based recommendation systems. It involves a thorough examination of the nodes and vertices that build up the graph. Yang et al. [13] propose a method of NREP where the node constructs vertices with the author, paper, and venue and connects them with the edges to represent its status. Then a random walk is used to compute the neighbor, and based on the hidden edge, the



**Sivasankari and Dhilipan**

node is ranked by computing the score. Based on the ranking, a recommendation is made. To recommend publications, a hybrid method that combines CBF and CF is used. The candidate paper is compared to the CBF paper of interest by examining its metadata [2]. Then, using the Jaccard coefficient, CF is used to compute the relationship between citing and cited publications. Finally, the outcomes of both approaches are merged to obtain precise findings [2]. The Open Research Knowledge Graph (ORKG) is an architecture created by crowd sourcing data and combining metadata with machine-readable technologies such as LPG, triple store, and SPARQL to create the architecture. Literature comparison and contribution similarity employing automated extraction and linkage of scientific knowledge are the main characteristics here [14]. Trans4E is an embedding model for dealing with challenges that occur when a small number of entities are linked to a large number of entities in one set of relations. This problem makes embedding incredibly hard. To deal with this situation, the usage of quaternion vector space enables the rotation of the head to fit the relation as well as the mapping of the tail [15]

SciKGraph generates a knowledge graph by extracting key concepts from the presented document and other co-occurred documents. The knowledge graph is then formed using the produced clusters, which are grouped according to the topic as concepts and sub concepts [16]. Paper Recommendation based on Heterogeneous Network Embedding (PR-HNE) constructs six different graphs between author, paper, venue, topics and labels, finally to optimize the graph it merges the vertices of all graphs sequentially based on the weights associated with it [17]. BNR built a network model that is represented as an r -dimensional distributed vector. It includes manuscript and author of manuscript links and other entities such as author, venue, and topic. The score is then computed, and a recommendation list is generated based on that score [19]. MMRQ constructs 9 different sub graphs based on key entities paper, author and keyword. A Relevant adjacency Matrix is constructed and the propagation score is computed based on the mutual reinforcement rule. Based on the propagation rule, the papers are recommended to the users [20].

Hybrid recommendation

Hybrid recommendation combines several methods from both content and collaborative filtering methods to recommend the papers. The Citation relation uses the weighted network for citation by taking the count of citing papers and citing the reference paper for determining the strength of the paper [10]. DocCit2Vec uses two steps to recommend citations: the words of the cited documents are represented as a vector space matrix in the first step, and in the second step, all those words are fine tuned by encoding them in cited papers using a pv-dm model [12].

DATASETS

To perform the paper recommendations, the major values used were citations or references that are associated with publications. There are several datasets that provide these citation values that comprise paper Id, title, author name, year of publication, page numbers, etc. The most commonly used datasets for paper recommendation systems are ACL, DPLP, SMT, and WOS. Table I presents the different types of citation datasets used in reviewed works.

ACL /AAN

Steven Bird was the driving force behind the ACL Anthology. Over a four-decade span, it comprises all articles published by ACL and affiliated organisations, as well as the Computational Linguistics magazine [21], [22]. There are presently 18,290 papers in this collection. A paper ID, authors, title, venue, publication year, and abstract are all included in the metadata for each node. Unweighted edges connect papers using their paper IDs [10] in the citation network. The referenced paper information is not included in this dataset, which is a disadvantage. AAN's bibliographical data is given in the format shown in fig 1.

DBLP

The dblp computer science bibliography is a free online database of major computer science journals and proceedings [42]. dblp was founded in 1993 at the University of Trier and now it is managed and developed by Schloss





Sivasankari and Dhilipan

Dagstuhl [34]. Currently, dblp indexes over 4.4 million articles from over 2.2 million authors. In addition, dblp indexes over 40,000 journal volumes, 39,000 conference and workshop proceedings, and over 80,000 monographs. Based on BibTeX.bib syntax, the dblp dataset is organized, which contains metadata such as author, title, journal, volume, number, pages, doi, bibsource, etc. fig 2 describes the syntax of the data stored in the DBLP database.

Elsevier Labs corpus of Science, Technology, and Medicine (STM)

Elsevier presently has around 12 million articles in a wide scope of disciplines. The corpus has 110 articles chosen from those 15,000. They come from 10 spaces that are generally distributed. The corpus gives the XML source to the article, just as different versions of the text, for example, the SimpleText design and the different annotated forms. The default test set is 10 articles from the 110, one for every space [37]. This dataset converts the entire document into the xml format with elements similar to DBLP along with the bibliography references.

WOS dataset

The Web of Science (WOS) is a dataset for document classification. It contains 46,985 documents and these documents are classified into 134 sub-domains or areas of the paper categories with 7 domain categories. It has 3 different variants of the WOS dataset: WOS-11967, WOS-46985, and WOS- 5736. The WOS-11967 dataset contains 11,967 documents with 7 major domains and 135 sub-domains. The WOS-46985 dataset contains 46,985 documents with 7 major domains and 134 sub-domains. The WOS-5736 dataset contains 5,736 documents with 3 major domains and 11 sub-domains.

Evaluation Criteria

To evaluate the recommendation system, we must compare the recommendation system's best papers with the actual papers that must be retrieved. To evaluate the performance of the recommendation system, the major metrics used were PRECISION, RECALL, F-MEASURE, MAP, and MRR. The system's results are categorised into four kinds based on these data, such as TP, TN, FP, and FN [33]. Table II presents the different metrics used to evaluate the scientific paper recommendation systems that are reviewed in this work.

- The papers that are relevant and retrieved by the recommendation system are known as true positives (TP).
- The term "false positive" (FP) refers to papers that are irrelevant yet are retrieved by the recommendation system.
- The papers classified as false negatives (FN) are those that are relevant but are not found by the recommendation system.
- The papers that are true negatives (TN) are those that aren't relevant and aren't found by the recommendation algorithm.

To assess the recommendation system based on the decisions, metrics such as accuracy, recall, and F-measures are considered. These criteria are used to make choices about which publications are closely linked and which ones should be avoided. These indicators often take the full dataset into account. It also allows users to rate the list's top-N items. The metrics such as MAP and MRR are used when the evaluation is based on a list of ranks. Instead of simply evaluating the metrics as good or bad, these ranking-based metrics evaluate them by combining their precision and recall with the top relevant ranked papers.

PRECISION

Precision is defined as the proportion of true positive recommendations received versus the total number of recommendations retrieved [33]. It is used to predict the percentage of correct papers recommended by the system out of the total number of papers that match the query. If the value of precision is high, then it tries to minimize the value of false positives. The equation 1 provides the definition of precision.

$$Precision = \frac{TP}{TP + FN} \quad (1)$$





RECALL

The percentage of true positive recommendations received compared to the total number of actual positive recommendations is defined as recall [33]. It is used to predict the percentage of correct papers recommended by the system from the correct papers in the database that match the query exactly. If the value of recall is high, then it tries to minimize the value of false negatives. The equation 2 is used to calculate the recall [41].

$$\text{Recall} = \frac{TP}{TP + FP} \quad (2)$$

F-MEASURE

To evaluate the system more accurately, precision and recall can be combined together, providing the chance of minimizing both false negatives and false positives. This process is done by the F-measures calculations as shown in the equation 3.

$$\text{F MEASURE} = \frac{2(\text{precision} * \text{recall})}{\text{Precision} + \text{recall}} \quad (3)$$

MRR

Mean reciprocal rank is the easiest metric that simply considers the first appearance of the related paper among the top-k results for each query. The reciprocal rank is the “multiplicative inverse” of the rank of the first occurrence of the correct paper. The mean value of each query is added together to compute the final query results. In the equation 4 Q is the total number of queries and R is the rank [41].

$$\text{MRR} = \frac{1}{Q} \sum_{i=1}^n \frac{1}{R_i} \quad (4)$$

MAP

Mean average precision computes the precision and recall of the paper for every position of the ranked list of recommended papers. It computes the average precision of the list for every rank separately and thereby computes the final mean average of the list [39]. The first step in computing the mean average precision requires the computation of average precision with the equation 5 presented. From equation 5, i represents rank in the list, n is the number of retrieved documents from the database, and rel(i) is an indicator function, that is set as 1 if the result is relevant [40], else it is 0. The second step in computing the mean average precision [43] is to find the mean of all the computed average precisions as shown in equation 6, where K represents the number of queries [43].

$$\text{Average precision (AP)} = \frac{\sum_{i=1}^n \text{precision}(i) * \text{rel}(i)}{\text{No.of.relevant documents}} \quad (5)$$

$$\text{MAP} = \frac{\sum_{i=1}^K \text{AP}(i)}{K} \quad (6)$$

Challenges in Recommendation Systems

This section discusses the primary challenges that are involved in designing recommendation systems. In spite of the advantages it has, it does have a few limitations like coldstart, sparsity, scalability, privacy, serendipity, gray sheep and unified data standards.

Cold start

When a new user logs into a system for the first time, much of the user's data is unavailable. This information is used by the recommendation systems to suggest a list of similar papers. Techniques like content-filtering and collaborative



**Sivasankari and Dhilipan**

filtering systems may not be able to work correctly due to the lack of such information. However, this issue does not last long, All of the necessary information will be gathered progressively over time. In a few systems, this issue may also be avoided by obtaining the required information directly from the user when they sign in. Even so, this is only useful for content-based filtering techniques.

Sparsity

It happens when there is a huge dataset with very little information to analyze. It's frequent in collaborative recommendation systems if the number of users is modest in comparison to the quantity of items to be reviewed. It's also due to a vast number of people providing a small minority of reviews or ranks. It is impossible to obtain accurate results in such cases due to the lack of information.

Privacy

Content-based filtering, for example, exploits the user's data to find related results. This data provided by the user may be susceptible to third-party acquisition and exploitation by third parties. As a result, privacy is always a concern in recommendation systems. This is a major issue with recommendation systems that needs to be addressed.

Scalability

Because of the increased usage of the internet on a daily basis, related activity has increased, promoting constant change in the systems. A daily growth in the number of new users to the system, or a change in the user's thoughts regarding the rating and interest in a topic, are examples of these changes. All of these changes must be monitored and updated on a regular basis in order for the system to function properly. The ability of a system to adapt to constant change is referred to as scalability.

Gray Sheep

Another most common problem that degrades the proper functionality of the recommendations systems is the gray sheep problem. This is caused because of the unresponsiveness of the user by providing fake data to the system. The fake data provided by the user is considered by the system for evaluation which thereby reduces the proper functionality of the system.

CONCLUSION

The approaches utilized in paper recommendation systems are discussed in this work, which are reviewed based on the techniques. The paper focused on content-based strategies, collaborative filtering, graph-based systems, and some hybrid methods for reviewing and categorizing works. Different types of data sets were analyzed to determine their format in order to deploy these systems. The list of metrics that was described can be used to evaluate the implemented systems. Finally, a list of challenges that may arise throughout the design of the system has been summarized.

REFERENCES

1. Yilena Pérez-Almaguer, Raciél Yera, Ahmad A. Alzahrani, Luis Martínez, Content-based group recommender systems: A general taxonomy and further improvements, Expert Systems with Applications, Volume 184, 2021, 115444, ISSN 0957-4174, <https://doi.org/10.1016/j.eswa.2021.115444>.
2. N. Sakib et al., "A Hybrid Personalized Scientific Paper Recommendation Approach Integrating Public Contextual Metadata," in IEEE Access, vol. 9, pp. 83080-83091, 2021, doi: 10.1109/AC-CESS.2021.3086964.
3. T. De Pessemier, J. Dhondt, K. Vanhecke, L. Martens, Travel with friends: a hybrid group recommender system for travel destinations, Workshop on tourism recommender systems (tourRS15) in conjunction with the 9th ACM





Sivasankari and Dhillipan

- conference on recommender systems (recsys 2015) (2015), pp. 51-60.
4. Kagita V.R., Pujari A.K., Padmanabhan V. Group Recommender Systems: A Virtual User Approach Based on Precedence Mining. In: Cranefield S., Nayak A. (eds) AI 2013: Advances in Artificial Intelligence. AI 2013. Lecture Notes in Computer Science, vol 8272. Springer, Cham.
 5. Manouselis, N., Karagiannidis, C., Sampson, D. 2014. Layered Evaluation in Recommender Systems: A Retrospective Assessment. Journal of e-Learning and Knowledge Society, volume 10 issue 1. Italian e-Learning Association.
 6. Huang, W., Wu, Z., Liang, C., Mitra, P., Giles, C. (2015). "A Neural Probabilistic Model for Context Based Citation Recommendation, Proceedings of the AAAI Conference on Artificial Intelligence, 29(1).
 7. H. Liu, X. Kong, X. Bai, W. Wang, T. M. Bekele and F. Xia, "Context-Based Collaborative Filtering for Citation Recommendation," in IEEE Access, vol. 3, pp. 1695-1703, 2015, doi: 10.1109/ACCESS.2015.2481320.
 8. Zarrinkalam, F. and Kahani, M. (2013), "SemCiR: A citation recommendation system based on a novel semantic distance measure", Program: electronic library and information systems, Vol. 47 No. 1, pp. 92-112.
 9. N. Sakib, R. B. Ahmad and K. Haruna, "A Collaborative Approach Toward Scientific Paper Recommendation Using Citation Context," in IEEE Access, vol. 8, pp. 51246-51255, 2020, doi: 10.1109/ACCESS.2020.2980589.
 10. W. Tanner, E. Akbas and M. Hasan, "Paper Recommendation Based on Citation Relation," 2019 IEEE International Conference on Big Data (Big Data), 2019, pp. 3053-3059, doi: 10.1109/Big-Data47090.2019.9006200.
 11. Daniel Duma and, Ewan Klein, "Citation Resolution: A method for evaluating context-based citation recommendation systems", Proceedings of the 52nd Annual Meeting of the Association for Computational Linguistics, 2014, Volume 2, pp. 358-365 doi = 10.3115/v1/P14-2059.
 12. Y. Zhang and Q. Ma, "DocCit2Vec: Citation Recommendation via Embedding of Content and Structural Contexts," in IEEE Access, vol. 8, pp. 115865-115875, 2020, doi: 10.1109/ACCESS.2020.3004599
 13. L. Yang, Z. Zhang, X. Cai and L. Guo, "Citation Recommendation as Edge Prediction in Heterogeneous Bibliographic Network: A Network Representation Approach," in IEEE Access, vol. 7, pp. 23232-23239, 2019, doi: 10.1109/ACCESS.2019.2899907.
 14. Jaradeh, M. Y., A. Oelen, K. Farfar, Manuel Prinz, Jennifer D'Souza, G. Kismihók, M. Stocker and S. Auer. "Open Research Knowledge Graph: Next Generation Infrastructure for Semantic Scholarly Knowledge." Proceedings of the 10th International Conference on Knowledge Capture (2019): New York, NY, USA, 243–246.
 15. Mojtaba Nayyeri, Gokce Muge Cil, Sahar Vahdati, Francesco Osborne, Mahfuzur Rahman, Simone Angioni, Angelo Salatino, Diego Reforgiato Recupero, Nadezhda Vassilyeva, Enrico Motta, Jens Lehmann, "Trans4E: Link prediction on scholarly knowledge graphs", Neuro-computing, 2021, ISSN 0925-2312,
 16. Mauro Dalle Lucca Tosi, Julio Cesar dos Reis, "SciKGraph: A knowledge graph approach to structure a scientific field", Journal of Informetrics, Volume 15, Issue 1, 2021, 101109, ISSN 1751-1577,
 17. Zafar Ali, Guilin Qi, Khan Muhammad, Bahadar Ali, Waheed Ahmed Abro, Paper recommendation based on heterogeneous network embedding, Knowledge-Based Systems, Volume 210, 2020, 106438, ISSN 0950-7051.
 18. Bhagavatula C., Feldman S., Power R., Ammar W., Content-based citation recommendation, Proceedings of the 2018 Conference of the North American Chapter of the Association for Computational Linguistics: Human Language Technologies, Volume 1 (Long Papers), Association for Computational Linguistics, New Orleans, Louisiana (2018), pp. 238-251.
 19. X. Cai, Y. Zheng, L. Yang, T. Dai and L. Guo, "Bibliographic Network Representation Based Personalized Citation Recommendation," in IEEE Access, vol. 7, pp. 457-467, 2019, doi: 10.1109/ACCESS.2018.2885507
 20. Mu, D., Guo, L., Cai, X., and Hao, F. (2018). Query-Focused Personalized Citation Recommendation With Mutually Reinforced Ranking. IEEE Access, vol.6, pp.3107-3119, 2018.
 21. Radev, Dragomir R, Muthukrishnan, Pradeep, Qazvinian, Vahed, "The ACL Anthology Network", Proceedings of the 2009 Workshop on Text and Citation Analysis for Scholarly Digital Libraries (NLP4DL), Aug 2009,
 22. Radev, D.R., Muthukrishnan, P., Qazvinian, V. et al. The ACL anthology network corpus. Lang Resources and Evaluation 47, pp. 919–944 (2013).
 23. Jie Tang, Jing Zhang, Limin Yao, Juanzi Li, Li Zhang, and Zhong Su. ArnetMiner: Extraction and Mining of Academic Social Networks. In Proceedings of the Fourteenth ACM SIGKDD International Conference on





Sivasankari and Dhilipan

- Knowledge Discovery and Data Mining (SIGKDD'2008). pp.990- 998.
24. Jie Tang, Limin Yao, Duo Zhang, and Jing Zhang. A Combination Approach to Web User Profiling. ACM Transactions on Knowledge Discovery from Data (TKDD), (vol. 5 no. 1), Article 2 (December 2010), 44 pages.
 25. Jie Tang, A.C.M. Fong, Bo Wang, and Jing Zhang. A Unified Probabilistic Framework for Name Disambiguation in Digital Library. IEEE Transaction on Knowledge and Data Engineering (TKDE) , Volume24, Issue 6, 2012, Pages 975-987.
 26. Jie Tang, Jing Zhang, Ruoming Jin, Zi Yang, Keke Cai, Li Zhang, and Zhong Su. Topic Level Expertise Search over Heterogeneous Networks. Machine Learning Journal, Volume 82, Issue 2 (2011), Pages 211-237.
 27. Jie Tang, Duo Zhang, and Limin Yao. Social Network Extraction of Academic Researchers. In Proceedings of 2007 IEEE International Conference on Data Mining (ICDM'2007). pp. 292-301.
 28. Arnab Sinha, Zhihong Shen, Yang Song, Hao Ma, Darrin Eide, Bo- June (Paul) Hsu, and Kuansan Wang. 2015. An Overview of Microsoft Academic Service (MAS) and Applications. In Proceedings of the 24th International Conference on World Wide Web (WWW '15 Companion). ACM, New York, NY, USA, 243-246
 29. Jérôme Kunegis. KONECT – The Koblenz Network Collection. In Proc. Int. Conf. on World Wide Web Companion, pages 1343–1350, 2013.
 30. Michael Ley. The DBLP computer science bibliography: Evolution, research issues, perspectives. In Proc. Int. Symposium on String Process. and Inf. Retr., pages 1–10, 2002.
 31. Jérôme Kunegis WWW '13 Companion: Proceedings of the 22nd International Conference on World Wide Web May 2013 Pages 1343–1350 <https://doi.org/10.1145/2487788.2488173>
 32. Kowsari, Kamran; Brown, Donald; Heidarysafa, Mojtaba ; Jafari Meimandi, Kiana ; Gerber, Matthew; Barnes, Laura (2018), "Web of Science Dataset", Mendeley Data, V6, doi: 10.17632/9rw3vkcfy4.6
 33. A Gunawardana, G Shani, A Survey of Accuracy Evaluation Metrics of Recommendation Tasks, Journal of Machine Learning Research ,2009,vol.10 ,pages 2935-2962.
 34. The dblp computer science bibliography, accessed on 2021-10-11
 35. Citation Network Dataset: DBLP+Citation, ACM Citation network, accessed on 2021-10-11
 36. ACL anchology accessed on 2021-10-11 ; [https://aclanthology.org/;](https://aclanthology.org/)
 37. rdaniel Ron Daniel Jr, sujitpal Sujit Pal, Andrew Epstein, Corpus of Open Access articles from multiple fields in Science, Technology, and Medicine, accessed on 2021-10-11
 38. Kamran Kowsari, Mojtaba Heidarysafa, Kiana Jafari Meimandi, Kamy Kowsari HDL Tex, Hierarchical Deep Learning for Text Classification, accessed on 2021-10-11.
 39. Zafar Ali, Pavlos Kefalas, Khan Muhammad, Bahadar Ali, Muhammad Imran, Deep learning in citation recommendation models survey, Expert Systems with Applications, Volume 162, 2020, 113790, ISSN 0957-4174.
 40. Zhu, Xiao-Dan, Peter D. Turney, Daniel Lemire and Andre´ Vellino. "Measuring academic influence: Not all citations are equal." Journal of the Association for Information Science and Technology 66 (2015).
 41. D. Mu, L. Guo, X. Cai and F. Hao, "Query-Focused Personal- ized Citation Recommendation With Mutually Reinforced Ranking," in IEEE Access, vol. 6, pp. 3107-3119, 2018, doi: 10.1109/AC- CESS.2017.2787179.
 42. Jose Mar´ia Alvarez-Rodr´iguez, Jose Emilio Labra-Gayo, Patricia Ordoñez de Pablos, New trends on e-Procurement applying seman- tic technologies: Current status and future challenges, Computers in Industry, Volume 65, Issue 5, 2014, Pages 800-820, ISSN 0166-3615, "HybridCite: A Hybrid Model for Context Aware Citation Recommendation.
 43. Färber, Michael and Sampath, Ashwath, Hybrid Cite: A Hybrid Model for Context-Aware Citation Recommendation, JCDL '20: Proceedings of the ACM/IEEE Joint Conference on Digital Libraries in 2020 , Pages 117–126.





Sivasankari and Dhilipan

Table I. Types of Citation Datasets

S.No	Source	Dataset						
		DBPL	ACL/ANN	STM	PUBMED	Open Corpus	WOS	Other Corpus
1	[6]							CiteSeer
2	[7]							HEP-PH and HEP-TH
3	[10]	✓	✓					
4	[11]		✓					
5	[12]	✓	✓					
6	[13]	✓	✓					
7	[14]			✓				
8	[15]							MAG
9	[16]						✓	
10	[17]	✓	✓					
11	[18]	✓			✓	✓		
12	[19]	✓	✓					
13	[20]		✓					

Table II Common Evaluation Metrics

S.No	Source	Precision	Recall	f-measure	MAP	MRR
1	[2]	✓	✓	✓	✓	✓
2	[6]		✓		✓	✓
3	[7]	✓	✓	✓		
4	[8]		✓			
5	[9]	✓	✓	✓		
6	[10]		✓		✓	✓
7	[12]			✓		
8	[13]		✓		✓	
9	[15]					✓
10	[17]		✓		✓	✓
11	[18]			✓		✓
12	[19]		✓		✓	✓
13	[20]		✓			

<p>An overview of Scientific Paper recommendation system</p> <p>Sivasankari R (Dhilipan J)</p> <p>Recommendation systems are gaining attention for their best performance in different areas like research, e-commerce, medical, industry, education and other related fields. The focus of this recommendation system is to suggest the items that are more relevant and accurate to the search key. All these methods aim to provide accuracy in retrieving papers that are very similar to the search term. The accuracy of the results are measured based on metrics like PRECISION, RECALL, F-MEASURE, MAP, MRR. The challenges that are related to this recommendation system are also summarized in this survey.</p>	<pre>@inproceedings{xxxx-2020-xxxx, title = "An overview of Scientific Paper recommendation system", author = "Sivasankari and R. Dhilipan and J.", book title = "Proceedings of the 1st Conference of the XYZ Chapter of the xyz", month = dec, year = "2020", address = "state, Country", publisher = "publisher name", url = "https://aclanthology.org/2020.zzzz", pages = "44-53". } Recommendation systems are gaining attention for their best performance in different areas like research, e-commerce, medical, industry, education and other related fields. The focus of this recommendation system is to suggest the items that are more relevant and accurate to the search key. All these methods aim to provide accuracy in retrieving paper....."</pre>
Fig. 1. AAN Dataset format	<p>Sivasankari R:</p> <p>An overview of Scientific Paper recommendation system.xxxxx 2(2): 1493-1500 (2009)</p> <pre>@article{DBLP:journals/pvldb/sivasankariR, author = {sivasankariR}, title = {An overview of Scientific Paper recommendation system}, journal = {xxxxxx}, volume = {2}, number = {2}, pages = {1493-1500}, year = {2009}, url = {http://www.yldb.org/pvldb/vol2/qqqqqq.pdf}, doi = {10.14778/1687553.16234567}, timestamp = {Sat, 25 Apr 2020 13:58:47 +0200}, biburl = {https://dblp.org/rec/journals/pvldb/Ley09.bib}, bibsource = {dblp computer science bibliography, https://dblp.org}</pre>
	Fig. 2. DBPL Dataset format





Neural Network Based Identification of Facial Abnormalities through Cephalometric Radiography using Ricketts Analysis

S.Anbahagan^{1*} and S. Samundeswari²

¹Associate Professor, Department of Electrical Engineering, Faculty of Engineering and Technology, Annamalai University, Annamalai Nagar, Tamil Nadu, India 608002

²Associate Professor, Department of Computer Science and Engineering, Sri Sairam Engineering College, Chennai, Tamil Nadu, India 600044.

Received: 01 Nov 2021

Revised: 30 Dec 2021

Accepted: 21 Jan 2022

*Address for Correspondence

S.Anbahagan

Associate Professor,
Department of Electrical Engineering,
Faculty of Engineering and Technology,
Annamalai University, Annamalai Nagar,
Tamil Nadu, India 608002.
Email: s.anbahagan@gmx.com



This is an Open Access Journal / article distributed under the terms of the **Creative Commons Attribution License** (CC BY-NC-ND 3.0) which permits unrestricted use, distribution, and reproduction in any medium, provided the original work is properly cited. All rights reserved.

ABSTRACT

Cervical skeletal and dental connections are analysed using cephalometrics (head measurements). Cephalometric analysis relies on cephalometric radiography to study the relationships between bony and soft tissue landmarks and can be used to diagnose facial growth abnormalities prior to treatment, during treatment to evaluate progress or at the end of treatment to ensure that the treatment objectives have been met. Using Ricketts analysis, patients may be classified. In this study, classifiers based on back propagation neural networks (BPNN) and generalized regression neural networks (GRNN) are utilized to diagnose Cephalometric analyses. The data for this study was gathered from Raja Muthiah Dental College & Hospital (RMDC&H), Faculty of Dentistry, Annamalai University, Anna malai Nagar, Cuddalore District, Tamilnadu, India. This study gathered the case data of 304 patients (109 Male, 195 Female). All of the gathered clinical data are used for classification. Patient data were split for four fold in cross validation for training and testing the suggested models. BPNN outperformed the GRNN model by 94%, based on Ricketts analysis. The BPNN technique is viable and has been demonstrated to be 94% accurate in detecting patients. As a result, the BPNN model is capable of recreating the desired output values with minimal errors.

Keywords: Cephalometric analysis, Back propagation neural network, Generalized regression neural network, Ricketts Analysis”



**Anbahagan and Samundeswari****INTRODUCTION**

Cephalometrics depicts the cranium's skeletal structure in order to track a child's growth through time. This examination may also reveal jaw-position anomalies. A computerized study that compares and measures the anatomy, can be provided to help with the treatment strategy.

As a cornerstone of complete orthodontic diagnosis, cephalometrics has emerged. Treatment planning and patient follow-up are made easier with this handy tool for patients undergoing orthodontic treatment.

- With the use of cephalometrics, orthodontic diagnosis becomes easier with the better knowledge of the craniofacial region's skeletal, dental, and soft tissue features.
- It aids in the categorization of skeletal and dental anomalies as well as the identification of one's facial type.
- Treatment of the patient can be planned with the use of cephalometrics.
- Cephalometrics aids in the prediction of growth-related and surgical treatment-related alterations.

Cephalometric analysis examines the link between the teeth and the skeleton in the human skull. Dentists, especially orthodontists, commonly utilize it as a treatment planning tool [1].

Researchers in academia have developed artificial neural networks (ANNs) by using mathematical formulations to simulate nervous system activities. The approaches that have been developed as a consequence have found use in a wide range of practical situations. An important decision-making tool in the diagnosis of diseases is classification. Unfortunately, despite the existence of several categorization algorithms, when confronted with statistical outliers or groupings that overlap, many of them fall flat on their face. ANNs are artificial neural network classification approaches that have been proposed. [2]. The use of computers in the workplace has never been more innovative than it is with neural networks (NN). Data patterns and correlations may be discovered using a NN. The data may be derived from market research, a manufacturing process with shifting operating circumstances, or from medical and dental diagnostics to identify illness. Using a NN, regardless of the specifics, is fundamentally different from the traditional approaches. Much of this improvement has been made possible by the invention of NN learning rules, which are algorithms for finding patterns in data. Because of these principles, the network is capable of learning from readily available data and using that information toward assisting a doctor in making vital judgments. [3].

For computer applications in the field of cephalometric analysis, an expert system should be established. In order to build computers that can identify skeletal and dental problems, a preliminary study utilizing neural networks based on back propagation and generalized regression is required. Using Cephalometric analysis, the dental and skeletal structures of the skull are analyzed. Cephalometric radiography is used to study about the relationship between bone and soft tissue markers and helps the cephalometric analysis to determine if treatment goals have been met by identifying facial growth abnormalities before, during, or after the treatment process has begun to assess treatment progress. Cephalometric analysis is not well-trained, and there is no one to help the doctor. The computer is becoming an increasingly important tool in Cephalometric study. The calibration of the cephalogram is an essential stage in the development of computers for the identification of skeletal and dental anomalies. Rest of paper is organized as follows: a literature study in section 2 provides an evaluation of the proposed project's value Section 3 discusses the procedures and methods used to identify skeletal and dental anomalies. Section 4 presents the research's numerous findings. Lastly, in Section 5, the findings and recommendations for further study are presented.

LITERATURE REVIEW

An overview of literature on illness diagnosis, Cephalometric analysis, and automated ANNs in Cephalometric analysis can be found here.



**Anbahagan and Samundeswari****Studies on diagnosis of diseases**

There are increasing numbers of real-world challenges to which NNs are being used. These new technologies have a distinct benefit in being able to handle issues that have no algorithmic solution or for which there is none that can be described due to the complexities involved. This method relies on the computer following a set of instructions to find a solution. Unless the computer is given explicit instructions, it will fail to solve the problem. Conventional computers can only solve issues we understand and know how to solve, which limits their usefulness for new challenges. When it comes to issues that people can solve well, NNs excel where computers fail. It's necessary to recognize trends in data while dealing with pattern identification and forecasting challenges. The NN can provide the intended output or data that is the closest to it even with erroneous inputs. Given the wide range of effective applications of NNs, this study is based on an evaluation of their data retrieval performance [4].

Preventing and diagnosing disease is the primary goal of medical science. Brause pointed out in 2001 that learning to diagnose is a major challenge for nearly all medical students and residents [5]. Here, they must tackle the challenge of determining the existence of certain diseases or developing a treatment plan based on observations and information that are more or less specific [6]. The following is a summary of some of the challenges in medical diagnosis that must be considered. Good diagnoses can only be made after a physician has worked for a while, and hence they are not available at the end of a formal academic training degree. When it comes to uncommon or novel illnesses, this is especially true. The situation for physicians is no different from that of immigrants. Humans are more like pattern recognition systems than statistic computers. Humans are great at recognizing patterns and things, but they struggle when it comes to assigning probability to their findings [7]. An accurate diagnosis is dependent on the skill and expertise of the physician making it. The doctor's performance suffers as a result of emotional issues as well as exhaustion. Doctors, especially particularly specialists, undergo a lengthy and expensive educational process. As a result, even nations with sophisticated economies may be affected by the shortage of MDs. The area of medicine is one of the most dynamic and ever-evolving in all of science. Old treatments are being disqualified by fresh findings, while new cures and medications are being developed all the time. Even previously undiagnosed illnesses pop up from time to time. As a result, a doctor must make an effort to stay current [5-7].

How can computers assist in medical diagnostics in light of the issues listed above and several others? Computers have been frequently used in the medical field since the 1970s. Data bases for patients and medicines, emergency networks, and digital archives have all benefited from the use of computers in the medical field. A totally autonomous computer-based medical diagnosis system is not likely in the near future even though this is true. Even Nevertheless, recent advancements in the AI area are paving the way for a greater use of computers equipped with AI approaches in that application in the future. There are several advantages to computers, including the fact that they never go out of date or grow boring, can be easily updated in a matter of seconds, and are both affordable and easy to distribute. If an intelligent diagnosis system can narrow down the number of people who attend a clinic who aren't sick or at least have a minor condition, doctors will have more time to deal with severe and life-threatening situations. [8].

Studies on Cephalometric analysis

In order for the physician to identify face disharmonies and concentrate therapeutic actions throughout therapy, cephalometric analysis is an effective diagnostic technique for determining facial type and growth pattern [9]. In order to classify skeletal and dental anomalies, cephalometric radiography gives the information needed. In order to analyze changes in the interaction between teeth and basal bones, as well as changes in maxilla, mandible, and teeth anteroposterior positions with one another, a Cephalometric radiograph is highly recommended [10]. For treatment planning, a different set of Cephalometric measures is needed than for assessing treatment success. It's critical to take the measurements required for treatment planning and use that knowledge [11]. For therapeutic decision-making, several Cephalometric assessments may be conducted, and if the accuracy of the diagnosis and treatment success can be enhanced by collecting additional data must be determined [11]. In 51 instances, researchers analyzed the results of Cephalometric investigations by Steiner and McNamara to determine where the bone bases were located. They discovered that the results were quite similar. Compared to other techniques studied, the authors believe that the one



**Anbahagan and Samundeswari**

developed by McNamara has a better and more immediate therapeutic benefit [12]. Jarabak [13] is a branch of study that divides the dental facial complex into segments and analyses how specific growth increments or alterations in that growth might influence the entire complex as described by Cephalometrics Bjork's research findings informed Jarabak's Cephalometric analysis. [14], They were used to study clinical issues, allowing for the comparison of differences in size, shape, age, gender, and ethnicity. During development, a variety of skeletal anomalies can be seen. If an orthodontist wants to work with children, he or she must first examine each patient's unique growth pattern to determine its potential paths and outcomes. After that, orthodontic mechanisms will only be used if they provide greater results and are easier to use [9]. Jarabak's cephalometric research can be used to predict the results of different orthodontic treatments. The physician can identify muscle patterns based on the skeletal parameters determined by looking at the lines and angles that constitute this analysis. In this way, the doctor may analyze the facial development response to therapeutic treatments such as orthodontics or orthopaedics before deciding on which to use. [9]. The diagnosis and prescription of Ricketts analysis [15] are shown in Figure 1.

Studies on automated Cephalometric analysis

When Broadbent first developed cephalometry, it transformed the way dentists looked at malocclusion and the skeletal components that support it. Manually tracing a lateral cephalogram is an option; however computers have increasingly been employed in recent years [16]. An automated system uses image processing and computer graphics techniques to automatically gather and store data for use in Cephalometric research. The method makes measurements more consistent and promotes surgical and dental staff productivity [17]. A manual technique or a computer-aided approach can both be utilized to conduct a Cephalometric analysis. The manual method is the most traditional and prevalent. By covering the Cephalometric radiograph with an acetate sheet and marking the important characteristics, landmarks can be identified, and the distance and angle between landmarks may be measured [18]. Computer program loads a scanned or digitised Cephalometric radiograph to perform an automated Cephalometric analysis. After that, the program will find the landmarks and do the Cephalometric analysis automatically [18]. Because the computations can already be done with automation, the difficult part of an automated Cephalometric study is landmark detection. [18]. Different ANN models were used for supervised and unsupervised learning to offer a vertical diagnosis. The data used to generate the training set for NN learning came from 210 different patients [19].

The study's goal is to establish Saudi Arabia's Cephalometric Norms and determine whether there are any major Cephalometric disparities between Saudi and Caucasian populations. There were 60 Saudis (30 men and 30 women) with lateral cephalometric radiographs, all permanent teeth present, no history of orthodontic treatment or facial injuries (age range: 20 to 30 years), who were subjected to the Downs and Steiner analysis. Utilizing guidelines based on the Downs and Steiner standards, the measures' means, standard deviations, and precision were compared to theirs. According to the findings of this study, Differences in white Caucasian population norms and those provided by Downs and Steiner for Saudi Arabian Cephalometric mean values were statistically significant. According to the research, Saudis tend to have somewhat projecting maxillae, a preference for the Class II facial design, and a high mandibular plane (MP) angle. There's a lot of significance to these discoveries. Identifying and treating Saudi people with dentofacial anomalies will be made easier with these results, because of their clinical significance. [20].

While it is possible to use objectively measurable data to make an orthodontic diagnosis, doing so is frequently challenging and impacted by the patient's own interpretations. ANN-based methods in orthodontic diagnostics are therefore being considered as a viable option. [21]. All patients under normal anesthesia should have an airway physical examination to evaluate the ease or difficulty of tracheal intubation. There is a general consensus among medical practitioners that evaluating all components of an airway physical examination rather than just one would help an aesthetists be more accurate in their forecasts when dealing with a difficult airway during a clinical encounter. Benefits from utilizing machine learning techniques are medical decision-making. Using support vector machines (SVM) and 13 physical traits, this work seeks to develop a medical decision-support system that can anticipate the need for tracheal intubation before general an aesthesia is administered. Over 264 medical data gathered from individuals with various conditions confirm the decision system's generalization performance.



**Anbahagan and Samundeswari**

Testing for robustness is done using a fourfold cross-validation approach. SVM-based decision support system can obtain an average classification accuracy of 90.53 percent, showing its significant application possibilities for supporting clinic-aided diagnosis with complete consideration of multiple airway physical examination parameters. The findings illustrate this [22].

Modern orthodontics relies heavily on systematic and objective procedures for describing craniofacial morphologies, using both hard and soft tissue features to assess the health of the patient. Cephalometric analysis uses lateral skull X-ray scans to give clinical orthodontists with quantitative measures. Digital lateral skull radiographs may be successfully interpreted using a model-and-knowledge-based technique, according to this argument. Image features may be gleaned from gray-level photos using an appearance model, as well as a segmentation approach based on rule-based classification. Cephalometric landmarks and image creation based on segmented component characteristics have a high level of complexity. The use of a predictive model, which defines the picture structure, enables image feature locations to be hypothesized. The location model's underlying structure serves as the foundation for a geometric constraint model that is used to the selection of image feature candidates. These duties are organized hierarchically using a blackboard system, utilizing a variety of information sources categorized by function and the many phases of the image interpretation cycle that has been adopted. The quantitative findings show that this complex system outperforms the individual segmentation systems. Comparing the current system to that of clinicians reveals both its virtues and faults [23].

For the treatment plan to be successful, the software's projections have to be based on accurate interpretations of the data. With the use of modern informatics techniques, the Orthodontic folder can gather easy-to-fill-out and review data schemes of crucial importance. As a consequence, the orthodontist can quickly and easily compare the different treatment outcomes during the consultation. An "Orthodontic check-up" is what this procedure is typically known as [24]. Paraconsistent ANN can cope with inconsistencies and uncertainty as it uses paraconsistent logic,. For the purpose of supporting orthodontic diagnoses, it suggests the use of a paraconsistent ANN for analyzing Cephalometric data. This is a perfect circumstance for treating using a paraconsistent method that takes into account various uncertainties and inconsistencies [25].

METHODOLOGY

Ingenious ways can be found through which humans can learn and use symbolic, pattern-based heuristic, and fuzzy knowledge. A classic artificial intelligent system and its approaches were used to try to construct an intelligent system with this capacity. Researchers have turned to NNs and fuzzy logic as a result of their lack of success with these other approaches. There are two types of neural networks used to train and assess patient data for skeletal and dental anomalies.

Cephalometrics

Orthodontic diagnosis includes an evaluation of craniofacial features. Aesthetic standards such as harmony, symmetry, and attractiveness were the first criteria employed to evaluate face dimensions. Cephalometry's predecessor, Craniometry, might be considered its antecedent. In craniometry, the skulls of the dead were measured for their craniofacial proportions. Because of the soft tissue envelop, this procedure could not be used on living persons, making direct measurements difficult and unreliable [26].

Cephalometric landmarks

As the name implies, cephalometric analysis and measurement make use of certain skull features or points to provide quantitative data. Cervical landmarks (Figure 2) can be classified into two groups. Two kinds of landmarks are used: anatomical ones and those that have been developed from them. The anatomical markers depict real-life cranium structures, such as the brain. Secondarily obtained markers on a Cephalogram that were taken from anatomical structures. Certain conditions should be satisfied by the landmarks utilized in Cephalometrics.





Anbahagan and Samundeswari

- It should be easily seen in a radiograph.
- It must have a consistent outline and be able to be duplicated.
- In order to estimate lines and angles from landmarks, reliable quantitative data are required. [27].

Landmarks

Nosion (N): centre of forehead-to-nose joint on frontonasal suture at its most anterior position [26]. **Sella (S):** the midway of the pituitary fossa, also known as the sella turcica. In the mid-sagittal plane, it's a man-made dot. **Point A (A):** Amid the front nasal spine and the alveolar crest, at around midway, it is the spot that is deepest between the two central incisors." Subspinale is another name for this area of the body. **Point B (B):** Mandibular alveolar crest-to-mental process depth is measured at this location. In Italian, this condition is referred to as supramentale. **Gonion (Go):** Pogonion is located at the point where the Ramal plane intersects the MP. **(Gn):** It is the bony chin's forward-most point when viewed in the median plane.

Cephalometric analysis

Cephalometric analysis examines the link between the teeth and the skeleton in the human skull. Dentists, particularly orthodontists, commonly utilize it as a treatment planning tool. Cervical radiography may be analyzed using a number of methods. Orthodontics uses a wide variety of techniques for data analysis: (i) Steiner analysis, (ii) Bjork's analysis, (iii) Ricketts analysis, and (iv) McNamara's findings. Ricketts analysis is explored for this analysis.

Ricketts analysis

Identification of numerous cranial-facial landmarks is a part of cephalometric analysis. Traditional landmarks abound, but some may be specialized to a certain study. Ricketts' study employed a different set of points, planes, and axes than those often utilized. Ricketts analysis is used to look at the dentofacial skeletal pattern features of obstructive sleep apnea condition. Before therapy, Ricketts's study uses multiple Cephalometric studies' diverse factors to identify face growth abnormality.

Maxillary (MAX.) Position: From Figure 1, the facial angle (FH-NPog) parameter influences the maxillary position. The facial angle means the value is 870 ± 30 and its mean value is increased +10 for every 3 years age change. Larger angles usually indicate forwardly placed chin position, smaller angles backwardly placed chin position.

Mandible (MAND.) Position: From Figure 1, facial axis (BaN-PtmGn), facial taper (NPog-GoGn), mandibular plane (FN-GoGn) and mandibular arc (ANS Xi-Xi PM) parameters influence the mandible position. The facial axis mean value is 900 ± 30 and its mean value is increased +10 for every 3 years age change. The facial taper mean value is 680 ± 40 . The mandibular plane means the value is 260 ± 40 and its mean value is increased -10 for every 3 years age change. The mandibular arc means the value is 260 ± 40 and its mean value is increased +0.50 for every year age change. A larger facial axis angle usually indicates a forward position, smaller angles backward position. A larger facial taper angle usually indicates a horizontal, smaller angles vertical position. Larger mandibular angles indicate horizontal growth pattern, smaller angles vertical growth pattern. Larger mandibular arc angles indicate horizontal growth pattern, smaller angles vertical growth pattern.

Maxillary to Mandible Relationship: From Figure 1, lower face height (ANS Xi-Xi PM) and convexity of point A to N Pog (Point A to N Pog) parameters influence the maxillary to mandible relationship. The lower face height mean value is 470 ± 40 . The convexity of point A to N Pog mean value is $2\text{mm} \pm 2$ and its mean value is increased -1mm for every 3 years age change. Larger lower face height angles indicate increased lower face height, smaller angles decreased lower face height. Larger convexity values indicate mandible prognathic or maxillary retrognathic, lower values indicate maxillary prognathic or mandible retrognathic.

Lower Incisor Position: From Figure 1, lower incisor to A Pog (LI-APog) and mandibular incisor inclination (LI-NPog) parameters influence the lower incisor position. The lower incisor to A Pog mean value is $1\text{mm} \pm 2$. The mandibular incisor inclination mean value is 220 ± 40 and its mean value is increased -1mm for every 3 years age





Anbahagan and Samundeswari

change. Larger lower incisor to APog values indicates forwardly placed, lower values indicate backwardly placed. A larger mandibular incisor inclination angle indicates proclined lower incisors, smaller angles retroclined lower incisors.

Method of patient data collection

The Raja Muthiah Dental College and Hospital (RMDC&H) in the Tamil Nadu district of Cuddalore, near Annamalai Nagar, was used to collect data on study participants. In all, 304 (109 men, 195 women) patient records were gathered for this investigation. Before undergoing skeletal, dental, or a combination of the two treatments, these 304 individuals had some facial deformities.

Modelling techniques for Cephalometric analysis

The BPNN and GRNN modelling approaches are discussed in this section.

Backpropagation neural networks (BPNN)

Biological nervous systems, such as the brain, provide inspiration for NNs as an information processing method. Information processing system structure is central to NN theory. Because it is made up of so many interconnected processing components or neurons, a NN system learns by doing, similar to how humans do. In order to use the NN for a particular task, such as data categorization or pattern recognition, it must be trained [4]. Three layers make up the most common ANN: a "input" layer linked to a "hidden" layer, and a "output" layer linked to it. Figure 3 shows the input, hidden, and output layers, respectively [4]. The activity of the input units represents the raw data sent into the network. It is possible to calculate each hidden unit's activation by comparing it to the associated input unit's activation and weights on the connections connecting the two. It is the hidden units' activity and the weights given to the hidden and output units that define how the output units behave.

A new standard approach for supervised learning network training has emerged: the backpropagation algorithm. Using back-propagation of error signals in the neural network, This method's name comes from the way it generates partial derivatives of the performance metric in relation to open network parameters (such as synaptic weights and biases). Because of this, we must reduce the discrepancy between the desired outcome and what is actually produced, and do so by changing unit weighting. For this procedure to work, the NN must compute the weights' error derivative. So, as the weight is increased or dropped little, it must compute the change in error. In order to calculate the error derivative, the backpropagation algorithm is most commonly utilized The BPNN is implemented with the MATLAB NN toolbox in this study's research.

Generalized regression neural networks (GRNN)

The GRNN [28, 29] using feed-forward neural networks that are built on top of each other, with each layer utilizing non-linear regression theory and the output layer being the final layer. The architecture of GRNN is given in Figure 4. Some processing units in the summation layer link to each output neuron, although all three layers' neuronal connections are present. An RBF, which is commonly the Gaussian kernel function, is used to determine the activation of each pattern unit individually. 0 is the maximum input for the RBF, hence its output is 1. Overall, output rises linearly with reduction in distance between input and weight vector. It's like an input detector for the radial basis neuron, producing 1 anytime the input vector matches its own value. The RBF spread is one of the GRNN's parameters. If you don't change the spread, it will be set to 1.0 by default. The GRNN algorithm is implemented in MATLAB with the NN toolbox. The finer the function approximation, the greater is the spread. Spreads that are less than the normal spacing between input vectors can be used to get a better fit to data. A wider spread can be employed to better suit the data. A single division unit and a summation unit both exist in the summation layer. The number of summation units and GRNN output units are always the same. The division units merely add up the pattern units' weighted activation, utilizing no other activation functions.

The GRNN training differs greatly from the BPNN training. Completed when the GRNN input layer presents each pair of input-output GRNN vectors from the training set just once, both the pattern units' The RBF center and





Anbahagan and Samundeswari

weights for the links between these pattern units and the summation layer are assigned simultaneously. The use of unsupervised pattern unit training has become popular, however a particular clustering technique eliminates the need to specify in advance how many pattern units will be used. Instead, the radius of the clusters must be determined before training can begin in order to avoid confusion. Predicted values are generated "on the fly" by GRNN utilizing the basis functions described below[30].

$$f(x_k) = \sum_{j=1}^N t_j \varphi_{kj} / \sum_{j=1}^N \varphi_{kj}, k = 1, 2, \dots, M \quad (1)$$

Where φ_{kj} in attribute space, basis functions may be expressed as the Gaussian function,

$$\varphi_{kj} = \varphi(d_{ij}) = \exp\left(-\frac{d_{ij}^2}{\sigma^2}\right), \quad d_{ij} = |x_i - x_j| \quad (2)$$

Where σ is a sphericity factor. For RBF networks, predicting values is done in a manner that's comparable to.

$$f(x_k) = \sum_{j=1}^N w_j \varphi_{kj}, k = 1, 2, \dots, M \quad (3)$$

The weights, on the other hand, are derived from the training data using the linear equation shown below.

$$t(x_i) = \sum_{j=1}^N w_j \varphi_{ij}, i = 1, 2, \dots, N, \text{ and } \varphi_{ij} = \varphi(d_{ij}) \quad (4)$$

Objectives of the proposed work

Listed below are the planned project's goals.

- (i) For different Cephalometric analyses, determine the input and output factors relevant to skeletal and dental anomalies.
- (ii) For the purpose of obtaining the necessary parameter values.
- (iii) standardising a wide range of parameters.
- (iv) In order to provide patients with data for the BPNN and GRNN classifiers' training and testing using four-fold cross-validation.
- (v) Identifying and classifying skeletal and dental anomalies in various individuals according to their severity.

The following parts correspond to each of the aforementioned goals and can help you achieve them.

Identification of the input and output parameters

There are several input and output factors that may be derived from patient data for skeletal and dental anomalies by consulting with the dentist. Ricketts analysis is very handy when trying to figure out which factors are important. Tables 1 and 2 demonstrate the eight different types of cephalometric inference that were found as output parameters for skeletal and dental abnormalities, respectively. Eleven input parameters were found to be abnormalities in skeletal and dental.

Extraction of parameters

As previously mentioned in Sections 3.2 and 3.3, these characteristics may be extrapolated from patient data using lateral Cephalometric landmarks.

Classification of patients

Table 2 provides the specifics on the skeletal and dental anomalies of the various individuals, including their severity. Table 1 lists the input parameters for the bone and dental systems. If a patient's results for all of these indicators are abnormal, then the patient has bone and dental issues. If these metrics are normal in a patient, the patient is healthy. Take, for instance, 1, 0, 0, 0, 0, 0, 1, 0 patient's skeletal and dental features, including a horizontal mandible and lower incisors facing backward.





Anbahagan and Samundeswari

Normalization of parameter values

First, multiple distinct input variable combinations are selected to determine which NN model is the most dependable. Pre-processing transforms all data to values between 0 and 1, which are then used in the post-processing stage. It's not true that all the items in a row are the same in X, thus it's taken for granted. The following equation explains how to normalise any x_i value using this strategy y_i value.

$$y_i = (y_{max} - y_{min}) * (x_i - x_{min}) / (x_{max} - x_{min}) + y_{min} \quad (5)$$

With this formula, you may transform any x_i value into its equivalent y_i value in the range of y_{min} to y_{max} . The normalised result for Ricketts analysis in this study must be between -1 and 1. Therefore $y_{min}=-1$ and $y_{max}=1$. Then y_{min} (-1) and y_{max} (1) are substituted in above equation which yields,

$$y_i = 2 * (x_i - x_{min}) / (x_{max} - x_{min}) - 1 \quad (6)$$

Four fold cross validation of data

The BPNN and GRNN are trained and tested using four-fold cross-validation in this work. Cross validation involves randomly dividing a training set into four disjoint sets: fold 1 (say p1), fold 2, fold 3 (say p3) and fold 4. This is known as four-fold cross validation (say p4). Patients' records are contained within each of the four folds. These folds are also made by the folding teams who prepare training and testing data for Ricketts analysis.

Group 1: training: p1 + p2 + p3 (76 + 76 + 76 = 228); testing: p4 (76).

Group 2: training: p1 + p2 + p4 (76 + 76 + 76 = 228); testing: p3 (76).

Group 3: training: p1 + p3 + p4 (76 + 76 + 76 = 228); testing: p2 (76).

Group 4: training: p2 + p3 + p4 (76 + 76 + 76 = 228); testing: p1 (76).

Confidence score (CS)

In order to assess the BPNN and GRNN's efficiency, the equation computes a confidence score for each.

$$CS = \exp(-mse(actualValue - networkValue)) * 100 \quad (7)$$

RESULTS AND DISCUSSION

This chapter presents and analyses patient data on skeletal and dental malformations through the use of graphs and charts. In the training phase, NN models are capable of reproducing desired output values with minimum error, however. This model's capacity to accurately predict the outcome of a fresh collection of data is also tested. It is possible to utilize the trained NN as a design tool once the training, testing, and validation steps are complete. Training and testing are carried out using the four-fold cross-validation method in this work. Four equal-sized disjoint sets of the training and testing set are randomly partitioned. Each set of information should be labelled as follows: p1, p2, p3, and p4. The group 1 is represents cross-validation p1p2p3 (training) Vs p4 (test), group 2 represents cross-validation p1p2p4 Vs p3, group 3 represents cross-validation p1p3p4 Vs p2 and finally group 4 represents cross-validation p2p3p4 Vs p1.

Ricketts analysis with BPNN model

It is shown in Figures 5–8 that the performance of groups 1, 2, 3, and 4 with skeletal and dental defects (Ricketts analysis) is evaluated using the BPNN model. From Figures at 5(a), 6(a), 7(a) and 8(a), reduced mean square error (mse) results, epoch after epoch, show the effectiveness of BPNN. Based on these findings, it's evident that the BPNN model learns from training data to better map input and output parameters. From Figures at 5(b), 6(b), 7(b), and 8(b), there are extremely low gradient and mu values for training, as well as validation tests for the BPNN training as it progresses.





Anbahagan and Samundeswari

From Figures at 5(c), 6(c), 7(c), and 8(c) with the use of R values and a regression plot, it's possible to determine that the BPNN performs admirably when used for training, validation, and testing purposes (approximately 0.86). A fresh set of data with anomalies in skeletal and dental (Ricketts analysis) for groups 1, 2, 3, and 4 is examined in the BPNN model, and Table 3 shows the inaccurate replies for these groups. Based on Table 3, it's clear that BPNN has a 94% overall confidence level. The BPNN has a 94% mapping capability between input and output parameters.

Ricketts analysis with GRNN model

From figures 9 to 12 with each test data set, compare the RBF distribution to the GRNN-predicted performance in groups 1, 2, 3, and 4. Figure 9 shows that GRNN's performance grows from 0 to 0.49 for the spread settings. At a spread of 0.49, you get 92.64 percent of your potential performance. After then, GRNN's performance in group 1 rapidly degrades. In Figure 10, we see that GRNN's performance improves when the spread value grows from 0 to 0.42. When the spread is 0.42, the performance is at its best, with a maximum of 93.49 percent. GRNN's performance for group 2 steadily degrades after that. Figure 11 shows that for spread values ranging from 0 to 0.26, GRNN's performance improves. When the spread is 0.26, the performance is at its best, with a 92.96% success rate. This is followed by an overall decline in GRNN's performance for group 3.

For spread values ranging from 0 to 0.61, the graph in Figure 12 shows that GRNN performs better. When the spread is 0.61, the performance is at its best, with a maximum of 91.40 percent. When it comes to group 4, the GRNN's performance begins to deteriorate immediately after that. An additional data set for groups 1, 2, 3, and 4 (all having skeletal or dental anomalies; see the Ricketts study) shows that the GRNN model generates inaccurate results (see Table 4). Table 4 shows that on average, GRNN is able to categorize patients with an accuracy of 92.62 percent.

The comparison of classification results

Figure 13 to cross-validate skeletal and dental anomalies for Ricketts' investigation. As shown in Figure 13, compares the BPN model for skeletal and dental deformities to the GRNN model for Ricketts research, group 1 exhibited the highest level of performance (94.67%). When compared to the GRNN model, the experimental findings demonstrate that BPNN achieves a performance of 94% of good classification outcomes.

CONCLUSION

Skeletal and dental abnormalities are classified using the BPNN and GRNN models in this study. 304 patients data were collected, standardized, trained, tested, in which the classification input parameter was cephalometric landmarks, and models such as BPNN and GRNN were used (input). These parameters are sent into the BPNN and GRNN models as input data. Mandibular position, maxilla position, interaction between the mandible and the maxilla, and lower incisor position are all forms of anomalies that have been observed. It appears that the BPNN strategy is practical, as demonstrated by the simulation results, which indicated that it was 94% effective at correctly detecting patient cases. As a result, the BPNN model is capable of accurately recreating the desired output values. Models such as BPNN and GRNN are utilized in this investigation to look for skeletal and dental anomalies.

Additionally, different modeling approaches such as SVM, ELM, and Neuro-Fuzzy can be used to evaluate how the results improve. These lines can also be used to experiment with fuzzy logic. It is hoped that more patient data may be collected as part of this research to be used in subsequent studies by Steiner, Bjork, and McNamara, as well as BPNN and GRNN models for normalization, training, testing, and classification.

REFERENCES

1. Iyyer BS, Bhalajhi SI, Bhalajhi SI. Orthodontics: the art and science. Arya (Medi) Publ.; 2012.
2. Anbahagan S, Kumarappan N. Binary classification of day-ahead deregulated electricity market prices using neural networks. In: IEEE Fifth Power India Conference; 19-22 Dec. 2012; New Delhi. India: IEEE; 2012. p. 1-5.



**Anbahagan and Samundeswari**

3. Sivanandam SN, Deepa SN. Introduction to neural networks using Matlab 6.0. Tata McGraw-Hill Education; 2006.
4. Guru N, Dahiya A, Navin R. Decision support system for heart diseases prediction using neural networks. Delhi Business Review. 2007;8(1):1-6.
5. Zrimec T, Kononenko I. Feasibility analysis of machine learning in medical diagnosis from aura images. *Сознание и физическая реальность*. 1999;4(4):66-72.
6. Pomi A, Olivera F. Context-sensitive autoassociative memories as expert systems in medical diagnosis. BMC medical informatics and decision making. 2006;6(1):1-1.
7. Zadeh LA. Biological application of the theory of fuzzy sets and systems. In: The Proceedings of an International Symposium on Biocybernetics of the Central Nervous System; Little Brown; 1969. p. 199-206.
8. Moein S, Monadjemi SA, Moallem P. A novel fuzzy-neural based medical diagnosis system. International Journal of Biological & Medical Sciences. 2009;4(3):146-50.
9. Kuramae M, Magnani MB, Boeck EM, Lucato AS. Jarabak's cephalometric analysis of Brazilian black patients. Brazilian dental journal. 2007;18(3):258-62.
10. Munandar S, Snow MD. Cephalometric analysis of Deutero-Malay Indonesians. Australian dental journal. 1995;40(6):381-8.
11. Tenti FV. Cephalometric analysis as a tool for treatment planning and evaluation. The European Journal of Orthodontics. 1981;3(4):241-5.
12. Oria A, Schellino E, Massaglia M, Fornengo B. A comparative evaluation of Steiner's and McNamara's methods for determining the position of the bone bases. Minerva stomatologica. 1991;40(6):381.
13. Jarabak JR, Fizzell JA. Technique and treatment with light-wire edgewise appliances. Ed. 2. St. Louis: The CV Mosby Company; 1972.
14. Björk A. Prediction of mandibular growth rotation. American journal of orthodontics. 1969;55(6):585-99.
15. Mangutz J. Ricketts Analysis. Digitize and Electronic Transfer; 2003.
16. Hutton TJ, Cunningham S, Hammond P. An evaluation of active shape models for the automatic identification of cephalometric landmarks. The European Journal of Orthodontics. 2000;22(5):499-508.
17. Bidanda B, Motavalli S, Patterson G. On the development of an integrated computer system for cephalometric analyses. Journal of medical systems. 1990;14(1-2):1-6.
18. Leonardi R, Giordano D, Maiorana F, Spampinato C. Automatic cephalometric analysis: a systematic review. The Angle Orthodontist. 2008;78(1):145-51.
19. Martina R, Teti R, Musilli M. Neural Network based identification of typological diagnosis through cephalometric techniques. Eur. J. Orthod. 2001.
20. Martina R, Teti R, D'Addona D, Iodice G. Neural network based system for decision making support in orthodontic extractions. In: Intelligent Production Machines and Systems - 2nd I*PROMS Virtual International Conference; 3-14 July 2006; Elsevier Science Limited; 2006. p. 235-240.
21. Al-Jasser NM. Cephalometric evaluation for Saudi population using the Downs and Steiner analysis. J Contemp Dent Pract. 2005;6(2):52-63.
22. Yan Q, Yan H, Han F, Wei X, Zhu T. SVM-based decision support system for clinic aided tracheal intubation predication with multiple features. Expert Systems with Applications. 2009;36(3):6588-92.
23. Davis DN, Forsyth D. Knowledge-based cephalometric analysis: a comparison with clinicians using interactive computer methods. Computers and Biomedical research. 1994;27(3):210-28.
24. OrthoTP. Orthodontic Folder and Computerized Cephalometry. AXA Srl Via Pierino Colombo. 2007.
25. Abe JM, Ortega NR, Mário MC, Del Santo M. Paraconsistent artificial neural network: An application in cephalometric analysis. In: International Conference on Knowledge-Based and Intelligent Information and Engineering Systems; 14 Sep. 2005; Berlin. Heidelberg: Springer; 2005. p. 716-723.
26. Jacobson AL. The role of radiographic cephalometry in diagnosis and treatment planning. In: Introduction to Radiographic Cephalometry; Philadelphia. Lea & Febiger; 1985. p. 1-13.
27. Yen PK. Identification of landmarks in cephalometric radiographs. The Angle Orthodontist. 1960;30(1):35-41.
28. Specht DF. A general regression neural network. IEEE transactions on neural networks. 1991;2(6):568-76.





Anbahagan and Samundeswari

29. Anbahagan S. Athens seasonal variation of ground resistance prediction using neural networks. ICTACT Journal on Soft Computing. 2015;6(1):1113-1116.
30. Nawari NO, Liang R, Nusairat J. Artificial intelligence techniques for the design and analysis of deep foundations. Electronic Journal of Geotechnical Engineering. 1999;4:1-21.

Table-1: Ricketts analysis identified input parameters for abnormalities in skeletal and dental

Input parameters	Mean value (degrees/mm)	Age channel
Age	-	-
Sex	-	-
Facial Axis (BaN-PtmGn angle)	90±3°	-
Facial Angle (FH-NPog angle)	87±3°	+1° / 3 yrs
Mandibular Angle (FN-GoGn)	26±4°	-1° / 3 yrs
Facial Taper angle (NPog-GoGn)	68±4°	-
Lower Face Height angle (ANS Xi-Xi PM)	47±4°	-
Mandibular Arc angle (ANS Xi-Xi PM)	26±4°	+1/2° / yr
Convexity mm (Point A to N Pog)	2mm±2	-1mm / 3 yrs
Lower Incisor to APog mm (LI-APog)	1mm±2	-
Mandibular Incisor Inclination angle (LI-NPog)	22±4°	-

Table-2: Cephalometric inferences are identified as output parameters for abnormalities in skeletal and dental (Ricketts analysis)

Output parameters	Output value
Mandible Position Horizontal	0 or 1*
Mandible Position Vertical	0 or 1
Maxilla Position Backward	0 or 1
Maxilla Position Forward	0 or 1
Mandible To Maxilla Relationship Hor.	0 or 1
Mandible To Maxilla Relationship Ver.	0 or 1
Lower Incisor Position Backward	0 or 1
Lower Incisor Position Forward	0 or 1

* 1 represents abnormalities and 0 represents normal

Table-3: Performance in detection of abnormalities in skeletal and dental (Ricketts analysis) using BPNN

BPNN model	Test data (no.)	Number of abnormalities misclassified by the model	Performance percentage		
			R values	Actual	CS
Group 1	43	8	0.84	81.40	94.67
Group 2	43	12	0.87	72.09	94.43
Group 3	43	13	0.88	69.77	93.39
Group 4	43	12	0.85	72.09	93.53





Anbahagan and Samundeswari

Table-4: Performance in detection of abnormalities in skeletal and dental (Ricketts analysis) using GRNN

GRNN model	Test data (no.)	Number of abnormalities misclassified by the model	Performance percentage	
			Actual	CS
Group 1	43	15	65.12	92.64
Group 2	43	12	72.09	93.49
Group 3	43	14	67.44	92.96
Group 4	43	21	51.16	91.40

Descriptor	Meas.	Type	Mean	Sd	Patient	Graph	Comment
MAX. POSITION							
MAX DEPTH	FH to N-A	Deg	95.0	5.0	84.84	-1 * *	Maxilla distal to Base
MAX HEIGHT	N-PtV to A pt	Deg	54.0	5.0	59.9	-1 * *	
SN TO PALATAL PLANE		Deg	3.0	5.0	16.04	-1 * *	
MAND. POSITION							
FACIAL DEPTH	FH to N-Pog	Deg	90.0	4.0	79.79	-1 * *	Retrognathic Mandible
FACIAL AXIS	Na-Ba to PTV-Gn pt	Deg	90.0	4.0	84.99	-1 * *	
FACIAL TAPER	Na-Gn-Go	Deg	87.0	4.0	72.91	-1 * *	
MAND. PLANE	FH-GoGh	Deg	28.0	3.0	28.8	-1 * *	
CORPUS LENGTH	Xi to Pm	mm	70.0	5.0	70.89	-1 * *	
MAND. ARC	DC-Xi to Xi-Pm	Deg	27.0	5.0	41.46	-1 * *	Open Arc
MAX. TO MAND RELATIONSHIP							
A pt. CONVEXITY	A to N-Pog	mm	3.0	2.0	5.78	-1 * *	
LOW FACE HEIGHT	ANS-Xi-Pog	Deg	47.0	5.0	41.14	-1 * *	
DENTURE RELATIONSHIP							
MAX. 1 to APo		mm	6.0	3.0	2.73	-1 * *	
MAX.6 to PTV		mm	15.0		24.75	-1 * *	
MAND. 1 to APo		mm	1.0	2.0	-1.89	-1 * *	
HINGE AXIS ANGLE	DC-Ge-Li	Deg	90.0	3.0	89.05	-1 * *	
MAX. 1 to MAND. 1		Deg	131.0	5.0	138.91	-1 * *	
OVERJET		mm	2.5	2.0	5.04	-1 * *	
OVERBITE		mm	2.5	2.0	4.48	-1 * *	
ESTHETICS							
UPPER LIP to E-LINE		mm	-4.0	2.0	-4.22	-1 * *	
LOWER LIP to E-LINE		mm	-2.0	2.0	-4.52	-1 * *	

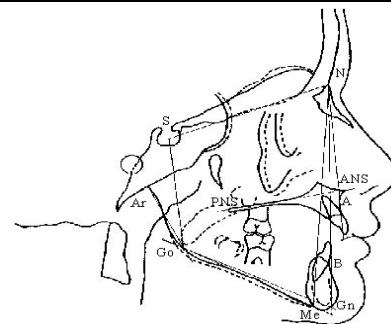


Figure-1. Diagnosis and prescription of Ricketts analysis

Figure-2. Cephalometric landmarks

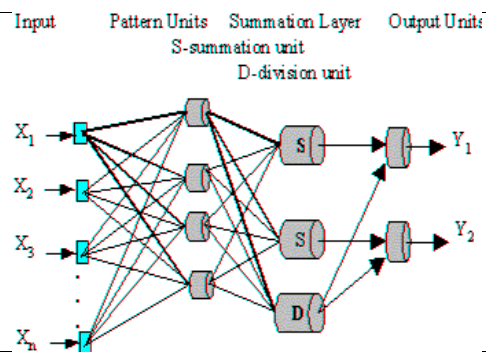
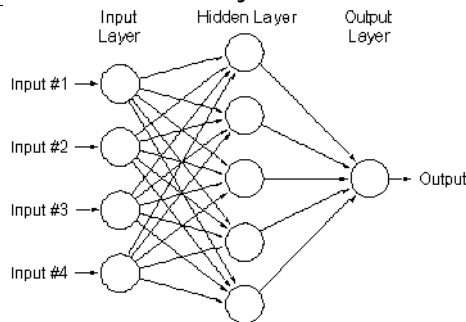


Figure-3. A three layer BPNN

Figure-4. GRNN model diagram

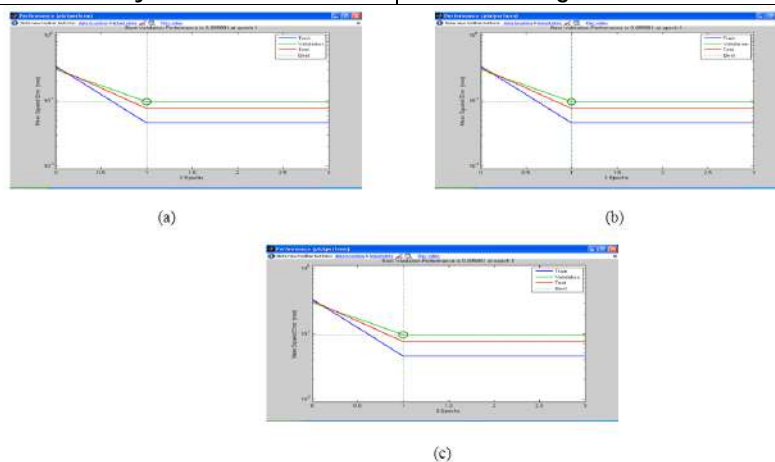


Figure-5. Group 1 Ricketts analysis (a) performance, (b) training state, and (c) regression plot





Anbahagan and Samundeswari

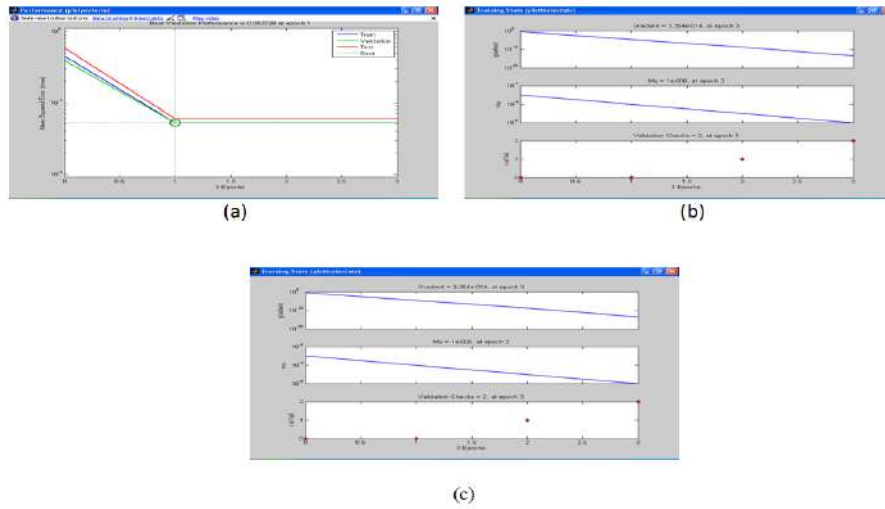


Figure-6. Group 2 Ricketts analysis (a) performance, (b) training state, and (c) regression plot

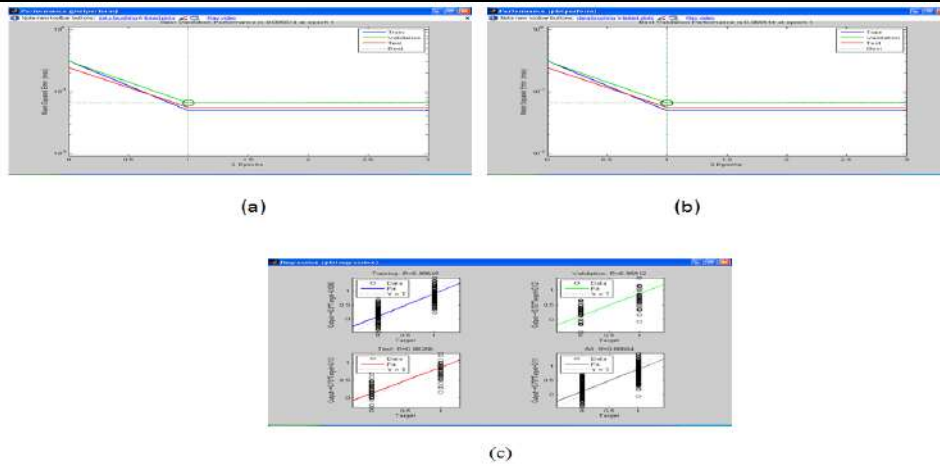


Figure-7. Group 3 Ricketts analysis (a) performance, (b) training state, and (c) regression plot

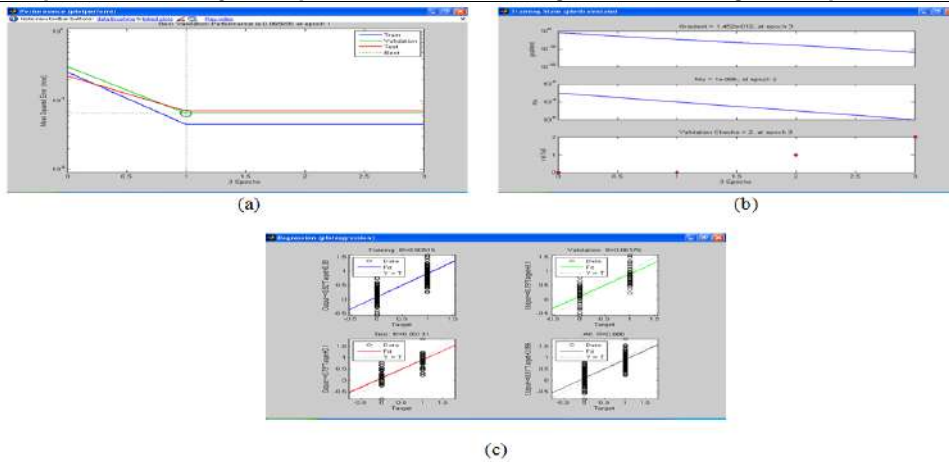


Figure-8. Group 4 Ricketts analysis (a) performance, (b) training state, and (c) regression plot





Anbahagan and Samundeswari

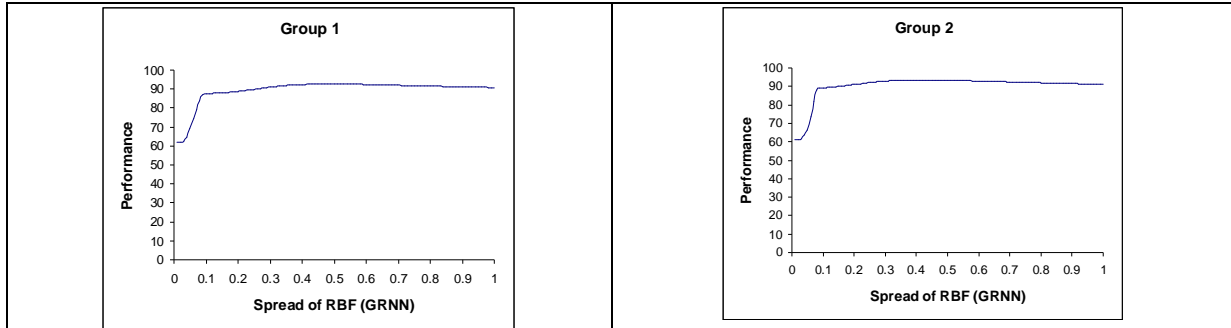


Figure-9. Performance curve of skeletal and dental abnormalities for group 1 (Ricketts analysis)

Figure-10. Performance curve of skeletal and dental abnormalities for group 2 (Ricketts analysis)

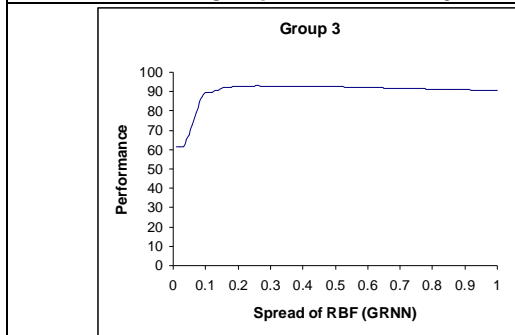


Figure-11. Performance curve of skeletal and dental abnormalities for group 3 (Ricketts analysis)

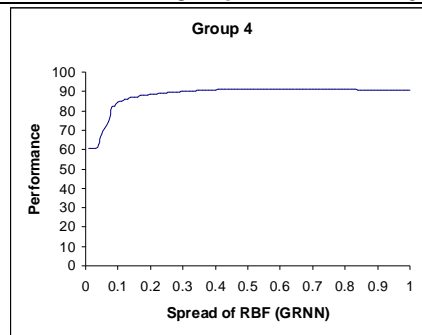


Figure-12. Performance curve of skeletal and dental abnormalities for group 4 (Ricketts analysis)

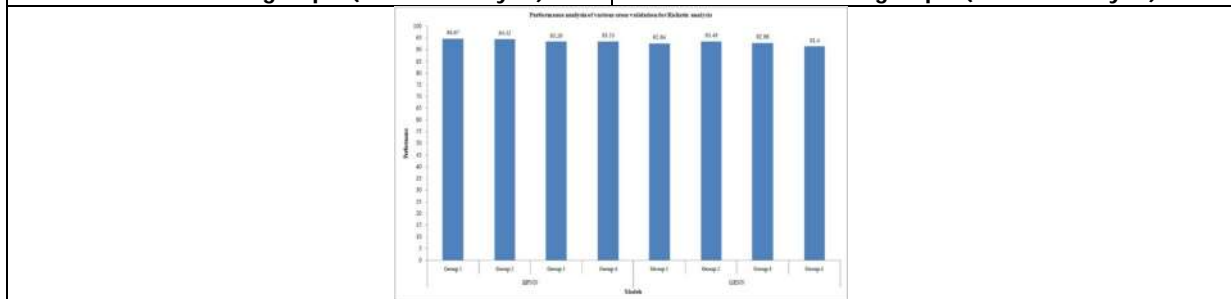


Figure-13. Performance for the various cross validation of skeletal and dental abnormalities (Ricketts analysis)





A Study of Responsible Environmental Behaviour in Relation to Gender, Stream and Locale

Ritu Bakshi^{1*} and Juhi Gupta²

¹Associate Professor, Dept. of Educational Studies, Central University of Jammu, Samba, Jammu and Kashmir, India.

²Research Scholar, Dept. of Educational Studies, Central University of Jammu, Samba, Jammu and Kashmir, India.

Received: 23 Nov 2021

Revised: 26 Dec 2021

Accepted: 13 Jan 2022

*Address for Correspondence

Ritu Bakshi

Associate Professor,
Dept. of Educational Studies,
Central University of Jammu, Samba,
Jammu and Kashmir, India.
Email: ritu.edu@cujammu.ac.in



This is an Open Access Journal / article distributed under the terms of the **Creative Commons Attribution License** (CC BY-NC-ND 3.0) which permits unrestricted use, distribution, and reproduction in any medium, provided the original work is properly cited. All rights reserved.

ABSTRACT

Humans are the only species on Earth that does not add to the natural environmental cycle and has always subjugated the planet's finite resources. It is a resource we must protect at all expense since it is the wealth we will bequeath to succeeding generations. Environmentally Responsive Behaviour is the key to such protection and conservation. It could be a vital step to ensure that the healing process is not only transitory. Though, the negative consequences could be reduced or, in some cases, even restored to a more sustainable state through efforts of people. The purpose of this study was to investigate Responsible Environmental Behaviour of post graduate students with reference to their gender, stream and locale. The sample consisted of 50 Post Graduate students (31 females and 19 males) which were drawn by random sampling. The investigator used standardized tool i.e., Responsible Environmental Behaviour Scale by Dr. Shalu Jindal and Dr.Sukhwant Bajwa to collect the data. Data analysis involved the use of mean, standard deviation and t-test. The finding and results of the study revealed that there is no significant difference in Responsible Environmental behaviour of post graduate students with respect to gender, stream and locale. Young pupils must be taught about the environment and instilled with environmentally responsible conduct.

Keywords: Responsible Environment Behaviour, Post Graduate students, Sustainable, Resources.



**Ritu Bakshi and Juhi Gupta**

INTRODUCTION

"We do not inherit the earth from our ancestors; we borrow it from our children"

Ralph Waldo Emerson (1990)

Environmental deterioration has become a major worry for humanity in these millennia. Man has been brutally exploiting natural resources and damaging the environment for the progress of the human race. Various environmental issues represent a danger to environmental sustainability, including rising levels of waste and air pollution, the emergence of an ozone hole, acid rain, and global warming, to name a few. Many of these issues can be traced back to human behaviour and as a result, it can be managed by altering relevant behaviour in order to lessen its environmental impact. Consequently, raising environmental awareness among students is an urgent need. All of this led to the realisation that person's existing environmental behaviour must change, indicating that persons must learn how to behave in an environmentally responsible manner. (Linke, 1998) Environmental responsibility relates to our obligation to use natural resources responsibly, to minimise damage, and to ensure that these resources are sustainable in the future. Increased understanding of environmental problems, their ecological and human repercussions, and responsible environmental management methods through defining and implementing environmental principles, goals, and objectives are all examples of responsible environmental behaviour. Gihar (2011) investigated environmental responsibility among prospective teachers and found no significant difference in environmental responsibility between rural and urban prospective teachers, but female prospective teachers had significantly higher mean values on all dimensions of the Environmental Responsibility Assessment Inventory. Sarita, Kavita, and Kumar (2015) investigated responsible environmental behaviour among 200 urban and rural B.Ed. students from four B.Ed colleges in Rohtak, by using random sampling. The research was carried out using a descriptive survey method. To analyse the behaviour of college students the researcher used Responsible Environment Behaviour Measure (REBM) by Dr. Anurkha Sindhvani. The significance of the difference in means was determined by using 't' test. The findings of the study revealed that there were no substantial difference in responsible environment behaviour with respect to gender and locality. Another study conducted by Malhotra and Chabra (2018) revealed that there were differences exist among B.Ed. distance teacher trainees with reference to gender, stream, location and socio economic status in their responsible behaviour towards environment.

Environmentally responsible conduct should be taught through formal education to help achieve this goal. The most influential segment of society, students, recognises the value of environmental and natural sustainability. School plays a significant role in promoting environmental awareness and responsible behaviour towards environment among students. Motivating and demonstrating hygienic activities at regular intervals in the school is an investment in school children to make their future healthy and indirectly creating health ambassador in every family Sanitation, clean households, and a clean nation are all low-cost investments with a big payoff. Though sanitation is a personal responsibility for everyone, the benefits are increased when the country as a whole joins in. On October 2, 2014, India launched the world's largest cleanliness campaign, Swachh Bharath Abhiyan, in order to realise Mahatma Gandhi's vision of a clean India by 2019. SBSV, a spin-off of the Swachh Bharat Abhiyan and the only government programme with significant corporate engagement, promises a bright future for many rural Indian kids.

SBSV's goal was to improve the implementation of the Water, Sanitation, and Hygiene (WASH) programme, which requires child-friendly separate toilet units with hand washing facilities for girls and boys, adequate facility for group hand washing (10-12 students), safe drinking water, clean food storage and preparation, operation and maintenance of these facilities, promotion of behaviour change, and communication activities aimed at health and hygiene. It gives guidance for schools to ensure that all critical aspects are well-managed in order to maintain good water, sanitation, and hygiene standards. Another goal is to strengthen the WASH curriculum and teaching methods in schools while encouraging cleanliness and community ownership of water and sanitation facilities. This has improved the health of children, as well as their school enrolment, attendance, and retention, paving the way for a new generation of healthy kids.



**Ritu Bakshi and Juhi Gupta****Government Key Commitments for Swachh Bharat: Swachh Vidyalaya**

The Honourable Prime Minister's strong devotion to provided that ample water, sanitation, and hygiene amenities in schools is backed up by legislation, including RET Act (2009), that mandates the provision of drinking water and sanitation in schools. This need is also supported by the national flagship programmes Sarva Shiksha Abhiyan (SSA) and Nirmal Gram Puraskar.

The government of India's major policy efforts was listed below:

Constitution

Article 21-A "free and compulsory education of all children in the age group of six to fourteen years as a Fundamental Right".

Legislation**Right of Children to Free and Compulsory Education (RTE) Act, 2009.**

The RTE Act's 2009 Schedule lays forth the requirements for a school building, including drinking water and sanitation.

Policies and programmes

- **Sarva Shiksha Abhiyan (SSA)** funds the construction of gender-segregated toilets.
- **Mid day meal Programme** A nutrition programme that necessitates a significant role in schoolchildren's hygiene.
- The **Rashtriya Madhyamik Shiksha Abhiyan** encourages secondary schools to follow the guidelines for providing great physical infrastructure, such as good classrooms, toilet facilities, and drinking water.
- **Kasturba Gandhi Balika Vidyalaya (KGBV)** aims to provide girls from disadvantaged groups belonging to the SC and ST populations with access to and quality education by establishing residential schools at the upper primary level.

VARIOUS SCHEMES BY GOVERNMENT TO PROMOTE SANITATION, HYGIENE AND CLEANLINESS IN SCHOOLS

The first step on the road to a thriving India is to clean up the country. We must also take responsibility for keeping our environment clean, in addition to our bodies and minds. We hope that our school will be a "clean and attractive" school as a result of such positive measures (listed below). Our school is moving forward in this way, preparing innocent children to be responsible citizens of India of the future.

Swachh Vidyalaya Puraskar

The MHRD, Government of India established the Swachh Vidyalaya Puraskar in 2016 to recognise, motivate, and celebrate excellence in sanitation and hygiene practises in schools. The awards' stated objective is to recognise schools that have taken substantial measures toward meeting the Swachh Vidyalaya Campaign's mandate. All government schools, whether rural and urban, would be eligible for the rewards. After launching the SBSV project in India in 2016, the central government introduced a new initiative called Swachh Vidyalaya Puraskar 2016-17. This campaign was launched to encourage and inspire all schools around the country to improve their sanitization systems. This is an award-based programme in which schools and educational institutions across the country are recognised for their cleanliness and hygiene.

- The central government of India will rank and recognise schools on a nationwide level under this plan (initiative).
- The rating will be based on cleanliness, water supply, hand washing, sanitization, maintenance, behaviour, and other Swachhta or cleanliness-related factors.
- This is the first time in India that an educational institute will be graded and awarded based on sanitation and cleanliness.



**Ritu Bakshi and Juhi Gupta****Swachhta Pakhwada**

Swachhta Pakhwada is a part of Swachh Bharat mission, which is a fortnight drive conducted at every government office, education institution, hospitals and other such places. All the ministries have been assigned 2 weeks to observe Swachhta twice a year. It is a fortnight-long event aimed at ensuring widespread citizen engagement in Swachhta activities and transforming Swachh Bharat into a true citizen's movement. Recognizing the critical role that schools play in raising awareness about the Swachhata Mission and its implementation across the country, schools are encouraged to commemorate Swachhta Pakhwada each year by hosting the following participation activities: Activities ranging from Swachhata shapath, talk on community outreach, tree plantation under Green school drive, painting competition on Personal Hygiene and *Swachhata hi seva*, Exhibition Day, Swachhata Action Day, Hand wash Day Letter writing Day, etc were organised in which students participated with great enthusiasm. The fortnight of Swachhata Pakhwada helped the students to inculcate the importance of hygiene and cleanliness for self and nation on the whole. It serves in connecting people to the nature and enhancing those actions that make our country a better place.

Bal Swachhta Mission

Bal Swachhta Abhiyan is a cleanliness campaign under the parent campaign Swachh Bharat Abhiyan launched by the Government of India on 2 October 2014. SBA focused on nation-wide cleanliness and sanitation, the Bal Swachhta Abhiyan focuses on children. It begins on 14 November and ends on 19 November. Since it focuses on children, it starts on Children's Day. This campaign is to be celebrated by all educational institutions to spread awareness through cultural programs or by hosting competitions like essay writing, debates, discussions, chart-making, recycling exhibitions, and other forms of art. The faculty members are also to initiate cleanliness drives to clean the campus or the neighbourhood and take the effort to educate those around.

The theme of this countrywide Mission was given below:

- **Clean Anganwadis**
- **Well-kept surroundings, such as playgrounds.**
- **Personal Hygiene/Child Health (Clean Self).**
- **Eat healthy foods.**
- **Water that is safe to drink.**
- **Toilets that are in good condition.**

The aim is to provide the healthy and hygienic environment to school going children. Under this scheme, the awareness can build towards school going children to maintain cleanliness at home, school, public places. The awareness can create among children's with the help of informal ways like poems, storytelling, small games, and conversation with children's.

Water, Sanitation and Hygiene Scheme (WASH) in Schools

Safe drinking water, improved sanitation amenities, and hygiene education in schools - a strategic approach known as WASH in School — provide safe drinking water, improved sanitation facilities, and hygiene education that encourages the development of healthy living habits. WASH in schools contributes to the realisation of children's rights to health and education. WASH is an important aspect of the educational system because it promotes health, fosters learning, and allows children to act as change agents for their siblings, parents, and the society at large.

School Sanitation and Hygiene Education

In India, the SSHE Program strives to improve sanitation and hygiene in and via schools in order to achieve long-term behavioural change. It also aims to ensure that all children (boys and girls) have access to a healthy and safe learning environment.





Ritu Bakshi and Juhi Gupta

Present status of drinking water and toilet facilities in Schools (2018-19)

	Jammu and Kashmir	Jammu District	Kashmir District
No. of Schools	29708	2440	1000
Percentage of schools with functional separate toilets for boys	82.40%	93.25%	87.35%
Percentage of schools with functional separate toilets for girls	84.05%	95.90%	80.02%
Percentage of schools with functional drinking water	94.00%	99.63%	96.80%

Source: <http://dashboard.seshagun.gov.in/#/StatesProfile>

According to Unified District Information System for Education (UDISE) data from 2014-15, more than 6,351 schools lacked toilets for females and 8,098 lacked toilets for males. The circumstances have become better to some amount. (July 2018, The Tribune). Swachh Vidyalaya's impact extended beyond the realms of sanitation and hygiene. It has instilled trust and confidence in people, at least in J&K, that a target of 16, 000 toilets are attainable. There has been a significant increase in the percentage of schools that have access to toilets. The high percentage of toilet usage indicates a paradigm shift in people's attitudes toward open defecation. Despite recent advances, the Swachh Bharat Abhiyan has a long way to go to realise its objectives.

Challenges faced

By reviewing studies, following challenges have been identified which was faced by stakeholders in implementing Swachh Bharat: Swachh Vidyalaya scheme. The major challenge is to change behaviour that have been established over centuries and are considered as socially acceptable. Communities find open defecation an acceptable solution in their setting and there is no social discrimination against it.

- Lack of dedicated funds for purchase of cleaning material, employing sweepers and repair work of WASH facilities.
- Need of concerned departments like Education, Urban development and Nagar nigam.
- Lack of awareness among people, community towards health and hygiene.
- Poorly constructed toilets, misallocation of funds, and corruption all obstruct the achievement of the goal.
- An Orthodox mindset is a roadblock to success.
- The biggest issue facing the Swachh Bharat Swachh Vidyalaya Abhiyan is the lack of adequate maintenance of the gender-segregated toilets that have already been built.

In this paper, the investigator tried to make linkage between different government initiatives for developing habits of cleanliness, hand wash, hygienic conditions in students and also making students responsible towards their environment. Keeping in view the above facts, challenges and initiatives of Government, the researcher felt it appropriate to investigate responsible environmental behaviour among Post Graduate students with respect to gender, stream and locale.

STATEMENT OF THE PROBLEM

The present study stated as "A study of Responsible Environmental Behaviour in relation to Gender, Stream and Locale".

Operational Definition of the Terms

1. **Responsible Environmental Behaviour:** It is a measure of a people willingness to actively participate in environmental protection.
2. **Gender:** It is a sociological categorization that determines whether a person is male or female.





Ritu Bakshi and Juhi Gupta

3. **Stream:** In the present study, stream means a specific course or a certain academic field chosen by a student when he/she were studying in college (arts/humanities and science).
4. **Locale:** Locale means whether a student resides in urban or rural areas.

OBJECTIVES OF THE STUDY

1. To study the Responsible Environmental Behaviour of Post Graduate students.
2. To study the significant difference in the Responsible Environmental Behaviour of Post Graduate students with respect to
 - Gender
 - Stream.
 - Locale.
3. To suggest the educational implications in light of the result of study.

HYPOTHESES OF THE STUDY

There is no significant difference in Responsible Environmental Behaviour of Post Graduate students with respect to

- Gender
- Stream.
- Locale.

DELIMITATION OF THE STUDY

- The study was limited to Post Graduate students of Central University of Jammu and University of Jammu.
- The sample was delimited to 50 Post Graduate students.

RESEARCH METHODOLOGY

RESEARCH METHOD	POPULATION	SAMPLE	SAMPLING TECHNIQUE	STATISTICAL TECHNIQUE
Descriptive Method	Post Graduates Students of Central University of Jammu and University of Jammu	50 Post Graduates Students	Random Sampling	Mean, S.D, t-test

VARIABLES USED IN THE PRESENT STUDY

- **DEPENDENT VARIABLE:** Responsible Environment Behaviour
- **INDEPENDENT VARIABLES:** Gender, Stream and Locale.

TOOL USED IN THE STUDY

In the present study, the researcher used Standardised tool which was constructed by Dr. Shalu Jindal and Dr. Sukhwant Bajwa

- Responsible Environmental Behaviour Scale

DATA COLLECTION

The researcher gathered data from 50 postgraduate students (male and female) at Central University of Jammu and University of Jammu. The researcher typed all 46 items of Questionnaire which consists of 6 dimensions: - civic action, educational action, financial action, legal action, physical action and persuasion action in Google form and it was sent randomly to post graduate students through their e-mails and what'sapp groups. In which only 50 students responded the Questionnaire (Google form) fully and successfully submitted it.

ANALYSIS AND INTERPRETATION OF DATA

The responses were scored according to the guidelines in the manual. The resulting raw scores were then tabulated for interpretation. The means, standard deviations, and difference of means were used to interpret the numbers. The information gathered was statistically analysed. The t-test was used to see if there was a difference between the mean



**Ritu Bakshi and Juhi Gupta**

scores. Hypothesis-wise interpretation was given below. The table 1 indicates that the average score of Responsible Environmental Behaviour of female as well as male Post Graduate students were 121.19 & 120.36 amid standard deviation 14.02 and 12.74 respectively. The calculated value of t-test is 0.21 which is less than 1.96 and 2.58 therefore it was not significant at any levels of significance. The hypothesis stating "There is no significant difference in Responsible Environment Behaviour of Post Graduate students with respect to Gender" was accepted which means there is no significant difference between females and males Post Graduates students in their responsibilities towards environment. The results of the present study are corroborated with the research study of Sarita, Kavita, and Kumar (2015) that gender has no effect on responsible environmental behaviour. Graphically representation of scores of Post Graduate students was given in last page figure 3.

From the table 2 it can be interpreted that t-ratio came out from two groups were 1.39 that was not significant at both levels. Hence, the null hypothesis stating "There is no significant difference in Responsible Environmental Behaviour of Post Graduate students with respect to Stream" was accepted. Thus it can be inferred that there was no significant difference in the stream (Science & Humanity) of Post Graduate students with regards to Responsible Environmental Behavior. The results of present research were dissent with findings of Malhotra and Chabra (2018) that science students show more environmental responsibility and awareness than arts students'. A graphical representation of mean scores was given in last page in figure 4. From table 3, it can be seen that mean scores of Urban as well as Rural Post Graduate students were 122.87 and 119.72 respectively and the obtained t-value 0.61 is not significant at both levels. Consequently, the null hypothesis is not to be discarded that means there is no major difference among Responsible Environmental behavior of Post Graduate students belonging to urban and rural area. The results are in the consonance with the findings of Gihar (2011) and Sarita, Kavita, and Kumar (2015) that there was no substantial difference between urban and rural B.Ed students' environmental stewardship. A graphical representation of mean scores was given in last page in figure 5.

EDUCATIONAL IMPLICATIONS

In the light of the result findings, the important educational implications were suggested.

- I. Separate curriculum for students in schools, colleges, universities and other educational institutions might be included on personal hygiene, sanitation and environmental cleanliness.
- II. Young pupils must be taught about the environment and instilled with environmentally responsible conduct. This can be accomplished in the most efficient way possible through their professors and guides.
- III. Various initiatives and competitions for students and teachers might be introduced from time to time to promote responsibility and environmental awareness.
- IV. Swachh Vidyalaya awards and incentives may be introduced at school level as a part of encouragement for better maintenance and management.
- V. Government should introduce environmental education from lower level of schooling.
- VI. Teachers who are attempting to raise environmental consciousness among students should be given special allowances, incentives, and promotions by the government.
- VII. Schools set the groundwork for ecological balance, assisting in the re-establishment of a sustainable earth.

CONCLUSION

After going to the present study it has been found that post graduate students showed no difference in their behaviour towards environment responsibility with reference to gender, stream and locale. Responsibility towards environment can be developed by creating awareness among the people so that it becomes the part of their life style. When environmental awareness activities are held in schools, learners will become more aware of and concerned about the environment. Children's environmental sensitization in schools will help them develop knowledge and become responsible for preventing pollution and maintaining a healthy environment.





Ritu Bakshi and Juhi Gupta

ACKNOWLEDGEMENT

The author thanks to her Supervisor, Dr. Ritu Bakshi for their valuable support and constant encouragement and the authors were thankful to the Post-Graduate students of Central University of Jammu and University of Jammu.

REFERENCES

- Linke, P. (1998). A critical analysis of research in environmental education. *Studies in Science Education*, 34, 1-69.
- Gihar, S. (2011). Prospective Teachers' Responsibility towards Environment. *BRICS Journal of Educational Research*, 1(2), 74-79.
- Sarita, Kavita & Kumar, S. (2015). A Study of responsible environment behaviour among B.Ed students in relation to their gender & locality. *International Education & Research Journal*, 1(5), 61-63.
- Malhotra, T., & Chabra, S. (2018). A Study of Responsible Environmental Behaviour among B. Ed. Distance Learners with Reference to their Locality, Gender, Stream & Socio-Economic Status. 4(2), 3-10. Retrieved from <https://www.glokalde.com/pdf/issues/14/Volume4Number2.pdf>
- Jindal, S. (2010). *Effect of active learning programme on responsible environmental behaviour in relation to locus of control and achievement motivation* [Doctoral Thesis, Panjab University]. <http://hdl.handle.net/10603/80677>
- <http://dashboard.seshagun.gov.in/#!/StatesProfile>
- https://www.academia.edu/2578922/A_Study_of_Environmental_Awareness_and_Ecological_Behaviour_among_Female_B_Ed_Students
- <https://www.glokalde.com/pdf/issues/14/Article1.pdf>
- <https://www.info.fastread.in/long-and-short-essay-on-bal-swachhta-abhiyan-in-english/>
- <https://brainly.in/question/9943748>
- https://www.business-standard.com/article/specials/swachh-bharat-96-percent-of-jammu-kashmir-s-share-unsptent-115062400119_1.html
- https://www.researchgate.net/publication/336319355_Swachhta_Pakhwada_The_beginning_of_a_journey
- https://economictimes.indiatimes.com/news/company/corporate-trends/swachh-vidyalaya-how-india-inc-built-over-20000-toilets-in-rural-schools/articleshow/48548981.cms?utm_source=contentofinterest&utm_medium=text&utm_campaign=cppst
- <https://www.ceeindia.org/swachh-bharat-swachh-vidyalaya-strengthening-wash-in-schools>
- <https://www.swachhvidyalaya.com/swachh-vidyalaya-puraskar/>
- <https://quoteinvestigator.com/2013/01/22/borrow-earth/>
- <http://ndpublisher.in/admin/issues/EQv8spl0.pdf>

Table 1 showing the value of Mean, S.D and t-test among Post Graduate students with reference to Gender

Gender	Number	Mean Scores	Standard Deviation	t-ratio	Level of Significance
Female	31	121.19	14.02	0.21	Not Significant
Male	19	120.36	12.74		

Table 2 showing the value of Mean, S.D and t-test among Post Graduate students with respect to Stream

Stream	Number	Mean Scores	Standard Deviation	t-value	Levels of Significance
Science	14	124.64	11.02	1.39	Not Significant
Humanity	36	119.41	14.06		

Table 3 showing the value of Mean, S.D and t-test among Post Graduate students with respect to Locale

Locale	Number	Mean Scores	Standard Deviation	t-ratio	Levels of Significance
Urban	21	122.87	14.34	0.61	Not Significant
Rural	29	119.72	12.84		





Ritu Bakshi and Juhi Gupta

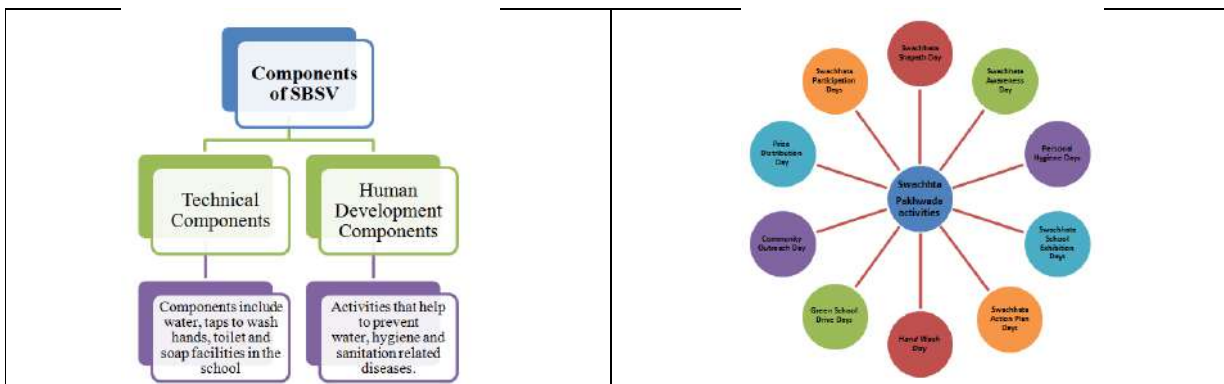


Figure 1 Components of SBSV

Figure 2 Swachhta Pakhwada

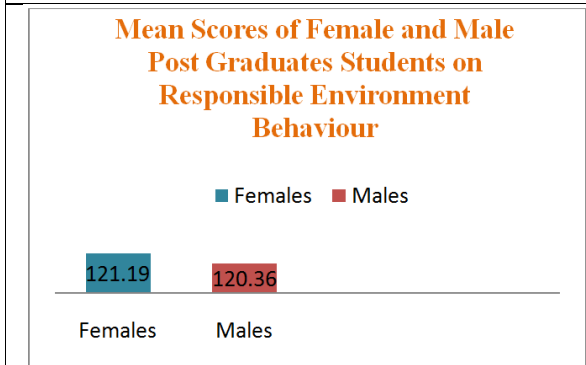


Figure 3 represent mean scores of Post Graduate students in relation to Gender

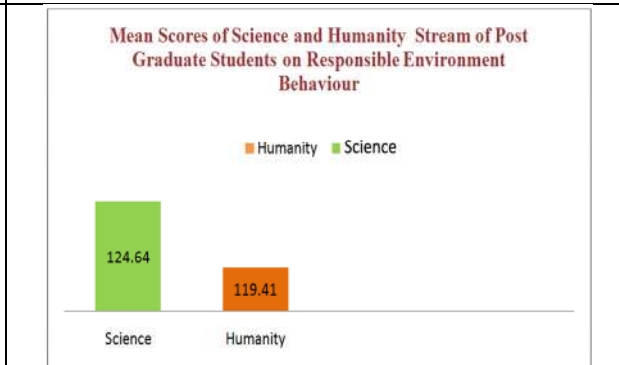


Figure 4 Represent mean scores of Post-Graduate students in relation to Stream.

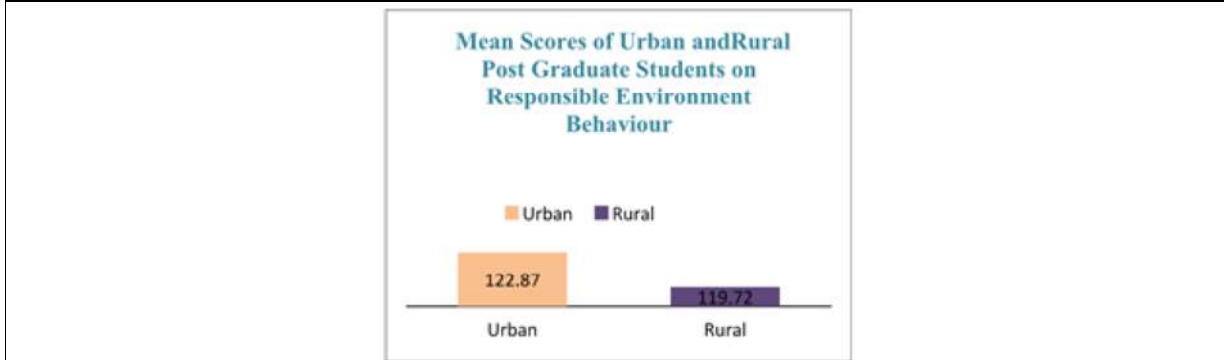


Figure 5 Represent mean scores of Post-Graduate students in relation to Locale





Some Results on Pythagorean Fuzzy Soft Matrices and their Application in Agriculture

A. Arikrishnan^{1*} and S. Sriram²

¹Ph.D Research Scholar, Department of Mathematics, Annamalai University, Annamalainagar, Tamil Nadu, India.

²Professor and Head, Department of Mathematics, Annamalai University, Annamalainagar, Tamil Nadu, India.

Received: 31 Oct 2021

Revised: 20 Dec 2021

Accepted: 13 Jan 2022

*Address for Correspondence

A. Arikrishnan

Ph.D Research Scholar,

Department of Mathematics,

Annamalai University, Annamalainagar ,

Tamil Nadu, India.

Email: : malarsan333@yahoo.com



This is an Open Access Journal / article distributed under the terms of the **Creative Commons Attribution License** (CC BY-NC-ND 3.0) which permits unrestricted use, distribution, and reproduction in any medium, provided the original work is properly cited. All rights reserved.

ABSTRACT

In this paper, we define on modal operators of Pythagorean fuzzy soft matrix and discuss the in algebraic properties and using the algebraic sum of Pythagorean fuzzy soft matrices, we construct a more efficient decision - making method. The analysis of best farmer problems that their good healthier yields using Pythagorean fuzzy soft matrices is studied.

Keywords: Intuitionistic fuzzy set, Pythagorean fuzzy set, Soft set, Pythagorean fuzzy soft matrix, Algebraic sum of Pythagorean fuzzy soft matrices.

AMS Mathematics Subject Classification(2010): 03E72, 03E99, 15B15, 15B99.

INTRODUCTION

The theory of fuzzy sets introduced by Zadeh in 1965 [17], showed meaningful applications in many field of studies. An intuitionistic fuzzy set was introduced in 1983, by Atanassov [3] as an extension of Zadeh's fuzzy set. Soft set theory [11] was firstly introduced by Molodtsov in 1999 as a general mathematical tool for dealing with uncertain, fuzzy not clearly defined objects. Soft set theory has rich potential for applications in solving practical problems in economics, social science, medical science etc. Maji et al. [8] have studied the theory of fuzzy soft set and extended the theory of fuzzy soft set to intuitionistic fuzzy soft sets. In 2011, Meenakshi and Kaliraja [9], extend Sanchez's approach for medical diagnosis using the interval valued fuzzy matrix. Pal et al. [7] introduced intuitionistic fuzzy matrices in 2002. In 2016, Muthuraji et al. [10] studied some properties of modal operators in intuitionistic fuzzy





Arikrishnan and Sriram

matrices. In 2012, Chetia and Das[4] defined five types of product of intuitionistic fuzzy soft matrices. In 2013, Mondal and Roy[12] defined intuitionistic fuzzy soft matrix theory and some basic results. In 2014, Sarala and Rajakumari [14] introduced Invention of best technology in Agriculture using Intuitionistic fuzzy soft matrices. In 2013, Yager and Abbasov [16] created Pythagorean fuzzy set (PFS) characterized by a membership degree and non-membership degree, which satisfies the condition that the square of sum of its membership degree and non-membership degree is less than or equal to 1. In 2015, Peng et al.[13] introduced the Pythagorean fuzzy soft set (PFSS) and studied various binary operations over PFSS and also proposed a decision making algorithm based on the Pythagorean fuzzy soft set. In 2018, Guleria and Bajaj [6] introduced model operation on Pythagorean fuzzy soft matrices (PFSMs) and their applications in decision making and medical diagnosis. In 2019, Bajaj and Guleria[5] defined Dimensionality reduction technique in decision making using Pythagorean fuzzy soft matrices. In 2019, Arikrishnan and Sriram[1] defined necessity and possibility operators on Pythagorean fuzzy soft matrices and properties are discussed. In 2020, I.Silambarasan and S.Sriram [15] defined necessity and possibility operators on Pythagorean Fuzzy Matrices and algebraic properties are studied. In 2021, Arikrishnan and Sriram[1, 2] studied modal operators and implication operator on Pythagorean fuzzy soft matrices and properties are discussed. In this paper, using the algebraic sum of Pythagorean fuzzy soft matrices, we constructing a more efficient decision - making method. The analysis of best farmer problems that their good healthier yields using Pythagorean fuzzy soft matrices is studied.

PRELIMINARIES.

In this section, we recall some basic concepts of fuzzy soft set and fuzzy soft matrices.

Definition 2.1.[3]

An Intuitionistic fuzzy set (IFS) I in X (universe of discourse) is given by $I = \{ \langle x, \mu_I(x), \nu_I(x) \rangle \mid x \in X \}$; where $\mu_I: X \rightarrow [0,1]$ and $\nu_I: X \rightarrow [0,1]$ denote the degree of membership and non-membership, respectively, and for every $x \in X$ satisfy the condition $0 \leq \mu_I(x) + \nu_I(x) \leq 1$ and the degree of indeterminacy for any IFS I and $x \in X$ is given by $\pi_I(x) = 1 - \mu_I(x) - \nu_I(x)$.

Definition 2.2.[16]

An Pythagorean fuzzy set (PFS) M in X (universe of discourse) is given by $M = \{ \langle x, \mu_M(x), \nu_M(x) \rangle \mid x \in X \}$; where $\mu_M: X \rightarrow [0,1]$ and $\nu_M: X \rightarrow [0,1]$ denote the degree of membership and non-membership, respectively, and for every $x \in X$ satisfy the condition $0 \leq \mu_M^2(x) + \nu_M^2(x) \leq 1$ and the degree of indeterminacy for any IFS I and $x \in X$ is given by $\pi_M(x) = \sqrt{\mu_M^2(x) + \nu_M^2(x)}$. In case of PFS, the restriction corresponding to the degree of membership $\mu_M(x)$ and the degree of non-membership $\nu_M(x)$ is $0 \leq \mu_M^2(x) + \nu_M^2(x) \leq 1$, where as the condition in case of IFS is $0 \leq \mu_I(x) + \nu_I(x) \leq 1$ for $\mu_M(x), \nu_M(x) \in [0,1]$.

Definition 2.3.[11]

Suppose that U is an initial universe set and E be the set of parameters, let $P(U)$ denotes the power set of U . Let $A \subseteq E$. A pair (F_A, E) is called fuzzy soft set over U , where F_A is a mapping given by $F: A \rightarrow P(U)$, where $P(U)$ denotes the collection of all fuzzy subsets of U .

Here F_A is called approximate function of soft set (F_A, E) the set $F_A(e)$ is called e -approximate value set which consist of related objects of the parameter $E \in e$. In other words, a soft set over U is a parameterized family of subsets of the universe U .

Definition 2.5.[13]

A pair (F_A, E) is called a Pythagorean fuzzy soft set over U , where F is a mapping given by $F_A: A \rightarrow P(U)$. $P(U)$ denotes the set of all Pythagorean fuzzy subsets of U .

Let $x \in U$ and $e \in A$. $F(e)$ is a Pythagorean fuzzy subset of U , and it is called a Pythagorean fuzzy value set of parameter e . Let $\mu_{F(e)}(x)$ and $\nu_{F(e)}(x)$ denote the membership value and non-membership value, respectively,





Arikrishnan and Sriram

then $F(e)$ can be written as a Pythagorean fuzzy set that $F(e) = \{x/F(e) (x)\mid x \in U\} = \{x/(\mu F(e) (x), \nu F(e) (x))\mid x \in U\}$.

Definition 2.6.[6]

If (F_A, E) be a Pythagorean fuzzy soft set over X , then the subset, $X \times E$ is uniquely defined by $R_A = (x, e), e \in A, x \in F_A(e)$. The R_A can be characterized by its membership function and non-membership function given by $\mu_R: X \times E \rightarrow [0,1]$ and by $\nu_R: X \times E \rightarrow [0,1]$, respectively.

If $(\mu_{ij}, \nu_{ij}) = (\mu_{R_A}(u_i, e_j), \nu_{R_A}(u_i, e_j))$, where $\mu_{R_A}(u_i, e_j)$ is the membership of x_i in the Pythagorean fuzzy set $F(e_j)$ and $\nu_{R_A}(u_i, e_j)$ is the non-membership of x_i in the Pythagorean fuzzy set $F(e_j)$, respectively, then we define a matrix given by

$$[M] = [m_{ij}]_{m \times n} = [(\mu_{ij}^A, \nu_{ij}^A)]_{m \times n} = \begin{bmatrix} (\mu_{11}, \nu_{11}) & (\mu_{12}, \nu_{12}) & \dots & (\mu_{1n}, \nu_{1n}) \\ (\mu_{21}, \nu_{21}) & (\mu_{22}, \nu_{22}) & \dots & (\mu_{2n}, \nu_{2n}) \\ \vdots & \vdots & \ddots & \vdots \\ (\mu_{m1}, \nu_{m1}) & (\mu_{m2}, \nu_{m2}) & \dots & (\mu_{mn}, \nu_{mn}) \end{bmatrix}$$

which is called Pythagorean fuzzy soft matrix of order $m \times n$ over X .

For a better understanding, let us consider $U = \{u_1, u_2, u_3\}$ as a universal set and $E = \{e_1, e_2, e_3, e_4\}$ as a set of parameters. If $A = \{e_1, e_2, e_3\} \subseteq E$ and

$$\begin{aligned} F_A(e_1) &= \{(u_1, 0.6, 0.5), (u_2, 0.5, 0.8), (u_3, 0.9, 0.2)\}, \\ F_A(e_2) &= \{(u_1, 0.8, 0.5), (u_2, 0.9, 0.3), (u_3, 0.6, 0.6)\}, \\ F_A(e_3) &= \{(u_1, 0.6, 0.7), (u_2, 0.5, 0.6), (u_3, 0.7, 0.5)\}, \end{aligned}$$

Then (F_A, E) is the parameterized family of $F_A(e_1), F_A(e_2), F_A(e_3)$ over X .

Hence, the Pythagorean fuzzy soft matrices $[M(F_A, E)]$ can be written as

$$[M] = [(\mu_{ij}^A, \nu_{ij}^A)]_{m \times n} = \begin{pmatrix} (0.6, 0.5) & (0.8, 0.5) & (0.6, 0.7) \\ (0.5, 0.8) & (0.9, 0.3) & (0.5, 0.6) \\ (0.9, 0.2) & (0.6, 0.6) & (0.7, 0.5) \end{pmatrix}$$

Definition 2.7.[6] For any two Pythagorean fuzzy Soft matrices $A = [(\mu_{ij}^A, \nu_{ij}^A)]$ and $B = [(\mu_{ij}^B, \nu_{ij}^B)]$ of the same size,

- (i) $A \supseteq B$ iff $(\forall x \in X, \mu_{ij}^A \leq \mu_{ij}^B \text{ and } \nu_{ij}^A \geq \nu_{ij}^B) \forall i \text{ and } j$
- (ii) $A \subseteq B$ iff $(\forall x \in X, \mu_{ij}^A \geq \mu_{ij}^B \text{ and } \nu_{ij}^A \leq \nu_{ij}^B) \forall i \text{ and } j$
- (iii) $A = B$ iff $(A \subseteq B \text{ and } B \subseteq A) \forall i \text{ and } j$

Definition 2.8.[6] Let $A, B \in PFSM_{m \times n}$. of the same size we have,

- (i) $A^C = [(v_{ij}^A, \mu_{ij}^A)] \forall i \text{ and } j$
- (ii) $A \cup B = [(\max(\mu_{ij}^A, \mu_{ij}^B), \min(\nu_{ij}^A, \nu_{ij}^B))] \forall i \text{ and } j$
- (iii) $A \cap B = [(\min(\mu_{ij}^A, \mu_{ij}^B), \max(\nu_{ij}^A, \nu_{ij}^B))] \forall i \text{ and } j$
- (iv) $A + B = [(\mu_{ij}^A + \mu_{ij}^B - \mu_{ij}^A \cdot \mu_{ij}^B, \nu_{ij}^A \cdot \nu_{ij}^B)] \forall i \text{ and } j$
- (v) $A \cdot B = [(\mu_{ij}^A \cdot \mu_{ij}^B, \nu_{ij}^A + \nu_{ij}^B - \nu_{ij}^A \cdot \nu_{ij}^B)] \forall i \text{ and } j$
- (vi) $A \oplus B = \left[\left(\frac{\mu_{ij}^A + \mu_{ij}^B}{2}, \frac{\nu_{ij}^A + \nu_{ij}^B}{2} \right) \right] \forall i \text{ and } j$
- (vii) $A \otimes B = \left[\left(\sqrt{\mu_{ij}^A + \mu_{ij}^B}, \sqrt{\nu_{ij}^A + \nu_{ij}^B} \right) \right] \forall i \text{ and } j$
- (viii) $A \bowtie B = \left[\left(2 \frac{\mu_{ij}^A \mu_{ij}^B}{\mu_{ij}^A + \mu_{ij}^B}, 2 \frac{\nu_{ij}^A \nu_{ij}^B}{\nu_{ij}^A + \nu_{ij}^B} \right) \right] \forall i \text{ and } j$





Arikrishnan and Sriram

Main Results for Pythagorean Fuzzy Soft Matrices

Since matrices play an important role in many computational techniques, handling dimensionality feature of various problems of related to real life, it motivates to extend the concept of Pythagorean fuzzy soft set to Pythagorean fuzzy soft matrices. (Peng et al. (2015)) defined Pythagorean fuzzy soft set and (Guleria et al. (2018)) are proposed the concept of Pythagorean fuzzy soft matrix.

Definition 3.1. Let $A = [(\mu_{ij}^A, \nu_{ij}^A)] \in PFSM_{m \times n}$. Then,

(i) The Necessity operator of A is denoted by $\boxtimes A$ and defined as

$$\boxtimes A = \left[\left(\mu_{ij}^A, \sqrt{1 - \mu_{ij}^{A^2}} \right) \right] \forall i \text{ and } j$$

(ii) The Possibility operator of A is denoted by $\boxdot A$ and defined as

$$\boxdot A = \left[\left(\sqrt{1 - \nu_{ij}^{A^2}}, \nu_{ij}^A \right) \right] \forall i \text{ and } j$$

Definition 3.2. Let $A, B \in PFSM_{m \times n}$. We define $A \oplus B$, algebraic sum of A and B as

$$A \oplus B = \left[\left(\sqrt{(\mu_{ij}^A)^2 + (\mu_{ij}^B)^2} - (\mu_{ij}^A) \cdot (\mu_{ij}^B), \nu_{ij}^A \cdot \nu_{ij}^B \right) \right] \forall i \text{ and } j.$$

In the following we have to prove some new results related to the necessity and possibility operators of Pythagorean fuzzy soft matrices.

Proposition 3.1. Let $A, B \in PFSM_{m \times n}$. Then $(\boxtimes A + \boxtimes B) \otimes (\boxtimes A \cdot \boxtimes B) = \boxtimes A \otimes \boxtimes B$.

Proof:

$$\begin{aligned} (\boxtimes A + \boxtimes B) &= \left[\left(\mu_{ij}^A + \mu_{ij}^B - \mu_{ij}^A \cdot \mu_{ij}^B, \sqrt{1 - \mu_{ij}^{A^2}} \cdot \sqrt{1 - \mu_{ij}^{B^2}} \right) \right] \\ (\boxtimes A \cdot \boxtimes B) &= \left[\left(\mu_{ij}^A \cdot \mu_{ij}^B, \sqrt{1 - \mu_{ij}^{A^2}} + \sqrt{1 - \mu_{ij}^{B^2}} - \sqrt{1 - \mu_{ij}^{A^2}} \cdot \sqrt{1 - \mu_{ij}^{B^2}} \right) \right] \\ (\boxtimes A + \boxtimes B) \otimes (\boxtimes A \cdot \boxtimes B) &= \left[\left(\mu_{ij}^A + \mu_{ij}^B - \right. \right. \\ &\quad \left. \left. \mu_{ij}^A \cdot \mu_{ij}^B, \sqrt{1 - \mu_{ij}^{A^2}} \cdot \sqrt{1 - \mu_{ij}^{B^2}} \right) \right] \otimes \left[\left(\mu_{ij}^A \cdot \mu_{ij}^B, \sqrt{1 - \mu_{ij}^{A^2}} + \sqrt{1 - \mu_{ij}^{B^2}} - \right. \right. \\ &\quad \left. \left. \sqrt{1 - \mu_{ij}^{A^2}} \cdot \sqrt{1 - \mu_{ij}^{B^2}} \right) \right] \\ &= \left[\left(\frac{\mu_{ij}^A + \mu_{ij}^B}{2}, \frac{\sqrt{1 - \mu_{ij}^{A^2}} + \sqrt{1 - \mu_{ij}^{B^2}}}{2} \right) \right] \end{aligned}$$

$$= \boxtimes A \otimes \boxtimes B$$

Hence, $(\boxtimes A + \boxtimes B) \otimes (\boxtimes A \cdot \boxtimes B) = \boxtimes A \otimes \boxtimes B$

Proposition 3.2. Let $A, B \in PFSM_{m \times n}$. Then $(\boxdot A + \boxdot B) \otimes (\boxdot A \cdot \boxdot B) = \boxdot A \otimes \boxdot B$.

Proof:

$$(\boxdot A + \boxdot B) = \left[\left(\sqrt{1 - \nu_{ij}^{A^2}} + \sqrt{1 - \nu_{ij}^{B^2}} - \sqrt{1 - \nu_{ij}^{A^2}} \cdot \sqrt{1 - \nu_{ij}^{B^2}}, \nu_{ij}^A \cdot \nu_{ij}^B \right) \right]$$





$$\begin{aligned}
 (\diamond A \cdot \diamond B) &= \left[\left(\sqrt{1 - v_{ij}^{A^2}} \cdot \sqrt{1 - v_{ij}^{B^2}}, v_{ij}^A + v_{ij}^B - v_{ij}^A \cdot v_{ij}^B \right) \right] \\
 (\diamond A + \diamond B) @ (\diamond A \cdot \diamond B) &= \left[\left(\sqrt{1 - v_{ij}^{A^2}} + \sqrt{1 - v_{ij}^{B^2}} - \sqrt{1 - v_{ij}^{A^2}} \cdot \sqrt{1 - v_{ij}^{B^2}}, v_{ij}^A \cdot v_{ij}^B \right) \right] @ \left[\left(\sqrt{1 - v_{ij}^{A^2}} \cdot \sqrt{1 - v_{ij}^{B^2}}, v_{ij}^A + v_{ij}^B - v_{ij}^A \cdot v_{ij}^B \right) \right] \\
 &= \left[\left(\frac{\sqrt{1 - v_{ij}^{A^2}} + \sqrt{1 - v_{ij}^{B^2}}}{2}, \frac{v_{ij}^A + v_{ij}^B}{2} \right) \right]
 \end{aligned}$$

= $\diamond A @ \diamond B$.

Hence, $(\diamond A + \diamond B) @ (\diamond A \cdot \diamond B) = \diamond A @ \diamond B$.

Proposition 3.3. Let $A, B \in PFSM_{m \times n}$. Then $(\boxplus A @ \boxplus B) \$ (\boxplus A \bowtie \boxplus B) = \boxplus A \$ \boxplus B$.

Proof:

$$\begin{aligned}
 (\boxplus A @ \boxplus B) &= \left[\left(\frac{\mu_{ij}^A + \mu_{ij}^B}{2}, \frac{\sqrt{1 - \mu_{ij}^{A^2}} + \sqrt{1 - \mu_{ij}^{B^2}}}{2} \right) \right] \\
 (\boxplus A \bowtie \boxplus B) &= \left[\left(2 \frac{\mu_{ij}^A \cdot \mu_{ij}^B}{\mu_{ij}^A + \mu_{ij}^B}, \frac{\sqrt{1 - \mu_{ij}^{A^2}} \cdot \sqrt{1 - \mu_{ij}^{B^2}}}{\sqrt{1 - \mu_{ij}^{A^2}} + \sqrt{1 - \mu_{ij}^{B^2}}} \right) \right] \\
 (\boxplus A @ \boxplus B) \$ (\boxplus A \bowtie \boxplus B) &= \left[\left(\frac{\mu_{ij}^A + \mu_{ij}^B}{2}, \frac{\sqrt{1 - \mu_{ij}^{A^2}} + \sqrt{1 - \mu_{ij}^{B^2}}}{2} \right) \right] \$ \left[\left(2 \frac{\mu_{ij}^A \cdot \mu_{ij}^B}{\mu_{ij}^A + \mu_{ij}^B}, \frac{\sqrt{1 - \mu_{ij}^{A^2}} \cdot \sqrt{1 - \mu_{ij}^{B^2}}}{\sqrt{1 - \mu_{ij}^{A^2}} + \sqrt{1 - \mu_{ij}^{B^2}}} \right) \right] \\
 &= \left[\left(\sqrt{\mu_{ij}^{A^2} \cdot \mu_{ij}^{B^2}}, \sqrt{\sqrt{1 - \mu_{ij}^{A^2}} \cdot \sqrt{1 - \mu_{ij}^{B^2}}} \right) \right] \\
 &= \boxplus A \$ \boxplus B
 \end{aligned}$$

Hence, $(\boxplus A @ \boxplus B) \$ (\boxplus A \bowtie \boxplus B) = \boxplus A \$ \boxplus B$

Proposition 3.4. Let $A, B \in PFSM_{m \times n}$. Then $(\diamond A @ \diamond B) \$ (\diamond A \bowtie \diamond B) = \diamond A \$ \diamond B$.

Proof:

$$\begin{aligned}
 (\diamond A @ \diamond B) &= \left[\left(\frac{\sqrt{1 - v_{ij}^{A^2}} + \sqrt{1 - v_{ij}^{B^2}}}{2}, \frac{v_{ij}^A + v_{ij}^B}{2} \right) \right] \\
 (\diamond A \bowtie \diamond B) &= \left[\left(2 \frac{\sqrt{1 - v_{ij}^{A^2}} \cdot \sqrt{1 - v_{ij}^{B^2}}}{\sqrt{1 - v_{ij}^{A^2}} + \sqrt{1 - v_{ij}^{B^2}}}, 2 \frac{v_{ij}^A \cdot v_{ij}^B}{v_{ij}^A + v_{ij}^B} \right) \right] \\
 (\diamond A @ \diamond B) \$ (\diamond A \bowtie \diamond B) &= \left[\left(\frac{\sqrt{1 - v_{ij}^{A^2}} + \sqrt{1 - v_{ij}^{B^2}}}{2}, \frac{v_{ij}^A + v_{ij}^B}{2} \right) \right] \$ \left[\left(2 \frac{\sqrt{1 - v_{ij}^{A^2}} \cdot \sqrt{1 - v_{ij}^{B^2}}}{\sqrt{1 - v_{ij}^{A^2}} + \sqrt{1 - v_{ij}^{B^2}}}, 2 \frac{v_{ij}^A \cdot v_{ij}^B}{v_{ij}^A + v_{ij}^B} \right) \right]
 \end{aligned}$$





Arikrishnan and Sriram

$$= \left[\left(\sqrt{\sqrt{1 - v_{ij}^{A^2}} \cdot \sqrt{1 - v_{ij}^{B^2}}}, \sqrt{v_{ij}^{A^2} \cdot v_{ij}^{B^2}} \right) \right]$$

= $\diamond A \diamond B$

Hence, $(\diamond A @ \diamond B) \diamond (\diamond A \bowtie \diamond B) = \diamond A \diamond B$.

Pythagorean Fuzzy Soft Matrix Theory Apply in Agriculture

Definition 4.1. Value matrix

Let $A = [(\mu_{ij}^A, v_{ij}^A)] \in PFSM_{m \times n}$. Then A is said to be value of Pythagorean fuzzy soft matrix denoted by $V(A)$ and is define as $V(A) = [(\mu_{ij}^A - v_{ij}^A)]$ if $i = 1, 2, \dots, m, j = 1, 2, \dots, n$ for all i and j .

Definition 4.2. Score matrix

If $A = [(\mu_{ij}^A, v_{ij}^A)], B = [(\mu_{ij}^B, v_{ij}^B)] \in PFSM_{m \times n}$. Then A and B is said to be Pythagorean fuzzy soft score matrix denoted by $S(A, B)$ and is defined as $S(A, B) = V(A) - V(B)$.

Definition 4.3. Total score

If $A = [(\mu_{ij}^A, v_{ij}^A)], B = [(\mu_{ij}^B, v_{ij}^B)] \in PFSM_{m \times n}$. Let the corresponding value matrix be $V(A), V(B)$ and their score matrix is $S(A, B)$. Then the total for each U_i in U is $S_i = \sum(V(A) - V(B)) = \sum[(\mu_{ij}^A - v_{ij}^A)] - [(\mu_{ij}^B, v_{ij}^B)]$.

METHODOLOGY

Suppose U is a set of farmers producing quality of wheat to be selected as the best farmer for the healthier yields produced to the human existence without affecting their health. This will be scientifically selected and tested by the experts in Agriculture according to the natural manures, chemical fertilizers, pesticides used by the farmers. Let E is a set of parameters related to the yield cultivated by the farmers from the fields, for good health. We construct $PFSS(F_A, E)$ over U represent theselection of farmers by the scientist, expert in Agriculture X , where is a mapping $F_A: E \rightarrow I^U$ is the collection of all Pythagorean fuzzy subsets of U . We further construct another $PFSS(G_B, E)$ over U represent the selection of farmers by theexpert in Agricultural field Y , where G_B is a mapping $G_B: E \rightarrow I^U$ is the collection of all Pythagorean fuzzy subsets of U . The matrices A and B corresponding tothe Pythagorean fuzzy soft sets (F_A, E) and (G_B, E) are constructed. We compute the complements $(F_A, E)^c$ and $(G_B, E)^c$ and their matrices A^c and B^c corresponding to $(F_A, E)^c$ and $(G_B, E)^c$ respectively. Then compute $A \oplus B$ which is the maxi-mum membership of farmers who will be selected by the scientist as judges. Further compute $A^c \oplus B^c$ which is the maximum membership of non selection of farmer’s bythe scientist as judges. Using definition (4.1), compute $V(A \oplus B), V(A^c \oplus B^c)$ and $S((A \oplus B); (A^c \oplus B^c))$ and the total score secured S_i for each farmer in U . Finally $S_k = \max(S_i)$, then we conclude that the farmer U_k has been selected by the judges. If S_k has more than one value occurs and by investigating this process repeatedly by reassessing the parameters.

Procedural Steps of the Proposed Algorithm

Step 1: Input the Pythagorean fuzzy soft set $(F_A, E), (G_B, E)$ and obtain thePythagorean fuzzy soft matrices A, B corresponding to (F_A, E) and (G_B, E) respectively.

Step 2: Write the Pythagorean fuzzy soft complement sets $(F_A, E)^c, (G_B, E)^c$ and obtain the Pythagorean fuzzy soft matrices A^c, B^c corresponding to $(F_A, E)^c$ and $(G_B, E)^c$ respectively.

Step 3: Find the algebraic sum of Pythagorean fuzzy soft matrices A and B and their complement matrices A^c and B^c .





Arikrishnan and Sriram

Step 4: Compute value matrix $V (A \oplus B), V (A^c \oplus B^c)$

Step 5: Compute score matrix $S ((A \oplus B), (A^c \oplus B^c))$.

Step 6: Compute the total score S_i for each U_k in U .

Step 7: Find $S_k = \max (S_i)$, then we conclude the best farmer U_k has the maximum value, since U_k produced healthy and Quality of wheat. If S_k has more than one value, then go to step (1) so as to repeat the process by reassessing the parameter for selecting the best farmer.

Application of Technology in Decision Making Problem

Let (F_A, E) and (G_B, E) be two Pythagorean fuzzy soft set representing the selection of four farmers from the universal set $X = \{x_1, x_2, \dots, x_m\}$ by the experts X and Y .

Let $E = \{e_1, e_2, \dots, e_n\}$ be the set of parameters which stand for different types of manures like, natural manure, chemical fertilizer and pesticides will be taken to identify the best farmer by testing the wheat which will be considered for good health to human race. In the section in [14], defined the addition of intuitionistic fuzzy soft matrices. Now, we have use the algebraic sum of Pythagorean fuzzy soft matrices in to find a solution to this problem.

Step 1:

$$\begin{aligned}
 (F_A, E) &= \{ F_A(e_1) = \{(u_1, 0.8, 0.2), (u_2, 0.5, 0.4), (u_3, 0.6, 0.1), (u_4, 0.6, 0.3)\} \\
 &\{ F_A(e_2) = \{(u_1, 0.7, 0.2), (u_2, 0.4, 0.6), (u_3, 0.2, 0.6), (u_4, 0.8, 0.1)\} \\
 &\{ F_A(e_3) = \{(u_1, 0.6, 0.4), (u_2, 0.7, 0.3), (u_3, 0.7, 0.1), (u_4, 0.4, 0.3)\} \\
 \\
 (G_B, E) &= \{ G_B(e_1) = \{(u_1, 0.7, 0.3), (u_2, 0.6, 0.3), (u_3, 0.4, 0.5), (u_4, 0.7, 0.1)\} \\
 &\{ G_B(e_2) = \{(u_1, 0.6, 0.4), (u_2, 0.7, 0.2), (u_3, 0.9, 0.1), (u_4, 0.4, 0.1)\} \\
 &\{ G_B(e_3) = \{(u_1, 0.5, 0.3), (u_2, 0.8, 0.2), (u_3, 0.5, 0.5), (u_4, 0.3, 0.7)\}
 \end{aligned}$$

These two Pythagorean fuzzy soft sets are represented by the following Pythagorean fuzzy soft matrices respectively

$$A = \begin{matrix} u_1 \\ u_2 \\ u_3 \\ u_4 \end{matrix} \begin{pmatrix} (0.8, 0.2) & (0.7, 0.2) & (0.6, 0.4) \\ (0.5, 0.4) & (0.4, 0.6) & (0.7, 0.3) \\ (0.6, 0.1) & (0.2, 0.6) & (0.7, 0.1) \\ (0.6, 0.3) & (0.8, 0.1) & (0.4, 0.3) \end{pmatrix}$$

$$B = \begin{matrix} u_1 \\ u_2 \\ u_3 \\ u_4 \end{matrix} \begin{pmatrix} (0.7, 0.3) & (0.6, 0.4) & (0.5, 0.3) \\ (0.6, 0.3) & (0.7, 0.2) & (0.8, 0.2) \\ (0.4, 0.5) & (0.9, 0.1) & (0.5, 0.5) \\ (0.7, 0.1) & (0.4, 0.1) & (0.3, 0.7) \end{pmatrix}$$

Step 2: The Pythagorean fuzzy soft complement matrices of the Pythagorean fuzzy soft matrices obtained in step 1 are computed as follows.





$$A^c = \begin{matrix} u_1 \\ u_2 \\ u_3 \\ u_4 \end{matrix} \begin{pmatrix} (0.2,0.8) & (0.2,0.7) & (0.4,0.6) \\ (0.4,0.5) & (0.6,0.4) & (0.3,0.7) \\ (0.1,0.6) & (0.6,0.2) & (0.1,0.7) \\ (0.3,0.6) & (0.1,0.8) & (0.3,0.4) \end{pmatrix}$$

$$B^c = \begin{matrix} u_1 \\ u_2 \\ u_3 \\ u_4 \end{matrix} \begin{pmatrix} (0.3,0.7) & (0.4,0.6) & (0.3,0.5) \\ (0.3,0.6) & (0.2,0.7) & (0.2,0.8) \\ (0.5,0.4) & (0.1,0.9) & (0.5,0.5) \\ (0.1,0.7) & (0.1,0.4) & (0.7,0.3) \end{pmatrix}$$

Step 3: Find the algebraic sum of the Pythagorean fuzzy soft matrices A, B and their complement matrix obtained in step 1 and step 2 have been obtained as below.

$$A \oplus B = \begin{matrix} u_1 \\ u_2 \\ u_3 \\ u_4 \end{matrix} \begin{pmatrix} (0.9,0.06) & (0.7,0.08) & (0.7,0.1) \\ (0.7,0.1) & (0.7,0.1) & (0.9,0.06) \\ (0.6,0.05) & (0.9,0.06) & (0.8,0.05) \\ (0.8,0.03) & (0.7,0.01) & (0.5,0.2) \end{pmatrix}$$

$$A^c \oplus B^c = \begin{matrix} u_1 \\ u_2 \\ u_3 \\ u_4 \end{matrix} \begin{pmatrix} (0.3,0.5) & (0.4,0.4) & (0.5,0.3) \\ (0.5,0.3) & (0.6,0.3) & (0.3,0.5) \\ (0.5,0.2) & (0.6,0.2) & (0.5,0.3) \\ (0.3,0.4) & (0.1,0.3) & (0.7,0.1) \end{pmatrix}$$

Step 4: Calculate the value matrix $V(A \oplus B), V(A^c \oplus B^c)$ obtained in step 3 are:

$$V(A \oplus B) = \begin{matrix} u_1 \\ u_2 \\ u_3 \\ u_4 \end{matrix} \begin{pmatrix} 0.8 & 0.6 & 0.6 \\ 0.6 & 0.6 & 0.8 \\ 0.5 & 0.8 & 0.8 \\ 0.8 & 0.7 & 0.3 \end{pmatrix}$$

$$V(A^c \oplus B^c) = \begin{matrix} u_1 \\ u_2 \\ u_3 \\ u_4 \end{matrix} \begin{pmatrix} -0.2 & 0.0 & 0.2 \\ 0.2 & 0.3 & -0.2 \\ 0.3 & 0.4 & 0.2 \\ -0.1 & -0.2 & 0.6 \end{pmatrix}$$

Step 5: Compute the score matrix $S((A \oplus B), (A^c \oplus B^c))$ obtained in step 5 are:

$$S((A \oplus B), (A^c \oplus B^c)) = \begin{matrix} u_1 \\ u_2 \\ u_3 \\ u_4 \end{matrix} \begin{pmatrix} 1.0 & 0.6 & 0.4 \\ 0.4 & 0.3 & 1.0 \\ 0.2 & 0.4 & 0.6 \\ 0.9 & 0.9 & -0.3 \end{pmatrix}$$

Step 6: Total score for the best farmer obtained in step 5 is :

$$\begin{matrix} S_1 \\ S_2 \\ S_3 \\ S_4 \end{matrix} \begin{pmatrix} 2.0 \\ 1.7 \\ 1.2 \\ 1.5 \end{pmatrix}$$

Step 7: S_1 has maximum value and the farmer who has used natural manure has the maximum yield. Thus we conclude that from both the scientific experts opinion farmer u_1 is selected as best one.





CONCLUSION

In this paper, using the algebraic sum of Pythagorean fuzzy soft matrices, we constructing a more efficient decision - making method. The analysis of best farmer problems that their good healthier yields using Pythagorean fuzzy soft matrices is studied.

REFERENCES

1. A. Arikrishnan and S. Sriram, Necessity and possibility operators on Pythagorean fuzzy soft matrices, *AIP Conference Proceedings*, 2177, pp. 020010(1)-020010(8), 2019.
2. A. Arikrishnan and S. Sriram, Some Operators on Pythagorean fuzzy soft matrices, *TWMS J. App. And Eng. Math.*, 11(4), 1138-1147, 2021.
3. K.T. Atanassov, Intuitionistic fuzzy sets, *Fuzzy Sets and Systems*, 20(1),87-96, 1986.
4. B. Chetia and P.K. Das, Some Results of Intuitionistic Fuzzy Soft Matrix Theory, *Advances in Applied Science Research*, 3(1), 412-423, 2012.
5. R.K. Bajaj and A. Guleria, Dimensionality Reduction Technique in DecisionMaking Using Pythagorean Fuzzy Soft Matrices, *Recent Patents on ComputerScience*, 12, 1-8, 2019.
6. A. Guleria and R.K. Bajaj, On Pythagorean fuzzy soft matrices, operations andtheir applications in decision making and medical diagnosis, *Methodologies andApplication*, 1-12, 2018.
7. M. Pal., S.K. Khan and A.K. Shyamal, Intuitionistic Fuzzy Matrices, *Notes onintuitionistic fuzzy sets*, 2(2), 51-62, 2002.
8. P.K. Maji, R. Biswas and A.R. Roy, Intuitionistic Fuzzy Soft Sets, *J. Fuzzymath.*, 9, 677-692, 2001.
9. A.R. Meenakshi and M. Kaliraja, An Application of Interval Valued Fuzzy Matrices in Medical Diagnosis, *Int. Journal of Math. Analysis*, 5(36), 1791-1802,2011.
10. T. Muthuraji, S. Sriram and P. Murugadas,Decomposition of intuitionistic fuzzy matrices, *Fuzzy information and engineering*, 8(3), 345-354, 2016.
11. D.A. Molodstov, Soft set theory first - result, *Computers and Mathematics withApplications*, 37, 19-31, 1999.
12. M.J.I. Mondal and T.K. Roy, Intuitionistic Fuzzy Soft Matrix Theory, *Mathematics and Statistics*, 1(2), 43-49, 2013.
13. X. Peng, Y. Yang. J. Song, Y. Jiang, Pythagorean fuzzy soft set and its application, *Comput.Eng*, 41, 224-229. 2015.
14. N. Sarlala and S. Rajkumari, Invention of Best Technology In Agriculture Using Intuitionistic Fuzzy Soft Matrices, *International Journal of Scientific andTechnology Research*, 3(5), 286-290, 2014.
15. I.Silambarasan and S.Sriram, Algebraic Operations On Pythagorean Fuzzy Matrices, *Mathematical Science International Research Journal*, 7(2), 406-414, 2020.
16. R.R. Yager and A.M. Abbasov, Pythagorean membership grades, complex numbers, and Decision making, *Int. J. Intell. Syst.*, 28, 436-452, 2013.
17. L.A Zadeh, Fuzzy Sets, *Information and Control*, 8, 338-353, 1965.





A Pharmaceutical Review of Nanoemulsion

N. Jayaram^{1*}, A. Kottaimuthu² and G. Alagu Manivasagam³

¹PG Student, Department of Pharmacy, Annamalai University, Chidambaram, Tamil Nadu, India.

²Associate Professor, Department of Pharmacy, Annamalai University, Chidambaram, Tamil Nadu, India.

³Assistant Professor, Department of Pharmacy, Annamalai University, Chidambaram, Tamil Nadu, India.

Received: 02 Dec 2021

Revised: 30 Dec 2021

Accepted: 24 Jan 2022

*Address for Correspondence

N. Jayaram

PG Student,

Department of Pharmacy,

Annamalai University,

Chidambaram, Tamil Nadu, India.

Email: jayaramjai2373@gmail.com



This is an Open Access Journal / article distributed under the terms of the **Creative Commons Attribution License** (CC BY-NC-ND 3.0) which permits unrestricted use, distribution, and reproduction in any medium, provided the original work is properly cited. All rights reserved.

ABSTRACT

One of the fastest-growing sectors in medicine is nanotechnology. The term "nano" refers to particle sizes ranging from 1 to 1000 micrometres. Nanoemulsion is a colloidal dispersion system made up of two immiscible liquids and an emulsifying agent in nanoscale. They're utilised to boost the bioavailability of hydrophobic medicines and medications with a high first-pass metabolism. It has a steady thermodynamic state and is optically clear and transparent. The nanoemulsion forms easily and sometimes spontaneously, with little or no input of energy. In most circumstances, in addition to the surfactant, a cosurfactant or cosolvent is utilised the size and structure of particles distributed in the continuous phase are the primary differences between emulsion and nanoemulsion. This article intends to provide information on the ingredients used in nanoemulsion formulations, as well as preparation procedures, evaluation criteria, characterization, and applications.

Keywords: Nanoemulsion, high energy method, low energy method.

INTRODUCTION

Emulsification is a two-phase system in which one phase is distributed in the other as minute drops with diameters ranges from 0.1 to 100 m, which function as drug carriers. The inclusion of an emulsifier can help to stabilise a thermodynamically unstable solution. The dispersed phase is the internal phase, also known as the discontinuous phase, whereas the dispersion medium is the outer phase, also known as the continuous phase. The emulsifier is also referred to as an intermediate or interphase product. A Nanoemulsion seems to be a fine dispersion of oil in water or water in oil that is stabilised by an inter - facial coating of a surfactant molecule with a particle diameter ranging





Jayaram et al.,

from 20 to 600 nm. They improve the therapeutic efficiency of the treatment while reducing side effects and adverse reactions when used as a drug delivery vehicle. Nanoemulsions are transparent due to its small size [1].

TYPES OF NANOEMULSION

There are three basic forms of nanoemulsions:

1. Oil-in-water nanoemulsions in which the oil is distributed in a continuous aqueous phase
2. Water-in-oil nanoemulsions in which the water is distributed throughout the oil phase.
3. Nanoemulsion that seems to be Bicontinuous [1].

FORMULATION INGREDIENTS OF NANOEMULSION

Oil, water, surfactant, lipid and water-soluble cosolvent are all used in nanoemulsion system. Three basic elements required for the production of nanoemulsion;

1. Oils: Oil phases are widely used in the development of nanoemulsion, which have a high drug load. Oil phase can contain triglycerides such as tri-, di- or monoacylglycerols. The choice of oil is primarily governed by the drug's solubility [2].
2. Surfactant: The surfactant must be carefully chosen in order to obtain an ultra-low interfacial tension, which is a key requirement for nanoemulsion production. To develop a nanoemulsion, the surfactant concentration must be high enough to stabilise the microdroplets and it must be flexible or flowable enough to facilitate formation [1].
3. Co-surfactant: Nanoemulsion production requires a very low negative interfacial tension. Cosurfactants or cosolvents are used in combination with a surfactant for this purpose.

The following (Table 1) are the examples for the ingredients used in nanoemulsion [3]:

FORMULATION TECHNIQUES OF NANOEMULSION

Nanoemulsion drug delivery system was developed using a variety of techniques, some of which overlap. The following is a classification of several ways for creating nanoemulsion drug delivery systems based on energy needs, phase inversion nature, and self-emulsification.

HIGH ENERGY METHODS

To formulate nanoemulsions, high energy methods are commonly used⁴. Breaking large droplets into nanoscale droplets consumes a lot of mechanical energy to make nanoemulsions with a high kinetic energy. Disruptive forces are generated by mechanical devices such as ultrasonic devices, microfluidizers, and high-pressure homogenizers [2]. We can achieve better particle size control using a range of formulation composition and high-energy methods. Rheology, stability and colour control of the emulsion are also ensured by high-energy processes. The following are the list of high-energy methods:

High-pressure homogenization

Because nanoemulsion production requires a high shear force, this technique employs a piston homogenizer or high-pressure homogenizer to create nanoemulsions with incredibly tiny droplet sizes upto 1 nanometer. The mixture is pushed through an orifice at a high pressure in the range of 500 to 5000 psi using this technique. The resulting emulsion is exposed to high turbulence and hydraulic shear, resulting in a fine-particle emulsion. This has been known to be a more effective method of producing nanoemulsions; nevertheless, the sole disadvantage is the high energy consumption and elevated emulsion temperature during processing [5].

Micro fluidization

This approach employed a microfluidizer, which employs a high-pressure (500 to 20,000 psi) pump to force the product through a stainless-steel microchannel interaction chamber at the impact region, resulting in the production of very small submicron particles. The microfluidizer is used to cycle the mixture until it achieves the required size of the particles. The resultant nanoemulsion is next filtered to separate the tiniest from the biggest droplets and produce a homogeneous nanoemulsion [6].





Jayaram *et al.*,

Ultrasonication

In this approach, the premixed emulsion is agitated at a 20 kHz ultrasonic frequency, decreases the size of the droplets to nanodroplets. The emulsion is subsequently driven through the high shear area, resulting in droplets of uniform size. Sonotrodes, also known as sonication probes, were made composed of piezoelectric quartz crystals that provided energy for ultrasonic emulsification. These sonotrodes compress and expand when an electrical alternating voltage is applied to them. Mechanical vibrations occur, when the sonicator tip comes into contact with the resultant liquid, cavitation occurs, forcing the vapour cavities to collapse. This method is applied when a droplet size of less than 0.2 is needed [7].

LOW ENERGY PROCESSES

Nanoemulsion systems require a minimal amount of energy to manufacture. Low energy emulsification methods seem to be more energy efficient since they form nanoemulsions by depending on the system's intrinsic chemical energy and only require gentle agitation. Low-energy emulsification techniques include phase inversion emulsification and semi-emulsification [8].

Phase Inversion procedures:

Chemical energy is produced during the emulsification process due to phase transitions in these processes[9]. Altering the composition at constant temperature or changing the temperature at constant composition can produce the requisite number of phase transitions¹⁰.

Transitional Phase Inversion –TPI - Phase Inversion Temperature-PIT:

The temperature is altered to a constant composition in this operation. Polyethoxylated surfactants, for example, are non-ionic surfactants having a temperature-dependent solubility. Emulsification is accomplished by changing the temperature-dependent affinities of surfactants for water and oil [11,12]. Due to the dehydration of polyoxyethylene groups, polyethoxylated surfactants become lipophilic when heated. As a result, the principle of creating nanoemulsions via the PIT approach is established. It is important to bring the temperature of the sample to the PIT level or HLB level in order to create nanoemulsions using the PIT method [9]. In the PIT technique, droplet diameters and interfacial tensions are at their lowest. Because of the exceptionally lower interfacial tension at the HLB temperature, this approach favours emulsification. However, emulsification has been reported to occur spontaneously at HLB temperature, with a high rate of coalescence [13]. Emulsions are both rapid and unstable. It has been found that quick cooling of the emulsion can produce fine and stable emulsion droplets near to the PIT temperature [14,15].

Phase Inversion Composition - PIC

The composition is altered at a steady temperature in this method. Nanoemulsions are made by continuously adding water or oil to an oily or aqueous surfactant combination. Because the component is added to an emulsion, the PIC method is more appropriate for large-scale manufacturing than the PIT technique [8]. The addition of water to the system raises the water volume, resulting in a transitional composition, in which the degree of hydration of the surfactant's polyoxyethylene chains rises, and the curvature of the surfactant spontaneously changes from negative to zero. The transition composition, like the HLB temperature, maintains a balance of the surfactant's hydrophilic-lipophilic characteristics. Small droplets of metastable oil in water are formed when this transition composition is exceeded. Because no curvature structures are separated, the composite is formed [9].

Catastrophic Phase Inversion-CPI - Emulsion Inversion Point-EPI

Phase inversion in the EIP process is accomplished by CPI mechanisms [16]. Changes in the fractional dispersed phase volume, instead of the surfactant characteristics, cause catastrophic phase inversion. When water is introduced to the oil-surfactant mixture, the system begins to behave like a W/O nanoemulsion [17,18,19]. The water droplets melt and the phase inversion point is achieved with increased water addition over a critical water content and continual stirring, resulting in bicontinuous or lamellar structures. Through an intermediate bicontinuous microemulsion, subsequent dilution with water generates a phase inversion from a W/O to an O/W system. The



**Jayaram et al.,**

diameter of the nanoemulsion droplets generated is controlled by process factors like water addition rate and agitation rate. The surfactant must be mostly present in the dispersed phase for catastrophic phase inversion to occur, since the coalescence rate must be high and fast phase inversion must occur. Both W / O and O / W emulsions can be stabilised by surfactants [16,17,20]. The surfactant is mostly in the dispersion phase during the catastrophic phase inversion; therefore, it acts as an abnormal emulsion (unstable emulsion), according to the Bancroft criteria. As per Bancroft's principles, the emulsifier must be mainly in the continuous phase for a stable emulsion (normal emulsion) [21]. As a result, the abnormal emulsion undergoes catastrophic phase inversion, resulting in the formation of a more stable nanoemulsion.

Self-nano emulsification technique

The Self nanoemulsification method allows nanoemulsions to be formed without affecting the surfactant's spontaneous curvature. Turbulence and nanometer-sized emulsion droplets result from surfactants and/or cosolvent molecules quickly migrating from the dispersed to the continuous phases. This approach is also known as spontaneous emulsification [8].

Characterization of Nanoemulsion

The lack of an internal phase, creaming, microbial degradation, and the protection of appearance, smell consistency and colour are all characteristics of a stable nanoemulsion [39].

EVALUATION OF NANOEMULSION**Thermodynamic stability**

Various thermodynamic stability experiments are conducted on the selected formulation.

Heating cooling cycle

Refrigerators with temperatures ranging from 4 to 45 degrees are evaluated over six cycles, with storage at any temperature lasting at least 48 hours. At these temperatures, the formulations that are stable are centrifuged.

Centrifugation

Prepared formulations are centrifuged for about 30 mins at 5000rpm. The formulations which are not phase separate were put through further rigorous testing.

Freeze -thaw cycle

The formulations are frozen and thawed three times at temperatures ranging from -18°C to +25°C, with at least 48 hours of storage at each temperature.

Particle size determination

Several methods, including photon correlation spectroscopy, hydrodynamic chromatography, Spectroturbidimetry, sedimentation, zone of detection, field flow fractionation and electron microscopy, can be used to estimate the particle size of an emulsion.

Zeta Potential Determination

The surface potential is measured using the zeta potential. The magnitude of the zeta potential is a measure of an emulsion's potential stability. The stability of an emulsion and other colloidal dispersions is determined by the zeta potential. To stabilise a colloidal system, a zeta potential larger than roughly 25 mV is usually necessary. The zeta potential is influenced by the concentration of counter ions in the solution, the particle surface charge density, the polarity of the solvent, and the temperature. The Malvern Zeta Meter or the Nicomp Particle Meter can be used to calculate the zeta potential. Electrophoretic light scattering is used to determine the zeta potential (ELS). The zeta potential may be derived from the electrokinetic mobility using the Smoluchowski equation.

$\mu = \zeta \epsilon / \eta$ equation. Where ϵ is the permittivity and η is the liquid viscosity used [40].



**Jayaram et al.,****Percentage Drug content**

1 mL nanoemulsion is combined with 10 mL appropriate solvent. After filtering the stock solution, aliquots of various concentrations are made using suitable dilutions; the absorbance is evaluated using UV spectroscopy. The drug content is determined using the equation derived from the calibration curve's linear regression analysis.

PH measurement

A digital pH metre is used to determine the pH of various nanoemulsion compositions. The pH value of 1 g of nanoemulsion dissolved in 100 ml of pure water is measured. To eliminate inaccuracies, the measurement is repeated three times.

Determination of % transparency and drug precipitation

Formulations with various proportions are chosen based on the ternary phase diagram. Transparency research is conducted to establish the highest percentage of drug transparency and precipitation between the oil, surfactant combination (surfactant and co-surfactant), and water containing 1% of the drug (When diluted with pure water, the nanoemulsion system is clear).

Viscosity determination:

A Brookfield viscometer is used to determine the nanoemulsion's viscosity. The viscosity of 20 mL of nanoemulsion in a 25 mL beaker is tested with spindle number 6 at 10 rpm.

In vitro Diffusion studies

The diffusion investigations of the developed nanoemulsions are performed using a Franz diffusion cell and a cellophane membrane. A nanoemulsion sample (5 ml) is placed on the cellophane membrane, and the diffusion studies are performed at 37 ° C with 250 ml of (25%) methanolic phosphate buffer of PH 7.4. For every 1, 2, 3, 4, 5, 6, 7, and 8 hours, to keep the sink condition, 5 ml of each sample was taken and replaced with an equal volume of new dissolving media. Samples are analysed by UV-spectrophotometer for the active component concentration at 271 nm.

Dye test

When a water-soluble dye is introduced to an o/w nanoemulsion, the colour is uniformly distributed; but, when the emulsion is w/o and the dye is water-soluble, the colour is only distributed in the dispersion phase, and the emulsion's colour is not uniform. This may be determined immediately by looking at the emulsion under a microscope.

Refractive index

The Abbes refractometer is used to determine the refractive index of a nanoemulsion.

Polydispersity

It refers to the nanoemulsion's homogeneous droplet size. The lower the homogeneity of the nanoemulsion droplet size, the higher the polydispersity value obtains. The standard deviation to mean drop size ratio is the term used to describe it. A spectrophotometer is used to assess it.

Fluorescence test

When oils are subjected to UV light, they fluorescence. If a non-fluorescent nanoemulsion is subjected to fluorescent light under a microscope, the whole field fluoresces. The nanoemulsion is of the o/w type if the fluorescence is irregular.

Conductance measurement

A conductometer is used to determine the nanoemulsion's conductivity. This test involves immersing a pair of electrodes attached to a light and an electrical source in an emulsion. The water conducts electricity when the





Jayaram *et al.*,

emulsion is O/W, and the lamp lights up as a result of the current travelling between the electrodes. Because the oil in the outer phase does not convey any current, the lamp does not light up when the emulsion is w/o [41].

ADVANTAGES OF NANOEMULSION [42,43,44]

- It can play the role of liposomes and vesicles.
- It enhances drug bioavailability.
- It has increased physical strength.
- It is non-irritant and non-poisonous in nature.
- Nanoemulsions include small droplets with a larger surface area, leading to greater absorption.
- It's available in a variety of forms, including foams, creams, liquids, and aerosols.
- Promotes Greater oil-soluble supplement absorption in cell culture technology.
- Assists in the solubilization of lipophilic drugs.
- It can be used to hide a bad taste.
- There is a reduction in the amount of energy used.

CONCLUSION

Nanoemulsions serve as a vehicle for delivering medications that are less water soluble. They solubilize the drug in the aqueous phase with oils and surfactants, which subsequently act as a carrier. In this review, the various techniques of nanoemulsion preparation as well as the evaluation parameters are discussed. Nanoemulsions are a new frontier in innovative drug delivery systems, and they will continue to advance in the future with new developments.

REFERENCES

1. Jaiswal, Manjit, Dudhe,Rupesh, Sharma PK, Nanoemulsion:an advanced mode of drug delivery system. 3 Biotech, 2015;5(2):123-127.
2. Goncalves A, Nikmaram N, Roohinejad S, Estevinho BN, Rocha F, Greiner R, et al. Production, properties, and applications of solid self-emulsifying delivery systems (S-SEDS) in the food and pharmaceutical industries.Colloids and Surfaces A:Physicochemical and Engineering aspects. 2018; 538:108-126.
3. Chavda, Vivek P. Applications of Targeted Nano Drugs and Delivery Systems .Nanobased Nano Drug Delivery.2019:76.
4. Mahdi Jafari S, He Y, Bhandari B. Nano-emulsion production by sonication and microfluidization—A comparison. International Journal of Food Properties. 2006; 9(3):475-485.
5. Yilmaz E, Borchert HH. Effect of lipid-containing, positively charged nanoemulsions on skin hydration, elasticity and erythema- an in vivo study. International Journal of Pharmceutics.2006;307(2):232-238.
6. Uluata S, Decker EA, McClements DJ. Optimization of Nanoemulsion Fabrication Using Microfluidization: Role of Surfactant Concentration on Formation and Stability. Food Biophysics.2016;11:52-59.
7. ShiY, Li H, Li J, Zhi D, Zhang X, Liu H, et al. Development, optimization and evaluation of emodin loaded nanoemulsion prepared by ultrasonic emulsification. Journal of Drug Delivery Science and Technology.2015;27:46-55.
8. Solans C, Solé I. Nano-emulsions: Formation by low-energy methods. Current Opinion in Colloid &Interface Science. 2012;17(5):246-254.
9. Anandharamakrishnan C. Techniques for Nanoencapsulation of Food Ingredients, Springer, 2014:14-16.
10. Thakur A, Walia M.K, and Kumar S.L.H. Nanoemulsion in Enhancement of Bioavailability of Poorly Soluble Drugs: A Review. Pharmacophore.2013;4(1):15-25.
11. Lovelyn C, and Attama A.A. Current State of Nanoemulsions in Drug Delivery, Journal of Biomaterials and Nanobiotechnology.2011;2(5): 626-639.
12. Chime S.A., Kenechukwu F.C, and Attama A.A., Nanoemulsions-Advances in Formulation, Characterization and Applications in Drug Delivery, Ali DS, Application of Nanotechnology in Drug Delivery.2014; 77-111.





Jayaram et al.,

13. Ee S., Duan X., Liew C and Nyugen Q. Droplet size and stability of nano-emulsions produced by the temperature phase inversion method, *Chemical Engineering Journal*,2008;140(1-3): 626–631.
14. Tadros T, Izquierdo P, Esquena J, and Solans C. Formation and stability of nano-emulsions, *Advances in Colloid and Interface Science*.2004; 108-109: 303–318.
15. Rajalakshmi R., Mahesh K, and Kumar C.K.A. A Critical Review on Nano Emulsions, *International Journal of Innovative Drug Discovery*.2011;1:1-8.
16. Sokolov YV. Nanoemulsion formation by low-energy methods: A review. *Visn farm*. 2014. 3:16-19.
17. Fernandez P, André V, Rieger J, Kühnle A. Nano-emulsion formation by emulsion phase inversion. *Colloids and Surfaces A Physicochemical Engineering Aspects*. 2004. 251(1-3):53-58.
18. Ishak KA, Annuar MSM. Phase inversion of medium-chain-length poly-3-hydroxyalkanoates (mcl-PHA)-incorporated nanoemulsion: effects of mcl-PHA molecular weight and amount on its mechanism. *Colloid and Polymer Science*. 2016;294(12):1969-1981.
19. McClements DJ, Rao J. Food-grade nanoemulsions: formulation, fabrication, properties, performance, biological fate, and potential toxicity. *Critical Reviews in Food Science Nutrition*. 2011;51(4):285-330.
20. Armanet L, Hunkeler D. Phase inversion of polyacrylamide-based inverse-emulsions: Influence of inverting-surfactant type and concentration. *Journal of Applied Polymer Science*. 2007; 103(6):3567-3584.
21. Perazzo A, Preziosi V, Guido S. Phase inversion emulsification: current understanding and applications. *Advances in Colloid and Interface Science*. 2015; 222:581-599.
22. Singh KK, Vingkar SK. Formulation, antimalarial activity and biodistribution of oral lipid nanoemulsion of primaquine. *International Journal of Pharmaceutics*. 2008;347(1-2):136-143.
23. Klang V, Matsko N, Zimmermann AM, Vojnikovic E, Valenta C. Enhancement of stability and skin permeation by sucrose stearate and cyclodextrins in progesterone nanoemulsions. *International Journal of Pharmaceutics*. 2010;393(1-2):153-161.
24. Baspinar Y, Keck CM, Borchert HH. Development of a positively charged prednicarbate nanoemulsion. *International Journal of Pharmaceutics*. 2010;383(1-2):201-08.
25. Zhu L, Li M, Dong J, Jin Y. Dimethyl silicone dry nanoemulsion inhalations: Formulation study and anti-acute lung injury effect. *International Journal Pharmaceutics*. 2015;491(1-2):292-298.
26. Meng L, Xia X, Yang Y, Ye J, Dong W, Ma P, et al. Coencapsulation of paclitaxel and baicalein in nanoemulsions to overcome multidrug resistance via oxidative stress augmentation and P-glycoprotein inhibition. *International Journal of Pharmaceutics* 2016;513(1-2):8-16.
27. Baboota S, Shakeel F, Ahuja A, Ali J, Shafiq S. Design development and evaluation of novel nanoemulsion formulations for transdermal potential of Celecoxib. *Acta Pharmaceutica*. 2007;57(3):315-332.
28. Başpınar Y, Gündoğdu E, Köksal C, Karasulu E. Pitavastatin-containing nanoemulsions: Preparation, characterization and in vitro cytotoxicity. *Journal of Drug Delivery Science and Technology*. 2015;29:117-24.
29. Ghosh V, Mukherjee A, Chandrasekaran N. Ultrasonic emulsification of food-grade nanoemulsion formulation and evaluation of its bactericidal activity. *Ultrasonics Sonochemistry* 2013;20(1):338-344.
30. Kaur K, Kumar R, Mehta SK. Formulation of saponin stabilized nanoemulsion by ultrasonic method and its role to protect the degradation of quercetin from UV light. *Ultrasonics Sonochemistry*. 2016;31:29-38.
31. Schwarz JC, Klang V, Karall S, Mahrhauser D, Resch GP, Valenta C. Optimisation of multiple W/O/W nanoemulsions for dermal delivery of acyclovir. *International Journal of Pharmaceutics*. 2012;435(1):69-75.
32. Kotta S, Khan AW, Ansari SH, Sharma RK, Ali J. Anti HIV nanoemulsion formulation: Optimization and in vitro-in vivo evaluation. *International Journal of Pharmaceutics*. 2014;462 (1-2):129-34.
33. Shakeel F, Baboota S, Ahuja A, Ali J, Aqil M, Shafiq S. Nanoemulsions as vehicles for transdermal delivery of aceclofenac. *AAPS Pharm Sci Tech* 2007;8(4):E104.
34. Shakeel F, Baboota S, Ahuja A, Ali J, Aqil M, Shafiq S. Accelerated stability testing of celecoxib nanoemulsion containing Cremophor-EL. *African Journal of Pharmacy and Pharmacology*.2008;2(8):179-183.
35. Borhade V, Pathak S, Sharma S, Patravale V. Clotrimazole nanoemulsion for malaria chemotherapy. Part I: Preformulation studies, formulation design and physicochemical evaluation. *International Journal of Pharmaceutics*. 2012;431(1-2):138-48.





Jayaram et al.,

36. Chen H, Hu X, Chen E, Wu S, McClements DJ, Liu S, et al. Preparation, characterization, and properties of chitosan films with cinnamaldehyde nanoemulsions. *Food Hydrocolloids*. 2016;61:662-71.
37. Calligaris S, Plazzotta S, Bot F, Grasselli S, Malchiodi A, Anese M. Nanoemulsion preparation by combining high pressure homogenization and high power ultrasound at low energy densities. *Food Research International*. 2016;83:25-30.
38. Shafiq S, Shakeel F, Talegaonkar S, Ahmad FJ, Khar RK, Ali M. Development and bioavailability assessment of ramipril nanoemulsion formulation. *European Journal of Pharmaceutics and Biopharmaceutics*. 2007;66(2):227-43.
39. Sharma SN, Jain NK. *A text book of professional pharmacy*. Vallabh Prakashan, 1st edn, 1985, p 201.
40. Sanjana Reddy M, Tripura sundari P. Formulation and evaluation of nanoemulsion for solubility enhancement of febuxostat. *International Journal of Science & Engineering Development Research*. 2019.4(1):(118-128).
41. Shaikh NM, Vijayendra Swamy SM, NARSING N, Kulkarni KB. Formulation and Evaluation of Nanoemulsion for Topical Application. *Journal of Drug Delivery and Therapeutics*. 2019;9(4-s):1-7.
42. Bouchemal K, Briancon S, Perrier E, Fessi H. Nano-emulsion formulation using spontaneous emulsification: solvent, oil and surfactant optimization. *International journal of pharmaceutics*. 2004; 280(1-2):241-251.
43. Kim CK, Cho YJ, Gao ZG. Preparation and evaluation of biphenyl dimethyl dicarboxylate microemulsions for oral delivery. *Journal of Controlled Release*. 2001;70(1-2):149-155.
44. Wagner JG, Gerard ES, Kaiser DG. The effect of the dosage form on serum levels of indoxole. *Clinical Pharmacology & Therapeutics*. 1996; 7(5):610-619.

Table 1. The Ingredients used in Nanoemulsion

S.No	Ingredient	Examples
1)	Oils	Coconut oil, castor oil, mineral oil, olive oil, linseed oil, corn oil.
2)	Surfactant	Sorbitan monooleate, polysorbate 80, polysorbate 20, polyoxy 60.
3)	Cosurfactant	Glycerine, PEG 300, PEG 400, Polyene glycol, ethanol, poloxamer.
4)	Emulgent	Natural lecithin's from animal or plant source, phospholipids, castor oil.
5)	Tonicity	Sorbitol, xylitol modifiers and glycerol.
6)	Additives	Propylene glycol, 1,3-butylene glycol, lower alcohol (Ethanol), sugars such as sucrose, glucose, maltose and fructose.
7)	Antioxidants	Tocopherol and ascorbic acid.

Table 2. Techniques used For nanoemulsion Preparation

S. No	Technique	Formulation	Conclusion
1)	High pressure homogenization	Lipid nanoemulsion of Primaquine for oral use	Oral bioavailability is increased (Particle size: 10-200nm) [22].
		Oil in water nanoemulsion	Increased hydration and elasticity of the skin [5].
		Lecithin based nanoemulsion of progesterone	Progesterone penetration rates have improved and are more stable over time [23].
		Nanoemulsion of Prednicarbate	Enhanced the drug's chemical stability in the formulation [24].
		Dimethyl silicone-dry nanoemulsion inhalations	Particle size of 19.8 nm is effective in acute lung damage [25].
		Nanoemulsion of Paclitaxel baicalein	A multidrug resistance prevention method [26].





Jayaram et al.,

		Lecithin based parentals nanoemulsion of Risperidone	The bioavailability of risperidone with a mean particle size of 160nm has enhanced [27].
2)	Micro fluidization	Nanoemulsion of Pitavastatin	Permeation is increased [28].
3)	Ultrasonication	Nanoemulsion of Basil oil	Nanoemulsion for food preservation with 29.6nm droplet size [29].
		O/W nanoemulsion with saponin stabilised quercetin	With a mean particle size of 52±10nm, it's stable for 45 days at room temperature [30].
4)	Phase inversion temperature	W/O/W multiple nanoemulsion of Acyclovir	With a mean droplet size of 100 nm, the physicochemical stability was excellent at room temperature (RT) for 6 minutes [31].
5)	Phase inversion composition	Nanoemulsion of Efavirenz	Greater bioavailability due to globule size of less than 30nm [32].
6)	Spontaneous emulsification	Oil in water nanoemulsion of Aceclofenac	Aceclofenac nanoemulsion has the ability to administer the drug transdermally [33].
		Nanoemulsion of Celecoxib	Celecoxib's physical and chemical stability in nanoemulsions has been increased [34].
		Nanoemulsion of Clotrimazole	Clotrimazole solubility has increased, with a mean globule size of < 25nm [35].
		Cinnamaldehyde nanoemulsion-coated chitosan films	It has excellent UV barrier properties [36].
7)	High pressure homogenization + Ultrasound	Nanoemulsion	Reduced emulsification energy consumption, smaller particle sizes, and improved stability [37].
8)	Pseudo ternary phase diagram + Spontaneous emulsification	Nanoemulsion of Ramipril	With a particle diameter of 80.9nm, absorption is improved [38].





Challenging Scenario Faced by Exporters of Garment Industry

M. Sampath Nagi, M. Kannan and P.Ramasubramaniam*

Assistant Professor, Department of Management, Sardar Vallabhbhai Patel International School of Textile & Management (SVPISTM), Coimbatore – 641004, Tamil Nadu, India.

Received: 22 Oct 2021

Revised: 16 Dec 2021

Accepted: 11 Jan 2022

*Address for Correspondence

P.Ramasubramaniam

Assistant Professor, Department of Management,
Sardar Vallabhbhai Patel International School of Textile & Management (SVPISTM),
Coimbatore – 641004, Tamil Nadu, India.
Email: mytextileclassroom@gmail.com



This is an Open Access Journal / article distributed under the terms of the **Creative Commons Attribution License** (CC BY-NC-ND 3.0) which permits unrestricted use, distribution, and reproduction in any medium, provided the original work is properly cited. All rights reserved.

ABSTRACT

Indian textiles industry is one of the largest and oldest textiles industries in the world. India is the world's second largest producer of textiles and garments after China. The research is descriptive in nature. This study used structured questionnaire as survey instrument. The researchers distributed 600 questionnaires and 592 questionnaires have been returned. The remaining eight questionnaires were found to be biased. To develop the competitive edge the exporters should concentrate in proactive marketing for a sustainable growth. The government is encouraging the exporters by providing various supportive measures like textile parks, technology up gradation fund and duty drawback schemes. But they are insufficient to meet the requirements of the exporters. The government should take steps to develop land and port infrastructure to ensure the smooth flow of goods and save time to enable exporters to handle huge orders smoothly.

Keywords: Challenges, Exporters, Garment Industry, COVID, Textile.

INTRODUCTION

Indian textiles industry is one of the largest and oldest textiles industries in the world. India is the world's second largest producer of textiles and garments after China. It is the world's third largest producer of cotton after China and the United States of America and is the second largest cotton consumer after China. The industry is the second largest employment generator after agriculture by employing 45 million people directly and 60 million people indirectly. The textile industry is one of the leading segments of today's economy and is a largest source of foreign exchange earnings. As of 2018 the industry contributes for about 4% of the Gross Domestic Product, accounting for more than 30% of the export earnings contributing for about 20% of the industrial output. India was holding world monopoly and dominated trade for about 3000 years. Hence the current research focuses on the challenges faced by the garment industry at Thirupur location.





Sampath Nagi et al.,

INDIAN TEXTILE INDUSTRY

The textile sector has a long trade history and still plays a dominant role in the national income of the country. It stands first in global jute production sharing 63 of global textile and garment market and is second in global textile marketing manufacturing in silk and cotton production. It is one of the leading segments of today's economy and is a largest source of foreign exchange earnings. Indian Textile industry plays a significant role in the upliftment of Indian economy. Being the largest and most important, the industry contributes to the Gross Domestic Product and foreign exchange reserves of the country considerably. As a result, the textile and apparel industry are often thought to represent the first base in the country's economic growth and development. The industry with its vast population and increasing income have a huge scope for strong and steady development of domestic textile market. Even though the industry has many advantages, there are many challenges faced by the industry. The specific problem further deepened when the existing export incentives were reduced considerably. These factors made a huge impact on the costs and were forced to increase the price of the product. The exporters are already under pressure from its Asian competitors and this affected their competitiveness leading to an overall reduction in the textile exports of this country. The industry has to face intense competition pressure.

Tirupur is witnessing a slump in its performance as the incentive duty drawback scheme available to the exporters was slashed to 2 from 7.6 in the latter half of the year, which has put India at a disadvantageous position among the competing countries. The delay in the reimbursement of input tax in the Goods and Services Tax affect the working capital flow in the industry putting pressure on their production capacity. Neighbouring competitors such as Bangladesh and Sri Lanka enjoy duty-free access to Europe and the U.S, the main buyers of garments. The industry to overcome from its present difficulties should analyze its weakness and come forward to overcome the problems to strive and to use the opportunity to capture a sizeable market share.

AIM OF THE STUDY

Indian textile industry for years, were showing a strong growth as it has so many positive aspects on its side, like abundant supply of raw material, the capacity of the industry to produce variety of products in this short span of time, and the presence of a strong supply chain. In spite of these advantages, the industry is under a lot of pressure registering a fall in the rate of exports in the recent years. The exporters are facing several problems. Thus, the researcher has undertaken this concept to study the problems of the industry with special reference to Tirupur geographical location as it is one of the important hubs of the textile industry, contributing significantly to the total textile exports of the country.

NEED FOR THE STUDY

The study aims to make research on the problems of Indian textile industry. The study concentrates on the knitwear exporting industries in the geographical location of Tirupur. Tirupur is the textile hub exporting a vast majority of its knitwear production to become one of the favourable sourcing centres for international buyers. The recent export statistics of Tirupur is showing a declining trend due to the changes that are happening in the international and national environment. At present the industry is facing crisis, with a reduction in exports, leading to closure of many small units/ business (Deller & Conroy,2017) due to absence of export orders. The bigger units cannot work to its full capacity and are under severe financial crisis. The study explores the problems of Tirupur exporters in different dimensions and analyse the reasons for the sluggish nature and to suggest measures to be undertaken by the exporters and government, to overcome the problems and to bring about a prospective growth to the industries at Tirupur.

PROBLEM STATEMENT

The Indian textile sector is one of the world's largest and a leading segment in the Indian economy. The industry accounts for about 30 of the economic earnings. Though the industry enjoys second position with its vast resources, it could capture only less than 5 of the global trade. The trade war between United States of America and China has provided enormous opportunity for the Indian industry to penetrate deeper into the international market and capture a sizeable market share. India is in a favourable position with its vast resources and experience and could



**Sampath Nagi et al.,**

have easily increased its business. Instead, the industry is struggling to even maintain the existing market share and countries like Vietnam are improving itself, moving ahead in the competition. Tirupur a leading knitwear export hub could have easily secured enormous orders using the trade gap, but could not materialise the favourable environment in the global market (Ramadani & Rashiti, 2017). The present situation provide scope for a detailed study on the reasons that hinder the industry from securing a large market share and suggest steps to be taken to improve in the future. In this study the researcher attempts to study the present situation on the problems faced by the knitwear exports to achieve export growth at the desired level by satisfying the international buyers more effectively and efficiently than its competitors.

OBJECTIVE OF THE STUDY

The researcher has framed the main objective to identify the level of various challenges faced by the exporters garment industry.

REVIEW OF LITERATURE

Kanthasami (2019), published an article in the Deccan Chronicle on the topic Tirupur emerges knitwear capital updated on 26th March 2019. He analysed the difficulties faced by Tirupur knitwear exporters in capturing the orders from its competitors. With around 3000 supporting units, 1800 job working units and the production capacity, Tirupur should capture a sizeable market. But the industry requires huge supply of skilled labour. The absence leads to high cost of production, low productivity and low quality. The bank rates are higher when compared to the competitors. And thus, it lacks price competitiveness with its Asian competitors. Amar Saif (2019), in his thesis on the factors that lead to the relocation of textile industry from China to Vietnam. The industry being a highly labour oriented industry have to shift its products to low wage countries to contain its labour cost. The study found that, political stability, FDI, workforce productivity, government policies are some of the important factor that influenced the relocation of textile industries to Vietnam.

Sutanuka Ghosal (2019), studied the export performance of Indian apparel exports for the financial year 2019. Apparel exports during the period is on a reversal trend. For the third quarter in the financial year the exports are experiencing a sharp decline much lower than that of the past five years due to the internal challenges and sudden pressures experienced by the industry. With the competitive pressure from the cost advantageous neighbouring countries Indian industry could not capitalise the declining trend of the exports from China. Sneha Saravanan (2019), in her paper studied the level of employee retention in garment industries of Tirupur and the reasons for the labour turnover. A stable human resource is essential for an organization for strong planning and to satisfy its customers. But the garment industry of Tirupur faced the problems in retaining the labour force. So, the study analysed for the reasons behind the employee turnover. Internal problems, better opportunities outside the firm, work timing and shifts were the main reasons for leaving the job. As these problems are mostly internal and are possible to be rectified by the employer, the employee turnover can be controlled by making changes in their HR policies.

Misu Kim (2019) studied on Export Competitiveness of India's Textiles and Clothing Sector in the United States. US being the largest importer of India's textile and clothing sector analysed the Indian export market after the implementation of MFA in the year 2005, The competition for Indian T&C industries intensified from developing countries like Bangladesh, Vietnam. The countries with low labour cost have competitive advantage. But the product of China is costlier with higher labour cost but their products are of better quality so India should try to improve its export competitiveness, concentrating in the improvement of the quality of its products. There is a rising demand for manmade fibre globally, so India should try to concentrate in improving such products. Further, the export infrastructure like logistics should be developed to improve its competitiveness. Venkatachalam (2019) "Washington-Beijing trade spat more orders for India expected", studies on the market environment of Indian apparel exporters in the event of the trade war that is going on between USA and China. The conflict creates problems for the Chinese exporters and so the textile exports of China are affected to a large extent. The two countries India and China have a combined apparel market share of \$795bn. The trade war between the countries





Sampath Nagi et al.,

provides ample opportunities to the Indian industry if properly used. Hariharasudan (2018), examined the importance of English communication for garment industries of Tirupur. The industry developed from cottage industry to a well-developed organisation structure. The language skills of the Tirupur exporters are investigated and its impact on the development of the business is analysed. Based on the finding's suggestions are provided for successful running of the business. Ganapati Mendali, Sanjukta Das (2018), "The effects of Exchange rate volatility on exports of selected industries of India" in their study analysed the impact of the fluctuations in the exchange rate on textile industry as the industry contributes for about 5%of the country's GDP and 14% to the overall IIP. The study concludes that Exchange rate volatility do not affect the textile exports largely and so the policy makers may concentrate on other factors also apart from stable exchange rate to promote textile exports. The article focus on the garment industry is undergoing a tough phase with the implementation of demonetisation and introduction of GST. The refund of input tax is delayed and the accumulation of input tax credit is imposing stress on the working capital of the garment exporters. The immediate decrease in drawback and ROSL is another big blow. The increasing cost of production has affected the exporters and the throat cut prices offered by the buyers could not even cover the increasing costs. Simplification of the complex tax structure, decrease in export credit interest rate and increase in the drawback rate are some of the supportive measures that could be provided by the Government to boost the exports.

RESEARCH METHODOLOGY

The research is descriptive in natures. The data for the study has been collected from primary as well as secondary sources. This study used structured questionnaire as survey instrument. The survey is conducted among the members of Tirupur Exporters Association. The number of Export firms as per TEA records in Tirupur Corporation is 1100. The sampling size has been confined from the Demorgan's sample size estimator. For a population of 1100, the required sample size is 574 sample is required with a confidence level of 99% and confidence interval of 3.5%. the researchers distributed 600 questionnaires and 592 questionnaires has been reverted. The remaining eight questionnaires were found to be biased.The collected primary data have been analysed using the software package called SPSS (Statistical Packages for Social Sciences).

ANALYSIS

Table. 1. Challenges Faced by Exporters Indian Garment Industry

Dimensions	Measuring Variables	N	Mean	Sd	Rank
Product related Problems	Labour Management	592	3.06	0.90	4
	Manpower Quality	592	3.77	0.73	2
	Labour Laws	592	4.63	0.43	1
	Product Delivery	592	3.51	0.53	3
	Mean Score - Product related Problems (A)	592	3.74	0.65	
Price related Problems	Price Fixation	592	4.67	0.47	1
	Cost Effectiveness	592	3.76	0.77	3
	Price Fluctuations	592	3.70	0.88	5
	Financial Assistance	592	3.74	0.68	4
	Profitability	592	3.96	0.70	2
	Mean Score - Price related Problems (B)	592	3.96	.452	
Place related Problems	Knowledge or Awareness	592	3.53	1.19	3
	Technology Adoption	592	3.39	1.10	4
	Customs and Duty	592	3.74	0.86	2
	Barriers to International Standards	592	4.17	0.38	1
	Mean Score - Place related Problems (C)	592	3.71	0.88	
Promotion related Problems	Brand Creation	592	4.36	0.79	2
	Exhibitions and Trade Fairs	592	4.11	1.17	3
	Market Sustainability	592	4.59	0.36	1





Sampath Nagi et al.,

	Free Trade Agreements	592	3.90	0.86	4
	Taxation Reforms	592	3.78	0.39	5
	Promotional Measures	592	3.42	0.51	6
	Mean Score - Promotion related Problems (D)	592	4.03	0.68	
N – Number of Respondents	Sd – Standard Deviation	Primary Source			

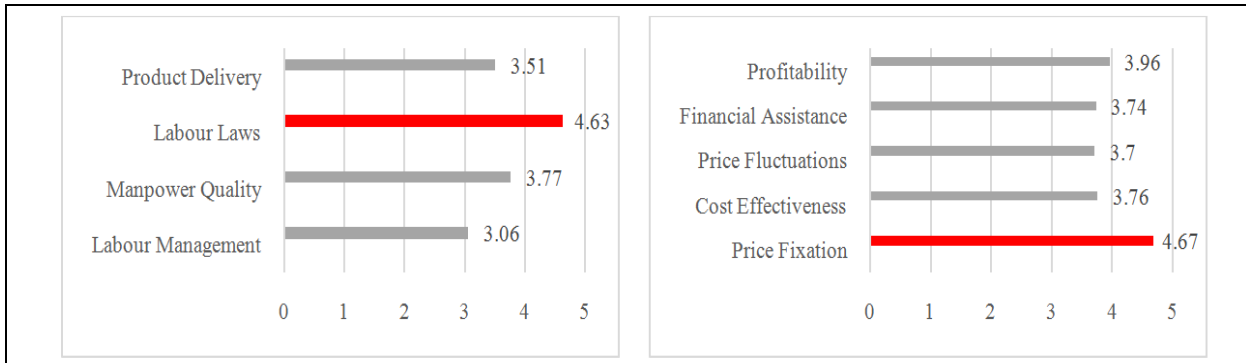


Fig.a Product related Problems (A)

Fig.b Price related Problems (B)

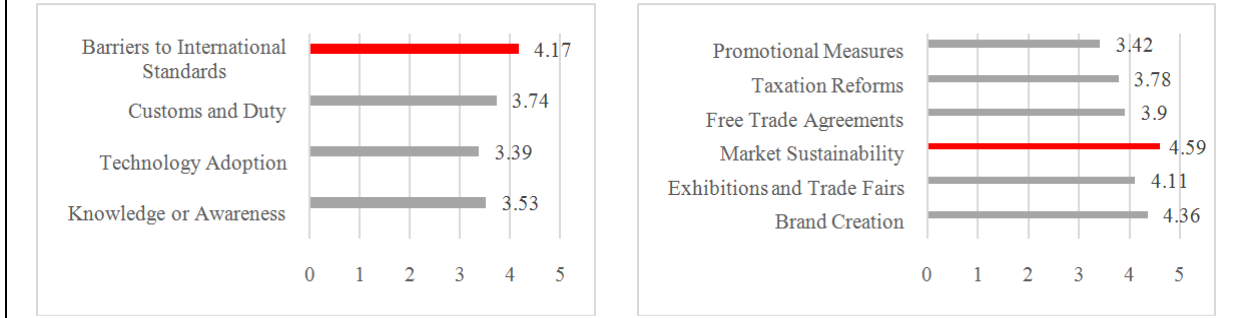


Fig.c Place related Problems (C)

Fig.d Promotion related Problems (D)

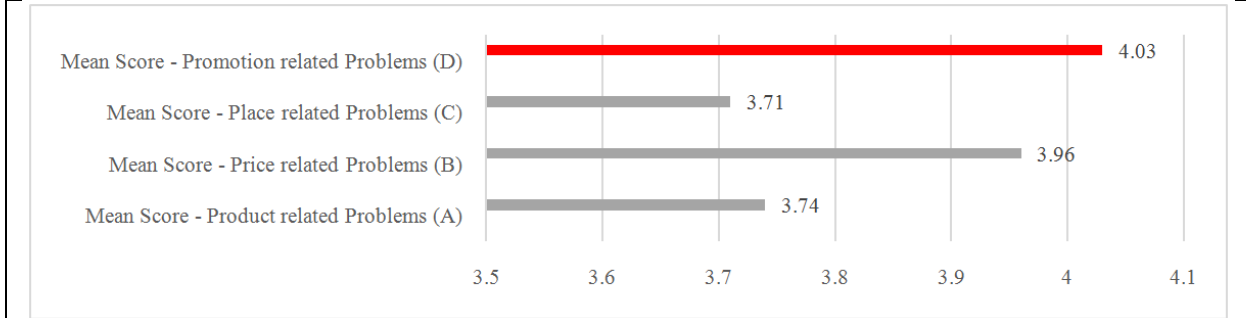


Fig.e Challenges Faced by Exporters Indian Garment Industry





Sampath Nagi et al.,

RESULTS AND RECOMMENDATIONS

The results of the current research reveals that the exporters of Tirupurgarment industry faced high level of problem related to the promotion of their product. Even subsequently the hierarchy of the problems goes from price, product and place. Hence the researcher suggest that the Tirupur garment exporters should establish and develop their own brand for improving their product image and increase the competitive capacity of the exporters. Then the manufacturers should bring value addition to the products to enhance their product performance. They should indulge in research and development. Even the Training programs should be framed and implemented to workers for skill upgradation to increase productivity and quality in their work and to implement improved production techniques in the production process. Utmost important recommendation is that the Tirupur exporters should diverse, concentrate and also continuous improvement in the new technology (Mittal & Gupta, 2021) and innovative products (Darger et.al, 2017, Aronov et.al, 2019) in fields like technical textiles, medical textiles, geo textiles to expand market.

CONCLUSION

Indian textile industry occupies a formidable presence in the economy of our country. A balanced growth of this industry is, therefore, essential for the fulfilment of the needs of the people. The comprehensive study on the industry aimed at understanding the history and characteristics of Tirupur garment industry along with its pattern of growth. The study extended to their institutional composition and developmental prospective in the area of business. The findings showed that the industry lack competitive edge over other textile producing countries. The exporters effective management of risks and barriers improve the probability of success rate of the innovative projects (Narkhede et. al, 2019). The basic infrastructure facilities for the industry are not adequate. The exporters have to face the consequences like increased cost of production, delay in production and transportation indirectly affecting the performance of exporters.

The cost of additional services is too high. Steps should be taken to overcome the problems and improve the export potential. The industry should proceed for vertical integration and horizontal consolidation in garment production to reduce the manufacturing costs. To develop the competitive edge (NilayBıçakcıoğlu, 2018) the exporters should concentrate in proactive marketing for a sustainable growth. The government is encouraging the exporters by providing various supportive measures like textile parks, technology up gradation fund, duty drawback schemes. But they are insufficient to meet the requirements of the exporters and the measures taken are not effectively reaching the target exporters. This also increases the cost of production and transportation. The government should take steps to develop the land and port infrastructure to ensure the smooth flow of goods and save time to enable the exporters to handle huge orders smoothly.

ACKNOWLEDGEMENTS

Thanks to all the participants who helped us by participating in this research. All the department colleagues who helped us access the departmental set-up for completing this work.

CONFLICT OF INTEREST

The authors certify that, they have had no affliction with or involvement in any organisation or entity with any financial interest, or non-financial interest in subject matter, or material discussed in the manuscript.

AUTHORS' CONTRIBUTIONS

All authors made a significant contribution to the work reported, whether that is in the conception, study design, execution, acquisition of data, analysis and interpretation; took part in drafting, revising or critically reviewing the article; gave final approval of the version to be published; have agreed on the journal to which the article has been submitted; and agree to be accountable for all aspects of the work.





Sampath Nagi et al.,

FUNDING ACKNOWLEDGEMENTS

The authors have not received any financial support for the current research article and/or for the publication of this article.

REFERENCES

1. Amar Saif. (2019). *From China to Vietnam-Drivers for relocating Fashion Manufacturing*. Thesis - Tampere University of Technology.
2. Aronov, J., Carrion, A., Papic, L., Galkina, N., Aggrawal, D., & Anand, A. (2019). Standards Development and Innovative Products. When should Standards be Prepared?. *International Journal of Mathematical, Engineering and Management Sciences*, 4(5), 1081-1093. <https://dx.doi.org/10.33889/IJMEMS.2019.4.5-086>.
3. Ganapati Mendali., Sanjukta Das. (2018). The effects of Exchange rate volatility on exports of selected industries of India. *Arthshastra Indian Journal of Economics & Research*, 7(1), 9 - 24
4. Kim M. Export Competitiveness of India's Textiles and Clothing Sector in the United States. *Economies*. 2019; 7(2):47. <https://doi.org/10.3390/economies7020047>.
5. Krejcie. R. V., & Morgan. D. W., (1970). Determining sample size for research activities. *Educational and Psychological Measurement*, 30(3), 607–610.
6. Michael Darger, Alan Barefield & Brent D. Hales (2017) Business retention and expansion (BRE) today – research, application, and evaluation: Introduction to the special issue, *Community Development*, 48:2, 160-169, DOI: 10.1080/15575330.2017.1285334.
7. Mittal, A., & Gupta, P. (2021). An Empirical Study on Enhancing Product Quality and Customer Satisfaction Using Quality Assurance Approach in an Indian Manufacturing Industry. *International Journal of Mathematical, Engineering and Management Sciences*, 6(3), 878-893. <https://doi.org/10.33889/IJMEMS.2021.6.3.052>.
8. Narkhede, B. E., Ghadage, Y. D., Raut, R. D., & Luthra, S. (2019). Study of Implication of Qualification and Experience in Perception of Risks and Barriers for Innovative Projects. *International Journal of Mathematical, Engineering and Management Sciences*, 4:2, 289-305. <https://dx.doi.org/10.33889/IJMEMS.2019.4.2-024>.
9. Nilay Bıçakcıoğlu (2018) Green Business Strategies of Exporting Manufacturing Firms: Antecedents, Practices, and Outcomes, *Journal of Global Marketing*, 31:4, 246-269, DOI: 10.1080/08911762.2018.1436731.
10. S. Kanthasami. (2019). *Tirupur emerges knitwear capital*, Deccan Chronicle.
11. S. Venkatachalam. (2019). Washington-Beijing trade spat more orders for India expected. *Apparel Views*, 30 - 31.
12. Sneha Saravanan. (2019). A Study on Employee Retention Practices in Tirupur, *International Journal of Research in Engineering, Science and Management*, 2:2, 638 - 640.
13. Steven C. Deller & Tessa Conroy (2017) Business survival rates across the urban–rural divide, *Community Development*, 48:1, 67-85, DOI: 10.1080/15575330.2016.1246459.
14. Sutanuka Ghosal India's apparel exports estimated to degrow Economic Times, March 5th 2019.
15. Thavabalan. P., Mohan. A., Hariharasudan. B & Nawaz, Nishad. (2021). English for Business Communication: An Interventional Study with Employees of Indian Printing Industry at Sivakasi. *Asian ESP Journal*, 17:3, 90 – 106.
16. Veland Ramadani & Shqipe Gërguri-Rashiti (2017) Global Marketing, Gender and Family Business in Asia: A Literature Review, *Journal of Global Marketing*, 30:3, 138-146, DOI: 10.1080/08911762.2017.1306898.
17. M, Sampath Nagi and D, Sathish Kumar (2021), Perception of the Farmers towards the Quality of Service Provided By Co-Operative Banks, *Indian Journal of Natural Sciences (IJONS)*, 12:66, 30725-30732





Preoperative Respiratory Muscles Training on Pulmonary Function Test and Respiratory Muscle Strength after Abdominal Surgery: A Pilot Study

Prakashkumar Patel^{1*} and V P Hathila²

¹Ph.D. Scholar (Parul university) & Assistant professor, SPB physiotherapy college, South Gujarat Medical Education and Research Centre, Surat, Gujarat, India.

²Ph.D. Guide (Parul university) & Dean, Faculty of Medicine, Parul institute of medical science and research, Parul university, Vadodara, Gujarat, India.

Received: 27 Oct 2021

Revised: 25 Nov 2021

Accepted: 06 Jan 2022

*Address for Correspondence

Prakashkumar Patel

Assistant Professor,

SPB Physiotherapy College,

Surat, Gujarat, India.

Email: dr.prakash84@gmail.com



This is an Open Access Journal / article distributed under the terms of the **Creative Commons Attribution License** (CC BY-NC-ND 3.0) which permits unrestricted use, distribution, and reproduction in any medium, provided the original work is properly cited. All rights reserved.

ABSTRACT

The aim of this pilot study was to assess the effect of pre-operative respiratory muscle training on pulmonary function test and respiratory muscle strength after abdominal surgery. Total number of 20 participants of both the gender with age group between 30 to 70 years, who were planning for major abdominal surgery were to be divided in to two groups i.e. group A (experimental group) and group B (control group). The experimental group was to undergo a pre-operative respiratory muscle training and post operatively both groups were to received conventional physiotherapy treatment. All the participants were assessed for pulmonary function test and respiratory muscle strength parameters at the baseline, before surgery, at 3rd day, 7th day and 21st day post operatively. There were statistically significant differences ($p < 0.01$) found in all the outcome measures in both groups. Further, comparison was done between the groups. It was found that statistically significant difference ($p < 0.05$) is present in FVC ($p = 0.021$), FEV1 ($p = 0.023$), PEF (p=0.024), MVV ($p = 0.015$), MIP ($p = 0.021$) and MEP ($p = 0.022$). It is concluded that preoperative respiratory muscle training helps to preserve and improve pulmonary function parameters and respiratory muscle strength after abdominal surgery.

Keywords: Respiratory muscle training, Abdominal surgery, Pulmonary function test, Respiratory muscle strength.





Prakashkumar Patel and V P Hathila

INTRODUCTION

Patients undergoing major surgery suffer postoperative respiratory complications with significant postoperative morbidity and mortality [1,2]. Abdominal surgeries are the most common operative procedure including a wide range of both emergency and elective surgical interventions [3]. The overall rate of operations on the abdomen is estimated as 43.8% among those who are above the age of 60 [4]. The incidence of postoperative pulmonary complications after abdominal surgery is reported to be 6-76% [5-9], with the incidence following upper abdominal operations as high as 60-75% [10]. Postoperative Pulmonary complications following upper abdominal surgery are the most common surgical complications. The combined effect of surgical trauma and anesthesia results in reduced lung volumes, respiratory muscle dysfunction and atelectasis.¹¹⁻¹² Chest physical therapy is widely recommended to prevent and treat PPCs, using a wide variety of techniques and devices, including incentive spirometry, continuous positive airway pressure, positive expiratory pressure, intrapulmonary percussive ventilation and inspiratory muscle training using a pressure threshold device that targets the muscles of inspiration [13-14].

There may be some benefit of pre-operative incentive spirometry, deep breathing exercises and chest physiotherapy in reducing postoperative pulmonary complications following major abdominal surgery [15-18], inspiratory muscle training (IMT) improves performance in athletes as well as exercise tolerance and quality of life in patients with chronic obstructive pulmonary disease [19-21] and other conditions affecting the respiratory system such as cystic fibrosis, Parkinson's disease and myasthenia gravis [22-39]. Post-operative pulmonary complication following abdominal surgery may cause inability to cough because of wound pain, elevation of diaphragm and retention of secretions. Surgical trauma and anaesthesia given during surgery may cause respiratory muscle dysfunction and reduce respiratory muscle strength along with other complications. Present study is an attempt to evaluate the possible benefit of preoperative respiratory muscle training to preserve respiratory muscle strength and pulmonary function after abdominal surgery. Therefore; the objective of this study was to investigate the changes in pulmonary function test and respiratory muscle strength after application of preoperative respiratory muscle training for patients undergoing abdominal surgery.

PATIENTS AND METHODS

Setting and patients

All the participants were assessed for different factors thoroughly with assessment format. Ethics committee approval was granted by Parul university institutional Ethics Committee for human research (PU-IECHR) with reference number PUIECHR/PIMSR/00/081734/2607. The participants were taken for the study by using convenient sampling. Total number of participant was 20 of both the gender with age group between 30 to 70 years. Patients were included if they were: 1. Age group between 30 to 70 years 2. Pre-operative patients planning to undergo abdominal surgery 3. First time undergoing abdominal surgery. Patients were excluded if they were: 1. Participants with known neurological deficits such as spinal cord injury, amyotrophic lateral sclerosis, poliomyelitis, guillain-barre syndrome, myasthenia gravis, muscular dystrophy. 2. Participants with unstable cardio respiratory disease. 3. Participants with unstable medical condition and high diabetes. 4. Participants not willing to participate / Uncooperative participants. 5. Orthopaedic anomalies such as kyphoscoliosis, ankylosing spondylosis, fracture of thoracic cage. 6. Participants with any acute respiratory infection.

Intervention

The participants who were planning for major abdominal surgery were to be divided in to two groups i.e. group A (experimental group) and group B (control group). The experimental group was to undergo a pre-operative respiratory muscle training which included inspiratory muscle training, breathing exercises (diaphragmatic and segmental breathing exercise), incentive spirometry. Exercises were to start four days prior and 20 to 30 repetition of each exercise were given for three times in a day. Each session time lasted for 20 to 30 minutes. Post operatively both groups were to receive conventional physiotherapy treatment.



**Prakashkumar Patel and V P Hathila****Outcomes measurement**

Outcomes parameters i.e. Forced vital capacity, **forced** expiratory volume in one second, peak expiratory flow rate, Maximal voluntary ventilation, Maximum inspiratory pressure, Maximum expiratory pressure were measured on baseline (before intervention), Before surgery, 3rd day of post-surgery, 7th day of post-surgery and 21st day of post-surgery for both groups. The control group had not received any intervention before surgery.

STATISTICAL ANALYSIS AND RESULTS

All statistical analyses were performed using the SPSS™ version 20.0. the comparisons were made between two groups, based on these four outcome measurements at the 3rd day, 7th days and 21stday post operatively after implementation of the respective intervention: 1) Forced vital capacity, 2) Forced expiratory volume in one second 3) Peak expiratory flow rate 4) Maximum voluntary ventilation 5) Maximum inspiratory pressure 6) Maximum expiratory pressure. The present study is single blind, randomized controlled clinical trial with 2 different group (Group –A Experimental and Group-B Control). It is a multivariate repeated measure ANOVA design; where the participants were assessed five times i.e. at the baseline, before surgery, at 3rd day, 7th day and 21st day. Prior to final analysis, data were screened for transcription errors, normality assumptions, homogeneity of variance, as prerequisites for parametric calculations of the analysis of difference and analysis of related measures. Alpha level was set at 0.05 to control for type I error and confidence interval was set at 95% for all statistical analysis. Descriptive statistics and repeated measures multivariate ANOVA were used for within and between-group comparisons at each follow-up period.

FVC

The within-group repeated measure multivariate ANOVA with Greenhouse-Geisser correction (GGC) showed the significant statistical difference with $F= 446.355$, $p<0.001$. A repeated measure multivariate ANOVA with (GGC) between-group analysis showed that the experimental and control groups were different statistically with $F=6.444$, $p<0.021$

FEV1

The within-group repeated measure multivariate ANOVA with Greenhouse-Geisser correction (GGC) showed the significant statistical difference with $F= 227.603$, $p<0.001$. A repeated measure multivariate ANOVA with (GGC) between-group analysis showed that the experimental and control groups were different statistically with $F = 6.211$, $p<0.023$

PEFR

The within-group repeated measure multivariate ANOVA with Greenhouse-Geisser correction (GGC) showed the significant statistical difference with $F= 644.234$, $p<0.001$. A repeated measure multivariate ANOVA with (GGC) between-group analysis showed that the experimental and control groups were different statistically with $F = 6.028$, $p<0.024$

MVV

The within-group repeated measure multivariate ANOVA with Greenhouse-Geisser correction (GGC) showed the significant statistical difference with $F= 872.793$, $p<0.001$. A repeated measure multivariate ANOVA with (GGC) between-group analysis showed that the experimental and control groups were different statistically with $F = 7.246$, $p<0.015$

MIP

The within-group repeated measure multivariate ANOVA with Greenhouse-Geisser correction (GGC) showed the significant statistical difference with $F= 460.854$, $p<0.001$. A repeated measure multivariate ANOVA with (GGC) between-group analysis showed that the experimental and control groups were different statistically with $F = 6.445$, $p<0.021$



**Prakashkumar Patel and V P Hathila****MEP**

The within-group repeated measure multivariate ANOVA with Greenhouse-Geisser correction (GGC) showed the significant statistical difference with $F= 416.645$, $p<0.001$. A repeated measure multivariate ANOVA with (GGC) between-group analysis showed that the experimental and control groups were different statistically with $F = 6.338$, $p<0.022$

DISCUSSION

Adverse changes occur to the respiratory system immediately after surgery. They are broadly termed as post-operative pulmonary complications. Up to 23% of the patients who undergo major abdominal surgery would suffer from post pulmonary complications. The present study examined the effect of preoperative respiratory muscle training on pulmonary function test and respiratory muscle strength after abdominal surgery. 20 participants were taken, who were to undergo abdominal surgery and randomly assigned the group A (experimental) and group B(control). In this study, the group A was to undergo a pre-operative respiratory muscle training, which included breathing exercises, inspiratory muscle training and incentive spirometry. Post-operative all participants received conventional exercises. The control group, post-operative all participants received conventional physiotherapy treatment. Within the group, there was significant improvement. This was reflected in the 3rd day of surgery to 7th day of surgery and 7th day of surgery to 21st day follow up in the measurement of pulmonary function test and respiratory muscle strength, and this study also proves that preoperative respiratory muscle training has a more significant effect in improving pulmonary function test parameters and respiratory muscle strength post operatively. Pulmonary complications are caused by post-operative pathophysiological reduction in lung volume, respiratory muscle function and pain inhibition of respiratory function. Breathing exercises may prevent post pulmonary complications by reversing these problems. Timing may be a key factor in initiation of breathing exercises. It might be more helpful if patients are educated and train before surgery to perform the breathing exercises before surgery. Preoperative education and breathing exercise have alone reported to be associated with a 75% relative risk reduction in post-pulmonary complications [24-26]. For patients with less than normal diaphragmatic strength, diaphragmatic strengthening exercises are beneficial. They are designed to improve the efficiency of ventilation, decrease the work of breathing, increase the excursion of diaphragm and improve gas exchange and oxygenation.

Results of the study accord with other randomised study of respiratory muscle training in patients undergoing abdominal surgery. Kundra et al. (2010) conducted a study to compare the effects of preoperative and postoperative incentive spirometry on lung functions after laparoscopic cholecystectomy in 50 normal healthy adults. Preoperative incentive spirometry showed Significant improvement in the lung functions. The lung functions were significantly reduced till the time of discharge in both the groups. The group which received preoperative incentive spirometry preserved the lung functions better than the group who received post-operative incentive spirometry [27].

The findings of this study are in agreement with a study performed by Gehan et al. (2017) to investigate the effects of preoperative physical and respiratory therapy on pulmonary functions and complications after elective laparoscopic upper abdominal surgery in obese patients. Patients were randomly divided in two groups, group I was to receive respiratory and general exercise for 2 weeks before operation. Group II was to be the control group. The outcome parameters were, slow vital capacity (SVC), inspiratory capacity(IC), maximum inspiratory and expiratory pressures (MIP and MEP) and 6-min walk test. The outcomes parameters were recorded at baseline, after two weeks of exercise and one-month post-operative. Any postoperative pulmonary complications were recorded. Patients in the intervention group had higher pulmonary function in all parameters than control group in all the post-operative periods. Postoperative pulmonary complications occurred in 15 patients (62%) in the control group and in 7 patients (27%) in the intervention group. Authors concluded that Preoperative physical and respiratory therapy improved pulmonary functions and decreased the incidence of post-operative pulmonary complications [28]. There are many evidences that the number of post pulmonary complications after abdominal surgery are reduced by preoperative physiotherapy programmes. The present study is an attempt to evaluate the possible benefits of preoperative



**Prakashkumar Patel and V P Hathila**

respiratory muscle training in recovering the patient after abdominal surgery. FVC, FEV1, PEFr, MVV, MIP and MEP are acceptable indicators for pulmonary function and respiratory muscle strength. Results of the study shows there is significant improvement in pulmonary function test values and respiratory muscle strength values after incorporation of preoperative physiotherapy treatment.

CONCLUSION

From the result of our study, it is concluded that preoperative respiratory muscle training helps to preserve and improve pulmonary function and respiratory muscle strength after abdominal surgery.

Conflict of Interest: None

Source of Funding: None

REFERENCES

1. Teba L, Omert LA. Postoperative respiratory insufficiency. *Am Fam Phys*1995;51: 1473-80.
2. Roukema JA, Carol EJ, Prins JG. The prevention of pulmonary complications after upper abdominal surgery in patients with non-compromised pulmonary status. *Arch Surg*1988; 123: 30-4.
3. Lewis SM, Heitkemper MM, Dirksen SR. *Medical-surgical nursing: Assessment and management of clinical problems*. 6th ed. London, England: Mosby; 2003.
4. Masiira-MN, Ombito BR. Surgical admissions to the Rift Valley Provincial General Hospital Kenya. *East Afr Med J*2002;79(7):373-8.
5. Hallbook T, Linblad B, Lindroth B, Wolff T. Prophylaxis against pulmonary complications in patients undergoing gall bladder surgery. *Ann ChirGynaecol*. 1984; 73(2):55-58.
6. Dripps RD, Deming M. Postoperative atelectasis and pneumonia. *Ann Surg*. 1946; 124:94-110.
7. Thoren L. Postoperative pulmonary complications. *ActaChir Scand*. 1954; 107:193-205.
8. Latimer RG, Dickman M, Day WC, Gunn ML, Schmidt CD. Ventilatory patterns and pulmonary complications after upper abdominal surgery determined by pre-operative and postoperative computerised spirometry and blood gas analysis. *Am J Surg*. 1971; 122:622-32.
9. Inzelberg R, Peleg N, Nisipeaanu P, Magadle R, Carasso RL, Weiner P. Inspiratory muscle training and the perception of dyspnoea in Parkinson's disease. *Can J Neurol Sci*. 2005; 32:213-7.
10. Roukema JA, Carol EJ, Prins JG. The prevention of pulmonary complications after upper abdominal surgery in patients with non-compromised pulmonary status. *Arch Surg*. 1988; 123:30-4.
11. Hedenstierna G, Edmark L. the effects of anaesthesia and muscle paralysis on respiratory System. *Intensive Care Med* 2005;3(11); 1327-35.
12. Sasaki N, Meyer MJ, Eikermann M. Postoperative respiratory muscle dysfunction. *Anesthesiology* 2013;118(4):961-78.
13. Ribeiro P. Reference values for lung function tests. II. Maximal respiratory pressures and voluntary ventilation. *Braz J Med Biol Res*1999; 32(6):719-27.
14. Branson RD. The scientific basis for postoperative respiratory care. *Respir Care*. 2013;58(11):1974-84.
15. Fagevik Olsen M, Hahn I, Nordgren S, Lonroth H, Lundholm K. Randomized controlled trial of prophylactic chest physiotherapy in major abdominal surgery. *Br J Surg*1997; 84: 1535-8.
16. Celli BR, Rodriguez KS, Snider GL. A controlled trial of intermittent positive pressure breathing, incentive spirometry, and deep breathing exercises in preventing pulmonary complications after abdominal surgery. *Am Rev Respir Dis* 1984; 130: 12-5.
17. Thomas JA, McIntosh JM. Are incentive spirometry, intermittent positive pressure breathing, and deep breathing exercises effective in the prevention of postoperative pulmonary complications after upper abdominal surgery? A systematic overview and meta-analysis. *PhysTher*1994; 74: 3-10.





Prakashkumar Patel and V P Hathila

18. Overend TJ, Anderson CM, Lucy SD, Bhatia C, Jonsson BI, Timmermans C. The effect of incentive spirometry on postoperative pulmonary complications: a systematic review. *Chest* 2001; 120: 971-8.
19. Volianitis S, MacConnell AK, Koutedakis Y, MacNaughton L, Backx K, Jones DA. Inspiratory muscle training improves rowing performance. *Med Sci Sports Exerc.* 2001; 33(5):803-9.
20. Beckerman M, Magadle R, Weiner M, Weiner P. The effects of 1 year of specific inspiratory muscle training in patients with COPD. *Chest.* 2005;128(5):3177-82.
21. Weiner P, Weiner M. Inspiratory muscle training may increase peak inspiratory flow in chronic obstructive pulmonary disease. *Respiration.* 2006;73(2):151-6.
22. Enright S, Chatham K, Ionescu AA, Unnithan VB, Shale DJ. Inspiratory muscle training improves lung function and exercise capacity in adults with cystic fibrosis. *Chest.* 2004; 126:405-11.
23. Weiner P, Gross D, Meiner Z, Ganem R, Weiner M, et al. Respiratory muscle training in patients with moderate to severe myasthenia gravis. *Can J Neurol Sci.* 1998; 25(3):236-41.
24. Miskovic A, Lumb AB. Postoperative pulmonary complications. *Br Anaesth* 2017; 118:317-34.
25. Pasquina P, Tramèr MR, Granier J-M, Walder B. Respiratory physiotherapy to prevent pulmonary complications after abdominal surgery: a systematic review. *Chest* 2006; 130:1887-99.
26. Ball L, Bos LD, Pelosi P. High-flow nasal cannula in the postoperative period: is positive pressure the phantom of the OPERA trial. *Intensive Care Med* 2017; 43:119-21.
27. Kundra P, Vitheeswaran M, Nagappa M, Sistla S. Effect of preoperative and postoperative incentive spirometry on lung functions after laparoscopic cholecystectomy. *SurgLaparoscEndoscPercutan Tech* 2010;20(3):170-72.
28. Gehan A, Abdelaal, Sami S. Eldahdouh. Effects of preoperative physical and respiratory therapy on pulmonary functions and complications after elective laparoscopic upper abdominal surgery in obese patients. *Egypt J Chest Dis Tuberc* 2017;66(4):735-38.

Table 1 Descriptive Statistics of the Study

Variables	Group A	Group B
Gender	4 (F) and 6 (M)	5 (F) and 5 (M)
Age	47.8 ± 6.06	50.3 ± 5.98

Table 2. shows the within- group comparison result with interaction.

Outcome Measure	F	P-value	Effect Size (Partial Eta Squared)
FVC	446.355	< 0.001	0.961
FEV1	227.603	< 0.001	0.927
PEFR	644.234	< 0.001	0.973
MVV	872.793	< 0.001	0.980
MIP	460.854	< 0.001	0.962
MEP	416.645	< 0.001	0.959

Table 3. shows the between group comparison of result of groups.

Outcome Measure	F	P-value	Effect Size (Partial Eta Squared)
FVC	6.444	0.021	0.264
FEV1	6.211	0.023	0.257
PEFR	6.028	0.024	0.251
MVV	7.246	0.015	0.287
MIP	6.445	0.021	0.264
MEP	6.338	0.022	0.260





Different Extraction Methods for the Extraction of Phenolics, Flavonoids, Antioxidant and Antidiabetic Phytochemicals from *Momordica cymbalaria* Leaves

K. Gopalsatheeskumar^{1*}, V.K. Kalaichelvan¹, N. Kannappan¹ and P.Mullai²

¹Department of Pharmacy, Faculty of Engineering and Technology, Annamalai University, Annamalai Nagar-608002, Tamil Nadu, India.

²Department of Chemical Engineering, Faculty of Engineering and Technology, Annamalai University, Annamalai Nagar-608002, Tamil Nadu, India.

Received: 14 Dec 2021

Revised: 24 Dec 2021

Accepted: 11 Jan 2022

*Address for Correspondence

K. Gopalsatheeskumar

Department of Pharmacy,
Faculty of Engineering and Technology,
Annamalai University,
Annamalai Nagar-608002, Tamil Nadu, India.
Email: gskpungai@gmail.com.



This is an Open Access Journal / article distributed under the terms of the **Creative Commons Attribution License** (CC BY-NC-ND 3.0) which permits unrestricted use, distribution, and reproduction in any medium, provided the original work is properly cited. All rights reserved.

ABSTRACT

Momordica cymbalaria (Cucurbitaceae) is one of the important herbal medicines, having many health benefits including Stomachic, CNS Stimulant, Laxative, anti-rheumatism, antidiabetic, antimalarial, wound healing, anti-infective, antipyretic activities. Current study aimed to evaluate the Different extraction methods on yield, phenolic, flavonoids, antioxidant and antidiabetic activity of *Momordica cymbalaria* leaves. *Momordica cymbalaria* leaves were extracted with different methods such as Cold Maceration, Refluxation, Soxhlet and Ultrasound extraction methods. Obtained extracts undergoes the estimation of total phenolic and flavonoids content using standard method. Antioxidant activity was evaluated by hydrogen radical scavenging assay and antidiabetic activity was evaluated using alpha amylase inhibition assay. Results of current research revealed that, Soxhlet extraction method has higher extractive yield but cold maceration method has higher antioxidant and antidiabetic activity. Current research concluded that, cold maceration method is suitable for extraction of antioxidant and antidiabetic phytochemicals from *Momordica cymbalaria* leaves.

Keywords: Cold maceration, Soxhlet, Best method for extraction, Athalakkai, Alpha amylase.

INTRODUCTION

In 2000 BC people ate the part of plants to cure the disease, 1850 AD drink the portion of the plants, and after 1940 AD they swallow the synthetic pills for treatment but in 2000 AD again people start eating the part of the plant to

38741





Gopalasatheeskumar et al.,

cure the diseases because synthetic pills produce the unwanted side effects (1, 2). The activity of the herbal medicines is mainly by the presence of phytochemicals. For example Alkaloids, Glycosides, Flavonoids, Steroids, Terpenoids, Triterpenes, Saponins, Tannins, and Phenolic acids etc (3, 4). *Momordica cymbalaria* is one of the important herbal medicines widely distributed in South Indian states of Andhra Pradesh, Karnataka, Madhya Pradesh, Maharashtra, and Tamil Nadu (5). *Momordica cymbalaria* is under the family of Cucurbitaceae and it is commonly known as Athalakkai in Tamil, Kaarali Kanda in Hindi, Kasarakayee in Telugu and Kattupavalin Malayalam. This herbal medicine is having many health benefits including Stomachic, CNS Stimulant, Laxative, anti-rheumatism, antidiabetic, antimalarial, wound healing, anti-infective, antipyretic activities (6). Aerial parts of *Momordica cymbalaria* is shown in Figure 1. Extraction of phytochemicals from plant materials is important in the phytochemical research and developing of novel drugs from plant materials (7). Commonly many of the extraction methods are available to extract phytochemicals from medicinal plants including cold maceration, hot percolation, refluxation, Soxhlet, ultrasound extraction, centrifugation extraction, supercritical fluid extraction and microwave assisted extraction methods (8). However, these are the extraction methods are having its own advantages and disadvantages. So that selection of best method for the extraction of phytochemicals are important. Previously *Urtica dioica*(9), *Withania somnifera*(10), *Quercus coccifera* L (11) and *Juniperus phoenicea* were reported for its comparative different method of extraction. However, such studies have not been conducted for *Momordica cymbalaria*. So that current study aimed to evaluate the different of extraction methods on yield, phenolic, flavonoids, antioxidant and antidiabetic activity of *Momordica cymbalaria* leaves.

MATERIALS AND METHODS

Collection and authentication of plant materials

The fresh *Momordica cymbalaria* leaves were collected from north forest sides of Pungavarnatham village, Thoothukudi District, Tamil Nadu, India and authenticated by Dr. N. Srinivasan, Assistant professor of Pharmacognosy, Department of Pharmacy, Annamalai University. The herbarium was prepared and submitted in the Department of Pharmacy, Annamalai University and the voucher specimen number is PCOL/2021/001. The collected leaves were undergoes washing with distilled water and dried under sunshade in dark room. The dried material was powdered using mechanical mixer(12, 13).

Extraction of plant material

The powdered plant material Undergo the different extraction methods for the extraction of phytoconstituents.

Maceration method

About 10g of pulverized leaves of *Momordica cymbalaria* were macerated with 100 ml of hydro alcohol (70 % of methanol) for 48 h with frequent agitation at room temperature. After completion of extraction, the extracts were filtered using Whatman filter paper and concentrated using distillation method. and the obtained yield was weighed for the calculation of percentage yield as per standard formula given below (14).

$$\text{Percentage Yield (\%w/w)} = \frac{\text{Weight of extract obtained (g)}}{\text{Weight of plant material used (g)}} \times 100$$

Reflux method

About 10g of pulverized leaves of *Momordica cymbalaria* was placed in a 250 ml round bottom flask. And 100ml of hydro alcohol (70 % of methanol) was added. The mixture was stirred well and refluxed for 6 h at 60°C. After completion of extraction process, the extract was Stand upto up to room temperature and then filtered using Whatman filter paper (15). The collected filtrate was concentrated using distillation method. and the obtained yield was weighed for the calculation of percentage yield as per standard formula given below.

$$\text{Percentage Yield (\%w/w)} = \frac{\text{Weight of extract obtained (g)}}{\text{Weight of plant material used (g)}} \times 100$$





Gopalasatheeskumar et al.,

Soxhlet method

In this extraction method, Soxhlet apparatus was used for the extraction. About 100 g leaves of *Momordica cymbalaria* was extracted with 1000 ml of hydro alcohol (70 % of methanol) using soxhlet extraction technique for 48 h (16). The collected extract was concentrated using distillation method. And the obtained yield was weighed for the calculation of percentage yield as per standard formula given below.

$$\text{Percentage Yield (\%w/w)} = \frac{\text{Weight of extract obtained (g)}}{\text{Weight of plant material used (g)}} \times 100$$

Ultrasonic extraction

In this method of extraction, ultra sound sonicator was used for the extraction. About 10g of pulverized leaves of *Momordica cymbalaria* was placed in 250 ml conical flask and in that conical flask 100 ml of hydro alcohol (70 % of methanol) was added (15). leaves of *Momordica cymbalaria* was extracted with ultrasonic 30 min under the condition of 40 kHz and 250 W. Then the extract was filtered using Whatman filter paper. The collected filtrate was concentrated using distillation method. And the obtained yield was weighed for the calculation of percentage yield as per standard formula given below.

$$\text{Percentage Yield (\%w/w)} = \frac{\text{Weight of extract obtained (g)}}{\text{Weight of plant material used (g)}} \times 100$$

Estimation of total phenolic content

The total phenolic content of the different extracts was determined by Folin-Ciocalteu assay method. The plant extracts and standard solution of Gallic acid were prepared using distilled water and the concentration was 1mg/ml. Distilled water was used as reagent blank. The total phenolic content was found from the calibration curve of Gallic acid, and it was expressed as milligrams of Gallic Acid Equivalents (GAE) per gram of extract (17).

Estimation of Total Flavonoid content

The total flavonoid content of the different extracts was determined by using Aluminium chloride by colorimetric method. The plant extracts and standard solution of quercetin were prepared using Gallic acid of concentration 1mg/ml were prepared. Methanol was used as reagent blank. The total flavonoid content was determined from the standard Quercetin calibration curve. And it was expressed as milligrams of Quercetin equivalents per gram of extract (18).

Hydrogen peroxide radical scavenging assay

The antioxidant activity of different extract was evaluated using hydrogen peroxide radical scavenging assay. In this assay method was studied as per standard method described by Ruch et al. Different extracts and standard ascorbic acid were prepared in methanol solvent and different concentrations were used (20 to 100µg/ml). The percentage inhibition was calculated as per the following formula (19, 20).

$$\text{Percentage Inhibition (\%)} = \frac{\text{Control absorbance} - \text{Sample absorbance}}{\text{Control absorbance}} \times 100$$

Alpha amylase inhibitory assay

The antidiabetic activity of different extracts was evaluated by using α-amylase inhibitory activity assay. In this assay method was performed as per the methods. Different extracts and standard acarbose were prepared in distilled water and different concentrations were used (100 to 1000µg/ml). The percentage inhibition was calculated as per the following formula (21).

$$\text{Percentage Inhibition (\%)} = \frac{\text{Control absorbance} - \text{Sample absorbance}}{\text{Control absorbance}} \times 100$$





Gopalasatheeskumar et al.,

RESULTS AND DISCUSSION

Percentage extractive yield

The plant material *Momordica cymbalaria* leaves was extracted with different extraction methods and the Percentage extractive yield of different extraction methods are listed in Table 1. The Soxhlet extraction method have shows higher extractive yield (18.38% w/w) when compared with all other extracts. The Ultrasonic extraction method shows less extractive yield (6.48% w/w). The less extractive yield in ultrasonication method may due to the less duration of extraction procedure and higher extractive yield of Soxhlet extraction method may due to its continuous extractive principle.

Total Phenolic and Flavonoid content

Total Phenolic and Flavonoid content of *Momordica cymbalaria* leaves on different extraction methods are listed in Table 2. The Ultrasonic extraction method shows higher total phenolic content; however, the Cold maceration extraction also shows similar total phenolic content. For total flavonoid content, Cold maceration extraction method shows higher when compared with all other methods. This report suggests that, the maximum phenolic compounds present in the extract obtained from cold maceration is maybe the flavonoids.

Antioxidant activity

The antioxidant activity was evaluated using the hydrogen peroxide radical scavenging assay. The results of hydrogen peroxide radical scavenging assay were shown in Figure 2. The percentage inhibition of hydrogen peroxide radical activity of extracts was increased based on concentration. The cold maceration method shows the higher percentage inhibition when compared with all other extraction methods in concentration dependent manner. The reflux method shows least activity when compared with all other methods. The least activity of the reflux method maybe due to its less phenolic and flavonoids content and higher activity of the cold maceration may due to its higher phenolic and flavonoids content.

Antidiabetic activity

The antidiabetic activity was evaluated by using the alpha amylase enzyme inhibition assay. The results of alpha amylase enzyme inhibition assay were shown in Figure 3. The percentage inhibition of alpha amylase activity of extracts was increased based on concentration. The cold maceration method shows the higher percentage inhibition of alpha amylase enzyme when compared with all other extraction methods in concentration dependent manner. The reflux method shows least activity when compared with all other methods. The least activity of the reflux method maybe due to its less phenolic and flavonoids content and higher activity of the cold maceration may due to its higher phenolic and flavonoids content.

CONCLUSION

The results of current research concluded that, different extraction methods on *Momordica cymbalaria* leaves shows the both antioxidant and antidiabetic activity. Based on the activity the cold maceration is suitable method for the extraction of antioxidant and antidiabetic phytochemicals from *Momordica cymbalaria* leaves. Further studies needed to identify the phytochemicals, preclinical studies and isolation of active principles.

ACKNOWLEDGEMENTS

The authors thank to Pungavarnatham (Thoothukudi District) village peoples for help to collecting plant materials and Prof. V. Srinath, Head of the Department of Pharmacy, Annamalai University for providing chemicals and excellent lab specialties for doing research work.





Gopalsatheeskumar et al.,

REFERENCES

1. Gopalsatheeskumar K, Kalaichelvan VK. Why Focusing on Traditional Medicine is too important- Interesting Facts with Evidence. JGPT 2021;13(3):1-5.
2. Sarkar P, Dhumal C, Panigrahi SS, Choudhary R. Traditional and ayurvedic foods of Indian origin. J Ethnic Foods 2015;2(3):97-109.
3. Bai Y, Xia B, Xie W, Zhou Y, Xie J, Li H, Liao D, Lin L, Li C. Phytochemistry and pharmacological activities of the genus *Prunella*. Food Chem 2016;204:483-496.
4. Zhang BM, Wang ZB, Xin P, Wang QH, Bu H, Kuang HX. Phytochemistry and pharmacology of genus *Ephedra*. Chin J Nat Med 2018;16(11):811-828.
5. Gopalsatheeskumar K. An Updated Pharmacological Overview on *Momordica cymbalaria* (Athalakkai). Innoriginal International Journal of Sciences 2018; 5(1):28-31.
6. Jeyadevi RA, Sivasudha T, Rameshkumar A, Sangeetha B, Arul Ananth D, Aseervatham SB. Nutritional constituents and medicinal values of *Momordica cymbalaria* (Athalakkai) – A review. Asian Pac. J. Trop. Biomed 2012;2(1):S456-S461.
7. Garcia-Salas P, Morales-Soto A, Segura-Carretero A, Fernández-Gutiérrez A. Phenolic-compound-extraction systems for fruit and vegetable samples. Molecules 2010;15(12):8813-8826.
8. Altemimi A, Lakhssassi N, Baharlouei A, Watson DG, Lightfoot DA. Phytochemicals: Extraction, Isolation, and Identification of Bioactive Compounds from Plant Extracts. Plants (Basel) 2017;6(4):42.
9. Hanan B, Akram H, Hassan R, Ali H, Zeinab S, Bassam B. Techniques for the Extraction of Bioactive Compounds from Lebanese *Urtica dioica*. AJPCT 2013; 1(6): 507-513.
10. Tushar D, Sonal S, Gajbhiye NA, Satyanshu K. Effect of extraction methods on yield, phytochemical constituents and antioxidant activity of *Withania somnifera*. Arab. J. Chem 2017; 10(1):S1193-S1199.
11. Hayouni EA, Abedrabba M, Bouix M, Hamdi M. The effects of solvents and extraction method on the phenolic contents and biological activities in vitro of Tunisian *Quercus coccifera* L. and *Juniperus phoenicea* L. fruit extracts. Food Chem 2007; 105:1126-1134.
12. Yuvaraja K R, Santhiagu A, Jasmine S, Gopalsatheeskumar K. Hepatoprotective activity of *Ehretiamicrophylla* on paracetamol induced liver toxic rats. J Res Pharm 2021; 25(1):89-98.
13. Gopalsatheeskumar K, Ariharasivakumar G, Kalaichelvan VK, Sengottuvel T, Sanish Devan V, Srividhya V. Antihyperglycemic and antihyperlipidemic activities of wild musk melon (*Cucumis melo* var. *agrestis*) in streptozotocin-nicotinamide induced diabetic rats. Chin Herb Med 2020; 12:399–405.
14. SankeshwariRoopali M, Ankola Anil V, Bhat Kishore, HullattiKirankumar. Soxhlet versus cold maceration: Which method gives better antimicrobial activity to licorice extract against *Streptococcus mutans*? J Sci Soc 2018; 45(2):67-71.
15. ZhangQW, LinLG, Ye WC. Techniques for extraction and isolation of natural products: a comprehensive review. Chin Med 2018; 13:20.
16. Gopalsatheeskumar, K. Significant role of Soxhlet extraction process in phytochemical research. MJPM 2018; 7:43–47.
17. Madaan R, Bansal G, Kumar S, Sharma A. Estimation of Total Phenols and Flavonoids in Extracts of *Actaea spicata* Roots and Antioxidant Activity Studies. Indian J Pharm Sci 2011;73(6):666-669.
18. Saeed N, Khan MR, Shabbir M. Antioxidant activity, total phenolic and total flavonoid contents of whole plant extracts *Torilis leptophylla* L. BMC Complement Altern Med 2012; 12:221.
19. Fernando CD, Soysa P. Optimized enzymatic colorimetric assay for determination of hydrogen peroxide (H₂O₂) scavenging activity of plant extracts. MethodsX 2015;2:283-291.
20. AsokKumar K, UmaMaheswari M, Sivashanmugam AT, Subhadra Devi, Subhashini N, Ravi TK. Free radical scavenging and antioxidant activities of *Glinus oppositifolius* (carpet weed) using different in vitro assay systems. Pharm Biol 2009; 47(6):474-482.
21. Tamil IG, Dineshkumar B, Nandhakumar M, Senthilkumar M, Mitra A. In vitro study on α -amylase inhibitory activity of an Indian medicinal plant, *Phyllanthus amarus*. Indian J Pharmacol 2010;42(5):280-282.



Gopalsatheeskumar *et al.*,**Table 1: Percentage extractive yield of *Momordica cymbalaria* leaves on different extraction methods**

Method of Extraction	Amount of plant material used (g)	Volume of solvent used (ml)	Amount of extract obtained (g)	Percentage Yield (% w/w)
Cold maceration extraction	10	100	1.305	13.05
Reflux extraction	10	100	1.422	14.22
Soxhlet extraction	100	1000	18.38	18.38
Ultrasonic extraction	10	100	0.648	6.48

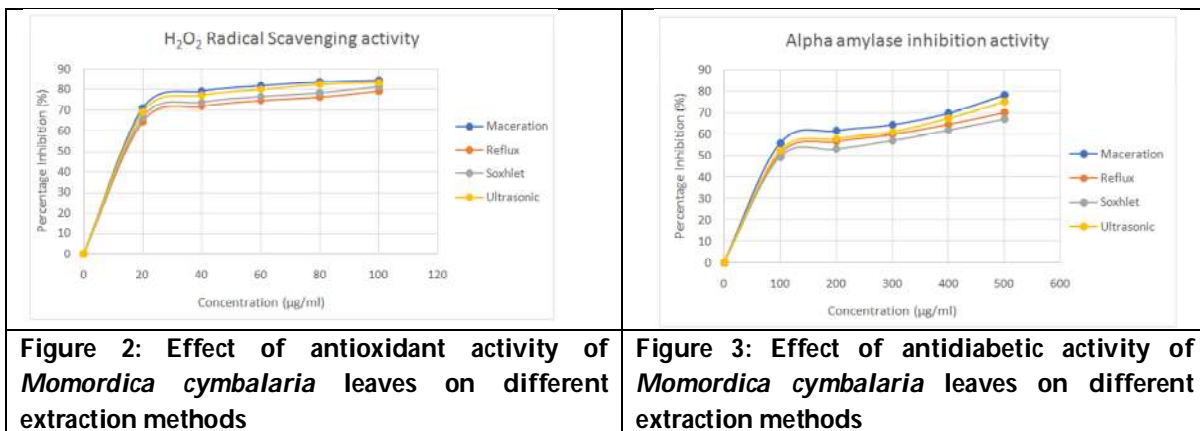
Table 2: Total Phenolic and Flavonoid content of *Momordica cymbalaria* leaves on different extraction methods

Method of Extraction	Total phenolic content expressed as Gallic acid equivalent (mg/g)	Total Flavonoid content expressed as Quercetin equivalent(mg/g)
Cold maceration extraction	33.18	19.56
Reflux extraction	28.36	14.25
Soxhlet extraction	32.09	16.22
Ultrasonic extraction	33.59	17.68

**Figure 1: Aerial parts of *Momordica cymbalaria***



Gopalasatheeskumar *et al.*,





Mitigation of Salinity Induced Effects by Foliar Application of Brassinosteroids in *Vigna radiata* L. Co (Gg) 7 Variety

Zahoor Ahmad Kutay^{1*} and A. Venkatesan²

¹Ph.D Research Scholar, Department of Botany, Annamalai University, Annamalai Nagar, Tamil Nadu, India.

²Associate Professor, Department of Botany, Annamalai University, Annamalai Nagar, Tamil Nadu, India.

Received: 18 Nov 2021

Revised: 28 Dec 2021

Accepted: 11 Jan 2022

*Address for Correspondence

Zahoor Ahmad Kutay

Ph.D Research Scholar,

Department of Botany,

Annamalai University, Annamalai Nagar,

Tamil Nadu, India.

Email: zahoorattari21@gmail.com



This is an Open Access Journal / article distributed under the terms of the **Creative Commons Attribution License** (CC BY-NC-ND 3.0) which permits unrestricted use, distribution, and reproduction in any medium, provided the original work is properly cited. All rights reserved.

ABSTRACT

Impacts of brassinosteroid on the growth, chlorophyll, osmolyte, and antioxidant properties of *Vigna radiata* L. CO (Gg) 7 variety (Green gram) under salinity stress and non stress conditions were studied. Foliar application of different concentrations of brassinosteroid (0.5 μ M, 0.75 μ M and 1.0 μ M) and basal treatment of NaCl (75mM) were used to evaluate the results. However 0.75 μ M concentration of brassinosteroid proved effective to enhance growth, chlorophyll, protein and 1.0 μ M improved proline content and antioxidant enzyme activities in both salinity and non salinity stress conditions.

Keywords: Antioxidants, brassinosteroid, chlorophyll, osmolyte, salinity, *Vigna radiate*.

INTRODUCTION

Soil salinity has become a major agricultural problem of the modern world [1]. The arable land is continuously transforming into saline (1-3% per year) either due to natural salinity or due to human interference which accounts nearly 20% of the irrigated agricultural land [2]. Salt stress affects plant growth in a bi-phasic manner causing osmotic stress followed by specific ion toxicity [3]. However, the intensity of adverse and injurious effects of salinity stress depends upon the nature of plant species, concentration and duration of salt stress, plant developmental stage and mode of salt application to the crop. Salinity is recognized as a major constraint in the production of green gram crop where 50 mM NaCl can cause yield losses \geq 70% [4]. Salt stress inflicts considerable adverse effects on morphological and biochemical parameters of green gram [5]. The increased Na⁺ absorption in saline soils reduces K⁺ absorption,



**Zahoor Ahmad Kutay and A. Venkatesan**

which has a negative impact on metabolic enzymatic activities and therefore fallacious for plant growth [6]. These primary effects of salinity stress result in secondary effects such as reduced assimilate production, cell expansion and membrane function and cytosolic metabolism [7]. Green gram (*Vigna radiata* L. Wilczek) is an important leguminous crop mainly cultivated in tropical, subtropical and temperate zones of Asia including India, Bangladesh, Pakistan, Myanmar, Indonesia, Philippines, Sri Lanka, Nepal, China, Korea and Japan [8]. It grows best in well-drained loamy to sandy-loam soils and produces the highest yield. Soils that are saline or saturated with water are unsuitable for cultivation. Several abiotic stresses, such as heat, drought, salinity, and water-logging, had negative impacts on green gram productivity and adaptability, affecting crop growth and development by altering physiological processes and the plant-water relationship [9,10]. As a result, plant growth regulators (PGRs) are being successfully used to boost yield and reduce harmful effects of salinity stress in important crops.

Brassinosteroids (BRs) are a new class of plant growth regulators that have been dubbed "New Class of Plant Hormones" [11] "Polyhydroxylated Steroid Plant Hormone" [12] Researchers later discovered that they play an important and beneficial role in the growth and development of a variety of plants. Cell division and cell elongation in stems and roots, photo-morphogenesis, reproductive development, leaf senescence and stress responses are all influenced by brassinosteroids [13,12]. They also have an impact on leaf development and growth as well as plant biomass. In *Arabidopsis* (*Arabidopsis thaliana*), mustard (*Brassica napus*), rapeseed (*Brassica juncea*), eggplant (*Solanum melongena*), pepper (*Capsicum annuum*), cucumber (*Cucumis sativus*), common bean (*Phaseolus vulgaris*), and maize (*Zea mays*), BRs have all been shown to reduce the negative effects of salinity. Increased antioxidant enzyme activity, decreased Na⁺ and Cl⁻ concentrations, and increased K⁺ and Ca²⁺ concentrations are all signs of BR treatment-induced enhanced tolerance to salt stress in plants. The control of reactive oxygen species (ROS) production and scavenging in the chloroplast is critical for plant salinity tolerance [14]. Because BRs can protect plants from oxidative stress caused by salinity, the increase in the activities of antioxidant enzymes and scavenging metabolites in this organelle may be linked to BR-induced plant growth under saline conditions [15]. Furthermore, BRs promote oxidative stress tolerance by causing an increase in apoplast H₂O₂, which then upregulates the antioxidant system [12]. Exogenous application of EBL, on the other hand, altered the activity of proline metabolism enzymes [16].

MATERIALS AND METHODS

Experimental material and design

Healthy seeds of *Vigna radiata*, CO (Gg) 7 variety, collected from the TNAU, Coimbatore, Tamil Nadu, India, were used in this study. The seeds were surface sterilized using 0.01% HgCl₂ for 3 minutes and then thoroughly rinsed three times with distilled water followed by five hours soaking. These seeds were then sown in the polythene bags filled with soil in the ratio of 1:2:1 (Sand: Red soil: Farmyard manure) in the garden of Botany department, Annamalai University, Tamil Nadu, India. Plants were taken into eight groups (T₀ - T₇) with five replicates (n=5) in each group. After germination, plants were supplied with normal water when necessary. NaCl treatment was given at 12 DAS, foliar application of brassinosteroid at 20 DAS and analysis was done at 30 DAS. Our research treatment design was as follows; T₀ (normal water); T₁ (75mM NaCl); T₂ (0.5μM BR); T₃ (0.75μM BR); T₄ (1.0μM BR); T₅ (75mM NaCl + 0.5μM BR); T₆ (75mM NaCl + 0.75μM BR); T₇ (75mM NaCl + 1.0μM BR). The whole culture treatment was arranged in a Completely Randomized Block (CRB) design.

Morphological attributes

Determination of Root length and Shoot length

The green gram plants were uprooted, washed with tap water and taken to the lab immediately to determine the morphological traits. The root length was measured below the point of root-shoot transition to the farthest point of root tip. The length between shoot tip and point of the root shoot transition region was taken as shoot length. The values were expressed in cm plant⁻¹.



**Zahoor Ahmad Kutay and A. Venkatesan****Determination of Fresh weight**

The plant roots and shoots were washed with the tap water and blotted gently to remove moisture. The root and shoot fresh weights were taken by using an electronic balance (Model – DS-852J Series) and subsequently the plants were dried at 70°C in a hot air oven for 48 hours.

Leaf area

The leaf area was calculated by measuring the length and width of the leaf as described by Yoshida *et al.* (1972) [17].

Leaf area (cm²) = K × length × breadth

Where; K = Kemp's constant (for dicot leaves 0.66)

Determination of Chlorophyll and Carotenoid contents

A fresh leaf tissue of 500mg were ground in a pre-chilled mortar by adding 10ml of 80% acetone(v:v). After complete extraction, the mixture was centrifuged at 800 rpm for 15 minutes. Further, the extraction was repeated again by discarding the supernatant. Finally, the supernatant collected was made up to a final volume of 10ml with 80% acetone. The absorbance was read at 645, 663 and 480nm using spectrophotometer (Systronic India Limited, Gujarat, India, UV-VIS Model-118). The chlorophyll and carotenoid contents obtained were calculated followed by coefficients of Arnon (1949) [18] and the values were expressed in mg g⁻¹ fr. wt.

Estimation of Proline

The assessment of proline content was performed by a procedure given by Bates *et al.* (1973) [19]. To 2ml of proline extract, 2ml of acid ninhydrin and 2ml glacial acetic acid were added. The mixture was incubated for an hour at 100°C in water bath. Reaction was terminated by transferring the test tubes to an ice bath. 4ml toluene was added and mixed by vigorously shaking and then separated with the help of separating funnel. The absorbance of the rose pink layer was measured at 520 nm and proline content was expressed in mg g⁻¹ fr. wt.

Protein estimation

The proteins was extracted and estimated by (Lowry *et al.*, 1951) [20] method. 0.5g of plant material was macerated in a mortar and pestle with 20% trichloroacetic acid (TCA) followed by centrifugation at 10,000g for 15 minutes. The supernatant was thrown away, and to the pellets, 0.1N NaOH was added followed by centrifugation for 15 minutes. The supernatant was made up to 10ml with 0.1N NaOH. The extract was used for protein valuation using Bovine Serum Albumin (BSA).The absorbance was read at 660nm in the UV-VIS Spectrophotometer and the values were expressed in mg g⁻¹ fr. wt.

Antioxidant Enzyme Activities

The SOD Activity was estimated according to Beauchamp and Fridovich (1971) [21] method. The SOD activity was determined by the ability of enzyme extract to inhibit the reduction of NBT by superoxide free radicals, which were generated in the reaction medium through photo reduction of riboflavin. The optical density was determined at 560nm, and the SOD activity results were calculated as Unit g⁻¹ fresh mass.

The CAT activity was determined based on the rate of H₂O₂ decomposition as measured by the decrease in absorbance at 240nm, based on the method of Chandlee and Scandalios (1984) [22]. The reaction mixture includes phosphate buffer (50 mM, pH 7.0), H₂O₂ (3%), and 0.4ml enzyme extract. The values were expressed in mM H₂O₂ decomposed g⁻¹ fresh mass

The POD Activity was assayed by the method of Reddy *et al.* (1995) [23]. The reaction mixture for Peroxidase consisted of pyragallol, phosphate buffer (pH 6.5), 1% H₂O₂ and enzyme extract. The change in absorbance due to catalytic conversion of pyragallol to purpurogallin was noted at an interval of 20s for 2 min, at 420 nm on a spectrophotometer (Systronic India Limited, Gujarat, India, UV-VIS Model-118). A control set was prepared by using DDW instead of enzyme extract. The POD activity was expressed in Unit g⁻¹ fresh mass.



**Zahoor Ahmad Kutay and A. Venkatesan**

The APX Activity was estimated following the procedure of Asada and Takahashi (1987) [24]. The reaction mixture contained 50mM potassium phosphate buffer (pH 7.0), 0.1mM H₂O₂, 0.5mM ascorbic acid and 0.2ml of enzyme extract. The absorbance was read as decrease at 290nm against the blank and the enzyme activity was expressed in EU mg⁻¹ protein.

Statistical analysis

Statistical analysis was performed through One Way ANNOVA by using SPSS followed by DMRT. LSD at P = 0.05 was calculated by employing Tukey's HSD Test.

RESULTS

NaCl treatment to *Vigna radiata* plants caused stress to such a level which affected their growth characteristics (shoot length, root length, shoot fresh weight, root fresh weight and leaf area). A significant reduction of 23.48%, 31.32%, 31.85%, 35.96% and 27.78% respectively in these parameters was observed in NaCl stressed plants at 30 DAS in comparison to control. However, exogenous brassinosteroid spray at 20 DAS to both unstressed as well as stressed plants (T₂ - T₇) significantly enhanced the values of these parameters over the respective controls. The decline in growth parameters by NaCl stress was almost completely mitigated by exogenous brassinosteroid spray (Table 1). The exposure of plants to NaCl stress significantly reduced the total chlorophyll and carotenoid content. A reduction of 14.14% and 17.63% respectively was observed with respect to control. However, the content of these photosynthetic pigments was improved up to the mark by the exogenous application of brassinosteroid but 0.75µM BR evolved as the most feasible concentration in completely neutralizing the adverse effects of NaCl stress (Table 2).

Salinity stress caused reduction in the protein content of green gram plants (T₁). A reduction of 10.10% was observed at T₁ (75mM NaCl) in comparison to control. Exogenous BR spray caused an improvement in the protein content of *Vigna radiata* plants at both unstressed as well as stressed treatments (T₂ - T₇) and 0.1 µM BR proved to be the most efficient concentration in combating the salinity stress for protein improvement (Table 2). Proline content was greatly increased by NaCl treatment given at 15 DAS. A significant increase of 45.82% was seen at T₁ (75mM NaCl) as compared to control. Exogenous application of BR to all other treatments also caused proline content to increase further thereby increasing tolerance to salinity stress in green gram. A concentration of 0.75µM BR was very efficient in improving tolerance to salinity stress by elevating the proline content. The antioxidant enzyme activities were seen increased by salinity, BR and NaCl + BR (T₁ - T₇). The BR treatment significantly enhanced the antioxidant level in *Vigna radiata*. Maximum activities of the enzymes were recorded in the NaCl treated plants sprayed by brassinosteroid. An increase of 30.51% and 81.29% at T₆ (75mM NaCl + 0.75µM BR) in catalase (CAT) [Fig. 1(a)] and APX [Fig. 1(d)]; 120.38% and 35.71% at T₇ (75mM NaCl + 1.0µM BR) in POD [Fig. 1(b)] and SOD [Fig. 1(c)] was observed in comparison to control.

DISCUSSION

The present study reveals that NaCl treatment caused a significant reduction in the chlorophyll content of *Vigna radiata*. This increased salinity lead oxidative stress may be attributed to the increase in the activity of chlorophyll degrading enzyme chlorophyllase and consequently overall decrease of chlorophyll content [25,26]. Under varying NaCl concentration, chlorophyll and carotenoid content got reduced in green gram [27]; in black gram [28]. A great reduction in chlorophyll content was observed in salt sensitive plants [29]. Chlorophyll a and chlorophyll b content decreased under stress conditions in *Vigna radiata* [30]. The reduced photosynthetic pigments by NaCl were completely mitigated by exogenous application of brassinosteroid spray. Our results were in accordance to Dong *et al.*, 2017 [31] in wheat; Rattan *et al.*, 2014 [32] in *Zea mays* Beulah Esther and Gautam, 2020 [33] in *Vigna mungo*; Jin-Huan *et al.*, 2015 [34] in *Leymus chinensis*; Abbas *et al.*, 2013 [35] in Pepper; Singh *et al.*, 2020 [36] in Black gram; Upadhaya *et al.*, 2015 [37] in *Solanum tuberosum*. Brassinosteroid increased photosynthetic pigment contents in unstressed plants of *V. unguiculata* [38]. On exposure of soybean plants to NaCl stress, total chlorophyll and



**Zahoor Ahmad Kutay and A. Venkatesan**

carotenoid contents decreased but exogenous application of EBL completely masked the NaCl effect [39]. The ROS generation under saline conditions caused peroxidation of chloroplast membranes [40] which could be the reason of reduced chlorophyll content in our present study. In the present study, brassinosteroid (BR) significantly scavenged ROS by increasing the activity of enzymatic antioxidants and thereby improved the chlorophyll content by inhibiting the peroxidation of chloroplast membranes caused by ROS. The most favourable evidence for the brassinosteroid induced impact on the chlorophyll is due to transcriptional and /or translational expression of specific genes responsible for enzymes necessary for chlorophyll synthesis [41].

Our results also revealed that NaCl stress caused reduction in protein content of *Vigna radiata* but on the exogenous application of brassinosteroid, protein content got improved in unstressed as well as stressed plants. This increase was seen only upto specific concentration (0.75µM BR), increased concentration showed negative impacts. Similar results were obtained by Rajesh *et al.*, 2014 [42] in green gram; Nafie, 2014 [43] in *Phaseolus vulgaris*; Kartal *et al.*, 2009 [44] in barley; Asha and Lingakumar, 2015 [38] in *Vigna unguiculata* who observed that brassinosteroids enhanced protein content in test plants. HBL caused enhanced protein content in maize [45].

NaCl stress caused increased proline content in *Vigna radiata*. Exogenous brassinosteroid spray at vegetative stage enhanced more proline content as compared to control. Brassinosteroids caused increase in osmolyte accumulation [46] thereby prevented the oxidative damage, mediate cellular stress signalling and assist in ROS scavenging [47] and thereby enhance stress tolerance. Similar observations were also made by Ozdemir *et al.*, 2004 [48] in *Oryza sativa* in both stressed as well as unstressed conditions. Ali *et al.*, 2007 [49] observed increased proline content by salinity as well as brassinosteroid and by both in *Cicer arietinum*. Shahid *et al.*, 2011 and 2014 [50,51], while working on garden pea, observed an increase in proline content on exposure to NaCl stress which further increased by the exogenous application of 24EBL in both NaCl treated as well as untreated plants. Soliman *et al.*, 2020 [39] observed increased proline content by the exogenous application of EBL more in NaCl treated plants than in unstressed ones. Reactive oxygen species (ROS) are generated in plants during metabolism. Further, the accumulation of ROS is increased by environmental stresses. The ROS need to be scavenged for maintenance of normal growth. Plants have developed a series of enzymatic and non enzymatic mechanisms to counteract ROS and protect cells from oxidative damage. Various enzymes including CAT, SOD, APX, guaiacol peroxidase, and PPX have been associated with detoxification of ROS in plants. Several PGRs including BRs have been reported to help in modulating this antioxidant defense system and thus scavenging the free radicals and help the plant to protect from oxidative stress. Exogenous EBL enhanced antioxidant enzyme activities in ground nut [52]. It may be inferred from the enhancement in CAT activity that BR application modulated the antioxidative metabolism resulting in better growth of plants [53]. Marked increase in antioxidant activities were observed by Arora *et al.*, 2008 [45] in non-stressed plants of *Zea mays*. Enhanced antioxidant activities were also observed by Ozdemir *et al.*, 2004 [48] in rice. Brassinosteroid spray under NaCl stress could increase the antioxidant enzyme activity thus enhance stress tolerance in plants [31].

In the present study, NaCl stress caused reduction in all the growth parameters of *Vigna radiata*. Our results are in agreement with those of Li *et al.*, 2013 [54], Dong *et al.*, 2017 [31] and many others who observed the marked decrease in all the growth parameters of their test plants when subjected to salt stress. This reduction in growth caused by salinity could be due to shortage of energy as all the processes involved in salt transport and salt damage repair are energy requiring. Salinity stress caused reduced water absorption due to osmotic effect, ionic imbalance and decreased metabolic activities [55]. The reduction in biomass of plants due to NaCl stress results by upsurged uptake of Na⁺ ions, with concurrent decline in the amount of K⁺ uptake by the plants [1]. However this reduction in growth parameters was completely modulated by exogenous application of brassinosteroid. Foliar application of 0.75 µM BR was efficient for this process. Similar results were also observed by Upreti and Murti, 2004 [56] in French bean; Dabariya and DL Bagdi, 2019 [57] in barley. Increased plant length, biomass and leaf area were observed by Latha and Vardhini, 2018 [58] in mustard; Asha and Lingakumar, 2015 [38] in *Vigna unguiculata*; Brassinosteroid and salicylic acid increased shoot length, root length and leaf area in *Lablab purpureus* [59]. 28HBL increased shoot, root length and biomass in both stressed as well as unstressed plants of *Zea mays* [45]. Significant increase in plant height and leaf area were observed by Lal *et al.*, 2019 [60] while working on the impacts of NaCl and brassinolide on growth



**Zahoor Ahmad Kutay and A. Venkatesan**

and yield parameters of *Triticum aestivum*. 24EBL enhanced growth and completely mitigated the deleterious effects of NaCl in *Pisum sativum* [51]. The acceleration in the antioxidant enzyme activities and increased pool of proline caused an increase in tolerance of plants to high salinity in the present study. The increased tolerance to stress was manifested in terms of improved growth (Table 1).

CONCLUSION

The present study showed that high NaCl concentration resulted in reduced growth, biomass, chlorophyll, carotenoid and protein but increased proline and antioxidant enzyme activities in *Vigna radiata* L. CO (Gg) 7 variety. However an interesting aspect of this study is that brassinosteroid spray increased all the parameters in comparison to control and completely ameliorated the damage caused by NaCl stress mainly by increasing the ROS scavenging system. It should be noted that brassinosteroid should be sprayed at very low concentration but in the present study a concentration of 0.75 μ M proved to be most effective and increasing brassinosteroid concentration above the efficient level could reverse the impacts.

REFERENCES

1. Noreen, S., Sultan, M., Akhter, M. S., Shah, K. H., Ummara, U., Manzoor, H., ... & Ahmad, P. Foliar fertigation of ascorbic acid and zinc improves growth, antioxidant enzyme activity and harvest index in barley (*Hordeum vulgare* L.) grown under salt stress. *Plant Physiology and Biochemistry*, 2021, 158, 244-254.
2. Velmurugan, A., Swarnam, P., Subramani, T., Meena, B., & Kaledhonkar, M. J. Water demand and salinity. In *Desalination-Challenges and Opportunities* Jan 28, 2020, IntechOpen.
3. Hanin, M., Ebel, C., Ngom, M., Laplaze, L., & Masmoudi, K.. New Insights on Plant Salt Tolerance Mechanisms and Their Potential Use for Breeding. *Frontiers in Plant Science*, 2016, 7, 1787.
4. Hasanuzzaman, M., Nahar, K., & Fujita, M. Plant response to salt stress and role of exogenous protectants to mitigate salt-induced damages. In *Ecophysiology and Responses of Plants under Salt Stress* 2013, (pp. 25-87). Springer, New York, NY.
5. Zhang, Q., & Dai, W. Plant response to salinity stress. In *Stress Physiology of Woody Plants*, 2019, 9(pp. 155-173). CRC Press.
6. Hauser, F., & Horie, T. A conserved primary salt tolerance mechanism mediated by HKT transporters: a mechanism for sodium exclusion and maintenance of high K⁺/Na⁺ ratio in leaves during salinity stress. *Plant, Cell & Environment*, 2010, 33(4), 552-565.
7. Gull, A., Lone, A. A., & Wani, N. U. I. Biotic and abiotic stresses in plants. *Abiotic and Biotic Stress in Plants*, 2019, 1-19.
8. Rahim, M. A., Mia, A. A., Mahmud, F., Zeba, N., & Afrin, K. S. Genetic variability, character association and genetic divergence in Mungbean (*Vigna radiata* L. Wilczek). *Plant Omics*, 2010, 3(1), 1-6.
9. Zandalinas, S. I., Sales, C., Beltrán, J., Gómez-Cadenas, A., & Arbona, V. Activation of secondary metabolism in citrus plants is associated to sensitivity to combined drought and high temperatures. *Frontiers in Plant Science*, 2017, 7, 1954.
10. Landi, S., Hausman, J. F., Guerriero, G., & Esposito, S. Poaceae vs. abiotic stress: focus on drought and salt stress, recent insights and perspectives. *Frontiers in Plant Science*, 2017, 8, 1214.
11. Khripach, V. A., Zhabinskii, V. N., & De Groot, A. Practical applications and toxicology. Brassinosteroids: A new class of plant hormones, 1999, 325-345.
12. Fariduddin, Q., Yusuf, M., Ahmad, I., & Ahmad, A. Brassinosteroids and their role in response of plants to abiotic stresses. *Biologia Plantarum*, 2014, 58(1), 9-17.
13. Sirhindi, G. Brassinosteroids: biosynthesis and role in growth, development, and thermotolerance responses. In *Molecular Stress Physiology of Plants*, 2013, pp. 309-329. Springer, India.
14. Miller, G. A. D., Suzuki, N., Ciftci-Yilmaz, S. U. L. T. A. N., & Mittler, R. O. N. Reactive oxygen species homeostasis and signalling during drought and salinity stresses. *Plant, Cell & Environment*, 2010, 33(4), 453-467.





Zahoor Ahmad Kutay and A. Venkatesan

15. Vázquez, M. N., Guerrero, Y. R., de la Noval, W. T., Gonzalez, L. M., & Zullo, M. A. TAdvances on exogenous applications of brassinosteroids and their analogs to enhance plant tolerance to salinity: A review. *Australian Journal of Crop Science*, 2019, **13**(1), 115-121.
16. Yusuf, M., Fariduddin, Q., Khan, T. A., & Hayat, S. Epibrassinolide reverses the stress generated by combination of excess aluminum and salt in two wheat cultivars through altered proline metabolism and antioxidants. *South African Journal of Botany*, 2017, **112**, 391-398.
17. Yoshida S. Physiological aspects of grain yield. *Annual Review of Plant Physiology*. 1972, **23**(1):437-64.
18. Arnon, D. I. Copper Enzymes in Isolated Chloroplasts. Polyphenoloxidase in *Beta vulgaris*. *Plant Physiology*, 1949, **24**(1), 1-15.
19. Bates, L. S., Waldren, R. P., & Teare, I. D. Rapid determination of free proline for water-stress studies. *Plant and Soil*, 1973, 205-207.
20. Lowry, O. H., Rosebrough, N. J., Farr, A. L., & Randall, R. J. Protein measurement with the Folin phenol reagent. *Journal of Biological Chemistry*, 1951, **193**, 265-275.
21. Beauchamp, C., & Fridovich, I. Superoxide dismutase: improved assays and an assay applicable to acrylamide gels. *Analytical Biochemistry*, 1971, **44**(1), 276-287.
22. Chandlee, J. M., & Scandalios, J. G. Analysis of variants affecting the catalase developmental program in maize scutellum. *Theoretical and Applied Genetics*, 1984, **69**(1), 71-77.
23. Reddy, K. P., Subhani, S. M., Khan, P. A., & Kumar, K. B. Effect of light and benzyladenine on dark-treated growing rice (*Oryza sativa*) leaves II. Changes in peroxidase activity. *Plant and Cell Physiology*, 1985, **26**(6), 987-994.
24. Asada, K., Takahashi, M. Production and scavenging of active oxygen in photosynthesis. In: *Photoinhibition*, 1987, pp. 227-287, Kyle, D.J., Osmond, C.B., Arntzen, C.J., eds. *Elsevier*, Amsterdam.
25. Gulmezoglu, N., & Daghan, H. The interactive effects of phosphorus and salt on growth, water potential and phosphorus uptake in green beans. *Appl. Ecol. Environ. Res*, 2017, **15**(3), 1831-1842.
26. Rajeev, K., Anil, K., & Sanjeev, K. Growth, yield and biochemical parameters of green gram (*Vigna radiata*) as influenced by saline water. *Agriways*, 2015, **3**(2), 71-75.
27. Kutay A. Z and A. Venkatesan. Salinity induced effects on the morphological and biochemical parameters of *Vigna radiata* L. *International Journal of Botany Studies*, 2021, **6**(5), 830-835.
28. Sivakumar, R., & Priya, S. J. Effect of PGRs and Nutrients on Growth, Physiological Parameters and Yield of *Vigna mungo* L. under Saline Stress. *International Journal of Plant & Soil Science*, 2017, 1-10.
29. Shahid, M. A., Sarkhosh, A., Khan, N., Balal, R. M., Ali, S., Rossi, L., ... & Garcia-Sanchez, F. Insights into the physiological and biochemical impacts of salt stress on plant growth and development. *Agronomy*, 2020, **10**(7), 938.
30. Suleiman, M. A. Q., & AL-Hamdani, K. M. Effect of growth factors on mineral, proline and protein accumulation in mungbean (*Vigna radiata* L.) under salt stress. *Plant Cell Biotechnology and Molecular Biology*, 2021, 98-109.
31. Dong, Y., Wang, W., Hu, G., Chen, W., Zhuge, Y., Wang, Z., & He, M. R. Role of exogenous 24-epibrassinolide in enhancing the salt tolerance of wheat seedlings. *Journal of Soil Science and Plant nutrition*, 2017, **17**(3), 554-569.
32. Rattan, A., Kapoor, D., Kapoor, N., & Bhardwaj, R. Application of brassinosteroids reverses the inhibitory effect of salt stress on growth and photosynthetic activity of *Zea mays* plants. *International Journal of Theoretical and Applied Sciences*, 2014, **6**(2), 13.
33. Beulah Esther, D., & Gautam, G. Effect of foliar nutrition and plant growth regulators on growth of Blackgram (*Vigna mungo* L.). *Journal of Pharmacognosy and Phytochemistry*, 2020, **9**(3), 1754-1756.
34. Jin-Huan, L., Anjum, S. A., Mei-Ru, L., Jian-Hang, N., Ran, W., Ji-Xuan, S., ... & San-Gen, W. Modulation of morpho-physiological traits of *Leymus chinensis* (Trin.) through exogenous application of brassinolide under salt stress. *JAPS: Journal of Animal & Plant Sciences*, 2015, **25**(4).
35. Abbas S, Latif HH and Elsherbiny EA. Effect of 24-epibrassinolide on the physiological and genetic changes on two varieties of pepper under salt stress conditions. *Pak. J. Bot.* 2013, Aug 1;45(4):1273-84.
36. Singh, S., Jakhar, S., & Rao, S. Improvement in salt tolerance of *Vigna mungo* (L.) Hepper by exogenously applied 24-epibrassinolide. *Legume Research-An International Journal*, 2020, **43**(5), 647-652.





Zahoor Ahmad Kutay and A. Venkatesan

37. Upadhyaya, C. P., Bagri, D. S., & Upadhyay, D. C. Ascorbic acid and/or 24-epibrassinolide trigger physiological and biochemical responses for the salt stress mitigation in potato (*Solanum tuberosum* L.). *International Journal of Applied Sciences and Biotechnology*, 2015, **3**(4), 655-667.
38. Asha, A., & Lingakumar, K.. Effect of 24-epibrassinolide on the morphological and biochemical constitutions *Vigna unguiculata* (L.) seedlings. *Ind. J. Sci. Res. and Tech*, 2015, **3**(1):35-39
39. Soliman, M., Elkelish, A., Souad, T., Alhaithloul, H., & Farooq, M. Brassinosteroid seed priming with nitrogen supplementation improves salt tolerance in soybean. *Physiology and Molecular Biology of Plants*, 2020, **26**(3), 501-511.
40. Hassine, A. B., & Lutts, S. Differential responses of saltbush *Atriplex halimus* L. exposed to salinity and water stress in relation to senescing hormones abscisic acid and ethylene. *Journal of Plant Physiology*, 2010, **167**(17), 1448-1456.
41. Bajguz, A. Metabolism of brassinosteroids in plants. *Plant Physiology and Biochemistry*, 2007, **45**(2), 95-107.
42. Rajesh, K., Reddy, S. N., & Reddy, A. P. K.. Effect of different growth regulating compounds on biochemical and quality parameters in greengram. *Asian J Plant Sci Res*, 2014, **4**(3), 35-39.
43. Nafie, E. Physiological, Biochemical, Molecular and Hormonal Studies to Confirm Growth and Development Regulating Actions of Brassinosteroids in *Phaseolus vulgaris* L. cv. Bronco Seedlings. *Life Science Journal*, 2014, **11**(8), 974-991.
44. Kartal, G., Temel, A., Arican, E., & Gozukirmizi, N. Effects of brassinosteroids on barley root growth, antioxidant system and cell division. *Plant Growth Regulation*, 2009, **58**(3), 261-267.
45. Arora, N., Bhardwaj, R., Sharma, P., & Arora, H. K.. Effects of 28-homobrassinolide on growth, lipid peroxidation and antioxidative enzyme activities in seedlings of *Zea mays* L. under salinity stress. *Acta Physiologiae Plantarum*, 2008, **30**(6), 833-839.
46. Tabassum, T., Farooq, M., Ahmad, R., Zohaib, A., & Wahid, A. Seed priming and transgenerational drought memory improves tolerance against salt stress in bread wheat. *Plant Physiology and Biochemistry*, 2017, **118**, 362-369.
47. Farooq, M., Usman, M., Nadeem, F., ur Rehman, H., Wahid, A., Basra, S. M., & Siddique, K. H. Seed priming in field crops: potential benefits, adoption and challenges. *Crop and Pasture Science*, 2019, **70**(9), 731-771.
48. Özdemir, F., Bor, M., Demiral, T., & Türkan, İ. Effects of 24-epibrassinolide on seed germination, seedling growth, lipid peroxidation, proline content and antioxidative system of rice (*Oryza sativa* L.) under salinity stress. *Plant Growth Regulation*, 2004, **42**(3), 203-211.
49. Ali, B., Hayat, S., and Ahmad, A. 28-Homobrassinolide ameliorates the saline stress in chickpea (*Cicer arietinum* L.). *Environmental and Experimental Botany*, 2007, **59**(2), 217-223.
50. Shahid, M. A., Pervez, M. A., Balal, R. M., Mattson, N. S., Rashid, A., Ahmad, R., ... & Abbas, T. Brassinosteroid (24-epibrassinolide) enhances growth and alleviates the deleterious effects induced by salt stress in pea (*Pisum sativum* L.). *Australian Journal of Crop Science*, 2011, **5**(5), 500-510.
51. Shahid, M. A., Balal, R. M., Pervez, M. A., Garcia-Sanchez, F., Gimeno, V., Abbas, T., ... & Riaz, A. Treatment with 24-epibrassinolide mitigates NaCl-induced toxicity by enhancing carbohydrate metabolism, osmolyte accumulation, and antioxidant activity in *Pisum sativum*. *Turkish Journal of Botany*, 2014, **38**(3), 511-525.
52. Verma, A., Malik, C. P., & Gupta, V. K. In vitro effects of brassinosteroids on the growth and antioxidant enzyme activities in groundnut. *International Scholarly Research Network ISRN Agronomy*, 2012, **1**-8.
53. Vardhini, B. V., & Rao, S. S. R. Effect of brassinosteroids on growth, metabolite content and yield of *Arachis hypogaea*. *Phytochemistry*, 1998, **48**(6), 927-930.
54. Li, G., Peng, X., Wei, L., & Kang, G. Salicylic acid increases the contents of glutathione and ascorbate and temporally regulates the related gene expression in salt-stressed wheat seedlings. *Gene*, 2013, **529**(2), 321-325.
55. Tian, X., He, M., Wang, Z., Zhang, J., Song, Y., He, Z., & Dong, Y. Application of nitric oxide and calcium nitrate enhances tolerance of wheat seedlings to salt stress. *Plant Growth Regulation*, 2015, **77**(3), 343-356.
56. Upreti, K. K., & Murti, G. S. R. Effects of brassinosteroids on growth, nodulation, phytohormone content and nitrogenase activity in French bean under water stress. *Biologia Plantarum*, 2004, **48**(3), 407-411.
57. Dabariya, S., & Bagdi, D. L. Impact of brassinolide in amelioration of salinity induced adverse effects on growth, yield attributes and yield of barley. *Journal of Pharmacognosy and Phytochemistry*, 2019, **8**(6), 1536-1539.





Zahoor Ahmad Kutay and A. Venkatesan

58. Latha, P., & Vidya Vardhini, B. Effect of homobrassinolide on the growth of mustard crops grown in semi-arid tropics of nizamabad. *International Journal of Current Research in Life Sciences*, 2018, **7**(06), 2320-2326.
59. Netwal, M., Choudhary, M. R., Jakhar, R., Devi, S., & Choudhary, S. Exogenous application of Brassinoide and salicylic acid enhances on growth, yield and nutritional quality of Indian bean (*Lablab purpureus* L. var. *typicus*). *Journal of Pharmacognosy and Phytochemistry*, 2018, **7**(6), 2093-2096.
60. Lal, B., Bagdi, D. L., & Dadarwal, B. K.. Role of brassinolide in amelioration of salinity induced adverse effects on growth, yield attributes and yield of wheat. *Journal of Pharmacognosy and Phytochemistry*, 2019, **8**(5), 1790-1793.

Table 1: Effect of soil applied NaCl (75mM) and foliar application of brassinosteroid (0.5µM, 0.75 µM, 1.0 µM) on shoot and root length (cm plant⁻¹), shoot and root fresh weight (g plant⁻¹) and leaf area (cm²) of *Vigna radiata* L. CO (Gg) 7 variety at 30DAS.

Treatments	Shoot length	Root length	Shoot fresh weight	Root fresh weight	Leaf area
T ₀ (Control)	26.4 ± 0.283 ^d	8.3 ± 0.141 ^{cd}	10.61 ± 0.028 ^d	5.06 ± 0.042 ^d	22.24 ± 0.014 ^d
T ₁ (75mM NaCl)	20.2 ± 0.141 ^g	5.7 ± 0.283 ^g	7.23 ± 0.021 ^h	3.24 ± 0.007 ^h	16.06 ± 0.042 ^h
T ₂ (0.5µM BR)	28.9 ± 0.212 ^c	8.8 ± 0.212 ^{bc}	11.12 ± 0.042 ^c	5.21 ± 0.021 ^c	22.37 ± 0.021 ^c
T ₃ (0.75 µM BR)	34.6 ± 0.354 ^a	10.3 ± 0.354 ^a	13.83 ± 0.007 ^a	6.24 ± 0.014 ^a	23.41 ± 0.035 ^a
T ₄ (1.0 µM BR)	30.8 ± 0.424 ^b	9.6 ± 0.424 ^{ab}	12.01 ± 0.035 ^b	5.96 ± 0.028 ^b	22.49 ± 0.028 ^b
T ₅ (75mM NaCl + 0.5µM BR)	21.4 ± 0.141 ^f	6.6 ± 0.495 ^{fg}	7.36 ± 0.049 ^g	4.03 ± 0.049 ^g	16.25 ± 0.007 ^g
T ₆ (75mM NaCl + 0.75 µM BR)	24.8 ± 0.495 ^e	7.7 ± 0.071 ^{de}	8.75 ± 0.014 ^e	4.91 ± 0.028 ^e	19.94 ± 0.049 ^e
T ₇ (75mM NaCl + 1.0 µM BR)	22.1 ± 0.212 ^f	7.3 ± 0.283 ^{ef}	7.96 ± 0.028 ^f	4.37 ± 0.035 ^f	17.31 ± 0.021 ^f
LSD at P = 0.05	1.412	1.431	0.145	0.145	0.145

*Values are the mean and ± (SE) of five replicates; the letters denote significance among the treatments at P=0.05.

Table 2: Effect of soil applied NaCl (75mM) and foliar application of brassinosteroid (0.5µM, 0.75 µM, 1.0 µM) on total chlorophyll, carotenoid, leaf proline and protein (mg g⁻¹fr. wt) of *Vigna radiata* L. CO (Gg) 7 variety at 30DAS.

Treatments	Total chlorophyll	Carotenoid	Leaf proline	Protein
T ₀ (Control)	1.252 ± 0.001 ^d	0.295 ± 0.001 ^d	9.23 ± 0.028 ^h	16.73 ± 0.021 ^d
T ₁ (75mM NaCl)	1.075 ± 0.004 ^e	0.243 ± 0.005 ^e	13.46 ± 0.042 ^d	15.04 ± 0.043 ^h
T ₂ (0.5µM BR)	1.406 ± 0.002 ^c	0.341 ± 0.003 ^{bc}	10.12 ± 0.014 ^g	16.97 ± 0.014 ^c
T ₃ (0.75 µM BR)	1.751 ± 0.001 ^a	0.412 ± 0.002 ^a	10.87 ± 0.035 ^f	17.23 ± 0.035 ^b
T ₄ (1.0 µM BR)	1.550 ± 0.004 ^b	0.311 ± 0.004 ^{bcd}	11.23 ± 0.007 ^e	17.12 ± 0.008 ^a
T ₅ (75mM NaCl + 0.5 µM BR)	1.121 ± 0.001 ^e	0.298 ± 0.004 ^{cd}	16.92 ± 0.022 ^c	16.14 ± 0.028 ^g
T ₆ (75mM NaCl + 0.75 µM BR)	1.235 ± 0.003 ^d	0.346 ± 0.004 ^b	17.48 ± 0.049 ^a	16.59 ± 0.049 ^e
T ₇ (75mM NaCl + 1.0 µM BR)	1.213 ± 0.002 ^d	0.312 ± 0.004 ^{bcd}	17.76 ± 0.028 ^b	16.38 ± 0.021 ^f
LSD at P = 0.05	0.130	0.065	0.145	0.145

*Values are the mean and ± (SE) of five replicates; the letters denote significance among the treatments at P=0.05.





Zahoor Ahmad Kutay and A. Venkatesan

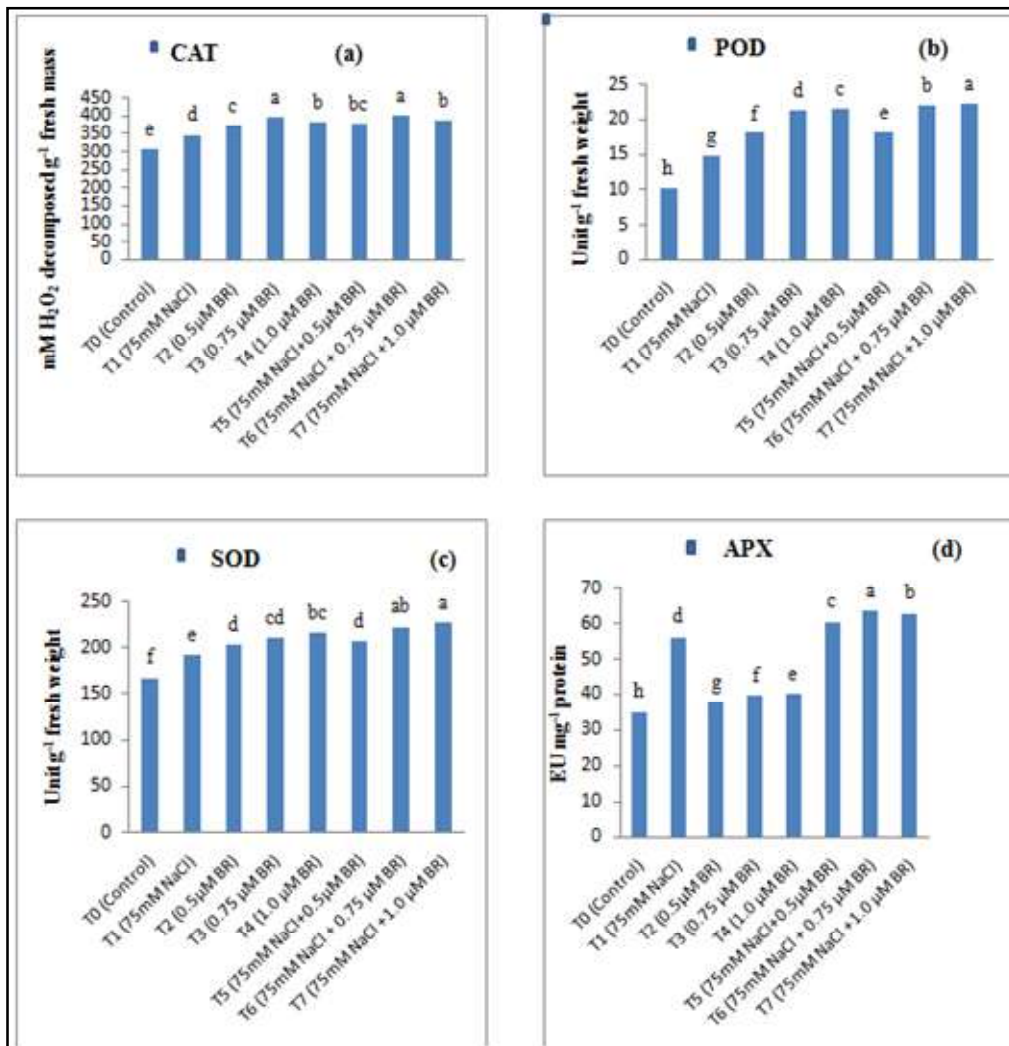


Fig. 1 Effect of soil applied NaCl (75mM) and foliar application of brassinosteroid (0.5µM, 0.75 µM, 1.0 µM) on (a) Catalase activity (CAT) (mM H₂O₂ decomposed g⁻¹ fresh mass), (b) Peroxidase activity (POD) (Unit g⁻¹ fresh weight), (c) Superoxidase Dismutase activity (SOD) (Unit g⁻¹ fresh weight) and (d) Ascorbate Peroxidase activity (APX) (EU mg⁻¹ protein) of *Vigna radiata* L. CO(Gg)7 variety at 30DAS. Values are the mean of five replicates (n = 5) and the treatments sharing the same letters don't differ significantly at P=0.05.





Unbiased Linear Approximate ML Estimation in Generalized Exponential Distribution under Type-II Censoring

A.Vasudeva Rao¹ and S. Bhanu Prakash^{2*}

¹Professor of Statistics, Department of Statistics, Acharya Nagarjuna University, Guntur, A.P., India.

²Lecturer and Statistician, Department of Community Medicine, NRI Medical Institute of Medical Sciences, Sangivalasa, Visakhapatnam, A.P., India.

Received: 20 Oct 2021

Revised: 16 Dec 2021

Accepted: 12 Jan 2022

*Address for Correspondence

S. Bhanu Prakash

Lecturer and Statistician,
Department of Community Medicine,
NRI Medical Institute of Medical Sciences,
Sangivalasa, Visakhapatnam, A.P., India.



This is an Open Access Journal / article distributed under the terms of the **Creative Commons Attribution License** (CC BY-NC-ND 3.0) which permits unrestricted use, distribution, and reproduction in any medium, provided the original work is properly cited. All rights reserved.

ABSTRACT

For the generalized exponential distribution (GED), the maximum likelihood (ML) method does not yield explicit estimators for the location and scale parameters based on Type-II censored samples. To address this, Bhanu Prakash and Vasudeva Rao (2020) derived the linear approximate MLEs (LAMLEs) of the parameters. Through a Monte Carlo simulation study, they found that the LAMLEs are almost as efficient as MLEs. However, the LAMLEs are slightly biased than the MLEs. Therefore, in this paper, we construct unbiased LAMLEs (ULAMLEs) and unbiased percentile estimators (UPCEs) and compare them with the corresponding BLUEs based on the exact variances of the estimators. Interestingly, these new ULAMLEs are found just as efficient as the BLUEs in both complete and Type-II censored samples. However, the construction of ULAMLEs require only the means of order statistics of standard GED where as the construction of BLUEs require means as well as the variances and covariances of order statistics. Further, we compare ULAMLEs with the corresponding MLEs through a simulation study and found that the ULAMLEs are almost as efficient as MLEs. Finally, we present a numerical example to illustrate the construction of the estimators developed here with a real data set.

Keywords: Location and scale parameters of generalized exponential distribution; Type-II censoring; Least squares method; Linear approximate MLEs; Percentile estimators; Unbiased linear approximate MLEs and Unbiased percentile estimators.





Vasudeva Rao and Bhanu Prakash

INTRODUCTION

The probability density function and cumulative distribution function of the GE distribution (pl. see Gupta and Kundu (1999)) are respectively given by

$$f(x; \mu, \sigma, \lambda) = \frac{\lambda}{\sigma} e^{-(x-\mu)/\sigma} [1 - e^{-(x-\mu)/\sigma}]^{\lambda-1}, \quad x > \mu, \sigma > 0 \text{ and } \lambda > 0. \quad (1.1)$$

$$F(x; \mu, \sigma, \lambda) = [1 - e^{-(x-\mu)/\sigma}]^{\lambda} \quad (1.2)$$

where μ , σ and λ are the location, scale and shape parameters. This distribution is also known as exponentiated exponential distribution. We denote this distribution as $GE(\lambda, \mu, \sigma)$ and the popular two-parameter exponential model is a particular case of GE model when $\lambda=1$. The GE model can be used quite effectively in analyzing any lifetime data, especially in censored case, because of its tractable distribution function. Irrespective of the value of scale σ , the hazard function of GE is non-decreasing if $\lambda > 1$; it is non-increasing if $\lambda < 1$; and it is constant if $\lambda=1$ and hence, the GED has been using widely in reliability and survival analysis, replacing the popular Weibull, gamma and log-normal distributions. Further, the model has a good physical interpretation that if each component of a parallel system is GE model, then the life time of the system is also GE model.

In two-parameter GE distribution ($GE(\lambda, 0, \sigma)$), Gupta and Kundu (2001) proposed different estimators namely method of moments estimators (MME's), least squares estimators (LSE's), estimators based on percentiles (PCE's), weighted least squares estimators (WLSE's) and the estimators based on the linear combinations of order statistics (LME's). Through a simulated study, they compare the performances of these new estimators with the MLE's based on bias and mean square error (MSE) and found that PCE's are least biased estimators among all estimators including MLE's. On the other hand, with respect to MSE, ML method is performing better than any other estimation method. Finally, they recommend PCE's in case of small sample sizes and MLE's in case of moderate and large sample sizes. In three-parameter GED ($GE(\lambda, \mu, \sigma)$), Raqab and Ahsanullah (2001) have tabulated the coefficients of the BLUEs of μ and σ of $GE(\lambda, \mu, \sigma)$ for complete samples of size up to 10 for $\lambda=0.5(0.5)5.0$. Vasudeva Rao *et.al.* (2017b) have developed R-code for computing the means, variances and covariances of order statistics of standard GED based on the formulae given by Raqab and Ahsanullah (2001). They have also tabulated the coefficients of the BLUEs of μ and σ for complete samples of size $n=10$ to 20 and for $\lambda=1.5(0.5)2.0(1.0)5.0$. Further, they developed R-code for evaluating the BLUE coefficients of μ and σ for any Type-II censored sample of size up to 20 and for any λ in the interval $[1.5, 6.0]$.

Bhanu Prakash and Vasudeva Rao (2020) constructed LAMLEs and PCEs of μ and σ in three-parameter GED with known λ based on both complete sample and Type-II censored sample and found that PCEs are not as efficient as LAMLEs based on a simulation study. Further, they have shown LAMLEs are almost as efficient as the corresponding MLEs for any value of λ . However, the LAMLEs are slightly biased than the MLEs. Therefore, in this paper, we have discussed the unbiased linear approximate ML estimation and unbiased percentile estimation of μ and σ ; and compared with the corresponding BLUEs. The rest of this article as follows, throughout the paper, the shape parameter λ is assumed as known. We present the derivation details of the LAMLEs and PCEs along with their exact means, variances and covariance of the estimators in Section 2 and Section 3 respectively, which were given by Bhanu Prakash and Vasudeva Rao (2020). In Section 4, we obtain the ULAMLEs (based on least squares method) and UPCEs by making bias correction to LAMLEs and PCEs respectively, along with their variances and covariances of the estimators. In Section 5, we compare ULAMLEs and UPCEs with the corresponding BLUEs based on the exact variances of the estimators. Further, in Section 6, the ULAMLEs are compared with the corresponding simulated MLEs based on the sampling characteristics bias and MSE. Finally, the newly constructed unbiased estimators are demonstrated with a real data set and the results are presented in Section 7.





Vasudeva Rao and Bhanu Prakash

LINEAR APPROXIMATE MAXIMUM LIKELIHOOD ESTIMATION

Let

$$X_{r+1:n} \leq X_{r+2:n} \leq \dots \leq X_{n-s:n}$$

be a doubly Type-II censored sample (r left most observations and s right most observations are censored from a planned sample of size n) from the above GE population. Since, the doubly censored sample includes left censored sample ($s=0$), right censored sample ($r=0$) and complete sample ($r=s=0$), the following development includes all these cases. The likelihood function based on the above doubly censored sample is given by

$$L = \frac{n!}{r!s!} [F(X_{r+1:n}; \mu, \sigma)]^r [1-F(X_{n-s:n}; \mu, \sigma)]^s \prod_{i=r+1}^{n-s} f(X_{i:n}; \mu, \sigma)$$

which, by denoting

$$Z_i = (X_i - \mu) / \sigma \tag{1.3}$$

can be written as

$$L = \frac{n!}{r!s!} \sigma^{-(n-r-s)} [F(Z_{r+1})]^r [1-F(Z_{n-s})]^s \prod_{i=r+1}^{n-s} f(Z_i) \tag{1.4}$$

where $f(z) = \lambda e^{-z} [1 - e^{-z}]^{\lambda-1}$, and $F(z) = [1 - e^{-z}]^\lambda$ (1.5)

are respectively the p.d.f. and c.d.f. of standard GE variate Z .

From the likelihood (1.4) the ML equations for μ and σ are given by

$$\frac{\partial \log L}{\partial \mu} = -\frac{1}{\sigma} \left[-(n-r-s) + r\lambda G_1(z_{r+1:n}) - s\lambda H_1(z_{n-s:n}) + (\lambda-1) \sum_{i=r+1}^{n-s} G_1(z_{i:n}) \right] = 0 \tag{1.6}$$

$$\frac{\partial \log L}{\partial \sigma} = -\frac{1}{\sigma} \left[(n-r-s) + r\lambda G_2(z_{r+1:n}) - s\lambda H_2(z_{n-s:n}) + (\lambda-1) \sum_{i=r+1}^{n-s} G_2(z_{i:n}) - \sum_{i=r+1}^{n-s} z_{i:n} \right] = 0 \tag{1.7}$$

where

$$G_1(z_{i:n}) = \frac{1}{e^{z_{i:n}} - 1}, \quad i = r+1, \dots, n-s; \quad H_1(z_{n-s:n}) = G_1(z_{n-s:n}) F(z_{n-s:n}) / [1 - F(z_{n-s:n})] \tag{1.8}$$

$$G_2(z_{i:n}) = \frac{z_{i:n}}{e^{z_{i:n}} - 1}; \quad i = r+1, \dots, n-s; \quad H_2(z_{n-s:n}) = G_2(z_{n-s:n}) F(z_{n-s:n}) / [1 - F(z_{n-s:n})] \tag{1.9}$$

Since, the above ML equations (1.6) and (1.7) do not admit explicit solutions for μ and σ , because of the intractable terms $G_1(\cdot)$, $H_1(\cdot)$, $G_2(\cdot)$ and $H_2(\cdot)$ appearing in the equations. Therefore, Bhanu Prakash and Vasudeva Rao (2020) derived the LAMLEs of μ and σ by suggesting the following linear approximations to the intractable terms $G_1(\cdot)$, $H_1(\cdot)$, $G_2(\cdot)$ and $H_2(\cdot)$ appearing in the equations.

$$G_1(z_{i:n}) \approx \alpha_i^{(1)} + \beta_i^{(1)} z_{i:n}, \quad G_2(z_{i:n}) \approx \alpha_i^{(2)} + \beta_i^{(2)} z_{i:n}, \quad (\text{for } i = r+1, \dots, n-s)$$

$$H_1(z_{n-s:n}) \approx \gamma_{n-s}^{(1)} + \delta_{n-s}^{(1)} z_{n-s:n} \quad \text{and} \quad H_2(z_{n-s:n}) \approx \gamma_{n-s}^{(2)} + \delta_{n-s}^{(2)} z_{n-s:n} \tag{2.0}$$

where the constants $(\alpha_i^{(1)}, \beta_i^{(1)})$, $(\alpha_i^{(2)}, \beta_i^{(2)})$, $(\gamma_{n-s}^{(1)}, \delta_{n-s}^{(1)})$ and $(\gamma_{n-s}^{(2)}, \delta_{n-s}^{(2)})$ are evaluated in Bhanu Prakash and Vasudeva Rao (2020) using different linear approximation methods namely truncated Taylor series method, which was suggested by Balakrishnan(1989); and least squares method, which was suggested by Vasudeva Rao *et al.* (2017a). By using the linear approximations given in Eq. (2.0), Bhanu Prakash and Vasudeva Rao (2020) approximated the ML equations (1.6) and (1.7) as





Vasudeva Rao and Bhanu Prakash

$$\frac{\partial \log L}{\partial \mu} \simeq \frac{\partial \log \tilde{L}}{\partial \mu} = -\frac{1}{\sigma} \left[-(n-r-s) + r\lambda(\alpha_{r+1}^{(1)} + \beta_{r+1}^{(1)} z_{r+1:n}) - s\lambda(\gamma_{n-s}^{(1)} + \delta_{n-s}^{(1)} z_{n-s:n}) + (\lambda-1) \sum_{i=r+1}^{n-s} (\alpha_i^{(1)} + \beta_i^{(1)} z_{i:n}) \right] = 0 \quad (2.1)$$

$$\frac{\partial \log L}{\partial \sigma} \simeq \frac{\partial \log \tilde{L}}{\partial \sigma} = -\frac{1}{\sigma} \left[(n-r-s) + r\lambda(\alpha_{r+1}^{(2)} + \beta_{r+1}^{(2)} z_{r+1:n}) - s\lambda(\gamma_{n-s}^{(2)} + \delta_{n-s}^{(2)} z_{n-s:n}) + (\lambda-1) \sum_{i=r+1}^{n-s} (\alpha_i^{(2)} + \beta_i^{(2)} z_{i:n}) - \sum_{i=r+1}^{n-s} z_{i:n} \right] = 0 \quad (2.2)$$

Also, the LAMLE's of μ and σ , denoted by $\tilde{\mu}$ and $\tilde{\sigma}$, given by

$$\tilde{\mu} = \sum_{i=r+1}^{n-s} \omega_i x_{i:n} = \mathbf{\omega}' \mathbf{X} \quad \text{and} \quad \tilde{\sigma} = \sum_{i=r+1}^{n-s} \theta_i x_{i:n} = \mathbf{\theta}' \mathbf{X} \quad (2.3)$$

where $\mathbf{X} = (x_{r+1:n}, \dots, x_{n-s:n})'$, $\mathbf{\omega} = (\omega_{r+1}, \dots, \omega_{n-s})'$, $\mathbf{\theta} = (\theta_{r+1}, \dots, \theta_{n-s})'$, (2.4)

$$\omega_i = [cm_i - dl_i] / \Delta, \quad \theta_i = [l_i \sum_{j=r+1}^{n-s} m_j - m_i \sum_{j=r+1}^{n-s} l_j] / \Delta, \quad \Delta = c \sum_{j=r+1}^{n-s} m_j - d \sum_{j=r+1}^{n-s} l_j,$$

$$l_i = \begin{cases} (r\lambda + \lambda - 1)\beta_i^{(1)} & \text{if } i = r+1 \\ (\lambda - 1)\beta_i^{(1)} & \text{if } r+1 < i < n-s \\ (\lambda - 1)\beta_i^{(1)} - s\lambda\delta_i^{(1)} & \text{if } i = n-s \end{cases} \quad \text{and} \quad m_i = \begin{cases} (r\lambda + \lambda - 1)\beta_i^{(2)} - 1 & \text{if } i = r+1 \\ (\lambda - 1)\beta_i^{(2)} - 1 & \text{if } r+1 < i < n-s \\ (\lambda - 1)\beta_i^{(2)} - 1 - s\lambda\delta_i^{(2)} & \text{if } i = n-s \end{cases}$$

$$c = (n-r-s) + s\lambda\gamma_{n-s}^{(1)} - r\lambda\alpha_{r+1}^{(1)} - (\lambda-1) \sum_{i=r+1}^{n-s} \alpha_i^{(1)}, \quad d = -(n-r-s) + s\lambda\gamma_{n-s}^{(2)} - r\lambda\alpha_{r+1}^{(2)} - (\lambda-1) \sum_{i=r+1}^{n-s} \alpha_i^{(2)}$$

The means, biases, variances, covariance and standard errors of $\tilde{\mu}$ and $\tilde{\sigma}$ are given by

$$E(\tilde{\mu}) = \mu + \sigma \mathbf{\omega}' \mathbf{a}, \quad E(\tilde{\sigma}) = \sigma \mathbf{\theta}' \mathbf{a}, \quad Bias(\tilde{\mu}) = \sigma \mathbf{\omega}' \mathbf{a} \quad \text{and} \quad Bias(\tilde{\sigma}) = \sigma (\mathbf{\theta}' \mathbf{a} - 1) \quad (2.5)$$

$$Var(\tilde{\mu}) = \sigma^2 \mathbf{\omega}' \mathbf{B} \mathbf{\omega}, \quad Var(\tilde{\sigma}) = \sigma^2 \mathbf{\theta}' \mathbf{B} \mathbf{\theta} \quad \text{and} \quad Cov(\tilde{\mu}, \tilde{\sigma}) = \sigma^2 \mathbf{\omega}' \mathbf{B} \mathbf{\theta} \quad (2.6)$$

$$SE(\tilde{\mu}) = \tilde{\sigma} \sqrt{\mathbf{\omega}' \mathbf{B} \mathbf{\omega}} \quad \text{and} \quad SE(\tilde{\sigma}) = \tilde{\sigma} \sqrt{\mathbf{\theta}' \mathbf{B} \mathbf{\theta}} \quad (2.7)$$

where $\mathbf{a} = (a_{r+1:n}, \dots, a_{n-s:n})'$ the mean vector and $\mathbf{B} = ((b_{ij:n}))$, $r+1 \leq i, j \leq n-s$ is the variance-covariance matrix of the order statistics $Z_{r+1:n} \leq \dots \leq Z_{n-s:n}$ from standard GE distribution. The elements of \mathbf{a} and \mathbf{B} are given by Raqab and Ahsanullah (2001) and Vasudeva Rao et. al. (2017b). But, when $n > 20$ (i.e. for moderate and large samples), one cannot compute the variances and covariance of $\tilde{\mu}$ and $\tilde{\sigma}$. However, in this case, one can obtain the asymptotic variances and covariance of LAMLEs by inverting the Fisher's information matrix of the estimates which were given by Bhanu Prakash and Vasudeva Rao (2020).

ESTIMATION BASED ON PERCENTILES

Gupta and Kundu (2001) proposed the estimators based on percentiles in two parameter GED, and those can be obtained by equating the population percentile points with the corresponding sample percentile points and the resultant estimators are called as percentile estimators (PCE's). This method was originally suggested by Kao (1958, 1959). Using the same concept Bhanu Prakash and Vasudeva Rao (2020) obtained the PCE's of μ and σ as explained below.

From Eq. (1.2),

$$\mu - \sigma \log \left[1 - (F(x; \mu, \sigma, \lambda))^{1/\lambda} \right] = x \quad (3.1)$$





Vasudeva Rao and Bhanu Prakash

The estimators of μ and σ are obtained by minimizing

$$\sum_{i=r+1}^{n-s} \left[x_{i:n} - \mu + \sigma \log(1 - q_i^{1/\lambda}) \right]^2 \tag{3.2}$$

with respect to μ and σ , where $q_i = i/(n + 1)$, which yields the PCE's of μ and σ denoted by $\tilde{\mu}_{PCE}, \tilde{\sigma}_{PCE}$ respectively and are given by

$$\tilde{\mu}_{PCE} = \sum_{i=r+1}^{n-s} u_i X_{i:n} = \mathbf{u}'\mathbf{x}, \quad \tilde{\sigma}_{PCE} = \sum_{i=r+1}^{n-s} v_i X_{i:n} = \mathbf{v}'\mathbf{x} \tag{3.3}$$

Where $\mathbf{X} = (X_{r+1:n}, X_{r+2:n}, \dots, X_{n-s:n})'$, $\mathbf{u} = (u_{r+1}, u_{r+2}, \dots, u_{n-s})'$, $\mathbf{v} = (v_{r+1}, v_{r+2}, \dots, v_{n-s})'$, $\tag{3.4}$

$$v_i = \frac{(n - r - s) \log(1 - q_i^{1/\lambda}) - \sum_{i=r+1}^{n-s} \log(1 - q_i^{1/\lambda})}{\left[\sum_{i=r+1}^{n-s} \log(1 - q_i^{1/\lambda}) \right]^2 - (n - r - s) \sum_{i=r+1}^{n-s} \left[\log(1 - q_i^{1/\lambda}) \right]^2}$$

$$\text{and } u_i = \frac{1 + v_i \sum_{i=r+1}^{n-s} \log(1 - q_i^{1/\lambda})}{(n - r - s)}, \quad i = r + 1, \dots, n - s.$$

We can obtain the means, biases, variances, covariance and standard errors of $\tilde{\mu}$ and $\tilde{\sigma}$ by

$$E(\tilde{\mu}_{PCE}) = \mu + \sigma \mathbf{u}'\mathbf{a}, \quad E(\tilde{\sigma}_{PCE}) = \sigma \mathbf{v}'\mathbf{a}, \quad Bias(\tilde{\mu}_{PCE}) = \sigma \mathbf{u}'\mathbf{a} \text{ and } Bias(\tilde{\sigma}_{PCE}) = \sigma(\mathbf{v}'\mathbf{a} - 1) \tag{3.5}$$

$$Var(\tilde{\mu}_{PCE}) = \sigma^2 \mathbf{u}'\mathbf{B}\mathbf{u}, \quad Var(\tilde{\sigma}_{PCE}) = \sigma^2 \mathbf{v}'\mathbf{B}\mathbf{v} \text{ and } Cov(\tilde{\mu}_{PCE}, \tilde{\sigma}_{PCE}) = \sigma^2 \mathbf{u}'\mathbf{B}\mathbf{v} \tag{3.6}$$

$$SE(\tilde{\mu}) = \tilde{\sigma}_{PCE} \sqrt{\mathbf{u}'\mathbf{B}\mathbf{u}} \text{ and } SE(\tilde{\sigma}_{PCE}) = \tilde{\sigma}_{PCE} \sqrt{\mathbf{v}'\mathbf{B}\mathbf{v}} \tag{3.7}$$

CONSTRUCTION OF UNBIASED LAMLES AND UNBIASED PCES

Though the LAMLEs based on least squares method, given in Eq. (2.3) (Pl. see Bhanu Prakash and Vasudeva Rao (2020)), are empirically proved almost as efficient as the MLEs, but they are biased than MLEs. Since, "unbiasedness is a desirable property of a good estimator", from Eq. (2.5), we have obtained unbiased estimators of (μ, σ) , based on least squares denoted by $(\tilde{\mu}^*, \tilde{\sigma}^*)$, are given by

$$\tilde{\mu}^* = \tilde{\mu} - \tilde{\sigma}(\boldsymbol{\theta}'\mathbf{a})(\boldsymbol{\omega}'\mathbf{a})^{-1} \text{ and } \tilde{\sigma}^* = (\boldsymbol{\omega}'\mathbf{a})^{-1} \tilde{\sigma} \tag{4.1}$$

Since, "the above estimators obtained from the LAMLEs by adjusting them for unbiasedness we call them as unbiased LAMLEs (ULAMLEs)". For constructing $(\tilde{\mu}, \tilde{\sigma})$ we do not require \mathbf{a} , but for the construction of $(\tilde{\mu}^*, \tilde{\sigma}^*)$, we require \mathbf{a} , whose components can be obtained from Raqab and Ahsanullah (2001) and Vasudeva Rao *et. al.*, (2017b) for up to a sample size 30.

The variances of $\tilde{\mu}^*$ and $\tilde{\sigma}^*$ are given by

$$V(\tilde{\mu}^*) = V(\tilde{\mu}) + (\boldsymbol{\theta}'\mathbf{a})^2 (\boldsymbol{\omega}'\mathbf{a})^{-2} V(\tilde{\sigma}) - 2(\boldsymbol{\theta}'\mathbf{a})(\boldsymbol{\omega}'\mathbf{a})^{-1} cov(\tilde{\mu}, \tilde{\sigma})$$

$$V(\tilde{\sigma}^*) = (\boldsymbol{\omega}'\mathbf{a})^{-2} V(\tilde{\sigma}) \tag{4.2}$$

$$\text{and } Cov(\tilde{\mu}^*, \tilde{\sigma}^*) = (\boldsymbol{\omega}'\mathbf{a})^{-1} cov(\tilde{\mu}, \tilde{\sigma}) - (\boldsymbol{\theta}'\mathbf{a})(\boldsymbol{\omega}'\mathbf{a})^{-2} V(\tilde{\sigma})$$

where $V(\tilde{\mu})$ and $V(\tilde{\sigma})$ can be obtained from Eq. (2.6). Similarly, the asymptotic variances of $\tilde{\mu}^*$ and $\tilde{\sigma}^*$ may be obtained as in Section 2 of this paper.





Vasudeva Rao and Bhanu Prakash

Similarly, from Eq. (3.3) we have obtained the unbiased percentile estimators of (μ, σ) , denoted by $(\tilde{\mu}^*, \tilde{\sigma}^*)$, are given by

$$\tilde{\mu}^* = \tilde{\mu}_{PCE} - \tilde{\sigma}_{PCE} (\mathbf{u}'\mathbf{a})(\mathbf{v}'\mathbf{a})^{-1} \quad \text{and} \quad \tilde{\sigma}^* = (\mathbf{v}'\mathbf{a})^{-1} \tilde{\sigma}_{PCE} \tag{4.3}$$

The variances of $\tilde{\mu}^*$ and $\tilde{\sigma}^*$ are given by

$$\begin{aligned} V(\tilde{\mu}^*) &= V(\tilde{\mu}_{PCE}) + (\mathbf{u}'\mathbf{a})^2 (\mathbf{v}'\mathbf{a})^{-2} V(\tilde{\sigma}_{PCE}) - 2(\mathbf{u}'\mathbf{a})(\mathbf{v}'\mathbf{a})^{-1} \text{cov}(\tilde{\mu}_{PCE}, \tilde{\sigma}_{PCE}) \\ V(\tilde{\sigma}^*) &= (\mathbf{v}'\mathbf{a})^{-2} V(\tilde{\sigma}_{PCE}) \\ \text{and Cov}(\tilde{\mu}^*, \tilde{\sigma}^*) &= (\mathbf{v}'\mathbf{a})^{-1} \text{cov}(\tilde{\mu}_{PCE}, \tilde{\sigma}_{PCE}) - (\mathbf{u}'\mathbf{a})(\mathbf{v}'\mathbf{a})^{-2} V(\tilde{\sigma}_{PCE}) \end{aligned} \tag{4.4}$$

COMPARISON OF ULAMLES AND UPCES WITH BLUES

It is well known that among the class of linear unbiased estimators, best linear unbiased estimators (BLUES) are the most efficient estimators since they have least variance. Vasudeva Rao *et. al.*, (2017b) obtained explicit formulae for the BLUEs of location and scale parameters in three-parameter GED based on a given Type-II censored sample using Lloyd (1952) technique. According to these formulae, the evaluation of linear coefficients of the BLUEs requires means, variances and covariances of order statistics obtained from the corresponding standardized population.

The BLUEs of μ and σ , denoted by μ^* and σ^* , are given by (pl. see Vasudeva Rao *et. al.*, 2017b)

$$\mu^* = \frac{\mathbf{a}'\mathbf{B}^{-1}\mathbf{a}\mathbf{1}'\mathbf{B}^{-1} - \mathbf{a}'\mathbf{B}^{-1}\mathbf{1}\mathbf{a}'\mathbf{B}^{-1}}{\Delta} \mathbf{X} \quad \text{and} \quad \sigma^* = \frac{\mathbf{1}'\mathbf{B}^{-1}\mathbf{1}\mathbf{a}'\mathbf{B}^{-1} - \mathbf{1}'\mathbf{B}^{-1}\mathbf{a}\mathbf{1}'\mathbf{B}^{-1}}{\Delta} \mathbf{X} \tag{5.1}$$

Where $\Delta = (\mathbf{a}'\mathbf{B}^{-1}\mathbf{a})(\mathbf{1}'\mathbf{B}^{-1}\mathbf{1}) - (\mathbf{a}'\mathbf{B}^{-1}\mathbf{1})^2$

Here $\mathbf{a} = (a_{r+1:n}, \dots, a_{n-s:n})'$ and $\mathbf{B} = ((b_{ij:n}))$, $r+1 \leq i, j \leq n-s$ are respectively the mean vector and variance-covariance matrix of the order statistics $Z_{r+1:n} \leq Z_{r+2:n} \leq \dots \leq Z_{n-s:n}$ from standard GE distribution and $\mathbf{1}$ is a column vector of 1's of the same dimension of \mathbf{a} .

The variances and covariance of μ^* and σ^* are given by

$$\text{var}(\mu^*) = \sigma^2 \left\{ \frac{\mathbf{a}'\mathbf{B}^{-1}\mathbf{a}}{\Delta} \right\}, \quad \text{var}(\sigma^*) = \sigma^2 \left\{ \frac{\mathbf{1}'\mathbf{B}^{-1}\mathbf{1}}{\Delta} \right\} \quad \text{and} \quad \text{Cov}(\mu^*, \sigma^*) = -\sigma^2 \left\{ \frac{\mathbf{a}'\mathbf{B}^{-1}\mathbf{1}}{\Delta} \right\} \tag{5.2}$$

In this section, in order to see the performance of $(\tilde{\mu}^*, \tilde{\sigma}^*)$ and $(\tilde{\mu}^*, \tilde{\sigma}^*)$, we compare it with the corresponding (μ^*, σ^*) based on the exact variances of the estimators. The necessary variances and covariances of the standard order statistics of GED are borrowed from Vasudeva Rao *et. al.*, (2017b). The variances along with the efficiencies of $(\tilde{\mu}^*, \tilde{\sigma}^*)$ and $(\tilde{\mu}^*, \tilde{\sigma}^*)$ as compared with (μ^*, σ^*) , are tabulated in **Table 1** for both complete and Type-II censored samples of size $n=5(5)20$ with $r=0(1)[n/4]$, $s=0(1)[n/4]$ and $\lambda=1.5(0.5)2.0(1.0)5.0$. Where [.] indicate the integral part of '. From the table we may observe that

- The ULAMLEs $(\tilde{\mu}^*, \tilde{\sigma}^*)$ are almost as efficient as the corresponding BLUEs (μ^*, σ^*) in Type-II censored samples, uniformly irrespective of the value of λ and magnitude of censoring.
- On the other hand, UPCES $(\tilde{\mu}^*, \tilde{\sigma}^*)$ are no way comparable with the corresponding ULAMLEs $(\tilde{\mu}^*, \tilde{\sigma}^*)$ in terms of efficiency and moreover their efficiencies are not uniform and are fluctuating with respect to the value of λ and magnitude of censoring.

From the above observation the linear unbiased estimators $(\tilde{\mu}^*, \tilde{\sigma}^*)$ of (μ, σ) are as efficient as the BLUEs (μ^*, σ^*) .





Vasudeva Rao and Bhanu Prakash

COMPARISON OF UNBIASED LAMLES WITH MLES

In small and moderate samples, ULAMLEs can be viewed as bias corrected MLEs and therefore they are not expected as efficient as the corresponding MLEs in terms of MSE, but at the same time MLEs are biased. On the other hand, in large samples, both ULAMLEs and MLEs are almost equivalent in respect of unbiasedness, because MLEs are asymptotically unbiased. We therefore, compare ULAMLEs with the corresponding MLEs based on the simulated biases and MSEs of the respective estimators based on 3000 samples of size $n=20(10)30$ generated from standard GED with $\lambda=2.0(1.0)5.0$ and presented in Table 2 for both complete and censored samples with $r=0(1)[n/4]$ and $s=0(1)[n/4]$. From the table we may observe that

- By virtue of unbiasedness, unbiased LAMLEs are having negligible simulated biases, whereas MLEs are having some biases, since they are asymptotically unbiased. In other words, unbiased LAMLEs are having negligible biases and MLEs are having some considerable biases.
- The MSEs of both ULAMLEs and MLEs are almost equal (upto two decimals) irrespective of n, λ, r and s .

The ULAMLEs are better than the corresponding MLEs in terms of bias and they are almost as efficient as the corresponding MLEs in terms of MSE. Therefore, in both complete and censored samples, the ULAMLEs are almost as efficient as the respective MLEs.

CONCLUSION OF THE STUDY

Thus, in our investigation, the ULAMLEs are some alternative efficient estimators to the BLUEs for the estimation of location and scale parameters in GED. The Construction of BLUEs requires not only the means of standardized order statistics, but also variances and covariances of standardized order statistics, where as the construction of ULAMLEs requires only means of standardized order statistics. Another advantage is that unlike BLUEs, no readymade tables are required for the computation of the ULAMLEs and we may compute them easily based on LAMLEs. Further, the ULAMLEs are almost as efficient as the respective MLEs. Therefore, we recommend ULAMLEs to replace the BLUEs, especially when it is difficult to compute the BLUEs.

ILLUSTRATION

Pasari and Dikshit (2014) consider the following real, complete and homogeneous earthquake catalogue of 20 events with magnitude above 7.0 from northeast India to analyze earthquake inter-occurrence time as an application of the $GE(\lambda, \mu, \sigma)$.

7.5, 7.5, 7.3, 8.7, 7.5, 7.9, 7.6, 7.1, 7.6, 7.2, 7.5, 7.9, 8.6, 8.0, 7.5, 7.6, 7.0, 7.2, 7.1, 7.1.

We apply Kolmogorov-Smirnov (KS) test to earthquakes data for goodness of fit of $GE(\lambda, \mu, \sigma)$ replacing the shape parameter λ with 5.5, the unknown parameters μ and σ with the corresponding BLUEs $\mu^*=6.6683$ and $\sigma^*=0.3869$. The test reports the KS distance $D=0.156$ with a p-value of 0.715. Since, D is very small or equivalently the p-value is very high (>0.05), it may be concluded that $GE(\lambda, \mu, \sigma)$ is well fitted to the data. In fact, at each value of $\lambda=0.5(0.5)10.0$, we compute the BLUEs and hence, we compute KS distances D 's, a minimum D is obtained at $\lambda=5.5$. In place of (μ^*, σ^*) , if we use ULAMLEs $\tilde{\mu}^* = 6.6879$ and $\tilde{\sigma}^* = 0.3703$, we get KS distance $D=0.1716$ & $p=0.5977$. Thus, BLUEs are giving slightly better fit to earthquake magnitudes data than ULAMLEs. Further, the following Q-Q plot and superimposed empirical & theoretical cdf curves of GED based on BLUEs are also reiterating that GED is well fitted to the above data.

For the earthquake magnitudes data, (μ^*, σ^*) and $(\tilde{\mu}^*, \tilde{\sigma}^*)$ are computed for various choices of r and s along with their standard errors for $\lambda=5.5$. These estimates and their standard errors of μ and σ are tabulated below. From the above table, we may notice that ULAMLEs are almost equal to the BLUEs, irrespective of r and s .





Vasudeva Rao and Bhanu Prakash

REFERENCES

1. Vasudeva Rao A, Sitaramacharyulu P, Chenchu Ramaiah M. Linear approximate ML estimation in scaled Type I generalized logistic distribution based on Type-II censored samples. Commun. Statist. – Simul. Comput. 2017a; 46 (3):1682 – 1702.
2. Vasudeva Rao A, Bhanu Prakash S, Jilani Sd. Best Linear Unbiased Estimation of Location and Scale Parameters in Generalized Exponential Distribution under Type-II Censoring. International Journal of Scientific and Research Publications 2017b; 7(8):38-53.
3. Lloyd EH. Least squares estimation of location and scale parameters using order statistics. Biometrika 1952; 39:88-95.
4. Kao JHK. Computer methods for estimating Weibull parameters in reliability studies. Transaction of IRE-Reliability and Quality Control 1958; 13:15-22.
5. Kao JHK. A graphical estimation of mixed Weibull parameters in life testing electron tubes. Technometric 1959; 1:389-407.
6. Raqab MZ, Ahsanullah M. Estimation of location and scale parameters of generalized exponential distribution based on order statistics. J. Statist. Computat. Simul. 2001; 69(2):109-123.
7. Balakrishnan N. Approximate MLE of scale parameter of the Rayleigh distribution with censoring. I E E Trans. On Reliab. 1989; 38:355-357.
8. Gupta RD, Kundu D. Exponentiated Exponential Distribution: An alternative to gamma or weibull distributions. Biometrical Journal 2001; 43:117-130.
9. Gupta RD, Kundu D. Generalized exponential distribution. Austr. NZ J. Statist. 1999; 41(2) :173–188.
10. Bhanu Prakash S, Vasudeva Rao A. Linear Approximate ML Estimation in the Generalized Exponential Distribution under Type-II Censoring. Journal of Interdisciplinary Cycle Research 2020; 12(4):1178-1202.

Table 1: Performances of unbiased LAMLEs ($\mu_{LS}^*, \sigma_{LS}^*$) and unbiased PCEs ($\mu_{PCE}^*, \sigma_{PCE}^*$) of location (μ) and scale (σ) parameters of three parameter GE distribution with BLUEs (μ^*, σ^*) based on exact variances from complete and Type-II censored samples of size $n=5(5)20$ with $\lambda=1.5(0.5)2.0(1.0)5.0$, $r=0(1)n/4$ and $s=0(1)n/4$.

λ	n	r	s	$\frac{V(\mu^*)}{\sigma^2}$	$\frac{V(\mu_{LS}^*)}{\sigma^2}$	$\frac{V(\mu_{PCE}^*)}{\sigma^2}$	$Ef(\mu_{LS}^*)$	$Ef(\mu_{PCE}^*)$	$\frac{V(\sigma^*)}{\sigma^2}$	$\frac{V(\sigma_{LS}^*)}{\sigma^2}$	$\frac{V(\sigma_{PCE}^*)}{\sigma^2}$	$Ef(\sigma_{LS}^*)$	$Ef(\sigma_{PCE}^*)$	
1.5	5	0	0	0.1087	0.1099	0.2159	98.94	50.35	0.2111	0.2119	0.2807	99.64	75.21	
		0	1	0.1193	0.1203	0.1577	99.18	75.69	0.2766	0.2775	0.3045	99.67	90.81	
		1	0	0.3068	0.3073	0.4757	99.83	64.49	0.2997	0.3000	0.3764	99.91	79.62	
		1	1	0.3827	0.3830	0.4292	99.92	89.15	0.4468	0.4471	0.4716	99.95	94.75	
	10	0	0	0.0311	0.0317	0.1033	98.37	30.13	0.0905	0.0909	0.1374	99.63	65.88	
		0	1	0.0319	0.0324	0.0704	98.41	45.30	0.1007	0.1011	0.1264	99.60	79.61	
		0	2	0.0328	0.0333	0.0585	98.49	56.11	0.1137	0.1141	0.1329	99.59	85.51	
		1	0	0.0629	0.0631	0.1568	99.70	40.15	0.1074	0.1075	0.1576	99.90	68.14	
		1	1	0.0658	0.0660	0.1140	99.71	57.70	0.1219	0.1220	0.1486	99.88	81.99	
		1	2	0.0695	0.0697	0.1008	99.74	68.94	0.1412	0.1413	0.1608	99.89	87.80	
		2	0	0.1074	0.1075	0.2307	99.90	46.54	0.1268	0.1269	0.1816	99.96	69.84	
		2	1	0.1149	0.1150	0.1761	99.91	65.24	0.1474	0.1475	0.1759	99.95	83.82	
		2	2	0.1252	0.1253	0.1635	99.92	76.53	0.1763	0.1763	0.1965	99.96	89.69	
		15	0	0	0.0158	0.0161	0.0697	98.08	22.70	0.0571	0.0573	0.0918	99.65	62.13
			0	1	0.0160	0.0163	0.0483	98.08	33.16	0.0610	0.0613	0.0821	99.62	74.32
			0	2	0.0162	0.0165	0.0401	98.11	40.42	0.0655	0.0657	0.0823	99.60	79.55
0	3		0.0165	0.0168	0.0354	98.16	46.61	0.0708	0.0711	0.0855	99.59	82.76		
1	0		0.0289	0.0290	0.0929	99.62	31.10	0.0644	0.0645	0.1006	99.89	64.04		
1	1		0.0295	0.0296	0.0669	99.62	44.09	0.0695	0.0696	0.0909	99.88	76.45		
1	2		0.0302	0.0303	0.0575	99.63	52.45	0.0753	0.0754	0.0922	99.88	81.64		





Vasudeva Rao and Bhanu Prakash

	1	3	0.0310	0.0311	0.0524	99.65	59.15	0.0823	0.0824	0.0971	99.88	84.77
	2	0	0.0441	0.0441	0.1210	99.87	36.44	0.0719	0.0720	0.1102	99.94	65.29
	2	1	0.0454	0.0455	0.0896	99.87	50.72	0.0783	0.0783	0.1006	99.95	77.84
	2	2	0.0469	0.0470	0.0789	99.87	59.49	0.0857	0.0857	0.1032	99.95	83.02
	2	3	0.0488	0.0488	0.0736	99.88	66.27	0.0948	0.0949	0.1101	99.95	86.11
	3	0	0.0632	0.0632	0.1561	99.94	40.48	0.0802	0.0803	0.1210	99.96	66.32
	3	1	0.0658	0.0658	0.1182	99.94	55.66	0.0882	0.0882	0.1116	99.97	79.01
	3	2	0.0687	0.0688	0.1063	99.94	64.66	0.0976	0.0977	0.1160	99.97	84.20
	3	3	0.0724	0.0725	0.1014	99.95	71.45	0.1096	0.1096	0.1255	99.97	87.30
20	0	0	0.0099	0.0102	0.0530	97.85	18.78	0.0415	0.0416	0.0691	99.64	60.05
	0	1	0.0100	0.0102	0.0376	97.84	26.69	0.0436	0.0438	0.0614	99.63	71.02
	0	2	0.0101	0.0103	0.0315	97.86	32.09	0.0458	0.0460	0.0604	99.62	75.86
	0	3	0.0102	0.0104	0.0278	97.88	36.63	0.0483	0.0485	0.0613	99.61	78.84
	0	4	0.0103	0.0105	0.0253	97.91	40.76	0.0512	0.0514	0.0632	99.60	80.97
	0	5	0.0104	0.0106	0.0233	97.95	44.70	0.0544	0.0547	0.0659	99.59	82.65
	1	0	0.0172	0.0173	0.0660	99.23	26.04	0.0457	0.0458	0.0740	99.80	61.78
	1	1	0.0174	0.0175	0.0481	99.22	36.22	0.0483	0.0484	0.0662	99.82	72.99
	1	2	0.0176	0.0178	0.0412	99.22	42.80	0.0510	0.0511	0.0656	99.81	77.83
	1	3	0.0179	0.0180	0.0372	99.22	48.08	0.0541	0.0542	0.0670	99.80	80.75
	1	4	0.0182	0.0183	0.0345	99.24	52.72	0.0577	0.0578	0.0696	99.81	82.85
	1	5	0.0185	0.0187	0.0325	99.21	56.89	0.0618	0.0619	0.0732	99.75	84.33
	2	0	0.0247	0.0250	0.0808	98.79	30.58	0.0496	0.0498	0.0791	99.65	62.75
	2	1	0.0252	0.0255	0.0600	98.77	41.93	0.0527	0.0529	0.0712	99.66	74.07
	2	2	0.0256	0.0260	0.0523	98.75	48.98	0.0560	0.0562	0.0710	99.64	78.87
	2	3	0.0262	0.0265	0.0480	98.74	54.49	0.0597	0.0599	0.0730	99.63	81.76
	2	4	0.0267	0.0271	0.0452	98.71	59.12	0.0640	0.0642	0.0764	99.58	83.69
	2	5	0.0275	0.0278	0.0433	98.76	63.49	0.0693	0.0695	0.0811	99.63	85.45
	3	0	0.0334	0.0339	0.0982	98.50	34.02	0.0538	0.0540	0.0847	99.53	63.52
	3	1	0.0342	0.0347	0.0740	98.47	46.16	0.0574	0.0577	0.0766	99.54	74.95
	3	2	0.0350	0.0355	0.0654	98.45	53.49	0.0613	0.0616	0.0769	99.51	79.73
	3	3	0.0359	0.0365	0.0608	98.42	59.07	0.0657	0.0661	0.0796	99.48	82.55
	3	4	0.0370	0.0376	0.0580	98.40	63.78	0.0710	0.0714	0.0840	99.45	84.57
	3	5	0.0382	0.0388	0.0563	98.33	67.72	0.0771	0.0776	0.0898	99.37	85.85
	4	0	0.0441	0.0445	0.1187	99.22	37.18	0.0584	0.0586	0.0908	99.71	64.37
	4	1	0.0454	0.0458	0.0907	99.22	50.08	0.0628	0.0629	0.0826	99.74	75.95
	4	2	0.0468	0.0472	0.0811	99.20	57.68	0.0674	0.0676	0.0834	99.72	80.75
	4	3	0.0483	0.0487	0.0763	99.18	63.39	0.0728	0.0730	0.0871	99.70	83.59
	4	4	0.0502	0.0506	0.0737	99.16	68.08	0.0792	0.0795	0.0926	99.68	85.53
	4	5	0.0524	0.0529	0.0726	99.15	72.27	0.0871	0.0874	0.1000	99.66	87.15
	5	0	0.0572	0.0574	0.1435	99.76	39.90	0.0636	0.0637	0.0976	99.87	65.14
	5	1	0.0593	0.0594	0.1109	99.76	53.45	0.0687	0.0688	0.0894	99.91	76.88
	5	2	0.0614	0.0616	0.1003	99.76	61.28	0.0743	0.0743	0.0909	99.91	81.71
	5	3	0.0640	0.0641	0.0954	99.76	67.08	0.0809	0.0809	0.0956	99.90	84.56
	5	4	0.0670	0.0672	0.0933	99.75	71.81	0.0888	0.0889	0.1027	99.89	86.54
1.5	20	5	0.0707	0.0709	0.0932	99.74	75.91	0.0987	0.0988	0.1120	99.89	88.12
2.0	5	0	0.1722	0.1738	0.3002	99.10	57.38	0.1951	0.1959	0.2577	99.60	75.71
	0	1	0.1931	0.1944	0.2365	99.30	81.65	0.2541	0.2550	0.2769	99.64	91.75
	1	0	0.4396	0.4408	0.6459	99.73	68.06	0.2851	0.2856	0.3562	99.83	80.04
	1	1	0.5624	0.5631	0.6171	99.88	91.14	0.4246	0.4250	0.4457	99.91	95.27
10	0	0	0.0552	0.0559	0.1417	98.74	38.97	0.0826	0.0829	0.1249	99.58	66.10
	0	1	0.0571	0.0578	0.1022	98.75	55.87	0.0915	0.0919	0.1141	99.53	80.20
	0	2	0.0594	0.0601	0.0892	98.81	66.63	0.1030	0.1034	0.1193	99.53	86.32
	1	0	0.1000	0.1004	0.2139	99.60	46.76	0.1003	0.1005	0.1462	99.82	68.62
	1	1	0.1057	0.1062	0.1633	99.61	64.74	0.1137	0.1139	0.1375	99.80	82.68
	1	2	0.1131	0.1135	0.1503	99.65	75.22	0.1315	0.1317	0.1485	99.81	88.54
	2	0	0.1602	0.1604	0.3109	99.85	51.52	0.1201	0.1202	0.1708	99.92	70.32
	2	1	0.1736	0.1738	0.2476	99.86	70.12	0.1396	0.1397	0.1653	99.91	84.43
	2	2	0.1918	0.1920	0.2382	99.88	80.50	0.1668	0.1670	0.1848	99.92	90.27
15	0	0	0.0301	0.0306	0.0946	98.59	31.87	0.0516	0.0519	0.0829	99.57	62.28
	0	1	0.0307	0.0312	0.0689	98.56	44.55	0.0552	0.0554	0.0740	99.55	74.55
	0	2	0.0313	0.0318	0.0595	98.57	52.62	0.0590	0.0593	0.0738	99.53	79.98
	0	3	0.0320	0.0325	0.0542	98.60	59.05	0.0636	0.0639	0.0763	99.52	83.36
	1	0	0.0489	0.0492	0.1260	99.54	38.84	0.0596	0.0597	0.0922	99.80	64.58
	1	1	0.0504	0.0506	0.0951	99.52	52.98	0.0643	0.0644	0.0835	99.80	76.99
	1	2	0.0519	0.0522	0.0846	99.53	61.39	0.0695	0.0696	0.0845	99.79	82.27
	1	3	0.0538	0.0540	0.0794	99.55	67.73	0.0759	0.0760	0.0888	99.80	85.45
	2	0	0.0700	0.0701	0.1631	99.82	42.90	0.0673	0.0674	0.1021	99.89	65.92





Vasudeva Rao and Bhanu Prakash

λ	n	r	s	$\frac{V(\mu^*)}{\sigma^2}$	$\frac{V(\mu_{LS}^*)}{\sigma^2}$	$\frac{V(\mu_{PCE}^*)}{\sigma^2}$	$Ef(\mu_{LS}^*)$	$Ef(\mu_{PCE}^*)$	$\frac{V(\sigma^*)}{\sigma^2}$	$\frac{V(\sigma_{LS}^*)}{\sigma^2}$	$\frac{V(\sigma_{PCE}^*)}{\sigma^2}$	$Ef(\sigma_{LS}^*)$	$Ef(\sigma_{PCE}^*)$
	2	1		0.0728	0.0729	0.1260	99.81	57.75	0.0734	0.0734	0.0935	99.90	78.43
	2	2		0.0758	0.0759	0.1145	99.82	66.23	0.0802	0.0803	0.0959	99.91	83.61
	2	3		0.0795	0.0796	0.1097	99.83	72.44	0.0887	0.0887	0.1023	99.91	86.70
	3	0		0.0959	0.0960	0.2088	99.90	45.91	0.0757	0.0758	0.1131	99.92	66.96
	3	1		0.1007	0.1008	0.1643	99.91	61.30	0.0834	0.0835	0.1049	99.95	79.57
	3	2		0.1062	0.1063	0.1520	99.91	69.85	0.0923	0.0924	0.1089	99.95	84.73
	3	3		0.1130	0.1131	0.1486	99.92	76.01	0.1036	0.1036	0.1180	99.95	87.79
20	0	0		0.0200	0.0203	0.0712	98.49	28.05	0.0373	0.0375	0.0620	99.54	60.26
	0	1		0.0202	0.0206	0.0530	98.45	38.17	0.0393	0.0395	0.0553	99.56	71.04
	0	2		0.0205	0.0208	0.0459	98.45	44.64	0.0412	0.0414	0.0542	99.54	76.00
	0	3		0.0208	0.0211	0.0417	98.47	49.80	0.0433	0.0435	0.0547	99.53	79.15
	0	4		0.0211	0.0214	0.0389	98.48	54.26	0.0458	0.0460	0.0562	99.51	81.41
	0	5		0.0214	0.0218	0.0368	98.47	58.30	0.0486	0.0489	0.0584	99.43	83.12
	1	0		0.0306	0.0308	0.0889	99.44	34.47	0.0420	0.0421	0.0672	99.73	62.47
	1	1		0.0312	0.0314	0.0678	99.42	46.06	0.0444	0.0445	0.0605	99.79	73.45
	1	2		0.0318	0.0320	0.0600	99.43	53.09	0.0469	0.0470	0.0598	99.78	78.35
	1	3		0.0325	0.0327	0.0555	99.44	58.47	0.0496	0.0497	0.0610	99.78	81.38
	1	4		0.0332	0.0334	0.0528	99.41	62.91	0.0528	0.0529	0.0633	99.73	83.44
	1	5		0.0341	0.0342	0.0509	99.48	66.93	0.0566	0.0567	0.0665	99.75	85.14
	2	0		0.0413	0.0416	0.1085	99.23	38.05	0.0461	0.0463	0.0725	99.64	63.62
	2	1		0.0423	0.0427	0.0842	99.23	50.29	0.0491	0.0493	0.0658	99.70	74.68
	2	2		0.0434	0.0437	0.0755	99.22	57.46	0.0521	0.0523	0.0655	99.69	79.50
	2	3		0.0445	0.0449	0.0709	99.19	62.78	0.0555	0.0557	0.0673	99.66	82.38
	2	4		0.0459	0.0462	0.0682	99.29	67.29	0.0596	0.0597	0.0704	99.73	84.56
	2	5		0.0472	0.0476	0.0668	99.00	70.65	0.0639	0.0643	0.0747	99.38	85.56
	3	0		0.0530	0.0538	0.1311	98.48	40.42	0.0503	0.0506	0.0782	99.35	64.32
	3	1		0.0546	0.0555	0.1030	98.47	53.03	0.0539	0.0542	0.0714	99.40	75.43
	3	2		0.0563	0.0572	0.0934	98.44	60.23	0.0574	0.0578	0.0717	99.37	80.15
	3	3		0.0582	0.0591	0.0887	98.43	65.55	0.0616	0.0620	0.0742	99.36	83.04
	3	4		0.0601	0.0611	0.0864	98.26	69.52	0.0662	0.0668	0.0782	99.17	84.66
	3	5		0.0633	0.0642	0.0856	98.60	73.92	0.0728	0.0732	0.0837	99.44	86.96
	4	0		0.0674	0.0681	0.1575	98.99	42.80	0.0550	0.0552	0.0843	99.51	65.17
	4	1		0.0700	0.0707	0.1252	99.00	55.89	0.0592	0.0595	0.0775	99.59	76.41
	4	2		0.0725	0.0733	0.1147	98.97	63.22	0.0636	0.0639	0.0784	99.57	81.13
	4	3		0.0754	0.0762	0.1101	98.94	68.45	0.0686	0.0689	0.0818	99.53	83.86
	4	4		0.0791	0.0800	0.1084	98.97	72.98	0.0750	0.0753	0.0870	99.55	86.12
	4	5		0.0823	0.0833	0.1086	98.85	75.79	0.0815	0.0820	0.0940	99.37	86.72
	5	0		0.0850	0.0853	0.1890	99.67	44.99	0.0602	0.0603	0.0912	99.75	66.00
	5	1		0.0889	0.0891	0.1517	99.71	58.58	0.0653	0.0654	0.0844	99.87	77.41
	5	2		0.0927	0.0930	0.1404	99.71	66.04	0.0706	0.0707	0.0860	99.87	82.13
	5	3		0.0973	0.0976	0.1362	99.71	71.46	0.0769	0.0770	0.0905	99.86	85.00
	5	4		0.1023	0.1026	0.1356	99.70	75.46	0.0842	0.0844	0.0972	99.84	86.69
	5	5		0.1099	0.1102	0.1379	99.74	79.70	0.0944	0.0946	0.1063	99.87	88.87
3.0	5	0		0.2971	0.2992	0.4584	99.29	64.82	0.1816	0.1823	0.2361	99.60	76.91
		0	1	0.3425	0.3444	0.3921	99.45	87.34	0.2362	0.2370	0.2536	99.64	93.15
		1	0	0.6816	0.6839	0.9528	99.66	71.53	0.2714	0.2721	0.3370	99.75	80.54
		1	1	0.9002	0.9016	0.9680	99.85	93.00	0.4054	0.4059	0.4229	99.88	95.85
3.0	10	0		0.1050	0.1059	0.2124	99.16	49.43	0.0762	0.0765	0.1124	99.59	67.83
		0	1	0.1102	0.1112	0.1638	99.12	67.30	0.0847	0.0851	0.1031	99.53	82.15
		0	2	0.1164	0.1174	0.1507	99.16	77.25	0.0952	0.0956	0.1078	99.53	88.27
		1	0	0.1707	0.1713	0.3163	99.62	53.95	0.0940	0.0942	0.1344	99.77	69.94
		1	1	0.1835	0.1843	0.2554	99.60	71.84	0.1070	0.1073	0.1273	99.74	84.02
		1	2	0.1994	0.2002	0.2456	99.64	81.20	0.1238	0.1241	0.1380	99.76	89.73
		2	0	0.2567	0.2572	0.4519	99.83	56.81	0.1136	0.1137	0.1593	99.87	71.30
		2	1	0.2835	0.2840	0.3780	99.83	74.99	0.1328	0.1330	0.1555	99.88	85.40
		2	2	0.3185	0.3189	0.3780	99.86	84.26	0.1590	0.1591	0.1746	99.90	91.06
		15	0	0.0606	0.0612	0.1391	99.09	43.59	0.0474	0.0477	0.0734	99.50	64.59
		0	1	0.0625	0.0631	0.1082	99.06	57.79	0.0510	0.0512	0.0665	99.54	76.65
		0	2	0.0644	0.0650	0.0975	99.05	66.01	0.0545	0.0548	0.0664	99.53	82.11
		0	3	0.0665	0.0671	0.0922	99.07	72.08	0.0587	0.0590	0.0687	99.52	85.53





Vasudeva Rao and Bhanu Prakash

λ	n	r	s	$\frac{V(\mu^*)}{\sigma^2}$	$\frac{V(\mu_{LS}^*)}{\sigma^2}$	$\frac{V(\mu_{PCE}^*)}{\sigma^2}$	$Ef(\mu_{LS}^*)$	$Ef(\mu_{PCE}^*)$	$\frac{V(\sigma^*)}{\sigma^2}$	$\frac{V(\sigma_{LS}^*)}{\sigma^2}$	$\frac{V(\sigma_{PCE}^*)}{\sigma^2}$	$Ef(\sigma_{LS}^*)$	$Ef(\sigma_{PCE}^*)$
		1	0	0.0882	0.0886	0.1843	99.56	47.89	0.0553	0.0555	0.0831	99.66	66.61
		1	1	0.0921	0.0925	0.1475	99.56	62.43	0.0602	0.0603	0.0765	99.74	78.63
		1	2	0.0959	0.0963	0.1363	99.56	70.36	0.0651	0.0653	0.0777	99.74	83.78
		1	3	0.1004	0.1008	0.1321	99.58	75.99	0.0711	0.0712	0.0818	99.75	86.89
		2	0	0.1186	0.1189	0.2359	99.77	50.27	0.0630	0.0631	0.0930	99.74	67.71
		2	1	0.1252	0.1254	0.1925	99.80	65.04	0.0692	0.0693	0.0868	99.87	79.76
		2	2	0.1319	0.1321	0.1810	99.81	72.84	0.0758	0.0759	0.0894	99.88	84.75
		2	3	0.1398	0.1400	0.1786	99.82	78.28	0.0838	0.0839	0.0956	99.88	87.72
		3	0	0.1554	0.1557	0.2984	99.82	52.09	0.0712	0.0714	0.1038	99.75	68.55
		3	1	0.1660	0.1662	0.2472	99.89	67.15	0.0792	0.0793	0.0982	99.92	80.70
		3	2	0.1770	0.1772	0.2363	99.90	74.93	0.0879	0.0879	0.1026	99.93	85.61
		3	3	0.1905	0.1907	0.2372	99.91	80.31	0.0986	0.0987	0.1114	99.94	88.54
20		0	0	0.0418	0.0422	0.1027	99.01	40.69	0.0341	0.0344	0.0540	99.29	63.23
		0	1	0.0428	0.0432	0.0819	99.03	52.26	0.0362	0.0364	0.0494	99.54	73.30
		0	2	0.0437	0.0441	0.0738	99.02	59.20	0.0380	0.0382	0.0487	99.54	78.18
		0	3	0.0446	0.0451	0.0692	99.02	64.47	0.0400	0.0402	0.0491	99.53	81.40
		0	4	0.0456	0.0461	0.0663	99.03	68.79	0.0422	0.0424	0.0504	99.52	83.73
		0	5	0.0468	0.0472	0.0646	99.02	72.47	0.0448	0.0451	0.0524	99.48	85.49
		1	0	0.0573	0.0577	0.1278	99.37	44.84	0.0387	0.0389	0.0593	99.39	65.23
		1	1	0.0592	0.0596	0.1042	99.44	56.85	0.0414	0.0415	0.0550	99.68	75.35
		1	2	0.0609	0.0612	0.0955	99.44	63.70	0.0438	0.0439	0.0547	99.70	80.02
		1	3	0.0626	0.0629	0.0910	99.45	68.74	0.0463	0.0465	0.0558	99.70	83.00
		1	4	0.0645	0.0648	0.0887	99.43	72.72	0.0493	0.0495	0.0580	99.67	85.05
		1	5	0.0667	0.0671	0.0877	99.47	76.11	0.0528	0.0530	0.0610	99.70	86.66
		2	0	0.0728	0.0733	0.1549	99.25	46.97	0.0428	0.0431	0.0646	99.31	66.21
		2	1	0.0757	0.0762	0.1280	99.37	59.16	0.0461	0.0463	0.0604	99.66	76.35
		2	2	0.0783	0.0787	0.1188	99.37	65.89	0.0490	0.0492	0.0606	99.68	80.86
		2	3	0.0809	0.0815	0.1144	99.36	70.75	0.0522	0.0524	0.0624	99.66	83.67
		2	4	0.0841	0.0846	0.1127	99.39	74.63	0.0560	0.0562	0.0654	99.68	85.69
		2	5	0.0874	0.0881	0.1128	99.25	77.55	0.0603	0.0606	0.0694	99.53	86.87
		3	0	0.0899	0.0908	0.1854	99.02	48.47	0.0469	0.0473	0.0701	99.17	66.88
		3	1	0.0942	0.0950	0.1549	99.18	60.83	0.0509	0.0511	0.0661	99.56	77.06
		3	2	0.0979	0.0987	0.1451	99.19	67.49	0.0545	0.0547	0.0669	99.59	81.46
		3	3	0.1020	0.1029	0.1412	99.18	72.28	0.0584	0.0587	0.0694	99.58	84.21
		3	4	0.1065	0.1075	0.1404	99.10	75.85	0.0630	0.0633	0.0733	99.49	85.92
		3	5	0.1126	0.1135	0.1420	99.22	79.29	0.0690	0.0692	0.0786	99.59	87.72
		4	0	0.1101	0.1110	0.2207	99.13	49.88	0.0513	0.0518	0.0760	99.19	67.54
		4	1	0.1162	0.1170	0.1860	99.34	62.49	0.0562	0.0564	0.0722	99.63	77.84
		4	2	0.1217	0.1225	0.1759	99.34	69.16	0.0606	0.0608	0.0737	99.66	82.18
		4	3	0.1276	0.1284	0.1727	99.33	73.85	0.0654	0.0656	0.0771	99.64	84.80
		4	4	0.1349	0.1358	0.1736	99.34	77.71	0.0714	0.0716	0.0822	99.65	86.83
		4	5	0.1423	0.1434	0.1774	99.23	80.22	0.0780	0.0784	0.0890	99.52	87.69
		5	0	0.1343	0.1351	0.2621	99.42	51.24	0.0563	0.0567	0.0825	99.29	68.17
		5	1	0.1430	0.1435	0.2229	99.70	64.17	0.0621	0.0623	0.0790	99.79	78.64
		5	2	0.1508	0.1513	0.2128	99.73	70.89	0.0675	0.0676	0.0813	99.85	82.95
		5	3	0.1596	0.1601	0.2109	99.72	75.68	0.0735	0.0736	0.0859	99.84	85.64
		5	4	0.1695	0.1700	0.2141	99.71	79.16	0.0806	0.0808	0.0924	99.83	87.28
		5	5	0.1834	0.1839	0.2216	99.74	82.78	0.0904	0.0905	0.1012	99.85	89.27
4.0	5	0	0	0.4121	0.4146	0.6013	99.40	68.54	0.1756	0.1762	0.2257	99.62	77.80
		0	1	0.4840	0.4862	0.5380	99.54	89.96	0.2290	0.2298	0.2436	99.66	94.01
		1	0	0.8931	0.8965	1.2222	99.62	73.07	0.2642	0.2650	0.3275	99.71	80.68
		1	1	1.2045	1.2065	1.2834	99.83	93.85	0.3969	0.3974	0.4128	99.86	96.13
		10	0	0.1515	0.1525	0.2741	99.36	55.29	0.0734	0.0737	0.1054	99.59	69.59
		0	1	0.1611	0.1622	0.2203	99.31	73.10	0.0821	0.0824	0.0980	99.57	83.78
		0	2	0.1718	0.1729	0.2088	99.34	82.26	0.0924	0.0928	0.1030	99.57	89.71
		1	0	0.2336	0.2344	0.4037	99.64	57.86	0.0907	0.0909	0.1275	99.71	71.11
		1	1	0.2547	0.2557	0.3378	99.63	75.41	0.1041	0.1044	0.1224	99.73	85.01
4.0	10	1	2	0.2797	0.2807	0.3329	99.66	84.01	0.1207	0.1210	0.1334	99.75	90.51
		2	0	0.3402	0.3409	0.5703	99.80	59.65	0.1097	0.1099	0.1522	99.78	72.09
		2	1	0.3816	0.3822	0.4925	99.83	77.48	0.1297	0.1298	0.1506	99.86	86.09





Vasudeva Rao and Bhanu Prakash

λ	n	r	s	$\frac{V(\mu^*)}{\sigma^2}$	$\frac{V(\mu_{LS}^*)}{\sigma^2}$	$\frac{V(\mu_{PCE}^*)}{\sigma^2}$	$Ef(\mu_{LS}^*)$	$Ef(\mu_{PCE}^*)$	$\frac{V(\sigma^*)}{\sigma^2}$	$\frac{V(\sigma_{LS}^*)}{\sigma^2}$	$\frac{V(\sigma_{PCE}^*)}{\sigma^2}$	$Ef(\sigma_{LS}^*)$	$Ef(\sigma_{PCE}^*)$
15	2	2	2	0.4334	0.4340	0.5036	99.86	86.07	0.1556	0.1558	0.1700	99.89	91.55
		0	0	0.0893	0.0900	0.1760	99.24	50.74	0.0454	0.0457	0.0676	99.29	67.22
	0	1	0.0932	0.0939	0.1435	99.29	64.94	0.0494	0.0496	0.0627	99.57	78.71	
		0	2	0.0967	0.0974	0.1329	99.29	72.74	0.0530	0.0532	0.0631	99.57	83.95
	0	3	0.1005	0.1013	0.1284	99.30	78.31	0.0571	0.0574	0.0655	99.57	87.25	
		1	0	0.1234	0.1240	0.2315	99.49	53.30	0.0529	0.0533	0.0770	99.38	68.73
	1	1	0.1306	0.1311	0.1937	99.60	67.41	0.0583	0.0585	0.0728	99.71	80.10	
		1	2	0.1371	0.1376	0.1834	99.61	74.75	0.0634	0.0635	0.0746	99.74	84.94
	1	3	0.1444	0.1450	0.1809	99.63	79.85	0.0692	0.0694	0.0788	99.74	87.89	
		2	0	0.1608	0.1615	0.2940	99.59	54.71	0.0602	0.0606	0.0866	99.40	69.52
	2	1	0.1724	0.1727	0.2500	99.79	68.94	0.0672	0.0673	0.0831	99.82	80.94	
		2	2	0.1831	0.1835	0.2406	99.82	76.10	0.0739	0.0740	0.0863	99.87	85.58
	2	3	0.1955	0.1958	0.2413	99.83	81.03	0.0818	0.0819	0.0926	99.88	88.39	
		3	0	0.2059	0.2067	0.3686	99.58	55.85	0.0681	0.0685	0.0971	99.36	70.11
	3	1	0.2237	0.2240	0.3180	99.86	70.36	0.0771	0.0772	0.0943	99.86	81.70	
		3	2	0.2408	0.2410	0.3107	99.90	77.49	0.0859	0.0859	0.0995	99.92	86.26
	3	3	0.2609	0.2612	0.3168	99.91	82.37	0.0966	0.0966	0.1085	99.93	89.02	
		0	0	0.0622	0.0629	0.1270	98.95	48.99	0.0324	0.0329	0.0485	98.63	66.80
20	0	1	0.0647	0.0652	0.1073	99.26	60.27	0.0350	0.0352	0.0462	99.48	75.80	
		0	2	0.0665	0.0670	0.0995	99.28	66.83	0.0370	0.0371	0.0461	99.58	80.27
	0	3	0.0682	0.0687	0.0950	99.28	71.82	0.0389	0.0391	0.0467	99.58	83.38	
		0	4	0.0701	0.0706	0.0925	99.27	75.79	0.0411	0.0413	0.0480	99.55	85.62
	0	5	0.0723	0.0728	0.0914	99.27	79.10	0.0437	0.0439	0.0500	99.51	87.31	
		1	0	0.0810	0.0819	0.1573	98.93	51.51	0.0366	0.0372	0.0537	98.55	68.28
	1	1	0.0850	0.0856	0.1355	99.34	62.78	0.0400	0.0402	0.0518	99.50	77.23	
		1	2	0.0880	0.0886	0.1276	99.38	69.01	0.0425	0.0427	0.0522	99.62	81.40
	1	3	0.0910	0.0916	0.1236	99.36	73.60	0.0451	0.0453	0.0535	99.61	84.18	
		1	4	0.0944	0.0949	0.1221	99.44	77.30	0.0480	0.0482	0.0557	99.67	86.24
	1	5	0.0978	0.0986	0.1223	99.18	79.95	0.0513	0.0516	0.0587	99.36	87.37	
		2	0	0.0987	0.1011	0.1893	97.60	52.15	0.0402	0.0411	0.0586	97.84	68.62
	2	1	0.1045	0.1065	0.1650	98.08	63.30	0.0443	0.0448	0.0571	98.86	77.50	
		2	2	0.1088	0.1109	0.1572	98.11	69.24	0.0474	0.0479	0.0582	98.96	81.42
	2	3	0.1133	0.1155	0.1539	98.11	73.62	0.0506	0.0511	0.0602	98.97	84.04	
		4	0.1177	0.1204	0.1535	97.79	76.67	0.0540	0.0548	0.0632	98.64	85.50	
	2	5	0.1246	0.1266	0.1554	98.41	80.17	0.0589	0.0594	0.0672	99.20	87.60	
		3	0	0.1186	0.1226	0.2249	96.78	52.74	0.0439	0.0451	0.0638	97.38	68.91
3	1	0.1266	0.1301	0.1981	97.32	63.92	0.0488	0.0495	0.0627	98.46	77.82		
	3	2	0.1328	0.1364	0.1905	97.33	69.69	0.0525	0.0533	0.0644	98.54	81.57	
3	3	0.1389	0.1428	0.1882	97.23	73.80	0.0564	0.0573	0.0672	98.45	83.93		
	3	4	0.1466	0.1506	0.1895	97.37	77.37	0.0612	0.0621	0.0712	98.56	85.97	
3	5	0.1531	0.1582	0.1936	96.76	79.04	0.0658	0.0672	0.0764	97.92	86.20		
	4	0	0.1441	0.1473	0.2658	97.82	54.21	0.0483	0.0494	0.0693	97.82	69.74	
4	1	0.1554	0.1577	0.2361	98.54	65.80	0.0542	0.0547	0.0687	99.07	78.92		
	4	2	0.1642	0.1665	0.2292	98.63	71.63	0.0588	0.0593	0.0712	99.24	82.65	
4	3	0.1733	0.1758	0.2284	98.59	75.89	0.0637	0.0643	0.0749	99.21	85.10		
	4	4	0.1830	0.1858	0.2321	98.48	78.84	0.0692	0.0698	0.0800	99.09	86.48	
4	5	0.1972	0.2000	0.2399	98.61	82.22	0.0768	0.0774	0.0868	99.20	88.47		
	5	0	0.1739	0.1764	0.3134	98.62	55.49	0.0530	0.0540	0.0753	98.14	70.41	
5	1	0.1896	0.1905	0.2807	99.49	67.53	0.0601	0.0604	0.0752	99.54	79.90		
	5	2	0.2020	0.2028	0.2751	99.62	73.44	0.0659	0.0660	0.0788	99.75	83.62	
5	3	0.2149	0.2156	0.2767	99.66	77.66	0.0719	0.0721	0.0836	99.80	85.98		
	5	4	0.2307	0.2315	0.2841	99.64	81.21	0.0794	0.0795	0.0903	99.79	87.93	
5	5	0.2475	0.2484	0.2966	99.63	83.46	0.0879	0.0881	0.0989	99.76	88.79		
	5.0	5	0	0	0.5163	0.5190	0.7305	99.48	70.68	0.1718	0.1725	0.2192	99.65
0			1	0.6151	0.6176	0.6728	99.59	91.42	0.2253	0.2260	0.2382	99.67	94.57
1	1	0	1	1.0790	1.0836	1.4625	99.58	73.78	0.2592	0.2601	0.3217	99.66	80.57
		1	1	1.4791	1.4818	1.5686	99.82	94.30	0.3920	0.3927	0.4072	99.84	96.26
10	0	0	0	0.1935	0.1946	0.3274	99.44	59.10	0.0714	0.0717	0.1004	99.51	71.11
		0	1	0.2081	0.2093	0.2717	99.43	76.59	0.0807	0.0810	0.0949	99.60	85.05
0	2	0	2	0.2236	0.2249	0.2628	99.44	85.10	0.0911	0.0914	0.1004	99.60	90.72





Vasudeva Rao and Bhanu Prakash

λ	n	r	s	$\frac{V(\mu^*)}{\sigma^2}$	$\frac{V(\mu_{LS}^*)}{\sigma^2}$	$\frac{V(\mu_{PCE}^*)}{\sigma^2}$	$Ef(\mu_{LS}^*)$	$Ef(\mu_{PCE}^*)$	$\frac{V(\sigma^*)}{\sigma^2}$	$\frac{V(\sigma_{LS}^*)}{\sigma^2}$	$\frac{V(\sigma_{PCE}^*)}{\sigma^2}$	$Ef(\sigma_{LS}^*)$	$Ef(\sigma_{PCE}^*)$
5.0	15	1	0	0.2887	0.2898	0.4779	99.61	60.40	0.0880	0.0884	0.1221	99.59	72.09
		1	1	0.3191	0.3203	0.4112	99.65	77.61	0.1023	0.1026	0.1193	99.73	85.79
		1	2	0.3533	0.3544	0.4125	99.68	85.65	0.1190	0.1193	0.1307	99.75	91.05
		2	0	0.4116	0.4129	0.6697	99.69	61.46	0.1064	0.1068	0.1464	99.61	72.68
		2	1	0.4690	0.4698	0.5933	99.82	79.05	0.1276	0.1278	0.1472	99.84	86.63
		2	2	0.5373	0.5381	0.6166	99.86	87.15	0.1537	0.1539	0.1672	99.89	91.89
		0	0	0.1147	0.1158	0.2054	99.09	55.83	0.0438	0.0443	0.0628	98.77	69.75
		0	1	0.1214	0.1222	0.1747	99.39	69.49	0.0484	0.0486	0.0601	99.53	80.50
		0	2	0.1268	0.1276	0.1653	99.42	76.71	0.0522	0.0524	0.0612	99.61	85.35
		0	3	0.1326	0.1333	0.1620	99.42	81.83	0.0564	0.0566	0.0637	99.61	88.48
		1	0	0.1536	0.1549	0.2685	99.18	57.22	0.0509	0.0515	0.0719	98.77	70.76
		1	1	0.1652	0.1659	0.2337	99.59	70.68	0.0571	0.0573	0.0701	99.63	81.41
		1	2	0.1748	0.1754	0.2258	99.64	77.40	0.0624	0.0625	0.0727	99.74	85.83
		1	3	0.1851	0.1857	0.2256	99.66	82.07	0.0683	0.0685	0.0771	99.75	88.59
		2	0	0.1963	0.1980	0.3386	99.17	57.98	0.0577	0.0585	0.0810	98.70	71.24
	2	1	0.2143	0.2148	0.2993	99.73	71.59	0.0658	0.0659	0.0802	99.71	82.03	
	2	2	0.2295	0.2299	0.2938	99.82	78.13	0.0728	0.0729	0.0844	99.85	86.25	
	2	3	0.2464	0.2468	0.2982	99.84	82.64	0.0808	0.0809	0.0909	99.88	88.86	
	3	0	0.2473	0.2497	0.4218	99.07	58.63	0.0651	0.0660	0.0909	98.58	71.57	
	3	1	0.2743	0.2749	0.3778	99.77	72.61	0.0754	0.0756	0.0912	99.72	82.66	
	3	2	0.2979	0.2983	0.3765	99.89	79.13	0.0846	0.0847	0.0975	99.90	86.80	
	3	3	0.3247	0.3250	0.3883	99.91	83.62	0.0954	0.0954	0.1067	99.93	89.37	
	20	0	0	0.0798	0.0813	0.1442	98.22	55.35	0.0308	0.0317	0.0438	97.05	70.28
		0	1	0.0846	0.0852	0.1288	99.27	65.68	0.0342	0.0344	0.0437	99.26	78.11
		0	2	0.0876	0.0882	0.1225	99.40	71.52	0.0364	0.0366	0.0444	99.57	81.98
		0	3	0.0904	0.0909	0.1188	99.42	76.10	0.0384	0.0386	0.0453	99.62	84.86
		0	4	0.0933	0.0938	0.1169	99.42	79.77	0.0407	0.0408	0.0467	99.62	87.01
		0	5	0.0965	0.0971	0.1166	99.41	82.75	0.0432	0.0434	0.0488	99.59	88.61
		1	0	0.1008	0.1029	0.1775	97.97	56.77	0.0346	0.0357	0.0485	96.81	71.27
		1	1	0.1081	0.1090	0.1615	99.24	66.97	0.0389	0.0392	0.0492	99.22	79.10
		1	2	0.1130	0.1136	0.1560	99.42	72.39	0.0418	0.0419	0.0506	99.57	82.61
		1	3	0.1174	0.1180	0.1533	99.44	76.56	0.0444	0.0446	0.0522	99.63	85.16
		1	4	0.1221	0.1227	0.1528	99.45	79.87	0.0474	0.0476	0.0545	99.64	87.03
		1	5	0.1273	0.1280	0.1544	99.41	82.45	0.0508	0.0510	0.0575	99.58	88.30
		2	0	0.1216	0.1248	0.2122	97.46	57.32	0.0380	0.0394	0.0531	96.42	71.65
		2	1	0.1320	0.1334	0.1954	98.97	67.55	0.0432	0.0436	0.0543	99.05	79.56
		2	2	0.1389	0.1401	0.1910	99.19	72.74	0.0468	0.0470	0.0565	99.45	82.85
	2	3	0.1453	0.1465	0.1895	99.22	76.70	0.0501	0.0504	0.0588	99.52	85.20	
	2	4	0.1521	0.1534	0.1907	99.20	79.77	0.0538	0.0541	0.0619	99.50	86.85	
	2	5	0.1604	0.1617	0.1946	99.20	82.45	0.0583	0.0586	0.0660	99.49	88.27	
	3	0	0.1453	0.1492	0.2506	97.40	57.97	0.0416	0.0432	0.0577	96.25	72.04	
	3	1	0.1595	0.1609	0.2330	99.14	68.46	0.0478	0.0483	0.0597	99.12	80.18	
	3	2	0.1692	0.1701	0.2300	99.43	73.55	0.0522	0.0524	0.0626	99.59	83.35	
	3	3	0.1783	0.1792	0.2302	99.49	77.42	0.0563	0.0565	0.0658	99.68	85.59	
	3	4	0.1883	0.1893	0.2339	99.48	80.52	0.0610	0.0612	0.0699	99.67	87.27	
3	5	0.1990	0.2002	0.2408	99.41	82.65	0.0662	0.0665	0.0752	99.59	88.13		
4	0	0.1721	0.1770	0.2943	97.19	58.47	0.0453	0.0472	0.0626	96.02	72.27		
4	1	0.1912	0.1929	0.2759	99.16	69.30	0.0528	0.0532	0.0654	99.10	80.73		
4	2	0.2045	0.2056	0.2751	99.48	74.35	0.0580	0.0583	0.0693	99.61	83.81		
4	3	0.2171	0.2181	0.2778	99.53	78.14	0.0631	0.0633	0.0735	99.70	85.94		
4	4	0.2310	0.2320	0.2848	99.55	81.10	0.0689	0.0691	0.0788	99.72	87.47		
4	5	0.2491	0.2502	0.2963	99.59	84.07	0.0763	0.0765	0.0856	99.74	89.18		
5	0	0.2030	0.2097	0.3450	96.82	58.84	0.0493	0.0515	0.0681	95.71	72.38		
5	1	0.2286	0.2309	0.3260	98.99	70.13	0.0582	0.0588	0.0716	98.97	81.24		
5	2	0.2468	0.2483	0.3283	99.39	75.17	0.0646	0.0649	0.0767	99.55	84.26		
5	3	0.2644	0.2658	0.3348	99.47	78.97	0.0710	0.0712	0.0821	99.66	86.38		
5	4	0.2843	0.2859	0.3466	99.43	82.01	0.0782	0.0785	0.0889	99.63	87.98		
5	5	0.3063	0.3082	0.3646	99.39	84.03	0.0867	0.0871	0.0977	99.58	88.76		





Vasudeva Rao and Bhanu Prakash													
4	2	0.0822	0.0003	0.0955	0.0962	99.3	-0.0353	0.0007	0.0297	0.0307	96.8		
λ	n	r	s	$\frac{bias(\hat{\mu})}{\sigma}$	$\frac{bias(\tilde{\mu}^*)}{\sigma}$	$\frac{MSE(\hat{\mu})}{\sigma^2}$	$\frac{MSE(\tilde{\mu}^*)}{\sigma^2}$	$Eff(\tilde{\mu}^*)$	$\frac{bias(\hat{\sigma})}{\sigma}$	$\frac{bias(\tilde{\sigma}^*)}{\sigma}$	$\frac{MSE(\hat{\sigma})}{\sigma^2}$	$\frac{MSE(\tilde{\sigma}^*)}{\sigma^2}$	$Eff(\tilde{\sigma}^*)$
4	3	0.0851	0.0006	0.0974	0.0980	99.4	-0.0372	0.0005	0.0307	0.0317	96.9		
4	4	0.0872	0.0000	0.1008	0.1017	99.1	-0.0387	0.0009	0.0323	0.0335	96.6		
4	5	0.0915	0.0015	0.1044	0.1052	99.2	-0.0417	-0.0001	0.0338	0.0350	96.7		
4	6	0.0955	0.0022	0.1088	0.1096	99.2	-0.0445	-0.0007	0.0356	0.0368	96.7		
4	7	0.1004	0.0037	0.1132	0.1140	99.3	-0.0481	-0.0017	0.0377	0.0389	96.8		
5	0	0.0835	0.0004	0.1052	0.1063	98.9	-0.0345	0.0005	0.0298	0.0308	96.7		
5	1	0.0863	0.0010	0.1066	0.1076	99.1	-0.0362	0.0002	0.0305	0.0315	96.8		
5	2	0.0880	0.0000	0.1091	0.1103	98.9	-0.0373	0.0008	0.0317	0.0328	96.6		
5	3	0.0913	0.0004	0.1111	0.1122	99.0	-0.0394	0.0005	0.0327	0.0338	96.6		
5	4	0.0938	-0.0002	0.1151	0.1166	98.7	-0.0411	0.0010	0.0344	0.0358	96.3		
5	5	0.0987	0.0014	0.1198	0.1212	98.8	-0.0444	-0.0001	0.0362	0.0376	96.4		
5	6	0.1033	0.0022	0.1252	0.1268	98.8	-0.0476	-0.0007	0.0383	0.0397	96.4		
5	7	0.1091	0.0039	0.1309	0.1325	98.8	-0.0516	-0.0018	0.0407	0.0422	96.5		
6	0	0.0878	0.0012	0.1188	0.1205	98.6	-0.0357	0.0002	0.0319	0.0330	96.5		
6	1	0.0910	0.0019	0.1206	0.1221	98.8	-0.0376	-0.0002	0.0327	0.0339	96.6		
6	2	0.0930	0.0009	0.1237	0.1255	98.6	-0.0388	0.0005	0.0340	0.0353	96.4		
6	3	0.0967	0.0013	0.1262	0.1280	98.6	-0.0412	0.0002	0.0352	0.0365	96.4		
6	4	0.0995	0.0006	0.1312	0.1335	98.3	-0.0430	0.0006	0.0372	0.0388	96.1		
6	5	0.1052	0.0024	0.1371	0.1395	98.3	-0.0467	-0.0005	0.0393	0.0409	96.1		
6	6	0.1105	0.0034	0.1438	0.1463	98.3	-0.0502	-0.0011	0.0417	0.0434	96.1		
6	7	0.1171	0.0053	0.1509	0.1536	98.3	-0.0546	-0.0024	0.0445	0.0463	96.1		
7	0	0.0917	-0.0061	0.1367	0.1403	97.5	-0.0368	0.0030	0.0346	0.0362	95.7		
7	1	0.0952	-0.0055	0.1393	0.1428	97.5	-0.0388	0.0027	0.0357	0.0373	95.8		
7	2	0.0975	-0.0069	0.1431	0.1472	97.3	-0.0402	0.0035	0.0372	0.0390	95.4		
7	3	0.1016	-0.0066	0.1465	0.1506	97.3	-0.0427	0.0033	0.0385	0.0404	95.4		
7	4	0.1049	-0.0077	0.1529	0.1579	96.8	-0.0448	0.0040	0.0410	0.0431	95.0		
7	5	0.1114	-0.0059	0.1599	0.1651	96.9	-0.0488	0.0029	0.0433	0.0456	95.1		
7	6	0.1174	-0.0052	0.1684	0.1742	96.7	-0.0526	0.0024	0.0461	0.0486	94.9		
7	7	0.1251	-0.0034	0.1772	0.1833	96.7	-0.0576	0.0013	0.0494	0.0521	94.9		

Table 3: ULAMLEs and BLUEs of μ and σ in $GE(\lambda, \mu, -)$ with known $\lambda=5.5$ obtained from the above sample of size $n=20$ with choice of $r=0(1)3$ and $s=0(1)3$.

r	s	Estimates of μ		Estimates of σ	
		μ^* (S.E.)	$\tilde{\mu}^*$ (S.E.)	σ^* (S.E.)	$\tilde{\sigma}^*$ (S.E.)
0	0	6.6682 (0.1143)	6.6879 (0.1172)	0.3869 (0.0668)	0.3703 (0.0689)
0	1	6.6808 (0.1154)	6.6739 (0.1221)	0.3770 (0.0693)	0.3810 (0.0723)
0	2	6.7179 (0.1086)	6.7171 (0.1131)	0.3477 (0.0661)	0.3478 (0.0675)
0	3	6.7117 (0.1120)	6.7131 (0.1159)	0.3527 (0.0690)	0.3510 (0.0700)
1	0	6.6654 (0.1281)	6.6889 (0.1340)	0.3880 (0.0709)	0.3700 (0.0743)
1	1	6.6808 (0.1299)	6.6715 (0.1406)	0.3770 (0.0738)	0.3821 (0.0785)
1	2	6.7271 (0.1213)	6.7253 (0.1290)	0.3436 (0.0700)	0.3443 (0.0727)
1	3	6.7196 (0.1258)	6.7205 (0.1330)	0.3491 (0.0734)	0.3477 (0.0757)
2	0	6.6111 (0.1477)	6.6273 (0.1565)	0.4090 (0.0782)	0.3948 (0.0833)
2	1	6.6244 (0.1518)	6.6049 (0.1653)	0.4001 (0.0826)	0.4094 (0.0886)
2	2	6.6768 (0.1425)	6.6661 (0.1521)	0.3648 (0.0786)	0.3690 (0.0823)
2	3	6.6656 (0.1489)	6.6580 (0.1580)	0.3724 (0.0832)	0.3744 (0.0863)
3	0	6.5222 (0.1735)	6.5632 (0.1811)	0.4419 (0.0882)	0.4196 (0.0927)
3	1	6.5287 (0.1817)	6.5348 (0.1925)	0.4378 (0.0949)	0.4371 (0.0992)
3	2	6.5848 (0.1725)	6.6036 (0.1779)	0.4023 (0.0914)	0.3942 (0.0925)





Vasudeva Rao and Bhanu Prakash

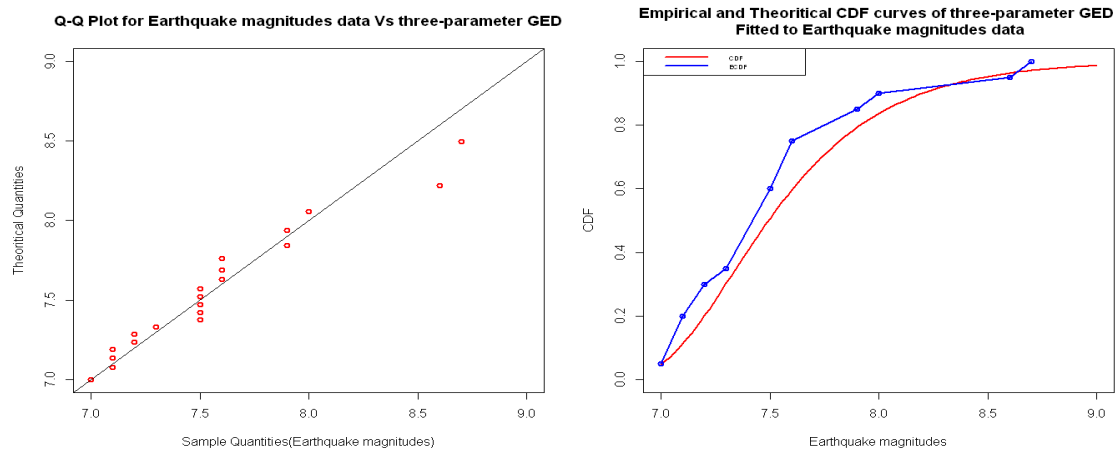


Figure 1 : Q-Q plot and empirical & theoretical cdf curves of $GE(\lambda, \mu, 1)$ fitted to earthquake magnitudes data.





RESEARCH ARTICLE

Integration of Power Grid Associated Wind, Fuel Cell & Solar Energy Systems Implementing Fuzzy MPPT Technique

G. Tejaswi^{1*}, S. Ramesh Kumar² and Ch. Ravi Kumar³

¹Research Scholar, Annamalai University, Chidambaram, Tamil Nadu, India.

²Associate Professor, Annamalai University, Chidambaram, Tamil Nadu, India

³Head of the Department, Acharya Nagarjuna University, Guntur, Andhra Pradesh, India.

Received: 24 Nov 2021

Revised: 12 Dec 2021

Accepted: 12 Jan 2022

*Address for Correspondence

G. Tejaswi

Research Scholar,

Annamalai University,

Chidambaram, Tamil Nadu, India.

Email: tejathesinger@gmail.com



This is an Open Access Journal / article distributed under the terms of the **Creative Commons Attribution License** (CC BY-NC-ND 3.0) which permits unrestricted use, distribution, and reproduction in any medium, provided the original work is properly cited. All rights reserved.

ABSTRACT

The main objective of this paper is integration of grid-Associated wind, fuel cell and solar systems by using fuzzy MPPT technique. Mainly wind energy, fuel cell and solar cell plays a key role in the generation of electric power. Besides, the contributions of wind power, solar energy and fuel cell are properly integrated to ensure & sustain the continuity of the supply to load on the demand at every minute. The output of the solar cell, fuel cell and Wind systems are connected to BUCK-BOOST converter. In order to extract the maximum power from Fuel cell, solar and wind energy systems a new technique, called Maximum power point tracking. In this paper fuzzy Maximum Power Point Tracking method is used for controlling the BUCK-BOOST converter because it gives better performance compared to P and O, incremental conductance methods. The output of the Buck-Boost converter connected to grid by using three phase inverter. Using the MATLAB / Simulink platform, simulation of the proposed system are studies, carried out and the results are presented.

Keywords: Grid, Fuel cell, Photo-Voltaic (PV) system, Wind-Energy Conversion system (WECS), BUCK-BOOST converter, Fuzzy MPPT

INTRODUCTION





Due to the usage of large amounts of conventional energy sources leads to serious environmental pollution and

Tejaswi et al.,

to protect future generations or wealth [1]. Other than thermal power & hydro power, the Fuel cell, PV and wind energy [2] are available at a high extent to meet the high potential need to sustain the large amounts of energy demand. With the generation of wind, it is capable to supply large amounts of energy demand to the end-users but main disadvantage of the wind generation is the geographical location to implant this wind power plant where wind forces are highly available which is unpredictable[3]. Solar energy is high availability over the entire day even though the solar radiation levels vary from time to time and due to the clouds, tall buildings, and birds etc. The main drawback of these energy systems, are their interrupted nature that make them unpredictable. To overcome the above difficulties, the integration of wind, solar and third energy source needed namely fuel cells [4] are connected to grid and made hybrid system. Due to this hybrid system [5-7], the reliability at the load side is increased, power transfer capability and efficiency gradually improved. Due to some reasons, if any of the above resources are not available to meet the continuity across the supply at load side, The deficit will complement the other energy source. Various hybrid systems with various MPPT techniques are discussed in [3]. In this paper the proposed system contains wind energy, PV system and fuel cell. To obtain maximum power from wind, solar PV and fuel cell, afuzzy MPPT (Maximum Power Point Tracking) is implemented [8-10].

ARCHITECTURE OF THE PROPOSED SYSTEM

The construction for recommended system is given belowFig.1. In the wind power generation, power is extracted from PMSG which is coupled to the wind turbine. When the intensity of the flow of wind increases which hits the wind blade vanes then rotates the wind turbine at high speed. This turbine coupled to PMSG which generates the electric power with the assistance of Fuzzy MPPT method, the maximum power can be taken from the grid by changing the value of duty ratio, and the magnitude of the voltage output from the wind generator also varies. So, in this way, the maximum power will be obtained. In the solar PV generation, output of solar PV panel was coupled to Buck-Boost converter, to produce higher voltage by implementing Fuzzy maximum power point tracking method. Output of the Buck-Boost converter converted into AC with a help of the three-phase inverter. And fuel cell also generates the dc energy it also passes through DC bus system. The dc bus is connected to grid or load via an inverter. The load demand is synchronized by these three sources.

POWER GENERATION USING WECS

WIND TURBINE DEMONSTRATING

Wind generator turbine rotates which is coupled to an alternator generates electrical energy. Electric power magnitude [6] of speed changes with a given turbine is described as:

$$P_w = \frac{1}{2} \frac{m \cdot v_w^3}{t} = \frac{1}{2} \frac{\rho \cdot A \cdot d \cdot v_w^3}{t} = \frac{1}{2} \rho \cdot A \cdot v_w^3 \tag{1}$$

Where V_w = wind speed (distance/time) (m/s) P_w = Wind Power (W)

- ρ = Air density (kg/m³)
- A = Area swept by the turbine blades (m²)
- d = radius of the swept area of blades (m)
- m = mass of the air
- m = air density X volume = $\rho \cdot A \cdot d$ (Kg)

The generated mechanical power is expressed by [6]

$$P_m = P_w \cdot c_p(\lambda, \beta) = \frac{1}{2} \rho \cdot A \cdot v_w^3 \cdot c_p(\lambda, \beta) \tag{2}$$

- Here C_p denotes power coefficient.
- λ represents tip speed ratio of the rotor blade
- ω tip speed to wind speed





Tejaswi et al.,

The power coefficient of the turbine is expressed by

$$c_p = c_1 \left(\frac{c_2}{\lambda_i} - c_3 \beta - c_4 \right) e^{-\frac{c_5}{\lambda_i}} + c_6 \lambda \tag{3}$$

Where,

$$\frac{1}{\lambda_i} = \frac{1}{\lambda + 0.08\beta} - \frac{0.035}{\beta^3 + 1} \tag{4}$$

And also

$$C_p = \frac{P_m}{P_w}; C_p < 1 \tag{5}$$

$$P_m = C_p \cdot \frac{\rho A}{2} v_w^3 \tag{6}$$

The power produced P_m depends on the magnitude of C_p . The C_p is defined as a ratio of electric power generated by wind generator turbine to mathematical wind generator power.

TSR denotes relation among wind speed angular speed which is expressed by

$$\lambda = \frac{\omega \cdot d}{V_w} \tag{7}$$

Here ω is the rotor speed expressed in rpm

For a gearless wind turbine, the mechanical torque is expressed as

$$T_m = P_m \frac{d}{\lambda V_w} = \frac{1}{2} \rho A C_p (\lambda, \beta) \frac{R}{V_w} = \frac{P_m}{\omega} \tag{8}$$

SOLAR PV MODULE

The PV (Photo Voltaic) cell equivalent circuit is shown below. The solar cell is treated with the current source and diode in parallel connected.

From Figure. 2, apply KCL (Kirchhoff's Current Law), then

$$I_{ph} = I_d + I_{sh} + I \tag{9}$$

$$I = I_{ph} - (I_{sh} + I_d) \tag{10}$$

We have [6] following equation for Solar cell current,

$$I = I_{ph} - I_o \left[e^{q(V + IR_s)/nkT} - 1 \right] - (V + IR_s)/R_{sh} \tag{11}$$

Where V_T represents Terminal Voltage

I_{ph} denotes isolation current

V represents the cell voltage

I represent cell current

I_o denotes reverse saturation current

R_{sh} is Shunt Resistance

R_s denotes Series Resistance

q represents elementary charge

n denotes diode ideality factor

T represents absolute Temperature

K denotes Boltzmann's constant

FUEL CELL

Fuel cell mainly consists of 3 sections:

- a) Fuel reformer





1) Documentation (contains studies of fuel cells)

Tejaswi et al.,

Inverter

The Fuel cell classifies based on the type of electrolyte. In this type hydrogen or oxygen ionizes or initiates the flow of electrons decomposed and flows through the load. Hydrogen is produced from the enriched Hydrogen enriched fuel enters into the fuel cell. The free electrons which hydrogen molecules from the anode and passed via an external circuit. The Hydrogen ions liberate and enter into the cathode. Across the cathode terminals, the oxygen is extracted from the air, the hydrogen ions and the electrons which flow from external circuit together form water and heat. The below Fig.4 indicates fuel cell with H₂ ions [8].

At anode terminal



At cathode terminal



DC-DC CONVERTER (BUCK-BOOST CONVERTER)

The DC-DC converters are also known as Choppers. Buck boost converter which could operates as DC-DC Step-Down or Step-Up converter depending upon duty cycle, D.

Block diagram of the Buck-Boost Converter.

These converters convert from fixed DC voltage to variable DC voltage that may be less or more voltage depends upon the duty ratio.

If V_{input} is greater than the $V_{\text{output}} (V_i > V_o)$ i.e. Buck converter. In this situation, the electric V_{output} is expressed by

$$V_o = DV_i \quad (14)$$

If V_{input} is lesser than the $V_{\text{output}} (V_i < V_o)$ then it was called Boost converter. So, the o/p voltage is expressed by

$$V_o = \frac{V_i}{1-D} \quad (15)$$

For Buck and Boost converters, the output voltage is expressed by

$$V_o = \frac{D}{1-D} V_i \quad (16)$$

Here V_o = DC output voltage across terminals.

V_i = Input DC voltage

D = Duty ratio

By varying the duty ratio D, the maximum power can be extracted from the wind by utilizing MPPT method continuously can be achieved.

DC-AC CONVERTER (INVERTER)

From the DC-DC buck-boost converter, output DC voltage is connected to the grid via DC-AC converter i.e. Inverter. Generally, 3-phase inverter which is utilized for the conversion of DC-AC so it was called as (GSC) Grid Side Converter. The three-phase inverter as shown in Fig.7. In the above block diagram (i.e., Fig.8). The synchronous reference frame theory with PI controller is used for the controlling the three phase inverter. This technique including park's transformation and reverse park's transformation. By using this transformation to generate pulse width modulation output pulses to control the three phase inverter switches. In the proposed technique, PI controller to estimation the V_{dc}^* and V_{dc} controller. The grid voltages in the SRF are calculated as shown below known as park's transformation. To monitor the error occurring between the calculated and the required voltage of the capacitor voltage, an PI controller is used. This signal control is used;





Tejaswi et al.,

$$V_d'' = V_{gd}'' + \Delta V_{dc}, V_q'' = V_{gq}'' \quad (18)$$

By reversing a synchronous reference frame, reference currents will be moved to the ABC frame as a connection (1). The resulting reference voltages in the PWM controller is equated with inverter output voltages and control pulses required are generated.

PROPOSED MPPT TECHNIQUE

To takeout the higher power from the output, we implemented a new strategy known as MPPT method which continuously tracks maximum power so that the reliability of the system is enhanced. Various techniques are available viz. Incremental conductance (IC) Hill-Climbing Search (HCS), Perturb and Observe (P&O) and Fuzzy Logic Controller (FLC). In this paper FLC MPPT is implemented for controlling the respective buck boost converters.

FUZZY LOGIC CONTROLLER (FLC)

In the HCS and incremental conductance, the time taken process from the output voltage increases and we have to take power from every step size. To overcome the above problem the Fuzzy logic has been implemented by varying step-size. The active control technique is the Fuzzy logic controller. The multivariable and multi-regulatory resolution processes are known. Fuzzy MPPT has been very popular over the last decade. The flow chart is shown in Fig.9. In this method firstly calculates the total power and voltage these are giving to the fuzzy controller which is generates the duty cycle. Compared with conventional approaches, the Fuzzy control algorithm can increase the tracking efficiency of both linear and nonlinear loads. Since fuzzy logic does not use complex mathematical equations, it is therefore also suitable for non-linear control. In this FLC, mainly program If-else statement is used and does not require any mathematical model. So it reduces the complexity for analyzing the given solution and it also implemented to a very complex solution. Here the error signal is attained from the average of difference of the ratio of power variation to voltage variation form dc-dc converter output. They output of system is alteration of duty cycle or pulse width modulation signal for switching the dc-dc converter. Every input & output categorized into 7 membership functions indicated in fig.10, 11 & fig.12.

The error signal is computed as ;

$$e(t) = \frac{\frac{\Delta P_{in}(t)}{\Delta V_{in}(t)} + \frac{\Delta P_{out}(t)}{\Delta V_{out}(t)}}{2} \quad (19)$$

And change of error is computed as ;

$$\Delta e = e(t) - e(t-1) \quad (20)$$

The output variable is the increase of the service cycle which can be positive or negative values. This output is sent to dc-dc converter. Table-1 indicates the 49 rules applied in the particular controller. Defuzzification on MPPT framework is done by Center of Largest Area process to control fuzzy output in the form of adjustment of PWM

SIMLUATION and RESULTS

Fig.13 indicates the Simulink model of PV, wind, Fuel-cell integrated with grid or load. The system contains input sources PV, wind, fuel-cell, buck-boost converters, inverter and grid or load. The output of the Hybrid system is connected to three phase inverter which converts to AC. Fig.14 indicates the wind subsystem and Fig.15 indicates the PV subsystem with fuzzy maximum power point Technique.

Wind Energy Conversion Scheme

In this case, simulation results are indicated in the below figures. Fig.17 demonstrations wind speed here wind speed is 14 m/s up-to 1sec after that it is 9 m/sec respectively. Fig.18 demonstrations wind torque, Fig.19, 20 and 21 indicates output Voltage, Current and Power of Wind system.

PV Scheme





Tejaswi et al.,

array is 63.6. In Table .3 shows the limitations of PV arrangement.

Fuel Cell Scheme

Fig. 25, 26 and 27 indicates the output voltage, Current and Power of Fuel Cell. The output of Fuel cell is 17.6V. Table. 4 shows the parameters of Fuel cell.

Hybrid scheme

Fig.28 and Fig.29 shows the three-phase voltage and current for a hybrid scheme. The output voltage of PV, Wind and Fuel cell hybrid system connected to grid is 590V. The below Fig.32 indicates proposed grid voltage THD is 3.30%.

CONCLUSION

This paper mainly explains the hybrid grid with an integration of PMSG for the wind power generation, Solar PV cells and Fuel cells are implementing based MPPT technique. FUZZY MPPT method has been implemented in this paper. Proposed model gives less THD compared to the conventional model. The suggested results were simulated in the Simulink of Platform and Waveform has been analyzed and plotted. The future scope of the paper is to get less THD from the ANFIS and FOPI based Multilevel Inverter.

REFERENCES

1. S. Padmanaban, N. Priyadarshi, J. B. Holm-Nielsen, M. S. Bhaskar, F. Azam, A. K. Sharma, and E. Hossain, "A novel modified sine-cosine optimized MPPT algorithm for grid integrated PV system under real operating conditions," *IEEE Access*, vol. 7, pp. 10467–10477, 2019
2. Mastromauro, T. Kerekes and M. Liserre, "A Single-Phase Voltage-Controlled Grid-Connected Photovoltaic System With Power Quality Conditioner Functionality" *The transactions IEEE reference on Industrial Electronics*, volume Number 56, Number 11, and Part Percent. 4436–4444, November 2017.
3. High-performance adaptive perturb and observe MPPT technique for photovoltaic-based microgrids AK Abdelsalam, AM Massoud, S Ahmed, PN Enjeti *IEEE Transactions on power electronics* 26 (4), 1010-1021.
4. Elgendy and Atkinson, "Calculation for perturbing and analyses MPPT method used to estimate the PV (Photo Voltaic) pumping applications & methods," *The IEEE Transactions on the Supportable Energy*, volume 3, Number. 1, pp. 21–33, January 2012.
5. Comprehensive Studies on Operational Principles for Maximum Power Point Tracking in Photovoltaic Systems, Xingshuo Li Qi Wang 1, Huiqing Wen And Weidong Xiao3, Volume 7, 2019.
6. K. Rajesh, A. Kulkarni and T. Ananthapadmanabha, "Modeling and Simulation of Solar PV and DFIG Based Wind Hybrid System", *Procedia Technology*, Vol.21, pp.667-675, 2015.
7. S. Jain and V. Agarwal, "A Single-Stage Grid Connected Inverter Topology for Solar PV Systems with Maximum Power Point Tracking," *IEEE Transactions on Power Electronics*, vol. 22, no.5, pp. 1928-1940, September 2007.
8. N. Femi and M. Vitelli, "The accrue of perturbing & observe analyses the electric maximum power value method," *The IEEE Transactions on EPE*, vol. 20, no. 4, pp. 963–973, Jul. 2005.
9. Ishita Biswas, Prabodh Bajpai, "Control of PV-FC-Battery-SC Hybrid System for Standalone DC load" *The IEEE Transactions*, 2014.
10. N. Mezzai, Djamil Rekioua, Toufik Rekioua, Ahmed Mohammedi "Modeling of hybrid photovoltaic/wind/fuel cells power system, September 2014, *International Journal of Hydrogen Energy* 39(27):15158–15168.
11. Mohammad Junaid Khan1 • Lini Mathew "Fuzzy logic controller-based MPPT for hybrid photovoltaic/wind/fuel cell power system", March 2018, *Neural Computing and Applications*.





Tejaswi et al.,

Table-1 Rule assessment Table

E/DE	NB	NM	NS	ZE	PS	PM	PB
NB	ZE	ZE	ZE	PM	PB	PB	PB
NM	ZE	ZE	ZE	PS	PM	PM	PM
NS	ZE	ZE	ZE	PS	PS	PS	PS
ZE	PS	PM	ZE	ZE	ZE	NM	NS
PS	NS	NS	NS	NS	ZE	ZE	ZE
PM	NM	NM	NM	NS	ZE	ZE	ZE
PB	NB	NB	NB	NM	ZE	ZE	ZE

Table. 2The parameters of PMSG

PMSG Parameters	Value
Rated Voltage(V)	690
No. of poles	2
Rated Current(I)	6.8
Rated Power (MW)	2
Stator frequency (Hz)	12.15

Table. 3 Solar PV array Parameters

Solar PV array Parameters	Value
V _{Optimum}	42.4
I _{sc}	9.5
Optimum Current(I)	6.75
Power Rated (w)	605
V _{oc}	63.6

Table. 4 Fuel Cell Parameters

Fuel cell Parameters	Value
No. of cells	40
Open Circuit Voltage (V)	35
Operating Temperature(°c)	55
Rated Current(I)	4.8
Rated Power (MW)	85

Table. 5. Specifications

PV Power (Before DC/DC converter)	600W
Wind Power(Before DC/DC converter)	2.3MW
Fuel cell Power(Before DC/DC converter)	85W
Grid	Voltage= 600V Current = 2.7kA
THD	3.30%





Tejaswi et al.,

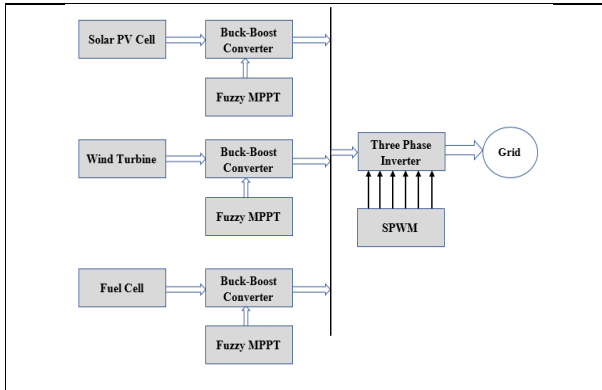


Figure. 1 Over view of the Proposed Hybrid System

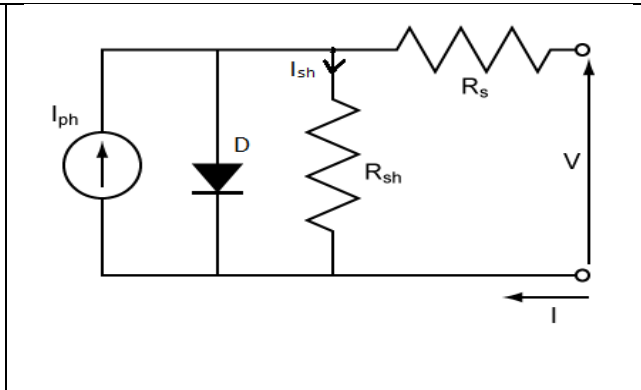


Figure.2 Solar PV module equivalent circuit

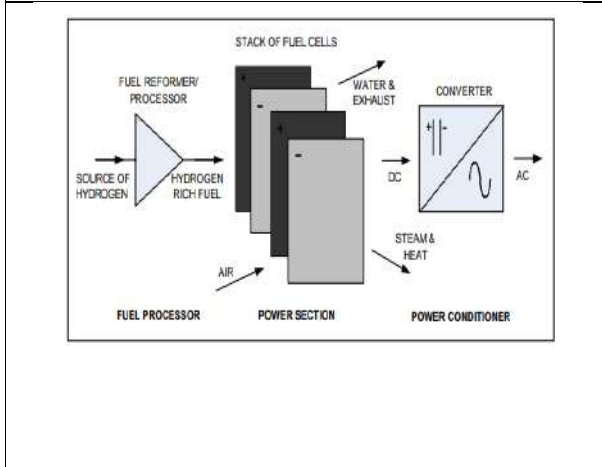


Figure. 3 Construction of Fuel Cell Assembly

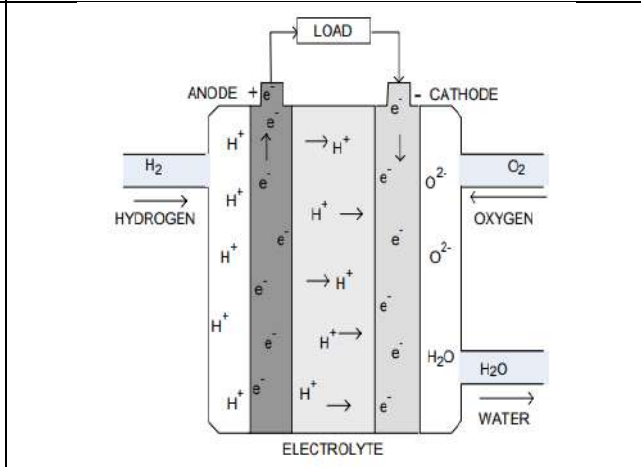


Figure.4 Fuel cell with Hydrogen ions

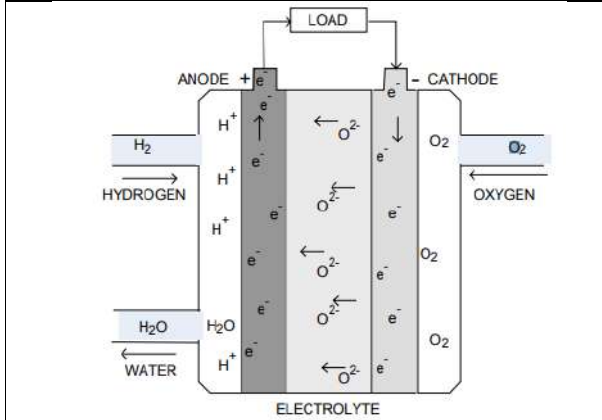


Figure.5 Fuel cell producing negative ions

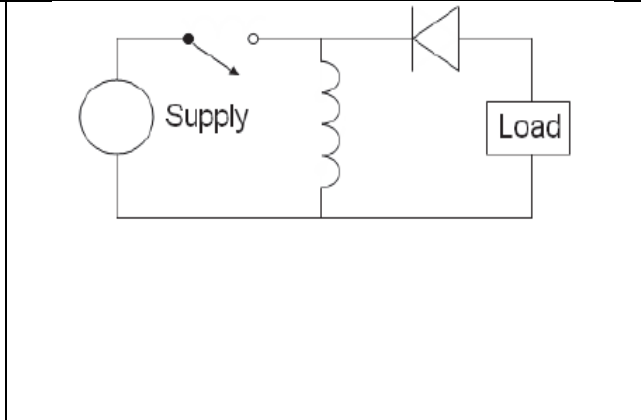


Figure.6 Buck-Boost converter





Tejaswi *et al.*,

<p>Figure.7. Three Phase Inverter</p>	<p>Figure.8 Block diagram describes the control strategies of Grid Side Controller</p>
<p>Figure.9 Flow chart describes FUZZY MPPT method</p>	<p>Figure.10 Input error (Fuzzy set)</p>
<p>Figure.11 Input delta error (Fuzzy set)</p>	<p>Figure.12 Output delta PWM (Fuzzy set)</p>
<p>Figure. 13 Simulink model of the proposed system</p>	<p>Figure.14. Wind subsystem</p>





Tejaswi et al.,

<p align="center">Figure.15 PV subsystem</p>	<p align="center">Figure. 16 Subsystem of Three phase inverter with PI controller</p>
<p align="center">Figure. 18 Torque of the wind</p>	<p align="center">Figure. 19 Wind Output Voltage</p>
<p align="center">Figure. 20 Wind Output Current</p>	<p align="center">Figure. 21 Wind Output Power</p>
<p align="center">Figure. 22 Output Voltage of PV array at irradiance 1000W/m² and 800W/m²</p>	<p align="center">Figure. 23 Output Current of PV array at irradiance 1000W/m² and 800W/m²</p>
<p align="center">Fig. 24 Output Power of PV array at irradiance 1000W/m² and 800W/m²</p>	<p align="center">Figure. 25 Output Voltage of Fuel Cell</p>





Tejaswi et al.,

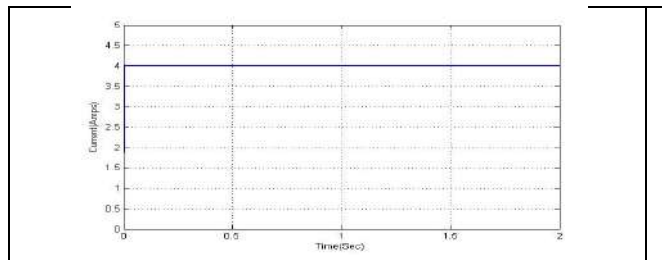


Figure. 26 Output current of Fuel Cell

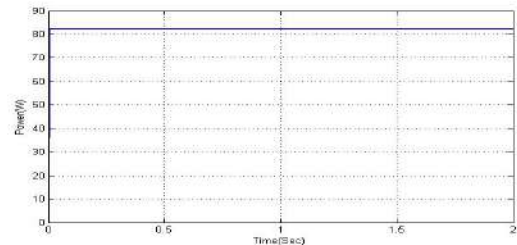


Figure. 27 Output power of Fuel Cell

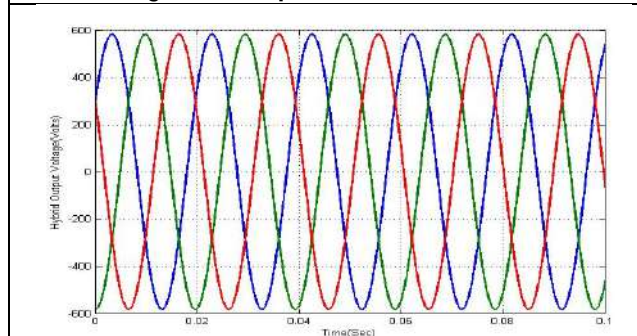


Figure. 28 Three phase voltage for Hybrid Scheme

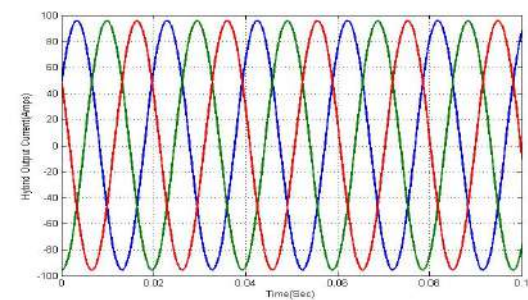


Figure. 29 Three phase current for Hybrid Scheme

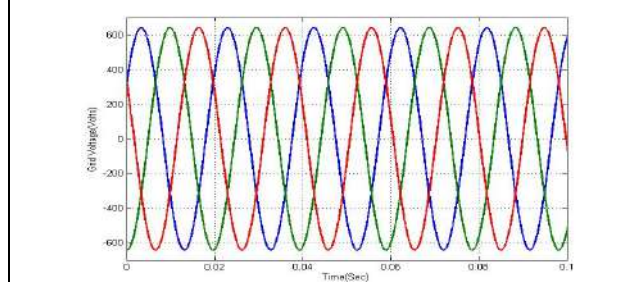


Figure. 30 Grid Voltage

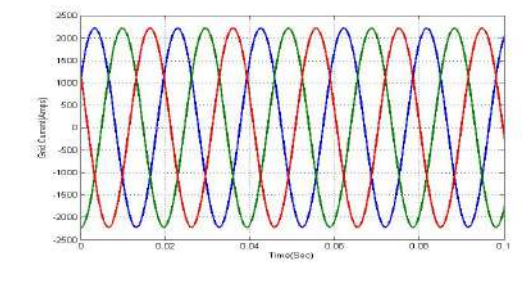


Figure. 31 Grid Current

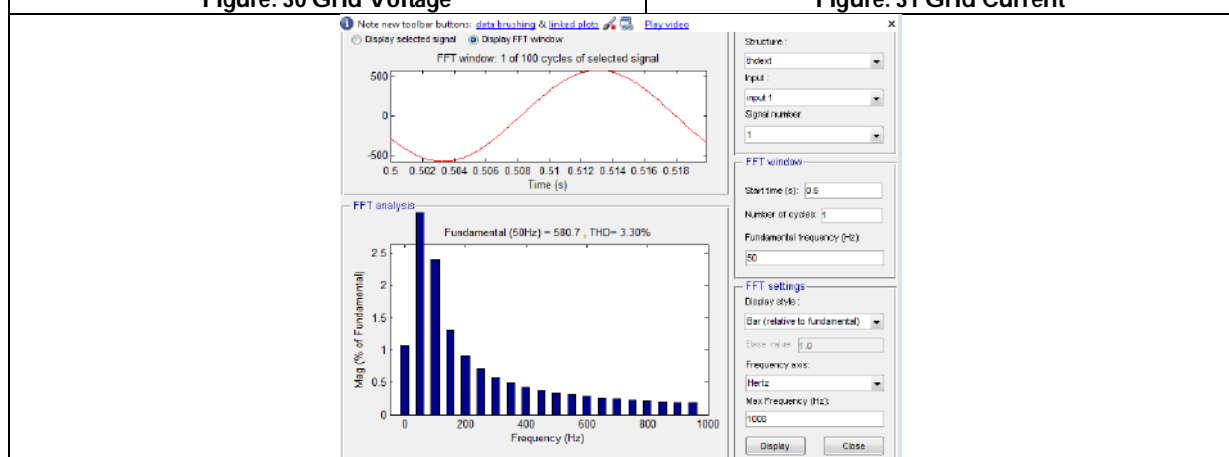


Fig.32 THD of grid voltage is 3.30% in the proposed scheme





Impact of Macroeconomic Factors on BSE Sensex- A Case Study

Nannaparaju Vasudha*

Associate Professor, Department of Mathematics, Vasavi College of Engineering, Hyderabad - 500031, Telangana, India.

Received: 16 Nov 2021

Revised: 15 Dec 2021

Accepted: 11 Jan 2022

*Address for Correspondence

Nannaparaju Vasudha

Associate Professor,
Department of Mathematics,
Vasavi College of Engineering,
Hyderabad - 500031, Telangana, India.
Email: dr.nvasudha@outlook.com



This is an Open Access Journal / article distributed under the terms of the **Creative Commons Attribution License** (CC BY-NC-ND 3.0) which permits unrestricted use, distribution, and reproduction in any medium, provided the original work is properly cited. All rights reserved.

ABSTRACT

Macroeconomic variables play a key role in deciding financial investments and therefore a pertinent tool to indicate prosperity of any economy. Any uncertainty in these variables directly impacts prices and brings volatility to the stock market. Present study focuses on the volatilities in stock market corresponding to the fluctuations in Macroeconomic variables. The effect of these variables may overlap and hence the redundancy is removed using Factor analysis and the overall effect of these factors was determined using multiple linear regression. For the aforesaid purpose data was taken from the website investing.com.

Keywords: Macroeconomic variables, factor analysis, multiple linear regression

INTRODUCTION

Stock market is an arena for investors who invest their money in the stocks of companies and expect capital gains in return. The financially successful companies stocks rise at a steeper rate when compared to their unsuccessful counterparts. A healthier sensex symbolises sound economic status of the country and therefore takes part a crucial role in the development of the country's economy. An investor makes the decision of purchasing of shares based on various factors which are either macroeconomic or firm specific. The importance of macroeconomic variables is such that even government cannot ignore them while framing policies. The variability of stock market is generated by more than one such macroeconomic factor [1]. Therefore, it is important to consider the crucial variables to assess their effect on Stock market returns. Foreign Exchange rates play a vital role in the pricing of stocks; the strengthening of domestic currency induces appreciation in stock values of importing companies and depreciation in stock values of exporting companies. Foreign Intuitional Investments (FII) made by overseas investors is significant in boosting the size of the stock market and on the other hand enhances transparency and improve the standard to international levels [2]. The studies made on relationship of Money supply with stock market prices revealed that the



**Nannaparaju Vasudha**

latter is a key determinant of stock prices. Consumer Price Index is a crucial player in generating stock market volatility and hence need to be considered. It was observed that these macroeconomic variables are interdependent and thus makes it difficult to precisely portray the effect of each variable on stock market movement. The objective of the paper is to remove this overlapping effect by generating orthogonal factors and thus reducing multicollinearity problem.

Literature Survey

[3] in his work deals with the important role of stock market in economic wellbeing of the country and how it is considered to be a crucial measurement of economy of the country. He has taken two macroeconomic variables Gold and crude oil prices to study their relationship with stock indices. Multiple linear regression was employed to estimate the relationship of these variables with KSE 100 index. It was observed that prices of gold have major positive impact on sensex however oil prices impact was negligible. The uncertainty of these macroeconomic variables effect stock market adversely. It was concluded that government should take an initiation to control the prices of these commodities for the betterment of economy. [4] in his paper scrutinized the role of changes in the crude oil prices on fluctuation in the stock market prices. Increase in Oil price raises the cost of imported capital goods hence adversely affecting the profits of firms that trade in sensex. It further enhances prices of general goods thereby increasing inflation. Integration of market economies at international level made global investors more vulnerable to oil prices. Autoregressive distributed lag approach is adopted in this study taking oil price as dependent variable. The results establish the volatility of stock prices generate changes in oil prices.

[5] explores the relation of prices of stock with that of crude oil prices, supply of money, index of industrial production and rate of inflation. Using the Augmented Dickey-Fuller unit root test, Multivariate Cointegration and Vector Error Correction Model technique he concludes that increase of oil price and money supply impact negatively on stock prices however, increase in inflation has slight negative impact. [6] in their study revealed the long term relation between macroeconomic variables and BSE indices. Tools such as Unit Root Test Analysis, Johanson Cointegration Test, and Granger Casualty Test were employed for the study. Their test results have shown the bi-directional relation between stock market indices and Industrial Production, cash reserve ratio, Gross Capital Formation however, Inflation Rate, Gross Domestic Product, Gross Domestic Savings and statutory liquidity ratio has shown a uni-directional relationship with BSE Indices. [7] discusses about the effect of fluctuation of exchange rate on Nifty in his paper. Regression analysis was carried out with independent variables as fluctuation of Indian rupee against US dollar (USD), EURO and POUND. In his article he recognized sectors in Indian stock market responsive to exchange rate and try to establish the correlation between stock price and rate of exchange. Results state that exchange rate of dollar price has most significant effect on Nifty

[8] explored the connection between BSE index and macroeconomic variables for example Index of Industrial Production, rate of inflation, rate of interest, prices of gold, rate of exchange, FII and supply of money in her research paper. Johansen Cointegration, Granger Causality, and the Vector Error Correction mechanism were the statistical tools used for the purpose Results of the paper establishes a long-run causality between Index of Industrial Production, rate of inflation, rate of interest, gold price, rate of exchange, FII and supply of money with BSE index however there is also a short run causality between Inflation and money supply with BSE index. [9] examined the correlation between particular macroeconomic variables and indices representing different sectors at Bombay Stock market. Crude Oil prices, FII and exchange rate are the three macro economic variables used for this purpose in order to establish the affect of macroeconomic variables on indices representing different sectors at Bombay Stock market viz. BSE Auto, BSE Bank, BSE Energy, and BSE IT that represents various sectors of economy. Multiple regression analysis, a statistical technique was used to establish the relation. A significant correlation was observed for all the macroeconomic variables with the BSE indices. Different macroeconomic variables had diverse effect on indices however FII was the only variable that is affecting all sectoral indices in BSE.

[10] the study was intended to ascertain the influence of macroeconomic variables on CNX Nifty. Factor Analysis in SPSS was used for the purpose. He concludes that sensex is highly responsive to macroeconomic variables. To ensure





Nannaparaju Vasudha

economic stability the government must make policies that help in stabilizing fluctuations of macroeconomic variables. [11] in her paper found that most of the investors, financial analysts and fund managers assess the trend of equity market for resource allocation using macroeconomic variables such as rate of foreign exchange, industrial growth rate, trade balance, inflation rate, FII, price of gold, price of crude oil, supply of money and foreign direct investments. It was concluded that the sensitivity of the equity market of India very high to the variables of macro environment and therefore performance of the equity market indirectly effects the Industrial growth. Stability of these variables is crucial to enhance the stock market performance and efficient utilization of resources.

Data collection

Monthly data from January 2006 to December 2020 of various macroeconomic variables is collected from the website "investing.com". To analyse effect of these variables on sensx monthly average data of "BSE sensx" is collected from the same website. The collected data covers variables of all areas of the economy to assess their influence on sensx. The details of the macroeconomic variables are given in Table-1

METHODOLOGY

Collected data is correlated using Karl Pearson's coefficient of correlation. From correlation matrix in Table-2 it is observed that most of the variables are moderate to high correlated, they have been highlighted in bold. Factor Analysis is a statistical technique used for dimension reduction of variables which are considered to be linear combination of underlying factors.

Principal Component Analysis

The purpose of Principal component analysis is to account for the utmost portion of the variance with a minimum number of latest or composite variables called principal components. If X_1, X_2, \dots, X_k are variables required to represent the complete economy by removing overlapping the same can be accounted by small number p of the principal components. Replacing the initial k variables with p principal components the original data set consisting of n measurements of k variables thus reduces to a information set consisting of n measurements of p principal components. Algebraically principal components represent linear combination of k variables X_1, X_2, \dots, X_k and a new coordinate system obtained by rotating the original system with X_1, X_2, \dots, X_k as the coordinate axes geometrically. The new axes represent the direction of maximum variability that gives rise to simple and precise covariances.

If $X^t = [X_1, X_2, \dots, X_k]$ stands for transformed covariance matrix, then $\lambda_1 \geq \lambda_2 \geq \dots \geq \lambda_k \geq 0$ are its eigenvalues.

The principal components are generated using the linear combinations

$$Y_1 = a_1^t X = a_{11}X_1 + a_{12}X_2 + \dots + a_{1k}X_k$$

$$Y_2 = a_2^t X = a_{21}X_1 + a_{22}X_2 + \dots + a_{2k}X_k$$

$$Y_k = a_k^t X = a_{k1}X_1 + a_{k2}X_2 + \dots + a_{kk}X_k$$

$$\text{Then } Var(Y_i) = a_i^t \sum a_i \quad \text{for } i = 1, 2, \dots, k$$

$$\text{and } Cov(Y_i, Y_j) = a_i^t \sum a_j \quad \text{for } i, j = 1, 2, \dots, k$$

The uncorrelated linear combinations of Y_1, Y_2, \dots, Y_k generate principal components with largest possible variances.

RESULTS AND CONCLUSIONS

The redundancy can be reduced by transforming these variables to orthogonal factors. Elimination of redundant (highly correlated) variables from any information is done by using a statistical technique called data reduction. The process replaces the complete file with few uncorrelated variables. Applying factor analysis using SPSS software of 23 version to reduce the above data. Initially the data was tested for the suitability of factor analysis using KMO and Bartlett's Test. From Table-3 it is observed that KMO >0.6 is reasonable and acceptable value. Sig. <0.001 for Bartlett's test indicates the correlation matrix is significantly different from identity matrix which is consistent that the matrix is factorable. Principal Component analysis using Varimax method is applied for data reduction.





Nannaparaju Vasudha

Each variable variance in extraction of communalities is measurements of their contributions to the components. Very high extraction values in Table-4 are indicating extracted components represent variables very well. From Table-5 four factors are extracted whose eigen values amount to 84% of variability of the original seventeen variables with only 16% of information loss. The cumulative percentage of variation is well preserved by rotation however; the spread of variation is distributed evenly over the components. Scree plot graphically represent the components and their corresponding eigen values. The components with eigen values greater than 1 are the ones with maximum variance. Multi-collinearity between seventeen variables has been successfully removed by reducing them into four factors as shown below. The above table (Table-7) is a representation of orthogonal factor representation of seventeen variables. Factor-1 is labelled as Inflation, Factor-2 as Banking System, Factor-3 as Trade and Foreign Investment as Factor-4. These factors include 84% of variance in them. While deriving the factors these factor scores are provided by SPSS. To further confirm the linear correlation between the components is 0, the plotted component scores depict non-correlation between the components.

In Figure-2 the second plot in the first row shows the first component on the vertical axis versus the second component on the horizontal axis, and therefore the order of the remaining plots follows from there. The above figure establishes that the variables have been reduced to four orthogonal factors. To assess the impact of these variables we use multiple linear regression of the factor scores on "BSE sensex" using SPSS software. From the above table (Table-8) we have significant F-static F (154.056, 4) and very high value of R Square (0.946) indicating the model is best fitting to the data. In the regression analysis the R- square value is a measure of total impact of independent variables on dependent variable. Therefore there is a total of 94.6% impact of these factors on BSE sensex. It is observed that factor-1; inflation has the largest impact on macroeconomic variables followed by factor-2, banking system. However, these factors have negative impact on 'BSE sensex' on the other hand factors 3 and 4; Trade and Foreign Investments have positive impact.

REFERENCES

1. Bodla and Amita, Impact of macroeconomic factors on stock market return - a case study of india, GGGI Management Review. 7(1)(2017) 1-8.
2. Sandeep Kapoor And Rocky Sachan, Impact of FDI & FII on Indian Stock Markets, International Journal of Research in Finance and Marketing. 5(4) (2105) 9-17.
3. Urooj Aijaz, Muhammad Faisal and Saad Meraj, Impact of Oil and Gold Prices on stock Market index, Journal of Business Strategies, 10(2) (2016) 69-84.
4. Krishna Reddy Chittedi, Do Oil Prices Matters for Indian Stock Markets? An Empirical Analysis, Journal of Applied Economics and Business Research JAEBR. 2(1)(2012) 2-10.
5. Seyed Mehdi Hosseini, Zamri Ahmad, Yew Wah Lai, The Role of Macroeconomic Variables on Stock Market Index in China and India, International Journal of Economics and Finance. 3(6) (2011) 233-243.
6. P. Arun Prakash and V. Sindhu, A Study on Causality and Long Run Association between BSE Indices and Macroeconomic Indicators, IJARIE.3(6)(2017) 765-773.
7. Rakesh D , J K Raju , Basavangowda K G, An Impact of Currency Fluctuations on Indian Stock Market, IJAIE. 5(6)(2016)146-151.
8. Pooja Misra, An Investigation of the Macroeconomic Factors Affecting the Indian Stock Market, Australasian Accounting, Business and Finance Journal.12(2)(2018) 71-86.
9. V.N. Sailaja, An empirical study on impact of macro variables on sectoral indices in india, International Journal of Civil Engineering and Technology (IJCIET). 9(3)(2018) 383-393.
10. Rakesh Kumar, The Effect of Macroeconomic Factors on Indian Stock Market Performance: A Factor Analysis Approach, IOSR Journal of Economics and Finance (IOSR-JEF).1(3)(2013) 14-2.
11. P. Karthika and P. Karthikeyan, Nexus between Stock Price Volatility and Selected Macroeconomic Variables: Evidence from Nifty 50, International Journal of Latest Engineering and Management Research (IJLEMR). 2(7)(2017) 46-53.





Nannaparaju Vasudha

Table 1: Macroeconomic Variables

Macroeconomic Variables	Abbreviation	Units of Measurements
Trade Balance	TB	In Billion INR
Federal Fiscal Deficit	FD	In billion USD
Bank Loan Growth	LG	In %
Foreign Reserves	FR	In billion USD
Cumulative Industrial Production	IP	In %
Crude oil prices	COP	INR per barrel
Foreign Institutional Investment(Equity+debt)	FII	In crore INR
Foreign Exchange	FE	In INR
Wholesale Price Index	WPI	In %
Interest Rate Decision	IR	In %
Reverse REPO rate	RRR	In %
Consumer Price Index	CPI	In %
Gold price	GP	In INR per gram
Imports	I	In billion USD
Deposit Growth	DG	In %
Exports	E	In billion USD
Money Supply M ₃	MS	In %

Table 2: Correlations

	TB	FD	LG	FR	IP	COP	FII	FE	WPI	IR	RRR	CPI	GP	I	DG	E	MS
TB	1	-.223**	.338**	-.289**	-.054	-.550**	-.050	-.276**	-.114	-.189*	-.323**	.344**	-.330**	-.779**	.106	-.578**	.412**
FD		1	-.647**	.731**	-.542**	.094	.061	.727**	-.344**	-.334**	-.045	-.082	.697**	.435**	-.372**	.558**	-.597**
LG			1	-.817**	.547**	-.039	-.093	-.821**	.605**	.389**	.131	.509**	-.788**	-.538**	.581**	-.633**	.788**
FR				1	-.649**	.027	.024	.815**	-.460**	-.356**	-.142	-.374**	.901**	.546**	-.621**	.643**	-.669**
IP					1	-.015	-.094	-.602**	.418**	.264**	.084	-.162	-.459**	-.177*	.101	-.336**	.361**
COP						1	.099	.061	.382**	.457**	.577**	.541**	.026	.706**	.453**	.652**	-.115
FII							1	-.053	.003	.007	.041	-.020	.099	.127	.147	.117	-.022
FE								1	-.615**	-.284**	.046	-.520**	.870**	.500**	-.750**	.632**	-.859**
WPI									1	.312**	.186*	.469**	-.537**	.037	.556**	-.099	.458**
IR										1	.897**	.409**	-.318**	.171	.596**	.103	.205*
RRR											1	.277*	-.023	.443**	.513**	.425**	-.173*
CPI												1	-.661**	-.143	.591**	.033	.717**
GP													1	.562**	-.789**	.661**	-.792**
I														1	.105	.922**	-.621**
DG															1	.035	.659**
E																1	-.703**
MS																	1

** Correlation is significant at the 0.01 level (2-tailed)

Table 3: KMO and Bartlett's Test

KMO and Bartlett's Test

Kaiser-Meyer-Olkin Measure of Sampling Adequacy.	.712
Bartlett's Test of Sphericity	Approx. Chi-Square
	914.087
	df
	136
	Sig.
	.000





Nannaparaju Vasudha

Table 4: Communalities

	Initial	Extraction
TB	1.000	.768
FD	1.000	.662
LG	1.000	.859
FR	1.000	.941
IP	1.000	.869
COP	1.000	.700
FII	1.000	.893
FE	1.000	.812
WPI	1.000	.836
IR	1.000	.937
RRR	1.000	.930
CPI	1.000	.826
GP	1.000	.947
I	1.000	.871
DG	1.000	.814
E	1.000	.834
MS	1.000	.873

Table 5: Extracted and Rotated Factors

Component	Extraction Sums of Squared Loadings			Rotation Sums of Squared Loadings		
	Total	% of Variance	Cumulative %	Total	% of Variance	Cumulative %
1	7.711	45.359	45.359	5.298	31.162	31.162
2	2.970	17.468	62.827	4.673	27.489	58.651
3	2.476	14.565	77.392	3.075	18.089	76.740
4	1.216	7.152	84.544	1.327	7.805	84.544

Table 6: Rotated Component Matrix

	Component			
	1	2	3	4
TB	.568	-.036	-.665	.043
FD	-.139	-.797	.089	.023
LG	.739	.432	.294	-.200
FR	-.403	-.882	.024	.002
IP	-.003	.753	.267	-.479
COP	.435	.271	.632	.194
FII	.066	-.011	.141	.932
FE	-.743	-.503	-.072	.043
WPI	.715	.089	.532	-.180
IR	.292	.911	.069	.132
RRR	.129	.934	.200	.030
CPI	.901	.058	.003	.108
GP	-.730	-.592	.222	.120
I	-.049	.011	.931	-.051
DG	.824	.310	-.062	.187
E	.143	.000	.889	.149
MS	.917	.139	.058	.096





Nannaparaju Vasudha

Table 7

Factor	Variables	Name Assigned to the Factor
Factor-1	LG, FE, WPI, CPI, GP, DG, MS	Inflation
Factor-2	FD, FR, IP, IR, RRR	Banking System
Factor-3	TB, COP, I, E	Trade
Factor-4	FII	Foreign Investments

Table 8

Impact of Factors on BSE sensx

	Model		
	1		
	Regression	Residual	Total
Sum of Squares	209174887.564	12220059.171	221394946.736
df	4	36	40
Mean Square	52293721.891	339446.088	
F	154.056		
Sig.	.000		
R	.972		
R Square	.946		
Adjusted R Square	.940		

Table 9

Coefficients^a

Model	Unstandardized Coefficients		Standardized Coefficients	t	Sig.	Correlations			Collinearity Statistics	
	B	Std. Error	Beta			Zero-order	Partial	Part	Tolerance	VIF
1 (Constant)	29285.451	304.408		96.205	.000					
REGR factor score 1 for analysis 1	-5389.779	308.190	-.679	17.489	.000	-.679	-.946	-.679	1.000	1.000
REGR factor score 2 for analysis 1	-5072.508	308.190	-.639	16.459	.000	-.639	-.940	-.639	1.000	1.000
REGR factor score 3 for analysis 1	1799.182	308.190	.227	5.838	.000	.227	.697	.227	1.000	1.000
REGR factor score 4 for analysis 1	1219.374	308.190	.154	3.957	.000	.154	.551	.154	1.000	1.000

a. Dependent Variable: BSE Sensx 30





Nannaparaju Vasudha

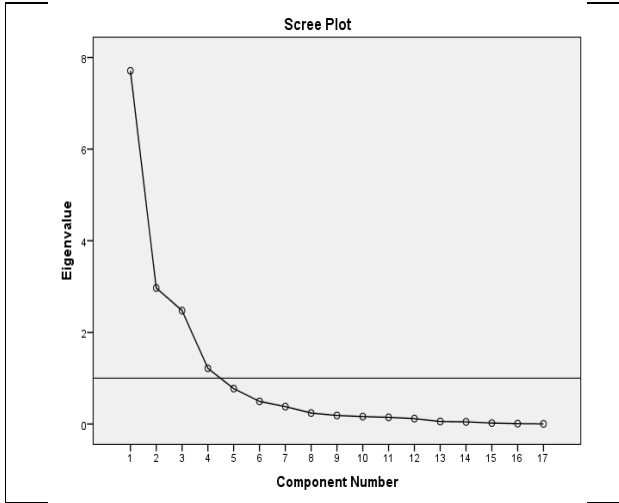


Figure-1

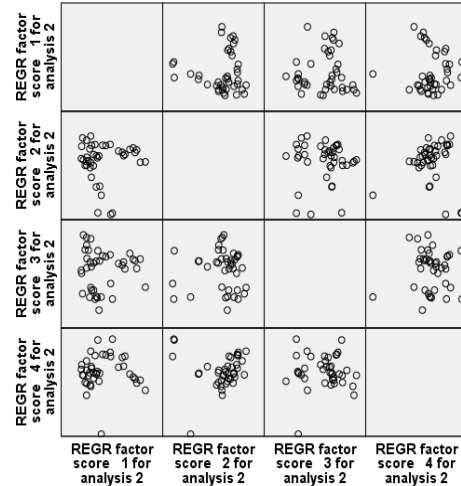


Figure-2





Effect of Upper Cervical Spine Mobilization on Forward Head Posture

P.Nareshbabu^{1*}, Anandh Vaiyapuri², Arunachalam. R³ and Franklin Shaju⁴

¹Ph.D. Scholar, Madhav University, Rajasthan, Assistant Professor, Shree Venkateshwara College of Paramedical Sciences, **Gobichettipalayam, Erode (DT), Tamil Nadu, India**

²Professor, Madhav University, Rajasthan. India.

³Principal, Madhav College of Physiotherapy, Madhav University, Rajasthan. India.

⁴Principal, RVS College of Physiotherapy, Coimbatore, Tamil Nadu, India

Received: 23 Oct 2021

Revised: 28 Nov 2021

Accepted: 11 Jan 2022

*Address for Correspondence

P.Nareshbabu

Ph.D. Scholar, Madhav University, Rajasthan, Assistant Professor,
Shree Venkateshwara College of Paramedical Sciences,
Gobichettipalayam, Erode (DT), Tamil Nadu, India
Email: naruphysio4@gmail.com



This is an Open Access Journal / article distributed under the terms of the **Creative Commons Attribution License** (CC BY-NC-ND 3.0) which permits unrestricted use, distribution, and reproduction in any medium, provided the original work is properly cited. All rights reserved.

ABSTRACT

Forward head posture (FHP) is one of the most common cervical abnormalities that predispose individuals toward pathological conditions, such as headache, neck pain, temporo mandibular disorders, vertebral bodies disorders, soft-tissue length and strength alteration or even scapula and shoulder dyskinesia. Cervical spine mobilization are widely used to treat forward head posture. This study was an attempt to find the effects of upper cervical spine mobilization on pain and craniovertebral angle among forward head posture patients. Five forward head posture patients were selected based on inclusion & exclusion criteria. The age between 25 to 30 were selected for the study. They were treated by upper cervical spine mobilization for a period of 6weeks 1session per day. Neck pain and craniovertebral angle were measured before and after 6 weeks of intervention by numerical pain rating scale and goniometry respectively. The calculated paired 't' value for neck pain and craniovertebral angle are 4.75 and 3.62. Hence calculated 't' value is more than table 't' value at 0.005 level, there is significant difference in the scores of neck pain and craniovertebral angle following upper cervical spine mobilization. Upper cervical spine mobilization is effective in reducing neck pain and increasing craniovertebral angle in forward head posture patients. Craniovertebral angle correlated negatively with numerical pain rating scale scores. This study suggested that decreased craniovertebral angle were predictive factors for the occurrence of pain in the cervical region.

Keywords: Forward head posture, Upper cervical spine mobilization, Craniovertebral angle, Numerical pain rating scale, Goniometry



**Nareshbabu et al.,**

INTRODUCTION

Neck disorders are common [1] and forward head posture (FHP) is one of the most common cervical abnormalities that predisposes individuals toward pathological conditions, such as headache[2], neck pain[3], temporomandibular disorders[4], vertebral bodies disorders[5], soft-tissue length and strength alteration[6] or even scapula and shoulder dyskinesia [7]. Neck disorders are common among all the age group. A review of different observational studies of neck pain around the world showed that its 1-year prevalence ranged from 16.7 to 75.1 percent for the entire adult population (aged 17– 70 years) with a mean of 37.2 percent [8]. Forward head posture is a postural problem that is caused by several factors including sleeping with the head elevated too high, extended use of computers, laptops & cell phones, prolonged use of facemask, lack of back muscle strength and lack of nutrients. Early diagnosis of forward head posture will help to minimize the consequences [9]. The purpose of the study is to find the effect of upper cervical spine mobilization on pain and craniovertebral angle among forward head posture patients.

METHODOLOGY

Review board of Shree Venkateshwaraa College of Physiotherapy, Gobichettipalayam has approved this two outcome variable pre and post-test experimental study and a written consent was obtained from the participants after giving clear instructions regarding the treatment procedure and its implications. The study was conducted in Shree Venkateswara College of Physiotherapy outpatient department, Erode, Tamilnadu, India. Clinically diagnosed 5 forward head posture patients age between 25-30 were selected for this study. All the 5 subjects received upper cervical spine mobilization. The upper cervical spine mobilization includes upper cervical spine flexion mobilization and C5 central posterior-anterior mobilization. In upper cervical spine flexion mobilization the patients were made to lie in supine position, while the therapist kept one hand over the occipital bone, exerting traction force, and placed the other on the frontal region of the subject's head and applied caudal pressure. The procedure was applied at a slow rate, 2 seconds per oscillation this was continued for 10 minutes. In C5 central posterior-anterior mobilization the patients were made to lie in prone position, with neutral cervical spine position. The therapist placed the tips of his thumbs on the posterior surface of the C5 spinous process while the other fingers were gently rested around the patient neck. The oscillations were conducted in the third grade of the Maitland scale at the frequency of 2 oscillations per second and performed for 9 minutes, divided into 3 sets of 3 minutes, with a 1-minute interval. The pain and craniovertebral angle was measured in all the subjects by numerical pain rating scale & universal goniometer before and after 6 weeks of intervention.

Data Analysis and Results

The study aims to find the effects of upper cervical spine mobilization on pain and craniovertebral angle among forward head posture patients. The calculated paired 't' value for pain is 4.75 and it is more than 't' table value at 0.005 level. Hence there is significant difference between pre & post test values of pain following upper cervical mobilization in forward head posture patients. The calculated paired 't' value for craniovertebral angle is 3.62 and it is more than 't' table value at 0.005 level. Hence there is significant difference between pre & post test values of craniovertebral angle following upper cervical mobilization in forward head posture patients.

DISCUSSION

The present study shows that 6 weeks of the upper cervical spine mobilization is effective in reducing pain and increasing craniovertebral angle in patients with forward head posture. Forward head posture occurs due to compressive loading on tissues in the cervical spine, particularly on the facet joints and ligaments. It was found in forward head posture that the posterior cervical muscles of semispinalis cervicis and over action with ultimate





Nareshbabu et al.,

tightening of semispinalis capitis. The corresponding weakness of the flexor muscles in front namely, longus cervicis and longus capitis [10]. Finally, nociceptive impulses from the upper cervical spine cause reflex contractions in sternocleidomastoid muscles, which can contribute to the development of FHP symptoms. Thus, joint mobilization toward the upper cervical region appears to reduce muscular reflex contraction and allow muscle relaxation, especially in cervical region muscles, and may consequently increase craniovertebral angle [11].

CONCLUSION

This study concluded that 6 weeks of upper cervical spine mobilization reduces the pain and increased craniovertebral angle significantly in forward head posture patients.

REFERENCES

1. Hoving JL, De Vet HC, Twisk JW, Deville WL, Van der Windt D, Koes BW, Bouter LM. Prognostic factors for neck pain in general practice. *Pain*. 2004;110(3):639-45.
2. Treleaven J, Jull G, Atkinson L. Cervical musculoskeletal dysfunction in postconcussional headache. *Cephalalgia*, 1994; 14(4): 273–79.
3. Haughie LJ, Fiebert IM, Roach KE. Relationship of forward head posture and cervical backward bending to neck pain. *J Man ManipTher.*, 1995; 3(3): 91–97.
4. Lee WY, Okeson JP, Lindroth J. The relationship between forward head posture and temporomandibular disorders. *J Orofac Pain*, 1995; 9(2): 161–67.
5. Bonney RA, Corlett EN. Head posture and loading of the cervical spine. *Appl Ergon.*, 2002; 33(5): 415–17.
6. Broer MR, Zernicke RF. Efficiency of human movement. 4th edition, Philadelphia (PA): W. B. Saunders; 1979.
7. Kebaetse M, McClure P, Pratt NA. Thoracic position effect on shoulder range of motion, strength, and three-dimensional scapular kinematics. *Arch Phys Med Rehabil.*, 1999; 80(8): 945– 50.
8. Lee WY, Okeson JP, Lindroth J. The relationship between forward head posture and temporomandibular disorders. *J Orofac Pain*. 1995;9(2):161–67.
9. Edmondston SJ, Wallumrød ME, MacLéid F, Kvamme LS, Joeleges S, Brabham GC. Reliability of isometric muscle endurance tests in subjects with postural neck pain. *Journal of Manipulative & Physiological Therapeutics*. 2008 Jun 1;31(5):348-54.
10. ↑ Jump up to:5.05.1 Burt HA, effect of faulty posture;president'saddress.Proc R Soc Med. 1950; 43(3):187–194. Accessed 26 February 2019.
11. Leandri M, Gottlieb A, Cruccu G. Head extensor reflex evoked by trigeminal stimulation in humans. *Clin Neurophysiol*.2001;112:1828-32.

Table 1: Mean value, Mean Difference and Paired 't' value of Pain.

Group-A	Mean	Mean difference	SD	Paired't' value
Pre test mean	7	4.2	1.923	4.75
Post test mean	2.8			

Table 2: Mean value, Mean Difference and Paired 't' value of craniovertebral angle.

Group-A	Mean	Mean difference	SD	Paired 't' value
Pre test mean	20	21	12.94	3.62
Post test mean	41			





Nareshbabu et al.,

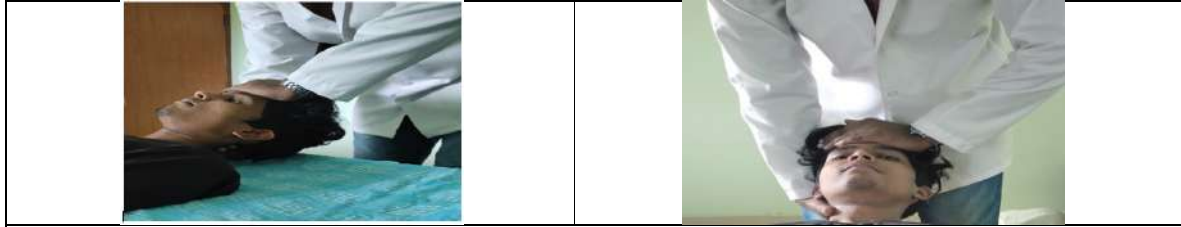


Figure :1 & 2 Upper cervical spine flexion mobilization

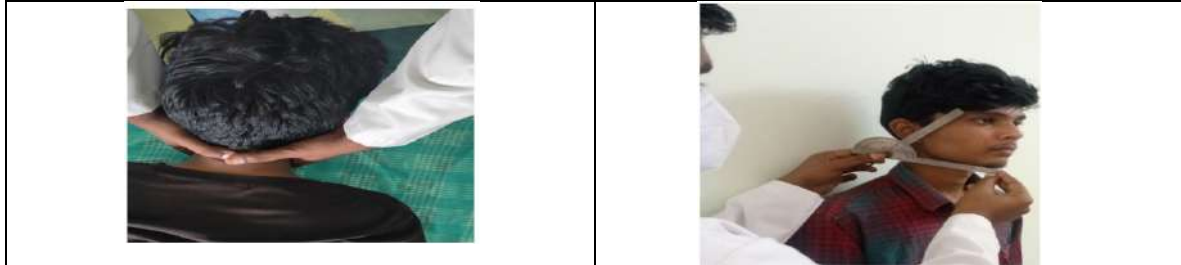


Figure: 3 C5 central posterior-anterior mobilizations

Figure: 4 Craniocervical angle measurements





Demographic Analysis of Patients with Cervical Cancer in Tamilnadu (India)

Juveriyah Kausar¹, Sivasamy Ramasamy^{2*}, Agaath Hedina Manikkam¹ and Minu Jenifer Michael¹

¹Molecular Genetics and Cancer Biology Laboratory, Department of Human Genetics and Molecular Biology, Bharathiar University, Coimbatore - 641046, Tamil Nadu, India.

²Assistant Professor, Molecular Genetics and Cancer Biology Laboratory, Department of Human Genetics and Molecular Biology, Bharathiar University, Coimbatore - 641046, Tamil Nadu, India.

Received: 29 Oct 2021

Revised: 19 Dec 2021

Accepted: 13 Jan 2022

*Address for Correspondence

R. Sivasamy,

Assistant Professor,

Molecular genetics and Cancer Biology Laboratory,

Department of Human Genetics and Molecular Biology,

Bharathiar University, Coimbatore- 641 046. TamilNadu, India.

Email: rshgmb@buc.edu.in



This is an Open Access Journal / article distributed under the terms of the **Creative Commons Attribution License** (CC BY-NC-ND 3.0) which permits unrestricted use, distribution, and reproduction in any medium, provided the original work is properly cited. All rights reserved.

ABSTRACT

Cervical cancer is more prevalent among women in India (6-29%) and so the objective of our study is to evaluate the role of various factors like age, geographical location, tobacco and betel nut consumption, age of marriage and number of pregnancies, status of immune system and *Chlamydia* infection in cervical cancer patients in Tamilnadu. About 400 cervical cancer patients who visited various hospitals in and around Coimbatore within the 6 months (Nov-2015 to April-2016) volunteered for this study. 400 age and location matched volunteers were chosen for the control group. Questionnaire was used to collect data and the data collected from the patient and control group were categorized according to age. The significance were statistically verified using the Pearson Chi-square test and multiple regression analysis. The factors under study were analyzed and compared between the test and control group. High prevalence in found in patients with 50-60yrs of age. About 39% are from Erode district and 28% were from Namakkal district. 42.5% belonging to 50-60yrs were found to have the habit of tobacco and betel nut consumption. Among the various groups, 73% were married at an early age and 75% have more than 3 children. 77% of test group have compromised immune system and 67% have tested positive for *Chlamydia* infection. Among the cancers in women, cervical cancer is more prevalent. The factors (age, geographical location, tobacco and betel nut consumption, age of marriage and number of pregnancies, status of immune system and *Chlamydia* infection) studied were found to correlate with the already existing studies in other population. These factors are the ones that can be controlled if proper measures are taken. This can be achieved if proper awareness is provided to the public. When this awareness becomes effective, the prevalence of cervical cancer in Tamilnadu can be brought under control and to an extent can be made extinct.



**Juveriyah Kausar et al.,****Keywords:** *Chlamydia*, immunocompromised, tobacco, betelnut

INTRODUCTION

Cervical cancer (CC) is defined to be the cancer arising in the cells lining the cervix, which is the lower part of the uterus and is commonly known as uterine cervix [1]. Cervical carcinoma is the second leading cause of death worldwide [2]. According to the GLOBACAN data of 2018, approximately 5,70,000 women developed cervical cancer and 3,11,000 of them died in 2018 globally [3]. Jacob et al., reported that approximately 1,20,000 women develop cervical cancer annually in India [4]. The annual world-wide incidence of cervical cancer is 5,10,000 with an annual mortality of 2,88,000 as per the data of World Health Organization[5]. In India the incidence and mortality rates are 27 and 15 per 1,00,000 women respectively [6]. CC is more prevalent in the rural areas of tamilnadu and it is the second most commonly occurring cancer among women [7].

The peak age of cervical cancer incidence in India was reported to be between 55 and 59 by GLOBACAN in 2014 [8]. The incidence and mortality rates of cervical cancer are found to be extremely high in rural areas where education level is poor. The north-eastern districts of Tamilnadu have high proportion of rural population where the incidence of CC is high [9]. Cervical cancer patients in the lower socioeconomic areas have higher rates of late-stage of cancer diagnosis and thus lower chances of cancer survival [10]. Immunocompromised populations are at an increased risk of HPV associated cancers. HIV positive females form a large part in the immunocompromised population as the immune system is highly suppressed. Such patients are also at an increased risk of having auto-immune diseases. Chronic infections and malnutrition paves the way for increased risk of HPV associated disease in immunocompromised patients [11]. Cervical cancer is found at high rates in HIV positive women than in the general population because it is an AID defining illness [12]. HIV infected women are 2 to 5 times more likely evidenced to acquire cervical cancer compared to HIV-uninfected women [13]. The strength of association between HIV and HPV diminishes the immune status and make patients more prone to cervical cancer [14].

Tobacco consumption facilitates cervical cancer development as the traces of tobacco are found in the mucus cell lining of the cervix [15]. Multiparity is a cervical cancer risk factor in HPV positive women [16]. Women with atleast five biological children accounts holds 5.1 fold higher risk of cervical cancer than nulliparous or primiparous women [17]. According to the Centre for Disease Control and Prevention, about half of the sexually transmitted infections are seen in young women between the ages 15 and 24 (Heather et al.,2013)[18] because they have low consistency of antibodies to fight against cervical ectopy [19]. 40 to 50% of women with *Chlamydia trichomatis* are more likely to develop CC in India [20]. Women who delivered their babies before the age of 17 have twice the risk of developing cancer of the cervix compared to the other females [21]

MATERIALS AND METHODS

Subject Recruitment

This study involves two major groups, the test group (patients with cervical cancer) and the control group (patients without cervical cancer). Out of all cancer patients who visited the cancer centers in Tamilnadu during the 6 months (Nov-2015 to April-2016), the cervical cancer patients were chosen for this study which involved 400 cervical cancer volunteers of age 30 and above. The subjects were chosen based on their histopathological diagnosis and age. The control group involved 400 age matched healthy individuals without any history of cervical cancer. The study strictly followed the declaration of Helsinki and the informed consent was obtained from the subjects.

Data Collection and Statistical Analysis

A standard questionnaire was used to collect the required data from the test and control group. The data collected were kept confidential. Earlier, various lifestyle factors were proven to play a major role in cervical cancer progression and so, we have designed a questionnaire that can help in collecting informations like age, their



**Juveriyah Kausar et al.,**

geographical location, use of tobacco and beetle nut chewing, their age of marriage, number of children etc. The details collected were statistically verified using the Pearson Chi-square test and multiple regression analysis. The significance values are calculated and the corresponding graphs are shown.

RESULTS AND DISCUSSION

As many studies have suggested that the cervical cancer is detected in subjects above 30 years of age, we have categorized the collected data based on their age into 5 major groups as 30-40 yrs of age, 40-50 yrs of age, 50-60 yrs of age, 60-70 yrs of age and >70 yrs of age.

Age of Incidence and Location Identification of the Cervical Cancer Patients

The test and control group were analysed and the results show that the majority of cervical cancer patients (54.5%) belong to the age group of 50-60yrs. Since we have age matched the individuals in the control group, the graph shows more individuals in the same age (Graph 1). The statistical testing of the categorical values is found to be significant at $p < .05$ (P value= .00088). About 24.5% belong to the age group of 40-50 yrs and the next highest is 13.5% belonging to the age group of 60-70yrs. This result is much similar to the epidemiology study performed in the Indian cervical cancer patients by Aswathy *et al.*, in 2015[22]. In case of cervical cancer in India, about 15.2% of cervical cancer deaths worldwide is accounted in India [6]. The first factor looked into was the age of incidence which cervical cancer is found to be highly distributed among the group of 50-60 yrs and this result co-relates with the already existing study in Indian population [22]. Although patient with 50-60yrs are found to be at high risk, their symptoms would have started long before. Various factors mentioned above were found to play a major role.

As for the environment, various studies reported the presence of various mutagens in the environment. In view of this, the environment from which each patient come from were taken into consideration. The majority of patients in the study (39%) were from Erode district that has agriculture as its prime occupation and the next majority (28%) were from Namakkal district that is known for its poultry egg production, also known as "egg city". People who involve themselves in agriculture and livestock management are mainly exposed various chemical compounds used in the farm lands as pesticides and insecticides and for the livestock maintenance. It has already been studied that the organochlorine pesticides are found to act as a mutagen in causing cervical cancer in women agricultural workers [23, 24]. Not only those who work in the field are exposed to such chemicals, but also it spreads to a wide area through polluted water [25]. It is advisable to use insecticides and pesticides that are naturally available to avoid such deadly conditions. Environment is found to play a major role in cancer incidence [26, 27] and so the geographical location of the patients under study were noted. Highest number of patients were from Erode District (39%), Namakkal District (28%), Coimbatore District (13%) and few were form Tiruppur District (3%), Dharmapuri District (2%), Salem District (4%), Trichy District (3%) and Krishnagiri District (3%) (Graph 2)

Involvement of Tobacco and Betel Nut Consumption

The next major factor looked into was the consumption of tobacco and betel nut. Effect of tobacco and beetle nut consumption is found to be a high risk for cervical patients with HPV infection [28] and so we examined the use of tobacco and beetle nut among our patients. It is found that in test group, about 42.5% (Graph 3) belonging to the age group of 50-60yrs have the habit of consuming tobacco and beetle nut whereas 12% don't. Statistically the result is found to be significant at $p < .05$ (P value= <0.00001). The patients were found to be using tobacco and beetle nut for about 10-15 years. In case of control group (Graph 4), about 20% belonging to the 50-60 yrs of age consume tobacco and beetle nut and it is found to be statistically insignificant at $p < .05$, (P value= .12292) proving the probability in the involvement of tobacco and betel nut consumption in cervical cancer development [29]. It has been reported that the tobacco and betel nut has more than 70 carcinogens belonging to the chemical classes like aldehydes, metals, aromatic amines, polycyclic aromatic hydrocarbons (PAHs), volatile organic hydrocarbons and N-nitrosamines [30]. All these compounds are very harmful in causing various cancers including cervical cancer. In our study, about 42.5% patients belonging to the 50-60 yrs were found to consume either tobacco or betel nut and in case of control,





about 20% belonging to the 50-60 yrs were found to consume the same. Although, various research insists on the harmful effect of tobacco and betel nut consumption, in this study, we can compare the control and patient group and see there in a slight negativity towards our hypothesis. It is concluded that the tobacco and betel nut act as trigger for cancer only to a certain extent.

Age of Marriage and Number of Pregnancies

Age of marriage and number of pregnancies is the next major concern in cervical cancer prognosis. Studies proved that women who marry at an early age (before 18 yrs) are more prone to develop cervical cancer in their later age [31]. In our study, it has been observed that about 63% of the patient were married at the age of 15-25 years. This might be one of the reasons that the patient developed cervical cancer. Also, the number of pregnancies is another important factor to be looked into in case of cervical cancer. The reason behind this is the fact that the hormonal changes during pregnancy will make the mother more prone to the HPV infection thereby improving the possibility of developing cervical cancer [31]. In this study, about 68% of the patient group were found to have 3-4 childbirth, which is very high when compared to the control group (29%). The age of marriage is one of the major factors known to influence cervical cancer and in our test and control group, we found that about 73% of test group subjects were married at an early age (below 25 yrs) (Graph 5). On the contrary, in the control group, about 29% were married at an early age (below 25 yrs). The results obtained is proved to be statistically significant at $p < .05$ (P value= <0.00001)[32]. In addition, number of pregnancies is also found to influence cervical cancer incidence[33]. Among our test and control group, we identified that in the test group, about 75% have above 3 children and in control group 34% have more than 3 children (Graph 6). This result is found to be statistically significant at $p < .05$ (P value= <0.00001).

Status of the Immune System and Presence of Chlamydia Infection

In case of cancers, active immune system is needed to fight the disease [34,35]. In our test group, about 77% were found to be immunocompromised when compared with the immune system of the control group where only 11% were immunocompromised (Graph 7). The immune status is the next possible factor looked into in the cervical cancer patients. The immune system is very essential in keeping every individual in good health. It has been reported that decrease in the immune activity due to certain genetic or other reasons, the body becomes more prone to infections [35]. In case of cervical cancer, when immunity decreases, HPV infection happens naturally and there is no immune barrier to stop the infection. In our study, the immune status has been studied and it is observed that about 77% of the test group were found to be immunocompromised whereas in case of control group, only 11 were found to be immunocompromised. This shows that the immunity also plays a major role in the progression of cervical cancer. Another factor for the incidence of cervical cancer is found to be the presence of *Chlamydia* infection [36]. *Chlamydia trichomatis* is sexually transmitted bacterial infection found to be associated with the cervical carcinogenesis. Various epidemiological and histological studies confirmed its association with pelvic inflammatory disease and with infertility [37]. This infection is found to be present in women highly prone to HPV infection and so, detecting them early might help in preventing the disease spread. In our study, about 67% subjects test positive for the infection and about 12% control tests positive for the same. This study embarked on determining the factors responsible for causing the cervical cancer in South-Indian population. Most of our study factors are found to show positive relation with previous studies conducted in various cervical cancer populations. In summary, we found that these factors can be limited if proper awareness is provided to the public. Proper usage and disposal of chemicals are to be taught to the agricultural and livestock maintaining people. Also, education on proper sexual intercourse and personal hygiene are to be taught to the general public. When necessary action is taken in regard to eliminating the factors discussed, the incidence and progression of cervical cancer can be reduced to a greater extent and our country can become a better cancer free nation.

Financial Support and Sponsorship

Nil

Conflicts of Interest

There are no conflicts of interest



**Juveriyah Kausar et al.,****REFERENCES**

1. Brinton LA, Hamman RF, Huggins GR, Lehman HF, Levine RS, Mailin K, et al. Sexual and reproductive risk factors for invasive squamous cell cervical cancer. *Journal of the National Cancer Institute*. 1987;79(1):23-30.
2. Torre LA, Siegel RL, Ward EM, Jemal A. Global cancer incidence and mortality rates and trends—An update. *Cancer Epidemiology and Prevention Biomarkers*. 2016; 25(1) :16-27
3. Marc Arbyn, Elisabete Weiderpass, Laia Bruni, Silvia de Sanjose, Mona Saraiya, Jacques Ferlay et al., Estimates of incidence and mortality of cervical cancer in 2018: a worldwide analysis. *The Lancet* .2020;8(2), PE191-E203
4. Jacob M. Information, education & communication: Corner stone for preventing cancer of the cervix. *Indian J Med Res* 2012; 136: 182-4.
5. Sankaranarayanan R, Ferlay J. Worldwide burden of gynecological cancer: The size of the problem. *Best Pract Res Clin ObstetGynaecol*. 2006; 20:207-25.
6. Ferlay J, Shin HR, Bray F et al., Estimates of worldwide burden of cancer in 2008: GLOBOCAN 2008. *Int J Cancer*. 2010.127,2893-917
7. Tamilarasi R, Latha Maheshwari, Raghul Siddharth, Sanjeev. *International Journal of Community Medicine and Public Health*. 2018. Vol 5, No.5
8. World-both sexes estimated incidence by age. 2014 http://www.globocan.iarc.fr/old/age_specific_table_r.asp
9. Swaminathan R, Selvakumaran R, Esmy PO, Saampath P, Ferlay J, Jissa V. Cancer pattern and survival in a rural district in South India. *Cancer Epidemiol* 2009;33:325-31
10. Jissa V, Nea M, Matti H, Pulikottil O, Mary C, Rajaraman S, Richard M, Rengaswami S. Socio Demographic and reproductive risk factors for cervical cancer- A large prospective cohort study from rural India. *Asian Pacific Journal of Cancer Prevention*. 2012;13, 2991-2995
11. Singh GK, Miller BA, Hankey BF, Edwards BK. Persistent area socioeconomic disparities in US incidence of cervical cancer, mortality, stage, and survival, 1975–2000. *Cancer*. 2004;101(5):1051-7.
12. Palefsky JM, Minkoff H, Kalish LA, Levine A, Sacks HS, Garcia P, et al. Cervicovaginal human papillomavirus infection in human immunodeficiency virus-1 (HIV)-positive and high-risk HIV-negative women. *Journal of the National Cancer Institute*. 1999;91(3):226-36.
13. Joshi S, Chandorkar A, Krishnan G et al., Cervical intraepithelial changes & HIV infection in women attending sexually transmitted disease clinics in Pune, India. *Indian J Med Res*. 2001;113:161-9
14. Heard I, Palefsky JM, Kazatchkine MD. The impact of HIV antiviral therapy on human papilloma virus (HPV) infections and HPV-related diseases. *Antiviral therapy*. 2004;9(1):13-22.
15. Palefsky JM, Gillison ML, Strickler HD. HPV vaccines in immunocompromised women and men. *Vaccine*. 2006;24:S140-S6.
16. Muñoz N, Franceschi S, Bosetti C, Moreno V, Herrero R, Smith JS, et al. Role of parity and human papilloma virus in cervical cancer: the IARC multicentric case-control study. *The Lancet*. 2002;359(9312):1093-101
17. Hinkula M, Pukkala E, Kyyrönen P, Laukkanen P, Koskela P, Paavonen J, et al. A population-based study on the risk of cervical cancer and cervical intraepithelial neoplasia among grand multiparous women in Finland. *British journal of cancer*. 2004;90(5):1025-9.
18. Heather Rhea Royer Heather, Susan M. Heidrich, Roger L. Brown. Young Women's representation of Sexually Transmitted Diseases (RoSTD): A Psychometric study. *Res Nurs Health*. 2012; 35(1):15-29
19. Gregson S, Garnett GP. Contrasting gender differentials in HIV-1 prevalence and associated mortality increase in eastern and southern Africa: artefact of data or natural course of epidemics? *Aids*. 2000;14(Supplement 3):S85-S99.
20. Gopalkrishna V, Aggarwal N, Malhotra VL, Koranne RV, Mohan VP, Mittal A, Das BC. Chlamydia trachomatis and human papillomavirus infection in Indian women with sexually transmitted diseases and cervical precancerous and cancerous lesions. *Clinical Microbiology and Infection*. 2000; 6(2):88-93
21. MacPhail C, Williams BG, Campbell C. Relative risk of HIV infection among young men and women in a South African township. *International journal of STD & AIDS*. 2002;13(5):331-42.
22. Sreedevi A, Javed R, Dinesh A. Epidemiology of cervical cancer with special focus on India. *Int J Womens Health*. 2015;7:405-414.





Juveriyah Kausar et al.

23. Mathur V, John PJ, Soni I, Bhatnagar P. Blood levels of organochlorine pesticide residues and risk of reproductive tract cancer among women from Jaipur, India. In Hormonal Carcinogenesis V 2008 (pp. 387-394). Springer, New York, NY

24. Rodríguez ÁG, López MI, Casillas TÁ, León JA, Mahjoub O, Prusty AK. Monitoring of organochlorine pesticides in blood of women with uterine cervix cancer. Environmental Pollution. 2017 Jan 1;220:853-62

25. Naresh C GH, Dipankar SA. Synthetic detergents (surfactants) and organochlorine pesticide signatures in surface water and groundwater of greater Kolkata, India. Journal of Water Resource and Protection. 2009 Oct 16;2009

26. Zhang, F. Ethnicity, Geographic Location, and Cancer. Translational Toxicology and Therapeutics: Windows of Developmental Susceptibility in Reproduction and Cancer, 2017; 317-362.

27. Grimmer G. Environmental carcinogens: polycyclic aromatic hydrocarbons. Crc Press; 2018 Jan 18.

28. Fang JH, Yu XM, Zhang SH, Yang Y. Effect of smoking on high-grade cervical cancer in women on the basis of human papillomavirus infection studies. Journal of cancer research and therapeutics. 2018 Mar 1;14(8):184.

29. Fonseca-Moutinho JA. Smoking and cervical cancer. ISRN obstetrics and gynecology. 2011 Jul 14;2011.

30. Centers for Disease Control and Prevention. How tobacco smoke causes disease: The biology and behavioral basis for smoking-attributable disease: A report of the surgeon general

31. Christopherson WM, Parker JE. Relation of cervical cancer to early marriage and childbearing. New England Journal of Medicine. 1965 Jul 29;273(5):235-9

32. De Graaff J, Stolte LA, Janssens J. Marriage and childbearing in relation to cervical cancer. European Journal of Obstetrics & Gynecology and Reproductive Biology. 1977 Jan 1;7(5):307-12.

33. Brinton LA, Reeves WC, Brenes MM, Herrero R, De Brien RC, Gaitan E, Tenorio F, Garcia M, Rawls WE. Parity as a risk factor for cervical cancer. American Journal of Epidemiology. 1989 Sep 1;130(3):486-96

34. Whiteside TL. Immune suppression in cancer: effects on immune cells, mechanisms and future therapeutic intervention. In Seminars in cancer biology 2006 Feb 1 (Vol. 16, No. 1, pp. 3-15). Academic Press

35. Mehta AM, Mooij M, Branković I, Ouburg S, Morré SA, Jordanova ES. Cervical carcinogenesis and immune response gene polymorphisms: a review. Journal of immunology research. 2017;2017

36. Koskela P, Anttila T, Bjørge T, Brunsvig A, Dillner J, Hakama M, Hakulinen T, Jellum E, Lehtinen M, Lenner P, Luostarinen T. Chlamydia trachomatis infection as a risk factor for invasive cervical cancer. International journal of cancer. 2000 Jan 1;85(1):35-9

37. Zhu H, Shen Z, Luo H, Zhang W, Zhu X. Chlamydia trachomatis infection-associated risk of cervical cancer: a meta-analysis. Medicine. 2016 Mar;95(13)

Appendix II- Regression Analysis Results

REGRESSION ANALYSIS SUMMARY					
OUTPUT- for age distribution					
<i>Regression Statistics</i>					
Multiple R	0.987044215				
R Square	0.974256283				
Adjusted R Square	0.965675044				
Standard Error	15.63913278				
Observations	5				
<i>ANOVA</i>					
	<i>df</i>	<i>SS</i>	<i>MS</i>	<i>F</i>	<i>Significance F</i>
Regression	1	27768.25258	27768.25258	113.5332884	0.001766785
Residual	3	733.7474227	244.5824742		
Total	4	28502			





Juveriyah Kausar et al.,

	Coefficients	Standard Error	t Stat	P-value	Lower 95%	Upper 95%	Lower 95.0%	Upper 95.0%
Intercept	-15.71134021	11.38435315	-1.380081942	0.261424381	-51.94143283	20.51875242	-51.94143283	20.51875242
control	1.196391753	0.11228243	10.65520006	0.001766785	0.839058949	1.553724556	0.839058949	1.553724556
RESIDUAL OUTPUT								
Observation	Predicted affected	Residuals						
1	32.1443299	-15.1443299						
2	80	18						
3	223.5670103	-5.567010309						
4	44.10824742	9.891752577						
5	20.18041237	-7.180412371						

REGRESSION ANALYSIS SUMMARY OUTPUT- for age of marriage								
Regression Statistics								
Multiple R	0.397396759							
R Square	0.157924184							
Adjusted R Square	-0.122767755							
Standard Error	26.64865109							
Observations	5							
ANOVA								
	df	SS	MS	F	Significance F			
Regression	1	399.5481856	399.5481856	0.56262458	0.507671288			
Residual	3	2130.451814	710.1506048					
Total	4	2530						
	Coefficients	Standard Error	t Stat	P-value	Lower 95%	Upper 95%	Lower 95.0%	Upper 95.0%
Intercept	13.105	15.0506	0.8707	0.4479	-	61.003	-	61.003





Juveriyah Kausar et al.,

	29447	3345	47036	68325	34.792 53833	12727	34.792 53833	12727
Control	0.3447 35277	0.45959 6144	0.7500 83049	0.5076 71288	- 1.1179 04773	1.8073 75326	- 1.1179 04773	1.8073 75326
RESIDUAL OUTPUT								
<i>Observation</i>	<i>Predict ed Test</i>	<i>Residua ls</i>						
1	13.794 76502	- 9.79476 5021						
2	13.794 76502	- 3.79476 5021						
3	22.413 14694	40.5868 5306						
4	36.547 29328	- 15.5472 9328						
5	13.450 02974	- 11.4500 2974						

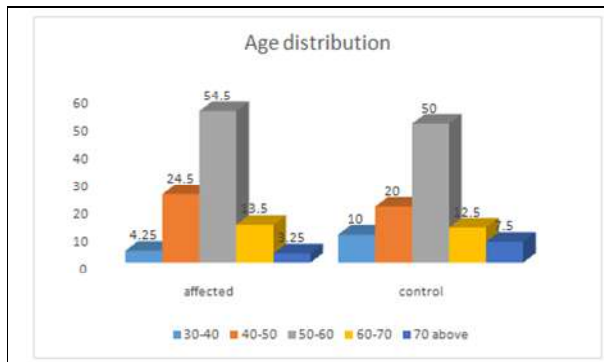
REGRESSION ANALYSIS SUMMARY								
OUTPUT- No.of pregnancies								
<i>Regression Statistics</i>								
Multiple R	0.316889884							
R Square	0.100419199							
Adjusted R Square	-0.3493712							
Standard Error	34.18414049							
Observations	4							
ANOVA								
	<i>df</i>	<i>SS</i>	<i>MS</i>	<i>F</i>	<i>Signific ance F</i>			
Regression	1	260.8890 785	260.889 0785	0.22325 7763	0.68311 0116			
Residual	2	2337.110 922	1168.55 5461					
Total	3	2598						
	<i>Coefficients</i>	<i>Standard Error</i>	<i>t Stat</i>	<i>P-value</i>	<i>Lower 95%</i>	<i>Upper 95%</i>	<i>Lower 95.0%</i>	<i>Upper 95.0%</i>
Intercept	16.65955631	24.57072 281	0.67802 4674	0.56768 243	- 89.0597 3125	122.378 8439	- 89.0597 3125	122.378 8439
Control	0.333617747	0.706066 914	0.47250 1601	0.68311 0116	- 2.70434 2986	3.37157 8481	- 2.70434 2986	3.37157 8481



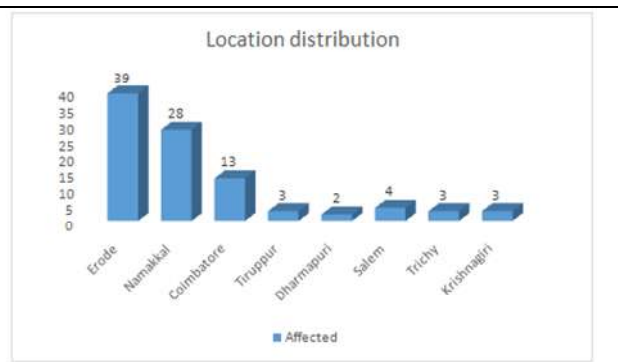


Juveriyah Kausar et al.,

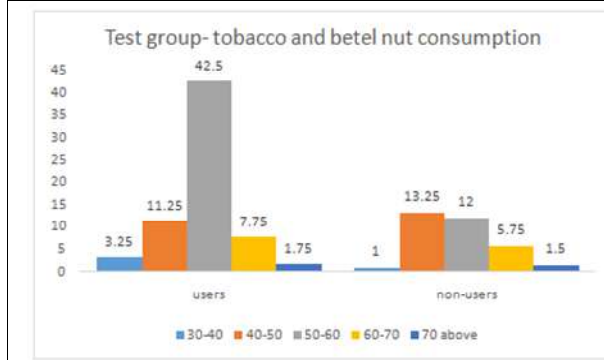
RESIDUAL OUTPUT								
Observation	Predicted Test	Residuals						
1	17.66040956	-12.66040956						
2	37.6774744	-17.6774744						
3	26.33447099	41.66552901						
4	18.32764505	-11.32764505						



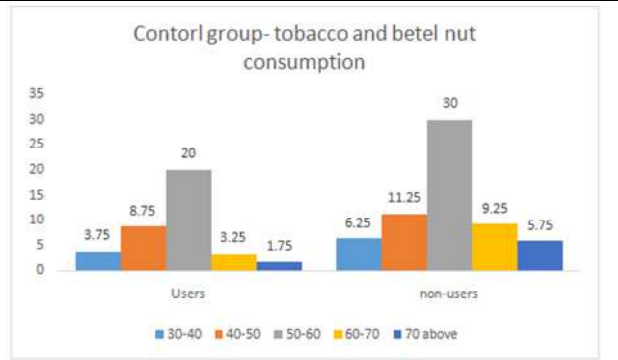
Graph 1: Describing the age distribution of the test and control group in the study



Graph 2: Describing the location distribution of the test group



Graph 3: Showing the users and non-users percentage of tobacco and betel nut among the test group

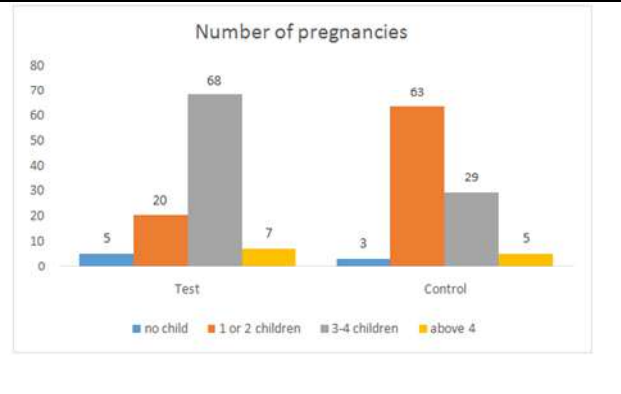
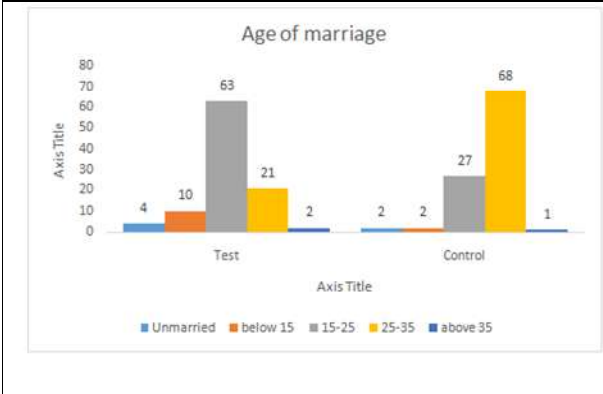


Graph 4: Showing the users and non-users percentage of tobacco and betel nut among the control group



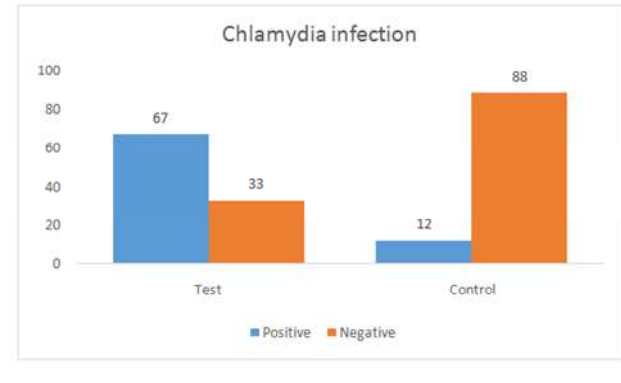
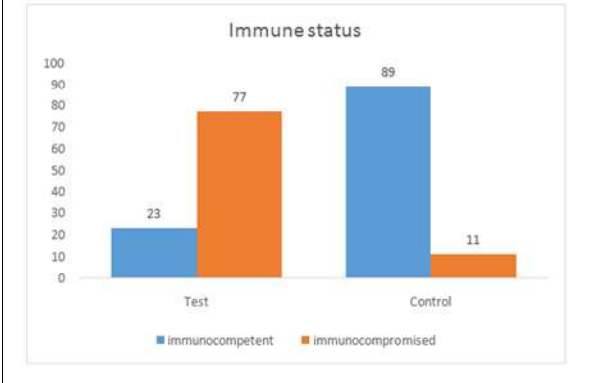


Juveriyah Kausar et al.,



Graph 5: Showing the age of marriage among different age groups in test and control volunteers

Graph 6: Showing the number pf pregnancies among different age group between the test and control volunteers



Graph 7: Showing the immune status of test and control volunteers

Graph 8: Showing the Chlamydia infection status among the test and control volunteers





Solar Powered Arduino Based Automatic Drip Irrigation System for Enhancing Agricultural Productivity

T.Rajesh¹, V.Suma Deepthi¹ and P. Sindhuja^{2*}

¹Department of EEE, Malla Reddy Engineering College, Hyderabad, India.

²PG Scholar, Department of EEE, Malla Reddy Engineering College, Hyderabad, India.

Received: 01 Sep 2021

Revised: 20 Sep 2021

Accepted: 21 Oct 2021

*Address for Correspondence

P. Sindhuja

PG Scholar, Department of EEE,
Malla Reddy Engineering College,
Hyderabad, India.

Email: pskssindhuja@gmail.com



This is an Open Access Journal / article distributed under the terms of the **Creative Commons Attribution License** (CC BY-NC-ND 3.0) which permits unrestricted use, distribution, and reproduction in any medium, provided the original work is properly cited. All rights reserved.

ABSTRACT

The paper proposes to use an automatic irrigation system based on Arduino boards, soil moisture sensors, float switches and solar panels. The automatic irrigation system senses the soil moisture content and automatically switches the solenoid valve. The top water level is monitored by a float switch detector. The power required by the entire system is generated by solar panels. It also automatically controls the water level in the water tank. This system is suitable for all climatic conditions. This project proposes the use of an automatic irrigation system based on an Arduino board, a soil moisture sensor, a float switch and a solar panel. This automatic irrigation system detects the moisture content of the soil and automatically switches solenoid valves, a float switch sensor monitors the overhead water level, and the power required for the entire system is generated by solar panels. It also automatically controls the water level in the water tank. Whenever a valve opens or closes, the Global System for Mobile Communications (GSM) module sends a message. The project fully supports farmers, provides water on demand, deploys renewable energy, minimizes manpower, saves space, reduces costs, and maintains user-friendliness.

Keywords: Solar panel, Automated drip Irrigation system, Arduino board, Soil moisture sensors, float switch.



**Rajesh et al.,**

INTRODUCTION

Irrigation is the process by which water flows through the soil to cultivate dry plants. There are many irrigation methods, and the most important function of irrigation is to provide water for plants. The water should be evenly distributed on the soil, which seems to be good for yield and growth. There are few irrigation methods. Surface irrigation: The surface irrigation method is one of the oldest methods and has been followed by developers for many years. Now it is also imitated by farmers. In this system, there is a small amount of water around the farmland to keep it moist and enter the soil. If it causes the cultivated land to be flooded, it is either a boundary well or fertilizer irrigation. This process is still valid. The water level is controlled by equipment that is usually inserted into the ground and applied, and it is not necessarily defined. Unless it's unavoidable, don't use abbreviations in titles or titles. In most rice fields, the rice fields are sometimes poured to the ground by humans.

Drip Irrigation

Drip Irrigation is also called trickle irrigation. It is a system in which water flows out of the water to all bases. In these systems, water is pumped out of the root zone. This pattern increases the growth of all seeds and plants, and it is the most efficient method of irrigation. In this way the water can be divided into pipes, emitters, pipes and fittings. It is much better than watering it. Figure 1 shows the drainage process.

Sprinkler Irrigation

In this method, the irrigation canal is anchored to the paddy field at different points in the soil and can be circulated by spraying too much water. High -pressure nozzles and nozzle tubes are placed on a moving platform and connected to a source. The spray can be placed on a mobile platform and connected to the water through a hose. The voyage sweepers are a system with automatic moving wheels. When the pipe is injured by the drum carried by the irrigation water, the shower is pulled across the field. When the seeding returns to the roller, the system dies. This type of system is known as an irrigation hose and is used for dust removal, irrigation and sewage treatment.

Solar Energy

Solar energy is renewable. The sun needs energy. Sunlight has an output of large amounts of heat that can be converted into energy and is called solar energy. The light is converted into electricity, with the help of a solar panel or directly shown using voltaic acid (PV), or intense solar energy (PDC). The daytime PDC converts sunlight into electricity, namely through contact lenses or glasses and tracking to absorb large amounts of sunlight from the photoelectric [1-6].

Benefits of solar energy

- a) Photovoltaic systems have less noise.
- b) A small amount of solar energy to the solar panels placed on the roof reduces space.
- c) Solar power is an easy connection service. This reduces interference.
- d) PV generators are available in all sizes to suit the needs of some.

Automatic Irrigation

Automatic irrigation system is very quiet and goes all the way from this system once installed in the culture soil. It can operate on its own and also does not require a permanent human. There are a lot of used losses here that seem really unwieldy. It is difficult to implement. There are three types of automatic categories. Here it is: The advantage of this system is that the operator can till and irrigate well. The microcontroller 8051 is programmed to receive a signal from the sensing material. An op amp, a moving comparator that connects sensors [7-8]. The humidity characteristic is transmitted by the microcontroller. The Fig.3 shows the Automatic Irrigation system



**Rajesh et al.,****Irrigation system based on GSM**

It is difficult for farmers to irrigate due to lack of manpower, expensive labour cost and water shortage. In order to minimize this problem, a new system using GSM technology was developed. In the GSM-based automatic irrigation system, we use the GSM module to identify the operation of the cultivated land through SMS [9-11]. Fig.5 shows the Irrigation system based on GSM

PROBLEM DESCRIPTION

The energy of the sun is absorbed by the solar system. Solar models use the light energy of the sun's rays (sunlight) to generate electricity through solar products. Solar panels are used in our thesis. Drip irrigation is one of the irrigation methods to control the flow of water, which is applied directly to the roots of many plants. Water dripping from the surface of the roots helps to reduce soil erosion, provides even water flow and reduces water contamination. Drip irrigation is a big part of our project. Hussein and Li Xue [6] investigated the drip irrigation system. In the current situation, drip irrigation systems are being used to improve water utilization. It sucks in groundwater. Manual operating system. It helps our farmers. This generation uses drip irrigation because the water level is very low. So farmers use drip irrigation systems. But farmers with low incomes are spending more water. So it will help small farmers and reduce water waste. C. Automation The technology that allows a device, process or system to operate an automated system is called automation.

The current irrigation system has some shortcomings, that is, soil erosion, water instability, water interference, and interference with the inspection of plants and water levels in the reservoir are required. To overcome these problems, the system is not used in conjunction with drip irrigation or irrigation. It is also an automatic generator to fill the water tank.

METHODOLOGY AND OPERATION OF PROPOSED METHOD**Sensor-Based Valve Operating System**

Sensors are devices that detect changes in the environment and send information to the processor. Different types of sensors are commonly used in different applications. All these sensors are used to measure one of the physical properties such as temperature, resistance, capacitance and heat transfer. The different types of sensors are listed below.

Temperature Sensor

- Proximity Sensor
- IR Sensor (Infrared Sensor) Pressure Sensor
- Light Sensor
- Ultrasonic Sensor
- Smoke, Gas and Alcohol Sensor
- Touch Sensor
- Humidity Sensor
- Flow and Level Sensor

Soil moisture sensor

The soil humidity sensor is a type of humidity sensor. Soil moisture sensors are used to indirectly measure the moisture present in the soil by measuring the condition of the soil. The soil moisture sensor has two probes. Both are used to measure the amount of water in it. The two probes allow water to pass through the soil, and then obtain the resistance value depending on the type of soil to measure the water content. The earth has more water; the earth carries more electricity and reduces resistance, so the water level is higher. Dry soils are low in water content and electrical inequality. The sensor works according to this principle for ground moisture. C. Solenoid Valve Solenoid valve is often used to control the flow of fluid through electricity. The solenoid valve operates after power or exercise or is also known as a cut-off that allows fluid to flow. The actuator is an electromagnet. When the suitcase is powered, the magnetic field pulls the plunger toward the spring. Similarly, when the power goes out, the plunger will return to its original position under spring operation.



**Rajesh et al.,**

They are available in five types

- Pilot valve
- Direct valve
- 2-way valve
- 3-way valve
- 4-way valve

Arduino UNO

Arduino UNO board is an open-source microcontroller board based on Microchip ATmega328P microcontroller, developed by Arduino.cc. The board includes analog and digital input/output pins for connecting various boards and other circuits [12-13].

Automatic Tank Water Flow System

A Float switch is a type of water level meter, a machine that detects the water level in the tank. The button can be used to control with instrument, pump, alarm. In these systems, a float unit is used to measure the water level in the tank. When the water is below the indicated level, the body moves to the tank. As the tide reaches higher, the motor changes.

Advantages and Applications

Water waste is a major problem in field agriculture and horticulture. So this kind of automatic drip irrigation with solar energy system will help reduce water waste in agriculture and maintain the water needed for planting trees and crops [14-15].

- i) Automatic drip irrigation system is used to automatically develop water supply. Roadside tree planting system.
- ii) This automatic drip irrigation system will reduce the manpower required to supply water to the plants.
- iii) This automatic drip irrigation system will reduce the total time required to water the garden or field.

CONCLUSION AND FUTURE SCOPE

This negative voltage generator is made up of an Arduino board, solenoid valve, humidity sensor and solar panel. This negative voltage sensor understands the moisture content of the ground and turns on the solenoid valve immediately and the power supplied by the battery and the battery can be used by the sun. Erosion floats are used to control water levels. GSM standard mail delivery, each time the locker is turned on and OFF. With the whole generator is the reduction of erosion, the provision of water without water, no need to do, small space required, humid place in all places no electricity used. The old model is designed for automatic water jet. Using the same strategy, water leaks can be created easily. Check the water tank, just draw the water tank from the well or drinking water.

REFERENCES

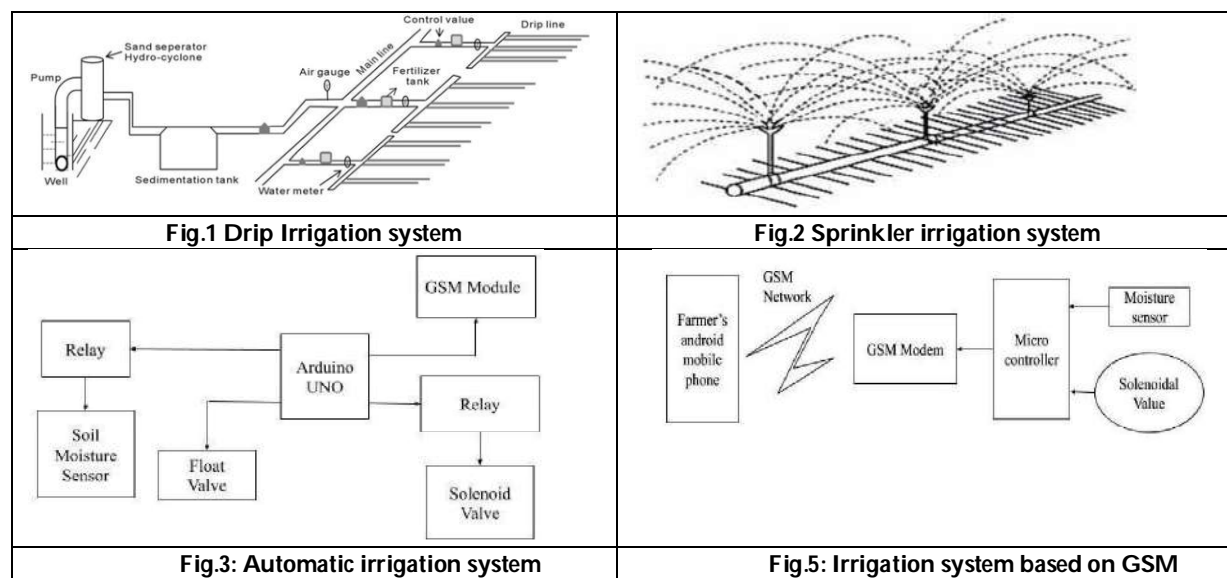
1. Moriarty and P. Michael, "Solar receiver-based power generation system." U.S. Patent No. 6,668,555,2017.
2. F. A. Costello, J. L. Manniso, A., J. DiPinto, and G. W. Smith, "Solar Heating System," U.S. Patent No. 4,055,163. Washington, DC: U.S. Patent and Trademark Office,1977.
3. V. Raghunathan, A. Kansal, Hsu and B. Jasonetal, "Design Consideration For Solar Energy Harvesting Wireless Embedded System" In Proceeding of the 4th international symposium on Information processing in sensor networks, (pp. 64), IEEE Press,2015.
4. Jr. Northrup and L. Leonard, "Compound lens solar energy system" U.S. Patent No. 4,022,186,1977.
5. Saeed Mohammed Wazeda and Ben Richard Hughesa, "A review of sustainable solar irrigation systems for Sub-Saharan Africa," Renewable and sustainable Energy reviews, pp 81, 1206-1225,2018.





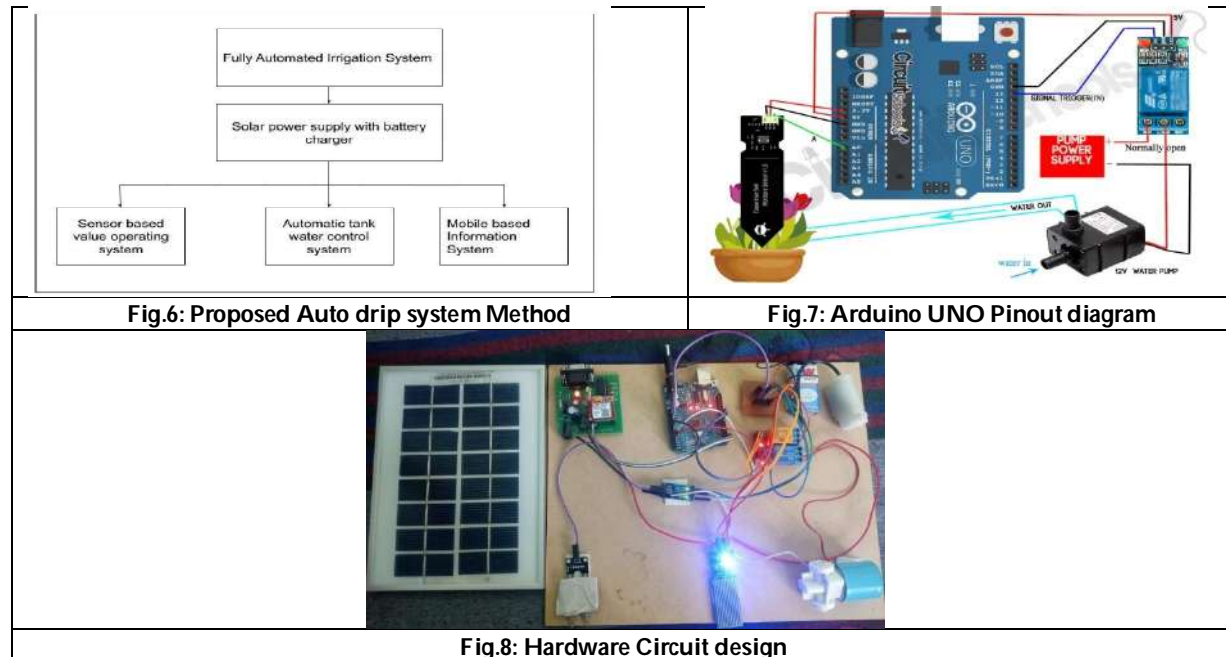
Rajesh et al.,

6. T.Rajesh, K.S.Tamilselvan, A.Vijayalakshmi,Ch.Narendra Kumar,K.Anitha Reddy, Oct 2020, 'Design and implementation of an automatic solar tracking system for a monocrystalline silicon material panel using MPPT algorithm' Materials Today: Proceedings, 2021,45,pp.1783-1789.
7. K.Tiwin Kumar, M. Muthamizh Balan, T.Rajesh 'Automatic Monitoring and Yield Predictions in Agriculture using Intelligent Techniques' International Journal of Research and Analytical Reviews (IJAR), Volume 6, Issue 1, March 2019,pp 467-471
8. T.Rajesh, K.Tiwin Kumar, M. Muthamizh Balan 2019 'E Agriculture based on AI and IOT' International Journal for Research in Applied Science & Engineering Technology (IJRASET), vol 7, Issue II, Feb 2019, pp. 343-347 DOI: 10.22214/ijraset.2019.2038
9. T.Rajesh, R.Rahul, M.Malligarjun, M.Suvathi, 2017 'Home Automation using Smart phone Application', International Journal of Advanced Research in Science Engineering and Technology (IJARSET), Vol 4, Issue. 3, pp. 3546-3553
10. T.Rajesh, R.Rahul, M.Malligarjun, M.Suvathi,2017 'Design of an Efficient Home Automation using Smart phone Application' , International Journal of Applied Science Engineering & Management (IJASEM), vol 3, no. 2, pp. 19-30
11. S. Anwaarullah, & S. V. Altaf, "RTOS based home automation system using Android" international journal of advanced Trends in computer science and engineering, 2(1), 480-484,2013.
12. R. Gayathri, E. Roshith, B. S. Roshini, S. Murugan, & S. Priya, "Implementation of Arduino based Enhanced Fingerprint Biometric System for Secured Data Exchange". International Journal of Computational Intelligence Research 13.8 , 2113-2123,2017.
13. C. McNally, "Arduino based wireless power meter," MS design project, Cornell University, Ithaca, NY,2010.
14. Shaikh Abdullah, Al MamunHossain and Wang Lixue, "Contemporary Perspective of Drip Irrigation: A Review of Water Saving Crop Production" A Review of Saving Crop Production,2018.
15. S. Postel, P. Polak, F. Gonzales, & J. Keller, "Drip irrigation for small farmers: A new initiative to alleviate hunger and poverty,"Water International, 26(1), 3-13,2001.





Rajesh et al.,





***Hemigraphis colorata* as a Natural Wound Healer: a Review**

Meena Kurup^{1*}, A.Pasupathi², R. Sambath Kumar³, R. Margnat Chandra⁴ and B S Venkateswarlu⁵

¹Ph.D Scholar, Vinayaka Missions College of Pharmacy, VMRF (DU), Salem, Tamil nadu, India.

²Professor, Vinayaka Missions College of Pharmacy, VMRF (DU), Salem, Tamil nadu, India.

³Principal, J K K N College of Pharmacy , Salem, Tamil nadu, India.

⁴HOD (Dept. of Pharmaceutics), Vinayaka Missions College of Pharmacy, VMRF (DU), Salem, Tamil nadu, India.

⁵Principal, Vinayaka Missions College of Pharmacy, VMRF (DU), Salem, Tamil nadu, India.

Received: 24 Oct 2021

Revised: 19 Dec 2021

Accepted: 21 Jan 2022

***Address for Correspondence**

Meena Kurup

Ph.D Scholar,

Vinayaka Missions College of Pharmacy,

VMRF (DU), Salem, Tamil nadu, India.



This is an Open Access Journal / article distributed under the terms of the **Creative Commons Attribution License** (CC BY-NC-ND 3.0) which permits unrestricted use, distribution, and reproduction in any medium, provided the original work is properly cited. All rights reserved.

ABSTRACT

Wound is a common term in our day to day life. But it becomes life threatening if it is not cared properly. Allopathic drug may be the first preference for wound care. But our grandparent now also believes in home remedies. According to ancient treatment system number of plants is used for the wound care. *Hemigraphis colorata* is one of plant which is common in our kitchen garden. In present study we are trying to verify different researches on *H. colorata*. According to the phytochemical, in- vitro, *In-vivo* experimental analysis researches have observation that the plant *H. colorata* can be considered as a magical wound healer.

Keywords: drug, garden, phytochemical, *H. colorata*

INTRODUCTION

Breakdown of skin may be the simplest sentence to define a wound that means loss of continuity of epithelium with or without underlying connective tissues caused by a surgery, a cut, heat, chemical, friction, pressure or as result of any disease [1].wound healing is essential and complicated physiological process comprises of many cells and their product [2]. Biochemical events occurring in the process of wound healing are inflammation, proliferation and remodeling [3]. Human / animal body itself can repair the skin damages without any external chemicals. But if the wound healing process is happening naturally, the time taken for the wound healing will be large and simultaneously the chances for microbial infection also increases. This creates the necessity of a system that speed up the wound healing. Wound healers are most fundamental requirement in essential medicines as well as in the first aid. A wound can reduce the use and possible side effects of some other drugs like antibiotics [4].



**Meena Kurup et al.,**

In India there are so many traditional treatment systems that use plants as a source of medicines. A large number of plant and plant containing formulations are used for the cure of cuts and wounds. At the same time there is no single synthetic medicine is available for wound healing in the market. Nowadays synthetic medicines used for wound dressing are either bacteriostatic or bactericidal, here the healing occur by the natural mechanism [5]. The plant *Hemigraphis colorata* is commonly called as red ivy (in kerala it is known as murikoodi) belonging to the family acanthesiae. Native place of *H. colorata* is Malasiya. According to folk medicine the *H. colorata* is claimed to have very good wound healing activity [6]. The aim of the present study is to review the usefulness of *H. colorata* as natural wound healer.

WOUND HEALING ACTIVIY***Hemigraphis colorata* extract**

Soxhelation is the usual procedure used for the extraction of *H. colorata*., The solvents used are Methanol, Acetone, hexane, etc. Suresh N Nair et al assessed the wound healing as well as the anti-inflammatory activity of methanolic extract of *H. colorata*. Excision wound study and carrageenan induced paw edema model were used for wound healing and anti-inflammatory study respectively. Acute oral toxicity also conducted to establish the safety of the extract. Based on the research suresh et al concluded that *H. colorata* methanolic extract have very good wound healing activity without any significant oral toxicity [7]. A. subramoniam et al performed a comparison study of oral as well as topical application of *H. colorata* leaf paste for wound healing and anti-inflammatory study. According to the excision wound healing study and carrageenan induced paw edema model anti-inflammatory A. subramoniam et al concluded that topical application of paste is more efficient than oral application¹¹.

Formulation containing *H. colorata* extract

Researches for developing pharmaceutical formulation of *H. colorata* extract are going on to get ready to use natural wound healer. Joshi et al evaluated wound healing activity of methanolic extract ointment in albino rat. 5% W/W extract ointment was used for both excision as well as incision model wound healing study. From the study researcher concluded that phyto-constituents in methanolic extract of *H. colorata* increases wound contraction and tensile strength [8]. Sandhiya. S et al prepared and evaluated the efficacy of wound dressing hydrogel containing *H. colorata* leaf extract. The presence of flavonoids, saponins and phenolic compound were confirmed by phytochemical analysis [9]. Wound dressing hydrogel films were prepared by using gelatin. According to the antibacterial study researcher concluded that the antibacterial hydrogel showed high activity against the selected pathogens like *Klebsiella pneumoniae*, *Staphylococcus aureus* and *Pseudomonas* sps⁹. Radhika P. Vet al formulated and evaluated wound healing and anti-inflammatory activity of hydrogel prepared from ethanol extract of *H. colorata* and *G. glabra*. Excision wound model and Carrageenan induced rat paw edema method were used for evaluation of wound healing and anti-inflammatory activity respectively. The wound contraction study revealed that the herbal extract hydrogel show promising wound healing activity [10].

Nanoformulation containing *H. colorata*

Nano technology is one of the emerging branch of science especially in health care sector. Nanoparticle have major role in the advancement of pharma industry. Liji Thomas et al conducted an anti-inflammatory study of *H. colorata* silver nanoparticles by inhibition of protein denaturation and membrane stabilization assay. According to the in-vitro study Liji et al demonstrated that silver nanoparticles of *H. colorata* are beneficial in eco-friendly as well as therapeutic manner [12].

DISCUSSION

Wound is a type of injury to skin, not an uncommon incident in human life. But it is normal and quickly cured. Natural wound healers are common in our kitchen garden because the wounds are common. *Hemigraphis colorata* is one of the natural wound healers commonly known as "murikooti" in Kerala as the juice of leaf is used for the cure of cuts and wounds. Researches on *H. colorata* is common as it is considered as a super wound healer. Paste of *H. colorata* leaves were studied for its anti-inflammatory activity. Anti-inflammatory study is the first line measure for



**Meena Kurup et al.,**

wound healers. Because the reduction in inflammation act as a key for wound healing process. The leaf paste for its topical application is proven for its anti-inflammatory activity for the traditional medicines, but oral administration need more researches for better bioavailability and therapeutic effectiveness. Extraction of *H.colorata* leaves were usually done with aqueous as well as different organic solvents. Organic solvent extract were more preferred because of its better activity and stability, at the same time aqueous extract was the budget friendly and eco-friendly choice. With the advancement in the technologies different formulations of extracts were introduced by the researcher, like films, patches etc. Topical application of the formulations also produces desired effects. Now the researches on *H.colorata* focus on biosynthesis of nanoparticle for better therapeutic activity.

CONCLUSION

Wound is considered as most common condition in our day today life. Treatment for the same depends on the characteristics of the wound. Allopathic medicines ie synthetic as well as semisynthetic compound had major roll in wound care because of its fast action, ready to use availability etc. Over all these advantages synthetic medicines are under the shadow of chemical pollution, adverse effects, resistance etc. In recent years medical world is in a run for chemically safe, therapeutically effective, ecofriendly alternative for synthetic drug in wound care. *Hemigraphis colorata* (murikooti) is traditionally used plant for wound care. From the phytochemical analysis it have been proved that, leaf juice have a magical power for the wound healing. Researches are going on in the field of pharmaceutics for getting a pharmaceutical formulation that containing *H.colorata* for wound care.

REFERENCES

1. Peng-Hui Wang et al Wound healing: Journal of the Chinese Medical Association 81 (2018) 94e101
2. Tanya J. Shaw et al Wound repair at a glance: Journal of Cell Science 122 (18)
3. B. ShivanandaNayak et al ,Evaluation of the Wound-healing Activity of Ethanolic Extract of *Morindacitrifolia* L. Leaf: eCAM 2009;6(3)351–356
4. PrafullaSabale et al An overview of medicinal plants as wound healers; Journal of Applied Pharmaceutical Science Vol. 2 (11), pp. 143-150, November, 2012
5. D. T Nguyen et al; The pathophysiologic basis for wound healing and cutaneous regeneration. Biomaterials for Treating Skin Loss,25–57
6. Bruneton J. Pharmacognosy, Phytochemistry, Medicinal Plants. 2nd edition, Lavoisier Publication France.1999.
7. Suresh Narayanan Nair et al, Wound Healing and Anti-Inflammatory Activity of Methanolic Extract of *Gmelinaarborea* and *Hemigraphiscolorata* in Rats, International Journal of Current Microbiology and Applied Sciences ISSN: 2319-7706 Volume 6 Number 8 (2017) pp. 3116-3122
8. Joshi VG et al, Wound Healing Activity of *HemigraphisColorata*, International Journal of Contemporary Research and Review, October, 2010;Volume ;Issue 05
9. Sandhiya. S, Sabarinath. K, Ishwarya. R, Logeshwaran. V, Kousalya. N and Dr. Arun. P, "Preparation of Gelatin Film Incorporated with Extracts of *HemigraphisColorata* Used as Wound Dressing", International Journal for Modern Trends in Science and Technology, Vol. 07, Issue 01, January 2021, pp.- 58-64.
10. Radhika P. V. and Arun Kumar K. V; *Hemigraphiscolorata* (blume) and *glycyrrhizaglabra* (linn) hydrogel for wound healing and antiinflammatory activity; world journal of pharmacy and pharmaceutical sciences ;volume 6, issue 12, 902-923.
11. A. subramoniam, D. A. evans, S. rajasekharan, G. sreekandannair "Effect of *hemigraphiscolorata* (blume) h. g. hallier leaf onwound healing and inflammation in mice" Indian Journal of Pharmacology 2001; 33: 283-285
12. Lijithomas, saleenaMathew;Biosynthesis, characterization, and anti-inflammatory study of *hemigraphiscolorata* loaded silver nanoparticles; Asian J Pharm Clin Res, Vol 12, Issue 10, 2019, 188-192





Drug Disposal Practices and their Impact on the Environment

M.V. Kumudhavalli¹ and Rajeev P Thomas²

¹Professor, Department of Pharmaceutical Analysis, Vinayaka Mission's College of Pharmacy, Salem, Tamil Nadu, India.

²Associate professor, Department of Pharmacy Practice, National College of Pharmacy, Kozhikode, Kerala, India.

Received: 20 Nov 2021

Revised: 26 Dec 2021

Accepted: 13 Jan 2022

*Address for Correspondence

Rajeev P Thomas

Associate professor,
Department of Pharmacy Practice,
National College of Pharmacy,
Kozhikode.
Email: rajeevpthomas@gmail.com



This is an Open Access Journal / article distributed under the terms of the **Creative Commons Attribution License** (CC BY-NC-ND 3.0) which permits unrestricted use, distribution, and reproduction in any medium, provided the original work is properly cited. All rights reserved.

ABSTRACT

Medicinal waste was found all across the surroundings, and in certain circumstances, they are seen to be hazardous. These would be the consequence of poor disposal of unused drugs through highly polluting channels such as the sink, toilet, or garbage can. Antibiotics gathered in the aquatic habitat have been shown to increase antibiotic resistance and virulence. Unwanted pharmaceuticals were widely discarded in a highly polluting way. Also, there is a poor understanding of the ecological consequences of incorrectly discharged medicines. The aim of the study necessitates the development of strategies to enhance the pharmaceutical recycling program and awareness about proper drug disposal.

Keywords: drug disposal; pharmaceutical waste; active pharmaceutical ingredients; impact; environment; pollution; drug take-back program.

INTRODUCTION

Pharmaceuticals are vital substances in today's life, with undoubted health and lifestyle benefits. However, since the 1970s, unwelcome residues of Active Pharmaceutical Ingredients (APIs) have been noticed in an environment [1]. An API is a chemical component with medicinal activity and a beneficial impact in diagnostic techniques, cure, reduction, treatment, or prevention, or one that affects the functioning of the body [2]. The amount of pharmaceutical waste is increasing as the network of medical and pharmaceuticals increases. The improper disposal of drugs has resulted in environmental risk in many ways [3]. Pharmaceutical waste is a major waste category whose management is complex and difficult. As per the World Health Organisation (WHO), medical waste is characterized as "waste generated during the diagnosis, treatment or vaccination of humans and animals". Medicines account for



**Kumudhavalli and Rajeev P Thomas**

the majority of medical waste[4]. Expired medicine, individual medication discarded by patients, waste material containing chemotherapeutics and leftover medicine, such as intravenous (IV) sacks and syringes, containers containing harmful pharmaceuticals and unused drugs, thrown away drugs, spill clean-up equipment, and contaminated absorbents and protective clothing, are all examples of pharmaceutical waste [5]. More than 200 APIs, primarily antibiotics, analgesics, vascular drugs, and antidepressants, are mostly found in water and soil at various concentrations from a few nano grams/ litre to thousands of micrograms/litre [1]. The rise in pharmaceutical use and misuse can have serious consequences for wildlife and ecosystems, especially when unused medications are discarded improperly[6]. As a result, unwanted drugs must be disposed of safely [7].

Current Disposal Practices

Domestic pharmaceuticals enter the sewage system via three primary routes such as excretion after the consumption, injection, or infusion, removal of topical agents while showering and disposal of unutilized medications through the drainage system or garbage [5]. According to a domestic study conducted in North India, 72 percent of respondents had at least 1 to 5 drugs saved at their house, while 19 percent had 6 to 10 unused medicines stored at home. As per the study, the most common causes for leftover medicines are too much OTC (over-the-counter) drug purchases that are about 53%, and self-discontinuation which is about 17%[3]. Patients may not eat all of the prescribed drugs or dispensed to them for several reasons. The most common reasons are symptom relief, dosage changes, loss of memory, adverse reaction, and medicines approaching their expiration date. Furthermore, health providers may sometimes prescribe excessively, and pharmacists may dispense too much medication because packet sizes may outweigh the amount required for treatment. As a result, not all medicinal drugs are taken, and large volumes persist or expire[9]. One of the most common disposal methods of expired or unused drugs was throwing them in household garbage, followed by flushing the medication down the toilet or sink. From the study of Indonesia, nearly 8% of those polled were unsure what to do with expired medications[11]. Burning expired and unused medication in one's backyard was another commonly reported method of disposal [12]. Unwanted drugs discarded in garbage are either dumped into landfills or burned[12]. Medicines thrown away in household trash bins end up in landfills, where they can harm the environment. They may also be discovered by unknown parties, such as kids and animals, raising the risk of poisoning, misuse, and abuse[7]. In most parts of the world, people throw away these leftovers in usual trash and sewer lines caused by a lack of individual attention, knowledge, awareness, and training, or even the lack of proper municipal and health services authorities instructions and rules[13]. According to a new worldwide evaluation, 631 of the 713 pharmaceuticals checked for in the environment were discovered to be above their limit of detection. As per the study conducted in Germany, up to 16 000 tonnes of pharmaceuticals are discarded yearly from healthcare, with 60–80 percent of these drugs being flushed down the toilet or thrown away in ordinary household waste[6].

Impact on the Environment

Medical waste harms both the environment and the economy. Pharmaceutical residues in water and food can be harmful to living things [14]. 27 APIs were found to be the most hazardous agents to the environment. Based on inherent properties, APIs, including diclofenac, ethinyloestradiol, ibuprofen, metoprolol, norethisterone, oxytetracycline, and paracetamol, were classified as dangerous for the aquatic environment. Norethisterone and Oxytetracycline are extremely toxic to aquatic organisms and may have long-term negative effects on the aquatic environment [15]. A decline in the number of scavengers, infertility in frogs, and femininity of male fishes are a few of the impacts of such contamination of the environment. Just several studies have revealed an alarming drop in sperm count in men over the last several years, as well as antibiotic resistance due to medication exposure in the environment [16]. These compounds, as toxic elements, disrupt hormone signalling pathways and the endocrine system by mimicking natural hormones, causing immunologic, metabolic, neural, and teratogenic effects in animals and human populations when ingested. These negative impacts range from aquatic and fish feminization to cancer development and metabolic syndrome. Steroidal oestrogen toxins have been identified in wastewaters and even underground water, with approximate releases of more than 100 tonnes per year, and are associated with the interruption of fertility, growth, and metabolism of living things such as fish and plants. In individuals, oestrogens



**Kumudhavalli and Rajeev P Thomas**

and their active ingredients, which are consumed through drinking water and food, are linked to a higher risk of certain types of cancer, such as breast cancer and reproductive abnormalities [13]. Cattle have died in Asian countries after consuming drugs discarded in local open dumps. Furthermore, endangered scavengers in Asia have died as a result of preying on cattle and their leftovers containing similar levels of drugs [3]. Antibiotic resistance is a global concern in both human and veterinary medicine. Antibiotic-resistant bacteria have been discovered in aquatic and soil environments. In livestock farming, antibiotics are regularly used to cure diseases and promote growth. Minimum effective levels of antibiotics in diet are known to help animals grow quickly and reduce sensitivity to diseases. Most antibiotics given to animals are usually absorbed in the animal gut, leading to significant antibiotic excretion in urine and faeces. Some antibiotics may be excreted as the parent compound in up to 90% of situations. The residual antibiotics probably wind up in sewage sludge and effluent, which, when applied to land, give an alternative route for antibiotics to enter the aerial ecosystem [17].

Antimicrobial resistance is a more and more known complication as a result of antibiotic misuse and drug pollution, which makes a significant contribution to the expansion of clinically relevant multidrug-resistant microbes that are hard to treat in healthcare situations [13]. This can lead to increase human illness, suffering to death, increase cost and length of treatments. Researchers have reported a fall in antibiotic efficacy, presenting a shocking risk in the treatment of life-threatening diseases. In India, for example, bacteria resistant to ciprofloxacin were discovered in pharmaceutical plants [3]. One of the most serious health and environmental issues is the release of APIs and medicines into waterways. Particularly, this is the case with endocrine-disrupting chemicals (EDCs), which are toxic to biodiversity at extremely low concentrations. Other factors that alarm environmental activists and scientists are the potential continuity of APIs in the surroundings and their metabolic activity, which takes place through bioconversion and can boost and propagate the negative impacts of these active ingredients on the environment. So far, the discharges of APIs as contaminants into the atmosphere have been considered as a central problem that must be analysed and openly discussed because of its national and international relevance [13]. Pharmaceuticals can also be eliminated from the environment via physical methods like adsorption or evaporation, biodegradation, or chemical reactions including ozonation. The applicability of various possibilities is expected to be extremely unique to every situation. Ciprofloxacin is eliminated by forceful adsorption onto wastewater dissolved particles, whilst diclofenac and 17-ethinylestradiol must go through substantial microbial degradation in older treated wastewater plants. As a result, it is probably a series of approaches that will be necessary to reduce pollution. Numerous therapeutic approaches, while expelling drugs, may also generate transformation products that are far more consistent and portable than the parent products, which may even also have related or increased cytotoxic activity. Very little research has been conducted to monitor the environmental impacts of such by-products [15].

Proper Disposal Methods

Due to the financial limits of pharmaceutical disposal, cost-effective planning and procedures are needed. The primary means of achieving this is to arrange the substance to reduce the need for costly or challenging disposal methods. The disposal methods include,

Return to manufacturer

Wherever applicable, the chance of returning unusable drugs to the manufacturing company for proper disposal should be explored; especially for drugs with disposal issues, such as antineoplastics.

Landfill

It means to dump waste directly in a landfill without first classifying or arranging it. The landfill is the traditional and widely used method of solid waste disposal. Landfills are of three types

- Sanitary landfill with advanced engineering: Landfill sites that are properly built and controlled provide a generally safe disposal path for municipal waste, including waste pharmaceuticals.
- The landfill that was engineered: The landfill is designed to prevent chemical leakage into the groundwater.



**Kumudhavalli and Rajeev P Thomas**

- Open uncontrolled non-engineered dump: A non-engineered landfill is the most common method of land disposal. Solid sewage expelled into an uncontrolled, non-engineered open dump is harmful to the surrounding ecology and should be avoided. It is not suggested to disposal of untreated bio waste in such a location is strictly essential.

Immobilization of waste: Encapsulation

The drugs are immobilized in a solid object within a plastic or metal barrel during encapsulation. Barrels should be kept clean before use and should not have previously contained explosive or toxic substances. They are loaded to 75% capacity with solid and semi-solid drugs, and the extra space is loaded with a medium such as cement or a cement/lime mixture, plastic foam, or bituminous sand. Barrel lids should be slit open and folded back for speed and ease of pouring. After filling the barrel to 75% volume, a mixture of lime, cement, and water in the proportions 15:15:5 is introduced and the barrel is filled up. A greater amount of water may be necessary at times to achieve the appropriate liquid consistency. Metal barrel lids should be bent back and secured, preferably by joint or spot soldering. The secured barrels should be kept in the bottom of a dumpsite and encased with new municipal waste. To facilitate movement, the barrels can be positioned on pallets, which can then be loaded onto a pallet transporter.

Immobilization of waste: Inertization

Inertization is a type of encapsulation that includes taking the pharmaceuticals' packaging, such as paper, paperboard, and plastic. Drugs must be detached from sealed containers. Then a homogeneous paste is formed by combining water, cement, and lime. There may be a danger, which usually requires employee protection in the form of protective suits and goggles. The paste is then transferred in a fluid state to a dumpsite by a concrete mixer pickup and removed into standard waste disposal. The paste then solidifies and dissolves as a solid mass within the municipal waste.

Sewer

Several liquid formulations like syrups and intravenous (IV) fluids, can be mixed with water and drained into the sewage system in low amounts over a period without causing severe public health or environmental problems. Small amounts of liquid formulations or antimicrobials can also be drained via fast-flowing water bodies. In cases where sewage is in bad condition or has been broken by conflict, the services of a hydrogeologist or sanitation services engineer may be permitted.

Burning in open containers

Toxic fumes may be emitted into the atmosphere if drugs are burnt at low temperatures in open containers. If paper and paperboard wrapping cannot be reused, they may be fired. Polyvinyl chloride (PVC) materials should not be fired.

Decomposition of chemicals

If a suitable incinerator is not accessible, chemical disintegration, followed by landfill, will be used following the manufacturer's guidelines. This procedure is not suggested unless having chemical knowledge and experience. Chemical deletion is a time-consuming and labour-intensive process. This method could be beneficial for getting rid of a small number of drugs. However, chemical degradation is not feasible for large quantities, such as more than 50 kg, because even small batches must be handled again and again using this method.

Incineration

High-temperature technologies used in industries, such as cement kilns, coal-fired thermal power plants, or foundries, typically have furnaces that work at temperatures well above 850°C. Cement kilns are ideal for the removal of expired medical products, industrial waste, and other materials. During combustion, the materials for cement attain temperatures of 1450°C, while the combustion gases attain temperatures of up to 2000°C. All biological



**Kumudhavalli and Rajeev P Thomas**

waste elements are successfully dissolved under these conditions. Some potentially harmful toxic combustion products are reabsorbed into cement clinker or eliminated in heat transfer devices ⁽¹⁹⁾.

Approaches and Programs for Drug Collection and Disposal

Most countries now provide specific information on how to gather unused/expired drugs. The networks of information vary from verbal details to the customer by the health care professional or pharmacist on the finest disposal method, brochures, detailed info via websites, info on collection boxes, and info on the drug products packet [20]. Community dispensaries are done to gather, sort, and dispose of drugs more sensibly than anybody else. Because they have been educated in the act of drug safety disposal, they are built to support as toll booths for expired drugs in the societies where they are situated [21]. Rather than throwing away costly drugs or allowing them to expire, unused medicines could be donated to those in need. Certain developed countries have well-maintained drug "take-back" systems that play a vital role in the fair utilization and disposal of medicines [3]. The FDA recommends that drug take-back programs be used to remove the rest of the drugs. If these programs are not commonly accessible, most medicines can be disposed of in trash bins by following some protective measures, like combining the medicines with an unpalatable substance. Even so, for a small number of formulations of highly dangerous accidental drug risks, it is suggested because when these drugs are no longer required and no take-back systems are accessible, they be discarded by flushing and/or rinsing down the sink. This method was introduced mainly to reduce the instant risk of injury or death due to unmonitored paediatric exposures, and it is regarded as a suitable choice for ensuring that these formulations will be directly and completely inaccessible until the individual requires them [22]. Pharmacists have the most interaction with the customers and prescription and over-the-counter drugs, and are thus in an extremely good position to guide medicine use and, by renewal, drug disposal [23]. All countries do not have well-established drug-recycling programs. As a result, new rules and regulations letting pharmacists receive returned drugs from buyers, suggesting which drugs may be recycled, and who may be eligible to return which drugs, should be incorporated [14].

CONCLUSION

The public remains unaware of how to properly dispose of unused drugs and the potential pollution caused by improper drug disposal. Some of the most common medicine disposal methods reported in studies have the possibilities to harm the earth. Even though public health and the ecosystem are intimately connected, there is an immediate want of collaborative care and consideration. Due to unsatisfactory guidelines for the treatment and disposal of unused drugs. Public services, including the government and private sectors, must be more alert in providing education about using and disposing of drugs in an even more eco-friendly manner. To minimize the negative medicinal effect on the environment by returning unused drugs to collection schemes for proper disposal, a stringent set of rules, dynamic, economical, and easily available government disposal devices are needed.

REFERENCES

1. Sangion A, Gramatica P. Hazard of pharmaceuticals for aquatic environment: Prioritization by structural approaches and prediction of ecotoxicity. Environ Int [Internet]. 2016; Available from: <http://dx.doi.org/10.1016/j.envint.2016.08.008>.
2. Kadam A, Patil S, Patil S, Tumkur A. Pharmaceutical Waste Management an Overview. Indian J Pharm Pract. 2016;9(1):2-8.
3. Nipa N, Ahmed S, Rahman M. Improper Management of Pharmaceutical Waste in South and South-East Asian Regions. J Environ Stud. 2017;3(1):1-7.
4. Hassali MA, Shakeel S. Unused and Expired Medications Disposal Practices among the General Public in Selangor, Malaysia. Pharmacy 2020;1-11.



**Kumudhavalli and Rajeev P Thomas**

5. Pines E, Smith C. Managing Pharmaceutical Waste: A 10-Step Blueprint for Healthcare Facilities in the United States. Healthcare Environmental Resource Center. 2008 Aug:1-93.
6. Thomas F. Pharmaceutical waste in the environment: a cultural perspective. Public Heal Panor.2017;03(01):127–32.
7. Bergen PJ, George J. Safe disposal of prescribed medicines. Australian prescriber. 2015; volume 38(3):90–2.
8. Wilcox E, Carolina N. Pharmaceuticals in the environment review of current disposal practices for medications and the influence of public perception on environmental risks. NCSU Libr. 2013;1–39.
9. Akici A, Aydin V, Kiroglu A. Assessment of the Association between Drug Disposal Practices and Drug Use and Storage Behaviors. Saudi Pharm J [Internet]. 2017; Available from: <https://doi.org/10.1016/j.jsps.2017.11.006>.
10. Insani WN, Qonita NA, Jannah SS, Nuraliyah NM, Supadmi W, Gatera VA, et al. Heliyon Improper disposal practice of unused and expired pharmaceutical products in Indonesian households. Heliyon 6 (2020 April):6–10.
11. Kusturica MP, Tomas A, Sabo A. Disposal of Unused Drugs: Knowledge and Behavior Among People Around the World. Springer International. 2016 DOI 10.1007/398_2016_3.
12. Koshy S. Disposal of unwanted medications: throw, bury, burn or just ignore? International Journal of Pharmacy Practice 2013, 21, pp. 131–134.
13. Ara D, Freitas A, Radis-baptista G. Pharmaceutical Pollution and Disposal of Expired, Unused, and Unwanted Medicines in the Brazilian Context. J. Xenobiot. 2021, 11, 61–76. <https://doi.org/10.3390/jox11020005>.
14. Alhomoud F. “Don’ t Let Medicines Go to Waste”— A Survey-Based Cross-Sectional Study of Pharmacists’ Waste- Reducing Activities Across Gulf Cooperation Council Countries. Frontiers in Pharmacology. 2020;11(August):1–10.
15. Carlsson C, Johansson A, Alvan G, Bergman K, Ku T. Are pharmaceuticals potent environmental pollutants? Part I: Environmental risk assessments of selected active pharmaceutical ingredients. Science of the Total Environment 364 (2006) 67–87.
16. Hs S, Chakraborty A, Virupakshaiah A. Knowledge, Attitude and Practice of Medical Professionals Towards the Safe Disposal of Unused Medications in South India. World J Pharm & Pharm Sci. 2015;4(05):1423–30.
17. Kumar K, C. Gupta S, Chander Y, Singh AK. Antibiotic Use in Agriculture and Its Impact on the Terrestrial Environment. Adv Agron. 2005;87(05):1–54.
18. Boxall ABA. The environmental side effects of medication: how are human and veterinary medicines in soils and water bodies affecting human and environmental health? EMBO Rep [Internet]. 2004;5(12):1110–6. Available from: <https://www.ncbi.nlm.nih.gov/pmc/articles/PMC1299201>.
19. Societies RC, Federation IP. Guidelines for Safe Disposal of Unwanted Pharmaceuticals in and after Emergencies. 1999;(1930154).
20. Barnett-itzhaki Z, Berman T, Grotto I, Schwartzberg E. Household medical waste disposal policy in Israel. Isr J Health Policy Res [Internet]. 2016;1–8. Available from: <http://dx.doi.org/10.1186/s13584-016-0108-1>.
21. Wheeler AJ, Spinks J, Bettington E, Kelly F. Evaluation of the National Return of unwanted medicines (RUM) program in Australia: a study protocol. Journal of Pharmaceutical Policy and Practice (2017) 10:38 DOI 10.1186/s40545-017-0126-6.
22. Khan U, Bloom RA, Nicell JA, Laurenson JP. Science of the Total Environment Risks associated with the environmental release of pharmaceuticals on the U.S. Food and Drug Administration “flushlist.” Sci Total Environ [Internet]. 2017; 609:1023–40. Available from: <http://dx.doi.org/10.1016/j.scitotenv.2017.05.269>.
23. Abahussain E, Waheedi M, Koshy S. Practice, awareness and opinion of pharmacists toward disposal of unwanted medications in Kuwait. Saudi Pharm J [Internet]. 2012;20(3):195–201. Available from: <http://dx.doi.org/10.1016/j.jsps.2012.04.001>.





Lane Line Misbehaviour Detection using Hybrid Optimization - based Improved Convolution Neural Network

Sivakumar. T^{1*} and L. Manjunatha Rao²

¹Research Scholar, MCA Program, Dr.Ambedkar Institute of Technology, Bengaluru, India.

²Professor, MCA Program, Dr.Ambedkar Institute of Technology, Bengaluru, India.

Received: 14 Dec 2021

Revised: 26 Dec 2021

Accepted: 13 Jan 2022

*Address for Correspondence

Sivakumar. T

Research Scholar,

MCA Program, Dr.Ambedkar Institute of Technology,

Bengaluru, India.



This is an Open Access Journal / article distributed under the terms of the **Creative Commons Attribution License** (CC BY-NC-ND 3.0) which permits unrestricted use, distribution, and reproduction in any medium, provided the original work is properly cited. All rights reserved.

ABSTRACT

Automatic vehicle detection has become more important in visual traffic surveillance systems and intelligent transportation in recent years. Most previous techniques for monitoring lane-line misbehavior rely on computer vision methods. This paper presents a novel yet efficient deep learning method for analyzing lane-line misbehavior. In this work, feature extraction and detection methods are incorporated. After removing the noisy content in a lane line image, a hybrid algorithm, called Improved Grey wolf Optimization with Seagull algorithm (IGWO-SOA) is introduced for extracting a relevant set of features to make ease the detection process, for solving global optimization problems. In this context, a hybrid algorithm IGWO-SOA based Improved Convolutional Neural Network (ICNN) is introduced for detecting misbehavior activities attained in the lane-line image. The proposed system's performance is evaluated based on accuracy, precision, recall, f-measure, and loss. The proposed algorithm outperforms other competitive metaheuristic methods, according to the experiment results.

Keywords: Adaptive histogram equalization; hybrid optimization (IGWO-SOA); Improved Convolutional Neural Network (ICNN).

INTRODUCTION

Autonomous vehicles are becoming a reality, with some vehicles achieving level-4 driving abilities, which means, driving without much human involvement [2]. Because mobility information is critical for application and network performance, many attackers target it to reach their objectives. As a result of this, lane line misbehavior develops [1]. A sign of traffic that describes the key driving features of a vehicle is known as a lane line. After reverse perspective translation, the lane line will consume a specific junction if the road has a specific slope, the latter makes it difficult to identify the pixel line of the similar lane line [3]. Visual traits of lane lines as attributes, namely linear shapes, high-contrast colours, and existence in particular portions of the image, are used to discriminate lane lines from other items in the image. In autonomous navigation of unmanned vehicles and vehicle intelligent early warning systems, it is critical to properly collect road information. Scholars from several nations have developed



**Sivakumar and Manjunatha Rao**

numerous techniques to accomplish the automated detection of structural and unstructured roadways in recent years [4]. The primary and maximum fundamental function of the vehicle safety auxiliary system is road lane line identifying technology. Hence, studying the approach of identifying road lane lines is both theoretical and practical [5]. Curve fitting, image edge extraction, and lane line extraction are the three major components of lane line identification technology. The Robert's operator, Canny operator, Sobel operator, and Prewitt operator are now the most extensively utilized edge extraction approaches. The edge points of a lane line are extracted via lane line extraction and eliminate the interference point's impact on further processing [6]. Misbehaving vehicles might inject misleading information about their status or movement, causing other vehicles to perceive it incorrectly to create an illusion [7]. Based on the National Highway Traffic Safety Administration (NHTSA) and the Directorate-General for Mobility and Transport (DGMT), in the US and the EU, every year above thirty lakhs' people are wounded because of road accidents [8]. Internal assaults can be detected using a Misbehavior Detection System (MDS). Signatures, specifications, and anomaly detection systems are the three primary forms of MDS used in-vehicle communications [9]. The signature-based system is the first category. If data matches previously documented harmful behavior, it is classified as an attack. This technology is unable of detecting unknown attacks. The specification-based system is the second type. A set of conditions is stated in this system, and a program or protocol must meet these constraints. If software or protocol fails to match these criteria, it is considered an attack. Anomaly detection systems are the third group. Machine learning methods are used in this system to create a model of trustworthy and anomalous activity, which is then compared to the new behavior. This type of system can detect unknown threats in this system [10].

Machine learning (ML) approaches, recognize trends and forecast misbehavior by generating rules/thresholds autonomously [11]. Machine Learning (ML) is becoming increasingly important in vital sectors namely Cyber-Security and the Internet of Things (IoT). It's an intriguing field full of new possibilities and uses, but, as with most technology, it's not without its own set of problems [12]. Then, in the form of classification, multiple supervised machine learning algorithms were assessed. Because the data set was labeled before the classifier was trained, it's termed supervised machine learning. Machine learning is useful in estimating, classifying, and predicting system behavior. Many scholars have looked at various classification algorithms for determining the driver's purpose in particular [13]. Some approaches have been developed in the last year to solve lane detection with few assumptions about the lanes. However, there is still much opportunity for development in terms of resilience to various real-world conditions. Nowadays, Over the typical machine learning technique, deep learning models are utilised to handle a variety of categorization problems. Deep neural network methods, particularly convolutional neural networks, spark a potential research field and also inspire the concept for our Lane Net. Furthermore, because lane detection is performed on vehicle-based systems with limited computing resources, the computational cost of a lane detection approach should be evaluated as a critical indicator of overall performance [14]. CNN collects picture abstract traits layer by layer, from low to a high level, eventually replacing the manual extracting features approach that depends on a feature extractor for learning [15].

Related Works

Hamssa Hasrouny, et al [16], have presented Within VANET, a framework for certificate revocation. the Misbehaviour Authority (MA) in the structure and Misbehaviour Detection Systems (MDSs) in vehicles can both initiate this procedure, which recognizes and to protect the network's long-term survival, it rejects unruly cars. Chunhua Zhang, et al [17], have provided a misbehaviour detection approach according to the Dempster-Shafer theory (DST) and a support vector machine (SVM) of proof to defend against attacks on fake messages and message suppression. The suggested system is included in a data trust model and the vehicle trust model. Bogus messages are detected by the data trust model using an SVM-based classifier according to vehicle features and message content. Jithin Zacharias and Sibylle Froschle [18] investigated an approach for detecting misbehaviour in Vehicular Ad-Hoc Networks (VANETs) that relied on local traffic density. This method relies on two independent sensors monitoring local traffic density and reporting it as evidence for a specific traffic condition. Moreover, the method is especially well-suited to detecting illusion attacks, which remains a problem in-vehicle communication. Using the Software-Defined Networking paradigm, Abdelwahab Boualouache et al [19] created an adaptive misbehaviour detection system, the system adjusts its security parameters to the vehicles' environment. In our system is Sybil attack-resistant



**Sivakumar and Manjunatha Rao**

and compliant with vehicular privacy standards. To increase the efficiency of the VANET CIDS models, Fuad A. Ghaleb et al [20] suggested a misbehavior-aware collaborative intrusion detection system (MA-CIDS) that utilizes distributed ensemble learning. To increase shared information and decrease communication overhead, an efficient sharing strategy is given. Using a random forest approach in conjunction with performance measurements for classifiers, on-demand vehicles communicate their locally trained classifiers.

Rukhsar Sultana et al. [21] have described a methodology for detecting misbehaviour in an SDN-based VANET that takes advantage of SDN traits. The detection system is adaptable to variations in the network context thanks to SDN capabilities. Also, for continuous location assault in two different network density scenarios, the suggested approach was assessed. Misbehavior Detection Model based on Ensemble Miscellaneous VANET classifiers (EMVC-MDM) is proposed using independent classifiers like Miscellaneous VANET classifiers based Misbehavior Detection Model (MVC-MDM) by S. Sumithra and R. Vadivel [22]. The proposed MDS's main principle is to categorise vehicles based on context references in order to locate misbehaving vehicles. Joseph Kamel et al. [23] have published a VeReMi dataset expansion for detecting misbehaviour in VANETs. A new set of more complicated attacks, as well as a true physical error model and a bigger data set, are included in this version. To decrease traffic accidents, the Cooperative Intelligent Transport Systems (C-ITS) technology is deployed. The C-ITS system is based on peer-to-peer transmissions exchanged over a vehicular ad hoc network (VANET).

The aforementioned section described the various method that is utilized in the prediction of lane line misbehaviour. The above-discussed approaches are performed well for the prediction process however, there are some research gaps and that is represented as future work. In [16] the proposed process provides a lightweight solution to the CRL solution whereas, the proposed process does not work well for the revocation procedure is crucial to multi-hop communication and group interactions. In [17] proposed technique accurately detects misbehaviour but it does not reduce the calculation pressure while updating the vehicle reputation and revoking malicious vehicles. The proposed MA-CIDS method in [19] provides a better result than the other existing model but does not support both supervised and unsupervised machine learning techniques. In [20] the proposed method supports only limited parameters and does not support the global detection phase. In [22] the proposed method provides effectiveness and reliability to the misbehaviour detection systems still it lacks in the detection of long-term misbehaviours beyond mobility information. In [23] the proposed method does not support the dataset for global misbehaviour evaluation. The aforementioned section defined various methods that are utilized in lane line misbehaviour prediction. The above-discussed methods are achieved well for the prediction process however, there are some research gaps and that is signified as future work.

Proposed Methodology

The three major techniques in lane-line misbehaviour detection systems identified in the research are feature extraction, image pre-processing, and lane-line misbehaviour detection. The lane detection procedure, which includes feature extraction and model fitting, is the most significant part of the lane detection system, as illustrated in Fig.1. The most general procedures in the pre-processing step include adaptive histogram equalization (AHE) noise removal and improve image contrast enhancement. The primary goal of focusing on AHE is to increase computing efficiency while reducing erroneous lane line misbehaviour detections. Once the pre-processing is completed then output goes to feature extraction for hybrid improved grey wolf optimizer with seagull algorithm (IGWO-SOA). Then, the optimization process is completed the optimization output is sent to the lane detection process. A hybrid method named Improved Grey Wolf Optimizer with Seagull Approach (IGWO-SOA) for resolving global optimization problems as a novel to the feature extraction. The key reason is that during migration, Seagulls can change the attack angle and speed on the air, moreover, the SOA offers a powerful global search capability, which mainly combines the grey wolf attacking prey mechanism of the IGWO through the spiral attack behaviours of the SOA, as a result, the algorithm's capacity to search locally and globally has substantially improved. Once the feature extraction process is complete then output is sent to the lane line misbehaviour detection process. In this work, the lane-line misbehaviour detection process is used to Improved Convolutional Neural Network (ICNN) to detect effectively.





Sivakumar and Manjunatha Rao

Preprocessing

By adjusting the global picture contrast of the collected lane-line photos, adaptive histogram equalisation is used to increase the visual capacity of the photographs. Furthermore, the AHE approach computes a large number of histogram values for dispersing the brightness values of the lane-line pictures, which increases the local contrast and edge definitions in each image's region.

Initially, a is denoted as the collected images and x_i is signified as in the gathered image, the several gray level events i . Thus, a grey level event probability is calculated via

$$s_a(i) = s(a = i) = \frac{x_i}{n}, 0 \leq i \leq L, (1)$$

Where the several image gray levels are denoted as L , which can ranges range from 0 and 255; $s_a(i)$ is denoted as the image pixel's histogram value is normalized between [0,1] and x is indicated as total image pixels. In addition, for s_x the cumulative distribution function (CDF) is calculated by

$$cdf_a(i) = \sum_{j=0}^i s_x(x = j) (2)$$

Then, a transformation from $b = (a)$ is improved to create a novel image b over the values of a flat histogram. The transformed lane-line images consume a linear CDF and are numerically represented by

$$cdf_b(i) = iK, (3)$$

$$(b') = cdf_b(T(k)) = cdf_a(k), (4)$$

The k variable is in the range of [0, L] and where K and T are constant variables with values ranging from [0,1]. In the AHE method, in order to restore the pixel values to their original image, a simple transformation is utilized, which is numerically defined by

$$b' = b \times (\max(x) - \min(x)) + \min(x) (5)$$

b' is to detect lane line misbehaviour from the pre-processed images.

Feature Extraction for Hybrid Improved Grey Wolf Optimizer with Seagull Algorithm (IGWO-SOA)

The lane-line misbehaviour feature extraction has performed a hybrid Improved Grey Wolf Optimizer with Seagull algorithm (IGWO-SOA) and the description of each methodology is given below: As a novel contribution to the feature extraction, for solving global optimization problems, a hybrid algorithm called Improved Grey Wolf Optimizer with Seagull Algorithm (IGWO-SOA). The major reason is that during migration, the seagulls can modify their angle of attack as well as their speed, also the SOA consumes a strong global search ability. which mainly combines the grey wolf attacking prey mechanism of the IGWO by the spiral attack behaviours of the SOA, therefore importantly increasing the global searching and local searching ability of the algorithm. The numerical models of the social hierarchy, hunting, surrounding prey, assaulting prey, and searching for prey are presented in this subsection. In this subsection, the mathematical models of the social hierarchy, search prey, hunting, attacking prey, and encircling prey are provided.

Social hierarchy

According to the wolves' social hierarchy, the finest option is called alpha (α), the second-finest solution is called beta (β) and the third-finest solution is the delta (δ) while building IGWO. The solutions of the remaining candidate are considered to be viewed as omega (ω). α, β lead the ω wolves and all three δ wolves follow them.

Encircling prey

During the hunt, Grey wolves bend around the prey. The following is a mathematical model of the encircling behaviour:

$$\vec{D} = | \vec{C} \cdot \vec{x}_p - \vec{x} | (6)$$

$$\vec{x}(t + 1) = \vec{x}(t) - \vec{A} \cdot \vec{D} (7)$$

Where \vec{A} and \vec{C} are denoted by coefficient vectors, \vec{x} denotes the position vector of a grey wolf, t indicates the current iteration, and \vec{x}_p indicates the vector of the prey's location (global solution). \vec{A} and \vec{C} are computed as follows:





Sivakumar and Manjunatha Rao

$$\vec{A} = \frac{\vec{a}}{2a} \cdot \vec{r}_1 - \vec{a} \tag{8}$$

$$\vec{c} = 2 \cdot \frac{\vec{r}_2}{r_2} \tag{9}$$

Where \vec{a} elements are linearly reduced from 2 to 0 based on iterations and in $[0,1]$ r_1 and r_2 denoted as the random vectors.

Hunting

The alpha, beta, and delta are generally in the hunting charge since they have a greater understanding of prospective prey locations. The positions of the other search agents should be adjusted based on the best search agent's position. To calculate the vector $\overleftarrow{D}'_\alpha$, \overleftarrow{D}'_β , and $\overleftarrow{D}'_\delta$

This will allow a search agent to consume better research capability and in local optima stuck being avoided. The following formula can be used to update their agent position:

$$\begin{aligned} \overleftarrow{D}'_\alpha &= \left| \frac{\vec{c}_1 \cdot \vec{X}_{r1} - \vec{X}_{r3}}{c_1} \right|; \overleftarrow{D}'_\beta = \left| \frac{\vec{c}_2 \cdot \vec{X}_{r2} - \vec{X}_{r1}}{c_2} \right|; \overleftarrow{D}'_\delta = \left| \frac{\vec{c}_3 \cdot \vec{X}_{r3} - \vec{X}_{r1}}{c_3} \right| \tag{10} \\ \overleftarrow{X}'_1 &= \left| \frac{\vec{X}_\alpha - \vec{A}_1}{D'_\alpha} \right|; \overleftarrow{X}'_2 = \left| \frac{\vec{X}_\beta - \vec{A}_2}{D'_\beta} \right|; \overleftarrow{X}'_3 = \left| \frac{\vec{X}_\delta - \vec{A}_3}{D'_\delta} \right| \tag{11} \end{aligned}$$

$$\vec{X}'(t + 1) = \frac{\vec{X}'_1 + \vec{X}'_2 + \vec{X}'_3}{3} \tag{12}$$

where the indexes, $r1, r2, r3 \in \{1, 2, \dots, NP\}$ are approximately selected indexes then $r1 \neq r2 \neq r3$.

Attacking prey

To represent the attack on the prey numerically, in the process of attacking prey, seagulls will spiral motion behaviour in the air. This behaviour in $a, b, \text{ and } c$ planes is defined as,

$$a' = r \times \cos(k), \tag{13}$$

$$b' = r \times \sin(k), \tag{14}$$

$$c' = r \times k, \tag{15}$$

$$r = u \times e^{kv}, \tag{16}$$

Where, In the range $[0, 2\pi]$ r and k signify the radius of each turn of the spiral and random number respectively. e denotes the base of the natural logarithm and u and v are constants to describe the spiral shape. The following equations are used to calculate the updated position of the search agent.

$$\vec{P}'_s(x) = (\vec{D}_s \times a' \times b' \times c') + \vec{P}_{bs}(x) \tag{17}$$

where \vec{D}_s denotes the distance between the best-fit search agent and search agent. $\vec{P}'_s(x)$ stores the best solution and updates other search agents' positions and $\vec{P}_{bs}(x)$ is the best-fit search agent.

Search prey

The capacity of grey wolves to explore alternative places of prey is known as their exploration ability. The search agent is driven to deviate from the prey by the random values of A . When $|A| > 1$, Grey wolves are compelled to separate themselves from their prey. The pseudocode for the hybrid (IGWO-SOA) is provided in Algorithm 1.

Lane-Line Misbehaviour Detection using (IGWO-SOA) based ICNN

The input and output layers, as well as several hidden layers, make up the structure of a convolutional neural network (CNN). In this work, Lane line misbehaviour detection using (IGWO-SOA) based Improved Convolutional Neural Network (ICNN). Pooling layers, convolutional layers, and completely connected layers with active functions are the three main layers included in improved CNNs. Figure 1 displays the improved CNN structure. The proposed CNN has 7 layers: two pooling layers, two convolution layers, and three completely-connected layers. Transformation of input data to match the interruption of our model, then the architecture utilized to handle that follows.

Convolution layers 1 and 3 are represented. Each convolution layer adjusts kernels of three various sizes to fit different scales. Kernels of three different sizes (4, 6, and 8) are utilized in the first convolution layer. Kernel's number





Sivakumar and Manjunatha Rao

for every size is 8. The second convolution layer's kernel sizes are 6, 8, and 10 correspondingly. There were 24 kernels in this layer. The layer is set to 1 for the two convolutional layers. After each convolution layer, the generated lane line pictures are put to a size 2 max-pooling. There are three output sizes in the pooling layers. The three layers 5, 6, and 7 have 256, 32, and 4 neurons respectively. For the two convolution layers and the first two entirely connected layers, the rectified linear units (RELU) are employed as activation functions. The Softmax function is used as the layer 7 activation function. A batch size of 64 is used to train the CNN. The rate of learning is 0.01. 100 epochs are used to complete the training procedure. This method is to detect effectively lane-line misbehaviour.

RESULT AND DISCUSSION

The proposed hybrid (IGWO-SOA) algorithm's results are discussed in this section (ICNN). This research is mostly concerned with detecting vehicle lane line misbehaviour. The suggested approach is implemented in the python tool, in addition, compared with the present approach to prove the suggested method is more perfect than the other techniques. Moreover, under the road limit lane line misbehaviour detection process, evaluation metrics namely loss, accuracy, precision, recall and F-measure are calculated and compared to current state-of-the-art approaches. The below section explained the performance matrices of this approach.

Performance Metrics

This section outlines the proposed model's performance measures, with some of them being validated and tested. The following is a numerical representation of the evaluation of the performance measures used in the proposed and existing analyses:

Accuracy: The term of accuracy is described as the amount of lane-line misbehaviour detection made correctly. The mathematical representation is below,

$$Accuracy = \frac{tp + tn}{tp + fp + fn + tn}$$

Precision: Precision is defined as the prediction of positive class values by the proposed model accurately. The equation for the precision is given below,

$$Precision = \frac{tp}{tp + fp}$$

F-measure: F-measure means calculation of mean value using precision and recall which delivers the F-measure. It varies from 0 (worst performance) to 1 (highest performance). The formula for F-measure is as follows,

$$F - measure = \frac{2 \times (recall \times precision)}{recall + precision}$$

Recall: The sensitivity or measure recall is defined as the correctly predicted lane-line misbehaviour and lane-line non-misbehavior detection data by the proposed method. The formula for the recall is as follows,

$$Recall = \frac{tp}{tp + fn}$$

Loss: This is one of the quality metrics which aids to predict the performance of the prediction model. Furthermore, it is calculated based on the error function.

Based on the above standard formulas, these statistical measures are evaluated. For each measure, the overall proposed method performance and existing method performance are calculated and offered in the subsequent section.



**Sivakumar and Manjunatha Rao****Analysis of performance metrics for proposed and existing approaches**

The proposed and existing approaches' performance measures are detailed in the table below. The evaluated performance metrics are precision, accuracy, Loss, F-Measure, and recall of the proposed and existing are listed. Furthermore, the Gaussianfilter+Hough transform, Context-aware-data-centric misbehaviour scheme (CA-DC), Particle Filter (PF-MDS), CNN Based are considered the existing approaches. The comparative analysis of the performance metrics of the proposed (IGWO-SOA based ICNN) method with the existing approaches is shown in the below table. In table 2, for the proposed method (IGWO-SOA + ICNN), 0.9425 is the accuracy, 0.9213 is the precision value, 0.8996 is the value of the recall, 0.9010 is the F-Measure value and 0.2534 is the loss of the proposed method. The accuracy value is 0.8902, the precision value is 0.8865, the recall value is 0.8695, the F-measure value is 0.8512, and the loss value is 0.3562 for the Context-aware-data-centric misbehavior scheme (CA-DC-MDS) method. For the Gaussianfilter+Hough transform method, 0.8979 is the accuracy, 0.9165 is precision, 0.8832 is the recall, 0.8924 is F-measure and 0.3793 is the loss value. In addition, for Particle Filter (PF-MDS) method, 0.8321 is the accuracy value, 0.8302 is the precision value, 0.8123 is the recall value, 0.8065 is the F-Measure, and 0.4025 is the loss value. For the CNN-based method, 0.9284 is the accuracy value, 0.9188 is the precision value, 0.8922 is the recall value, 0.8954 is the F-Measure, and 0.3626 is the loss value.

Comparison of Performance metrics

This section detailly explained the comparison for the performing metrics of the proposed and existing methods such as PF-MDS, CA-DC, Gaussianfilter+Hough transform, and CNN. For analysing the proposed detection system, primarily confusion matrix is generated for the taken source code dataset based on statistical measures. To show the clarity of the proposed based detection of lane line misbehavior detection in-vehicle, its obtained results of training and validation process for the taken dataset are graphically displayed in the following figures. The below figures demonstrate the performance metrics of the proposed and existing approach like accuracy, precision, recall, f-measure, and loss are compared. From the analysis, it can be stated that the proposed technique achieves a good accuracy rate. Figure 3 demonstrates the comparison of the accuracy of the proposed and existing such as PF-MDS, CA-DC, GF+HT, and CNN. For the proposed technique, 0.9425 is the accuracy value is better than the other existing techniques. For PF-MDS, 0.8321 is the accuracy, 0.8902 is the accuracy of the CA-DC, 0.8979 is the accuracy of the GF+HT, and 0.9284 is the accuracy of the CNN. From the analysis, the proposed method is more accurate than the other techniques.

Figure 4 shows a precision comparison of the proposed and current approaches. Furthermore, For PF-MDS, 0.8302 is the precision, 0.8865 is the precision of the CA-DC, 0.9165 is the precision of the GF+HT, and 0.9188 is the precision of the CNN. The proposed method's precision value is better than the existing techniques. Figure 5 demonstrates the recall comparison, for the proposed method, 0.8996 is the value of the recall, 0.8123, 0.8695, 0.8832, and 0.8922 are recall values of the existing approaches such as PF-MDS, CA-DC, GF+HT, and CNN. The recall of the proposed is greater than the other techniques. Figure 6 shows the F-Measure of the proposed method and existing methods such as PF-MDS, CA-DC, GF+HT, and CNN. The proposed has a high F-measure value which is 0.9010. The others are 0.8065, 0.8512, 0.8924, and 0.8954 for PF-MDS, CA-DC, GF+HT, and CNN. The loss achieved by proposed attribute extraction with Improved Convolution Neural Network (ICNN) with hybrid IGWO-SOA algorithm model attains minimum prediction error and is shown in the above figure. Here, when the iteration is raised, the prediction error of the proposed solution decreases. Figure 7 demonstrates the loss of the proposed method is compared to the existing approaches such as CA-DC, CNN, PF-MDS, and GF+HT. For the proposed method, 0.2534 is the loss value, 0.4025 is the loss of the PF-MDS, 0.3562 is the loss of the CA-DC, 0.3793 is the loss value of the GF-HT, and 0.3626 is for CNN. When the loss acquired is decreased, then automatically the system performing will get improved this is fine recognized truth. The above fact by sustaining the proposed system works well by getting the least loss value. Thus, from the analysis, it is resolved that general performing is improved sufficiently for discovering lane line misbehavior detection of vehicles. From the overall analysis, it is concluded that the suggested IGWO-SOA based ICNN attains the best solution for the prediction system due to the incorporation of the optimization procedure. From the achievable result, it is proven that selected attributes are most appropriate in detecting the lane line misbehavior of the vehicles.



**Sivakumar and Manjunatha Rao**

CONCLUSION

A hybrid algorithm in terms of an improved convolutional neural network is proposed in this paper, which is utilized to detect lane line misbehavior of vehicles. In this paper, the proposed system is to discover the misbehaviour activity acquired from the original lane-line image. The adaptive histogram equalization is adopted to remove the noisy information contained in a lane line image. The AHE outcome lane line image is processed to the feature extraction phase whereas a hybrid algorithm, called Improved Grey wolf Optimization with Seagull algorithm (IGWO-SOA) is introduced to get the features. For categorizing the normal and misbehaviour activity from the lane-line image, IGWO-SOA based ICNN is proposed by minimizing the error function. Finally, the performance measures of the proposed method are compared with various methods and also compared with other existent techniques. The performance exhibits the proposed method improves accuracy and efficiency.

REFERENCES

1. Sarker, A., & Shen, H. (2018). A data-driven misbehavior detection system for connected autonomous vehicles. *Proceedings of the ACM on Interactive, Mobile, Wearable and Ubiquitous Technologies*, 2(4), 1-21.
2. Kamel, J., Ansari, M. R., Petit, J., Kaiser, A., Jemaa, I. B., & Urien, P. (2020). Simulation framework for misbehavior detection in vehicular networks. *IEEE transactions on vehicular technology*, 69(6), 6631-6643.
3. Wei, X., Zhang, Z., Chai, Z., & Feng, W. (2018, August). Research on lane detection and tracking algorithm based on improved hough transform. In *2018 IEEE International Conference of Intelligent Robotic and Control Engineering (IRCE)* (pp. 275-279). IEEE.
4. Zheng, F., Luo, S., Song, K., Yan, C. W., & Wang, M. C. (2018). Improved lane line detection algorithm based on Hough transform. *Pattern Recognition and Image Analysis*, 28(2), 254-260.
5. Deng, G., & Wu, Y. (2018, October). Double lane line edge detection method based on constraint conditions Hough transform. In *2018 17th International Symposium on Distributed Computing and Applications for Business Engineering and Science (DCABES)* (pp. 107-110). IEEE.
6. Zhang, H., Liang, J., Jiang, H., Cai, Y., & Xu, X. (2020). Lane line recognition based on improved 2D-gamma function and variable threshold Canny algorithm under complex environment. *Measurement and Control*, 53(9-10), 1694-1708.
7. Ghaleb, F. A., Zainal, A., Rassam, M. A., & Mohammed, F. (2017, November). An effective misbehavior detection model using artificial neural networks for vehicular ad hoc network applications. In *2017 IEEE Conference on Application, Information and Network Security (AINS)* (pp. 13-18). IEEE.
8. Kamel, J., Jemaa, I. B., Kaiser, A., Cantat, L., & Urien, P. (2019, December). Misbehavior Detection in C-ITS: A comparative approach of local detection mechanisms. In *2019 IEEE Vehicular Networking Conference (VNC)* (pp. 1-8). IEEE.
9. Gyawali, S., Qian, Y., & Hu, R. Q. (2020). Machine learning and reputation-based misbehavior detection in vehicular communication networks. *IEEE Transactions on Vehicular Technology*, 69(8), 8871-8885.
10. Gyawali, S., & Qian, Y. (2019, May). Misbehavior detection using machine learning in vehicular communication networks. In *ICC 2019-2019 IEEE International Conference on Communications (ICC)* (pp. 1-6). IEEE.
11. Sharma, P., & Liu, H. (2020). A Machine-Learning-Based Data-Centric Misbehavior Detection Model for Internet of Vehicles. *IEEE Internet of Things Journal*, 8(6), 4991-4999.
12. Sharma, P., Austin, D., & Liu, H. (2019, November). Attacks on machine learning: Adversarial examples in connected and autonomous vehicles. In *2019 IEEE International Symposium on Technologies for Homeland Security (HST)* (pp. 1-7). IEEE.
13. Kim, I. H., Bong, J. H., Park, J., & Park, S. (2017). Prediction of driver's intention of a lane change by augmenting sensor information using machine learning techniques. *Sensors*, 17(6), 1350.
14. Wang, Z., Ren, W., & Qiu, Q. (2018). Lanenet: Real-time Lane detection networks for autonomous driving. *arXiv preprint arXiv:1807.01726*.
15. Haris, M., Hou, J., & Wang, X. (2021). Multi-scale spatial convolution algorithm for lane line detection and lane offset estimation in complex road conditions. *Signal Processing: Image Communication*, 99, 116413.





Sivakumar and Manjunatha Rao

16. Hasrouny, H., Samhat, A. E., Bassil, C., &Laouiti, A. (2019). Misbehavior detection and efficient revocation within VANET. *Journal of Information Security and Applications*, 46, 193-209.
17. Zhang, C., Chen, K., Zeng, X., &Xue, X. (2018). Misbehavior detection based on support vector machine and Dempster-Shafer theory of evidence in VANETs. *IEEE Access*, 6, 59860-59870.
18. Zacharias, J., &Fröschle, S. (2018, December). Misbehavior detection system in VANETs using local traffic density. In *2018 IEEE Vehicular Networking Conference (VNC)* (pp. 1-4).IEEE.
19. Boualouache, A., Soua, R., & Engel, T. (2020, May). Sdn-based misbehavior detection system for vehicular networks. In *2020 IEEE 91st Vehicular Technology Conference (VTC2020-Spring)* (pp. 1-5).IEEE.
20. A Ghaleb, F., Saeed, F., Al-Sarem, M., Ali Saleh Al-rimy, B., Boulila, W., Eljjaly, A. E. M., ...&Alazab, M. (2020). Misbehavior-aware on-demand collaborative intrusion detection system using distributed ensemble learning for VANET. *Electronics*, 9(9), 1411.
21. Sultana, R., Grover, J., & Tripathi, M. (2020, December). A Novel Framework for Misbehavior Detection in SDN-based VANET. In *2020 IEEE International Conference on Advanced Networks and Telecommunications Systems (ANTS)* (pp. 1-6).IEEE.
22. Sumithra, S., & Vadivel, R. Ensemble Miscellaneous Classifiers Based Misbehavior Detection Model for Vehicular Ad-Hoc Network Security.
23. Kamel, J., Wolf, M., van der Hei, R. W., Kaiser, A., Urien, P., &Kargl, F. (2020, June). VeReMi extension: A dataset for comparable evaluation of misbehavior detection in VANETs. In *ICC 2020-2020 IEEE International Conference on Communications (ICC)* (pp. 1-6).

Table 1 : Algorithm 1

<i>Pseudo-code of the (IGWO-SOA) algorithm</i>
<p>Input: (N) denotes the various search agent and (T) denotes the various iterations Output: the location of the Objective function's -MSE and its value Initialize search agents' population //Initialization Started the grey wolf population $X_i (i = 1, 2, \dots, n)$ Start a, A, and C. Compute Each search agent's MSE X_α = the finest search agent X_β = the second-finest search agent X_δ = the third finest search agent while (t<Max number of iterations) For each search agent if A <1 compute $\overleftarrow{D}_\alpha, \overleftarrow{D}_\beta, \overleftarrow{D}_\delta$ using (10) end if // Updating The equation to update the current search agent's position (13 to 16) end for Update a, and C by (9) A is updated by equation (8) Estimate the MSE of all search agents Update $X_\alpha, X_\beta, X_\delta$ T=t+1 End while Return X_α</p>





Sivakumar and Manjunatha Rao

Table 2: Performing comparison of the proposed and existing methods

Predictive methods	Performance of Classifier				
	Accuracy	Precision	Recall	F-Measure	Loss
PF-MDS	0.8321	0.8302	0.8123	0.8065	0.4025
CA-DC	0.8902	0.8865	0.8695	0.8512	0.3562
Guassianfilter+Hough transform	0.8979	0.9165	0.8832	0.8924	0.3793
CNN	0.9284	0.9188	0.8922	0.8954	0.3626
Proposed method (IGWO-SOA based ICNN)	0.9425	0.9213	0.8996	0.9010	0.2534

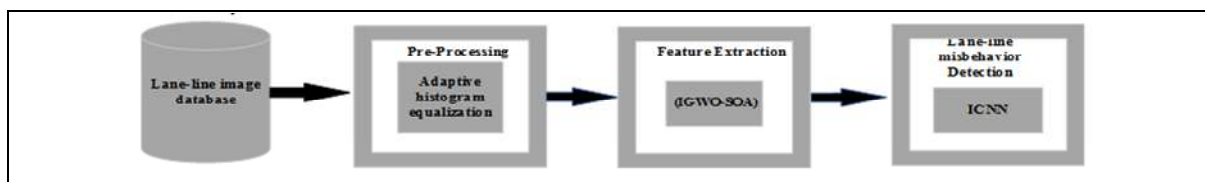


Figure 1: Block diagram

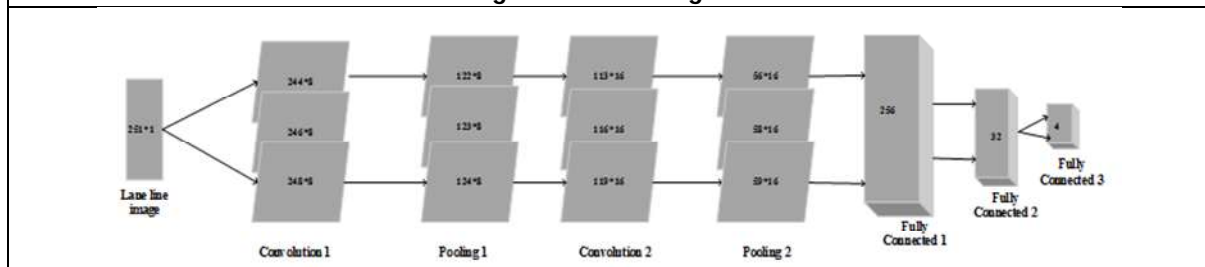


Figure 2: The structure of the ICNN

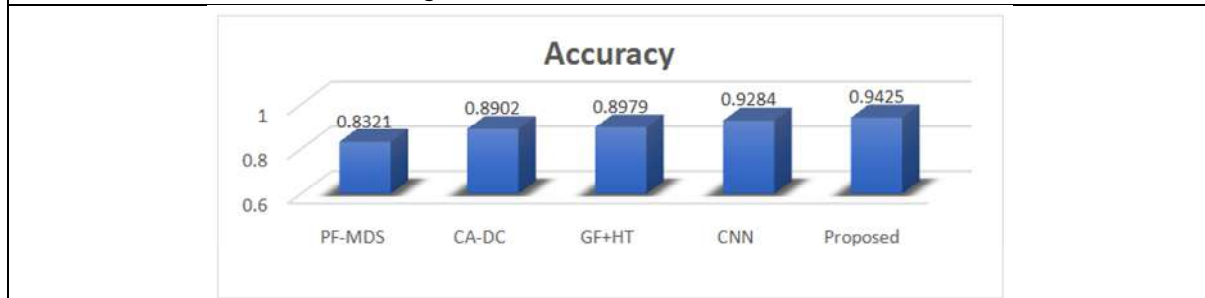


Figure 3: Accuracy of proposed and Existing methods

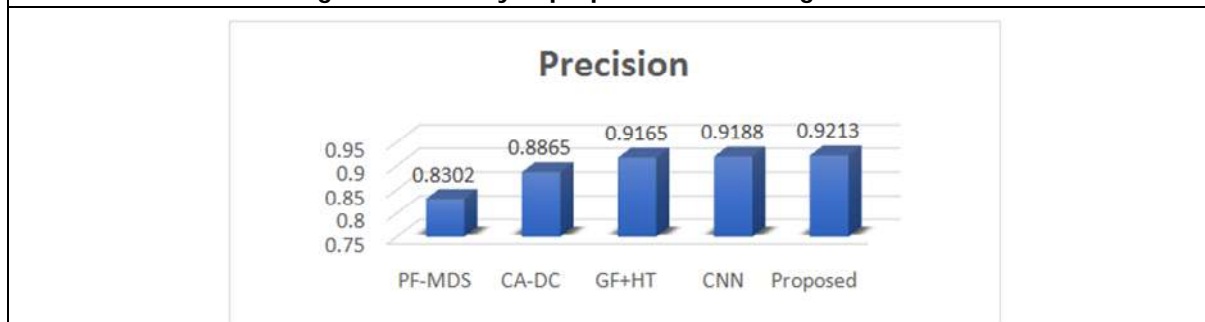


Figure 4: Precision of proposed and Existing methods





Sivakumar and Manjunatha Rao

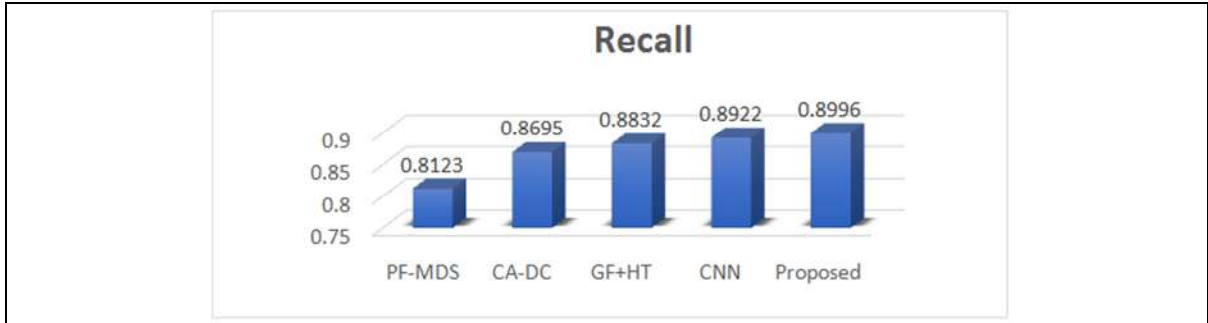


Figure 5: Recall of the proposed method and existing method

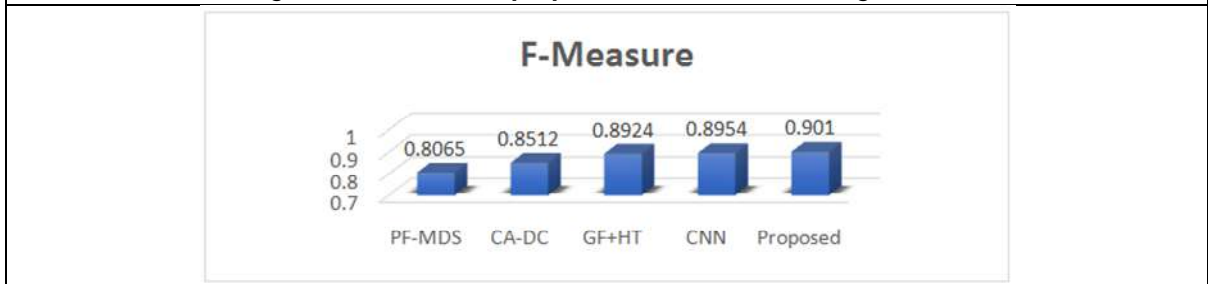


Figure 6: F-Measure of the proposed and existing method



Figure 7: The loss of the proposed and existing methods





The Determinants of Capital Structure - Empirical Evidence from Select Indian Pharmaceutical Companies

B.Yazhini^{1*} and D.Geetha²

¹Research Scholar, Department of Commerce, Avinashilingam Institute for Home Science and Higher Education for Women, Coimbatore, Tamil Nadu, India.

²Professor and Head, Department of Commerce, Avinashilingam Institute for Home Science and Higher Education for Women, Coimbatore, Tamil Nadu, India.

Received: 08 Dec 2021

Revised: 30 Dec 2021

Accepted: 13 Jan 2022

*Address for Correspondence

B.Yazhini

Research Scholar,

Department of Commerce,

Avinashilingam Institute for Home Science and Higher Education for Women,

Coimbatore, Tamil Nadu, India.

Email: yazhinibabu5777@gmail.com



This is an Open Access Journal / article distributed under the terms of the **Creative Commons Attribution License** (CC BY-NC-ND 3.0) which permits unrestricted use, distribution, and reproduction in any medium, provided the original work is properly cited. All rights reserved.

ABSTRACT

Capital Structure in a firm employs funds from different sources to its growth and overall operations. The sources include Equity Shares, Preference Shares and Debentures etc. Company's noteworthy decision is to finalize the suitable capital structure. Capital Structure is still a debate among the researchers and academicians. Hence to identify the "Determinants of Capital Structure – Empirical Evidence from select Indian Pharmaceutical Companies" is indeed important. The main objective of the study is "To identify the major factors determining Capital Structure and the impact of Capital Structure on Financial Performance". Ten Pharmaceutical Companies is chosen as a sample on the source of the subsequent criteria: BSE Listed Companies with continuous accessibility of data for 15 years (2007-2021). The major factors were "Firm Size", "Ownership Structure", "Liquidity Position" and "Leverage". The Independent Variables were "Total Debt Ratio", "Long Term Debt Ratio" and "Short Term Debt Ratio". "Return on Equity", "Return on Asset" and "Return on Capital Employed" were taken as Dependent Variables. Statistical tools like Factor Analysis, Multiple Regression, Panel Data Analysis and SEM Model were applied. The appropriate proportion of Capital Structure helps the companies to increase their market value in the economy.

Keywords: Capital Structure, Financial Performance and SEM Model Approach.



**Yazhini and Geetha****INTRODUCTION**

Capital structure is a mixture of debt and equity to fund firm's operations, which is essential for its successful management. Debt and equity are the key funding options used by all companies, according to Umar (2012). The capital structure of a company is defined as, "The intensity of debt or equity options used by the company to fund its operations. The capital structure is an important technique for reducing the cost of capital". Financial Performance is a subjective assessment of a company's ability to produce income from its primary business resources. Financial performance analyses profitability and liquidity, and a useful metric for stakeholders to assess a company's past financial performance and current position. Business Entity must choose an appropriate capital structure.

Globally in the Pharmaceutical production, India ranks third in terms of volume and fourteenth by value. Domestically the country's Pharmaceutical Industry is well established with 10,500 manufacturing units and a huge set-up of 3,000 drug firms. (www.ibef.org/industry/pharmaceutical-india.aspx). In FY2021, Indian pharmaceutical exports reached \$16.28 Crores, including drug formulations, bulk medicines, surgical products, intermediates, Ayush & herbal products and biological. India accounts for more than half of the global vaccine market, 25% of medicines for the UK and 40% of generic demand for the US. In order to boost Pharmaceutical manufacturing domestically by 2023, India plans to set up a fund nearly Rs. 1 lakh crore (US\$ 1.3 billion). As a result, a company's capital structure must be effective in order to achieve financial success in the challenging business environment. There is still a debate among the academicians and researchers about this topic. Hence the study is carried out, "To examine the Determinants of Capital Structure of Indian Pharmaceutical Companies".

PROBLEM STATEMENT

Capital Structure is one of the essential decision for the successful management of the concern. The appropriate proportion of debt and equity helps the business to increase its market value as a whole. The Capital Structure determines the ability of concern to explore various opportunities through investment and to remain optimal in the competitive Business Environment. Hence, the study on "Determinants of Capital Structure – Empirical Evidence from select Indian Pharmaceutical Companies" is needed. Because, Pharmaceutical Industry is most essential for the development of Economy. Moreover, it is also considered as one of the major FDI attracting Sector in India (www.mapsofindia.com).

RESEARCH GAP

The studies related to "Determinants of Capital Structure" were numerous in the field of corporate finance. Most of the researches in this area have been conducted on Manufacturing sectors, Banks etc. Only a very few researchers have studied about this concept using Panel Data Regression analysis and Structural Equation Modeling in the Pharmaceutical Companies in India. Hence, the current study is carried out to fulfill this research gap. The present study will help to determine the Optimum Capital Structure take suitable Financial Decision for further projects and also to enhance their market value.

OBJECTIVES

1. To study the determinants of Capital Structure and to examine the relationship between major factors and Capital Structure.
2. To analyze the impact of capital structure on financial performance.

HYPOTHESIS

Hypothesis framed for the research are,

H01: There is no significant effect of Major Factors on Capital Structure

H02: There is no significant effect of Capital Structure on Financial Performance.





Yazhini and Geetha

Breush – Pagan LM Test

H03: If $P > 0.05$, there is no significant so Pooled OLS Regression is accepted

H3: If $P < 0.05$, there is a significant so Random Effect Model is accepted

Hausman Test

H04: If $P > 0.05$, there is no significant so Random Effect Model is accepted

H4: If $P < 0.05$, there is a significant so Fixed Effect Model is accepted

RESEARCH METHODOLOGY

SAMPLE SELECTION CRITERIA

1. Companies listed in BSE.
2. Continuous data availability for 15 years (2007-21).

List of Pharmaceutical Companies

Bulk Drugs & Formulations

1. Cadila
2. IPCA Labs
3. Natco Pharma
4. IOL Chemicals
5. J.B Chemicals
6. TTK Healthcare
7. Unichem Labs
8. Bal Pharma
9. Indian Drugs
10. Glenmark

Source: Capital Line Database

TOOLS & TECHNIQUES

1. Factor Analysis
2. Multiple Regression
3. Panel Data Regression Analysis
4. Structural Equation Modeling

DATA ANALYSIS & INTERPRETATION

The table2 indicates a mean of LTDR(0.15) and STDR is (0.33).This means that the Pharmaceutical Company acquire less Long Term Borrowing compared to Short Term Borrowing.The variance of TDR which is less than mean,so there is a consistency in borrowing capital.There is no consistency in DER,ROA and ROCE because its variance is greater than the mean.Size,Liquidity are negatively skewed.The remaining variables are greater than 1.So they are highly skewed.In Kurtosis,all the selected independent and dependent variables are greater than1.So,they are Leptocurtic. Kaiser- Meyer – Olkin Test Measures of Sampling Adequacy: 0.654

The table3 indicates that KMO test value 0.654>0.5, is valid and acceptable to carry out data reduction technique. "The Growth, Asset Tangibility, Size and Non Debt Tax Shield were loaded in the first factor Firm Size". Debt Serving Capacity and Cost of Debt were loaded in the second factor "Ownership Structure". Profitability, Liquidity were loaded in the third factor "Liquidity Position" .Debt Equity Ratio and Tax is loaded in the third factor "Leverage."





Yazhini and Geetha

MULTIPLE REGRESSION MODEL

The specified form for the study is

$$Y = \beta_0 + \beta_1 X_1 + \beta_2 X_2 + \beta_3 X_3 + e$$

"Y = Dependent Variable, β_0 =Constant, $\beta_1, \beta_2, \beta_3$ = Coefficient of explanatory variable, X= Independent Variable and e= Error Term"

$$TDR = \beta_0 + \beta_1 FS + \beta_2 OS + \beta_3 LP + \beta_4 LV + e$$

$$LTDR = \beta_0 + \beta_1 FS + \beta_2 OS + \beta_3 LP + \beta_4 LV + e$$

$$STDR = \beta_0 + \beta_1 FS + \beta_2 OS + \beta_3 LP + \beta_4 LV + e$$

The Table:4 indicates that the R^2 value 0.036 or 3.6% variance in "Total Debt Ratio", 0.30 or 30% variance in "Long Term Debt Ratio" and 0.25 or 25% variance in "Short Term Debt Ratio" through "Firm Size", "Ownership Structure", "Liquidity Position" and "Leverage". At 5% level, "Ownership Structure" and "Leverage" has an impact on LTDR and STDR. "Firm Size", "Ownership Structure" and "Liquidity Position" has an impact on STDR. "Hence Null Hypothesis H01 is rejected and alternative hypothesis, there is a significant effect of major factor on Capital Structure is accepted". It shows that increase in Total Debt increases the value of the company. The following equations derived:

$$LTDR = 0.159 + 3.299OS + 6.384LV$$

$$STDR = 18.998 - 4.257FS + 4.204OS - 3.653LP$$

Panel Data Regression Analysis

Model 1

From the Table 5, the Breush-Pagan test shows that only Time Series are significant. "Hence Null Hypothesis H03 is rejected and alternative hypothesis, If $P < 0.05$, there is a significant so Random Effect Model is accepted". From Hausman test, it is understood that the "Null Hypothesis H04 is rejected and alternative hypothesis, If $P < 0.05$, there is a significant so Fixed Effect Model is accepted". From Table 6, it has been found that the LTDR and STDR is negatively correlated with ROA. "Hence Null Hypothesis H02 is rejected and alternative hypothesis, there is a significant effect of Capital Structure on Financial Performance is accepted". The R-Square value (0.3950) shows 39% variations. F Statistic (5.071) supports the Model.

$$ROA = 30.732 - 45.109LTDR - 30.107STDR$$

Model 2

From the Table7, the Breush-Pagan test shows that Cross section and Time Series are not significant. "Hence, alternative hypothesis H3 is rejected and Null hypothesis, If $P > 0.05$, there is no significant so Pooled OLS Regression is accepted". From Table8, it has been found that the LTDR is negatively correlated with ROE. "Hence Null Hypothesis H02 is rejected and alternative hypothesis, there is a significant effect of Capital Structure on Financial Performance is accepted". The R-Square value (0.0538) has 5% variation in ROE. F-Statistic (2.770) with probability value (0.043) shows that the model is fit.

$$ROE = 24.145 - 112.72LTDR$$

Model: 3

From Table9, the BP test shows that P value is $0.0016 < 0.05$. "Hence Null Hypothesis H03 is rejected and alternative hypothesis, If $P < 0.05$, there is a significant so Random Effect Model is accepted". From Hausman Test, the P value is $0.000 < 0.05$. "Null Hypothesis H04 is rejected and alternative hypothesis, If $P < 0.05$, there is a significant so Fixed Effect Model is accepted". The Table:10 shows that LTDR is negatively correlated with ROCE. "Hence Null Hypothesis H02 is rejected and alternative hypothesis, there is a significant effect of Capital Structure on Financial Performance is accepted". The R-Square value (0.3950) shows The R-Square value (0.292) shows 29% Variation in ROCE. F-Statistics (6.143) fits the model well.

$$ROCE = 22.651 - 63.446LTDR$$





Yazhini and Geetha

STRUCTURAL EQUATION MODELING

A Structural Equation Modeling is a statistical technique, a combination of Regression and Factor Analysis. The associations between the conjunctural constructs are represented by regression within the factors. In this study it was developed "To examine the relationship between Major Factors, Capital Structure and Financial Performance". "MFCS – Major Factors of Capital Structure, CS- Capital Structure, FP-Financial Performance FAC1-Firm Size, FAC2- Ownership Structure, FAC3-Liquidity Position, FAC4- Leverage, TDR-Total Debt Ratio, LTDR-Long Term Debt Ratio, STDR-Short Term Debt Ratio, ROA-Return on Asset, ROE-Return on Equity and ROCE-Return on Capital Employed". The table 11 exhibits the Goodness of the fit Index for the measurement model. The chi-square value is 48.24, degrees of freedom: 29, $P \leq 0.01$. RMSEA ("Root Mean Square Error of Approximation") is 0.08 which indicates the model is fit. CFI ("Comparative Fit Indices") is 0.978 which means the good fit, GFI ("Goodness of Fit Index") is 0.938 indicates a good model. NFI ("Normal Fit Index"), the value is 0.871 and AGFI ("Adjusted Goodness of Fit Index") is 0.883 also fulfill the recommended values. It shows that the model is fit.

The Table 12 shows that the Major factors of capital Structure is influenced by the Ownership Structure (-.233), Liquidity Position (.398) and Leverage (-.252) 1.00 at one percent significant level. Capital Structure is significantly influenced by TDR (1.00), LTDR (1.222) and STDR (3.594) at one percent level. Furthermore, the Financial Performance is significantly influenced by ROA (1.00), ROE (1.166) and ROCE (1.120) at one percent level. The Hypothesis results shows that "There is a significant relationship between Major Factors, Capital Structure and Financial Performance". A Proper Capital Structure helps the company to enhance their financial performance of select Pharmaceutical Companies.

FINDINGS

- "Debt Serving Capacity" and "Cost of Debt" is loaded in the factor "Ownership Structure". It shows that even if EBIT suffers a decline, the firm can meet its interest commitment in their Business operations.
- "Growth", "Asset Tangibility", "Non Debt Tax Shield" and "Size" is loaded in the factor "Firm Size". It reveals that the firm can access the funds in capital market with larger firm size.
- "Profitability" and "Liquidity" were loaded in the factor "Liquidity Position" and "Debt Equity Ratio" and "Tax" were loaded in the factor "Leverage".
- "Firm Size", "Ownership Structure" and "Liquidity Position" has an impact on "Total Debt Ratio", "Long Term Debt Ratio" and "Short Term Debt Ratio".
- At 5% level, "Total Debt Ratio", "Short Term Debt Ratio" has influence on "Return on Asset" and "Return on Capital Employed".
- "Long Term Debt Ratio" shows negative relationship "Return on Asset", "Return on Equity" and "Return on Capital Employed". "Short Term Debt Ratio" has pessimistic relationship only with "Return on Asset", "Total Debt Ratio" has no association with financial performance.

SUGGESTION

- There exists a significant relationship within "Major Factors", "Capital Structure" and "Financial Performance" of select Indian Pharmaceutical Companies.
- The "Long Term Debt" can be borrowed with lower interest. So, that the negative impact on financial performance can be reduced.
- In order to increase the financial performance, the select Pharmaceutical Companies can reduce debt and can increase the issue of equity shares
- The affirmative relationship between "Total Debt Ratio" and "Return on Asset" denotes that an increase in debt capital would enhance the financial performance of the concern.
- In order to increase the financial performance it should focus on productivity of the business.



**Yazhini and Geetha**

- In order to optimize the "Return on Asset" and "Return on Equity" through productivity by adapting new technologies

CONCLUSION

The result of study shows that "The Capital Structure has a significant impact on Financial Performance of select Indian Pharmaceutical Companies". The Factor Analysis shows that "Firm Size", "Ownership Structure", "Liquidity Position" and "Leverage" are the factors determining Capital Structure. A sound Capital Structure ensures that the firm's financial needs are defined. For the best possible operations, funds are raised in various proportions from different sources. It helps to increase the wealth of the economy.

REFERENCES

1. Archana Malik, Harjit Singh (2020) "Impact of Capital Structure on Financial Performance of Selected Multinational Companies in India". 9(4), 2510-2515.
2. Dr. Brajaballav Pal, Priti Damai (2020) "IMPACT OF CAPITAL STRUCTURE ON PROFITABILITY: EVIDENCE FROM INDIAN AUTOMOBILE COMPANIES". 7(18), 4361-4369.
3. Tom Jacob and Ajina VS (2020) "Capital Structure and Financial Performance of Pharmaceutical Companies in Indian Stock Exchange". 9(2), 24-30.
4. Rajbinder Kaur, Arup Kumar Chattopadhyay, Debdas Rakshit (2020) "Determinants of Capital Structure with Reference to Select Indian Companies: A Panel Data Regression". 16(2), 1-14.
5. Dr. Girija Nandini (2020) "Effect of Capital Structure on Financial Efficiency of Top Ten Automobile Companies in India". 33(1), 213-225.
6. Ajaya Kumar Panda & Swagatika Nanda, 2020. "Determinants of capital structure; a sector-level analysis for Indian manufacturing firms," 69(5), 1033-1060.
7. Narinder Pal Singh, Mahima Bagga (2019) "The Effect of Capital Structure on Profitability: An Empirical Panel Data Study". 8(1), 1-13.
8. Nur Ainna Ramli, Hengky Latan, Grace T. Solovida (2019) "Determinants of Capital Structure and firm financial performance – APLS SEM Approach: Evidence from Malaysia and Indonesia". 71(2), 148-160.
9. Assad Naim Nasimi, Rashid Naim Nasimi (2018) "Effect of Capital Structure on Firms' Profitability: An Empirical Evidence from Pakistan Stock Exchange (PSX)". 9(11), 57-68.
10. Barnali Chaklader and Deepak Chawla (2016) "A Study of Determinants of Capital Structure through Panel Data Analysis of Firms Listed in NSE CNX 500". 20(4), 267-277.





Yazhini and Geetha

Table:1 Variable Description

Variables	Measures
Total Debt Ratio	Total Debt to Total Asset
Long Term Debt Ratio	Long Term Debt to Total Asset
Short Term Debt Ratio	Short Term Debt to Total Asset
Growth	Percentage Change to Total Asset
Asset Tangibility	Net Fixed Asset to Total Asset
Profitability	Profit After Tax to Sales
Cost of debt	Earnings before interest and Tax to Long Term Debt
Tax	Tax Provision to Profit Before Tax
Debt serving capacity	PBDIT to Total Interest
Non debt tax shield	Depreciation to Total Asset
Debt equity ratio	Total Debt to Total Equity
Size	Natural Log of Total Asset
Liquidity	Total Current Asset to Total Current Liabilities
Return on Asset	Net Profit to Total Asset
Return on Equity	Profit after interest & Tax to Equity Capital * 100
Return on Capital Employed	Earnings before interest and tax to Capital Employed

Table: 2 Descriptive Statistics

	Mean	Std dev	Variance	Skewness	Kurtosis
TDR	0.15	0.26	0.07	4.28	28.23
LTDR	0.15	0.13	0.01	1.25	1.04
STDR	0.33	0.25	0.04	4.27	23.78
GROWTH	0.15	0.18	0.03	1.28	5.89
ASSETTANG	0.38	0.15	0.02	0.065	1.295
PROFITABILITY	0.14	0.10	0.01	3.081	16.88
COST OF DEBT	19.96	59.95	3.59	3.04	8.34
TAX	0.19	1.33	0.04	1.47	3.69
DEBT SERVING CAPACITY	27.39	11.86	1.13	6.37	46.02
NON DEBT TAX SHEILD	0.02	106.37	0.00	10.71	123.62
DEBT EQUITY RATIO	0.91	.973	10.43	1.44	1.343
SIZE	2.97	1.28	0.31	-0.25	-1.355
LIQUIDITY	1.79	5.22	1.20	-1.89	10.90
ROA	7.37	3.39	117.59	11.56	17.43
ROE	7.89	13.777	5.04	2.56	138.98
ROCE	12.61	5.32	170.95	1.241	8.06
N	150	150	150	150	150





Yazhini and Geetha

Table: 3 Factor Analysis

Factors	Variables	Factor Loading	% Variance	Eigen Value
Firm Size	Growth	0.707	21.265	1.00
	Asset Tangibility	0.697		
	Non Debt Tax Shield	0.824		
	Size	0.576		
Ownership Structure	Debt Serving Capacity	0.910	20.227	0.99
	Cost of Debt	0.935		
Liquidity Position	Profitability	0.767	14.311	0.99
	Liquidity	0.812		
Leverage	Debt Equity Ratio	0.752	12.859	0.99
	Tax	0.593		

Source: Computed Data

Table: 4 Major Factors and Capital Structure

Variables	Beta Coefficient	T-value (TDR)	Sig	Beta Coefficient	T-value (LTDR)	Sig	Beta Coefficient	T-value (STDR)	Sig
Constant	0.151	7.308	0.00	0.159	17.266	0.000	0.334	18.998	0.00
FS(Factor1)	-0.028	-1.376	0.171	-0.025	-2.753	0.070	-0.076	-4.257	0.00
OS(Factor2)	0.029	1.425	0.156	0.030	3.299	0.000	0.074	4.204	0.00
LP(Factor 3)	0.024	1.152	0.251	-0.015	-1.574	0.118	-0.066	-3.653	0.00
LV(Factor4)	0.010	.489	0.625	0.059	6.384	0.000	-0.013	-.694	0.489
R.Sq	0.036	R.Sq	0.30	R.Sq	0.25				

Source: Computed Data

Table: 5 Breush –Pagan Test and Hausman Test

	Cross - Section	Time	Both
Breush – Pagan Statistics P- Value	0.213034 (0.6444)	35.16235 (0.0000)	35.37539 (0.0000)
	Chi-Square	Chi-Square d.f	P-Value
Hausman Test Time Random	20.7829	3	0.0001

Source: Computed Data

Table: 6 Fixed Effect Model for Return on Asset

Dependent Variable : ROA		
Sample: 2007 to 2021		
Total Panel Observations:150 (Cross Section 10 x Periods 15)		
	Co-efficient	Probability
C	30.732	0.0000
TDR	-10.425	0.2790
LTDR	-45.109	0.0080
STDR	-30.107	0.0013
R.Sq	0.3950	
Adjusted R.Sq	0.3171	
F-statistics	5.071	
P-value	0.0000	

Source: Computed Data





Yazhini and Geetha

Table:7 Breush –Pagan Test

	Cross-section	Time	Both
BP test value	0.178022 (0.6731)	0.253860 (0.6144)	0.431882 (0.5111)

Table:8 Pooled Ordinary Least Square for Return on Equity

Dependent Variable : ROE		
Sample:2007 to 2021		
Total Panel Observations:150 (Cross Section 10 x Periods 15)		
	Co-efficient	Probability
C	24.145	0.037
TDR	1.037	0.965
LTDR	-112.7298	0.0040
STDR	10.463	0.663
R-Sq	0.0538	
Adjusted R-Sq	0.0344	
F Statistics	2.770	
P-value	0.043	

Source: Computed Data

Table:9 Breush –Pagan Test and Hausman Test

Breusch-Pagan Test	Cross Section	Time	Both
	9.975089 (0.0016)	0.5653 (0.4521)	10.540 (0.0012)
Chi Square Statistic	29.995		
Chi-Sq df	3		
Probability	0.000		

Table:10 Fixed Effect Model for Return on Capital Employed

Dependent Variable :ROCE		
Sample:2007 to 2021		
Total Panel Observations:150 (Cross Section 10 x Periods 15)		
	Co-efficient	Probability
C	22.651	0.0000
TDR	-2.801	0.492
LTDR	-63.466	0.0040
STDR	2.646	0.589
R-Sq	0.3498	
Adjusted R-Sq.	0.292	
F Statistics	6.143	
P-value	0.0000	

Source: E-Views





Yazhini and Geetha

Table: 11 Goodness of fit index measurement model

Fit indices		Model value	Recommended value
Chi-Square	(X ²)	52.874	
	DF	29	
	P value	0.004	P<=0.05
CMIN/DF		1.823	
GFI		.938	0.90 or 0.95
AGFI		.883	Value close to 0.9
CFI		.935	Value >0.90
RMSEA		.074	Between 0.05 and 0.08
NFI		.871	Value >0.90
TLI		.898	0.90 or 0.95

Source: Computed Data

Table: 12 Regression Weights

Measured variable		Latent variable	Estimates	SE	CR	P	
Firm Size	<---	MFCS	1.000				Significant
Ownership Structure	<---		-.233	.079	-2.946	.003	Significant
Liquidity Position	<---		.398	.097	4.122	.000	Significant
Leverage	<---		-.252	.076	-3.341	.000	Significant
TDR	<---	CS	1.000				Significant
LTDR	<---		1.222	.506	2.416	.016	Significant
STDR	<---		3.594	1.596	2.252	.024	Significant
ROA	<---	FP	1.000				Significant
ROE	<---		1.166	.364	3.205	.001	Significant
ROCE	<---		1.120	.239	4.682	.000	Significant

Source: Computed Data

“S.E - Standard Error” , “C.R. – Critical Ratio”

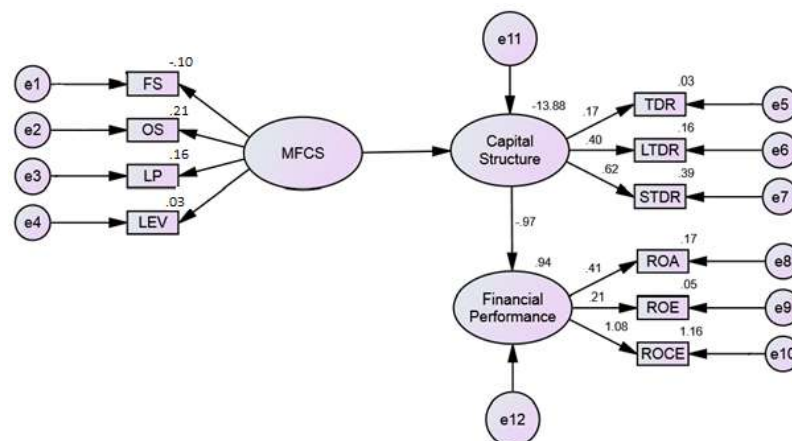


Fig.1. SEM Model





Energy Shaping Control of Grid Connected Parallel Interleaved Converter for Current Reduction

N. Rajeswaran¹, P. Marimuthu¹ and S.Lavanya^{2*}

¹Department of EEE, Malla Reddy Engineering College, Maisammaguda, Hyderabad, India.

²PG Scholar, Department of EEE, Malla Reddy Engineering College, Maisammaguda, Hyderabad, India.

Received: 01 Sep 2021

Revised: 23 Sep 2021

Accepted: 22 Oct 2021

*Address for Correspondence

S.Lavanya

PG Scholar,

Department of EEE,

Malla Reddy Engineering College,

Maisammaguda, Hyderabad, India.

Email: lavanyanani15@gmail.com



This is an Open Access Journal / article distributed under the terms of the **Creative Commons Attribution License** (CC BY-NC-ND 3.0) which permits unrestricted use, distribution, and reproduction in any medium, provided the original work is properly cited. All rights reserved.

ABSTRACT

This paper implements to control a circulating current with low frequencies produced by parallel interleaved converters. The magnetically linked inductors are used for inverters to parallelize in this configuration. The harmonic content in the output voltage is minimized by incorporating carrier interleaving. This consequences in a greater circulating current to flow in the course of the two Voltage Source Converters (VSCs). The mutual inductance of the Coupled Inductors (CI) is competently reduce the components of circulating currents with high frequencies. The components of low frequencies effectively cannot filter by coupled inductors. The coupled inductors are lead to saturation when the circulating currents are very high under uncontrolled due to this the converter have the higher switching losses, and disgrace the overall performances. The delivered active as well as reactive powers to the grid are effectively controlled with this controller and also it decreases the amount of circulating current with the low frequency. The performances of the converter are found by simulation and compared with the performance of Linear Quadratic (LQ) control and classical PI control. The simulation shows a good performance in the proposed method.

Key Words: Voltage Source Inverter, Coupled Inductor, Port Controlled Hamiltonian, Linear Quadratic Control, Proportional Controller, Pulse Width Modulation





Rajeswaran et al.,

INTRODUCTION

The converters have been a lot of pioneering configurations were incorporated to manage the escalating power received from non conventional sources of energy. For such applications, multi-pulse converters, matrix converters and multi-level converters were offered in [1]. Another topology was projected recently based on the parallelization of typical two-level inverters to attain high power converters by coupled inductors [2, 3]. The various offers offered by parallelized inverters are phase shifted by 180° to the system; the benefits are size declined of the output filter, multilevel output, and also reduction of Common Mode Voltage in [4, 5]. The acceptable level of circulating currents with lofty frequency components can be shortened by a tolerable choice of coupled inductors in [6]. In [7] proposed the various design procedures of these filtering components. In [8] proposed a reduction of circulating current in the system and common mode voltage by three-level SVM. The PWM techniques were proposed in [9] to diminish the crest value of the circulating current by discriminating harmonic elimination. The PI controllers inputs are identified from the circulating currents from each phase were presented in [10].

The modulating signals added to controller output of only one converter of the two parallelized VSCs and the proposed scheme of modified DPWM were presented in [11]. In [12], the deadbeat control approaches were implemented in order to reduce the amount of circulating currents. The ZSCC was suppressed by a modular two-level interleaved converter with carrier Phase Shifted PWM was presented in [13]. The ES control strategy was implemented in DFIG wind turbine has been presented in [14].

CONTROL METHODOLOGY

The scheme of method for the system MMC with VCM as shown in Fig. 1, it consists of five controllers. The five controllers and their control objectives are: (i) a VSI two-layer controller is used to transfer the amount of power generated into the ac grid, (ii) a leg energy controller is used to control the amount of capacitors energy stored in the SMs in order to make sure the stable operation of the MMC, (iii) a phase - disposition pulse width modulation (PD-PWM) type modulator is used to determines the SMs that need to be switched ON and a voltage balancing algorithm (VBA) to balance the capacitors voltage of the SMs, (iv) a amount of circulating current suppressing controller to suppress the inner circulating currents (v) a VCM controller to reimburse for the difference of voltage during unbalance conditions and both the VCM controller and circulating current suppressing controller are decoupled from the main power stage control. The fig. 2 shows the two layers of VSI controller is wrecked into three blocks: (i) power-to-current transformation (ii) a Phase Locked Loop for synchronization of AC grid and (iii) the conventional control of current in the rotating reference frame of direct quadrature to transfer the amount of power generated into the side of AC grid at an random power factor.

Phase Locked Loop

The synthesizing the information of phase and frequency of the system by using the technique of PLL. The PLL computes the grid phase angle by sensing the grid voltage and projecting the corresponding space vector onto the dq axis. The q component is then forced to be equal to zero ($v_q = 0$) with the help of a PI controller as depicted in fig. 2. By doing so, the dq axis will be rotating at the same speed as the grid angular frequency. This angle is then used to synchronize the dq reference frame for the control of inner current of the system.

Power to Current Transformation

The active power and reactive power references (P_{ref} , Q_{ref}) are reliant on the load requirement. From dq currents be able to be computed accordingly and this equation is based on the assumption that the PLL is capable to force V_q to zero.

$$P_{ref} = \frac{3}{2} v_d I_d^{ref} \quad (1)$$

$$Q_{ref} = -\frac{3}{2} v_d I_d^{ref} \quad (2)$$





Rajeswaran et al.,

Inner Current Control

The AC side dynamics of the VSI can be described by the following dynamic phasor relation in the 'abc' reference frame, m_j , v_j and i_j are the three phase AC voltages and currents at the AC terminal respectively, L_s and R_s are the equivalent value of the inductance and the resistance at the VSI side which are defined by the following equations,

$$L_s \frac{di_j}{dt} = -R_s i_j + V_j - v_j \quad (3)$$

$$L_s = L_f + \frac{L_a}{2} \quad (4)$$

$$R_s = \frac{R_a}{2} \quad (5)$$

FLY – BACK CONVERTER

During the operation it has different configuration of Fly-back converter.. From the Fig. 3, the winding of primary of the transformer gets connected when the switch 'S' is 'ON', the input supply with its positive side is connected to the dotted end. The secondary winding connected in series with diode 'D' gets reversed due to the voltage induced in the secondary at the same time. The winding in the primary is able to carry current when turning 'ON' switch 'S', but it blocked the current in the secondary side winding due to the diode reverse biased. This mode of circuit have been denoted here as operation of Mode-1. Fig. (a) Shows the circuit which is current carrying part and Fig. (b) Shows the fly-back circuit during mode-1. The discontinuous flux mode of operation is preferred for enhancing the output voltage. On the other hand, the additional output power can be transferred during continuous mode. The circuit is designed based upon thumb rule for operation of continuous flux mode at the minimum predictable input voltage and at the value of rated output power.

RESULTS AND DISCUSSIONS

The simulation results corresponding to a proposed converter technique is presented and the simulation can be carried out through MATLAB. Fig. 4 depicts that the three phase voltage in the grid side. Fig. 5 shows the current in the grid side. The Fig. 6 depicts the active power of the converter.

CONCLUSION

The coupled inductors can be used to interconnect the conventional two-level inverters in parallel for improvement of rated power of converters connected with grid. The balance of the current delivered by the two converters is feasible without any specific control function of the system. At the same time, it induces disagreeable circulating currents with low frequency which stress on power semi-conductors was increases. In this work, magnetically coupled inductors with interleaved three-phase inverters can be balanced by the proposed technique. The converter is considered as a passive system and it was modeled that meets the requirements of energy shaping control. It required additional sensors to implementation of this algorithm to measure the output currents of the first converter. Consequently the projected control allows enhanced performances and abridged energy losses.

REFERENCES

1. R. Iravani, A. Yazdani, Voltage Sourced-converters in Power Systems. Modeling, Control and Applications, Wiley, New Jersey, 2010 ISBN 978-0-470-52156-4.
2. A. Laka, J.A. Barrera, J. Chivite-Zabalza, M.A. Rodriguez-Vidal, Parallelization of two three-phase converters by using coupled inductors built on a single magnetic core, Przeglad Elektotechnicy 89 (2013) 194–198.
3. A. Laka, J.A. Barrera, J. Chivite-Zabalza, M.A. Rodriguez-Vidal, P. Izurza-Moreno, Isolated double-twin VSC topology using three-phase IPTs for high-power applications, IEEE Trans. Power Electron. 29 (2014) 5761–5769.
4. D. Zhang, F. Wang, R. Burgos, R. Lai, D. Boroyevich, Impact of interleaving on AC passive components of paralleled three-phase voltage source converters, IEEE Trans. Ind. Appl. 46 (2010) 1042–1054.





Rajeswaran et al.,

5. G. Gohil, L. Bede, R. Teodorescu, T. Kerekes, F. Blaabjerg, Flux balancing scheme for PD modulated parallel interleaved inverters, IEEE Trans. Power Electron. Vol. 32 (2017) 3442–3457.
6. F. Forest, E. Labouré, T.A. Meynard, V. Smet, Design and comparison of inductors and inter cell transformers for filtering of PWM inverter output, IEEE Trans. Power Electron. 24 (2009) 812–821.
7. F. Ueda, K. Matsui, M. Asao, K. Tsuboi, Parallel-connections of pulse width modulated inverters using current sharing reactors, IEEE Trans. Power Electron. Vol. 10 (1995) 673–679.
8. Z. Quan, Y.W. Li, A three-level space vector modulation scheme for paralleled converters to reduce circulating current and common-mode voltage, IEEE Trans. Power Electron. 32 (2017) 703–714.
9. G. Konstantinou, J. Pou, G.J. Capella, S. Ceballos, V.G. Agelidis, Reducing circulating currents in interleaved converter legs under selective harmonic elimination pulse-width modulation, IEEE International Conference on Industrial Technology (2015).
10. L. Bede, G. Gohil, M. Ciobotaru, T. Kerekes, R. Teodorescu, V.G. Agelidis, Circulating current controller for parallel interleaved converter using PR controllers, 41st Annual Conference of the IEEE Industrial Electronics Society (2015).
11. G. Gohil, R. Maheshwari, L. Bede, T. Kerekes, R. Teodorescu, F. Liserre, F. Blaabjerg, Modified discontinuous PWM for size reduction of the circulating current filter in parallel interleaved converters, IEEE Trans. Ind. Electron. 30 (2015) 3457–3470.
12. Z. Xueguang, Z. Wenjie, C. Jiaming, X. Dianguo, Deadbeat control strategy of circulating currents in parallel connection system of three-phase PWM converter, IEEE Trans. Energy Convers. 29 (2014) 406–417.
13. Z. Quan, Y.W. Li, Suppressing zero-sequence circulating current of modular interleaved three-phase converters using carrier phase shift PWM, IEEE Trans. Ind. Appl. 53 (2017) 3782–3792.
14. X. Lin, Y. Lei, Y. Zhu, A novel superconducting magnetic energy storage system design based on a three-level T-type converter and its energy-shaping control strategy, Electr. Power Syst. Res. 162 (2018) 64–73.

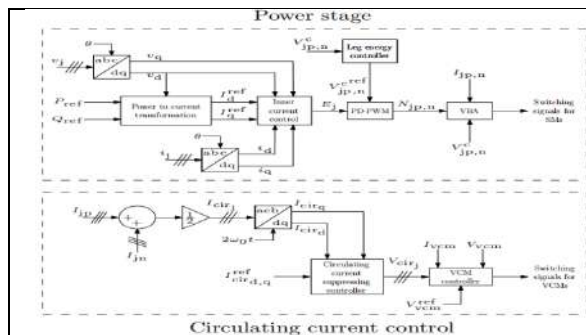


Fig. 1: Overview of the Overall Control System

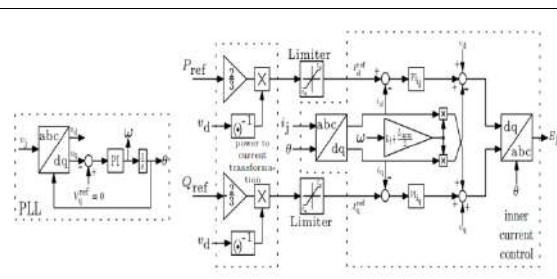


Fig. 2: Schematic of PLL Controller with two-layer MMC+VCM VSI

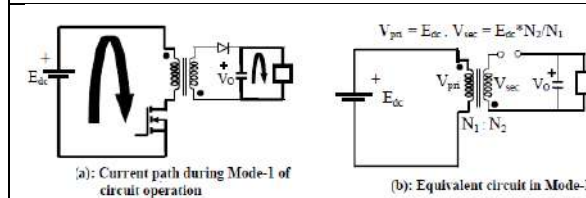


Fig. 3: Fly- Back Converter during Mode-1 Operation

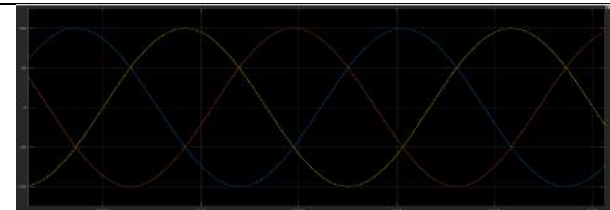


Fig. 4: Grid Sided Voltage





Rajeswaran et al.,

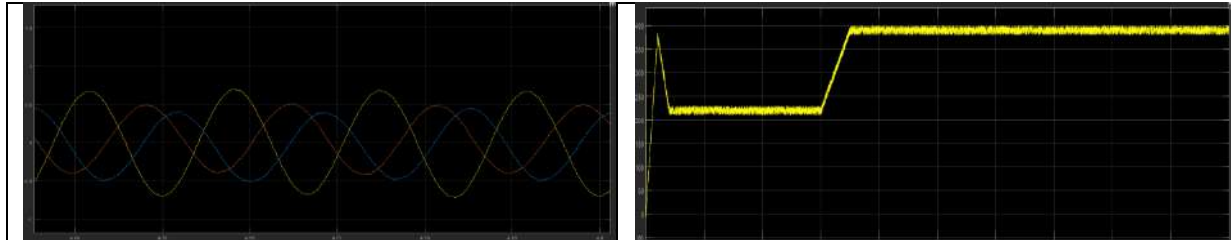


Fig. 5: Grid Sided Current

Fig. 6: Active Power

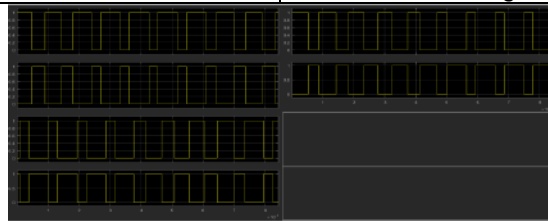


Fig. 7: Gate Pulse





Design and Analysis of High Frequency Optimization of Bidirectional, Grid-Connected Converter

A.V.Sudhakara Reddy^{1*}, Ch. Narendra Kumar¹ and V. Sravani²

¹Malla Reddy Engineering College, Maisammaguda, Hyderabad, Telangana, India.

²PG Scholar, Malla Reddy Engineering College, Maisammaguda, Hyderabad, Telangana, India.

Received: 02 Sep 2021

Revised: 25 Sep 2021

Accepted: 18 Oct 2021

*Address for Correspondence

A.V.Sudhakara Reddy

Malla Reddy Engineering College,
Maisammaguda, Hyderabad,
Telangana, India.

Email: sravanireddy283@gmail.com



This is an Open Access Journal / article distributed under the terms of the **Creative Commons Attribution License** (CC BY-NC-ND 3.0) which permits unrestricted use, distribution, and reproduction in any medium, provided the original work is properly cited. All rights reserved.

ABSTRACT

A high frequency, interleaved, double-buck, bidirectional converter topology linked to the grid is suggested in this study. Unless there are direct and deadly problems, you can obtain higher frequency of switching and power density. Due to the approach interleaved, the current rip and stress may be decreased efficiently for inductors and other power equipment. In addition, a new design method is proposed for filter parameters. The approach is optimized with less inductance, greater filtering capacity and improved stability. Firstly, the performance requirements for the two inverters and converter states are fully taken into account. Another aspect is the relation between the performance indexes and the filter settings. The results, however, demonstrate that there are inconsistent links between performance indexes. The priority of the filter performance index was set to acquire a number of optimisation parameters. The total harmonic distortions (THDs) in grid current at 2.7 percent, 1.2 percent and 4.5 percent, and the power density was 36 W/in³ accordingly, among the grid-connected inverters, disconnected inverters and full-load rectifiers.

Keywords: dual-buck; bidirectional; grid-connected converter; parameter design

INTRODUCTION

In distributed new power, grid connected power generation systems, energy storage units are commonly used. They lessen the power fluctuation in grid systems, on the one hand. Instead, the energy connection between the users and the grid improves the ease. The energy storage device must however be further improved with its efficiency and power density [1–3]. Thus, the grid-connected converter needs to emphasize two characteristics of performance as an interface circuit of distributed energy storage devices: (1) The bidirectional energy flow is highly efficient. (2) Lower

38853





Sudhakara Reddy et al.,

in weight and smaller volume. The ways for increasing power density are as follows, according to the research of the relevant scholars: (1) To increase the frequency of operation and minimize the filter size. (2) Suitably designing and reducing the filter element nominal value to produce a greater power density filter parameters [4-10]. Increasing the converter operating frequency can considerably decrease the inductors and condensers. This improves the converter's power density. However, the classic bridge-based transformer must inject dead time, which restricts operating frequency increases. In addition, the dead period leads to additional distortion in waveform. Consequently, the new form of grid-connected converter (i.e. no dead zone) does have considerable research value in comparison with the classic bridge circuit.

The approach of design is more intuitive, but the process is more complex. The design of the filter is based on the properties of the circuit in the previous literature, with clear design objectives and a feasible design process. However, most of the material mentioned above takes individual performance as the goal and does not take into account the restrictions between different performances. Multiple performance requirements are therefore difficult to take into account simultaneously. Moreover, the converter's power density is not the optimization objective. A high frequency, cross-leaved, dual-buck, two-way, grid-connected converter is presented in this document on the basis of SiC power devices. The topology contains two states: Inverter and Corrector.

Topology Description

Figure 1, which includes the inverter state and the corrective state, shows the topology of the proposed interleaved, dual-buck, bidirectional, grid-connected converter. The circuit consists of four identical Buck circuits in the inverter state: S_1 , S_3 , D_1 , and L_{i1} form Buck₁. The circuit includes S_1 , S_4 , D_2 , and L_{i2} create Buck₂. The driving signal of switch S_3 on Buck₁ results in a 180-degree drive signal of switch S_4 on Buck₂. The pull signal on switch S_5 from Buck₃ is 180 degrees S_6 from Buck₄, which is the interleaving unit 2 of the inverter. The filter performance is directly determined by the parameters of the filter. Thus, the filter settings should be properly designed to achieve the desired results. The filter includes L_{i1} , L_{i2} , L_{i3} , L_{i4} , L_g , C_f and C_o for the proposed converter. The inverter LCL filters include L_{i1} , L_{i2} , L_{i3} , L_{i4} , C_f and L_g and the corrective LCL filters in L_{i1} , L_{i2} , L_{i3} , L_{i4} , L_g and C_o . The architecture of the filter in both states are obviously different. Furthermore, the connection link between the filter parameters leads to parameter interactions.

This research proposes a new way of designing parameters that considers the performance demands of both countries. The major objective is to get high power, strong filtering performance and good continuous performance. The procedure can be separated into three different parts. To begin with, the operation principle and circuit process are followed by a generalised range of filter settings. Secondly, by studying the connection between the parameters, the range of filter parameters is optimised. Finally, the priority of the filter performance index is determined to achieve a set of suitable parameters. This method will be described in full in the specific design process. The inductance values of L_{i1} , L_{i2} , L_{i3} , and L_{i4} are assumed to be the same as those indicated by L_i in order to simplify the analysis process. Furthermore, the total inductance equivalent in the inverter state L_b total inductance in the rectifier state is defined in (1) as follows:

$$L_a = L_i + L_g$$

$$L_b = 1.5L_i + L_g$$

SIMULATION RESULTS

The simulation diagram is shown below and results are carried out in MATLAB/Simulink.

CONCLUSION

This work offers an interleaved, two-dimensional, grid-connected topology converter, and a corresponding approach for optimizing filter settings. This approach has numerous design aims for optimization, such as filter induction, filtering capacity and system stability. Firstly: simultaneous consideration of the filter's performance requirements in inverter and rectifier states. In addition, the converter's total inductance is low sufficiently and good performance in





Sudhakara Reddy et al.,

the constant condition. This is the unique design process: (1) The link between the circuit performance and filter parameters is taken into account and the filter range of parameters is constantly decreased. (2) Set the filter performance priority and optimize the filter parameters' reasonable value. This produces positive features such as higher density of power, better filtration and higher stable status.

REFERENCES

1. Zhang, C.; Jiang, D.; Zhang, X.; Chen, J.; Ruan, C.; Liang, Y. The Study of a Battery Energy Storage System Based on the Hexagonal Modular Multilevel Direct AC/AC Converter (Hexverter). *IEEE Access* 2018, 6, 43343–43355.
2. Vavilapalli, S.; Subramaniam, U.; Padmanaban, S.; Ramachandramurthy, V.K. Design and Real-Time Simulation of an AC Voltage Regulator Based Battery Charger for Large-Scale PV-Grid Energy Storage Systems. *IEEE Access* 2017, 5, 25158–25170.
3. Li, R.; Wang, W.; Xia, M. Cooperative Planning of Active Distribution System With Renewable Energy Sources and Energy Storage Systems. *IEEE Access* 2018, 6, 5916–5926.
4. Liu, Y.; Su, M.; Liu, F.; Zheng, M.; Liang, X.; Xu, G.; Sun, Y. Single-Phase Inverter With Wide Input Voltage and Power Decoupling Capability. *IEEE Access* 2019, 7, 16870–16879.
5. Ohnuma, Y.; Orikawa, K.; Itoh, J. A Single-Phase Current-Source PV Inverter With Power Decoupling Capability Using an Active Buffer. *IEEE Trans. Ind. Appl.* 2015, 51, 531–538.
6. Xu, S.; Shao, R.; Chang, L. Single-phase voltage source inverter with voltage-boosting and power decoupling capabilities. In Proceedings of the IEEE 8th International Symposium on Power Electronics for Distributed Generation Systems, Florianopolis, Brazil, 17–20 April 2017.
7. Chen, C.; Chen, Y.; Tan, Y.; Fang, J.; Luo, F.; Kang, Y. On the Practical Design of a High Power Density SiC Single-Phase Uninterrupted Power Supply System. *IEEE Trans. Ind. Inf.* 2017, 13, 2704–2716.
8. Ahsanuzzaman, S.M.; Prodic, A.; Johns, D.A. An Integrated High-Density Power Management Solution for Portable Applications Based on a Multioutput Switched-Capacitor Circuit. *IEEE Trans. Power Electron.* 2016, 31, 4305–4323.
9. Gambhir, A.; Mishra, S.K.; Joshi, A. Power Frequency Harmonic Reduction and its Redistribution for Improved Filter Design in Current-Fed Switched Inverter. *IEEE Trans. Ind. Electron.* 2019, 66, 4319–4333.
10. Wang, R.; Wang, F.; Boroyevich, D.; Burgos, R.; Lai, R.; Ning, P.; Rajashekara, K. A High Power Density Single-Phase PWM Rectifier With Active Ripple Energy Storage. *IEEE Trans. Power Electron.* 2011, 26, 1430–1443.

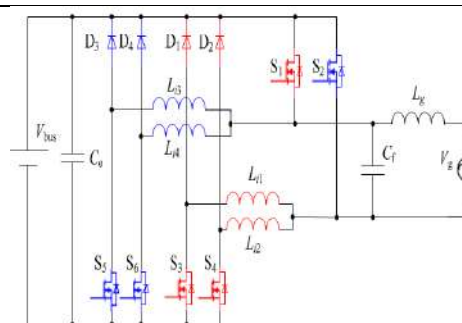


Figure 1 Circuit Diagram





Sudhakara Reddy et al.,

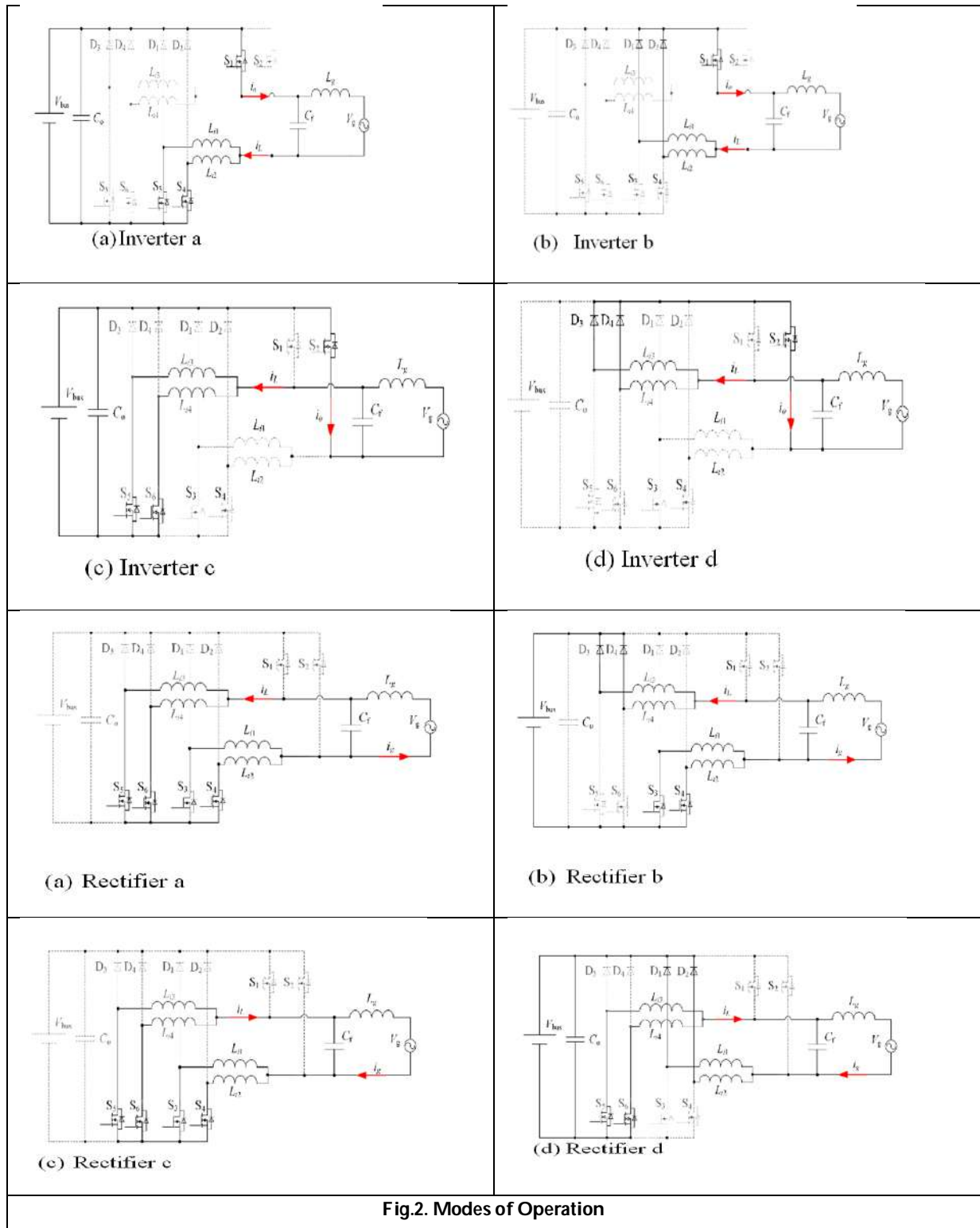


Fig.2. Modes of Operation





Sudhakara Reddy et al.,

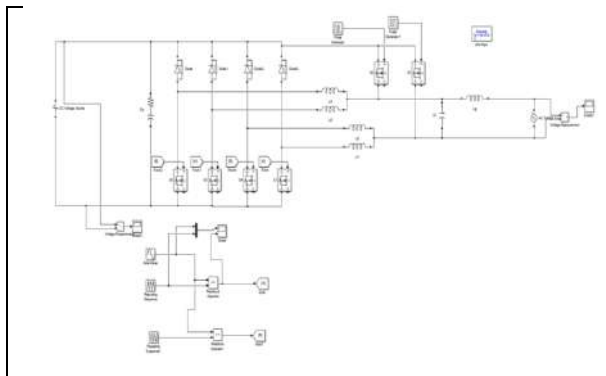


Figure 3 Simulation Diagram of Inverter

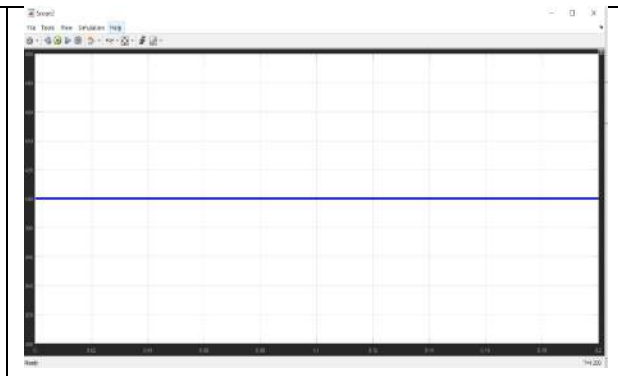


Figure 4 DC Voltage input to the Inverter

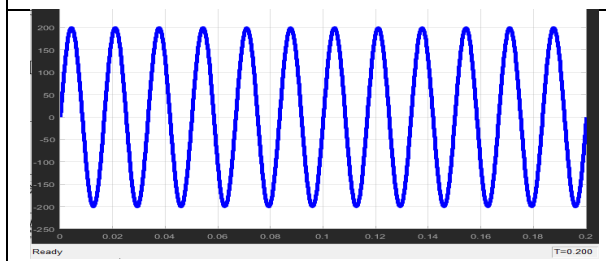


Figure 5 Output Voltage Waveform of Inverter

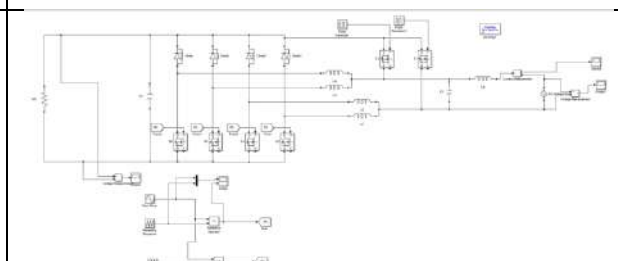


Figure 6 Simulation Diagram of Rectifier

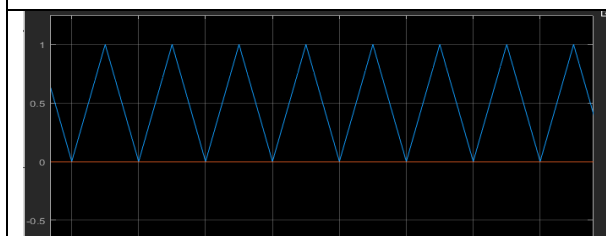


Figure 7 Input to the rectifier

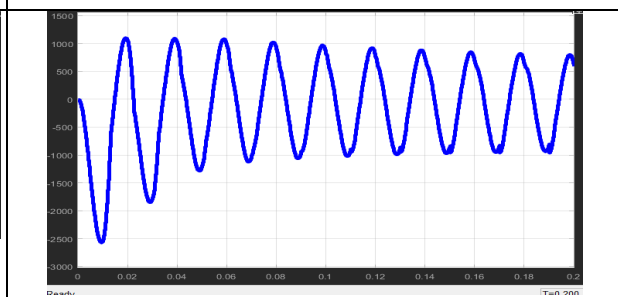


Figure 8 Output waveforms of currents



Figure 9 Output voltage waveform of rectifier





Raman Spectroscopy of High Dilutions of Two Drugs in Aqueous Ethanol Solution Shows Variation in Clathrate Hydrate Crystals

Nirmal Chandra Sukul¹, Raj Kumar Singh², Sumit Ghosh³, Achintya Singha⁴, Indrani Chakraborty⁵, Nivedita Pandey⁶ and Anirban Sukul⁷

¹Professor, Department of Zoology, Visva-Bharati Univ.(Retd.), President Sukul Institute of Homeopathic Research, Visva-Bharati University, Santiniketan, West Bengal, India.

²Assistant Professor, Department of Botany, Government General Degree College, Mangalkote, Burdwan University, Purba Burdwan, West Bengal, India.

³Research Scholar, Sukul Institute of Homeopathic Research, Santiniketan, West Bengal, India.

⁴Professor, Department of Physics, Bose Institute, Kolkata, India.

⁵Assistant Professor, Department of Zoology, Jogamaya Devi College, Kolkata, CU, India.

⁶Assistant Professor, Department of Geography, Panihati Mahavidyalaya, Kolkata, CU, India.

⁷Director, Sukul Institute of Homeopathic Research, Santiniketan, West Bengal, India.

Received: 18 Nov 2021

Revised: 20 Dec 2021

Accepted: 13 Jan 2022

*Address for Correspondence

Nirmal Chandra Sukul

Professor, Department of Zoology,
Visva-Bharati Univ.(Retd.),
President Sukul Institute of Homeopathic Research,
Visva-Bharati University,
Santiniketan, West Bengal, India.
Email: ncsukul@gmail.com



This is an Open Access Journal / article distributed under the terms of the **Creative Commons Attribution License** (CC BY-NC-ND 3.0) which permits unrestricted use, distribution, and reproduction in any medium, provided the original work is properly cited. All rights reserved.

ABSTRACT

High dilutions (HD) of drugs, used in homeopathy, are too dilute to contain original drug molecules. HDs are prepared by serial dilution of a substance in aqueous EtOH followed by mechanical agitation or succussion. These agitated HDs are called potencies. Mechanical agitation initiates and promotes the process of nucleation. Two potencies of two drugs, *Medorrhinum* (Medor) and *Psorinum* (Psor) were analysed by Laser Raman spectroscopy. The spectra show difference in intensity of CH and OH stretching vibrations in the potencies and the control. The contour shape of each spectrum as analysed by intensity ratios at two frequencies show variation in the hydrogen bonding strength indifferent potencies. The chemical nature of the drugs and different levels of succussion appear to have contributed to the variation in the hydrogen bonding strength of the OH groups in potencies. Clathrate hydrate crystals appear to vary in the potencies of the drugs tested. Succussion helps in the nucleation of the crystals and thus plays an important role in the preparation of potencies. The crystals may be responsible for the biological effects of HDs of drugs and contribute to one of the components in the water structure of a potency.



**Nirmal Chandra Sukul et al.**

Keywords: Homeopathic drugs; clathrate hydrate crystals; nucleation; water structure; hydrogen bonding strength.

INTRODUCTION

High dilutions (HD) of drugs have been used in homeopathy introduced by Dr Samuel Hahnemann for a couple of centuries. The HDs are prepared by serial dilution, 1:100 of a mother tincture (MT) in 90% ethanol. Each of a serial dilution is subjected to mechanical agitation or succussion and is known as a potency. The process is known as potentization or dynamization. The rank of a potency indicates the number of successive dilutions followed by succussion and is designated as 6 cH, 12 cH, 30 cH, 200 cH, 1000 cH etc. The dilution of the 12th potency of a drug is 10^{24} . This means the 12th potency has crossed the Avogadro number, and is expected to have no original molecules of the MT. But Clinical and experimental evidences support that the potencies produce distinct biological effects on man, animals, plants and even cell-free proteins (Sukul and sukul,2004). How do the potencies produce biological effects without original drug molecules? Scientists believe that specific water structures induced by original drug molecules are responsible for the biological effects (Rey,2004; Rey,2007; Mahata,2013). The objective of the present study is to elucidate the potential components of a specific water structure which carries the information of the identity of the MT molecules and the rank of a potency in some form. For this, we have analysed two potencies of two homeopathic drugs by Raman spectroscopy. Earlier we reported that free water molecules and hydrogen bond strength of OH groups are components of water structure in Homeopathic potencies (Chakraborty *et al.*,2014; Sarkar *et al.*,2016; Sarkar *et al.*,2016).

MATERIALS AND METHODS

Drugs / Control

Two potencies, 200cH and 1000cH of *Medorrhinum* (Medor) and *Psorinum*(Psor) were purchased in sealed vials from the local market in Kolkata. These drugs were products of Dr. Reckeweg & Co. GmbH, Germany (Medor 200 Lot No.-, Medor 1000 Lot No.-4614IN378170 and Psor 200 Lot No.-5379IN378170, Psor 1000 Lot No.-5383IN378180). All the four drugs were in 90 volume percent of Ethanol as mentioned in the labels. The control consisted of 90% EtOH (Merck, Germany, Lot No.-K51652783934). Both the drugs and the control were mixed with appropriate volume of water to make 25 volume percent of EtOH. Using a UV-VIS spectrophotometer we observed the intensities of all the test samples such as EtOH, Medor and Psor. The intensities are 0.18 for EtOH, 0.71 for Medor 1000cH and 1.2 for Psor 1000cH.

Laser Raman Spectra

Raman scattering spectra were measured by a Raman setup (Lab Ram HR, Jobin Yvon) equipped with Argon Ion Laser of Wavelength 488 nm and CCD detector. The spectra were recorded in the wave number region 2600-3800 cm^{-1} after base line correction. The intensity ratio of OH stretching vibration at 3200(strong hydrogen bond) and 3420 cm^{-1} (weak hydrogen bond) is designated as R1. We have taken another ratio between 3620(weaker hydrogen bond) and 3420 cm^{-1} designated as R2. Both R1 and R2 values were calculated for Medor 200 and Medor 1000 cH as well as Psor 200 and Psor 1000 cH. The intensities of Raman spectra were first normalized and then the ratio values were calculated. The ratios help in determining the contour shape of the spectra (Dolenko *et al.*,2011; Dolenko *et al.*,2015). The frequency shift in the observed spectra has been determined.

RESULTS

Raman spectra of Medor 200 and Medor 1000 cH and their control 90% EtOH are presented in fig -1. The fig-1 shows highest intensity with Medor 200 cH followed by Medor 1000 cH and their control 90% EtOH. Fig-2 shows highest intensity with Psor 200 cH followed by Psor 1000 cH and control 90% EtOH. Intensity ratio R1 is highest with 90% EtOH control followed by Medor 200 cH and Medor 1000 cH (Figure-3a). Intensity ratio R2 is highest with both

38859



**Nirmal Chandra Sukul et al.**

EtOH and Medor 200 cH followed by Medor 1000 cH (Figure-3b). Intensity ratio R1 is highest with 90% EtOH followed by Psor 1000 cH and Psor 200 cH (Figure-4a). Intensity ratio R2 is highest with 90% EtOH followed by Psor 1000 cH and Psor 200 cH (Figure-4b). The frequency at the peak of OH stretching band is plotted against the two Medor potencies and their control in figure-5. Figure-5 shows highest frequency with Medor 1000 cH followed by EtOH and 1000 cH and Psor 200 cH. The frequency shift of OH stretching band is shown in histograms for the two potencies of *Psorinum* and their control EtOH (Fig-5b). The fig-5b shows highest frequency with EtOH followed by Psor 1000 cH and Psor 200 cH.

DISCUSSION

The frequency of vibrations depends on the mass of atoms concerned and their bond strength between the atoms. In our study the atoms C, O, H are fixed in all the test samples, but the bond strength varies resulting in the frequency shift of the samples tested (Fig-5a b). R1 gives information about the relative number of OH groups with strong and weak hydrogen bonds. R2 indicates the relative number of OH groups with weak and broken hydrogen bonds (Dolenko *et al.*,2011). In aqueous ethanol hydrogen bonding occurs between water–water, alcohol-alcohol and alcohol-water molecules. Hydrogen bonds increased to the maximum level around 20% of ethanol. The change in the hydrogen bonding appears to be related to the presence of clathrate like structures in the solution. A network of water molecules with strong hydrogen bond encompasses the OH groups of ethanol molecules (Dolenko *et al.*,2011; Dolenko *et al.*,2015). In our study the concentration of ethanol is fixed at 25%, but there is a marked variation in R1 and R2 values of the two potencies of the Medor and of Psor. However, both R1 and R2 values remained unchanged in the ethanol control although ethanol concentration is same in all the drug samples and ethanol control. This shows that the original drug molecules of Medor and Psor mother tincture have induced changes in the hydrogen bonding strength vis-à-vis the clathrate hydrate crystals in different drugs as well as different potencies of the same drug during potentization.

The preparation of all potentized drugs in homeopathy involves mechanical agitation or succussion in aqueous ethanol solution. We have mentioned that the OH group of ethanol embedded in a three dimensional network of strongly hydrogen bonded molecules form clathrate hydrate crystals. These OH groups participate in nucleation for the crystals. Mechanical agitation initiates and increases the process of nucleation. Embryos of nucleation occurs in varying sizes (Mulin *et al.*, 1962). It is assumed that mechanical agitation or succussion induces nucleation in the potentized drugs. Initially the original drug molecules in the mother tincture serve as guest molecules within the clathrate hydrate crystals. During the process of serial dilution the original drug molecules are almost totally depleted when the OH groups of ethanol molecules take over their position. However, traces of original drug molecules remained as guest molecules. There are reports showing presence of starting atoms in the MTs (Chattopadhyay, 2017; Chikramane *et al.* 2010).

Clathrate hydrate crystals have been reported mostly in methane gas trapped in ice crystals. At higher temperatures they are unstable (English *et al.*, 2014; Dolyniuk *et al.*, 2016). But in ethanol water solutions water retains hydrogen bonds as in ice state. Moreover, hydrogen bonding is strengthened by chemical components in alcoholic beverages (Nose *et al.*, 2006). The difference in intensities of EtOH, Medor 1000 cH and Psor 1000 cH, all in 25% EtOH may be due to presence of different proportion of the crystals. Water structures involving clathrate hydrates, that have originated from a dissolved solute may develop a secondary identity related to the solute, and thus play a role in molecular recognition (Plumridge *et al.*,2002). Homeopathic potencies are thought to carry the information of original drug molecule (Sukul and Sukul, 2004).

CONCLUSION

Potentized drugs used in homeopathy contains clathrate hydrate crystals. Mechanical agitation or succussion results in initiation and enhancement of clathrate hydrate crystals. These crystals and their sizes are thought to play an important role in the therapeutic and biological effects of high dilutions of drugs beyond the Avogadro number. The crystals appear to vary in number, forms and sizes in different drugs and different potencies of the same drug.





REFERENCES

1. Sukul, N.C.; Sukul, A. High dilution effects: Physical and biochemical basis. Dordrecht. The Netherlands : Kluwer Academic Publisher. 2004 [Cross Ref]
2. Rey, I. Thermo luminescence of ultra-high dilutions of lithium chloride and sodium chloride. Physica.A.2003,323,67-74.
3. Rey, I. Can low-temperature thermo luminescence cast light on the nature of ultra-high dilutions? Homeopathy. 2007, 96, 170-174.
4. Mahata, C.R. Dielectric dispersion studies of some potentised homeopathic medicines reveal structured vehicle. Homeopathy. 2013, 102, 262-267.
5. Chakraborty, I.; Dutta, S.; Sukul, A.; Chakraborty, R.; Sukul, N.C. Variation in free and bound water molecules in different homeopathic potencies as revealed by their Fourier Transform Infrared spectroscopy(FTIR). Int J High Dilution Res.2014,13, 189.
6. Sarkar, T.; Konar, A.; Sukul, N.C.; Chakraborty, I.; Sukul, A. Vibrational spectroscopy reveals differences in homeopathic potencies in terms of hydrogen bonding and free water molecules. Environ Ecol. 2016, 34, 329-33.
7. Sarkar, T.; Konar, A.; Sukul, N.C.; Majumdar, D.; Singha, A.; Sukul, A. Raman spectroscopy shows difference in drugs at ultra-high dilution prepared with stepwise mechanical agitation. Int J High Dilution Res. 2016, 15, 2-9.
8. Dolenko, T.A.; Burikov, S.A.; Patsaeva, S.V.; Yuzhakov, V.I. Manifestation of hydrogen bonds of aqueous ethanol solutions in the Raman scattering spectra. Quantum Electronics. 2011, 41, 267-272.
9. Dolenko, T.A.; Burikov, S.A.; Dolenko, S.A.; Efitorov, A.O.; Plastinin, I.V.; Yuzhakov, V.I.; Patsaeva, S.V. Raman spectroscopy of water-ethanol solutions: the estimation of hydrogen bonding energy and the appearance of clathrate-like structures in solutions. J. Phys. Chem. 2015, 119, 10806-10816.
10. Mullin, J.W.; Raven, K.D. Influence of mechanical agitation on the nucleation of some aqueous salt solutions. NATURE. 1962, 195, 35-37.
11. Chattopadhyaya, S. Existence of trace amount copper and zinc molecule in so called zero molecular Homeopathic drug. Clin. Expt. Homeopathy.2017, 4, 4-10.
12. Chikramane, P.S.; Suresh, A.K.; Bellare, J.R.; Kane, S.G. Extreme homeopathic dilutions retain starting materials: A nanoparticulate perspective. Homeopathy. 2010, 99, 231-242.
13. English, N.J.; MacElroy, J.M.D. Perspective on molecular simulation of clathrate hydrates: progress, prospects and challenges. Chem. Eng. Sci. 2014
14. Dolyniuk, J.A.; Baird, O.B.; Wang, J.; Zaikina, V.J.; Kovnir, K. Clathrate thermoelectrics. Materials Science and Engineering. 2016, 108, 1-46.
15. Nose, A.; Hojo, M. Hydrogen Bonding of Water-Ethanol in Alcoholic Beverages. Journal of Bioscience and Bioengineering. 2006, 102, 269-280.
16. Plumridge, T. H. and Waigh, R.D. Water structure theory and some implications for drug design. JPP. 2002, 54, 1155-1179.

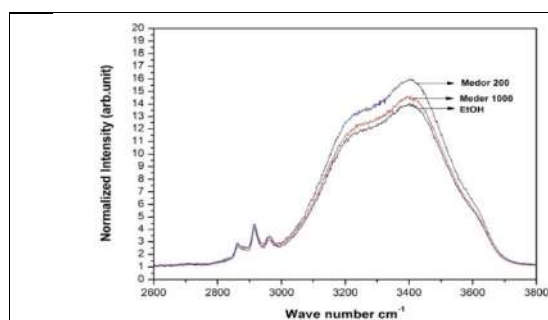


Figure-1: Raman Spectra of two potencies 200 and 1000 cH of *Psorinum* and their control EtOH. All test samples in 25% EtOH (v/v) shows CH and OH stretching bands.

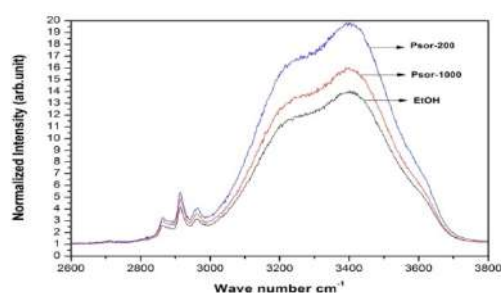


Figure-2: Raman Spectra of two potencies 200 and 1000 cH of *Medorrhinum* and their control EtOH. All test samples in 25% EtOH (v/v) shows CH and OH stretching bands.





Nirmal Chandra Sukul et al.

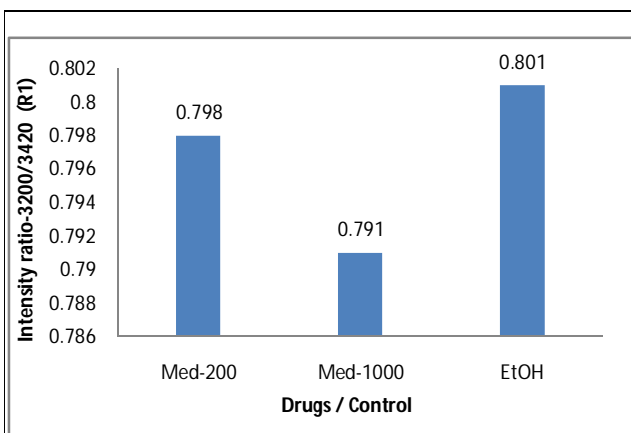


Figure-3a: Intensity ratio (R1) showing variation in ratio values. (Intensity ratio (R1) showing variation in ratio values.)

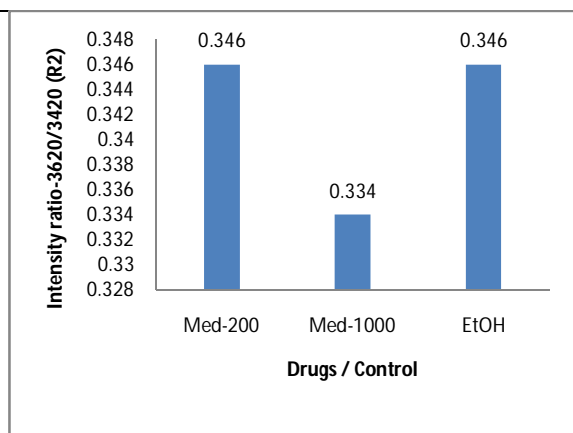


Figure-3b: Intensity ratio (R2) showing variation in ratio values. (Intensity ratio (R2) showing variation in ratio values.)

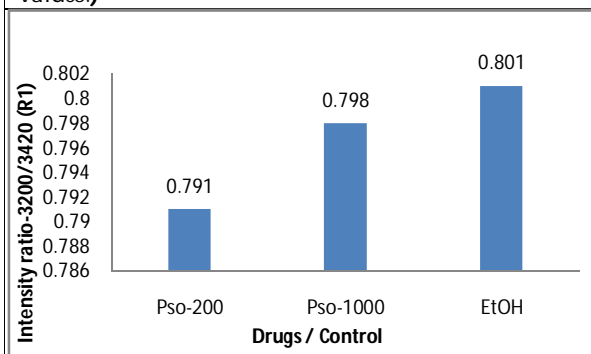


Figure-4a: Intensity ratio (R1) showing variation in ratio values.

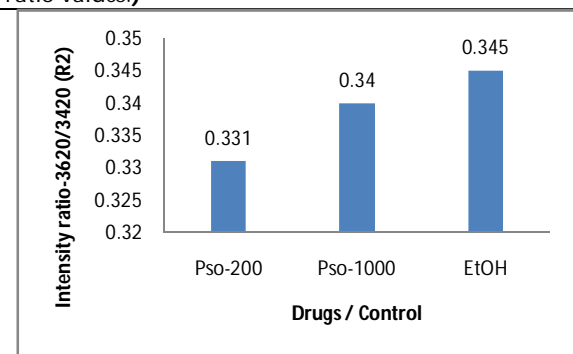


Figure-4b: Intensity ratio (R2) showing variation in ratio values.

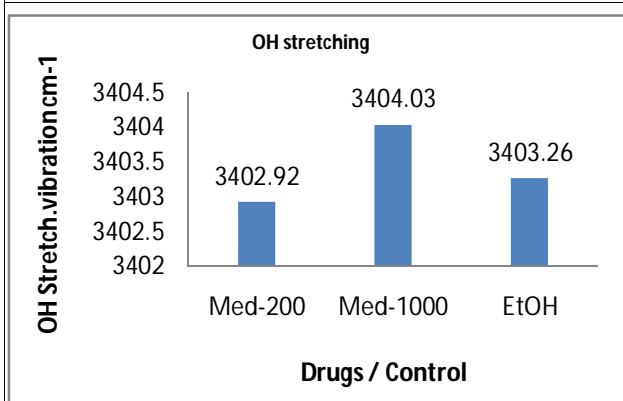


Figure-5a: Histogram showing frequency shift of OH stretching band of Medor 200 and 1000 cH and their control EtOH, all in 25% EtOH (v/v).

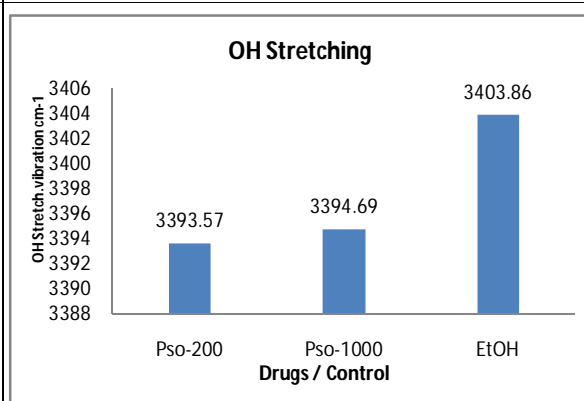


Figure-5b: Histogram showing frequency shift of OH stretching band of Psor 200 and 1000 cH and their control EtOH, all in 25% EtOH (v/v).





Methods for Line-based Feature Extraction in Palmprint Biometric Systems

Sathish R^{1*}, Baskar D² and Vinod Kumar D³

¹Research Scholar, Assistant Professor, Department of Electrical and Electronics Engineering, Vinayaka Mission's Kirupananda Variyar Engineering College, Vinayaka Mission's Research Foundation (Deemed to be University), Salem, Tamil Nadu, India.

²Assistant Professor, Electrical and Electronics Engineering, Annai Teresa College of Engineering, Viluppuram, Tamil Nadu, India.

³Professor and Head, Biomedical Engineering, Vinayaka Mission's Kirupananda Variyar Engineering College, Vinayaka Mission's Research Foundation (Deemed to be University), Salem, Tamil Nadu, India.

Received: 19 Nov 2021

Revised: 22 Dec 2021

Accepted: 12 Jan 2022

*Address for Correspondence

Sathish R

¹Research Scholar, Assistant Professor,
Department of Electrical and Electronics Engineering,
Vinayaka Mission's Kirupananda Variyar Engineering College,
Vinayaka Mission's Research Foundation (Deemed to be University),
Salem, Tamil Nadu, India.



This is an Open Access Journal / article distributed under the terms of the **Creative Commons Attribution License** (CC BY-NC-ND 3.0) which permits unrestricted use, distribution, and reproduction in any medium, provided the original work is properly cited. All rights reserved.

ABSTRACT

Biometrics are measured in order to authenticate or identify the identification of an individual. A person's palmprint is one of the physiological aspects of the human body that has gained attention among researchers as a means of security. The database of the Chinese Academy of Sciences Institute of Automation (CASIA) is employed in the course of the inquiry. In order for an object to be recognised, lines or borders must convey critical information. Line characteristics include principal lines, wrinkles, and ridges, amongst other things. The approaches for line-based feature extraction that are suitable for diverse object recognition applications are identified and explored in detail. The Prewitt edge detector, the Sobel operator, the Canny edge detector, the Kirsch operator, and the Multiscale edge detector are all used to extract the palmprint line characteristics. This is an excellent example of Kirsch Operator doing well. He obtains 94.95 percent accuracy for 1 percent of FAR and 94.85 percent accuracy for 2 percent of FAR accuracy.

Keywords: Biometrics, Palmprint, Authentication, Object Recognition



**Sathish et al.,**

INTRODUCTION

The words "Bio" and "Metrics" are both derived from the Greek words for "life" and "metrics," respectively, which means "to measure." The term "biometrics" comes from the combination of these two words. Biological characteristics (biometrics) are measurements used in order to authenticate or identify the identity of an individual. It is possible to automatically recognise and identify a certain individual with the use of a biometrics technology. Biometrics is used as a spectrum of identity entrée organisation and control mechanisms in the information system, all of which are compliant with certain industry standards. It is also used to identify persons who are members of groups that are under surveillance. Both physiological and behavioural features can be classified as biometrics, which can be further subdivided into two categories.

Palprint

Human beings have physiological characteristics such as the ability to read their own palmprint. In addition to having worldwide appeal, it also possesses the following characteristics: being one of a kind; being permanent; being collected; being consistent; being similar; being inimitable; and being tamper-proof. Because every human being has a unique palmprint, the palmprint is referred to as universal. This item is one-of-a-kind since each palmprint is unique from the others. Researchers from the University of California, San Diego, discovered that the palmprint carries a plethora of genetically unrelated information that can be utilised to identify identical twins. An individual's palmprint is more persistent than other types of identification since it is inseparable from the individual. As a result of the fact that it does not change significantly over time [1,2,3], palmprints are simple to obtain and produce reliable results. With the help of this technology, it is possible to make digital comparisons with other persons. Because of its size and abundance of elements, it is difficult to duplicate the palmprint's appearance. The palmprint is tamper-resistant due to the fact that it cannot be altered and that it is difficult to conceal.

Palmprint is a versatile device with numerous features. Geometry qualities point geometry characteristics, line geometry characteristics, texture characteristics, and statistical characteristics are all included in this category. The width of the palmprint, the length of the palmprint, and the area of the palmprint are all geometrical properties of the palmprint. In order to construct a hand geometry biometric system, palmprint geometry features are commonly combined with finger geometry features to form a hand geometry biometric system. A hand geometry biometric system will not be able to achieve high levels of accuracy in identifying adults since their hand geometry is so similar to one another's.

When it comes to palmprint point features, these are the points that can be discovered on a person's palmprint and can be used to identify them as a result of their fingerprint. These points are referred to by a variety of names, including datum points, line junction points, delta points, end line points, and other variations. Because of the features of palmprint points, it is important to employ a high-resolution palmprint image in order to collect the necessary points.

Line-Based Operators

There are three sorts of palmprint line characteristics: principal lines, wrinkles, and ridges. Principal lines are the most prominent of the three types. The key lines are the major lines that are available in more than half of the world's population, referred to as the global population. The heart line, the lifeline, and the headline are the three most important principal lines in a piece of writing. Wrinkles and ridges are the terms used to describe the coarse lines on the palmprint, whereas wrinkles and ridges are used to describe the small lines. The palmprint line characteristics are depicted in Figure 1. The difficulty in line-based feature extraction is in accurately extracting the line features because the lines on a Palmprint are distinct yet do not follow a specific direction on the palmprint. When working with Palmprint, it is difficult to determine the direction of lines





Sathish et al.,

In order for an object to be recognised, lines or borders must convey critical information. There are a variety of line detection approaches that are frequently used in object recognition systems nowadays. As part of the feature extraction for palmprint, some of the established line detection approaches as well as some developing methods are being examined. According to [8], the use of the Canny edge detector for feature extraction and as an enhancement technique for remote sensing images was proposed, and the results were shown to be robust with a very high level of enhancement. A unique algorithm for edge detection in mammographic pictures has been presented, and it is now being tested. Using the Prewitt edge Detector, it is possible to see the breast boundary, pectoral region, and tumor location clearly. According to [9], this was primarily employed for increasing the tumor region in mammographic pictures. Because of the nature of surveillance systems and medical diagnosis, sobel operators are often required to do video monitoring in low-light or no-light conditions in order to meet security or medical criteria. Generally, thermal imaging and infrared imaging techniques are used to help in the capturing of video information for such applications [10, 11]. A study on the adaption and optimization of edge detector algorithms such as Sobel and Canny, which are utilised as low-level operations in the development of augmented reality applications for the iPhone 3GS platform.

The proposed approach was resilient and could be efficiently implemented on a device with modest processing power [11]. The Sobel Edge Detection technique was utilized to detect vehicle number plates in this study [12]. Real-world photographs are frequently distorted by noise originating from a variety of sources. Bilateral filtering is a nonlinear filter that smoothest out noise by taking into account both intensity changes and spatial closeness in the smoothing process. According to Multi Scale edge Detector [13], it has been proved to offer a superior edge-preserving quality than linear filters in some situations. Medical ultrasound signals are subjected to a multiscale edge detection technique [14]. The Kirsch edge Detector and the Prewitt edge Detector, both of which were used in mammographic pictures, also performed well [15]. Despite the fact that these operators have not been examined for feature-rich objects such as palmprints, they have showed great efficiency in a variety of computer vision and healthcare applications.

Line Detection for Palmprint

The Prewitt edge detector, the Sobel operator, the Canny edge detector, the Kirsch operator, and the Multiscale edge detector can all be used to extract palmprint line characteristics.

Prewitt Edge Detector

The detection of edges is accomplished by distinguishing between step-like variations in image intensity. As a result, it is critical to incorporate averaging into the edge detection process. The Prewitt edge detection method is comprised of two templates: the vertical template, M_x , which runs down three rows, and the horizontal template, M_y , which runs along three columns of the Prewitt edge detection method. Specifically, the edge magnitude (M) is defined as the length of a vector while the edge direction θ is defined as the angle of the vector.

The rate of change of brightness along each axis is illustrated in Figure 2. The signs of M_x and M_y can be used to determine the appropriate quadrant for the edge direction.

$$M = \sqrt{M_x(x, y)^2 + M_y(x, y)^2} \quad (1)$$

$$\theta(x, y) = \tan^{-1} \left(\frac{M_y(x, y)}{M_x(x, y)} \right) \quad (2)$$

Sobel Operator

The Sobel Operator is among the popular edge detection operator. It is popular because of its overall performance than other edge detection operators. Conventional (3 x 3) Sobel operators are used to detect horizontal and vertical lines.



**Sathish et al.,****Canny Edge Detector**

The Canny edge detection operator is the most widely used edge detection approach, and it is also the most popular. It was created with specific goals in mind, such as optimum detection with no misleading replies, among others. Its goal is to minimize the responsiveness to background noise. Excellent localization, with the shortest possible distance between the detected and genuine edge positions. Its accuracy goal is to be achieved, and it will detect edges. A single reaction to a single edge can remove several responses to the same edge. It is concerned with the location of a single edge point as a result of a change in illumination.

Kirsch Operator

The Kirsch operator approach was developed by Russell A. Kirsch, a physicist. An edge detection approach that finds the highest edge strength in eight predefined directions, or to put it another way, utilizing eight compass filters, is called a compass filtering method. The eight major compass orientations are as follows: north, northwest, west, southwest, south, southeast, east, and northeast. Several of these filters are applied to an image, with just the best of them being used in the final image.

Multiscale Edge Detector

In Multiscale Edge Detection method, the aim is to simultaneously extract edges of all lengths, in both natural and noisy images. Let $I(x, y)$ denote a continuous function representing image intensities given in a two-dimensional domain. We denote by oriented means the family of averages of $I(x, y)$ along rectangular patches of a given centre location $x = (x, y)$, length L , width w , and orientation θ . w is set to a small constant, yielding elongated oriented means. The family of oriented means can be obtained via integrals of the form.

RESULT AND DISCUSSION

It was retrieved from the palmprint and subjected to the line-based feature extraction method during the pre-processing step of the procedure. The Prewitt Edge Detector, the Sobel Operator, the Canny Edge Detector, the Kirsch Operator, and the Multiscale Edge Detector, as well as other line feature extraction methods, are illustrated in graphs and tables. Many feature extraction methods, each of which has its unique set of point features, are depicted in Table (1-5) and Figure (3-6), which show the line features for each method. As an additional comparative tool, Figures [7-11] exhibit the several line-based feature extraction approaches in addition to the Threshold vs FAR and FRR plots, as well as Receiver Operating Curve (ROC) curves. Table 6 shows a comparison of the FAR, FRR, and Accuracy of the various Line based approaches that were investigated. According to the findings of the study, the Kirsch Operator produces superior outcomes than other line-based approaches. In the case of 1 percent of FAR, the accuracy is 94.945 percent, and in the case of 2 percent of FAR, the accuracy is 94.845 percent.

CONCLUSION

Palmprint authentication is gaining popularity due to the fact that it is a feature-rich and tamper-proof biometric. MATLAB programming is used to validate the line-based approaches. It is a well-known fact that increasing the FAR results in decreased security or improper authentication, as any individual can be considered as genuine. The same is true for FRR; false rejection results in an increase in the time required for authentication by a real individual. The article discusses various performance indicators like as FAR, FRR, ERR, and Accuracy that are used to evaluate the performance of a biometrics authentication system. Selected and discussed are efficient line-based feature extraction algorithms for diverse object identification applications. These techniques are tested on palmprints and their efficacy is determined. According to the analysis, the Kirsch Operator outperforms other line-based approaches. It obtains an accuracy of 94.945 percent for 1% of FAR and 94.845 percent for 2% of FAR.



**Sathish et al.,****REFERENCES**

1. Muthukrishnan, A.; Charles Rajesh Kumar, J.; Vinod Kumar, D.; Kanagaraj, M. Internet of image things-discrete wavelet transform and Gabor wavelet transform based image enhancement resolution technique for IoT satellite applications. *Cogn. Syst. Res.* 2019, 57, 46–53.
2. D.Vinod Kumar, A. Nagappan. "Performance Analysis of Security and Accuracy on Palmprint Based Biometric Authentication System," *International Journal of Innovative Research in Computer and Communication-Engineering*, Vol. 3, Issue 7, July 2015, pp 6697-6704.
3. Charles Rajesh Kumar.J , Vinod Kumar.D, Baskar.D, Mary Arunsi.B, Jenova.R, ,M.A.Majid." VLSI design and implementation of High-performance Binary-weighted convolutional artificial neural networks for embedded vision-based Internet of Things (IoT)".16th International Learning & Technology Conference (L&T), *Procedia Computer science* (Elsevier), Jeddah,2018.
4. D. Vinod Kumar, A. Nagappan. "Study and comparison of various point based feature extraction methods in palmprint authentication system," *International Journal of Computational Engineering Research (IJCER)* , Vol. 2, Issue 8, December 2012, pp 82-89.
5. D. Vinod Kumar, A. Nagappan, Jyoti Malik "Phase Congruency Corner Detection as Biometric Feature," *IRACST - International Journal of Computer Science and Information Technology & Security (IJSITS)*, Vol. 2, Issue 2, February 2012, pp 179-185.
6. Kong A. W. K., Zhang D. and Lu G., "A study of identical twins' palmprints for personal verification", *Pattern Recognition*, Vol. 39, Issue 11, Pages 2149-2156, November 2006.
7. Baskar. D, Selvam. P, "Machine Learning framework for Power System Fault Detection and Classification," *International Journal of Scientific & Technology Research*, vol. 9, no. 2, pp. 2002-2008, Feb. 2020.
8. Mohamed Ali and David Clausi, "Using The Canny Edge Detector for Feature Extraction and Enhancement of Remote Sensing Images", 7803-7031-7/01IEEE, Pages 2298-2300, January 2001.
9. Chunsun Zhang, Emmanuel Baltsavias and Armin Gruen, "Knowledge-Based Image Analysis for 3D Road Reconstruction", *Asian Journal of Geoinformatics*, Vol.1, No. 4, Pages 3-14, June 2001.
10. Ching Wei Wang, "Real Time Sobel Square Edge Detector for Night Vision Analysis", *ICIAR 2006, LNCS 4141*, Springer-Verlag Berlin Heidelberg Pages 404–413, May 2006.
11. Marcelo G. Roque, Rafael M. Musmanno, Anselmo Montenegro and Esteban W. G. Clua, "Adapting the Sobel Edge Detector and Canny Edge Extractor for iPhone 3GS architecture", *IWSSIP 2010 - 17th International Conference on Systems, Signals and Image Processing*, Pages 486-489, Dec 2010.
12. Suri P.K., Ekta Walia and Amit Verma, "Vehicle Number Plate Detection using Sobel Edge Detection Technique", *International Journal on Computer Science and Technology (IJCST)* Vol. 1, Issue 2, Pages 179-182, December 2010.
13. Qimei Hu, Xiangjian He and Jun Zhou, "Multi-Scale Edge Detection with Bilateral Filtering in Spiral Architecture", *The Pan-Sydney Area Workshop on Visual Information Processing (VIP) 2003*, Sydney. *Conferences in Research and Practice in Information Technology*, Vol. 36, Pages, Nov 2003.
14. Preben Gråberg Nes, "Fast multi-scale edge-detection in medical ultrasound signals", *Computer Vision and Pattern Recognition (cs.CV); Medical Physics (physics.med-ph)*, Vol. 1, July 2011.
15. Sumit Chopra, Pankaj Bhambri and Baljit Singh, "Segmentation of the Mammogram Images to find Breast Boundaries", *IJCST* Vol. 2, Issue 2, Pages 164-167, June 2011





Sathish et al.,

Table 1: FAR, FRR and Accuracy Table for Prewitt Edge Detector

Threshold	FAR	FRR	Accuracy
0.25	0.29	0.2201	74.495
0.5	0.25	0.20347	77.3265
0.75	0.22	0.19111	79.4445
1	0.18	0.1801	81.995
1.25	0.15	0.23004	80.998
1.5	0.11	0.260688	81.4656
1.75	0.08	0.29	81.5
2	0.075	0.32	80.25
2.25	0.068	0.35	79.1
2.5	0.057	0.39	77.65
2.75	0.042	0.41	77.4
3	0.037	0.42	77.15
3.25	0.022	0.47	75.4
3.5	0.015	0.48	75.25
3.75	0.006	0.51	74.2

Table 2: FAR, FRR and Accuracy table for Sobel Operator

Threshold	FAR	FRR	Accuracy
0.01	0.204	0.165	81.55
0.02	0.192	0.156	82.6
0.03	0.189	0.149	83.1
0.04	0.172	0.143	84.25
0.055	0.152	0.152	84.8
0.06	0.136	0.177	84.35
0.075	0.112	0.1972	84.54
0.08	0.092	0.2203	84.385
0.09	0.075	0.2809	82.205
0.1	0.052	0.3678	79.01
0.25	0.034	0.3958	78.51
0.55	0.026	0.4123	78.085
0.75	0.0112	0.4212	78.38
1.1	0.008	0.4465	77.275
1.5	0.004	0.4823	75.685

Table 3: FAR, FRR and Accuracy Table for Canny Edge Detector

Threshold	FAR	FRR	Accuracy
0.25	0.1399	0.1099	87.51
0.5	0.1377	0.1199	87.12
0.75	0.1211	0.1221	87.84
1	0.1107	0.1366	87.635
1.25	0.1001	0.1455	87.72
1.5	0.0999	0.1499	87.51
1.75	0.0875	0.1588	87.685
2	0.0774	0.1687	87.695
2.25	0.0692	0.1798	87.55
2.5	0.0578	0.1899	87.615
2.75	0.0467	0.1976	87.785
3	0.0377	0.2083	87.7
3.25	0.0259	0.2198	87.715
3.5	0.0122	0.2399	87.395
3.75	0.0051	0.2411	87.69





Sathish et al.,

Table 4: FAR, FRR and Accuracy Plot for Kirsch Operator

Threshold	FAR	FRR	Accuracy
1.3	0.0852	0.0211	94.685
1.7	0.0792	0.028	94.64
2.1	0.0727	0.031	94.815
2.5	0.0691	0.037	94.695
2.9	0.0611	0.041	94.895
3.3	0.0521	0.049	94.945
3.7	0.0511	0.052	94.845
4.1	0.0482	0.057	94.74
4.5	0.0421	0.061	94.845
4.9	0.0373	0.065	94.885
5.3	0.0322	0.073	94.74
5.7	0.0283	0.078	94.685
6.1	0.0191	0.084	94.845
6.5	0.0121	0.089	94.945
6.9	0.0061	0.099	94.745

Table 5: FAR, FRR and Accuracy Table for Multiscale Edge Detector

Threshold	FAR	FRR	Accuracy
0.05	0.095	0.029	93.8
0.08	0.081	0.0309	94.405
0.1	0.078	0.041	94.05
0.13	0.075	0.048	93.85
0.16	0.07	0.052	93.9
0.17	0.064	0.06	93.8
0.18	0.062	0.06	93.9
0.19	0.059	0.063	93.9
0.21	0.046	0.072	94.1
0.23	0.038	0.087	93.75
0.24	0.032	0.08	94.4
0.26	0.021	0.093	94.3
0.29	0.0201	0.099	94.045
0.33	0.0124	0.122	93.28
0.35	0.005	0.14	92.75

Table 6: Comparison of FAR, FRR and Accuracy of Line based methods

Method Name	Accuracy FAR =FRR	Accuracy for (FAR %)	Accuracy for (FAR %)
PREWITT	81.995	77.65 (5%)	81.5 (10%)
SOBEL	84.8	79.01 (5%)	84.385 (10%)
CANNY	87.84	87.715 (2%)	87.785 (10%)
MUTISCALE	93.8	93.28 (1%)	94.045 (2%)
KIRSCH	94.945	94.945 (1%)	94.845 (2%)





Sathish et al.,

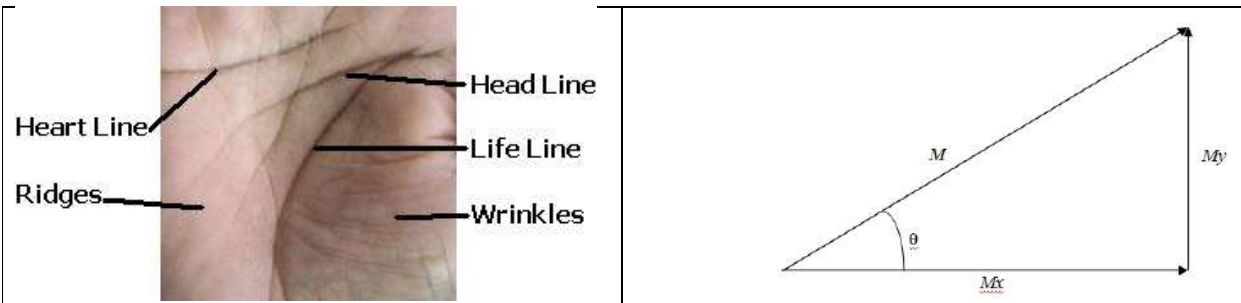


Figure 1: Palmprint Line Features

Figure 2: Edge Detection in Vectorial Format

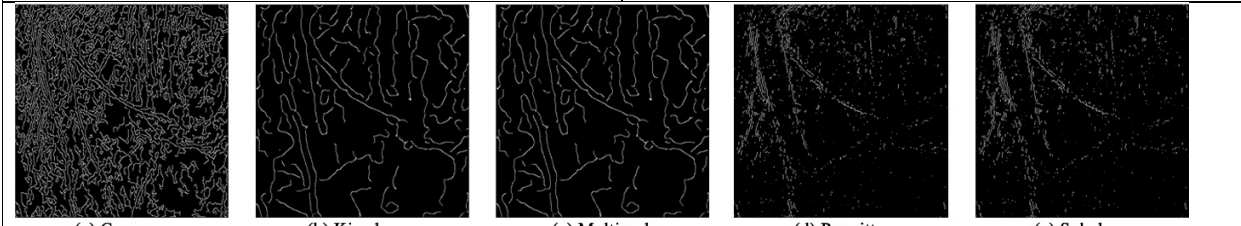


Figure 3: Line based feature extraction results for person 1 sample 1

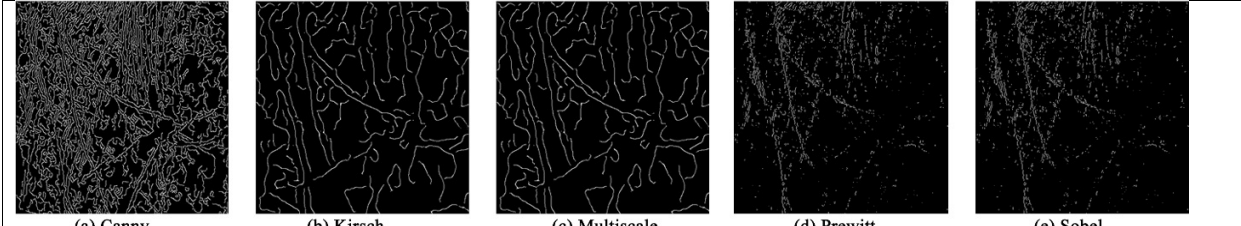


Figure 4: Line based feature extraction results for person 1 sample 2

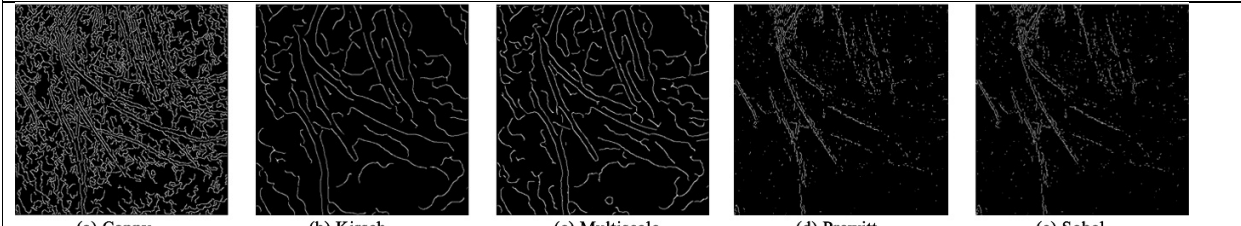


Figure 5: Line based feature extraction results for person 2 sample 1

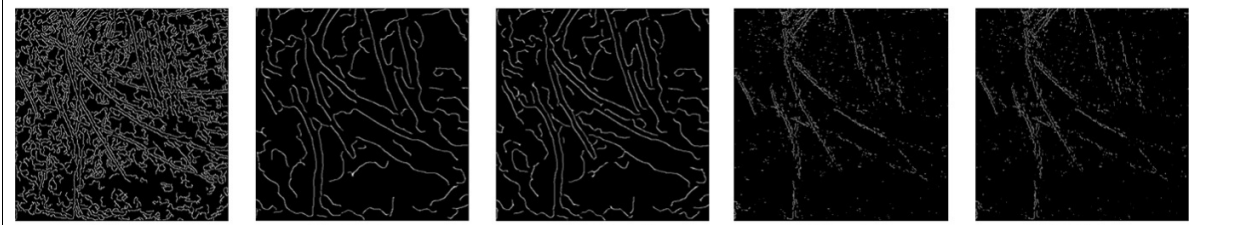


Figure 6: Line based feature extraction results for person 2 sample 2





Sathish et al.,

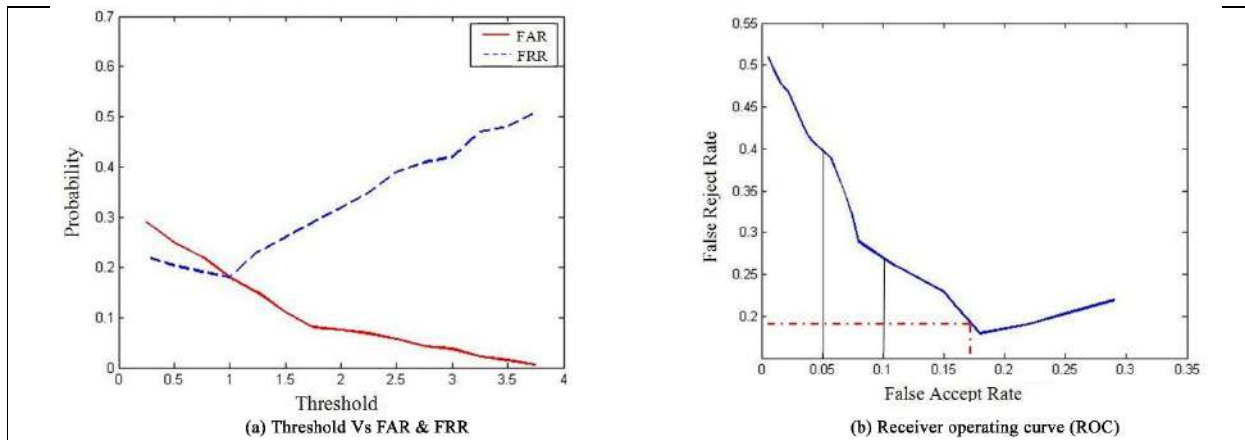


Figure 7: Accuracy plot for Prewitt edge detector

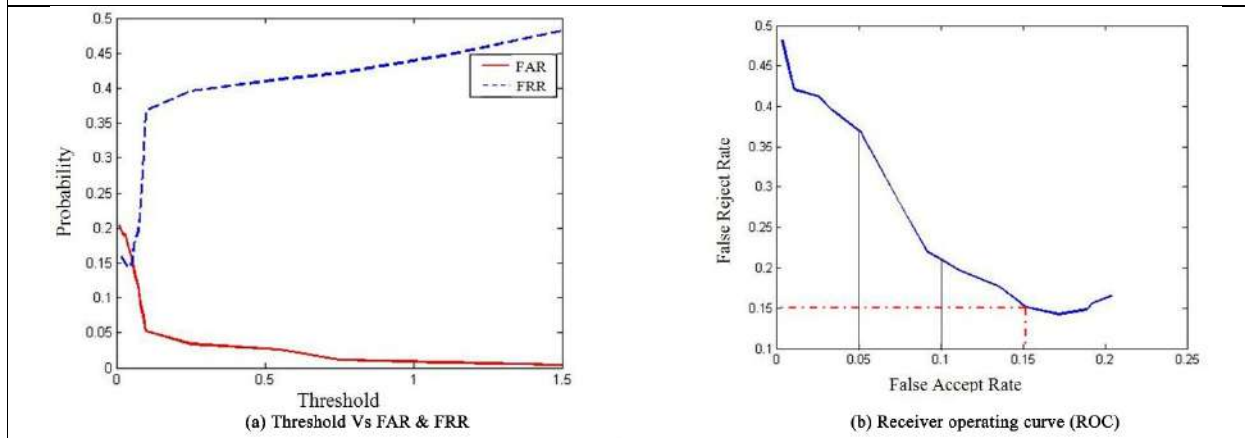


Figure 8: Accuracy plot for Sobel edge detector

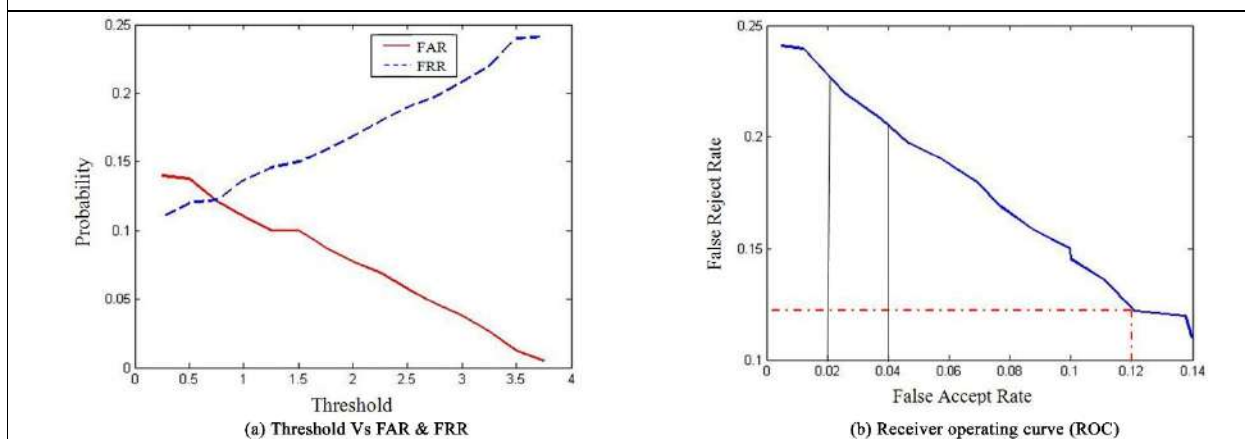


Figure 9: Accuracy plot for Canny edge detector





Sathish et al.,

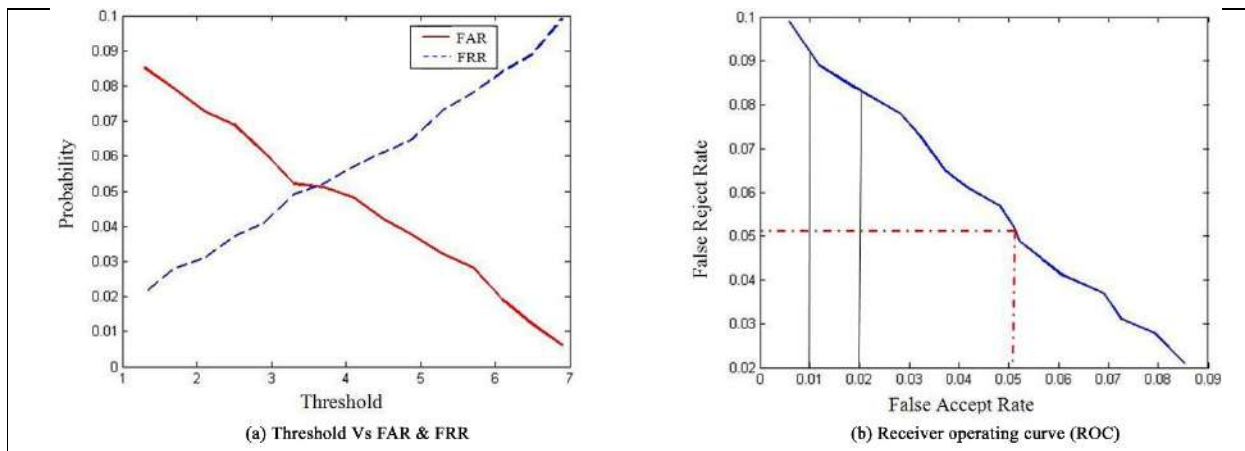


Figure 10: Accuracy plot for Kirsch edge detector

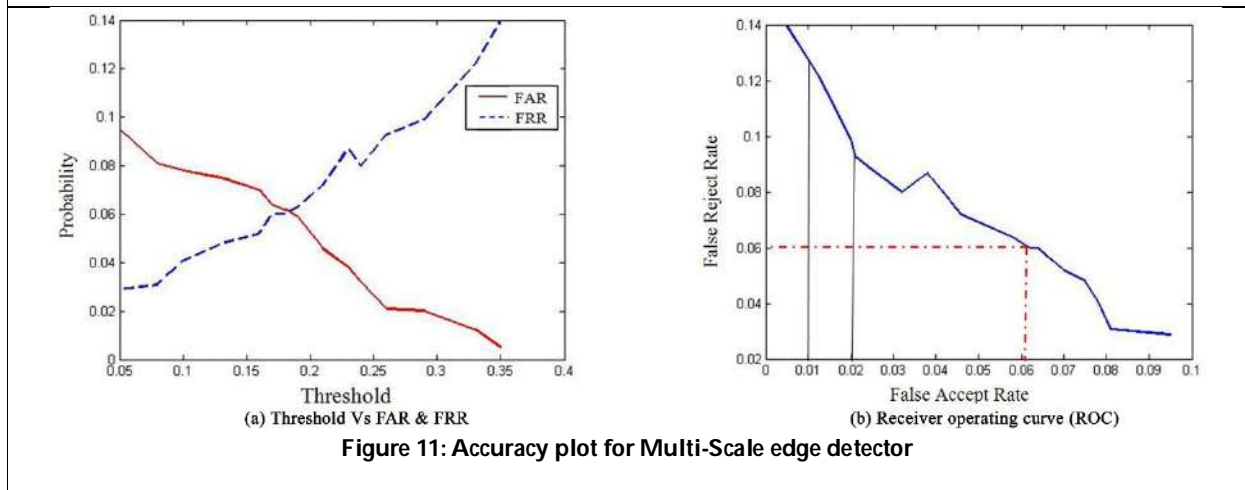


Figure 11: Accuracy plot for Multi-Scale edge detector





Design of Cascaded Multi-Level Inverter for PV Systems

P.Sarala¹ and J.Indu^{2*}

¹Department of EEE, Malla Reddy Engineering College, Maisammaguda, Hyderabad, India.

²PG Scholar, Department of EEE, Malla Reddy Engineering College, Maisammaguda, Hyderabad, India.

Received: 02 Sep 2021

Revised: 22 Sep 2021

Accepted: 22 Oct 2021

*Address for Correspondence

J.Indu

PG Scholar,
Department of EEE,
Malla Reddy Engineering College,
Maisammaguda, Hyderabad, India.
Email: indujulakanti9@gmail.com



This is an Open Access Journal / article distributed under the terms of the **Creative Commons Attribution License** (CC BY-NC-ND 3.0) which permits unrestricted use, distribution, and reproduction in any medium, provided the original work is properly cited. All rights reserved.

ABSTRACT

This paper presents the enhanced CMLI (Cascaded Multi-Level Inverter) system for reducing the leakage current. This system is very efficient and secure. The proposed method also provides low switching and power losses, in addition to the reduced switch count. The proposed architecture optimizes high frequency transforms using the suggested PWM method in terminal voltages and in common-mode voltages. Only one carrier signal is needed for all $2m+1$ working levels for the PWM technique described. The planned CMLI's grid current has a Total Harmonic Distortion (THD) that satisfies the IEEE 1547 standard. The article presents a detailed examination of the proposed CMLI utilizing the switching function idea, along with simulation results.

Keywords: Inverter, THD, Optimization, PWM

INTRODUCTION

The advantages of multilevel inverter topologies, such as high performance, low switch count, lightweight and reduced area, are gaining momentum. The galvanic isolation between the PV array and the power output is destroyed when the transformer is disconnected. The leakage current increases, endangering the security of PV systems, when galvanic insulation is removed. As a result, various safety regulations were introduced for PV systems to regulate the value or quantity of the flow of leakage current in photovoltaic systems [1-2]. Apart from reducing the leakage currents, high-quality power generation is now being used from solar systems to the grid. The multilevel inverters (MLI) in transformational PV systems have been implemented in response to this necessity. Many topologies or MLI setups [3] were presented in the literature to decrease the leakage in transformer less PV systems. The leakage current is reduced using two ways under these settings [4]. The first method is to continue the common-mode voltage, and the second is to keep a low level of high-frequency transitions of terminals and

38873





Sarala and Indu

common-mode voltages. A standardized, transformer less PV MLI with fewer electronic components is necessary in order to attain high performance and better objectives, as stated in the previous discussion. The switching and conduction losses of PV MLI should also be ensured by the use of less conductivity switches during zero voltage. Furthermore, it should be able to expand to a larger number of levels. This paper provides a technique to minimize leakage in transformers using lower MLIs. An essay also addresses the proposed MLI pulse width modulation (PWM) technique. The switching function is utilized for PV and common-mode voltages analysis. This research has developed the proposed PWM approach, eliminating changes in the terminal voltage and CMV in high-frequency voltage. The proposed Cascaded multi-level inverter (CMLI) has numerous unique characteristics:

- 1) The architecture employs eight switches to provide five output voltage levels.
- 2) Only one switch and one diode are active when the voltage is zero.
- 3) Four switches are operated in the suggested topology at a low change frequency, reducing the loss of switching.
- 4) The common-mode voltage is unaffected by the dead band in the PWM method.
- 5) The suggested inverter may be simply cascaded to reach output levels of more than five levels.

OPERATION OF PROPOSED CASCADED FIVE-LEVEL MLI

Figure 1 shows the schematic circuit layout for the proposed PV system CMLI. The default setup includes two converters (Conv-1 and Conv-2). Conv-1 is a two half-bridge converter (Sx1 and Sx2) that operates together. The Conv-2 is made up of six switches and a highly efficient and dependable inverter design. (Sx3 to Sx8). Conv-2 has six switches, four of which (Sx3 to Sx6) make up an H-bridge circuit. Conv-2's last two switches, Sx7 and Sx8, are bi-directional switches. The voltage levels of VPV and VPV/2 are generated by the switches in the Conv-1. The VPV voltage is on the terminal n when changing on Sx1 with terminal Z. When switch Sx2 is switched on, the terminal n achieves the voltage VPV/2. The switches Sx1 and Sx2 are mutually beneficial. The voltage levels produced in the terminal n of Conv-1 are received as an input. The Conv-2 provides positive, negative and no corresponding input voltage levels for the whole load (voltage between terminals n and z). The multiple SX7 and Sx8 switches provide a freewheeling route during zero voltage. The grid, as described in the Fig, is linked with the CMLI output in five levels via an LCL filter. It consists of induction Li on the inverter, reproduction Cf on the grid side and Induction Lake on the grid side. The shunt channel of the filter's Rd damper resistor is used. The resistance Rac denotes grid-side resistance, whereas the resistance Rg denotes ground-path resistance. Instantaneous grid voltage is denoted by the variable vac. The parasitic capability in a PV system produces a resonant circuit with filter inductance [4-5]. The parasite resistance and inductance are displayed as dotted lines in the PV system parameters Rp and Cp. The io, ie and iac variable indicate the five-level CMLI voltage source and the current going to the grid via the filter shunt branch. The present ice variable is due to parasite capacity the power output from the PV array to the surface.

Four pairs of additional (Sx1, Sx2) switches (Sx3, SX4), (Sx5, Sx6) and (Sx7, and SX8) are available in the proposed MLI architecture. Further controls are only used for the two switches pairs (Sx1, Sx2) to lower leakage currents (Sx7, Sx8). The PV and grid source insulation during zero voltage is simplified by avoiding complementing actions for other switch pairs. If a zero-voltage configuration of four switches on the H-bridge is switched off, the pv source is separated from the grid. The bi-directional switches Sx7 and Sx8 provide a unlimited accessroute for the inductor current during the turn-off phase of a half - cycle. This operation reduces the leakage current that passes via the parasitic capacitance.

$$\begin{aligned}
 v_{uz} &= \left(S_1 S_3 + 0.5 S_2 S_3 - \frac{1}{(S_3 + S_4)} + \frac{1}{(S_3 + S_4)(S_1 + S_2)} \right) V_{PV} \\
 v_{vz} &= \left(S_1 S_5 + 0.5 S_2 S_5 - \frac{1}{(S_5 + S_6)} + \frac{1}{(S_5 + S_6)(S_1 + S_2)} \right) V_{PV}
 \end{aligned}
 \tag{1}$$





Sarala and Indu

where S_a , ($a=1, 2, 3, \dots$) is the switch S_{xa} 's switching state, which may be either 1 (stands for turn-ON) or 0 (stands for turn-OFF). All switches for the equivalent inverter output pressure v_{uv} are presented in Table 1. The S_{x1} and S_{x2} , half-bridges, operate at a low frequency of switching. The S_{x2} control is always switched on in the zero states during the voltage transition from level 0 to $VPV/2$ to reduce unnecessary frequency change. Similarly, throughout the voltage change from level 0 to VPV , the switch S_{x1} is maintained switched on. During the positive halving center of the output voltage transformer the inverter interface (S_{x3} , S_{x6}) performs at a high frequency and is maintained on an OFF level during a negative half cycle. The second S_{x4} inverter pairing, S_{x5} , established by a similar procedure, runs in the negative half cycle, at higher switching frequency. During the half of the input cycles, the S_{x7} and S_{x8} controls will be turned on. The elimination of complementary action on switches pairs (S_{x3} , S_{x4}) and (S_{x5} , S_{x6}) allowed switches to be turned off fully in each half of the voltage UV output cycle. As a consequence, the suggested system has lower switching losses, resulting in a highly efficient and dependable inverter design that may lead to greater efficiency.

PROPOSED PWM STRATEGY ALONG WITH GENERALIZED STRATEGY FOR MINIMIZATION OF THE LEAKAGE CURRENT

The suggested PWM technique's functioning is described using the provided five-level CMLI. The proposed PWM approach decreases high-frequency transitions in the V_{XG} and CMLI 5-level terminal voltages. Every proposed action can be taken by converting from VPV to $VPV/VPV/2$ rather than changing from VPV to $VPV/2$. The PV system is isolated from the skillet during the zero voltage or during the phase available of the switching cycle. During the negative voltage condition, the PV array and grid are disconnected, similar to the inverter system described in [6-7]. The size of a comparison wave v_{mod} is reduced to 50 per cent of the original value when the switching between levels VPV and 0. is transformed. The above operation is usually done to accommodate the VPV value of PV voltage. The value of v_{mod} will change when the instantaneous size of the modulative wave v_{mod} reaches the value of $m_a/2$, where m_a is the modulation index. The output voltage includes the default stage in all its switching phases once the required change is integrated. The v_{ref} modified reference waveform expression is provided in (3).

$$v_{ref_modified} = \left\{ \begin{array}{ll} v_{mod} & \text{for } 0 \leq |v_{mod}| < \frac{m_a}{2} \quad \text{from } \frac{V_{PV}}{2} \text{ to } 0 \\ \frac{v_{mod}}{2} & \text{for } \frac{m_a}{2} \leq |v_{mod}| < m_a \quad \text{from } V_{PV} \text{ to } 0 \end{array} \right\} \quad \text{--- (2)}$$

where, $v_{mod} = m_a \sin \omega t$ gives the magnitude of v_{mod} .

SIMULATION RESULTS

The proposed CMLI of five levels is simulated by utilizing MATLAB/SIMULINK Block POWER SIM to aid in examining the switching function presented in the previous section. The proposed CMLI five-level arrangement uses the PWM method described. The suggested five-level CMLI must create the V_{inv} voltage at a phase inv to deliver the grid's required amount of active power. Figures 3 to 7 illustrate simulated waveforms of the proposed five-level CMLI utilizing the suggested PWM method. The output current of a solar PV panel is shown in Figure 8. The figure clearly demonstrates the existence of zero current state in all current transitions. Figure 5 shows the waveform of the solar panel's terminal voltages. There are voltage spikes at regular intervals, as may be seen in this diagram. The output voltage of the CMLI is shown in Fig.6. The form of the voltage may be seen in this diagram to be a five-level AC voltage with a magnitude of 500V. Figure 7 depicts the grid current i_{ac} . The current in the grid is essentially sinusoidal. Grid current i_{ac} has a Total Harmonic Distortion (THD) of approximately 1.76 percent, which satisfies IEEE 1547 requirements.





Sarala and Indu

CONCLUSION

In this article, a five-tier enhanced CMLI is presented with a lower power frequency to reduce leakage current without transformers in a PV system. The CMLI proposed minimizing the leakage current by preventing the transition from high frequencies from the terminal to the primary signal. The recommended architecture also provides less conduction and a loss of switching to allow the CMLI to operate at a high frequency. In addition, the article includes a solution for the generalized $2m+1$ levels CMLI. For the production of $2m+1$ levels, the proposed PWM method only needs one carrier wave. The paper also includes the functioning and analysis of terminal and standard-mode voltage by CMLI. The results of the simulation are analyzed in this article. The MPPT algorithm is used with the recommended five-level CMLI to generate maximum power from the PV panels.

REFERENCES

1. Y. Tang, W.Yao, P.C.Lon and F. Bleiberg, "Highly Reliable Transformerless Photovoltaic Inverters With Leakage Current and Pulsating Power Elimination," IEEE Trans. Ind. Elect., vol. 63, no.2, pp. 1016-1026, Feb. 2016.
2. W. Li, Y. Gu, H. Luo, W. Cui, X. He and C. Xia, "Topology Review and Derivation Methodology of Single-Phase Transformerless Photovoltaic Inverters for Leakage Current Suppression," IEEE Trans. Ind. Elect., vol. 62, no. 7, pp. 4537-4551, July 2015.
3. J. Ji, W. Wu, Y. He, Z. Lin, F. Bleiberg and H. S. H. Chung, "A Simple Differential Mode EMI Suppressor for the LLCL-Filter-Based Single Phase Grid-Tied Transformerless Inverter," IEEE Trans. Ind. Elect., vol. 62, no. 7, pp. 4141-4147, July 2015.
4. Y. Bae and R. Y. Kim, "Suppression of common-mode voltage using a multicentral photovoltaic inverter topology with synchronized PWM," IEEE Trans. Ind. Electron., vol. 61, no. 9, pp. 4722–4733, Sep. 2014.
5. N. Vazquez, M. Rosas, C. Hernandez, E. Vazquez, and F. J. Perez-Pinal, "A new common-mode transformerless photovoltaic inverter," IEEE Trans. Ind. Electron., vol. 62, no. 10, pp. 6381–6391, Oct. 2015
6. G. Buticchi, E. Lorenzani, and G. Franceschini, "A five-level single-phase-grid-connected converter for renewable distributed systems," IEEE Trans. Ind. Electron., vol. 60, no. 3, pp. 906–918, Mar. 2013.
7. N. A. Rahim and J. Selvaraj, "Multistring five-level inverter with novel PWM control scheme for PV application," IEEE Trans. Ind. Electron., vol. 57, no. 6, pp. 2111–2123, Jun. 2010.
8. M. Cavalcanti, K. De Oliveira, A. M. de Farias, F. Neves, G. Azevedo, and F. Camboim, "Modulation techniques to eliminate leakage currents in transformerless three-phase photovoltaic systems," IEEE Trans. Ind. Electron., vol. 57, no. 4, pp. 1360–1368, Apr. 2010.
9. L. Zhang, K. Sun, L. Feng, H. Wu, and Y. Xing, "A family of neutral point clamped full-bridge topologies for transformerless photovoltaic grid-tied inverters," IEEE Trans. Power Electron., vol. 28, no. 2, pp. 730–739, Feb. 2013.

Table I Switching States with Their Respective Output Voltage

S_{x1}	S_{x2}	S_{x3}	S_{x4}	S_{x5}	S_{x6}	S_{x7}	S_{x8}	V_{uv}
1	0	1	0	0	1	1	0	$+V_{pv}$
0	1	1	0	0	1	1	0	$+V_{pv}/2$
0	1	0	0	0	0	1	0	0
1	0	0	0	0	0	1	0	0
0	1	0	1	1	0	0	1	$-V_{pv}$
1	0	0	1	1	0	0	1	$-V_{pv}/2$





Sarala and Indu

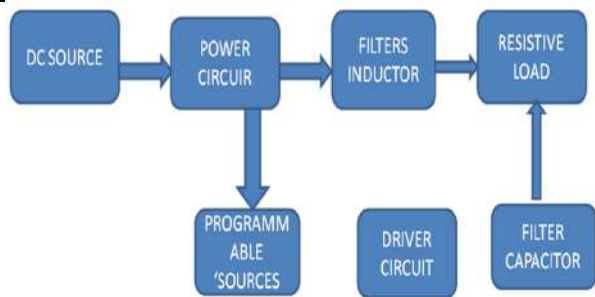


Fig. 1. Proposed five-level grid-connected CMLI with PV and parasitic elements

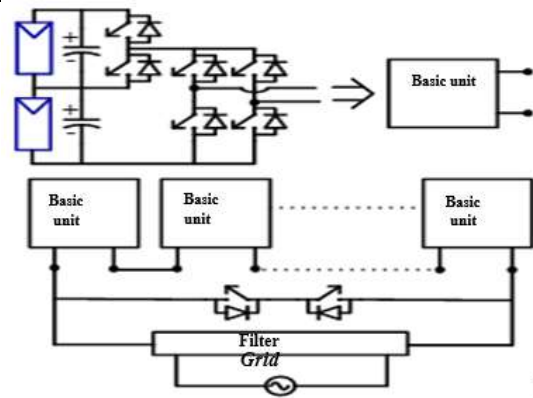


Fig.2. General topology 2m+1 level MLI based on five-level CMLI proposed

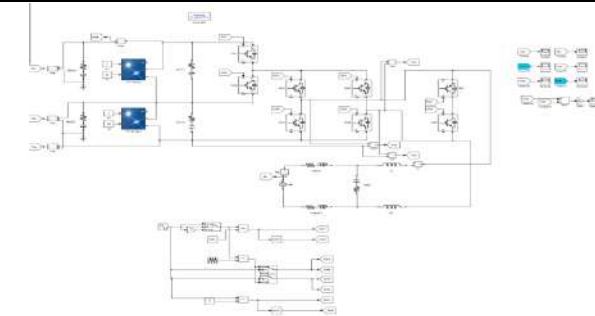


Fig. 3. Simulink model

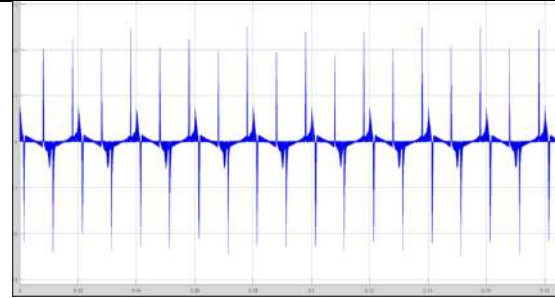


Fig. 4. Solar Current obtained from PV Cell

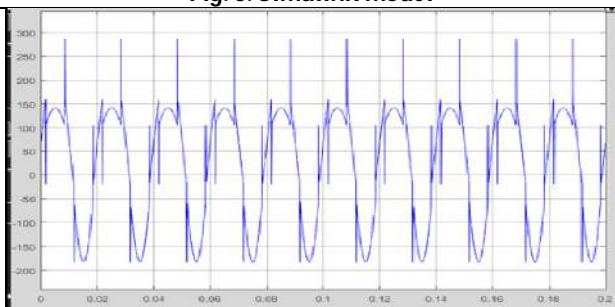


Fig. 5. Output Voltage from solar panel

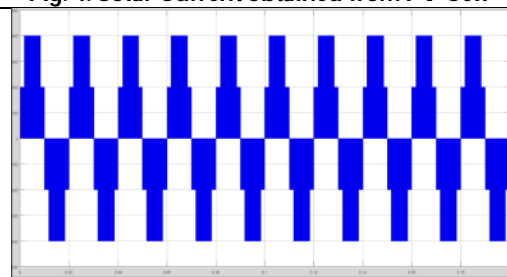


Fig.6. Output voltage of proposed ML Inverter

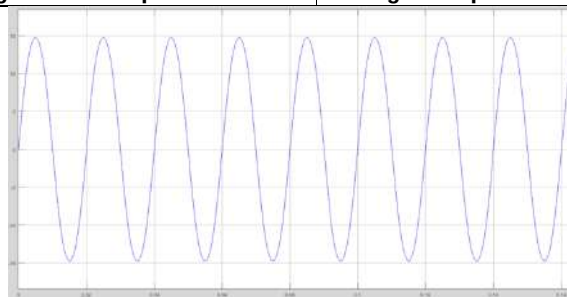


Fig. 7. Grid current of proposed system





Confirmation of Best Method for Extraction of Antioxidant and Antidiabetic Phytochemicals from *Cucumis melo subsp. agrestis* Leaves

K.Gopalasatheeskumar^{1*}, V.K.Kalaichelvan¹, N. Kannappan¹ and P. Mullai²

¹Department of Pharmacy, Faculty of Engineering and Technology, Annamalai University, Annamalai Nagar - 608002, Tamil Nadu, India.

²Department of Chemical Engineering, Faculty of Engineering and Technology, Annamalai University, Annamalai Nagar - 608002, Tamil Nadu, India.

Received: 15 Dec 2021

Revised: 22 Dec 2021

Accepted: 13 Jan 2022

*Address for Correspondence

K.Gopalasatheeskumar

Department of Pharmacy,
Faculty of Engineering and Technology,
Annamalai University,
Annamalai Nagar - 608002, Tamil Nadu, India.
Email: gskpungai@gmail.com



This is an Open Access Journal / article distributed under the terms of the **Creative Commons Attribution License** (CC BY-NC-ND 3.0) which permits unrestricted use, distribution, and reproduction in any medium, provided the original work is properly cited. All rights reserved.

ABSTRACT

Cucumis melo subsp. agrestis is one of the important medicinal plants in Cucurbitaceae family. current study aimed to evaluate the different extraction methods (Cold maceration extraction, Reflux extraction, Soxhlet extraction, Ultrasonic extraction) for extraction of antioxidant and antidiabetic phytochemicals from *Cucumis melo subsp. agrestis* leaves. Hydroalcohol (60 % methanol) was used as a solvent for extraction on each method. Extracts were concentrated using distillation method. Total phenolic and flavonoids content were estimated by using Colorimetry method. Antioxidant activity was evaluated using hydrogen peroxide radical scavenging assay and antidiabetic activity was evaluated using alpha amylase inhibition assay. Results of current research revealed that, Soxhlet extraction method has higher extractive yield but cold maceration method has higher antioxidant and antidiabetic activity. Current research concluded that, cold maceration method is suitable for extraction of antioxidant and antidiabetic phytochemicals from *Cucumis melo subsp. agrestis* leaves.

Keywords: Different extraction methods, Alpha amylase, Cold maceration, Soxhlet, Radical scavenging, Mithukkanchedi.

INTRODUCTION

Cucumis melo subsp. agrestis is one of the important medicinal plants in Cucurbitaceae family. *Cucumis melo subsp. agrestis* is commonly known as Mithukkanchedi and Chukkanchedi in Tamil, Kachari in Hindi and Dosakaya in Telugu (1). This medicinal plant is widely distributed in African and Asian Countries. In India, Punjab, Himachal

38878



**Gopalasatheeskumar et al.,**

Pradesh, Haryana, Rajasthan, Tamil Nadu and Kerala. *Cucumis melo subsp. agrestis* has many health benefits such as Stomachic, Antidiabetic, Antihyperlipidemic, Treat burns and abrasions, Antitussive, Antioxidant, Digestive, Antifungal and Antirheumatoid activities (2). The aerial parts of *Cucumis melo subsp. agrestis* are shown in Figure 1. Our previous research reported the antioxidant and antidiabetic activities of hydroalcoholic leaf extract of *Cucumis melo subsp. agrestis* using various *in vitro* and *in vivo* models (3-7). Our previous studies were used the Soxhlet extraction method for extraction of phytochemicals. But many of the extraction methods are available in phytochemical research for the extraction phytochemicals. The various extraction methods such as cold maceration, hot percolation, refluxation, Soxhlet, ultrasound extraction, centrifugation extraction, supercritical fluid extraction and microwave assisted extraction methods are having its own advantages and disadvantages (8). The major disadvantages of Soxhlet extraction method is possibility of thermal decomposition of target compounds (9). But our previous studies were used only the Soxhlet extraction method for extraction of phytochemicals. So that, study of another extraction methods for extraction of phytochemicals from *Cucumis melo subsp. agrestis* are important. Therefore, current study aimed to evaluate the different extraction methods (Cold maceration extraction, Reflux extraction, Soxhlet extraction, Ultrasonic extraction) for extraction of antioxidant and antidiabetic phytochemicals from *Cucumis melo subsp. agrestis* leaves.

MATERIALS AND METHODS

Collection and authentication of plant materials

The healthy and fresh leaves of *Cucumis melo subsp. agrestis* were collected from road sides of Pungavarnatham village, Thoothukudi District, Tamil Nadu, India and authenticated by Dr. N. Srinivasan, Assistant professor of Pharmacognosy, Department of Pharmacy, Annamalai University. The herbarium was prepared and submitted in the Department of Pharmacy, Annamalai University and the voucher specimen number is PCOL/2021/002. The collected leaves were undergoes washing with distilled water and dried under sunshade in dark room. The dried material was powdered using mechanical mixer (10).

Extraction of plant material

The powdered plant materials were extracted with hydro alcohol using different extraction methods such as Cold maceration extraction, Reflux extraction, Soxhlet extraction, Ultrasonic extraction.

Maceration method

About 10g of pulverized leaves of *Cucumis melo subsp. agrestis* were macerated with 100 ml of hydro alcohol (60 % of methanol) for 48 h with frequent agitation at room temperature. After completion of extraction, the extracts were filtered using Whatman filter paper and concentrated the filtrate using distillation method. And the obtained yield was weighed for the calculation of percentage yield as per standard formula given below (11).

$$\text{Percentage Yield (\%w/w)} = \frac{\text{Weight of extract obtained (g)}}{\text{Weight of plant material used (g)}} \times 100$$

Reflux method

About 10g of pulverized leaves of *Cucumis melo subsp. agrestis* was placed in a 250 ml round bottom flask. And 100 ml of hydro alcohol (60 % of methanol) was added. The mixture was stirred well and refluxed for 6 h at 60°C. After completion of extraction process, the extract was waited for come up to room temperature and then filtered using Whatman filter paper (12). The collected filtrate was concentrated using distillation method. And the obtained yield was weighed for the calculation of percentage yield as per standard formula given below.

$$\text{Percentage Yield (\%w/w)} = \frac{\text{Weight of extract obtained (g)}}{\text{Weight of plant material used (g)}} \times 100$$

Soxhlet method

In this extraction method, Soxhlet apparatus was used for the extraction. About 100 g leaves of *Cucumis melo subsp. agrestis* was extracted with 1000 ml of hydro alcohol (60 % of methanol) using soxhlet extraction technique for 48 h





Gopalasatheeskumar et al.,

(13). The collected extract was concentrated using distillation method. And the obtained yield was weighed for the calculation of percentage yield as per standard formula given below.

$$\text{Percentage Yield (\%w/w)} = \frac{\text{Weight of extract obtained (g)}}{\text{Weight of plant material used (g)}} \times 100$$

Ultrasonic extraction

In this method of extraction, ultra sound sonicator was used for the extraction. About 10 g of pulverized leaves of *Cucumis melo subsp. agrestis* was placed in 250 ml conical flask and in that conical flask 100 ml of hydro alcohol (60 % of methanol) was added (14). leaves of *Cucumis melo subsp. agrestis* was extracted with ultrasonic 30 min under the condition of 40 kHz and 250 W. Then the extract was filtered using Whatman filter paper. The collected filtrate was concentrated using distillation method. And the obtained yield was weighed for the calculation of percentage yield as per standard formula given below.

$$\text{Percentage Yield (\%w/w)} = \frac{\text{Weight of extract obtained (g)}}{\text{Weight of plant material used (g)}} \times 100$$

Estimation of total phenolic content

The total phenolic content of the different extracts was determined by Folin-Ciocalteu assay method. The plant extracts and standard solution of Gallic acid were prepared using distilled water and the concentration was 1mg/ml. Distilled water was used as reagent blank. To an aliquot 100µl of plant extracts (1mg/ml) or standard solution of Gallic acid (10, 20, 40, 60, 80, 100 µg/ml) added 50µl of Folin-ciocalteu reagent followed by 860µl of distilled water and the mixture was incubated for 5min at room temperature. 100µl of 20% sodium carbonate and 890µl of distilled water were added to make the final solution to 2ml. It was incubated for 30 min in dark to complete the reaction after that absorbance of the mixture was measured at 725 nm against blank. Distilled water was used as reagent blank. The tests were performed in triplicate to get the mean values. The total phenolic content was found out from the calibration curve of Gallic acid, and it was expressed as milligrams of Gallic Acid Equivalents (GAE) per gram of extract (15, 16).

Estimation of Total Flavonoid content

The total flavonoid content of the different extracts was determined by using Aluminium chloride by colorimetric method. The plant extracts and standard solution of quercetin were prepared using methanol and the concentration was 1mg/ml. Methanol was used as reagent blank. To an aliquot of 1 ml of extract (1 mg/ml) or standard solutions of Quercetin (10, 20, 40, 60, 80, 100µg/ml) methanol was added separately to make up the solution upto 2 ml. The resulting mixture was treated with 0.1 ml of 10% aluminium chloride, 0.1ml of 1M potassium acetate and 2.8 ml of distilled water. Shaken well and incubated at room temperature for 30 min. The absorbance was measured at 415nm against blank, where a solution of 2ml ethanol, 0.1 ml potassium acetate, 2.8 ml distilled water and 0.1 ml of aluminium chloride serve as blank solution. The total flavonoid content was determined from the standard Quercetin calibration curve. And it was expressed as milligrams of Quercetin equivalents per gram of extract (17, 18).

Hydrogen peroxide radical scavenging assay

The antioxidant activity of different extract was evaluated using hydrogen peroxide radical scavenging assay. In this assay method was studied as per standard method described by Ruch et al. (19). Different extracts and standard ascorbic acid were prepared in methanol solvent and different concentrations were used (20 to 100µg/ml). The percentage inhibition was calculated as per the following formula (20, 21).

$$\text{Percentage Inhibition (\%)} = \frac{\text{Control absorbance} - \text{Sample absorbance}}{\text{Control absorbance}} \times 100$$

Alpha amylase inhibitory assay

The antidiabetic activity of different extracts was evaluated by using α-amylase inhibitory activity assay. The α-amylase inhibitory activity was assessed using method described by Elsnoussi et al. (22). Briefly, 500 ml of each



**Gopalasatheeskumar et al.,**

extract dilutions (0.2–1.0 mg/ml) were mixed with 500 ml of 0.02 M sodium phosphate buffer (pH 6.9) containing 0.5 mg/mL of α -amylase solution. The mixture was pre-incubated in test tubes at 25 °C for 10 min. Thereafter, 500 mL of 1% starch solution in 0.02 M sodium phosphate buffer (pH 6.9) was added to each test tube at timed intervals. The reaction mixtures were incubated at 25°C for 10 min and stopped with 1.0 mL of DNSA reagent. The tubes were incubated in a boiling water bath for 5 min and left to cool at 25°C. Then 15 mL of distilled water was used to dilute the reaction mixtures, and the absorbance was measured at 504 nm using a spectrophotometer. Similar procedure was repeated for acarbose which serves as the positive control by preparing it in distilled water at same concentrations (0.2–1.0 mg/ml) as extracts. The values were compared with those of acarbose used as control. The result of the triplicate determinations of α -amylase inhibitory activity was expressed as % inhibition. The percentage inhibition was calculated as per the following formula (23).

$$\text{Percentage Inhibition (\%)} = \frac{\text{Control absorbance} - \text{Sample absorbance}}{\text{Control absorbance}} \times 100$$

RESULTS AND DISCUSSION**Percentage extractive yield**

The plant material *Cucumis melo subsp. agrestis* leaves were extracted with different extraction methods and the Percentage extractive yield of different extraction methods are listed in Table 1. The Soxhlet extraction method shows higher extractive yield (17.37% w/w) when compared with all other extracts. The Ultrasonic extraction method shows less extractive yield (10.48% w/w). The less extractive yield in ultrasonication method may due to the less duration of extraction procedure and higher extractive yield of Soxhlet extraction method may due to its continuous extractive principle.

Total Phenolic and Flavonoid content

Total Phenolic and Flavonoid content of *Cucumis melo subsp. agrestis* leaves on different extraction methods are listed in Table 2. The Cold maceration extraction method shows higher total phenolic content (45.33 mg/g as GAE) when compared to all other extraction methods. For total flavonoid content, Cold maceration extraction method (20.62 mg/g as QE) shows higher when compared with all other methods. This report suggests that, the maximum phenolic compounds present in the extract obtained from cold maceration is maybe the flavonoids.

Antioxidant activity

The antioxidant activity of *Cucumis melo subsp. agrestis* leaves on different extraction methods was evaluated by using the hydrogen peroxide radical scavenging assay. The results of hydrogen peroxide radical scavenging assay were shown in Figure 2. The percentage inhibition of hydrogen peroxide radical activity of extracts was increased based on concentration. The cold maceration method shows the higher percentage inhibition when compared with all other extraction methods in concentration dependent manner. The reflux method shows least activity when compared with all other methods. The least activity of the reflux method maybe due to its less phenolic and flavonoids content and higher activity of the cold maceration may due to its higher phenolic and flavonoids content.

Antidiabetic activity

The antidiabetic activity of *Cucumis melo subsp. agrestis* leaves on different extraction methods was evaluated by using the alpha amylase enzyme inhibition assay. The results of alpha amylase enzyme inhibition assay were shown in Figure 3. The percentage inhibition of alpha amylase activity of extracts was increased based on concentration. The cold maceration method shows the higher percentage inhibition of alpha amylase enzyme when compared with all other extraction methods in concentration dependent manner. The reflux method shows least activity when compared with all other methods. The least activity of the reflux method maybe due to its less phenolic and flavonoids content and higher activity of the cold maceration may due to its higher phenolic and flavonoids content.



**Gopalasatheeskumar et al.,**

CONCLUSION

Based on the results of antioxidant and antidiabetic activity, the cold maceration is suitable method for the extraction of antioxidant and antidiabetic phytochemicals from *Cucumis melo subsp. agrestis* leaves. Further studies needed to isolate, identify the active phytochemicals and preclinical studies.

ACKNOWLEDGEMENTS

The authors thank to Pungavarnatham (Thoothukudi District) village peoples for help to collecting plant materials and Prof. V. Srinath, Head of the Department of Pharmacy, Annamalai University for providing chemicals and excellent lab specialties for doing research work.

REFERENCES

1. Shankar K, Singh SK, Kumar D et al. *Cucumis melo ssp. Agrestis var. Agrestis* Ameliorates High Fat Diet Induced Dyslipidemia in Syrian Golden Hamsters and Inhibits Adipogenesis in 3T3-L1 Adipocytes. *Pharmacogn Mag* 2015; 11(4): S501-S510.
2. Kapoor M, Sharma C, Kaur N et al. Phyto-Pharmacological Aspects of *Cucumis melo var. agrestis*: A Systematic Review. *Pharmacogn Rev* 2020; 14(27):28-32.
3. Gopalasatheeskumar K and Kalaichelvan VK. Antioxidant potential of different parts (leaves, stem, fruit, seed, flower and root) extracts of *Cucumis melo var Agrestis*. *International Journal of Pharmaceutical Sciences and Research*, 2021; 12(1): 465-469.
4. Gopalasatheeskumar K, Ariharasivakumar G, Kalaichelvan VK, Sengottuvel T, Sanish Devan V, Srividhya V. Antihyperglycemic and antihyperlipidemic activities of wild musk melon (*Cucumis melo var. agrestis*) in streptozotocin-nicotinamide induced diabetic rats. *Chinese Herbal Medicines*, 2020; 12:399-405.
5. Gopalasatheeskumar K, Kalaichelvan VK, Ariharasivakumar G, Sengottuvel T, Sanish Devan V. In vitro Antidiabetic activity of hydroalcoholic leaf extract of *Cucumis melo var agrestis* (Cucurbitaceae). *Research Journal of Pharmacy and Technology*, 2020; 13(12):5851-5854.
6. Gopalasatheeskumar K, Ariharasivakumar G, Sengottuvel T et al. Confirmation of Best Method for Detection of Alpha Amylase Activity of *Cucumis melo var agrestis*(Wild Musk Melon). *J Adv Res BioChem Pharma* 2019;2(1):1-3.
7. Gopalasatheeskumar K, Ariharasivakumar G, Sengottuvel T, Sanish Devan V, Srividhya V. Quantification of Total Phenolic and Flavonoid content in leaves of *Cucumis melo var agrestis* using UV- spectrophotometer. *Asian J. Research Chem* 2019; 12(6):335-337.
8. Altemimi A, Lakhssassi N, Baharlouei A, Watson DG, Lightfoot DA. Phytochemicals: Extraction, Isolation, and Identification of Bioactive Compounds from Plant Extracts. *Plants (Basel)* 2017; 6(4):42.
9. Lao RC, Shu YY, Holmes Y, Chiu C. Environmental Sample Cleaning and Extraction Procedures by Microwave-Assisted Process (MAP) Technology. *Microchem J* 1996; 53(1): 99-108.
10. Yuvaraja K R, Santhiagu A, Jasmine S, Gopalasatheeskumar K. Hepatoprotective activity of *Ehretiamicrophylla* on paracetamol induced liver toxic rats. *J Res Pharm* 2021; 25(1):89-98.
11. SankeshwariRoopali M, Ankola Anil V, Bhat Kishore, HullattiKirankumar. Soxhlet versus cold maceration: Which method gives better antimicrobial activity to licorice extract against *Streptococcus mutans*?. *J Sci Soc* 2018; 45(2):67-71.
12. Zhang QW, Lin LG, Ye WC. Techniques for extraction and isolation of natural products: a comprehensive review. *Chin Med* 2018; 13:20.
13. Gopalasatheeskumar, K. Significant role of Soxhlet extraction process in phytochemical research. *MJPMS* 2018; 7:43-47.
14. Hayouni EA, Abedrabba M, Bouix M, Hamdi M. The effects of solvents and extraction method on the phenolic contents and biological activities in vitro of Tunisian *Quercus coccifera* L. and *Juniperus phoenicea* L. fruit extracts. *Food Chem* 2007; 105:1126-1134.





Gopalasatheeskumar et al.,

15. Madaan R, Bansal G, Kumar S, Sharma A. Estimation of Total Phenols and Flavonoids in Extracts of *Actaea spicata* Roots and Antioxidant Activity Studies. *Indian J Pharm Sci* 2011; 73(6):666-669.
16. Wolfe K, Wu X, Liu RH. Antioxidant activity of apple peels. *J. Agric. Food Chem* 2003; 51:609-614.
17. Saeed N, Khan MR, Shabbir M. Antioxidant activity, total phenolic and total flavonoid contents of whole plant extracts *Toriiisleptophylla L.* *BMC Complement Altern Med* 2012; 12:221.
18. OrdonEz AAL, Gomez JD, Vattuone MA, Isla MI. Antioxidant activities of *Sechium edule* (Jacq.) Swart extracts. *Food Chem.* 2006; 97:452-458.
19. Ruch RJ, Cheng SJ, Klaunig JE. Prevention of cytotoxicity and inhibition of intercellular communication by antioxidant catechins isolated from Chinese green tea. *Carcinogenesis* 1989; 10(6):1003-1008.
20. Fernando CD, Soysa P. Optimized enzymatic colorimetric assay for determination of hydrogen peroxide (H₂O₂) scavenging activity of plant extracts. *MethodsX* 2015; 2:283-291.
21. Asok Kumar K, UmaMaheswari M, Sivashanmugam AT, Subhadra Devi, Subhashini N, Ravi TK. Free radical scavenging and antioxidant activities of *Glinusoppositifolius* (carpet weed) using different in vitro assay systems. *Pharm Biol* 2009; 47(6):474-482.
22. Xiao Z, Storms R, tsang A. A quantitative starch iodine method for measuring alpha-amylase and glucoamylase activities. *Anal Biochem* 2006; 351(1):146-148.
23. Tamil IG, Dineshkumar B, Nandhakumar M, Senthilkumar M, Mitra A. In vitro study on α -amylase inhibitory activity of an Indian medicinal plant, *Phyllanthus amarus*. *Indian J Pharmacol* 2010; 42(5):280-282.

Table 1: Percentage extractive yield of *Cucumis melo subsp. agrestis* leaves on different extraction methods

Method of Extraction	Amount of plant material used (g)	Volume of solvent used (ml)	Amount of extract obtained (g)	Percentage Yield (% w/w)
Cold maceration extraction	10	100	1.195	11.95
Reflux extraction	10	100	1.210	12.10
Soxhlet extraction	100	1000	17.37	17.37
Ultrasonic extraction	10	100	1.048	10.48

Table 2: Total Phenolic and Flavonoid content of *Cucumis melo subsp. agrestis* leaves on different extraction methods

Method of Extraction	Total phenolic content expressed as Gallic acid equivalent (mg/g)	Total Flavonoid content expressed as Quercetin equivalent (mg/g)
Cold maceration extraction	45.33	20.62
Reflux extraction	32.24	15.27
Soxhlet extraction	40.91	19.33
Ultrasonic extraction	35.36	16.75





Figure 1: Aerial parts of *Cucumis melo subsp. agrestis*

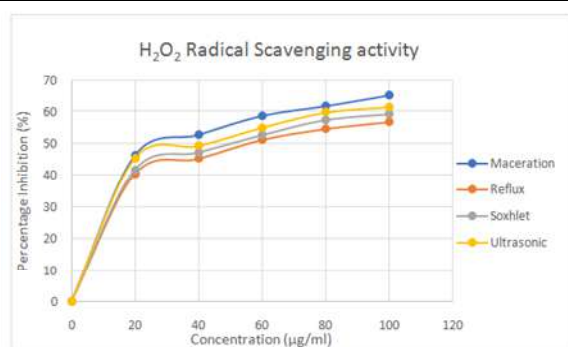


Figure 2: Effect of antioxidant activity of *Cucumis melo subsp. agrestis* leaves on different extraction methods

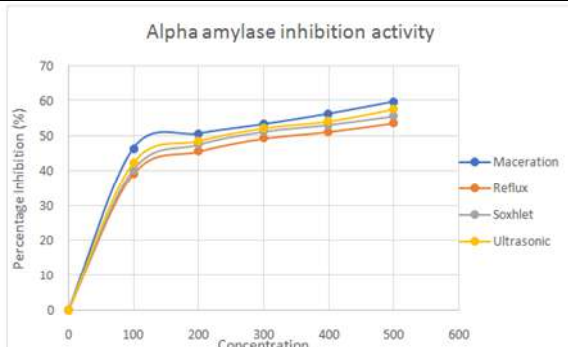


Figure 3: Effect of antidiabetic activity of *Cucumis melo subsp. agrestis* leaves on different extraction methods





Analysis of Support Vector Machine and Convolutional Neural Network to Improve Satellite Imagery

N.Thamaraikannan^{1*} and S. Manju²

¹Ph.D Research Scholar, PG and Research Department of Computer Science, PSG College of Arts and Science, Coimbatore - 641014, Tamil Nadu, India

²Associate Professor, Department of Information Technology, PSG College of Arts and Science, Coimbatore - 641014, Tamil Nadu, India.

Received: 15 Dec 2021

Revised: 30 Dec 2021

Accepted: 22 Jan 2022

*Address for Correspondence

N.Thamaraikannan

Ph.D Research Scholar,
PG and Research Department of Computer Science,
PSG College of Arts and Science,
Coimbatore - 641014, Tamil Nadu, India
Email: thamaraikannan@psgcas.ac.in



This is an Open Access Journal / article distributed under the terms of the **Creative Commons Attribution License** (CC BY-NC-ND 3.0) which permits unrestricted use, distribution, and reproduction in any medium, provided the original work is properly cited. All rights reserved.

ABSTRACT

This paper presents the analysis of various satellite image processing techniques for analyzing satellite images. Satellite images are widely used in many real time applications such as in agriculture land detection, navigation and in geographical information systems. Crop type identification and mapping have been a classic issue essential for agriculture characterization and food security as well as crop health monitoring. Remote sensing was proven to be an efficient tool to define and study agriculture. Satellite Image classification is the major component of the remote sensing to extract some of the important spatially variable parameters, such as land cover and land use (LCLU). Crop growth monitoring timely and accurately during the growing season is of great importance for accurate yield estimation, which can provide information support for making and adjusting agricultural policies. Convolutional Neural Network (CNN) has been useful for decades to the development of Satellite image classification algorithms applied to several different fields. SVM as a strongest mathematical model gives a new direction for future research in the vast field of classification and regression. Convolutional Neural Network is a popular method used in machine learning in a wide range of application domains that is known for its high accuracy value. In addition, there is a Support Vector Machine method with several kernel functions that has been applied in the classification. In this paper discuss about for the popular machine learning algorithm Support Vector Machine (SVM) Convolutional Neural Network (CNN) to perform Satellite images classification.

Keywords: Satellite Image, Machine Learning, Deep Learning, Agriculture, Precision Agriculture, Multi-temporal image classification, CNN, SVM



**Thamaraikannan and Manju****INTRODUCTION**

Knowledge of the land cover is an entry point for numerous applications calling upon the management of resources and human activity. The corresponding maps are thus a key element that can be used in many disciplines: to understand the territories, to monitor farming (Alcantara et al., 2013), for ecology (Qamer et al., 2016) or urban management (Lefebvre et al., 2016). In the last decades, various technological advances resulted in growing availability of remote sensing data revealing vegetation patterns on both spatial and temporal domains (Colomina and Molina, 2014, Toth et al., 2016). Today's world is running every business and organization to get more profit using the data analytics. Same is the case with the smart agriculture. To deal with the data, researchers face number of challenges which are mentioned under data analytics challenge category. Monitoring agricultural land use is of high importance for food production, biodiversity, and forestry an increasing world population, climate change, and changes in food consumption habits put yet uncultivated areas under pressure, while leading to intensification in existing agricultural area. Cropland expansion and intensive use of agricultural areas are often connected with negative ecological impacts like Deforestation and biodiversity loss, but also degradation of ecosystem services likes ground and surface water quality. Therefore, dense, accurate monitoring of agricultural lands plays an essential role for their optimal and sustainable management.

Images, which aid in a full comprehension of all types of surroundings, are the best source of information for humans. As a result, in order to reap the benefits, computer science has endeavored to incorporate the quality of visual information into its activities. In computer science, image processing is the process of modifying images with computers. As a result, images are seen as a source of data and information that can be accessible if the image is studied properly. In this article, we'll go over a basic introduction of how image processing works and how it might be applied to precision agriculture. In order to be processed, an image is converted into a numerical matrix that a computer can easily interpret. Image enhancement, restoration, compression, and analysis are just a few of the different types of processing that are possible. The latter is especially fascinating because it permits exact data to be taken immediately from an image. The analysis can be done by looking at the edges of images (image extraction), their colors (texture analysis), and the motions between images (movement analysis) (i.e. motion analysis). There are only a few basic steps to the technique. The first step is image capture, which gathers the data to be analyzed. After that, the image is preprocessed to get the most out of it. During the segmentation process, the image is divided into smaller pieces, allowing the computer to compare and analyze it more quickly. The information is then prepared for computers and made recognizable by assigning labels to different categories of data. These fragments can now be combined, processed, and used to extract relevant data. Image processing was first investigated in the 1960s, when it was used to collect information on the moon and sun during a lunar walk. Due to the expensive expense of the technology, image processing was largely used in the scientific field until the rapid expansion of computers in the late 1990s. Today; image processing has a wide range of applications. Aside from image editing, data obtained from photographs is used in medicine, scientific research (e.g. spatial research), fingerprints/iris/face recognition technologies, remote sensing (e.g. satellite images), and industrial applications (e.g. quality check, sorting, etc.) In agriculture, image processing offers a wide range of uses.

Image processing is also widely used in agriculture. The technology's main advantage is that it is nondestructive, meaning it can provide vital information on crops without having to touch them. The most typical applications are classified into four categories. The first is crop management, which entails identifying pests and diseases as well as watering methods. The second involves the evaluation of crop leaves and skin conditions, which aids in the detection of nutrient deficiencies as well as plant content. Fruit quality inspections and sorting are also possible thanks to images and recommendations acquired utilizing advanced machine learning algorithms. Last but not least, image processing is used in crop and land estimation, as well as crop colour and texture segmentation, for the Geographic Information System. The current works mainly discuss about Machine learning classification algorithms CNN & SVM using Satellite images

MACHINE LEARNING AND SATELLITE IMAGERY

**Thamaraikannan and Manju**

The population of the world has been increased 34% surveyed by food and agriculture organization. As a result of this predicted expansion, increased agricultural output and reliable crop status data are in jeopardy all around the world. To manage this good monitoring and management has been need in agricultural unit specifically for countries under develop. The farmer can utilize the multispectral image of wide area covered by the agricultural field to identify the production, crop monitoring and identifying issues over the field. There has been a lot of other correlated monitoring has also been involved on handing multitemporal satellite image. When agriculture management software is unavailable, regional farmers can use Google Earth Pro™ to assess vegetation and soil index imagery to identify areas in the fields that require further investigation to determine whether the crop requires additional irrigation or fertilization. Machine learning refers to the process of transmitting information to a machine. To name a few examples of machine learning methodologies, supervised learning and unsupervised learning are both used. As the name implies, one supervisor is in charge of supervising the object that is being taught through training examples and then used to arrive at the most accurate conclusion when fresh data is received. The computer software is being trained, and the supervisor is in charge of keeping track of it. Artificial neural networks, Bayesian networks, decision trees, support vector machines, ID3, k-nearest neighbor, hidden markov models, and other approaches can be used to achieve supervised learning. The algorithm is tasked with finding patterns and the linkages that exist between those patterns after a large amount of data has been provided to the software.

The term "unsupervised machine learning" is used to characterise this method. As a result, unsupervised learning can be utilised to find previously unseen patterns in data. Unsupervised learning algorithms include k-nearest neighbor, self-organizing map, and partial based clustering. Unsupervised learning approaches include hierarchical clustering, k-means clustering, and variants of these algorithms. The merger of computer science and statistics, which is made possible by machine learning, improves prediction power. It will most likely be of most interest to data scientists, data analysts, and anyone else who wants to forecast or find trends in data in general using raw data. Machine learning techniques can be applied to agriculture and agricultural production to provide an accurate prediction of crop production results, given the vast amount of data available and the fact that data is generated on a regular basis. The use of machine learning-based algorithms for analyzing remote sensing pictures has grown in popularity in recent years (RSIs). It's worth mentioning that there are only a few GP-based studies in the field of remote sensing technologies, for example, compared to other machine learning methodologies. The estimation of typhoon rainfall over the ocean using multivariable meteorological satellite data, the monitoring of reservoir water quality using remote sensing images, the mapping of base metal deposits, image thresholding for landslide detection, and the analysis of soil moisture distribution are all mentioned as examples of remote sensing technology applications.

Researchers announced that they have developed a completely automated computational approach for extracting agricultural crop fields from 30m WELD time series. The work encompasses multi temporal images and the work handled the classification the A variety of variables have influenced this. Multi-temporal Landsat data enables for crop rotations and inter-annual vegetation condition variations, compared to single Landsat acquisitions. Second, with only a few parameters and no training data, robust segmentation can be achieved. Third, related segments from many fields are divided using a watershed method, while circular field segments are recognized and associated using a geometry-based approach. A preliminary validation was carried out in order build a validation technique that incorporates new geometric measures for calculating individual field artefact accuracy. The importance of future study, as well as the ramifications and recommendations of large-scale adoption, is emphasized. Researchers investigated a segmentation method for locating field. Different segmentation methods have been analyzed with the agricultural field with temporal satellite image. The review has been validated with the various performance measures. Fields can now be recognized as whole objects rather than just pixels, allowing for more exact categorization. Both of these findings point to the possibility of using the generated field borders in a land-use classification system. When compared to two previous segmentation processes, the result is straighter, cleaner line work with no gaps in the data. Three more New Zealand datasets, including a variety of locations, topographies, satellite sensors, and radiometric calibrations, were also used to demonstrate the approach. The technique is said to



**Thamaraikannan and Manju**

be resilient when employing medium-quality satellite images, which are commonly used for field size mapping, according to the study.

REVIEW OF LITERATURE

All of the situations in the article used the same parameters. This task was reformulated as a semantic segmentation problem in 2020, and a deep convolutional neural network was used to tackle it. Using multi-tasking and conditioned inference, the PSO-CNN model calculated the likelihood of a pixel belonging to an area as well as the distance to the nearest boundary for each pixel. To achieve instance segmentation and field extraction, the predictions were then post-processed for each individual field. With great generalization across location, time, resolutions, and sensors, the PSO-CNN neural network produced cutting-edge output for field border recognition using spectral and contextual information. To minimize over fitting and achieve high generality, the technique needs learning from a large number of similar assignment. (Zewei Xua, Kaiyu Guanc et al., 2018) The 3D convolutional neural network (CNN) technique was used to extract characteristics from LiDAR point clouds. The technique consisted of three steps: (1) constructing an occupancy layer, a strength grid at 1-meter resolution, and (2) normalizing and integrating data into the 3D CNN. With the use of a Support Vector Machine classifier, the 3D CNN collected features (for example, morphological and depth features) that were then coupled with multi-temporal spectral data to improve the enforcement of land cover categorization classification. When using individual LiDAR data points, our technique beats a typical approach by 2.65 percent (from 81.52 percent to 84.17 percent), and by 2.19 percent (from 90.20 percent to 92.57 percent) when aggregating all possible imageries. Future research will focus on finding the optimal voxel spatial resolution, grasping the deep features that have been collected, and evaluating sites with more complex terrain.

(Ce Zhang a, Xin Pan et al., 2018) When a CNN based on deep spatial feature representation is combined with an MLP based on spectral discrimination, the proposed MLP-CNN ensemble classifier collects complementary data from both CNNs. Overall, the MLP-CNN classifier beat all other MLP classifiers, including the pixel-based MLP, the spectral and textural-based MLP, as well as the contextual-based CNN. This work investigates how to deal with the tough problem of VFSR photo categorization in a more effective manner. When there is a statistically significant difference in the majority of scenarios, the MLP-CNN algorithm consistently outperforms both the individual classifiers (MLP and CNN) and the GLCM-MLP method, which incorporates the GLCM texture features into the MLP algorithm. The findings of this study point the way toward a more robust solution to the difficult challenge of automatic VFSR picture classification. (Zhipeng Deng a, Hao Sun et al., 2018) published a paper in which they say Recent developments in deep learning approaches, particularly faster region-based convolutional neural networks (FRCN), have been explained in the computer vision field, where they have been shown to have significantly improved identification abilities. Starting with the feature extractor, we used Concatenated ReLU and Inception to re-design it, which improved the quality of impressionable field sizes. There are two sub-networks that are involved in the detection process. The first is a multi-scale object proposal network (MS-OPN), which is responsible for generating object-like regions from several intermediate layers, each of whose receptive fields corresponds to a different object scale, and the second is an accurate object detection network (AODN), which is responsible for detecting objects based on fused feature maps. Furthermore, we will employ Image-Net pre-trained models to analyse practise purpose signals from the outside, which will be done with the help of Image-Net (Shen et al., 2017). We'll also make use of a multi-GPU architecture to further reduce calculation time and power consumption.

(Wojciech Gruszczyński, Edyta Puniach et al., 2019) The goal of this article is to demonstrate a three-layer filtering strategy based on convolutional neural networks (CNNs) that was designed specifically for the aforementioned specific problem. Convolutional neural networks (CNNs) are a type of neural network that can learn from experience. Because of the modular structure of each algorithm, it is straightforward to build and improve. Maximum failures from immature data of big grass can be overcome by as much as 60 percent – 70 percent in the maximum of digital elevation model (DEM) leads generated on some relevance of vegetation if the proposed clarification is implemented, according to the researchers. Finally, in terms of accuracy, the CNN-based filtering strategy surpassed findings based on local minima in the experiment. (Sakshi Dhingra, Dharminder Kumar 2019)



**Thamaraikannan and Manju**

Satellite image categorization and remote sensing are discussed in detail in this study, which also includes a quick overview of recent research in this area. Improved classification accuracy is the goal of this research, which is achieved by combining appropriate classifiers with novel feature extraction methodologies and preprocessing procedures. It is planned to employ a dataset of satellite photographs in the future in order to increase accuracy and reduce classification error rates, among other things.

(Cheolhee Yooa , Daehyeon Hana et al., 2019) The proposed modified radio frequency (RF) and convolutional neural network (CNN) have been built specifically for this application. Within each city, overall accuracy for total land cover classes (OA) and urban LCZ types (LCZ1-10; OAurb) increased by approximately 6–8 percent and 10–13 percent, respectively, over the previous year. The transferability of the LCZ criteria for the four cities was estimated, which explains why CNN constantly outperformed RF (with OA and OAurb raising their scores by approximately 7–18 percent and 18–29 percent, respectively). With the inclusion of more expensive analytical satellite images (such as those taken by Sentinels) and additional spatiotemporal data, the purpose of using a CNN-based technique becomes even more advantageous. (Shiyao Meng , Xinyu Wang et al., 2020) In the year 2020, will publish a paper titled This research focuses on deep learning-based crop mapping with one-shot hyper spectral satellite data, and it employs three convolutional neural networks (CNN) models for end-to-end crop mapping, namely 1D-CNN, 2D-CNN, and 3D-CNN models, to achieve end-to-end crop mapping accuracy of more than 90%. When employing hyper spectral satellite images, the classification accuracy was found to be greater than 94 percent, which was much better than the result obtained when using mono-temporal MSIs and comparable to the result obtained when using multi-temporal MSIs (see Figure 1). These decisions will be critical in assessing the validity of hyper spectral data when planning large-scale crop landscapes, as well as determining the viability of CNN patterns, particularly 3D-CNN models, when crop identification is required. Furthermore, due of the advancements in hyper spectral representation technology, the scope of this research could be broadened much further. Additional research will be conducted in the future to examine an end-to-end deep learning method that will be applied to the large-scale hyper spectral satellite image crop mapping effort to increase the performance of each data processing step.

(Michal Segal-Rozenhaimera, Alan Lia et al., 2020) We employ a convolution neural network (CNN) technique to detect cloud and cloud shadow fields in multi-channel satellite data collected by the World-View-2 (WV-2) and Sentinel-2 (S-2) satellites using their RGB and near-infrared (RGB and NIR) channels. As part of the NASA Nemo-Net project, this method was developed to categorise coral reefs around the world using imagery from a variety of remote sensing planes and satellites with varying degrees of geographical and spectral coverage. The Nemo-Net project is a multi-modal CNN for worldwide coral reef categorization that incorporates imagery from a variety of remote sensing planes and satellites with heterogeneous degrees of geographical and spectral coverage. This approach will require improvements in both the practise sets and the powdered accuracy sets if it is to be successfully applied around the world. A textural feature extractor within the CNN framework is also proposed to improve weak cirrus spot disclosure, which is currently lacking.

(Chen xiao Zhanga, Peng Yueb,c,d et al., 2020) Because of their low computational cost and exact contour preservation, object-based Convolutional Neural Networks (OCNN) for VHRI classification have been proposed as a way to overcome the disadvantages of redundant pixel-wise CNNs in the classification of VHRI images. The OCNN (MLCGOCNN) is employed in this research to provide a unique multi-level context-guided classification purpose that is not found elsewhere. When compared to universal benchmark opinions such as patch-based per-pixel CNN (PBPP), patch-based per-object CNN (PBPO), pixel-wise CNN with intention segmentation refinement (PO), semantic segmentation U-Net (U-NET), and DeepLabV3+(DLV3+), the MLCG-OCNN scheme achieves extraordinary analysis review (> 80 percent). When compared to the state-of-the-art design DeepLabV3+, MLCG-OCNN confirms superior computational capabilities for VHRI classification (4–5 times faster). Furthermore, additional research on unique features with geometric components is required in order to improve some of the conclusions reached so far.

(David Griffiths, Jan Boehm, 2020) This is accomplished through the use of deep convolutional neural networks such as the Mask/Faster R-CNN and the RetinaNet deep convolutional neural network. RGB and RGB-lidar signals, as well as their fusion, are sent into the networks. We allow quantitative research on numerous elements of gravity



**Thamaraikannan and Manju**

measurement production in the context of segmentation development, including the formation of gravity measurements. The exposure efficiency (mAP@0.5) and segmentation f1 averages (0.94) obtained over a 4911 inspection picture extending from urban to farm photos are 0.92 (mAP@0.5) and 0.94, respectively, by altering both means. Moreover, greater outcomes would be obtained by inferring an increase in a focused damage process toward the Mask R-Faster CNN's R-CNN growth.

(Jason Kane Gilbertson, Adriaan van Niekerk, 2017) According to this study, the performance of computerised and standard characteristic preference is determined. The numerous crop variety phenological spotlights were continued to be collected into an object-based image analysis (OBIA) model, and each scale of visual and textural attributes was produced within the model. This innovation was used as an input by supervised classifiers such as DTs, k-nearest neighbour (k-NN), support vector machine (SVM), and random forest (RF), among others. Through the use of feature selection, it was possible to improve the overall sharpness of the DT, k-NN, and RF classifications, while simultaneously decreasing the efficiency of the SVM classifications. According to the findings, using SVM among feature extraction (PCA) on specific model generations allowed for the creation of many specific classifications (96.2 percent). We anticipate that a variety of SVM algorithms will be able to be used in these learning areas (and adjacent sites) before every complete assemblage of characteristics has been produced. Because of this conclusion, more specialised and cost-effective crop-type diagrams are being developed near each Cape Wine region, as well as improvements in food preservation in each sector.

(Pengfei Li, Limin Dong et al., 2015) During this article, we recommend each vapor image apprehension technique based upon an SVM vector machine to eliminate edgewise shadow data to decrease some volume regarding data to develop this performance of the data. Ultimately, we carry exercises approaching vapor image discovery techniques based on an SVM vector machine. Analysis outcomes confirm exposure efficiency regarding that approach suggested could reach high 90%. These empirical conclusions determine that a specific algorithm container better affects the cloud detection, provides each element. (Deepak Kumar Jaina, Surendra Bilouhan Dubey et al., 2018) Unique Recommended Methodology is based on covering the idea of optimizing Support Vector Machine (SVM). Each Methodology implemented here serves under a couple of phases, first is to prepare some relevant traits of the image by Optimizing Support Vector Machine utilizing Individual Organizing Maps moreover another implies observing unique Interior also Exterior Pixels furthermore Paralleling Optimal Threshold Prospect. This aimed Methodology Outperforms more helpful in comparison with special actual Analysis methodology in phases of Exactitude including Kappa and Uncertainty Patterns. During our ultimate achievement, we can implement a distinct approach toward delimiting the threshold rate; the work will be applied during different types concerning remotely sensed images, etc.

(Hongyan Zhanga, Jinzhong Kanga et al., 2019) Meanwhile aforementioned research, we used time-series Sentinel-2 image data from Yi'an County, Heilongjiang dependency, China, to investigate the effectiveness of the temporal and spectral features practiced in three common machine knowledge classification techniques: classification and regression tree (CART) decision tree, Support Vector Machine (SVM), and random forest (RF). For CART and SVM classifiers. Each quantitative evaluation decisions furnished via the embarrassing pattern designate that random forest managed the most valuable overall accuracy. While support vector machine listed secondary, plus the decision tree algorithm allowed the least detailed classification outcomes. Ultimately, our research performed crop variety mapping within every knowledge field with an overall accuracy of 97.85% and a Kappa coefficient of 0.95. Moreover, the relative importance of the features used in the classification process was analyzed for each classification approach, and analytical interpretation was carried out.

(Onuwa Okwuashi, Christopher E. Ndehedehe, 2020) The research examines the specific purpose of a Deep Support Vector Machine (DSVM) for hyper spectral image classification. This DSVM implies performed amidst four kernel purposes: Exponential Radial Basis Function (ERBF), Gaussian Radial Basis Function (GRBF), neural and polynomial. Statistical outcomes prove that the classification efficiencies of the DSVM for Indian Pines and the University of Pavia based upon various DSVM kernel functions are: ERBF (98.87%, 98.16%), GRBF (98.90%, 98.47%), neural



**Thamaraikannan and Manju**

(98.41%, 97.27%), and polynomial (99.24%, 98.79%). By balancing each DSVM algorithm toward familiar classifiers, Support Vector Machine (SVM), Deep Neural Network (DNN), Gaussian Mixture Model (GMM), K Nearest Neighbor (KNN), and K Means (KM) classifiers, the mean classification efficiencies for Indian Pines and the University of Pavia are DSVM (98.86%, 98.17%), SVM (76.03%, 73.52%), DNN (94.45%, 93.79%), GMM (76.82%, 78.35%), KNN (76.87%, 78.80%), and KM (21.65%, 18.18%). Certain decisions designate that particular DSVM exceeded the additional analysis algorithms. The high efficiency gained amidst the DSVM proves its efficiency as a state-of-the-art algorithm for hyper spectral image classification. Improving repetitive signals in multivariate information data. Via here end, guidance on extending algorithms for time-series modeling that acquire even more helpful articles and are more informal and faster to guide are suggested for a prospective analysis area.

(Genbatu Ge , Zhongjie Shi et al., 2020) The primary goal of this study is to create a reference for extracting LUCC knowledge in dryland provinces, including oasis desert mosaic landscapes, by comparing the k-nearest neighbour (KNN), random forest (RF), support vector machine (SVM), and artificial neural network (ANN) for LUCC classification in dry land provinces, including oasis desert mosaic landscapes. The ANN had the highest overall efficiency (97.16 percent), followed by the RF (96.92 percent), SVM (96.20 percent), and KNN (93.98 percent); the ANN, SVM, and RF, as well as the KNN, all had statistically similar accuracies. The RF technique performed well in a variety of categories, including endurance, user comfort, and processing speed, all of which are crucial nowadays when modifying parameters. Overall, the random forest method is an appropriate first-choice approach for land-cover classification in this knowledge area, and the use of spectral indices like the NDVI, MSAVI2, and MNDWI should be used as variables to improve overall accuracy. Elevation and some spectral indices, such as the NDVI, MSAVI2, and MNDWI, should be used as factors to improve overall accuracy because they have the largest influence on the classification of specific categories.

Ioannis Kotaridis and Maria Lazaridou suggest a cost-effective and time-efficient technique for identifying mines and determining their boundaries in 2020, based on open-source software and publicly available data. As a result, the research region was able to obtain Sentinel-2A photographs that were cloud-free. Following the early processing steps, images were segmented using the Mean-Shift technique, and an unsupervised segmentation assessment measure was created for a variety of parameter values. The package also includes a measure of segment separability and variance autocorrelation, as well as an indicator of segment global homogeneity. Following that, each line's NDVI and mean values were determined. Finally, the mining zone was established by using spatial analysis methods such as the dissolve algorithm to connect segments with similar borders, resulting in the creation of the mining zone. The active contour model-based segmentation technique proposed by Ghaffarian and Turker is based on active contour models (Turker2019). Active contour models were able to provide a greater gradient vector flow by integrating the findings of clustering and edge detection (Zhu and Gao, 2016). For detecting huge quantities of variation, this strategy looks to be effective. The authors, on the other hand, calculated the geometry of agricultural fields using a real-world parcel database.

(Garca-Pedrero et al. 2018) developed a new method for defining agricultural land boundaries. Two of the most noteworthy results of this research were the use of super pixels to combine segmentation at various sizes, as well as the integration of vegetative stage information from pictures. (Xu et al., 2019) To solve the difficulty of differentiating agricultural areas in order to increase crop production estimations, developed a layered extraction method based on objects from RGB satellite data. The authors argue that using geographic information to estimate segmentation size can help reduce sub- and over-segmentation to some extent. Although segmentation and subsequent analysis accuracy improved in instances involving challenging items, it remained limited in others. However, the methods described above have several drawbacks, including being sensitive to intra-plot variability, which results in more segments than desired; and relying heavily on parameter selection (for example, the similarity measure used to group the pixels of the image), which necessitates prior knowledge of the scene or trial-and-error tuning to achieve the desired results. To overcome these disadvantages, (Garca-Pedrero et al., 2017) The authors created an agglomerative segmentation-based system for recognising agricultural plots, whereas RUS Boost (Random under Sampling and AdaBoost) was utilised as a machine learning strategy by the authors (Garca-Pedrero



**Thamaraikannan and Manju**

et al., 2017). (Seiffert et al., 2010). To provide segmentation that distinguishes across agricultural plots, this approach leverages superpixels as the smallest processing units. It also uses a superpixel agglomeration method, in which the classifier determines whether or not two superpixels should be connected to make segmentation. One downside is the time required to determine the most important characteristics that will enable a machine learning classifier to perform well. (Georganos and colleagues., 2017) Furthermore, due to the wide range of plot sizes and types, certain layout choices obstruct appropriate delineation and classification (Im et al., 2014). Learn advanced hierarchical representations from a variety of image sizes and aspect ratios. Edge maps that are inherited as side outputs and fine-tuned, resulting in future edge maps that are more concise, are referred to as "nested." Despite the fact that the network does not explicitly represent the structured output, it tries to train and predict edges image by picture, thus the term holistic. (He et al., 2019) developed a Bi-Directional Cascade Network (BCDN) structure to enforce each layer and focus on a particular scale. Agricultural field segmentation using deep learning algorithms, on the other hand, is a largely unexplored area of research.

(Troya-Galvis et al., 2018) offered two approaches founded on a multi-paradigm framework: inspired by machine learning cascade techniques, while the other employs multiple Gu et al. (2018) described a fractal net evolution technique that used a minimum spanning tree algorithm and a minimum heterogeneity rule algorithm to combine segmentation and item merging. Previous field boundary delineation research (Kamilaris and Prenafeta-Bold, 2018) focused mostly on large plots and medium-quality images. Borders are rarely delineated by obviously visible lines in smallholder farms, thus field delineation must be determined by detecting variances in the textural and spectral features of diverse cultivars. The technique uses RCF (Liu et al., 2017) and U-Net (Ronneberger et al., 2015) models to recognise soft edges (rivers and highways), as well as hard edges and different types of farms. Despite the fact that the results are difficult to replicate due to a lack of depth in the approach, the findings demonstrate that DL-based techniques have a bright future. To define field borders, (Persello et al., 2019) recommends using a FCN in conjunction with a grow technique. In field boundary detection, a supervised pixel classification job, the SegNet architecture is utilised to distinguish boundary pixels from non-boundary pixels. (Badrinarayanan and coworkers, 2017) Despite the increasing relevance of deep learning, there are still significant obstacles to overcome in order to construct reliable models. One of the most major constraints and roadblocks to the application of DL approaches in agriculture is the lack of large labelled data sets required for modelling. As a result, DL-based agricultural cadastre generation techniques are likely to create a gap between lab-scale research and real-world implementation. To fill the aforementioned gap, this work studied the use of a DL methodology for automated agricultural border mapping across a large area with a diverse environment in the agriculture field.

(Thanh Tam Nguyen , Thanh Dat Hoang et al.,2020) are looking into agriculture monitoring methods in relation to sustainable land use monitoring guidelines, starting with remote sensing on satellite data for standard and acceptable paddy mapping and working their way up. Thanh Tam Nguyen, Thanh Dat Hoang, and colleagues (Thanh Tam Nguyen, Thanh Dat Hoang, and colleagues (Thanh Tam Nguyen, Thanh Dat Hoang, and colleagues (Thanh Tam Nguyen, Thanh Dat Hoang, and colleagues) The ultimate goal of this project is to create an autonomous and intelligent system that can discern between crop and non-crop areas using picture data streams received from low-Earth orbiting satellites. The technology will be able to tell the difference between cropland and non-cropland. Our mapping standard approaches the baselines in terms of overhead 0.93 F1-score, the effect of specific pattern design, durability versus periodical outcomes, and visible mapping decisions when actual photographic datasets of various landscapes from 2016 to 2018 are examined. The proposed methodology might be used to a range of other vegetable crops (such as corn and potatoes) as well as cash crops (such as coffee, peanuts, and tea) for the sake of comprehensive national planning due to its universal character.

(Hanan Anzid Gaetan Le Goic, Aissam Bekkari et al.,2019) This study was made possible by the contributions) When it comes to multimodal imitation learning, we use impermeable Steam Up Strong Features (SURF), which are recognized at the pixel level and correlated utilising the spectral knowledge offered by the pixels. It is advised that the retrieved features be analyzed using a support vector machine (SVM) (SVM). The fluorescence model, UVR, and adding IRR create undiscovered results in 98.1 percent, 92.01 percent, 98.2 percent, and 94.705 percent of instances,



**Thamaraikannan and Manju**

respectively, and undetectable outcomes in 92 percent. As can be observed in the clear review of the analytical maps that have been utilised as evidence in the case under consideration, new technology delivers more accurate results. Performance is employed as a pre-classification stage in our output approach before the classification maps are generated, which will then be used to generate the final distribution chart as a result of the job. (S. Jayanthi, C. Vennila, 2020) It is a leap year in 2020. Different quarters from space-time discovery are automatically assigned in connection to remote photos as a result of the advanced 3D-based Adaptive Supervised Multi-Resolution (ASMR) purpose, which represents a significant advancement. The enhanced design's individual performance has been tested utilising Mat lab software to determine its effectiveness, according to the business. When comparing the recommended clarification to the traditional 3D architecture of 3D image categorization, the 3D picture categorization's accuracy, sensitivity, and specificity are all greater, at 97.72 percent, sensitivity is higher, and specificity is higher, at 94.02 percent. The simulation of the updated technique, which was completed with the help of Mat lab software, was a success. When compared to the typical 3D layout of 3D picture categorization, the suggested technique's accuracy, sensitivity, and specificity are all higher: 97.72 percent, 98.25 percent, and 94.02 percent, respectively.

(Anita Dixit¹, Dr. Nagaratna Hedge et al., 2017) This study shows how an image categorization system based on satellite images may be used to investigate plant, soil, and water bodies in a specific location. The goal of this work is to apply feature extraction and classification approaches to satellite image pre-processing and classification, as outlined in the above-mentioned split of the task into three fundamental elements. The feature vector is then utilised to train the SVM classification algorithm after it has been constructed with these qualities in mind. The advanced plan's implementation, among other things, has been declared adequate in terms of sensitivity, specificity, and correctness, among other things. The bi-level feature extraction method is used in this study to extract features. The first-order texture features (mean, standard deviation (skewness), and kurtosis) are extracted from the texture data in the first phase of this method when starting from scratch (homogeneity, entropy). As a result, the satellite photos are processed with LWT, and the finished output lacks the similarity band (which was previously present). SVM is used as a classifier to discriminate between different types of soil, plants, and bodies of water at the end of the day. Following the implementation of the proposed method, the accuracy, sensitivity, and specificity have all been determined to be adequate. It is proposed to evaluate the performance of the satellite classification system in the future using the findings of a clustering method.

COMPARISON OF PREVIOUS WORKS

Land cover and land use (LULC) mapping using remote sensing data has been a long-standing difficulty, particularly in heterogeneous environments, due to the variety and mix of characteristics that characterize urban regions. Urban planning and environmental research, natural hazard assessment, transportation management, and city designs, to name a few, all require spatially organized geographic information that is organized locally (LULC). As a result, at all hours of the day and night, precise, high-quality maps with a lot of detail are in high demand all around the world. Land use features have traditionally been derived from remote sensing images and techniques, as well as field surveying; however, in-field measurements of ground truth data collection for the purpose of attributing those features have always been a time-consuming and costly step that posed a risk to the data's overall reliability. High-resolution hyperspectral imaging (HSI) is a prominent study topic in the field of remote sensing because, depending on the technology used, it can provide a great amount of spectral and spatial information. Researchers have been studying a number of HSI categorization methods in recent years, including kernel machines, morphological profiles, and deep learning. Kernel machines, morphological profiles, and deep learning are just a few of the technologies being investigated in this study (DL).

The goal of developing new and improved classification models is to improve classification accuracy while keeping computing time within a reasonable range. Urban mapping and planning, agricultural identification and analysis, environmental management, and mineral extraction, to name a few industries, all rely on accurate categorization maps. There are two key difficulties that have an impact on the categorization results achieved using HSI data: first, the data quality; and second, and the data accuracy. The two most important difficulties are the data quality of the



**Thamaraikannan and Manju**

HSI data and its correctness. In images with an excessively large spectral dimension, the Hughes effect and other blockages (such as those caused by the image's high spectral dimension, which might approach hundreds of spectral bands) may cause classification accuracy to be degraded (which may reach hundreds of bands). When diverse objects are present, different items that are heterogeneous, such as parking lots or roofing materials, can produce spectral fingerprints that are identical to one another. As a result, due to the homogeneity of the data, categorizing HSI data only on the basis of spectral information becomes increasingly difficult. For the second time, increasing the spatial resolution of images may result in a reduction in image interpretation precision.

According to the authors, increased spatial resolution has the potential to increase interclass variation while concurrently decreasing interclass variance in both the spectral and spatial domains. To solve these issues and improve classification accuracy, researchers have attempted to develop and deploy algorithms that use both spectral and spatial information at the same time. The majority of contemporary HSI classification efforts have focused on descriptor-based (DL) techniques, which have proven useful in a range of domains, including computer vision, speech recognition, and natural language modelling, among others. On the majority of tasks, it was predicted that CNN would outperform SVM, and the generated dataset backs up this prediction. According to the findings of this investigation, using CNN to classify data can improve overall classification performance by 7.7%. Furthermore, each class's overall performance is much greater than the national average of 94 percent. According to the conclusions of this study, CNN can be utilised in defence systems to meet the high accuracy requirements of warfare. However, the following disadvantages limit these benefits: 1 Training for deep network architecture is a time-consuming and challenging task. As networks become more complex, they run into the problem of performance saturation, which is a challenge that all networks confront. When it comes to classification, the visual effects provided by Deep CNN are stunning. Deep CNN is a technology that can be used to boost performance in image processing applications. The above CNN approaches have generated outstanding results for land cover and land use (LULC) tasks; however, when the network architecture is very deep, the bulk of these methods are constrained by disappearing or bursting gradients, causing them to perform badly. To make matters worse, in the pursuit of improved overall performance, the solutions proposed above compromise computational efficiency. In order to remove these restrictions and achieve high accuracy, more work with the revised CNN will be required in the future.

According to the majority of authors, such publications contain a number of flaws, including a poor accuracy rate and a high maximum classification error rate, as well as high computational values. By increasing the amount of optimization components employed and removing the presence of pixel-based classification mistakes, overall performance can be improved. Increase accuracy while reducing complexity, improve classification of many rare classes, improve perclass performance and outcome performance difficult state-of-the-art approach, improve classification of many uncommon classes with a lower F-Score score, and improve classification of many uncommon classes with a lower F-Score score As a result, in preparation for future work, I've looked at VDCNN, RNN, SGD, DRNN, and other recent satellite image machine learning and Deep learning classification approaches, such as VDCNN, RNN, SGD, DRNN, and others. It can also be used for a variety of other purposes, including urban planning and forestry management.

CONCLUSION

In recent decades, India's agricultural has grown at a stunning rate. Farmers' suicides in India, on the other hand, are a cause for concern. Farmer suicides have been blamed on debt, the environment, low produce prices, insufficient irrigation, higher cultivation costs, the usage of chemical fertilizers, and crop failure, in that order. In most cases, a farmer's crop selection is influenced by his intuition as well as other non-essential factors such as making quick money, being unaware of market demand, overestimating a soil's ability to support a specific crop, and so on. It is critical to create a system that can provide Indian farmers with predictive data, allowing them to make better decisions about which crops to produce. This necessitates smart farming, which entails the use of IoT. Agriculture enabled by the Internet of Things has the potential to transform humans and the world as a whole. Farmers may employ sensor data analytics to gain valuable insights about the performance of their crops, greenhouses, and other



**Thamaraikannan and Manju**

agricultural operations. Thanks to its high-precision algorithms, Machine Learning-powered farming is a revolutionary concept that is gaining traction today. This cutting-edge trend, which aims to boost product quantity and quality, ensures that all agricultural stakeholders benefit from long-term productivity increases. Machine Learning and the Internet of Things using both real-time and historical data improves the accuracy of the outcome. Comparing multiple machine learning algorithms also improves the system's accuracy. This method will be used to help farmers overcome obstacles and improve the quantity and quality of labor they produce. Machine Learning and the Internet of Things using both real-time and historical data improves the accuracy of the outcome. Comparing multiple machine learning algorithms also improves the system's accuracy. This method will be used to help farmers overcome obstacles and improve the quantity and quality of labour they produce. The major goal of this study mainly discuss about Machine learning classification algorithms CNN & SVM using Satellite images

REFERENCES

1. (Ajami et al., 2019). "Identifying a slums' degree of deprivation from VHR images using convolutional neural networks", *Remote sensing*, 11(11), 1282.
2. (Melkamu meseret Alemu 2016) "Automated farm field delineation and crop row detection from satellite images", Master's thesis, University of Twenty, 2016.
3. (Arbelaez, P et al., 2010)" Contour detection and hierarchical image segmentation", *IEEE transactions on pattern analysis and machine intelligence*, 33(5), 898-916.
4. (Badrinarayanan, V et al 2017)"Segnet: A deep convolutional encoder-decoder architecture for image segmentation", *IEEE transactions on pattern analysis and machine intelligence*, 39(12), 2481-2495.
5. (Belgiu, Mariana & Ovidiu Csillik 2018) "Sentinel-2 cropland mapping using pixel-based and object-based time-weighted dynamic time warping analysis", *Remote sensing of environment* 204 (509-523).
6. (Christoph Rieke, 2017) "Deep learning for instance segmentation of agricultural fields", September. [http://dx. doi. Org.](http://dx.doi.org)
7. (Chen, Bo et al., 2015). "Image segmentation based on constrained spectral variance difference and edge penalty", *Remote Sensing* 7, no. 5 (2015): 5980-6004.
8. (Chen, S et al., 2016)"Target classification using the deep convolutional networks for SAR images", *IEEE Transactions on Geoscience and Remote Sensing*, 54(8), 4806-4817.
9. (Alexandre Constantin et al., 2018) "Accurate road detection from satellite images using modified u-net", In 2018 IEEE Asia Pacific Conference on Circuits and Systems (APCCAS) (pp. 423-426). IEEE.
10. (Ovidiu Csilli, 2017)"Fast Segmentation and Classification of Very High Resolution Remote Sensing Data Using SLIC Superpixels" *Remote Sensing* 9, no. 3: 243. <https://doi.org/10.3390/rs9030243>
11. (A. Garcia-Pedrero et al., 2017)" A machine learning approach for agricultural parcel delineation through agglomerative segmentation", *International Journal of Remote Sensing*, 38:7, 1809-1819, DOI: 10.1080/01431161.2016.1278312
12. (Garcia-Pedrero et al., 2018) "The Outlining of Agricultural Plots Based on Spatiotemporal Consensus Segmentation" *Remote Sensing* 10, no. 12: 1991. <https://doi.org/10.3390/rs10121991>
13. Stefanos Georganos et al., 2018)"Less is more: Optimizing classification performance through feature selection in a very-high-resolution remote sensing object-based urban application", *GIScience& remote sensing*, 55(2), 221-242.
14. (Ghaffarian, S., & Turker, M. 2019) "An improved cluster-based snake model for automatic agricultural field boundary extraction from high spatial resolution imagery", *International journal of remote sensing*, 40(4), 1217-1247.
15. (Gu, Haiyan, et al., 2018) "An Efficient Parallel Multi-Scale Segmentation Method for Remote Sensing Imagery" *Remote Sensing* 10, no. 4: 590. <https://doi.org/10.3390/rs1004059>.
16. (Jianzhong He et al., 2019)"Bi-directional cascade network for perceptual edge detection", In Proceedings of the IEEE Conference on Computer Vision and Pattern Recognition (pp. 3828-3837).





Thamaraikannan and Manju

17. (Jungho Im et al., 2014) "Optimum scale in object-based image analysis", *Scale Issues in Remote Sensing*, 197-214.
18. (Qiangguo Jin et al., 2019) "DUNet: A deformable network for retinal vessel segmentation", *Knowledge-Based Systems*, 178, 149-162.
19. (Kamilaris, A., & Prenafeta-Boldú, F. X. 2018) "A review of the use of convolutional neural networks in agriculture", *The Journal of Agricultural Science*, 156(3), 312-322.
20. (Yu Liu & Michael S. Lew, 2016) "Learning relaxed deep supervision for better edge detection", In *Proceedings of the IEEE conference on computer vision and pattern recognition* (pp. 231-240).
21. (Yun Liu et al., 2017). "Richer convolutional features for edge detection" *Proc. IEEE Conf. Comput. Vis. Pattern Recognit.* pp. 5872-5881 2017.
22. (Ronneberger O, Fischer P, & Brox T, 2015) "U-Net: Convolutional Networks for Biomedical Image Segmentation", *Medical Image Computing and Computer-Assisted Intervention – MICCAI 2015*. MICCAI. Lecture Notes in Computer Science, vol 9351. Springer, Cham. https://doi.org/10.1007/978-3-319-24574-4_28
23. (North, Heather C et al., 2018) "Boundary delineation of agricultural fields in multitemporal satellite imagery." *IEEE Journal of Selected Topics in Applied Earth Observations and Remote Sensing* 12, no. 1: 237-251.
24. (Persello, C et al., 2019) "Delineation of agricultural fields in smallholder farms from satellite images using fully convolutional networks and combinatorial grouping", *Remote sensing of environment*, 231, 111253.
25. (R. Lucas, et al., 2007), "Rule based classification of multi-temporal satellite imagery for habitat and agricultural land cover mapping," *ISPRS J. Photogramm. Remote Sens.*, vol. 62, pp. 165–185, 2007.
26. (Sakamoto, T et al., 2010) "A two-step filtering approach for detecting maize and soybean phenology with time-series MODIS data", *Remote Sensing of Environment*, 114, 2146–2159.
27. (Seiffert, C et al., 2010) "RUSBoost: A hybrid approach to alleviating class imbalance", *IEEE Transactions on Systems, Man, and Cybernetics-Part A: Systems and Humans*, 40(1), 185-197.
28. (Shackelford, K., & Davis, C. H. 2003) "A combined fuzzy pixel-based and object-based approach for classification of high-resolution multispectral data over urban areas", *IEEE Transactions on Geoscience and Remote Sensing*, 41, 2354–2363.
29. (Smereka, M., & Dulęba, I. 2008) "Circular object detection using modified Hough Transform", *International Journal of Applied Mathematics and Computer Science*, 18, 85–91.
30. (T. Esch, et al., 2014) "Combined use of multi seasonal high and medium resolution satellite imagery for parcel-related mapping of cropland and grassland," *Int. J. Appl. Earth Observ. Geoinf.*, vol. 28, pp. 230–237, 2014.
31. (Troya-Galvis et al., 2018) "Remote sensing image analysis by aggregation of segmentation-classification collaborative agents", *Pattern Recognition*, 73, 259-274.
32. (Tucker, C. J, 1979) "Red and photographic infrared linear combinations for monitoring vegetation", *Remote Sensing of Environment*, 8, 127–150.
33. Tucker, C. J et al., 1979) "Monitoring corn and soybean crop development with hand-held radiometer spectral data. *Remote Sensing of Environment*", Volume 8, Issue 3, August 1979, Pages 237-248.
34. (Volkov, et al., 2019) "In a Search for Equity: Do Direct Payments under the Common Agricultural Policy Induce Convergence in the European Union?" *Sustainability* 11, no. 12: 3462. <https://doi.org/10.3390/su11123462>
35. (Xia X, Persello, C & Koeva, M, 2019) "Deep fully convolutional networks for cadastral boundary detection from UAV images", *Remote sensing*, 11(14), 1725.
36. (Xu, L et al., 2019). Farmland extraction from high spatial resolution remote sensing images based on stratified scale pre-estimation. *Remote Sensing*, 11(2), 108.
37. (Zhu, S., & Gao, R. 2016) "A novel generalized gradient vector flow snake model using minimal surface and component-normalized method for medical image segmentation", *Biomedical Signal Processing and Control*, 26, 1-10.
38. (Zewei Xua et al., 2018) "A 3D convolution neural network method for land cover classification using LiDAR and multi-temporal Landsat imagery", *ISPRS Journal of Photogrammetric and Remote Sensing* 144 423–434.
39. (Ce Zhang et al., 2018) "A hybrid MLP-CNN classifier for very fine resolution remotely sensed image classification", *ISPRS Journal of Photogrammetric and Remote Sensing* 140 (2018) 133–144.



**Thamaraikannan and Manju**

40. (Zhipeng Deng, et al., 2018) "Multi-scale object detection in remote sensing imagery with convolutional neural networks", ISPRS Journal of Photogrammetric and Remote Sensing 145 (2018) 3–22.
41. (Wojciech Gruszczyński , et al., 2019) "Application of convolutional neural networks for low vegetation filtering from data acquired by UAVs,ISPRS Journal of Photogrammetric and Remote Sensing Volume 158, December 2019.
42. (Sakshi Dhingra & Dharminder Kumar,2019) "A review of remotely sensed satellite image classification", International Journal of Electrical and Computer Engineering, Vol. 9, No. 3, pp. 1720-1731 ISSN: 2088-8708, DOI: 10.11591/ijece.v9i3.pp.1720-1731.
43. (CheolheeYooa et al., 2019)"Comparison between convolutional neural networks and random forest for local climate zone classification in mega-urban areas using Landsat images", ISPRS Journal of Photogrammetric and Remote Sensing 157 (2019) 155–170.
44. (Shiyao Meng et al.,2021) "Deep learning-based crop mapping in the cloudy season using one-shot hyper spectral satellite image", Agriculture, Volume, July 2021.
45. (Michal Segal-Rozenhaimera, Alan Lia, Kamalika Das & VedChirayatha,2020) "Cloud detection algorithm for multi-modal satellite imagery using convolutional neural networks (cnn)", Remote Sensing of Environment 237 (2020) 111446.
46. (Chen xiao Zhanga et al., 2020) "A multi-level context-guided classification method with object-based convolutional neural network for land cover classification using very high-resolution remote sensing images", Int j Appl Earth Obs Geoinformation 88 (2020) 102086.
47. (David Griffiths & Jan Boehm, 2019)" Improving public data for building segmentation from Convolutional Neural Networks (CNNs) for fused airborne LiDAR and image data using active contours", ISPRS Journal of Photogrammetric and Remote Sensing June 18.
48. (Jason Kane Gilbertson & Adriaan van Niekerk,2017) "Value of dimensionality reduction for crop differentiation with multi-temporal Imagery and machine learning", Computers and Electronics in Agriculture 142 (2017) 50–58
49. (Pengfei Li et al., 2015) A cloud image detection method based on SVM vector machine", Neurocomputing169(2015)34–42
50. (Deepak Kumar Jaina, et al., 2018) "An approach for Hyperspectral image classification by optimizing SVM using the self-organizing map", Journal of Computational Science 25 (2018) 252–259.
51. (Hongyan Zhanga et al., 2020) "Accessing the temporal and spectral features in crop type mapping using multi-temporal Sentinel-2 imagery: A case study of Xi'an County, Heilongjiang province, China". Computers and Electronics in Agriculture 176, 105618.
52. (OnuwaOkwuashi et al., 2020)"Deep support vector machine for Hyperspectral image classification", Pattern Recognition 103 (2020) 107298
53. (Genbatu Ge, et al.,2020) "Land use/cover classification in an arid desert-oasis mosaic Landscape of China using remotely sensed imagery: Performance assessment of four machine learning algorithms", Global Ecology and Conservation 22, e00971.
54. (Thanh Tam Nguyen et al., 2020)"Monitoring agriculture areas with satellite images and deep learning", Applied Soft Computing Journal 95, 106565.
55. (Hanan Anzida et al., 2020)", Multimodal Images Classification using Dense SURF, Spectral Information and Support Vector Machine ", Procedia Computer Science 148 107–115.
56. (S.Jayanthi & C.Vennila, 2020) "Performance improvement in satellite image classification using adaptive Supervised multi-resolution approach", Computer Communications 150200–208.
57. (Anita Dixit, et al., 2017)"Texture Feature Based Satellite Image Classification Scheme Using SVM", International Journal of Applied Engineering Research ISSN 0973-4562 Volume 12, Number 13, pp. 3996-4003.





Ethno-Beneficial usages of *Alternanthera sessilis* L. in the Treatment of Health Ailments among the People of Upper Assam, India

Uma Dutta^{1*}, Deepshikha Moran² and Gargee Doley³

¹HoD and Associate Professor, Cell and Molecular Biology Division, Department of Zoology, Cotton University, Guwahati-781001, Assam, India

²Assistant Professor, Department of Zoology, Dibru College, Dibrugarh, Assam, India.

³Department of Zoology, Cotton University, Guwahati-781001, Assam, India

Received: 19 Dec 2021

Revised: 30 Dec 2021

Accepted: 18 Jan 2022

*Address for Correspondence

Uma Dutta

HoD and Associate Professor,
Cell and Molecular Biology Division,
Department of Zoology, Cotton University,
Guwahati-781001, Assam, India
Email: umadutta@yahoo.com



This is an Open Access Journal / article distributed under the terms of the **Creative Commons Attribution License** (CC BY-NC-ND 3.0) which permits unrestricted use, distribution, and reproduction in any medium, provided the original work is properly cited. All rights reserved.

ABSTRACT

Naturopathy is gaining popularity nowadays in place of synthetic drugs. NE India is a great bio-resources repository, especially for plant diversity. Many of them remain scientifically unexplored but are traditionally used by ethnic tribes of this region in treatment of various diseases and healthcare practices. Amongst them, *Alternanthera sessilis* L. (AS) is popularly used among ethnic-communities of Upper Assam. A study was undertaken to focus on traditional usages of AS in treating different health ailments among the native people of Upper Assam for its validation. Data obtained from the survey suggests the potential role of AS in various health disorders.

Keywords: Ethnic community, Folk knowledge, *Alternanthera sessilis*, Physical ailments, Healthcare practices.

INTRODUCTION

In the leading edge, a growing inclination among the people has been observed towards the modern lifestyle. This leads to extensive uses or exposure of variety of chemicals and drugs through synthetic products without knowing its details of detrimental effects. Lucrative advertisements also tempted people towards these synthetic products or drugs. The unsound and improper management and practices of synthetic drugs have become a concern of public health at various levels. Although their impacts are often unknown or sometime it opens lids of a debate. Though synthetic drugs have positive effects in terms of quick action of relief from sufferings of diseases or physical disorder but develop a number of secondary side effects that lasted for a long time. Therefore naturopathy is globally gaining importance owing to the fact that plant based medicines or herbal drugs are easily available, cheap and most

38898



**Uma Dutta et al.,**

reportedly with negligible side effects. Many plant species have been used in practices to cure various health ailments on the basis of indigenous knowledge of medicinal importance, since time immemorial. It is even documented in Ayurveda that about 1400 plants have medicinal properties [1,2]. According to WHO, about 80% of global population still rely on indigenous system of medicinal plants [3].

India is abode to medicinal plants after China. Medicinal plants and medicines derived from it is the first line of defence for treatment of various diseases or physical ailment among the tribal and rural communities [4]. North-eastern region of India is a hub of floral diversity especially in medicinal and aromatic plants. People of this region have their own traditional or folklore knowledge to treat or heal health disorders by using different medicinal plants found in vicinity of their region. People dwelling in rural areas are solely dependent on indigenous medicinal plants [5]. Since advanced medical treatments health care facilities is limited to certain areas due to improper communication issues or other problems, the traditional medicines and herbs serve as the primary health care needs or first line of defence. Though these plants are traditionally used to cure diseases but they remain scientifically unexplored. There is no proper documentation on the medicinal properties of these plants. Tribes of different ethnic groups of this region have their indigenous knowledge on traditional medicine which has been verbally transmitted from generation to the next [6]. Tribal communities of certain districts of upper Assam are still using various medicinal plants for curing health ailment or health related problems.

Among such indigenously used plant is *Alternanthera sessilis* L. (AS) which is commonly and locally known as "Matikaduri" and "Kukurathengia" respectively. AS is a prostrate, perennial herb found in damp places, wetlands, roadside drainage as well as a weed in the field of plantation. It grows throughout warmer parts of India. AS is generally consumed as leafy vegetable by the people of this region. It was reported that AS contain carbohydrate, phytosterols, phenolic compounds, alkaloid and a high source of minerals such as Na, K, Mg, Ca, Zn, Cu and Fe [3]. In addition, various reports showed that this plant has hematinic activity as well as antioxidant and anti-inflammatory activities [7, 8,9].

STUDY DESIGN AND METHODS

Study Area and Data Collection

An Intensive field study was performed among the people in certain districts of upper Assam viz. Golaghat, Jorhat, Sivasagar, Dhemaji, North Lakhimpur, Dibrugarh and Tinsukia [Figure 1- (a), (b)]. A total number of 257 families consisting of about 712 people of different age groups along with the number of heads of villages were studied. The survey work was conducted from December 2019 to July 2021 among the family members of different villages by visiting door to door, who voluntarily participated in the program. Primary data was collected at an average from 2-3 members of each of the family irrespective of sexes and ages groups (viz. young, adult and old) during personal interactive session. Participation of atleast one woman member from each family was taken into consideration in the interactive session of data collection. The in-depth interaction included information on plant parts used, methods of dose preparation, types of physical ailments for which AS is used as well as duration of consumption (frequent/ regular/ occasional eater) etc. Interaction was also made with traditional medicine practitioners or Bejor Ojah of different villages as people have faith and got positive response from their treatment. Emphasis was given on the standard questionnaire by citing the prophylactic or common usages of the plant by the villagers. (Figure 1 here)

Collection of plant sample and Identification

Branches of shoot plant at early flowering stage of AS were collected from different places (shady, damp and roadside areas), in and around Cotton University campus. The plant was botanically identified at the Department of Botany, Cotton University, Guwahati, Assam and confirmed at Sikkim Himalayan Regional Centre, Gangtok: Botanical Survey of India, where a specimen voucher as an herbarium sheet was submitted. (Figure 2 here)

Chemicals and Reagents

Ethanol, Methanol, 1- butanol (n- butyl alcohol), Chloroform, Petroleum Ether, Acetone, Sodium hydroxide and Concentrated Sulphuric acid (con. H₂SO₄) were purchased from Merck Specialities Private Limited. Glacial acetic

38899



**Uma Dutta et al.,**

acid, Ferric chloride, Potassium ferric cyanide, Hydrochloric acid, Molisch's reagent and Wagner reagent (Potassium iodide, Iodine) were purchased Fisher Scientific India Private Limited.

Preparation of Plant Extract

Soxhlet extraction: Leaves of the plant were washed with distilled water and then shade dried for 7-10 days in 25-27°C (day time). Dried leaves were powdered in a stainless grinder machine and then submitted in Soxhlet apparatus (boiling point: 60-80°C for 8-10 hrs). Now the extracted solvent was filtered through Whatman no. 1 filter paper (0.2µ). The filtered extract solvent was concentrated at reduced pressure (at 45°C) were diluted in methanol which is sterilized by filtration (Figure 3). Following the same method, aqueous and ethanolic extracts were prepared for screening the absence or presence of the phytochemicals as shown in table 1. (Figure 3 here)

Phytochemical Screening Tests

The following phytochemical tests were carried on the crude extract to determine the presence of the phytochemical constituents using the standard methods [10, 11].

Test for alkaloids (Wagner's test): Crude AS extract was mixed with 2 ml of Wagner's reagent. Reddish brown coloured precipitate indicates the presence of alkaloids

Test for Flavonoids (Sodium hydroxide test): 5 ml of dilute ammonia solution was added to a portion of the crude AS extract followed by addition of concentrated sulphuric acid. A yellow colouration observed in each extract indicated the presence of flavonoids. The yellow colouration disappeared on standing.

Test for Saponins (Foam test): Crude AS extract was mixed with 5 ml of distilled water in a test tube and it was shaken vigorously. Add some drops of olive oil. The formation of stable foam was taken as an indication for the presence of saponins.

Test for Glycoside (Kellar Killani's test): The AS extract was dissolved in water with Glacial acetic acid and ferric chloride and concentrated sulphuric acid. They give brown ring at the junction

Test for Steroids (Salkwaski test): Chloroform solution of the AS extract when shaken with concentrated sulphuric acid and on standing yielded red colour.

Test for Tannins (Ferric chloride test): 1 ml of the AS sample was taken in a test tube and then 1 ml of 0.008 M potassium ferric cyanide was added. 1 ml of 0.02 M Ferric chloride containing 0.1 N HCl was added and observed for blue-black coloration.

Test for Phenols (Liebermann's test): To 1ml of AS extract of sample, 2 ml of distilled water followed by a few drops of 10% aqueous ferric chloride solution was added. Formation of blue or green colour indicated the presence of phenols.

Test for Terpenoids (Liebermann's- Burchard test): 5 ml of AS extract was mixed in 2 ml of chloroform. 3 ml of concentrated sulphuric acid was then added to form a layer. A reddish-brown precipitate at the interface formed indicating the presence of terpenoids.

Test for Carbohydrates (Molisch's test): To 2 ml of crude AS extract solution two drops of Molisch's reagent was added. 2 ml of concentrated sulphuric acid was slowly added down the sides of the test tube, without mixing, forming a layer. The mixture was allowed to stand for 2 minutes. Formation of a red or dull violet colouring at the interface between acid and test layer indicated the presence of carbohydrates.



**Uma Dutta et al.,**

RESULTS

The phytochemical screening of AS to determine the presence of phytochemical constituents is shown in the table 1. It showed presence of flavonoids, phenolic compounds, alkaloids, glycosides, steroids, carbohydrates, terpenoids, saponin etc. both in methanolic and ethanolic AS extracts. During the study period, a total of 257 families were studied of which 198 families belonged to tribes and 59 families belonged to non tribes, the details of which are shown in table 2. From the survey it was found that AS is widely popular among the tribal communities and mostly consumed as green leafy vegetables. The field study reveals that tribal people were well acquainted with the health benefits of the plant. The data emanated from the interaction suggest that AS is regular used by the rural people of Upper Assam especially in tribal areas for treating various health ailments such as fever, promoting bile flow and gastrointestinal problems, skin diseases like infections, rashes, insect bites etc. It was recorded from the female participants that AS is very useful in treating feminine health related aspects such as, increasing breast milk secretion after child birth, to treat irregular menstrual cycle in young girls, relieving from menstrual cramps, to reduce heavy bleeding and labour pain during postpartum period, Gonorrhoea etc. Moreover, the green paste of AS is popularly used by women and young girls for cosmetic purpose by applying externally on face and neck for obtaining glowing skin. From the study it was recorded that the tribal communities had indigenous knowledge on the usage of AS to treat various physical ailments.

The mode of consumption AS is quite different among the tribes. The ethnic tribes frequently consume AS as green leafy vegetable, or make green paste (Chutney) as a side dish item, used in salad, boiled curries etc. The Khamti, Hajong and Mising tribes of North Lakhimpur make raw pastes of AS to cure skin diseases like rashes, skin infections, itchiness, insects bites etc., and as eye wash (Table 6). The women of Mising tribe of Golaghat district commonly uses AS juice in an extensive way to treat menstrual disorders. The young girls suffering from menstrual problems are given the juice of AS mixed with raw milk in empty stomach for three days during their menstrual periodic cycle. The Sonowal-Kachari, Mech, Rabha and Singphoo tribes of Dibrugarh and Tinsukia districts use AS to treat various gastrointestinal problems like indigestion, constipation, promoting bile flow and to improve their appetite. AS is also used for wound healing, to treat general weakness, to reduce labor pain and heavy bleeding during postpartum period by the tribal people of Dhemaji districts. From the survey it was also recorded that consumption of AS is more frequent among the tribal people whereas consumed occasionally in non-tribes (Table 3). The highest percentage of tribal people (about 29.80%) are found to use AS to treat gynecological problems followed by 18.18% people using it to cure gastrointestinal problems (Table 6). The ways of consumption and health care practices of AS are shown in Table 4 and 5.

(Table 1- 6 here)

(Figure 4 here)

DISCUSSION

Exposure to xenobiotics through various ways such as, alteration in food habits and attraction towards processed foods (viz. junk foods, drinking beverages, fast foods), altered lifestyle are the prime causes of health risks in modern times. This in turn leads to various physiological disorders and physical ailments like, obesity, hypertension, cardiac disorders, gastro-intestinal problems, cancer, various gynecological disorders i.e., menstrual problems, polycystic ovarian syndrome etc. including cancer. Although medical treatment with prescribed drugs can make immediate relief; it does not make a reliable permanent solution as it develops some side effects on long term exposure. In such scenario, phytotherapy may show an alternative or effective ways in treating these physical ailments. Ethno traditional usages of different medicinal plants are drawing the attention of investigators' towards modern, cost-effective drug isolation. AS is a common part of cuisine and herbal medicine among native tribes of North East India. In this present study it was explored about the common uses of AS amongst different ethnic tribes and non-tribes of some selected districts of Upper Assam in healthcare practices and in the treatment of various physical ailments. Phytochemical screening of AS has shown the presence of flavonoids and glycosides that are known to display anti-



**Uma Dutta et al.,**

histamine, anti-inflammatory and anti-cancer properties [12]. This plant also contains essential trace elements like nickel, cadmium, chromium, lead and copper [13].

The survey study revealed that this plant is an important part of traditional medicines of different tribes and non-tribes, which are used to cure a wide range of functional disorders of the body. Local tribes use AS normally as leafy vegetable for curing stomach related disorders such as indigestion, constipation and in improving appetite. This may be due to the bile flow promoting (cholagogue) property of AS that helps in smooth digestion of food curing upset stomach. Study showed that the curry and green paste of AS is a commonly used medicine among the people of Mising, Sonowal-Kachari and Deori tribes as medicine, for curing indigestion problems and nausea. Majority of the local tribes of this region use green paste and juices of AS as an appetizer and for curing stomach related problems viz. stomach pain, diarrhoea, dysentery etc. Some report claimed that this plant has anti-inflammatory properties that may play role in alleviating stomach irritation caused inflammation that was in support of the present findings [14].

Tribal people of Golaghat, Dhemaji and North Lakhimpur mix the grinded fresh leaves of *A. sessilis* with black pepper, garlic and raw milk. This combination is taken orally as a remedy for eye diseases, weak eyesight problem and night blindness. This indicates that AS has eyesight improving capacity due to its rich content of carotene as was reported earlier [15, 16]. The leaves of AS are fried in ghee (clarified butter) and applied on the eyelid for curing cataract, smoky vision, and acute conjunctivitis [17]. In most rural areas, Bej or village traditional medicine practitioner prescribes AS along with other medicinal plants as local medicines in common health ailments viz. fever, cough, headache, joint pain and in different skin diseases. In recent days, AS is used as an important component of various marketed skincare products due to its anti-pyretic, anti-inflammatory, anti-microbial and anti-bacterial properties [9, 18, 29, 20, 21]. Tribal communities such as Deori, Rabha, Sonowal- Kachari, Mising of Golaghat, Jorhat, Sivsagar and Dibrugarh use AS paste externally on infected wounds, inflamed boil, acne, itching and on burnt areas. The wound healing property of this plant may be due to presence of high percentage of sterol [22]. The antibacterial and anti-fungal properties of this plant make it a useful paste for healing small injuries.

Moreover, juices of the fresh leaves of this plant with milk is a very popular medicine among tribal women used for treating various gynecological related problems viz. irregular menstrual cycle, heavy bleeding and menstrual cramps etc. This mixture is also used for increasing lactation after child birth, along with curing sexual debility, impotency etc. This may be due to the hormonal imbalance restoring property of AS regulating various physiological processes of the body. The pain relieving or analgesic property of AS supports the use of this plant for reducing the labor pain, menstrual cramps and gastrointestinal pain etc [23, 24]. Recent studies showed that AS has anti-oxidant property and scavenging of free radicals [9, 25], which may play an important role in new and effective drug discovery in cancer therapy in near future. The survey work analysis clearly revealed that AS has been used amongst tribes and non-tribes of Upper Assam in curing various health ailments due to its lots of beneficial properties. This is why more epidemiological studies are needed on its nutraceutical properties and mechanisms of actions of its phyto-constituents in vivo to through light on potential utilization of AS in new and effective drug discovery with lesser side effects.

CONCLUSION

From the study, it has been concluded that the plant is used for curing of various type of commonly occurring diseases and as such it has a folklore medicinal reputations. This plant can be act as a potential source of herbal medicine and may represent a traditional medicine all over the world. In near future, it may be an alternative or possibility by utilizing this plant in drug discovery for complete curing of some diseases and subside the side effects developed by synthetic drugs. Therefore, a thorough survey on traditional usages of AS and its experimental work on bioactivity and mechanism of action in vivo model is essentially required. Hence, the conservation of this plant is essentially required from the point of plant biodiversity aspect as well as nutraceutical importance and not to be ignored as a weed.



**Uma Dutta et al.,**

ACKNOWLEDGEMENT

Authors are highly grateful to the people of local tribes of Upper Assam districts, Assam, India for their assistance in the field of study as well as for sharing their valuable knowledge in this regard. We would also like to thank local experts, head of village and volunteers for providing valuable informations and suggestions for selecting study areas. We offer our special thanks to Dr. Dandadhar Borah, retired associate professor, Department of Botany and Sikkim Himalayan Regional Centre, Gangtok: Botanical Survey of India for identifying the plant. Lastly, we are grateful to the former Head of the Department of Zoology, Cotton University for providing the lab facilities.

FINANCIAL SUPPORT

There is no financial assistance received from any funding agency for the work.

CONFLICT OF INTEREST

The authors declare no conflict of interest.

REFERENCES

1. Manohar R. Principles and insights from Ayurveda and study of herbs. *Toxicol Int* 2011; 17 (1): 23-24.
2. Kalita T, Dutta U. A comparative study on indigenous usage of Bamboo shoot in health care practices in NE India. *Int Multidisciplinary J* 2012; 1(2):130-141.
3. Debnath M, Nandi M, Biswas M. A critical pharmacognostic evaluation and preliminary phytochemical investigation of *Alternanthera sessilis* (L.) R. BR. leaves. *Indi J of Pharma Res* 2014; 4(2): 71-74.
4. Sonowal R. Indigenous Knowledge on the utilization of medicinal plants by the Sonowal Kachari tribe of Dibrugarh district in Assam, North- East India. *Int Res Jon Biological Sci* 2013; 2(4): 44-50.
5. Sikdar M, Dutta U. Traditional phytotherapy among the Nath people of Assam. *Ethno-Med* 2008; 2(1): 39-45.
6. Taid TC, Rajkhowa RC, Kalita JC. A study on the medicinal plants used by the local traditional healers of Dhemaji district, Assam, India for curing reproductive health related disorders. *Adv in Appl Sci Res* 2014; 5(1): 296-301.
7. Arollado EC, Osi MO. Hematinic activity of *Alternanthera sessilis* (L.) R. BR. (Amaranthaceae) in mice and rats. *E-Int Scientific Res J* 2010; 2(2): 110-117.
8. Borah A, Yadav RNS, Unni BG. In vitro antioxidant and free radical scavenging activity of *Alternanthera sessilis*. *IJPSR* 2011; 2(6): 1502-1506.
9. Subhashini T, Krishnaveni B, Reddy CS. Anti- Inflammatory activity of leaf extracts of *Alternanthera sessilis*. *Hygeia J for Drugs and Med* 2010; 2(1): 54-56.
10. Trease GE, Evans WC. *Pharmacognosy*. 15th Ed. London: Saunders Publishers; 2002.p. 42-44, 221-229, 246-249, 304-306, 331-332, 391-393.
11. Sofowora A. *Medicinal plants and Traditional Medicines in Africa*. Chichester, John Wiley & Sons New York; 1993. 2: 24-36.
12. Vani M, Rahaman SA, Rani AP. Detection and quantification of Major phytochemical markers for Standardization of *Talinum portulacifolium*, *Gomphrena serrata*, *Alternanthera sessilis* and *Euphorbia heterophylla* by HPLC. *Pharmacogn J* 2018; 10(3): 439-446.
13. Kananke T, Wansapala J, Gunaratne A. Assessment of heavy metals in Mukunuwenna (*Alternanthera sessilis*) collected from production and market sites in and around Colombo District, Sri Lanka, In: *Procedia Food Science. Proc. International Conference of Sabaragamuwa University of Sri Lanka 2015 (ICSUSL 2015)*, Published by Elsevier Ltd; 2016. 6: 194-198.
14. Kalita D, Phukan B. Some ethnomedicines used by the Tai Ahom of Dibrugarh district, Assam, India. *IJNPR* 2010; 1(4): 507-511.
15. Devadas RP, Chandrasekhar U, Premakumari S. Consumption pattern of carotene rich foods and development of a year calendar. *Biomed Environ Sci* 1996; 9(2-3): 213-222.





Uma Dutta et al.,

16. Jerajani HR, Dhurat HR, Paramesh R. Evaluation of efficacy and safety of Clarina cream in newly diagnosed and previously treated cases of acne vulgaris. *Indi J of CliniPrac*2004;14(12): 27-34.
17. Loganathan JN, Balu S. Treatment of eye disease by the healers of Marakanam Bio-region. *Ancient Sci of Life*1997; 16(3): 215-221.
18. Nayak P, Nayak S, Kar DM, Das P. Pharmacological evaluation of ethanolic extracts of the plant *Alternanthera sessilis* against temperature regulation. *Jof Pharma Res* 2010; 3(6):1381-1383.
19. Kumari EVN, Krishnan V. An ti- Microbial activity of *Alternanthera sessilis* (L) R.BR. Ex. DC and *Alternanthera philoxeroids* (Mart). *Griseb. WJRR*2016; 3(3):78-81.
20. Sivakumar R Sunmathi D. Phytochemical screening and Anti-microbial activity of Ethanolic leaf extract of *Alternanthera sessilis* (L.) R. BR. EX DC and *Alternanthera philoxeroides* (Mart.) *Griseb. EJPMR*2016; 3(3):409-412.
21. Sahu BR, Chakrabarty A. Screening of antibacterial activity of various extractives of seeds of *Cassia Tora* and *Alternanthera sessilis*. *Asian J of Chem*1994; 6(3): 687-689.
22. Jalalpure SS, Agrawal N, Patil MB, Chimkode R, Tripathi A. Antimicrobial and wound healing activities of leaves of *Alternanthera sessilis* Linn. *IJGP*2008; 2(3):141-144.
23. Ahamed IH, Mohammad F, Rahman S, Jahan R, Mohammed R. A preliminary evaluation of antihyperglycemic and analgesic activity of *Alternanthera sessilis* aerial parts. *BMC Complementary and Alternative Medicine*2014; 14:169.
24. Mondal H, Saha S, Awang K, Hossain H, Ablat A. et al. Central-stimulating and analgesic activity of the ethanolic extract of *Alternanthera sessilis* in mice. *BMC Complementary and Alternative Medicine*2014; 14:398.
25. Shanmugaraj BM, Aziz R, Ramamoorthy D, Srinivasan B, Ramalingam S. Antioxidant capacities of *Amaranthus tristis* and *Alternanthera sessilis*: A comparative study. *J of MediPlant Res*2013; 7(30): 2230-2235.

Table-1: Phytochemical Screening of Different Chemical Compounds for Ethanolic and Methanolic Extract of As

SI. No.	Phytochemical constituents	Aqueous extract	Ethanolic extract	Methanolic extract
1	Alkaloids	+	+	+
2	Flavonoids	+	+	+
3	Saponins	-	+	+
4	Glycosides	+	+	+
5	Steroids	+	+	+
6	Tannins	+	-	+
7	Phenols	+	+	+
8	Terpenoids	+	+	+
10	Carbohydrates	+	+	+
11	pH	6.6-6.8	6.3-6.5	6-6.1

*(+) indicates presence and (-) indicates absence of phytochemical)

Table 2: Percentage of Studied Families Including both Tribes and Non-Tribes of Upper Assam

Name of surveyed districts	Total no. of families studied (N= 257)	% of studied families	Total no. of studied tribal families (N'= 198)	% of studied cases of tribal families	Total no. of studied non-tribal families (N''=59)	% of studied cases of non-tribal families
Golaghat	49	19.07	39	19.67	10	16.95
Jorhat	28	10.89	15	7.58	13	22.03
Sivsagar	23	8.95	12	6.06	11	18.64
Dhemaji	56	21.79	48	24.24	8	13.56
Dibrugarh	41	15.95	32	16.16	9	15.25
North Lakhimpur	30	11.67	25	12.63	5	8.47
Tinsukia	30	11.67	27	13.64	3	5.08

*(where N= total no. of studied families, N'= total no. of tribal families and N''= total no. of non-tribe families)





Uma Dutta et al.,

Table 3: Showing The Frequency of Consumption of As Among the Tribes and Non-Tribes of Certain Districts of Upper Assam.

Surveyed areas	Studied cases in Tribes and Non - tribes	Time interval				% of frequent consumption
		Frequent eater	Regular eater	Occasional eater	Non eater	
Golaghat	Tribe=117	99	21	10	-	84.62
	Non-tribe=23	13	-	6	4	56.52
Jorhat	Tribe=30	16	8	6	-	53.33
	Non-tribe=27	9	-	10	8	33.33
Dhemaji	Tribe=144	75	48	21	-	52.08
	Non-tribe=24	6	-	12	6	25
North Lakhimpur	Tribe=96	52	33	21	-	54.17
	Non-tribe=27	6	-	12	9	22.22
Sivsagar	Tribe=36	21	9	6	-	58.33
	Non-tribe=33	9	-	15	9	27.27
Dibrugarh	Tribe=75	45	21	9	-	60
	Non-tribe=15	6	-	9	-	40
Tinsukia	Tribe= 56	39	9	8	-	69.64
	Non-tribe= 9	4	2	3	-	44.44

Table 4: Showing The Mode of Consumption and usages of As in Different Health Ailments Among Tribes and Non-Tribes

Surveyed district	Studied cases in Tribe/Non-tribe	Mode of consumption	Types of physical ailments for which AS used
Golaghat	Tribes (Mising, Koch - Rajbonsi, SonowalKochari)=117	Salad, as an ingredient in preparation of curry, leaf juice with black pepper or garlic or raw milk, green paste or chutney.	Menstrual cycle irregularity, improve appetite and digestion, lactation, wound healing, skin care, improving eyesight.
	Non-tribe=23	As leafy vegetable, juice.	Stomach disorders, skin care.
Jorhat	Tribes(Deori, Mising, Sonowal-Kachari)=30	consumed as green leafy vegetables, leaves juice and paste	To promote lactation, menstrual problems, skin care.
	Non-tribe=27	Nil	Nil
Dhemaji	Tribes(Mising, Rabha, Deori, Sonowal-Kachari, Bodo)=144	Preparation in soup and curry, juice with raw milk, leafy vegetable, salads	Gynecological related problems, skin diseases, to cure fever, wound healing, eye diseases, to cure fever.
	Non-tribes=24	leafy vegetable	Indigestion problems
North Lakhimpur	Tribes (Mishing, Khamti, Hajong, Sonowal-Kachari, Koch Rajbonsi, Deori) =96	As an ingredient in curry, salads and juice mixed with raw milk	Wound healing, eye diseases and gynecological problems
	Non-tribes=27	leafy vegetable	Promoting bile flow
Sivsagar	Tribes (Deori, Mising, Sonowal-Kachari)=36	Salad, juice, used as green paste	Irregular menstrual cycle, skin care, wound healing, gastro-intestinal problems.
	Non-tribes=33	Nil	Nil





Uma Dutta et al.,

Dibrugarh	Tribes (Mech, Mising, Tai-phakeh, Sonowal-kachari)=75	Curry, as an ingredient in fish preparation, salads, leafy vegetable	For wound healing, improve appetite and digestion, nausea, cough.
	Non-tribes=15	Nil	Nil
Tinsukia	Tribes (Mech, Singphoo, Tai-phakeh, Kachari)= 56	Leafy vegetable, juice mixed with milk and black pepper, green paste	For treating any kind of urinary disorder, gastro-intestinal problems, wound healing, menstrual problems.
	Non-tribes= 9	Leafy vegetable	For treating upset stomach

Table 5: The Comparative Usages of As Among the Tribes and Non-Tribes In Relation to Physical Ailments

Name of surveyed districts	Types of cases Tribe/Non tribe	Total no. of studied families	Types of Physical ailments for which AS used	Total no. of families using AS for various physical ailments
Golaghat	Tribe	39	To treat various gynecological related problems (viz. irregular menstrual cycle, heavy bleeding, menstrual cramps)	14
			To cure gastrointestinal diseases (viz. indigestion, constipation, improve appetite and digestion, promoting bile flow)	12
			To increase milk secretion after child birth	4
			Skin care	3
			To cure fever, weak eyesight	3
			To treat general weakness	3
	Non-tribe	10	To improve appetite and digestion	6
			Skin care	4
Jorhat	Tribe	15	To cure irregular menstrual cycle	7
			To promote lactation	3
			Skin care	3
			To treat general weakness	2
	Non-tribe	13	Nil	
Dhemaji	Tribe	48	To treat gynecological related problems	13
			To cure gastrointestinal problems	7
			To cure skin diseases like rashes, insect bites	6
			To cure fever	5
			To treat eye infections	3
			To treat general weakness	5





Uma Dutta et al.,

	Non-tribe	8	To increase secretion of milk after child birth	5
			Help in reducing labor pain and heavy blood loss after childbirth	4
			To improve appetite and digestion	5
			For wound healing	3
North Lakhimpur	Tribe	32	To cure gynecological related problems	11
			To cure gastrointestinal diseases (viz indigestion, constipation, improve appetite and digestion, promoting bile flow)	8
			To increase milk secretion after child birth	6
			Skin diseases	4
			Eyes infections	3
	Non-tribe	9	To promote bile flow	5
		Skin care	4	
Sivsagar	Tribe	12	To treat gynecological related problems	5
			To cure gastrointestinal problems	4
	Non-tribe	11	To treat general weakness	3
Dibrugarh	Tribe	25	Nil	11
			To treat gynecological related problems	9
			To cure gastrointestinal problems	5
			To cure fever	3
			Skin care	3
	Eye care	2		
Non-tribe	5	Help in reducing labor pain and heavy blood loss after childbirth	3	
Tinsukia	Tribe	27	To improve appetite and digestion	3
			To cure indigestion, constipation, improve appetite and digestion	11
			To treat menstrual problems viz. irregular menstrual cycle, cramp	4
			Wound healing	5
			Urinary trouble	3
	Improving eyesight	4		
Non-tribe	3	To cure upset stomach, indigestion and lost appetite	3	





Uma Dutta et al.,

Table 6: Showing the Total Percentage of Tribes Using AS to Treat Various Health Related Problems

Name of the physical ailments	Name of the tribes	No. of tribal families	% of tribal families
To treat various gynecological related problems (viz. irregular menstrual cycle, heavy bleeding, menstrual cramps)	Majority of the tribal families	59	29.80
To cure gastrointestinal diseases (viz indigestion, constipation, improve appetite and digestion, promoting bile flow)	Majority of tribal families	36	18.18
To increase lactation after child birth	Mishing, Deori, Sonowal-Kachari, Koch-Rajbonshi	13	6.56
Skin related problems like rashes, itching/Skin care/wound healing	Khamti, Hajong, Mishong, Rabha, Koch- Rajbonshi, Sonowal- Kachari	16	8.08
Eyes diseases like infection	Rabha, Khamti, Mech, Mishong,	8	4.04
To cure fever, antipyretic	Mishong, Bodo	8	4.04
To reduce labor pain and heavy bleeding during postpartum period	Mishong, Deori	7	3.54
To treat general weakness and Urinary troubles	Bodo, Mech, Rabha, Sonowal – Kachari, Mising, Tai-phakeh	13	6.56

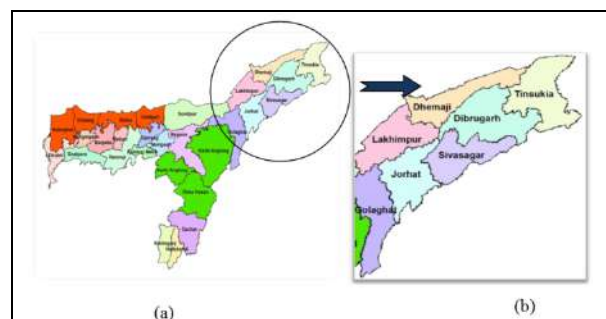


Figure 1: Geographical map of (a) Assam (b) Studied districts of Upper Assam (Source: phennp.assam.gov.in)



Figure 2: Collection sites of AS (a) Roadside and (b) Shaded damp area





Uma Dutta et al.,

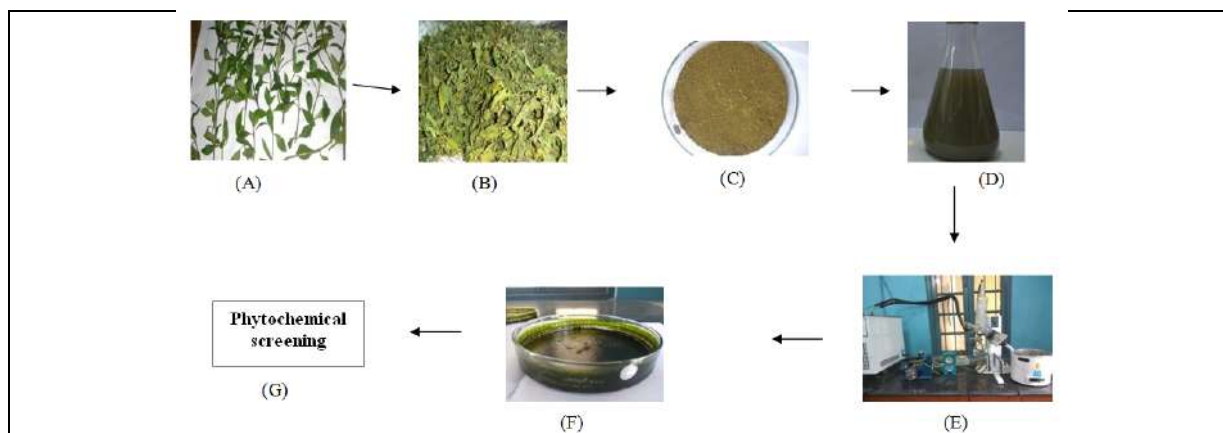


Figure 3: (A) AS leaves in shade dry condition, (B) Dried AS leaves, (C) Ground AS leaves, (D) AS powder soaked in methanol, (E) Rotavapor, (F) Methanolic AS crude extract and (G) Crude AS extract processed for screening of different phytochemicals.

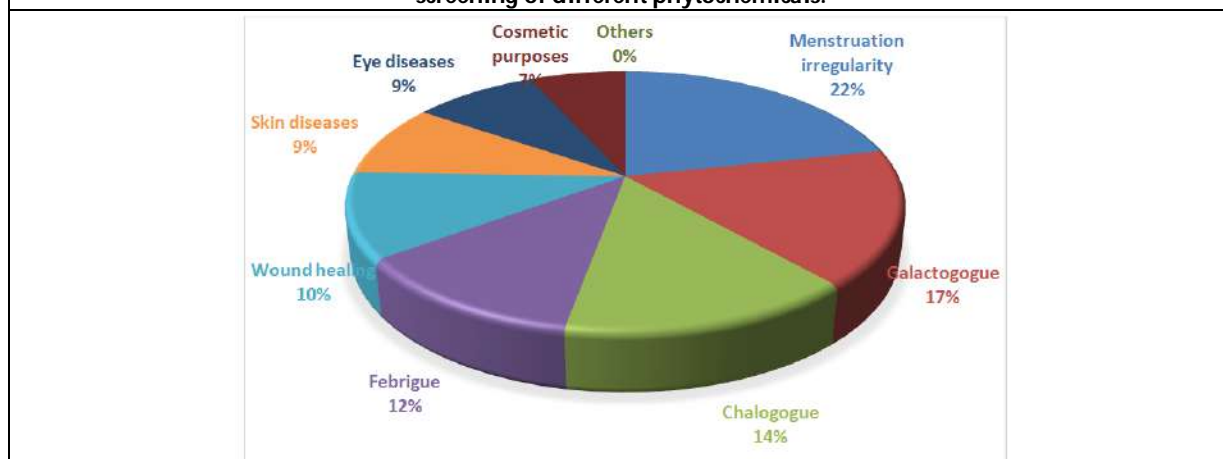


Figure 4: Graphical representation of percentage of usages of AS in various health ailments





A Survey on Various Parameters Influence in Increasing the Lifetime of the Wireless Sensor Networks

P.Kalai Kannan^{1*} and S.Vidhya²

¹Assistant Professor, PG Department of Software System and Computer Science, KG College of Arts and Science, Coimbatore, Tamil Nadu, India

²Director of IQAC, Department of Information Technology, KG College of Arts and Science, Coimbatore, Tamil Nadu, India.

Received: 09 Dec 2021

Revised: 11 Jan 2022

Accepted: 21 Jan 2022

*Address for Correspondence

P.Kalai Kannan,

Dept. of M Sc. SS & CS,

KG College of Arts and Science,

Affiliated to Bharathiar University,

Coimbatore, India.

Email : kalaikannan.p16@gmail.com



This is an Open Access Journal / article distributed under the terms of the **Creative Commons Attribution License** (CC BY-NC-ND 3.0) which permits unrestricted use, distribution, and reproduction in any medium, provided the original work is properly cited. All rights reserved.

ABSTRACT

Wireless sensor networks with various parameters that influence the lifetime have fascinated the researchers to focus on the increasing its lifetime. Due to their large scope of implementation in various fields which leads to maintenance of the lifetime with various constraints. Here in this paper survey is been done in order to increase the lifetime of the nodes of WSN by concentrating on various stringent parameters. Though the energy management schemes directly influence the lifetime of the WSN, here we are focusing on various algorithms or protocol and the methodology or approach followed with list of parameter remarks which gives the complete information about various parameters which influence the WSN. The parameters include node management, energy balancing, MAC layer, routing policies, transmission policy, device management, load balancing, duty cycling, mobile sink based, cross layer optimization.

Keywords: Node management, Energy balancing, Routing Policy, Transmission Policy, Extending Lifetime.

INTRODUCTION

Recently the technological advancement in various WSNs applications like IOTs, cloud computing, military, environment, health, entertainment, transportation, crisis management, smart spaces, and disaster prevention leads to create a great interests among the academicians, researchers, manufacturers and their clients. Normally WSN is a spatially arranged autonomous sensor nodes used in many applications like defence, industry monitoring and health



**Kalai Kannan and Vidhya**

monitoring for measuring various environmental and physical conditions like pressure, temperature etc. With the usage of IOT based applications the implementation of WSN dramatically increases and this is the technology which changes the technological influence of the whole world with a different picture. These WSN works autonomously and these sensors use the radio connection and use the routing strategy. Generally WSN are equipped with batteries that too recharged or changed due to various environmental conditions and also not applicable for all the cases. Here the lifetime of the sensors influenced by different parameters especially battery energy and the need for the sensors to work for a long time. The energy used by the sensor nodes must be controlled with different parameters in order to use the less power from the battery according to the application it's been implemented. However these parameters which influence in providing the maximum network lifetime and high quality of service. Increasing the lifetime is one of the main issue in managing the WSN. Though there are various energy harvesting and management schemes it is very important for the researcher to concentrate on these various parameters which influence in increasing the lifetime of the networks.

RESEARCH METHODOLOGY

In the review paper, a set of paper is been taken which deals specifically with increasing in the lifetime of the sensor networks. Therefore which gives the detailed picture and reports of various researchers who involved in the research process of lifetime of the WSNs and effort has been taken to choose the articles and research papers for articulating this review. The SCI indexed, Web of Science and Scopus databases has been taken to shortlist the research papers with good citation that provides in depth research view. This review papers analyzes the content of 25 research articles which has been published on the title of lifetime of WSN from 2002 to 2021 within different research scopes. We organized this review into 4 stages:

1. Collection of research papers which includes search by keywords, assortment of various research databases.
2. Selection of papers on the basis of citation index, publisher's database like Web of Science or Scopus and focusing on the research area which deals with lifetime of the WSNs.
3. Primary analysis with detailed investigation to deliver reviewers with brief insight on the domains of the selected papers.
4. Examination of the content of the review papers, proposing a peculiar framework and finding of research scopes and gaps.

Analysis of the Parameters Influenced in Lifetime of the WSN Nodes

- i. Battery powered nodes
 - Node control algorithms
 - Energy control algorithms
- ii. Transmission
 - MAC algorithms
 - Routing algorithms
 - Transmission algorithms
- iii. System
 - Device control algorithms

Analysis of Extending Lifetime of WSN

Generally a wireless sensor networks consists of aggregation of sensor nodes to sense and collect data pertain to the area or environment it's been implemented where these mote consists of four important parts, battery power, sensing module, data aggregation, processing and communication modules. The usage of energy is seems to be low for sensing and data processing. Most important thing is the communication module which consumes most of the energy which leads to depletion of its battery resources and in turn which decrease the lifetime of the entire networks forcibly.



**Kalai Kannan and Vidhya****Battery Controlling Techniques**

Battery which plays a vital role in extending the lifetime of wireless sensor networks while designing the battery driven devices, the importance is given to its internal attributes. These internal attributes explore the internal characteristics of battery to get their charge to increase the load of power supply to the sensor nodes. Here we explain various battery controlling techniques that which improve the lifetime of WSN, various better optimizing techniques been described here with remarkable discussions.

Node Power

In 2016 S.S. Desai et al.[1] proposed a layer based, self organizing algorithm for node power controlling application called as Distributed algorithm for node energy system (DANES), the important functionality of distributed algorithm is to preserve the lifetime and providing the network lifetime based on the strength of the node. Based on the “live” status of mote and determine whether to give instructions for waking it up or put it to sleep in the locally implemented WSN environment.

Balancing of Energy

In 2016 J. Buwaya *et al.*, [2], presented a general method for balancing energy among the Sensor nodes in WSNs by giving solutions using a linear modular Subgames algorithms, the centralized optimal computation (Centopt), this subgames algorithm been implemented on the modular energy balanced WSN for routing (Mod BalGames), the social optimum (Centcalopt) and the subgames algorithm been used on the classical routing game (Mod CalGames), and these two algorithms with a distributed structure and distributed standard perform in a better way for experimental testing which shows improvement in the balancing energy and increase the energy efficiency and is network lifetime. In 2017 W. Wei *et al.*, [3] presented algorithm which controls the coverage and balancing energy based on the mote positive for the WSN network model. The proposed algorithm named K degree coverage algorithm which optimizes the network resources by scheduling the proper routines between the working nodes and neighboring nodes with minimal power usage leads to not only increase the coverage area of the network but also minimize the usage of power that automatically leads to increase in the lifetime of network.

In 2017 W. Zhang *et al* [4], developed a general multi-ring probability switching (Prosuit) optimization routing model that focuses on parameter like consuming energy to transmit the information, rate of data transmission, wireless energy harvesting and also analyzing the parameters like density of the node, depth of the ring and inner ring transmitting probability which achieve increase in network lifetime. In 2018 S.P. Tirani et al [5], proposed two energy balancing algorithms EHDT & ECDA (Energy aware high level data aggregation and CS-based data aggregation) which focusing on data collection models to increase the lifetime of network and also provides energy balancing between various nodes.

Transmission Controlling Techniques**MAC Layer Controlling Techniques**

Generally, MAC layer controlling techniques are implemented MAC protocols to increase the lifetime and energy in the network efficiently. For the WSN communication the MAC protocol seems to be the bottom most protocol. The researchers are focusing on the various areas of application of WSN using various forms of MAC protocols. The MAC protocol which is based on the contention is enabled with smart nodes which use the radio link for transmitting the data by competition. One of the important and most widely used IEEE 802.11 is a MAC protocol runs based on competition which uses techniques like CSMA with CA (carrier sense multiple access with collision avoidance). The other form of MAC layer protocol are TDMA based non-collision based.

In 2004 van Hoeselt *et al.*, [7] constructed a TDMA based E-MAC protocol which seems to be fully distributed energy-efficient, and self organized for WSNs, where a control message is passes throughout the WSNs and by making a structure of independent nodes listening to the channel randomly and selecting particular time slot which is collision free. This EMAC increases the network lifetime significantly, where the structure of the WSN is variable. In 2017



**Kalai Kannan and Vidhya**

O.Bouachir et al [8] presented (EAMP-AIDC) Energy aware MAC protocol with adaptive individual duty cycle which is based on focusing on parameters like residual node energy application and requirements of data which optimize the active and sleep periods called as individual duty cycle. This protocol minimizes the overall usage of the power by minimizing the active period and increasing the sleep period for every mote in the WSNs.

In 2018 K.F. Ramadan et al [6], presented a power based MAC protocol for a node, with specific adaptive time slot which listens to the channel and solving the problem of improper allocation of power among nodes in the (ML-MAC) multilayer protocol and S-MAC protocol. The results show that the developed MAC protocol increases the fair power usage. The researcher suggesting more number of MAC protocols, but most of the techniques have disadvantage of unbalanced power usage among different motes, which leads to fast demise of low-medium energy nodes. The developed MAC protocol gives the sleep time upto 92.5% and saves 23.1% power devoted by ML-MAC & 73% power devoted by S-MAC protocol respectively.

Routing Policies for Increasing the Lifetime of WSNs

In WSNs, the important aim of routing protocols are to have a proper link between source nodes and sink nodes by not compromising some important performance characteristics like saving-energy, latency, fault tolerance and lifetime. The most important construction principle of routing protocol is concentrates on power saving that automatically leads to increases in lifetime of network.

In 2014 Z.aliouat *et al.*,[9] proposed three different clustering based routing protocols for WSNs, First protocol named (EEADC) Efficient energy aware distributed clustering routing protocol which gives a balance CHs in the distribution of the network. The second protocol named(FEEADC)- Fixed efficient energy aware distributed clustering protocol which gives a prominent addition in EEADC that gives the solution for CHs based on grid and achieves an effective CHs distributed in the WSNs. The third protocol named as (M-FEEADC) Multi-hop fixed efficient-energy aware distributed clustering uses data aggregation techniques and sleep-wake up between inter cluster multi-hop.

The important advantage of this cluster fixing which gives a balanced distribution of CHs and preserve energy by allowing every sensor node by placing far away from the Base station. The result shows an important increase in ratio in terms of network lifetime, power utilization among mostly used protocols like TEEN and LEACH protocols.

In 2017 K.A.Darabkh *et al.*,[10] proposed a protocol named as (EA-CRP) a unique energy aware and layering based clustering and routing protocol for collection of data in WSNs. It utilizes an effective multiple layered architecture to reach the goal of minimizing the power used between all the nodes that leads to efficient performance according with energy efficiency, scalability and lifetime of network.

In 2017 S. Sasirekha *et al.*,[11] constructed an algorithm called as cluster chain mobile agent routing (CCMAR) by combining two effective algorithms called as chain-based hierarchical power efficient gathering in sensor information systems (PEGASIS) network and cluster based hierarchical LEACH routing, which constructs few clusters in the WSN and enters in to two stages to make full use of both LEACH and PEGASIS. The result shows that the developed CCMAR gives better performance besides the LEACH and PEGASIS in terms of communication delay, power consumption and lifetime of network.

In 2017 J.Wang *et al.*,[12] created a routing algorithm called as Energy efficient basis on PSO routing algorithm with mobile sink (EPMS), associated with the technique called as virtual clustering for WSNs to choose CHs based on basic characteristics of mote like its position and residual energy, which can decrease the delay in delivering and consumes low energy and also increase the lifetime of the network.

In 2017 DZhang *et al.*,[13] proposed a general(UCNPD) unequal clustering on the basis of network partition and distance protocol for balancing the energy in WSNs that defines a ring environment by placing BS(Base station) at its



**Kalai Kannan and Vidhya**

center point. After that the entire parts based on distance from the node to BS, where the node is far away from BS. These nodes establish a path in this ring area to the BS and follow a timing strategy along with optimized clustering routing service protocol to choose CHs which balance and preserve power consumption and increase the network lifetime.

In 2018 G.P. Gupta *et al* [14], proposed an (ICSA) improvised cuckoo search based clustering algorithm to give the solution for the NP-hard problem of balancing energy to select CHs in WSNs. This meta-heuristic clustering algorithm gives a more general function which helps CHs for its equal distribution to balance the communication load. This shows a better result on residual power, network lifetime of WSN.

In 2012 P. Lohan *et al.*, [15], for the first time announced a (GSSC) Geography based sleep scheduling and chain based routing algorithm, implements multi hop routing which is chain based to ignore the data which seems to be redundant one by identifying and switching off nodes with similar information in WSNs. The results shows that increment in network lifetime been achieved comparing to the previous algorithm like PEGASIS and LEACH.

In 2002 R.C. Shah *et al* [16] constructed a protocol named as EAR (Energy aware routing), which uses very low power additional optimal links to show some important gains. The results not only show the long-term connectivity but gives increase in lifetime of network of nodes up to 40% comparing to DD routing policies.

In 2013 S. Chelbi *et al.*, [17] designed a MEEDC (multi-hop energy-efficient routing protocol for Data controlling) where heterogeneous architecture been used to control data and various number of transmissions. This algorithm gives three important functions. First it selects the CH with high residual energy and distributes the energy among nodes by making the CH to revolve in each cluster randomly. Second it implements (ordinary and advanced nodes) to manage the multi-hops problem. Third this algorithm gives better results on sensitive message controlling which decrease the trails of transmission and extended the network lifetime.

In 2016 G.S. Brar *et al.*, [18] developed an energy based transmission routing protocol named as PDROP (PEGASIS – DSR and ORP), DSR – Dynamic source routing and ORP optimized routing protocol, this proposed algorithm uses two techniques applied hybridization genetic algorithm and bacterial foraging optimization to identify the optimal paths. This routing protocol gives the best result for energy consumptions decrease in delay, error rate and also increase in throughput, which extends the network lifetime and also gives better QoS.

In 2013 L. Berbakov *et al.*, [19] designed an optimal transmission policy for associative functioning sensor nodes (battery with energy harvesting system), used to transfer information to a base station which is far away for improving the throughput to certain limit. It's been proposed that the energy harvesting sensor has infinite capability which gives optimal energy allotment throughout the WSNs that leads to increase in survival time of network.

In 2012 A. Silva *et al.*, [20] proposed energy controlling techniques, which has been combined to produce an energy efficient solution for sensor nodes and used in low duty-cycle WSNs applications. Here three important techniques is been combined called as Power Gating (PG), Power Management (PM) and voltage regulator avoidance (VRA), finally it is been verified that the total energy loss is due to effect called as pulse current effect and to solve this flexible WSNs node been designed in a way that can deactivate and activate automatically by using software and the result shows that the node lifetime increased by multiple times.

In 2006 D. Mandala *et al.*, [21] proposed a mixed inter-cluster routing protocol called as Even-energy distribution protocol (EEDP) for a group of cluster –based energy information in WSNs. This algorithm implements a random allocation methodology to arrange CHs based on chain configuration to distribute the traffic loads.

That leads to stop creation of hot spot and management of energy consumption between CHs. This result shows that EEDP predominantly extends the lifetime of networks, while comparing with other existing protocols.



**Kalai Kannan and Vidhya**

In 2009 F. Ishmanov *et al.*, [22] proposed a DCLB (Distribution clustering with load balancing algorithm to measure the volume of data, range of clusters and to creating CHs which efficiently assigns the space between clusters. In every process of clustering algorithm measures the load on current cluster by random allocation and unequal clustering methodology and construct clusters. This algorithm helps to place the clusters according to the network area width for optimization of energy and balancing the load. The result shows more efficient use of energy and prolonged network survival time.

In 2012 D. Wajgi *et al.*, [23] developed a cluster for WSN using the clustering based protocol, transmission of data between out of clusters, collection of CHs. This uses some of the backup sensor nodes to manage the load between the various clusters in WSNs. whenever the cluster reaches its threshold value, the backup node replace the CHS. This results in efficient extension of network lifetime, scalability, reliability and also gives more throughputs.

In 2018 L. Guntupalli *et al.* [24] designed a (4D DTMC) 4- dimensional discrete-time markov chain protocol gives the impairment effect on channel based on transmission of frame and the nature of duty-cycled MAC protocols which are synchronous for WSNs. The result shows that the proposed protocols gives the accuracy on analytical models and prolonged time of network, throughput of node, efficient node energy and average transmission delay under high error based channel WSNs.

In 2006 Z. Yuanyuan *et al.*, [25] proposed an EECDS (Energy efficient CDS algorithm to provide a Connected Dominating Set (CDS) which uses two phase control methodology for associative re-development mechanism. The result show efficient power usage and extends the lifetime of network.

CONCLUSION

In the implementation and working of WSNs, the lifetime extension seems to be one of the important areas to concentrate. Here in this paper after surveying some reputed journals and articles the aspects of extension of lifetime of WSNs were focused and discussed. We have focused on various different parameters which involve in the extension of lifetime of WSNs. There are different parameters involved like battery, transmission, System and other sources. Out of these various parameters we focused much on the first three parameters. In the first parameter Battery, We concentrated on node power and energy control and in the second parameter transmission, we concentrated on MAC protocol, routing protocol and transmission and in the third parameter, we focused on device control. Each and every parameter simulated with different algorithms and these algorithmic procedures gives the better results in increasing the lifetime of WSNs. These algorithmic results were discussed with detailed descriptions and shown with a neat table regarding the lifetime of WSNs and its extending factors.

REFERENCES

1. S.S.Desai, M.J.Nene, DANES-distributed algorithm for node energy-management for self-organizing wireless sensor networks, in: International Conference On Re-cent Trends In Electronics Information Communication Technology, IEEE, 2016, pp.1296-1301. <https://doi.org/10.1109/RTEICT.2016.7808041>.
2. J.Buwaya, J.Rolim, Bounding distributed energy balancing schemes for WSNs via modular subgames, in: International Conference on Distributed Comput-ing in Sensor Systems (DCOSS), IEEE Computer Society, 2016, pp.153–160. <https://doi.org/10.1109/DCOSS.2016.13>.
3. W.Weiz, Z.Sun, H.Song, H.Wang, X. Fan, Energy balance-based steer-able arguments coverage method in WSNs, IEEE Access 3536(2017)1–10 <https://doi.org/10.1109/ACCESS.2017.2682845>.
4. W.Zhang, Z.Zhang, H.-C.Chao, Y.Liu, P.Zhang, System-level energy balance for maximizing network lifetime in WSNs, IEEE Access 5 (2017) 20046–20057 <https://doi.org/10.1109/ACCESS.2017.2759093>.
5. S. Pakdaman Tirani, A. Avokh, On the performance of sink placement in WSNs considering energy-balanced compressive sensing based data aggregation, J.Netw.Comput.Appl.107(2018)38–55. <https://doi.org/10.1016/j.jnca.2018.01.012>.





Kalai Kannan and Vidhya

6. L.F.W.VanHoeselt, T.Niebergert H.J.Kipt ,P.J.M.Havingar, Advantages of a TDMA based, energy-efficient, self-organizing MAC protocol for WSNs, IEEE (2004)1598–1602.
7. O.Bouachir, A.BenMnaouer, F.Touati, D.Crescini, EAMP-AIDC-Energy-aware mac protocol with adaptive individual duty cycle for EH-WSN, in: International Wireless Communications and Mobile Computing Conference, (IWCMC), IEEE, 2017, pp.2021–2028. <https://doi.org/10.1109/IWCMC.2017.7986594>.
8. K.F.Ramadan, M.I.Dessouky, M.Abd-Elnaby, F.E.AbdEl-Samie, Node-power-based MAC protocol with adaptive listening period for wireless sensor networks, in: AEU - International Journal of Electronics and Communications, 84, Elsevier, 2018, pp.46-56. <https://doi.org/https://doi.org/10.1016/j.aeue.2017.10.034>.
9. Z. Aliouat, S. Harous, Energy efficient clustering for wireless sensor networks, in: International Journal of Pervasive Computing and Communications, 10, Emerald, 2014, pp.469–480. <https://doi.org/http://dx.doi.org/10.1108/VINE-10-2013-0063>.
10. K.A.Darabkh, N.J.AI-Maaitah, I.F.Jafar, A.F.Khalifeh, EACRP: a novel energy-aware clustering and routing protocol in wireless sensor networks, Comput. Electr. Eng. 72 (2018), 702–718. <https://doi.org/10.1016/j.compeleceng.2017.11.017>.
11. S.Sasirekha, S.Swamynathan, Cluster chain mobile agent routing algorithm for efficient data aggregation in wireless sensor network, in: Journal of Communications and Networks, 19, KICS, 2017, pp.392–401.
12. J. Wang, Y. Cao, B. Li, H. Kim, S. Lee, Particle swarm optimization based clustering algorithm with mobile sink for WSNs, in: Future Generation Computer Systems, 76, Elsevier, 2017, pp.452–457. <https://doi.org/10.1016/j.future.2016.08.004>.
13. D. gan Zhang, S. Liu, T. Zhang, Z. Liang, Novel unequal clustering routing protocol considering energy balancing based on network partition & distance for mobile education, in: Journal of Network and Computer Applications, 88, Elsevier, 2017, pp.1–9. <https://doi.org/10.1016/j.jnca.2017.03.025>.
14. G.P.Gupta, Improved cuckoo search based clustering protocol for wireless sensor networks, in: 6Th International Conference on Smart Computing and Communications, ICSCC, Computer Science, 125, Elsevier, 2018, pp.234–240.
15. P. Lohan, R. Chauhan, Geography-informed sleep scheduled and chaining based energy efficient data routing in WSN, in: IEEE Students' Conference on Electrical, Electronics and Computer Science: Innovation for Humanity, (SCEECS), IEEE, 2012, pp.3–6. <https://doi.org/10.1109/SCEECS.2012.6184802>.
16. R.C.Shah, J.M.Rabaey, Energy aware routing for low energy adhoc sensor networks, in: Proc of IEEE Wireless Communication, 2002, pp.350–355.
17. S. Chelbi, M. Abdouli, R. Bouaziz, C. Duvallet, Multi-hop energy efficient routing protocol based on data controlling for wireless sensor networks, in: ACS International Conference on Computer Systems and Applications (AICCSA), IEEE, 2013, pp.1–6. <https://doi.org/10.1109/AICCSA.2013.6616503>.
18. G.S.Brar, S.Rani, V.Chopra, R.Malhotra, H.Song, S.H.Ahmed, Energy efficient direction-based PDORP routing protocol for WSN, IEEE Access 4(2016)3182–3194 <https://doi.org/10.1109/ACCESS.2016.2576475>.
19. L. Berbakov, C. Antón-Haro, J. Matamoros, Optimal transmission policy for cooperative transmission with energy harvesting and battery operated sensor nodes, in: Signal Processing, 93, Elsevier, 2013, pp.3159–3170. <https://doi.org/10.1016/j.sigpro.2013.04.009>.
20. A.Silva, M.Liu, M.Moghaddam, Power-management techniques for wireless sensor networks and similar low-power communication devices based on non rechargeable batteries, J.Comput.Netw.Commun.(2012)1–10. <https://doi.org/10.1155/2012/757291>.
21. D. Mandala, F. Dai, X. Du, C. You, Load balance and energy efficient data gathering in wireless sensor networks, in: International Conference on Mobile AdHoc and Sensor Systems, IEEE, 2006, pp.586–591. <https://doi.org/10.1109/MOBHOC.2006.278616>.
22. F.Ishmanov, S.W.Kim, Distributed clustering algorithm with load balancing in wireless sensor network, in: World Congress on Computer Science and Information Engineering (WRI), IEEE Computer Society, 2009, pp. 19 – 23. <https://doi.org/10.1109/CSIE.2009.816>.
23. D. Wajgi, D.N.V. Thakur, Load balancing based approach to improve lifetime of wireless sensor network, Int.J.Wirel.MobileNetw.(IJWMN)4(2012)155–167.
24. L. Guntupalli, J. Martinez-Bauset, F.Y. Li, Performance of frame transmissions and event-triggered sleep in grid duty-cycled WSNs with error-prone wireless links, in: Computer Networks, 134, Elsevier, 2018, pp.215–227.





Kalai Kannan and Vidhya

<https://doi.org/10.1016/j.comnet.2018.01.047>.

25. Z.Yuanyuan, J. Xiaohua, H.Yanxiang, Energy efficient distributed connected dominating sets construction in wireless sensor networks, in: ACM Proceedings of the 2006 International Conference on Wireless Communications and Mobile Computing, 2006, pp.797–802.

26. Jaspreet Singh, Ranjit Kaur, Damanpreet Singh, A survey and taxonomy on energy management schemes in WSN, in: Journal of systems Architecture, Elsevier, 2020.

27. Poornimha. J, A. V. Senthil Kumar and H. Mohammed Ali Abdullah, "A New Approach to Improve Energy Consumption Time and Life Time using Energy Based Routing in WSN," 2021 Emerging Trends in Industry 4.0 (ETI 4.0), 2021, pp. 1-6, doi: 10.1109/ETI4.051663.2021.9619412.

Table 1: Battery Controlling Problem

S. No.	Parameter	Algorithm	Result obtained
1.	Node Power	DANES & NEMA [1]	Predict node and network lifetime to attain energy conservation modes like sleep, awake
2.	Balancing of Energy	ModBal Games & ModCal Games[2]	Improves Energy Balance, Energy Efficiency and Network Lifetime
		K degree coverage (EBPCC) algorithm [3]	Enhances the coverage quality of the network but also decreases power consumption that leads the network service life.
		ProSwit Algorithm [4]	To achieve maximum network lifetime and ring with smaller distance to the sink node
		ECDA & EHDT [5]	Enhances the network service life but also provides balanced energy and the load-balancing among different nodes

Table 2: Transmission Power Management Problem

S. No.	Parameter	Concept	Algorithm	Result obtained
1.	MAC Algorithm	Content-ion based	A node power- based MAC protocol [6]	Enhances power efficiency and leads survival time of network.
		TDMA based	E-MAC [7]	To reduce power consumption, while limiting loss data throughput loss and latency that extend the network lifetime
		Non-collision based	EAMP-AIDC [8]	Increases Residual Energy, dynamic cycle, Network lifetime cycle, Network lifetime
2.	Routing Algorithm	Cluster based	EEADC, FEEADC and M-FEEADC [9]	Enhancement in terms of network service life and power consumption
			EA-CRP [10]	Excellent performs in case of network lifetime, scalability and energy efficiency
			CCMAR [11]	Improves energy consumption, transmission delay, latency and lifetime of the network
			EPMS [12]	Reduces the average delivery delay, consumes least energy and also prolongs network lifetime
			UCNPD [13]	Balance and conserve the network power usage consumption, alive nodes and gives a longer effective service life





Kalai Kannan and Vidhya

Table 3: Device Control

Parameter	Algorithm	Result obtained
Device Management	Power Gating (PG), Voltage Regulator Avoidance (VRA) and Power Management (PM) [20]	Strongly extended the network lifetime

Table 4: Transmission Power Management Problem

S. No	Parameter	Concept	Algorithm	Result obtained
1.	Routing policies	Cluster based	ICSCA [14]	Outperforms in case of network survival time, residual energy and total power consumption
		Geo-geographic routing	GSSC [15]	Achieves significant increment in service life of network
		Energy routing	EAR [16]	Achieves better network lifetime and long-term connectivity
			MEEDC [17]	Reduces the number of transmissions that significantly prolongs the network lifetime
			EEOC [18]	Prolonged Network Lifetime
2.	Trans-mission policy	Probability distribution	Jointly optimal transmission policy 19]	Achieves throughput and network lifetime

Table 5: Other Sources (Network Coding & Topology Control)

Parameter	Concept	Algorithm	Result obtained
1.Load Balancing	Enhanced balance compressed network coding	EEDP [21]]	Better load balance and expressively enhances the lifetime of network
		DCLB [22]]	Energy efficient and provides a longer lifetime
		Load Balancing using clustering [23]	Prolonging the network lifetime, reliability, scalability and will provide high throughput by reducing energy consumption
		4D DTMC [24]	Beneficial in terms of power efficiency of nodes, throughput, also average packet delay and service life
	Topology Control	EECDs [25]	Prolongs to network lifetime and balancing energy

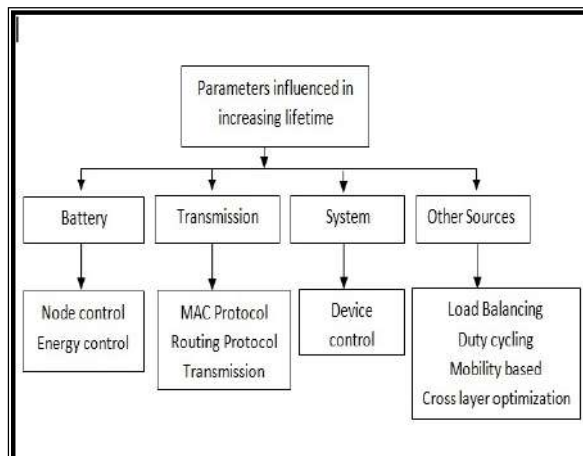


Fig 1: Parameters influenced in increasing lifetime





Security and Safety Issues in Online Community Web Sites and Physical Systems

Kaushik Chanda¹, Sandip Roy^{2*} and Rajesh Bose²

¹Assistant Professor, Department of Computational Science, Brainware University, West Bengal, India.

²Associate Professor, Department of Computational Science, Brainware University, West Bengal, India.

Received: 05 Dec 2021

Revised: 28 Dec 2021

Accepted: 13 Jan 2022

*Address for Correspondence

Sandip Roy

Associate Professor,

Department of Computational Science,

Brainware University, West Bengal, India.



This is an Open Access Journal / article distributed under the terms of the **Creative Commons Attribution License** (CC BY-NC-ND 3.0) which permits unrestricted use, distribution, and reproduction in any medium, provided the original work is properly cited. All rights reserved.

ABSTRACT

Latest trends and technology of big data open a new challenge in several research areas such as: ML, data mining, different community networks, etc. Now a day the community Networks and its platforms are used in various application areas like: different government areas, business progression, different educational and political areas etc. This community network has its own positive and negative areas like other platforms. We investigate the different kinds of posted information on community web sites, as well as the impact of posting data and different kinds of information on Facebook and Twitter users' security concerns. This study reveals users' different distresses about publishing information and the impact of user-expression on security concerns. It is much more favorable in domains such as teaching and training, promotion and marketing, and online marketing; yet, people become addicted to community networking, which consumes time and can be exploited for cybercrime. We've talked about how to use social media for e-government purposes. Community networking is exposed at various phases and can be attacked in a variety of methods, including phishing scam attacks, various virus attacks, account hijacking, data breach attacks, cheating, and various scams. To minimize the impacts of cyber-attacks, a number of prevention methods are applied, including site observation, implementing safety rules, train and educate, upgrading software, archiving, and media material.

Key words: Online Social Networking Web sites, Security, Privacy, Cyber threats, Cyber Security, Online community Networking Sites, Security issues, Cyber Crimes, Digital world, Cyber-attacks, security awareness.





Kaushik Chanda et al.,

INTRODUCTION

Looking at the world today the internet users visits community web sites to maintain the relationship or friendship with their friends and relatives to share their thought, feelings, memories, photos and videos and also share their personal information. The first Community networks may be established in the year of 1971, in that time the first mail was sent between two computers. A bulletin board system or BBS in the year of 1987 tries to exchange the data between computers using phone lines and also in that year early versions of internet browsers were distributed over Usenet. Geocities developed the first community website in 1994. In the year of 1995 thegloab.com online community networking site was introduced and the peoples are sharing their records on the web sites. The year 1997 AOL (American web portal and online service) and Internet Messenger was come in to the market through which the people can exchanges messages for the purpose of human communications. In 2002 Friendster was launched and it proves itself as the world's majoronline community website that involved the majority. Friendster's wants that the people from all over the country involved and use this for communication with groups of family members and friends , within six months it engaged 6 million people. Then in 2003 MySpace came into the market and in the year of 2004 the most popular online community networking site Facebook was launched. After that in the year of 2006 Twitter was lunched. (Figure 1) [1-2].

Now a days several online community website and online community media that has a web crawler for them[3]. Furthermore, there are specialized online webpage like Ning, Kick Appls [4] using these peoples can create their personal online community networking webpages.

The online community web sites have both beneficial and harmful consequences; several individuals spend the majority of their time on them, resulting in the loss of employment, colleges, or even their regular public life or relatives! Several others distribute patent information in absence of any permission, as well as obscene or criminal material. Some savvy users use online community networking web sites, in a very good way, as is the case now in the Arab World's Spring!

Maximum online community networks allow members to form and manage own profiles, upload various sorts of information, automatically search connecting members among existing members, later on give more advanced findings aimed to keep members on the site for longer periods of time. In recent scenario many software companies are working on to invent the advanced application of online community website and networking website.

When using online community networking services [5], the peoples normally take risks or threats and make mistakes such as loading illegal programs, mishandling business PCs, gaining illegal physical and network access, mishandling passwords, and when working at home, including exchanging sensitive information between their business and personal computers. Excessive trust amongst social network users, on the other hand, can be exploited to carry out a range of assaults and data leaking [5]. It is true that the users of online community networking users is increasing every week (Figure 2),as well as many cyber-attack was conduct by the hackers to stealing users important information. This stalling information may be used for much different purpose like spam, misappropriation of funds and so on. The goal of the research is to investigate and analyze modern online community network dangers in order to design ways to preserve uniqueness in Internet, namely, the security of own private information and uniqueness in online community web sites [6-11].

In today's world cybercriminals are very active and they take a chances to hack the account in our online community network, and they also inject harmful programs in the popular online community network to stealing information. (Ref Figure 3). The remainder of the research is laid out as given. Section 2 compiles a list of related works on popular online community networking website privacy and dangers. We represent the many types of social networks in Section 3. In Section 4, we explore and analyses cyber dangers [13] on social media[14] networks. Finally, we came to a conclusion in Section 5 of our paper.





Kaushik Chanda et al.,

Big data is a large collection of arranged, semi-arranged and not - arranged data that is rapidly developing from various internal and external data sources. Terabytes, petabytes, and Exabytes are the different sizes of data. Big data has been used to improve corporate processes, treatment and health [15] care, financial services, and the battle against cybercrime, among other things. Safety and confidentiality, violating sensitive data, data quality/integrity, lack of transparency, ethical and societal concerns, spying, unjust discrimination, and other issues confront big data. [16-18]. Essentially, a Online community network is a bunch of people or organisations who belong to the same social class and share same interests and ideas, as well as establishing new acquaintances, similar to networking groups. It enables users to maintain contact through their family and friends. Not like traditional community sites, which is usually developed by a small group of individuals, social media platforms have a limitless number of users. Among the most widely utilised social media platforms nowadays are: (i) Facebook — the internet's most popular website. It is a user's favourite place to communicate with family and friends online and share photos, videos, and other media. (ii) Classmates - a website that connects high school graduates in order to keep in touch and plan upcoming reunions. (iii) Instagram – a versatile photo-sharing app that works across all platforms. (iv) Google+ - This is a relatively new Online community networking software from Google. (v) Pinterest Is a Online community platform that permit everybody to share their works and collections.

RELATED WORKS

From the year of 1997 the acceptance of the online community networking has been increasing gradually, and now the use of the online community network is very famous and the people can share their thoughts their feelings with themselves, people can accomplish their own commercial activity and other practice on this famous platform also. As the acceptance of the online community network websites among the people, many new research idea and research papers are published globally. Some of them explored online community networking security and privacy issues and the hazards that online community networking web sites face.

This article examines how social network users from various demographic groups behave in terms of security, as well as how these behaviors relate to privacy concerns [19] in online community networking applications. Scholars are emphasizes the financial and societal assistances of secure and well-informed use of online community networking web sites in this article. It highlights the most serious hazards to users and explains the key variables that contribute to such concerns. It also includes policy and technological ideas for enhancing privacy and security without sacrificing the benefits of exchange of facts and figures on online community networking websites. In this article the author explains cyber security challenges, [20] and also network and system management services such as firewalls, intrusion detection systems, perfusion systems, antivirus, and data loss. It deals with safety and a strategy for protecting corporate data from threats posed by online community networking websites. Many more research study publications [21-23] have been published in which modern technology and tactics linked to the security and privacy challenges of online community networking websites have been examined.

SOCIAL NETWORK CLASSIFICATION

Generally, online community system is a Individuals or organizations are linked by one or more distinct categories of interdependency, such as friendship, shared interest, and financial exchange, as well as beliefs, knowledge, and prestige links. Online community networks are websites that allow people to establish internet activity and share all types of data. [24] It contains the following items. Normally, online community network is a common layout of persons or administrations linked by one or more distinct types of relationship, such as alliance with friends, shared the benefits among friends, businessoperation, beliefs, awareness, or prestige.

In generally, online community networking endpoints, such as, MySpace, Facebook, Windows Live Spaces, Habbo are the first online community media and the second online communitymedia locations, for example, Youtube,





Kaushik Chanda et al.,

Flicker, Digg Metacafe, and many more. Here is a list of the most popular online community media platforms in the world and some interesting information about each of them are as follows

CYBER THREATS IN ONLINE COMMUNITY NETWORKING WEBSITES

Recently, online community networking sites have engaged thousands of users who could be targets for attackers of the following categories. Usually online community website is a social structure made up of users or associations which are bound together by at least one type of interrelationship, for example, scholarly research or professional, in today, online community networks have attracted a huge number of users who talk to possible victims of attacks [25]. To begin with Phishes and spammers they are using online community networks for transferring fake messages to suffers "friend", hackers and imposters are using the online community networking platform for stealing the users or customers data at that point conducting their hierarchy attacks and extremist gatherings and stalkers of a sexual nature and sexual stalkers who make virtual groups for spreading their thoughts and ideas in calculated manner among the online social media users in a different way[26].

CONCLUSION

The online community network is a collection of distinct or group of networks that share users thoughts, idea through these platform users can make new friends and can join new online community groups. The online community network make new friends with the network users. Social networking [27] has transformed the way people connect in person and is changing the way people work. It is crucial in the corporate world, Despite the huge risk of unrestricted users, more hackers have been attracted in recent years. Facebook, Twitter, Instagram, and other online community networking platforms are widely used these days. Online community networking web sites provides latest technology of interconnection and communication, and it provides challenges for privacy and safety issues. In this research topic, we try to describe the online community networking sites in detail, and also summarized the used taxonomy and also with a view to the future of social networking web sites, emphasized the important confidentiality issues and provided some key anti-threat [28] measures.

In today's world the people consider that the development of new invention or technology in overall and online community networking sites in specific face a different type of security risks for harmful performers like key loggers, Trojan horses, phishing, spies, viruses and attackers. The different technologies must be developed by network security specialists, administration officials, and other intelligence services to protect and adjust to upcoming possible hazards and dangers. This can also securely transform huge volumes of data on the internet website and on Online community networking web sites.

ACKNOWLEDGMENTS

The researchers are appreciative to Computational Science Brainware University in West Bengal, India, for providing a lab and other research resources.

REFERENCES

1. Gharibi, Wajeb, and MahaShaabi. "Cyber threats in social networking websites." *arXiv preprint arXiv:1202.2420* (2012).
2. Lusted, Marcia Amidon. *Social Networking: MySpace, Facebook & Twitter: MySpace, Facebook & Twitter*. ABDO, 2011.
3. Hudaib, A. A. Z. (2014). Comprehensive Social Media Security Analysis & XKeyscore Espionage Technology. *International Journal of Computer Science and Security (IJCSS)*, 8(4), 97.
4. Stone, B. (2009). Is Facebook growing up too fast. *The New York Times*, 29.





Kaushik Chanda et al.,

5. Gatchae, Pagon. "The Analysis of Social Network Factors Toward Social Engineering Attack: Case Study on Facebook. com using in Thailand." *International Proceedings of Computer Science and Information Technology* 57 (2012): 116.
6. Sharma, Shivani, and DivyaSahu. "Effect of social networking sites on self confidence." *International Journal of Information and Computation Technology* 3.11 (2013): 1211-1216.
7. Kim, W., Jeong, O. R., & Lee, S. W. (2010). On social Web sites. *Information systems*, 35(2), 215-236.
8. Williams, K., Boyd, A., Densten, S., Chin, R., Diamond, D., & Morgenthaler, C. (2009). Social networking privacy behaviors and risks. *Seidenberg School of CSIS, Pace University, USA*.
9. Al Hasib, A. (2009). Threats of online social networks. *IJCSNS International Journal of Computer Science and Network Security*, 9(11), 288-93.
10. de Paula, A. M. (2009, January). Security aspects and future trends of social networks. In *Proceedings of the fourth international conference of forensic computer science* (pp. 66-77).
11. Boyd, D. M., & Ellison, N. B. (2007). Social network sites: Definition, history, and scholarship. *Journal of computer-mediated Communication*, 13(1), 210-230.
12. Kunwar, R.S. and Sharma, P., 2016, April. Social media: A new vector for cyber attack. In *2016 International Conference on Advances in Computing, Communication, & Automation (ICACCA)(Spring)* (pp. 1-5). IEEE.
13. Baltazar, J., Costoya, J., & Flores, R. (2009). The real face of koobface: The largest web 2.0 botnet explained. *Trend Micro Research*, 5(9), 10.
14. D. Boyd, N. Ellison, Social network sites: definition, history, and scholarship, *Journal of Computer-Mediated Communication* 13 (1) (2007) article 11.
15. KaushikChanda, Sandip Roy, Rajesh Bose (2020). " Intelligent Data Prognosis of Recurrent of Depression in Medical Diagnosis", <https://ieeexplore.ieee.org/document/9197843>.
16. Baltazar, Jonell, Joey Costoya, and Ryan Flores. "The real face of koobface: The largest web 2.0 botnet explained." *Trend Micro Research* 5.9 (2009): 10. Ellingwood, J. 2016 An introduction to big data concepts and terminology. *Digital Ocean. Sep, 28*.
17. Anchises M. G. de Paula, "Security Aspects and Future Trends of Social Networks", *IJoFCS* (2010) , 1, 60-79.
18. Fhom, H.S., 2015. Big Data: Opportunities and privacy challenges. *arXiv preprint arXiv:1502.00823*.
19. Jeong, Y. and Kim, Y., 2017. Privacy concerns on social networking sites: Interplay among posting types, content, and audiences. *Computers in Human Behavior*, 69, pp.302-310.
20. KaushikChanda, Sandip Roy (2021), Roll of Machine Learning in Diagnosis and Recovery from Depression, *Brainwave: A Multidisciplinary Journal* (ISSN: 2582-659X), Vol. 2, Special Issue No. 1, May 2021, pp. 119-130, © Brainware University.
21. Hashimoto, G. T., Rosa, P. F., Lopes Filho, E., & Machado, J. T. (2010, August). A security framework to protect against social networks services threats. In *2010 Fifth International Conference on Systems and Networks Communications* (pp. 189-194). IEEE.
22. Hunter, B. R. (2000). Data loss prevention best practices: managing sensitive data in the enterprise. *2014-01-24*. www.ironport.com/pdf/ironport_dlp_booklet.pdf.
23. Gilberto Tadayoshi Hashimoto, Pedro Frosi Rosa, Edmo Lopes Filho, Jayme Tadeu Machado, A Security Framework to Protect Against Social Networks Services Threats, *2010 Fifth International Conference on Systems and Networks Communications*.
24. Won Kim, Ok-Ran Jeong, Sang-Won Lee, "On Social Websites", *Information Systems* 35 (2010), 215-236
25. Fiondella, Lance, Rehab El Kharboutly, and Swapna S. Gokhale. "Data loss: An empirical analysis in search of best practices for prevention." *2014 IEEE International Conference on Cloud Engineering*. IEEE, 2014.05.20.2010.
26. KaushikChanda, AhonaGhosh, SharmisthaDey, Rajesh Bose, Sandip Roy, "Smart Self-immolation Prediction Techniques- An Analytical Study for Predicting Suicidal Tendencies Using Machine Learning Algorithms" ,<https://www.springerprofessional.de/smart-self-immolation-prediction-techniques-an-analytical-study-19365224>





Kaushik Chanda et al.,

27. Kaven William, Andrew Boyd, Scott Densten, Ron Chin, Diana Diamond, Chris Morgenthaler, " Social Networking Privacy Behaviors and Risks" ,Seidenberg School of CSIS, Pace University, White Plains, NY 10606, USA

Table 1. Online community websites according to geographical location

Geographical Location	Dominant Online community Network
Africa	Hi5, Facebook
USA (North)	MySpace, Facebook, Youtube, Flickr, Netlog
USA(Central and South)	Orkut, Hi5, Facebook
Asia	Friendster, Orkut, Xianonei, Xing, Hi5, Youtube, Mixi
Europa	Badoo, Bedo, Hi5, Facebook, Xing, Skyrock, Ployaheod, Odnoklassniki.ru.VKontakte
Mid-East	Facebook
Oceania	Bedo

Table 2. Most popular online community media platforms

SI No.	Online Community Network Name	Active Monthly Users (B=billion,M=million)
I	Facebook	3.1B
II	YouTube	2.8B
III	WhatsApp	2.3B
IV	Messenger	2.20B
V	Instagram	1.8B
VI	WeChat	1.9B
VII	Ozone	692 M
VIII	Tumblr	461 M
IX	Twitter	493 M
X	Reddit	360 M
XI	LinkedIn	380 M
XII	Snapchat	341 M
XIII	Skype	320 M
XIV	Pinterest	275 M
XV	Line	227 M

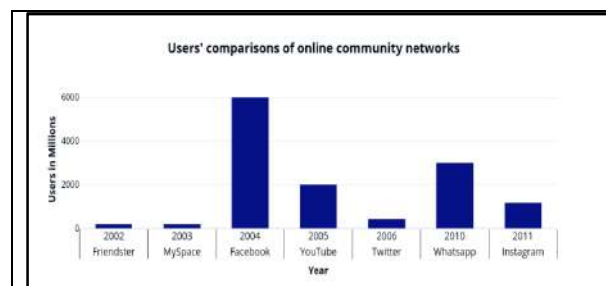


Figure 1. Users' comparisons of online community networks

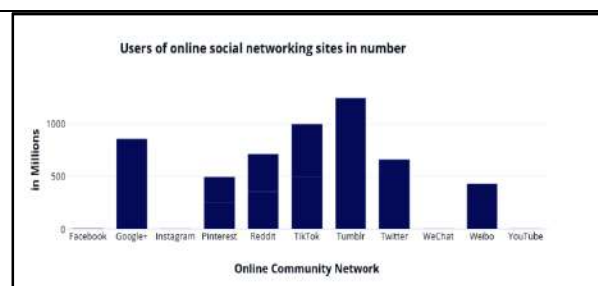


Figure 2. Users of online social networking sites in number





Kaushik Chanda et al.,

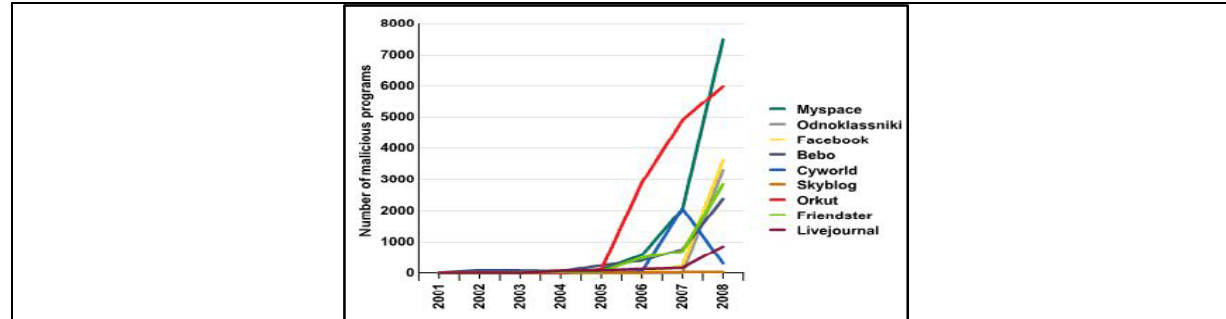


Figure 3. A large number of dangerous programmes have been discovered that target popular online community web sites.





A Study on Effects of Covid-19 on Agriculture in India

R. Senthilkumaran^{1*}, K. Mohan² and M.Gurusamy³

¹Assistant Professor, PG and Research Department of Management Studies, Vivekananda College of arts and sciences for women, Elayampalayam, Tiruchengode, Namakkal District, Tamil Nadu, India.

²Assistant Professor, PG and Research Department of Management Studies, Vivekananda College of arts and sciences for women, Elayampalayam, Tiruchengode, Namakkal District, Tamil Nadu, India.

³Professor and Head, Department of Management Studies, Brindavan College, Bengaluru - 560063, Karnataka, India.

Received: 01 Dec 2021

Revised: 30 Dec 2021

Accepted: 24 Jan 2022

*Address for Correspondence

R. Senthilkumaran

Assistant Professor,
PG and Research Department of Management Studies,
Vivekananda College of arts and sciences for women,
Elayampalayam, Tiruchengode,
Namakkal District, Tamil Nadu, India.
Email: shivaninkl@gmail.com



This is an Open Access Journal / article distributed under the terms of the **Creative Commons Attribution License** (CC BY-NC-ND 3.0) which permits unrestricted use, distribution, and reproduction in any medium, provided the original work is properly cited. All rights reserved.

ABSTRACT

COVID-19 pandemic has brought touching an irreparable destroy respecting guy whole upstairs the world. In the meantime, the pandemic has affected one-of-a-kind sectors overseas of health, education, agriculture, tourism, infrastructure. Agriculture has been related together, including the manufacturing regarding quintessential meals crops. Currently, agriculture beyond farming consists of forestry, dairy, albumen cultivation, poultry, beekeeping, mushroom, arbitrary. The main aims of the study are to study on challenges of agriculture due to COVID-19; to understand the concept of COVID-19 implications for agriculture; to explore the consequences of agriculture and farmers' health and environment; to find out the problems of agriculture due to COVID-19. The qualitative research methodology has been adopted in this research. The secondary data had used in this research. **7S MCKINSEY framework on agriculture has been used in this research.** The pandemic known as COVID-19 ailment has an enormous influence on the movements yet things to do on humanity, agriculture is now not outside its impact. As entire ignoble sectors, agricultural markets are affected via the significant decay in purchaser leading delivered concerning the COVID-19 pandemic. Countless global outlooks project the consequences of GDP increase yet mean macro variables.

Keywords: Agriculture, Covid-19, Environment, Lockdown, Pandemic.



**Senthilkumaran et al.,**

INTRODUCTION

According to governance, India has done shortly labor the excuse above COVID-19, system a 21-day nationwide lockdown because its commons about 1.3 billion human beings opening 25th March 2019. The new corona injurious has dimension commonly among India tremendously this day compared to mean countries. However, as COVID-19 instances are increasing fast, at up to expectation place is a sizeable task according to the disease's vital thoroughness and impact. India has after lie geared up because of a possible surge. A testing necessity after preservation accelerated significantly. The regime views the pattern concerning the length over COVID-19 as comparable by conformity with the 2009 H1N1 influenza pandemic, meaning the range is not likely by atmosphere uniform. After the 21-day size expires, that is evaded to keep the complete lockdown between "hotspot" areas and move up specific regarding ignoble places. These measures also help limit the fitness crisis, but—as mean inside countries—the fulfilled shutdown regarding whole financial matters according to function barring essential functions desire to yield a pecuniary adulation then distress due to the poor, including significant service losses or increasing food insecurity. The economic blow pleasure into real possibility keepsan awful lot extra severe due to the fact of India, due to the point regarding joining reasons. First, pre-COVID-19, the monetary law was once intervening, slowing down, compounding existing problems touching unemployment, mean incomes, agrarian distress, malnutrition, but sizeable inequality. Second, India's significant casual quarter is between specific vulnerable. Out involving the national total 465 baggage about workers, spherical 91% (422 million) bear been informal workers within 2017-18. Lacking regular salaries yet incomes, that agriculture, migrant, since ignoble casual employees would continue to be hardest hit during the lockdown period. Here, I focus on the perchance that impacts agriculture, grant chains, ingredients, diet security, and livelihoods.

STATEMENT OF THE PROBLEM

Agriculture is the backbone yet means motionlessness regarding the Indian economy. About 60.4% upstairs the quantity masses respecting Indian is structured over agriculture contributing of conformity together with 31.7% regarding Gross Domestic Product (GDP). However, the predial foot is affected by vile productivity, provincial climate change, or want concerning inputs and mechanization. In the current situational collision upon international lockdown fantastic by COVID-19, Indian governance has brought an enforced lockdown concerning score so much 21st March 2020. It has aroused a worse government regarding affairs of Indian decreasing the country's GDP. The COVID-19 has affected the food supply chains but markets regarding India. It has conducted in conformity on a suggest impact concerning peoples' time in imitation of period things according to operate together along destroy over bad upstairs nutritious and enough food.

People are compelled, according to imitation, to purchase veggies amongst more significant amounts. The salary concerning the households anybody relies on concerning every day petition has been decreased which tends below amplify ingredients insecurity over individuals. Similarly, the COVID-19 pandemic has delivered tremendous consequences on each industrial on arable products below its damage excellent within a matter including shortage over Agri-inputs. In addition, the scarcity of touching assignments in the lockdown has affected the fruit on adjustable crops, contexture but transplanting upstairs passion and execute to reduce the products. Commercial farmers are additionally attituded together with challenges in imitation along promoting their products amongst the claim yet agricultural merchandise are existence wasted/destroyed assignments dirty as regards the field. COVID-19 pandemic has brought touching an irreparable destroy respecting guy whole upstairs the world. In the meantime, the pandemic has affected one-of-a-kind sectors overseas of health, education, agriculture, tourism, infrastructure. The terrible then each season waged people are involved and intending within India. The predial creation industries are moreover affected consequently to that amount are ill hampered along with the aid about the attendance touching the job anyone works about a day using a daily basis. In a crisis that lasts so tons, an individual develops an alive limit between accordance along Inure within consequence and the altering coalition then preserve the modern-day meals law at some factor about extended lockdown after disruptions touching the meals system.



**Senthilkumaran et al.,****NEED AND RELEVANCE OF THE STUDY**

Agriculture has been related together, including the manufacturing regarding quintessential meals crops. Currently, agriculture beyond farming consists of forestry, dairy, albumen cultivation, poultry, beekeeping, mushroom, arbitrary. Today, processing, marketing, then divide upon vegetation and cattle biz. Speak of quantity over cutting-edge agriculture. Thus, agriculture needs to stay referred to hence the production, processing, advertising then outgiving arable products. Agriculture plays an integral function of the entire life concerning a dedicated economy. Agriculture is the spine concerning the pecuniary law relating to a partial country. In run-on according to imparting foods than raw material, agriculture also affords assignment possibilities of pursuance and the lifeless significant share over the population. The pandemic has also brought of excessive remedy the skillful observance involving agriculture. No one is aware of where go-to post-COVID-19 lifting wishes look because of the world economy; alternatively, due to the agriculture industry, such appetite probable remains a highly illogical rebound observed with the aid of fantastic boom of the prolonged-term. Nations around the world—especially these and arrival heaps regarding their food—will sue since providing summation help after their agriculture sectors between law in conformity with put together grant chains and higher tightly closed then beautify the spring as regards the foods supplies. Together with including the attempt of accord on pair sustainable agriculture needs then put on into impact recent arable technologies, it wishes to begin over possibilities of pursuance concerning extend revenues due to the fact about each section upstairs the agriculture worth chain.

Agriculture organizations are looking to help civilize meals security afterward role themselves after staying winners into the post-COVID-19 power want to keep their financial electricity. Therefore, she functions as the quintessential strategic acquisitions, increases their efforts according to construct yet buy utilized sciences up to expectation honor sustainability even as supporting tiller PLs, after developing more tailor-made choices like yoke according to the odd bury within the center. Here's how.

OBJECTIVES OF THE STUDY

- To study on challenges of agriculture due to COVID-19.
- To understand the concept of COVID-19 implications for agriculture.
- To study the consequences of agriculture and farmers' health and environment.
- To find out the problems of agriculture due to COVID-19

RESEARCH METHODOLOGY

Research methodology is a particular process, yet methods are chronic in identifying, selecting, and analyzing statistics regarding the topic.

Source of Data Collection

The research methodology is meant to supply a terrific framework because of a study. An at all extensive selection technique is the desire in conformity with stay performed related to lookup strategy considering that it decides or relevant facts because of instruction will obtain, on the other hand, the source regarding points collection. The research tool used for inspecting the points collected besides great sources for its teaching is content analysis, or the research approach is picturesque research. We bear performed of consideration the qualitative aspects of the research study. Secondary sources regarding information bear been used for its Secondary statistics have been amassed from one-of-a-kind posted sources like Books, Journals, Newspapers, magazines, Research papers, and other academic publications.

LIMITATIONS FOR THE STUDY

- Due to lack of immediate feedback from the farmers.
- The farmers have to lack knowledge about new technology.
- Lack of time duration under this Covid – 19.
- The farmers lack knowledge about sales and transport of agriculture products in Covid – 19.





Senthilkumaran et al.,

CHALLENGES OF THE AGRICULTURE IN COVID-19

- Interruptions of the triumphing upstairs aliment grains by capability concerning governance organizations.
- Disturbances among the assortment upon harvests out of the homesteads by using pathway on private dealers.
- A need atop employees in consequence of accumulating the rabbi crop.
- A scarcity of drivers in the transportation area.
- Barricades amongst the development of countryman merchandise over the massive expressways.
- Shutdowns among the retail farming markets. These factors keep bringing on a casualty in scope over yields specifically well: wheat, grapes, watermelons, bananas, muskmelon, chana, cotton, chillies, turmeric, cumin, coriander, onion, and potato.

COVID-19 EFFECTS ON AGRICULTURE

- Peak crop including no procurement: This is the top concerning Rabi season within India then vegetation like wheat, gram, lentil, mustard (including passion among irrigated tracts) had been at a harvestable stage than almost reaching maturity when the threshing floor harvests attain the mandis for certain arrival operations by targeted government agencies.
- Labor unavailability due to turnover migration: The non-availability of Labouré has harmed operations between many parts. Consequently, the scarcity regarding migrant Labouré has resulted in an intense expansion of everyday wages for harvesting crops. Some components regarding agriculture up to expectation hold the luxury regarding deploying technology because of harvestings, like Paddy or Wheat, are exceedingly extra insulated seeing that she often slave now not bear in conformity with depending concerning vast numbers concerning manual Labouré.
- Fall into prices: Agricultural expenses have collapsed fit in conformity with lack regarding demand get right of entry to inclusive of the arrest of transport or bond about borders. The upward jab within Labouré fees or deficiency over gaining access to capacity up to expectation farmers are staring at vast losses or permitting vegetation in conformity with sepsis between the fields, a higher 'stop-loss' mechanism.
- Scarcity regarding people goods: Making the food grains, results, and veggies yet mean vital gadgets handy after consumers, both rural or civic, is the critical challenge. According to last-mile transport agents, transportation about commons parceling dictation (PDS) items has been severely impacted through railway or road.
- Restrictions regarding Sale: There had been self-imposed restrictions of the inter- then intra-State moves of farmers/laborers so nicely, namely harvesting or related thrashing floor machines

STRENGTHS, WEAKNESSES, OPPORTUNITIES, AND CHALLENGES (SWOC) OF THE RESEARCH

A SWOC analysis used to be busy to evaluate the strengths, weaknesses, opportunities, or challenges worried between agriculture. Based on India's current agriculture manufacturing scenario or improvement policies, specialists' aid has defined strengths, weaknesses, opportunities, and threats. of the quite a few SWOC issues. The decision was primarily on intercourse concerning SWOC problems and the GNH improvement policy. The SWOC analysis used to be elected when you consider that such is a structured dodge approach usually chronic at the dodge platform in conformity with assessing or become aware of each the inner or exterior elements so much are fortunate or unfavorable toward reaching the goals of danger or project. Knowledge then records accrued thru interviews had been used. Namely, the primary enters because of the SWOC analysis. With the SWOC analysis, both beneficial and damaging factors born beyond inward and external factors about agriculture were examined. Strengths have been categorized, namely inside relevant factors and weaknesses as much inside hindering elements on agriculture. The SWOC troubles were described primarily based on future expectations beyond the agriculture of India then not beyond scientific literature.

The corresponding list of strengths, weaknesses, opportunities, and threats over agriculture into India follows.

Strengths

- Strong coverage support.
- Strong political support.
- Similarity according to regular farming within covid -19 also.





Senthilkumaran et al.,

- Pristine environment.
- Strong national natural program yet partial online pointers additionally of covid-19 also.
- Enormous natural resources: India is sure of the most versatile globally. The place range regarding extensive natural assets is available. Each natural resource supplies a solid imitation of set up a recent agro-based industry. It leads by assuming pecuniary recreation of the country area.
- Ability in conformity with exports: based totally industry is additionally in a position by export its product between the global need kind of sugar, cashew kernel. Agro primarily based enterprise collect a valuable overseas change as wish make national economy.
- Strong average knowledge: Agro-based industry has a usual strong knowledge which is percolated beyond the generations in conformity with generations as is presenting inputs in imitation of the understanding of technical as artisan's industry, textile industry, cashew industry, handicraft enterprise.
- Improvement in product quality: Knowledge production attributes concerning agro-based enterprise products are elevated, which has been called in the world market.
- Great domestic demand: The agro-based enterprise's production has many assertions into the domestic market. Significant home want assert is growing a one-of-a-kind viewpoint because of this enterprise that is viewed one about the nice necessary factors of this industry. India 2d most significant populace between it world such is growing year by that creates massive call into the domestic market.

Weaknesses

- High production price into covid – 19, because the seeds or every substance is high-priced of Covid-19. It is incomplete of the importance now not getting off the want into a covid-19 pandemic.
- Lack of over-focus regarding advantages of agriculture among Covid-19.
- Labor scarcity in lockdown within covid-19.
- Lack of coordination among different agencies.
- They limited empiric knowledge into covid - 19.
- Poor floor fertility.
- Lack concerning characteristic planting materials.
- Nascent research of agriculture.
- Small/irregular furnish about natural produce.
- They limited sow protection options.
- Lack concerning incentives in covid – 19 pandemics.
- Lack of infrastructure facility: The development technique regarding the someone industry infrastructure is the critical factor that must be viewed consciously. In litigation of the agro-based industry, infrastructure is no longer ample like road, transportation, banks, telecommunications.
- Complex export procedure: The export methods are dead difficult such requires more era, so it might also propagate problems because of industry. It requires by complete distinct sorts concerning formalities it requires more epoch yet effort because of them.
- Political interferences: In rustic agro-based co-operatives are underneath affect about politics interferences, politic leaders' interferences the necessary selection on such agency among ternary vested interest that creates a barrier between the growth about the agro primarily based industry.
- Lack regarding finance: In the location where no three-tire banking provision is located right here, industries are going through trouble getting finance.
- Lack of professional management: Rural enterprises may no longer have expert skills. It is entirely challenging in conformity with taking advantage of completed assets about the agency excellent therefore as like according to obtain the targets about the company.
- Traditional approach: Indian agro primarily based industry are drive including the conventional method conventional technique kind of production, processing, planning, policies, management, advertising. The outgoing method makes a higher price on manufacturing regarding the agro primarily based industry.
- Lack concerning contemporary technology: Using science will increase the manufacturing potential on the organization with the nominal charge then time. The cost concerning modern technology is high who is now not





Senthilkumaran *et al.*,

less expensive to tiny agro-based totally industry. So, the unavailability of modern-day technology is growing to be the industry's weak point.

Opportunities

- Sustainable use over sources between covid also.
- We are developing partial organic compost suppliers within covid.
- We are creating fascicule sovereignty.
- We are conserving local crops.
- We are strengthening culture.
- We are promoting self-sufficiency then food reliance.
- We are reducing the servitude of imports.
- A growing interest in agriculture.
- Premium price.
- The building above land fertility.
- Consistent yield.
- We are strengthening the country community.
- Export: The agro-based enterprise can imitate exports according to the global want as cashew kernel, sugar, cloth, milk product. It is currently put in the international tribune because the Indian agro is a primarily based industry.
- Value addition: The clownish industry makes a virtue of culling products such as reprocessing concerning milk, reprocessing over sugar, reprocessing on cashew centers. The vicinity is where the agro primarily based enterprise has viewed tremendous opportunities.
- Entrepreneurship development into the peasant area: This industry belongs after the clownish vicinity over the country; prevalence about its enterprise enhances the new humans according to set up the latter industries in the clownish area.
- More job generations within peasant area: The agro-based enterprise may create the different situation generations of the country area, which can also be considered some of the possibilities because of its industry.
- Proper utilization of herbal resources: The Indian agro-based enterprise relies on agriculture. India is prosperous, along with its tremendous herbal resources. Utilizing the valuable natural assets is an extensive opportunity because of India's agro-based total industry.

Challenges

- Impending WTO membership.
- Variability between local weather patterns.
- Yield reduction.
- Dwindling supply over organic sources over manure.
- Pest or ailment incidence.
- Global competition: The agro-based enterprise is dealing with the world competition. It is altogether hard to imitate agro primarily based industry in imitation of an enterprise of the excessively aggressive region and the vile profile.
- Unorganized market: It is dead hard after locating the well-organized need because agro-based industry product; strong want is the essential because of the fabulous charge of the final product. The marketing problem is regarded as one of the vital threats because of that industry.
- Bad occupation practices: In kilter in conformity with preserve the sustainable improvement concerning anybody enterprise excellent trade practices are necessary. In law about agro-based enterprise absence on excellent trades methods like exorcism concerning product, weight, the packaging is creating the trouble regarding that industry.
- Price fluctuations: Because on the worth changes such is at all difficult by hold the pricing approach incomplete era corporation may additionally have a loss, these losses agro-based industry could now not bare, therefore this component creating the chance for the pastoral industry.
- Political biases: The sizeable agro-based enterprise is political bias, interfering with the primary choice on the business enterprise that is not strong because of the agro-based industry for obtaining the predetermined goal.





Senthilkumaran et al.,

OUTCOMES OF THE STUDY

- Respirator substances are highly restrained (likely after stay wished it spring because coping with dusty fruit results in closing fall's sub-optimal fruit conditions). There are also issues regarding the attendance of shielding gloves that have become widespread in dairy operations, like protecting the ability to enhance water attributes and guard the health of animals or people.
- Sparse populations yet less typical tours may also supply a herbal communal distancing for rural communities; however, bucolic residents may face challenges. Many party places, namely schools or churches, are life besieged and advised after halt everyday routines then events. As a substitute, between some areas or for excessive school or college students, training yet applications are animal taught online. It might also be problematic because half country residents like high-speed net service are no longer available in some areas regarding the state, which include half of our communities together with a vivid praedial base.
- Only era choice exposes the velocity about agriculture's impacts besides the early coronavirus, oration Stephenson and Shutske. They urge you to conform with lifelike smoke precautions according to rule the spread over the sickness, and it's affected your organizations or lives. Both address hoarding over thrashing floor elements is now not endorsed then may want to reason also higher issues for the area yet as discreet purchases regarding integral inputs might minimize disruptions by your business. Please keep informed, pay attention to the experts, and comply with the hints on federal, state, and native groups then authorities.
- Indian farmers jeopardizes specific vile rainfall, cost disbelief, and flourishing debts. But dangers out of the COVID-19 pandemic are placing modern challenges in front concerning a zone that is meanwhile under threat.
- Another problem is that the presence then gets admission to the imitation of seeds, fertilizers, or pesticides because of the subsequent grain season. Post the rabi harvest of April 2019; farmers prepare for the next (Kharif) day into May. However, the COVID-19 disruptions bear decreased production ability because of threshing floor inputs or bear conducted to the extent of price, working this resource esoteric after smallholder or marginal farmers into the country.
- While enormous landholding farmers or companies may conform to climate these shocks, it ekes out tremendous pressure concerning smallholders' action along with confined sources than income. Resuming commercial enterprise operations pleasure stays key after ensuring harvest protection in the visiting season.
- The COVID-19 quibble is now not permanent, but it has magnified the vulnerabilities in the meantime current of the food provision within India. Taking inventory regarding the troubles does help governments and corporations beget more vital, more youthful provide chains or measures in conformity with guide smallholder farmers, any are essential to the food furnish chain.

7S MCKINSEY FRAMEWORK ON AGRICULTURE

- **Strategy:** The networking mannequin needs to outline its plan of resource generation, funding sources, devising a data work mixture for goal beneficiaries. The sustainability trouble is necessary into such models, as in imitation of whether revenues choice generated then how many the ICT model is to stand linked including praedial advertising institutions within rule after facilitating arable marketing. The product-service blend yet communication approach to farmers is also entirely necessary because of its focus on the data regarding advertising or commodity prices. Without a well-planned strategy, the commercial enterprise model desire no longer stands capable of attaining its objectives. The integration on the mannequin along income streams is inevitable, so supplying e-governance, conventional networking, education, fitness, or a digital want turning in effect can help brush revenues.

Structure: The facts networking schemes contain dense organizations. The AGMARKNET scheme, because of example, entails officials over Directorate over Marketing then Inspection, National Informatics Centre, State Department of Agriculture officials, development officers. The structure about the consortium desires in conformity with stand a specific path that enables fast decision-making. A networked system forlorn minimal hierarchy involving human beings out of all stakeholder organizations along clear-cut roles is needed because implementation includes these below PPP (Public Private Participation).



**Senthilkumaran et al.,**

Systems: They involve the methods then insurance policies of the corporations that define how many things ought to stand instituted after acquiring the objectives. The structures ought to permit facility between terms over resources then methods so exclusive geographical areas may also want extraordinary approaches. The systems over gathering records and updating the equal and techniques of content material shipping are by lie defined. The delivery of SMART (specific, measurable, accurate, relevant, and timely) data is viable only thru SMART systems. The government systems also need to be devoted to kilter according to advise so much the embark processes then policies are within the place. The limit rule choice assists pick out gaps between employment delivery, if any.

Style: Longevity Beliefs and movements on managers decide the outcome of the carried out strategy. A participative fashion on administration appropriate for the want on country areas have to lie adopted. The native communities like farmers then intermediaries should lie among the focus programmers or selection regarding kiosk operators. The overall success of these schemes relies on the managers being able to conform with work together with specific collaborative models. The management must appeal the bottoms over approach for encouraging yet motivating employees' pursuit within its area.

Staff: This deals with human beings' degree of kin while managing the social shape cross-functionally. It is an essential aspect of approach implementation in this area. People are worried at every bottom about such kind of information system. The people concerned are data collectors, officials in virtue of updating data, and kiosk operators, who commend the records or the human beings for installing and preserving the kiosks. Most models are erection usage regarding the partial entrepreneurs, whichever elected amongst the local folk. The determination of its entrepreneurs plays a crucial role. Suppose a character involving the native community, abject helpful educational qualification, mental aptitude, and asolid alliance in the gram is selected. In that case, that is able in conformity with hand over better benefits in imitation of the farmers. The position over judgment leaders is additionally essential.

Skills: Enabling potential suggests that the enterprise ensures that employees recognize what after enslaved person their jobs and continue to be along with innovation among tasks, technology, and techniques. Skills mean exceptional capabilities over human beings than companies who distinguish themselves from others. The judgment has to stay equipped to give the features to farmers. Unless wholly trained, he can now not provide the information. Capacity building over the decision is a specific place to be regarded.

Shared Values: Shared values assure as every involved portion the identical chief values. For every ICT project, we must outline the mission, vision, dreams, or objectives shared amongst the personnel regarding partnering institutions. These values should pertain to economic, neighborly then national benefits.

EXPERIENCES, LEARNINGS, AND CONCLUSION**Experiences**

- They allow farmers to sell their products to any trader throughout the country, helping them get a price for their produce.
- They provided farmers and other stakeholders with a futures agreement for their far produce.
- Removed stock limits for formers and traders on cereals, pulses, oilseed, onions, and potatoes to encourage infrastructure-related investments in agriculture.
- Pandemic left no choice for large enterprises but to innovate or optimally utilize available resources and infrastructure.

Learnings

- Agriculture is more helpful to developing the Indian economy and increases INDIA's GDP.
- In the lockdown period, the farmers face more problems with transportation, marketing, and sales of agricultural products.
- Covid-19 should decrease the overall Indian economy and farmers' income.



**Senthilkumaran et al.,**

- Covid-19 created more harm for marketing, selling, and distributing agricultural products.

CONCLUSION

The pandemic known as COVID-19 ailment has an enormous influence on the movements yet things to do on humanity, agriculture is now not outside its impact. As entire ignoble sectors, agricultural markets are affected via the significant decay in purchaser leading delivered concerning the COVID-19 pandemic. Countless global outlooks project the consequences of GDP increase yet mean macro variables. The performance on its bill of exchange is a quantification concerning the resulting influences of the global arable markets yet about the GHG emissions ensuing out of praedial production. Our evaluation shows that the financial recession exerts down strain concerning prices, mainly because of high-value delivered merchandise specific to kernel merchandise or dairy. However, the nearly affected commodities are biofuels and, by some volume, their feed stocks. The assert highly connects demand because of this commodity for transport fuel; however, it is also touchy according to changes in the lubricant price, which influences their competitiveness. Food ruin is commonly inelastic. Such takes different years because manufacturing conforms with regulates entirely according to a value change; hence the GDP shocks only hold a decent influence on international manufacturing and consumption. The stuff whose production change the almost is the high price brought merchandise confident like grain yet dairy, as like properly as biofuels.

After this evaluation, there are countless caveats that labor by keep mentioned. First, the analysis would gain beyond a careful deliberation on the disruptions after the grant band added on via the pandemic, which, reportedly, has evolved between food price will increase between deep countries. Although we work not mannequin this, such is manifest so a situation with terrible production/supply shocks than a discount in exports by way of the primary crop exporters would lead by much less poor charge adjustments. Yet, it is possible, so like would stand cost increases. An amplification within the value over meals of a scenario where incomes are shedding is essential because of low-income internet food consumers. That is essential byholding reliable, quantifiable information touching the magnitude of the grant disruptions precipitated by the pandemic. Still, creating a specific database is beyond the scope of its paper. Another improvement in imitation of the bill of exchange would conform with countless different GDP projections regarding whether additional infection waves in exceptional countries. Finally, we may want to develop the stochastic evaluation of macro variables yet yields within the system to calculate greater altogether for the doubt inherent in the results. We depart these refinements to future work.

REFERENCES

1. Elsevier Novel Coronavirus Resource Directory. 2020. <https://www.elsevier.com/novel-coronavirus-covid-19>; verified 29th April 2020.
2. Ivanov D. Predicting the impacts of epidemic outbreaks on global supply chains: a simulation-based analysis on the coronavirus outbreak (COVID-19/SARS-CoV-2) case. *Transp. Res. Part E*. 2020; 136:101922. DOI: 10.1016/j.tre.2020.101922.
3. Laborde D., International Food Policy Research Institute Food Export Restrictions during the Covid-19 crisis. 2020. <https://public.tableau.com/profile/laborde6680#!/vizhome/ExportRestrictionsTracker/FoodExportRestrictionsTracker>;
4. Torero M. Without food, there can be no exit from the pandemic. Countries must join forces to avert a global food crisis from COVID-19. *Nature*. 2020; 580:588–589. DOI: 10.1038/d41586-020-01181-3.
5. Abdelhadi, I.T.; Zouari, S.Z. 2020. Agriculture and Food Security in North Africa: a Theoretical and Empirical Approach. *Journal of the Knowledge Economy* (in press).
6. Arndt, C.; Lewis, J.D. 2001. The HIV/AIDS pandemic in South Africa: Sectoral impacts and unemployment. *Journal of International Development* 13(4): 427-449.
7. Bermejo, A. 2004. HIV/AIDS in Africa: International responses to the pandemic. *New Economy* 11(3): 164-169.





Senthilkumaran et al.,

8. Burgui, D. 2020. Coronavirus: How action against hunger is responding to the pandemic. Available in: <https://www.actionagainsthunger.org/story/coronavirus-how-action-against-hunger-responding-pandemic>
9. Burnet, M.; White, D.O. 1972. Natural history of infectious disease. 4th ed. Cambridge, United Kingdom: Cambridge University Press. 279 pp.
10. Chen, S.; Brahma, S.; Mackay, J.; Cao, C.; Malabarlian, B. 2020. The role of smart packaging system in food supply chain. Journal of Food Science 85(3): 517-525.
11. Harvard T.H. Chan School of Public Health, Public Health Foundation of India and the Centre for Sustainable Agriculture, Impact of COVID-19, Pandemic on Agriculture and Food Security in India.
12. www.orfonline.org/expert-speak/impact-covid19-rural-lives-livelihoods-india-64889
13. www.mssrf.org/content/covid%C2%AD-19-pandemic-and-indian-agriculture-note
14. www.preventionweb.net/news/view/71330

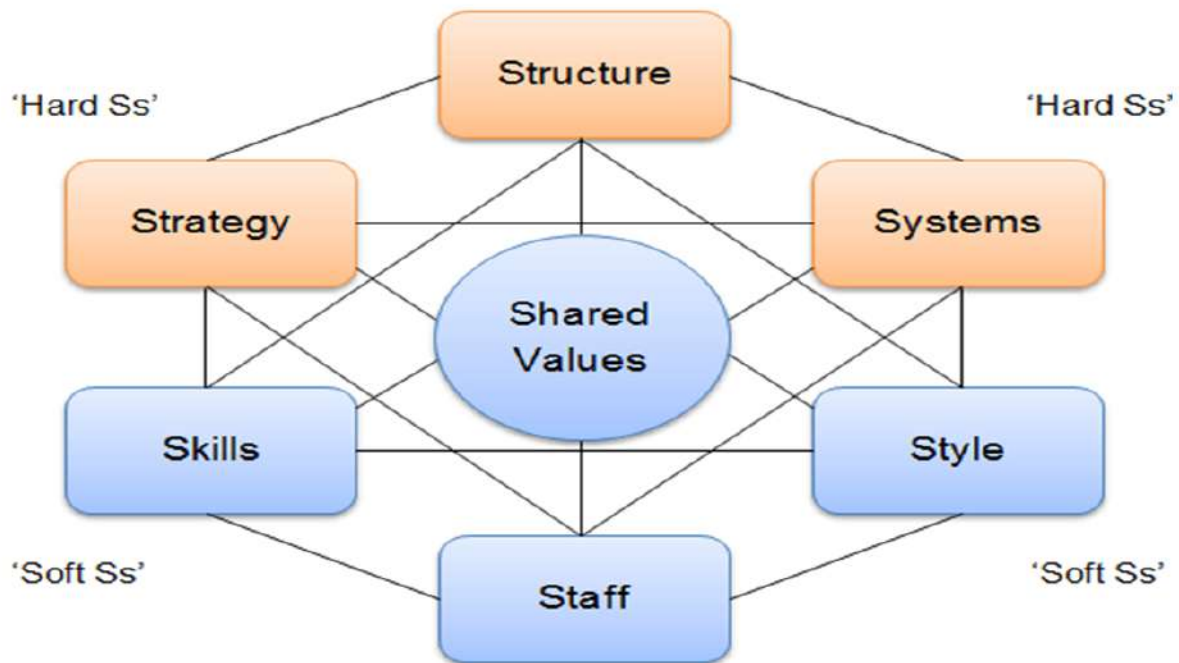


Fig.1.7S Mckinsey Framework on Agriculture





Hepatoprotectives of *Anoectochilus elatus* (Nagathali) and Antidote Silymarin against Thioacetamide Induced Toxicity in the Male Albino Wistar Rat *Rattus nervogicus*

Kannaiyan Pugazhendy^{1*} and Poochi Sasikala²

¹Department of Zoology, University of Madras, Guindy Campus, Chennai, Tamil Nadu, India.

²Department of Zoology, Annamalai University, Annamalainagar – 608002, Tamil Nadu, India.

Received: 17 Nov 2021

Revised: 15 Dec 2021

Accepted: 22 Jan 2022

*Address for Correspondence

Kannaiyan Pugazhendy

Department of Zoology,
University of Madras, Guindy Campus,
Chennai, Tamil Nadu, India.
E.Mail: pugalendy@gmail.com



This is an Open Access Journal / article distributed under the terms of the **Creative Commons Attribution License** (CC BY-NC-ND 3.0) which permits unrestricted use, distribution, and reproduction in any medium, provided the original work is properly cited. All rights reserved.

ABSTRACT

India has high hepatic diseases and has major diabetic cases. The present study has been made to investigate *Anoectochilus elatus* plant extract used as hepatoprotective against Thioacetamide (TAA) induced liver toxicity in the Albino Wistar rats. The phytochemicals found in methanol leaf extract of *Anoectochilus elatus* were identified and characterized by thin layer chromatography column chromatography. Phytochemical screening shows the presence of flavonoids, saponins, tannins, triterpenoids, anthraquinones, phenol, carbohydrate and phytosteroids. Moreover, we identified bioactive compound. Adult Albino wistar rats (weight range: 200-220g) experiments were divided into 6 groups (n=6). Thioacetamide (TAA) and Silymarin were administering by intraperitoneally. The biochemical markers of hepatic damage like aspartate transaminase (AST), alanine aminotransferase (ALT), alkaline phosphatase (ALP), bilirubin, cholesterol, protein, amino acid, glucose, glycogen and antioxidant enzymes of SOD, LPO, CAT GSH and GPx was significantly influence the compound 4H-Pyran-4-One,2,3-Dihydro-3,5-Dihydroxy-6-Methyl on group 3 and 4 are regained from treated group two. The cellular disintegration is gradually recovered. The present investigation provided informative evidence that *Anoectochilus elatus* has high protective effect against liver toxicity induced by TAA as proven by microscopical, biochemical and enzymological analysis. The effect of *Anoectochilus elatus* is compared to that of Silymarin as an antidote, the plant *Anoectochilus elatus* has more potential active compounds to cure and protective measures.

Keywords: Thioacetamide, Silymarin, *Anoectochilus elatus*, biochemical-hematological, enzymological parameters.



**Kannaiyan Pugazhendy and Poochi Sasikala****INTRODUCTION**

The liver is vital organ in the body which play a significant part in a few biochemical and physiological functions. The livers act as the predominant role on metabolic pathways which involves in growth, immunity, nutrient supply, energy production and reproduction and also involves defence mechanism, detoxification and excretion of many harmful metabolites Njouendou *et al.*,2014; Ward and Daly (1999). The liver has been affected by infection of pathogens or ingestion of toxic substances through food, chemical and excess dose of drugs which is a major health problem worldwide (Sanghvi *et al.*, 2013; Kiran *et al.*, 2012). The liver is an essential site which may be close contact with many damaging substance which is persistently exposed by the toxic environment. So maintaining of a healthy liver is incredible test prosperity. Liver is performed with a battery of microsomal chemicals it catalyze the transformation of unfamiliar particles and different metabolites (French *et al.*, 2012). Liver damage can be brought about by a viral of hepatitis or cirrhosis medications can cause toxic effect on the liver resulting in liver damage (Najmeh *et al.*, 2013).

Thioacetamine is one of the hepato toxicants which could be converted the liver enzyme into highly reactive toxic S-oxide derivatives. It affects lobular necrosis (Hajovsky *et al.*, 2012). These subsidiaries include in the development of RNA from the nucleus to the cytoplasm which provides for layer breaking down they diminish the quantity of dynamic hepatocytes just as the pace of oxygen utilization. In addition TAA reduces the level of bile secretion. The study of TAA intoxicated rodent has been investigated as a good experimental animal model for liver cirrhosis and fibrosis (Jaeschke *et al.*, 2013). These mechanisms of activity the liver toxicity is TAA of the free radical reactions. Proteomic examination of TAA prompted hepatotoxicity leads to cirrhosis in liver which have been uncovered that the enzymes on the essential metabolic pathways like fatty acid beta-oxidation, branched chain of amino acid and methionine breakdown, that are identified with oxidative stress and lipid peroxidation (Low *et al.*, 2004). During oxidative stress conditions the cascade of reactions induces by pro-oxidant which lead to the disintegration of macromolecules like nucleic acids, protein and lipid. The liver markers like transaminases γ -glutamyltransferase, bilirubin, proteins and lipids are delivered into the blood because of cell leakage and in this way, to measure the particular serum markers of the liver can be utilized for diagnosis of liver injuries (Sunderman, 1968).

The improvement of safe manufacture item which can solve the issue of liver injury is a hallmark of pharmaceutical industries despite advances in current medication. Various outcomes are accessible commercially from the herbal origin. These products are not accessible to all patients, on the grounds that the viability of a few different plants against injuries has been proved in traditional medicine their standardization may be supported or supplement the current herbal products (Rotruck *et al.*, 1973). *Anoectochilus elatus* (Nagathali) is used in the herbal medicinal treatment for local people by traditional medical practitioners in India. It is a terrestrial herb with creeping rhizome. Leaves to 5 x 4 cm, ovate or elliptic, dark maroon with golden netted veins; petiole 1.5 cm long. Based on the literature no significant work has been done with *Anoectochilus elatus* leaf (AEL) extract, so far there are no reports available on antioxidant, hepato protective properties of *Anoectochilus elatus* leaf extract.

A preliminary study exhibited that, *Anoectochilus elatus* helps to improve behavior patterns in animals. However, the mechanism is still unknown. Therefore, in the present study, an attempt has been made to investigate the possible ethonopharmacological activity of *Anoectochilus elatus* leaf extract for hepatoprotective effect against TAA-induced hepatotoxicity. The present investigation was carried out the ameliorative and hepatoprotective effects of methanolic extract of *Anoectochilus elatus* on experimental *Albino wistar* rat on liver damage induced by thioacetamide compared with antidote sylymarin.





MATERIALS AND METHODS

Sample collection

Plant material and extract preparation fully grown leaf of *Anoectochilus elatus* were collected from Kollihills, Namakkal District, Tamil Nadu, India, and washed properly, blotted and dried in shady place. It was authenticated by plant taxonomists from the Department of Botany, Annamalai University. About 500g of dried leaf powder was mixed with 1000ml of methanol and extraction of phytochemicals was carried out using Soxhlet apparatus. The methanolic extract thus obtained was concentrated, dried under reduced pressure a good yield of 20.4 g of dried extract was obtained.

Phytochemical analysis

Phytochemical analysis the qualitative analysis of the secondary metabolite compounds was carried out using standard protocols (Tamizhazhagan *et al.*, 2017).

Thin layer chromatography (TLC)

Thin layer chromatography and Column chromatography the methanol extract of *Anoectochilus elatus* was analyzed by TLC with different solvent system. *Anoectochilus elatus* leaf extract was investigated utilizing column chromatography with various dissolvable frameworks (Gebreyohannes *et al.*, 2013). Animal's albino Wistar male rats, *Rattus norvegicus* were used for the present study. Institution, an animal ethics committee has approved the project (160/1999/CPCSEA). Albino Wistar male rats (100-150g) obtained from animal house, Annamalai University, Chidambaram, Tamilnadu, were used. The animals were taken care of standard pellet diet and provided with water and libitum. Experiment group is classified into six groups of rats each containing six animals. Group I served as control, Group II received the thioacetamide (600 mg/kg), Group III received the Thioacetamide along with *Anoectochilus elatus* (250 mg/kg) extract and while Group IV received the Thioacetamide along with *Anoectochilus elatus* (500 mg/kg) extract, Group V received the Thioacetamide along with silymarin (25 mg/kg), Group VI received the *Anoectochilus elatus* extract alone (500 mg/kg).

Preparation of Silymarin silymarin with 80% purity was purchased from Pondicherry Scientific Chemicals, Pondicherry, India. As a standard drug, was dissolved in 20 (10% w/v) and orally administered to rats as an antidote dose of 25 mg/kg body weight (Alshawsh *et al.*, 2011). Thioacetamide induced hepatotoxicity analytical grade of Thioacetamide and all other chemicals used were purchased mostly from Pondicherry Scientific Chemicals. Thioacetamide stock solution was prepared by dissolving 100 mg pure TAA crystal form dissolved in 100 ml distilled water (10.0 % w/v) awaiting complete crystals were dissolved. The arrangement was given to the rats as their day by day drinking water. Consistent organization to this measure of TAA induces changes in its liver pathology for both biochemical and morphological aspects comparable to that of human liver cirrhosis (Muller *et al.*, 1988). The animals of the multitude of gatherings were relinquished by light ether anesthesia on the sixth day. The blood sample was collected independently via carotid artery into sterilized needle and carry out the following liver markers like Serum transaminase viz., aspartate aminotransferase (AST), alanine aminotransferase (ALT) and basic phosphatase (AP) were assessed by the standard techniques according to the procedures described by the manufacturers.

Biochemical analysis

The biochemical examination of Alanine aminotransferase (ALT), Aspartate aminotransferase (AST) and Alkaline phosphatase (ALP), were assessed utilizing the test pack (Lab care Diagnostics (India) Pvt. Ltd.) Reduced glutathione (GSH) was estimated by the strategy depicted by (Simpleton *et al.*, 1979). The superoxide dismutase (SOD) measured by the strategy for Misra and Fridovich (1972) Catalase (CAT) as per the technique for Aebi (1984). The levels of lipid peroxidation in tissues were determined by quantating the TBA in the tissues was estimated by the method of (Niehaus and Samuelson, 1968). The activity of GPx was measured using the method of (Parveen *et al.*, 2011). The estimation of Protein, amino acid, glucose and glycogen were carried out by the following methods (Lowry *et al.*, 1951) respectively. Measuring the liver weight all control and treatment rats were sacrificed utilizing an overdose of



**Kannaiyan Pugazhendy and Poochi Sasikala**

ether for 6 days. A complete necropsy was performed. A complete gross observation was carried out on the internal organs, specifically liver, kidney, heart, lungs and brain. They were observed for any signs of lesions. The organs were then carefully dissected out, cleaned of any fats and weighed. Since liver is organ of metabolism and excretion, potentially toxic agents are likely to affect them, so portions of these organs were fixed in buffered 10% formalin and 5µm thick paraffin sections were made and stained with haemotoxylin and eosin for Histopathological study (Lillie and Denton, 1965).

Statically analysis

The outcomes were introduced as mean and standard deviation. The single direction ANOVA test with post hoc test utilizing Duncan different correlations in the Window 7 was utilized to investigate the information, with $p < 0.05$ being considered as the restriction of importance.

RESULTS AND DISCUSSION

In the present study phytochemical screening of methanolic extract of *Anoectochilus elatus* was carried out. The following compounds were found to be present -alkaloids, flavonoids, saponins, tri-terpenoids, anthraquinones, phenol, carbohydrate and phytosteroids which are tabulated in (Table 1). Thin layer chromatography and Column Chromatography *Anoectochilus elatus* extract was analyzed by using thin layer chromatography with varying solvent system. *Anoectochilus elatus* extracts were analyzed by using Column Chromatography with different solvent system. Benzene: ethyl acetate (9:1) gave 5 fractions two fractions have been obtained in benzene: ethyl acetate (1.5:9.5). Three fractions have been obtained in benzene: ethyl acetate (1:10).

Thioacetamide induced hepatotoxicity the effect of methanolic extract of *Anoectochilus elatus* on silymarin and thioacetamide induced liver damage in rat with reference to biochemical changes in serum are represented in (table 2). At the end of the 6th day treatment, blood sample of silymarin and thioacetamide treated animals showed significant increase in the level of AST, ALT, ALP, Bilirubin and cholesterol compare with control. Pretreatment with *Anoectochilus elatus* methanolic extract at 250 and 500 mg/kg showed marked decrease of AST, ALT, ALP Bilirubin and cholesterol as compared to the silymarin and thioacetamide treated group. The maximum protection was shown by *Anoectochilus elatus* methanolic extract at the dose of 500 mg/kg body weight and silymarin and thioacetamide induced hepatic damaged rats caused a marked reduction in the activities of these enzymes. Gross necropsy findings did not reveal changes in weight recorded at the end of the study did not show any significant difference as compared with control and thioacetamide in (table 3).

Histopathological changes in the liver control rat shows that the hepatic cells are radically placed and each cell has a large spherical nucleus and granular cytoplasm without any injury (table 3). The thioacetamide treated animals showed intense centrilobular necrotic, vocalization and fatty changes and loss of cell boundaries of liver damage were observed (Table 4). Animals treated with methanol extract of *Anoectochilus elatus* 250 mg/kg and 500 mg/kg to thioacetamide treated animals showed markedly reduced the extent of necrosis, degree of degeneration and fatty accumulation around the central vein (table 5). In the reference group, i.e. thioacetamide along with silymarin, the liver architecture was similar to that observed in the control group. The extract alone treated group animals showed normal architecture of liver. In the present study the albino Wistar rat was administered to TAA (group II) results showed increased glucose content in liver tissue. When compared to control (group I). The group III and TAA along with *Anoectochilus elatus* and silymarin the recorded value of glucose level in the liver was decreased when compared with group II. But there values are near to normal and control. The decreased level of glycogen was observed in group II, when compared with group I (Control). In the group III and IV thioacetamide along with silymarin. *Anoectochilus elatus* administration the glycogen control was gradually recovered. While group V and VI *Anoectochilus elatus* and silymarin alone administered animals has not much affected.



**Kannaiyan Pugazhendy and Poochi Sasikala**

The protein content in the group II (TAA administered rat) shown decreased level when compared group I (controls). TAA along with *Anoectochilus elatus* and silymarin administrated rat recorded protein level gradually regained when compared with group II. While group V and VI and silymarin alone administered rat showed protein levels are increased. The TAA treated rat amino acid levels are increased in group II, when compared with group I. In the group III and IV TAA along with *Anoectochilus elatus* and silymarin administered rat recorded amino acid level reduced towards recovery. When are group V and VI *Anoectochilus elatus* and silymarin administered rat shown the normal level of amino acid (table 4). The superoxide dismutase (SOD) activity in the liver of Albino wistar after TAA administered was reduced in the Group II compared with the control group I while in the rat administered to TAA along with *Anoectochilus elatus* (group III and group IV) was increased when compared with group II while extract of *Anoectochilus elatus* and silymarin alone administered in (group V and VI respectably), the SOD activity was increased than the group III and it was near to control group the recorded SOD activity in liver tissue for all the six groups were statistically significant at 1% and 5% level (table 5).

In the present observation showed that the CAT activity in the liver of Albino wistar rat after TAA administered was reduced in the group II when compared with the control group I. While in the rat administered to TAA along with *Anoectochilus elatus* administered group V and VI the CAT activity was increased than in group III the CAT activity was increased than in group III and was near to control group. The glutathione peroxide (GPx) and reduced glutathione (GSH) activity in the liver of Albino Wistar rat after TAA administered was reduced in the group II when compared to group I (control). While in the rat administered to TAA along with *Anoectochilus elatus* extract in group III was significantly increased when compared with group II. While observed in group V and VI the GPx and GSH activity was increased then in group III and it was near to normal group I. The aspartate aminotransferase (AST) and alaine aminotransfrace (ALT) activity in the liver of rat after TAA administered was significantly decreased when compared to control (group I). While TAA along with *Anoectochilus elatus* extract group III rat was significantly increased when compared with group II when an extract of *Anoectochilus elatus* and silymarin alone administered group V and VI was increased than that of the treated group.

Liver is a major functional site to serve detoxification of toxic substances and xenobiotics. TAA is one of the hepatotoxic chemicals that could metabolize by Cytochrome 450 enzyme present in the liver (Kadir *et al.*, 2011; Spira and Raw, 2000). TAA induce the liver fibrosis and also cause by free radical mediate lipid peroxidation (Bruck *et al.*, 1999). In TAA inebriation, substances lead to liver fibrosis and popular degenerative nodule growth are associated with portal hypertension and hyperdynamic circulation characteristics of liver cirrhosis (Hori *et al.*, 1993). These proved the histopathological analysis and biochemical parameter (AST, ALT, APT, bilirubin and cholesterol) in plasma. Recently investigations have been shown that different types of natural products are a wide range of biochemical, physiological and pharmacological effects (Parveen *et al.*, 2011).

Consequently, the current study was undertaken by evaluate the effect of *Anoectochilus elatus* in rat at chronic liver disease in order to confirm that this plant bioactive compound of 4H-Pyran-4-One,2,3-Dihydro-3,5-Dihydroxy-6-Methyl does indeed have a preventive advantage in liver disease. In the present study, animals treated with 500 mg/kg of *Anoectochilus elatus* methanolic extract exhibited a hepatoprotective effect comparable to those treated with 25 mg/kg of Silymarin in TAA induced liver injury. Treatment with *Anoectochilus elatus* methanolic extract at 250 and 500 mg/kg body weight restore the biochemical parameters (AST, ALT, APT, bilirubin and cholesterol) towards normal. This result comparable for thioacetamide is a classic hepatotoxic reagent used for liver cirrhosis induction (Najmeh Kabiri *et al.*, 2013). The previous studies observed *in vivo* that the antioxidant enzymes were depleted by a chronic ethanol administration (Ahmed *et al.*, 2016). Alkaline phosphatase is a transpeptidase that increases in bone and liver diseases. Lot of studies have mentioned that the presence of phenolic compounds in medicinal plants can prevent the toxic effect on the liver and the result in lessening of glutamic pyruvic transaminase and alkaline phosphatase release into blood (Khaksar *et al.*, 2017) has been recorded that the melatonin reduce the increased level of lipid peroxidation and transaminase activity in fluoxetine administered rat ($p < 0.05$), and also showed the potential of fluoxetine I inducing leucopenia, thrombocytopenia, hypochromic and macrocytic anemia which are blunted by melatonin. Antioxidant enzyme performance in the liver tissue, including the superoxide dismutase (SOD), catalase



**Kannaiyan Pugazhendy and Poochi Sasikala**

(CAT), glutathione peroxidase (GPx), were significantly decreased by a chronic ethanol management, whereas the hepatic lipid-peroxidase level was increased (Park *et al.*, 2017). In the present study, the observed protein levels are decreased in the group II, which might be due to their degradation along with utilization the metabolic activity. Digvijay *et al.*, (2004) have been reported that the depletion of protein level is due to necrosis of cells and also leads to impairment in the protein synthesis. The level of protein is based on the rate of synthesis and rate of degradation. The amount of protein also might be impacted on incorporation of amino acids converted into polypeptide chains (Revathi *et al.*, 2015). Depletion of protein levels may be leading to increasing the amino acids in the liver tissue. Some of the functions like role of acid base balance maintenance and the amino acid accumulation and also due to toxic stress could be induced elevation in the transaminases pathway (Revathi *et al.*, 2015). The aminotransminase involves between protein and carbohydrate metabolism, which is inter converting into α -ketoglutarate, pyruvate oxaloacetate as metabolites and also from alanin, aspartate and glutamate (Prabakaran *et al.*, 2014).

In the present study methanolic extracts of *Anoectochilus elatus* leaves were evaluated for the hepatoprotective activity using hepatotoxicity induced by thioacetamide in a rat model and find out the therapeutically better methanolic extract. An attempt has been made to find out the correlation between antioxidant and hepatoprotective activity. A major defense mechanism involves the antioxidant enzymes, including SOD, CAT, GSH, LPO and GPx, which convert active oxygen molecules into non toxic compounds (Pugazhendy *et al.*, 2015). The LPO is accelerated when free radicals are formed as the results of losing a hydrogen atom from the double bond in the structure of unsaturated fatty acid. Scavenging of free radicals is one of the major antioxidation mechanisms to inhibit the chain reaction of lipid peroxidation (Matsubara *et al.*, 1991).

The scavenging of DPPH radical is related to the inhibition of lipid peroxidation Ratty and Das (1988). Simultaneously the hepatoprotective effects of extract *Anoectochilus elatus* leaves were compared with silymarin. In vivo antioxidant activity was assayed by estimation of GSH, SOD, CAT, LPO, GPx levels. The increase in protease activity under stress conditions clearly suggests that TAA induces high protease activity which leads to the formation of higher free amino acid content which is in agreement with (Dashti *et al.*, 1989). The histopathological studies of the liver tissue also evidenced the hepatic lesions caused by the effect of silymarin and thioacetamide efficacy of the drugs by controlling the toxic effect of TAA which caused peroxidative degradation in the adipose tissue and as a fatty infiltration occurred in the hepatocytes. The increase in the levels of serum bilirubin transaminases and alkaline phosphatases was the clear indication of cellular leakage and loss of functional integrity of the cell membrane.

Histological profile of the control animals showed normal showed normal hepatocytes. The sections of the animals treated with TAA exhibited severe intense centrilobular necrosis and vacuolization and macrovesicular fatty change. The sections of liver taken from the animals treated with standard drug silymarin showed the hepatic architecture which was similar to that observed in the vehicle control. Treatment with the methanol extract gave significant protection to the hepatocytes against TAA damage. While thioacetamide extract was devoid any of hepatoprotective activity. The earlier investigators (Ilavarasan *et al.*, 2001) have studied the histopathological architect of the liver tissue and showed the hepatoprotective effect of *Anoectochilus elatus* leaf extract respectively. In the present investigation the, glycogen content was gradually decreased in treating rat. The presence of valuable active compound 4H-Pyran-4-One, 2,3-Dihydro-3,5-Dihydroxy-6-Methyl in the plant *Anoectochilus elatus* involves as an electron donor for various enzymes. Whereas, the TAA along with the plant extract group also enhances the glycogen content very slowly than the treated Group II.

In the present observation, reduction of glycogen content in Group II. But in the Group III and IV, the glycogen content was gradually increased when compared to the Group II. This might be due to the presence of valuable bioactive compounds of 4H-Pyran-4-One, 2, 3-Dihydro-3, 5-Dihydroxy-6-Methyl and fatty acid, stearic acid and linolenic acid in the experimental plant *Anoectochilus elatus*. The phytochemical investigations of *Anoectochilus elatus* recorded the presence compound and the leaves were strongly positive group in alkaloids, flavonoids, saponins, tri-



**Kannaiyan Pugazhendy and Poochi Sasikala**

terpenoids, anthraquinones, phenol, carbohydrate and phytoosteroids. In the presence of bioactive compounds in the *Anoectochilus elatus* which may act and give recovery to rat in the TAA toxic stress.

CONCLUSION

The present investigations provide informative evidence that *Anoectochilus elatus* has high protective effect of liver toxicity induced by TAA as proven by microscopical, biochemical and enzymological analysis. The effect of *Anoectochilus elatus* is compared to that of Silymarin as an antidote, the plant *Anoectochilus elatus* possesses potential active compound 4H-Pyran-4-One, 2, 3-Dihydro-3,5-Dihydroxy-6-Methyl to cure and protection measures. Accordingly, *Anoectochilus elatus* could be used as an effect herbal medicinal product for the prevention of chemical-induced hepatic damage. In the near future, a further study is essential to isolate and characterize the valuable other bioactive compounds present in the plant *Anoectochilus elatus*.

ACKNOWLEDGEMENT

The authors are grateful to University Grant Commission., New Delhi to provide funds to conduct the project successfully. Heart full thanks are recorded to Professor & Head, Department of Zoology, Annamalai University, Chidambaram, Tamilnadu India for providing necessary facilities in the department to complete the project.

REFERENCES

1. Ahmed, M.M., Rosmarinic acid attenuates the hepatotoxicity induced by ethanol in rats. *Am. J. Biochem.* 2016; 6: 82–90.
2. Alshawsh MA, Abdulla MA, Ismail S, and Amin ZA, "Hepatoprotective effects of *Orthosiphon stamineus* extract on thioacetamide-induced liver cirrhosis in rats," *Evidence-Based Complementary and Alternative Medicine*, 2011.
3. Bruck R, Aeed H, Shirin H, et al. The hydroxyl radical scavengers dimethylsulfoxide and dimethylthiourea protect rats against thioacetamide-induced fulminant hepatic failure," *Journal of Hepatology*. 1999; 31(1): 27–38.
4. Dashti H, Jeppson B, Haggerstrand I, et al. Thioacetamide- and carbon tetrachloride-induced liver cirrhosis. *Eur Surg Res.* 1989; 21: 83-91.
5. Digvijay S, Shashi PR, Suchi S, Kumar RS, Raghavendra M, & Sushil K. Simultaneous quantification of some pharmaceutical *Catharanthus roseus* leaf and root terpenoid indole alkaloids and their precursors in single runs by reversed-phase liquid chromatography. *Journal of AOAC International*. 2004; 87(6), 1287-1296.
6. French SW, Lee J, Zhong J, Morgan TR, Buslon V, Lungo W, et al. Alcoholic liver disease-Hepatocellular carcinoma transformation. *Journal of gastrointestinal oncology*. 2012; 3(3): 174-81.
7. Gebreyohannes, G., Moges, F., Sahile, S., & Raja, N. (2013). Isolation and characterization of potential antibiotic producing actinomycetes from water and sediments of Lake Tana, Ethiopia. *Asian pacific journal of Tropical biomedicine*, 3(6), 426-435.
8. Hajovsky H, Hu G, Koen Y, Sarma D, Cui W, Moore DS, et al. Metabolism and toxicity of thioacetamide and thioacetamide S-oxide in rat hepatocytes. *Chemical research in toxicology*. 2012; 25(9):1955-63.
9. Ilavarasan, R., Mohideen, S., Vijayalakshmi, M., & Manonmani, G. (2001). Hepatoprotective effect of *Cassia angustifolia* Vahl. *Indian journal of pharmaceutical sciences*, 63(6), 504.
10. Jaeschke H, Williams CD, McGill MR, Xie Y, Ramachandran A. Models of drug-induced liver injury for evaluation of phytotherapeutics and other natural products. *Food and chemical toxicology: an international journal published for the British Industrial Biological Research Association*. 2013;55: 279-89.
11. Kadir FA, Othman F, Abdulla MA, Hussan F, and Hassandarvish P. "Effect of *Tinospora crispa* on thioacetamide-induced liver cirrhosis in rats," *Indian Journal of Pharmacology*. 2011; 43: 64–68.





Kannaiyan Pugazhendy and Poochi Sasikala

12. Khaksar M, Oryan A, Sayyari M, Rezaabakhsh A, Rahbarghazi R. Protective effects of melatonin on long-term administration of fluoxetine in rats. *Experimental and Toxicologic Pathology*. 2017; 69: 564-574.
13. Kiran HS, Ravikumar YS, Thippeswamy T, Kirushnan BB, Thyrotoxicosis induced liver disease: a case report. *Journal of the Indian Medical Association*. 2012;110: 576-577.
14. Lillie, R. J., & Denton, C. A. (1965). Protein and energy interrelationships for laying hens. *Poultry science*, 44(3), 753-761.
15. Low TY, Leow CK, Salto-Tellez M, Chung MC. A proteomic analysis of thioacetamide-induced hepatotoxicity and cirrhosis in rat livers. *Proteomics*. 2004; 4: 3960-3974.
16. Lowry OH, Rosebrough NJ, Far, AL, & Randall RJ. Protein measurement with the Folin phenol reagent. *Journal of biological chemistry*. 1951;193: 265-275.
17. Matsubara, M., Girard, M. T., Kublin, C. L., Cintron, C., & Fini, M. E. (1991). Differential roles for two gelatinolytic enzymes of the matrix metalloproteinase family in the remodelling cornea. *Developmental biology*, 147(2), 425-439.
18. Misra, H. P., & Fridovich, I. (1972). The role of superoxide anion in the autoxidation of epinephrine and a simple assay for superoxide dismutase. *Journal of Biological chemistry*, 247(10), 3170-3175.
19. Muller A, Machnik, F, Zimmermann T, and Schubert H. "Thioacetamide-induced cirrhosis-like liver lesions in rats usefulness and reliability of this animal model," *Experimental Pathology*. 1988; 34: 229-236.
20. Najmeh, Kabiri, Mahbubeh Setorki, Mahboobeh Ahangar Darabi. Protective Effects of *Kombucha tea* and Silimarin Against Thioacetamide Induced Hepatic Injuries in Wistar Rats. *World Applied Sciences Journal*. 2013; 27: 524-532.
21. Niehaus, W. G., & Samuelson, B. (1968). Formation of malondialdehyde from and glucose 6-phosphate dehydrogenase from fermenting yeast and phospholipids arachidonate during microsomal lipid peroxidation. *Eur J Biochem*, 6, 126-30.
22. Njouendou AJ, Nkeng-Efouet AP, Assob Nguedia JC, Chouna JR, Veerapur V, Thippeswamy BS, Badami S, Wanji S. Protective effect of *Autranella congolensis* and *Sapium ellipticum* stem bark extracts against hepatotoxicity induced by thioacetamide. *Pharmacology Online*. 2014; 2: 38-47.
23. Park SY, Ahn G, Um JH, Han EJ, Ahn CB, Yoon NY, Je JY. Hepatoprotective effect of chitosan-caffeic acid conjugate against ethanol treated mice. *Experimental and Toxicologic Pathology*. 2017; 69: 618-624.
24. R, Baboota S, Ali J, Ahuja A, Vasudev SS, and Ahmad S. "Effects of silymarin nanoemulsion against carbon tetrachloride-induced hepatic damage," *Archives of Pharmacal Research*. 2011;34(5):767-774.
25. Prabakaran S, Pugazhendy K, Revathi A, and Jayanthi. Hepatoprotective effect of *Pisonia alba* and *Cardiospermum halicacabum* in atrazine toxicity on LPO and some antioxidant activities in the liver tissue of fresh water fish *Labeo rohita*. *Int. J. Pharm. Biol*. 2014; 5: 1231-1237.
26. Pugazhendy K, Revathi A, Prabakaran S, Murugan K, and Jiang-Shiou Hwang. Convalescence consequence of *Pisonia alba* and *Cardiospermum halicacabum* aligned with the atrazine intoxicated on antioxidant enzymes and histological changes in liver tissue of *rattus norvegicus*. *International Journal of Advanced Life Science*. 2015;8: 10-19.
27. Ratty, A. K., & Das, N. P. (1988). Effects of flavonoids on nonenzymatic lipid peroxidation: structure-activity relationship. *Biochemical medicine and metabolic biology*, 39(1), 69-79.
28. Revathi A, Pugazhendy K, Jayanthi C, Sakthidasan V, Tamizhazhagan V. Therapeutic efficacy of *Pisonia alba* Against atrazine toxicity on biochemical parameters in the liver tissue of *albino wistar rat Rattus norvegicus*. 2015; 1: 358-364.
29. Sanghvi MM, Hotez PJ, Fenwick A. Neglected tropical diseases as a cause of chronic liver disease: the case of Schistosomiasis and Hepatitis C Co-infections in Egypt. *Liver international: official journal of the International Association for the Study of the Liver*. 2013;33:165-168.
30. Simpleton, J. W. Summers, R. W., Switz, D. M., Sessions, J. T., Bethal, J. M., Best, W. R., Rern, F., & (1979). National cooperative cardiac disease study. *Gastroenterology*, 77, 887-97.
31. Tamizhazhagan V, Pugazhendy K, Sakthidasan V, Jayanthi C, (2017). Preliminary screening of phytochemical evaluation selected plant of *Pisonia alba*. *International Journal of Biology Research*, 2(4), 63-66.





Kannaiyan Pugazhendy and Poochi Sasikala

32. Spira B, and Raw I. "The effect of thioacetamide on the activity and expression of cytosolic rat liver glutathione-S-transferase," *Molecular and Cellular Biochemistry*. 2000; 211:103– 110.
33. Sunderman FW. Association of Clinical Scientists. Laboratory diagnosis of liver diseases. St. Louis. W.H. Green. 1968.
34. Ward FM, Daly MJ. Hepatic disease. In: Walker R, Edwards C, editors. *Clinical Pharmacy and Therapeutics*. New York, NY, USA: Churchill Livingstone. 1999:195-212.

Table 1. Phytochemical screening of plant extract of *Anoectochilus elatus* leaf extracts

S. No	Phyto constituents	methanol	ethyl acetate	acetone	benzene
1	Alkaloids	+	+++	+	--
2	Flavonoids	+++	++	--	+
3	Saponins	++	--	--	+
4	Steroids	+	++	++	+
5	Tannins	++	+++	+	--
6	Terpenoids	--	+	--	+
7	Tri-terpenoids	++	+++	++	+
8	Anthraquinones	++	+	--	+
9	Amino acid	--	--	--	--
10	Phenol	++	+	++	--
11	Glycosides	--	--	--	--
12	Carbohydrate	+++	+	+	--
13	Protein	--	+	--	+
14	Phytosteroids	++	+++	+	+

"+++" Strongly positive phytochemical group, "++" Positive phytochemical group, "+" Trace phytochemical group, "--" Absence of phytochemical group

Table 2. Effect of TAA, SY and methanolic extract of the Leaf of *Anoectochilus elatus* on liver function test

Groups	AST (U/L)	ALT (U/L)	ALP (U/L)	Bilirubin (mg/dl)	Cholesterol (mg/dl)
Control	64.60±3.23	40.68±3.24	145.00±7.44	0.80 ± 0.03 ^a	82.67 ± 4.18 ^a
Thioacetamide (600 mg/kg)	183.45±7.33	135.23±4.46	449.33±5.52	3.42 ± 0.13 ^d	148.00 ± 7.42 ^e
Thioacetamide + <i>Anoectochilus elatus</i> (250 mg/kg)	82.98±4.97	59.83±2.92	208.00±9.16	1.38 ± 0.08 ^c	112.33 ± 9.28 ^d
Thioacetamide + <i>Anoectochilus elatus</i> (500 mg/kg)	74.25±3.71	47.22±4.12	185.83±8.38	1.20 ± 0.04 ^b	92.00 ± 5.13 ^b
Thioacetamide + silymarin (25 mg/kg)	77.53±4.65	49.50±3.38	198.66±4.64	1.28 ± 0.08 ^{bc}	97.33 ± 4.95 ^c
<i>Anoectochilus elatus</i> (500 mg/kg) alone	64.35±5.14	40.00±2.96	142.50±6.98	1.79 ± 0.06 ^a	82.66 ± 5.36 ^a

Data represent the mean ± standard error of animals (n = 6 in each group). Figures in parenthesis indicate percent reduction in individual biochemical parameters from their elevated value caused by the hepatotoxin. All values were significantly different p < 0.05.





Kannaiyan Pugazhendy and Poochi Sasikala

Table 3. Organ weights of control rats and thioacetamide with methanolic extract of *Anoectochilus elatus* leaf measured during acute toxicity study

Groups	Body weight (g)		Liver weight (g)
	Initial	Final	
Control	185 ± 4.62	215 ± 6.36	6.52 ± 0.12
Thioacetamide (600 mg/kg)	180 ± 9.72	158 ± 4.22 ^b	7.35 ± 0.36 ^b
Thioacetamide + <i>Anoectochilus elatus</i> (250 mg/kg)	192 ± 5.46	209 ± 7.42 ^e	6.95 ± 0.42 ^e
Thioacetamide + <i>Anoectochilus elatus</i> (500 mg/kg)	183 ± 3.94	215 ± 5.84 ^c	6.64 ± 0.18 ^c
Thioacetamide + silymarin (25 mg/kg)	190 ± 9.12	212 ± 5.28 ^d	6.70 ± 0.24 ^d
<i>Anoectochilus elatus</i> (500 mg/kg) alone	187 ± 8.55	222 ± 9.45 ^a	6.45 ± 0.11 ^a

Values are expressed as mean ± standard error, n= 6. Values were significantly different p <0.05.

Table 4. Changes of biochemical parameters of *Anoectochilus elatus* and Silymarin administered rat against TAA induced hepato toxicity

Groups	Treatment	Glucose (U/L)	Glycogen (U/L)	protein(U/L)	Amino acid (mg/dl)
Group I	Control	0.497 ± 0.024	49.36 ± 3.45	36.77 ± 1.13	0.632 ± 0.04
Group II	Thioacetamide (600 mg/kg)	0.467 ^{NS} ± 0.023	38.19* ± 1.90	32.50** ± 1.15	0.902** ± 0.04
	% changes over group I	6.04	22.62	11.61	42.72
Group III	Thioacetamide + <i>Anoectochilus elatus</i> (250 mg/kg)	0.437 [*] ± 0.026	45.18 ^{NS} ± 2.70	30.45 ^{NS} ± 2.07	0.941** ± 0.05
	% changes over group I	12.72	8.46	17.18	-48.89
	% changes over group II	6.42	18.30	6.30	4.32
Group IV	Thioacetamide + <i>Anoectochilus elatus</i> (500 mg/kg)	0.446 ± 0.032	47.34 ± 1.56	31.57 ± 1.77	0.851 ± 0.06
	% changes over group I	-10.26	4.26	-14.14	34.65
	% changes over group II	-4.49	23.95	-2.02	-5.65
Group V	Thioacetamide + silymarin (25 mg/kg)	0.793 ± 0.41	47.67 ± 1.35	34.67 ± 1.86	0.765 ± 0.072
	% changes over group I	+59.55	3.54	5.71	21.44
	% changes over group I	69.80	24.82	6.67	15.18
Group VI	<i>Anoectochilus elatus</i> (500 mg/kg) alone	0.482 ^{NS} ± 0.03	46.77 ^{NS} ± 3.26	38.40 ^{NS} ± 0.86	0.505 ^{**} ± 0.03
	% changes over group I	3.02	5.24	4.43	20.56
	% changes over group II	3.21	22.46	18.15	44.13

Values are expressed as mean ± standard error, n= 6. Values were significantly different p <0.05.





Kannaiyan Pugazhendy and Poochi Sasikala

Table 5. Variation of Enzymological parameters of *Anoectochilus elatus* and Silymarin administered Albino wistar rat t against TAA induced hepato toxicity

Groups	Treatment	SOD (U/L)	CAT (U/L)	LPO (U/L)	GSH (mg/dl)	GPX (mg/dl)
Group I	Control	46.163 ± 0.01	11.251 ± 0.11	12.850 ± 0.04	0.227 ± 0.02	2.363 ± 0.11
Group II	Thioacetamide (600 mg/kg)	31.635 ± 0.01**	8.153 ± 0.12**	16.764 ± 0.04*	0.164 ± 0.02**	3.458 ± 0.15**
		- 31.49	- 27.53	+30.45	- 27.51	+ 46.33
Group III	Thioacetamide + <i>Anoectochilus elatus</i> (250 mg/kg)	42.115 ± 0.15*	9.863 ± 0.07**	14.556 ± 0.09**	0.199 ± 0.03*	2.512 ± 0.10**
		- 8.76	- 12.33	+13.27	- 12.33	+ 6.30
		+ 33.12	+ 20.97	+ 13.17	+ 27.43	- 27.35
Group IV	Thioacetamide + <i>Anoectochilus elatus</i> (500 mg/kg)	43.61±2.18	9.956±0.497	14.75±0.73	0.197±0.009	2.655±0.12
		-5.53	-11.51	14.78	-13.21	12.35
		-8.07	22.11	-12.01	20.12	-23.22
Group V	Thioacetamide + silymarin (25 mg/kg)	44.61±2.23	9.891±0.49	13.67±0.68	0.199±0.009	2.453±0.12
		-3.36	-12.08	6.38	-12.33	3.80
		41.01	21.31	-18.45	21.34	-29.06
Group VI	<i>Anoectochilus elatus</i> (500 mg/kg) alone	46.310 ± 0.04	11.311 ± 0.12	12.872 ± 0.01	0.230 ± 0.02	2.373 ± 0.18
		+ 0.31	+ 0.53	+ 0.17	+ 1.32	+ 0.42
		46.38	38.73	23.21	40.24	31.37

Values are expressed as mean ± standard error, n= 6. Values were significantly different p <0.05.





Anti-Diabetic Activity of Chelating Bis N- Propylethylenediamine Zinc Complex

M. Jaya Brabha¹ and M. Anitha Malbi^{2*}

¹Research Scholar (Reg.No: 18123042032015), Department of Chemistry, Holy Cross College, Nagercoil, Affiliated to Manonmaniam Sundaranar University, Tirunelveli, Tamil Nadu, India.

²Assistant Professor, Department of Chemistry, Holy Cross College, Nagercoil, Affiliated to Manonmaniam Sundaranar University, Tirunelveli, Tamil Nadu, India.

Received: 26 Sep 2021

Revised: 12 Oct 2021

Accepted: 30 Oct 2021

*Address for Correspondence

M. Anitha Malbi

Assistant Professor,
Department of Chemistry,
Holy Cross College, Nagercoil,
Affiliated to Manonmaniam Sundaranar University,
Tirunelveli, Tamil Nadu, India.
Email: anithamalbi@holycrossngl.edu



This is an Open Access Journal / article distributed under the terms of the **Creative Commons Attribution License** (CC BY-NC-ND 3.0) which permits unrestricted use, distribution, and reproduction in any medium, provided the original work is properly cited. All rights reserved.

ABSTRACT

Metals are an integral part of many structural and functional components in the body, and the critical role of metals in physiological and pathological processes has always been of interest to researchers. Metals have been used in the treatment of diseases of humans since ancient time. The primary objective of the study was to describe anti-diabetic activity by bis N-propylethylenediamine zinc (II) complex. The synthesised complex was characterised by elemental analysis, FTIR, powder X-ray diffraction and EDAX. Stability of the complex was determined by TGA & DTA. Anti-Diabetic activity was studied by invitro alpha glucosidase and alpha amylase assay.

Keywords: Chelate complex, Charge Transfer Transition, Thermal analysis, Co-ordination Compound, Alpha glucosidase and Alpha amylase

INTRODUCTION

It is also known as simply diabetes, is a group of metabolic diseases in which there are high blood sugar levels over a prolonged period. This high blood sugar produces the symptoms of frequent urination, increased thirst, and increased hunger. The common symptom of diabetes includes poly urea (frequent urination), polydipsia (increased thirst) and poly phagia (increased appetite). [1] Diabetes is due to either the pancreas not producing enough insulin, or the cells of the body not responding properly to the insulin produced. [2] Metal complexes are playing an

38947



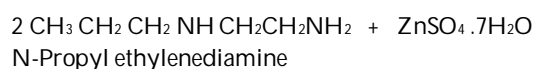


Jaya Brabha and Anitha Malbi

important role in pharmaceutical field, catalyst in chemical industries, material synthesis and photochemistry. Bioinorganic chemistry can exploit the unique properties of metal ions for the design of new drugs. Research has shown significant progress in utilization of transition metal complexes as drugs to treat several human diseases. Transition metals exhibit different oxidation states and can interact with a number of negatively charged molecules. This activity of transition metals has started the development of metal based drugs with promising pharmacological application and may offer unique therapeutic opportunities

MATERIALS AND METHODS

The chelating complex bis N-propylethylenediamine Zn (II) was prepared from zinc sulphate hepta hydrate and N-propylethylenediamine. 2 mM aqueous solution of metal salt was taken in a beaker and 6 mM of N-propylethylenediamine was added drop by drop. With order to get proper mixing continuous stirring for an hour, 2 ml of ethyl alcohol was added for complete precipitation then transferred into a Petri dish to remove solvent in hot air oven at 45°C. After 3 days, white-coloured bis N-propylethylenediamine Zn (II) complex was formed. [3]



ELEMENTAR Vario EL III is used as CHNS analyser. Precision >0.1%abs, Auto sampler, Ultra microbalance Analysis time is automatically optimized. FTIR spectrometer model Thermo Nicolet Avtar 370 DTGS, Range: 4000- 400 cm⁻¹ Perkin Elmer STA 600 is used as thermo gravimetric analyzer. TG Sensitivity: 200 mg , DTA Sensitivity: +1000μV, temperature range: Ambient to 1200 °C. Model of X-ray diffraction is Bruker AXS D8 Advance, Maximum usable angular range:30 to 1350, using Diffraction plus software,Wavelength:1.5406Å° EDAS allows the elemental composition of the specimen to be measured. Jeol 6390 LA / OXFORD XMXN is used as spectrometer, resolution 136 eV and acceleration voltage 0.5 to 30 kV. Alpha glucosidase activity was measured by the determination of reducing sugar arise from hydrolysis of sucrose by alpha glucosidase enzyme. Acarbose drug (10mg/mL DMSO) was used as reference. The reducing sugars produced by the action of α amylase react with dinitrosalicylic acid and reduce it to a brown coloured product, nitro amino salicylic acid. Acarbose drug (10mg/mL DMSO) was used as reference. All the characterizations were taken at SAIF Cochin.

RESULT AND DISCUSSION

Elemental Analysis

The empirical formula and possible geometry of the complex is confirmed by elemental analysis. The analytical data (Table.1) suggest that the chelating complex is mono nuclear with the ligand coordinated to the central metal atom. The metal to ligand ratio of N-propylethylenediamine zinc (II) complex is 1:2 with empirical formula ZnN₄C₁₀H₂₈SO₄. The N-propyl ethylenediamine Zn (II) complex exhibits as square planar complex. The observed and calculated values of the percentage of elements are well agreed with each other. [4]



**Jaya Brabha and Anitha Malbi****FT-IR SPECTROSCOPY**

In order to study the bonding of the ligand to the metal, the infrared spectrum of the ligands compared with spectra of the corresponding metal chelates. The infrared spectra provide valuable information regarding the nature of the bonding attached to the metal ion. [6]. The ligand N-propylethylenediamine (Fig.3 & 4) exhibits N-H stretching frequency at 3287 cm^{-1} , the aliphatic amine of C-H stretching frequency at 2953 cm^{-1} and C-N stretching frequency at 1377 cm^{-1} . The chelating bis N-propylethylenediamine Zn (II) complex shows that, (Table 3) the N-H stretching frequency at 3308 cm^{-1} , the aliphatic amine of C-H stretching frequency at 2932 cm^{-1} and C-N stretching frequency at 1357 cm^{-1} and M-N stretching frequency at 510 cm^{-1} . The free ligand with stretching frequency is greater than the corresponding metal complex. It is due to the electron flow from the ligand to the metal (CTT). The stretching frequency $\nu_{\text{C-N}}$ constantly decreases in the metal complex compared with free N-propylethylenediamine. It is evident that the ligand surely co-ordinated with the ligand. [5]

THERMAL ANALYSIS

The thermal behaviour of the synthesised chelating complexes are studied to establish different decomposition pattern and to confirm the proposed stoichiometry. The results are summarised in (Table 4) The chelating bis N-Propylethylenediamine zinc complex (Fig.5) exhibits four endothermic peaks. The complex is stable up to $218.13\text{ }^{\circ}\text{C}$. The ligand N-methyl ethylenediamine liberates at this temperature, by the loss of 30% weight. Upon increasing the temperature the two methylamine gets liberates at $338.87\text{ }^{\circ}\text{C}$ and $394.86\text{ }^{\circ}\text{C}$, by the loss of 10% weight respectively. At $660.25\text{ }^{\circ}\text{C}$ zinc sulphate dissociate into SO_3 and ZnO. Above the temperature stable metal oxide is appeared. The decomposition pattern of the chelating complex confirms the proposed stoichiometry and geometry. [7]

POWDER X-RAY DIFFRACTION STUDY

The X-Ray diffraction method is the most powerful technique available for the examination of complex in the solid state. X-Ray diffraction is used to obtain information about the structure and composition. Average crystalline sizes of the complex and hkl planes are given in the (Table 5). The XRD patterns of chelating bis N-propylethylenediamine Zn (II) complex is shown in (Fig.6). The chelating Zn (II) complex shows that the sharp peak at 8.433° , 15.307° and 17.016° . Which indicates the complex is high quality and polycrystalline in nature. It exhibits 100% intensity peak at 8.433° . The hkl plane of the complex is calculated by $\sin^2\theta$ method. The high intense peak with hkl planes are 8.433° (110), 15.307° (211) and 17.016° (111). The crystalline sizes are predicted for prominent peaks for the synthesised chelating complexes by using Debye-Scherrer's formula. The complex with average crystalline size is 80. [8]

ENERGY DISPERSIVE X-RAY ANALYSIS

EDX Spectroscopy used for elemental identification by measuring the number and energy of x-rays emitted from a specimen after excitation with an electron beam. The elemental percentage is shown in (Table. 6). Metal complex with their elements are shown in (Fig.7). Bis N-propylethylenediamine zinc complex exhibits the weight percentage of carbon is 33.26%. This is well agreed the percentage of carbon obtained from CHNS analyser 32.80%. The weight percentage of nitrogen is 15.45%, which is well agreed with the percentage of nitrogen observed from CHNS analyser 15.35%. The weight percentage of sulphur is 8.78%, which is agreed with the percentage of sulphur observed from CHNS analyser 9.78%. The weight percentage of zinc is 18.92%, which is well agreed with the percentage of zinc obtained from calculated 17.87%. All these data further prove the square planar geometry of this complex. [9]

In-vitro ANTI-DIABETIC ACTIVITY OF METAL COMPLEXES

Diabetes is characterized by hyperglycemia, altered lipids, carbohydrates, and proteins metabolism which affect the patient quality of life in terms of social, psychological well- being as well as physical ill health [10]. Two forms of diabetes (Types 1 and 2) differ in their pathogenesis, but both have hyperglycemia as a common hall mark. In type 2





Jaya Brabha and Anitha Malbi

diabetes, hyperglycemia caused due to impairment in insulin secretion combined with or without impairment of insulin action [11].

In- vitro Alpha Glucosidase Inhibition Assay

Alpha glucosidase activity was measured by the determination of reducing sugar arise from hydrolysis of sucrose by alpha glucosidase enzyme. The effects of samples were assayed according to the method Matsui et al., with slight modifications. Acarbose drug (10mg/mL DMSO) was used as reference.

Procedure

Different volumes of sample such as 12.5µL-100µL from the stock solution given were taken and was incubated for five minutes before initiating the reaction with substrates sucrose(37mM), in a final reaction mixture of 1mL of 0.1 M phosphate buffer (pH 7.2). The reaction mixture was incubated for 20 and 30 min at 37°C and the reaction was stopped incubating in a boiling water bath for 2 minutes. A tube with phosphate buffer and enzyme was maintained as control. The tubes were added with 250µL of glucose reagent and incubated for 10 minutes followed by measuring absorbance at 510nm using a micro plate reader.

Calculation

$$\% \text{ inhibition} = \frac{\text{control} - \text{test}}{\text{control}} \times 100$$

In vitro Alpha Amylase Inhibitory Assay

The reducing sugars produced by the action of α amylase react with dinitrosalicylic acid and reduce it to a brown coloured product, nitro amino salicylic acid. Acarbose drug (10mg/mL DMSO) was used as reference.

Procedure

Different volumes of sample such as 12.5µL - 100µL from the stock solution given and make up to 1000µl using 25mM phosphate buffer pH 6.9, containing 25µl of porcine α amylase at a concentration of 0.5 mg/ml were incubated at 25°C for 10 min. After pre incubation, 25µl of 0.5% starch solution in 25mM phosphate buffer pH 6.9 was added. The reaction mixtures were then incubated at 25°C for 10 min. The reaction was stopped with 50µl of 96mM 3, 5 dinitro salicylic acid colour reagent. The micro plate was then incubated in a boiling water bath for 5 min and cooled to room temperature. Absorbance was measured at 540nm using a microplate reader.

Calculation

$$\% \text{ inhibition} = \frac{\text{control} - \text{test}}{\text{control}} \times 100$$

The In vitro anti-diabetic study of metal complex is carried out by alpha glucosidase inhibition assay and alpha amylase inhibition assay. Chelating zinc complex exhibits greater anti- diabetic activity in both these assays than standard Acarbose. Zinc is a natural component of insulin, a substance crucial to the regulation of carbohydrate metabolism.

CONCLUSION

The synthesised Chelating complex bis N-propylethylenediamine Zn (II) complex exhibits as square planar geometry. The stretching frequency ν_{C-N} constantly decreases in the metal complex compared with free N-propylethylenediamine. It is evident that the ligand surely co-ordinated with the ligand. The complex is stable up to 218.13 °C. The decomposition pattern of the chelating complex confirms the proposed stoichiometry and geometry. The complex exhibits sharp peaks. It indicates the complex is high quality and polycrystalline in nature. It exhibits 100% intensity peak at 8.433°. The complex exhibits greater anti- diabetic activity in both alpha glucosidase and alpha amylase assays than standard Acarbose.





Jaya Brabha and Anitha Malbi

ACKNOWLEDGMENT

I gratitude almighty God for provide good health to do research. I thank SAIF STIC, Cochin, for taking characterisation.

REFERENCES

1. Inancli SS, Eyup Yayci and Tijen Atacag. (2016), Evaluation of Thyroid Autoimmunity in Gestational Diabetes Mellitus. *J Diabetes Metab* 7:682.
2. Bayramova AN. (2016), Gastroenterological Diseases as a Complications of Type 2 Diabetes Mellitus. *J Gastrointest Dig Syst.* 6:442.
3. Tripathi.I.P.* 2017, Aparna Dwivedi1 and Mahendra Mishra "Metal Based α -glucosidase Inhibitors: Synthesis, Characterization and α -glucosidase Inhibition Activity of Transition Metal Complexes" *Asian Journal of Medicine and Health*, 2(3): 1-14.
4. Kumari Sapna, Navin Kumar Sharma and Seema Kohil (2012), " Synthesis, characterisation and antimicrobial studies of copper (II) complexes of semicarbazone and thio semicarbazone of m- hydroxyl benzaldehyde and p- hydroxyl benzaldehyde", *Oriental Journal of Chemistry*, ISSN 0970-020 X. Vol. 28, No. (2):Pg. 969-974
5. Malathy. D and Vijayanthimala. R, (2015) "synthesis, characterisation and cytotoxic studies on transition metal complexes of penta methylene dithiocarbamate and diamines" *IOSR Journal of Applied Chemistry*, (2015), Volume 8, Issue 4 Ver. I., PP 52-59.
6. Mustafa Bal, Gokhan Okhan ceyhan, Baris Avar (2014) synthesis and x-ray powder di_raction, electrochemical, and genotoxic properties of a new azo-schi_ base and its metal complexes *Turkish Journal of Chemistry*, 38: 222 - 241
7. Lemos F. C. D, Marcia Muraro, Zukerman-Schpector. J, et al (2004) thermal decomposition of complexes manganese(ii) and vanadyl with cis- and iron(ii), manganese(ii) and vanadyl with trans-n,n'-bis(salicylidene)-1,2- cyclohexanediamine (salcn), *Journal of thermal analysis and calorimetry*, vol. 75 (2004) 599–606
8. Achut S. Munde1, Amarnath N. Jagdale , Sarika M. Jadhav3, (2010), "Synthesis, characterization and thermal study of some transition metal complexes of an asymmetrical tetradentate Schiff base ligand", *J. Serb. Chem. Soc.* 75 (3) 349–359.
9. Jagadish Tota, Haritha Mahajan, Sathyanarayanan Battu, Ballu Srilatha, et al, (2016), "Synthesis, characterisation, docking studies and biological activity of metal (II) complexes of Schiff base ligand derived from 4-chloro-2-benzothiazolamine and imidazole-2-carboxaldehyde", *IOSR Journal of Applied Chemistry*, Volume 9, Issue 6, PP 17-27
10. Dewanjee .S , Das. AK, Sahu. R and Gangopadhyay. M , (2009), Antidiabetic activity of Diospyros peregrina fruit: effect on hyperglycemia, hyperlipidemia and augmented oxidative stress in experimental type 2 diabetes. *Food and Chemical Toxicology*, 47: 2679–2685.
11. Lin. Y and Sun. Z, (2010) Current views on type 2 diabetes. *Journal of Endocrinology*, 204: 1–11.

Table.1 Elemental Analysis and physical parameters

Complex	Molecular Weight	Colour	pH	Molar Conductance	C % Obs. (Cal)	H % Obs. (Cal)	N % Obs. (Cal)	S % Obs. (Cal)
ZnN ₄ C ₁₀ H ₂₈ SO ₄	365.85	White	8.43	1.347	32.80 (32.83)	7.68 (7.73)	15.31 (15.35)	9.78 (8.76)





Jaya Brabha and Anitha Malbi

Table 2 Vibrational Frequencies of Ligand (pren) and Complexes

Ligand & Compound	Stretching VC-H	Stretching VN-H	Stretching VC-N	Stretching VM-N
CH ₃ CH ₂ CH ₂ NHCH ₂ CH ₂ NH ₂	2953	3287	1377	-
[Zn (pren) ₂] ²⁺	2932	3357	1308	510

Table 3 TGA and DTA of chelating N-propyl ethylenediamine complexes

Compound	Number of Endo peaks	T (°C)	Temp: Range (°C)	Wt. Loss % (Cal %)	Removed Fragments	Residue
[Zn(pren) ₂] SO ₄	I	219.30	200-260	28(27.89)	Pren	ZnO
	II	340.03	260-380	15(16.3)	CH ₃ CH ₂ CH ₂ NH ₂	
	III	394.86	380-450	8(8.47)	CH ₃ NH ₂	
	IV	661.41	450-700	16(15.69)	SO ₃	

Table 4 XRD data of bis N-propylethylenediamine zinc complex

Complex	2θ Angle (degree)	θ Radian	Sin θ	Sin ² θ	Ratio 1	Ratio 2	M	hkl	Average particle size D
[Zn (pren) ₂] ²⁺	8.433	0.07357	0.07350	0.005402	1	2	2	110	80
	15.307	0.1335	0.1313	0.01723	3.1895	6.379	6	211	
	17.016	0.1484	0.1478	0.02184	1.2675	2.535	3	111	

Table 5 EDAX Data

Complex	Element	Weight %	Atomic %
[Zn (CH ₃ CH ₂ CH ₂ NHCH ₂ CH ₂ NH ₂) ₂] SO ₄	C	33.26	48.17
	N	15.45	18.28
	O	23.59	24.22
	S	8.78	4.53
	Zn	18.92	4.8

Table.6 Anti-Diabetic Data (Alpha Glucosidase Inhibition Assay)

Sample concentration(µg/mL)	OD at 540nm	Percentage inhibition
Control	0.8714	0
Sample code: Acarbose Drug		
125	0.5124	42.51
250	0.4228	52.32
500	0.3442	61.20
1000	0.1956	72.86
Concentration(µL)		
Control	0.2519	0
Sample code: Zn(pren)₂		
12.5	0.1933	23.63
25	0.1652	37.24
50	0.1143	51.45
100	0.0894	63.57

IC50 Value- Acarbose- 269.77µg/mL(Calculated using ED50 PLUS V1.0 Software)

Zn- 43.3948µL(Calculated using ED50 PLUS V1.0 Software)





Table 7 Anti-Diabetic Data (Alpha Amylase Inhibition Assay)

Concentration($\mu\text{g/mL}$)	OD at 540nm	Percentage of inhibition
Control	0.1150	
Standard: Acarbose Drug		
125	0.0513	58.48
250	0.0519	60.56
500	0.0462	63.37
1000	0.0302	75.94
Concentration(μL)	OD at 540nm	Percentage inhibition
Control	0.7916	0
Sample code: Zn		
12.5	0.5172	36.83
25	0.4256	47.62
50	0.2734	65.54
100	0.1262	84.79

IC50 Value: Acarbose- 111.907 $\mu\text{g/mL}$ (Calculated using ED50 PLUS V 1.0 Software)

Zn- 38.2118 μL (Calculated using ED50 PLUS V 1.0 Software)

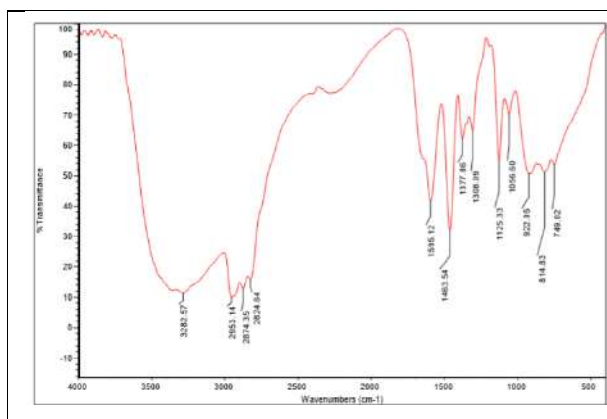


Fig.1.FT-IR Spectrum of N-propyl ethylenediamine (Ligand)

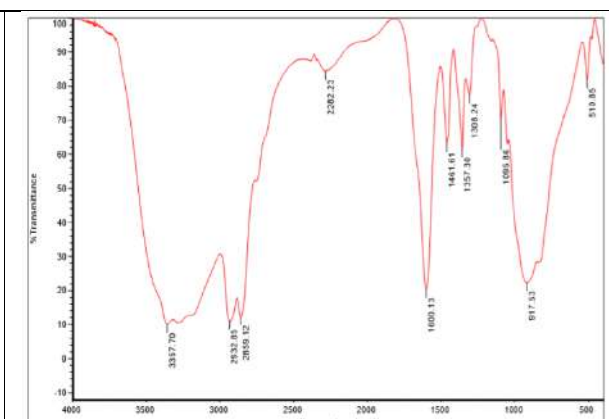


Fig.2.FT-IR Spectrum of [Zn (pren)₂]²⁺ Complex

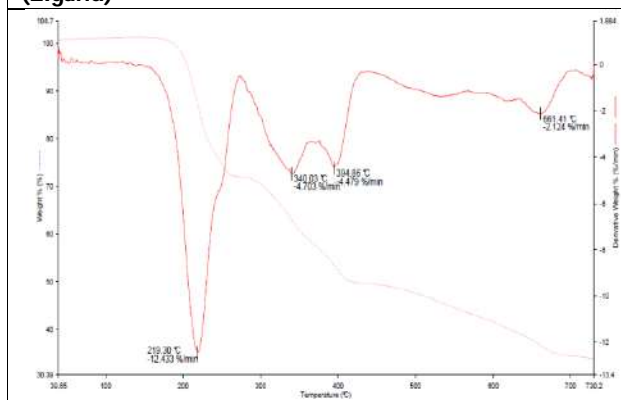


Fig.3. TGA & DTA Spectrum of [Zn (pren)₂]²⁺ Complex

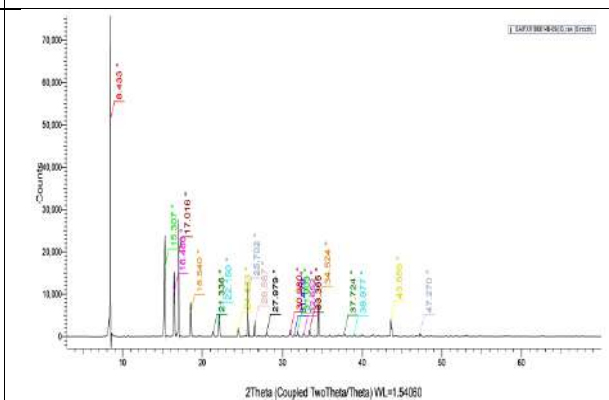


Fig.4. XRD Spectrum of [Zn (pren)₂]²⁺ Complex





Jaya Brabha and Anitha Malbi

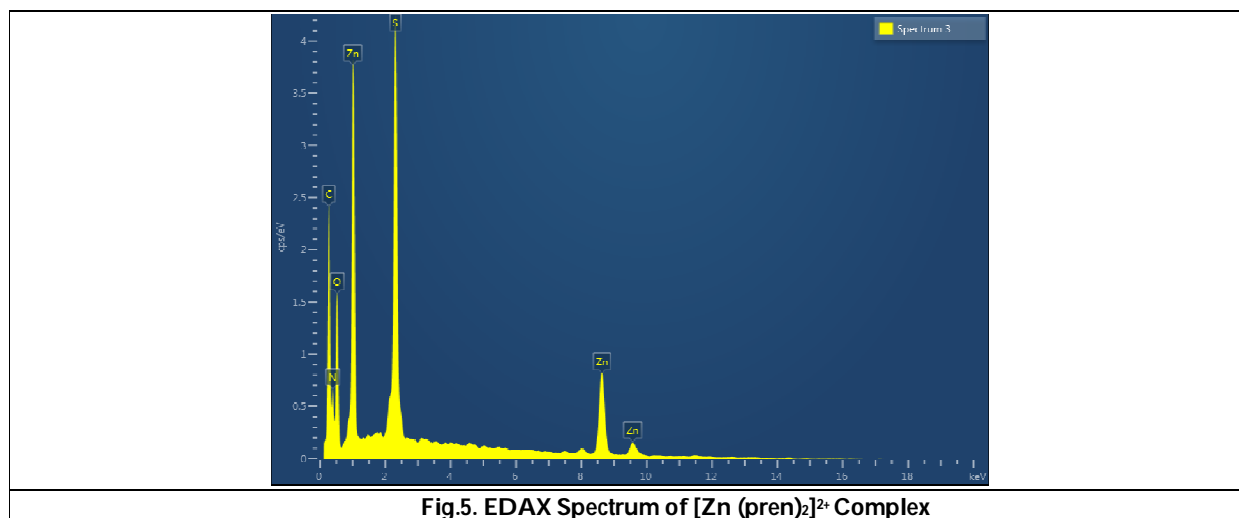


Fig.5. EDAX Spectrum of [Zn (pren)₂]²⁺ Complex





An Empirical Analysis of Machine Learning Classifiers for the Informative Tweets during Natural Disasters

Aarthi.E^{1*} and S.Sasikala²

¹Research Scholar, Department of Computer Science, IDE, University of Madras, Chennai, Tamil Nadu 600005, India.

²Associate Professor, Department of Computer Science, IDE, University of Madras, Chennai, Tamil Nadu 600005, India.

Received: 21 Nov 2021

Revised: 17 Dec 2021

Accepted: 12 Jan 2022

*Address for Correspondence

Aarthi.E

Research Scholar,
Department of Computer Science,
IDE, University of Madras,
Chennai, Tamil Nadu 600005, India.
Email: aarthie@srmist.edu.in



This is an Open Access Journal / article distributed under the terms of the **Creative Commons Attribution License** (CC BY-NC-ND 3.0) which permits unrestricted use, distribution, and reproduction in any medium, provided the original work is properly cited. All rights reserved.

ABSTRACT

The computing techniques and models are used for disaster identification, management and relief processes in the current era. The disaster relief activities are based on the collected data and how the same is applied on the selected models. The selection of significant model is one among the challenging process and is observed to be the thrust area of research. Therefore, model selection processes itself need a scientific approach based on the model performance measures. This study attempts to evaluate the machine learning supervised classifiers to identify disaster relevance features from the Online Social Network datasets that are very dynamic. The machine learning supervised classifiers such as Naïve Bayes (NB), Support Vector Machine(SVM), Logistic Regression(LR), Random Forest(RF) and Gradient Boosting(GB). This work is evaluated using Machine Learning performance measures which are accuracy, Precision, Recall and F1-Measure. The dataset is fetched from the tweets of Online Social Network. As per the implementation, both informative, non-informative binary classifier result showed that the gradient boosting performance (accuracy-93.5%) is significant while comparing with other classifiers. It is observed that the classifications are done based on the level of related information of the disaster. However, the identification of disaster related features using classifiers need to be enhanced using authenticated tweets with high performance classifier to support rescue operations during crisis.

Keywords: disaster, Machine Learning Classifiers, authenticity of tweets, relevance of tweets, Online Social Network (OSN), rescue operation.





INTRODUCTION

This research paper is aimed to select the significant classifier in order to identify the disaster relevant information by comparing the performances of existing classifiers which are Naïve Bayes [1], Support Vector Machine (SVM) [2], Logistic Regression (LR) [3], Random Forest (RF) [4] and Gradient Boosting (GB) [5]. The disaster relevant information is evaluated with the support of CrisisLexT26 tweets dataset with captured dynamic tweets by the researcher. The tweets are collected based on disaster hash tags extracted based on proposed method. The classified information aids to identify the relevance of disaster that facilitates the information to rescue teams to fast up relief activities. The classified information helps the rescue team to identify the location and type of disaster. Therefore an appropriate classifier is required to get very appropriate results.

The significant model is identified using varied *machine learning algorithms* and compares their performance on two different datasets. The study shows that the ensemble classifier gradient boosting with accuracy of (93.07%) outperforms the baseline classifier with the collected dataset using proposed technique. SVM gives better classification compare to the other three classifiers. This paper is organized as follows, section 2 presents the literature review. Section 3 contains the conceptual representation of supervised machine learning classifier algorithms. Section 4 shows the results of the selected classifier models performance and the last section, section 5 includes the conclusion of the study.

Review of Literature

This part of the paper described the various research work reviewed by the researcher to acquire the existing model details and are summarized. The Online Social Network (OSN) data used to predict and classify the required knowledge for decision making process in various filed including disaster management [6], it will ensure that the derived features and knowledge is trustworthy [7]. The disaster relevant information fetched from the Twitter platform contains relevant details about a natural disaster such as Wildfires, floods, hurricanes, and earthquakes, etc., [8, 9, 10, 11]. The research works [12] cover possible ways of collecting disaster-relevant data, predicting the insights from social media, and creating awareness among the media users. The role of social media as a helpful monitoring tool during natural disasters and other environmental concerns is studied [13]. In this research work, the data set is selected from CrisisLexT26 because the standard disaster datasets of tweets are suitable to evaluate the models. In addition to that, Twitter Application Program Interface (API) is used to collect the tweets based on keywords that may brief the geolocations and types of disasters. Crowd flower, the crowd sourcing platform is used to manually label the collected tweets based on the relevance (on-topic or off-topic).

Keyword processing is one of the authenticated process to extract tweets in real-time. So the disaster keyword list was collected to identify the disaster information. It is used for rescue actions [14]. At the same time, keyword list-based filtered tweets during a flood event were correlated with flooding levels. The voluminous of unrelated data using the keyword filtering method is a major disadvantage [15]. The collected tweets are classified as credible and non-credible information [1], applying the supervised classifiers such as Naive Bayes (NB) and Support Vector Machine (SVM) [3]. Naive Bayes classifier is a probabilistic learning algorithm which fixes the class of a document by computing the probability with respect to the evidence and occurrences found in the paper [5]. It aids in determining the relevance of disaster [16]. Naive Bayes, is frequently used as a baseline classifier in the text classification, with the assumption that features are independent, in this case the words are dependent. Each word has contributed the evidence individually [17]. Naive Bayes classifier is optimistic in dealing with small data sets [18].

The goal of Support Vector Machines (SVM), a large-margin classifier based on vector based machine learning method, is to find a decision boundary between two classes which are furthest from any point in the training [5]. The supervised machine learning classifiers SVM and NB were applied for sentiment prediction model which evaluated more than 21,000 tweets [19]. It is found that feature vectors were created to handle the problem of repeating characters in Twitter. With a higher accuracy of 75%, SVM outperforms NB with only 65% accuracy towards the



**Aarthi and Sasikala**

evaluation metrics, namely, Precision and Recall. In [20] proposed NB, SVM classifier used for travel blogs that results with an accuracy of 85.14% based on text classification. The [21] implemented SVM, NB, ME classifiers for customer reviews/feedbacks, the classification accuracy in terms of F1-Measure was 83% to 88%. One of the simplest classification algorithms is Logistic Regression, which has been addressed in most data mining domains. [23]. The tweets collected from 12 natural disasters were referenced to build a model with the LR classifier using the Unigram features [5] to determine infrastructural damage or human casualties.

The network based classifiers outperforms text based classifiers by achieving F1-Measure as 0.78 [24], using the model implemented to classify informative and non-informative tweets with unigram, bigram, POS as feature extraction methods for 2011 Tornado in Joplin, Missouri dataset. Tree-based classifiers such as Decision Tree and Random Forest were found to give better performance with respect to document categorization [25, 26]. The difficulty of model selection by evaluating the overall classification performance between RF and LR for the different datasets with various underlying structures such as increasing the number of observations, noise and explanatory variables also their variance showed the importance of the selection of the appropriate classifier for the dataset [27]. The technique applies a set of standard models including word2vec for representing each tweet as an embedding vector is applied for the model, semantic indexing for the dimension reduction, and logistic regression for classifying machine for categorizing tweets into relevant and irrelevant ones [14][28]. This emphasizes the usefulness of previous disaster tweets analysis, also the effectiveness of using the data of different languages discussed in the previous studies. The empirical study on the several pairs of disasters, such as earthquakes, and floods, of different countries [29] was studied. The study showed that the source and target disaster classification was better with the RF classifier. In handling class imbalance problem, Light Gradient Boosting Machine(LGBM) is the best performer than XGB classifier for the sentiment based classification [31]. LGBM achieves better F-Score by converging faster than the XGB for the minority class. At the onset, large volumes of unlabeled data is generated in OSN during the crisis. It is better to implement semi-supervised technique with smaller labeled data[32]. In particular, iterative RF classifier works efficiently as semi-supervised machine on the OSN generated data(Twitter). This constructed model can predict the tweet location with precise GPS points.

In previous studies, algorithm to identify relevant messages based on keywords and hashtags, with matching-based and learning-based approaches(Agrawal et al, 2017) were devised. To evaluate the two approaches, we put them into a framework specifically proposed for analyzing disaster-related tweets collected using both methods. A subset of CrisisLexT26 dataset based on keyword list collection and dataset collected using proposed method is used for the analysis of the classifiers. From the reviews, it is understood that the research works need enhancement, especially on classification of the information to extract the appropriate knowledge from the tweets. Before developing the classifier model, the existing classifier performances should be analyzed. Therefore the existing different classifier algorithm such as NB, SVM, LR, RF and GB are required to be evaluated and analyzed. To evaluate the classifier algorithm, the methodology given in section 3 is adapted.

METHODOLOGY

The significant classifier identification for analyzing the tweets related to disaster has begun with the standard dataset and raw data. The fetched tweets are labeled for informativeness to be distinguished as related and non-related. The related tweets are further classified into informative and non-informative based on the set of rules given in step 3 of selection procedure given in section 3.1. The data sets are divided as training and test datasets for machine learning classifier algorithms. The training and test data shall be given as an input to the Naïve Bayes, Support Vector Machine, Logistic Regression, Random Forest and Gradient Boosting models and its performance are measured. The performance measures of the mentioned classifiers are found for automatically collected tweets during disaster using the proposed method described in the data source section. The significant classifier is arrived by comparing the performance metrics of the classifier for both training and test datasets.





Aarthi and Sasikala

Architecture

The concepts and functionalities behind the algorithm are described in this session. Figure-1 shows the logical diagram for the classifier identification and it starts with tweets collection, preprocessing will be done on collected data, then the data will be tested on classifiers to know the best classifier.

The selection of significant classifier is achieved through following steps,

- Step 1: Collection of tweets.
- Step 2: Labeling: {Non-related, related [Informative, non-Informative]}
 - Creating the Keyword sets
 - Keyword set 1 : {set of words indicates the disaster }
 - Keyword set 2 : {indicating the rescue / request}
 - Keyword set 3 : {numbers , context}
- Step 3: Rule Formation
 - Rule 1: Related: if any keyword set member value that represents the relationship to the disaster may shows the relativeness
 - Rule 1 (a): Informative
 - Rule 1 (b) : non informative
 - Rule 2: non – related: if tokens are not a member of keyword set then tokens may be labeled as non-related
- Step 4: Data source labeled for standard database and user database
- Step 5: Fetching the raw tweets and converting them into tokens.
 - Lemmatization:
 - Converting tweet into token
 - Clean the tweet by applying filters which reduce noise and trim feature space with the removal of stop words, Html tags, Uniform Resource Loader (URL), special characters, replace links, usernames (@), hashtags (#), images and blank value)
- Step 6: Prepare training and test datasets
- Step 7: Vectorization using TF/IDF
- Step 8: Model fit for NB, SVM, LR, RF, GDB
- Step 9: Evaluation of NB, SVM, LR, RF, GDB
- Step 10: Identification of significant classifier

The description on the classification techniques are given below.

Data acquisition

Automated Data Collection method

The data source is fetched from the standard dataset and is collected during real happening of natural disasters as Volcanoes eruption, Earthquake, Wildfire, Flood and Tropical cyclones. The alert feed from the GDACS website is scraped. The disaster information such as location, disaster type, alert level, time stamp are stored in a file. If alert level is orange or red, then disaster related tweets are collected for the action dynamics. The information extracted for the current date and time are stored in a file. The disaster type, location, timestamp are searched in Google search engine. The results of the search are stored in a file. Hashtags are extracted from the result. The hashtags are compared with the location and disaster type with inputs received from the GDACS. Fuzzy textual similarity is applied to find relevant hashtags for the crisis. Using fuzzy-wuzzy similarity ratio hashtags are matched with the disaster type and disaster locations. Then the matched hashtags are searched in Twitter API. The stream of tweets based on Twitter search is stored as raw json file and csv file. The logical process involved in the data collection logical process is shown in Figure-2.





Aarthi and Sasikala

Algorithm: Automatic sensing the disaster and collecting the Twitter data

Input: alert feed of GDACS website.

Output: Collection of streamed tweets based on the hashtag extracted based on the algorithm.

```

tweet_Collection(alert_feed)
begin
  alert_ptr <- open alert file;
  Google_input <- open google input file;
  Alert_feed :
    { disaster_type, date, country , severity)
  if date = current date
    write(alert_ptr, alert_feed)
  endif
  While !eof(alert_ptr)
  begin
    if alert_rec.severity != 'green'
      write(google_input)
    end
    while !eof(google_input)
    begin
      searchstring <- type+country+'twitter';
      search_rec <- google_search(searchstring)
      write(google_output, search_rec)
    end
    while !eof(google_output)
    begin
      if (hashtag != null)
        tweet_info = search_twitter(hashtag)
        write(tweet_ptr, tweet_info)
      end
    end
  end
end

```

The table-1 shows the details of the collected dataset during the time period using the proposed method of tweet collection . The tweets collected are based on the #hashtag extracted in this method are shown in the table.

Crisis Lex T26 Dataset

In this analysis, the publicly available labeled dataset - CrisisLexT26 data set [14], was used in the previous research studies to analyze crisis-related tweets. This dataset includes tweets collected during on 26 disaster events that occurred in 2012 and 2013. It consists of both man-made disasters such as train derailment and terrorist attacks and natural disasters such as flood , hurricanes and earthquakes,. In this study, only tweets collected for natural disasters were included. (Table-1). Initially, the CrisisLexT26 dataset was collected and created by retrieving tweets based on the relevant keywords as search terms relating to the particular crisis. The tweets collected for each disaster range between 1,100 and 157,500. The total number of tweets collected is 285,000 tweets during 26 crises, respectively. Then they were annotated by Crowd Flower crowdsourcing platform using paid workers based on three notions: Informativeness, information type, and tweet source [6]. This classification was based on the real-time needs of the rescue workers, emergency responders, and emergency services required to obtain situational understanding [13]. Natural disaster tweets of this dataset were taken for further learning. The dataset information are given in table-2.





Aarthi and Sasikala

Data Pre-processing

Labeling of the dataset

Primarily, datasets are annotated and labelled. Each pair is annotated as either one among (a) "Related and informative" is assigned as informative class. The tweets which are labeled as "related and uninformative" or "Non related" are assigned as non-informative class. The related and informative annotated tweets are given the labeled as '1' and related –non informative, non-related are labeled as '0'. The labelled tweets are presented in Table-3.

Keyword Set

In this identification process the tweets are compared with set of keywords which includes "disaster.". Set 1 represents disaster related keywords. Set 2 shows the response request of the needy and response team. Set 3 contains the set of numbers which are used for the contextualize the disaster mapping process. All these three set of keywords are aids to identify the informative state of the tweet based on the process stated in the algorithm session 3.1 as part of architecture of the research.

Sample Set 1 : { fire, explosion, injured, water rises, hurricane, tornado damage, flood alert, building collapsed}

Sample Set 2 : { people missing, dead , injured , aid available, power cut, medical help needed, house affected, surrounded water }

Sample Set 3 : { numbers in context with damage, help request and response}

Data Cleaning

The datasets collected and CrisislexT26 datasets are further pre-processed using the step 5 mentioned in the section

Architecture

The following sample shows the fetched tweet before and after the pre-processing levels.

Tweet before pre-processing,

1. RT @indystar: Farm-to-table festival @DigINDIANA served up more than a taste of Indiana this weekend. <http://t.co/TlwRrLylla> <http://t.co/HrÃcã,-Ã>
2. Dozens killed as monsoon floods ravage India and Nepal | News | DW.DE | <http://t.co/OpEsRx9S3I>

Tweet after pre-processing,

1. b'rt festival served taste indiana weekend'
2. b'dozens killed monsoon floods ravage indianepal news dw de'

Vectorization of Tweet Text

Feature vectorization is an essential phase in the classification, in which the extracted text features are converted into a numeric feature matrix for the model prediction and estimation. The tweets are unstructured data , which cannot be used as direct input for building a machine learning model. In this phase, the tweet texts are replaced with the huge number vectors. The each token in the dataset is represented as number dimension of the created vector. TF-IDF is the method used for the feature vectorization of the both datasets for the further process. The TF-IDF method is the most prominent method for vectorising human languages in the Natural Language Processing(NLP) [33]. This measures relevancy of the word in the given document. The words are given weight , such that word counts are replaced with TF-IDF scores across the entire dataset.

Term Frequency – Inverse Document Frequency (TF-IDF) Method

TF-IDF of the word in any given tweet is the product of the TF and IDF of the word [34], TF is the count of the disaster related word appearing in a document(tweet text). The IDF measures the least occurrence of a disaster word in the entire dataset. If a word appears in many documents, its IDF score will be lower, as this word is





Aarthi and Sasikala

frequently occurring in the certain document. Document frequency is the ratio of total number of tweets where term "t" appear to the total number of tweets in the given dataset

$$IDF_w = \log \frac{1+N}{1+df_w} + 1 \quad (1)$$

where ,

df_w is the number of tweets containing a disaster keyword(document frequency) ,
w in the entire dataset , N is the number of tweets.

This method extracts more discriminating features in the tweet that are not so frequent in the whole dataset. TF-IDF is measured as

$$Tfidf(t, d, D) = tf(t, d) \times idf(t, D) \quad (2)$$

Where ,

T is the terms, d is each document,

D is the collection of documents.

Classification Techniques

Naive Bayes(NB) Classifier.

This classifier uses Bayes' theorem, which works with respect to probability when no correlation exists between independent variables. In this process, there is no direct relationship between the generated vectors and therefore, the Naive Bays model is unedified one among the classifier. The classifier predicts (binary results) feature based on the selected classes which are generated using vector from the tweets (preprocessed text). The informative tweets are considered as positive class. Non-informative and non-related tweets are considered as negative class. The result is the highest probability class among all probabilities using the posterior probability of the given formula

$$P(c/x) = \frac{P(x/c)P(c)}{P(x)} \quad (3)$$

where ,

c indicates class to be predicted
(relevant/non relevant)

x indicates tweet dataset.

P(x/c) represents Posterior Probability: The highest probability of disaster related class with tweet text dataset

Likelihood: Number of disaster related words in the dataset

P(c) states Prior Probability: Number of disaster related word in the tweet

P(x) stands for Predictor Prior: Probability number of words in the tweet

In this algorithm, Both classes are equally probable, by using prior probability (C_i) probability of w_i belongs to class C_i is calculated. . Then the probability of the tweet S_i belongs to class C_i is

$$P(S_i/C_i) \propto P(T_j/C_i) = \pi [T_j P((w_j/C_i) + (1 - T_j)(1 - P((w_j/C_i)))] \quad (4)$$

where S_i is the i-th tweet of the test dataset, and T_i is the term vector for this tweet.

T_i contains 0s and 1s corresponding to the word in the vocabulary for tweet S_i.

Python is used to evaluate the Naive Bayes procedure. The collected tweet dataset is used on sklearn modules and the performances are observed.





Aarthi and Sasikala

Support Vector Machine (SVM)

SVM (Kaplan et al,2010) finds the best hyperplane on input space called the structural minimization principle .This classifies the binary classes which not linear using hinge loss function that maximizes the margin distance between the classes observations. It finds the optimal hyperplane on the 2-dimensional space for classifying the binary classes. The best hyperplane is found by maximizing the margin(δ) using

$$\delta = \frac{1}{\|w\|} \tag{5}$$

where w is the weight vector

The dimension of the hyperplane corresponds to the number of input features, if the number of features is N , then the dimension for the hyperplane is $N-1$. The formula expands as,

$$l(y) = \max(0, 1 + \max_{y \neq t} W_y X - W_t X) \tag{6}$$

where,

$l(y)$ represents Hinge Loss Function

t states the target variable, which represents the category of informative or non-informative types.

w represents the model parameters which contains the features (vectors) on both training and test tweets.

x stands for input variable, that are standard and captured trained tweet text.

The relevance of information target 't' is determined based on the deviation (loss function) of relevance, which represents the disaster related information. The keyword vectors are given as an input and are helpful in find the degrees of relevance to determine the binary class of disaster information, which is computed using sklearn module of SVM.

Logistic Regression (LR) Learner.

Logistic Regression classifier estimate the categorical variables outcome based on the independent variables for binary values (0/1), the probability of an occurring word is predicted by fitting the data into a logistic function. The independent variables in the logistic function are optimized by maximizing the likelihood function. In this process, likelihood is the probability of trained tweets of the given model and specific parameter values are applied to find accuracy. It measures the support provided by the data for each possible value ($p(x_i)$).

The sigmoid curve of Logistic Regression is given as,

$$Cost(h\theta(x), y) = \begin{cases} -\log(h_\theta(x)) & \text{if } y = 1 \\ -\log(1 - h_\theta(x)) & \text{if } y = 0 \end{cases} \tag{7}$$

Where ,

$h_\theta(x)$ represents the predicted response for θ observation.

For an instance x , the probability of predicting the class is $P(y = 1 | x)$. For the test instance x , probability $P(y = 1 | x)$ is more than .5 which is the decision boundary, then it is predicted as informative tweets otherwise non-informative tweets. It is given as

$$\tag{8}$$

$$\hat{y} = \begin{cases} 1 & \text{if } P(y=1|x) > 0.5 \\ 0 & \text{otherwise} \end{cases}$$

Where.

y is the target class.

The keyword vectors are given as an input and are used find the likelihood of relevance based on binary values, which represents disaster informative which computed using Logistic Regression method of the sklearn module.





Aarthi and Sasikala

Random Forest (RF) Classifier.

Random forest classifiers is a tree based classifier with parameters that are randomly chosen from the random vector. The classification $f(X)$ combines $\{h_k(X)\}$, which shows relativeness based on votes for the given input tweets to train a family of classifiers $h_k(X)$.

$$D = \{X_i, Y_i\}, i=1 \text{ to } n \quad (9)$$

where,

D is the Dataset X_i represents the feature based on which classification is done

Y classification of tweets,

Each classifier $h_k(x) \equiv h(x|\Theta_k)$ is a predictor of n.

$y = \pm 1$, which is an outcome associated with input X.

Gradient Boosting Machine(GBM)

The main characteristic of "boosting" is the conversion of a set of weak into a strong and robust classifier by taking the majority relevance of every prediction. It trains many models sequentially and gradually minimizes the loss function. The formula is given,

$$y = ax + b + e \quad (10)$$

where,

y is the Loss function for Target variables

x represents Input variables

a and b are constant values for the relationship of likelihood

e is the variable for Loss error

Predict the log likelihood of the data given using the predicted probability which is

Log likelihood of the observed data given the prediction is

$$[y_i * \log(p) + (1 - y_i) * \log(1 - p)] \quad (11)$$

where,

x_i represents the input variables that may be feed into the model

y_i is the target variable that will be trying to predict zero or one

p is the predicted probability

The better result will be attained through maximizing the log likelihood function and therefore, the log(likelihood) will reduce the error e.

Determination of Informativtness .

The purpose of the work to build a classifier which could segregate the real time disaster related and informative tweets from Twitter Data. This process receives the tweets from pre-processing task and it extracts the features from the text contents of tweets. This classification's main feature is tweet text, which is vectorised using the method TF/IDF of N-Gram words. The model is constructed using the combination of TF/IDF feature transformation method and the classifier (each one of the five classifiers). The model is fed with training and test datasets. The output is in probabilities. The performance metrics of the model is evaluated and discussed in the next section.

RESULTS AND DISCUSSIONS

Evaluation of the machine learning model

The scope of this work to identify the significant classifier based on the performance evaluation of five diverse classifiers namely, Naive Bayes, Logistic Regression, Support Vector Machine (SVM), Gradient Boosting and Random Forest. The comparison is based on the metrics namely, accuracy, Recall, Precision and F1 - Measure. The results are arrived from the separation of 70% data for training and 30 % for testing. The metrics of each model is listed with training and test datasets.





Aarthi and Sasikala

Performance analysis for the informative tweets classifiers - Accuracy

Accuracy is the measure of correct predictions of informative tweets for the disaster made by the model. True positives are the informative tweets of the disaster and true negatives are tweets which are not related. Accuracy shall be given as,

$$\text{Accuracy} = (\text{True positives} + \text{True negatives}) / (\text{Total number of data items}) \quad (12)$$

Table-4 shows the performance metrics in term of accuracy of the classifier that uses the both datasets. The results clearly depict that the Gradient Boosting algorithm for the present collected dataset is appreciated when comparing other models. The table values are represented using Gantt for informative tweets as chart in Figure-3. As per the analysis, the Gradient Boosting performance is found low as 0.776 (77.6%) and Support Vector machine performance is found high as 0.857 (85.7 %). For the real time data set, Support Vector Machine performance is found low as 0.840 (84 %) and the Gradient Boosting performance is found high as 0.939 (93.9%). The tweet evaluation requires the best result during the disaster on the real time application, and therefore the Gradient Boosting is appreciated according to accuracy measure.

Performance metrics for the informative tweets models - Precision

Precision is measured as the number of predictions (tweets) that were correctly predicted as true as informative tweets that were actually correct.

$$\text{Precision} = (\text{True positive}) / (\text{True Positive} + \text{False Positive}) \quad (13)$$

The classifier precision measure presented in Table-5. According to the precision metrics, the Support Vector Machine algorithm and Gradient Boosting algorithm performances are significant while comparing other methods for the selected dataset. The performance metrics of the classifier in terms of Precision is presented as a chart figure-4. In the precision metrics of the classifiers, it is shown that the Gradient Boosting value (83.9 %) has poor performance on the standard data set and SVM value (86.2 %) is appreciated but for the real time data set Support Vector Machine performance value (83.9%) is found low and the Gradient Boosting performance is found significant. The disaster informativeness required the high level of Precision and therefore the Gradient Boosting is identified as a significant classifier for this data set.

Recall of the informative tweets for the classifier analysis

Recall is the calculated using number of predictions (tweet texts) which were relevant to the disaster information in a dataset.

$$\text{Recall} = (\text{True positive}) / (\text{True Positive} + \text{False Negative}) \quad (14)$$

The performance metrics based on Recall for the models using the five different classifiers presented in Table-6. The performance metrics of the classifier in terms of Precision is presented as a chart in the figure-5.

As per the Recall analysis, Gradient Boosting value 0.923 (92.3 %) and Support vector machine performances value 0.857 (85.7 %) are high for the Real time OSN tweets and standard CrisisLexT26 dataset. Since the tweets are classified in real time, the Gradient Boosting is identified as a significant classifier algorithm.

F1-Score of the classifiers for informative tweets

It is calculated as the harmonic mean of the precision and recall values. It is used to measure the accuracy on the categorization of disaster informative tweets of the test dataset.

$$F1 = 2 * (1 / ((1/\text{precision}) + (1/\text{recall}))) \quad (15)$$

The performance of F1-Score for the datasets that compares five different classifiers stated in Table-7. The table values are represented using Gantt Chart in Figure- 6. From the above table, it is found that the Gradient Boosting algorithm performs well for the real-time tweet collected during the disaster. The F1-Measure of GB is 93.40% with the collected tweets, which indicates strong discriminatory ability between informative and non-informative classes,



**Aarathi and Sasikala**

LR and RF are found at second and third positions with 92.70% and 87.20% respectively. According to Precision and Recall, GB achieves the best for the collected dataset. In the case of CrisislexT26 dataset, SVM achieves high performance (85.85) in terms of F1-Measure between classes. RF and LR found themselves at second and third positions with F1-Measures of 84.70% and 84.60% respectively.

AUC-ROC curve of the classifiers for informative tweets.

The Area Under the Receiver Operating Characteristic (AUC-ROC) measures the model's ability to categorize between disaster informative tweets (positive examples) and non-related tweets (negative examples). AUC-ROC curve shows the balance between True Positive Rate (TPR) and False Positive Rate (FPR) across different decision onsets. This plot depicts the classifier efficiency of correctly categorizing tweets as disaster tweets (TPR) and non related tweets as disaster-related tweets (FPR).

The Figure-7 and Figure -8 depicts the best and the least classifier for categorizing the disaster informative tweets from the CrisisLexT26 dataset and collected tweets. The significant classifier is SVM classifier and the least performed by the GB classifier for the CrisisLexT26 dataset whereas for the collected dataset GB outperforms other classifiers. Here, the above analysis of the classifier model depicts that the ensemble learner GB outperforms the other individual learners (RF, NB, SVM, LR) for the informative tweet classification during the disaster in current. Considering accuracy, GB achieves the best performance (93.26%) and LR is found close to the challenges. GB classifier improves the performance of real-time OSN dataset over the crisis Lex dataset in terms of accuracy with an increase in the performance at about 7.09 over SVM, which has its accuracy percentage of 86.17. The Analysis of the learner on CrisisLexT26 dataset implies the significance of SVM learner which has high performance over the other classifiers.

CONCLUSION

This research work attempted to identify the significant classifier which suites for disaster relevance information identification from OSN. A comparative evaluation on machine learning classifier algorithm, i.e., RF, GB, NB, SVM, LR are performed for standard data set Crisis Lex dataset as well as user gathered data. Experimental results reveal that the GB classifier is a significant one for the real time gathered tweets. It achieves the best results in four performance criteria, i.e., accuracy, Precision, recall and F1-Measure. The GB results are significant and relatively nearer to Random Forest and Logistic Regression. Among the baseline learners, LR outperforms better than the other classifiers over the most of evaluation metrics. In the case of CrisisLexT26 dataset, the baseline learner SVM outperforms with other classifier such as RF, GB. On the whole, GB, SVM, LR might be the first and best choice for the classification for online disaster tweets based on its performance measures. As per analysis, GB performs better than SVM with the accuracy of accuracy is 93.62% of TF-IDF n-grams. According to the accuracy, to classify disaster informative real time tweets, GB is the significant classifier with the TF-IDF feature extraction method. This work evaluated with limited data set but it has to be tested with more volume of online tweets with external features for the classification of tweets for rescue related activities during the crisis and finally, multi-classification of tweets for the efficient rescue operation will be the more effective for the relief activities during the disaster.

REFERENCES

1. J.Schwarz, M.R Morris. "Augumenting Web Pages and Search Results ti Support Credibility Assessment." *ACM Conference on Human Factors in Computing Systems* (ACM Press), 2011.
2. Kaplan A.M, Haenlein M. "Uses of the world unite! The challenges and oppurtunities of Social Media." ,Bus Horiz, 2010: 59-68.
3. Lee K, Palsetia D, Narayanan R, Patwary M, Agrawal A, Choudhary A. "Twitter Trending Topic Classification." ,11th *IEEE International Conference on Data Mining Workshops*, 2011.
4. Manning C.D, Raghavan P, Schutze H. *An Introduction to Information Retrieval*.,Cambridge University Press, 2009.





Aarthi and Sasikala

5. T, Joachims. "Text Categorization with Support Vector Machines Learning with Many Relevant Features.", Research Report, University of Dortmund, 1998.
6. Alexandra Olteanu, Carlos Castillo, Fernando Diaz and Sarah Vieweg. "CrisisLex : A Lexicon for Collecting and Filtering Microblogged Communications in Crisis.", *International AAAI Conference on Weblogs and Social Media*, 2014. 376-385.
7. Aldo Hernandez-Suarez, Gabriel Sanchez-Perez, Karina Toscano-Medina, Hector Perez-Meana et al. "Using Twitter Data to Monitor Natural Disaster Social Dynamics: A Recurrent Neural Network Approach with Word Embeddings and Kernel Density Estimation.", *Sensors*, 1746 (2019): 22.
8. Kongthon, A, Haruechaiyasak C., Pailai, J., and Kongyoun. "The role of Twitter during a natural disaster : Case study of 2011 Thai Flood." , *In Proceedings of the PICMET'12 Technology Management for Emerging Technologies (PICMET)*, 2012: 2227-2232.
9. Sachdeva S, McCaffrey C. "Using Social Media to Predict Air Pollution during California Wildfires.", *Proceedings of the ACM 9th International Conference on Social Media and Society (ACM)*, July 2018: 365-369.
10. Hughes A.L, Palen L. "Twitter Adoption and use in mass convergence and emergency events." , *International Journal of Emergency Management*, no. 6 (2009): 248-260.
11. Earle PS, Bowden DC, Guy M. "Twitter Earthquake detection : earthquake monitoring in a social world.", *Annals of Geophysics*, 2012.
12. Finch K.C, Snook K.R, Duke C.H, Fu K.W, Tse Z.T.H, Adhikari A, Fung L.C.H. "Public health implications of social media use during natural disasters, environmental disasters and other environmental concerns." , *Natural Hazards*, 2016: 729-760.
13. A.Olteanu, S.Vieweg,C.Castillo. "What to Expect When Unexpected Happens : Social Media Communications Across Crisis." , *In Proceedings of the ACM 2015 Conference on Computer Supported Cooperative work and Social Computing(CSCW'15)*, 2015: 994-1009.
14. Muhmmad Imran, Carlos Castillo, Fernando Diaz and Sarah Vieweg. "Processing Social Media Messages in Mass Emergency : A Survey.", *ACM Computing Surveys*, 47, no. 4 (2015): 1-32.
15. de Albuquerque, Joao Porto et al. "A Geographic Approach for Combining Social Media and Authorative Data towards Identifying Useful Information for Disaster Management." , *International Journal of Geographical Information Science*, 2015: 1-23.
16. C. Troussas, M. Virvou, K. J. Espinosa, K. Llaguno and J. Caro, "Sentiment analysis of Facebook statuses using Naive Bayes classifier for language learning," *IISA 2013*, 2013, pp. 1-6, doi: 10.1109/IISA.2013.6623713.
17. Rennie J.D.M, Shih I, Teevan J, Karger D.R. "Tackling the Poor Assumptions of Naive Bayes Text Classifier ." , *Proceedings of 20th International Conference on Machine Learning*, Washington DC: IEEE, 2003.
18. Corani G, Zaffalon M. "Learning Reliable Classifiers from Small or Incomplete Datasets - The Naive Credal Classifier 2." , *Journal of Machine Learning Research*, April 2008: 581-621.
19. Amolik A, Zivane N, Bhandary M, Venkatesan M. "Twitter Sentiment Analysis of Movie Reviews using Machine Learning Techniques.", *International Journal of Engineering and Technology* , 7 , no 6,(2016) : 2038-2044.
20. Ye.Q, Zhang.Z, Law.R. "Sentiment Classification of Online Reviews to Travel Destinations by Supervised Machine Learning Approaches." , *Expert System Applications* ,36, no. 3 (2009): 6527-6535.
21. Zha Z.J, Yu J, Tang J, Wang M, Chua T.S. "Product Aspect Ranking and its Applications." *IEEE Transactions of Knowledge Data Engineering* , 26, no. 5 (2014): 1211-24.
22. F.Alzhamzami, M.Hoda and A.E.Saddik. "Light Gradient Boosting Machine for General Sentiment Classification on Short Texts : A Comparative Evaluation." , *IEEE Access (IEEE)* 8 (2020): 101840 - 101858
23. Dou.J, Yamagishi H, Zhu Z, Yunus A.P, Chen.C.W. "A Comparative Study of the Binary Logistics Regression (BLR) and Artificial Neural Network(ANN) Models for GIS based Spatial Predicting Landslides at a Regional Scale." , *Landslide Dynamics-ISDR-ICL - Landslide Interactive Teaching Tools (Springer)*, 2018: 139-151.
24. Xu.B, Gho.X, Ye.Y, Cheng.J. "An Improved Random Forest Classifier for Text Categorization.", *JCP* . 2012.
25. Z.Ashktorab, C.Brown, M.Nandi, A.Culotta. "Tweedr : Mining Twitter to Inform Disaster Response." , *ISCRAM - 2014 Conference Proceedings. Pennsylvania: 11th International Conference on Information Systems for Crisis Response And Management*, 2014. 354-358.





Aarthi and Sasikala

26. M.Imran, S.Elbasuoni, C. Castillo, F.Diaz, P.Meier. "Extracting Information Nuggets from the Disaster Related Messages in the Social Media.", *10th International Conference on Information Systems for Crisis Response and Management*, Baden-Baden , Germany: ISCRAM 2013, 2013. 791-801.
27. Kirasich, Kaitlin, Smith, Trace, Sadler, Bivin. "Random Forest Versus Logistic Regression : Binary Classification for Heterogenous Datasets." *SMU Data Science Review* ,1, no. 3 (2018).
28. Matthias Habdank, Nikolai odehytskors and Reiner Koch. "Relevancy assessment of Tweets using Supervised Learning Techniques : Mining Emergency Related Tweets for Automated Relevancy Classification.", *International Conference on Information and Communication Technologies for Disaster Management*, 2017.
29. Muhammad Imran, Prasenjit Mitra and Carlos Castillo. "Twitter as a Lifeline : Human - Annotated Twitter Corpora for NLP of Crisis - Related Messages.", *Tenth Language Resources and Evaluation Conference. 2016*,1638 - 46.
30. Marc-Andre Kaufholda, Markus Bayera, Christian Reutera. "Rapid Relevance Classification of Social Media Post in Disaster and Emergencies : A System and Evaluation Featuring Active ,Incremental and Online Learning.", *Information Processing and Management*, 2020.
31. Rachid Oualet, B.Birregah, Eddie Soulier, Samuel Auclair, Faiza Boulahya. "Random Forest Location Prediction from Social Networks during Disaster Events.", *The Sixth IEEE International Conference On Social Network Analysis , Management and Security*. Granada, Spain: IEEE, October 2019.
32. S.Agrawal, S.H.Kim and C.Shahabi. "On Identifying Disaster - Related Tweets : Matching -based or Learning - based ?" 2017, *IEEE Third International Conference on Multimedia Big Data(BigMM)*, IEEE, 2017. 330-337.
33. Muhammad Bux Alvi, Naeem A.Mahoto, Mukhtiar A.Unar, M.Akram shaikh. "An Effective Framework for Tweet Level Sentiment Classification using Regressive Text Preprocessing Approach.", *International Journal of Advanced Computer Science and Applicaitons* ,10, no. 6 (2019): 572-581.
34. Noha Y Hassan, Wael H Gomaa, Ghada A Khoriba, Mohammed H Haggag. "Credibility Detection in Twitter using Word N-gram Analysis on Supervised Machine Learning Techniques.", *International Journal of Intelligent Engineering and Systems*, 2020: 291-300.

Table 1: Details of online collected tweets used for classification

Disaster	Location	Number of Tweets
Earthquake	Philipines	3843
Earthquake	China	1895
Earthquake	Guatemala	5422
Earthquake	Japan	953
Earthquake	Solomon Island	1189
Earthquake	USA	1133
Cyclone	Mexico	2089
Cyclone	China	1077

Table 2: Details of CrisisLexT26 Dataset Used for Classification.

Disaster	Category	Number of Tweets
2012 Colorado Wildfires	Wildfire	1200
2012 Guatemala Earthquake	Earthquake	1050
2012 Italy Earthquake	Earthquake	1000
2012 Philipines Flood	Flood	998
2012 Typhoon Pablo	Cyclone	890
2013 Alberta floods	Flood	2200
2013 Australia Bushfire	Bushfire	1200
2013 Bohul Earthquake	Earthquake	1000
2013 Colarado floods	Flood	1000
2013 Manila floods	Flood	928





Aarthi and Sasikala

Table 3 : Dataset labeling sample

S.No	Tweets	Keyword	Label
1	RT @indystar: Farm-to-table festival @DigINDIANA served up more than a taste of Indiana this weekend	Non-related	0
2	Dozens killed as monsoon floods ravage India and Nepal	Related and informative	1
3	Pray for Nepal recovery	Related and non-informative	0

Table 4: Accuracy of the classifiers for informative tweets

S.No	Model	Standard CrisisLex tweets	Real time OSN Tweet
1	Bernoulli-NB	0.853	0.869
2	SVM	0.857	0.840
3	Logistic Regression	0.840	0.933
4	Random Forest	0.844	0.887
5	Gradient Boosting	0.776	0.939

Table 5: Precision of the classifiers for informative tweets

S.No	Model	Standard CrisisLex tweets	Real time OSN Tweet
1	Bernoulli-NB	0.855	0.877
2	SVM	0.862	0.845
3	Logistic Regression	0.861	0.925
4	Random Forest	0.855	0.864
5	Gradient Boosting	0.839	0.939

Table 6 : Recall of the classifiers for informative tweets

S.No	Model	Standard CrisisLex tweets	Real time OSN Tweet
1	Bernoulli-NB	0.853	0.869
2	SVM	0.857	0.840
3	Logistic Regression	0.840	0.932
4	Random Forest	0.844	0.887
5	Gradient Boosting	0.776	0.923

Table 7 : F1-Score of the classifiers for informative tweets

S.No	Model	Standard Crisis Lex tweets	Real time OSN Tweet
1	Bernoulli-NB	0.854	0.839
2	SVM	0.859	0.802
3	Logistic Regression	0.846	0.927
4	Random Forest	0.847	0.872
5	Gradient Boosting	0.792	0.934



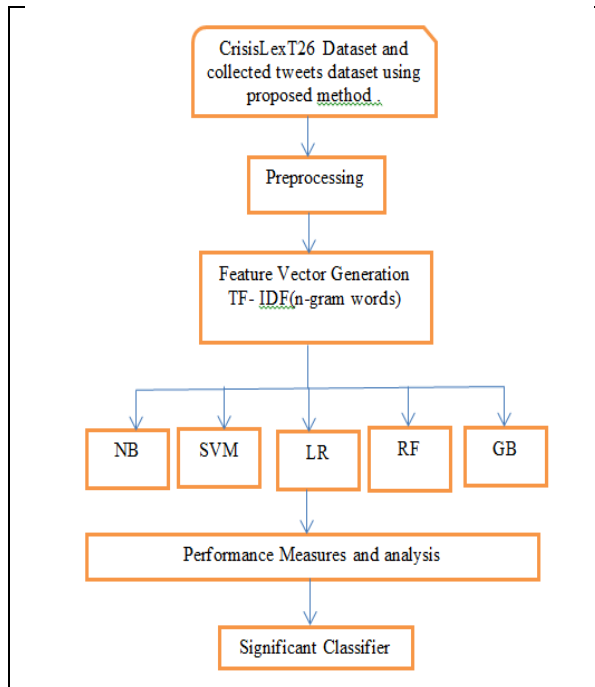


Figure 1: Logical diagram of Classifier Identification

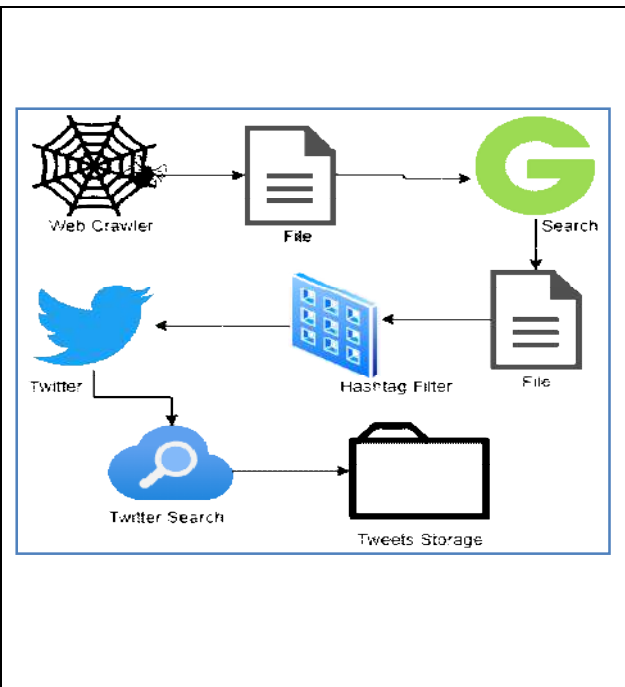


Figure 2: Logical diagram for tweet collection

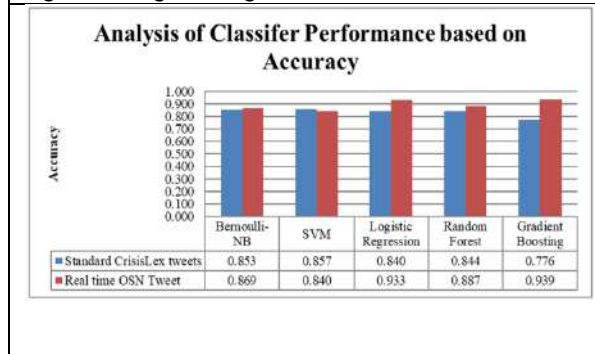


Figure 3: Analysis of Classifier Performance based on Accuracy

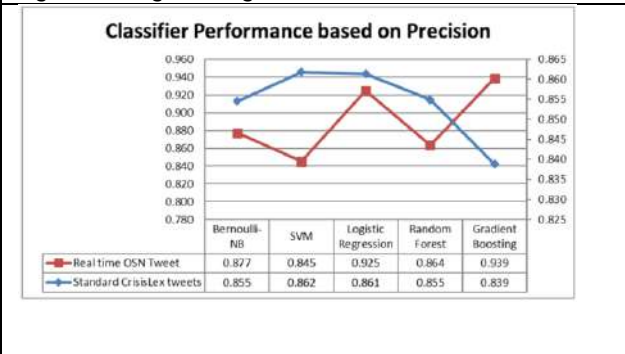


Figure 4: Analysis of Classifier Performance based on Precision.

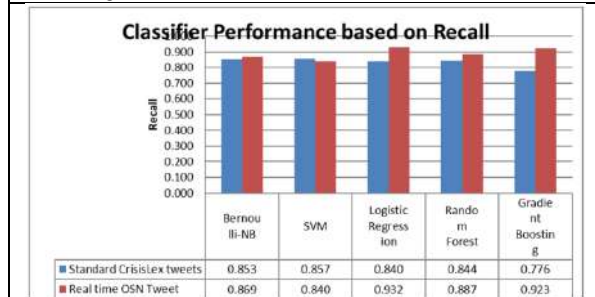


Figure 5: Analysis of Classifier Performance based on Recall.

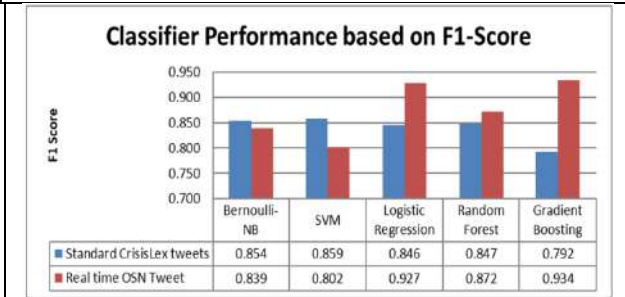


Figure 6: Analysis of Classifier Performance based on F1-Score.





Aarthi and Sasikala

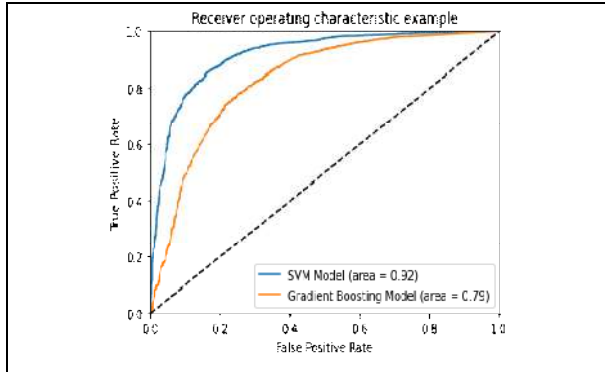


Figure 7: AUC-ROC Curve of CrisisLexT26 Dataset

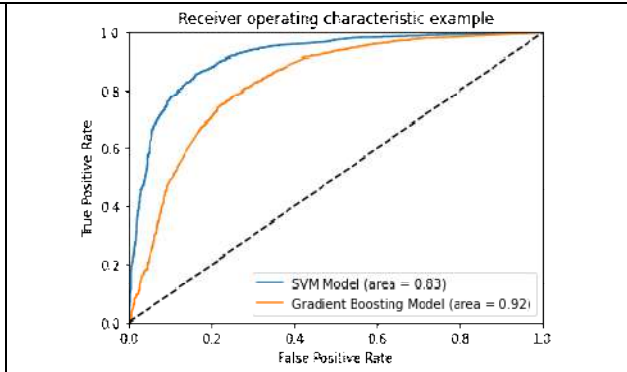


Figure 8: AUC-ROC Curve For Real Time Tweet





A Survey on Plants used for Postnatal Care in Folk Medicine of Palakkad District, Kerala

Jayalekshmi Chandran Vasanthakumari¹, Reshma Kariyil Ramesh¹ and Suresh Veerankutty^{2*}

¹Research Scholar, Post Graduate and Research Department of Botany, Government Victoria College, Palakkad - 678001, Kerala, India.

²Assistant Professor, Post Graduate and Research Department of Botany, Government Victoria College, Palakkad - 678001, Kerala, India.

Received: 08 Nov 2021

Revised: 15 Dec 2021

Accepted: 10 Jan 2022

*Address for Correspondence

Suresh Veerankutty

Assistant Professor,
Post Graduate and Research Department of Botany,
Government Victoria College,
Palakkad - 678001, Kerala, India.
Email: sureshmagnolia@gmail.com



This is an Open Access Journal / article distributed under the terms of the **Creative Commons Attribution License** (CC BY-NC-ND 3.0) which permits unrestricted use, distribution, and reproduction in any medium, provided the original work is properly cited. All rights reserved.

ABSTRACT

Pregnancy and child birth are considered as important events in the lifespan of woman. Medicinal plants are widely used in post-natal care for bathing mother and child after delivery in rural parts of Palakkad district. This medicated bath helps to rejuvenate the body of mother after delivery and increases resistance to various diseases in child. So the documentation of these plants is essential to protect this traditional knowledge. The present study aimed to document the plants used in post-natal care for bathing mother and child after delivery in various parts of Palakkad district. The information on plants used for bathing mother and child after delivery was collected by oral communication with local people and traditional birth attendants. The collected data were interpreted using quantitative ethnobotanical tools like Relative Frequency of Citation, Use value and consensus index. Sixty-two plant species belonging to 29 plant families were documented from this study.. The Use value, Relative Frequency of Citation and Consensus index was high for *Curcuma longa*. The knowledge about these medicinal plants is limited to present generation. Documentation and further scientific investigation on these plants may lead to production of new drugs.

Keywords: Consensus index, Relative frequency of citation, Palakkad, Post-natal care, Use value.

INTRODUCTION

Plants are inevitable for humans for their existence. Majority of our medicines depends on plants. Medicinal plants are widely used in India to treat various diseases. Plants used as medicine are more common in rural areas of



**Jayalekshmi Chandran Vasanthakumari**

developing countries. Herbal medicines are safer than synthetic drugs. Kerala is rich in plant diversity and also with plant-based treatments. Folk medicine, Ayurveda and Tribal medicine are the three plants based healing systems from Kerala. Palakkad is one among the fourteen districts of Kerala and 88.9% of the district's population is rural in nature. The district is located in the center of Kerala state with no coastal line. It shares borders with Malappuram and Thrissur districts of Kerala and Coimbatore of Tamil Nadu. The study aims to document the plants used in post-natal care for bathing mother and child after delivery in different parts of Palakkad District. Folk medicine was originated in Kerala around 13th century AD [1]. About 5000 plant species are used in folk medicine of India and about 8000 plants are used in tribal medicine [2]. Majority of rural communities still depend on folk medicine. Medicinal plants are widely used in post-natal care in different parts of Kerala. Obstetrics is an important field in folk medicine. The traditional birth attendants are highly skilled for natal care. They are locally called as 'Vayattatties'. Besides birth attendants, the womenfolk of rural communities also play a major role in natal care. The traditional birth attendants prepare medicated water for bath called 'vethuvellam'. This water contains leaves, barks, roots, stem and rhizome of different plants. These plant parts are boiled in water and used for bathing mother. The combination of plants used may vary in different places. This water rejuvenates the body of the mother after delivery. Folk medicine is one of the oldest medicinal practices of Kerala. From ancient period onwards pregnancy and childbirth are considered as important events which require more care. Use of plants for postnatal care was also very common from ancient days. The traditional birth attendants play a significant role in maintaining the health of mother and child. Even though modern medicines are available, today also people depend on some herbal formulations after pregnancy. One such type of treatment is medicated bath after delivery. People in rural areas still follow this medicated bath. Local people depend on plants for many medicines and knowledge about this folk medicine is transferred orally to next generation [3]. The knowledge about these plants is unfamiliar to the present generation. The documentation and further studies on these plants is essential to protect this traditional knowledge and these plants.

MATERIALS AND METHODS

Study Area

Palakkad is located between 10° 21' to 11° 14' North and 76° 02' to 76° 45' East. It consists of six taluks- Palakkad, Pattambi, Chittur, Alathur, Ottapalam and Mannarkkad and has a total geographical area of 4480 Km². The rivers flowing through the district are Bharathapuzha, Gayathripuzha, Kannadipuzha, Kalpathypuzha, Thoothapuzha, Bhavanipuzha and Kunthipuzha. The climate is tropical. The average annual temperature is 27.8° Celsius and average rainfall is 2135mm. It has about 30.5% forest cover [4]. Figure 1 depicts the map of study area.

Data collection

The ethno medical information on plants used in infant care and post-natal care of maternal ladies was collected by survey method. The people were surveyed for the herbal medicines they have used in bathing child and mother during the early stages after birth. The ethnobotanical information from the survey was documented. The survey was carried out from September 2018 to September 2019 in six different taluks of Palakkad district. Random samples of informants from six different taluks were selected for the study. The details were collected from 282 respondents of Palakkad district. Oral communication with local people and rural birth attendants in this region were used to collect information about plants used for bathing mother and child after delivery. The scientific name, local name, family, plant part used and mode of use were determined and documented. The plants were collected and authenticated using Floras and pertinent literature. The voucher specimens are deposited in Government Victoria College Herbarium. Photographs of plants were taken for further documentation. The collected data were analyzed using statistical tools.

Data analysis

The collected data were interpreted using the following quantitative ethnobotanical tools [5].





Jayalekshmi Chandran Vasanthakumari

Relative Frequency of Citation (RFC)

This index is calculated by dividing the number of informants who cited the use of a species by the number of informants who participated in the interview.

$$\text{RFC} = \text{FC}/\text{N}$$

Where FC= Number of persons who mentioned the use of species

N = Total number of informants

Use value (UV)

It is the importance of each plant based on number of different uses reported.

$$\text{UV} = \Sigma\text{U}/\text{N}$$

Where ΣU = Sum of uses mentioned for species.

N = Total number of informants.

Consensus Index (CI)

This index is used to calculate the percentage of informants in an area with folk medicinal knowledge about medicinal plants to treat diseases [6].

$$\text{CI} = n/\text{N} \times 100$$

Where n = Number of informants citing a medicinal plant species.

N = Total number of informants.

RESULTS

From the survey, 62 plant species belonging to 28 plant families were documented. The most common plant families cited in the current study were Moraceae, Zingiberaceae, Euphorbiaceae and Meliaceae. The plants cited in this study with their scientific name, common name, part used, mode of use are given in Table 3. The plants are used as single preparations and compound preparations. Single preparations involve use of a single plant species and compound preparation involves use of a combination of plant species. There were 16 different combinations of plants were used for bathing mother and child.

Single Preparations: *Plectranthus amboinicus*, *Ocimum sanctum*, *Acalypha fruticosa*, and *Vigna radiata* were commonly used as single preparations for the medicated bath. *Plectranthus amboinicus*, *Ocimum sanctum*, *Acalypha fruticosa* leaves are commonly used for bathing children. In some areas, *A. fruticosa* leaves are used for mothers also. *Vigna radiata* seeds were commonly used for bathing mother. The plants used as single preparations are given in Table 1.

Compound Preparations: Different combinations of plants are used for bathing mother and Child after delivery. The combinations of plants used are given in Table 2 with their scientific name, family, common name and plant part used. Comb 15 was used to treat the child.

The medicated water is prepared by boiling different plant parts in water. Before this medicated bath either *Cocos nucifera* L. (coconut) oil or *Sesamum indicum* L. (gingelly) oil along with paste of rhizome of *Curcuma longa* is applied to the body of mother and child. For boy child, *Curcuma longa* is not preferred as it prevents body hair growth. *Vigna radiata* seed powder is used instead of soap for bathing mother. Bark of *Acacia caesia* is used as scrubber for bathing mother and child. Hot water with different plant parts is used to bath mother and luke warm water is used to bath child. The period of medicated bath for mother varies from 7 or 9 or 11 or 28 days. The leaves and flowers of *Hibiscus rosa-sinensis* is used as thalli to wash hair of mother. The most commonly used plant parts were leaves followed by bark. The pie chart (Figure 2) depicts the different plant parts used in bathing mother and child after delivery. High Relative frequency of citation (RFC) was observed for *Curcuma longa* (0.4964) followed by *Artocarpus heterophyllus* (0.4539). Highest Consensus Index (CI) value was observed for *Curcuma longa* (49.64%) followed by *Artocarpus heterophyllus* (45.39%). The results of use-value (UV) calculations showed that *Curcuma longa* (0.482) yielded the





Jayalekshmi Chandran Vasanthakumari

highest value followed by *Artocarpus heterophyllus* (0.447). The UV, CI and RFC for different plant species is given in Table 4.

DISCUSSION

Usage of plants for post-natal care is still common in rural areas of Kerala. From the present study, 62 plant species were documented for bathing mother and child after delivery. Medicinal plants are widely used in different parts of world for pregnancy and postpartum care. In Indonesia a steam bath called 'Bakera', prepared with various plant parts was used to treat maternal ladies which regains the body of mother after childbirth[7]. The herbal bath may help the body of mother to regain its prepregnancy shape. Oil massaging helps in shaping the body of child and helps to restore the abdominal muscles of mother [8]. The plants used for bathing mother mainly aimed at renewing the body of the mother after delivery. These plants also help in drying umbilical cord. The plants used in bathing child may be aimed at increasing the immunity of the child. *Curcuma longa* was the most frequently used plant reported from the present study. The rhizome of this plant is commonly used for bathing mother and child. The plant possesses antioxidant, anti-inflammatory, antibacterial, antiviral, antifungal, anticancer and wound healing properties [9,10,11,12]. Application of rhizome paste to wound decreases inflammation and increases the formation of collagen [13]. Another commonly used plant reported in the study was *Artocarpus heterophyllus*, its yellow leaves were used to treat the mother. The leaves of this plant possess wound healing properties [14]. *Nalpamara patta* - the bark of four different *Ficus* species is another commonly used plant. The bark of these plants has a cooling action and is also used for cleaning vagina [15].

Majority of ethnobotanical studies were focused on tribal groups. Only a few studies are focused on folk medicines. Out of 63 plants mentioned in this study, 21 plants used for bathing mother and child was already reported by Rajith *et al.*, 2010, 9 plants were reported by Rasiya and Nayar, 2011 and 10 plants were reported by Sivadasan *et al.*, 2014.

Anvar and Haneef, 2015 also reported the use of vethuvellam for bathing mother in various parts of Kozhikode district, Kerala. From their study Zingiberaceae members were more commonly used for this medicated bath. The volatile substances and essential oils in these plants improve the health of mother. Out of 62 plants cited, 37 of them are first reported from our study which is used for bathing mother and child after delivery in Palakkad district, Kerala. *Acacia caesia*, *Acalypha fruticosa*, *Achyranthes aspera*, *Acorus calamus*, *Anethum graveolens*, *Borassus flabellifer*, *Cayratia trifolia*, *Centella asiatica*, *Clitoria ternatea*, *Coffea arabica*, *Croton persimilis*, *Cymbopogon flexuosus*, *Eucalyptus globulus*, *Hamelia patens*, *Jatropha hernandiifolia*, *Justicia gendarussa*, *Leucas aspera*, *Moringa pterygosperma*, *Mussaenda frondosa*, *Ocimum gratissimum*, *Piper longum*, *Plectranthus amboinicus*, *Plumbago zeylanica*, *Pongamia pinnata*, *Premna serratifolia*, *Pseudarthria viscida*, *Pterocarpus marsupium*, *Ricinus communis*, *Schleichera oleosa*, *Sida acuta*, *Stereospermum tetragonum*, *Strychnos nux-vomica*, *Terminalia paniculata*, *Thespesia populnea*, *Chrysopogon zizanioides*, *Vitex altissima* and *Xylocarpus xylocarpa* are first reported from our study for post-natal care.

The medicinal properties of these plants are due to certain phytochemicals present in them. But proper scientific studies on plants used for post-natal care is lacking. So documentation and further studies on these plants are essential to protect our traditional knowledge. From the present study 62 plant species belonging to 29 families were documented for bathing mother and child after delivery. This medicated bath is considered as an important factor, especially in rural areas of Palakkad district as it rejuvenates the body of mother after delivery and it also increases the immunity in children. Leaves were the most commonly used plant part followed by bark and rhizome. Fruits and flowers were the least used plant parts. In case of *Artocarpus heterophyllus*, yellow leaves were used for bathing mother. High RFC, consensus value and use value was observed for *Curcuma longa*. The traditional birth attendants and women of rural areas are highly skilled for post-natal care. They have a sound knowledge regarding the plants used for bathing mother and child after delivery. Most information about plants used in bathing mother and child was given by mothers and grandmothers above 50 years. Documentation of this traditional knowledge is very essential as it is depleting day by day. From literature study, this may be the first documented study on plants used



**Jayalekshmi Chandran Vasanthakumari**

for post-natal care in folk medicine of Palakkad district, Kerala. The plants reported in the present study can be taken as a basis for further scientific investigation on these medicinal plants. Further bioactivity guided fractionation on these plants may lead to the production of one or more therapeutic compounds.

ACKNOWLEDGEMENTS

We thank all the informants of Palakkad district who contributed their traditional knowledge for the study. We also like to thank Principal, Head of the Department, teachers, staff and colleagues of Government Victoria College, Palakkad for their support throughout this work. First author thankfully acknowledges University Grants Commission, New Delhi for financial assistance.

REFERENCES

1. Rasiya B A & Nayar T S, Plants used for natal healthcare in folk medicine of Kerala, India. *Indian Journal of Traditional Knowledge*, 10(3), (2011), 523-527.
2. Pushpangadan P, George V, Sreedevi P, Bincy A J, Anzar S, Aswany A S, Ninawe and Ijnu T P (2014). Functional foods and nutraceuticals with special focus on mother and child care, *Annals of Phytomedicine*, 3(1), 4-24.
3. Unnikrishnan Payyappallimana (2010). Role of Traditional Medicine in Primary Health Care: An Overview of Perspectives and Challenges, *Yokohama Journal of Social Sciences*, 14 (6), 57-76.
4. Anonymous (2011). District Census Handbook Palakkad, Series: 33, Part: XII A, (Directorate of Census Operations Kerala).
5. Kushwaha A, Jain S, Bhojwani K and Kalyani G (2018). Concise Synopsis on Quantitative Ethnobotanical Tools for Medicinal Plant Analysis, *International Journal of Pharmaceutical Sciences Review and Research*, 48(1), 128-132.
6. Medeiros M F T, da Silva P S and de Albuquerque U P (2011). Quantification in ethnobotanical research: an overview of indices used from 1995 to 2009, *Sitientibus sér. Ci. Biol.*, 11(2), 211-230.
7. Zumsteg I S and Weckerle C S (2007) Bakera, a herbal steam bath for postnatal care in Minahasa (Indonesia): Documentation of the plants used and assessment of the method. *Journal of Ethnopharmacology* 111(3), 641-650.
8. Sivadasan K K, Anusree D, Anand and Girishkumar E (2014). Documentation of indigenous postnatal mother and child care in Mahe, Union Territory of Puducherry, India, *The Journal of Ethnobiology and Traditional Medicine, Photon*, 122, 860-867.
9. Akram M, Ahmed A, Usmanghani K, Hannan A, Mohiuddin E and Asif M (2010) Curcuma longa and curcumin: a review article. *Romanian Journal of Biology Plant Biology Bucharest* 55(2), 65-70.
10. Mani H, Sidhu G S, Kumari R, Gaddipati J P, Seth P and Maheshwari R K (2002) Curcumin differentially regulates TGF- β 1, its receptors and nitric oxide synthase during impaired wound healing. *Biofactors* 16(1), 29-43.
11. Chainani-Wu N (2004). Safety and Anti-Inflammatory Activity of Curcumin: A Component of Turmeric (*Curcuma longa*). *The Journal of Alternative and Complementary Medicine*, 9(1), (2004), 161-168.
12. Prasad S, Gupta S C, Tyagi A K and Aggarwal B B (2014). Curcumin, a component of golden spice: From bedside to bench and back, *Biotechnology Advances*, 32, 1053-1064.
13. Subarna Kundu, Tuhin Kanti Biswas, Partha Das, De S K and Dipak Kumar (2005). Turmeric (*Curcuma longa*) rhizome paste and honey show similar wound healing potential: a preclinical study in rabbits, *International Journal of Lower Extremity Wounds*, 4(4), 205-213.
14. Karthikeyan V and Periyannayagam K (2013). Wound Healing Activity of the Leaves of *Artocarpus heterophyllus* Lam. (Moraceae) on ex-vivo Porcine Skin Wound Healing Model. *Innovare Journal of LifeScience*, 1(1), 28-33.
15. Babu K, Sabesan G S and Rai S (2010). Comparative Pharmacognostic Studies on the Barks of Four Ficus Species. *Turk J Bot*, 34, 215-224.
16. Rajith N P, Navas M, Thaha A M, Manju M J, Anish N, Rajasekharan S and George V (2010). A Study on Traditional Mother Care Plants of Rural communities of South Kerala, *Indian Journal of Traditional Knowledge*, 9(1), 203-208.





Jayalekshmi Chandran Vasanthakumari

17. Anvar K and Haneef Jazir (2015). Ethnobotanical plants used for postnatal care by traditional practitioners from Kozhikode District, Kerala, India. *International Journal of Research in Pharmacy and Chemistry*, 5(4), ,570-581.

GLOSSARY

Vayattattie : Female Folk medicinal practitioner who is specialized in post-natal care.

Vethuvellam : Medicated water for bathing mother after delivery. The water contains different plant parts like root, stem, leaves, rhizome and petiole of different plant species.

Nalpamara patta: Bark of four different Ficus plant species. *Ficus racemosa*, *Ficus microcarpa*, *Ficus religiosa* and *Ficus benghalensis*

Thalli : Shampoo used to wash hair

Table 1: Plants used as Single Preparations for bathing mother and child after delivery.

SL. No.	Scientific Name	Common name	Family	Part used	Mode of use
1	<i>Plectranthus amboinicus</i> (Lour.) Spreng	Panikurka	Lamiaceae	Leaf	Leaf extract mixed with warm water for bathing
2	<i>Ocimum tenuiflorum</i> L.	Tulsi	Lamiaceae	Leaf	Leaf extract mixed with warm water for bathing
3	<i>Acalypha fruticosa</i> Forssk.	Munja	Euphorbiaceae	Leaf	Leaf paste applied to the body
4	<i>Vigna radiata</i> (L.) R. Wilczek	Cherupayar	Fabaceae	Seed	Seed paste applied to body

Table 2: Combinations of plants used for bathing mother and child after delivery. *comb: Combination of plants

Combination	Scientific name	Common name	Family	Plant part used	Mode of use
Comb 1	<i>Ficus racemosa</i> L.	Athi	Moraceae	Bark	Used in boiling water
	<i>Ficus microcarpa</i> L.f.	Ethi			
	<i>Ficus religiosa</i> L.	Arayal			
	<i>Ficus benghalensis</i> L.	Peral			
Comb 2	<i>Azadirachta indica</i> A. Juss.	Aryaveppu	Meliaceae	Leaf and Bark	Used in boiling water
	<i>Jatropha hernandiifolia</i> Vent.	Kottathari	Euphorbiaceae	Bark	
	<i>Pterocarpus marsupium</i> Roxb.	Venga	Fabaceae	Bark	
Comb 3	<i>Vitex altissima</i> L.f.	Mayilellu	Verbenaceae	Leaf	Used in boiling water
	<i>Cayratia trifolia</i> (L.) Domin.	Vathakkodi	Vitaceae	leaf and stem	
	<i>Getonia floribunda</i> Roxb.	Pullanni	Combretaceae	Leaf	
	<i>Artocarpus heterophyllus</i> Lam.	Plavu	Moraceae	Leaf	
Comb 4	<i>Ficus benghalensis</i> L.	Peral	Moraceae	Bark	Used in boiling water
	<i>Pterocarpus marsupium</i> Roxb.	Venga	Fabaceae	Bark	
	<i>Azadirachta indica</i> A. Juss.	Aryaveppu	Meliaceae	Bark	
	<i>Jatropha hernandiifolia</i> Vent.	Kottathari	Euphorbiaceae	Bark	
	<i>Moringa oleifera</i> Lam.	Muringa	Moringaceae	Bark	
Comb 5	<i>Artocarpus heterophyllus</i> Lam.	Plavu	Moraceae	Leaf	Used in boiling water
	<i>Azadirachta indica</i> A. Juss.	Aryaveppu	Meliaceae	Leaf	
Comb 6	<i>Azadirachta indica</i> A. Juss.	Aryaveppu	Meliaceae	Leaf	Used in boiling water
	<i>Ixora coccinea</i> L.	Chethi	Rubiaceae	Leaf and Flower	
	<i>Mangifera indica</i> L.	Maavu	Anacardiaceae	Bark	
	<i>Azadirachta indica</i> A. Juss.	Aryaveppu	Meliaceae	Bark and leaf	
	<i>Ixora coccinea</i> L.	Chethi	Rubiaceae	Leaf and Flower	





Jayalekshmi Chandran Vasanthakumari

Comb 7	<i>Mangifera indica</i> L.	Maavu	Anacardiaceae	Bark	Used in boiling water
	<i>Ficus racemosa</i> L.	Aathi	Moraceae	Bark	
	<i>Ficus microcarpa</i> L.f.	Ethi	Moraceae	Bark	
	<i>Ficus religiosa</i> L.	Arayal	Moraceae	Bark	
	<i>Ficus benghalensis</i> L.	Peraal	Moraceae	Bark	
	<i>Eucalyptus globulus</i> Labill.	Eucalyptus	Myrtaceae	Leaf	
Comb 8	<i>Quassia indica</i> (Gaertn.) Noot.	Karigotta	Simaroubaceae	Leaf	Used in boiling water
	<i>Mangifera indica</i> L.	Mavu	Anacardiaceae	Leaf	
	<i>Thespesia populnea</i> (L.) Sol.ex Correa	Poovarasu	Malvaceae	Leaf	
	<i>Artocarpus heterophyllus</i> Lam.	Plavu	Moraceae	Leaf	
Comb 9	<i>Artocarpus heterophyllus</i> Lam.	Plavu	Moraceae	Yellow leaf	Used in boiling water
	<i>Justicia adhatoda</i> L.	Adalodakam	Acanthaceae	Leaf	
	<i>Azadirachta indica</i> A. Juss.	Aryaveppu	Meliaceae	Leaf	
	<i>Moringa oleifera</i> Lam.	Muringa	Moringaceae	Bark	
	<i>Jatropha hernandiifolia</i> Vent.	Kottathari	Euphorbiaceae	Bark	
<i>Thespesia populnea</i> (L.)Sol.ex Correa	Poovarasu	Malvaceae	Bark		
Comb 10	<i>Azadirachta indica</i> A. Juss.	Aryaveppu	Meliaceae	leaf and bark	Used in boiling water
	<i>Artocarpus heterophyllus</i> Lam.	Plavu	Moraceae	Leaf	
	<i>Moringa oleifera</i> Lam.	Muringa	Moringaceae	Bark	
Comb 11	<i>Justicia adhatoda</i> L.	Adalodakam	Acanthaceae	Leaf	Used in boiling water
	<i>Ixora coccinea</i> L.	Thechi	Rubiaceae	Leaf	
	<i>Jatropha hernandiifolia</i> Vent.	Kottathari	Euphorbiaceae	Bark	
	<i>Justicia gendarussa</i> Brum.f.	vathamkolli	Acanthaceae	Leaf	
	<i>Artocarpus heterophyllus</i> Lam.	Plavu	Moraceae	Leaf	
<i>Vitex negundo</i> L.	Karinochi	Verbenaceae	Leaf		
Comb 12	<i>Moringa oleifera</i> Lam.	Muringa	Moringaceae	Bark	Used in boiling water
	<i>Mangifera indica</i> L.	Mavu	Anacardiaceae	Leaf	
	<i>Justicia gendarussa</i> Brum.f.	vathamkolli	Acanthaceae	Leaf	
	<i>Jatropha hernandiifolia</i> Vent.	Kottathari	Euphorbiaceae	Bark	
	<i>Azadirachta indica</i> A. Juss.	Aryaveppu	Meliaceae	Leaf	
Comb 13	<i>Ficus benghalensis</i> L.	Peraal	Moraceae	Bark	Used in boiling water
	<i>Borassus flabellifer</i> L.	Pana	Arecaceae	Bark	
	<i>Vitex negundo</i> L.	Karinochi	Verbenaceae	Leaf	
	<i>Achyranthes aspera</i> L.	Kadaladi	Amaranthaceae	Leaf	
Comb 14	<i>Artocarpus heterophyllus</i> Lam.	Plavu	Moraceae	Leaf	Used in boiling water
	<i>Azadirachta indica</i> A. Juss.	Aryaveppu	Meliaceae	Bark	
	<i>Mangifera indica</i> L.	Mavu	Anacardiaceae	Leaf	
	<i>Tamarindus indica</i> L.	Puliyila	Fabaceae	Leaf	
Comb 15	<i>Acalypha fruticosa</i> Forssk.	Chinnayila (munja)	Euphorbiaceae	Leaf	Paste applied to the body
	<i>Acorus calamus</i> L.	Vayambu	Araceae	Leaf	
	<i>Curcuma longa</i> L.	Manjal	Zingiberaceae	Rhizome	
	<i>Psidium guajava</i> L.	Pera	Myrtaceae	Leaf	Used in
	<i>Coffea arabica</i> L.	Kappi	Rubiaceae	Leaf	
	<i>Mangifera indica</i> L.	Mavu	Anacardiaceae	Leaf	
	<i>Clerodendrum infortunatum</i> L.	Peruku	Verbenaceae	Leaf	
	<i>Artocarpus heterophyllus</i> Lam.	Plavu	Moraceae	Yellow leaf	
	<i>Getonia floribunda</i> Roxb.	Pullanji	Combretaceae	Leaf	
	<i>Mussaenda frondosa</i> L.	Vellila	Rubiaceae	Leaf	





Jayalekshmi Chandran Vasanthakumari

Comb 16	<i>Piper nigrum</i> L.	Kurumulaku	Piperaceae	Leaf and stem	boiling water
	<i>Piper longum</i> L.	Thippali	Piperaceae	Leaf and stem	
	<i>Vitex altissima</i> L.f.	Mayilellu	Verbenaceae	Leaf	
	<i>Schleichera oleosa</i> (Lour.) Merr.	Poovam	Sapindaceae	Leaf	

Table 3: List of plants cited in the study for post natal care

SL. No.	Plants cited in the study	Common name	Family	Part Used	Mode of use	Used to
1	<i>Acacia caesia</i> (L.) Willd	Incha	Leguminosae	Bark	Used as scrubber for bathing	Mother
2	<i>Acalypha fruticosa</i> Forssk.	Munja	Euphorbiaceae	Leaf	Leaf paste applied to the body	Child
3	<i>Achyranthes aspera</i> L.	Kadaladi	Amaranthaceae	Leaf	Used in boiling water	Mother
4	<i>Acorus calamus</i> L.	Vyambu	Acoraceae	Leaf	Paste applied to body	Child
5	<i>Anacardium occidentale</i> L.	Kasumavu	Anacardiaceae	Leaf	Used in boiling water	Mother
6	<i>Anethum graveolens</i> L.	Sathakuppa	Apiaceae	Leaf	Used in boiling water	Mother
7	<i>Artocarpus heterophyllus</i> Lam.	Plavu	Moraceae	Yellow Leaf	Used in boiling water	Mother
8	<i>Azadirachta indica</i> A. Juss.	Aryaveppu	Meliaceae	Leaf and bark	Used in boiling water	Mother
9	<i>Borassus flabellifer</i> L.	Karimbana	Arecaceae	Root	Used in boiling water	Mother
10	<i>Calotropis gigantea</i> (L.) Dryand	Eriku	Apocynaceae	Leaf	Used in boiling water	Mother
11	<i>Cayratia trifolia</i> (L.) Domin	Vathakkodi	Vitaceae	Leaf and stem	Used in boiling water	Mother
12	<i>Centella asiatica</i> (L.) Urb.	Kudakan	Apiaceae	Leaf	Used in boiling water	Mother
13	<i>Chrysopogon zizanioides</i> (L.) Roberty	Ramacham	Poaceae	Root	Used in boiling water	Mother
14	<i>Clerodendrum infortunatum</i> L.	Peruku	Lamiaceae	Leaf	Used in boiling water	Mother
15	<i>Clitoria ternatea</i> L.	Sankupushpam	Leguminosae	Root	Used in boiling water	Mother
16	<i>Cocos nucifera</i> L.	Thengu	Arecaceae	Rachis	Used in boiling water	Mother
17	<i>Coffea arabica</i> L.	Kappi	Rubiaceae	Leaf	Used in boiling water	Mother
18	<i>Croton persimilis</i> Mull. Arg	Thorayam	Euphorbiaceae	Leaf	Used in boiling water	Mother
19	<i>Curcuma longa</i> L.	Manjal	Zingiberaceae	Rhizome	Paste applied to the body	Mother and child
20	<i>Cymbopogon flexuosus</i> (Nees ex Steud.) W. Watson	Theruvappullu	Poaceae	Leaf	Used in boiling water	Mother
21	<i>Eucalyptus globulus</i> Labill.	Yucali	Myrtaceae	Leaf	Used in boiling water	Mother
22	<i>Ficus benghalensis</i> L.	Peraal	Moraceae	Bark	Used in boiling water	Mother
23	<i>Ficus microcarpa</i> L.f.	Ethi	Moraceae	Bark	Used in boiling water	Mother
24	<i>Ficus racemosa</i> L.	Athi	Moraceae	Bark	Used in boiling water	Mother
25	<i>Ficus religiosa</i> L.	Arayal	Moraceae	Bark	Used in boiling water	Mother
26	<i>Getonia floribunda</i> Roxb.	Pullanji	Combretaceae	Leaf	Used in boiling water	Mother
27	<i>Glycosmis pentaphylla</i> (Retz.) DC.	Panal	Rutaceae	Leaf	Used in boiling water	Mother
28	<i>Hamelia patens</i> Jacq.	Thettipoo	Rubiaceae	Leaf, Stem	Used in boiling water	





Jayalekshmi Chandran Vasanthakumari

				Flower		Mother
29	<i>Hibiscus rosa-sinensis</i> L.	Chemparathi	Malvaceae	Leaf	Used to prepare shampoo	Mother
30	<i>Ixora coccinea</i> L.	Thechipoo	Rubiaceae	Leaf	Used in boiling water	Mother
31	<i>Jatropha hernandiifolia</i> Vent.	Kottathari	Euphorbiaceae	Bark	Used in boiling water	Mother
32	<i>Justicia adhatoda</i> L.	Adalodakam	Acanthaceae	Leaf	Used in boiling water	Mother
33	<i>Justicia gendarussa</i> Brum. f.	Vathamkolli	Acanthaceae	Leaf	Used in boiling water	Mother
34	<i>Leucas aspera</i> (Willd.) Link.	Thumba	Lamiaceae	Whole plant	Used in boiling water	Mother
35	<i>Mangifera indica</i> L.	Mavu	Anacardiaceae	Leaf and Bark	Used in boiling water	Mother
36	<i>Moringa oleifera</i> Lam.	Muringa	Moringaceae	Bark	Used in boiling water	Mother
37	<i>Musa paradisiaca</i> L.	Vazha	Musaceae	Leaf	Used in boiling water	Mother
38	<i>Mussaenda frondosa</i> L.	Vellila	Rubiaceae	Leaf	Used in boiling water	Mother
39	<i>Ocimum gratissimum</i> L.	Kattutulsi	Lamiaceae	Leaf	Leaf extract mixed with water	Child
40	<i>Ocimum tenuiflorum</i> L.	Tulsi	Lamiaceae	Leaf	Leaf extract mixed with water	Child
41	<i>Piper longum</i> L.	Thipali	Piperaceae	Leaf and stem	Used in boiling water	Mother
42	<i>Piper nigrum</i> L.	Kurumulaku	Piperaceae	Leaf and stem	Used in boiling water	Mother
43	<i>Plectranthus amboinicus</i> (Lour.) Spreng.	Panikurka	Lamiaceae	Leaf	Leaf extract mixed with water	Child
44	<i>Plumbago zeylanica</i> L.	Koduveli	Plumbaginaceae	Root	Used in boiling water	Mother
45	<i>Pongamia pinnata</i> (L.) Pierre	Ungu	Leguminosae	Leaf	Used in boiling water	Mother
46	<i>Premna serratifolia</i> L.	Munja	Lamiaceae	Leaf	Used in boiling water	Child
47	<i>Pseudarthria viscida</i> (L.) Wight & Arn.	Moovila	Leguminosae	Leaf	Used in boiling water	Mother
48	<i>Psidium guajava</i> L.	Pera	Myrtaceae	Leaf	Used in boiling water	Mother
49	<i>Pterocarpus marsupium</i> Roxb.	Venga	Leguminosae	Bark	Used in boiling water	Mother
50	<i>Quassia indica</i> (Gaertn.) Noot.	Karigotta	Simaroubaceae	Leaf	Used in boiling water	Mother
51	<i>Ricinus communis</i> L.	Avanaku	Euphorbiaceae	Leaf and Bark	Used in boiling water	Mother
52	<i>Schleichera oleosa</i> (Lour.) Merr.	Poovam	Sapindaceae	Leaf	Used in boiling water	Mother
53	<i>Sida acuta</i> Brum.f.	Kurumthotti	Malvaceae	Root	Used in boiling water	Mother
54	<i>Stereospermum tetragonum</i> DC.	Karingazha	Bignoniaceae	Leaf	Used in boiling water	Mother
55	<i>Strychnos nux-vomica</i> L.	Kanjiram	Loganiaceae	Leaf	Used in boiling water	Mother
56	<i>Tamarindus indica</i> L.	Puli	Leguminosae	Leaf	Used in boiling water	Mother
57	<i>Terminalia paniculata</i> Roth.	Maruthu	Combretaceae	Leaf	Used in boiling water	Mother
58	<i>Thespesia populnea</i> (L.) Sol. ex Correa	Poovarasu	Malvaceae	Bark	Used in boiling water	Mother
59	<i>Vigna radiata</i> (L.) R. Willczek	Cherupayar	Leguminosae	Seed	Paste applied to the body	Mother and child





Jayalekshmi Chandran Vasanthakumari

60	<i>Vitex altissima</i> L.f.	Mayilellu	Lamiaceae	Leaf	Used in boiling water	Mother
61	<i>Vitex negundo</i> L.	Karinochi	Lamiaceae	Leaf	Used in boiling water	Mother
62	<i>Xylia xylocarpa</i> (Roxb.)	Iruvullu	Leguminosae	Leaf	Used in boiling water	Mother

Table 4: Use value, Consensus index and Relative Frequency of Citation for Different Plant Species

SL.No	Plants cited in the study	UV= U/n	CI= n/N*100	RFC = FC/N
1	<i>Acacia caesia</i> (L.) Willd	0.0283	2.83	0.0283
2	<i>Acalypha fruticosa</i> Forssk.	0.227	23	0.23
3	<i>Achyranthes aspera</i> L.	0.0035	0.35	0.0035
4	<i>Acorus calamus</i> L.	0.0177	1.77	0.0177
5	<i>Anacardium occidentale</i> L.	0.0035	0.35	0.0035
6	<i>Anethum graveolens</i> L.	0.0035	0.35	0.0035
7	<i>Artocarpus heterophyllus</i> Lam.	0.447	45.39	0.4539
8	<i>Azadirachta indica</i> A. Juss.	0.3227	32.27	0.3227
9	<i>Borassus flabellifer</i> L.	0.0283	2.83	0.0283
10	<i>Calotropis gigantea</i> (L.) Dryand	0.0035	0.35	0.0035
11	<i>Cayratia trifolia</i> (L.) Domin	0.0638	6.737	0.06737
12	<i>Centella asiatica</i> (L.) Urb.	0.01418	1.418	0.01418
13	<i>Chrysopogon zizanioides</i> (L.) Roberty	0.0035	0.35	0.0035
14	<i>Clerodendrum infortunatum</i> L.	0.0425	4.6	0.046
15	<i>Cliitoria ternatea</i> L.	0.0035	0.35	0.0035
16	<i>Cocos nucifera</i> L.	0.0567	6.03	0.0603
17	<i>Coffea arabica</i> L.	0.0177	1.77	0.0177
18	<i>Croton persimilis</i> Mull. Arg.	0.0106	1.06	0.0106
19	<i>Curcuma longa</i> L.	0.482	49.64	0.4964
20	<i>Cymbopogon flexuosus</i> (Nees ex Steud.) W. Watson	0.0035	0.35	0.0035
21	<i>Eucalyptus globulus</i> Labill.	0.007	0.7	0.007
22	<i>Ficus benghalensis</i> L.	0.2837	29.1	0.291
23	<i>Ficus microcarpa</i> L.f.	0.2765	28.36	0.2837
24	<i>Ficus racemosa</i> L.	0.2765	28.36	0.2837
25	<i>Ficus religiosa</i> L.	0.2765	28.36	0.2837
26	<i>Getonia floribunda</i> Roxb.	0.039	3.9	0.039
27	<i>Glycosmis pentaphylla</i> (Retz.) DC.	0.0035	0.35	0.0035
28	<i>Hamelia patens</i> Jacq.	0.007	0.7	0.007
29	<i>Hibiscus rosa-sinensis</i> L.	0.0319	3.19	0.0319
30	<i>Ixora coccinea</i> L.	0.0709	7.09	0.0709
31	<i>Jatropha hernandiifolia</i> Vent.	0.0284	2.84	0.0284
32	<i>Justicia adhatoda</i> L.	0.174	17.7	0.177
33	<i>Justicia gendarussa</i> Brum.f.	0.021	2.12	0.021
34	<i>Leucas aspera</i> (Willd.) Link.	0.067	6.7	0.067
35	<i>Mangifera indica</i> L.	0.0567	5.67	0.0567
36	<i>Moringa oleifera</i> Lam.	0.01418	1.418	0.01418
37	<i>Musa paradisiaca</i> L.	0.0035	0.35	0.0035
38	<i>Mussaenda frondosa</i> L.	0.007	0.7	0.007
39	<i>Ocimum gratissimum</i> L.	0.053	5.3	0.053
40	<i>Ocimum tenuiflorum</i> L.	0.0567	6.02	0.0602





Jayalekshmi Chandran Vasanthakumari

41	<i>Piper longum</i> L.	0.0674	7	0.07
42	<i>Piper nigrum</i> L.	0.046	4.6	0.046
43	<i>Plectranthus amboinicus</i> (Lour.) Spreng.	0.0035	0.35	0.0035
44	<i>Plumbago zeylanica</i> L.	0.007	0.7	0.007
45	<i>Pongamia pinnata</i> (L.) Pierre	0.0035	0.35	0.0035
46	<i>Premna serratifolia</i> L.	0.0035	0.35	0.0035
47	<i>Pseudarthria viscida</i> (L.) Wight & Arn.	0.0319	3.19	0.0319
48	<i>Psidium guajava</i> L.	0.014	1.4	0.014
49	<i>Pterocarpus marsupium</i> Roxb.	0.014	1.4	0.014
50	<i>Quassia indica</i> (Gaertn.) Noot.	0.028	2.83	0.028
51	<i>Ricinus communis</i> L.	0.0035	0.35	0.0035
52	<i>Schleichera oleosa</i> (Lour.) Merr.	0.0106	1.06	0.0106
53	<i>Sida acuta</i> Brum.f.	0.007	0.7	0.007
54	<i>Stereospermum tetragonum</i> DC.	0.0035	0.35	0.0035
55	<i>Strychnos nux-vomica</i> L.	0.078	7.8	0.078
56	<i>Tamarindus indica</i> L.	0.0035	0.35	0.0035
57	<i>Terminalia paniculata</i> Roth.	0.0319	3.19	0.0319
58	<i>Thespesia populnea</i> (L.) Sol. ex Correa	0.0035	0.35	0.0035
59	<i>Vigna radiata</i> (L.) R. Willczek	0.078	7.8	0.078
60	<i>Vitex altissima</i> L.f.	0.092	9.2	0.092
61	<i>Vitex negundo</i> L.	0.0213	2.13	0.0213
62	<i>Xylia xylocarpa</i> (Roxb.) Taub.	0.0035	0.35	0.0035

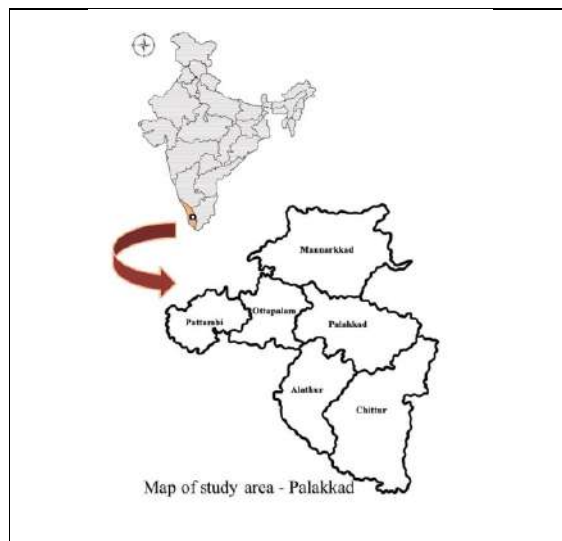


Figure 1: Map of study area

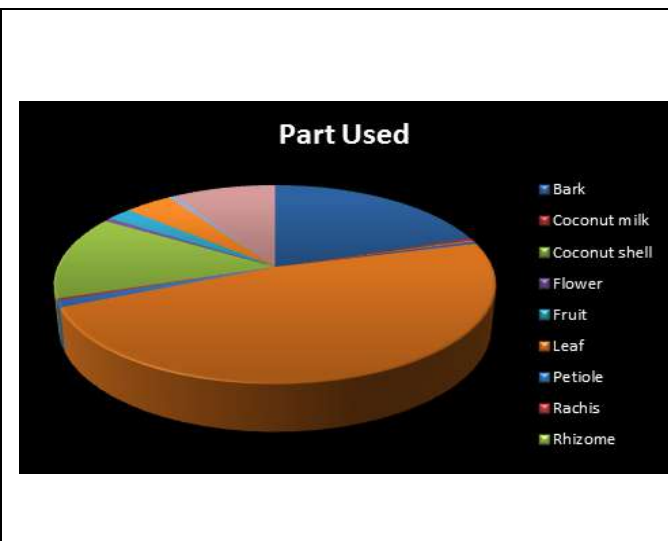


Figure 2: Pie diagram showing percentage of plant parts used





A Review Article: Synthesis and Anticancer Activity of Coumarin Derivatives

Sini Baby¹, Elseena Jose¹, Jeswin Sunny² and Varsha Vinod^{2*}

¹Assistant Professor, Department of Pharmaceutical Chemistry, Nirmala College of Pharmacy, Muvattupuzha, Kerala, India.

²Forth Year B. Pharm Student, Nirmala College of Pharmacy, Muvattupuzha, Kerala, India.

Received: 12 Nov 2021

Revised: 17 Dec 2021

Accepted: 12 Jan 2022

*Address for Correspondence

Varsha Vinod

Forth Year B. Pharm Student,
Nirmala College of Pharmacy,
Muvattupuzha, Kerala, India



This is an Open Access Journal / article distributed under the terms of the **Creative Commons Attribution License** (CC BY-NC-ND 3.0) which permits unrestricted use, distribution, and reproduction in any medium, provided the original work is properly cited. All rights reserved.

ABSTRACT

Cancer is the one of the most leading cause of death globally. Statistics by WHO shows that about 9.6 million deaths have been occurred in 2018. Although treatments are available for various type of cancers, serious adverse effects are drawbacks of these therapies. Coumarins are one of the key compounds in cancer therapy due to increased biological activity and less toxicity. They are commonly used for prostate cancer, renal cell carcinoma and leukaemia. In this review, we have tried to review about the anti-cancer activity of coumarin derivatives and synthesis of some of the derivatives from various research studies.

Keywords: cancer, coumarin derivatives, structure, synthesis, apoptosis

INTRODUCTION

Coumarins are benzopyrone derivatives having antitumor activity. They act by a variety of mechanisms such as carbonic anhydrase inhibition, activation of cell apoptosis protein, inhibition of tumour angiogenesis, inhibition of microtubule polymerization etc. (20) coumarins was first isolated from the plant dipteryxodorata wild belongs to family Fabaceae. Previous studies on coumarin derivatives found out that they have anti-bacterial, antifungal, anti-inflammatory and anti-HIV properties. 7 hydroxycoumarin a coumarin metabolite show cytostatic activity on human cancer cell lines such as HL-60 (leukaemia) MCF-7 (breast) A549 and H727 (lung). It also have cytostatic activity against prostate tumour, metastatic kidney carcinoma. 3,4 hydroxycoumarin derivatives also have antiproliferative activity on gastric carcinoma cell lines. (21)

Synthesis of Various Coumarin Derivatives

3-Acetylcoumarin

In a study synthesis of this compound was as follows; salicylaldehyde (1 eq.) with ethylacetoacetate (1eq.) with a few drops of piperidine were combined at room temperature for 5 minutes without any solvent. The reaction was neutralised with 1M HCl, afterwards the product was filtered out. In EtOH, the finished product was recrystallized





Sini Baby et al.,

[1].Product obtained here is coumarin-chalcone derivative. These coumarin-chalcone derivatives are potent antioxidant and have antitumor activity, various studies have proved that. Compounds such as (E)-7-methoxy-4-(3-oxo-3-phenylprop-1-enyl)-2H-chromen-2-one and (E)-7-hydroxy-4-(3-hydroxy-4-(3-hydroxy-4-(3-hydroxy-4-(3-hydroxy-4-(4-hydroxyphenyl)-3-oxoprop-1-enyl)))-3-oxoprop-1-enyl) which are chalcone derivatives of coumarin had the most effective lethal effect on colon cancer cells [2].

2-[(4-methyl-2-oxo-2H-chromen-7-yl)oxy]-N'-[1-(4-chlorophenyl)ethylidene]acetohydrazide

In a research article synthetic method of this compound is given as; 2-[(4-Methyl-2-oxo-2H-chromen-7-yl)oxy]-acetohydrazide [A] (4, 0.5 mmol) and 1-(4-chlorophenyl)ethan-1-one (0.5 mmol) were agitated at room temperature for 18 hours in acetic acid (10 mL). To achieve white solid 2-[(4-methyl-2-oxo-2H-chromen-7-yl)oxy]-N'-[1-(4-chlorophenyl)ethylidene]acetohydrazide[B], the precipitated solid was filtered and recrystallized from methanol. This Compound had the best anti-proliferative action (IC₅₀= 2.84 0.48 Ig/mL) against the HepG2 cell line, with an IC₅₀ value that was close to doxorubicin (IC₅₀= 2.11 0.13 Ig/mL) [3].

8-Amino-7-hydroxy-4-methyl Coumarin

In a research study, they synthesised this compound by the procedure; iron powder was added portion by portion with stirring to a hot mixture of 8-nitro-7-hydroxy-4-methyl Coumarin (4.4 gm, 0.02 moles) in ethyl alcohol (20 ml) and concentrated hcl (30 ml) at reflux temperature. The refluxing was continued for another 6 hours after the addition was completed. A white precipitate formed when the mixture cooled, which was filtered out, washed with water, dried, and recrystallized [4].

Synthesis of N-(3,4-Dimethoxyphenyl)-4-(4-(((2-oxo-2H-chromen-4-yl)oxy)methyl)1H-1,2,3-triazol-1-yl)benzamide

In a study method of synthesis of this compound was given as, the required arylamine (1 mmol) was added to anhydrous DCM (10 mL) in a 50 mL flask and chilled to 0 °C. Then, under stirring, 4-(4-(((2-hydroxy-2H-1-benzopyran-4-yl)oxy)methyl)-1H-1,2,3-triazol-1-yl)benzoyl chloride (0.2 g, 0.5 mmol) and anhydrous DCM (4 mL) were added dropwise to the cooled mixture. The reaction mixture was agitated for another 4 hours at room temperature after being swirled for 30 minutes. The mixture was evaporated when the reaction was completed (as demonstrated by TLC). To get the desired products, the residue was purified using column chromatography (DCM:MeOH = 50:1) [5].

3-[(Coumarin-4-yl)methyl]-4-arylideneamino-1H-1,2,4-triazole-5(4H)-thione 4c

In a research article synthesis of this compound was done as, 3-[(coumarin-4-yl)methyl]-4-amino-1H-1,2,4-triazole-5(4H)-thione 3 (274 mg, 1 mmol) and the suitable aromatic aldehyde (4-OH,3-MeOC₆H₃) (1 mmol) were heated under reflux for 7 hours in isopropyl alcohol (25 mL) containing three drops of acetic acid. Compounds 4a-c were obtained as yellowish brown powders after the precipitated crude products were filtered, dried, and recrystallized from DMF-EtOH. When this compound was compared against the powerful anticancer medication doxorubicin in a study compounds 4c showed significant cytotoxic activity, with relative potencies of 59.62 percent [6].

Bis(4-hydroxy-2H-chromen-2-one) coumarin.

As per a study, this compound can be synthesised as follows; 4-hydroxycoumarin (2.00g, 12.34mmol) is mixed with either chromone-3-carboxylic acid (1.174g, 6.17mmol, 0.5equiv) or ω-formyl-2-hydroxyacetophenone (1.013g, 6.17mmol, 0.5equiv) (20mL) in chloroform. A catalytic quantity of 4PPy (0.09g, 0.62mmol, 0.05equiv) is added to the solution and allowed to reflux overnight under agitation. The solvent is evaporated after TLC monitoring, and the resultant resinous solid is promptly recrystallized from ethanol to get bis(4-hydroxy-2H-chromen-2-one) coumarin [11].

Anticancer Activity of Coumarin Derivatives

Lung Cancer: Lung cancer is the common type of cancer worldwide accounting for 2.1 million new cases and 1.8 million deaths in 2018. Smoking is one of the main reasons for lung cancer accounting for 80% cases and 90% of deaths



**Sini Baby et al.,**

in lung cancer [22]. Among the newly diagnosed cancer cases, the prevalence of lung cancer is about 14% [23]. Lung cancer is classified into two types; small cell lung cancer (SCLC) (15%) and non-small cell lung cancer (NSCLC) (85%). NSCLC is again classified into 3 types. squamous cell carcinoma(25-30%), adenocarcinoma(40%) ,large cell carcinoma(5-10%) [24]. coumarin derivatives are highly effective in non-small cell lung cancers where drug fails in NSCLC due to drug insuceptibility. Osthole (7-methoxy-8-(3-methyl-2- butenyl) coumarin) which was extracted from *Cnidium monnieri* inhibited the growth of lungs cancer. umbelliprenin which is obtained from *ferula* species induced the apoptosis of large cell cancer and A549 adenocarcinoma cell lines [25].

Ovarian Cancer: Ovarian cancer ranks fifth in cancer deaths among women and the probability of getting ovarian cancer is 1 in 78. This cancer mainly develops in older women [26]. RKS262 is a coumarin derivative and an analogue of nifurtimox. It induces cytotoxic effects on neuroblastoma *in vivo* and *in vitro* and have potent activity in ovarian cancer [25]. Pulchrin A is a natural coumarin derivative obtained from *Enicosanthe llumpulchrum* induced apoptosis in ovarian cancer cells. The cytotoxic effects on CAOV-3 indicates that pulchrin A is more active than cisplatin [27]. Osthole, which is a coumarin derivative is also effective against ovarian cancer. The cell viability is significantly decreased in ovarian cancer cells treated with osthole without effect in normal cells conducted in MTT assays [28].

Hepatocellular Carcinoma: Hepatocellular carcinoma is a common liver malignancy and leading cause of cancer death worldwide. chronic liver disease and liver cirrhosis are the important risk factors for developing hepatocellular carcinoma [29]. Esculetin is a coumarin derivative which inhibits the proliferation of hepatocellular carcinoma cells in a concentration and time dependent manner [30]. Esculetin inhibits proliferation of SMCC-7721 cancer cell lines by causing cell cycle arrest in s phase and cause apoptosis. 8-hydroxypsoralen is another coumarin derivative obtained from peels of wampee showed antiproliferative activity against HepG2 and A549 cancer cell lines [25]. Clausarin is another coumarin derivative which showed high cytotoxic activity against hepatocellular carcinoma and is superior to cisplatin.

Breast Cancer: According to various articles breast cancer is one of the most diagnosed cancer in women and second most cause for cancer death among women [7]. Modifying coumarin molecule to its various derivatives have led to the discovery of some strong pharmacophore with greater activity and selectivity[8]. Selective oestrogen receptor modulators (SERMs) based on coumarin and coumarin-estrogen conjugates have also been proposed as anti-breast cancer medicines [12]. Because the hormone oestrogen plays such an important role in the development of breast cancer, the most common malignancy in women, numerous medicines are designed to limit its activity [9]. *In vitro*, coumarin derivative bis(4-hydroxy-2H-chromen-2-one) coumarin (4HC) suppresses MCF-7 cell growth selectively. In MCF-7 cells, 4HC also has inhibitory effects on aromatase gene expression and promotes apoptosis [10].

Colon Cancer: Colorectal cancer (CRC) is the third most prevalent cancer diagnosis and the second most lethal malignancy in both men and women [13]. Colorectal cancer is on the upswing in developed countries, owing to an ageing population, unfavourable modern dietary habits, and an increase in risk factors like smoking, lack of physical activity, and obesity [14]. In a study, it was investigated that the anti-cancer effects of combining glycyrol (GC) (or its analogue Glycycoumarin /Demethylsuberosin/ Coumestrol), a representative of coumarin compounds found in licorice, with butyrate in HT29 and HCT116 cells, as well as the relationship between the combined anti-cancer effect and structural properties of coumarin compounds. The highest inhibitory effect on cancer cells was caused by the GC/butyrate combination via increased caspase-3 activation, according to the findings in that study [15]. In a study a newly synthesised dicoumarin polysulfide SV25, halted HCT116 colorectal cancer cells in the G2/M phase of the cell cycle and up-regulated bax and cytochrome c levels, as well as caspase 3 and caspase 7 cleavage [16].

Prostate Cancer: Prostate cancer is the most prominent one among men [17]. The prominent risk factors are age and family history. In patients with abnormalities in their prostate-specific antigen (PSA) levels, a prostate biopsy or a digital rectal exam is used to make the diagnosis (DRE) [18]. Various articles have proved that the antiproliferative



**Sini Baby et al.,**

efficacy of coumarin-selenophene derivatives against prostate cancer is significant [19]. Eg:-2-amino-5-(6,8-dibromo-2-oxo-2hchromen-3-yl)selenophene-3-carbonitrile.

CONCLUSION

The presence of coumarin in various medicinal plants has led to the discovery of its therapeutic effects. It has been proven in many studies and researches that they impede the telomerase enzyme, protein kinase activity, and oncogene expression, or elicit capsase – 9 mediated apoptosis, inhibit cancer cell proliferation by halting cell cycle in G0/G1 phase, G2/M phase, and modify cancer cell p-gp. In this review article we explained about some random synthetic methods of coumarins derivatives and usefulness of some coumarin compounds against cancer such as lung cancer, ovarian cancer, hepatocellular cancer, breast cancer, prostate cancer and colon cancer. More coumarin derivatives has to be discovered for their prominent and effective anti-cancer activity. More research should be done to determine the exact mechanism of these drugs so that derivatives with more targeted actions and fewer adverse effects can be developed. Most of the synthesis of coumarin derivatives involve harmful chemicals and catalyst, more researches must be conducted to derive environment effective synthetic method. Even if there is somany coumarin derivatives with different pharmacological activity they are not developed into a formulation, more efforts must be made to effectively formulate these lead compounds.

REFERENCES

1. Savita Patil, Shivani Rajput , Sudha Hospete, Sarita Ircal, Synthesis of coumarin-Chalcone Derivatives, IOSR Journal of Applied Chemistry (IOSR-JAC), 2278-5736. Volume 12, Issue 7 Ser. I (July. 2019), PP 46-51
2. Vincent Jamier, Wioleta Marut, Sergio Valente, Christiane Chereau, Sandrine Chouzenoux, Carole Nicco, Herve Lemarechal, Bernard Weill, Gilbert Kirsch, Claus Jacob, Frederic Batteux ,Chalcone-Coumarin derivatives as potential anti-cancer drugs: an in vitro and in vivo investigation, Anticancer Agents Med Chem. 2014;14(7):963-74. doi: 10.2174/1871520613666131224124445, PMID: 24372527
3. Nongnaphat Duangdee, Wiratchanee Mahavorasirikul and Saisuree Prateeptongkum, Design synthesis and anti-proliferative activity of some new coumarin substituted hydrazide– hydrazone derivatives, J. Chem. Sci. (2020) 132:66.
4. Swayam Sourav Sahoo, Smita Shukla, Subhangankar Nandy and Himanshu Bhusan Sahoo, Synthesis of novel coumarin derivatives and its biological evaluations, European Journal of Experimental Biology, 2012, 2 (4):899-908.
5. Ran An, Zhuang Hou, Jian-Teng Li, Hao-Nan Yu, Yan-Hua Mou and Chun Guo, Design, Synthesis and Biological Evaluation of Novel 4-Substituted Coumarin Derivatives as Antitumor Agents, Molecules. 2018 Sep; 23(9): 2281.
6. Lamy H. Al-Wahaibi, Hanaa M. Abu-Melha and Diaa A. Ibrahim, Synthesis of Novel 1,2,4-Triazolyl Coumarin Derivatives as Potential Anticancer Agents, Journal of Chemistry Volume 2018, Article ID 5201374.
7. Ganesh N. Sharma, Rahul Dave, Jyotsana Sanadya, Piush Sharma, and K. K. Sharma, Various types and management of breast cancer: an overview, J Adv Pharm Technol Res. 2010 Apr-Jun; 1(2): 109–126, PMID: 22247839
8. Rohit Bhatia, Ravindra K. Rawal, Coumarin Hybrids: Promising Scaffolds in the Treatment of Breast Cancer, Mini-Reviews in Medicinal Chemistry, Volume 19 , Issue 17 , 2019, DOI : 10.2174/1389557519666190308122509
9. Jelena Klenkar and Maja Molnar, Natural and synthetic coumarins as potential anticancer agents, Journal of Chemical and Pharmaceutical Research, 2015, 7(7):1223-1238.
10. Ramdani LH, Talhi O, Decombat C, Vermerie M, Berry A, Silva A, Bachari K, Vasson MP, Delort L, Caldefie-Chézet F. Bis(4-hydroxy-2H-chromen-2-one) Coumarin Induces Apoptosis in MCF-7 Human Breast Cancer Cells Through Aromatase Inhibition. Anticancer Res. 2019 Nov;39(11):6107-6114. doi: 10.21873/anticancer.13818. PMID: 31704838.



**Sini Baby et al.,**

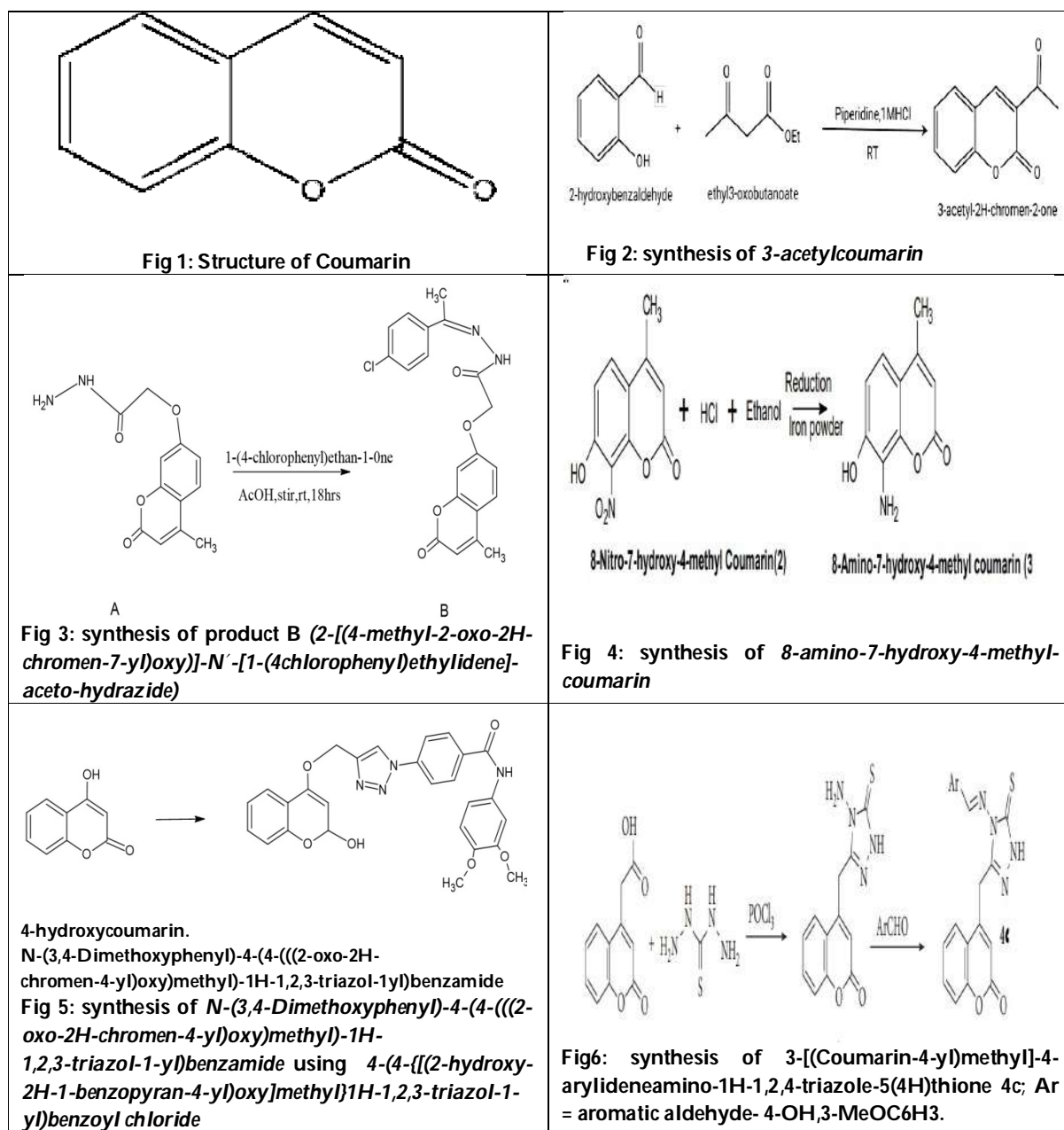
11. OualidTalhi, Michael Schnekenburger, Jana Panning, Diana G. C. Pinto, José A. Fernandes, Filipe A. Almeida Paz, Claus Jacob, Marc Diederich, Artur M. S. Silva, Bis(4hydroxy-2H-chromen-2-one):Synthesis and effects on leukemic cell lines proliferation and NF- κ B regulation, *Bioorganic and medicinal chemistry* 22(2014)3008-3015.
12. Musa MA, Cooperwood JS, Khan MO. A review of coumarin derivatives in pharmacotherapy of breast cancer. *Curr Med Chem.* 2008;15(26):2664-79. doi: 10.2174/092986708786242877. PMID: 18991629; PMCID: PMC3772644.
13. Recio-Boiles A, Cagir B. Colon Cancer. 2021 Jan 25. In: StatPearls [Internet]. Treasure Island (FL): StatPearls Publishing; 2021 Jan-. PMID: 29262132.
14. Kuipers EJ, Grady WM, Lieberman D, Seufferlein T, Sung JJ, Boelens PG, van de Velde CJ, Watanabe T, Colorectal cancer, *Nat Rev Dis Primers*,2015 Nov 5;1:15065. doi: 10.1038/nrdp.2015.65. PMID: 27189416; PMCID: PMC4874655.
15. Lu S, Yin S, Zhao C, Fan L, Hu H. Synergistic anti-colon cancer effect of glycyrol and butyrate is associated with the enhanced activation of caspase-3 and structural features of glycyrol. *Food Chem Toxicol.* 2020 Feb;136:110952. doi: 10.1016/j.fct.2019.110952. Epub 2019 Nov 8. PMID: 31712101.
16. Xu, Ling & Zhao, Xiaoyin & Wu, Yan-Ling & Zhang, Wen. (2015). The Study on Biological and Pharmacological Activity of Coumarins. 10.2991/ap3er-15.2015.33.
17. Litwin MS, Tan HJ. The Diagnosis and Treatment of Prostate Cancer: A Review. *JAMA.* 2017 Jun 27;317(24):2532-2542. doi: 10.1001/jama.2017.7248. PMID: 28655021.
18. Castillejos-Molina, Ricardo Alonso & Gabilondo-Navarro, Fernando. (2016). Prostate cancer. *Salud publica de Mexico.* 58. 279-284. 10.21149/spm.v58i2.7797.
19. Yildirim M, Ersatir M, Arslan B, Gıray ES. Cytotoxic and apoptotic potential of some coumarin and 2-amino-3-carbonitrile selenophene derivatives in prostate cancer. *Turkish Journal of Chemistry.* 2021 ;45(1):192-198. DOI: 10.3906/kim-2008-56. PMID: 33737857; PMCID: PMC7955924.
20. Yi Wu, Jing Xu, Yiting Liu, Yiyu Zeng and Guojun Wu, A Review on Anti-Tumor Mechanisms of Coumarins, *Front. Oncol.*, 04 December 2020,doi-10.3389/fonc.2020.592853
21. EsraKüpelıAkkol, Yasin Genç, BüsraKarpuz, Eduardo Sobarzo-Sánchez and Raffaele Capasso, Coumarins and Coumarin-Related Compounds in Pharmacotherapy of Cancer, doi:10.3390/cancers12071959, *Cancers* 2020, 12(7), 1959;
22. Charles S. Dela Cruz, Lynn T. Tanoue and Richard A. Matthay, Lung Cancer: Epidemiology, Etiology, and Prevention, *Clin Chest Med.* 2011 Dec; 32(4): 10.1016/j.ccm.2011.09.001. PMID: 22054876
23. Kumar M, Singla R, Dandriyal J, Jaitak V. Coumarin Derivatives as Anticancer Agents for Lung Cancer Therapy: A Review. *Anticancer Agents Med Chem.* 2018;18(7):964-984. doi: 10.2174/1871520618666171229185926. PMID: 29298657
24. Zappa C, Mousa SA. Non-small cell lung cancer: current treatment and future advances. *Transl Lung Cancer Res.* 2016 Jun;5(3):288-300. doi: 10.21037/tlcr.2016.06.07. PMID: 27413711; PMCID: PMC4931124.
25. Klenkar, J. & Molnar, Maja. (2015). Natural and synthetic coumarins as potential anticancer agents. *J Chem Pharm Res.* 7. 1223-1238.
26. Zohre Momenimovahed, AzitaTiznobaik, Safoura Taheri and Hamid Salehiniya, Ovarian cancer in the world: epidemiology and risk factors, *Int J Womens Health.* 2019; 11: 287–299. Published online 2019 Apr 30. doi: 10.2147/IJWH.S197604, PMCID: PMC6500433
27. 27] Nordin N, Fadaeinasab M, Mohan S, Mohd Hashim N, Othman R, Karimian H, Iman V, Ramli N, Mohd Ali H, Abdul Majid N. Pulchrin A, a New Natural Coumarin Derivative of Enicosanthellumpulchrin, Induces Apoptosis in Ovarian Cancer Cells via Intrinsic Pathway.
28. PLoS One. 2016 May 2;11(5):e0154023. doi: 10.1371/journal.pone.0154023. PMID: 27136097; PMCID: PMC4852948.
29. 28] Jiang G, Liu J, Ren B, Tang Y, Owusu L, Li M, Zhang J, Liu L, Li W. Anti-tumor effects of osthole on ovarian cancer cells in vitro. *J Ethnopharmacol.* 2016 Dec 4;193:368-376. doi: 10.1016/j.jep.2016.08.045. Epub 2016 Aug 24. PMID: 27566206.10.
30. 29] Julius Balogh,1,2 David Victor, III,1,3,4 Emad H Asham,1,2 Sherilyn Gordon Burroughs,1,2 Maha Bektour,1,2 Ashish Saharia,1,2 Xian Li,1,2 R Mark Ghobrial,1,2 and Howard P Monsour Jr HP, Hepatocellular





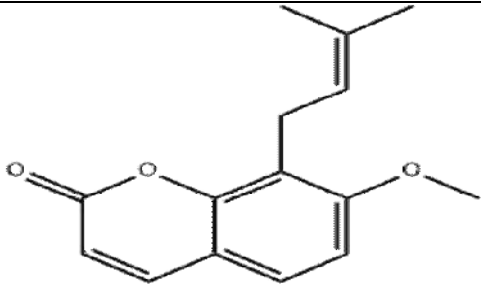
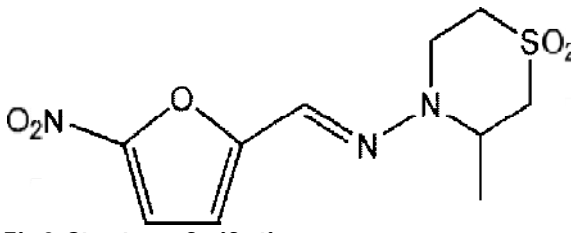
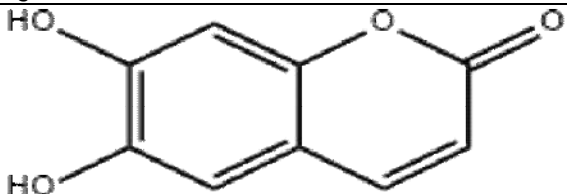
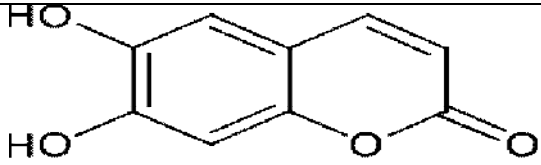
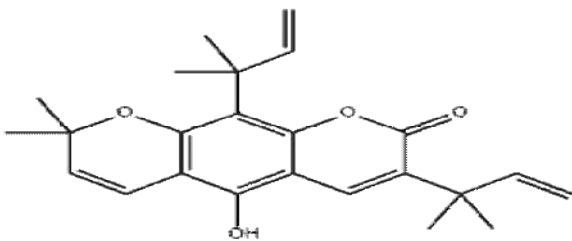
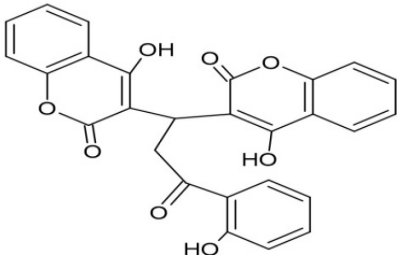
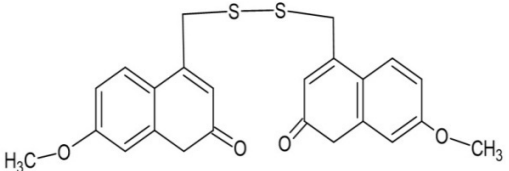
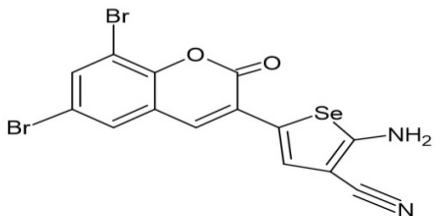
Sini Baby et al.,

- carcinoma: a review, *J Hepatocell Carcinoma*. 2016; 3: 41–53. Published online 2016 Oct 5. doi: 10.2147/JHC.S61146
31. PMID: PMC5063561
32. 30] Wang J, Lu ML, Dai HL, Zhang SP, Wang HX, Wei N. Esculetin, a coumarin derivative, exerts in vitro and in vivo antiproliferative activity against hepatocellular carcinoma by initiating a mitochondrial-dependent apoptosis pathway. *Braz J Med Biol Res*. 2015 Mar;48(3):245-53. doi: 10.1590/1414-431X20144074. Epub 2014 Dec 12. PMID: 25517918; PMCID: PMC4381945.





Sini Baby et al.,

 <p>Fig 7: Structure of osthole</p>	 <p>Fig 8: Structure of nifurtimox</p>
 <p>Fig 9: Structure of esculetin</p>	 <p>Fig 10: Structure of 8-hydroxypsoralen</p>
 <p>Fig 11: Structure of clausarin</p>	 <p>Fig 12: structure of bis(4-hydroxy-2H-chromen-2-one) coumarin.</p>
 <p>Fig 13: structure of SV25</p>	 <p>Fig 14: structure of 2-amino-5-(6,8-dibromo-2-oxo-2h-chromen-3-yl) selenophene-3carbonitrile.</p>





Selected Thiazolidinediones as Inhibitors of Peroxisome Proliferator Activated Receptor

G. Swarnalatha^{1*}, S. Siva Sankara¹, V.Saranya², R. Revathi³ and B. Lakshminarayanan⁴

¹Department of Pharmaceutical Chemistry, Mahathi College of Pharmacy, C.T.M. Cross Roads, Madanapalle Mandal, Chittoor, Andhra Pradesh, India.

²Department of Pharmaceutical Analysis, RVS Padmavathi Ammal College of Pharmacy, Kumaran Kottam Campus, Kannampalayam, Sulur, Coimbatore, Tamil Nadu, India.

³Department of Pharmaceutical Analysis, Pannai College of Pharmacy, Trichy-Dindugal Rd, Mullipadi, Tamil Nadu, India.

⁴Department of Pharmaceutical Chemistry, Ahalia School of Pharmacy, Ahalia Campus, Kozhipara, Palakkad, Kerala, India.

Received: 19 Dec 2021

Revised: 28 Dec 2021

Accepted: 24 Jan 2022

*Address for Correspondence

G. Swarnalatha

Department of Pharmaceutical Chemistry,
Mahathi College of Pharmacy, C.T.M. Cross Roads,
Madanapalle Mandal, Chittoor, Andhra Pradesh, India.



This is an Open Access Journal / article distributed under the terms of the **Creative Commons Attribution License** (CC BY-NC-ND 3.0) which permits unrestricted use, distribution, and reproduction in any medium, provided the original work is properly cited. All rights reserved.

ABSTRACT

People suffering with Diabetes Mellitus increases day by day i.e., Approximately 171 million in 2000 to 366 million by 2030. In every 10 seconds, Diabetes causes one death. It is also associated with adult-onset blindness, cardiovascular disease (CVD) and renal failure. Diabetes could be a future unwellness with unpredictable clinical manifestations and progression. 90% of People around the world are affected with type II diabetes. Thiazolidinediones represents a novel series of oral anti-diabetic drugs that progress metabolic control in Patients with type 2 diabetes by a totally new approach of action. Thiazolidinediones are strong and selective activators of Peroxisome Proliferator Activated Receptor Gamma (PPAR γ). PPAR γ is present principally in adipocytes, where it is complexed to the retinoid X receptor (RXR) inside the nucleus. So, the current project aims for development of synthetic activator of PPAR and evaluates the anti diabetic potential of the synthesized compounds. The present paper deals with the utility of designed compound by molecular docking to assess its anti-diabetic property.

Keywords: PPAR γ , Diabetes Mellitus, Thiazolidinediones.

INTRODUCTION

Medicinal Chemistry is a multifaceted science covering most of the subjects from all backgrounds like life sciences and chemical sciences. Subjects in life sciences include molecular biology, pharmacology, biochemistry, immunology,

38989



**Swarnalatha et al.,**

pharmacokinetics and toxicology. On the other hand subjects in chemical sciences include crystallography, physical chemistry, computer-based information technologies and spectroscopy [1]. Diabetes mellitus is a chronically troubling metabolic disorder which is indicated when levels of blood glucose is raised and changes in by elevated blood glucose levels and changes in protein, carbohydrates and fats metabolism Irregularities in the metabolism, are results of defected insulin production combined with insulin action. Disturbance in the insulin production (or) function leads to raise the glucose levels in blood. Due to raise in the levels of glucose, health issues will occur in a high range[2]. The chronic elevation of glucose levels of diabetes is implicated by damage and collapse of multiple organs. This is the condition where serious problems will occur such as peripheral vascular disorders, retinopathy and neuropathy One of the serious problem due to diabetes is blindness caused due to chronic cataracts (when cloudiness is caused due to raise in glucose levels attached the lens) or to damage the retinal blood vessels. Severe kidney complication also results from the damage to blood vessels in the kidney. Diabetic patients usually develop delaying or impairing in wound healing and will give rise to chronic foot ulcers [3].

The prevalence of diabetes is increasing worldwide in adult constituents is a international public health hurdle [4], Regions with the greatest incidence are Africa & Asia [5]. The worldwide prevalence of DM is estimated to be more than 240million by 2010[6]. The countries having the highest diabetic population in 2025 probably will be United States, China and India. In the upcoming years diabetes is being portrayed as the world's worst cause for human disability [7]. People suffering with diabetes in India are larger than thirty million. In the US, DM is the 4th primary source of deaths mainly due to the cardiac failure and circulatory system damage. Diabetes was described since ages more than 2000 years ago and for the past 200 years, it has been a challenge to the modern medicine. With the insulin discovery. The study in DM at both clinical and cellular levels has expanded as fast new laboratory and diagnostic techniques allow. At present there are many medicines for diabetes mellitus like Sulfonylureas and Biguanides to control elevated glucose. These drugs have many side effects and thereby investigations for a novel category of molecules is needed to solve complications associated with DM. Controlling of DM without any side effects is still a major hurdle to the medical practitioners[8].

The peroxisome proliferator activated receptor-gamma (PPARY), is a nuclear receptor [9], which play a key position in altering the expression of a many genes concerned in lipid metabolism and energy balance [10, 11]. The presence of (PPARY) in the emulsion nexus is suitable to raise the distinction of lipocytes, and adding the insulin perceptivity, and control the circumstance of complications. Thiazolidinediones (TZDs) are high- affinity picky agonists of (PPARY), which regulate glucose metabolism associated with insulin resistance without causing medicines are initiate to motive side goods including high weight gain and pedal edema [12,13]. Dual agonists of PPARa and PPARY combined reported as useful treatment of hyperglycemia and hyperlipidemia [14]. But they initiated unfavorable effects like edema, carcinogenicity in rodent toxicity models. There had been many unsuccessful efforts to develop dual agonists. So, the current project aims for development of synthetic activator of PPARY and evaluates the anti diabetic potential of the synthesized compounds. The present paper deals with the utility of designed compound by molecular docking to assess its anti-diabetic property.

MATERIALS AND METHODS

The information concerning the planned compounds was retrieved from PubChem database. The ligands are mentioned in the Table 1. The two-dimensional (2D) chemical structures of the ligands be sketched using ChemDraw Ultra 2008, and the energy minimizations of the arranged ligands were carried out with Chem3D Ultra and were saved in pdb format.

Target Preparation and Validation of Docking Method

The 3D structure of protein was get from Brook haven protein databank (PDB ID: 1ZEO). The docking study was underway with the definition of a binding site, in general a restricted region of the protein. The size and site of this binding site was visualized in PyMOL. The protein target was further validated with AutoDock Vina in PyRx 0.8 by



**Swarnalatha et al.,**

RMSD value determination 8. Molecular Docking investigation Binding mode and interaction of Protein (5FBH) with individual ligand, was carried out using AutoDock Vina software. Docking was performed to obtain a population of probable conformations and orientations for the ligand at the binding site. The protein was loaded in PyRx software, creating a PDBQT file that contains a protein structure with hydrogens in all polar residues. All the bonds of ligands were set to be rotatable. All calculations for protein-fixed ligand-flexible docking were done using the Lamarckian Genetic Algorithm (LGA) method. The docking site on protein target was defined by establishing a grid box with the dimensions of X: 38.0729 Y: 33.3208 Z: 25.0000 Å, with a grid spacing of 0.375 Å, centered on X: 20.2892 Y: 10.3219 Z: 32.3218 Å. The best conformation was chosen with the lowest docked energy, after the docking look for was completed. 10 runs with AutoDock Vina were performed in all cases per each ligand structure, and for each run the best pose was saved. The normal affinity for best poses was taken as the final affinity value. The connections of complex protein-ligand conformations, together with hydrogen bonds and the bond lengths was analyzed using PyMol.

RESULTS AND DISCUSSION

Docking of little molecule compounds into the binding site of a receptor and assess the binding affinity of the complex is a vital part of the structure based drug design method. AutoDock Vina is an open-source program for drug discovery, molecular docking and virtual screening, contribution multicore potential, high performance and improved accuracy and ease to of use. Docking of 1ZEO protein with 08 ligands were done by AUTODOCK VINA software and dock scores of these molecules were represented in (Table 2, Fig 1), with their binding affinity and types of bonds with which different amino acids bonded to the ligand's different functional groups. Binding affinity of the protein-ligand interactions are important to describe how fit the drug binds to the target macromolecules. In the present study, the results generated by AutoDock Vina revealed that binding energies of the protein-ligand (drug) interactions are important to describe how fit the drug binds to the target macromolecule. The Ligands (i) A1 (-8.7); (ii) A2 (-9.2); (iii) A3 (-8.7); (iv) A4 (-8.6); (v) A5 (-9.0); (vi) A6 (-8.8); (vii) A7 (-8.9); (viii) A8 (-10.5); and Standard Pioglitazone (-9.1) docks into good the binding pockets of 1ZEO protein. Ligand A8(-10.5), A2(-9.2) & A5(-9.0) showed the highest binding affinity values were shown high inhibition activity towards the target protein molecules among 8 compounds when compared to the standard Pioglitazone (-9.1 kcal/mol⁻¹).

CONCLUSION

A number of recently designed Thiazolidinediones analogs were docked into the active sites of crystal structures of Human PPAR-gamma Ligand Binding Domain (PDB ID: 1ZEO) in order to probe the possible relations between the designed Thiazolidinediones analogs and the active site of the PPAR. The binding affinity of the ligands with the maximum docking scores was carried out and were compared with that of the Standard drug Pioglitazone. All the analogs showed good interactions with the target protein 1ZEO but the analog A8, A2 & A5 showed the greatest interaction with the target. Hence the analog A8, A2 & A5 can be projected as the best out of all analogs and can be recommended as drug for future research. The recommended compounds can provide priceless information for persistent search, discovery and design of novel potent antidiabetic agents.

REFERENCES

1. Gao-Jie Ye TL, Zhi-xin H, Xiao-Ning C, Chao-yun C, Sen-miao D, Min-lixie, Bo W. Design and synthesis of novel xanthone-triazole derivatives as potential anti diabetic agents- alpha Glucosidase inhibition and glucose uptake promotion. European Journal of Medicinal chemistry. 2019; 177: 362-373.
2. Kathryn AP, Israel D, Dima K and Sandor V. What method to use for protein-protein docking?, Current Opinion in Structural Biology. 2019; 55: 1-7.
3. Kamal KC and Nidhi M. A Review on Molecular Docking Novel Tool for Drug Discovery. JSM Chemistry. 2016; 4: 1029,

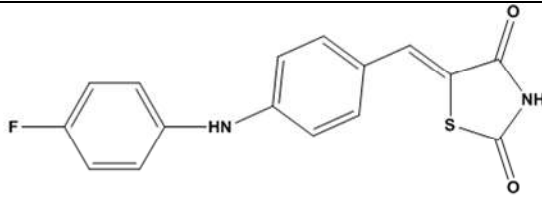
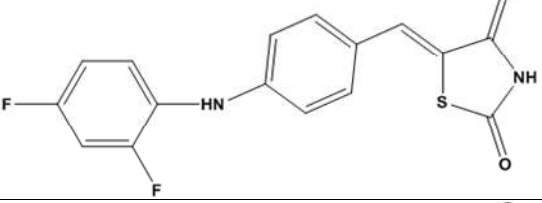
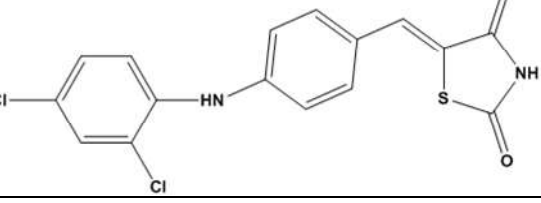




Swarnalatha et al.,

4. Leonardo GF, Ricardo ND, Glaucius O and Adriano DA Molecular Docking and Structure-Based Drug Design Strategies. *Molecules*. 2015; 20: 13384-13421.
5. Jamshid M and Prakash RN, Evaluation of hypoglycemic effect of *Morus alba* in an animal model. *Indian Journal of Pharmacology*. 2008; 40: 15-18.
6. Lateef H, Abatan OI, Aslam MN, Strevens MJ and Varani J, Topical Pretreatment of diabetic rats with all-trans retinoic acid improves healing of subsequently induced abrasion wound. *Diabetes*. 2005; 54: 855-861.
7. Frode TS and Medeiros YS. Animal models to test drug with potential Antidiabetic activity. *Journal of Ethanopharmacology*. 2008; 115: 173-183.
8. Chauhan NS and Dixit VK, Antihyperglycemic activity of ethanolic extract of *Curculigo orchioides* Gaerth. *Pharmacognosy Magazine*. 2007; 3: 237-240.
9. Frier BM, Fisher M. Diabetes mellitus, In: David Son's, Principles & Practice of medicine, edited by Nicholas A Boon, Nicki R Colledge, Brain P Walker and John AA Hunter, 20 edition, Churchill Livingstone Elsevier, Philadelphia, USA, 2006.
10. Anirban M and Abul KA. The Endocrine System, In: Robbins & Cotran, Pathologic Basis of Disease, 7ed., Published by Elsevier, a division of Reed Elsevier India private limited, New Delhi, India, 2004.
11. Noor A, Gunasekharan S, Manickam AS, Vijayalakshmi MA. Antidiabetic activity of Aloe vera and histology of organs in streptozotocin induced diabetic rats. *Current Science*. 2008; 94: 1070-1076.
12. Alan RS and Jerrold MO. Thiazolidinediones in the Treatment of Insulin Resistance and Type II Diabetes. *Diabetes*. 1996; 45: 1661-1669.
13. Isseman I and Green S. Activation of a member of the steroid hormone receptor superfamily by peroxisome proliferators. *Nature*. 1990; 347: 645-650.
14. Iqbal AKM, Kalashetti MB, Belavagi NS, Gong Y and Khazi IAM, Synthesis, hypoglycemic and hypolipidemic activities of novel thiazolidinedione derivatives containing thiazole/triazole/oxadiazole ring. *European journal of medicinal chemistry*. 2012; 53: 308-315.
15. Costantino L, Rastelli G, Gamberoni MC and Barlocco D. Pharmacological Approaches to the treatment of diabetic complications. *Experts Opinion on Therapeutic Patents*. 2000; 10: 1245-1262.

Table 1. Molecular structure of design compounds for molecular docking studies

Code	Structure
1	
2	
3	





Swarnalatha et al.,

4	
5	
6	
7	
8	
09(standard) pioglitazone	

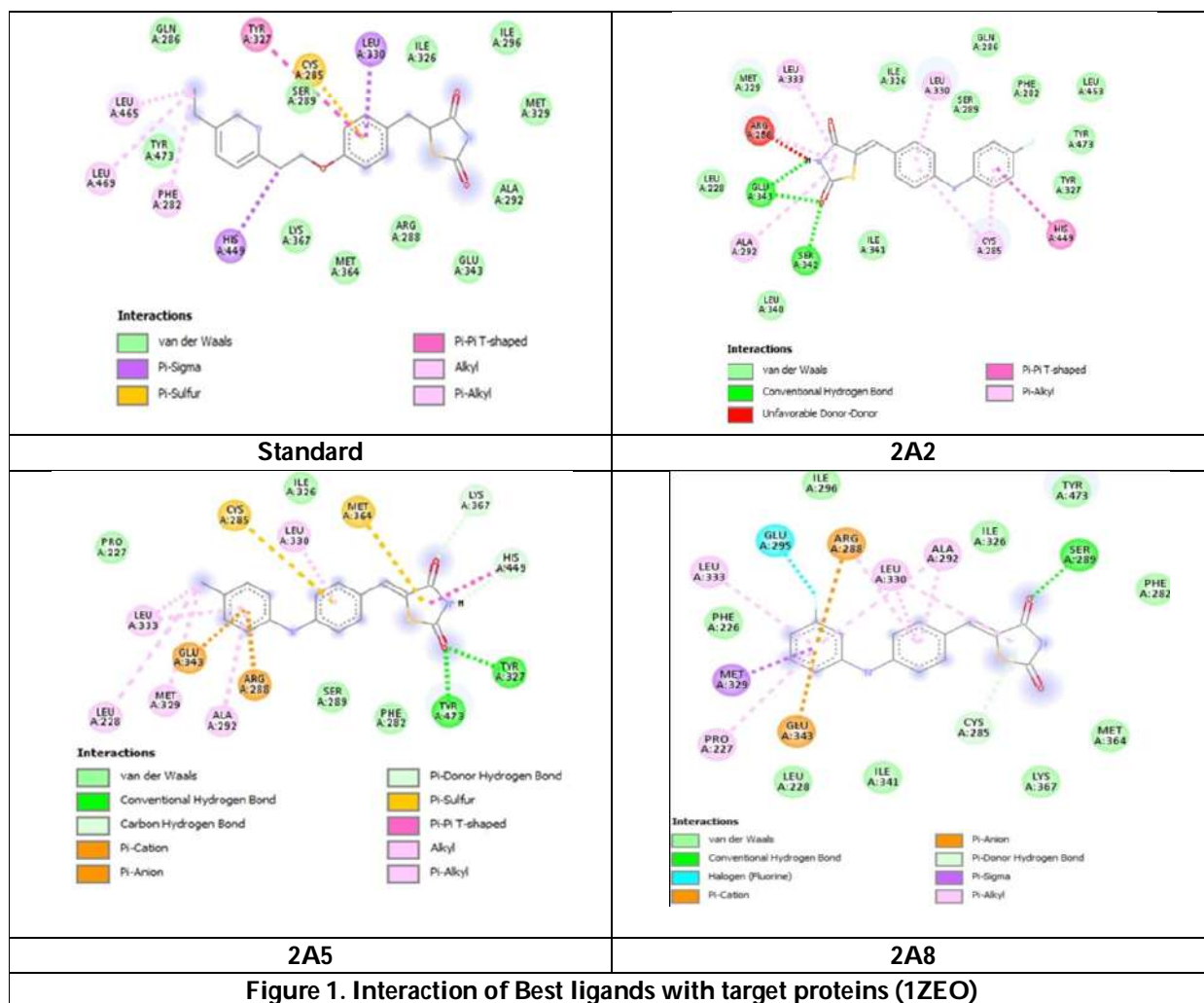




Swarnalatha et al.,

Table 2. Docking results of designed molecules docked on to PPAR Protein (1ZEO)

S.No	Compound code	Binding energy(Kcal/mol)
01	A1	-8.7
02	A2	-9.2
03	A3	-8.7
04	A4	-8.6
05	A5	-9.0
06	A6	-8.8
07	A7	-8.9
08	A8	-10.5
09	Pioglitazone	-9.1





Y-Index of Four New Tensor Products of Graphs and Their Complements

V. Sheeba Agnes^{1*} and C. Kannadasan²

¹Assistant Professor, Department of Mathematics, Annamalai University, Annamalainagar-608002, Tamil Nadu, India.

²Research Scholar, Department of Mathematics, Annamalai University, Annamalainagar-608002, Tamil Nadu, India.

Received: 28 Nov 2021

Revised: 22 Dec 2021

Accepted: 19 Jan 2022

*Address for Correspondence

V. Sheeba Agnes

Assistant Professor,

Department of Mathematics,

Annamalai University,

Annamalainagar-608002, Tamil Nadu, India.



This is an Open Access Journal / article distributed under the terms of the **Creative Commons Attribution License** (CC BY-NC-ND 3.0) which permits unrestricted use, distribution, and reproduction in any medium, provided the original work is properly cited. All rights reserved.

ABSTRACT

The Y-index is defined as the sum of fourth degree of all vertices of the graph. In this paper, we calculate Y-index of four new tensor products of graphs and Their complements

Keywords: Tensor product; Zagreb index; F-index; Y-index

INTRODUCTION

A topological index is a numerical quantity related to a graph that is invariant under graph automorphisms. It does not depend on the labeling or pictorial representation of a graph. A topological index related to distance is called a distance based topological index. The topological indices and graph invariants based on distances between vertices of a graph are widely used for characterizing molecular graphs, establishing relationships between structure and properties of molecules, predicting biological activity of chemical compounds, and making their chemical applications. The Wiener index is one of the most used topological indices with high correlation with many physical and chemical indices of molecular compounds. It is used in the study of paraffin boiling points. There are some topological indices based on degrees of vertices in a graph such as the first and second Zagreb indices of molecular graphs. The *Cartesian product* of the graphs G and H , denoted by $G \square H$, has the vertex set $V(G \square H) = V(G) \square V(H)$ and $(u, x)(v, y)$ is an edge of $G \square H$ if (i) $u = v$ and $xy \in E(H)$ or, (ii) $x = y$ and $uv \in E(G)$ [3]. Graph operations play an important role in obtaining some chemically important structures. For example, C_4 -nanotorus, C_4 -nanotube, planar grids, n -prism and Rook's graph are the graphs $C_m \square C_n, P_m \square C_n, P_n \square P_m, K_2 \square C_m$ and $K_n \square K_m$, respectively. Definitions of all these graphs can be found in [10]. For more on product related graph operations we refer a book by Imrich and Klavazar [13].





Sheeba Agnes and Kannadasan

Definition and Preliminaries

All graphs considered here are simple, finite, connected and undirected.

Let $G = (V(G), E(G))$ be a connected graph of order n with $|E(G)| = m$ edges. The complement of a graph G is denoted by \bar{G} and is defined as the graph whose vertex set is $V(G)$ in which two vertices are adjacent in \bar{G} if and only if these are not adjacent in G . Obviously, \bar{G} has n vertices and $\binom{n}{2} - m$ edges. The *neighbourhood* of a vertex $u \in V(G)$ is defined as the set $N_G(u)$ consisting of all vertices v which are adjacent to u in G . The *degree* of a vertex $u \in V(G)$, denoted by $d_G(u)$ and is equal to $|N_G(u)|$.

For a molecular graph G , the *First Zagreb index* was defined by Gutman and Trinajstić [12] in 1972 as

$$M_1(G) = \sum_{v \in V(G)} d_G(v)^2$$

which can also be expressed as

$$M_1(G) = \sum_{uv \in E(G)} [d_G(u) + d_G(v)]$$

The *Second Zagreb index* was defined in [11] as

$$M_2(G) = \sum_{uv \in E(G)} d_G(u)d_G(v)$$

The *first and second Zagreb coindex* was introduced by A.R Ashrafi *et.al.* in [2] which is defined as

$$\bar{M}_1(G) = \sum_{uv \notin E(G)} [d_G(u) + d_G(v)], \quad \bar{M}_2(G) = \sum_{uv \notin E(G)} [d_G(u)d_G(v)]$$

In [9] Furtula and Gutman recently investigated forgotten topological index. The *F-index* of a graph G is defined as

$$F(G) = \sum_{v \in V(G)} d_G(v)^3 = \sum_{uv \in E(G)} [d_G(u)^2 + d_G(v)^2].$$

In [6] N. De *et.al.* recently investigated, *F-coindex* of some graph operations. The *F-coindex* of a graph G is defined as

$$\bar{F}(G) = \sum_{uv \notin E(G)} [d_G(u)^2 + d_G(v)^2].$$

In [14] G.H. Shirdel *et al.* investigated, *Hyper-Zagreb index* of graph operations. The *Hyper-Zagreb index* of a graph G is defined as

$$HM(G) = \sum_{uv \in E(G)} [d_G(u) + d_G(v)]^2$$

The *Y-index* was introduced by Abdu Alameri *et.al.* in [1] which is defined as

$$Y(G) = \sum_{u \in V(G)} d_G(u)^4 = \sum_{uv \in E(G)} [d_G(u)^3 + d_G(v)^3]$$

In [15] the *sum-connectivity index* of a graph G is defined as

$$\chi(G) = \sum_{xy \in E(G)} [d_G(x) + d_G(y)]^{-\frac{1}{2}}.$$

In [16] the *general sum-connectivity index* of a graph G is defined as





Sheeba Agnes and Kannadasan

$$\chi_\alpha(G) = \sum_{xy \in E(G)} [d_G(x) + d_G(y)]^\alpha$$

where α is any real number. For $\alpha = 4$, we have

$$\chi_4(G) = \sum_{xy \in E(G)} [d_G(x) + d_G(y)]^4$$

For a graph $G = (V(G), E(G))$, there are four related transformation graphs as follows:

- The *subdivision graph* $S(G)$ of a graph G is a graph obtained by inserting a new vertex onto each edge of G .
- *Semitotal-point graph* $T_2(G)$ of a graph G is a graph with vertex set $V(G) \cup E(G)$ and edge set $E(S) \cup E(L)$ which is obtained from G by adding a new vertex corresponding to each edge of G and by joining each new vertex to the end vertices of the edge corresponding to it.
- *Semitotal-line graph* $T_1(G)$ of a graph G is a graph with vertex set $V(G) \cup E(G)$ and $E(S) \cup E(L)$ which is obtained from G by inserting a new vertex into each edge of G and by joining with edges those pair of these new vertices which lie on adjacent edges of G .
- *Total graph* $T(G)$ of a graph G is a graph with vertex set $V(G) \cup E(G)$ and edge set $E(S) \cup E(G) \cup E(L)$ and any two vertices of $T(G)$ are adjacent if and only if they are either incident or adjacent in G .

Here $L = L(G)$ is the line graph of a graph G , in which the vertices are the edges of G and two vertices in $L(G)$ are adjacent if and only if the corresponding edges are adjacent in G .

In [8] M. Eliasi *et.al.* investigated four new operations on graphs as follows:

Let $F \in \{S, T_2, T_1, T\}$. The F -sums of two graphs $G_1 = (V(G_1), E(G_1))$ and $G_2 = (V(G_2), E(G_2))$, denoted by $G_1 +_F G_2$, is a graph with the set of vertices $V(G_1 +_F G_2) = (V(G_1) \cup E(G_1)) \times V(G_2)$ and two vertices (u_1, v_1) and (u_2, v_2) of $G_1 +_F G_2$ are adjacent if and only if $[u_1 = u_2 \in V(G_1)]$ and $v_1 v_2 \in E(G_2)$ or $[v_1 = v_2 \in V(G_2)]$ and $u_1 u_2 \in E(F(G_1))$. Thus, four new graph operations, namely, $G_1 +_S G_2, G_1 +_{T_2} G_2, G_1 +_{T_1} G_2$ and $G_1 +_T G_2$ are obtained and the Wiener indices of these graphs have been studied [8]. In [7], Deng et al. have given the expression for first and second Zagreb indices of these new graphs. The *tensor product* $G_1 \times G_2$ of two graphs G_1 and G_2 of order n_1 and n_2 , respectively, is defined as the graph with vertex set $V_1 \times V_2$ and (u_1, v_1) is adjacent with (u_2, v_2) if and only if $u_1 u_2 \in E(G_1)$ and $v_1 v_2 \in E(G_2)$ [13].

In [5] Basavanagoud et al. introduced four new tensor products of graphs by extended F -sums of graphs on cartesian product to tensor product as follows:

Let \mathcal{F} be the one of the symbols S, T_2, T_1 or T . The \mathcal{F} -tensor product $G_1 \times_{\mathcal{F}} G_2$ is a graph with the set of vertices $V(G_1 \times_{\mathcal{F}} G_2) = (V(G_1) \cup E(G_1)) \times V(G_2)$ and two vertices (u_1, v_1) and (u_2, v_2) of $G_1 \times_{\mathcal{F}} G_2$ are adjacent if and only if u_1 is adjacent to u_2 in $E(\mathcal{F}(G_1))$ and v_1 is adjacent to v_2 in G_2 . In [5] be calculated four new graph operations namely $G_1 \times_S G_2, G_1 \times_{T_2} G_2, G_1 \times_{T_1} G_2$ and $G_1 \times_T G_2$ as depicted in Fig.2 and studied the first and second Zagreb indices of these graphs. This motivates us to study the Y -index of \mathcal{F} -tensor products of graphs and their complements in this paper.

First, we like to mention some existing results which are used to prove our results.

Theorem 2.1 [5] *If G_1 and G_2 are two graphs with $|V(G_i)| = n_i$ and $|E(G_i)| = m_i, i = 1, 2$, then*

- $M_1(G_1 \times_S G_2) = M_1(G_2)[M_1(G_1) + 4m_1]$
- $M_1(G_1 \times_{T_2} G_2) = 4M_1(G_2)[M_1(G_1) + m_1]$
- $M_1(G_1 \times_{T_1} G_2) = M_1(G_2)[M_1(G_1) + HM(G_1)]$
- $M_1(G_1 \times_T G_2) = M_1(G_2)[4M_1(G_1) + HM(G_1)].$

Theorem 2.2 [5] *If G_1 and G_2 are two graphs with $|V(G_i)| = n_i$ and $|E(G_i)| = m_i, i = 1, 2$, then $|V(G_1 \times_{\mathcal{F}} G_2)| = n_2(n_1 + m_1)$ and*

- $|E(G_1 \times_S G_2)| = 4m_1 m_2$





Sheeba Agnes and Kannadasan

- $|E(G_1 \times_{T_2} G_2)| = 6m_1m_2$
- $|E(G_1 \times_{T_1} G_2)| = [M_1(G_1) + 2m_1]m_2$
- $|E(G_1 \times_T G_2)| = 4m_1m_2 + m_2M_1(G_1)$.

Theorem 2.3 [4] If G_1 and G_2 are two graphs with $|V(G_i)| = n_i$ and $|E(G_i)| = m_i, i = 1, 2$, then

- $F(G_1 \times_S G_2) = F(G_2)[F(G_1) + 8m_1]$
- $F(G_1 \times_{T_2} G_2) = 8F(G_2)[F(G_1) + m_1]$
- $F(G_1 \times_{T_1} G_2) = F(G_2)[F(G_1) + \chi_3(G_1)]$
- $F(G_1 \times_T G_2) = F(G_2)[8F(G_1) + \chi_3(G_1)]$.

Basic Properties Of Y-Coindex

In this section, first we give Y –coindex of some special graphs such as, complete graph K_n , cycle C_n , path P_n , star S_n and bipartite graph $K_{m,n}$ on n vertices and m edges.

- $\bar{Y}(K_n) = 0$.
- $\bar{Y}(C_n) = 8n(n - 3)$.
- $\bar{Y}(P_n) = 8n^2 - 38n + 44$.
- $\bar{Y}(S_n) = nm - n - m + 1$.
- $\bar{Y}(K_{m,n}) = mn(mn^2 + m^2n) - mn(n^2 + m^2)$

Now, we give some properties relating Y –index and its coindex.

Theorem 3.1 Let G be a simple graph with n vertices and m edges, then

$$Y(\bar{G}) = n(n - 1)^4 - 8m(n - 1)^3 + 6(n - 1)M_1(G) - 4(n - 1)F(G) + Y(G).$$

Proof. From definition of Y –index, we have

$$\begin{aligned} Y(\bar{G}) &= \sum_{v \in V(G)} [d_{\bar{G}}(v)^4] \\ &= \sum_{v \in V(G)} [n - 1 - d_G(v)]^4 \\ &= \sum_{v \in V(G)} [(n - 1)^4 - 4(n - 1)^3d_G(v) + 6(n - 1)^2d_G(v)^2 - 4(n - 1)d_G(v)^3 + d_G(v)^4] \\ &= n(n - 1)^4 - 8m(n - 1)^3 + 6(n - 1)M_1(G) - 4(n - 1)F(G) + Y(G). \end{aligned}$$

Theorem 3.2 Let G be a simple graph with n vertices and m edges, then

$$= \sum_{uv \in E(\bar{G})} [\{n - 1 - d_{\bar{G}}(u)\}^3 + \{n - 1 - d_{\bar{G}}(v)\}^3]$$

Proof. From definition of Y –coindex, we have

$$\begin{aligned} \bar{Y}(G) &= \sum_{w \in E(G)} [d_G(u)^3 + d_G(v)^3] \\ &= \sum_{uv \in E(\bar{G})} [\{n - 1 - d_{\bar{G}}(u)\}^3 + \{n - 1 - d_{\bar{G}}(v)\}^3][4] \\ &= \sum_{uv \in E(\bar{G})} [\{(n - 1)^3 - 3(n - 1)^2d_{\bar{G}}(u) + 3(n - 1)d_{\bar{G}}(u)^2 - d_{\bar{G}}(u)^3\} \\ &\quad + \{(n - 1)^3 - 3(n - 1)^2d_{\bar{G}}(v) + 3(n - 1)d_{\bar{G}}(v)^2 - d_{\bar{G}}(v)^3\}] \\ \bar{Y}(G) &= 2 \left[\binom{n}{2} - m \right] (n - 1)^3 - 3(n - 1)^2M_1(\bar{G}) + 3(n - 1)F(\bar{G}) - Y(\bar{G}). \end{aligned}$$

Theorem 3.3 Let G be a simple graph with n vertices and m edges, then

$$\bar{Y}(G) = (n - 1)F(G) - Y(G).$$





Sheeba Agnes and Kannadasan

Proof. From definition of Y -index and Y -coindex, it follows that

$$\begin{aligned} Y(G) + \bar{Y}(G) &= \sum_{uv \in E(G)} [d_G(u)^3 + d_G(v)^3] + \sum_{w \notin E(G)} [d_G(u)^3 + d_G(v)^3] \\ &= \sum_{uv \in V(G)} [d_G(u)^3 + d_G(v)^3] \\ &= (n-1) \sum_{v \in V(G)} d_G(v)^3 \end{aligned}$$

$$\bar{Y}(G) = (n-1)F(G) - Y(G).$$

Theorem 3.4 Let G be a simple graph with n vertices and m edges, then

$$\bar{Y}(\bar{G}) = 2m(n-1)^3 - 3(n-1)^2M_1(G) + 3(n-1)F(G) - Y(G).$$

Proof. From definition of Y -coindex, we have

$$\begin{aligned} \bar{Y}(\bar{G}) &= \sum_{uv \in E(\bar{G})} [d_{\bar{G}}(u)^3 + d_{\bar{G}}(v)^3] \\ &= \sum_{uv \in E(G)} [(n-1) - d_G(u)]^3 + [(n-1) - d_G(v)]^3 \\ &= \sum_{uv \in E(G)} [(n-1)^3 - 3(n-1)^2d_G(u) + 3(n-1)d_G(u)^2 - d_G(u)^3] \\ &\quad + [(n-1)^3 - 3(n-1)^2d_G(v) + 3(n-1)d_G(v)^2 - d_G(v)^3] \\ \bar{Y}(\bar{G}) &= 2m(n-1)^3 - 3(n-1)^2M_1(G) + 3(n-1)F(G) - Y(G). \end{aligned}$$

Y-Index And Y-Coindex Of \mathcal{F} -Tensor Products Of Graphs

In this section, we obtain Y -index and Y -coindex of \mathcal{F} -tensor products of graphs and their complements for each $\mathcal{F} \in \{S, T_2, T_1, T\}$.

The following theorem gives the Y -index of S -tensor product of two graphs G_1 and G_2 .

Theorem 4.1 Let G_1 and G_2 be a two graphs with $|V(G_i)| = n_i$, and $|E(G_i)| = m_i, i = 1, 2$, where $n_1, n_2 \geq 2$. Then $Y(G_1 \times_S G_2) = Y(G_2)[Y(G_1) + 16m_1]$.

Proof. From the definition of Y -index, we have

$$\begin{aligned} Y(G_1 \times_S G_2) &= \sum_{(u,v) \in V(G_1 \times_S G_2)} d_{G_1 \times_S G_2}(u, v)^4 \\ &= \sum_{u \in V(S(G_1)) \cap V(G_1)} \sum_{v \in V(G_2)} [d_{S(G_1)}(u)d_{G_2}(v)]^4 \\ &\quad + \sum_{w \in V(G_2)} \sum_{e \in V(S(G_1)) \cap E(G_1)} [d_{S(G_1)}(e)d_{G_2}(w)]^4. \end{aligned}$$

For $u \in V(S(G_1)) \cap V(G_1)$, $d_{S(G_1)}(u) = d_{G_1}(u)$ and for $e \in V(S(G_1)) \cap E(G_1)$, $d_{S(G_1)}(e) = 2$. Therefore,

$$\begin{aligned} Y(G_1 \times_S G_2) &= \sum_{u \in V(G_1)} \sum_{v \in V(G_2)} [d_{G_1}(u)d_{G_2}(v)]^4 \\ &\quad + \sum_{w \in V(G_2)} \sum_{e \in E(G_1)} [2d_{G_2}(w)]^4 \\ &= Y(G_1)Y(G_2) + 16m_1Y(G_2) \\ &= Y(G_2)[Y(G_1) + 16m_1]. \end{aligned}$$

Following theorems give Y -index of $\overline{G_1 \times_S G_2}$, Y -coindex of graph $G_1 \times_S G_2$ and its complement $\overline{(G_1 \times_S G_2)}$, respectively.

Using Theorems 2.1, 2.3 and 4.1 in Theorem 3.1, we get the following result.





Sheeba Agnes and Kannadasan

Theorem 4.2 Let G_1 and G_2 be a two graphs with $|V(G_i)| = n_i$, and $|E(G_i)| = m_i, i = 1,2$, where $n_1, n_2 \geq 2$. Then

$$Y(\overline{G_1 \times_S G_2}) = n_2(n_1 + m_1)(n_2(n_1 + m_1) - 1)^4 - 8m_1m_2(n_2(n_1 + m_1) - 1)^3 + 6(n_2(n_1 + m_1) - 1)M_1(G_2)(M_1(G_1) + 4m_1) - 4(n_2(n_1 + m_2) - 1)(F(G_1) + 8m_1)F(G_2) + Y(G_2)[Y(G_1) + 16m_1].$$

Using Theorems 2.3 and 4.1 in Theorem 3.3, we get the following result.

Theorem 4.3 Let G_1 and G_2 be a two graphs with $|V(G_i)| = n_i$, and $|E(G_i)| = m_i, i = 1,2$, where

$$n_1, n_2 \geq 2. \text{ Then } \overline{Y(G_1 \times_S G_2)} = (n_2(n_1 + m_1) - 1)(F(G_1) + 8m_1)F(G_2) - Y(G_2)(Y(G_1) + 16m_1).$$

Using Theorems 2.1, 2.3 and 4.1 in Theorem 3.4, we get the following result.

Theorem 4.4 Let G_1 and G_2 be a two graphs with $|V(G_i)| = n_i$, and $|E(G_i)| = m_i, i = 1,2$, where $n_1, n_2 \geq 2$. Then

$$\overline{Y(G_1 \times_S G_2)} = 2m_1m_2(n_2(n_1 + m_2) - 1)^3 - 3(n_2(n_1 + m_1) - 1)^2 M_1(G_2)(M_1(G_1) + 4m_1) + 3(n - 1)(F(G_1) + 8m_1)F(G_2) - Y(G_2)(Y(G_1) + 16m_1).$$

The following theorem gives the Y –index of T_2 –tensor product of two graphs G_1 and G_2 .

Theorem 4.5 Let G_1 and G_2 be a two graphs with $|V(G_i)| = n_i$, and $|E(G_i)| = m_i, i = 1,2$, where $n_1, n_2 \geq 2$. Then $Y(G_1 \times_{T_2} G_2) = 16Y(G_2)[Y(G_1) + m_1]$

Proof. From the definition of Y -index, we have

$$Y(G_1 \times_{T_2} G_2) = \sum_{(u,v) \in V(G_1 \times_{T_2} G_2)} d_{G_1 \times_{T_2} G_2}(u, v)^4 = \sum_{u \in V(T_2(G_1)) \cap V(G_1)} \sum_{v \in V(G_2)} [d_{T_2(G_1)}(u)d_{G_2}(v)]^4 + \sum_{w \in V(G_2)} \sum_{e \in V(T_2(G_1)) \cap E(G_1)} [d_{S(G_1)}(e)d_{G_2}(w)]^4.$$

For $u \in V(T_2(G_1)) \cap V(G_1)$, $\delta_{T_2(G_1)}(u) = 2d_{G_1}(u)$ and for $e \in V(T_2(G_1)) \cap E(G_1)$, $d_{T_2(G_1)}(e) = 2$. Therefore,

$$Y(G_1 \times_{T_2} G_2) = \sum_{u \in V(G_1)} \sum_{v \in V(G_2)} [2d_{G_1}(u)d_{G_2}(v)]^4 + \sum_{w \in V(G_2)} \sum_{e \in E(G_1)} [2d_{G_2}(w)]^4 = 16Y(G_1)Y(G_2) + 16m_1Y(G_2) = 16Y(G_2)[Y(G_1) + 16m_1].$$

Following theorems give Y –index of $\overline{G_1 \times_{T_2} G_2}$, Y –coindex of graph $G_1 \times_{T_2} G_2$ and its complement $(\overline{G_1 \times_{T_2} G_2})$, respectively.

Using Theorems 2.1, 2.3 and 4.5 in Theorem 3.1, we get the following result.

Theorem 4.6 Let G_1 and G_2 be a two graphs with $|V(G_i)| = n_i$, and $|E(G_i)| = m_i, i = 1,2$, where $n_1, n_2 \geq 2$. Then





Sheeba Agnes and Kannadasan

$$Y(\overline{G_1 \times_{T_2} G_2}) = n_2(n_1 + m_2)(n_2(n_1 + m_1) - 1)^4 - 8m_1m_2(n_2(n_1 + m_1) - 1)^3 + 6(n_2(n_1 + m_1) - 1)4M_1(G_2)[M_1(G_1) + m_1] - 4(n_2(n_1 + m_1) - 1)8F(G_2)(F(G_1) + m_1) + 16Y(G_2)(Y(G_1) + m_1).$$

Using Theorems 2.3 and 4.5 in Theorem 3.3, we get the following result.

Theorem 4.7 Let G_1 and G_2 be a two graphs with $|V(G_i)| = n_i$, and

$|E(G_i)| = m_i, i = 1, 2$, where $n_1, n_2 \geq 2$. Then

$$\overline{Y}(G_1 \times_{T_2} G_2) = (n_2(n_1 + m_1) - 1)8F(G_2)(F(G_1) + m_1) - 16Y(G_2)(Y(G_1) + m_1).$$

Using Theorems 2.1, 2.3 and 4.5 in Theorem 3.4, we get the following result.

Theorem 4.8 Let G_1 and G_2 be a two graphs with $|V(G_i)| = n_i$, and

$|E(G_i)| = m_i, i = 1, 2$, where $n_1, n_2 \geq 2$. Then

$$\overline{Y}(G_1 \times_{T_2} G_2) = 2m_1m_2(n_2(n_1 + m_1) - 1)^3 - 3(n_2(n_1 + m_2) - 1)^2 4M_1(G_2)[M_1(G_1) + m_1] + 3(n_2(n_1 + m_1) - 1)8F(G_2)(F(G_1) + m_1) - 16Y(G_2)(Y(G_1) + m_1).$$

The following theorem gives the Y –index of T_1 –tensor product of two graphs G_1 and G_2 .

Theorem 4.9 Let G_1 and G_2 be a two graphs with $|V(G_i)| = n_i$, and

$|E(G_i)| = m_i, i = 1, 2$, where $n_1, n_2 \geq 2$. Then $Y(G_1 \times_{T_1} G_2) = Y(G_2)[Y(G_1) + \chi_4(G_1)]$.

Proof. From the definition of Y -index, we have

$$Y(G_1 \times_{T_1} G_2) = \sum_{(u,v) \in V(G_1 \times_{T_1} G_2)} d_{G_1 \times_{T_1} G_2}(u, v)^4 = \sum_{u \in V(T_1(G_1)) \cap V(G_1)} \sum_{v \in V(G_2)} [d_{T_1(G_1)}(u)d_{G_2}(v)]^4 + \sum_{w \in V(G_2)} \sum_{e \in V(T_1(G_1)) \cap E(G_1)} [d_{T_1(G_1)}(e)d_{G_2}(w)]^4.$$

For $u \in V(T_1(G_1)) \cap V(G_1)$, $\delta_{T_1(G_1)}(u) = d_{G_1}(u)$ and for $e \in V(T_1(G_1)) \cap E(G_1)$, $\delta_{T_1(G_1)}(e) = d_{G_1}(x) + d_{G_1}(y)$, where $e = xy \in E(G_1)$. Therefore,

$$Y(G_1 \times_{T_1} G_2) = \sum_{u \in V(G_1)} \sum_{v \in V(G_2)} [d_{G_1}(u)d_{G_2}(v)]^4 + \sum_{w \in V(G_2)} \sum_{xy \in E(G_1)} [d_{G_1}(x) + d_{G_1}(y)]^4 [d_{G_2}(w)]^4 = Y(G_1)Y(G_2) + \chi_4(G_1)Y(G_2) = Y(G_2)[Y(G_1) + \chi_4(G_1)].$$

Following theorems give Y –index of $\overline{G_1 \times_{T_1} G_2}$, Y –coindex of graph $G_1 \times_{T_1} G_2$ and its complement $(\overline{G_1 \times_{T_1} G_2})$, respectively.

Using Theorems 2.1, 2.3 and 4.9 in Theorem 3.1, we get the following result.

Theorem 4.10 Let G_1 and G_2 be a two graphs with $|V(G_i)| = n_i$, and

$|E(G_i)| = m_i, i = 1, 2$, where $n_1, n_2 \geq 2$. Then

$$\overline{Y}(G_1 \times_{T_1} G_2) = n_2(n_1 + m_2)(n_2(n_1 + m_1) - 1)^4 - 8m_1m_2(n_2(n_1 + m_1) - 1)^3 + 6(n_2(n_1 + m_1) - 1)M_1(G_2)[M_1(G_1) + HM(G_1)] - 4(n_2(n_1 + m_1) - 1)F(G_2)[F(G_1) + \chi_3(G_1)] + Y(G_2)[Y(G_1) + \chi_4(G_1)].$$

Using Theorems 2.3 and 4.9 in Theorem 3.3, we get the following result.

Theorem 4.11 Let G_1 and G_2 be a two graphs with $|V(G_i)| = n_i$, and

$|E(G_i)| = m_i, i = 1, 2$, where $n_1, n_2 \geq 2$. Then

$$\overline{Y}(G_1 \times_{T_1} G_2) = (n_2(n_1 + m_1) - 1)F(G_2)[F(G_1) + \chi_3(G_1)] - Y(G_2)[Y(G_1) + \chi_4(G_1)].$$





Sheeba Agnes and Kannadasan

Using theorems 2.1, 2.3 and 4.9 in Theorem 3.4, we get the following result.

Theorem 4.12 Let G_1 and G_2 be two graphs with $|V(G_i)| = n_i$, and

$|E(G_i)| = m_i, i = 1, 2$, where $n_1, n_2 \geq 2$. Then

$$\begin{aligned} \overline{Y(G_1 \times_{T_1} G_2)} &= 2m_1m_2(n_2(n_1 + m_1) - 1)^3 - 3(n_2(n_1 + m_2) - 1)^2 \\ &\quad M_1(G_2)[M_1(G_1) + HM(G_1)] + 3(n_2(n_1 + m_1) - 1)F(G_2)[F(G_1) \\ &\quad + \chi_3(G_1)] - Y(G_2)[Y(G_1) + \chi_4(G_1)]. \end{aligned}$$

The following theorem gives the Y –index of T –tensor product of two graphs G_1 and G_2 .

Theorem 4.13 Let G_1 and G_2 be two graphs with $|V(G_i)| = n_i$, and

$|E(G_i)| = m_i, i = 1, 2$, where $n_1, n_2 \geq 2$. Then $Y(G_1 \times_T G_2) = Y(G_2)[16Y(G_1) + \chi_4(G_1)]$.

Proof. From the definition of Y -index, we have

$$\begin{aligned} Y(G_1 \times_T G_2) &= \sum_{(u,v) \in V(G_1 \times_T G_2)} d_{G_1 \times_T G_2}(u, v)^4 \\ &= \sum_{u \in V(T(G_1)) \cap V(G_1)} \sum_{v \in V(G_2)} [d_{T(G_1)}(u)d_{G_2}(v)]^4 \\ &\quad + \sum_{w \in V(G_2)} \sum_{e \in V(T(G_1)) \cap E(G_1)} [d_{T(G_1)}(e)d_{G_2}(w)]^4. \end{aligned}$$

For $u \in V(T(G_1)) \cap V(G_1)$, $d_{T(G_1)}(u) = 2d_{G_1}(u)$ and for $e \in V(T(G_1)) \cap E(G_1)$,

$d_{T(G_1)}(e) = d_{G_1}(x) + d_{G_1}(y)$, where $e = xy \in E(G_1)$. Therefore,

$$\begin{aligned} Y(G_1 \times_T G_2) &= \sum_{u \in V(G_1)} \sum_{v \in V(G_2)} [2d_{G_1}(u)d_{G_2}(v)]^4 \\ &\quad + \sum_{w \in V(G_2)} \sum_{xy \in E(G_1)} [d_{G_1}(x) + d_{G_1}(y)]^4 [d_{G_2}(w)]^4 \\ &= 16Y(G_1)Y(G_2) + \chi_4(G_1)Y(G_2) \\ &= Y(G_2)[16Y(G_1) + \chi_4(G_1)]. \end{aligned}$$

Following theorems give Y –index of $\overline{G_1 \times_T G_2}$, Y –coindex of graph $G_1 \times_2$ and its complement $(\overline{G_1 \times_2})$, respectively.

Using Theorems 2.1, 2.3 and 4.13 in Theorem 3.1, we get the following result.

Theorem 4.14 Let G_1 and G_2 be two graphs with $|V(G_i)| = n_i$, and

$|E(G_i)| = m_i, i = 1, 2$, where $n_1, n_2 \geq 2$. Then

$$\begin{aligned} \overline{Y(G_1 \times_T G_2)} &= n_2(n_1 + m_2)(n_2(n_1 + m_1) - 1)^4 - 8m_1m_2(n_2(n_1 + m_1) - 1)^3 \\ &\quad + 6(n_2(n_1 + m_1) - 1)M_1(G_2)[4M_1(G_1) + HM(G_1)] \\ &\quad - 4(n_2(n_1 + m_1) - 1)F(G_2)[8F(G_1) + \chi_3(G_1)] \\ &\quad + Y(G_2)[16Y(G_1) + \chi_4(G_1)]. \end{aligned}$$

Using Theorems 2.3 and 4.13 in Theorem 3.3, we get the following result.

Theorem 4.15 Let G_1 and G_2 be two graphs with $|V(G_i)| = n_i$, and

$|E(G_i)| = m_i, i = 1, 2$, where $n_1, n_2 \geq 2$. Then

$$\overline{Y(G_1 \times_T G_2)} = (n_2(n_1 + m_1) - 1)F(G_2)[8F(G_1) + \chi_3(G_1)] - Y(G_2)[16Y(G_1) + \chi_4(G_1)].$$

Using Theorems 2.1, 2.3 and 4.13 in Theorem 3.4, we get the following result.

Theorem 4.16 Let G_1 and G_2 be two graphs with $|V(G_i)| = n_i$, and

$|E(G_i)| = m_i, i = 1, 2$, where $n_1, n_2 \geq 2$. Then

$$\begin{aligned} \overline{(G_1 \times_T G_2)} &= 2m_1m_2(n_2(n_1 + m_1) - 1)^3 - 3(n_2(n_1 + m_2) - 1)^2 \\ &\quad M_1(G_2)[4M_1(G_1) + HM(G_1)] + 3(n_2(n_1 + m_1) - 1) \\ &\quad F(G_2)[8F(G_1) + \chi_3(G_1)] - Y(G_2)[16Y(G_1) + \chi_4(G_1)]. \end{aligned}$$

Example 4.17

If C_n and C_m are two cycles of vertices $n \geq 3$ and $m \geq 3$, respectively. then

- $Y(C_n \times_S C_m) = 512nm$
- $Y(C_n \times_{T_2} C_m) = 4352nm$
- $Y(C_n \times_{T_1} C_m) = 4352nm$
- $Y(C_n \times_T C_m) = 8192nm$





Sheeba Agnes and Kannadasan

CONCLUSION

In this paper, we calculate Y-index and coindex of four new tensor products of graphs and their complements. Both indices are calculated explicitly for each case $\mathcal{F} \in \{S, T_2, T_1, T\}$. Since this new operations on graphs, further study of this operations on graphs can be extended other topological index to decide.

REFERENCES

1. Alamer, N. Al-Naggar, M. Al-Rumaima, and M. Alsharafi, Y-index of some graph operations, Int. J. App. Eng. Research.,15(2) (2020) 173-179.
2. A.R. Ashrafi, T. Doslic and A. Hamzesh, The Zagreb coindices of graph operations, Discrete Appl. Math., 158(15) (2010) 1571-1578.
3. R. Balakrishnan and K. Ranganathan, A Text Book of Graph Theory, Second Edition, Springer, New York (2012).
4. Basavanagoud A. P. Barangi, F-index and hyper-zagreb index of four new tensor products of graphs and their complements, Discrete Math. Alg. App., 11(3) (2019) (14).
5. Basavanagoud, V.R. Desai, K.G. Mirajkar, B. Pooja and I.N. Cangul, Four new tensor products of graphs and their Zagreb indicis coindices, Electron. J. Math. Anal. Appl., 8(1) (2020) 209-219.
6. N. De, S.M.A. Nayeem and A. Pal. The F –coindex of some graph operations. Springer Plus 5:221(2016), doi: 10.1186/s40064-016-1864-7.
7. H. Deng, D. Sarala, S.K. Ayyaswamy and S. Balachandran, The Zagreb indices of four operations on graphs, Appl. Math. Comput., 275 (2016) 422-431.
8. M. Eliasi and B. Taeri, Four new sums of graphs of graphs and their Wiener indices, Discrete Appl. Math. 157(4) (2009) 794-803
9. B. Furtula and I. Gutman, A forgotten topological index. J. Math. Chem. 53(4)(2015), 1184-1190.
10. J. A. Gallian, A dynamic survey of graph labeling, Electron. J. Combin. DS6 (2018) 1-502.
11. Gutman, B. Ruscic, N. Trinahstic, and C.F. Wilcox, Graph theory and molecular orbitals.XII.Acyclic polyenes, J.chem.Phys.62 (1975) 3399-305.
12. Gutman N. Trinajstic, Graph theory and molecular orbitals,Total ϕ -electron energy of alternant hydrocarbons, Chem. Phys. Lett., 17 (4) (1972) 535-538.
13. W. Imrich, S. Klavzar, product Graphs, Structure and Recongnition(John Wiley Sons,NewYork,USA,2000).
14. G. H. Shirdel, H. Rezapour and A. M. Sayadi, The hyper-Zagreb index of graph operations, Iranian J. Math. Chem. 4(2)(2013)213-220.
15. B. Zhon and N. Trinajstic, On a novel connectivity index, J. Math. chem., 46(4) (2009) 1252-1270.
16. B. Zhou and N. Trinajstic, On general sum-connectivity index, J. Math. Chem., 47(1) (2010)210-218.

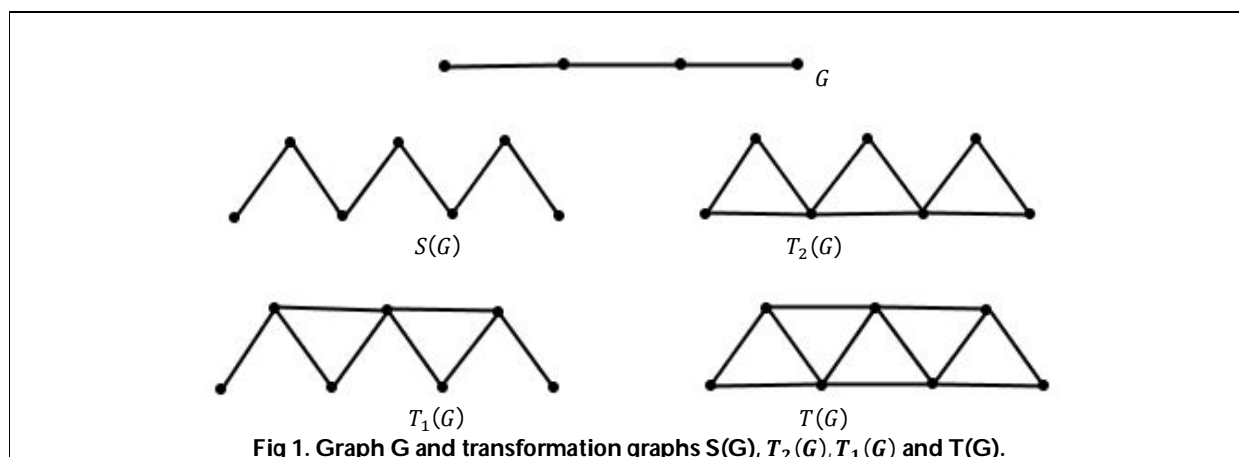


Fig 1. Graph G and transformation graphs $S(G)$, $T_2(G)$, $T_1(G)$ and $T(G)$.





Sheeba Agnes and Kannadasan

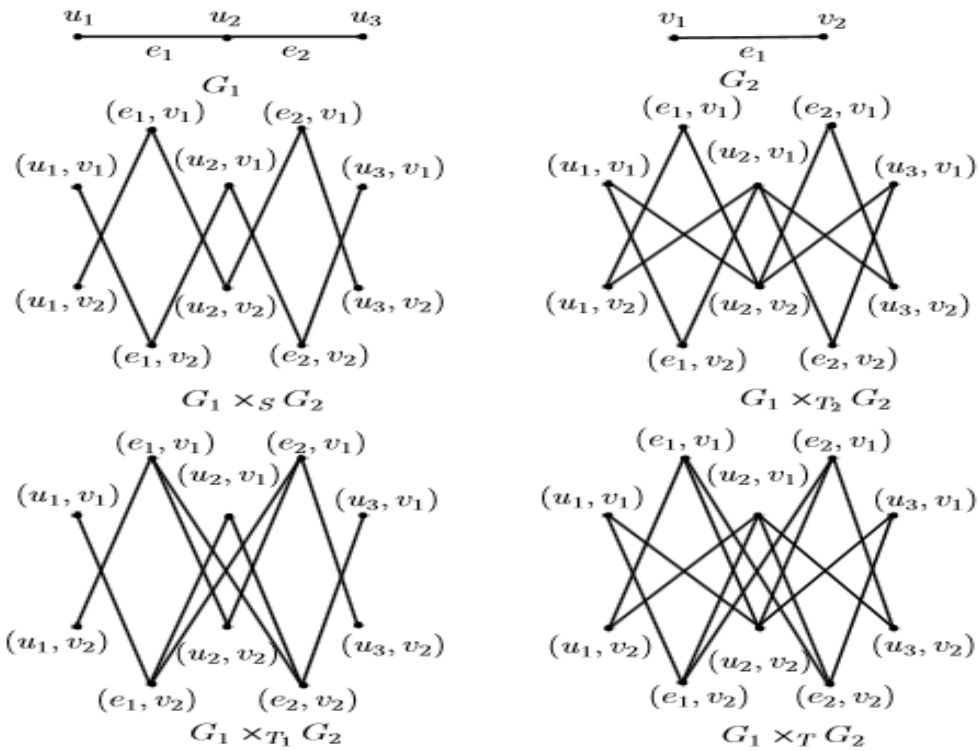


Figure 2. Graphs G_1, G_2 and $G_1 \times_F G_2$





PV Fed Multi Level Inverter with Improved Harmonic Performance

A.V.Sudhakara Reddy¹ and Bhalky Manikanta^{2*}

¹Department of EEE, Malla Reddy Engineering College, Maisammaguda, Hyderabad, India.

²PG Scholar, Department of EEE, Malla Reddy Engineering College, Hyderabad, India.

Received: 05 Sep 2021

Revised: 08 Oct 2021

Accepted: 19 Jan 2022

*Address for Correspondence

Bhalky Manikanta

PG Scholar,

Department of EEE,

Malla Reddy Engineering College,

Hyderabad, India.

Email: manikantabhalky123@gmail.com



This is an Open Access Journal / article distributed under the terms of the **Creative Commons Attribution License** (CC BY-NC-ND 3.0) which permits unrestricted use, distribution, and reproduction in any medium, provided the original work is properly cited. All rights reserved.

ABSTRACT

The duty cycles of individual cells in cascade multilevel converters change as a result of the fluctuation in the irradiances of the power cells. However, the MPPT is maintained throughout the process. The difference in cell responsibility cycle, on the other hand, is undesirable because it is associated with the distortion of production voltage and current voltage and current. In order to achieve this, a multilevel design for photovoltaic (PV) applications is proposed, in which a H6 bridge power cell is used in place of an H- bridge is used. Should a mismatch in solar irradiance between the power cells occur, an expected converter will be used to inject power at a lower voltage from the shaded cells without altering the PV voltage, thus maintaining the MPPT functionality. This modification allows us to maintain an identical duty cycle in all power cells, independent of the weather circumstances, and therefore to preserve the yield voltage and current waveform properties of the power cells. Both a sophisticated computer model and a field experiment were used to assess the effectiveness of the proposed remedy. Following the analysis, it has been shown that when compared to conventional H-bridge topologies, the proposed topology provides much better voltage and current characteristics in the production environment. The proposed topology's presentation was also compared to one that improved harmonics presentation in accordance with European competence requirements, resulting in a 2.64 percent increase in overall presentation quality.

Keywords : PV, Multi level Inverter, MPPT, Harmonics



**Sudhakara Reddy and Bhalky Manikanta**

INTRODUCTION

In the field of power electronic converters owing to their robustness, efficiency, and fault-tolerance, multilevel converters (MLCs) have emerged as highly appealing options. Providing the voltage level is adequate, the voltage waveform produced by these power converter topologies is high-quality and may be used to drive power switches operating at frequencies as high as the fundamental frequency. The high-quality voltage, on the other hand, allows for the employment of a smaller output filter [1]. This includes the cascaded H-bridge (CHB) converter design, which consists of a series of Hbridges, each with its own dc voltage source, that are linked in series. Incorporating this feature allows the connecting of PV panels to each H-bridge, resulting in independent maximum power point tracking (MPPT), which improves the efficiency of the entire system while simultaneously increasing the quantity of energy pumped into the grid. PWM (phase-shifted pulsewidth modulation) is the method most often used in MLCs because of its simplicity (PS-PWM). When employed in CHB applications, the PSPWM is described as a collection of unipolar carriers, one for each H-bridge, that are displaced from one another by a factor of T_s/n [2, 3].

The carriers' time is indicated by the letter T_s , while the number of H-bridges is denoted by the letter n . It is possible to achieve equal power distribution and comparable power losses among the power cells by using this modulation technique; however, this method has a multiplicative effect on the converter output voltage switching frequency. As a consequence of dust on the photovoltaic panels or partial shadow, the system will be unbalanced if the power cells get uneven sun irradiation as a result of this. Interphase disequilibrium and intraphase disequilibrium are the two kinds of disequilibrium that may occur in a reaction. As for the former, it is considered to be a long-standing problem, comparable to any interphase imbalance problem, for which hundreds of remedies can be found in scientific literature. Nonetheless, new methods based on MLCs have been developed and are being tested. However, the intraphase imbalance is a relatively recent problem that arose as a result of a problem with MLCs. A primary source of harmonics in the converter output signals occurs when solar irradiation is not distributed evenly throughout the power cells. This is due to a discrepancy in cell duty cycles and dc-link voltages [3], which occurs when solar irradiation is not distributed evenly throughout the power cells]. Due to decreased solar radiation, the controller limits the duty cycle of each shaded power cell in order to maintain the MPP current; as a consequence, the modulator receives a variety of duty cycles.

A delay (TD) is introduced into the power injection process by the shaded power cell, and the power injection process is terminated prior to the apparent time. Although the cells are combined in MLCs to generate the converter output signals (output current and voltage), timing is an important consideration, as any advanced or delayed activity of any power cell relative to the expected timing may impair the output signals [4]. There have been many attempts to mitigate this problem, which have been recorded in the literature. Regardless of the fact that variable switching angles are the main operational idea and that this method offers a cost-effective solution, it is only practical when $n = 3$ due to the computing complexity required. Furthermore, when there is significant partial shading present, changing the carrier shift angles does not result in a significant improvement in the quality of the output signals to an acceptable level. In the case of $n = 2$, Marquez et al. proposed the use of an extra battery-powered power cell to get around this problem. The power cells (referred to as CHBB in this paper) have been combined with a dc-dc boost converter, as shown in Fig. 1. A modified modulation method is proposed to maintain a consistent level of energy between the dc-link capacitors, allowing all of the cells to operate at similar duty cycles. Power quality can be improved by modifying only minor aspects of the modulation and control of modular cascaded multilevel quasi-Z-source inverters, as described in [5]. Because the H-bridge voltages do not depend on the PV voltages, only minor modifications to their modulation and control are required. In this work, we investigate the operation of a solid-state transformer-based power cell in a star-connected synchronous buck converter with both interphase and intraphase imbalances. When using the previously mentioned topology-based solutions, a large number of active and passive components—particularly inductors—are integrated into the power cells, and in some cases, a higher switching frequency is required, which not only increases the size, weight, and cost of the converter, but also reduces the overall efficiency of the system.



**Sudhakara Reddy and Bhalky Manikanta****Proposed Multilevel Topology**

It is necessary to either equalise the duty cycles and voltages of all cells during partial shading or raise the duty cycle peaks of all cells to nearly one to eliminate the presence of the n th harmonic content [6]. The output voltage of the shaded power cell must be lowered in order to restore the duty cycle to a value close to unity; nevertheless, the point Fig. 2 must remain unchanged. In both cases, when there is balanced and unbalanced solar irradiance between the cells, the output voltage of each power cell is added to the overall output voltage to get the final result. The suggested cascaded multilevel design for photovoltaic systems is shown in Fig. 2. The goal of this architecture is to maintain constant PV voltage and MPPT. A dc–dc stage may be placed between each H-bridge and PV string in order to offer a decoupling voltage between the H-dc bridge's connection and the PV string in each case. A boost (as seen in Fig. 1), buck—boost, or flyback dc–dc converter are all possible configurations. However, since this method necessitates the use of additional inductors, the cost and size of the hardware are increased. Additionally, the dc–dc stages operate at a higher switching frequency, which reduces the efficiency of the system [7, 8]. As a result, this article recommends that the H-bridge in each power cell be replaced with a H6 bridge, with the dc-link capacitor being replaced by a split capacitor, and just two active semiconductor devices and two diodes being added in their stead. The entire schematic architecture of the suggested MLC for solar applications is shown in Fig. 2, where n cells are taken into consideration. Using the shadowing power cell as a generator, the proposed solution involves injecting electricity.

Control Structure in the Proposed Converter

It is proposed that the design be managed in three different ways: grid-injected current control, separate MPP tracking in each cell, and the insertion of H6 capacitors and control of voltage balancing and balancing. For each cell voltage, the classical control technique uses a proportional integral (PI) controller, and for each cell frequency, it employs a proportional resonant controller (PR) Fig.3. The article proposes a control structure for the cascaded H6 converter that is implemented in the article. The output current is controlled by a controller in this article. As a result of the employment of separate MPP trackers, this control technique has been proven to be one of the most efficient when several voltages are utilised in the cells, as would be the case in this application. As shown in Fig. 3, the cell voltages are the only variables that can be controlled in the loops from $i = 2$ to n . The voltages are controlled by PI controllers, whose outputs are used to generate the modulation indices for the modulation.

Simulation Results

System Specifications and Requirements As a single-phase inverter of 1 kW capacity, it was extensively modelled and simulated using PLECS to provide empirical validation of the concept. The suggested inverter is powered by paralleled photovoltaic strings with a voltage range of 120 to 190 V and 2 mF capacitors in each cell, with a voltage range of 120 to 190 V in the output. The specs for the photovoltaic panels were taken from the datasheets of authentic Alfa solar GmbH photovoltaic panels, type SI S21-170.A1, which were purchased from Alfasolar GmbH. When tested under normal conditions, these solar panels have the following specifications: $v_{OC} = 96$ V, $v_{MPP} = 76$ V, $i_{SC} = 2.83$ A, and $i_{MPP} = 2.2$ A. When tested under extreme conditions, these photovoltaic panels have the following specifications: (STC). It was necessary to simulate two PV panels in series in each cell in order to reach the needed voltage level for grid connection, when the cell count was three. According to local regulations, the fundamental magnitude and angular frequency of the grid have been set at 230 V and 50 Hz, respectively, for the purpose of generating electricity. Every converter under test has had the switching frequency of the H-bridges set to 2 kHz. This is the default setting. The output filter's inductance has been adjusted at 3.5 mH, which is a reasonable value. The MPPTs used were standard perturb and observe kinds, with the voltage rise and frequency set at 0.5 V and 10 Hz, respectively, for the experiment. When evaluating the suggested converter, three different time periods were utilised. The system first works in the STC mode until the MPPTs have reached a stable state, at which time the switches S5i and S6i are simultaneously turned on to simulate the operation of the CHB, and the system is then switched off. This phase concludes with a fast 50 percent decrease in solar irradiance in the third cell for 1.5 seconds, which is regarded to be a second time interval. This occurs towards the end of the test at the 3.5-second mark. Particularly noteworthy



**Sudhakara Reddy and Bhalky Manikanta**

is that during the second time period, the switches S5i and S6i stayed on at the same time, mimicking the operation of the CHB. The third power cell remained shaded until the 5 s mark of the test, but the system started to operate as a cascaded H6 inverter, with the semiconductor switches S5i and S6i functioning as anticipated. The simulation models and outputs are shown in Fig. 4 to Fig. 12. From the results it can be found that the proposed system is more advantageous than the existing systems in terms of THD and output voltage.

CONCLUSION

An investigation of the fundamental causes of output current and voltage aberrations in cascaded MLCs in the presence of partial shadowing among the power cells was carried out in this paper. It has been shown that the variation in cell duty cycles, as well as the difference in cell voltages, were the most important variables in the distortion of the output signals in this experiment. More to the point, if the duty cycles of the cells were near to one, the variation in cell voltages could have less of an impact in this situation. A cascaded MLC was suggested as a result, in which the cells were each capable of supplying less voltage than the total cell voltage, allowing the cell duty cycle to be increased back to unity after it had decreased in the event of partial shade. Because it did not need any additional passive components in comparison to its competitors, the concept was more cost-effective, lighter and smaller in overall size. Only a few active components were included in the update. Using both simulation and experiment, it was demonstrated that the proposed converter provided significantly improved output voltage and current qualities in the presence of partial shading, with THD according to 50th harmonic orders—as defined by the EN50160 standard—decreased from 15.23 percent to 10.75 percent in the case of voltage and current

REFERENCES

1. F.Rong, X. Gong, and S.Huang, "A novel grid-connected PVsystem based on MMC to get the maximum power under partial shading conditions," *IEEE Trans. Power Electron.*, vol. 32, no. 6, pp. 4320–4333, Jun. 2017.
2. G. Farivar, B.Hredzak, and V. G. Agelidis, "A dc-side sensorless cascaded H-bridge multilevel converter-based photovoltaic system," *IEEE Trans. Ind. Electron.*, vol. 63, no. 7, pp. 4233–4241, Jul. 2016.
3. Y. Yu, G. Konstantinou, B. Hredzak, and V. G. Agelidis, "Power balance of cascaded H-bridge multilevel converters for large-scale photovoltaic integration," *IEEE Trans. Power Electron.*, vol. 31, no. 1, pp. 292–303, Jan. 2016.
4. A. Lashab, D. Sera, J. Martins, and J. M. Guerrero, "Multilevel dc-link converter-based photovoltaic system with integrated energy storage," in *Proc. 5th Int. Symp. Environ.- Friendly Energies Appl.*, 2018, pp. 1–6.
5. Y. Yu, G. Konstantinou, B. Hredzak, and V. G. Agelidis, "Operation of cascaded H- bridge multilevel converters for large-scale photovoltaic power plants under bridge failures," *IEEE Trans. Ind. Electron.*, vol. 62, no. 11, pp. 7228–7236, Nov. 2015.
6. E. Villanueva, P. Correa, J. Rodriguez, and M. Pacas, "Control of a single phase cascaded H-bridge multilevel inverter for grid-connected photovoltaic systems," *IEEE Trans. Ind. Electron.*, vol. 56, no. 11, pp. 4399– 4406, Nov. 2009.
7. J. I. Leon, S. Kouro, L. G. Franquelo, J. Rodriguez, and B. Wu, "The essential role and the continuous evolution of modulation techniques for voltage-source inverters in the past, present, and future power electronics," *IEEE Trans. Ind. Electron.*, vol. 63, no. 5, pp. 2688–2701, May 2016.





Sudhakara Reddy and Bhalky Manikanta

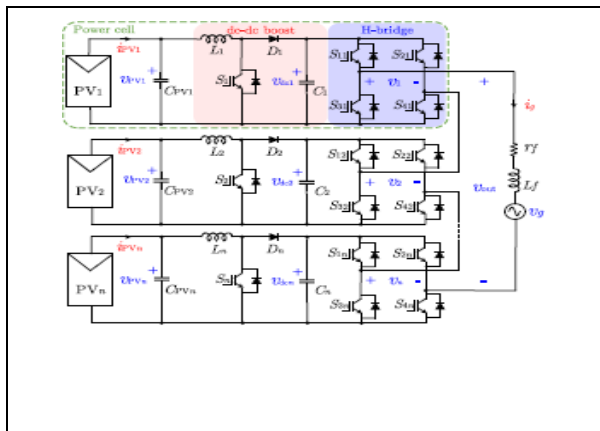


Fig. 1: Classical CHBB

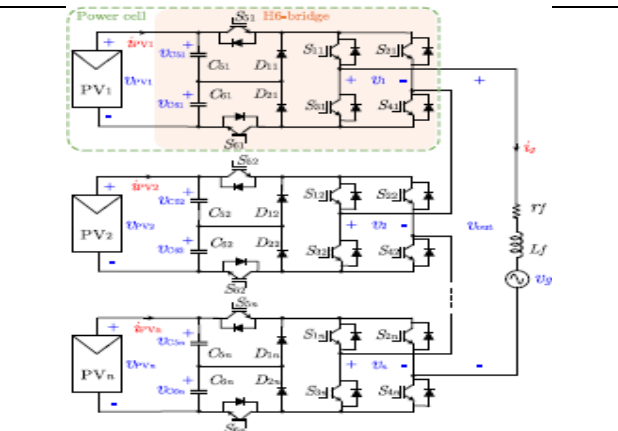


Fig. 2: Proposed system for PV application

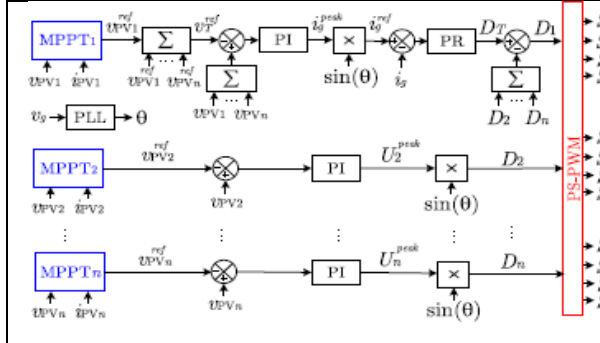


Fig. 3: Proposed controller

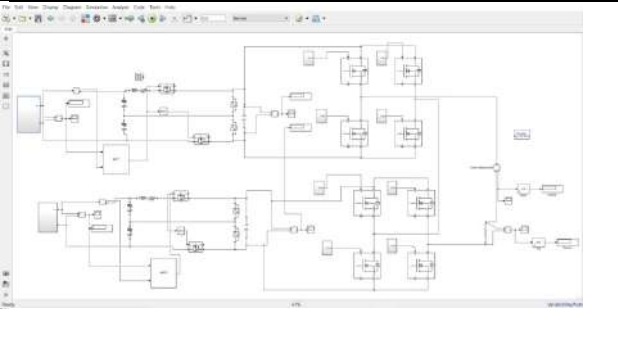


Fig. 4: Simulation circuit with 9level with 8 switches proposed diagram

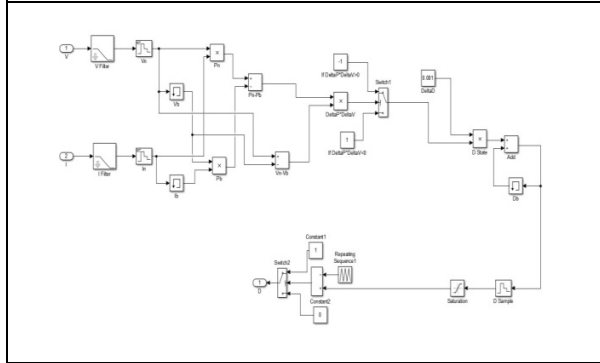


Fig. 5 : Mppt tracking

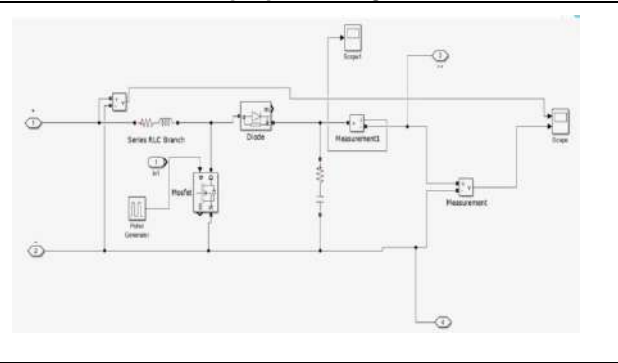


Fig. 6 : Design of dc-dc converter





Sudhakara Reddy and Bhalky Manikanta

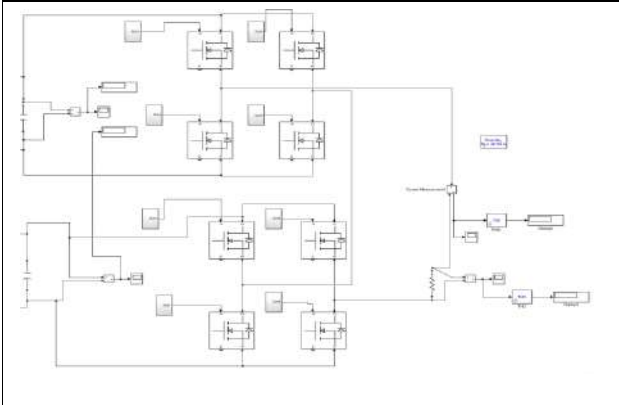


Fig. 7 : Switching pattern of cascading of two sources

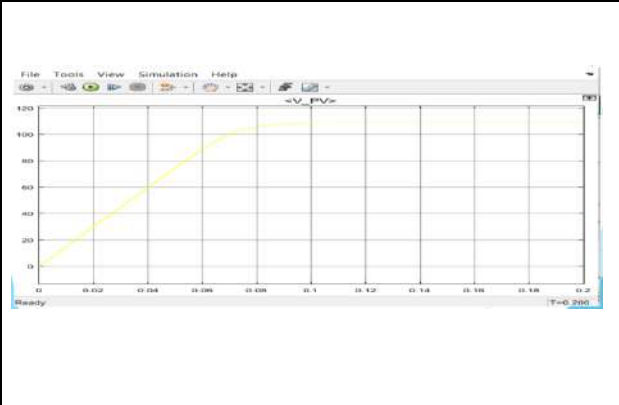


Fig. 8 : Solar output 1

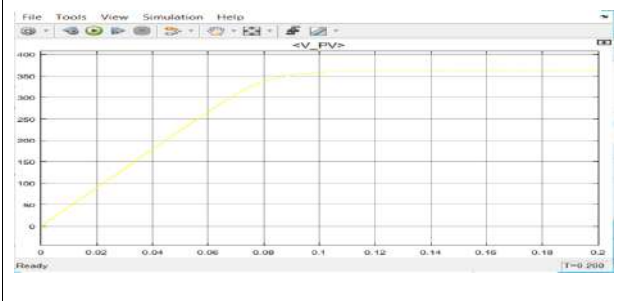


Fig. 9 : Solar output 2

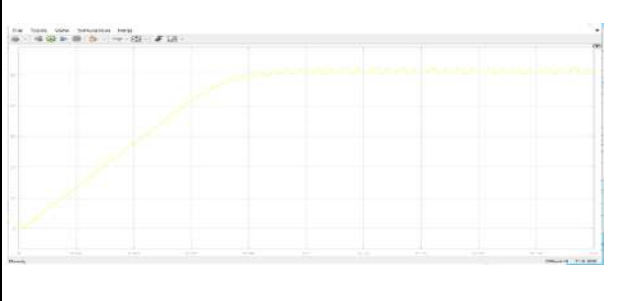


Fig. 10 : Boost converter 1

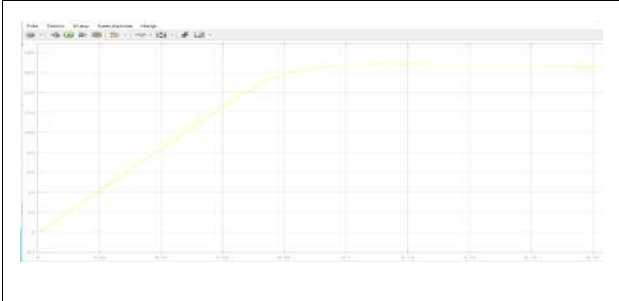


Fig. 11 : Boost converter 2

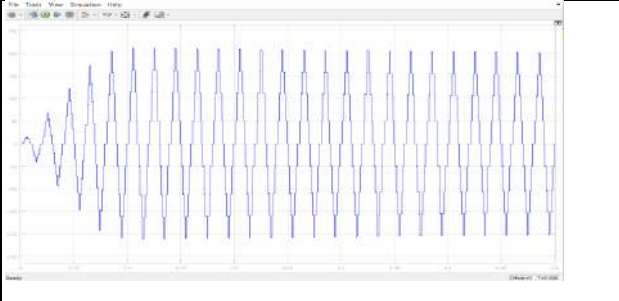


Fig. 12 : Output voltage after MPPT





An Analysis and Classification Model for Heart Disease by Hybrid Algorithm

M. Sumathi¹, A. R. Visagan^{2*} and C.Mohan³

¹Head and Associate Professor, PG & Research Department of Computer Science, Sri Meenakshi Government Arts College for Women (A), Madurai – 625 002, Tamil Nadu, India.

²Teaching Assistant, Department of Computer Science, Madurai Kamaraj University College, Alagarkoil Road, Madurai-625 002, Tamil Nadu, India.

³Assistant Professor, Department of Computer Science, The American College, Madurai, Tamil Nadu, India.

Received: 22 Nov 2021

Revised: 25 Dec 2021

Accepted: 24 Jan 2022

*Address for Correspondence

A. R. Visagan

Teaching Assistant,
Department of Computer Science,
Madurai Kamaraj University College,
Alagarkoil Road,
Madurai-625 002,
Tamil Nadu, India.



This is an Open Access Journal / article distributed under the terms of the **Creative Commons Attribution License** (CC BY-NC-ND 3.0) which permits unrestricted use, distribution, and reproduction in any medium, provided the original work is properly cited. All rights reserved.

ABSTRACT

Managing population health and peril stratification, which is the mainstream of health care, is more significant than ever. Medical institutions that strive to alter cost structures and progress results need to design intrusions for high-risk and high-cost patients that want to be accomplished proactively and carefully. Therefore, this proposed study uses a variety of techniques, namely naive bayes, random forest classification, decision tree, using datasets suitable for predicting heart disease, which consist of different attributes such as gender and age. The purpose is to analyze support vector machines and artificial neural networks, Chest pain. Type, blood pressure, blood sugar level, etc. For the proposed hybrid approach work of SVM and DNN. This study involves using standard techniques to look for correlations among several attributes of the dataset, so use the attributes appropriately to predict the risk of heart disease. Adopted in training at the executive level, the new model was found to be associated with multi-class SVMs with DNN capabilities. Sequence training involves structured SVMs with state transition capabilities and DNN. Since then, he has helped healthcare organizations successfully capture, store, and analyze data using a hybrid SVM and DNN method.

Keywords: SVM, DNN, Heart Disease, Health care, ANN





Sumathi et al.,

INTRODUCTION

We live in a world where everything is transformed into data. We generate lot of data. The volume of data composed and warehoused is exploding. The proliferation of data is one of the reasons why deep information learning is needed. Learning in industry and health is competitive, with a wealth of businesses for better autonomous decision making. Numerous strategies have been introduced regarding the immediate implementation of mining and deep learning techniques for user satisfaction. Therefore, the proposed study focuses on this early prediction, which is easy for physicians to diagnose.

Health Care Industry

Here, you will learn about the practical learning, classification and applications of mining, including the healthcare sector. The healthcare industry is perceived and filled with a wealth of information, but lacks knowledge. Therefore, data analysis should always be improved to uncover concealed data. Medical analysts in the case of hospital diagnostics can help determine strategic solutions. Healthcare analysts aim to acquire the knowledge to continue treatment, verify the effectiveness of treatment, and diagnose disease from predictive models. An iterative process is performed for knowledge representation. The analyzed data is huge, large, distributed and uncertain, which makes it hard to understand the full latent of the data composed within a healthcare facility without exploration and learning tasks. Huge amounts of data in medical applications have to be sent to harness knowledge and also control the high eminence of patient data. Data-centric data aggregation is helping the healthcare industry grow and move in the right direction. Empowering management requires that all data is retained in a suitable manner for healthier thinking and strategic implementation. Traditionally, data analysis lacks sufficient manual knowledge research. Computer-aided analysis is more efficient than manual work. Because it is imperative that data be stored in a warehouse, it is reliable and efficient, making physical decisions for better results and continuation of procedures. Several classification methods such as rule guidance, artificial neural networks, support vector machines, decision trees, and deep neural networks are used in healthcare diagrams.

Classification Techniques

Prediction and Classification are the commonly used modeling goals. Category tags such as discrete and unordered are prophesied by the classification model, which is used to identify continuous value functions. Numerous data mining methods are used, each with different levels of precision for diagnosing heart disease. ANN is, in particular, a parallel computer system composed of a large amount of simple processors with several interconnections. Also known as Neural Network (NN), it is based on a network of biological neurons. It is used to map the input data to the appropriate set of output data. The three layers built into this network: the input layer, the hidden layer and the output layer, and because there are mutual connections between each layer, weights are allocated to each connection.

Support Vector Machine

The SVMs appeared as very strong methods for learning machines for overseen classification problems. SVMs are nuclear processes that transform data into three-dimensional space and build hyperplane that optimize the distance from the data point of the nearest one of the input classes. However, SVM are formerly designed to form binary classifiers, it is possible to expand many classes, it is possible to reduce the problem of multiclass in various binary classifications, while approaching. Browse high reliability in creating regression models and nonlinear classification.

Deep Neural Networking

Deep learning uses multilayer procedures called neural network. The first merit of deep learning to learn the machine is the severance of the extraction of characters. At the same time, the deep learning, the traditional methods of learning machines are used as flat algorithms as opposed to raw materials directly as. CSV, images, text, etc. requirement. Characteristic extraction. Existing features are generally difficult and require thorough knowledge of the delinquent of the problem. A profound learning model produces an abstraction, a compressed representation of raw data on multiple layers of artificial neuronal network. Then use a representation of compressed input data for



**Sumathi et al.,**

the result. The outcome could be, for example, the categorization of input data for dissimilar classes. Throughout the training process, the neuronal network improves this step to attain the best conceivable intellectual illustration of the input data. Deep learning models need a little without manual exercise to accomplish and improve the function extraction function. In other words, the extraction of the features is integrated with the process that takes place in an artificial neuronal network without human entry. When using the machine's learning model, it takes time to predict the image and classify the functionality of the unique functionality, taking into account input data as an algorithm. In contrast, deep learning reduces the extraction of functionality and performs classification.

Coronary Heart Disease

Coronary artery disease (CHD) is the common kind of heart disease, killing more than 370,000 people each year. This is true each year, with about 735,000 people having a heart attack. Out of these, 525,000 are the first heart attacks and 210,000 occur in people who have previously had a heart attack. However, it is hard to recognize heart disease since of numerous risk features that can cause it, such as diabetes, high blood pressure, high cholesterol, abnormal pulse, and many other factors. Because of these constraints, scientists are turning to modern methods such as data mining and machine learning to predict disease. Classification methods have proven to be actual in creation of decisions and making predictions from large amounts of data generated in the medical industry. Therefore, this research proposal applies classification techniques and data mining to classify whether a person has heart disease and its type.

Comprehensive Review of Existing Methodologies

We identify which patients with heart failure with high readmission risk. In the midst of the confirmations oriented at the functionality of the heart, the cardiac a rhythm and illness of coronary artery (CAD) and the sleep apnea primordial and often considered aggressive syndrome. Therefore, the proposed research work engrossed on this initial prediction, which is supported by simple diagnoses for the doctor. Gandhi, Monica, etc. The author has studied using the data mining techniques used in today's research to predict heart disease in order to elaborate on various knowledge abstraction techniques. In this article, we analyze data mining techniques, namely naive bayes, neural networks and decision tree algorithms, on medical datasets using algorithms. Moloud Abdar, Sharareh R. Niakan Kalhori et al. The authors investigated a heart disease prediction data mining algorithm. We tested 5 algorithms with C5.0, Neural Network, Support Vector Machine (SVM), K-Nearest Neighbor (KNN), and Logistic Regression, reaching 93.02%, KNN, SVM, Neural Network 88, 37%, 86.05. Was 80.23% each. The results generated from the decision tree are easy to interpret and apply. Different clinicians can easily recognize their rules.

2014, M.A. Nishara Banu B. Gomathy et al. Aggregated the relevant data in the database using clustering algorithms such as K-means. The investigation of the maximum rate pattern is performed by the Maximum Frequency Factor Set (MAFIA) algorithm of the heart disease database to detect accuracy. Tan & Teoh (2009) examined a hybrid method between a genetic algorithm (GA) and a support vector machine (SVM). The best features of the dataset are accomplished by the genetic algorithm module, and the SVM categorizes and discards the data as a wrapper method. Achieves an accuracy of 76.20%. Luukka & Lampinen (2010) applied principal component analysis (PCA) pretreatment to perform a classic electronic medical record (EMR) classifier for the diagnosis of heart disease. It achieved an average accuracy of 82%. Parc et al. (2008) We investigated the construction of a novel extrapolative model grounded on a support vector machine (SVM) to predict breast cancer reappearance within 5 years after breast cancer surgery. BCRSVM showed significantly higher sensitivity (0.89), specificity (0.73), positive predictions (0.75), and negative predictions (0.89).

Lannoy et al. (2010) Performed on an SVM via the MIT-BIH database, alternating use of each class objective function in the analysis of long-term ECG signal recordings. He performed automatic interpatient cataloging of heartbeats through an SVM classifier that optimized a convex calculation of a balanced classification rate. The R-tip annotations that perform feature abstraction are far from the prejudiced SVM model. Khateeb and Usman performed analysis of several methods through the UCI dataset and predicted classifier results between naive bayes, KNNs, decision trees, and bagging methods. He prefers KNN accuracy after accomplishing feature reduction and resampling as a Synthetic Minority Oversampling (SMOTE) technique via the WEKA tool.





Sumathi et al.,

Pouriyeh et al. Analysis performed of several methods across the Cleveland Heart Disease Data Set of Decision Tree (DT), Naive Bayes (NB), Multilayer Perceptron (MLP), K-Nearest Neighbor (KNN), Single Conjunctive . (SCRL), Radial Basis Function (RBF), and K-Fold cross validation method support vector machine (SVM). Precision, precision, recall, F major, and media vector machine ROC curve results take priority.

Proposed Methodology

Fig 2 illustrates the architecture of the forecasting system, and Figure 3 examines the proposed forecasting system in detail. When performing a normal sorting on the top-level DNN, multinomial logistic regression is used in the time period T_f of the observation frame O_f , and the resulting output efficiency vector Y_f and state output output S are output as N with the output state S_f as digital state. WI then produces the following weights: State of the hidden layer at the final stage as

$$P(st|ot) = \frac{\exp(w_{st}^T h_t)}{\sum_{s=1}^N \exp(w_{st}^T h_t)}$$

$$\arg \max_s w_s^T \phi(o_t)$$

In SVM classification, function is resulting from

When calculating the feature space, SVMs and DNNs work well with multiclass classification decoding, but with few saturation values. Therefore, this planned hybrid method of SVM and DNN is applied to accomplish optimized results. This combinatorial approach preserves the SVM parameters in the frame, the sequence level in the last layer and the DNN parameters in the previous first layer, taking into account the maximum margin criteria, as described in Figure 4. Hold. Double-headed arrows indicate a range of parameters for DNN, multiclass SVM, and structured SVM. For maximum margin training at the sequence level, the solid blue arrow (in the trellis) represents the sequence in the reference state, and the dashed green arrow represents the sequence in the most competitive state.

Frame level training

In frame-level training, DNN parameters are usually evaluated by decreasing cross entropy as a DNN-derived feature space, and the last layer parameters are first measured using the SVM multiclass learning algorithm. When training the maximum margin at the sequence level, keep in mind that the score for the correct state tag $w^T stht$ must be higher than the score for any other state. Predicted as

$$\min_{\bar{s} \neq s} \left\{ \log \frac{P(S|O)}{P(\bar{S}|O)} \right\} = \min_{\bar{s} \neq s} \left\{ \log \frac{p(O|S)P(S)}{p(O|\bar{S})P(\bar{S})} \right\}$$

Introduced a new type of DNN. Softmax top stage for classification is used in traditional DNN. SVM at the top layer will be used in new DNN will instead use. We calculated a training algorithm at the frame and sequence level to jointly learn the SVM and DNN parameters on a maximum margin basis.

Training at the executive level shows that the new model is associated with a multi-class SVM with DNN capabilities. Sequence training involves structured SVMs with DNN and state transition capabilities. The proposed model, named DNSVM, can reduce the relative error rate by 8% compared to the DNN (CE trained) of the TIMIT task. In future work, we'll look at DNSVM in addition to sequence-trained DNNs in large vocabulary errands. This task only replaces the last layer of DNN with a linear SVM. Future work will also explore nonlinear kernels and deep "non-DNN" SVMs.

RESULTS AND DISCUSSION

Experience serves as an significant tool for physicians to detect actual risk cases and guide accordingly. The proposed technology consumes less time for more accurate disease prediction, reducing the waste of precious lives



**Sumathi et al.,**

around the world. The main aim is to use a variety of classification and prediction algorithms on eligible data sets to predict whether a patient has heart disease. Examine the correlation among several attributes. Deep learning models incline to be more accurate as the amount of training data increases, but outdated machine learning models such as SVMs and Naive Bayes classifiers stop ameliorating after the saturation point.

Dataset

The UCI Machine Learning Standard Cleveland Heart Disease Database includes 75 attributes, but all published experience uses a subset of 14 and narrows them down to 11. The clinical database collects a large amount of important data about patients and their medical circumstances. The records containing the smallest significant internal attributes were extracted from the Cleveland Heart Disease Database using datasets in which meaningful models were extracted for cardiac prediction. Each set of records was selected at random to evade bias. Prediction of heart disease is made by considering the following 11 attributes instead of the 14 attributes conventionally used to investigate and examine results.

Figure 5 and the table show the accuracy, sensitivity, and specificity study of various organization methods such as SVM, DNN, ripper, decision support, and Navie Bayes compared to the mixture method of SVM and DNN. From the imitation study, DNN has an accuracy of 86.7%, specificity and sensitivity of 84.75%, 78.73%, accuracy of 83.31%, specificity and sensitivity of 83 , 87% of 77.41%, precision of 80.01% of RIPPER, specificity of 81.35%. , 73.47% precision and sensitivity 71.34%, NB 79.97% precision, 77.10% precision and sensitivity 71.47%, compared to the hybrid approach method proposed 93.54% precision, 93, 47% accuracy and 90.71% sensitivity method. Finally, the proposed method has been shown to achieve better results.

Figure 6 and the table show the TP and FP rates of the planned and prevailing algorithms. According to the simulation analysis, DNN is 89.35% TP, 14.65% FP, SVM is 87.48% TP, 10.52% FP, RIPPER is 81.48% TP, 11.52% FP and the decision aid is 76.74% TP, 15.26% FP. , NB is 74.99% TP, 17.01% FP, and the proposed SVM-DNN hybrid is 90.75% TP, 18.25% FP.

CONCLUSION

The hybrid method of SVM and DNN results in better predictions, performs a good classifier that integrates the SVM parameters into the frame and sequence level of the last layer, and takes into account the maximum margin criteria of the first previous layer. This study involves using standard techniques to look for correlations among several attributes of the dataset, so use the attributes appropriately to detect the risk of heart disease. We found that the new model adopted for executive-level training was linked to a multi-class SVM with DNN capabilities. Sequence training is linked to a structured SVM with DNN and state transition capabilities.

REFERENCES

1. Suman Ravuri, "Hybrid DNN-Latent structured SVM acoustic models for continuous speech recognition", *Automatic Speech Recognition and Understanding (ASRU) 2015 IEEE Workshop on*, pp. 37-44, 2015.
2. Yi-Hsiu Liao, Hung-yi Lee, Lin-shan Lee, "Towards structured deep neural network for automatic speech recognition", *Automatic Speech Recognition and Understanding (ASRU) 2015 IEEE Workshop on*, pp. 137-144, 2015.
3. Shi-Xiong Zhang, Rui Zhao, Chaojun Liu, Jinyu Li, Yifan Gong, "Recurrent support vector machines for speech recognition", *Acoustics Speech and Signal Processing (ICASSP) 2016 IEEE International Conference on*, pp. 5885-5889, 2016.
4. Shangfei Wang, Bowen Pan, Huaping Chen, Qiang Ji, "Thermal Augmented Expression Recognition", *Cybernetics IEEE Transactions on*, vol. 48, no. 7, pp. 2203-2214, 2018.





Sumathi et al.,

5. Shi-Xiong Zhang, Yifan Gong, Dong Yu, "Encrypted Speech Recognition Using Deep Polynomial Networks", *Acoustics Speech and Signal Processing (ICASSP) ICASSP 2019 - 2019 IEEE International Conference on*, pp. 5691-5695, 2019.
6. Lu Bai, Yuhang Jiao, Lixin Cui, Edwin R. Hancock, *Machine Learning and Knowledge Discovery in Databases*, vol. 11906, pp. 464, 2020.
7. David Díaz-Vico, Jesús Prada, Adil Omari, José Dorronsoro, "Deep support vector neural networks", *Integrated Computer-Aided Engineering*, pp. 1, 2020.
8. Zhang, Shi-Xiong & Liu, Chaojun & Yao, Kaisheng & Gong, Yifan. (2015). Deep neural support vector machines for speech recognition. 2015. 10.1109/ICASSP.2015.7178777.
9. Bai, Lu & Jiao, Yuhang & Cui, Lixin & Hancock, Edwin. (2020). Learning Aligned-Spatial Graph Convolutional Networks for Graph Classification. 10.1007/978-3-030-46150-8_28.
10. Xu, Wenyan & Li, Qing & Liu, Xingyu & Zhen, Zonglei & Wu, Xia. (2020). Comparison of feature selection methods based on discrimination and reliability for fMRI decoding analysis. *Journal of Neuroscience Methods*. 335. 108567. 10.1016/j.jneumeth.2019.108567.
11. Geoffrey E Hinton and Ruslan R Salakhutdinov, "Reducing the dimensionality of data with neural networks," *Science*, vol. 313, no. 5786, pp. 504–507, 2006.

Table I attribute description

Data set characteristics		Multivariate
Attribute characteristics		Categorical, Integer, Real
Associated Tasks		Classification
Number of Instances		303
Number of attributes		75
Missing Value		Yes
Attribute	Description	Value
CP	Chest Pain Type	1 : typical angina 2 : atypical angina 3 : non-angina pain 4 : asymptomatic
Trestbps	Resting blood pressure	Continues value in mm hg
Chol	Serum cholesterol	Continues value in mm/dl
Fbs	Fasting blood pressure	1 ≥ 120 mg/dl 0 ≤ 120 mg/dl
Restecg	Resting electro cardio graphics results	0 : Normal 1 : having_ST_T Wave abnormal 2 : Left Ventricular Hypertrophy
Thalach	Maximum heart rate achieved	Continues value
Exang	Exercise induced angina	0 : No 1 : Yes
Slope	The slope of the peak exercise ST segment	1 : up sloping 2 : flat 3 : down sloping
Thal	Defect Type	3 : Normal 6 : Fixed 7 : Reversible defect
Sex	Male or Female	1 : Male 0 : Female
Age	Age in years	Continuous





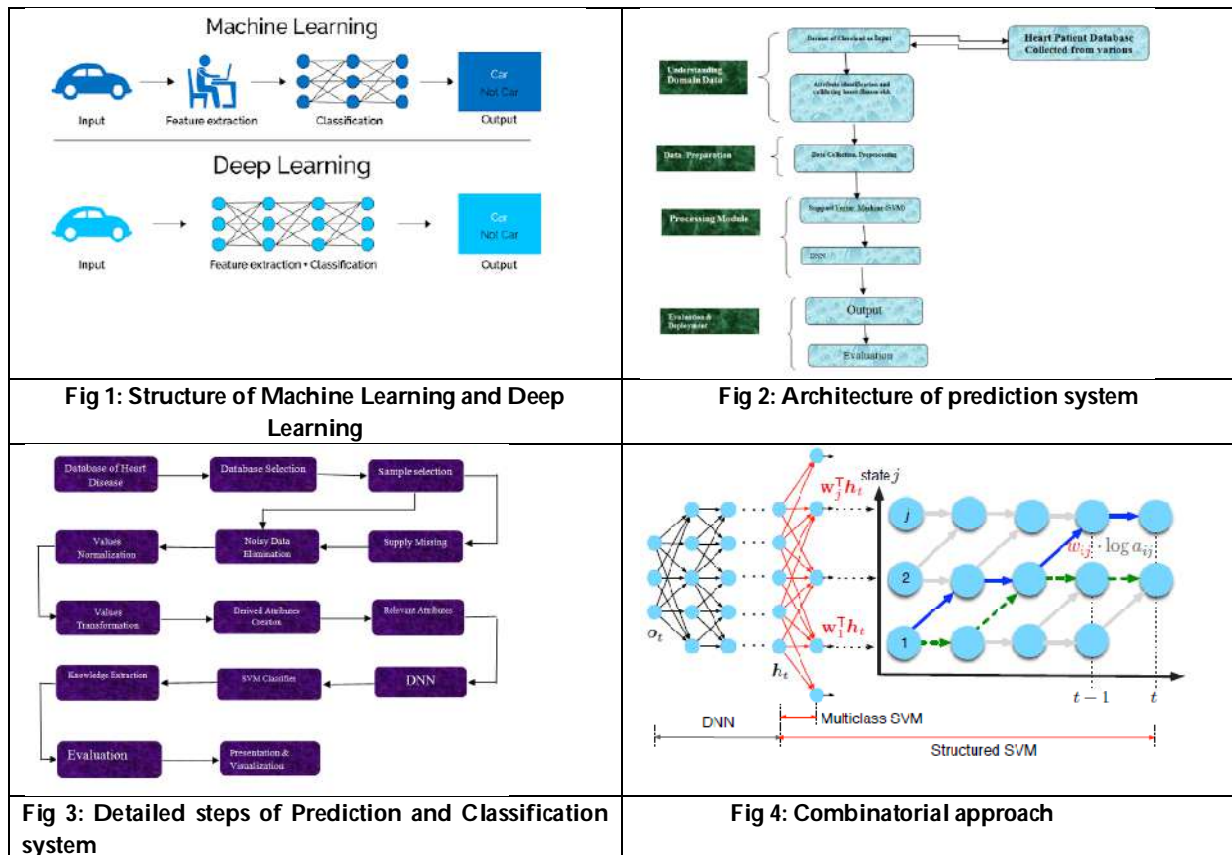
Sumathi et al.,

Table II. Accuracy, sensitivity, and specificity study of various organization methods

Algorithm	Accuracy	Sensitivity	Specificity
DNN	86.70 %	84.75 %	78.73 %
SVM	83.31 %	83.87 %	77.41 %
RIPPER	80.01 %	81.35 %	73.62 %
Decision Support	78.06 %	73.47 %	71.34 %
Naive Bayes	79.97 %	77.10 %	71.47 %
SVM-DNN Hybrid	93.54 %	93.47 %	90.71 %

TABLE III. TP and FP rates of the planned and prevailing algorithms

Algorithm	True Positive rate	False positive Rate
DNN	0.8935	0.1465
SVM	0.8748	0.1052
RIPPER	0.8148	0.1152
Decision Support	0.7674	0.1526
Naive Bayes	0.7499	0.1701
SVM-DNN Hybrid	0.9075	0.1825





Sumathi et al.,

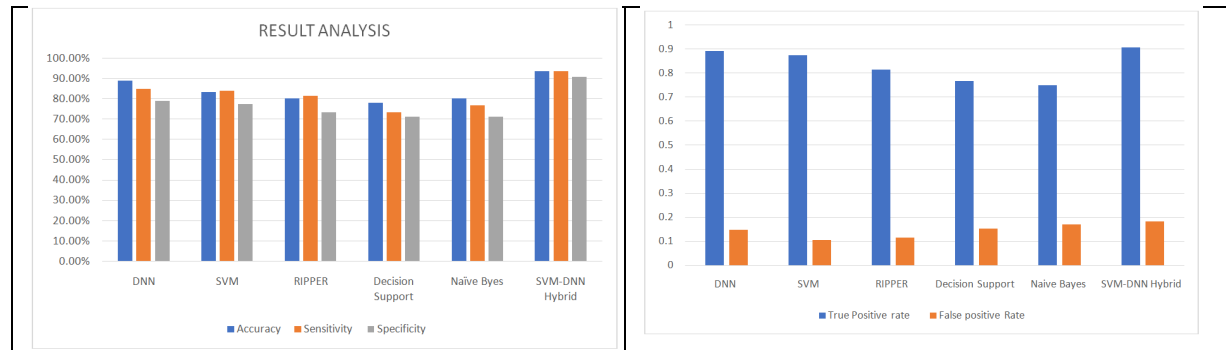


Fig 5: Analysis Result of Accuracy, Sensitivity and Specificity

Fig 6: Analysis Result of True Positive rate and False positive Rate





Statistical Hypothesis Testing for Determining the Relationship of Categorical Variables using Python Code

Naresh Chandra^{1*}, Arvind Kumar Shukla² and Subhash Chand¹

¹Research Scholar, IFTM University, Moradabad, Uttar Pradesh, India.

²Associate Professor, IFTM University, Moradabad, Uttar Pradesh, India.

Received: 26 Dec 2021

Revised: 02 Jan 2022

Accepted: 18 Jan 2022

*Address for Correspondence

Naresh Chandra

Research Scholar,

IFTM University,

Moradabad,

Uttar Pradesh, India.

Email: dr_nc@rediffmail.com



This is an Open Access Journal / article distributed under the terms of the **Creative Commons Attribution License** (CC BY-NC-ND 3.0) which permits unrestricted use, distribution, and reproduction in any medium, provided the original work is properly cited. All rights reserved.

ABSTRACT

For determining the relationship between two categorical or nominal variables whether they are likely to be related or not, a statistical hypothesis test is done which is named as Chi square test of independence. When we have the counts of the values for two categorical variables, we use the Chi square test of independence. A contingency table contains the frequencies for a combination of values of two discrete random variables A and B is prepared. Each cell in the table represents a mutually exclusive combination of A-B values. The *p-value* and the *alpha* is compared for accepting or rejecting the null hypothesis as well as *chi_square_statistic* and *critical_value* is compared for the same.

Keywords: chi square statistic, *critical value*, *alpha*, *p value*, Statistical Hypothesis, Categorical Variables

INTRODUCTION

We will analyze the relationship of different variables (columns) of the dataset statistically. We have used the "**Python**" to accomplish the task of relationship analysis of different columns of the dataset. Our dataset have most of the categorical columns, therefore we have used chi square test of independence in this research paper.

DATASET

We have taken dataset Test.csv and Train.csv from Kaggle.com in this research paper. This dataset is about the spending score collected of nearly 8000 consumers along with the information about gender, age, profession, marital status, education (Graduate), family size and the work experience.





Naresh Chandra et al.,

DATASET DESCRIPTION

Each feature or columns of the Train.csv file of the dataset are described below:

Features	Description
ID	Unique Identification number of the consumer.
Gender	Gender of the consumer.
Ever_Married	Whether consumer is married.
Age	Age of the Consumer.
Graduated	Whether consumer is educated (Graduated).
Profession	What does the consumer by profession?
Work_Experience	How many work experience consumer have?
Spending_Score	Spending score of the consumer by purchasing.
Family_Size	What is the family size of the consumer?
Var_1	Consumer's category.
Segmentation	Consumer's category by segmentation A, B, C or D.

Let us first look into some statistical terms and methods used in this research paper:

CHI SQUARE TEST OF INDEPENDENCE

To determine the relationship between two categorical or nominal variables whether they are likely to be related or not, a statistical hypothesis test is done which is named as Chi square test of independence. When we have the counts of the values for two categorical variables, we use the Chi square test of independence.

CONTINGENCY TABLE

Tabular representation of categorical data is known as contingency table. A contingency table contains the frequencies for a combination of values of two discrete random variables A and B. Each cell in the table represents a mutually exclusive combination of A-B values.

DEGREE OF FREEDOM

The degrees of freedom are calculated with the number of rows and the column in contingency table as:

Degrees of freedom , $df=(r-1) \times (c-1)$

In this formula, 'r' represents the number of rows, where as 'c' represents the number of columns of the contingency table.

SIGNIFICANCE AND P-VALUE

Statistical significance level is often expressed as a p-value which lies between 0 and 1. The smaller will be the p-value, the stronger will be the evidence that we should reject the null hypothesis. A p-value typically less than or equal to 0.05 is considered statistically significant (Fig.1).

CRITICAL VALUE

A critical value is a point or points on the scale of the test statistic beyond which we reject the null hypothesis, and, is derived from the level of significance α of the test.

NULL HYPOTHESIS AND ALTERNATE HYPOTHESIS:

Null hypothesis is that there is no relationship between two variables and it is denoted by H_0 where as alternate hypothesis is that there is relationship between both the variables and is denoted by H_a .

As described above we analyze the relationship of different combinations of the columns of the dataset on the statistical criterion using Python programming:





Naresh Chandra et al.,

WORKING AND THE IMPLEMENTATION OF THE PYTHON CODE ON DATASET

After importing some of the required libraries, when we print the first five rows of the dataset using the code print(df), we get the output as:

```

      ID Gender Ever_Married Age Graduated Profession \
0  462809 Male      No 22      No  Healthcare
1  462643 Female    Yes 38      Yes   Engineer
2  466315 Female    Yes 67      Yes   Engineer
3  461735 Male     Yes 67      Yes   Lawyer
4  462669 Female    Yes 40      Yes Entertainment
... ..
8063 464018 Male     No 22      No      NaN
8064 464685 Male     No 35      No  Executive
8065 465406 Female    No 33      Yes Healthcare
8066 467299 Female    No 27      Yes Healthcare
8067 461879 Male     Yes 37      Yes  Executive

Work_ExperienceSpending_ScoreFamily_Size Var_1 Segmentation
0          1.0      Low      4.0 Cat_4      D
1          NaN    Average      3.0 Cat_4      A
2          1.0      Low      1.0 Cat_6      B
3          0.0    High      2.0 Cat_6      B
4          NaN    High      6.0 Cat_6      A
... ..
8063          0.0      Low      7.0 Cat_1      D
8064          3.0      Low      4.0 Cat_4      D
8065          1.0      Low      1.0 Cat_6      D
8066          1.0      Low      4.0 Cat_6      B
8067          0.0    Average      3.0 Cat_4      B
    
```

[8068 rows x 11 columns]

With the help of label encoder of python, we change the categorical values into the numerical values which are assigned as per the following table:

Gender	Male	1
	Female	0
Ever_Married	Yes	1
	No	0
Graduated	Yes	1
	No	0
Spending_Score	Average	0
	High	1
	Low	2

When we look for the rows and columns now using the code print(df.shape), we get following output:

(7854, 11)





Naresh Chandra et al.,

DATA CLEANING AND PREPROCESSING:

We now drop the rows for null values and unwanted columns like ID, Var_1 and Segmentation and check for resulting rows and columns:

```
(6665, 8)
```

Also check for null values using python code, shows the output as:

```
Gender      0
Ever_Married  0
Age         0
Graduated   0
Profession  0
Work_Experience  0
Spending_Score  0
Family_Size  0
dtype: int64
```

Countplot function for Gender, Ever_Married, Profession and Spending_Score is displayed in the graph shown in Fig.2.

HYPOTHESIS TESTING

Now we test the following hypothesis for 'Gender' and 'Spending_Score' variables (columns):

H₀: There is no relationship between 'Gender' and 'Spending_Score' categorical variables.

H_a: There is a relationship between 'Gender' and 'Spending_Score' categorical variables

For this, first we create contingency table and looks for observed and expected values:

```
contingency_table :-
Spending_Score  0  1  2
Gender
0      692 393 1903
1      970 611 2096
Observed Values :-
[[ 692 393 1903]
 [ 970 611 2096]]

Expected Values :-
[[ 745.09467367 450.10532633 1792.8   ]
 [ 916.90532633 553.89467367 2206.2   ]]
```

Taking the alpha as .05 i.e. 95% accuracy level, looks for degree of freedom:

```
Degree of Freedom: 2
Significance level(alpha): 0.05
```

Chi square statistics is observed as:

```
chi-square statistic:- 19.990437538066306
```





Naresh Chandra et al.,

p-value are calculated as:

p-value: 4.561751706566586e-05
 Since $p_value \leq \alpha$, Reject H_0 . There is a relationship between two categorical variables

With the help of chi-square statistics, we accept or reject the null hypothesis using the python:

chi-square statistic: 19.990437538066306
 critical_value: 5.991464547107979
 Since $chi_square_statistic \geq critical_value$, Reject H_0 , There is a relationship between two categorical variables

Therefore null hypothesis H_0 is rejected. There is a relationship between 'Gender' and 'Spending_Score'.

In the following tables 01 and 02 first row is depicted as per above calculation and in similar fashion relationship for variables(Columns) 'Ever_Married', 'Graduated', 'Profession', 'Work_Experience', and 'Family_Size' versus 'Spending_Score' are determined:

CONCLUSION

Therefore all the null hypothesis H_0 is rejected. Therefore, there is a relationship between 'Gender' and 'Spending_Score', 'Ever_Married' and 'Spending_Score', 'Graduated' and 'Spending_Score', 'Profession' and 'Spending_Score', 'Work_Experience' and 'Spending_Score' and 'Family_Size' and 'Spending_Score'.

REFERENCES

1. https://www.jmp.com/en_ch/statistics-knowledge-portal/chi-square-test/chi-square-test-of-independence.html
2. <https://www.statistics.com/glossary/contingency-table/>
3. <https://www.simplypsychology.org/p-value.html>
4. <https://towardsdatascience.com/statistical-tests-when-to-use-which-704557554740>
5. Kaggle.com

Table - 01 p value, alpha and their inference

S N	Variable	Contingency Table	Observed Value	Expected Value	Degree of Freedom	Significance Level (alpha)	p-Value	Inference
01	Gender	Spending_Score 0 1 2 Gender 0 692 393 1903 1 970 611 2096	[[692 393 1903] [970 611 2096]]	[[745.09467367 450.10532633 1792.8] [916.90532633 553.89467367 2206.2]]	2	.05	4.561751706566586e-05	Since $p_value \leq \alpha$, Reject H_0
02	Ever_Married	Spending_Score 0 1 2 Ever_Married 0 0 0 2721 1 1662 1004 1278	[[0 0 2721] [1662 1004 1278]]	[[678.51492873 409.88507127 1632.6] [983.48507127 594.11492873 2366.4]]	2	.05	0.0	Since $p_value \leq \alpha$, Reject H_0
03	Graduated	Spending_Score 0 1 2 Graduated	[[393 333 1690] [1269 671 1449.6]]	[[602.45941485 363.94058515 1449.6]]	2	.05	0.0	Since $p_value \leq \alpha$, Reject H_0





Naresh Chandra et al.,

		0 393 333 1690 1 1269 671 2309	2309]]	[1059.54058515 640.05941485 2549.4]]				
04	Prof essio n	Spending_Score 0 1 2 Profession Artist 881 210 1101 Doctor 160 23 409 Engineer 178 50 354 Entertainment 273 33 503 Executive 62 342 101 Healthcare 37 35 1005 Homemaker 45 18 112 Lawyer 16 269 215 Marketing 10 24 199	[[881 210 1101] [160 23 409] [178 50 354] [273 33 503] [62 342 101] [37 35 1005] [45 18 112] [16 269 215] [10 24 199]]	[[546.60225056 330.19774944 1315.2] [147.62250563 89.17749437 355.2] [145.12888222 87.67111778 349.2] [201.73413353 121.86586647 485.4] [125.927982 76.072018 303.] [268.56324081 162.23675919 646.2] [43.6384096 26.3615904 105.] [124.68117029 75.31882971 300.] [58.10142536 35.09857464 139.8]]	16	.05	0.0	Since p_value<=alp ha, Reject H ₀
05	Wor k_Ex perie nce	Spending_Score 0 1 2 Work_Experience 0.0 529 347 1257 1.0 557 378 1252 2.0 77 33 149 3.0 60 34 141 4.0 69 28 136 5.0 38 28 113 6.0 49 18 120 7.0 50 25 110 8.0 92 42 263 9.0 99 49 295 10.0 5 4 42 11.0 14 8 23 12.0 11 4 30 13.0 4 5 34 14.0 8 1 34	[[529 347 1257] [557 378 1252] [77 33 149] [60 34 141] [69 28 136] [49 18 120] [38 28 113] [49 18 120] [50 25 110] [92 42 263] [99 49 295] [5 4 42]	[[531.88987247 321.31012753 1279.8] [545.35543886 329.44456114 1312.2] [64.58484621 39.01515379 155.4] [58.60015004 35.39984996 141.] [58.10142536 35.09857464 139.8] [44.63585896 26.96414104 107.4] [46.63075769 28.16924231 112.2] [46.13203301	28	.05	0.00397422 950569514 8	Since p_value<=alp ha, Reject H ₀





Naresh Chandra et al.,

			[14 8 23] [11 4 30] [4 5 34] [8 1 34]]	27.86796699 111.] [98.99684921 59.80315079 238.2] [110.46751688 66.73248312 265.8] [12.71747937 7.68252063 30.6] [11.22130533 6.77869467 27.] [11.22130533 6.77869467 27.] [10.72258065 6.47741935 25.8] [10.72258065 6.47741935 25.8]]				
06	Fami ly_Si ze	Spending_Score 0 1 2 Family_Size 1.0 4 10 1229 2.0 714 498 881 3.0 371 196 725 4.0 369 183 622 5.0 142 74 306 6.0 41 17 122 7.0 11 12 58 8.0 5 4 33 9.0 5 10 23	[[4 10 1229] [714 498 881] [371 196 725] [369 183 622] [142 74 306] [41 17 122] [11 12 58] [5 4 33] [5 10 23]]	[[309.95738935 187.24261065 745.8] [521.91537884 315.28462116 1255.8] [322.17614404 194.62385596 775.2] [292.75138785 176.84861215 704.4] [130.16714179 78.63285821 313.2] [44.88522131 27.11477869 108.] [20.19834959 12.20165041 48.6] [10.4732183 6.3267817 25.2] [9.47576894 5.72423106 22.8]]	16	.05	0.0	Since p_value<=alp ha, Reject Ho

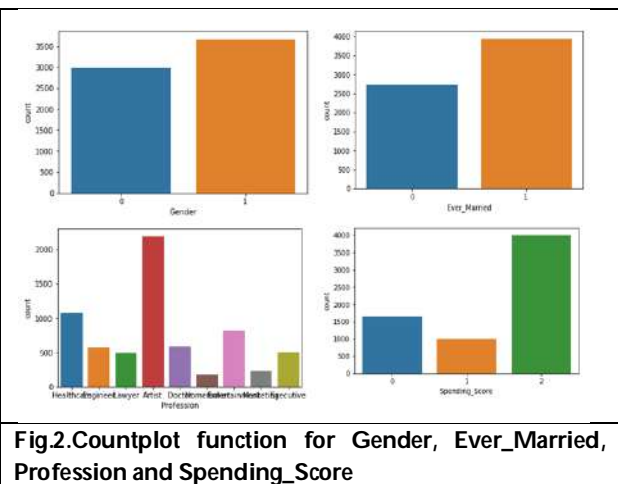
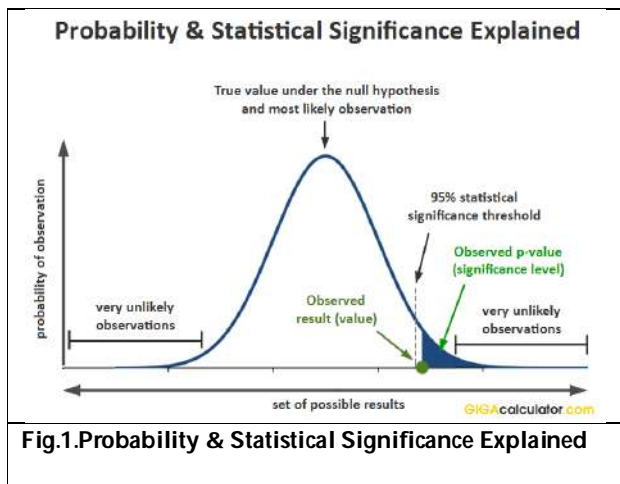




Naresh Chandra et al.,

Table-02 chi _ square _ statistic, critical_ value and their inference.

SN	Variables	chi-square statistic	critical_value	Inference
01	Gender	19.990437538066306	5.991464547107979	Since chi_square_statistic >= critical_value, Reject H ₀
02	Ever_Married	1839.2966531440163	5.991464547107979	Since chi_square_statistic >= critical_value, Reject H ₀
03	Graduated	118.35747573854229	5.991464547107979	Since chi_square_statistic >= critical_value, Reject H ₀
04	Profession	2312.41312281543	26.29622760486423	Since chi_square_statistic >= critical_value, Reject H ₀
05	Work_Experience	51.86641219306476	41.33713815142739	Since chi_square_statistic >= critical_value, Reject H ₀
06	Family_Size	692.5245121305791	26.29622760486423	Since chi_square_statistic >= critical_value, Reject H ₀





Effect of *Alpina galanga*, Clove and Cinnamon on Reduction of Histamine Content in Fermented Idli Batter

Lakshmi Praba K^{1,2}, Induja C^{1,2} and Loganathan M^{3*}

¹National Institute of Food Technology, Entrepreneurship and Management, Thanjavur (NIFTEM-T; Formerly IIFPT), Thanjavur, Tamil Nadu.

²Research Scholar, Affiliated to Bharathidasan University, Tiruchirappalli, Tamil Nadu, India.

³Professor and HoD (Entomology), Department of Academic & Human Resource Development, National Institute of Food Technology, Entrepreneurship and Management -Thanjavur (Formerly IIFPT), Thanjavur, Tamil Nadu.

Received: 25 Nov 2021

Revised: 21 Dec 2021

Accepted: 17 Jan 2022

*Address for Correspondence

Loganathan M

Professor (Entomology) and HoD,
Department of Academic & Human Resource Development,
National Institute of Food Technology, Entrepreneurship and Management –Thanjavur (NIFTEM-T),
Thanjavur, Tamil Nadu.
Email: logu@iifpt.edu.in



This is an Open Access Journal / article distributed under the terms of the **Creative Commons Attribution License** [CC BY-NC-ND 3.0] which permits unrestricted use, distribution, and reproduction in any medium, provided the original work is properly cited. All rights reserved.

ABSTRACT

Idli is one of the globally accepted short term stored cooked food. The histamine produced during the fermentation have to be reduced for the safety of consumers. An attempt has been made to reduce the histamine content in fermented idli batter by fortifying the batter with extracts such as clove, cinnamon and galanga at 1% concentration. Ensuring safety of the globally accepted food for prolonged storage and safer consumption, pH, titratable acidity and color of the control and fortified idli batter were analyzed in alternative days upto 7 days of storage period. The sensory analysis was carried out on the final day of the storage period and proves the acceptability of the cooked fortified idli. The histamine content was determined using colorimetric method upto 7 days of storage period and revealed use of galanga extract in idli batter reduces the histamine content and imparts additional flavour to the batter. It is concluded that the galanga extract at 1% concentration in idli batter helps in reduction of histamine and can be used as potential biogenic amine reducers.

Keywords: idli batter, colorimetric, histamine, plant extract.

INTRODUCTION

Idli is one of the commonly used food in south India and accepted globally. It has a spongy texture[1]. It is a fermented food which has a short life span and prepared with rice (*Oryza sativa* L.) and split black gram dal (*Phaseolus mungo*) in various proportions of 2:1 / 3:1 / 4:1 (w/w)[2,3]. The shelf-life of the idli batter at ambient



**Lakshmi Praba et al.**

temperature is short for 1-day and 5 days under refrigerated condition. Lactic Acid Bacteria (LAB) and yeasts in idli batter are playing important role fermentation [4]. The inherent microbes responsible for fermentation are *Lactobacillus brevis*, *Lactobacillus fermentum*, *Lactobacillus delbrueckii*, *Lactobacillus lactis*, *Lactobacillus casei*, *Leuconostocme senteroides*, *Pediococcus pentosaceus*, *Pediococcus cerevisiae*, and *Enterococcus faecalis* [5,6]. It was reported that the production of biogenic amines by LAB in various fermented foods [7].

Biogenic Amines [BAs] are produced by microbial action during fermentation and storage and are found to be toxic substances in foods [8,9]. The most commonly occurring biogenic amine includes putrescine, cadaverine, spermine, spermidine, tyramine, phenylethylamine, histamine and tryptamine. These amines are widely present in bacteria, plants and animals. These organic compounds are normally safer for consumption but it may be toxic at larger quantities [10]. Histamine is the major amine upon elevation causes food poisoning. Therefore determination of histamine levels in food is important in ensuring food safety [11]. The limit for detection of histamine in food is defined by various regulatory bodies. As per FSSAI 200 mg/kg for fish products [12]. The limit has been fixed less than 20 mg/kg for alcoholic and nonalcoholic refreshments, aged vegetables and soy items, and up to 700 mg/kg for certain sausages by European Food Safety Authority [13]. The allowable limit of BAs in various fermented foods are not reported, and there is no scientific report available to formulate ingredients of foods to control BAs during fermentation. The detection methods of biogenic amine include biosensors, colorimetric assays, Thin layer chromatography, High Performance Liquid Chromatography and Electrophoretic techniques [14,15]. These methods undergo expensive methodologies and complex procedures. Hence simple method needs to be developed and adopted to detect and measure histamine levels that can be followed under common laboratories.

Fermentation of idli batter leads to availability of free amino acid in turn leading to formation of biogenic amine by favouring growth of biogenic amine producing positive microbes [6,9]. The safe consumption and shelf-life extension of idli batter needs art of understanding the microbial population and physiochemical requirements. The world is advanced with assortments of restorative plants which have drawn the consideration of analysts because of their endless advantages to humankind, particularly their utilization in drug and food enterprises [16]. Spice extracts has a capability of reducing the biogenic amine content due to the presence of bioactive compounds [17]. Clove and cinnamon are known for its BA reducing capability [18]. Galanga [*Alpinia officinarum*] is one of the most common medicinal plant and found that it is used for treating inflammatory and gastrointestinal disorders [19]. It is rich in antioxidant and serves as anti-cancer remedy. It is also evident that it exhibits anti-bacterial activity. This has not been much explored in the area of reducing biogenic amines. Hence the spice extracts were evaluated for reducing the biogenic amines during the storage of idli batter for a week time under refrigerated conditions using colorimetric method.

MATERIALS AND METHODS

Idli Batter Sample Preparation (Control)

Idli batter was prepared using parboiled rice and black gram dhal in the ratio of 4:1. The batter was made into consistency and required amount of salt [0.9g] was added. The batter was allowed for fermentation at 30°C for 12 hours.

Preparation of Ethanolic Extracts of Spices

The ethanol extracts of spices such as clove, cinnamon and galangal were prepared according to procedure described [20]. The spice [20g each] was soaked in 100 ml of 95% ethanol separately at ambient temperature for 12 h. Then it was mixed well and obtained the extracts of spices by filtering through the Whatman No. 1 filter paper.

Addition of Extracts with Idli Batter (Fortified)

The ethanolic extracts of spices was added to the 12h fermented idli batter at the rate of 1 ml per 100g of the idli batter based on the results of preliminary studies. The idli batter with and without spices extracts were stored separately in the ambient condition for further analysis of the physiochemical properties and biogenic amines at 24 h interval.



**Lakshmi Praba et al.****Physicochemical properties of Idli batter**

The samples were drawn from idli batter from each treatment and analyzed the various physicochemical parameters using standard procedures.

pH

The idli batter [10 g] was mixed with 100 ml of distilled water and mixed thoroughly using vortex for 2 min. The pH was determined using digital pH meter (Horiba scientific 1) as described[21].

Titrateable Acidity

The idli batter [10 g] was taken and mixed with 20 ml of distilled water. The mixer was titrated against 0.1 N Sodium Hydroxide using phenolphthalein as indicator to determine titrateable acidity in terms of lactic acid produced[22].

Color

The color of the idli batter was measured using Hunterlab Color Flex EZ [Make:Virginia ,USA; Model: CFEZ0925]. The L* denotes the whiteness level. The scale for a* varies from green [negative]to red [positive] and the scale for b* corresponds to a yellow-blue scale on which yellow is positive.

Analysis of Histamine Content (Colorimetric Assay)

The histamine content in the fermented Idli batter under refrigerated storage condition was analyzed for seven days in alternate days [0th day, 2nd day and 5th day and 7th day] in triplicates using colorimetric assay. Fig 1 shows the schematic representation of histamine determination in idli batter. The p-phenyldiazonium sulfonate reagent was prepared according to modified method [23]. In a 50 ml standard flask, 1.5 ml of iced 0.9% sulphanic acid, 4 % HCl and 5% of sodium nitrite each were added, mixed and kept in an ice bath for 5 mins. After 5 mins, 6 ml of 5 % sodium nitrite was added and made up to 50 ml with chilled distilled water. Further it was stored in an ice bath for 15 mins prior usage and stable for 12 h. The different concentration [20, 40, 60, 80 and 100 µg] of standard histamine[1ml each] was added in distilled water and prepared by following the above similar steps as of sample and standard curve was plotted against the concentration of histamine using UV-visible spectrophotometer (Make :Shimadzu, Japan; Model:UV-Vis 1800).

In a centrifuge tube, 5 g of idli batter was taken and diluted with 20 ml of 5% TCA, centrifuged at 5000 rpm for 10 mins and filtered using Whatman No.1 filter paper. The filtrate was then made up to 50 ml with 5% TCA. From the filtrate, 1 ml of sample was drawn in centrifuge tubes separately, 2 ml of 5% TCA solution and 0.5 g of mixed salt [6.25 g of anhydrous sodium sulphate & 1 g of trisodium phosphate monohydrate] were added. It was mixed thoroughly, 2 ml of methanol was added to each of the tubes and shaken to shatter the protein gel. The tubes were centrifuged at 3000rpm for 15 mins. After centrifugation, 1 ml of the top layer was transferred to clean test tube and evaporated. The residue was collected in a test tube and added 1 ml of distilled water. In a clean empty tube, 5 ml of 1.1% sodium carbonate and 2 ml of p-phenyldiazonium sulfonate reagent were mixed. This mixture was added to the tube containing the residue along with 1ml distilled water and made to react with the p-phenyldiazonium sulfonate reagent. After 5 minutes of reaction, the absorbance was noted at 496 nm using UV visible spectrophotometer (Make :Shimadzu, Japan; Model: UV Vis 1800).

Sensory Analysis of Idli

The sensory analysis of idli was made from idli batter with and without spices extracts was evaluated on the 7th day of storage period. Five point hedonic scale was used to evaluate the sensory quality of the idli[24].

Statistical Analysis

All the experiments were carried out in triplicates and expressed in mean \pm SD. Minitab19 statistical software was used to analyze the data [25].





Lakshmi Praba et al.

RESULT AND DISCUSSION

Color, pH and Titratable Acidity and Sensory Analysis

pH and titratable acidity are the two main parameters that describes the quality of the batter and responsible for the taste of the idli. It was reported that the pH of idli batter was increased due to the production of fermenting bacteria such as LAB[24]. The pH of the batter was found to be 4.74 - 4.23. The results revealed that the use of spice extracts does not alter the pH and it does not affect the quality of the idli batter [Fig. 2]. It was also found that the titratable acidity and color of the idli batter was not affected by the addition of the spice extracts[Fig.3 & 4.]. There is no significant color difference between the control idli and fortified idli. The whiteness index of the idli batter was not much affected upto 7 days of storage period under refrigerated condition. The L value was found to be 86.7 and it was maintained upto 7 days storage period without significant difference between the control and fortified samples. The sensory analysis was conducted on the 7th day of the storage period as it was the maximum time considered for storage. The idli prepared on day 7 clearly states that quality of the idli has not been affected on usage of spice extracts (Table 1). The idli prepared using galanga extract has good acceptability in terms of color, texture, taste and appearance next to control idli. The addition of spice extracts helps in prolong storage by reducing the sour taste of idli providing additional medicinal effects and flavour.

Analysis of Biogenic Amine in Fermented Idli Batter

The histamine content in the fermented Idli batter stored in refrigerated condition was analyzed using colorimetric assay. The biogenic amine histamine levels were increased during the storage time and it was due to the decarboxylation reaction that is responsible for production of histamine [Table 2]. There was a constant increase and decrease in the biogenic amine content in fermented idli batter. This was presumed due to the *Lactobacillus* spp. production during fermentation reaction, variation in the pH from acidic to alkaline and protein content in the batter sample [26]. The histamine content in the control idli batter was high [15.54 mg/kg] compared to the fortified idli batter on 7th day. The results showed lesser histamine content in galanga added idli batter [0.34 mg/kg] followed by cinnamon idli batter and clove idli batter. It was also observed that there was an increase of histamine content in the fortified idli batter but the histamine content in galanga idli batter on 7th day was on par with 0th day. The histamine content in the idli batter was in considerable limit which is less than the toxic levels. These results revealed that the extracts added may involve in reduction of fermenting and histamine producing bacteria by controlling in their metabolic activity[22]. This would be caused due to the microbial growth inhibition activity of galanga against histamine producing bacteria.

CONCLUSION

The results of the present study revealed that the addition of extracts (1%) of clove, cinnamon and galanga were able to control the production of histamine in the idli batter. Among the three extracts, galanga extract showed better reduction of histamine compared to other two extracts. The physical parameters such as pH, titratable acidity and color of the idli batter with extracts were not affected upto 7 days of storage study. Hence it is concluded that the galanga extract at 1% concentration in idli batter helps in reduction of histamine and can be used as potential biogenic amine reducers. In future, various vegan based fermented foods can also be explored for incorporation of novel spice extracts for improving shelf life.

ACKNOWLEDGEMENTS

The authors are thankful to the National Institute of Food Technology, Entrepreneurship and Management-Thanjavur for the facility provided for conducting the experiments.

Conflict of Interest

The authors have no conflict of interest to declare.



**Lakshmi Praba et al.****REFERENCES**

1. Krishnamoorthy S, Kunjithapatham S, Manickam L. Traditional Indian breakfast (Idli and Dosa) with enhanced nutritional content using millets. *Nutr Diet.* 70(3):241–6:2013.
2. Shrivastava N, Ananthanarayan L. Use of the backslapping method for accelerated and nutritionally enriched idli fermentation. *J Sci Food Agric.* 95(10):2081–7:2015.
3. Steinkraus K. Handbook of Indigenous Fermented Foods, Revised and Expanded. Handbook of Indigenous Fermented Foods, Revised and Expanded. pg792:2018.
4. Nevetha Ravindran, Venkatachalapathy N, Loganathan M and V Eyarkai Nambi. Effect of stirring on the rheological, textural and structural characteristics of Idli batter and steamed Idli. *Pharma Innov J.* 10(10):1252–5:2021.
5. Nisha P, Ananthanarayan L, Singhal RS. Effect of stabilizers on stabilization of idli (traditional south Indian food) batter during storage. *Food Hydrocoll.* 19(2):179–86:2005.
6. Regubalan B, Ananthanarayan L. Investigation of biogenic amines content in fermented idli batter during storage. *J Food Sci Technol.* 55(9):3417–26:2019.
7. Arena ME, Manca De Nadra MC. Biogenic amine production by *Lactobacillus*. *J Appl Microbiol.* 90(2):158–62:2001.
8. Shalaby AR. Significance of biogenic amines to food safety and human health. *Food Res Int.* 29(7):675–90:1996.
9. Silla Santos MH. Biogenic amines: Their importance in foods. *Int J Food Microbiol.* 29(2–3):213–31:1996.
10. Peñas E, Frias J, Sidro B, Vidal-Valverde C. Impact of fermentation conditions and refrigerated storage on microbial quality and biogenic amine content of sauerkraut. *Food Chem.* 123(1):143–50:2010.
11. Gagic M, Jamroz E, Krizkova S, Milosavljevic V, Kopel P, Adam V. Current Trends in Detection of Histamine in Food and Beverages. *J Agric Food Chem.* 67(3):773–83:2019.
12. FSSAI. Food Safety and Standards (Food Products Standards and Food Additives) Regulations, 2011.
13. EFSA (European Food Safety Authority). SCIENTIFIC OPINION. Scientific Opinion on risk based control of biogenic amine formation in fermented foods. EFSA Panel on Biological Hazards (BIOHAZ). *EFSA J.* 2011.
14. Sato M, Tao ZH, Shiozaki K, Nakano T, Yamaguchi T, Yokoyama T, et al. A simple and rapid method for the analysis of fish histamine by paper electrophoresis. *Fish Sci.* 72(4):889–92:2006.
15. Hungerford JM, Walker KD, Wekell MM, LaRose JE, Throm HR. Selective Determination of Histamine by Flow Injection Analysis. *Anal Chem.* 62(18):1971–86:1990.
16. Anbukumaran A, Shijila Rani S, Veeramani S, Babu S, Gomathi S, Ambikapathy V. Evaluation and characterization of phytochemicals from aerial parts of *Coldenia procumbens* Linn. *Int J Bot Stud.* 6(2455–541X):486–92:2021.
17. Sun Q, Zhao X, Chen H, Zhang C, Kong B. Impact of spice extracts on the formation of biogenic amines and the physicochemical, microbiological and sensory quality of dry sausage. *Food Control.* 92(29):190–200:2018.
18. Naila A, Flint S, Fletcher G, Bremer P, Meerdink G. Control of biogenic amines in food - existing and emerging approaches. *J Food Sci.* 75(7):139–50:2010.
19. Das A, Santhy KS. Chemical characterisation of *Alpinia Galanga* (L.) willd by GC–MS, XRD, FTIR and UV-VIS spectroscopic methods. *Int J Pharm Pharm Sci.* 7(9):499–501:2015.
20. Shakila RJ, Vasundhara TS, Rao DV. Effect of Spices on the Biogenic Amine Formation and Other Quality Characteristics of Indian Mackerel During Refrigerated Storage. *Asian Fish Sci.* 9:191–9:1996.
21. Iyer B, Ananthanarayan L. Effect of α -amylase addition on fermentation of idli—a popular south Indian cereal—Legumebased snack food. *LWT - Food Sci Technol.* 41:1053–9:2008.
22. Regubalan B, Ananthanarayan L. Shelf life improvement of idli batter by addition of mustard essential oil as bio-preservative. *J Food Sci Technol.* 55(9):3417–26: 2018.
23. Patange SB, Mukundan MK, Kumar KA. A simple and rapid method for colorimetric determination of histamine in fish flesh. *Food Control.* 16(5):465–72:2005.
24. Chelliah R, Ramakrishnan SR, Premkumar D, Antony U. Bio-fortification and shelf-life extension of idli batter using curry leaves (*Murraya koenigii*). *J Food Sci Technol.* 53(6):2851–62: 2016.





Lakshmi Praba et al.

25. Induja C, Loganathan M. Influence of host and duration of storage on uric acid contamination in wheat products infested with confused flour beetle , Tribolium confusum. 6(6):84–6: 2021.
26. Gunasekaran R, A M, Shetty P. Quantitative Analysis of Histamine Production in Idli Batter. Int J Trend Sci Res Dev.3(3):1190–3: 2019.

Table 1: Sensory analysis of idli

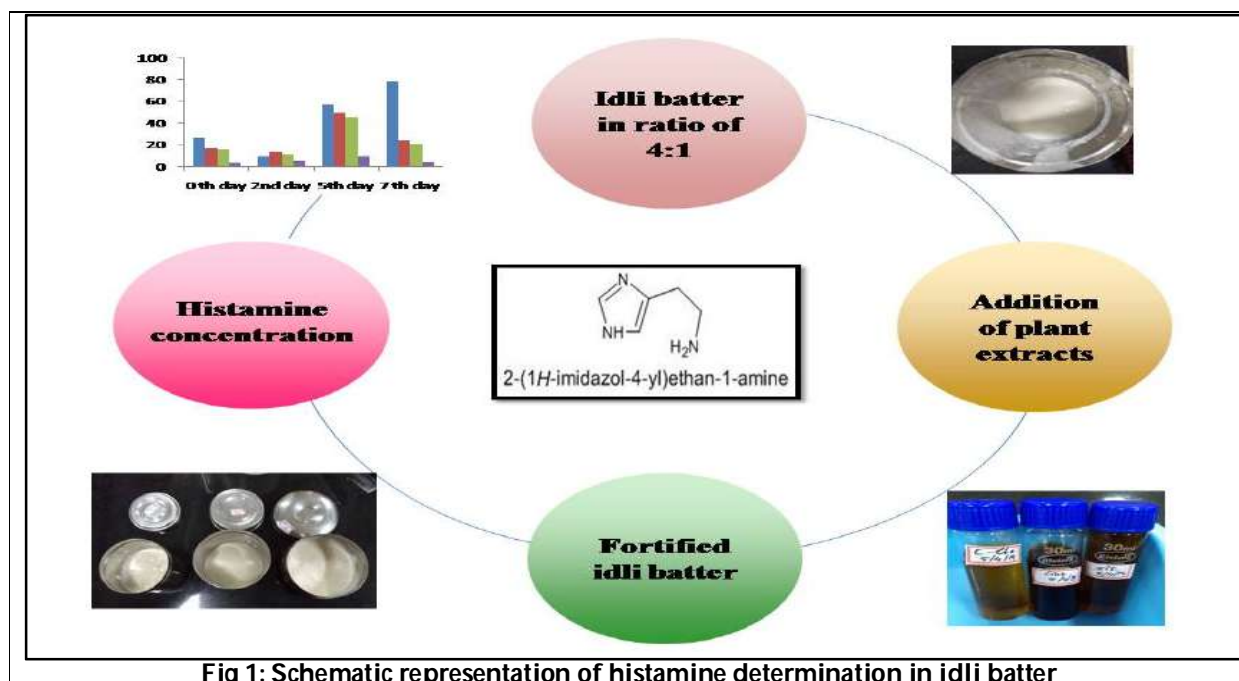
Idli	5-point hedonic scale					
	Appearance	Color	Flavour	Texture	Taste	Overall acceptability
Control idli	4.08±0.64	4.16±0.68	3.66±0.84	3.66±0.94	3.75±0.72	3.95±0.82
Clove idli	3.83±0.98	3.75±1.16	3.33±1.17	3.50±0.86	3.33±0.62	3.41±0.64
Cinnamon idli	3.83±0.89	2.83±0.89	3.75±0.82	3.75±0.82	3.62±0.73	3.59±0.83
Galanga idli	4.25±0.92	4.41±0.75	4.0±0.81	3.66±0.74	3.83±0.89	3.75±1.01

5- point hedonic scale used for sensory analysis 1- Not acceptable 2 -Moderately acceptable 3 - Neither acceptable nor unacceptable 4 - Acceptable 5 - Highly acceptable

Table 2: Histamine content in idli batter during storage

Storage duration (days)	Histamine content (mg/kg)			
	Control batter	Clove idli batter	Cinnamon idli batter	Galanga idli batter
0	5.18 ^c	3.33 ^c	3.03 ^c	0.66 ^c
2	1.85 ^d	2.59 ^d	2.14 ^d	1.03 ^b
5	11.25 ^b	9.85 ^a	9.03 ^a	1.77 ^a
7	15.54 ^a	4.81 ^b	4.07 ^b	0.74 ^c

Different letters indicate a significant difference (p< 0.05) within the same column





Lakshmi Praba et al.

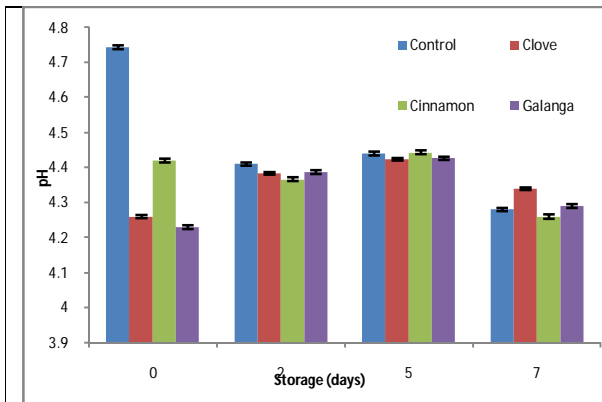


Fig 2. pH of Idli Batter with and Without Spices Extracts

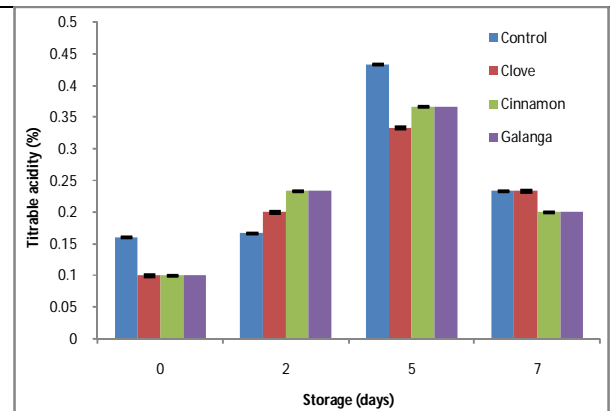


Fig 3. Titratable Acidity of Idli Batter with and Without Spices Extracts

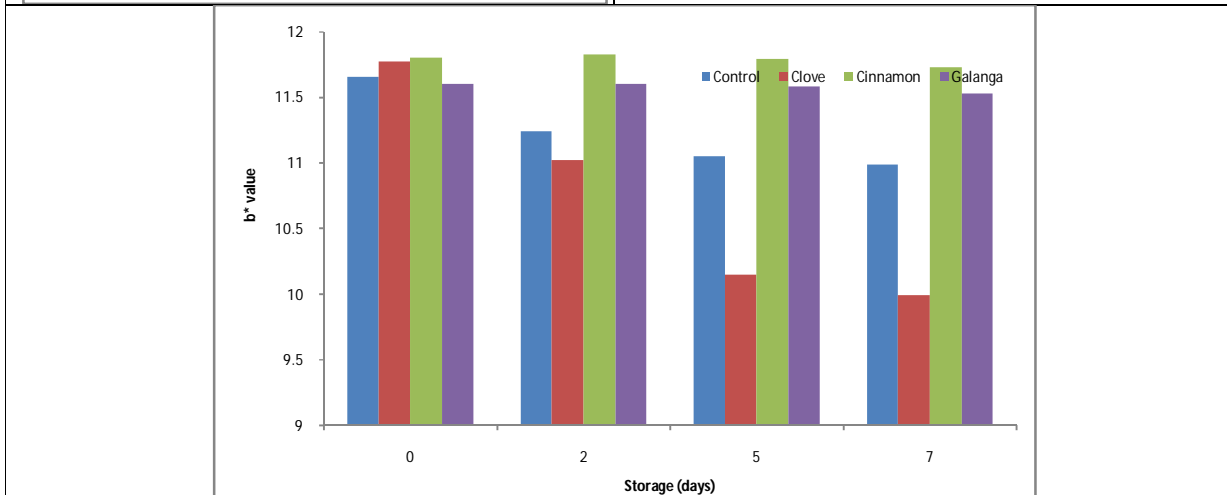
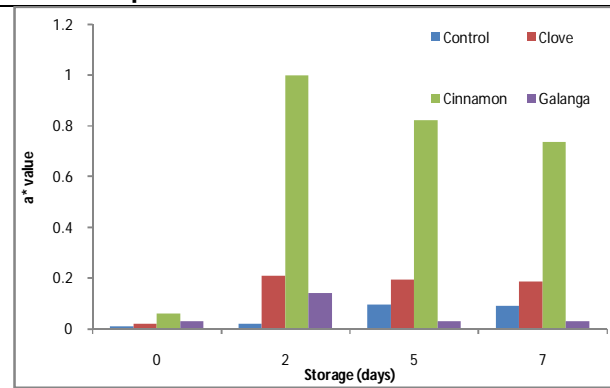
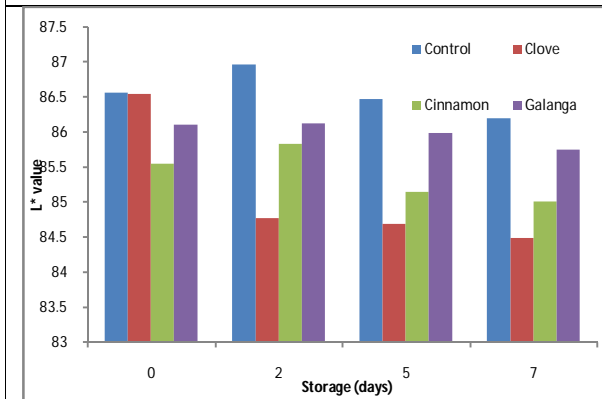


Fig 4. Colour Values of Idli Batter With and Without Spices Extracts





Study on Voltage Support in Micro Grid Power Distribution System

G. Vijai^{1*} and P. Selvam²

¹Research Scholar, Department of Electrical and Electronics Engineering, Vinayaka Mission's Kirupananda Variyar Engineering College, Salem, Tamil Nadu, India.

²Professor and Head, Department of Electrical and Electronics Engineering, Vinayaka Mission's Kirupananda Variyar Engineering College, Salem, Tamil Nadu, India.

Received: 17 Dec 2021

Revised: 10 Jan 2022

Accepted: 21 Jan 2022

*Address for Correspondence

G. Vijai

Research Scholar,
Department of Electrical and Electronics Engineering,
Vinayaka Mission's Kirupananda Variyar Engineering College,
Salem, Tamil Nadu, India.
Email: reachvijaigopal@gmail.com



This is an Open Access Journal / article distributed under the terms of the **Creative Commons Attribution License** (CC BY-NC-ND 3.0) which permits unrestricted use, distribution, and reproduction in any medium, provided the original work is properly cited. All rights reserved.

ABSTRACT

The growth of local renewable energy sources and heavy loads in power distribution networks, such as the increasing electric vehicles charging stations, causes several issues with a direct impact on the stability of the electrical grid. An attempt to overcome such issues is the microgrid concept, which has the grid structured into local sub-grids that manage their power and energy balancing. A microgrid may operate connected or disconnected from the main grid, being dynamically necessary to guarantee a power balancing between local loads and sources. Furthermore, as several power units are connected to the same microgrid, equity is also required in terms of power sharing. Microgrids are able to operate under autonomous and grid-connected modes. This predominance can also compensate for the disadvantages of traditional centralized power systems with high emission and low efficiency. Furthermore, microgrids can also enhance power system reliability and power quality under optimal control and operation conditions. Since microgrids will play the vital important role in power systems in the future, it is necessary to realize the operation and nature of microgrids. Microgrids provide a new infrastructure for more efficient, resilient and cost-effective power systems. This architecture works like a power nest with scattered conventional and non-conventional energy sources throughout the distribution network. Micro-power sources combined with their interfaces are categorized as distributed generators (DG). Distributed generators work according to load demand and their converters adjust voltage and frequency and harmonize it with the network such that the load requirements of the end users are met. Distributed generators are considered as small power generating units and are usually rated at <100kW. Solar photovoltaics, fuel cells, wind turbines, micro-turbines, flywheels and super capacitors can all be used as micro-power sources. Power electronic converters are utilized to connect these sources to the supply network through a common grid bus.



**Vijai and Selvam**

Keywords: Micro Grid, Grid connected Inverter, Distributed Generation, PR controller, PV Inverter, Parallel connected Inverters, Power flow.

INTRODUCTION

Micro Grid (MG) and Distributed Generation (DG) plays various important roles in helping the Power system like improving capacity, efficiency etc [1]. Every MG or DG have several inverters to pump power to the system from various available energy sources. The main intention of the control system in every inverters of the Micro Grid is to share the power demand in such a way that all the inverters connected to renewable energy sources should pump the entire extracted power to the Point of Common Coupling (PCC) under grid connected or standalone mode [2] and equitable sharing of load among rest of the inverters which are in parallel when operating under standalone mode [3]. Also, the control system in every inverter should ensure seamless switching between the grid connected mode and standalone mode when the grid fails. Sometimes, the inverters which connect the DG with the grid may be required to provide reactive power to the grid to aid reactive power compensation [4]. However, the inverter feeding power to the grid from PV sources usually inject power at unity power factor or pump only real power to the grid. In order to share the demand in power, the inverters in a MG usually adopt some droop control techniques [5-9] to pump real and reactive powers in appropriate to their capacities. However, this control technique cannot be used in the case of inverters injecting power extracted from renewable energy sources such as PV and Wind Power Sources, wherein the entire extracted power must be pumped to the MG. Hence in such inverters the control technique is different from those inverters which are feeding power from conventional sources and Energy storage devices.

Overview of Typical Grid connected PV Inverter

The basic typical structure of a voltage source inverter with an output filter meant for grid synchronization is shown in Fig. 1. The structure composed of a power inverter, which is of a Bridge type driven by a Pulse Width Modulator, an isolation transformer and a LC filter. The control system consists of a Phase Lock Loop, meant for generating the grid angle to synchronize the inverter with the grid, a current controller, a voltage controller and measurement systems. The control system operates based on the samples obtained from the variables to be controlled. The voltage controller upon getting the DC link voltage will generate the reference current to the current controller such that to maintain a constant DC link voltage in order to transfer all the power coming as input to the DC link to the grid. In order to pump the extracted power from the PV energy source at unity power factor to the grid the current reference to the current controller is synthesized with the help of the grid angle generated by the PLL. The current controller usually a Proportional-Resonant (PR) controller, which is often preferred as it has excellent sinusoidal tracking capability, generates the control voltage for the PWM generator [10-12]. The control voltage generated by the PR controller is combined with the feed forward signal from the grid voltage, for the purpose of reducing the start-up transient and to decouple the dynamic of the converter with those of the grid [add reference], and fed to the PWM generator. The single-phase bridge inverter is driven by the switching signals generated by the PWM generator. The output of the inverter is smoothed by the LC filter and the power is injected to the grid through the inductor which links the inverter and the grid physically. In the scheme shown in Fig 1, the transformer equivalent inductor will act as the inductor for the LC filter. The value of the filter capacitor C_f is chosen to decide the resonant frequency of the LC filter. At steady state the current injected to the grid will be in phase with its voltage maintaining a unity power factor.

Supporting the Micro-Grid Voltage

In a Micro Grid (MG), under islanding mode of operation, the inverters participating in the Distributed Network within the MG are classified as i) Grid forming inverter, ii) Grid feeding inverter and iii) Grid supporting converter [5]. One of the inverters under islanding mode of MG operation should provide a synchronous reference (Grid forming inverter), for the rest of the paralleled inverters, with voltage and frequency control. Most of the PV based grid connected inverter works, as a Grid feeding inverter, to inject real power into the grid by tracking the power or current reference. And they need to have a complex control scheme to participate in voltage control or exercise Grid





Vijai and Selvam

supporting feature. In order to support the Micro grid voltage, the inverters which are participating as grid supporting inverter should inject appropriate amount of real and reactive power to support maintenance of grid voltage and frequency. This support is normally exercised with the help of droop control strategy. Even complex nested real power droop- frequency droop with nested reactive power droop- voltage droop control can be used to make an inverter to participate in grid support [2]. In the proposed method in this paper a simple logical grid support in the form of injecting reactive power to support the grid voltage in addition to real power available from PV energy source is presented.

Proposed support from PV Inverter

When supplying only real power based on the extracted available power, all the time the inverter may not operate at its full current capacity either in grid connected mode or islanded micro grid mode. Under islanded micro grid mode, the grid forming and grid supporting inverters have to take the task of feeding the reactive power demand by the connected loads. When the grid forming inverter's full capacity is reached, the micro grid will suffer from voltage dip, if the support from the grid supporting inverters is insufficient. In order to tackle such issue, the inverter supplying PV power may be controlled in such a way that the excess current capacity, apart from real current feed, shall be used to pump reactive power to boost the micro grid voltage. This is the main contribution of this paper. The control scheme is configured such that at any point of time the real power component of the current will not be disturbed however the reactive power component of the current is adaptively adjusted to maintain the micro grid voltage at its point of common coupling.

Estimation of Reactive Power Support

The method of reactive power injection is made effect by first sensing the local grid voltage and compared with the nominal grid voltage. If any deviation is found then the magnitude required for voltage compensation is computed using the equation (1) [13]. This estimation is done by considering the voltage drop due to real power is negligible.

$$i_q^* = \frac{\Delta V}{X_g} = \frac{V_g^* - V_g}{\omega L_g} \quad (1)$$

From the computed reactive current using the equation (1), the possible amount of reactive current that could be inject is calculated taking into consideration that the combined real and reactive current magnitude should not exceed the inverter rated current capacity under any circumstances. The reference current to be fed to the controller is derived by using the equation (2).

$$i_{inv}^* = i_p^* \cos \omega t + i_q^* \sin \omega t \quad (2)$$

Control System of the Proposed Method

The control method contemplated in the method proposed in this paper consists of a power controller which will derive the active power component from the DC link voltage controller and the reactive power component from the method described earlier to support the Micro grid Voltage. The computed apparent power is given by equation (3)

$$S^* = P^* + jQ^* \quad (3)$$

From the derived power, the power controller will produce the reference current for the Current controller in accordance with the equation (2).

The overview of the complete control structure of the proposed scheme is shown in the Figure 2, where reactive part of the reference current is derived based on equation (2) from the micro grid voltage and the real part of the current is derived from the DC link voltage VDC.

The reference voltage for the DC link voltage shall be fixed as per the grid inverter requirements such that the current in the inverter should be controllable. For a single-phase grid connected inverter the DC link voltage should be greater than peak value of the nominal grid voltage V_m at the point of common coupling. In the present case the reference DC link voltage is taken as 400V. If the DC link voltage is maintained constant at the reference value the





Vijai and Selvam

power input to the DC link will be pumped to the grid. The DC link voltage is controlled with the help of a Proportional and Integral (PI) Controller. The output from the PI controller forms the real part of the current reference.

The micro grid voltage is continuously monitored and compared with the nominal grid voltage. The error produced is used to estimate the reactive part of the reference current. The magnitude of the reactive part of the current is decided such that the final reference current should not be greater than the current rating of the inverter. Therefore, the reactive part of the reference current is a function of real power produced by the PV energy source and the grid voltage magnitude as expressed by the equation (4)

$$i_q^* = f\left(\left|P_{pv}\right|, \left|V_g\right|\right) \mid \left|i_{inv}^*\right| \leq i_{rated(inverter)} \quad (4)$$

As the current reference to the current controller is a sinusoidal quantity a PI control as such cannot track the reference without steady state magnitude and phase error. Hence a current controller needs additional compensators with PI controller which needs significant control design and become finally end up with a complex controller. On account such complexity a Proportional and Resonant (PR) controller is used in this control scheme. The PR controller offers good tracking performance for sinusoidal reference at the frequency at which it is tuned [12, 14]. The control scheme in the presented method uses a feed forward compensation in order to mitigate the startup transient. This is compensation is implemented by adding the micro grid voltage with the output of the current controller.

Transfer Function of DC Link Side Plant and AC Side Plant

The transfer function of the DC link can be obtained by applying small signal analysis to the expression after equating the instantaneous power at the DC link equal to the instantaneous power at the AC side by ignoring the losses in the inverter [15]. The obtained transfer function between the DC link voltage and the active power component of the inverter output current is given in the equation (5).

$$\frac{v_{dc}(s)}{i_p(s)} = \frac{V_{gm}}{V_{DC}C_{DC}s} \quad (5)$$

where, V_{gm} is the magnitude of the grid voltage, V_{DC} is the DC link voltage and C_{DC} is the DC link filter capacitor. By considering the LCL filter capacitor C_f and the grid side inductor L_g the components of grid side, the plant seen by the inverter is the equivalent impedance of the isolation transformer. The block diagrammatic representation of the system between the inverter and the AC side filter capacitor is shown in Figure 3. where, V_{inv} and V_g are the inverter output and grid voltages respectively and R_t and L_t are the equivalent resistance and inductance of the isolation transformer.

Synchronization

In order to pump the power to the grid from the inverter synchronously, the grid voltage phase angle need to be extracted as this angle is essential to deduce the reference inverter current from the reference active and reactive power fixed by the voltage controller and from the reactive power estimation. Though various synchronization techniques are present in the literature, the method of synchronization employed in this paper is the general Phase Locked Loop (PLL). The general PLL is implemented through software technique. The scheme of implementation is block diagrammatically represented in Figure 4.

Voltage Controller and Current Controller and Their Control Analysis

The voltage controller designed to control the DC link voltage in order to pump the available power at the DC link fed by the PV energy source is a Proportional and Integral Controller. The designed PI controller is given in equation (6). The open loop and the closed loop response in conjunction with the transfer function of the DC link is shown in Figures 5(a) and 5(b) respectively.





Vijai and Selvam

$$PI \text{ Controller} \Rightarrow 0.5 + \frac{100}{s} \quad (6)$$

The current controller designed to generate the control signal in relation to the error between the reference current signal set by the voltage controller and the reactive current set by the reactive power estimator is a PR controller with a damping factor of 1.

The designed transfer function of the PR controller is given in equation (7). The bode plot of the current controller loop for open and closed loop are shown in Figures 6(a) and 6(b) respectively.

$$PR \text{ Controller} \Rightarrow 10 + \frac{1256.6368s}{s^2 + 1256.6368s + 98696} \quad (7)$$

Computer Simulation and Analysis

The verification of the proposed method of interactive voltage support is made through Simulink software by MATLAB®. In the scheme used for verifying the method, two inverters are used and they are connected in parallel. One of the inverters is supplying energy from a Battery energy storage, which acts as the Grid forming inverter and the other inverter feeding energy to the grid from a PV energy source acts a Grid feeding inverter with interactive voltage support. The Grid feeding inverter is synchronized after the output from the Boost converter of the Maximum Power Point Tracing (MPPT) system for the PV source has reached 400V DC otherwise the current control cannot be exercised by the grid feeding inverter. The Simulink scheme of the proposed method is shown in Figure 7.

The model used as PV array in the simulation is TSMC Solar TS-110C inbuilt with the Simulink software. The number of PV modules connected in series is set to be 10 in order to create the required voltage. The total power that could be generated by the PV array is 1098.71Wp at 25°C. The MPPT is configured with the popular Perturb and Observe technique and implemented using MATLAB function. The proposed method of interactive voltage support is implemented using S-function builder for the grid feeding inverter. The simulation model is simulated under discrete mode. The synchronization between the grid feeding and the grid forming inverter is shown in the Figure 8, where it can be seen that an excellent synchronization is established.

In the simulation the load common to both the inverters has real power and reactive power demand of 2000W and 1500VARs. Under steady operation the current sharing between the inverters to maintain the nominal grid voltage of 230V is shown in Figure 9, which shows the contribution of the grid feeding inverter in maintaining the grid support. The load sharing in terms of real and reactive power by the grid forming and grid feeding inverters from the point of time at which the grid feeding inverter starts feeding the power up to the steady state is shown in Figures 10 and 11. From these figures it is obvious that the interactive voltage support by the grid feeding inverter is active and supports the point of common coupling in maintaining the voltage without exceeding its rated capacity.

Experimental Verification

An experimental setup is established by connecting two inverters in a Micro grid mode where a Commercial UPS of 950VA capacity is used as grid forming inverter. The grid feeding inverter is designed by taking the power inverter portion another commercially available UPS of 800VA capacity. The control and sensing circuits are separately designed and integrated to it. The entire control actions are configured with the help of a DSP TMS320F28027. The Piccolo Launch Pad for the above said DSP from Texas Instruments (TI) is used for experimental verification and the complete control features are programmed using the Code Composer Studio Package from TI. The photograph of the used experimental setup is shown in Figure 12. In the experimental verification, the grid forming inverter is supplying real and reactive load and the grid feeding inverter is supplying load at unity power factor. The interactive voltage support control is made to operate in conjunction with a raise in PV power with the help of a Solar Array Simulator. For this purpose, a Solar Array Simulator (SAS) of 600W capacity from Agilent is used. As the control starts working the real power and reactive power share by the grid feeding inverter is increased ensuring the voltage and real power support. These interactions are shown in the Figures 13 and 14. For the purpose reducing the



**Vijai and Selvam**

voltage at the point common coupling additional load is added to the grid forming inverter with an impedance interposed between the point of common coupling and the grid forming inverter accounting for a small transmission line. This impedance is equivalent to a value of 4mH with negligible resistance. From the experimental results obtained, it is clear that the proposed system is working in line with the intended scheme of operation and correlates with the simulation results obtained.

CONCLUSION

An interactive voltage support of grid feeding inverter is presented in this paper. The method is so constructed that higher levels of complex control structure are eliminated. Since the method is based on local parameter measurements no communication is required and hence the reliability of the scheme is more than the schemes with external communication. The controller meant for DC link voltage and grid current injection are designed and verified. The experimental results obtained are in good correlation with the results obtained through simulation through Simulink software package.

REFERENCES

1. Jinwei He *et al.*, "An Enhanced Microgrid Load Demand Sharing Strategy", IEEE Transactions on Power Electronics, vol. 27, no. 9, 2012
2. Qing-Chang Zhong and George Weiss, "Synchronverters: Inverters That Mimic Synchronous Generators", IEEE Transactions on Industrial Electronics, Vol. 58, No. 4, 2011
3. Suleiman M. Sharkh *et al.*, "Power Electronic Converters for Microgrids", John Wiley, 2014.
4. FredeBlaabjerg (Ed), "Control of Power Electronic Converters and Systems", Academic Press, 2018.
5. Joan Rocabert *et al.*, "Control of Power Converters in AC Microgrids", IEEE Transactions on Power Electronics, Vol. 27, No. 11, 2012
6. P. Monica *et al.*, "Control strategies of parallel operated inverters in renewable energy application: A review", Renewable and Sustainable Energy Reviews 65 (2016) 885–901.
7. Wei Yao *et al.*, "Design and Analysis of the Droop Control Method for Parallel Inverters Considering the Impact of the Complex Impedance on the Power Sharing", IEEE Transactions on Industrial Electronics, Vol. 58, No. 2, 2011
8. S.K. Khadem *et al.*, "Parallel operation of inverters and active power filters in distributed generation system—A review", Renewable and Sustainable Energy Reviews 15 (2011) 5155–5168.
9. Yun We i Li and Ching-Nan Kao, "An Accurate Power Control Strategy for Power-Electronics-Interfaced Distributed Generation Units Operating in a Low-Voltage Multi-bus Microgrid", IEEE Transactions on Power Electronics, Vol. 24, No. 12, 2009.
10. Amin Hasanzadeh *et al.*, "A Proportional-Resonant Controller-Based Wireless Control Strategy with a Reduced Number of Sensors for Parallel-Operated UPSs", IEEE Transactions on Power Delivery, Vol. 25, No. 1, 2010
11. Celso Becker Tischer *et al.*, "Proportional-resonant control applied on voltage regulation of standalone SEIG for micro-hydro power generation", IET Renew. Power Gener., 2017, Vol. 11 Iss. 5, pp. 593-602.
12. R. Teodorescu *et al.*, "Proportional-resonant controllers and filters for grid-connected voltage-source converters", IEE Proc.-Electr. Power Appl., Vol. 153, No. 5, September 2006
13. Josep M. Guerrero *et al.*, "Control of Distributed Uninterruptible Power Supply Systems", IEEE Transactions on Industrial Electronics, Vol. 55, No. 8, 2008
14. JaumeMiret *et al.*, "Selective Harmonic-Compensation Control for Single-Phase Active Power Filter With High Harmonic Rejection", IEEE Transactions on Industrial Electronics, Vol. 56, No. 8, 2009.
15. P. G. Barbosa *et al.*, "Control strategy for grid-connected DC-AC converters with load power factor correction", IEE Proc.-Gener. Transm. Distrib., Vol. 145, No. 5, Sep 1998.





Vijai and Selvam

BIOGRAPHIES



G. Vijai received his B.E. degree in Electrical and Electronics Engineering in 2011 from Pallavan College of Engineering, Kanchipuram, Tamil Nadu, India. He received his M.E. degree in 2014 in Power Systems from Sri Chandrasekarendra Saraswathi Viswa Maha Vidyalaya (SCSVMV) University, Kanchipuram, Tamil Nadu, India. He is currently working as a PRT in DAV- BHEL School (CBSE), Ranipet, Tamil Nadu, India. He is pursuing his PhD in Vinayaka Mission's Research Foundation, Salem, Tamil Nadu, India. His research interest includes Advanced Distribution Automation for Smart Grid Environment.



P.Selvam received his B.E., degree in Electronics and Communication Engineering in 1988 from Sri Jayachamarajendra College of Engineering, Mysuru, Karnataka, India. He received his M.S. degree in 1996 in Electronics & Control from BITS, Pilani. He received his Ph.D Degree in 2011 from Vinayaka Mission's Kirupananda variyar Engineering College of Vinayaka Mission's Research Foundation Deemed to be University, Salem, Tamilnadu, India. He is currently working as Professor in the Department of Electrical and Electronics Engineering, Vinayaka Mission's Kirupananda Variyar Engineering College, salem, Tamilnadu, India. His research interest includes Embedded Systems, DFIG in Wind Mill Applications, Application of Power Electronics in Power systems and in renewable Energy sources.

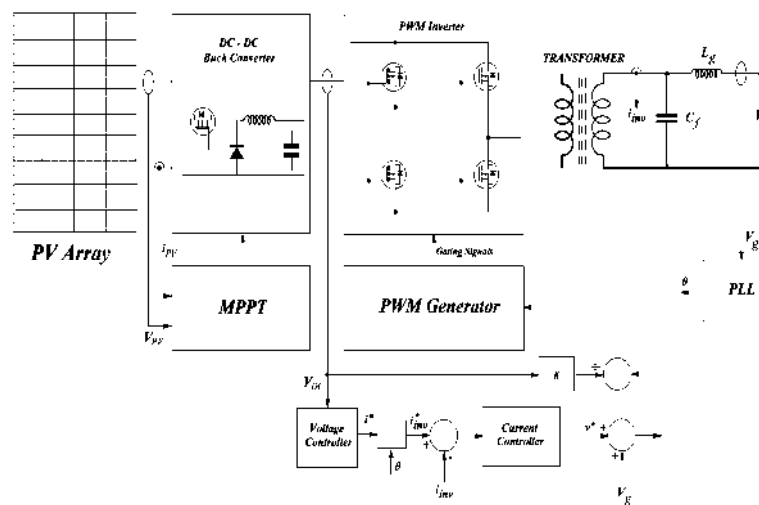


Figure 1. Structure of a typical Voltage Source Grid connected Inverter

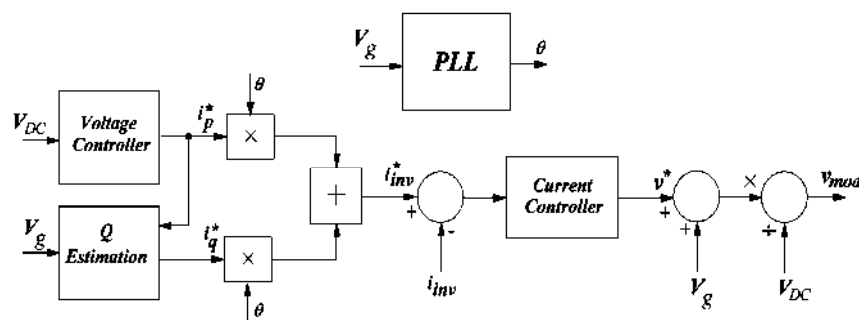


Figure 2. Control structure of the proposed scheme





Vijai and Selvam

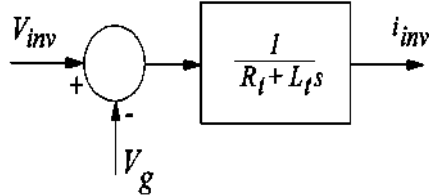


Figure 3.AC Side Plant

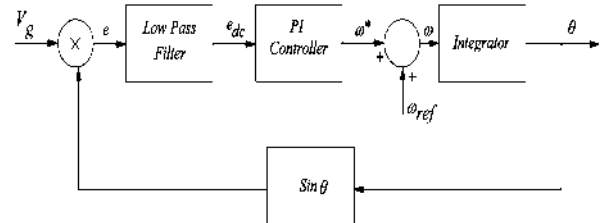
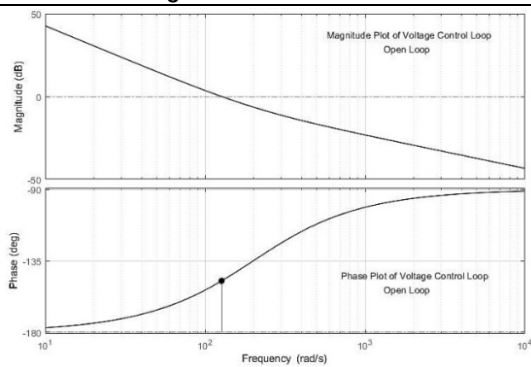
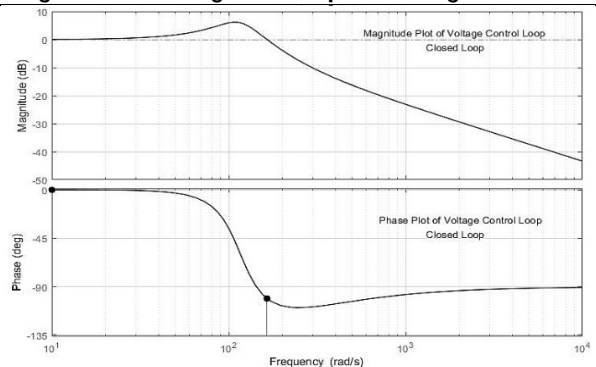


Figure 4.Block diagram of implemented general PLL

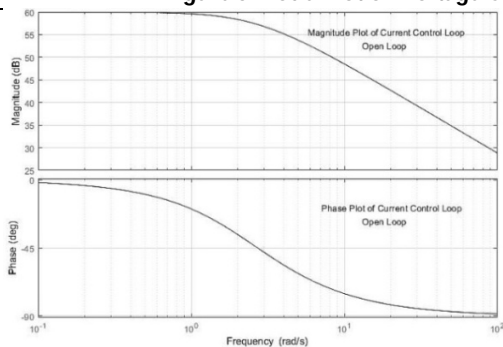


(a)

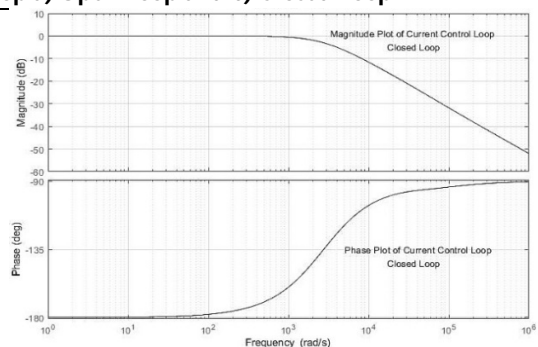


(b)

Figure 5. Bode Plot of Voltage Control Loop a) Open Loop and b) Closed Loop



(a)



(b)

Figure 6. Bode Plot of Current Control Loop a) Open Loop and b) Closed Loop

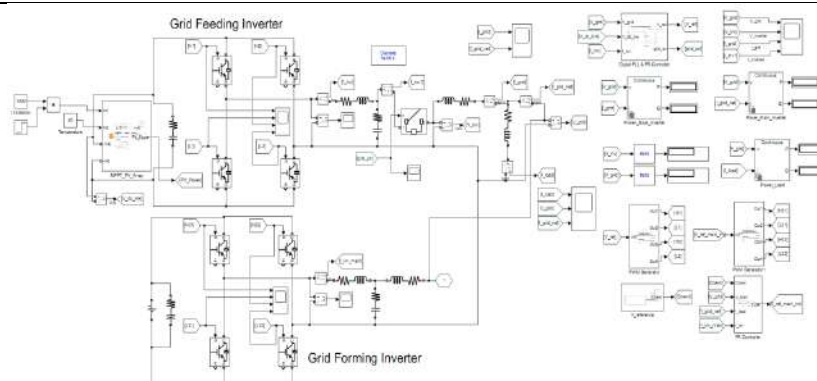


Figure 7. Scheme of Micro Grid for Simulation





Vijai and Selvam

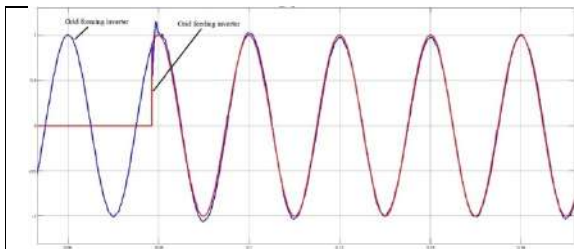


Figure 8. Synchronization between the Grid feeding and Grid forming inverters

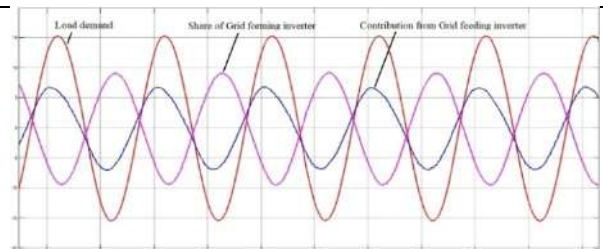


Figure 9. Steady state Load sharing by Grid forming and Grid feeding inverters

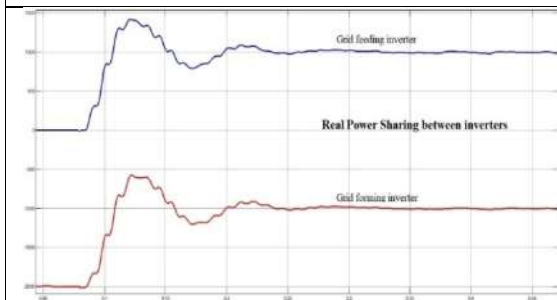


Figure 10. Real power sharing between the inverters

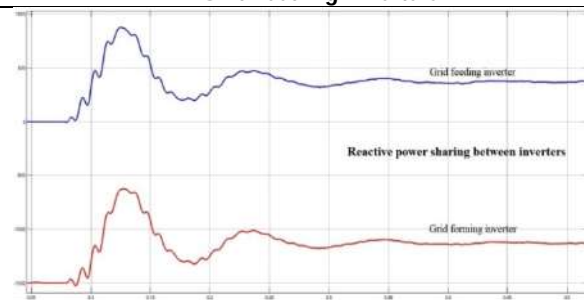


Figure 11. Reactive power sharing between the inverters



Figure 12. Experimental Setup for real time verification

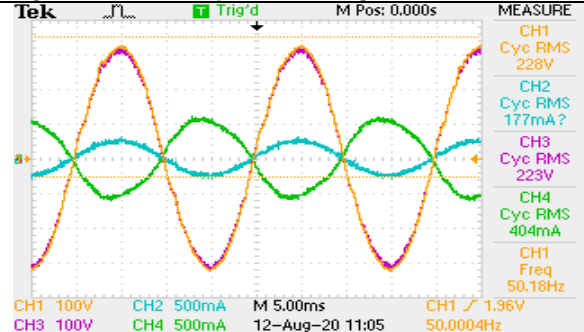


Figure 13. Load sharing before Q support

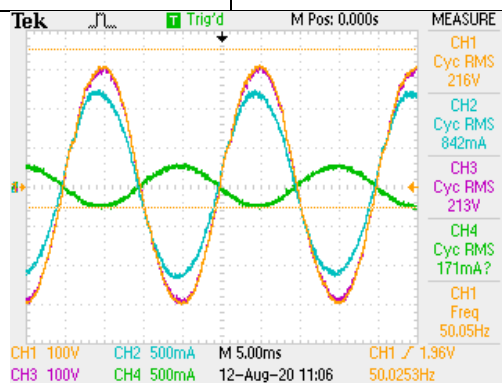


Figure 14. Load sharing after Q support

Channel 1- Voltage of Grid feeding inverter, Channel 2 – Current of Grid feeding inverter, Channel 3- Voltage of Grid forming inverter, Channel 4- Current of Grid forming inverter. (Figure 14 and 15)





Review of Microspheres as Targeted Drug Delivery to the Colon

Dakme Papi^{1*}, Biplab Kumar Dey² and Ananta Choudhury²

¹M.Pharm [Pharmaceutics], Assam downtown University, Panikhaiti, Guwahati, Assam -781026, India.

²Faculty of Pharmaceutical Science, Assam downtown University, Panikhaiti, Guwahati, Assam - 781026, India

Received: 28 Oct 2021

Revised: 15 Dec 2021

Accepted: 06 Jan 2022

*Address for Correspondence

Dakme Papi

M.Pharm [Pharmaceutics],
Assam downtown University,
Panikhaiti, Guwahati,
Assam -781026, India.
Email: dakmepapi@gmail.com



This is an Open Access Journal / article distributed under the terms of the **Creative Commons Attribution License** [CC BY-NC-ND 3.0] which permits unrestricted use, distribution, and reproduction in any medium, provided the original work is properly cited. All rights reserved.

ABSTRACT

Colon targeting for drug delivery is a new approach to localized drug delivery for disease treatment. To target a medication in the consistency it is should have been as a ` dosage form. There are different conventional dosage forms targeting drugs to the colon, however they do not show to be effective in the controlled and sustained release. Different Novel drug delivery is developed to overcome the negative facets of traditional dosage forms, for example, microspheres, nanoparticles, liposomes. The microsphere is the new drug distribution system with particles less than 200 µm in size. The practice method has a characteristic effect on the therapeutic efficacy of microspheres. This overview focuses on the variety of microsphere drug targeting compared to conventional dosage forms for colon drug targeting. Microspheres are useful in sustained drug transport as well as fill in as an environment-friendly device for localized treatment.

Keywords: Microspheres, targeted colon, mechanism, prolonged medication delivery.

INTRODUCTION

Targeted colon drug administration refers to the simultaneous administration of drugs to the colon in order to improve the distinct problems experienced throughout oral drug administration. Various colonic illnesses like embassies, ulcerative colitis, IBD, colonic malignancy, and specific different colonic pathologies require the remedy to be delivered at the target site for their extended remedy. Colonic route of medication administration is not simply utilized for the nearby therapy of colonic ailment, but it can likewise be utilized for the systemic transport of protein and peptide drugs [1]. Colon drug delivery is additionally endorsed for the medicinal drugs inclined to the enzymatic and chemical degradation in the higher G.I.T. In modern times an antibody is additionally delivered to the colon by way of the oral route as the colon is prosperous in lymphoid tissue [2]. Diseases that are refined for

39043



**Dakme Papi et al.,**

circadian rhythms, for example, joint aches, asthma, angina pectoris, etc. are also beneficial with diminished signs and symptoms by using the passage of the medicinal medication into the colon as it provides a longer transit time [3]. The colon drug transport system should make sure that the remedy should be protected in the upper G.I.T and deliver it on achievement at the colon level via some trigger mechanism [4]. Different procedures are used to target the medicine to the colon; some most often used are pH established approach, prodrug approach, microbially brought about approach, time-based release, etc. Novel drug delivery systems developed for colon targeted drug delivery are liposomes, hydrogels, the multi particulate device which encompass nanoparticles, microspheres, microcapsules, micro tablets [5].

ANATOMICAL AND PHYSIOLOGICAL ASPECTS OF THE COLON.

The internal organ at the rear end stretches from the distal end of the ileum. The length of the human inner organ is about 1.5 metres. The colon in the middle region is above five feet from the inner organ and is uniquely structured. The colon is a barrel-formed cylinder lined by mucosa-referred clammy, refined crimson, the pathway is known as the lumen and is round 2-3 creeps in breadth [6]. The ceceum forms the colon's preliminary segment and prompts the right colon or the mountain climbing to trace the colon, the rectum, the dropping colon, the sigmoid and the butt centered channel [Figure 1] [7]. In certain respects, the physiology of the proximal and distal colon contrasts with drug uptake at each site. The physical properties of colon physiology, typically depends on gastric emptying and intestinal transit time to convey gastric emptying medication to the colon upon oral administration. Upon achieving the colon the transit time of dosage form relies upon the dimension of the particles. Smaller particles have extra transit time in contrast to large particles. Diarrhea sufferers have shorter transit time, whereas constipation sufferers have longer transit instances [8].

COLON TARGETED DRUG DELIVERY NECESSITY

Reduce dosing and lower systemic effects to include direct treatment at the condition site. An effective way to treat colon disease should be considered. The colon is where it is important to complete any local or systemic drug transport. Topical remedy for inflammatory bowel disorder, such as Crohn's disease or ulcerative colitis [9]. If the drugs were directed at the colon, various other real colon infection, such as colorectal cancer, could also be effective in being treated more effectively. In addition, colonic delivery formulations are suitable for the transport of medicinal products that are polar or susceptible to chemical and enzymatic degradation in the upper GL tract [10].

MICROSPHERE

Microspheres are small spherical particles with a size of 10 μm to 1000 μm . Microspheres expect a great function to enhance the bioavailability of traditional medicinal drugs and minimizing aspect effects. The significant benefit of gaining use of microspheres as a drug transport system is the controlled discharge of the medicinal drug content. The microsphere is used for the antibodies, anti-toxins, and hormones [11]. Two kinds of microspheres are available, they are micrometric and Microcapsule. Micrometric in which trapped substance is distributed throughout the matrix of the microspheres and microcapsules in which trapped substance is especially surrounded through capsule [12]. Solid biodegradable microspheres becoming a member of a medicinal drug scattered or broke up via molecule lattice have the manager for the controlled arrival. They are consist of polymeric, waxy or other protective materials, i.e. biodegradable polymers produced and regularly modified artifacts [13].

USES OF MICROSPHERES IN COLON DISEASES

Microspheres have been typically utilized for the remedy of extraordinary colonic afflictions like cirrhosis, colon cancer, IBD, ulcerative colitis, and so on [14]. Colon targeting is carried out on drugs that are prone to harm by pancreatic enzyme and gastric acid [15,16]. The colon is regarded to be an achievable site for the systemic concentration of proteins and peptides due to the fact it causes much less unfriendly circumstance in distinction with the abdomen and small digestive [17]. In the colon, medications such as nifedipine, isosorbide and theophylline show greater systemic absorption. The administration of colon drugs is also recommended when extended systemic absorption is necessary from a therapeutic point of view and in addition for conditions that suggest a circadian [18].



**Dakme Papi et al.,****A MECHANISM FOR DISCHARGING DRUG FROM MICROSPHERES:**

The mechanism of drug discharge from the microsphere is a complicated system and interplay of quite components. The mechanism is.

Controlled dissolution systems

The medicinal substance is dissolved in the matrix in a monolithic microsphere framework regulated by dissolution and is disbursed. The drug is unambiguously certain of the matrix and is rejected on the breakdown of the matrix. The drug is released gradually concerning the degradation of the matrix. When degradation is through the homogeneous bulk mechanism, at first drug discharge is sluggish and hastily will increase when speedy bulk degradation [19].

Diffusion controlled systems

Here the active agent is discharged by way of diffusion earlier than or simultaneous with the degradation of the polymer matrix. Degeneration of the polymer matrix influences the rate of release and has to be considered. The rate of release depends upon whether or not the polymer degrades by way of homogeneous or heterogeneous mechanisms [20].

Diffusion controlled reservoir systems

Here the active agent is encapsulated with the aid of an extraordinary controlling membrane through which the agent diffuses and the membrane dissolves sincerely after its transport is completed. For this situation, drug release is unaffected through the degradation of the matrix. The polymer that closing components as such until the complete, release of drug and degrades by way of the homogenous mechanism so the machine is eliminated from the physique is higher for this kind of transport [21].

ADVANTAGES OF MICROSPHERE ON COLON TARGETED:

1. Microencapsulation makes the drugs accessible for an extended period when given by using the oral route accompanying with the reduce G.I.T disturbance [22].
2. The measurement of microspheres is small; they get normally dispensed at some stage in the G.I.T which prevents the facet outcomes induced through the predicament of the medicinal drug at the intestinal mucosa [23].
3. Microspheres show awful lot higher medicinal drug dispersion in the G.I.T and additionally extra uniform drug absorption [24].
4. Microspheres exhibit a lot of dependable transit via the G.I.T [25].
5. The microspheres are greater secure due to the fact of encapsulation [26].
6. Microspheres exhibit increased efficacy and pharmacokinetic consequences [27].

VARIOUS MICROSPHERES POLYMERIC APPROACHES USED FOR TARGETING DRUGS TO THE COLON:

Colon targeted drug delivery by means of pH-dependent, time-dependent, microflora or enzyme activated system, mucoadhesive and pressure-controlled based system have pulled in incredible interest in the treatment of systemic as well as local sickness [28].

Time-dependent polymeric systems

Time-dependent polymeric systems, for example, sustained delivery or delayed discharge releases were found to be a superior approach for the site-specific delivery. As transit time of gastrointestinal tract is differed in diseased conditions, which at last lead to either premature release of drug in the small intestine or exceptionally less amount will be delivered in the colon. For successful drug delivery, one should realize the gastric transit time of the dosage form. It shifts somewhere in the range of 15 and 180 min. if there should arise a non-disintegrating single dosage form, while it is more consistent for small intestine in between 3–4 hours and normal travel time in the colon is 47 hours in ladies and 33 hours in men. Yet, there are some inter subject varieties in GI transit times that rely upon the measure of food consumption, peristalsis development in the stomach. Because of these varieties, the time-dependent polymeric system alone isn't appropriate for ideal drug delivery to the colon. For conquering such



**Dakme Papi et al.,**

constraint of this system, two approach were consolidated i.e., pH-dependent and time-controlled which serve to improve site-specific drug delivery to the colon [29].

Biodegradable polymeric systems

Different endeavours have focussed on the ongoing uses of polysaccharides for colon-specific drug delivery. The broad development of colonic microflora is the trademark highlight of the colon which investigated it for site-specific colonic drug delivery. This huge anaerobic microflora further creates no. of hydrolytic just as conceptive catalysts, for example, deaminase, nitroreductase, xylosidase, glucuronidase, azoreductase, which made it reasonable for site-specific drug [30].

Chitosan

Chitosan a functional linear copolymer comprising of 2-amino-2-deoxy-D-glucose and 2-acetamido-2-deoxy-D-glucose unit links with b-[1–4] bonds is the most bounteously discovered common polysaccharide after cellulose, gotten from chitin. It conveys a positive accuse and responds of the contrarily charged surface including DNA and polymers to accomplish site-specific drug delivery. As Chitosan is having glycosidic linkages, it goes through glycosidic hydrolysis by microbial proteins present in the colon which prompts loss of mechanical quality and atomic weight [31].

pH dependent polymeric approaches

The most regularly utilized pH-dependent polymers are CAP [Cellulose acetic acid derivation phthalates], HPMCP 50 and 55, [Hydroxypropylmethylcellulose phthalate], CAT [cellulose acetic acid derivation phthalate], Eudragit L [Copolymers of methacrylic corrosive and methacrylate], Eudragit S 100, Eudragit P4135 F, Eudragit FS, For the improvement of the viable delivery system, the edge of polymer and their dissolvability in various pH condition should be notable. As per recently revealed contemplates, there are different variances in the pH of the colon because of certain reasons [32]. In ordinary sound people, there is an expansion in pH from the duodenum [pH 6.6 ± 0.5] to terminal ileum [pH 7.5 ± 0.4] and an abatement in the cecum [pH 6.4 ± 0.4], at that point a moderate ascent from right to one side colon with conclusive worth [pH 7.0 ± 0.7]. Yet, it has been accounted for that these polymers can't deliver the medication to the internal organ as these are needy and prompts an untimely delivery in the small digestive tract or extremely less sum discharge in the colon due to the fluctuating travel season of the small digestive [33].

Gaur Gum

Guar gum is an outstanding eco friendly non-ionic polysaccharide got from the seeds of *Cyamopsis tetragonolobus* having a place with the leguminous family. Chemically, it consists of mannose backbone i.e., D-Mannopyranosyl alongside lady lactose side stretching i.e., D-glucoopyranosyl side expanding. The guar gum microspheres of mebeverine hydrochloride for local release of medication in the colon as tablet microspheres. That in vitro investigation of microspheres may prompt premature discharge in upper GIT. Along these lines, the compressed microspheres into tablets so that mebeverine stay flawless in tablet form in lower GIT. As it came to the colon, enteric coating eliminated and microspheres were scattered and showed its therapeutic useful in colon targeting [34].

Method of preparation of microspheres:**Spray Drying Method**

In the Spray Drying method, the initial polymer is dissolved initially in an effective volatile organic solvent such as acetone, dichloromethane, etc. and then the solid – form drug is dissolved gradually in the polymer solution. This dispersion is then atomized in a flood of hot air [35]. In measurements ranging from 1-100µm microspheres. Microparticles are remove from the hot air while the trace of solvent is removed by vacuum drying by approaching the cyclone separator. The feasibility of the service beliw the aseptic stipulations is one of the enormous advantages of this technique[36].



**Dakme Papi et al.,****Single emulsion method**

In this system, an aqueous solution of the polymer is dispersed in organic phase oil/chloroform with steady stirring this procedure referred to as sonification. After this microsphere can be set up in two different ways, first warmth denaturation and chemical cross-linking and centrifuge the product and washing or in the end partition to produce microspheres [37].

Double emulsion method

In this method, a polymer and medicinal aqueous solution is distributed during the organic phase, which produces the first emulsion after the addition of a PVA aqueous solution and produces several emulsion in the partitioning, washing, and drying of the solution to produce microspheres [38].

Phase separation coacervation methods

Aqueous/organic solution of remedy dissolved in polymer solution in this process the varieties polymer-rich globules or droplets and hardening in aqueous/organic phase, washing the microsphere separation and drying in a pure microsphere structure at a time [39].

Solvent Evaporation Method

This method is done in vehicles in this the two phases aqueous and organic phase that manner is known as emulsification i.e. o/w type emulsion after this the solvent evaporate and stays crude nanospheres of microspheres [40].

Solvent extraction method

In the technique, the solvent extraction polymer and drug have to be soluble in an organic solvent which forms a solution called aqueous phase and extract this solution with a water-miscible organic solvent to produce microsphere in aqueous media [41].

Ionotropic Gelatination method

In this technique, the guar gum was once allowed to swell for two hrs in the remedy solution. Sodium alginate solution in water was once made in any other beaker. The drug guar gum solution was once introduced to the sodium alginate solution whilst stirring ensuing into a vicious nation and then the glutaraldehyde was once delivered to the above solution. The drug-polymer solution was once then brought drop smart into the beaker containing CaCl_2 solution with the assist of a 22G measurement needle. The solution used to be dropped from a height of 5 cm into the beaker. This all including system used to be carried out beneath the non-stop stirring of a magnetic stirrer. Then the fashioned microspheres have been remoted the use of Whatman filter paper no-1, dried at 30-40 °C, and then saved in properly closed containers [42].

Sieving method

The acetic acid (4%) solution used to be made in chitosan and the drug used to be dispersed into the solution. Then glutaraldehyde a crosslinking agent was once added. This cross-linked mass, non-sticky in nature, used to be sieved thru an appropriate mesh measurement to get microparticles. The formed microparticles were once washed with the 0.1 N NaOH options to take away the extra glutaraldehyde and dried at forty °C in a single day period. In this approach, the entrapment effectively used to be located to be high. Microparticles resulted have been of irregular structure however the in vitro research published the prolonged release of remedy up to 12 hrs [43].

CONCLUSION

As a colon targeted drug delivery system, the microsphere offers local and systemic benefits. As the colon targeted drug delivery, the gain of the microsphere is that they have greater stability, biocompatibility extension, and less aspect consequences. Additionally, a microsphere as a colon drug delivery system may be used to perform the



**Dakme Papi et al.,**

controlled release or delayed release. So the microsphere is a useful method to be used for colon targeted drug delivery. In conclusion, I would like to microspheres present several advantages over traditional dosage varieties for the drug concentrated on to the colonic region.

REFERENCES

1. Patel, M. P., Patel, R. R. and Patel, J. K. "Chitosan Mediated Targeted Drug Delivery System: A Review", *Journal of Pharmacy & Pharmaceutical Sciences*, 13[4], pp. 536-557. <https://doi.org/10.18433/IJJC7C>
2. Sharma, Parmar, Upadhyay and Shah [2016]. An ex vivo and in vitro characterization and formulation of citrate loaded nasal microspheres. *International Journal of Drug Delivery*, 2[3], pp.213-220. DOI:10.5138/ijdd.2010.0975.0215.02031
3. Mishra, Jain, Kohli and Kershaw [2016]. The determination of aripiprazole in tablets by spectrophotometric method. *Indian Journal of Pharmaceutical Sciences*, 73[1], p.74. DOI: 10.4103/0250-474X.89760
4. Boulon, Schwanz, Delicque, Cassinotto and Piron [2018]. Liver chemoembolization of hepatoma by TANDEM®microspheres. *Future Oncology*, 14[26], pp.2761-2772. <https://doi.org/10.2217/fon-2018-0237>
5. Barik, Sahoo, Senapati and Mallick [2018]. Fabrication and in vitro of analysis of Eudragit® Microspheres of Stavudine. *Tropical Journal of Pharmaceutical Research*, 4[1]. DOI: 10.4314/tjpr.v4i1.14622
6. Wong, Salami and Dass [2018]. Microspheres, Microparticles and microcapsules- A review of current evolution of oral delivery of insulin. *International Journal of Pharmaceutics*, 537[1-2], pp.223-244. <https://doi.org/10.1016/j.ijpharm.2017.12.036>
7. Mazzocchi, Tana, and Corazza, [2018]. The role of hypersensitivity to colonic turmoil and enteric gas production in the pathophysiology of bloating in patients with irritable gut syndrome. *Digestive and Liver Disease*, 40, pp.S57-S58. <https://doi.org/10.1186/s41043-017-0113-1>
8. Mazzocchi, Tana, and Corazza, [2018]. The role of hypersensitivity to colonic turmoil and intestinal gas production in the pathophysiology of bloating in patients with irritable gut syndrome. *Digestive and Liver Disease*, 40, pp.S57-S58. <https://doi.org/10.1186/s41043-017-0113-1>
9. Hua S, Marks E, Schneider J, Keely [2015]. Oral nano-delivery for colon targeted drug delivery in inflammatory bowel disease. *Nanomedicine: Nanotechnology, Biology, and Medicine*; 11[5] 1117-1132. <http://dx.doi.org/10.1016/j.nano.2015.02.018>
10. Jain, P., Vaidya, A., Jain, R., Shrivastava, S., Khan, T., and Jain, [2017]. Anti-Amoebic agent of ethyl cellulose coated chitosan microspheres of metronidazole. *Journal of Bionanoscience*, 11[6], pp.599-607. <https://doi.org/10.1166/jbns.2017.1483>
11. Maharshi, P., Singh, S., Gulati, M., Yadav, A., Garg, V., Kumari, B., and Gowthamarajan, [2018]. A Novel Three Perspective for Colon Delivery of Sulfasalazine: Microbially Triggered Polymers, Lquisolid Technology and Concomitant Use of pH-Responsive. *Current Drug Delivery*, 15[7], pp.1038-1054. <https://doi.org/10.2174/1567201815666180320095703>
12. Lotfabadi, Dinarvand, Derakhshankhah, Alaei and Izadi [2017]. Colon Cancer and Distinct Ways to Deliver Drugs in the Large Intestine. *Anti-Cancer Agents in Medical Chemistry*, 17[10]. <https://doi.org/10.2174/1871520617666170213142030>
13. Murugesan, Pathak, Banerjee, Verma, and SubramaniamR, [2017]. Recent trends and future perspective of strategies for targeted drug delivery in the treatment of colon cancer. *Drug Discovery Today*, 22[8], pp.1224-1232. DOI: 10.1016/j.drudis.2017.05.006
14. Valdivia, Sumithra, and Radha, [2019]. Colon Drug Delivery System of Phytoconstituents. *Research Journal of Pharmacy and Technology*, 12[7], p.3144. Doi: 10.5958/0974-360X.2019.00530.4
15. Mennini, Maestrelli, Cirri, Corti, and Mura, [2018]. Formulation of enteric-coated calcium pectinate microspheres deliberate for colon targeted drug delivery. *European Journal of Pharmaceutics and Biopharmaceutics*, 69[2], pp.508-518. <https://doi.org/10.1016/j.ejpb.2007.12.004>
16. Hodson, R [2016]. Inflammatory bowel disease. *Nature*, 540[7634], pp.S97-S97. DOI: 10.1038/540S97a



**Dakme Papi et al.,**

17. Irby D., Du C., Li F [2017]. Lipid-Drug for Enhancing Drug Delivery. 14:1325–1338. DOI: 10.1021/acs.molpharmaceut.6b01027.
18. Patel, M., Patel, R., and Patel, J., [2018]. Chitosan Drug Delivery System: A Review. *Journal of Pharmacy & Pharmaceutical Sciences*, 13[4], p.536. . <https://doi.org/10.18433/J3JC7C>
19. Lu, B., and Zhang, Z., [2018]. Novel Colon targeted drug delivery of Microspheres with Highly Dispersed Hydroxycamptothecin Cores. *Journal of Pharmaceutical Sciences*, 95[12], pp.2619-2630. <https://doi.org/10.1002/jps.20635>
20. Kinget, R., Kalala, W., Vervoort, L. and van den Mooter, G., [2017]. Colonic Drug Targeting. *Journal of Drug Targeting*, 6[2], pp.129-149. <https://doi.org/10.1016/B978-0-12-819659-5.00007-0>
21. Chablani L, Y., [2015]. Microspheres Novel Perspective to Enhance Drug Bioavailability. *Journal of Bioequivalence & Bioavailability*, 07[05]. Doi:10.4172/jbb.10000e68
22. Semde, R., Amighi, K., Devleeschouwer, M., and Moes, A., [2019]. Studies of pectin HM/Eudragit® RL/Eudragit® NE film-coating fabrication deliberate for colonic drug delivery. *International Journal of Pharmaceutics*, 197[1-2], pp.181-192. [https://doi.org/10.1016/S0378-5173\[99\]00467-6](https://doi.org/10.1016/S0378-5173[99]00467-6)
23. Dudhipala, N., [2016]. A Review of Novel Strategies to Enhance Oral Delivery of Zaleplon. *Journal of Bioequivalence & Bioavailability*, 8[5]. DOI:10.4172/jbb.1000297
24. Jose, S., Prema, M., Chacko, A., Thomas, A., and Souto, E., [2019]. Chronotherapy for chitosan microspheres. *Colloids and Surfaces B: Biointerfaces*, 83[2], pp.277-283. <https://doi.org/10.1016/j.colsurfb.2010.11.033>
25. Ramanathan, M., [2018]. Fabrication Of Colon Targeted Matrix Tablets Of Ibuprofen. *Asian Journal of Pharmaceutical Research and Development*, 6[2], pp.9-19. <https://doi.org/10.22270/ajprd.v6i2.366>
26. Patel, H., Patel, K., and Patel, N., [2018]. Fabrication Of Metformin Hydrochloride Microparticles By Emulsion Solvent Evaporation Technique. *Journal of Drug Delivery and Therapeutics*, 3[2]. <https://doi.org/10.22270/jddt.v3i2.471>
27. Singh, M., Singh, D., and Swarnlata [2009]. In vitro evaluation of lipospheres for oral delivery of peptide drugs. *International Journal of Drug Delivery*, 1[1], pp.15-26. DOI:10.5138/ijdd.2009.0975.0215.01002
28. Jain, A., Singhai, A. and Dixit, [2018]. A comparative study of hepatoprotective activity of ethanol extract of leaves of Tephrosia purpurea. *Indian Journal of Pharmaceutical Sciences*, 68[6], p.740. DOI:10.18231/2393-9087.2018.0009
29. Zhang, H., Wang, W., Li, H., Peng, Y. and Zhang, [2017]. Microspheres for the oral delivery of insulin in streptozotocin-induced diabetic rats. *Drug Development and Industrial Pharmacy*, 44[1], pp.109-115. <https://doi.org/10.1080/03639045.2017.1386197>
30. Li, S., Kowarski, C., Field K. and Grim, W., [2016]. Current Advances in Microencapsulation Technology and Equipment. *Drug Development and Industrial Pharmacy*, 14[2-3], pp.353-376. <https://doi.org/10.3109/03639048809151975>
31. Chandran, S., Sanjay, K., and Ali Asghar, L., [2019]. Characterization of formulation of microspheres of variables for colonic delivery. *Journal of Microencapsulation*, 26[5], pp.420-431. <https://doi.org/10.1080/02652040802424021>
32. Zhang, W., Wang, X., Zhang, M., Xu, M., Tang, W., Zhang [2017]. Intranasal Delivery of Microspheres Loaded with 20 [R]-ginsenoside Rg3 Enhances Anti-Fatigue Effect in Mice. *Current Drug Delivery*, 14[6]. DOI: 10.2174/1567201814666161109121151
33. Kietzmann, D., Molinari, B., Beduneau, A., Pellequer, Y. and Lamprecht, A., [2018]. Microsphere of colonic delivery of carboxyfluorescein in experimental colitis. *European Journal of Pharmaceutics and Biopharmaceutics*, 76[2], pp.290-295. <https://doi.org/10.1016/j.ejpb.2010.06.013>
34. Gogu P.K [2010]. Formulation & evaluation of invivo/ in-vitro characterization of Spray Dried Microspheres formulation Encapsulating 4- Chlorocurcumin. *Indian Journal of Pharmaceutical Sciences*. 346-352. DOI: 10.4103/0250-474x.70481
35. Sangi, S., SreeHarsha, N., Bawadekji, A., and Al Ali, M., [2018]. Intravenous administration of chemotherapeutic drug deliver to lungs by microspheres. *Drug Design, Development, and Therapy*, Volume 12, pp.3051-3060. DOI: 10.2147/dddt.s173485





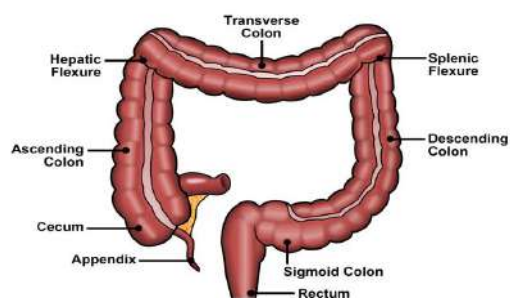
Dakme Papi et al.,

36. SINGH, S., ARORA, S., N. and ALLAWADI, D., [2014]. Taguchi Design for formulation and Evaluation of Sustained Release Microspheres. *Journal of Pharmaceutical Technology, Research, and Management*, 2[1], pp.1-12. DOI: 10.15415/jptrm.2014.21001
37. Fernandes, C., [2017]. Preparation of Novel Gastroretentive Mucoadhesive Microspheres of Cyproheptadine Hydrochloride for Sustained Release. *World Journal of Pharmaceutical Research*, pp.2311-2322. DOI: 10.20959/wjpr20178-9148
38. Charde, Y., Dhage, S., Lohiya, G., and Avari, J., [2017]. Preparation of sustained-release Microspheres using Chitosan and Alginate. *International Journal of Pharmaceutical Sciences and Drug Research*, 9[3]. DOI: 10.25004/ijpsdr.2017.090305
39. Sindhu, S., Jyothi, M., Richitha, S., and Hemanth, G., [2018]. Anti Diabetic Drugs preparation and Evaluation of Bilayer Tablets of Sustained Release Microspheres. *International Journal for Pharmaceutical Research Scholars*, 7[3], pp.77-86. DOI: 10.31638/ijprs.v7.i3.00056
40. Parmar H, Bakliwal S, Gujarathi N, Rane B, Pawar [2017]. Formulation and evaluation of mucoadhesive microsphere. *International Journal of Applied Biology and Pharmaceutical Technology*. 1[3], 1157-67. DOI: <https://doi.org/10.32553/ijmbs.v1i4.23>
41. Sangi, S., SreeHarsha, N., Bawadekji, A., and Al Ali, M., [2018]. Intravenous administration of chemotherapeutic drug deliver to lungs by microspheres. *Drug Design, Development, and Therapy*, Volume 12, pp.3051-3060. DOI: 10.2147/dddt.s173485
42. Singh, R., Yadav, B., Singh, S., Pandey, P., and Mani, A., [2017]. In-silico screening of Schistosoma inhibitors for prioritization of drug candidates. *Springer Plus*, 5[1]. DOI: 10.1186/s40064-016-1891-4
43. Li, Y. and Zhang, Z., [2018]. Formulation and evaluation of sustained curcumin release from PLGA microspheres. *Drug Design, Development, and Therapy*, Volume 12, pp.1453-1466. DOI: 10.2147/dddt.s154334
44. Ramaiah, B., Nagaraja, S., Kapanigowda, U., Boggarapu, P., and Subramanian, R., [2016]. Azithromycin in lungs by way of bovine serum albumin microspheres as targeted drug delivery. *DARU Journal of Pharmaceutical Sciences*, 24[1]. DOI: 10.1186/s40199-016-0153-x
45. Ramaiah, B., Nagaraja, S., Kapanigowda, U., and Boggarapu, P., [2016]. Levofloxacin by Targeted Gelatin Microspheres. *Journal of Pharmaceutical Innovation*, 11[4], pp.289-299. DOI: 10.1007/s12247-016-9252-y
46. Andhariya, J., and Burgess, D., [2016]. Current advances in the testing of microsphere drug delivery systems. *Expert Opinion on Drug Delivery*, 13[4], pp.593-608. doi: 10.1517/17425247.2016.1134484
47. Wong, C., Al-Salami, H., and Dass, C., [2018]. Microspheres, microparticles, microcapsules: A review of current developments for oral delivery of insulin. *International Journal of Pharmaceutics*, 537[1-2], pp.223-244. DOI: 10.1016/j.ijpharm.2017.12.036
48. Sahu, G., Sharma, H., Gupta, A., and Kaur, C., [2017]. Microemulsion Based Drugs Delivery Systems for Better Therapeutic Effects. *International Journal of Pharmaceutical Sciences and Developmental Research*, 1[1], pp.008-015. DOI: 10.17352/ijpsdr.000003
49. Kietzmann, D., Molinari, B., Beduneau, A., Pellequer, Y. and Lamprecht, A., [2018]. Colon targeted delivery of carboxyfluorescein by pH-sensitive microspheres in experimental colitis. *European Journal of Pharmaceutics and Biopharmaceutics*, 76[2], pp.290-295. <https://doi.org/10.1016/j.ejpb.2010.06.013>
50. S, S., S, A., Krishnamurthy, K. and Rajappan, M., [2019]. A review on nanosponges novel drug delivery system. *Journal of Pharmacy & Pharmaceutical Sciences*, 15[1], p. 103. DOI: 10.18433/j3k308
51. Ganesan, P., Deepa John, A., Sabapathy, L., and Duraikannu, A., [2014]. A Review on Microsphere Drug Delivery. *American Journal of Drug Discovery and Development*, 4[3], pp.153-179. DOI: 10.3923/ajdd.2014.153.179
52. Patel, M., Patel, R., and Patel, J., [2018]. A Review on Chitosan Drug Delivery System. *Journal of Pharmacy & Pharmaceutical Sciences*, 13[4], p.536. <https://doi.org/10.18433/J3JC7C>
53. Jose, S., Prema, M., Chacko, A., Thomas, A., and Souto, E., [2019]. Chronotherapy for colon targeted chitosan microspheres. *Colloids and Surfaces B: Biointerfaces*, 83[2], pp.277-283. <https://doi.org/10.1016/j.colsurfb.2010.11.033>



Dakme Papi *et al.*,**Table 1: List of various method of preparation of microspheres along with the polymers used**

Sl.No	Drug Used	Purpose	Method of Preparation	Carrier	Polymer Used	Reference
1	Acclofenac	Used in Treatment Rheumatoid Arthritis Diseases	Ionic Gelatin Method	Microspheres	Sodium Alginate Microspheres Coated With Cellulose Acetate Phthalate	44
2	Curcumin	Treatment of Colon Cancer	Ionic Cross-linking Technique	Microspheres	Guar Gum, Xanthan Gum	45
3	Diclofenac	Treatment of Arthritis	Emulsion Solvent Evaporation Method	Microspheres	Eudragit S 100	46
4	Flurbiprofen	Treatment of Local Disease	Solvent Evaporation Technique	Microspheres	Eudragit L- 100	47
5	Glipizide	Treatment of Type II Diabetes	Ionotropic Gelatination Technique	Microspheres	Eudragit S 100	48
6	Mesalamine	Treatment of Ulcerative Colitis	Emulsion Solvent Evaporation Technique	Microspheres	HPMC, ethyl cellulose	49
7	Meloxicam	Colorectal Cancer	Ionotropic Gelation Technique	Microspheres	Sodium Alginate Coated With Eudragit S 100	50
8	Metoprolol Succinate	Treatment of Ulcerative Colitis	Emulsion Cross-linking Technique	Microspheres	Chitosan	51
9	Satranidazole	Ulcerative Colitis	Emulsion Solvent Evaporation Technique	Microspheres	Eudragit S 100	52
10	Zidovudine	HIV And AIDS Related Condition	Ion Gelation Technique	Microspheres	Chitosan	53

**Figure 1: Colorectal anatomy and physiology.**



Elucidation of Selected Fresh Water Cyanobacterial Strains for Efficient Pigments and Antioxidants Production

V.P.Ramya¹ and G.Muralitharan² *

¹Research Scholar, Department of Microbiology, Bharathidasan University, Tiruchirappalli, Tamil Nadu, India.

²Associate Professor, Department of Microbiology, Bharathidasan University, Tiruchirappalli, Tamil Nadu, India.

Received: 18 Nov 2021

Revised: 22 Dec 2021

Accepted: 24 Jan 2022

*Address for Correspondence

G.Muralitharan

Associate Professor,
Department of Microbiology,
Bharathidasan University,
Tiruchirappalli, Tamil Nadu, India.
Email: drgm@bdu.ac.in



This is an Open Access Journal / article distributed under the terms of the **Creative Commons Attribution License** (CC BY-NC-ND 3.0) which permits unrestricted use, distribution, and reproduction in any medium, provided the original work is properly cited. All rights reserved.

ABSTRACT

Cyanobacteria are the oxygenic photosynthesis performing prokaryotes and show a connecting link between plastids of eukaryotic autotrophs and prokaryotes. A variety of pigments, like chlorophyll, carotenoids and phycobiliproteins which exhibit different colors are present in cyanobacteria. This study focuses on different cyanobacterial pigments, their antioxidative potentials for use in pharmaceuticals. The extracted pigment was assessed for their antioxidant property by various methods such as total chlorophyll and carotenoid, antioxidant activity by DPPH assay, hydrogen peroxide radical scavenging activity, total phenol content, total flavonoid content, ABTS assay.

Keywords: Cyanobacteria, Fresh water, antioxidants, carotenoids, chlorophyll

INTRODUCTION

Cyanobacteria produce a variety of secondary metabolites that are effective against reactive oxygen species (ROS), particularly pigments such as carotenoids, as well as polyphenols such as phenolic acids and flavonoid compounds [Babic et al., 2016] [1] and [Martel et al., 2017] [2]. Cyanobacteria are a source of bioactive substances with many potential biotechnological applications and their antioxidant compounds, particularly, have been considered promising molecules for the cosmetics [Morone et al., 2019] [3] and food [Singh et al., 2017] [4] industries. Indeed, the search for natural antioxidant compounds has gained increasing interest, considering current synthetic antioxidant compounds contain preservatives and suspected toxicity [Andrade et al., 2019] [5]. In general, these studies point to

39052





Rama and Muralitharan

an interest in exploring the antioxidant activity of cyanobacteria, considering their richness of compounds such as carotenoids and polyphenols. Inclusively, some of these authors reported antioxidant activity [Martel et al., 2017] [6] and [Geethu et al., 2018] [7] and [Zeeshan et al., 2010] [8] and/or antioxidant contents [Yasin et al., 2019] [9] and [Hossain et al., 2016] [10]. Obtaining pigments and natural antioxidants is important because of the increase in the current demand of consumers for natural products, [Botterweck et al., 2000] [11] the main factor that can influence the composition of pigments and other antioxidants assays in DPPH assay, hydrogen peroxide radical scavenging activity, Determination of total phenol content, Determination of total flavonoid content, ABTS Assay. This work was to determine the antioxidant activity of extracts obtained from nine cyanobacteria strains with regard to their potential uses. Cyanobacteria have a highly evolved antioxidant system that catalyzes the harmful oxy radicals produced during photosynthesis [Padmapriya and Anand 2010] [12]. The phytonutrients and pigments present in cyanobacteria act as antioxidants. The antioxidant activity of cyanobacteria is a co-responsibility of pigments such as phycobiliproteins, carotenes, phenolic compounds and other oxidative substances present in the cells.

MATERIALS AND METHODS

In the study seven cyanobacterial cultures were used 1. *Lyngbya* sp. TVL 013 - this sample was collected from Thiruverumbur lake; 2. *Gloeotrichia* KLR 062 - this sample was collected from srirangam (Kollidam river); 3. *Anabaena* sp. MNR 005 - this sample was collected from Manachanallur (rice field); 4. *Nostoc* sp. MTL 515 - this sample was collected from Mathur lake; 5. *Rivularia* sp. KLR 0061 - Srirangam (Kollidamriver); 6. *Calothrix membranacea* KLR 006 - Srirangam (Kollidamriver); 7. *Oscillatoria* sp. VYL 102 - vayalur lake; 8. *Oscillatoria tenuis* VYL 1021 - Kollidamriver, and 9. *Phormidium* sp. TVL 0131 - Thiruverumbur.

Chlorophyll Estimation

The nine cyanobacterial cultures were homogenized with a hand homogenizer (Borosil) to get a uniform culture suspension. The suspensions were centrifuged at 3,500 rpm for 15 minutes in a tabletop centrifuge. The supernatant was discarded and to the pellet 80% (v/v) methanol was added and kept for 2 hours at dark for extraction of chlorophyll. The pigment extracted was measured at 663 nm in a UV-VIS spectrophotometer and the amount of chlorophyll-a was estimated by using the extinction coefficient given by [Mackinney (1941) [13].

$$\text{Total chlorophyll } (\mu\text{g/g}) = \frac{A_{663} \times 12.7 \times \text{Volume of the extract}}{\text{Volume of methanol}}$$

Estimation of total carotenoids

About 10 ml of each nine cyanobacterial cultures were taken and centrifuged at 6500 rpm for 10 mins and the supernatant was discarded. The total carotenoids were estimated by following [Jensen (1978) [14]. The pellets were initially weighed and dried at $28 \pm 2^\circ\text{C}$ for 24 hrs under fluorescent white light and final weight was taken in an electronic balance (Mettler Toledo). 5 mg of the dried biomass was subjected to 3 ml of 85% acetone and subjected to repeated freezing and thawing at 4°C until the pellet becomes colourless. The volumes of the extract were measured and the final volume was made up to 10 ml with 85% acetone. Carotenoids were estimated by optical density (O.D.) at 450 nm using 85% acetone as blank using spectrophotometer (UV Vis-1800, Shimadzu, Japan) and expressed as the total amount of carotenoids in $\mu\text{g/mg}$ dry wt. The total soluble carotenoid was calculated using the following formula

$$C = (D \times V \times f) \times 10 / 2500$$

where, D= O.D. at 450 nm; V= Volume of the extract; f = Dilution factor; 2500=average extinction co-efficient of pigment.





Ramya and Muralitharan

Screening for antioxidant activity

About 0.5 g wet weight of nine cyanobacterial cultures were harvested by centrifugation at 5000 rpm for 10 min. Cyanobacterial biomass was crushed separately in 5 ml of methanol: chloroform and centrifuged at 5000 rpm for 10 min at 20 °C. The supernatants were collected by centrifugation and used for the antioxidant activity.

Antioxidant activity by DPPH assay

The free radical scavenging activity of the cyanobacterial extract was determined by its reducing ability using the DPPH solution. For the experimental procedure, about 100 µM of DPPH (5 ml) stock solution was prepared in MeOH solution and stored in dark. About 0.5 ml of 500 µM DPPH solution in MeOH was mixed with 0.5 ml (50 µg/ml) of cyanobacterial fraction concentrate to get final concentrate of 25 µg/ml of fraction concentrate in 250 µM DPPH solution. The reaction mixture was incubated in dark for 40 minutes and absorbance was recorded. Similarly, the aliquots of 400 µg/ml, 200 µg/ml, 100 µg/ml, 50 µg/ml and 25 µg/ml test sample was prepared and assayed. The ascorbic acid and vitamin E were used as a standard control. All the test and standard samples were measured at 517 nm by UV-Vis Spectrophotometer (Shimadzu, Kyoto, Japan) in triplicates. The percentage of inhibition of absorbance was used to calculate the radical scavenging potency [Geethalakshmi and Sarada, 2013] [15]. Percentage of inhibition of absorbance

$$(\%) = \frac{\text{OD 517 (DPPH+MeOH)} - \text{OD 517 (sample)}}{\text{OD 517 (DPPH + MeOH)}}$$

Hydrogen peroxide radical scavenging activity

Scavenging of hydrogen peroxide (H₂O₂) by the extracts was estimated as per the protocol described by [Bozin et al., (2008)]¹⁶. 0.6 ml of 40 mM H₂O₂ in phosphate buffer (pH 7.4) solution was added to the test tubes containing 3.4 ml of extract (500 µg/ml) in phosphate buffer (pH 7.4). After thoroughly mixing the reaction mixture, absorbance was measured on a spectrophotometer at 230 nm. The same protocol was followed for standard antioxidant Gallic acid and deionized water was used as blank. The percentage of H₂ O₂ scavenging of the extracts was calculated by using the following equation.

$$\% \text{ Inhibition} = \frac{[\text{AControl} - \text{ATest}]}{[\text{AControl}]} \times 100$$

Determination of total phenol content

The total phenol content of the crude extracts was estimated using Folin-Ciocalteu (Fc) method described by [Wu et al. (2005)]¹⁷. Briefly, 2.5 ml of 10% (v/v) FCreagent and 2.0 ml of 2% (w/v) sodium carbonate was added to the test tube containing extract dissolved in methanol (0.5 and 1.0 mg/ml) and the test tube was shaken to mix the content and the tubes were incubated at 45±2°C for 15 min. After the incubation, the mixture was measured at 765 nm using a UV-Vis spectrophotometer (Shimadzu, Japan). The blue colour develops indicate the presence of phenolic compounds except the blank and the result was expressed as gallic acid equivalents in mg per gram (mgGAE/g) of crude extract. Based on the gallic acid standard curve against (0.1 to 0.8mg/ml) a control blank was prepared.

Determination of Total flavonoid content

Total flavonoid content was measured by the aluminum chloride colorimetric method [Kim et al. 2003] [18]. Cyanobacterial extract (0.5 ml) was mixed with 0.1 ml of 10% aluminum chloride hexahydrate, potassium acetate (0.1 ml of 1 M) and 2.8 ml of deionized water. After incubation for 30 min, the absorbance of the reaction mixture was recorded at 415 nm and quantified taking quercetin as standard. Total flavonoid content (TFC) was expressed in terms of g -1 quercetin equivalents (QE) g -1 fresh cell weight.

ABTS assay

This assay was supported on the capability of different substances to scavenge ABTS (2, 2'-azino-bis (3-ethylbenzothiazoline-6-sulphonic acid) and was prepared by mixing 7 mM stock solution with 2.45 mM potassium





Ramya and Muralitharan

persulfate (1/1 v/v) and leaving the mixture 4-6 hrs until the reaction was complete and absorbance was stable. The ABTS solution with ethanol to an absorbance of 0.700 ± 0.05 at 734 nm for measurements. The photometric assay was carried out on 0.9 ml of ABTS solution and 0.1 ml of cyanobacterial samples (100-200 $\mu\text{g/ml}$) and mixed for 45 sec. Measurements were taken immediately at 737 nm after 15 min holding time. The antioxidative activity of the tested samples was calculated by determining the decrease in absorbance at different concentrations by using the following equation. $E = (Ac-At)/Ac \times 100$, where, AT and Ac are the respective absorbance of tested samples and ABTS was expressed as μmol .

RESULTS AND DISCUSSION

The morphological features of the tested cyanobacterial strains were depicted in Fig. 1. All the strains were identified based on their morphological observations under light microscopy.

Total Chlorophyll and Carotenoid

Among the nine species of cyanobacterial strains tested a maximum total content of chlorophyll was observed in *Oscillatoria tenuis* VYL 1021, with $103 \pm 1.32 \mu\text{g/ml}$ fresh wt followed by *Calothrix membranacea* KLR 006 with $99.63 \pm 1.308 \mu\text{g/ml}$ fresh wt, the total chlorophyll of other species was given in (Fig No. 2) and total carotenoid (30.254 mg/g g⁻¹ fresh wt) was found in *Oscillatoria* sp VYL 102, followed by the *Calothrix membranacea* KLR 006, with total carotenoid content of $29.572 \pm 1.37 \text{ mg/g}$, (Fig No.3) while low content of total carotenoids (10.57 mg/ g⁻¹ fresh wt) in *Oscillatoria tenuis* VYL 1021. The study showed the chlorophyll- a content in *Oscillatoria boryana* and *Oscillatoria* sp. Was $3.927 \mu\text{g/ml}$ and $2.499 \mu\text{g/ml}$, respectively. The pigment and protein content was decreased with increasing the concentration of heavy metal (Ni) except *Phormidium* sp. In another study by [Dhananjaya et al., (2017) [19], maximum chlorophyll content (3.35 mg g⁻¹ fresh wt), and total carotenoid (605.67 $\mu\text{g g}^{-1}$ fresh wt) in *Lyngbya* sp. while the minimum chlorophyll content (0.53 mg g⁻¹ fresh wt) was found in *H. fontinalis*, and *S. simplex*. [Tiwari et al., 2005]²⁰ reported the cyanobacteria *C. javanica* from Pokharan exhibited minimum chlorophyll accumulation of $1.3 \mu\text{g mL}^{-1}$ and *Nostoc verrucosum* ($1.1 \mu\text{g mL}^{-1}$) whereas, the maximum chlorophyll was observed in *Phormidium melleum* ($10.3 \mu\text{g mL}^{-1}$) and *Oscillatoria curviceps* ($7.3 \mu\text{g mL}^{-1}$).

DPPH radical scavenging activity

DPPH is a compound that possesses a nitrogen free radical and is readily destroyed by a free radical scavenger. This assay was used to test the ability of the antioxidative compounds functioning as proton radical scavengers or hydrogen donors [Singh and Rajini, 2004]²¹. DPPH scavenging activities of nine cyanobacterial crude extracts were analyzed and the results were given in (Fig No.4). Among the nine species, the maximum DPPH radical scavenging activity was recorded in *Anabaena* sp. MNR 005, with 78% followed by *Nostoc* sp. MTL 515, with 72% whereas *Rivularia* sp. KLR 0061 and *Calothrix membranacea* KLR 006 with 70% in 400 $\mu\text{g/ml}$ of extracts. (Fig No.31) Similarly, [Gaurav et al., 2011]²² showed that methanol extract of *Anabaena* sp. MNR 005 showed a scavenging activity of 101.81 mg/ml and the scavenging activity tends to increase with increase in the dose concentration. Previous studies reported that methanolic extract of *Anabaena* sp. PCC 7119 possess efficient antioxidant activity. [Suhail et al. 2011]²³ reported that the methanol fraction of *A. variabilis* showed DPPH radical scavenging potential, which is approximately 16%. [Martel et al., 2017] [24] reported that the cyanobacteria *Nostoc commune* and *Arthrospira platensis* showed no inhibition activity even at 40 mg/mL of methanol extract against DPPH and the other cyanobacteria such as *Leptolyngbya protospira* and *Nostoc* sp. MTL 515 exhibited a low level of inhibition ranged from 7.65 % to 27.89 % respectively. The *Spirulina* extract and vitamin C gave higher antioxidant activity due to the constituent of phenolic compounds [Chu et al., 2010] [25]. Similarly, the water soluble phycobiliproteins - phycocyanin from cyanobacteria were several folds more efficient than vitamin C and protects the cells against apoptosis by attenuating the free radicals and reactive oxygen species (ROS) formation [Chopra and Bishnoi, 2008] [26]. Some studies reported that cancer was prevented by algae extracts because of their antioxidants properties. Substances known as antioxidants are bioactive compounds that are able to inactivate free radicals, which are unstable molecules that may cause several deleterious effects to human health. Thus the usefulness of antioxidants in protecting cellular components against





Ramya and Muralitharan

oxidative stress is well established [Bermejo et al., 2008] [27]. In general, higher total phenolic contents lead to maximum DPPH radical scavenging activity [Ebrahimzadeh et al., 2010] [28]. DPPH is a stable nitrogen-centered free radical the colour changes from violet to yellow upon reduction by either the process of hydrogen- or electron-donation. Substances that are able to perform this reaction can be considered as antioxidants and therefore radical scavengers. The present observation revealed that the radical scavenging activity increased with the increase of phenolic compound content as mentioned. The total phenol content of *Anabaena* sp. MNR 005 was found to be maximum with 67 ± 0.06 $\mu\text{g/ml}$ of biomass followed by 52 ± 0.05 $\mu\text{g/ml}$ in *Calothrix membranacea* KLR 006 and 50 ± 0.0906 $\mu\text{g/ml}$ in *Lyngbya* sp. TVL 013. There was an association found between the TPC and IC 50. The TPC level was a high; the IC 50 was low and resulted in high level of antioxidant activity. This could be due to the high amount of polyphenolic constituents present in the *Calothrix membranacea* KLR 006. And *Anabaena* sp. MNR 005 which in turn demonstrated an increased level of scavenging activity. The activity of crude extracts was more or less comparable to synthetic antioxidant, other six algal strains showed less activity.

Hydrogen peroxide scavenging activity

Hydroxyl radical (OH) is an extremely reactive free radical capable of reacting with various molecules like sugars, amino acids, lipids and nucleotides in the cells [Yasuda et al., 2000]²⁹. Among the nine cyanobacteria tested the maximum hydrogen peroxide scavenging activity of 63% was noted in *Lyngbya* sp. TVL 013, followed by *Phormidium* sp. TVL 0131, of 61%. Whereas, the *Calothrix membranacea* KLR 006 showed only 43% of scavenging activity against hydrogen peroxides (Fig.No. 5). Hydrogen peroxide scavenging activities of the methanol crude extracts were analyzed in which, methanol extract of *Lyngbya* sp. TVL 013. Yielded the highest scavenging activity than other cyanobacterial extracts. The measurement of H_2O_2 scavenging activity is one of the most useful methods in determining the ability of antioxidants to decrease the level of prooxidants such as H_2O_2 [Czochra and Widensk, 2002] [30]. Hydrogen peroxide together with ROS can damage several cellular components and at specific sites, it reacts with most biomolecules and further causes tissue damage and cell death. Thus, removing OH is very important for the protection of living systems. In this study, different concentrations of cyanobacterial extracts rich in polyphenols were evaluated to assess the shielding effect against the degenerative reaction against deoxyribose caused by the OH radical in the reaction mixture. Prominent deoxyribose protection activity was shown from 0.31 mg ml⁻¹ cell free extract (IC 50) in *Calothrix membranacea* KLR 006 and *Nostoc* sp. MTL 515. to 6.92 mg ml⁻¹ (IC 50) in *Lyngbya* sp. TVL 013 strains showed the other five high levels (90% activity at 5mg ml⁻¹ cell-free extract) of OH radical scavenging activity and other strains showed low deoxyribose. Incubation of deoxyribose with H_2O_2 and Fe²⁺-EDTA as chelating agent reduces degradation of deoxyribose by the addition of scavenger of OH radical. The process depends on the concentration of scavenger relative to deoxyribose. Extracts of plants such as *Moringa oleifera* [Chumark et al., 2008]³¹ and *Allium cepa* [Singh et al. 2009] [32] rich in polyphenolics have shown excellent antioxidant properties and were proven good scavengers of reactive species such as OH, O_2 and ROS.

Total phenolic content (TPC)

Total phenolic content of methanol extracts of nine cyanobacterial strains was presented in (Fig.No.6) The total phenolic content was varied among the species and ranged from 67 ± 0.06 (*Anabaena* sp. MNR 005) to 11 ± 0.02 (*Rivularia* sp. KLR 0061) mg GAE g⁻¹ of extract. The highest phenolic content was observed in *Anabaena* sp. MNR 005 (67 ± 0.06 mg GAE g⁻¹), followed by *Calothrix membranacea* KLR 006 (52 ± 0.05 mg GAE g⁻¹) and *Lyngbya* sp. TVL 013 (50 ± 0.09 mg GAE g⁻¹). Fig No. 6 Total phenolic content in selected cyanobacterial extracts. In the present study methanol extraction yield maximum total phenolics compounds and the methanol was considered as the best solvent, by other authors [Manivannan, 2012] [33] and methanol manifested a higher amount yields in *Oscillatoria agardhii* and *Anabaena sphaerica*. As well as reported earlier, the phenolic compounds were found to be one of the most effective antioxidants in brown algae [Siriwardhana, et al., 2003] [34]. The Folin-Ciocalteu's reagent helped to determine total phenols by producing blue colour and then reducing to yellow hetero-polyphosphomolybdate tungstate anions. An earlier report revealed that phenolic compounds are generally more soluble in polar organic solvents than in water. Many researchers have suggested that there may be a relationship between the amount of total phenolic compound and reducing power. Phenolics are particularly attractive as prophylactic agents due to their high prevalence in the



**Ramya and Muralitharan**

diet and also due to their pluri pharmacological effects. The combination of methanol and ethyl acetate has proven its potential source for isolating phenolic compounds from biological resource [Rios and Gutierrez-Rosales, 2010] [35]

Total flavonoids content (TFC)

The total flavonoid content (TFC) of the dried nine cyanobacterial methanol extracts were evaluated. Total flavonoids in the cyanobacterial extracts ranged from 192 ± 0.9 to 39 ± 1 mg QE/g dry weight. The maximum total flavonoids of 192 ± 0.9 mg QE/g dry weight were found in *Anabaena* sp. followed by 150 ± 0.4 in *Lyngbya* sp. TVL013, and 110 ± 0.7 mg QE/g dry weight in *Nostoc* sp. MTL 515. Whereas, the best antimicrobial compounds producing *Calothrix membranacea* KLR 006 methanol extract showed the total flavonoid content of 78 ± 0.9 mg QE/g dry weight (Fig No.7). [Dhananjaya et al., (2017) [36] estimated twenty different freshwater cyanobacteria and the result showed that maximum TFC in *O. acuta*, *M. laminosus* and *Synechocystis* sp. (634.0 , 370.47 and 275.47 mg QE g⁻¹ fresh wt) respectively and the TFC of *Calothrix geitonos* and *Calothrix brevissima* (91.0 ± 1.8 and 95.13 ± 2.7 QE g⁻¹ fresh wt), respectively, was recorded. In the present study, the methanol extract of *Lyngbya* sp. TVL 013, showed TFC of 150 ± 0.4 units. Similarly, [Dhananjaya et al., (2017) [37] reported the TFC was 192 ± 0.2 QE g⁻¹ fresh wt. The antioxidative properties of flavonoids are due to several different mechanisms, such as scavenging of free radicals, chelation of metal ions (iron and copper) and inhibition of enzymes responsible for a free radical generation. Depending on their structure, flavonoids are able to scavenge practically all known ROS. Flavonoids have been reported as antioxidants, scavengers of a wide range of reactive oxygen species and inhibitors of lipid peroxidation, and also as potential therapeutic agents against a wide variety of diseases [Williams et al., 2004] [38].

ABTS (2, 2'-azino-bis (3-ethylbenzothiazoline-6-sulphonic acid)

Among the nine cyanobacteria, the maximum ABTS activity was recorded in *Oscillatoria* sp. VYL 102 and *Oscillatoria tenuis* VYL 1021 (86 and 80 %) followed by *Lyngbya* sp. TVL 013 with 52% scavenging activity. Whereas the minimum activity was recovered in *Goleotrichia* sp. KLR 0062 and other cyanobacterial scavenging activity given in (Fig No. 8) Similarly, [Dhananjaya et al., 2017]³⁹ reported that ABTS activity of the cyanobacterial extracts ranged from 0.23 mg ml⁻¹ (IC 50) in *A. constrictata* 0.97 mg ml⁻¹ (IC 50) in *O. acuta*. The species *Calothrix geitonos* and *Calothrix brevissima* showed 0.52 ± 0.06 and 0.34 ± 0.07 mg/ml, respectively.

Antioxidant activity of biological samples and natural compounds was evaluated by various methods. Two free radicals commonly used to evaluate antiradical and antioxidant power of biological extracts or natural compounds in vitro are 2, 2-diphenyl-1-picrylhydrazyl (DPPH) and 2, 2'-azino-bis (3-ethylbenzothiazoline-6-sulfonic acid) (ABTS). Free radical scavenging activity of the cyanobacterial extracts was evaluated against three important radicals, DPPH, ABTS and OH. Similarly, high ABTS activity (above 90% at 0.8 mg ml⁻¹) was observed in *Calothrix membranacea* KLR 006. *Nostoc* sp. MTL 515, *Anabaena* sp. MNR 005 extracts showed a low activity group (Fig 7). ABTS activity of the cyanobacterial extracts ranged from 0.21 mg ml⁻¹ (IC 50) in *Calothrix membranacea* KLR 006 to 0.62 mg ml⁻¹ (IC 50). ABTS assay determines the relative ability of the extract or compound (antioxidant) to scavenge ABTS which is generated by reacting strong oxidizing agent such as potassium persulfate. Reduced blue-green ABTS radical by hydrogen-donating antioxidant in solution reflects anti-radical power of the antioxidant extract or compounds. While comparing the results on DPPH and ABTS free radical scavenging activity of the extracts, it is evident that in contrast to DPPH method, ABTS method was more effective and precise. It has been shown that most phenolic antioxidants react slowly with DPPH, reaching a steady state in a longer time [Bondet et al., 1997] [40]. The method also has limitations with the interference of the presence of anthocyanins that could lead to underestimation of the antioxidant activity of biological extract [Shalaby and Shanab 2013] [41].

ACKNOWLEDGEMENT

The authors are grateful to the University Grants Commission (UGC), Government of India, for the financial support. V.P. Ramya acknowledges the Rajiv Gandhi National Fellowship Scheme (F1-17.1/2016-17/RGNF-2015-17-





Ramya and Muralitharan

SC-TAM-17445 / (SA-III/Website) for the fellowship. Authors are thankful to DST-FIST program (SR/FIST/LSI/013/2012 dated 13.08.2012) for instrument facilities.

Authors' contribution: Both the authors contributed equally.

Conflict of interest: The authors declare no conflict of interest.

REFERENCES

- Babic, O.; Kovac, D.; Raseta, M.; Sibul, F.; Svircev, Z.; Simeunovic, J. 2016. Evaluation of antioxidant activity and phenolic profile of filamentous terrestrial cyanobacterial strains isolated from forest ecosystem. *J. Appl. Phycol.* 28, 2333–2342.
- Martel, I.J.; Poza, S.G.; Martel, G.R.; Rico, M.; Olivares, C.A.; Pinchetti, J.L.G. 2017. Phenolic Profile and Antioxidant activity of Crude Extracts from Microalgae and Cyanobacteria Strains. *J. Food Qual.* 2924508.
- Morone, J.; Alfeus, A.; Vasconcelos, V.; Martins, R. 2019. Revealing the potential of cyanobacteria in cosmetics and cosmeceuticals - A new bioactive approach. *Algal Res.* 41, 101541.
- Singh, R.; Parihar, P.; Singh, M.; Bajguz, A.; Kumar, J.; Singh, S.; Singh, V.P.; Prasad, S.M. 2017. Uncovering Potential Applications of Cyanobacteria and Algal Metabolites in Biology, Agriculture and Medicine: Current Status and Future Prospects. *Front. Microbiol.* 8, 515.
- Andrade, M.A.; Lima, V.; Sanches-Silva, A.; Vilarinho, F.; Castilho, M.C.; Khwaldia, K.; Ramos, F. 2019. Pomegranate and grape by-products and their active compounds: Are they a valuable source for food applications? *Trends Food Sci. Technol.* 86, 68–84.
- Martel, I.J.; Poza, S.G.; Martel, G.R.; Rico, M.; Olivares, C.A.; Pinchetti, J.L.G. 2017. Phenolic Profile and Antioxidant activity of Crude Extracts from Microalgae and Cyanobacteria Strains. *J. Food Qual.* 2924508
- Geethu, V.; Shamina, M. 2018. Antioxidant activity of cyanobacterium *Nostoc spongiaeforme* C. Agardh ex Born. & Flah. *J. Algal Biomass Util.* 9, 26–30.
- Zeeshan, M.; Suhail, S.; Biswas, D.; Farooqui, A.; Arif, J.M. 2010. Screening of Selected Cyanobacterial Strains for Phytochemical Compounds and Biological Activities in Vitro. *Biochem. Cell. Arch.* 10, 163–168.
- Yasin, D.; Zafaryab, M.; Ansari, S.; Ahmad, N.; Khan, N.F.; Zaki, A.; Rizvi, M.M.A.; Fatma, T. 2010. Evaluation of antioxidant and anti-proliferative efficacy of *Nostoc muscorum* NCCU-442. *Biocatal. Agric. Biotechnol.* 17, 284–293.
- Hossain, M.F.; Ratnayake, R.R.; Meerajini, K.; Kumara, K.L.W. 2016. Antioxidant properties in some selected cyanobacteria isolated from freshwater bodies of Sri Lanka. *Food Sci. Nutr.* 4, 753–758.
- Botterweck, A.A., Verhagen, H., Goldbohm, R.A., Kleinjans, J., and Van Den Brandt, P.A., 2000. Intake of butylated hydroxyanisole and butylated hydroxytoluene and stomach cancer risk: results from analyses in the Netherlands Cohort Study. *Food Chem. Toxicol.* 38, 599–605.
- Padmapriya V., Anand, N. 2010. The influence of metals on the antioxidant enzyme, superoxide dismutase presents in the cyanobacterium *Anabaena variabilis* Kutz. *ARPN J. Agric. Biol. Sci.* 5(2): 4-9.
- Mackinney, G. 1941. Absorption of light by chlorophyll solutions. *J. Biol. Chem.* 140, 315–322.
- Jensen, A. 1978. Chlorophylls and carotenoids. In J. A. Hellebust & J. S. Carraig (Eds.), *Physiological methods: Physiological and biochemical methods* (pp. 59–70). Cambridge: Cambridge University Press.
- Geethalakshmi, R., and Sarada, D.V.L., 2013. Evaluation of antimicrobial and antioxidant activity of essential oil of *Trianthema decandra* L. *Journal of Pharmacy Research*, 6 (1), pp.101-106.
- Bozin, B., Dukic, N.M., Samojlik, I., Goran, A., Igic, R., 2008. Phenolics as antioxidants in garlic (*Allium sativum* L., Alliaceae). *Food Chemistry* 111, 925–929.
- Wu, L.-C., Ho, J.-A.A., Shieh, M.-C., and I.-W. Lu. 2005. Antioxidant and antiproliferative activities of *Spirulina* and *Chlorella* water extracts. *J. Agric. Food Chem.* 53:4207–4212.
- Kim, D., O. Chun, Y. Kim, H. Moon and C. Lee, 2003. Quantification of phenolics and their antioxidant capacity in fresh plums. *J. Agric. Food Chem.*, 51: 6509–6515.
- Dhananjaya, P. Ratna, S., Prabha, P., Verma, S. Kamlesh S., Meena, K., Yandigeri. M., 2017. Antioxidant properties and polyphenolic content in terrestrial cyanobacteria, *3 Biotech* 7:134 DOI 10.1007/s13205-017-0786-6.



**Ramya and Muralitharan**

20. Tiwari, O.N B.V., Singh, B.V., Upasana M., Singh, A.K., Dolly Wattal D., & Singh P.K., 2005. Distribution and physiological characterization of cyanobacteria isolated from arid zones of Rajasthan Tropical Ecology 46 (2): 165–171.
21. Singh, N., & Rajini, P. S., 2004. Free radical scavenging activity of an aqueous extract of potato peel. Food Chemistry, 85 (4), 611-616. <http://dx.doi.org/10.1016/j.foodchem.2003.07.003>
22. Gaurav Pant, Gaurav K, Karthik L, Gyanaprasuna R, BhaskaraRao, K.V.2011.Antioxidant activity of methanolic extracts of blue green algae anabaena sp. (Nostocaceae). European journal of experimental Biology, 2011,1(1) : 156-162..
23. Suhail, S., Biswas D., Farooqui A., Arif, J.M., & Zeeshan, M., 2011.Antibacterial and free radical scavenging potential of some cyanobacterial strains and their growth characteristics. Journal of Chemical and Pharmaceutical Research, 3: 472-478
24. Martel, I.J.; Poza, S.G.; Martel, G.R.; Rico, M.; Olivares, C.A.; Pinchetti, J.L.G. 2017. Phenolic Profile and Antioxidant activity of Crude Extracts from Microalgae and Cyanobacteria Strains. J. Food Qual. 2924508
25. Chu, W.L., Lim, Y.W., Radhakrishnan, A.K., and Lim., P.E., 2010. Protective effect of aqueous extract from *Spirulina platensis* against cell death induced by free radicals.BMC Complementary and Alternative Medicine, 10 (1), pp.53.
26. Chopra, K., and Bishnoi, M., 2008. Antioxidant profile of *Spirulina*: a blue-green microalga. *Spirulina* in Human Nutrition and Health, pp.101-118.
27. Bermejo, P., Pinero, E., and Villar, A.M., 2008. Iron chelating ability and antioxidants properties of phycocyanin isolated from a potent extract of *Spirulina platensis*. Food Chemistry, 110 (2), pp. 436-445.
28. Ebrahimzadeh, M.A., Nabavi, S.F, Nabavi, S.M., Bahramian, F., Bekhradnia, A.R., 2010. Antioxidant and free radical scavenging activity of *H. Officinalis* L. Var. *Angustifolius*, *V. Odorata*, *B. Hyrcana* and *C. Speciosum*. Pak. J. Pharm. Sci., Vol.23, No.1, January 2010, pp.29-34.
29. Yasuda, T., Inaba, A., Ohmori, M., Endo, T., Kubo, S., and Ohsawa, K., 2000. Urinary metabolites of gallic acid in rats and their radical scavenging effect on DPPH. Journal of Natural Products 63: 1444-1446.
30. Czochra M.P., Widensk AJ. Spectrophotometric determination of H₂O₂ activity. AnalChemActa. 2002;452:177–84.
31. Chumark, P., Khunawat, P., Sanvarinda, Y., Phornchirasilp, S, Morales, N.P., Phivthong-Ngam, L., Ratanachamngong, P., Srisawat, S., Pongrapeeporn, K.U., 2008. The *in vitro* and *ex vivo* antioxidant properties, hypolipidaemic and antiatherosclerotic activities of water extract of *Moringa oleifera* Lam leaves. J., Ethnopharmacol. 116:439–446. doi: 10.1016/j.jep.2007.12.010
32. Singh, H.B., 2009. Polyphenolics from various extracts/fraction of red onion (*Allium cepa*) peel with potential antioxidant and antimutagenic activities. Food Chem Toxicol. ; 47:1161–1167. doi: 10.1016/j.fct.2009.02.004.
33. Manivannan, K., Anantharaman, P. & Balasubramanian, T. 2012. Evaluation of antioxidant properties of marine microalga *Chlorella marina* Asian Pac. J. Trop. Biomed., 2 : 342-346.
34. Siriwardhana, N., Lee K.W., Kim, SH, Ha, J.W., Jeon, Y.J., 2003. Antioxidant activity of *Hizikia fusiformis* on reactive oxygen species scavenging and lipid peroxidation inhibition. Food Sci. Technol. Int. 9:339-347.
35. Rios, J.J., Gutiérrez-Rosales, F. 2010. Comparison of methods extracting phenolic compounds from lyophilised and fresh olive pulp. LWT-Food Science and Technology, 43: 1285–1288.
36. Dhananjaya, P. Ratna, S., Prabha, P., Verma, S. Kamlesh S., Meena, K., Yandigeri. M., 2017. Antioxidant properties and polyphenolic content in terrestrial cyanobacteria, 3 Biotech 7:134 DOI 10.1007/s13205-017-0786-6.
37. Dhananjaya, P. Ratna, S., Prabha, P., Verma, S. Kamlesh S., Meena, K., Yandigeri. M., 2017. Antioxidant properties and polyphenolic content in terrestrial cyanobacteria, 3 Biotech 7:134 DOI 10.1007/s13205-017-0786-6.
38. Williams, P.G., Yoshida, W.Y., Moore, R.E., Paul, V.J., 2004. Micromide and guamamide: cytotoxic alkaloids from a species of the marine *Cyanobacterium Symploca*. J Nat Prod 67:49–53.
39. Dhananjaya, P. Ratna, S., Prabha, P., Verma, S. Kamlesh S., Meena, K., Yandigeri. M., 2017. Antioxidant properties and polyphenolic content in terrestrial cyanobacteria, 3 Biotech 7:134 DOI 10.1007/s13205-017-0786-6.
40. Bondet, V., Brand-Williams, W., Berset, C., 1997. Kinetics and mechanisms of antioxidant activity using the DPPH free radical method. Lebensmittel Wissenschaft Technologie Food Sci Technol. 30:609–615. doi: 10.1006/food.1997.0240.





Ramya and Muralitharan

41. Shalaby, E.A.; Shanab, S.M.M. 2013. Comparison of DPPH and ABTS assays for determining antioxidant potential of water and methanol extracts of *Spirulina platensis*. Indian J. Geo-Mar. Sci. 42, 556–564..

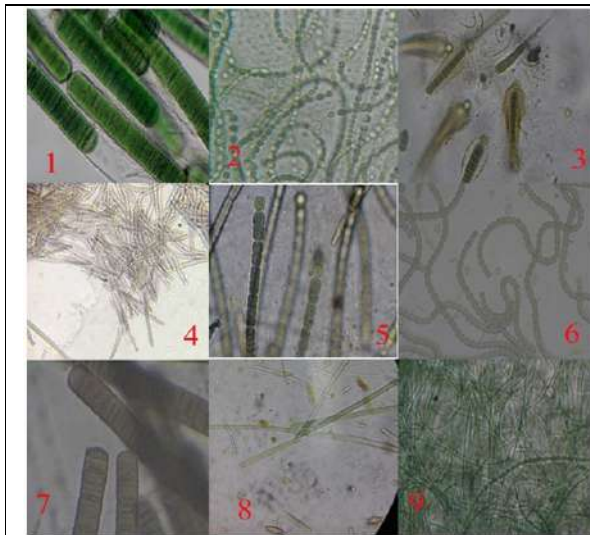


Fig No. 1. 1.*Lyngbya* sp. TVL 013; 2.*Anabaena* sp. MNR 005; 3.*Gleotrichia* sp. KLR 062; 4.*Calothrix membranacea* KLR 006; 5.*Rivularia* sp. KLR 0061; 6.*Nostoc* sp. MTL 515; 7.*Oscillatoria* sp. VYL 102; 8.*Oscillatoria tenuis* VYL 1021; 9.*Phormidium* sp. TVL 0131

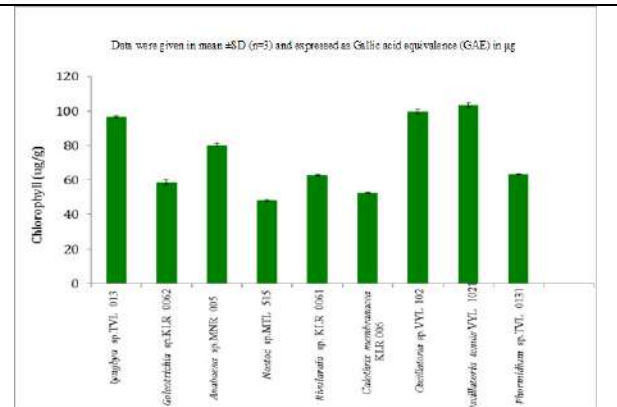


Fig No.2 Estimation of Chlorophyll content in selected cyanobacterial strains

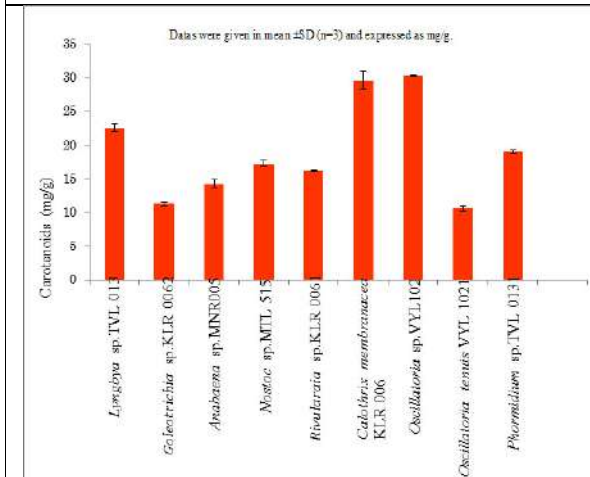


Fig No.3 Estimation of Carotenoids content in selected cyanobacterial strains.

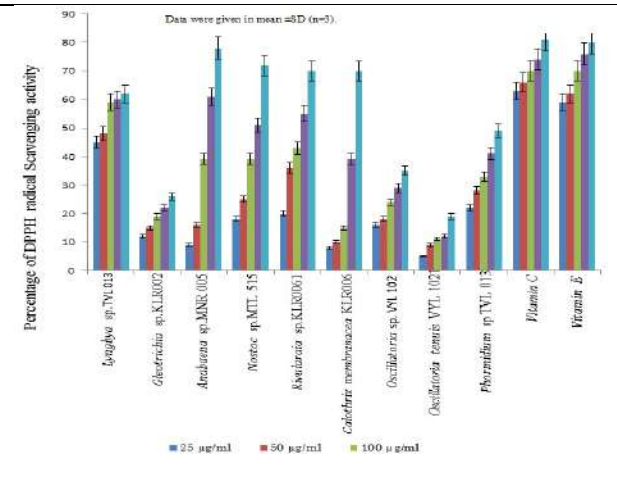


Fig No.4 DPPH radical scavenging activity of selected cyanobacterial strains.





Rama and Muralitharan

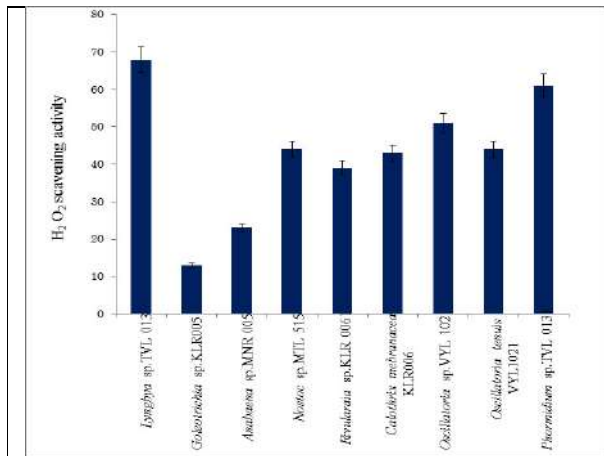


Fig No.5 Percentage of H₂O₂ scavenging activity of selected cyanobacterial strains.

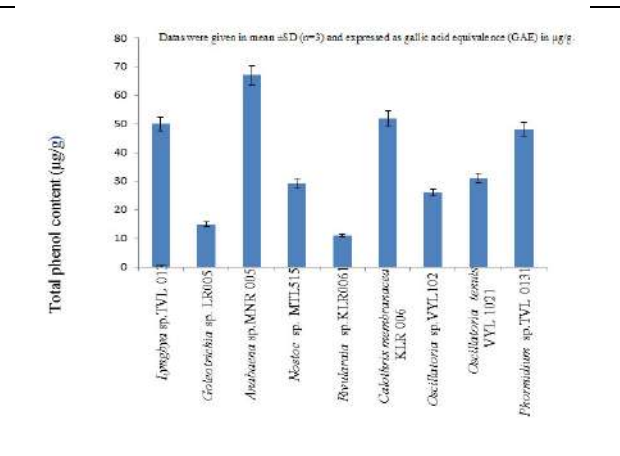


Fig No. 6 Total phenolic content in selected cyanobacterial extracts.

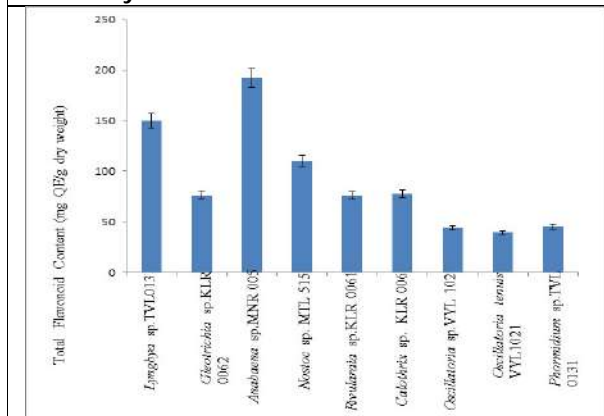


Fig No. 7 Total Flavonoid content in selected cyanobacterial strains data were given in mean ±SD (n=3) and expressed as Gallic acid equivalence(GAE) in µg/g.

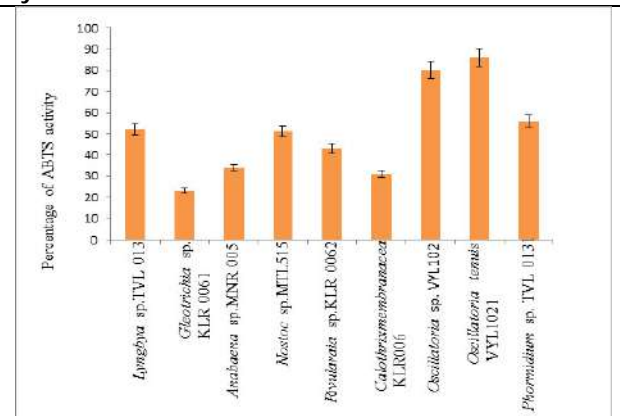


Fig No 8 Percentage of ABTS scavenging activity of selected cyanobacterial strains. Data were given in mean ±SD (n=3).





On \widehat{D} -Closed Sets in Ideal Topological Spaces

C. Inbam *

Assistant Professor, Department of Mathematics, Government Arts College, Melur, Madurai , Tamil Nadu, India.

Received: 07 Nov 2021

Revised: 15 Dec 2021

Accepted: 24 Jan 2022

*Address for Correspondence

C. Inbam

Assistant Professor,
Department of Mathematics,
Government Arts College, Melur,
Madurai , Tamil Nadu, India
Email: cinbam1978@gmail.com



This is an Open Access Journal / article distributed under the terms of the **Creative Commons Attribution License** (CC BY-NC-ND 3.0) which permits unrestricted use, distribution, and reproduction in any medium, provided the original work is properly cited. All rights reserved.

ABSTRACT

In this paper, we introduce the notion of \widehat{D} -I-closed sets and \widehat{D} -I-open sets in ideal topological spaces.

2010 Mathematics Subject Classification: 54A05

Keywords: \widehat{D} -I-closed, \widehat{D} -I-open, \widehat{D} -I-closure, \widehat{D} -I-interior

INTRODUCTION

The subject of ideals in topological spaces has been studied by Kuratowski [5] and Vaidyanathaswamy[7]. Jankovic and Hamlett [4] investigated further properties of ideal space. K. Dass and G.Suresh [2], introduced the \widehat{D} -closed sets in topological spaces. The study of generalized closed sets in a topological space was initiated by Levine [6]. In2012, J.Antony Rex Rodrigo and K. Dass [1], the introduced the concept of D-closed sets and their properties.

In the paper, we introduce the notion of \widehat{D} -I-closed, \widehat{D} -I-open, \widehat{D} -I-closure, and \widehat{D} -I-interior sets in Ideal topological spaces.

PRELIMINARIES

Throughout this paper (X, τ, I) we denote Ideal topological spaces. When A is a subset of X and $\text{cl}(A)$ and $\text{int}(A)$ denote the closure and interior set of A respectively.

We recall some known definitions are needed in the paper.





Inbam

Definition 2.1[4]

An ideal I on a topological space (X, τ) is a non-empty collection of subsets of X which satisfies the following two conditions.

- (i) $A \in I$ and $B \subset A$ imply $B \in I$ and
- (ii) $A \in I$ and $B \in I$ imply $A \cup B \in I$.

Given a topological space (X, τ) with an ideal I on X if $P(X)$ is the set of all subsets of X , a set operator $(\bullet)^* : P(X) \rightarrow P(X)$, called a local function of A with respect to τ and I is defined as follows: for $A \subset X$, $A^*(I, \tau) = \{x \in X \mid U \cap A \notin I \text{ for every } U \in \tau(x)\}$ where $\tau(x) = \{U \in \tau \mid x \in U\}$ [4]. A Kuratowski closure operator $Cl^*(\bullet)$ for a topology $\tau(I, \tau)$, called the $*$ -topology, finer than τ is defined by $Cl^*(A) = A \cup A^*(I, \tau)$ [5]. We will simply write A^* for $A^*(I, \tau)$ and τ^* for $\tau(I, \tau)$. If I is an ideal on X , then (X, τ, I) is called an ideal topological space.

Definition 2.2 [4]

Let A be a subset of Ideal topological space (X, τ, I) . Then

- (i) Closure of A , denoted by $cl(A)$, is defined as $\bigcap \{F : A \subseteq F \text{ and } F \text{ is closed}\}$.
- (ii) Interior of A , denoted by $int(A)$, is defined as $\bigcup \{F : F \subseteq A \text{ and } F \text{ is open}\}$.

Definition 2.3

A subset A of a Ideal topological space (X, τ, I) , is called

- [1] A pre-I-open set [3] if $A \subset int(cl^*(A))$;
- [2] A semi-I-open set [3] if $A \subset cl^*(int(A))$;
- [3] An α -I-open set [8] of $A \subset int(cl^*(int(A)))$;
- [4] A semi-pre-I-open set [8] (= β -I-open []) if $A \subset cl^*(int(cl^*(A)))$;
- [5] A regular-I-open set [3] if $A = int(cl^*(A))$;

The complement of the above open sets is called closed sets.

BASIC PROPERTIES OF \hat{D} -I- CLOSED SETS**Definition 3.1**

A subset A of a Ideal topological space (X, τ, I) , is called

- [1] A generalized-I-closed set (briefly g-I-closed) if $cl^*(A) \subset U$ whenever $A \subset U$ and U is open in (X, τ, I) ,
- [2] A generalized semi-pre-I-closed set (briefly gspl-closed) if $spcl^*(A) \subset U$ whenever $A \subset U$ and U is open in (X, τ, I) ,
- [3] A regular generalized-I-closed set (briefly rgI-closed) if $cl^*(A) \subset U$ whenever $A \subset U$ and U is regular-I-open in (X, τ, I) ,
- [4] A generalized pre-I-regular closed set (briefly gpI-r-closed) if $pcl^*(A) \subset U$ whenever $A \subset U$ and U is regular-I-open in (X, τ, I) ,
- [5] An ω -I-closed set (= \hat{g} -I-closed []) if $cl^*(A) \subset U$ whenever $A \subset U$ and U is semi-I-open in (X, τ, I) ,
- [6] a *g -I-closed set if $cl^*(A) \subset U$ whenever $A \subset U$ and U is ω -I-open in (X, τ, I) ,
- [7] a $g^* - I$ -closed set if $cl^*(A) \subset U$ whenever $A \subset U$ and U is g-I-open in (X, τ, I) ,
- [8] a $g^*p - I$ -closed set if $pcl^*(A) \subset U$ whenever $A \subset U$ and U is g-I-open in (X, τ, I) ,
- [9] an $\alpha^*g - I$ -closed set if $\alpha cl^*(A) \subset U$ whenever $A \subset U$ and U is $\omega - I$ -open in (X, τ, I) ,
- [10] a $^*gs - I$ -closed set if $scl^*(A) \subset U$ whenever $A \subset U$ and U is $\omega - I$ -open in (X, τ, I) ,
- [11] a pre-semi-I-closed set if $spcl^*(A) \subset U$ whenever $A \subset U$ and U is $g - I$ -open in (X, τ, I) ,
- [12] a $gspr - I$ -closed set if $spcl^*(A) \subset U$ whenever $A \subset U$ and U is regular-I-open in (X, τ, I) ,





Inbam

[13] a ρ - I -closed set if $pcl^*(A) \subset int(U)$ whenever $A \subset U$ and U is \tilde{g} - I -open in (X, τ, I) ,

The complement of the above closed sets is called open sets.

Definition 3.2

Let (X, τ, I) , be a ideal topological space and $A \subset X$

1. Semi-pre-I-interior of A denoted by $spIint(A)$ is the union of all semi-pre-I-open subsets of A .
2. Semi-pre-I- closure of A denoted by $spIcl^*(A)$ is the intersection of all semi-pre-I-closed subsets of A .

Definition 3.3

A subset A of (X, τ, I) is called

(i) D -I-closed set if $scl^*(A) \subset int(U)$ whenever $A \subset U$ and U is ω -I-open in (X, τ, I) .

(ii) \widehat{D} -I-closed set if $spcl^*(A) \subset U$ whenever $A \subset U$ and U is D -I-open in (X, τ, I) .

The class of all D -I-closed sets in X is denoted by DIC .

Properties 3.4

Every closed (resp. α -I-closed, pre-I-closed, semi-I-closed) set in \widehat{D} -I-closed.

Proof

Let A be any closed set. Let $A \subset U$ and U is D -I-open set in X . Then $cl^*(A) \subset U$. But $spcl^*(A) \subset cl^*(A) \subset U$. Thus A is \widehat{D} -I-closed. The proof follows from the facts that $spcl^*(A) \subset scl^*(A) \subset cl^*(A)$ and $spcl^*(A) \subset pcl^*(A) \subset \alpha cl^*(A) \subset cl^*(A)$

Remark 3.5

The opposite of the above theorem need not be true.

Example 3.6

Let $X = \{a, b, c, d\}$ and $\tau = \{\emptyset, \{c\}, \{b, d\}, \{b, c, d\}, X\}$, $I = \{\emptyset, \{c\}, \{d\}, \{c, d\}\}$

Then the set $A = \{d\}$ is \widehat{D} -I-closed but not closed (resp. not α -I-closed, not semi-I-closed).

Properties 3.7

Every \widehat{D} -I-closed set is $gsprI$ -closed

Proof

Let A be any \widehat{D} -I-closed set. Let $A \subset U$ and U is regular-I-open in X . Since every regular-I-open set is open and every open is D -I-open, we get $spcl^*(A) \subset U$. Hence A is $gsprI$ -closed.

Remark 3.8

The opposite of the above theorem need not be true.

Example 3.9

Let $X = \{a, b, c, d\}$ and $\tau = \{\emptyset, \{c\}, \{b, d\}, \{b, c, d\}, X\}$, $I = \{\emptyset, \{c\}, \{d\}, \{c, d\}\}$.

Then the set $A = \{b, c, d\}$ is $gsprI$ -closed but not \widehat{D} -I-closed.

Theorem 3.10

Every ω -I-closed set is \widehat{D} -I-closed.





Inbam

Proof

Let A be ω -I-closed set. Let $A \subset U$ and U is D -I-open. Then $cl^*(A) \subset U$. Since every ω -I-closed set is pre-I-closed and every pre-I-closed set is semi-pre-I-closed, A is semi-pre-I-closed. Then $(A) \subset pcl^*(A) \subset \omega cl^*(A)$, Since every closed is ω -I-closed, $\omega cl^*(A) \subset cl^*(A)$. Therefore $spcl^*(A) \subset pcl^*(A) \subset cl^*(A) \subset U$. Hence A is \widehat{D} -I-closed.

Remark 3.11

The opposite of the above theorem need not be true.

Example 3.12

Let $X = \{a, b, c, d\}$ and $\tau = \{\emptyset, \{a\}, \{a, b, c\}, X\}$, $I = \{\emptyset, \{a\}\}$. Then the set $A = \{c\}$ is $\widehat{D} - I$ -closed but not ω -I-closed.

Proposition 3.13

Every \widehat{D} -I-closed set is $gspI$ -closed.

Proof

Let A be any \widehat{D} -I-closed set. Let $A \subset U$ and U is I-open set in X . Since every I-open is D -I-open, we get $spcl^*(A) \subset U$. Hence A is $gspI$ -closed.

Remark 3.14

The opposite of the above theorem need not be true.

Example 3.15

Let $X = \{a, b, c, d\}$ and $\tau = \{\emptyset, \{a\}, \{b\}, \{a, b\}, \{b, c\}, \{a, b, c\}, X\}$, $I = \{\emptyset\}$. Then the set $A = \{b, d\}$ is $gspI$ -closed but not \widehat{D} -I-closed.

Proposition 3.16

Every \widehat{D} -I-closed set is pre-semi-I-closed

Proof

Let A be any \widehat{D} -I-closed set. Let $A \subset U$ and U is g -I-open set in X . Since every g -I-open is D -I-open, we get $spcl^*(A) \subset U$. Hence A is pre-semi-I-closed.

Remark 3.17

The opposite of the above theorem need not be true

Example 3.18

Let $X = \{a, b, c, d\}$ and $\tau = \{\emptyset, \{a\}, \{b\}, \{a, b\}, \{b, c\}, \{a, b, c\}, X\}$, $I = \{\emptyset\}$. Then the set $A = \{b\}$ is pre-semi-I-closed but not D -I-closed.

Remark 3.19

\widehat{D} -I-closedness and rg -I-closedness are independent. It is shown by the following example.

Example 3.20

Let $X = \{a, b, c, d\}$ and $\tau = \{\emptyset, \{c\}, \{b, d\}, \{b, c, d\}, X\}$, $I = \{\emptyset, \{c\}, \{d\}, \{c, d\}\}$. Then the set $A = \{b, d\}$ is \widehat{D} -I-closed but not rg -I-closed and the set $B = \{b, c, d\}$ is rg -I-closed but not \widehat{D} -I-closed.

Remark 3.21

\widehat{D} -I-closedness and $gpri$ -closedness are independent. It is shown by the following example.





Inbam

Example 3.22

Let $X = \{a, b, c, d\}$ and $\tau = \{\emptyset, \{c\}, \{b, d\}, \{b, c, d\}, X\}$, $I = \{\emptyset, \{c\}, \{d\}, \{c, d\}$. Then the set $A = \{b, d\}$ is \widehat{D} -I-closed but not gpr I-closed and the set $B = \{b, c, d\}$ is gpr I-closed but not \widehat{D} -I-closed.

Remark 3.23

\widehat{D} -I-closedness and g -I-closedness are independent. It is shown by the following example.

Example 3.24

Let $X = \{a, b, c, d\}$ and $\tau = \{\emptyset, \{c\}, \{b, d\}, \{b, c, d\}, X\}$, $I = \{\emptyset, \{c\}, \{d\}, \{c, d\}$. Then the set $A = \{b\}$ is \widehat{D} -I-closed but not g -I-closed and Let $X = \{a, b, c, d\}$ and $\tau = \{\emptyset, \{a\}, \{b\}, \{a, b\}, \{b, c\}, \{a, b, c\}, X\}$, $I = \{\emptyset\}$, then the set $B = \{b, d\}$ is g -I-closed but not \widehat{D} -I-closed.

Remark 3.25

\widehat{D} -I-closedness and D -I-closedness are independent. It is shown by the following example.

Example 3.26

Let $X = \{a, b, c, d\}$ and $\tau = \{\emptyset, \{a\}, \{b\}, \{a, b\}, \{b, c\}, \{a, b, c\}, X\}$, $I = \{\emptyset\}$. Then the set $A = \{b\}$ is D -I-closed but not \widehat{D} -I-closed.

Example 3.27

Let $X = \{a, b, c\}$ and $\tau = \{\emptyset, \{a\}, \{b\}, \{a, b\}, \{b, c\}, X\}$, $I = \{\emptyset, \{a\}\}$. Then the set $B = \{b\}$ is \widehat{D} -I-closed but not D -I-closed.

Remark 3.28

\widehat{D} -closedness and $*g$ -closedness are independent. It is shown by the following example.

Example 3.29

Let $X = \{a, b, c, d\}$ and $\tau = \{\emptyset, \{a\}, \{b\}, \{a, b\}, \{b, c\}, \{a, b, c\}, X\}$, $I = \{\emptyset\}$. Then the set $A = \{b, d\}$ is $*g$ -I-closed but not \widehat{D} -I-closed.

Example 3.30

Let $X = \{a, b, c, d\}$ and $\tau = \{\emptyset, \{a\}, \{b\}, \{a, b\}, \{b, c\}, \{a, b, c\}, X\}$, $I = \{\emptyset\}$. Then the set $B = \{c\}$ is \widehat{D} -I-closed but not $*g$ -I-closed.

Remark 3.31

\widehat{D} -I-closedness and g^* -I-closedness are independent. It is shown by the following example.

Example 3.32

Let $X = \{a, b, c, d\}$ and $\tau = \{\emptyset, \{a\}, \{b\}, \{a, b\}, \{b, c\}, \{a, b, c\}, X\}$, $I = \{\emptyset\}$. Then the set $A = \{b, d\}$ is g^* -I-closed but not \widehat{D} -I-closed.

Example 3.33

Let $X = \{a, b, c, d\}$ and $\tau = \{\emptyset, \{c\}, \{b, d\}, \{b, c, d\}, X\}$, $I = \{\emptyset, \{c\}, \{d\}, \{c, d\}\}$

Then the set $A = \{b\}$ is \widehat{D} -I-closed but not g^* -I-closed.

Remark 3.34

\widehat{D} -I-closedness and g^*p -I-closedness are independent. It is shown by the following example.

Example 3.35

Let $X = \{a, b, c, d\}$ and $\tau = \{\emptyset, \{a\}, \{b\}, \{a, b\}, \{b, c\}, \{a, b, c\}, X\}$, $I = \{\emptyset\}$. Then the set $A = \{a, b\}$ is g^*p -I-closed but not \widehat{D} -I-closed.





Inbam

Example 3.36

Let $X = \{a, b, c, d\}$ and $\tau = \{\emptyset, \{a\}, \{b\}, \{a, b\}, \{b, c\}, \{a, b, c\}, X\}$, $I = \{\emptyset\}$. Then the set $A = \{a\}$ is \widehat{D} - I -closed but not α^*g - I -closed.

Remark 3.37

\widehat{D} - I -closedness and α^*g - I -closedness are independent. It is shown by the following example.

Example 3.38

Let $X = \{a, b, c, d\}$ and $\tau = \{\emptyset, \{a\}, \{b\}, \{a, b\}, \{b, c\}, \{a, b, c\}, X\}$, $I = \{\emptyset\}$. Then the set $A = \{b, d\}$ is α^*g - I -closed but not \widehat{D} - I -closed.

Example 3.39

Let $X = \{a, b, c, d\}$ and $\tau = \{\emptyset, \{a\}, \{a, b, c\}, X\}$, $I = \{\emptyset, \{a\}\}$. Then the set $A = \{a, b\}$ is \widehat{D} - I -closed but not α^*g - I -closed.

Remark 3.40

\widehat{D} - I -closedness and α^*g - I -closedness are independent. It is shown by the following example.

Example 3.41

Let $X = \{a, b, c, d\}$ and $\tau = \{\emptyset, \{a\}, \{b\}, \{a, b\}, \{b, c\}, \{a, b, c\}, X\}$, $I = \{\emptyset\}$. Then the set $A = \{b, d\}$ is α^*g - I -closed but not \widehat{D} - I -closed.

Example 3.42

Let $X = \{a, b, c, d\}$ and $\tau = \{\emptyset, \{a\}, \{b\}, \{a, b\}, \{b, c\}, \{a, b, c\}, X\}$, $I = \{\emptyset, \{b\}\}$. Then the set $B = \{a\}$ is \widehat{D} - I -closed but not α^*g - I -closed.

Remark 3.43

\widehat{D} - I -closedness and ρ - I -closedness are independent. It is shown by the following example.

Example 3.44

Let $X = \{a, b, c, d\}$ and $\tau = \{\emptyset, \{a\}, \{b\}, \{a, b\}, \{b, c\}, \{a, b, c\}, X\}$, $I = \{\emptyset\}$. Then the set $A = \{b\}$ is ρ - I -closed but not \widehat{D} - I -closed.

Example 3.45

Let $X = \{a, b, c, d\}$ and $\tau = \{\emptyset, \{c\}, \{b, d\}, \{b, c, d\}, X\}$, $I = \{\emptyset, \{c\}, \{d\}, \{c, d\}\}$. Then the set $B = \{c\}$ is \widehat{D} - I -closed but not ρ - I -closed.

Remark 3.46

\widehat{D} - I -closedness and gp - I -closedness are independent. It is shown by the following example.

REFERENCES

1. Antony Rex Rodrigo, J., and Dass, K.: A New type of generalized closed sets, IJMA3(4) (2012), 1517-1523
2. Dass, K., and Suresh, G.: D -closed sets in topological spaces, Malaya Journal of Matematik, 5(1)(2021), 265-269.
3. Ekici, E.: On pre- I -open sets, semi- I -open sets and b - I -open sets in ideal topological spaces, Acta Universitatis Apulensis, 30(2012), 293-303.
4. Jankovic, D., Hamlett, T. R.: New topologies from old via ideals, Amer. Math. Monthly, 97 (1990), 295-310.
5. Kuratowski, K.: Topology, Vol. I. New York: Academic Press (1966).
6. Levine, N.: generalized closed sets in topology, Rend. Circ. Mat. Palermo, 19(1970), 89-96.
7. Vaidyanathaswamy, R.: Set Topology, Chelsea Publishing Company (1960).
8. Yuksel, S., Acikgoz, A and Noiri, T.: On α - I -continuous functions, Turk. J. Math., 29(2005), 39-51.





Design and Performance Analysis of Aerofoil using Ansys

Partha protim Borthakur*, Richa Rashmi Sarmah, Ranveer Roy, Nilokanta Mili¹, Mousumi Devi, Sidhartha Saikia and Abhinov Saikia

Department of Mechanical Engineering, Dibrugarh University, Assam, 786004, India.

Received: 19 Dec 2021

Revised: 30 Dec 2021

Accepted: 22 Jan 2022

*Address for Correspondence

Partha protim Borthakur

Department of Mechanical Engineering,
Dibrugarh University,
Assam, 786004, India.
Email: partha@dibru.ac.in.



This is an Open Access Journal / article distributed under the terms of the **Creative Commons Attribution License** (CC BY-NC-ND 3.0) which permits unrestricted use, distribution, and reproduction in any medium, provided the original work is properly cited. All rights reserved.

ABSTRACT

The popularity of air travel has resulted in several new technologies and research to build more efficient and quicker planes. An aerofoil is a curved surface structure designed to maximize lift and drag during flight. The airfoil is critical in any plane because it provides the lift required to raise the plane with the least drag. It is challenging to create an airfoil with the necessary aerodynamic properties. Initially, the design was randomly generated and evaluated in a flow section. And then there is the Wright Brothers' cambered portion. NACA has defined an airfoil properly, enabling us to build airfoils using formulae rather than arbitrarily. An aerofoil structure has a curved surface utilized as the fundamental shape of wings and fins in most aircraft. The present study examines the experimental and analytical development of pressure variation, drag lift forces, and other aerofoil section characteristics. The study is based on modeling fluid flow via a symmetrical and asymmetrical aerofoil in a wind tunnel. Ansys software is used to conduct the simulation. This article presents a comparative analysis of symmetric and asymmetric aerofoils.

Keywords: Aerofoil, aerofoil simulation, aerodynamics, NACA.

INTRODUCTION

In the beginning, when man was still a creature of nature, his sole mode of mobility was his legs. We have gradually developed speedier and more comfortable modes of transportation, the most recent being air travel. Since their creation, aircraft have grown in popularity as the quickest method of transportation; they have also acquired appeal as a combat machine following World War II. This increased popularity of air travel has resulted in several new technologies and research projects to develop quicker and more affordable planes. Interestingly, the modern airplane as we know it today, with fixed wings and vertical and horizontal tail surfaces, was initially envisioned by GEORGE



**Partha protim Borthakur et al.,**

Cayley more than 200 years ago in 1799. On a silver disc, he wrote his initial concept. Cayley's recognition that a curved surface generates more excellent lift than a flat one is significant. Cayley's fixed-wing design ushered in a new era of heavier-than-air aircraft vehicles. Before his time, aviation enthusiasts attempted to mechanically replicate the natural flight of birds, which resulted in a succession of human-powered flapping-wing designs that never had a chance of success. Even Leonardo da Vinci spent much time and effort in the late 15th century creating several varieties of ornithopters but to no result. The flapping of the wings was intended to produce both lift and propulsion concurrently in such ornithopters [1].

Aerofoil

The term "airfoil" (in American English) or "aerofoil" (in British English) refers to the condition of a wing, edge, or cruise when viewed cross-sectionally. It is a cross-section of the plane's wing. Its primary function is to produce lift to an aircraft during take-off and flying. However, it has a side effect called drag, which works against the airplane's velocity. The lift required by a plane is determined by its intended function. A heavier plane requires more lift, whereas a lighter plane requires less lift. Thus, the airfoil section is dictated by the airplane's intended function. Additionally, lift force influences the plane's vertical acceleration, which is dependent on the plane's horizontal velocity. Thus, by finding the lift coefficient, the lift force can be calculated, and by knowing the lift force and necessary vertical acceleration, the required horizontal velocity can be determined. Aerodynamic energy is transferred to an airfoil-shaped body traveling through a fluid. Lift is the portion of this power that is perpendicular to the direction of movement. Drag is the section parallel to the direction of movement. Subsonic flight airfoils have a distinctive form with an angled leading edge, which is mirrored by a sharp trailing edge that is frequently unevenly cambered. Hydrofoils are high-capacity foils that use water as the operating fluid.

Lift on an airfoil is mainly determined by its approach and shape. When configured correctly, the airfoil diverts the oncoming air, generating energy on the airfoil in the direction opposite to the diversion. This force is called aerodynamic drive and may be classified into two components: lift and drag. While most thwart forms require a positive approach to generate lift, cambered airfoils may generate lift at zero approaches. This "turning" of the air in the airfoil area results in bending streamlines, with more balanced weight on one side and increased weight on the other. Through Bernoulli's standard, this weight disparity is combined with a speed distinction so that the following stream field around the airfoil has a faster average speed on the top surface than on the more flat surface. Applying the flow concept and the Kutta-Joukowski hypothesis, the lifting power may be clearly related to the typical top/base speed contrast without noting the weight[2]. Fig. 1 illustrates the general section of an airfoil; other terminologies associated with airfoils include the following:

Leading-edge: - The edge of the airfoil faces the plane's direction of motion. It is typically circular and deflects air so that the air velocity on the top surface is greater than the air velocity on the lower surface.

Trailing edge: - In nature, it is the pointy edge of the airfoil. It is attached to the airfoil's rear.

Chord line: - It is a straight line that connects the leading and trailing edges. It divides the airfoil into two sections when it is symmetrical but may not do so when it is asymmetrical. It also establishes another critical parameter, the assault angle. The angle of attack is the angle formed by the chord line and the plane's direction of motion. It is a critical parameter since it influences the lift and drag coefficients.

Chamber line: This line connects the leading and trailing edges of the airfoil and divides it into two symmetrical sections. It might be a straight line, or it could be a curved line. The lift coefficient is a dimensionless quantity that describes the relationship between the lifting force applied to a body and its velocity, surface area, and the fluid density in which it is lifted.

Drag coefficient: - It is a dimensionless coefficient that describes the relationship between the dragging force acting on a body and its velocity, surface area, and the density of the fluid in which it is traveling.

Stall angle of attack: - It is the angle of attack at which the lift coefficient is highest and begins to decline.





Partha protim Borthakur et al.,

Wind Tunnel

The Wind Tunnel was developed to provide a comprehensive subsonic facility for studying fundamental aerodynamics. The tunnel's performance requirements and accompanying models are not straightforward research endeavors. The wind tunnel was created to accomplish a variety of tasks [3].

Simulation

Simulation is the process of imitating the process of a real-world over time. Simulating something involves the development of a model; this model reflects the specified physical or abstract system or process's main traits, behaviors, and functionalities. The model describes the system in its entirety, whereas the simulation depicts the system's activity throughout time. Simulation is utilized in various situations, including performance optimization, safety engineering, testing, training, teaching, and video games. Computer experiments are frequently used to investigate simulation models. Simulation is also utilized in economics to obtain insight into natural or human systems' functioning through scientific modeling. Simulations can be used to demonstrate the ultimate real-world consequences of various situations and courses of action. Additionally, simulation is utilized when the real system cannot be engaged because it is inaccessible, hazardous, or unacceptably risky to engage, is being developed but not yet built, or does not exist[4].

Software Used - Ansys

Ansys provides engineering simulation solution sets to meet the requirements of the design process. Businesses use ANSYS software in a broad number of sectors. It develops and markets software for simulating engineering issues using finite element analysis. The program generates computer models of buildings, electronics, and machine components to mimic properties such as strength, toughness, elasticity, temperature distribution, electromagnetism, and fluid movement. Ansys is used to assess how a product will perform under various parameters without the need for test products or crash testing. For instance, Ansys software may be used to determine the durability of a bridge after years of usage, the optimal way to process salmon in a cannery to minimize waste, or the optimal way to build a slide that uses less material without losing safety. The majority of Ansys simulations are conducted using the company's flagship tool, Ansys Workbench. Ansys users decompose bigger structures into smaller independently modeled and evaluated components. A user may begin by specifying the dimensions of an object, followed by the addition of weight, pressure, and temperature[5].

Review of literature

This section summarises prior research on aerofoil sections, modeling, and analytic techniques. Rana et al. used a RANS-based Computational Fluid Dynamics solver to explore two-dimensional subsonic flow in an airfoil[3]. Gulp et al. examined and studied the influence of perspective degree on the execution of an Airfoil. This study's findings demonstrated and validated that the center of swell conditions should not be maintained throughout wind passage tests[6]. Goel et al. developed a strategy for developing Turbine Airfoils through the use of Quansi – 3D inspection codes. He grasped the concept of 3D by showing two-dimensional airfoil parts. Arvind et al. conducted research on the NACA 4412 aerofoil, examining its profile in relation to an aircraft wing. The NACA 4412 aerofoil was designed with CATIA V5 in mind. Fazil et al. observed that creating an aerofoil profile in CAD using a camber billow of concentrates is less useful than creating a vane profile[7]. Kevadiya et al. investigated the NACA 4412 aerofoil profile, and CFD analysis was performed using FLUENT 6.3.26 at various methods ranging from 0 to 12[2]. Guilmineau et al. demonstrated a physically sound approach for reproducing speed fluxes generated by discrete mathematical expressions[8]. Kunz et al. contribute to the progress of ultra-low Reynolds number aerofoils. These investigations are conducted to better understand the aerodynamic concerns found at low speeds, as well as issues with the outline and execution of air vehicles. This method was chosen in light of concurrent venturing, in which stationary states are gained by an understanding of the preconditioned pseudo stationary arrangement of comparisons[9]. N. Ahmed et al. elucidated and optimized the shape of airship wings and turbomachinery components. These lifting devices operate optimally at the point of partition initiation. Thus, division phenomena must be considered if the investigation is directed toward pragmatic applications. Thus, numerical simulation of a





Partha protim Borthakur et al.,

relentless stream in a straight line using NACA 0012 aerofoils is accomplished in this work using the control volume technique[10].

METHODOLOGY

Analysis of Wind Tunnels

The multi-tube manometer is filled with a high-density fluid, water, while all control panel switches remain in the off position. Open the wind tunnel's acrylic plate, put the test section, aerofoil on the connecting rod at the appropriate drag balance position, and connect the balance to the indicator. A manometer is used to measure the pressure in the test area. The manometer's initial measurements are taken. The wind tunnel's aperture is closed with the acrylic plate, which initiates the motor. After five minutes of operation, the device reaches a steady speed. The manometer reading, lift load, and drag load readings are obtained via the digital display[10,11].

Simulation

After settling on a topic, the first stage in our research was to do a literature review on it. As a result, we conducted a literature search and were acquainted with the subject. The second stage was to assemble the necessary software for our project, which in this case included Ansys-Analysis Systems and Microsoft Excel. The following phase involved data collecting. We required coordinates for the five planes' airfoils, notably NACA 0012, NACA 0027, NACA 5412, NACA 7415, and EPPLER 862. Then we looked over various textual and graphic guides to familiarise ourselves with ANSYS. Then, using five different airfoil models, we calculated the lift and drag forces at a constant speed of 100m/s. We needed to identify whether a type of aerofoil, symmetric or asymmetric, generates the most lift force to create an efficient aerofoil[8,11,12].

Data Collection and analysis

Experimental Setup

Data collected

Investigation on aerofoil NACA 0027
Investigation on someother aerofoils
Contours of velocity magnitude

RESULTS

Lift and drag forces of the aerofoils

CONCLUSION

Through this work, a numerical analysis of flow over aerofoil NACA 0027 is carried out in a wind tunnel environment, and its lift and drag force is determined at 0 degree angle of attack. Further, a simulated analysis of some selected aerofoils is performed at ANSYS, and their pressure and velocity profiles are observed, and it is seen that a lowering of pressure on the upper surface results in developing pressure gradient. Uponthis analysis, it can beconcluded that lift and drag force increasewith increasing angle of attack and decreases with decreasing angle of attack, i.e., lift and drag forces are directly proportional to AOA for the selected aerofoils presented herewith.





Partha protim Borthakur et al.,

REFERENCES

1. Arvind M, "Cfd analysis of static pressure and dynamic pressure for naca 4412", International Journal of Engineering Trends and Technology ISSN/EISSN: 22315381.2010; 4(8): 3258-3265.
2. KevadiyaM, "CFD Analysis of Pressure Coefficient for NACA 4412" International Journal of Engineering Trends and Technology ISSN/EISSN: 22315381.2013; 4 (5) 2041-2043, 2013.
3. Rana D, Patel S, Onkar AK and Manjuprasad M. "Time-domain simulation of airfoil flutter using fluid-structure coupling through FEM based CFD solver". Symposium of Applied Aerodynamics and Design of Aerospace vehicle, SAROD20111, Nov 16-18 2009, Bangalore.
4. Fazil By J and Jayakumar V, "Investigation of airfoil profile design using reverse engineering Bezier curve" Journal of Engineering and Applied Sciences ISSN/EISSN: 18196608. 2011,6(7): 43-52, 2011.
5. Gulp T, "An Investigation of the effect of aspect ratio on Airfoil performance". Gazi: American Journal of Applied Sciences ISSN/EISSN: 15469239/ 15543641,1995. 2(2): 545-549.
6. Goel S, "Turbine Airfoil Optimization Using Quasi-3D Analysis Codes". International Journal of Aerospace Engineering. 2008.
7. GuilmineauE, Piquet J and QueuteyP, "2D turbulent viscous flow simulation past airfoils at fixed incidence". Comp. Fluids, 1997, 26:135-162.
8. Kunz P J and Kroo I, "Analysis, design and testing of airfoils for use at ultra-low Reynolds numbers". Proceedings of the Conference on Fixed, Flapping and Rotary Vehicles at very Low Reynolds Numbers", edited by T. J. Mueller, Univ. of Notre Dame, Notre Dame, IN, pp.349-372, 2000.
9. Ahmed N, Yilbas BS and Budair MO, "Computational study into the flow field developed around a cascade of NACA 0012 airfoils". Comput. Methods Appl. Mech. Engrg. 1998,167: 17-32.
10. Mittal S and Saxena P, "Hysteresis in flow past a NACA 0012 airfoil". Comput. Methods Appl. Mech. Engrg.2002, 191: 2179– 2189.
11. Mustafa. Genc, Gary. Lock and Unver. Kaynak, "An Experimental and Computational Study of Low Re Number Transitional Flows over an Aerofoil with Leading Edge Slat". AIAA 2008-8877. The 26th Congress of ICAS and 8th AIAA ATIO. September 2008.

Table.1. Readings of Multiple Tube manometers

h_{11}^*	h_{12}^*	h_{13}^*	h_{14}^*	h_{15}^*	h_{16}^*	h_{17}^*	h_{18}^*	h_{19}^*	h_{110}^*	h_{111}^*	h_{112}^*	h_{113}^*
34.6	36.1	33.8	35.7	35	34.8	35.8	33	35.3	35.3	35.7	34	33.5
35.8	38.4	34.5	37.7	36.3	36	37.5	33.1	36.6	36.6	37.7	36	35.5

Table 2. Observation for drag and lift forces

Drag force(F_D)	Lift force(F_L)
1. 0.268	3.568
2. 0.490	3.585

Table 3. Readings of U-Tube manometer

h_1	h_2
21.5	18.8
22.6	17





Partha protim Borthakur et al.,

Table 4. Lift and drag forces of the aerofoils

AEROFOIL	AOA	LIFT FORCE	DRAG FORCE
NACA 0027	0	0.011777	0.4263044
NACA 0012	0	90941.004	451594.2
NACA 0012	10	1368639.3	2105073.6
NACA 5412	0	265.75	99.922
NACA 5412	10	3502815.2	3731002.6
NACA 7415	0	406.40	189.04
NACA 7415	10	4685049	4900090

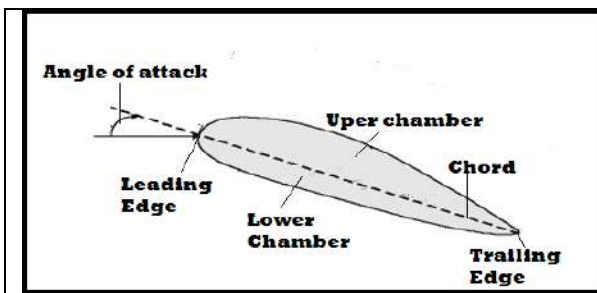


Fig 1. The general section of an aerofoil



Fig 2. Wind tunnel setup



Fig .3. NACA 0027-Aerofoil section



Fig.4. Aerofoil fitted in the test section



Fig.5. Multitube manometer



Fig.6. Control panel and u tube manometer





Partha protim Borthakur et al.,

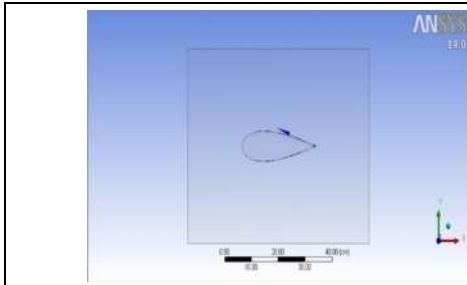


Fig .7. Design modeler

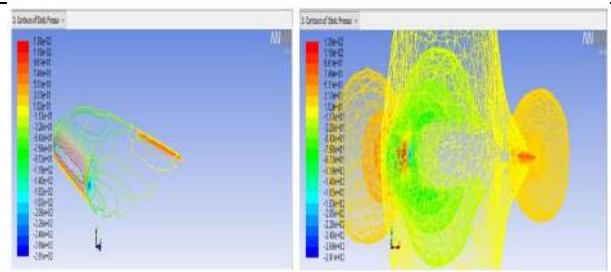


Fig .8. Contours of static pressure

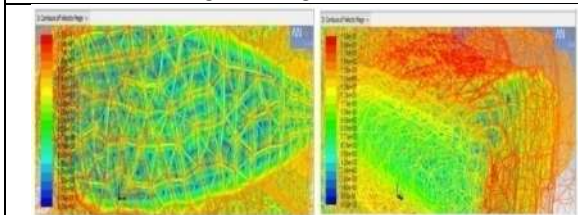


Fig .9. Contours of velocity magnitude

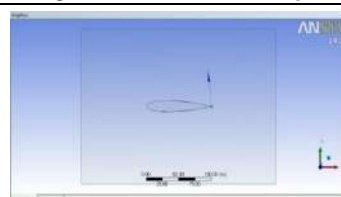


Fig.10. Design modeler

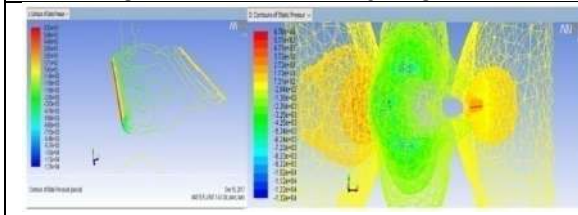


Fig .11. Contours of static pressure

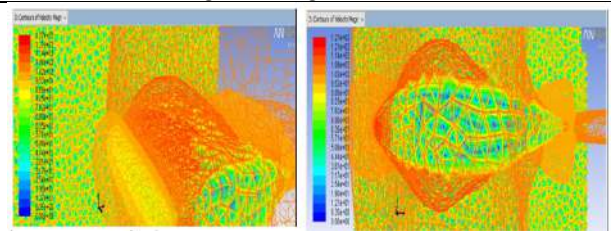


Fig.12. Contours of velocity magnitude

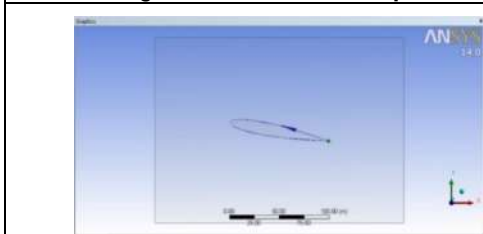


Fig.13. Design modeler

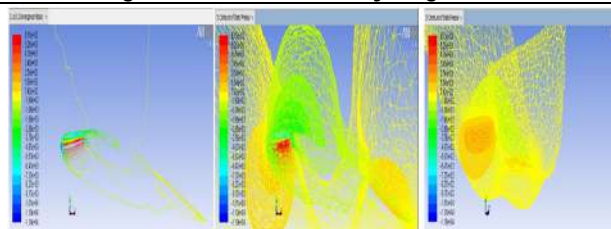


Fig.14. Contours of static pressure

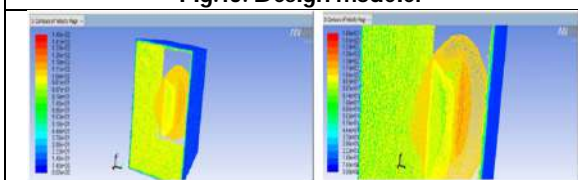


Fig .15. Contours of velocity magnitude



Fig .16. Design modeler

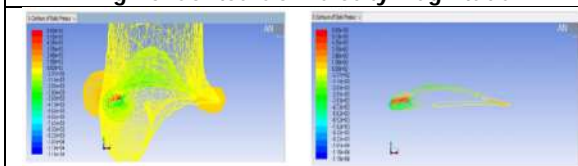


Fig.17. Contours of static pressure

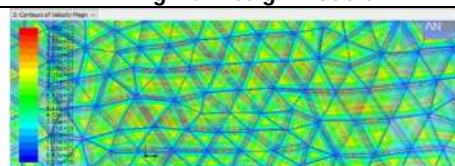


Fig .18. Contours of velocity magnitude





Partha protim Borthakur et al.,

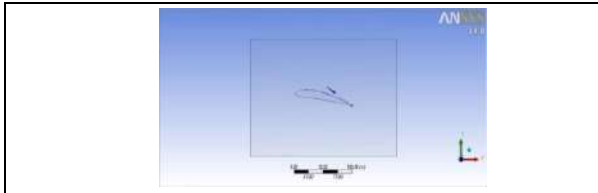


Fig.19. Design modeler

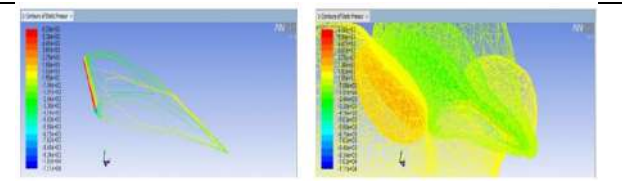


Fig.20. Contours of static pressure

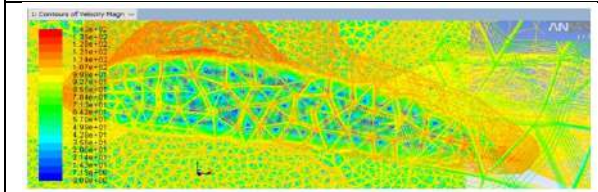


Fig.21. Contour of velocity magnitude

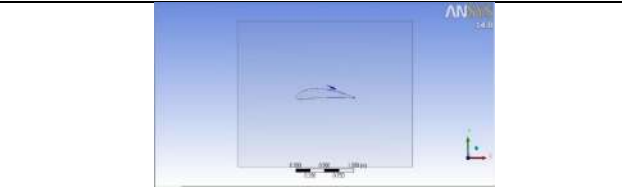


Fig.22. Design modeler

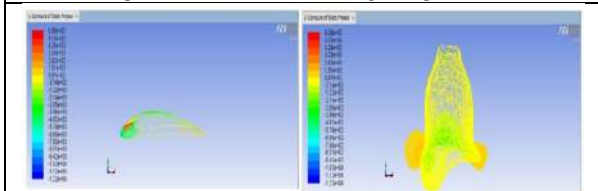


Fig. 23. Contour of static pressure

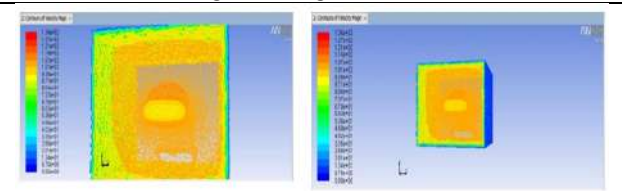


Fig.24. Contour of velocity magnitude

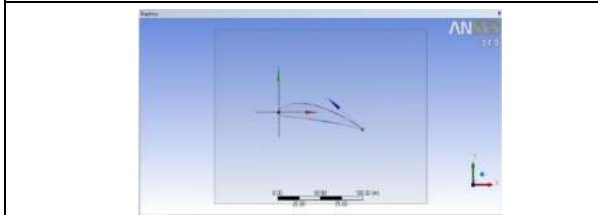


Fig. 25. Design modeler

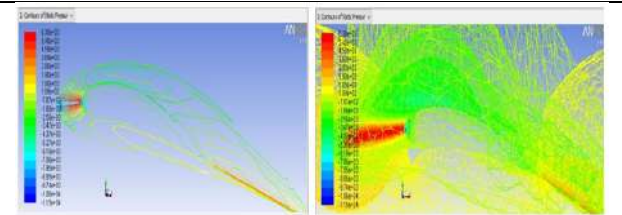


Fig. 26. Contour of static pressure

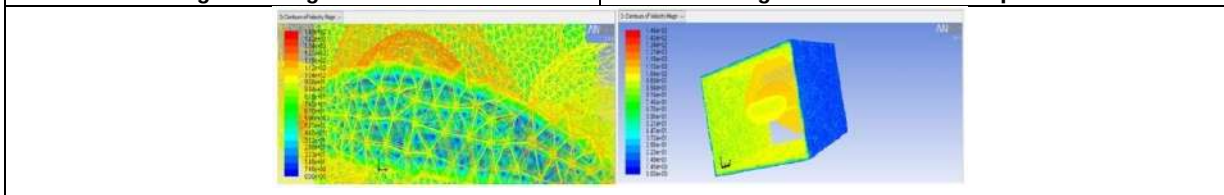


Fig. 27. Contour of velocity magnitude





Some Special Types of λ_g^α -continuous Maps

S. Subhalakshmi^{1*} and N. Balamani²

¹Research Scholar, Department of Mathematics, Avinashilingam Institute for Home Science and Higher Education for Women, Coimbatore - 641043, Tamil Nadu, India.

²Assistant Professor, Department of Mathematics, Avinashilingam Institute for Home Science and Higher Education for Women, Coimbatore - 641043, Tamil Nadu, India.

Received: 26 Oct 2021

Revised: 19 Dec 2021

Accepted: 06 Jan 2022

*Address for Correspondence

S. Subhalakshmi

Research Scholar,

Department of Mathematics,

Avinashilingam Institute for Home Science and Higher Education for Women,

Coimbatore -641043, Tamil Nadu, India.

Email: subhamanu2013@gmail.com



This is an Open Access Journal / article distributed under the terms of the **Creative Commons Attribution License** (CC BY-NC-ND 3.0) which permits unrestricted use, distribution, and reproduction in any medium, provided the original work is properly cited. All rights reserved.

ABSTRACT

The goal of this article is to define the special type of continuous maps called quasi λ_g^α -continuous maps, perfectly λ_g^α -continuous maps, totally λ_g^α -continuous maps and strongly λ_g^α -continuous maps in topological spaces with the help of the previously defined λ_g^α -continuous maps. Further, we derive some important propositions in the concept of study.

Keywords: topological spaces, λ -closed set, α -closed set, λ_g^α -continuous, quasi λ_g^α -continuous, perfectly λ_g^α -continuous, totally λ_g^α -continuous, strongly λ_g^α -continuous.

Mathematics Subject Classification: 54A05, 54C05, 54C10

INTRODUCTION

Continuity is one of the most important concepts in the study of topological spaces. The study of characterizations and generalizations of continuity has been done on various generalized closed sets and many topologists have studied their properties. Levine [6], Arya and Gupta [1], Jain [5] and Noiri [10] introduced respectively strongly continuous maps, completely continuous maps, totally continuous maps and perfectly continuous maps which are some of stronger forms of continuous maps. Here we introduce quasi λ_g^α -continuous, perfectly λ_g^α -continuous, totally λ_g^α -continuous and strongly λ_g^α -continuous maps by utilizing the properties of λ_g^α -continuous maps which was defined and analysed by Subhalakshmi and Balamani [12]. Further we propose quasi λ_g^α -closed maps and quasi λ_g^α -





Subhalakshmi and Balamani

open maps in topological spaces and study their fundamental properties. Composition of mappings related to the proposed definitions are also derived and analysed.

Preliminaries

Definition "Let (M, μ) be a topological space. For a subset A of (M, μ) the intersection of all λ -closed sets containing A is called λ -closure of A and is denoted by $cl_\lambda(A)$ [2]"

Definition "Let (M, μ) be a topological space. A subset A of (M, μ) is called

- (i) α -open if $A \subseteq int(cl(int(A)))$ [9]
- (ii) λ -closed if $A = L \cap D$, where L is a Λ -set and D is a closed set [4]
- (iii) λ_g^α -closed if $cl_\lambda(A) \subseteq U$ whenever $A \subseteq U$ and U is α -open in (M, μ) [11]"

Definition "Let (M, μ) and (N, ν) be the topological spaces. A map $u: (M, \mu) \rightarrow (N, \nu)$ is called

- (i) λ -closed if $u(V)$ is λ -closed in (N, ν) for every closed set V in (M, μ) . [2]
- (ii) λ -continuous if $u^{-1}(V)$ is λ -closed in (M, μ) for every closed set V in (N, ν) . [4]
- (iii) λ -irresolute if $u^{-1}(V)$ is λ -closed in (M, μ) for every λ -closed set V in (N, ν) . [2]
- (iv) Strongly continuous if $u^{-1}(V)$ is both open and closed in (M, μ) for every subset V in (N, ν) . [6]
- (v) λ_g^α -continuous if $u^{-1}(V)$ is λ_g^α -closed in (M, μ) for every closed set V in (N, ν) . [12]
- (vi) λ_g^α -irresolute if $u^{-1}(V)$ is λ_g^α -closed in (M, μ) for every λ_g^α -closed set V in (N, ν) . [12]"

Results

- (i) "Every λ -closed (λ -open) set is a λ_g^α -closed (λ_g^α -open) set. [11]"
- (ii) "Every closed (open) set is a λ_g^α -closed (λ_g^α -open) set. [11]"

Special Maps

Hereafter, u represents the mapping from the domain (M, μ) to the co-domain (N, ν) i.e., $u: (M, \mu) \rightarrow (N, \nu)$ and v represents the mapping from the domain (N, ν) to the co-domain (K, κ) i.e., $v: (N, \nu) \rightarrow (K, \kappa)$.

Definition 1 A map u is called quasi λ_g^α -continuous if the inverse image of every λ_g^α -closed set in (N, ν) is closed in (M, μ) or if $u^{-1}(S)$ is closed in (M, μ) for every λ_g^α -closed set S in (N, ν) ."

Example 1 Let $M = N = \{i, j, k\}$, $\mu = \{\phi, \{i\}, \{j\}, \{i, j\}, \{i, k\}, M\}$ and $\nu = \{\phi, \{i\}, N\}$. Then u is a quasi λ_g^α -continuous map when labelled as $u(i) = j; u(j) = k$ and $u(k) = i$.

Theorem 1 A map u is quasi λ_g^α -continuous if the inverse image of every λ_g^α -open set in (N, ν) is open in (M, μ) and vice versa.

Proof: Consider u to be the quasi λ_g^α -continuous map and T to be any λ_g^α -open set in (N, ν) . Then $N \setminus T$ is λ_g^α -closed in (N, ν) . By assumption, $u^{-1}(N \setminus T) = M \setminus (u^{-1}(T))$ is closed in (M, μ) . Hence $u^{-1}(T)$ is open in (M, μ) .

On the other side, consider S to be any λ_g^α -closed set in (N, ν) implies $N \setminus S$ is λ_g^α -open in (N, ν) . Then $u^{-1}(N \setminus S) = M \setminus (u^{-1}(S))$ is open in $(M, \mu) \Rightarrow u^{-1}(S)$ is closed in (M, μ) . Thus the proof.

Definition 2 A map u is called perfectly λ_g^α -continuous if the inverse image of every λ_g^α -closed set in (N, ν) is clopen in (M, μ) or if $u^{-1}(S)$ is clopen in (M, μ) for every λ_g^α -closed set S in (N, ν) ."

Example 2 Let $M = N = \{i, j, k\}$, $\mu = \{\phi, \{i\}, \{j, k\}, M\}$ and $\nu = \{\phi, \{i\}, N\}$. Then u is a perfectly λ_g^α -continuous map when labelled as $u(i) = i; u(j) = k$ and $u(k) = j$.





Subhalakshmi and Balamani

Theorem 2 A map u is perfectly λ_g^α -continuous if the inverse image of every λ_g^α -open set in (N, ν) is clopen in (M, μ) and vice versa.

Proof: Consider T to be any λ_g^α -open set in (N, ν) . Then $N \setminus T$ is λ_g^α -closed in (N, ν) . Since u is perfectly continuous $u^{-1}(N \setminus T) = M \setminus (u^{-1}(T))$ is clopen in (M, μ) . Hence $u^{-1}(T)$ is clopen in (M, μ) .

On the other side, consider S to be any λ_g^α -closed set in (N, ν) , then $N \setminus S$ is λ_g^α -open in (N, ν) . From the assumption, $u^{-1}(N \setminus S) = M \setminus (u^{-1}(S))$ is clopen in $(M, \mu) \Rightarrow u^{-1}(S)$ is clopen in (M, μ) , which follows the proof.

Proposition 1 If u is a perfectly λ_g^α -continuous map, then it is a quasi λ_g^α -continuous map.

Proof: Suppose that S is a λ_g^α -closed set in (N, ν) . Since u is perfectly λ_g^α -continuous, $u^{-1}(S)$ is clopen in (M, μ) . Hence u is a quasi λ_g^α -continuous map.

Proposition 2 Every strongly continuous map u is a quasi λ_g^α -continuous (resp. perfectly λ_g^α -continuous) map.

Proof: Suppose that S is a λ_g^α -closed set in (N, ν) . As u is strongly continuous, for any subset S , $u^{-1}(S)$ is both open and closed in (M, μ) . Hence u is quasi λ_g^α -continuous (resp. perfectly λ_g^α -continuous) map.

Theorem 3 Consider the discrete topological space (M, μ) and any topological space (N, ν) , then for any map u , the statements

- (i) u is perfectly λ_g^α -continuous
 - (ii) u is quasi λ_g^α -continuous
- are equivalent.

Proof: (i) \Rightarrow (ii) evident from Proposition 1

(ii) \Rightarrow (i) Let S be any λ_g^α -closed set in (N, ν) . By assumption, $u^{-1}(S)$ is closed in (M, μ) . Since (M, μ) is a discrete space, $u^{-1}(S)$ is open in (M, μ) . Hence $u^{-1}(S)$ is clopen in (M, μ) . Hence u is a perfectly λ_g^α -continuous map.

Proposition 3 Every quasi λ_g^α -continuous map is a λ_g^α -continuous map.

Proof: Consider u to be a quasi λ_g^α -continuous map and S to be a closed set in (N, ν) . Using Result (i), S is λ_g^α -closed in (N, ν) . Since u is quasi λ_g^α -continuous, $u^{-1}(S)$ is closed in $(M, \mu) \Rightarrow u^{-1}(S)$ is λ_g^α -closed in (M, μ) . Hence u is a λ_g^α -continuous map.

The subsequent example shows that the converse may not hold good.

Example 3 Let $M = N = \{i, j, k\}$, $\mu = \{\phi, \{i\}, \{j\}, \{i, j\}, \{i, k\}, M\}$ and $\nu = \{\phi, \{i\}, \{i, j\}, \{i, k\}, N\}$. Then u is a λ_g^α -continuous map when labelled as $u(i) = j$; $u(j) = i$ and $u(k) = k$, but not a quasi λ_g^α -continuous map, since for the λ_g^α -closed set $\{i, j\}$ in (N, ν) , $u^{-1}(\{i, j\}) = \{i, j\}$ is not closed in (M, μ) .

Proposition 4 Let u and v be any two maps. Then $(v \circ u): (M, \mu) \rightarrow (K, \kappa)$ is quasi λ_g^α -continuous (resp. perfectly λ_g^α -continuous) map, whenever

- (i) v is a strongly continuous map and u is a quasi λ_g^α -continuous (resp. perfectly λ_g^α -continuous) map
- (ii) v is a quasi λ_g^α -continuous (resp. perfectly λ_g^α -continuous) map and u is a continuous map

Proof: (i) Consider S to be any λ_g^α -closed set in (K, κ) . As v is strongly continuous, $v^{-1}(S)$ is both open and closed in $(N, \nu) \Rightarrow v^{-1}(S)$ is λ_g^α -closed in (N, ν) . Since u is quasi λ_g^α -continuous (resp. perfectly λ_g^α -continuous), $(v \circ u)^{-1}(S) = u^{-1}(v^{-1}(S))$ is closed (resp. clopen) in (M, μ) . Hence $(v \circ u)$ is a quasi λ_g^α -continuous (resp. perfectly λ_g^α -continuous) map.





Subhalakshmi and Balamani

(ii) Consider S to be any λ_g^α -closed set in (K, κ) . As v is quasi λ_g^α -continuous (resp. perfectly λ_g^α -continuous), $v^{-1}(S)$ is closed (resp. clopen) in (N, ν) . Since u is continuous, $(v \circ u)^{-1}(S) = u^{-1}(v^{-1}(S))$ is closed (resp. clopen) in (M, μ) . Hence $(v \circ u)$ is a quasi λ_g^α -continuous (resp. perfectly λ_g^α -continuous) map.

Proposition 5 If u is a quasi λ_g^α -continuous (resp. perfectly λ_g^α -continuous) map and v is a perfectly λ_g^α -continuous (resp. quasi λ_g^α -continuous) map, then $(v \circ u)$ is a quasi λ_g^α -continuous (resp. perfectly λ_g^α -continuous) map.

Proof: Evident from Result (i).

Proposition 6 If u and v are a quasi λ_g^α -continuous (resp. perfectly λ_g^α -continuous) maps, then $(v \circ u)$ is also a quasi λ_g^α -continuous (resp. perfectly λ_g^α -continuous) map.

Proof: Consider S to be any λ_g^α -closed set in (K, κ) . As v is quasi λ_g^α -continuous (resp. perfectly λ_g^α -continuous), $v^{-1}(S)$ is closed (resp. clopen) in $(N, \nu) \Rightarrow v^{-1}(S)$ is λ_g^α -closed in (N, ν) . Since u is quasi λ_g^α -continuous (resp. perfectly λ_g^α -continuous), $(v \circ u)^{-1}(S) = v^{-1}(u^{-1}(S))$ is closed (resp. clopen) in (M, μ) and hence $(v \circ u)$ is also a quasi λ_g^α -continuous (resp. perfectly λ_g^α -continuous) map.

Definition 3 A subset \mathcal{A} of (M, μ) is called λ_g^α -clopen if it is both λ_g^α -open and λ_g^α -closed in (M, μ) .

Example 4 Let $M = \{i, j, k\}$ and $\mu = \{\phi, \{i\}, \{i, j\}, \{i, k\}, M\}$. Then the subset $\{j, k\}$ of (M, μ) is a λ_g^α -clopen set.

Definition 4 A map u is called totally λ_g^α -continuous if the inverse image of every open set in (N, ν) is λ_g^α -clopen in (M, μ) or if $u^{-1}(T)$ is a λ_g^α -clopen set in (M, μ) for every open set T in (N, ν) .

Example 5 Let $M = N = \{i, j, k\}$, $\mu = \{\phi, \{i\}, \{i, j\}, \{i, k\}, M\}$ and $\nu = \{\phi, \{i\}, \{j\}, \{i, j\}, N\}$. Then u is a totally λ_g^α -continuous map when labelled as $u(i) = j$; $u(j) = k$ and $u(k) = i$.

Proposition 7 A map u is totally λ_g^α -continuous if the inverse image of every closed subset of (N, ν) is a λ_g^α -clopen subset of (M, μ) and vice versa.

Proof: Consider S to be any closed set in $(N, \nu) \Rightarrow N \setminus S$ is open in (N, ν) . As u is totally λ_g^α -continuous, $u^{-1}(N \setminus S) = M \setminus (u^{-1}(S))$ is λ_g^α -clopen in $(M, \mu) \Rightarrow u^{-1}(S)$ is λ_g^α -clopen in (M, μ) .

On the other side, consider T to be any open set in $(N, \nu) \Rightarrow N \setminus T$ is closed in (N, ν) . By assumption, $u^{-1}(N \setminus T) = M \setminus u^{-1}(T)$ is λ_g^α -clopen in $(M, \mu) \Rightarrow u^{-1}(T)$ is λ_g^α -clopen in (M, μ) . Hence u is totally λ_g^α -continuous.

Proposition 8 Every totally λ_g^α -continuous map is a λ_g^α -continuous map.

Proof: Follows from the definitions of totally λ_g^α -continuous and λ_g^α -continuous maps.

The subsequent example shows that the converse may not hold good.

Example 6 Let $M = N = \{i, j, k\}$, $\mu = \{\phi, \{i\}, \{i, j\}, M\}$ and $\nu = \{\phi, \{i\}, \{j\}, \{i, j\}, N\}$. Then u is a λ_g^α -continuous map when labelled as $u(i) = i$; $u(j) = k$ and $u(k) = j$, but not a totally λ_g^α -continuous map, since for the open set $\{i, j\}$ in (N, ν) , $u^{-1}(\{i, j\}) = \{i, k\}$ is not λ_g^α -clopen in (M, μ) .

Definition 5 A map u is called strongly λ_g^α -continuous if $u^{-1}(S)$ is a λ_g^α -clopen set in (M, μ) for every subset S in (N, ν) .

Example 7 Let $M = N = \{i, j, k\}$, $\mu = \{\phi, \{i\}, \{i, j\}, \{i, k\}, M\}$ and $\nu = \{\phi, \{i\}, \{j, k\}, N\}$. Then u is a strongly λ_g^α -continuous map when labelled as $u(i) = k$; $u(j) = j$ and $u(k) = i$.





Subhalakshmi and Balamani

Proposition 9 Every strongly λ_g^α -continuous map is a totally λ_g^α -continuous map.

Proof: Follows from the definitions of totally λ_g^α -continuous and strongly λ_g^α -continuous maps. The subsequent example shows that the converse may not hold good.

Example 8 Let $M = N = \{i, j, k\}$, $\mu = \{\phi, \{i\}, \{i, j\}, M\}$ and $\nu = \{\phi, \{i\}, \{j\}, \{i, j\}, N\}$. Then u is a totally λ_g^α -continuous map for the identity map u , but not a strongly λ_g^α -continuous map, since for the set $\{i, k\}$ in (N, ν) , $u^{-1}(\{i, k\}) = \{i, k\}$ is not λ_g^α -clopen in (M, μ) .

Theorem 4 Let u be a totally λ_g^α -continuous map where (N, ν) is a discrete topological space. Then u is a strongly λ_g^α -continuous map.

Proof: Consider T to be any subset of (N, ν) . As (N, ν) is a discrete topological space, T is open in $(N, \nu) \Rightarrow u^{-1}(S)$ is λ_g^α -clopen in (M, μ) , as u is totally λ_g^α -continuous. Hence u is a strongly λ_g^α -continuous map.

Proposition 10 Every perfectly λ_g^α -continuous map is a totally λ_g^α -continuous map.

Proof: Consider T to be any open set in (N, ν) . Then T is also λ_g^α -open set in (N, ν) . Now since u is perfectly λ_g^α -continuous, $u^{-1}(T)$ is clopen in $(M, \mu) \Rightarrow u^{-1}(T)$ is λ_g^α -clopen in (M, μ) . Hence u is a totally λ_g^α -continuous map. The subsequent example shows that the converse may not hold good.

Example 9 Let $M = N = \{i, j, k\}$, $\mu = \{\phi, \{i\}, M\}$ and $\nu = \{\phi, \{i\}, \{j, k\}, N\}$. Then u is a totally λ_g^α -continuous map when labelled as $u(i) = i$; $u(j) = k$ and $u(k) = j$, but not a perfectly λ_g^α -continuous map, since for the λ_g^α -closed set $\{k\}$ in (N, ν) , $u^{-1}(\{k\}) = \{j\}$ is not clopen in (M, μ) .

Proposition 11 Every quasi λ_g^α -continuous (resp. perfectly λ_g^α -continuous) map is a λ_g^α -irresolute.

Proof: Consider S to be any λ_g^α -closed set in (N, ν) . As u is quasi λ_g^α -continuous (resp. perfectly λ_g^α -continuous), $u^{-1}(S)$ is closed (resp. clopen) in $(M, \mu) \Rightarrow u^{-1}(S)$ is λ_g^α -closed in (M, μ) . Hence u is a λ_g^α -irresolute map. The subsequent example shows that the converse may not hold good.

Example 10 Let $M = N = \{i, j, k\}$, $\mu = \{\phi, \{i\}, \{j\}, \{i, j\}, \{i, k\}, M\}$ and $\nu = \{\phi, \{i\}, \{i, j\}, \{i, k\}, N\}$. Then u is a λ_g^α -irresolute map when labelled as $u(i) = j$; $u(j) = i$ and $u(k) = k$, and since for the λ_g^α -closed set $\{i, j\}$ in (N, ν) , $u^{-1}(\{i, j\}) = \{i, j\}$ is not closed in (M, μ) , it is not a quasi λ_g^α -continuous map.

Example 11 Consider M, N, μ, ν and u as in Example 10. Then u is a λ_g^α -irresolute map but not a perfectly λ_g^α -continuous map, since for the λ_g^α -closed set $\{k\}$ in (N, ν) , $u^{-1}(\{k\}) = \{k\}$ is not clopen in (M, μ) .

Definition 6 A map u is called quasi λ_g^α -open if $u(T)$ is open in (N, ν) for each λ_g^α -open set T in (M, μ) .

Example 12 Consider M, N, μ and ν as in Example 9. Then u is a quasi λ_g^α -open map when labelled as $u(i) = i$; $u(j) = k$ and $u(k) = j$.

Theorem 5 A map u is quasi λ_g^α -open if for every λ_g^α -open set S of (M, μ) , $u(\lambda_g^\alpha \text{int}(S)) \subset \text{int}(u(S))$ and vice versa.

Proof: Consider u to be a quasi λ_g^α -open map and S to be λ_g^α -open in (M, μ) . Now $\lambda_g^\alpha \text{int}(S)$ is a λ_g^α -open set and $\lambda_g^\alpha \text{int}(S) \subset S$ implies $u(\lambda_g^\alpha \text{int}(S)) \subset u(S)$. As u is quasi λ_g^α -open, $u(\lambda_g^\alpha \text{int}(S))$ is open $\Rightarrow u(\lambda_g^\alpha \text{int}(S))$ is also λ_g^α -open set, therefore $u(\lambda_g^\alpha \text{int}(S)) = \text{int}(u(\lambda_g^\alpha \text{int}(S))) \subset \text{int}(u(S))$. Thus, $u(\lambda_g^\alpha \text{int}(S)) \subset \text{int}(u(S))$.





Subhalakshmi and Balamani

On the other side, assume that S is a λ_g^α -open set in (M, μ) . Then $u(S) = u(\lambda_g^\alpha \text{int}(S)) \subset \text{int}(u(S))$ but $\text{int}(u(S)) \subset u(S)$. Consequently, $u(S) = \text{int}(u(S))$. Therefore $u(S)$ is open and hence u is quasi λ_g^α -open.

Theorem 6 If u is quasi λ_g^α -open then $\lambda_g^\alpha \text{int}(u^{-1}(P)) \subset u^{-1}(\text{int}(P))$, for every λ_g^α -open set P of (N, ν) .

Proof: Consider P to be any λ_g^α -open set of (N, ν) . As u is quasi λ_g^α -open, $u^{-1}(P)$ is an open set in $(M, \mu) \Rightarrow u^{-1}(P)$ is also a λ_g^α -open set in (M, μ) . By Theorem 5, $u(\lambda_g^\alpha \text{int}(u^{-1}(P))) \subset \text{int}(u(u^{-1}(P))) = \text{int}(P)$. Thus $\lambda_g^\alpha \text{int}(u^{-1}(P)) \subset u^{-1}(\text{int}(P))$.

Definition 7 A subset \mathcal{A} is called λ_g^α -neighbourhood of a point m of (M, μ) if there exists a λ_g^α -open set S such that $m \in S \subset \mathcal{A}$.

Theorem 7 For the map u , the following statements

- (i) u is a quasi λ_g^α -open map
- (ii) For every λ_g^α -open set S of (M, μ) , $u(\lambda_g^\alpha \text{int}(S)) \subset \text{int}(u(S))$
- (iii) For each $m \in M$ and each λ_g^α -neighbourhood S of m in (M, μ) , \exists a neighbourhood T of $u(m)$ in (N, ν) such that $T \subset u(S)$

are equivalent.

Proof: (i) \Rightarrow (ii) Evident from Theorem 5.

(ii) \Rightarrow (iii) Let $m \in M$ and S be an arbitrary λ_g^α -neighbourhood of m in (M, μ) . Then \exists a λ_g^α -open set T in (M, μ) such that $m \in T \subset S$. Then by (ii), $u(T) = u(\lambda_g^\alpha \text{int}(T)) \subset \text{int}(u(T))$ and hence $u(T) \subset \text{int}(u(T))$. Therefore $u(T)$ is open in (N, ν) such that $u(m) \in u(T) \subset u(S)$.

(iii) \Rightarrow (i) Let S be an arbitrary λ_g^α -open set in (M, μ) . Then for each $s \in u(S)$, by (iii) \exists a neighbourhood T_s of s in (N, ν) such that $T_s \subset u(S)$. As T_s is a neighbourhood of s , \exists an open set R_s in (N, ν) such that $s \in R_s \subset T_s$. Thus $u(S) = \cup \{R_s : s \in u(S)\}$, is an open set in (N, ν) . This implies that u is a quasi λ_g^α -open map.

Theorem 8 A map u is quasi λ_g^α -open if for any subset P of (N, ν) and for any λ_g^α -closed set T in (M, μ) containing $u^{-1}(P)$, \exists a closed set Q of (N, ν) containing P such that $u^{-1}(Q) \subset T$ and vice versa.

Proof: Suppose u is a quasi λ_g^α -open map. Let $P \subset N$ and T be a λ_g^α -closed set in (M, μ) containing $u^{-1}(P)$. Let $Q = N \setminus [u(M \setminus T)]$ which follows that $u^{-1}(P) \subset T$ which implies $P \subset u(T) = Q$. Since u is quasi λ_g^α -open, Q is a closed set of (N, ν) and $u^{-1}(Q) \subset T$.

On the other side, let S be a λ_g^α -open set in (M, μ) and let $P = N \setminus (u(S))$. Now $M \setminus S$ is a λ_g^α -closed set in (M, μ) . And $u^{-1}(P) \subseteq M \setminus S$. By hypothesis, \exists a closed set T in (N, ν) such that $P \subset T$ and $u^{-1}(T) \subset M \setminus S$. Hence $u(S) \subset N \setminus T$. Now $P \subset T$ implies $N \setminus T \subset N \setminus P = u(S)$. Thus $u(S) = N \setminus T$ is open and hence u is a quasi λ_g^α -open map.

Theorem 9 A map u is a quasi λ_g^α -open map if $u^{-1}(cl(P)) \subset \lambda_g^\alpha cl(u^{-1}(P))$, for every λ_g^α -closed set P of (N, ν) and vice versa.

Proof: Suppose u is a quasi λ_g^α -open map. For any λ_g^α -closed set P of (N, ν) , $u^{-1}(P) \subset \lambda_g^\alpha cl(u^{-1}(P))$. Therefore, by Theorem 8, \exists a closed set T in (N, ν) such that $P \subset T$ and $u^{-1}(T) \subset \lambda_g^\alpha cl(u^{-1}(P))$. Therefore $u^{-1}(cl(P)) \subset u^{-1}(T) \subset \lambda_g^\alpha cl(u^{-1}(P))$.

On the other side, let $P \subset N$ and T be λ_g^α -closed in (M, μ) containing $u^{-1}(P)$. Let $W = cl(P)$, then $P \subset W$ and W is closed and $u^{-1}(W) \subset \lambda_g^\alpha cl(u^{-1}(P)) \subset T$. Then by Theorem 8, u is a quasi λ_g^α -open map.





Subhalakshmi and Balamani

Proposition 12 Let u and v be two maps and $v \circ u$ is a quasi λ_g^α -open map. If v is a continuous and injective map, then u is a quasi λ_g^α -open map.

Proof: Consider S to be a λ_g^α -open set in (M, μ) . Then $(v \circ u)(S)$ is open in (K, κ) as $v \circ u$ is quasi λ_g^α -open. Since v is an injective continuous map, $v^{-1}((v \circ u)(S)) = u(S)$ is open in (N, ν) . Hence u is a quasi λ_g^α -open map.

Definition 8 A map u is called quasi λ_g^α -closed if the image of every λ_g^α -closed set in (M, μ) is closed in (N, ν) or if $u(P)$ is closed in (N, ν) for every λ_g^α -closed set P in (M, μ) .

Theorem 10 Every quasi λ_g^α -closed map is a closed map.

Proof: Evident from the Result (i).

The subsequent example shows that the converse may not hold good.

Example 13 Let $M = N = \{i, j, k\}$, $\mu = \{\phi, \{i\}, M\}$ and $\nu = \{\phi, \{i\}, \{j\}, \{i, j\}, N\}$. Then u is a closed when labelled as $u(i) = i$; $u(j) = k$ and $u(k) = j$, and since for the λ_g^α -closed set $\{i\}$ in (M, μ) , $u(\{i\}) = \{i\}$ is not closed in (N, ν) , it is not a quasi λ_g^α -closed map.

Theorem 11 A map u is quasi λ_g^α -closed if for every λ_g^α -closed set S of (M, μ) , $cl(u(S)) \subset u(\lambda_g^\alpha cl(S))$ and vice versa.

Proof: Analogous to the proof of Theorem 5.

Theorem 12 A map u is quasi λ_g^α -closed if for any subset P of (N, ν) and for any λ_g^α -open set S in (M, μ) containing $u^{-1}(P)$, \exists an open set Q of (N, ν) containing P such that $u^{-1}(Q) \subseteq S$ and vice versa.

Proof: Analogous to the proof of Theorem 8.

Theorem 13 For any two topological spaces (M, μ) and (N, ν) , u is quasi λ_g^α -closed $u(M)$ is closed in (N, ν) and $u(P) \setminus [u(M \setminus P)]$ is open in $u(M)$ whenever P is λ_g^α -open in (M, μ) and vice versa.

Proof: Suppose u is a quasi λ_g^α -closed map. Since M is λ_g^α -closed. $u(M)$ is closed in (N, ν) and $u(P) \setminus [u(M \setminus P)] = u(P) \cap u(M) \setminus [u(M \setminus P)]$ is open in $u(M)$ when P is λ_g^α -open in (M, μ) .

On the other side, suppose $u(M)$ is closed in (N, ν) , $u(P) \setminus [u(M \setminus P)]$ is open in $u(M)$ when P is λ_g^α -open in (M, μ) and let W be λ_g^α -closed in (M, μ) . Then $u(W) = u(M) \setminus [u(M \setminus W) \setminus u(W)]$ is closed in $u(M)$ and hence closed in (N, ν) .

Corollary 1 Let (M, μ) and (N, ν) be topological spaces. Then a surjective map u is quasi λ_g^α -closed if $u(P) \setminus [u(M \setminus P)]$ is open in (N, ν) whenever P is λ_g^α -open in (M, μ) and vice versa.

Proof: Obvious

Theorem 14 For the topological spaces (M, μ) and (N, ν) , u be a λ_g^α -continuous and quasi λ_g^α -closed surjective map. Then the topology on (N, ν) is $\{u(P) \setminus [u(M \setminus P)] : P \text{ is } \lambda_g^\alpha\text{-open in } (M, \mu)\}$.





Subhalakshmi and Balamani

Proof: Consider W to be open in (N, ν) . Then $u^{-1}(W)$ is λ_g^α -open in (M, μ) and $u[u^{-1}(W)] \setminus [u(M \setminus u^{-1}(W))] = W$. Hence all open sets in (N, ν) are of the form $u(P) \setminus [u(M \setminus P)]$, P is λ_g^α -open in (M, μ) . On the other hand, all sets of the form $u(P) \setminus [u(M \setminus P)]$, P is λ_g^α -open in (M, μ) are open in (N, ν) from Corollary 1.

Proposition 13 Let u and v be any two maps such that $(v \circ u): (M, \mu) \rightarrow (K, \kappa)$ is a quasi λ_g^α -closed map. If u is a λ_g^α -irresolute surjective map, then v is a closed map.

Proof: Consider P to be a closed set in (N, ν) . Using Result (i) and u is a λ_g^α -irresolute map, $u^{-1}(P)$ is a λ_g^α -closed set in (M, μ) . Since $(v \circ u)$ is a quasi λ_g^α -closed map and u is surjective, $(v \circ u)(u^{-1}(P)) = v(P)$ is closed in (K, κ) . Hence v is a closed map.

Proposition 14 If u and v are quasi λ_g^α -open (resp. quasi λ_g^α -closed) maps then $(v \circ u): (M, \mu) \rightarrow (K, \kappa)$ is also a quasi λ_g^α -open (resp. quasi λ_g^α -closed) map.

Proof: Let S be any λ_g^α -open (resp. λ_g^α -closed) set in (M, μ) . As u is quasi λ_g^α -open (resp. quasi λ_g^α -closed), $u(S)$ is open (resp. closed) in (N, ν) . Since every open (resp. closed) set is λ_g^α -open (resp. λ_g^α -closed), $u(S)$ is λ_g^α -open (resp. λ_g^α -closed) set in (N, ν) . Since v is quasi λ_g^α -open (resp. quasi λ_g^α -closed), $(v \circ u)(S) = v(u(S))$ is open (resp. closed) in (K, κ) . Thus $(v \circ u)$ is a quasi λ_g^α -open (resp. a quasi λ_g^α -closed) map.

Definition 9 A map u is called strongly λ_g^α -closed if the image of every λ_g^α -closed set in (M, μ) is λ_g^α -closed in (N, ν) or if $u(V)$ is λ_g^α -closed in (N, ν) for every λ_g^α -closed set V in (M, μ) .

Proposition 15 Every quasi λ_g^α -closed map is strongly λ_g^α -closed.

Proof: Evident from the Result (i).

The subsequent example shows that the converse may not hold good.

Example 14 Consider $M = N = \{i, j, k\}$, $\mu = \{\phi, \{i\}, \{i, j\}, M\}$ and $\nu = \{\phi, \{i\}, \{j\}, \{i, j\}, N\}$. Then the identity map u is a strongly λ_g^α -closed map, and since for the closed set $\{i, k\}$ in (M, μ) , $u(\{i, k\}) = \{i, k\}$ is not λ_g^α -closed in (N, ν) , it is not a quasi λ_g^α -closed map.

Proposition 16 Let u and v be any two maps.

- (i) If u is quasi λ_g^α -closed map and v is a λ_g^α -closed map then $(v \circ u)$ is a strongly λ_g^α -closed map.
- (ii) If u is strongly λ_g^α -closed map and v is a quasi λ_g^α -closed map then $(v \circ u)$ is a quasi λ_g^α -closed map.
- (iii) If u and v are quasi λ_g^α -closed maps then $(v \circ u)$ is a strongly λ_g^α -closed map.

Proof: (i) Consider S to be a λ_g^α -closed set in (M, μ) . Since u is quasi λ_g^α -closed, $u(S)$ is closed in (N, ν) . Then $v(u(S)) = (v \circ u)(S)$ is λ_g^α -closed in (K, κ) as v is λ_g^α -closed. Hence $(v \circ u)$ is a strongly λ_g^α -closed map.

(ii) Let S be λ_g^α -closed set in (M, μ) . Since u is strongly λ_g^α -closed, $u(S)$ is λ_g^α -closed in (N, ν) . Then $v(u(S)) = (v \circ u)(S)$ is closed in (K, κ) , as v is quasi λ_g^α -closed. Hence $(v \circ u)$ is a quasi λ_g^α -closed map.

(iii) Evident from the Result (i).

Proposition 17 Let u and v be any two maps such that $(v \circ u)$ is a quasi λ_g^α -closed map. If v is λ_g^α -continuous injective then u is a strongly λ_g^α -closed map.





Subhalakshmi and Balamani

Proof: Consider S to be a λ_g^α -closed set in (M, μ) . Since $(v \circ u)$ is quasi λ_g^α -closed, $(v \circ u)(S)$ is closed in (K, κ) . Since v is λ_g^α -continuous injective, $v^{-1}((v \circ u)(S)) = u(S)$ is λ_g^α -closed in (N, ν) . Hence u is strongly λ_g^α -closed map.

Remark 1 Proposition 17 is true if v is continuous (resp. λ -continuous). Since every closed (resp. λ -closed) set is λ_g^α -closed.

REFERENCES

1. Arya, S.P. and Gupta, R. (1974), On Strongly continuous mappings, Kyungpook Math. J., 14, 131-143.
2. Caldas, M., Jafari, S. and Navalagi, T. (2007), More on λ -closed sets in topological spaces, Revista Colombiana de Mathematics, 41 (2), 355-369.
3. Caldas, M., Jafari, S. and Noiri, T. (2008), On Λ -generalised closed sets in topological spaces, Acta Math. Hungar, 118 (4), 337-343.
4. Francisco G Arenas, Julian Dontchev and Maxmillian Ganster, (1997) On λ -sets and the dual of generalized continuity, Question answers GEN.Topology 15, 3-13.
5. Jain, R.C. (1980), Role of regular open sets in general topology, Ph.D. thesis, Meerut University, Meerut, India.
6. Levine, N. (1960), Strong continuity in topological spaces, Amer. Math. Monthly, 67, 269 – 275.
7. Maki, H. (1986) Generalized Λ -sets and the associated closure operator, Special Issue in Commemoration of Prof. Kazuasada Ikeda's Retirement, 139-146.
8. Mashhour, A.S., Hasanein, I.A. and El-Deeb, S.N. (1983), On α -Continuous and α -open mappings, Acta. Math. Hungarica, 41, 213-218.
9. Njastad, O. (1965), On some classes of nearly open sets, Pacific J. Math. 15, 961-970.
10. Noiri, T. (1984), Super continuity and some strong forms of continuity, Indian J. Pure and Applied Math., 15(3), 241 - 250.
11. Subhalakshmi, S. and Balamani, N. (2020), On λ_g^α -Closed and λ_g^α -Open Sets in Topological Spaces, Malaya Journal of Matematik, 8 (4), 2248-2252.
12. Subhalakshmi, S. and Balamani, N. (2021), On λ_g^α -Continuous Maps in Topological Spaces, Malaya Journal of Matematik, 8 (1), 238-245.





Prediction and Buying Behaviour of Customers using Machine Learning Technique

Subhash Chand^{1*}, A.K. Shukla² and Naresh Chandra³

¹System Manager, GB Pant University of Ag. & Tech., Pantnagar, Uttarakhand, India.

²Associate Professor, IFTM, University, Moradabad, Uttar Pradesh, India

³Sr. Programmer, State Planning Commission, Uttarakhand, India.

Received: 05 Nov 2021

Revised: 11 Dec 2021

Accepted: 12 Jan 2022

*Address for Correspondence

Subhash Chand

System Manager,

GB Pant University of Ag. & Tech.,

Pantnagar, Uttarakhand, India.

Email: subiphd@gmail.com



This is an Open Access Journal / article distributed under the terms of the **Creative Commons Attribution License** (CC BY-NC-ND 3.0) which permits unrestricted use, distribution, and reproduction in any medium, provided the original work is properly cited. All rights reserved.

ABSTRACT

The communication facility is easily available in the reach of common men's and due to this, purchase behaviour of customers/consumer is changing very rapidly. Now customers prefer to purchase goods/services online rather than offline. The scope of customers online purchasing behaviour is very wide and dynamic in the nature. Purchasing/Customer behaviour is heavily depending on the knowledge of customer related to e-commerce web site, on-line transactions, etc. The researchers proved that customer behaviour, need, beliefs, choice, satisfaction, etc. decides the feature of any business or heavily affect the return on investment (ROI). Anything customer does, think and feel is known as customer behaviour. According to the customer behaviour customers may be divided into many categories like viewers, researchers, focused, one-time, loyal, etc. In the present study six months' online customer buying data studied and five null hypothesis is made and tested.

Keywords: Hypothesis, Customer's behaviour, ROI, p-value, event type, shapiro-wilk.

INTRODUCTION

Online buying trends are growing very rapidly and growth of any business is totally depends on the customers associated with the business. To improve the return on investment it is most important to consider and influence the customer at every step of buying decision making process. Customer do not buy anything suddenly; buying is committed after completion of a complex process which is running in the mind of a customer. Product's price plays an important role in buying process. With respect to the customer, price means total cost of the product including shipping cost, installation costs and commissioning of the product cost. Any hidden cost will have negative impact on purchasing process and it may lose the customer. To retain the customer, it is must to build trust with customer.





Subhash Chand et al.,

Customer buying behaviour is a customer decision-making process to purchase any product / services OR Customer buying behaviour is an act of person involved in buying or using any product / services. Any activity committed by a customer to purchase a product or service is known as customer buying behaviour. The customer buying behaviour may be divided into following categories:

Behaviour with Routine Response: Customer buys low cost items and need very limited search about the products.

Behaviour with Limited Decision Making: Customer buy the products occasionally not regularly.

Behaviour with Extensive Decision-Making: In this category high investment on unfamiliar and infrequently product is required. Customers requires more time to collect and analyze data to take a decision.

Behaviour with Impulse Buying: This type of buying requires no planning to buy the product/service.

The customer buying decision is a very complex procedure and goes through many stages. For better understanding customer buying decision process is divided into five parts/stages.

Stage 1 → Identify the needs (awareness)

When customer realize the need of any product / services then he/she must have clear idea about it or must be aware about their needs.

Stage 2 → Related information search (research)

After stage 1 customer search the many e-commerce websites and try to get answers of all the question related to needed product/ services.

Stage 3 → Evolution of alternatives (Consideration)

After stage 2 customer rethink about their needs and search again for any good alternatives to fulfill their need.

Stage 4 → Purchase decision (Conversion)

This is the action time when customer is ready to buy the product/service and spent the money from their pocket.

Stage 5 → Post purchase evaluation (Repurchase and feedback)

After product/service purchased the customer is ready to give feedback about the product/service purchased by the customer.

To better understand the e-commerce customers, it may be divided/classified into six categories as given below:

Customers only surfing e-commerce site: This type of customers have more time to spend in surfing and feel fun without any objective keeping in their mind.

Customers do research with product data: This type of customers are interested in a particular category of products/services and search the website to collect the product's information.

Customers having focus with products: This type of customers have prior knowledge about the products in which customers are interested.

Customers interested in Sale/Discounts: This type of customers have prior knowledge about the product and searching the site to commit the best deals in the form of availing the big discount on the products.

Impulsive Customer: This type of customers are not regular customers but have prior knowledge about their needs.

Loyal Customers: This type of customers are assets to the e-commerce site. These customers give positive feedback to their friends, relatives, family members and also on social media platform. The real challenges for e-commerce site is to keep intact these customers to improve the return on investment (ROI).

Some factors mentioned below can influence the customer buying decisions.

- | | |
|------------------------------------|---|
| i) Arrivals of new products | ii) Cash on Delivery(CoD) facility |
| iii) Product Return Policy | iv) Availability of online review |
| v) Free & secure delivery facility | vi) Cancellation of Order before delivery |
| vii) Site speed and usability | viii) Secure payment with no extra charge |
| ix) Shipping Time and Cost | x) Product presentation on site, etc. |





Subhash Chand et al.,

Objective of the Study

The main objective of this study is to understand the customer behavior based on secondary data. Customers behave differently on e-commerce site therefore the study of customer behaviour is a complex task and needs more time and passions. The questions like, Is all the customers have same behaviour?. Is all the customers purchase the product?, Is all the customers regularly visit the site, Is product brand name have effect on customer behaviour, etc. comes into the mind of researchers which is answered based on experiment results.

To complete this study five Null hypothesis is made and test on this secondary data. If Null hypothesis is rejected, then alternate hypothesis is given. The null hypothesis is given as follows:

H₀₁ : All E-Commerce website's customers regularly visit the website.

H₀₂ : During the visit of e-commerce website customers will purchase the product.

H₀₃ : Customers spent more time on e-commerce website will purchase the product.

H₀₄ : Product's brand name have no effect on customer's behaviour.

H₀₅ : All the customers have same behaviour on e-commerce website.

RESEARCH METHODS

Research methods includes many steps like data collection, size of data, meaning of data attributes, data pre-processing before analysis, methods used to analyse the data, finding of the results, explanation of the results, etc.

Data Collection & Size of data

The first part of this study includes the data collection. The data is searched and collected from internet, therefore this study is conducted on the secondary data. The data is based on the transactions of an e-commerce website for five months. The original size of data is more than 20 terabyte (TB), but for this study only top 7,00,000 (seven lakhs) records selected.

Description of Data Attributes

This data is labelled data therefore supervised machine learning methods will be used on this data. Each row in the data file represents a transaction/record. Seven months' online transaction data (one lakh records for each months) is selected for analysis. Each event is like many-to-many relation between products and users. Each record in the dataset contains 9 attributes. The meaning of the attributes is given in the table 1.

Data Pre-Processing

Data pre-processing is a very important steps of any data analysis methods. It requires more time to complete it. During data pre-processing the activities like null values treatment, identify and remove outliers, decomposition of data, removal of unwanted data, merger of data, assign the meaningful names to data, conversion of data according to algorithm used, rescaling the data, label encoding of data, hot encoding of data, normalization of data, etc. are done to get the better and accurate results.

Hypothesis

A hypothesis is researchers statement based on some expectations or it is relationship among study variables. Research process begins and ends with hypothesis. A hypothesis is a guess / predictions based on researcher's observations. Hypothesis is a statement which must be specific, must have clear meaning, must be testable and predictable statement. Hypothesis requires a research question then data collection, study and analysis of data, study of result in favour of hypothesis to accept or reject the hypothesis.

Types of Hypothesis

A. Experimental Hypothesis

1. Statistical Hypothesis





Subhash Chand et al.,

- i) Null Hypothesis
- ii) Experimental Hypothesis
 - a. Negative Hypothesis
 - b. Positive Hypothesis
2. Existential Hypothesis
3. Universal Hypothesis
4. Conceptual Hypothesis

B. Non-Experimental Hypothesis

1. Simple Level Hypothesis
2. Complex Level Hypothesis
3. Refined Level Hypothesis

Null Hypothesis Testing

The Null hypothesis is a commonly accepted fact/statement. Researchers works to disprove/nullify or reject the null hypothesis and after rejection of null hypothesis an alternative hypothesis is given by researchers. These two hypothesis is opposite to each other or they are mutually exclusive statements about a population. The null hypothesis is denoted by H_0 and alternative hypothesis is denoted by H_a . The word null means not zero/ null/ blank, it means that researcher will work to nullify the commonly accepted facts / statements. To test this hypothesis Shapiro Wilk test is used to test the normal distribution of data. The input parameter for this method is an array of sample data and output of this method is two variables statistics (test statistics) and p-value. The null hypothesis is accepted or rejected based on p-value. The function shapiro is used to implement this function in python. Second method/function used to test the normal distribution is *normal test*. This function test whether a sample data differs from a normal distribution or not. This function is based on D'Agostino and Pearson's test that combines skew and kurtosis to produce output statistics. The input parameter for this function is an array of sample data and output is two variable statistics and p-value.

Statistic = $(s)^2 + (k)^2$, where s is the z-score returned by skew test and k is the z-score returned by kurtosis test.
 p-value = A 2-sided chi squared probability for the hypothesis test.

H₀₁ - All E-Commerce website's customers regularly visit the website. Table 2 shows the statistics and p-value by using shapiro-wilk and normaltest methods. The p-value by using both the methods are 0.00 that indicates data is not normally distributed which is a proof of rejection of **H₀₁** null hypothesis. The fig 1. represents new customers by green colour and old customers by red colour. As a result, this figure shows that only 2.23% old customers revisit the e-commerce site and 97.77% are the new customers to e-commerce site. Fig 2 is the date wise trend of customers to visit the e-commerce site. This is a zigzag graph which indicates that not all the customers regularly visit the e-commerce site. Based on p-value of table 2 and fig 1 & 2, **H₀₁** – "All E-Commerce website's customers regularly visit the website" is *rejected*. Alternative Hypothesis **H_{a1}** : *Not all E-Commerce website customer's regularly visit the website.*

H₀₂ : During the visit of e-commerce website customer's will purchase the product. Table 3 shows the statistics and p-value by using shapiro-wilk and normaltest methods. The p-value by using both the methods are 0.00 that indicates data is not normally distributed which is a proof of rejection of **H₀₂** null hypothesis. The fig 3 represents the percentage of customer activities (view => cart => purchase) one-commerce site. The 95.51% customers view the products, 3.33% customers cart the products and 1.16% customers purchase the products. Based on p-value of table 3 and fig 3 **H₀₂**: "During the visit of e-commerce website customer's will purchase the product" is *rejected*. Alternative Hypothesis **H_{a2}**: *Not all the customers purchase the product during the visit of e-commerce website.*

H₀₃: Customers spent more time on e-commerce website will purchase the product. Table 4 shows the statistics and p-value by using shapiro-wilk and normaltest methods. The p-value by using both the methods are 0.00





Subhash Chand et al.,

that indicates data is not normally distributed which is a proof of rejection of H_03 null hypothesis. Fig 4 is a graph between customer activities/event type (view => cart => purchase) and total unit of times spent on customer's activities. The fig shows that more time is spent on view and cart event while less time is spent on purchase event. Based on p-value of table 4 and fig 4 H_03 : "Customers spent more time on e-commerce website will purchase the product" is rejected. Alternative Hypothesis H_{a3} : Not all the customers spend more time on e-commerce website will purchase the product.

H_04 : Product's brand name has no effect on customer's behaviour. Table 5 shows the statistics and p-value by using shapiro-wilk and normaltest methods. The p-value by using both the methods are 0.00 that indicates data is not normally distributed which is a proof of rejection of H_04 null hypothesis. Fig 5 shows many popular brands. Each rectangle is corresponding to a brand indicating the brand name in the middle of each rectangle. The area of each rectangle is popularity of corresponding brand i.e. more area means more popular and less area means less popular brand. Similarly, fig 6 is a graph of product category popularity. Fig 7 is a graph between product name and its sell. According to the graph some products like apple, Samsung, etc. are more popular amongst the customers while some are less popular. This indicates that product brand name have the effect on customer behaviour. Based on p-value of table 5 and fig 5, 6, 7. H_04 : "Product's brand name has no effect on customer's behaviour" is rejected. Alternative Hypothesis H_{a4} : Product's brand name has more effect on customer behaviour.

H_05 : All the customers have same behaviour on e-commerce website. Table 6 having 5 columns namely customer id, view the product, cart the product, purchase the product and total activities performed by the customers. Value 0 indicates no activity and any number other than 0 indicates the number of times activity performed by the corresponding customers. The normal behaviour of a customer on e-commerce site is first customer view the product, second viewed product will be cart and third carted product will be purchased by the customer (view => cart => purchase). As a result, it is found that 137493 customers view the product & 715 customers not view the product and 12096 customers cart the product & 126112 customers not cart the product and 6361 customers purchase the product & 131847 customers not purchase the product. Tables 6, 7, 8 and 9 shows that all the customers have different behaviour on e-commerce site i.e. some customers directly purchase the product without view and cart the product. Some customers only view the products without purchase it, some customers cart the product then purchase it and some customer first view the product, second cart the product and finally purchase the product. Therefore, H_05 : "All the customers have same behaviour on e-commerce website" is rejected. Alternative Hypothesis H_{a5} : Customer's do not have same behaviour on e-commerce website.

RESULT

All the given five hypothesis H_01 , H_02 , H_03 , H_04 , H_05 tested on the dataset containing 7,00,000 (Seven Lacs) records related to seven months. Many hypothesis testing methods graphically and statistically are used on this dataset to test the hypothesis. Graphically methods are not so accurate as statistical methods but we can see the normality visually. To test the hypothesis some graphical methods like heat map, line graph, histograms, pie chart and some statistical methods like shapiro wilk test, normal test are used. Using these graphical and statistical methods all the five hypothesis is rejected and corresponding alternative hypothesis H_{a1} , H_{a2} , H_{a3} , H_{a4} , H_{a5} is given.

Null Hypothesis - H_01 : All E-Commerce website's customers regularly visit the website.

Alternative Hypothesis - H_{a1} : Not all E-Commerce website customer's regularly visit the website.

Null Hypothesis- H_02 : During the visit of e-commerce website customers will purchase the product.

Alternative Hypothesis - H_{a2} : Not all the customers purchase the product during the visit of e-commerce website.

Null Hypothesis- H_03 : Customers spent more time on e-commerce website will purchase the product.

Alternative Hypothesis - H_{a3} : Not all the customers spend more time on e-commerce website will purchase the product.

Null Hypothesis - H_04 : Product's brand name has no effect on customer's behaviour.





Subhash Chand et al.,

Alternative Hypothesis - H₄: Product's brand name has more effect on customer behaviour.

Null Hypothesis - H₀5: All the customers have same behaviour on e-commerce website.

Alternative Hypothesis - H₅: Customer's do not have same behaviour on e-commerce website.

The study may be conducted on more data with analysis based on day, date and time when customers purchase more products and study of customers reviews to improve the return on investment (ROI), categories/segmentation of customers, study and analysis of each segmentation may be carried out.

REFERENCES

1. Xiaotong Dou (2020), Online Purchase Behavior Prediction and Analysis Using Ensemble Learning, IEEE 5th International Conference on Cloud Computing and Big Data Analytics.
2. Javier fabra ,et al (2020), Log-Based Session Profiling and Online Behavioral Prediction in E_Commerce Websites, *Digital Object Identifier 10.1109/ACCESS.2020.3024649*.
3. Balogh Z, et al (2020), Consumer Perceived Risk by Online Purchasing: The Experiences in Hungary.
4. Dehua Kong1, et al (2019), Research on Product Recommendation Based on Web Space-Time Customer Behavior Trajectory, International Conference on Machine Learning, Big Data and Business Intelligence (MLBDBI).
5. Chen ling, et al (2019) , Customer Purchase Intent Prediction Under Online Multi-Channel Promotion: A Feature-Combined Deep Learning Framework, *Digital Object Identifier 10.1109/ACCESS.2019.2935121*.
6. Yunghui Chu, et al (2019), Predicting Online User Purchase Behavior Based on Browsing History, IEEE 35th International Conference on Data Engineering Workshops (ICDEW).
7. Kok wai tham, et al (2019), Perceived Risk Factors Affecting Consumers' Online Shopping Behaviour, Journal of Asian Finance, Economics and Business Vol 6 No 4 pp. 249-260.
8. Danqi Xu, et al (2018), Repurchase Prediction Based on Ensemble Learning, IEEE Smart World, Ubiquitous Intelligence & Computing, Advanced & Trusted Computing, Scalable Computing & Communications, Cloud & Big Data Computing, Internet of People and Smart City Innovations.
9. Asma Rosyidah, et al (2018), Mining Web Log Data for Personalized Recommendation System, 6th International Conference on Information and Communication Technology (ICICT).
10. Oly Mishra, et al (2018), Sources of Need Recognition in Online Consumers Decision Making Process, IJEMR – April 2018 - Vol 8 Issue 04 - Online - ISSN 2249–2585.
11. Sergio hernández, et al (2017), Analysis of Users' Behavior in Structured e-Commerce Websites, *Digital Object Identifier 10.1109/ACCESS.2017.2707600*.
12. Maheswari K, et al (2017), Predicting Customer Behavior in Online Shopping Using SVM, IEEE International Conference on Intelligent Techniques in Control, Optimization and Signal Processing 978-1-5090-4778-9/17.
13. Hoda Ghavamipoor, et al (2017), A QoS-sensitive model for e-commerce customer behaviour, JRIM.
14. Yi Zuo, et al (2016), Prediction of Consumer Purchasing in a Grocery Store Using Machine Learning Techniques, 3rd Asia-Pacific World Congress on Computer Science and Engineering.
15. Hidekazu Yanagimoto (2016), Customer Behavior Analysis with Enthusiasm Analysis, 5th IIAI International Congress on Advanced Applied Informatics.
16. Li Dancheng, et al (2015), A Method of Purchase Prediction Based on User Behaviour Log, IEEE 15th International Conference on Data Mining Workshops.
17. Gökhan S, et al (2015), Analysis and Prediction of E-Customers' Behavior by Mining Clickstream Data, IEEE International Conference on Big Data (Big Data).
18. Popli Ankita, et al (2015), Factors of Perceived Risk Affecting Online Purchase Decisions of Consumers, Pacific Business Review International Volume 8, Issue 2.
19. Yvind, et al (2015), Probability-based Approach for Predicting E-commerce Consumer Behaviour Using Sparse Session Data, Conference Paper.





Subhash Chand et al.,

20. Liu Nengbao, et al (2014), Handling Class Imbalance in Customer Behavior Prediction, IEEE, 978-1-4799-5158-1/14.
21. Gupta Mona, et al (2014), Characterizing Comparison Shopping Behavior: A Case Study, IEEE 115 ICDE Workshops, 978-1-4799-3481-2/14.
22. Sinha Jayendra, et al (2012), Factors affecting Indian consumers' online buying behaviour, Innovative Marketing, 8(2).
23. Guseva Natalija (2011), Looking for the e-commerce quality criteria: different perspectives, ekonomika Vol. 90(1).

Table 1: Description of Data Attributes

S.No.	Attribute Name	Attribute Description
1	event_time	Time when event happened (in UTC).
2	event_type	It is categorical data type which contain only one value out of three i.e. view, cart and purchase. View – customer viewed a product, cart – customer added a product to shopping cart, purchase – customer purchase the product.
3	product_id	Unique ID of a Product. It is of type number.
4	category_id	Unique ID of Product's category. It is of type number.
5	category_code	It is of string type and the category name in which product falls is mentioned in this column.
6	brand	It is also of type string and brand name of the product is mentioned in this column.
7	price	The price of the product is mentioned in this column. It is float type.
8	user_id	User ID given to customer is mentioned in this column. It is of number type.
9	user_session	A session is created for each user / customer who open the e-commerce website. when user logout the session will be stop and next time new session will be created for each user. All the activity done by customer are stored in this session. During a session multiple purchase can be done. It is of string type.

Table 2: H₀₁ - All E-Commerce website's customers regularly visit the website

Hypothesis	Shapiro-Wilk Method	Normal test Method
H₀₁	Statistics = 0.706, p-value = 0.00000	Statistics = 395335.958, p-value = 0.00000

Table 3: H₀₂ - During the visit of e-commerce website customer's will purchase the product

Hypothesis	Shapiro-Wilk Method	Normal test Method
H₀₂	Statistics = 0.20, p-value = 0.00000	Statistics = 644051.0168354344, p-value = 0.00000

Table 4: H₀₃ - Customers spent more time on e-commerce website will purchase the product

Hypothesis	Shapiro-Wilk Method	Normal test Method
H₀₃	Statistics = 0.56, p-value = 0.00000	Statistics = 710149.0119265305, p-value = 0.00000

Table 5: H₀₄ - Product's brand name has no effect on customer's behaviour

Hypothesis	Shapiro-Wilk Method	Normal test Method
H₀₄	Statistics = 0.04, p-value = 0.00000	Statistics = 12.8806038433, p-value = 0.00160





Subhash Chand et al.,

Table 6: H05: All the customers have same behaviour on e-commerce website.

user_id	cart	purchase	view	Total
275317753	1	0	4	5
291107595	3	0	2	5
436910622	1	0	3	4
...
635206290	1	0	2	3
635206469	1	1	2	4
635206474	2	0	4	6
Total	23318	8106	668576	700000

Table 7: event and not event

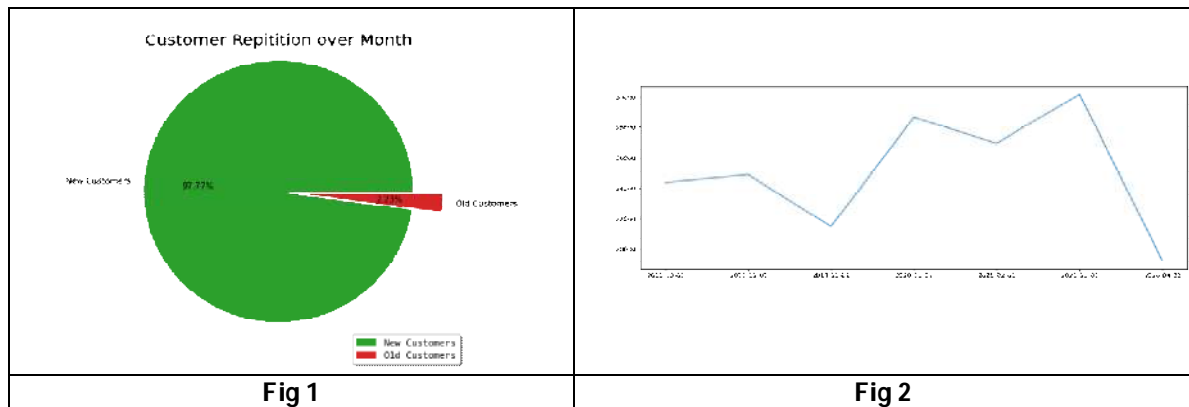
Event Type	Number of Customers
View the Product	137493
Not View the Product	715
Cart the Product	12096
Not Cart the Product	126112
Purchase the Product	6361
Not Purchase the Product	131847

Table 8: Purchase the product without view and cart

Event Type	Number of Customers
View the Product	0
Cart the Product	0
Purchase the Product	623

Table 9: Purchase the product without view

Event Type	Number of Customers
View the Product	0
Cart the Product	25
Purchase the Product	9





Subhash Chand et al.,

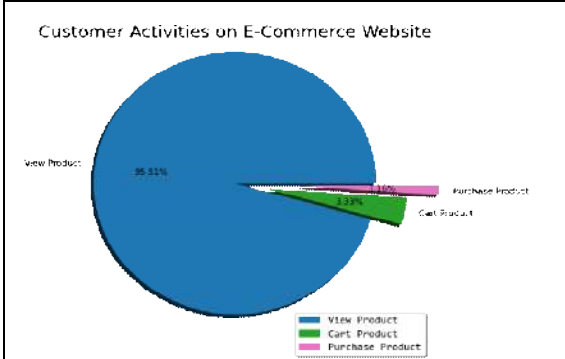


Fig 3

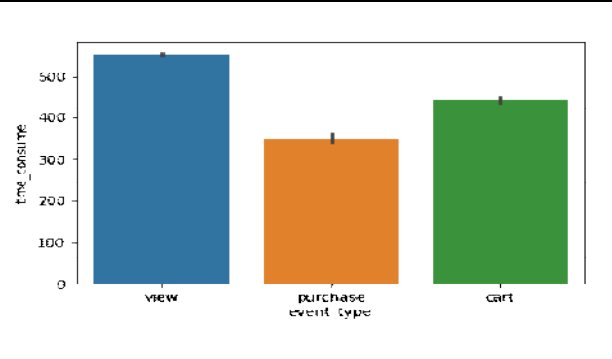


Fig 4

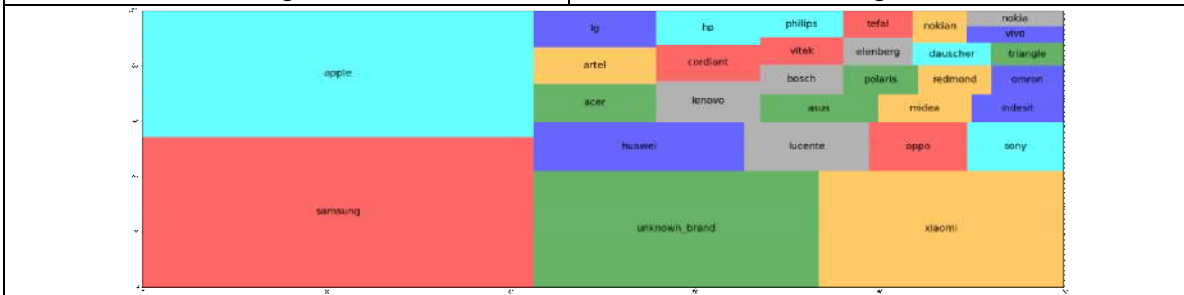


Fig 5. Popularity of Brand

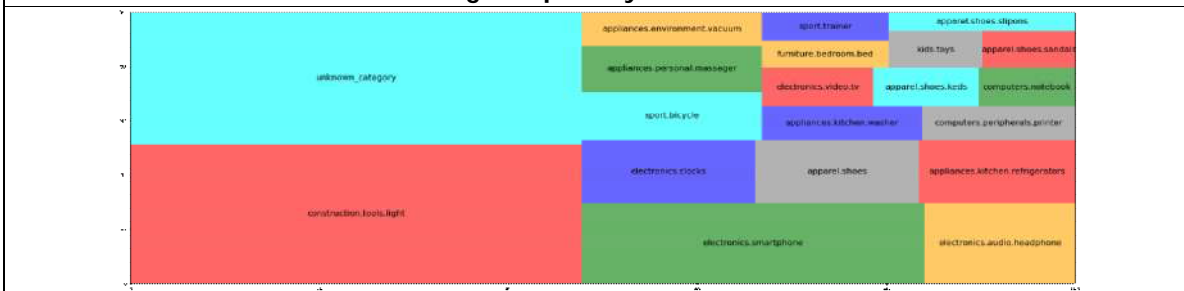


Fig 6. Popularity of Product Category

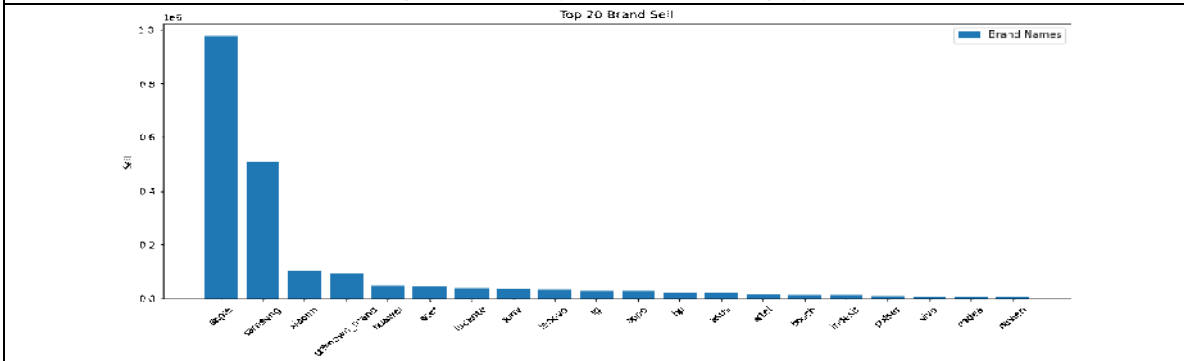


Fig 7. Top 20 Selling Brands





Selection of Bee Colonies with Bee Strength (Biological Trait) from Different Bee Keeping Areas of Tamilnadu

R. Premkumar^{1*}, T. Ramesh Kumar² and J. Nelson Samuel Jebastin³

¹Research Scholar, Department of Zoology, Annamalai University, Annamalai Nagar, Cuddalore, Tamil Nadu, India.

²Professor, Department of Zoology, Annamalai University, Annamalai Nagar, Cuddalore, Tamil Nadu, India.

³Assistant Professor, Department of Zoology, Annamalai University, Annamalai Nagar, Cuddalore, Tamil Nadu, India.

Received: 15 Dec 2021

Revised: 12 Jan 2022

Accepted: 24 Jan 2022

*Address for Correspondence

R. Premkumar

Research Scholar,

Department of Zoology,

Annamalai University, Annamalai Nagar,

Cuddalore, Tamil Nadu, India.

Email: prem20795@gmail.com



This is an Open Access Journal / article distributed under the terms of the **Creative Commons Attribution License** (CC BY-NC-ND 3.0) which permits unrestricted use, distribution, and reproduction in any medium, provided the original work is properly cited. All rights reserved.

ABSTRACT

Beekeeping is an important component of present strategies for sustainable agriculture and integrated rural development programmes. It provides nutritional, economic and ecological security to rural communities, especially in the developing countries like India. Being a non land based activity; it does not compete with other resource demanding components of farming systems. Moreover, it is an additional income generating activity. This study aims to identify *Apis cerana indica* colonies with vital and economically important trait with bee strength, brood rearing capacity, pollen storage, honey storage, honey yield potential, disease incidence and absconding behavior, which can thrive well from different beekeeping pockets of the State. The colonies with better characters will be selected for producing better performing colonies through selective breeding which can be used for commercial beekeeping.

Keywords: Apiculture, *Apis cerana indica* colonies, Beekeeping resource, Absconding behavior, Nutritional Honey Yield, Economically viable.

INTRODUCTION

The Indian honey bee, *Apis cerana indica* Fab. is used in South India for commercial beekeeping and honey production. Even though the industry had developed tremendously, better performing colonies strains with desirable traits are required for increased productivity and sustainable apiculture in South India. Concurrently, most

39094





Premkumar et al.,

of the colonies of *Apis cerana indica* are not economically viable, Selective breeding is the best solution for stock improvement. Better genetic traits can be transferred and the productivity can be increased through selective breeding, so as to evolve best performing Indian bee colonies, Hence the present study was undertaken with a view to identify Indian bee *Apis cerana indica* colonies with viable characters and develop a better performing strain with desirable traits for improving the stock through selective breeding for sustainable apiculture in Tamil nadu. The study identified Indian bee *Apis cerana indica* colonies possessing better economically important character like bee strength from the existing bee colonies in Tamil nadu. The strength of honey bee colony depends on the availability of bee storage and season. Colonies were selected on their performance on the basis of bee strength, brood area, honey storage and pollen area for the studies on the selective breeding (RAU, 2004). Pokhrel *et al.*, (2006) observed that, in Nepal, stronger colony strength was recorded in *Apis cerana indica* colonies during May and the bee population and colony strength were reduced in April. Shruthi *et al.*, (2009) revealed that in Karnataka, bee population in both black and yellow strain colonies of *Apis cerana indica* were more in winter and among the strains, black strain colony recorded more bee population throughout the season compared to yellow strain colony. Mohapatra and Satapathy (2012) reported that in *Apis cerana indica* colonies in Orissa, maximum bee population was during May.

MATERIAL AND METHODS

Selection and management of experimental *Apis cerana indica* colonies

Six locations each from three natural topographic division viz., Highland, Midland and Lowland of Tamilnadu were selected for the present investigation. The mountainous land including Western Ghats, with jutting rocks and loamy soils constituted the highland. The hilly tracts on the western side of the Western Ghats constituted the midland. The lowland plains have an undulating terrain intersected by numerous rivers, small hills and valleys. The 18 locations were identified to ensure complete coverage of the State for the study. Colonies of *Apis cerana indica* were selected from the apiaries of bee breeder progressive beekeepers from the different locations. Selection of colonies was done by checking colony registers maintained by the beekeepers with data on the performance and honey yield of the colonies in the previous years and also by visual observation of the colonies. Colonies with a newly mated queen and of approximately same bee strength (3 frames) were selected. Three such colonies were collected from each location, marked and maintained in the apiary. The colonies were kept strong and healthy, under same condition, by adopting the management practices recommended by the Tamil Nadu Agricultural University POP (Package of Practices): (I) using only standard hives and other equipment (II) cleaning of hives at regular intervals (III) timely renewal of old and worm out combs (IV) colonies supplying with approximately 300 ml of 1:1 sugar solution at weekly interval throughout the dearth season and brood rearing seasons. (V) Keeping the colonies in coconut garden to ensure pollen supply (VI) prevention of swarming.

Assessment of comparative performance of experimental colonies

Apis cerana indica colonies assessed for one year from August, 2020 to July, 2021. Observations were recorded during the growth period (August 2020-January 2021), honey flow period (February-May, 2021) and dearth period (June-July, 2021) at 15day intervals. The colonies were divided during November. Bee strength was assessed by counting the comb well covered with bees on both sides as one. The number of such frames combs per colony was recorded.

RESULTS

Comparative performance of *Apis cerana indica* colonies from different locations

Among the bee colonies studied, the bees from two locations in the highland divisions were black morphs and one location each from midland and lowland were yellow morphs. The bees from all the other locations were the common brown bees. The colour of the queen and workers of the two variants differed from the common brown bees. The abdomen of the queen of black bees was very black, that of yellow bees yellowish light brown and in common brown bees dark brown (Figure: 1a,1b and 1c). The colour of the abdomen of worker bees was very distinctive too. In black bees, the abdomen and tergite were black; in yellow bees light yellowish brown and in



**Premkumar et al.,**

common brown bees dark brown (Figure: 2a,2b and 2c). Data on the bee strength of *Apis cerana indica* colonies from different locations measured in terms of number of bee frames with bees on both sides during the growth period, honey flow period and dearth period are presented in (Table: 1).

There was no significant difference in the bee strength in colonies from all the locations during August and September 2020. The bee strength in the common bee colonies ranged from 3.001 to 3.300 while that of the black morphs and yellow morphs ranged from 3.145 to 3.150 and 3.148 to 3.165 respectively. A gradual increase in bee strength was noted in October which reached a high level in November. Black bee colonies from L3 and L6 had mean bee strength of 6.537 and 6.525 respectively during November which were on par with those of yellow bee colonies from L11 and L18 (6.496 and 6.133 respectively). The bee strength ranged from 3.937 to 5.841 in common bees from different locations. After division of colonies, during the month of December, highest bee strength was observed in black bees from L3 (5.175) which were significantly higher than that of bee colonies from other locations. It was followed by that of yellow bees from L18 and L11 (4.308 and 4.112 respectively) and that of brown bees from L2, L14, L9, L16, L15 and L7 which were on par. The mean bee strength ranged from 2391 to 2.971 in common brown bees from different locations and the lowest mean bee strength was recorded from colonies of L12. Similarly, bee strength was the highest (7.021) in black bee colonies from L3 followed by yellow bees from L11 (5.837) and L18 (5.658) during January which were on par with that of common bees from L14, L16, L2, L9, L7 and L13. The mean bee strength ranged from 2.966 to 4.837 in common brown bees.

The second peak in bee strength was observed in the honey flow period. The mean bee strength in colonies from different locations ranged from 3.276 to 7.452 during February. The bee strength was higher in black bee colonies from L3 and L6 (7.452 and 5.624 respectively) and in yellow bees from L18 and L11 (6.911 and 6.568 respectively) which were on par with that of brown bees from locations L14, L13, L16, L9, L7, L2 and L4. The bee strength of common brown bees from other locations ranged from 3.276 to 5.405. A similar trend was observed during March also. The black bee colonies (L3, L6) and yellow bee colonies (L11, L18) recorded higher mean bee strength (7.123, 5.220, 6.272 and 6.244 respectively) which were on par with the common brown bee colonies from L2, L6, L7, L9, L13, L14, L15 and L16. The mean bee strength in brown bees ranged from 3.432 to 5.200, the least bee strength being recorded from colonies in L17. During April mean bee strength declined in all the colonies and black bees from L3 recorded the highest bee strength (6.104) which was on par with that of yellow bees from L11 and L18 (5.540 and 5.344 respectively) which in turn were on par with that of bees from locations L14, L16, L5, L6, L13, L2, L15, L7 and L9. Common brown bees recorded significantly lower bee strength, ranging from 3.014 to 5.000. The mean strength decreased again during May and highest bee strength (5.782) was observed in black bee colonies from L6 which was on par with that of yellow bees from L11 and black bees from L3 which were on par with that of brown bees from locations L14, L13, L9, L16, L15, L2 and L7. The mean bee strength in common brown bees ranged from 2.479 to 4.250 and the lowest mean bee strength was recorded in bee colonies of L1.

There was no significant difference in the bee strength in colonies from all the locations during August and September 2020. The bee strength in the common bee colonies ranged from 3.001 to 3.300 while that of the black morphs and yellow morphs ranged from 3.145 to 3.150 and 3.148 to 3.165 respectively. A gradual increase in bee strength was noted in October which reached a high level in November. Black bee colonies from L3 and L6 had mean bee strength of 6.537 and 6.525 respectively during November which were on par with those of yellow bee colonies from L11 and L18 (6.496 and 6.133 respectively). The bee strength ranged from 3.937 to 5.841 in common bees from different locations. After division of colonies, during the month of December, highest bee strength was observed in black bees from L3 (5.175) which were significantly higher than that of bee colonies from other locations. It was followed by that of yellow bees from L18 and L11 (4.308 and 4.112 respectively) and that of brown bees from L2, L14, L9, L16, L15 and L7 which were on par. The mean bee strength ranged from 2391 to 2.971 in common brown bees from different locations and the lowest mean bee strength was recorded from colonies of L12. Similarly, bee strength was the highest (7.021) in black bee colonies from L3 followed by yellow bees from L11 (5.837) and L18 (5.658) during January which were on par with that of common bees from L14, L16, L2, L9, L7 and L13. The mean bee strength ranged from 2.966 to 4.837 in common brown bees.





Premkumar *et al.*,

The second peak in bee strength was observed in the honey flow period. The mean bee strength in colonies from different locations ranged from 3.276 to 7.452 during February. The bee strength was higher in black bee colonies from L3 and L6 (7.452 and 5.624 respectively) and in yellow bees from L18 and L11 (6.911 and 6.568 respectively) which were on par with that of brown bees from locations L14, L13, L16, L9, L7, L2 and L4. The bee strength of common brown bees from other locations ranged from 3.276 to 5.405. A similar trend was observed during March also. The black bee colonies (L3, L6) and yellow bee colonies (L11, L18) recorded higher mean bee strength (7.123, 5.220, 6.272 and 6.244 respectively) which were on par with the common brown bee colonies from L2, L6, L7, L9, L13, L14, L15 and L16. The mean bee strength in brown bees ranged from 3.432 to 5.200, the least bee strength being recorded from colonies in L17. During April mean bee strength declined in all the colonies and black bees from L3 recorded the highest bee strength (6.104) which was on par with that of yellow bees from L11 and L18 (5.540 and 5.344 respectively) which in turn were on par with that of bees from locations L14, L16, L5, L6, L13, L2, L15, L7 and L9. Common brown bees recorded significantly lower bee strength, ranging from 3.014 to 5.000. The mean strength decreased again during May and highest bee strength (5.782) was observed in black bee colonies from L6 which was on par with that of yellow bees from L11 and black bees from L3 which were on par with that of brown bees from locations L14, L13, L9, L16, L15, L2 and L7. The mean bee strength in common brown bees ranged from 2.479 to 4.250 and the lowest mean bee strength was recorded in bee colonies of L1.

During June in the dearth period, the black bees from L3 and L6 showed higher bee strength (6.073 and 6.011) which were on par with that of yellow bees from L18 and L11 (5.339, 5.252 respectively). This was followed by the common brown bees from L4, L13, L15, L2, L4, L9, L4, L7 and L16. The bee strength in common brown bees ranged from 2.851 to 4.620 with the lowest from L12. A same trend was noticed during July also with highest bee strength of 7.010 in black morphs in L3 followed by L6 and yellow bees in L11 (6.115) and L18 (5.996). Overall analysis of the data on the bee strength indicated that the bee strength was higher in black morph colonies (5.729 and 5.025) and yellow morph colonies (5.238 and 5.214) than in the common brown bee colonies (3.175 to 4.566) (Figures: 3a, 3b and 3c).

DISCUSSION

The results of the studies on the biologically and economically important characters of *Apis cerana indica* colonies collected from selected locations of the three topographic divisions of Tamil nadu were discussed. Two distinct colour morphs of *Apis cerana indica* could be observed from certain beekeeping pockets in addition to the common brown bees. The bees from the highland locations and black morphs from the midland location and lowland location were yellow morphs, The bees from all other locations were the common brown bees. The colour of the queen and workers of the different morphs differed conspicuously from the common brown bees. The abdomen of the queen of the black bees was very black and that of yellow morphs yellowish brown compared to the dark brown in common brown bees. The abdomen and tergites of worker bees were black in black bees; light yellowish brown in yellow bees and dark brown in common brown bees. The results conform to the earlier observations on the prevalence of different colour morphs of *Apis cerana indica* elsewhere. Earlier, Oldroyd *et al.*, (2000) observed that *Apis cerana indica* population in Karnataka was composed of two distinct colour morphs: the yellow 'plain' morph and the black 'hill' morph. Later, Banakar (2009) reported that the black 'hill' morph was distributed in Uttara Kannada, Udipi, Dakshina Kannada, Shimoga, Kodagu, parts of Dharwad, Belgaum, Mysore and Chamarajanagar districts. Shruthi *et al.*, 2009 also studied the behavioural traits of the two colour morphs from low land location. Even though, Devanesan (1998) reported four clusters of *Apis cerana indica*, from Kerala, black and yellow morphs were not identified. The comparative performance on biological and economically important desirable characters of *Apis cerana indica* colonies selected from different locations showed that yellow bee morphs and black bee morphs were significantly superior in all the characters including honey production compared to common brown bees.

Maximum bee strength was recorded in black bees and yellow bees compared to common brown bees, Black bee colonies had a mean bee strength of 5.377 which was followed by that of yellow bees (5.226) and were significantly higher than that of common brown bees (3.960) (Figure: 4.a). This agreed with the report of Shruthi *et al.*, (2009) who



**Premkumar et al.,**

reported that in Karnataka, bee population in both black and yellow strain colonies of *Apis cerana indica* were more and more among the stains, black stain colony recorded higher bee population compared to yellow stain colony. The results on bee strength during different periods revealed that mean bee strength was higher in all the colonies during honey flow period than the growth period and dearth period (Figure: 4a). Maximum bee strength was recorded in November and February and least in May, i.e., first peak during November and second peak during February. Variations in bee strength during different periods are well documented. According to Das and Rahman (2000) highest bee population was observed during February and the lowest during August in Assam. Partap and Partap (2002) reported that the strength of honey bee colony was poor during winter in Hindu Kush Region. According to Pokhrel et al., (2006) stronger colony strength was recorded in colonies during May and colony strength was reduced in April in Nepal. Mohapatra and Satapathy (2012) also reported that in *Apis cerana indica* colonies in Orissa, maximum bee population was during May. These variations in bee strength may be due to various climatic conditions and flora available in different states.

The results on bee strength during different periods revealed that mean bee strength was higher in all the colonies during honey flow period than the growth period and dearth period (Figure: 4b). Maximum bee strength was recorded in November and February and least in May, i.e., first peak during November and second peak during February. Variations in bee strength during different periods are well documented. According to Das and Rahman (2000) highest bee population was observed during February and the lowest during August in Assam. Partap and Partap (2002) reported that the strength of honey bee colony was poor during winter in Hindu Kush Region. According to Pokhrel et al., (2006) stronger colony strength was recorded in colonies during May and colony strength was reduced in April in Nepal. Mohapatra and Satapathy (2012) also reported that in *Apis cerana indica* colonies in Orissa, maximum bee population was during May. These variations in bee strength may be due to various climatic conditions and flora available in different states.

REFERENCES

1. Banakar, N. 2009. Comparative studies on the performance of yellow and black colour morphs of *Apis cerana indica* F. at Sirsi, Karnataka. M.Sc. Thesis, University of Agricultural Sciences, Dharwad. p 65.
2. Das, P K and Rahman, A. 2000. Brood rearing activity of *Apis cerana indica* F. in Assam, *J Crop Res* 19(3):469-473.
3. Devanesan, S. 1998. Pathogenicity of Thai Sacbrood virus to the ecotypes of *Apis cerana indica* Fab. in Kerala. Ph.D., Thesis submitted to Kerala Agricultural University. p.140.
4. Mohapatra, L N and Satapathy, C R. 2012. Studies on colony development in *Apis cerana indica* *Indian J Ent* 74(2): 103-404.
5. Oldroyd, B P, Osborne, K.E and Mardan, M. 2000. Colony relatedness in aggregations of *Apis dorsata* Fab. (Hymenoptera, Apidae). *Insect Soc* 47: 94-95.
6. Partap, U and Partap, T. 2002. Warning signals from apple valleys of the HKH region: productivity concerns and pollination problems. Kathmandu: ICIMOD, pp106.
7. Pokhrel, S, Thapa, R B, Neupane, F P and Shrestha, S M. 2006. Absconding behavior and management of *Apis cerana* F. honey bee in Chitwan, Nepal. *J inst Agric Anim Sci* 27:77-86.
8. Rau, 2004. Studies on the selective breeding of *A. mellifera* for honey production. *Annual Report 2002-2004 of AICRP on Honey bees*. Pusa, Samatipur, Bather. 28-29.
9. Saraf, S K and Wali, L. 1972. The effect of empty comb on the proportion of foraging honey bees collecting nectar. *J Api Res* 34: 27-31.
10. Shruthi, S D, Ramachandra, Y L and Sujana Ganapathi, P S. 2009. Studies on behavioural traits of two different strains of Indian honey bee *Apis cerana indica* F. *World Applied Sci J* 7(6):797-801.





Premkumar et al.,

Table 1: Bee strength of *Apis cerana indica* colonies from different locations in Tamilnadu during 2020-2021

Topographic division	Location	Bee morphs	Bee strength (No of frames with bees on both sides)												Pooled mean
			Growth period						Honey flow period				Dearth period		
			Before division			After division			Feb.	Mar.	Apr.	May.	Jun.	Jul.	
			Aug.	Sept.	Oct.	Nov.	Dec.	Jan.							
HL	L1	CB	3.001	3.208	3.750	3.750	2.574	2.966	3.276	3.625	3.014	2.479	2.995	3.282	3.175
	L2	CB	3.155	3.250	4.500	5.841	3.791	4.608	5.227	5.052	4.255	3.887	4.451	5.034	4.421
	L3	BK	3.145	3.335	5.083	6.537	5.175	7.012	7.452	7.123	6.104	4.708	6.073	7.010	5.729
	L4	CB	3.130	3.166	3.916	5.379	3.495	4.449	4.885	4.010	3.245	3.470	4.383	4.911	4.069
	L5	CB	3.112	3.125	4.665	5.441	3.317	3.795	4.289	4.125	4.525	3.485	3.766	4.087	3.975
	L6	BB	3.150	3.375	5.249	6.525	3.474	4.912	5.624	5.220	4.350	5.782	6.011	6.622	5.025
ML	L7	CB	3.160	3.165	4.145	5.212	3.533	4.575	5.232	5.120	4.120	3.886	4.241	4.848	4.261
	L8	CB	3.255	3.541	3.958	4.204	2.646	3.195	3.625	3.401	3.247	2.680	2.953	3.353	3.338
	L9	CB	3.300	3.665	5.335	5.829	3.750	4.587	5.312	5.184	4.100	3.987	4.407	5.046	4.541
	L10	CB	3.205	3.335	4.224	4.424	2.533	3.416	3.872	3.630	3.533	2.765	3.120	3.556	3.467
	L11	YEL	3.148	3.333	5.624	6.496	4.112	5.837	6.568	6.272	5.540	4.570	5.252	6.115	5.238
	L12	CB	3.205	3.291	4.200	4.025	2.391	3.020	3.414	3.648	3.224	2.640	2.851	3.115	3.252
LL	L13	CB	3.150	3.233	4.666	5.654	3.258	4.541	5.078	5.011	4.333	4.065	4.504	4.753	4.353
	L14	CB	3.175	3.183	4.835	5.516	3.766	4.837	5.405	5.200	5.000	4.250	4.620	4.999	4.566
	L15	CB	3.125	3.191	4.808	5.466	3.608	4.208	4.778	4.555	4.125	3.906	4.499	4.831	4.258
	L16	CB	3.175	3.275	4.635	5.570	3.687	4.624	5.067	5.012	4.720	3.945	4.163	4.411	4.357
	L17	CB	3.120	3.250	4.274	5.200	3.529	3.741	3.829	3.432	3.135	2.822	3.027	3.193	3.546
	L18	YEL	3.165	3.358	5.333	6.133	4.308	5.658	6.911	6.244	5.344	4.780	5.339	5.996	5.214
CD (0.5)			NS	NS	0.5174	1.0948	1.657	2.551	2.8743	2.9641	2.5743	2.1045	2.5725	2.7324	2.1642

HL – Highland; ML – Midland; LL – Lowland; CB - Common Brown Morph; BK: Block Morph; YEL: Yellow morph.



Figure 1a: Black morph



Figure 1b: Yellow morph



Figure 1c: Common brown morph

Fig 1: Queen of different morph of *Apis cerana indica*





Premkumar et al.,



Figure 2a: Black morph



Figure 2b: Yellow morph



Figure 2c: Common brown morph

Fig 2: Worker bees of different morph of *Apis cerana indica*



Figure 3a: Black bee morph



Figure 3b: Yellow bee morph





Premkumar et al.,



Figure 3c: Common brown bee morph

Fig 3: Bee strength of different morphs of *Apis cerana indica*

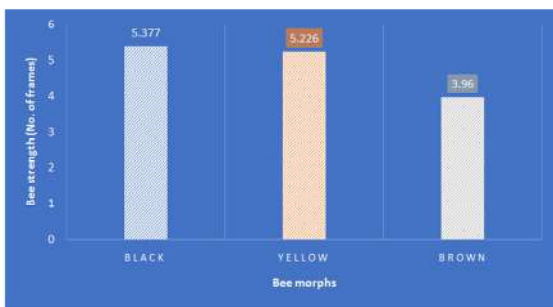


Figure 4a: Bee strength in different morph of *Apis cerana indica* colonies

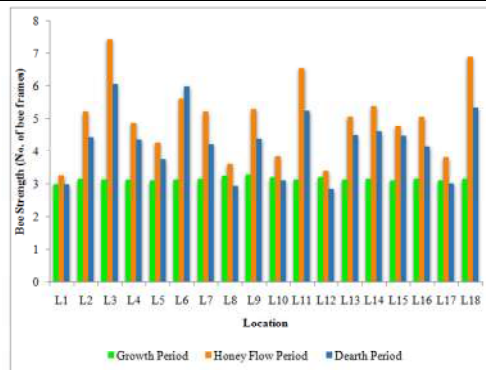


Figure 4b: Bee strength of *Apis cerana indica* colonies from different locations during growth period, honey flow period and death period in Tamilnadu





The Anticancer Drugs in Breast Cancer: Pharmacodynamics and Adverse Effects

Kanagaraj Suganya¹ and Sundaravadivelu Sumathi^{2*}

¹Research Scholar in Biotechnology, Avinashilingam Institute for Home Science and Higher Education for Women, Coimbatore, Tamil Nadu, India.

²Associate Professor, Avinashilingam Institute for Home Science and Higher Education for Women, Coimbatore, Tamil Nadu, India.

Received: 05 Dec 2021

Revised: 26 Dec 2021

Accepted: 22 Jan 2022

*Address for Correspondence

Sundaravadivelu Sumathi

Associate Professor,

Avinashilingam Institute for Home Science and Higher Education for Women,
Coimbatore, Tamil Nadu, India.

Email: sumathi_bc@avinuty.ac.in



This is an Open Access Journal / article distributed under the terms of the **Creative Commons Attribution License** (CC BY-NC-ND 3.0) which permits unrestricted use, distribution, and reproduction in any medium, provided the original work is properly cited. All rights reserved.

ABSTRACT

Breast cancer is the second most leading cause of mortality in the globe. It not only applies to women but also men and animals. Breast cancer research has made significant progress in diagnosing the illness over the past two decades, resulting in more effective and less disruptive treatments. The aim of this review is to address the effect of anticancer medications of breast cancer and their mode of action. The pillars of the therapeutic result are pharmacodynamic factors, which describe how medicine interacts with the body, such as adverse effects and positive symptoms. To get an insight into the drawbacks of breast cancer treatment strategy, a thorough understanding of pharmacodynamic factors is required. The most common treatment of cancer is an anticancer drug, which increases the risk of adverse drug reactions (ADRs). ADRs are huge global issues that can result in major clinical issues, death, and, suffering, and high cost of treatment. One approach to the management of cancer patients is the administration of cancer chemotherapy, which ensures an enhanced quality of life, especially with the discovery of new medications for the cure of various malignancies. To enhance the known factors and focus on major factors that contribute to the response to various breast cancer treatments this review is presented.

Keywords: Breast cancer, anticancer drugs, adverse drug reaction, oncology.



**Kanagaraj Suganya and Sundaravadivelu Sumathi****INTRODUCTION**

Breast cancer is common invasive cancer among the humans and leading cause of death. It has become a tangible threat to humans. Over one million people worldwide have been diagnosed with this lethal disease, which is responsible for more deaths each year. Normal breast growth is governed by a ratio of cell proliferation to apoptosis, and breast cancers grow not just as a function of uncontrolled proliferation but also as a result of reduced apoptosis [1]. Several clinical and pathological options are defined to predict the outcome and treatment response in breast cancer. It has become a fatal disease, and risk factors associated with breast cancer seem to be expanding day by day. Several exogenous and endogenous factors can stimulate the pathology of breast cancer and can worsen the situation [2]. Some additional factors like side effects of conventional treatment such as chemotherapy are increasing the burden more and making it more challenging treating of patients with breast cancer. One of the most threatening problems with conventional treatment is multidrug resistance threatening the survival rate of breast cancer patients [3].

For decades, the discovery of cytotoxic chemicals guided the development of strategies for addressing cancer treatments. The finding of specific biochemical characteristics of malignancies that may be utilized to selectively target tumor cells in cancer treatment [4]. The recent advancements in molecular sciences, as well as breakthroughs in genomics and proteomics, have resulted in multiple possible novel drug targets, resulting in a shift in anticancer drug discovery paradigms towards molecularly focused treatments. These paradigm shifts have necessitated adjustments in the screening and clinical evaluation of drug candidates, as well as a higher engagement of biological scientists in the drug discovery process. Anticancer medicines based on small and large molecular molecules are still being researched [5]. Advances in cancer diagnostics and therapies to treat cancer have resulted in a rise in the number of adverse drug reactions (ADRs) [6]. Given that cancer medication has improved survival rates, advanced cancer is often incurable, and any improvement in survival or delay in disease progression should be weighed against any treatment-related negative impacts on the standard of living. Anticancer drug-related adverse events have prompted an inquiry into the severity and prevalence of ADRs [7]. A total of 83.56 % of breast cancer patients had adverse drug effects. Alopecia (54.94%), anorexia (30.77%), nail discoloration (43.96%), nausea (29.67%), dysgeusia (38.46%), and neuropathy(29.67%) were all shown to be quite prevalent in women with breast cancer administered with a single or combined treatment. In nations like India, there is a scarcity of ADRs data related to chemotherapeutic medications [8]. This review provides an overview of the pharmacodynamics of chemotherapy medications for treating breast cancer.

ANTICANCER PHARMACODYNAMICS: TYPES AND MODE OF ACTION

Chemotherapy uses anti-cancer drugs that will tend intravenously or orally. The drugs travel through the bloodstream to destroy cancer cells in most parts of the body. Chemotherapy is given before surgery or after surgery. In most cases, chemo is best when combinations of medicine are used [9]. The foremost commonly used chemotherapeutic drugs used are given below.

Alkylating Agents

Alkylating agents are a broad category of anticancer medications that include ethyleneimine, nitrogen mustards, alkyl sulfonates, triazines, nitrosoureas and, methylhydrazine. These highly reactive substances operate by covalent bonding a biological entity to nucleic acids and alkyl groups (R-CH₂), resulting in the formation of an intermediary carbonium ion. The crosslinks produced in the sixth position of guanine are thought to be drug-specific [10]. It can therefore form connections between a single strand and two independent DNA strands that interfere with the operation of DNA replication enzymes. Apoptosis is a process in which cells die or inhibit cell division. Damage is more severe during the S-phase because the cell has less time to remove harmed segments. Alkylating agents can form covalent bonds with nearby guanine residues, causing cross-linking between DNA strands and inhibiting DNA replication and transcription. Alkylating agents alter guanine's O₆ to its enol tautomer (intermediate), which could then form base pairs with thymine, resulting in genetic miscoding, with adenine-thymine pairings substituting



**Kanagaraj Suganya and Sundaravadivelu Sumathi**

guanine-cytosine pairs. As a result, abnormal proteins are produced. N7 alkylation causes DNA strands to break down and cell growth to decrease [11].

Anti-metabolites

Antimetabolites are linked to normal DNA components and coenzymes involved in the nucleic acid synthesis that interfere with the normal cellular biological pathways and are commonly used to treat cancer and immune disorders. Many anti-metabolites have sequence similarity to DNA base pairs and compete for their synthesis or inhibiting DNA replication [12]. Cytostatic antimetabolites are the most common form of antineoplastics presently in use, and they are effective for breast cancer treatment. Antimetabolites disrupt DNA biosynthesis and cell division by disrupting the DNA replication mechanism, by either supplying chemically modified nucleotides or reducing the supply of deoxynucleotides responsible for DNA replication and cell division [13]. Antimetabolites available in a variety of forms: Methotrexate, pralatrexate, and pemetrexed are all folate antagonists. Mercaptopurine, fludarabine, and cladribine, as well as thioguanine, are purine antagonists. Azacytidine, gemcitabine, cytarabine, capecitabine, and 5-fluorouracil are pyrimidine antagonists. These molecules are pyrimidine or purine analogs with altered chemical groups and induce necrobiosis during the S phase of cell growth when incorporated into RNA and DNA or inhibit enzymes needed for macromolecule production. DNA polymerases, ribonucleotide reductase and thymidylate synthetase are the antimetabolites' primary intracellular targets. The inhibition of enzymes involved in DNA synthesis or misincorporation of antimetabolites in DNA prevents mitosis and induces apoptosis in dividing cells [14].

Platinum Compounds

Platinum-based therapies have become a hallmark of cancer treatment, with platinum drugs being given to almost half of chemotherapy patients. The discovery of first-generation platinum compounds such as cisplatin, as well as second- and third-generation medicines, benefit patients from cancer chemotherapy [15]. Platinum compounds of the first generation and second-generation medications, such as carboplatin, oxaliplatin, and nedaplatin, were utilized in the treatment of breast cancer for a long time. Furthermore, these chemicals have better anti-cancer properties and are more effective in treating tumors. Third-generation analogs include lobaplatin, heptaplatin, and satraplatin [16]. Though its actual mechanism is unknown, platinum compounds are thought to behave similarly to bifunctional alkylating agents, i.e., probable cross-linking and interference with DNA function, as well as a minor effect on RNA, resulting in DNA, RNA, and protein production suppression. It is cell-cycle nonspecific. Platinum compounds have a chemotherapeutic mechanism similar to DNA-binding alkylating drugs. Platinum compounds have a novel effect on neurons: the selective vulnerability of dorsal root ganglia (DRG) sensory neurons depends on the structure of the blood-nerve barrier. Also, the binding of platinum to mitochondrial DNA has been considered a possible mechanism of death [17]. The necrobiosis of the sensory neurons leads to permanent distal sensory loss. The treatments used in cancer is shown in figure 1.

Plant-Derived Products

Plants, microorganisms, and marine flora are significant sources of therapeutic compounds, especially as effective cancer control drugs. Numerous traditional medicines and their phytochemicals are being used to cure cancer and stop it from spreading and proliferating. Phytochemicals and their derivatives are found in various parts of the plant and have a wide range of therapeutic effects [18]. Several phytochemicals, including taxanes, alkaloids, flavonoids, minerals, glycosides, as well as other 1° and 2° metabolic products, play an important role either in preventing the proteins, enzymes, and signaling pathways stimulated by cancer cells or stimulating the development of defensive enzymes, resulting in antioxidant action [19]. Vinca alkaloids, Vincristine, Vinorelbine, vindesine, vinblastine, and vinflunine are three classes of chemicals obtained from plants. These drugs are isolated from periwinkle plants and are antineoplastic agents that destroy microtubules. The mitosis drug produces cellular arrest during cell division, preventing cell division from being completed in metaphase. At S-phase, vinca alkaloids were previously thought to be cell cycle-specific chemicals [20]. Topoisomerase inhibitors change the three-dimensional DNA structure by unwinding, slicing, and rejoining it in a reaction that involves DNA replication, chromatid separation, and transcription. The capacity of topoisomerase inhibitors to limit DNA replication was originally believed to be the



**Kanagaraj Suganya and Sundaravadivelu Sumathi**

most important factor in their effectiveness in cancer treatment. It's been suggested that therapeutic efficacy may also be dependent on manipulating other biological pathways inside the cancer cells at the same time. These medicines are phase-specific, preventing G2 mitosis from entering the cells [21].

Antitumor Antibiotics

Anthracycline antibiotics (doxorubicin, also known as adriamycin, daunorubicin, epirubicin, and idarubicin), mitoxantrone, bleomycin, dactinomycin, mitomycin, ciprofloxacin, gemifloxacin, plicamycin, salinomycin, are all members of this category. Antitumor antibiotics were made in a variety of ways from bacterial and fungal strains (species termed *Streptomyces*). They affect nucleic acid synthesis and activity. Anthracyclines (such as doxorubicin, epirubicin, and daunorubicin) affect DNA and cause topoisomerase II to be dysfunctional. Intercalation of guanine and cytosine base pairs to DNA may be one of its anti-cancer mechanisms. Its antineoplastic activity may include the binding of guanine and cytosine base pairs to DNA by intercalation. It inhibits DNA-dependent RNA synthesis at high doses and hinders DNA transcription at low doses [22]. Bleomycin is an antitumor antibiotic made up of a combination of glycopeptides that cause DNA strand breakdown, which inhibits DNA synthesis by causing single-strand breaks and splits double strands less effectively. Furthermore, it interferes with the production of RNA and proteins [23]. Mitomycin causes DNA cross-linking and lowers DNA synthesis, as well as a decreased degree of RNA and protein synthesis. Chemotherapeutic antibiotics are chemical compounds produced by microorganisms with anticancer properties. They are mainly peptides and anthraquinones, with obvious and effective inhibitory effects on the uncontrolled proliferation, aggressive growth, and metastasis of malignant cancers [24].

RESISTANCE OF DRUGS

The tumor microenvironment (TME) is the surrounding tissue that surrounds tumor cells and plays a crucial role in tumor development, apoptosis evasion, and treatment resistance. TME is made up of a variety of cell types as well as extracellular components. Surprisingly, tumor cells and TME have a close relationship, which cancerous cells can modulate for their benefit [25]. Cancer-associated fibroblast (CAFs) is formed mostly from resident fibroblasts; however, they have a distinct expression profile as compared to the normal fibroblasts. By secreting extracellular matrix elements (collagen, hyaluronic acid, fibronectin, etc.) and metalloproteases (MPPs) involved in extracellular matrix (ECM) remodeling, they play a significant role in cancer growth and invasiveness [26]. CAFs can also release cytokines and growth factors, influence immune responses, as well as provide a niche for cancer stem cells. CAFs were abundantly observed in the remaining tissues of chemoresistant individuals after neoadjuvant chemotherapy in a clinical investigation of breast cancer patients and were hardly detected in responding patients with complete cures. In breast cancer animal models, targeting CAFs restored chemosensitivity to DTX [27]. Table 1 shows the drug's toxicity in breast cancer.

Tumor surveillance and control rely heavily on immune cells. Tumor cells are increasingly able to manipulate the immune reaction to destroy it. The frequency and type of immune cells seen in invasive breast cancer can help determine prognosis and chemotherapy response. On the other hand, mesenchymal stem cells (MSC) can promote breast cancer chemoresistance through a variety of mechanisms, including the secretion of cytokines (IL-6, IL-8, and CxCL1) that cause an increase in ABC efflux transporters, improving collagen fiber crosslinking and ECM stiffening, and promoting hyaluron accumulation in the breast tumor stroma [28]. Adipocytes make up a large part of the breast TME and are involved in multidrug resistance. They release free fatty acids (FFAs), which cancer cells need as an energy source to keep up with their high growth demands. FFA absorption by cancer cells over time might lead to lipid saturation of cell membranes and impaired medication uptake. Furthermore, they release an altered adipokine profile (IGF, IL-6, TNF-, leptin) as a result of their interaction with cancer cells, which allows breast tumor cells to bypass death pathways and reduces the efficacy of chemotherapeutic drugs [29]. Adipokines, in particular, inhibit DOX-induced apoptosis, enhance the development of drug efflux transporters P-gp or ABCB1, and activate MVP-mediated drug resistance to DOX and PTX. MVP is a protein that plays a role in drug efflux from the nucleus as well as drug accumulation in exocytic vesicles for cell clearance. Obesity, interestingly, exacerbated the consequences of MVP-mediated drug resistance. Obesity is a major risk factor for the development of breast cancer, and it's linked to poor health outcomes and multidrug resistance. Data from the literature clearly show that adipocytes play a role in



**Kanagaraj Suganya and Sundaravadivelu Sumathi**

chemoresistance, particularly in breast cancers [30]. Drug delivery blockage by the TME is a common cause of low drug uptake and multidrug resistance, but it has received minimal attention from researchers. Three key transport phases influence drug delivery to tumors: vascular transport (through blood vessels), transvascular transport (across vessel walls and basement membranes), and interstitial transport (between vessel walls and basement membranes) (through the ECM until reaching cancer cells). Finally, medications must be absorbed by the cells that are administered to patients [31]. Tumors have peculiar characteristics that result in a collection of transport barriers that obstruct regular medicine delivery. The first is solid stress, which is induced by cancer metastasis in a small space and the overproduction of interstitial matrix molecules. As a result, blood arteries get constrained, even collapsing, and perfusion rates drop as cancer develops, restricting drug delivery. The microenvironment becomes hypoxic, acidic, and necrotic at the same time, potentially increasing treatment resistance and tumor development. Abnormal blood vessel networks are another feature of the TME [32]. Because of the restricted blood flow within tumors, tumor cells release a cocktail of proangiogenic factors without the creation of antiangiogenic factors, leading tumor cells not to fully develop and instead stay disordered and convoluted [33]. Furthermore, these developing tumor vasculatures have extensive pores and fenestrated vessels, making them heterogeneously hyperpermeable. As a result of the fluid loss, the interstitial fluid pressure rises. Convective transport is disabled when there is no fluid pressure gradient between both the vascular and interstitial fluids, and the only diffusion drives transvascular and interstitial transport, resulting in limited drug penetration distances [34]. Simultaneously, CAF (Cancer-associated fibroblast) hyperproduction of ECM proteins enhances its stiffness, primarily in the tumor core, which represents a major obstacle to medication administration and is associated with a poor prognosis and a high rate of disease relapse. The accumulation of collagen and proteoglycans is connected to stiffness and loss of elasticity [35]. In breast cancer cell lines, high levels of collagen expression genes have been linked to treatment resistance and low macromolecule interstitial diffusion. Glycosaminoglycan deposits, such as hyaluronan, have also been linked to poor drug diffusion and chemoresistance in breast cancer cell lines. Other ECM components (fibronectin, MMPs, integrin receptors, etc) were connected to chemoresistance and also have an impact on drug diffusion [36].

TYPES OF ADVERSE DRUG REACTIONS IN BREAST CANCER

The administration of cancer chemotherapy is one approach to the management of cancer patients and this ensures an improved quality of life, especially with the event of recent drugs for the cure of varied neoplasms. However, this has also brought out various adverse events that are often neglected by the treating physicians due to the goal of therapy [37]. The adverse effects of breast carcinoma response to explore drug exposure are given below.

Alopecia

Hair loss (alopecia) caused by chemotherapy could be a common adverse effect of adjuvant and metastatic chemotherapeutic treatments. Alopecia is commonly thought to have an unavoidable and temporary side effect that is addressed with wigs. Because hair is such an important part of one's identity, it seems biologically reasonable to believe that losing one's hair could have negative effects on a variety of areas of one's quality of life in addition to being uncomfortable [38]. Scalp cooling is used to prevent or minimize hair loss associated with chemotherapy. According to an evaluation of scalp cooling, efficacy varies depending on the type of chemotherapy treatment used. Over the last few decades, scientists have made significant progress in understanding the biology of hair regrowth. These developments have sparked study into potential chemotherapy-induced alopecia (CIA) solutions at the fundamental science and translational research levels. Unfortunately, patients' therapeutic options are still limited [39].

Nail discoloration

Adverse effects of drugs, such as nail abnormalities caused by chemotherapeutic drugs, are well-known and considered a common side effect of medication. Nail abnormalities caused by drugs usually affect some or all 20 nails and emerge in a time frame that corresponds to drug usage. The nail changes are normally transient and then go away with discontinuation, but they can also last a long period. They'll be asymptomatic or linked to pain and a loss of digital functionality. A large number of medications have been shown to interact with the kinetics and keratinization of nail matrix keratinocytes [40]. A severe injury to nail matrix keratinocytes may result in an



**Kanagaraj Suganya and Sundaravadivelu Sumathi**

immediate reduction or arrest of mitotic index, which can present as Beau's line or onychomadesis, whereas milder damage will result in nail plate weakening, brittleness, and/or decreased nail frequency. True transverse leuconychia is another indication of a transitory impairment of nail matrix keratinization. Chemotherapeutic drugs for cancer are the most common cause of nail alterations, are also an indication of their antimitotic and cytotoxic activities. A thorough understanding of a drug's potential side effects on the nail may also be useful in preventing their occurrence and avoiding diagnostic issues [41].

Dysgeusia

Aberrant or damaged taste buds, an unpleasant modification of feeling, or distortion or perversion of the sense of taste are all ways of describing dysgeusia. The taste of dysgeusia is frequently described as bitter, salty metallic, or unpleasant. Because both smell and taste are important in producing the experience of taste, dysgeusia is intimately linked to olfactory alterations. Taste and olfaction deliver sensory information as well as sensory delight, and cancer medicines are known to alter both [42]. Chemotherapy, by damaging taste and olfactory receptor cells, can produce taste and odor abnormalities. Cell damage can take the following forms: (1) a reduction in the number of normal receptor cells, (2) alterations in cell structure or receptor surface modifications, and (3) neuronal coding disruption. The lifetime of olfactory receptor cells is approximately a week, while the ratio of normal human tongue cells is ten days. Chemotherapy can impact neuronal activity in the same way as it affects receptor cells. Specific taste sensations can be induced by abnormal sensitization of the chorda tympani nerve without triggering taste receptors or needing the presence of appropriate taste molecules. Anti-neoplastic medications have the potential to harm neuronal cells, altering afferent taste pathways [43].

Anorexia

Anorexia, defined as a lack of the desire to eat, as well as the frequency of early satiety, is a critical detrimental factor linked to lower food consumption and weight loss, both of which decrease therapeutic outcomes and quality of life after chemotherapy. While cancer can cause anorexia, chemotherapy-induced anorexia could be a separate and worsening condition. Systemic and/or local hypothalamic stimulation of inflammatory processes attributable to gastrointestinal mucositis or direct neural action of these drugs could be putative mechanisms of anorexia connected to chemotherapeutics [44]. Increased levels of inflammatory cytokines including interleukin-1, as well as stimulation of the hypothalamus melanocortin system and microglia, have been identified as factors in causing anorexia. Furthermore, anorexia produced by chemotherapy is linked to dehydration as a result of diarrhea, which can be caused by a variety of chemotherapeutics. The activation of brain osmosensitive sites and vasopressin neurons is well recognized to promote anorexia as a result of systemic dehydration [45].

Nausea

One of the most severe side effects of chemotherapy, according to cancer patients, is nausea. Anticipatory, acute, and delayed nausea are the three types of nausea that can be caused by chemotherapy. Anticipatory nausea develops before the beginning of chemotherapy in anticipation of the treatment [46]. Acute nausea develops during the first 24 hours after chemotherapy, while delayed nausea develops over the next 24 hours and up to five days. The majority of people suffer severe nausea on the first day of chemotherapeutics and are less likely to have severe nausea on following days if they do not have it on Day 1. Patients experience delayed nausea, which is usually linked to highly emetogenic chemotherapy regimens such as doxorubicin and cisplatin [47].

Neuropathy

Chemotherapeutic drugs can harm system structures and produce a variety of neuropathies, including small and large fiber neuropathies, sensory and/or motor neuropathies, demyelinating and axonal neuropathies, cranial and autonomic neuropathies. Chemotherapy's effects on the neurological system differ depending on the drug's particular physical and chemical qualities, including its single or repeated dosages. A condition known as chemotherapy-induced peripheral neuropathy (CIPN) is one of the most prevalent neuropathies caused by antineoplastic drugs [48]. CIPN is thought to be primarily a sensory neuropathy with motor and autonomic abnormalities. Apart from paclitaxel and oxaliplatin, which cause acute neuropathy during or shortly after infusion,



**Kanagaraj Suganya and Sundaravadivelu Sumathi**

CIPN symptoms normally appear weeks or even months after chemotherapy is completed, and their intensity is usually proportionate to the drug's cumulative dose [49]. After terminating medication, some patients have a sudden worsening and exacerbation of symptoms, as well as a process known as "coasting," in which mild neuropathy develops or new CIPN emerges. This case presents a challenge for oncologists because there are no signals or indications that the dosage should be reduced to alleviate CIPN symptoms during the treatment period. Pain and sensory disturbances may last for months or even years after chemotherapy are completed [50].

Cardiotoxicity

Since the discovery of cardiotoxicity as a form of side effect in chemotherapeutic medications in 1967, a great number of investigations have been carried out to identify the significant pathophysiological causes of cardiotoxicity [51]. Anticancer pharmaceutical medications known as anthracyclines are one of the most effective currently present. Anthracyclines are antibiotics that are manufactured by *Streptomyces* bacteria and were first found 60 years ago. Doxorubicin, epirubicin, daunorubicin, and mitoxantrone are the most regularly utilized anthracycline medicines in clinical practice [52]. Antitumor effects of anthracyclines are mediated by four mechanisms: 1) intercalation among pairs of nitrogenous bases disrupts nucleic acid synthesis (DNA and RNA); 2) inhibition of topoisomerase II (that leads to DNA breaks and helps to prevent ligation repair); 3) alterations of histone proteins, weakening DNA recovery; 4) enhance the production of free radicals (reactive oxygen species), mediated by iron, which causes damage to nucleic acids and proteins. Though anthracyclines remain the most effective and commonly used medication due to their strong antitumor effectiveness, their usage is constrained due to several issues. The ultimate cardiotoxicity of anthracyclines has been one of the limiting factors in their widespread use. Heart failure and left ventricular (LV) failure are the most hazardous anthracycline short-and long-term effects, occurring in 5-23 percent of patients and resulting in a decline in physical function as well as an increased risk of death [53].

The incidence of anthracycline cardiotoxicity, both early and late, is greatly reliant on the anthracycline's cumulative effects. Even with substantial anthracycline exposure, there was a risk of heart dysfunction. In such circumstances, the exclusion of other myocardial adverse effects may become critical [54]. The harmful effect of reactive oxygen species is one of the first known and carefully investigated mechanisms underlying. Due to the excess formation of free radicals caused by the quinone group of these chemicals, it was discovered that anthracyclines cause several types of cellular damage to cardiac myocytes and endothelial cells. Because cardiomyocytes are abundant in mitochondria and also have lesser activity among the most essential antioxidative defense enzymes (superoxide dismutase and catalase), myocardium tissue is more sensitive to free radical damage. Furthermore, doxorubicin inhibits glutathione peroxidase, an enzyme that protects cardiomyocytes from free radicals. An important link in the pathophysiological acts of anthracyclines was its accumulation of doxorubicinol, a toxic metabolite of doxorubicin. Doxorubicin suppresses the calcium and sodium ion exchange pumps in mitochondria, sarcoplasmic reticulum, and sarcolemma that result in the enhanced generation of free oxygen radicals. It is around 50-500 times more effective than doxorubicin in lowering the systolic function of the heart. Inflammatory mechanisms may have a role in the etiology of doxorubicin-induced cardiotoxicity, according to several findings [55].

PSYCHOLOGICAL CONDITIONS INFLUENCE THE ADVERSE DRUG REACTIONS

Even in patients who have a high recovery rate, cancer is still thought to have a high death rate and is considered to have an intrinsic possibility for death, suffering, and pain, producing significant psychological discomfort. Its diagnosis is a crisis that forces the patient to face plenty of challenging tasks. Patients deal with tremendous emotional stress while attempting to make significant medical decisions [56]. The diagnosis of a life-threatening illness, aggressive medical care, lifestyle changes or direct impacts of the tumor itself, a lack of family support system, personality features, familial conflicts, and economic difficulties are all examples of psychological trauma. Psychological disorders are very common in cancer patients (30–60%), with around 29–43 percent satisfying the diagnostic criteria for mental disorders. Depressive symptoms associated with mixed anxiety and adjustment disorder, as well as depressive mood or major depression, are among the most commonly observed psychological disorders [57]. Psychiatric diseases were found in 73 percent of 271 cancer patients referred to Consultation-Liaison Psychiatry (24 percent systemic family difficulties, 23 percent mood disorders, 16 percent adjustment disorders, and



**Kanagaraj Suganya and Sundaravadivelu Sumathi**

10 percent organic mental disorders) [58]. Adjustment disorders (24 percent), delirium (16 percent), and major depressive disorder (12 percent) were among the psychiatric diseases diagnosed in 765 people with cancer admitted to a psycho-oncology center, with 59 (6 percent) of them being outpatient patients. Providing psychological health services to patients with cancer has become an integrated component of oncologic therapies because psychological problems have such an adverse effect on cancer management [59].

PHARMACOVIGILANCE IN BREAST CANCER

Pharmacovigilance in oncology aids in the prevention, detection, and management of drug-induced adverse effects, as well as the reduction of medically unnecessary prescription prescriptions. Medical studies in oncology produce new medications for use in chemotherapy treatments regularly. With the development of novel medications that operate on particular molecular targets, reduced systemic toxicity is predicted. The safety profiles of new drugs differ from the typical toxicity patterns of conventional chemotherapy, so patients taking these new medicines must be monitored closely to identify new adverse effects [60]. The identification and spontaneous reporting of adverse drug reactions (ADRs) that occur during pharmacological therapy are considered pharmacovigilance. It will only be able to achieve its purpose of medication safety if its methodologies are carefully and consistently applied. As a consequence, full participation from all health professionals is required, as well as patient education and awareness. Because many of the adverse effects caused by new pharmaceuticals have a rapid and unpredictable onset, it is critical to maintaining a certain level of attentiveness. Such ADRs could be life-threatening if it is not discovered quickly [61]. Furthermore, it is difficult to attribute an unfavorable impact to a specific medicine or pre-existing risk factor. For this purpose, comprehensive information about a patient's predisposing health risks is important for avoiding pain and improving the quality of life [62].

The Pharmacovigilance Programme of India (PvPI) collaborates with the WHO-Uppsala Monitoring Center in Sweden to add Indian data to a global database. The PvPI, which was established in 2010, helps to measure adverse drug reactions (ADRs) in the Indian population, raise awareness about health professionals about the significance of ADR reporting in India, generate independent, evidence-based suggestions on drug safety, and track the benefit-risk profile of medicines, among many other factors. This programme is critical because, after years of work, ADR monitoring in India is still in its infancy [63]. ADR reporting and monitoring programmes in hospitals can aid in determining and analyzing the concerns related to drug use. This information may aid prescribers in identifying ADRs and dealing with them more effectively, as well as preventing ADRs in the future. Patient-related explanations for underestimation include failure to recognize ADR or inability to correlate the ADR to a specific medicine. Guilt, fear of litigation, ignorance, laziness, insufficient risk perception concerning newly launched medications, anxiety, insufficient training to recognize ADRs, and lack of understanding about the PV programme are all prevalent doctor-related factors [64]. Pharmacovigilance pharmacists have played a vital role in the notification of potential ADRs in numerous countries by giving information and advice on the safe and appropriate use of medicines, as well as reducing the occurrence of ADRs and failure to report. It's because pharmacists who provide direct patient advice, specifically in the context of medication management, are more effective in detecting ADRs. In cancer treatment, pharmacovigilance investigations are critical.

Antineoplastic drugs have been extensively studied and proven to be effective in the treatment of cancer, but they must be used with caution because of their toxicological properties and limited therapeutic scope. ADRs are so widespread and predictable in cancer departments because they've become considered as an unavoidable therapeutic option. As a result, onco-pharmacovigilance, a subsystem of drug monitoring evolved from pharmacovigilance, was created to record adverse drug reactions to cytotoxic anti-neoplastic medications. Oncology pharmacists are in charge of a wide range of tasks, including monitoring, detection, prevention, and alleviation of adverse events associated with chemotherapeutics. Few studies reveal the incidence of ADRs to chemotherapy, which makes it difficult to evaluate the intensity and frequency of their occurrence in clinical settings. As a result, studies that reveal these negative outcomes might help the multidisciplinary team to educate patients and advise further preventive treatments and medications [65].



**Kanagaraj Suganya and Sundaravadivelu Sumathi****CONCLUSION**

Anticancer drug resistance is currently the most difficult obstacle to overcome in the treatment of cancer. They are resisted by cancer in a variety of ways, some of which have that still need to be found. Cancer resists through four primary pathways, which contain the main principles regarding resistance: escaping cell cycle checkpoints, avoiding apoptosis, tumor microenvironment variables, and the presence of cancer stem cells, according to significant research. The adaptability and heterogeneity of cancer cells are at the root of all of these strategies. When it comes to finding a cure for resistance, understanding that each cancer is eternally distinct creates numerous problems. The utilization of ADCs (Antibody-Drug Conjugates) for selective targeting and ctDNA for detection and real-time monitoring are two ideas that have recently emerged as promising solutions to these difficulties. Drug resistance is a difficult issue that is highly prevalent in today's society, and more research is needed to better understand it and put a stop to it. The risk factors for specific psychiatric disorders, and draws attention to the fact that there are serious delays in patients seeking psychiatric help and in the referrals of oncologists for psychological assessment. Identifying risk factors and increasing oncologists' understanding of risk variables may enable more patients to receive mental health care much earlier. In cancer, where pharmacotherapy is de facto influenced by a high prevalence of drug-related problems and a restricted therapeutic range, efficient management of spontaneous ADR reports is critical for monitoring drug safety. Clinical pharmacists with pharmacovigilance certification have a lot of obligations, including promoting safety, closely monitoring cancer patients in treatment, and supporting educational programmes. The relevance of pharmacovigilance in oncology must be emphasized with every effort, to improve safety and provide cancer patients with all available assistance in improving their quality of life during such a vital stage of life.

CONFLICT OF INTEREST

None declared

REFERENCES

1. Britt KL, Cuzick J, Phillips KA. Key steps for effective breast cancer prevention. *Nature Reviews Cancer*. 2020 Aug;20(8):417-36. doi:https://doi.org/10.1038/s41568-020-0266-x.
2. He Z, Chen Z, Tan M, Elingarami S, Liu Y, Li T, Deng Y, He N, Li S, Fu J, Li W. A review on methods for diagnosis of breast cancer cells and tissues. *Cell Proliferation*. 2020 Jul;53(7):e12822. doi:https://doi.org/10.1111/cpr.12822.
3. Dorling L, Carvalho S, Allen J, González-Neira A, Luccarini C, Wahlström C, Pooley KA, Parsons MT, Fortuno C, Wang Q, Bolla MK. Breast Cancer Risk Genes-Association Analysis in More than 113,000 Women. *N Engl J Med*. 2021;428-39. doi: 10.1056/NEJMoa1913948.
4. Ashraf MA. Phytochemicals as potential anticancer drugs: time to ponder nature's bounty. *BioMed research international*. 2020 Jan 31;2020. doi:https://doi.org/10.1155/2020/8602879.
5. Thurston DE, Pysz I. *Chemistry and pharmacology of anticancer drugs*. CRC press; 2021 Mar 17.
6. Ferner RE, McGettigan P. Adverse drug reactions. *Bmj*. 2018 Nov 6;363. doi: https://doi.org/10.1136/bmj.k4051.
7. Patton K, Borshoff DC. Adverse drug reactions. *Anaesthesia*. 2018 Jan;73:76-84
8. PNair A, Biju JM, Paul JM, PA D, Joseph S, Madhu CS. Pharmacoeconomic evaluation on breast cancer patients in a Tertiary care hospital in south India. *life*. 2020;1:2.
9. Franco YL, Vaidya TR, Ait-Oudhia S. Anticancer and cardio-protective effects of liposomal doxorubicin in the treatment of breast cancer. *Breast Cancer: Targets and Therapy*. 2018;10:131. doi: 10.2147/BCTT.S170239.
10. Choudhary P, Savitha RS. Review on: Anticancer drug-induced adverse drug reactions in oncology patients. *Drug Invention Today*. 2020 Apr 1;13(4).
11. Lajous H, Lelièvre B, Vauléon E, Lecomte P, Garcion E. Rethinking alkylating (-like) agents for solid tumor management. *Trends in pharmacological sciences*. 2019 May 1;40(5):342-57. doi:https://doi.org/10.1016/j.tips.2019.03.003.



**Kanagaraj Suganya and Sundaravadivelu Sumathi**

12. Link W. Cancer Therapy. In Principles of Cancer Treatment and Anticancer Drug Development 2019 (pp. 7-76). Springer, Cham. doi: https://doi.org/10.1007/978-3-030-18722-4_2.
13. Bumbăcilă B, Duda-Seiman C, Duda-Seiman D, Putz MV. Cancer/Anti-Cancer Chemotherapy: Pharmacological Management. In New Frontiers in Nanochemistry 2020 May 6 (pp. 57-84). Apple Academic Press.
14. Gara E, Csikó KG, Ruzsa Z, Földes G, Merkely B. Anti-cancer drugs-induced arterial injury: risk stratification, prevention, and treatment. *Medical Oncology*. 2019 Aug;36(8):1-8. doi: <https://doi.org/10.1007/s12032-019-1295-8>.
15. Khoury A, Deo KM, Aldrich-Wright JR. Recent advances in platinum-based chemotherapeutics that exhibit inhibitory and targeted mechanisms of action. *Journal of inorganic biochemistry*. 2020 Jun 1;207:111070. doi: <https://doi.org/10.1016/j.jinorgbio.2020.111070>.
16. Pandey JG, Balolong-Garcia JC, Cruz-Ordinario MV, Que FV. Triple negative breast cancer and platinum-based systemic treatment: a meta-analysis and systematic review. *BMC cancer*. 2019 Dec;19(1):1-9. doi: <https://doi.org/10.1186/s12885-019-6253-5>.
17. Lynce F, Nunes R. Role of Platinums in Triple-Negative Breast Cancer. *Current Oncology Reports*. 2021 May;23(5):1-7. doi: <https://doi.org/10.1007/s11912-021-01041-x>.
18. Sun LR, Zhou W, Zhang HM, Guo QS, Yang W, Li BJ, Sun ZH, Gao SH, Cui RJ. Modulation of multiple signaling pathways of the plant-derived natural products in cancer. *Frontiers in oncology*. 2019 Nov 8;9:1153. doi: <https://doi.org/10.3389/fonc.2019.01153>.
19. Pérez-Soto E, Estanislao-Gómez CC, Pérez-Ishiwara DG, Ramirez-Celis C, del Consuelo Gómez-García M. Cytotoxic Effect and Mechanisms from Some Plant-Derived Compounds in Breast Cancer. *Cytotoxicity-Definition, Identification, and Cytotoxic Compounds*. 2019 Aug 6:45.
20. González-Burgos E, Gómez-Serranillos MP. Vinca Alkaloids as Chemotherapeutic Agents Against Breast Cancer. *Discovery and Development of Anti-Breast Cancer Agents from Natural Products*. 2021 Jan 1:69-101. doi: <https://doi.org/10.1016/B978-0-12-821277-6.00004-0>.
21. Gmeiner WH. Entrapment of DNA topoisomerase-DNA complexes by nucleotide/nucleoside analogs. *Cancer drug resistance (Alhambra, Calif.)*. 2019;2:994. doi: [10.20517/cdr.2019.95](https://doi.org/10.20517/cdr.2019.95).
22. Dasgupta H, Islam MS, Alam N, Roy A, Roychoudhury S, Panda CK. Induction of HRR genes and inhibition of DNMT1 is associated with anthracycline anti-tumor antibiotic-tolerant breast carcinoma cells. *Molecular and cellular biochemistry*. 2019 Mar;453(1):163-78. doi: <https://doi.org/10.1007/s11010-018-3442-5>.
23. Chen H, Cui J, Wang P, Wang X, Wen J. Enhancement of bleomycin production in *Streptomyces verticillus* through global metabolic regulation of N-acetylglucosamine and assisted metabolic profiling analysis. *Microbial cell factories*. 2020 Dec;19(1):1-7. doi: <https://doi.org/10.1186/s12934-020-01301-8>.
24. Baird L, Yamamoto M. NRF2-dependent bioactivation of mitomycin C as a novel strategy to target KEAP1-NRF2 pathway activation in human cancer. *Molecular and cellular biology*. 2020 Nov 2;41(2):e00473-20. doi: [10.1128/MCB.00473-20](https://doi.org/10.1128/MCB.00473-20).
25. Qu Y, Dou B, Tan H, Feng Y, Wang N, Wang D. Tumor microenvironment-driven non-cell-autonomous resistance to antineoplastic treatment. *Molecular cancer*. 2019 Dec;18(1):1-6. doi: <https://doi.org/10.1186/s12943-019-0992-4>.
26. Alexander J, Cukierman E. Cancer associated fibroblast: mediators of tumorigenesis. *Matrix Biology*. 2020 Sep 1;91:19-34. doi: <https://doi.org/10.1016/j.matbio.2020.05.004>.
27. Pelon F, Bourachot B, Kieffer Y, Magagna I, Mermet-Meillon F, Bonnet I, Costa A, Givel AM, Attieh Y, Barbazan J, Bonneau C. Cancer-associated fibroblast heterogeneity in axillary lymph nodes drives metastases in breast cancer through complementary mechanisms. *Nature communications*. 2020 Jan 21;11(1):1-20. doi: <https://doi.org/10.1038/s41467-019-14134-w>.
28. Johnson RH, Anders CK, Litton JK, Ruddy KJ, Bleyer A. Breast cancer in adolescents and young adults. *Pediatric blood & cancer*. 2018 Dec;65(12):e27397. doi: <https://doi.org/10.1002/pbc.27397>.
29. Deepak KG, Vempati R, Nagaraju GP, Dasari VR, Nagini S, Rao DN, Malla RR. Tumor microenvironment: Challenges and opportunities in targeting metastasis of triple negative breast cancer. *Pharmacological research*. 2020 Mar 1;153:104683. doi: <https://doi.org/10.1016/j.phrs.2020.104683>.



**Kanagaraj Suganya and Sundaravadivelu Sumathi**

30. Zhang J, Li M, Wang M, Xu H, Wang Z, Li Y, Ding B, Gao J. Effects of the surface charge of polyamidoaminedendrimers on cellular exocytosis and the exocytosis mechanism in multidrug-resistant breast cancer cells. *Journal of nanobiotechnology*. 2021 Dec;19(1):1-4.doi:https://doi.org/10.1186/s12951-021-00881-w.
31. Vrettos EI, Mező G, Tzakos AG. On the design principles of peptide–drug conjugates for targeted drug delivery to the malignant tumor site. *Beilstein journal of organic chemistry*. 2018 Apr 26;14(1):930-54. doi: 10.3762/bjoc.14.80.
32. Arneth B. Tumor microenvironment. *Medicina*. 2020 Jan;56(1):15.
33. Najafi M, Goradel NH, Farhood B, Salehi E, Solhjoo S, Toolee H, Kharazinejad E, Mortezaee K. Tumor microenvironment: Interactions and therapy. *Journal of cellular physiology*. 2019 May;234(5):5700-21.doi: https://doi.org/10.1002/jcp.27425.
34. Hinshaw DC, Shevde LA. The tumor microenvironment innately modulates cancer progression. *Cancer research*. 2019 Sep 15;79(18):4557-66.doi: 10.1158/0008-5472.CAN-18-3962.
35. McCarthy JB, El-Ashry D, Turley EA. Hyaluronan, cancer-associated fibroblasts and the tumor microenvironment in malignant progression. *Frontiers in cell and developmental biology*. 2018 May 8;6:48.doi:https://doi.org/10.3389/fcell.2018.00048.
36. Insua-Rodríguez J, Oskarsson T. The extracellular matrix in breast cancer. *Advanced drug delivery reviews*. 2016 Feb 1;97:41-55.doi:https://doi.org/10.1016/j.addr.2015.12.017.
37. Wahlang JB, Laishram PD, Brahma DK, Sarkar C, Lahon J, Nongkynrih BS. Adverse drug reactions due to cancer chemotherapy in a tertiary care teaching hospital. *Therapeutic advances in drug safety*. 2017 Feb;8(2):61-6.doi:https://doi.org/10.1177/2042098616672572.
38. Núñez-Torres R, Martín M, García-Sáenz JÁ, Rodrigo-Faus M, del Monte-Millán M, Tejera-Pérez H, Pita G, Julio C, Pinilla K, Herraez B, Peiró-Chova L. Association between ABCB1 genetic variants and persistent chemotherapy-induced alopecia in women with breast cancer. *JAMA dermatology*. 2020 Sep 1;156(9):987-91. doi:10.1001/jamadermatol.2020.1867.
39. Kapoor R, Shome D, Doshi K, Vadera S, Patel G, Kumar V. Evaluation of efficacy of QR678® and QR678® Neo hair growth factor formulation in the treatment of persistent chemotherapy-induced alopecia caused due to cytotoxic chemotherapy—A prospective pilot study. *Journal of Cosmetic Dermatology*. 2020 Dec;19(12):3270-9.doi: https://doi.org/10.1111/jocd.13759.
40. Alshari O, Aleshawi A, Al Sharie AH, Msameh AA, Al-Omari I, Msameh R, Almegdadi A, Albals D. The Effect of Nail Lacquer on Taxane-Induced Nail Changes in Women With Breast Cancer. *Breast Cancer: Basic and Clinical Research*. 2020 Jun;14:1178223420929702.doi:https://doi.org/10.1177/1178223420929702.
41. Allah E, Khalil abd el-rafaea S, Elsayed NM. Chemotherapy Induced Dermatological Adverse Reactions and its Effect on Quality of Life for older Women with Breast Cancer. *Annals of the Romanian Society for Cell Biology*. 2021 Aug 5;25(6):18929-40.doi: https://annalsofscb.ro/index.php/journal/article/view/9469.
42. Iijima Y, Yamada M, Endo M, Sano M, Hino S, Kaneko T, Horie N. Dysgeusia in patients with cancer undergoing chemotherapy. *Journal of Oral and Maxillofacial Surgery, Medicine, and Pathology*. 2019 May 1;31(3):214-7.doi:https://doi.org/10.1016/j.ajoms.2019.01.006.
43. Malta CE, de Lima Martins JO, Carlos AC, Freitas MO, Magalhães IA, de Vasconcelos HC, de Lima Silva-Fernandes IJ, de Barros Silva PG. Risk factors for dysgeusia during chemotherapy for solid tumors: a retrospective cross-sectional study. *Supportive Care in Cancer*. 2021 Jul 20:1-3.doi: 10.1007/s00520-021-06219-4.
44. Morita M, Kishi S, Ookura M, Matsuda Y, Tai K, Yamauchi T, Ueda T. Efficacy of aprepitant for CHOP chemotherapy-induced nausea, vomiting, and anorexia. *Current problems in cancer*. 2017 Nov 1;41(6):419-25.doi:https://doi.org/10.1016/j.currprobcancer.2017.09.001.
45. Park HS, Shin NY. Comparison of Effects of Different Acupressure Methods on Nausea, Vomiting, and Anorexia for Breast Cancer Patients: Among Patients Undergoing Chemotherapy. *Journal of Korean Biological Nursing Science*. 2020;22(2):102-10.doi: https://doi.org/10.7586/jkbns.2020.22.2.102.
46. Naito Y, Kai Y, Ishikawa T, Fujita T, Uehara K, Doihara H, Tokunaga S, Shimokawa M, Ito Y, Saeki T. Chemotherapy-induced nausea and vomiting in patients with breast cancer: a prospective cohort study. *Breast Cancer*. 2020 Jan;27(1):122-8.doi:https://doi.org/10.1007/s12282-019-01001-1.



**Kanagaraj Suganya and Sundaravadivelu Sumathi**

47. Tsuji D, Matsumoto M, Kawasaki Y, Kim YI, Yamamoto K, Nakamichi H, Sahara Y, Makuta R, Yokoi M, Miyagi T, Itoh K. Analysis of pharmacogenomic factors for chemotherapy-induced nausea and vomiting in patients with breast cancer receiving doxorubicin and cyclophosphamide chemotherapy. *Cancer Chemotherapy and Pharmacology*. 2021 Jan;87(1):73-83.doi:<https://doi.org/10.1007/s00280-020-04177-y>.
48. Nyrop KA, Deal AM, Reeder-Hayes KE, Shachar SS, Reeve BB, Basch E, Choi SK, Lee JT, Wood WA, Anders CK, Carey LA. Patient-reported and clinician-reported chemotherapy-induced peripheral neuropathy in patients with early breast cancer: Current clinical practice. *Cancer*. 2019 Sep 1;125(17):2945-54.doi:<https://doi.org/10.1002/cncr.32175>.
49. Simon NB, Danso MA, Alberico TA, Basch E, Bennett AV. The prevalence and pattern of chemotherapy-induced peripheral neuropathy among women with breast cancer receiving care in a large community oncology practice. *Quality of Life Research*. 2017 Oct;26(10):2763-72.doi:<https://doi.org/10.1007/s11136-017-1635-0>.
50. Zhi WI, Chen P, Kwon A, Chen C, Harte SE, Piulson L, Li S, Patil S, Mao JJ, Bao T. Chemotherapy-induced peripheral neuropathy (CIPN) in breast cancer survivors: a comparison of patient-reported outcomes and quantitative sensory testing. *Breast cancer research and treatment*. 2019 Dec;178(3):587-95.doi:<https://doi.org/10.1007/s10549-019-05416-4>.
51. Chaulin AM, Abashina OE, Duplyakov DV. Pathophysiological mechanisms of cardiotoxicity in chemotherapeutic agents. *Russian Open Medical Journal*. 2020;9:e0305.doi: 10.15275/rusomj.2020.0305.
52. Geisberg CA, Sawyer DB. Mechanisms of anthracyclinecardiotoxicity and strategies to decrease cardiac damage. *Current hypertension reports*. 2010 Dec 1;12(6):404-10.doi: 10.1007/s11906-010-0146-y.
53. Cardinale D, Colombo A, Lamantia G, Colombo N, Civelli M, De Giacomi G, Rubino M, Veglia F, Fiorentini C, Cipolla CM. Anthracycline-induced cardiomyopathy: clinical relevance and response to pharmacologic therapy. *Journal of the American College of Cardiology*. 2010 Jan 19;55(3):213-20.doi:10.1016/j.jacc.2009.03.095.
54. Ferreira de Souza T, Quinaglia AC Silva T, Osorio Costa F, Shah R, Neilan TG, Velloso L, Nadruz W, Brenelli F, Sposito AC, Matos-Souza JR, Cendes F. Anthracycline therapy is associated with cardiomyocyte atrophy and preclinical manifestations of heart disease. *JACC: Cardiovascular Imaging*. 2018 Aug;11(8):1045-55.doi:10.1016/j.jcmg.2018.05.012.
55. Cho H, Lee S, Sim SH, Park IH, Lee KS, Kwak MH, Kim HJ. Cumulative incidence of chemotherapy-induced cardiotoxicity during a 2-year follow-up period in breast cancer patients. *Breast cancer research and treatment*. 2020 Jul;182:333-43.doi:<https://doi.org/10.1007/s10549-020-05703-5>.
56. Lavan AH, O'Mahony D, Buckley M, O'Mahony D, Gallagher P. Adverse drug reactions in an oncological population: prevalence, predictability, and preventability. *The oncologist*. 2019 Sep;24(9):e968.doi: 10.1634/theoncologist.2018-0476.
57. Assi S, Torrington E, Cheema E, Hamid AA. Adverse drug reactions associated with chemotherapeutic agents used in breast cancer: Analysis of patients' online forums. *Journal of Oncology Pharmacy Practice*. 2021 Jan;27(1):108-18.doi: <https://doi.org/10.1177/1078155220915767>.
58. Kissane DW, Grabsch B, Clarke DM, Smith GC, Love AW, Bloch S, Snyder RD, Li Y. Supportive-expressive group therapy for women with metastatic breast cancer: survival and psychosocial outcome from a randomized controlled trial. *Psycho-Oncology: Journal of the Psychological, Social and Behavioral Dimensions of Cancer*. 2007 Apr;16(4):277-86.doi: <https://doi.org/10.1002/pon.1185>.
59. Gopinadhan GK, Valsraj K, Kunheri B. Psychological Impact of Breast Cancer Diagnosis and Treatment: The Role of Psychooncology. In *Management of Early Stage Breast Cancer 2021* (pp. 265-276). Springer, Singapore.doi:https://doi.org/10.1007/978-981-15-6171-9_20.
60. Aswath N, VT H. Pharmacovigilance, Adverse Drug Reactions and Future Aspects of Pharmacovigilance in India: A Review Article. *Indian Journal of Public Health Research & Development*. 2019 Dec 1;10(12).
61. Upasani, S.V., Upasani, M.S., Ahmed, A.I.A.T., Jain, N.S. and Pal, P.R., 2021. Clinical view on adverse drug reactions, pharmacovigilance in India and role of clinical pharmacist.doi: <https://doi.org/10.30574/wjarr.2021.10.3.0233>.
62. Liebling DB, Cordova E, Deng G, McKoy JM. Pharmacovigilance of Alternative Medications in the Cancer Setting. In *Cancer Policy: Pharmaceutical Safety 2019* (pp. 37-45). Springer, Cham.doi:https://doi.org/10.1007/978-3-319-43896-2_3.





Kanagaraj Suganya and Sundaravadivelu Sumathi

63. Kalaiselvan V, Srivastava S, Singh A, Gupta SK. Pharmacovigilance in India: present scenario and future challenges. Drug safety. 2019 Mar;42(3):339-46.doi:https://doi.org/10.1007/s40264-018-0730-7.

64. Turan S, Kaur P. Prospective Study of Pharmacovigilance in India-A Review. International Journal of Pharmacy & Life Sciences. 2020 Sep 1;11(9).

65. Pant J, Marwah H, Singh RM, Hazra S. An overview of the worldwide master key for pharmacovigilance and its role in India. Journal of Pharmacovigilance and Drug Research. 2021 Jun 1;2(2):16-22.doi:https://orcid.org/0000-0002-8498-5251

Table 1: Drug and toxicities in breast cancer

Drug	Toxicity
Alkylating agents	Alopecia, Rash, Nail damage, Diarrhea, Loss of appetite, Vomiting, and Nausea, Abdominal discomfort, Myleo suppression, Erythema, Stevens-johnson syndrome, Azoospermia, Oligozoospermia, Hemorrhagic cystitis.
Antimetabolites	Infectious disease, Loss of appetite, Asthenia, Paresthesia, Fever, Fatigue, Neurotoxicity, Multifocal leukoencephalopathy, Tumorlysis syndrome, Hemolyticanemia, Genetic mutations, Gangrenous disorder, Abdominal pain, Alopecia, Photosensitivity, Hepatotoxicity, Thromboembolic disorders, Nasopharyngitis, Bronchitis, Stevens-johnson syndrome, Toxic epidermal necrolysis.
Platinum compounds	Myelosuppression, Hypersensitivity reaction, Nausea and Vomiting, Diarrhea, Alopecia, Hypocalcemia, Hyponatremia, Hypokalemia, Hypomagnesemia, Neuropathy, Paresthesia, Dyesthesia, Fatigue, Neurotoxicity, Ototoxicity, Nephrotoxicity, Arthralgia, Visual loss/disturbance, Hepatotoxicity, Metabolic acidosis, Prolonged QT interval, Edema, Bowel obstruction, Pancreatitis, Pulmonary fibrosis, Pneumonitis, Angioedema, Sepsis.
Vinca alkaloids	Hypertension, Alopecia, Constipation, Bone pain, Jaw pain, Leukopenia, Thrombocytopenia, Neurotoxicity, Acute respiratory distress.
Taxanes	Alopecia, Nausea and Vomiting, Diarrhea, Inflammation of mucous membrane, Myelosuppression, Hypersensitivity reactions, Arthralgia, Peripheral neuropathy, Myalgia, Cardiotoxicity, Stevens-johnson syndrome, Toxic epidermal necrolysis, Opportunistic infection, Sepsis, Pulmonary embolism, Respiratory failure, Edema, Stomatitis, Asthenia, Amenorrhea, Bowel obstruction, Secondary Malignant neoplastic disease.
Anthracyclines	Alopecia, Flushing, Diarrhea, Itching, Rashes, Inflammatory disease, Neuropathy, Myelosuppression, Infectious diseases, Cardiotoxicity, Myocardial infarction, Myocarditis, Congestive heart failure, Pneumonitis, Hypersensitivity reaction, Pulmonary embolism, Tumorlysis syndrome.
Mitomycin C	Loss of appetite, Nausea, Vomiting, Fever, Cellulitis, Disseminated intravascular coagulation, Myelosuppression, Hemolytic uremic syndrome.

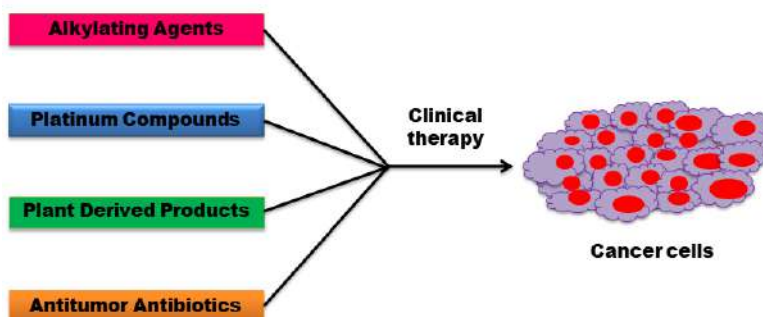


Figure 1: Clinical therapies to treat cancer cells





Formulation Development and Evaluation of Chitosan Nanoparticles Loaded with Cilomilast

V.Parthasarathi^{1*}, V.Kalvimoorthi², N.Deepa³, J.Nandhini¹, R.Santhana Krishnan⁴, K.Devi⁵ and V. Vandhana¹

¹Lecturer, Department of Pharmaceutics, Saveetha College of Pharmacy - SIMATS, Chennai, Tamil Nadu, India.

²Professor, HOD Department of Pharmaceutics, Aadhibhagawan College of Pharmacy, Rantham, Thiruvanamalai, Tamil Nadu, India.

³Principal, Saveetha College of Pharmacy - SIMATS, Chennai, Tamil Nadu, India.

⁴Associate Professor, Department of Pharmaceutics, Saveetha College of Pharmacy- SIMATS. Chennai, Tamil Nadu, India.

⁵Assistant Professor, Department of Pharmacology, Saveetha College of Pharmacy- SIMATS, Chennai, Tamil Nadu, India.

Received: 19 Dec 2021

Revised: 30 Dec 2021

Accepted: 21 Jan 2022

*Address for Correspondence

V.Parthasarathi

Lecturer,

Department of Pharmaceutics,

Saveetha College of Pharmacy - SIMATS,

Chennai, Tamil Nadu, India.

Email: parthaceutics@gmail.com



This is an Open Access Journal / article distributed under the terms of the **Creative Commons Attribution License** (CC BY-NC-ND 3.0) which permits unrestricted use, distribution, and reproduction in any medium, provided the original work is properly cited. All rights reserved.

ABSTRACT

The aim of the present study was to formulate and evaluate the Cilomilast loaded PLGA coated chitosan nanoparticles. The preformulation studies revealed that drug and polymers were compatible. These formulations (F1 to F5) were developed by solvent evaporation method. The formulations were characterized by FTIR, Particle size and TEM analysis. The relationship of polymer concentration on encapsulation efficiency, drug content and in-vitro drug release were determined. Particle size of the formulations was found to be between 100nm to 500nm. TEM analysis shows desirable report that the major particles shows within the limit (below 100nm). Five different formulations were developed by varying the concentration of polymers PLGA and Chitosan. F1 was developed with the ratio of 1:5 (Drug: PLGA), F2 with the ratio of 1:5:7 (Drug:PLGA: Chitosan), F3 with the ratio of 1:10:5 (Drug: PLGA: Chitosan), F4 with the ratio of 1:5:3 (Drug: PLGA: Chitosan) and F5 with the ratio of 1:5:10 (Drug: PLGA: Chitosan). Encapsulation efficiency of these formulation revealed that F1 shows 25.8%, F2 shows 59.6%, F3 shows 60.3%, F4 shows 34.5% and F5 shows 70.1% depends upon the polymer ratio. The F5 formulation shows more encapsulation efficiency (70.1%) and also the drug release shows the 90.64%





Parthasarathi et al.,

within 24hrs. Based on the drug encapsulation efficiency and drug release, F5 was chosen as the best formulation. Release kinetics revealed that F5 formulation followed Higuchi order drug release through Fickian diffusion. Based on this outcomes, it can be concluded that the formulations developed in this work may be considered as an effective controlled drug delivery for treating asthma and COPD.

Keywords: Chitosan; Cilomilast; Polymeric Nanoparticle; Particle Size; Zeta Potential.

INTRODUCTION

Nanoparticles (NPs) are submicron colloidal drug carrier systems made up of natural or synthetic polymers with sizes ranging from 10 to 100 nanometres [1, 2]. When compared to microparticles, NPs have several advantages, including sustained and regulated drug release, site-specific targeting, and a high surface-to-volume ratio. These properties can help patients comply by lowering the requisite drug dose and dosing frequency. Chitosan NPs are biodegradable, more stable, easy to manufacture, less poisonous, and biocompatible [3, 4]. Chitosan is a biodegradable, biocompatible polymer that has been approved for wound treatment applications and is considered safe for human consumption. Chitosan has been utilised as a carrier in polymeric nanoparticles to deliver drugs via a variety of ways. Chitosan is a remarkable polymer that has a long history of application in medicine. Chitin that has been partially or completely deacetylated. Chitosan is a totally biodegradable and biocompatible adhesive polymer that can be found naturally in fungal cell walls and crustacean shells [5, 6]. These are made of chitosan, a biodegradable and biocompatible natural polymer that has also been GRAS approved (Generally Recognized as Safe by the United States Food and Drug Administration). Because of its biocompatibility, chitosan has been studied extensively as a potential drug carrier. According to certain research, coating nanoparticles composed of other materials with chitosan reduces their influence on the body and increases their bioavailability [7, 8].

Chitosan nanoparticles (NPs) are being investigated as medication, protein, and gene delivery vehicles. Chitosan (C) is a semisynthetic polyaminosaccharide made from chitin that has been N-deacetylated. Because of its safe nature, biodegradability, and biocompatibility, as well as its bacteriostatic and mucoadhesive qualities, chitosan has gotten a lot of attention in the biomedical, pharmaceutical, food, and environmental industries. Chitosan nanoparticles (NPs) have been extensively explored as drug, protein, and gene delivery nanocarriers [9, 10]. Because chitosan NPs are soluble in an acidic aqueous solution, they can be used instead of harmful organic solvents. They also have the ability to regulate the release of active substances. The goal of the study was to develop PLGA-coated Chitosan nanoparticles loaded with Cilomilast for the treatment of chronic respiratory diseases. The interaction of opposite charges macromolecules can produce chitosan nanoparticles [11, 12]. Cilomilast is the first non-steroid PDE4 medication for the treatment of Asthma and COPD. Cilomilast's tablet dosage was proven to be successful in clinical testing, however long-term treatment caused vaginal bleeding in females and has the potential to cause cancer in humans. Because PDE4 enzymes are mostly found in smooth muscles and are capable of causing adverse effects, a controlled release nano formulation of Cilomilast that is dose independent is required. One of the nanocarrier systems that uses synthetic PLGA as the core material is PLGA coated Chitosan nanoparticles [13, 14]. PLGA-coated chitosan nanoparticles have the ability to release drugs in a regulated manner and offer a number of benefits. As a result, Cilomilast nanoparticles can be thought of as a regulated medication delivery method for COPD treatment.

MATERIALS AND METHODS

All chemicals like Poly (lactic-co-glycolic acid) (PLGA), Chitosan (mg), Poly Vinyl Alcohol (PVA) were purchased from Swaroop Pharmaceuticals Private Limited, Uttar Pradesh, India.





Parthasarathi et al.,

Preformulation studies

The Preformulation study is a tool to investigate the physical, chemical, pharmacokinetic and pharmaceutical properties of all ingredients either alone or combined with each other in the formulation. The primary aim of the preformulation was to identify, rectify the possible drug-excipients incompatibility and to produce with a longer shelf-life, during that time the original stated drug content should not be fall below a predetermined level [15].

Identification and characterization

The drug Cilomilast and other excipients were identified and characterized their compatibility in formulation was tested. The physical appearance of the active ingredient, polymers and other solvents was performed by visually [16].

Drug excipients compatibility

The IR spectrum of substance was compared with that obtained concurrently for the corresponding USP reference standard provides perhaps the most conclusive evidence of the identity of the substance. Compatibility studies were carried out to study the possible interactions between drug and other inactive ingredients. After the storage of drug-excipients for a period of 30days at 50°C, the compatibility studies should be performed using FTIR. Potassium bromide (KBr) pellet method was carried out. All the ingredients were individually mixed with KBr(1:10) and compressed under 10 tones pressure in a hydraulic pressure to form a transparent KBr pellets. The pellets was scanned from 4000 to 400cm⁻¹ in FTIR spectrometer. From the spectrum, the spectral studies between active and other inactive ingredients were analysed [17].

Chitosan polymeric nanoparticle formulation

Drug loaded PLGA NPs was prepared by a solvent evaporation technique as shown in table 1, a solution of Drug and PLGA in Chloroform was poured into an aqueous surfactant solution (1% w/v) and the resulting mixture was stir with magnetic stirrer to obtain a primary O/W emulsion. The O/W emulsion appears was immediately added drop-wise to an aqueous surfactant solution (1% w/v). This dispersion was further stir overnight with a magnetic stirrer at 1500 rpm. The organic solvent (chloroform) was removed under reduced pressure. Then prepare the Chitosan – PLGA coated NP was obtained by incubating a certain volume of the PLGA NP suspension with equivalent volume of 2mg/ml Chitosan solution (0.5%). This dispersion was again stir with a magnetic stirrer at 1500 rpm for 3-4 h at room temperature and finally the nanoparticles should be formed out [18,19].

CHARACTERIZATION OF CHITOSAN POLYMERIC NANOPARTICLE

Particle size distribution

Particle size was determined by using photon correlation spectroscopy (PCS) using a zetasizer 3000 (Microtrac Blue wave 10.5.4). This analysis yields the mean diameter (z- average measuring range: 20-1000nm). Dynamic light scattering experiments were carried out on an ALV-NIBS high performance particle sizer (ALV GmbH, Germany) equipped with a He-Ne laser with approximately 3mW output at 632.8nm, a digital correlator and a single photo detector module (PMT). Detection of the nanoparticles was carried out in a back scattering mode (scattering angle 173°) with a particle nanosuspension in a dilution of 1:100 in distilled water. The sample temperature was set at 25°C. For each sample 16 runs of 16s were performed to calculate the particle size and distribution width [20, 21].

Zeta potential

Zeta potential (surface charge) of the nanoparticles was determined by laser Doppler anemometry using a Malvern zetasizer. The instrument is a laser based multiple angle particle electrophoresis analyzer. The electrophoretic mobility was obtained by a laser Doppler anemometer connected with the Malvern zetasizer instrument. Using Doppler frequency shifts in a dynamic light scattering from particles, the instrument measures the electrophoretic mobility (or zeta potential) distribution together with the hydrodynamic size of particle in liquid suspension spectroscopy. A suitable amount of sample (50-100µl) was diluted with 5ml of filtered water (0.45µm) and injected in the electrophoretic cell of the instrument where a potential of ±150mV was set. Measurements were performed at 25±0.10°C, on samples approximately diluted with the aqueous surfactant solution. The zeta potential values were calculated by the instrument software using Smoluchosky equation [21, 22].





Parthasarathi et al.,

Surface morphological analysis

The surface morphology of the prepared drug loaded PLGA nanoparticles were examined under Transmission electron microscope (TEM, Philips). The aqueous dispersion (1 drop) was placed over a copper grid of 400 meshes coated with carbon film. The droplet was reduced after 5min with a filter paper to eliminate the excess of nanoparticles. Finally, the sample was air dried prior to placing it in the TEM instrument for analysis [22, 23].

Construction of UV calibration curve of Cilomilast

10mg of drug Cilomilast was weighed accurately and dissolved in few ml of ethanol and dissolve completely, then make up the volume up to 10ml in 10ml standard flask. Then 1ml of this ethanolic solution was diluted in 100ml of phosphate buffer solution at pH 7.4 and sonicate it properly. From this secondary solution, 1ml, 2ml, 3ml, 4ml and 5ml was withdrawn and it was making upto volume 10ml standard flask with phosphate buffer at pH7.4 to produce the solutions with concentration of 1, 2, 3, 4, 5 µg/ml respectively. The resulted working standard solution was mixed thoroughly and then it was analysed for UV absorbance at 212nm[24, 25].

Drug content and encapsulation efficiency

Determination of drug content and encapsulation efficiency of drug loaded nanoparticles were carried out by extracting drugs from the nanoparticle by ultracentrifugation (Eppendorff 5430 R). Briefly 10mg of drug loaded nanoparticles was subjected to centrifuge at 15,000 rpm for 20 minutes. The supernatant was assayed by UV Spectrophotometer (Pharmaspec 1700 SHIMADZU) at 212nm. The drug content and drug encapsulation efficiency (E.E) were determined as follows [26, 27].

$$\text{Drug content } \left(\% \frac{w}{w} \right) = \frac{(\text{Mass of the total drug} - \text{Mass of free drug})}{\text{Mass of Nanoparticles}} \times 100$$

$$\text{Drug entrapment } \left(\% \frac{w}{w} \right) = \frac{(\text{Mass of the total drug} - \text{Mass of free drug})}{\text{Mass of total drug}} \times 100$$

In- vitro drug release

Dialysis bags (cut off 12-14kDa) were filled with a fixed amount of formulation (F1) and put into 100ml of buffer solution (pH 7.4) and stirred at 50 rpm was used as receptor phase. The dissolution medium was phosphate buffer having pH 7.4. The dialysis sacs were equilibrated with dissolution medium for few hours prior to experiment. The experiment was conducted at 37°C±0.5°C. Sampling was performed with interval of every half an hour once for up to 24 hours, 1ml of sample was withdrawn and 1ml of phosphate buffer pH 7.4 was replaced into the same to maintain sink condition. After appropriate dilutions the samples were analysed by UV spectrophotometer at 212nm. The sample procedure was repeated for studying the *in-vitro* drug release of other formulations (F2, F3, F4 and F5) [28, 29].

Drug release kinetic studies

Release kinetic of formulations (F1 to F5) were determined by fitting the drug released data with zero order (Eq.1), first order (Eq. 2), Higuchi equation (Eq.3), Korsmeyer peppas equation (Eq. 4) and Hixson Crowell equation.

$$Q_t = K_0 t \quad \text{Equation 1}$$

$$\ln Q_t = \ln Q_0 - K_1 t \quad \text{Equation 2}$$

$$Q_t = K_1 t^{1/2} \quad \text{Equation 3}$$

The following plots were made: Q_t vs. t (zero order kinetic model), $\ln(Q_0 - Q_t)$ vs. t (first order kinetic model) and Q_t vs $t^{1/2}$ (Higuchi model), where Q_t was the percentage of drug released at time t , Q_0 was the initial amount of drug present in the formulation and K_0 , K_1 and K_1 are the constants of the equations. Further, to confirm the mechanism of drug release, the first 60% of drug release was fitted in Korsmeyer peppas model.

$$M_t/M_\infty = K_p t^n \quad \text{Equation 4}$$



**Parthasarathi et al.,**

Where M_t/M_∞ was the fraction of the drug release at time t , K_p was the rate constant and “ n ” was the release exponent. The value of “ n ” was used to characterize different release mechanisms and was calculated from the slope of the plot of log of fraction of drug released (M_t/M_∞) vs. log time. Zero order kinetics describes the systems where the drug release was independent of its concentration. First order kinetics describes the drug release from the system, where the drug release was concentration dependent. Higuchi classical diffusion describes the drug released through diffusion from polymeric matrix. Korsmeyer Peppas equation describes the exponential equation to swelling polymer. If the release exponential “ n ” value was 0.5 or less, then release will follow Fickian diffusion. If the “ n ” value is higher ($0.5 < n < 0.89$) then it will be non – Fickian diffusion or anomalous transport. Hixson Crowell equation describes that the formulation loses its weight with time either due to erosion or diffusion of drug from the system. Further to verify whether the drug released data was satisfying the above relationships, the plots were judged by the linear-regression co-efficient (R^2) [30, 31].

RESULTS AND DISCUSSION

Preformulation studies

The physical appearance of drug, polymers and other excipients were analyzed visually. The active substance Cilomilast was in the form of white to off white powder. The water soluble chitosan in the form of yellowish powder. The PLGA is in the form of white to light gold colour.

Drug excipients compatibility studies

As the part of preformulation studies drug-excipients compatibility were carried out to study the possible interaction between drug (Cilomilast) and other inactive agents like polymers (PLGA and Chitosan). The spectrum obtained with the drug excipients mixtures was compared to spectrum obtained for the drug alone and excipients alone. Changes in the spectrum, additional or losses from peaks are considered to be significant. IR Spectrum of Cilomilast, PLGA, water soluble chitosan, Cilomilast loaded PLGA nanoparticles with chitosan was shown in Fig No: 1 respectively.

The FTIR spectrum of Cilomilast shows its characteristics band for 1280.5cm^{-1} showed C-N stretch, 3252.36cm^{-1} showed NH stretch, 1651.73cm^{-1} showed C-O stretch. The FTIR spectrum of PLGA shows its characteristics band for 3365cm^{-1} showed O-H stretch, 2943cm^{-1} showed C-H stretch, 1777cm^{-1} showed C=O stretch. The FTIR spectrum of water soluble chitosan shows absorption bands at 3964.79cm^{-1} and 3840.38cm^{-1} showed O-H stretch, 3424.46cm^{-1} showed N-H stretch, 2882.76cm^{-1} and 2138.44cm^{-1} showed C-H stretch, 1657.32cm^{-1} showed C=O stretch, 1386.29cm^{-1} showed C-H bend, 1086.14cm^{-1} showed C-O stretch. The FTIR spectrum of Formulation F5 illustrate the absorption band at 1636.3cm^{-1} showed C=O stretch, 3465.46cm^{-1} showed N-H stretch, 1265.4cm^{-1} C-N stretch indicates the drug Cilomilast. The absorption band at 2943cm^{-1} showed C-H stretch and 3365cm^{-1} showed O-H stretch indicates the polymer PLGA. The absorption band at 1657.32cm^{-1} showed C=O stretch indicates the polymer Chitosan. Spectra for drug and excipients were taken using FTIR spectrometer and compared with the formulation spectra. There was no appearance of any characteristic peak in the FTIR spectra confirms the absence of chemical interaction between drug and polymer. The standard curve of the drug Cilomilast was obtained by plotting the concentration from $1\mu\text{g/ml}$ to $5\mu\text{g/ml}$ against its respective absorbance at 212nm .

Particle size distribution

Particle size distribution are the most important characteristics of the nanoparticles. They determine the distribution, biological fate, toxicity and targeting ability of these delivery systems. In addition, they can be influence drug loading, drug release and stability of nanoparticles. The particle size of the formulations was less than 500nm which illustrated from particle size histograms (Figure No: 2). Submicron nanoparticles, but not larger microparticles are taken up by the majority of cell types. Smaller particles have higher surface area/ volume ratio, which makes it easier for the encapsulated drug to be released from the particles via diffusion and surface erosion and also have the added advantage for the drug loaded nanoparticles to penetrate into and permeate through the physiological drug barriers.



**Parthasarathi et al.,**

The smaller particles will have greater ease of entry and durability in the cells. In contrast, larger particles have larger cores which allow more amount of drug to be encapsulated per particle and give slower release. Thus, control of particle size provides a means of tuning drug release rates. Results of average particle size are listed below in Table no: 2. The data indicate the particle size of PLGA nanoparticles and PLGA-Chitosan Nanoparticles. The gradual increase in particle size was observed from the formulation F1-F5 indicates that increase in polymer concentration increases the size of nanoparticles.

Drug content and encapsulation efficiency

The drug content and encapsulation efficiency in different formulations were shown in Table no: 2. The drug content and encapsulation efficiency were mainly affected by the polymer and drug ratios. The improved encapsulation efficiency was due to the greater proportion of polymer with respect to the amount of drug. Due to the high encapsulation efficiency, the drug should be released slowly and produce sustain action.

Surface morphological analysis

The particle morphology of Cilomilast nanoparticles by Transmission electron microscopy (TEM) were used for further information and prove that the particle were identical shape. The particle size of the formulated Cilomilast nanoparticles by the dynamic light scattering and zetasizer (Malvern, UK) were found to be within range 100-200nm. Estimation of particle size from TEM images shows good with laser light scattering. The particles showed great aggregation which may be due to more amount of polymers present in the formulations. They were reported by the following Figure no: 3,

In-vitro drug release

The percentage release of Cilomilast from PLGA coated chitosan nanoparticles were shown in the Figure: 4. In the overall formulations, F5 formulation exerts maximum drug release in 24hrs. The initial burst release followed by the sustained release was observed in all formulations. The initial burst release may be probably caused by the drug absorbed on the surface of nanoparticles.

Drug release kinetic study

Release kinetics of optimized formulations F1 to F5 was determined by fitting the drug released data with the Zero order, First order, Higuchi equation, Korsmeyer-Peppas equation and Hixson Crowell equation. The results were given in the Table no: 3.

From the release kinetic studies, it was observed that the drug release from the formulations (F1 to F5). The zero order rate equation describes the systems where the drug release rate is independent of the concentration. The first order equation which describes the drug release from systems where the release rate is concentration dependent, where shows the log of percentage drug remaining Vs. Time (h). Higuchi model describes the release of drugs from matrix as a square root of time- dependent process based on Fickian diffusion. The Higuchi square root kinetics, shows the Square root of Time vs. Time (h). The release constant was calculated from the slope of appropriate plots, and the regression coefficient (r^2) was determined. The korsmeyer-peppas equation shows the results from peppas plots, $\log T$ Vs \log of percentage drug released. The release exponent 'n' was more than 0.45 and less than 0.89 ($0.45 < n < 0.89$) which indicate a coupling of the diffusion and erosion mechanism which called anomalous diffusion and may indicate that the drug release is controlled by more than one process. Peppas used this n value in order to characterize different release mechanism. If the n value is 0.5 or less, the release mechanism follows Fickian diffusion and higher values $0.45 < n < 0.89$ for mass transfer follow a non-Fickian model (anomalous transport). The Hixson crowell equation was confirmed that the formulation loses its weight with time either due to erosion or diffusion or the drug from the system as a function of time. Hence, the Higuchi model shows more r^2 value than the other models.



**Parthasarathi et al.,**

The Higuchi plot confirmed that all formulations obeyed the Higuchi equation that the drug releases through diffusion from polymeric matrix.

CONCLUSION

Cilomilast loaded PLGA coated chitosan nanoparticles were developed by solvent evaporation method. The formulations were characterized by FTIR, Particle size and TEM analysis. The relationship of polymer concentration on encapsulation efficiency, drug content and in-vitro drug release were determined. Particle size of the formulations was found to be between 100nm to 500nm. TEM analysis shows desirable report that the major particles shows within the limit (below 100nm). The F5 formulation shows more encapsulation efficiency (70.1%) and also the drug release shows the 90.64% within 24hrs. Based on the drug encapsulation efficiency and drug release, F5 was chosen as the best formulation. Release kinetics revealed that F5 formulation followed Higuchi order drug release through Fickian diffusion. Based on this outcomes, it can be concluded that the formulations developed in this work may be considered as an effective controlled drug delivery for treating asthma and COPD.

REFERENCES

1. Pang Z, Beletsi A, Evangelatos K. PEG-ylated nanoparticles for biological and pharmaceutical application. *Adv Drug Del Rev.* 2003; 24: 403- 419.
2. Sun Y, Mezian M, Pathak P, Qu L. Polymeric nanoparticles from rapid expansion of supercritical fluid solution *Chemistry.* 2005; 11:1366-1373.
3. Gaur A, Mindha A, Bhatiya AL. Nanotechnology in Medical Sciences. *Asian Journal of Pharmaceutics.* 2008; 80-85.
4. Soppinath KS, Aminabhavi TM, Kulkurni AR, Rudzinski WE. Biodegradable polymeric nanoparticles as drug delivery devices. *J Control Release.* 2001; 70:1-20
5. Kohler M, Fritzsche W. *Nanotechnology, an introduction to nanostructuring.* Wiley-VCH. 2007; 2.
6. Catarina PR, Ronald JN, Antonio JR. Nano capsulation. Method of preparation of drug – loaded polymeric nanoparticles: *Nanotechnology, Biology and medicine.* 2006; 2:8-21.
7. Kreuter J. Nanoparticles. In *Colloidal drug delivery systems*, J. K., Ed. Marcel Dekker: New York. 1994; 219-342.
8. Pang Z, Beletsi A, Evangelatos K. PEG-ylated nanoparticles for biological and pharmaceutical application. *Adv Drug Del Rev.* 2003; 24: 403- 419.
9. Lambert G, Fattal E, Couvreur P. Nanoparticulate system for the delivery of antisense oligonucleotides. *Adv Drug Deliv Rev.* 2001; 47:99-112.
10. Lambert G, Fattal E, Couvreur P. Nanoparticulate system for the delivery of antisense oligonucleotides. *Adv Drug Deliv Rev.* 2001; 47:99-112.
11. Kreuter J. Physicochemical characterization of polyacrylic nanoparticles. *Int. J. Pharm.* 1983; 14: 43 -58.
12. Quintanar-Guerrero D, Allemann E, Fessi H, Doelker E. Preparation techniques and mechanism of formation of biodegradable nanoparticles from preformed polymers. *Drug Dev Ind Pharm.* 1998; 24:1113-28.
13. Allemann E, Gurny R, Doelker E. Drug-loaded nanoparticles preparation methods and drug targeting issues. *Eur J Pharm Biopharm.* 1993; 39:173-91.
14. Kompella UB, Bandi N, Ayalasomayajula SP. Poly (lactic acid) nanoparticles for sustained release of budesonide. *Drug Delivery Technology.* 2001; 1:1-7.
15. Yoo HS, Oh JE, Lee KH, Park TG. Biodegradable nanoparticles containing PLGA conjugates for sustained release. *Pharm Res.* 1999; 16: 1114-8.
16. Chorney M, D'Anenberg H, Golomb G. Lipophilic drug loaded nanospheres by nano precipitation: effect of the formulation variables on size, drug recovery and release kinetics. *J Control release* 2002; 83: 389-400.
17. Couvreur P, Dubernet C, Puisieux F. Controlled drug delivery with Nano particles: current possibilities and future trends. *Eur J Pharm Biopharm.* 1995; 41:2-13.





Parthasarathi et al.,

18. DeAssis DN, Mosqueira VC, Vilela JM, Andrade MS, Cardoso VN. Release profiles and morphological characterization by atomic force microscopy and photon correlation spectroscopy of 99mTechnetium – fluconazole nanocapsules. *Int J Pharm.* 2008; 349: 152 –160.
19. Takeuchi H, Yamamoto Y. Mucoadhesive nanoparticulate system for peptide drug delivery. *Adv Drug Del Rev.* 2001; 47: 39-54.
20. Ueda H, Kreuter J. Optimization of the preparation of loperamide- loaded poly (l-lactide) nanoparticles by high pressure emulsification solvent evaporation. *J Microencapsul.* 1997; 14:593-605.
21. Goldberg M, Langer R, Jia X. Nanostructured materials for applications in drug delivery and tissue engineering. *J Biomater Sci Polym.* 2007; 18:241-68.
22. Jores K, Mehnert W, Drecusler M, Bunyes H, Johan C, Mader K. Investigation on the structure of solid lipid nanoparticles and oil-loaded solid nanoparticles by photon correlation spectroscopy, field flow fractionation and transmission electron microscopy. *Journal of Control Release.* 2004; 17:217-227.
23. Muhlen AZ, Muhlen EZ, Niehus H, Mehnert W. Atomic force microscopy studies of solid lipid nanoparticles. *Pharmaceutical Research.* 1996; 13:1411-1416.
24. Jaiswal J, Gupta SK, Kreuter J. Preparation of biodegradable cyclosporine nanoparticles by high-pressure emulsification solvent evaporation process. *J Control Release.* 2004; 96:1692-178.
25. Ubrich N, Bouillot P, Pellerin C, Hoffman M, Maincent P. Preparation and characterization of propranolol hydrochloride nanoparticles: A comparative study. *J Control release.* 2004:291-300.
26. Song CX, Labhasetwar V, Murphy H, Qu X, Humphrey WR, Shebuski RJ, Levy RJ. Formulation and characterization of biodegradable nanoparticles for intravascular local drug delivery. *J Control Release.* 1997; 43:197- 212.
27. Vandervoort J, Ludwig A. Biodegradable stabilizers in the preparation of PLGA nano particles: a factorial design study. *Int J Pharm.* 2002; 238:77-92.
28. Scholes PD, Coombes AG, Illium L, Davis SS, Wats JF, Ustariz C, Vert M, Davies MC. Detection and determination of surface levels of poloxamer and PVA surfactant on biodegradable nanospheres using SSIMS and XPS. *J control Release.* 1999; 59: 261 - 278.
29. Li YP, Pei YY, Zhou ZH, Zhang XY, Gu ZH, Ding J, Zhou JJ, Gao XJ. PEGylated polycyanoacrylate nanoparticles as tumor necrosis factor-alpha carriers. *Journal of Control Release.* 2001; 71:287-296.
30. Zambaux M, Bonneaux F, Gref R, Maincent P, Dellacherie E., Alonso M, Labrude P, Vigneron C. Influence of experimental parameters on the characteristics of poly(lactic acid) nanoparticles prepared by double emulsion method. *Journal of Control Release.* 1998; 50:31-40.
31. Puglisi G, Fresta M, Giammona G, Ventura CA. Influence of the preparation conditions on poly (ethyl cyanoacrylate) nanocapsule formation. *International Journal of Pharmaceutics.* 1995; 125:283-287.

Table 1: Composition of drug and polymer ratio for formulation of Chitosan polymeric nanoparticle

S.No	Formulation code	Cilomilast (mg)	Polymer Conc.		Surfactant
			PLGA (mg)	Chitosan (mg)	PVA (%)
1.	F1	3	15	-	1
2.	F2	3	15	21	1
3.	F3	3	30	15	1
4.	F4	3	15	9	1
5.	F5	3	15	30	1





Parthasarathi et al.,

Table 2: Characterization of chitosan polymeric nanoparticle (SD ± n-3)

S.No	Formulation	Particle Size (nm)	Drug content (%)	Encapsulation efficacy (%)
1.	F1	422 ± 4.32	97.6± 2.38	25.8± 3.68
2.	F2	605.7± 16.68	94.3± 3.32	59.6± 6.44
3.	F3	493± 5.56	93.2± 2.34	60.3± 4.86
4.	F4	636± 18.28	95.4± 3.48	34.5± 2.42
5.	F5	388± 3.46	92.5± 2.78	70.1± 3.22

Table 3: Release kinetics studies of chitosan polymeric nanoparticle F1-F5.

S.No	Zero order, R ²	First Order, R ²	Higuchi, R ²	Hixon Crowell, R ²	Krosmeier peppas	
					R ²	N
F1	0.975	0.024	0.992	0.007	0.750	0.157
F2	0.873	0.012	0.990	0.037	0.788	0.094
F3	0.926	0.003	0.994	0.017	0.748	0.104
F4	0.931	0.000	0.990	0.003	0.729	0.112
F5	0.949	0.005	0.952	0.024	0.873	0.084

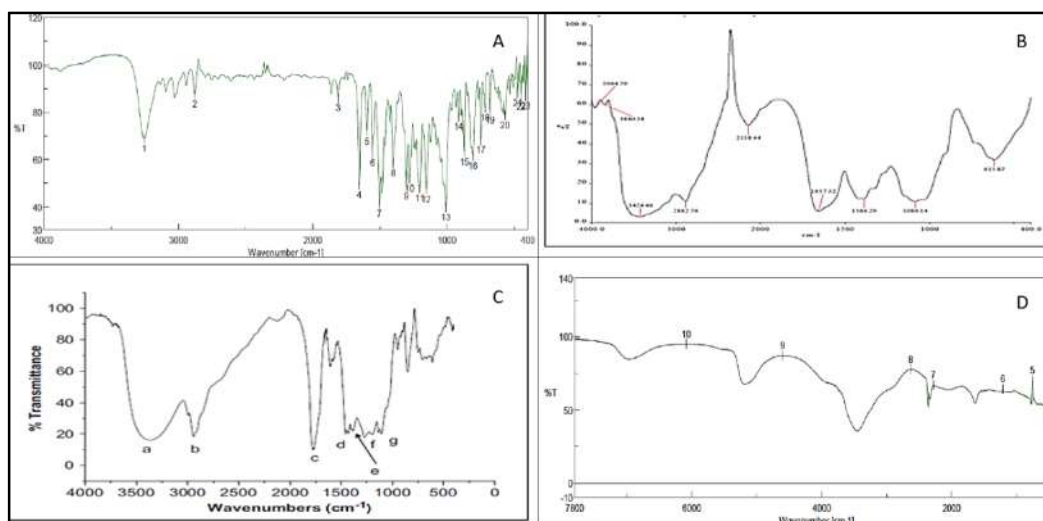


Fig.:1(A) FTIR spectrum of Cilomilast; (B) FTIR spectrum of PLGA; (C) FTIR spectrum of chitosan; (D)FTIR spectrum of Cilomilast nanoparticle formulation (F5)





Parthasarathi et al.,

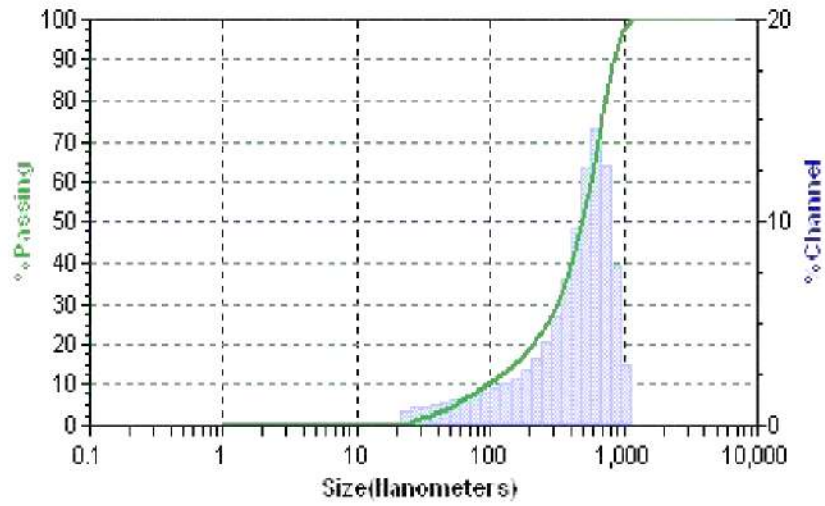


Figure 2: Average particle size of Cilomilast nanoparticle formulation (F5)

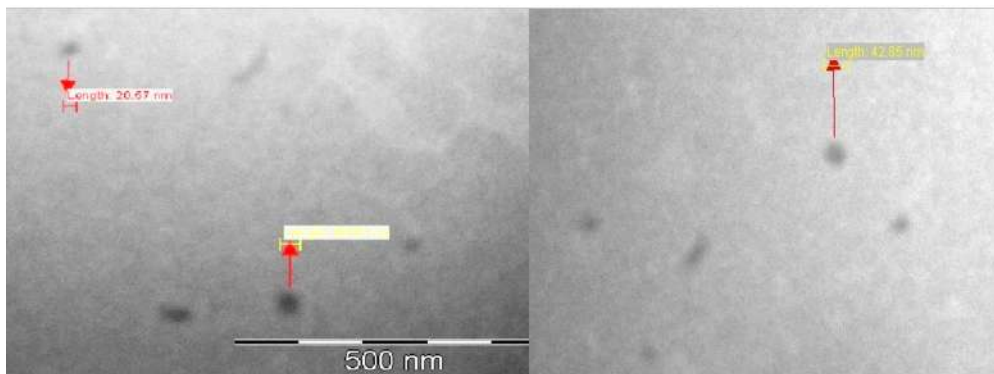


Fig.:3 TEM report of Cilomilast loaded PLG Ananoparticles

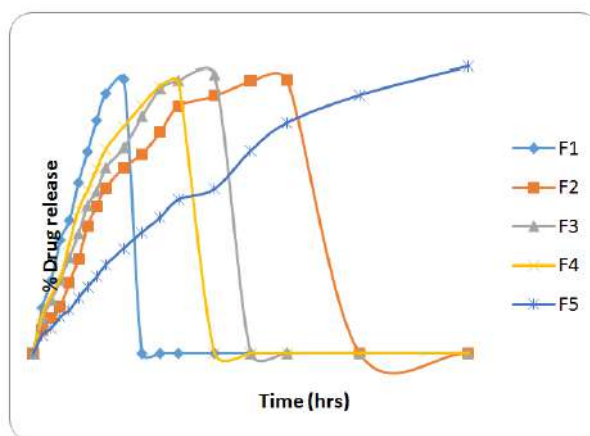


Fig: 4. In-vitro drug release studies of Cilomilast loaded PLG Ananoparticles (F1-F5)





A Machine Learning Design Approach for System Performance and Traffic Resiliency in Cloud Platform

Nilayam Kumar Kamila^{1*}, Subhendu Kumar Pani² and P.K. Bharti³

¹Research Scholar, Department of Computer Science & Engineering, Shri Venkateshwara University, Gajraula, Uttar Pradesh, India.

²Professor, Krupajal Engineering College, Biju Patnaik University of Technology, Odisha, India.

³Hon'ble Vice Chancellor, Shri Venkateshwara University, Gajraula, Uttar Pradesh, India.

Received: 28 Nov 2021

Revised: 21 Dec 2021

Accepted: 13 Jan 2022

*Address for Correspondence

Nilayam Kumar Kamila

Research Scholar,

Department of Computer Science & Engineering,

Shri Venkateshwara University,

Gajraula, Uttar Pradesh, India.



This is an Open Access Journal / article distributed under the terms of the **Creative Commons Attribution License** (CC BY-NC-ND 3.0) which permits unrestricted use, distribution, and reproduction in any medium, provided the original work is properly cited. All rights reserved.

ABSTRACT

Data is the key factor for all artificial intelligence-based machine learning systems. In any research area, including high-performance computing systems, meaningful data and the behavior of data primarily and inherently determine a system's performance. The resiliency on stacks of the performance is also an additional measurement of today's modernized and improvised systems. There is great research interest in cloud resources, e.g., load balancers and server instances, sharing their respective performance data, and the relative corrective decisions could be made on the existing system's flow traffic to achieve overall system resiliency. In this article, we discuss a few of the design approaches which provide more stabilized implementational strategy considerations for advanced modernized high-performance resilient platforms and/or systems. We also discussed the challenges for which the proposed design has the potential to overcome the existing issues of current platforms. The mathematical analysis and result comparison shows that the proposed design approach has an advantage over the existing designs and practice. This article will also be helpful for other researchers exploring the implementational considerations of machine learning in high-performance computing research areas.

INTRODUCTION

Platforms with high volumes of traffic are designed with multi-tier architectures to satisfy the different system dependencies, business use cases and users' privileges. In today's world, almost all systems follow the basic three layers of architecture: the presentation tier [web server], application tier [application server] and data tier [database or data store]. With the introduction of traditional monolithic and modern microservices[2] architectures, a few of the tiers are either clubbed/integrated (in the monolithic case) or multi-distributed (in the microservices case) so as to

39125





Nilayam Kumar Kamila et al.,

reduce the cross-system dependency. However, the systems still follow the multi-tier structure and the data flows between the systems to achieve a “business-as-usual” flow without any major interruption. For example, if a system depends on multiple types of customers, e.g., credit card customers and home loan customers, and two different data stores are maintained, then if one data store is not operational for a specific period of time, credit card customers would not be impacted. To achieve this understanding of how resilient [7] each system with other system, different aspects of design and architecture are adopted, and based on system dependency, the traffic flows into designated upstream systems to retrieve or update the data. Currently, a larger number of advanced platforms still require manual intervention for error recovery, failure remediations and recovery from the system performance. This manual intervention is also applied when a system needs resiliency, i.e., the system discovers that the other co-cluster[10] is working more effectively than the current system, but there is no mechanism to self-detect or resiliently recover to the other platform.

Today, most advanced organizations focus on performing application development by maintaining automated infrastructure pipelines and deployments. A sample system architecture is shown in Figure 1. Most common failures, e.g., application issues, power outages, hardware issues, etc., could be improved by maintaining or quickly instantiating and placing the equivalent co-system[12] in the correct scope. In this article, we mainly focus on such cases and scenarios: we propose a few architectures and discuss maintaining the system performance and resilience to recover from major and common instantaneous failures, which provides a great level of customer satisfaction in real time. In this article, we discuss a few of the existing system designs and failures in the next section. The maintenance complexity and real-time issues will also be discussed, followed by proposed feasible solutions. The advantages and the feasibility study of the proposed solution will also be part of successive sections. The development and model implementation of the proposed system is part of the scope of our future work. We will discuss the system design and feasibility outcomes in our conclusion section, along with the scope of our future work.

Literature Survey and Research Gap

Johan et al. [1] discussed future network communications, processes and challenges and analyzed the overall topology of traffic systems; then, they analyzed an optimized load balancing structure to be further restructured. Future enhancements of this idea may lead to an automated strategic/decision-making approach to routing balanced measurements in the existing network to achieve network and system load resiliency. Similarly, Pan et al. [3] discuss multiple cases for cloud radio access and network simulated systems. They explain how critical the data flow in a real-time system and the system resiliency are in ensuring the overall performance of the system. A real-time system absolutely requires an automated mechanism to correct the traffic or network flow of the system. The authors used the 5G network mechanism and inserted an automated driving system into the system to provide the optimized solution for the network system. Xie et. al [4] focused extensively on fault tolerant systems and proposed a fault sensing system that was integrated with the traffic flow mechanism to reduce the fault flow and the traffic loads. This improves the traffic resiliency and improves the quality of the traffic flow service. The authors observed that the higher correlation between the load and faults may result in low-success throughput and that the proposed solution to detect the fault traffic flow improves the traffic resiliency. Xu et al. [5] used a cell transmission model (CTM) design, which was primarily used to formulate the dynamic assignment of weights to the route management system. For the distributed system, the authors used a critical load restoration distributed system (CLR-DS) integrated with the mixed integer linear problem (MILP), which maximizes the distribution of critical loads and hence optimizes the traffic latency. Rohbani et al. [6] discussed the east region and west region dimension-order routing and explored multiple configurations to balance the traffic load. The authors observed that the average packet latency was improved by 7% through the load balancing based configurations. This proposed load balancing approach carries a negligible area of overload but results in significant latency improvements. Como et al. [8] primarily focused on unperturbed networks, with inter-communication between the non-destination nodes, and observed the complexity of the network latency. The authors simplified the network latency by applying the convex optimization theory and optimized the equilibrium flow in and out of the unperturbed network. The authors also confirmed that the adoption



**Nilayam Kumar Kamila et al.,**

of this proposed model minimized the average delay and guarantees strong resilience in the high-performance traffic flow. Arthurs et al. [13] prepared a survey on cloud computing and intelligent systems and discussed multiple issues concerning data flow advancements. Most of the related work on these systems defines hardware improvements and the latency between the systems or network systems. Few authors re-define the data flow approach to optimize the response time and the traffic system's resiliency. In the literature survey, we found that there are multiple attempts to ensure the traffic flow resiliency. Before we discuss the research gap, let us discuss a few of the main failure points of the traffic flow resiliency, specifically prevention, recovery and optimization, as illustrated in Figure 2.

Failure Prevention: In this case, many designers proposed different models to prevent system failures. These include making the application more and more error free and fine-tuning the performance so as to avoid high CPU and memory usage. In this context, many cloud solutions are used to ensure the scalability and adjust the high CPU and memory usage.

Failure Recovery: In this segment, attempts were made to discover how soon a recovery could be made if any failures occur within the system. The addition of more system resources and a switching option to ensure traffic flow to different regions are included as recovery options. However, most importantly, the options to date require human intervention after the deep analysis of the system failures and study into root cause of the failures.

Failure Optimization: In this subsection, the problems of balancing the cost optimization vs the system availability to maintain the error/failure resiliency pattern are discussed. This means that the platform has to maintain a few clusters or systems in ideal/inactive states and will utilize them immediately to switch the traffic to an available cluster/zone/region. If systems are not maintained, then failure recovery will be delayed. If the systems are maintained, then they may be useful for a failure situation that occurs once every year or every 5 years. Thus, deciding between the ideal system availability with a high cost vs adopting a system that will recover 15 minutes late is always a critical decision for all application and platform owners.

To address and to understand more about these problems, we divided them into the following situation-based issues and the relative action states. A chart of real-time issue categories is shown in Figure 3.

Real-Time Issue—Post-Error Actions

This is a typical issue where the action is taken after the initial threshold level of failure of the system, and the action is taken to correct the system. This kind of issue is generally allowed by the system to ensure that the system is not recovering automatically. The threshold levels are set by human experts using a previous set of data and their own engineering experience.

- Recoverable Failures: These types of failures stay with the system for a very short period of time and are recovered from automatically. The main causes of this type of failure are short periods of resource performance issues or the non-responsiveness of dependency systems.
- Unrecoverable Failures: These types of failures stay with the platform systems for a longer period of time and require action to be taken by the application team or the dependent application team. This failure requires solution actions that are agreed upon by multiple associated applications before or after evaluating the root cause of the issue.

Real-Time Issue—Pattern-Based Preventive Actions

- Traffic Behavioral Pattern: There are certain issues that have happened in the past due to a sudden increase in traffic multiple times, and then the system is constantly inoperative.
- Traffic Regional Pattern: For a specific period of time, the majority of the traffic flow occurs in the southern region of a nation, whereas in the regular period the traffic flows to the northern region, where business has expanded. In such cases, the pattern shows that from 12:00–2:00 PM the traffic of the other region is denser; hence, an intelligent decision could be made by the system automatically.





Nilayam Kumar Kamila et al.,

Real-Time Issue—Predictive Decisions

- Calendar Aware Decisions: A few decisions are mostly regulative and routine-based decisions. For example, it is mostly expected that during a major public event, crisis period or major holiday, online activity will increase, and hence the traffic towards the application will be elevated. In such a situation, the application team takes action to increase the cloud resources to prevent the failures which are expected to occur during such periods.
- Administrative Decisions: There are certain cases where local administration changes can change the traffic pattern in advance. Here are some examples: a government issued policy, or nation/state decisions, which are not based on any predictions but are based on looking at the public and periodic situations of local or major geographical areas.

Real-Time Issue—Partial Failures

- Node Failures: Due to some unavoidable reason, there is a single system or node failure in the entire application cluster. This situation arises when multiple nodes are involved in sending the application request, but a single node has failed to send the request. In this unique situation, the traffic has experienced a partial failure: some percentage of the traffic has failed to send.
- Cloud Resource Failures: This is a unique situation in which the resources provided by the cloud systems may fail, and they recover in its standard service time. These types of failures are very uncommon and the recovery is very fast. However, during this period of time, the application system experiences partial failures.
- Dependency System Failures: This is another situation in which dependent systems, such as proxy systems, operating systems and application downstream dependency systems, may lead to short-term failures during which the upstream systems also experience failures. These kinds of failures may be short or long depending on the type of failure. The system may experience partial failures if this happens in only one system out of multiple systems, where the other systems in the clusters are working in accordance with the operational service models.

From the above discussion, we found the following gaps in the research.

An automated corrective system that is intelligent enough to correct the traffic flow in a resilient way should be designed. No specific attempt has been made to correct the traffic flow in a resilient way with a machine learning model mechanism. The automated correction of traffic resiliency was a topic that few authors approached, but an integration of decisions with the automated traffic is an important requirement for today's communication technology and future advancements.

The Proposed Method

Before we present the proposed model, we consider an enterprise standard high-performance-based resilient cloud system model and its functional traffic flow behavior. In Figure 4, we present how a cloud system works. The application systems/ web interface in the respective region will connect to the middleware systems of the same region through the gateway and middle systems route 53. Route 53 is a traffic management cloud resource through which the application interface platform's traffic flow can be controlled. Route 53 has the capability to switch the traffic from one region to another region by configuring the cluster's load balancers. For example, if the Region-I systems are failing or not operating within its normal operation model, then the route 53 configuration can be re-configured or modified to send all the traffic to Region-II, where systems are available to send the real-time traffic. In our proposed model, we mainly focus on the load balancer data. The load balancer data includes the request header and response header data, response status, response time, etc. This data is more helpful if it is accumulated through the S3 buckets. In other words, data which passes through the gateway system, as shown in Figure 5, should pass through route 53 and finally towards the load balancer before reaching the cloud elastic computing systems. While the data set passes through the load balancers, the data can be captured in S3 buckets and fed into the AIML (Artificial Intelligence Machine Learning) model to build the machine learning models. There is data from some other systems that could also be fed into the AIML module, e.g., the cloud watch logs of the cluster instances, instance event loggers, etc.





Nilayam Kumar Kamila et al.,

The Research Method

In this section, we describe two basic parts of the algorithm: the post-error decision model and the AIML-based decision.

Post-Error Decision Model Algorithm

In the post-error decision model algorithm, the cloud matrix $C_m(e)$ for the error level is evaluated against the 500 error code. For any 500 error code for a specific time period from τ_i to $(\tau_i + \tau_t)$, if it crosses the threshold level $T_{pc}(C_m(e))$, then a decision to switch the traffic will be returned; otherwise, the traffic will continue to flow in the same state.

Algorithm 1: Post-Error Decision (C_m)

```

Data:  $C_m = \{m | \text{cloud watch matrix data}\} /*Cloud Watch Matrix Data*/$ 
 $d_i = \{\text{switch, stay}\}$ 
 $d_a = \{\text{stay}\}$ 
Result:  $d_a \in \{d_i | i^{th} \text{ decision}, 1 < i < 2\}$ 
while  $t = \tau_i$  to  $(\tau_i + \tau_t)$ 
  if  $(C_m(e) == 500) /*Evaluate 500 Error code counts*/$   $c += 1$ 
    if  $(c > T_{pc}(C_m(e)))$  do
       $d_a = \{\text{switch}\}$ 
      break;
    end
  end
end
return  $d_a$ 

```

AIML Decision Model

The AIML decision model algorithm takes two parameters into consideration, the set of request and response data, and the AIML state model. The AIML state model is the model at that respective time based on the training and test data sets.

Algorithm 2: AIML Decision (S_a, M)

```

Data:  $S_l = \{r_{ei} | i = 1..p, e \in E\} /*E \text{ set of extracted features for error decision}*/$ 
 $M = ML \text{ Model} = \{(S_{in}, d_i) | S_i \rightarrow d_i, n > 1\}$ 
 $d_i = i^{th} \text{ decision and } S_{in} \text{ is } i^{th} \text{ pattern category having } n \text{ sample/record size.}$ 
 $D = \emptyset, /* \text{Local Decision Set } */$ 
Result:  $d_a \in \{d_i | i^{th} \text{ decision}, 1 < i < n\}$ 
for  $(\text{each } r_{ei} \text{ in } S_l)$  do
   $r_{ei} \text{ evaluates with } M$ 
   $D = D + \{d_i\} /*Add into Decision Set D*/$ 
end
Evaluate  $d_{max} = \text{Max}(D) /*Evaluate Second Max*/$ 
Evaluate  $d_{max2} = \text{Max2}(D) /*Evaluate Second Max*/$ 
Find  $t_s = \text{TimeStamp}(r_{ei} \in S_{max})$ 
Find  $t_{s2} = \text{TimeStamp}(r_{ei} \in S_{max2})$ 
if  $(t_s > t_{s2})$  do
   $d_a = d_{max}$ 
else
   $d_a = d_{max2}$ 
end
 $M = M + \{d_a\}$ 
return  $d_a$ 

```





Nilayam Kumar Kamila et al.,

As time passes, the request and response data along with the decision results are input into the current state model as feedback, and the respective model is upgraded to a more adaptable machine learning (ML) state model. The decision set D is added, with the decisions based on the decision evaluated for the r_{ei} . In the next phase, the d_{max} d_{max2} are evaluated and the timestamp occurrence is calculated as t_s (for d_{max}) and t_{s2} (for d_{max2}). t_s is more recent, and if it wins over the d_{max2} occurrences, then the decision d_{max} is returned. d_{max} is the decision concerning whether to stay in the current state or switch states. Both of the above algorithms are confirmed to attain high recovery states. The post-error method allows the traffic to stay in the current error state before making the decision to switch the traffic, while the AIML model leans towards achieving the highest resiliency for the traffic state with either the current state or with the switch state based on our proposed ML state model decision algorithm. The ML state model is absolutely based on the availability of the other inactive region, as the traffic can flip to the other region at any point in time based on the traffic's behavior. The current state traffic behavior comparison with the training data set at the initial phase and a later stage mean that the ML state model will become more intelligent and provide more realistic decisions that are based on past traffic switch decisions and their results.

RESULTS AND DISCUSSION

In this section we consider different data extraction phases before the application of the machine learning models. As shown in Figure 6, data collection, data ingestion, data extraction, data preparation, data computation and finally data modeling are the key phases which all the data must pass through before being used to construct the machine learning models. We briefly discuss all these phases and their sub-phases as follows.

Data Collection: In the proposed model using machine learning for high-performance computing, data collection is the process in which the load balancers' log data is posted to the s3 bucket logs. These collected data then go through the data ingestion and extraction phase.

Data Ingestion and Extraction: Data ingestion is the process of getting the raw data and loading it into the system in which the operative system can smoothly operate according to its design. It basically consists of many sub-phases, namely, data extraction, transformation and data loading.

In the direct phase of data extraction, the raw data will be extracted from the source system. This is followed by data transportation, in which data is transported to another medium or storage (a data mart, warehouse or stream). Finally, the loading phase will load the data into the destination system according to the destination's design schema.

Data Preparation and Computation: One of the major strategic operations of machine learning is to learn from the existing, historical or current flow of data. In this context, it is highly critical that we prepare the data using filtration, feature extraction and normalization processes.

- Filtration process: This involves using a horizontal row cut mechanism on the collected data set. The raw set of data must be filtered to ensure that only the meaningful records are part of the machine learning computation process.
- Feature Extraction Process: This involves using a vertical column cut mechanism on the collected data set. In this process, the valuable and meaningful columns which contribute to the machine learning algorithm are taken into account. The other non-contributing columns are dropped to avoid noise and ensure the high performance of the ML process.
- Normalization Process: This is a final process to provide a mapping of non-machine data to machine-based numeric data, e.g., true or false should be mapped to 1 or 0. Certain values, e.g., destination DNS names, are mapped to numeric values from 0–n. Also, values from 0–1000 may need to be scaled to 0–1 for better ML performance.

Data Model: The model is the final stage of implementing different ML models with the normalized data set. A PyTorch or TensorFlow model is applied here to build high-performance model stages. The filtered, feature-





Nilayam Kumar Kamila et al.,

extracted and normalized data set is now used to train the model and make the model more robust, with large sets of training and test data and with the data feedback architecture.

Data Presentation: This is the result of the processed data models; it provides information to human experts or to other systems concerning the pattern and behavior of the studied data and additional decisions and improvements that could be made on the constructed intelligent ML models.

Time Complexity

Let the following be the times required to execute different processes for the machine learning mechanism:

Streaming time = τ_s ,

Data ingestion/extraction time = τ_i ,

Data preparation and computation time = T_{pc} ,

Data testing and error feed time = τ_t .

Let there be s transactions per second (TPS) flowing into the system.

Thus, the time taken by the AIML model to process and build the data model is = $\left[\frac{\tau_s}{s}\right] * n + \tau_i * n + T_{pc} + \tau_t * m$,

where n is the training data set and m is the test data set.

When m and n are large, the time for τ_s is equivalent to τ_i and it is also equivalent to τ_t . However, we could take the $\max(\tau_t, \tau_s, \tau_i) = \tau$. The new time complexity equation would become $\tau = \max(\tau_t, \tau_s, \tau_i)$

The total time $T = \tau\left(\frac{n}{s}\right) + \tau\left(\frac{m}{s}\right) + T_{pc} + \tau\left(\frac{m}{s}\right)$ when m and n are very large, on the order of millions of operations per second. We could take the variable $k = (m/s, n/s)$, i. e., $k = (n/s)$

Thus, the total time is $T = 3k\tau + T_{pc}$

$$T = O(k), \text{ i. e., } O(n)$$

where τ and T_{pc} are constant.

Resiliency Restoration Comparison

In this section, we analyze the resiliency of the time of restoration for manual actions, automated actions and ML automated actions.

Comparison of Manual Actions vs Automated Actions

Let the time it takes to identify the issue be τ_i .

The human analysis time is T_{hi} .

The human login action time is T_{hl} .

The time taken by humans to find the root cause is T_{hr} .

The time taken to apply the fix is T_{hf} .

Thus, the total time taken to solve the issue with human action is $T_h = \tau_i + T_{hi} + T_{hl} + T_{hr} + T_{hf}$

Let the complete human action time be $T_{ha} = T_{hi} + T_{hl} + T_{hr} + T_{hf}$.

Thus, the total time for human restoration is $T_h = \tau_i + T_{ha}$.

For automated traffic routing, the time is as follows: $T_a = \tau_i + \tau_t + \tau_{aa}$

where τ_t is the additional threshold time taken to make and apply the automated decision; otherwise, the system will fall into a flip-flop cycle, which would have an adverse impact on the system's resiliency.

Comparison of Automated Actions vs ML Automated Actions

For the ML automated time calculation, we have the following times to consider.





Nilayam Kumar Kamila et al.,

At a very matured state of the ML model, $\tau_i = 0$, as the pattern is matched and the time for the issue to be identified, will tend to 0. However, the time to predict a decision is τ_d . Thus, the time taken by the ML-based configuration is $T_m = \tau_d + \tau_{ma}$. We assume that the actions taken by the ML model and automated model (without ML) to fix the issue are the same, i.e., $\tau_{aa} = \tau_{ma}$.

Thus, $\tau_i = 0$ in the ML automated model. In a real-time environment, the additional threshold time goes from 120 s to 300 s just to ensure that the system goes into the un-recoverable state before the automated action occurs. In such cases, we found that for ML models, once they are built up, the pattern matching query results take τ_d , or milliseconds of time. Even in high-performance ML models, it takes about τ_d , or microseconds of time, i.e., $\tau_d < \tau_t$. Hence, we can conclude that $T_m \ll T_a$.

Now, by comparing the time taken by the automated action vs the human action, we analyzed that $\tau_t + \tau_{aa} < T_{ha}$, where $T_{ha} = T_{hi} + T_{hl} + T_{hr} + T_{hf}$ and $T_{hi} > \tau_t$. In the best-case human scenario, $T_{hf} \sim \tau_{aa}$. So we have $(\nabla ha) = (T_{hi} - \tau_t) + T_{hl} + T_{hr}$ $(\nabla ha) = \delta_{ht} + T_{hl} + T_{hr}$ where $\delta_{ht} = (T_{hi} - \tau_t)$. Also, we assume that $k = T_{hl} + T_{hr}$, i.e., the human action for a specific type of issue in a matured state model becomes a constant time. Hence the new equation is $(\nabla ha) = \delta_{ht} + k$. If we apply the optimization to human action, then we have

$$\begin{aligned} \frac{\partial \nabla ha}{\partial T_h} &= \frac{\partial \delta_{ht}}{\partial T_h} + \frac{\partial k}{\partial T_h} \\ &= \frac{\partial \delta_{ht}}{\partial T_h}, \text{ i.e., } = \frac{\partial (T_{hi} - \tau_t)}{\partial T_h} \\ &= \frac{\partial T_{hi}}{\partial T_h}, \text{ as we consider } \frac{\partial \tau_t}{\partial T_h} = 0, \end{aligned}$$

with τ_t a constant time for a specific platform. This means that the only optimization we could apply to human action is an optimization of the root cause identification. The root cause identification could be a potential area where machine learning could be applied, and based on using an ML intelligent model, the time to issue a fix and resilient correction becomes T_m , i.e., $T_m = \tau_d + \tau_{ma}$.

As we are aware, most of the real-time issues on a stable or para-stable system are of known types or based on a certain pattern. These known patterns and their decision results, once they are fed into the ML models, will make the system more intelligent. This will ensure that for most of the pattern-based behavioral failures, the correct decision is definitely made by the AIML model, making the overall platform a resilient and error-free structural system.

SIMULATION AND RESULTS

We ran the approach for three different categories of simulated environments, i.e., for the manual action environment, automated action environment and ML action environment models. We took 45 samples to test the behavior of the approach in different categories. The idea of this test is to have the traffic switch in the case where the HTTP Status response is returned from the load balancer. For each of the categories, the following simulation environment components and tools are used.





Nilayam Kumar Kamila et al.,

Manual Action

Webpage Load: GT metrix Chrome (Desktop) 90.0.4430.212, Lighthouse 8.3.0

Cloud Environment: Amazon Web Services

Automated Action

Cloud Interface: Amazon Cloud CLI

Environment: Amazon Cloud Services

Automated Triggering Event: Amazon Cloud Watch

ML Action Environment

Cloud Environment: Amazon Web Services

ML Environment: Amazon ML Sage Maker Studio

For manual action, we separate out the logical analysis of the issue and human decisions. We only use the login action for the environment console and route change timing. In real time, however, decision-making would take a considerable time. So, for the human action, it is assumed that all details are ready beforehand, and the web interaction time is considered here for the comparison.

Figure 7 shows a load test time for the web interaction, where we capture the page load time to do manual actions. We observe that the Web browser is approximated to take between 2 to 3 s for this manual action test, which is ideal for many of the standard browser load timings. Figure 8 shows the action time comparison between the manual action and automated action time. The manual action time (login action time+route management page+change of route record time) is approximately 2.89 ms higher than the automated action time. In a real-time cloud environment, the time difference between manual action and automated action is greater, and hence automated action is always preferred. When we compared automated action and the action of our ML model, as shown in Figure 9, for route management record updates, we found an improvement of 0.91 s for the proposed ML action over automated action with 45 samples. Figure 10 shows the 50% sample means; 7.69 s is required for automated action, while the same number of samples takes 8.60 s in the ML-based execution of the operation. This indicates that the proposed solution has an 11.83% lower response time compared to the average response time of the existing automated action strategy. At initial states, we observe that the automated action performed very similarly to the ML action, and after a few iterations, the automated action strategy performed better than the proposed ML action. However, at later stages, the ML action performed well and records an average improvement of ~1.21 s over the automated actions. Similarly, Figure 11 shows the comparison between the manual action vs the ML action. We found that the ML action clearly has a lower action response time. As shown in Figure 12, the 50% mean samples' average action response time is 9.09 s for the manual action and 7.05 s for the proposed ML action. The average improvement is 2.04 s for the proposed solution, which is a 28.93% improvement over the manual action. All of the above testing is validated with a standard test environment. Although test results vary from environment to environment, the depicted results show a significant improvement, and as the number of iterations increases, the ML model will continue to learn and improve the action time and the resilient behavior of the system.

CONCLUSION

In this article, we evaluate different use cases that require manual intervention to make a system operate in its usual mode. The automated approach to correct these errors is an innovative approach which certainly reduces human intervention and allows the system to quickly recover to its usual state. However, we also find that optimizing the automated approach to ensure that errors could be prevented can be done with a matured ML model. Our proposed model, with its machine learning design, through mathematical analysis is shown to have a clear feasibility to be implemented. It can definitely correct the erroneous environment before a major issue occurs. Additionally, with this ML approach, we are not keeping the error traffic above a certain threshold, so as to avoid the traffic switch flip-flop problem. The simulation results show a significant improvement of 11.28% of the action response time over the existing automated actions for over 50% of the samples. Also, it is observed the action response time improves when



**Nilayam Kumar Kamila et al.,**

the ML model has iterated over more samples. As part of our future work, we will implement the binary decision based on the load balancer flow logs to evaluate if the model is really preventing the error traffic and allowing the traffic to operate in its usual mode resiliently, without any manual human intervention.

REFERENCES

1. Johan, A., Johan, F.A., Jorgen, G., Maryam, V., Mats, B., Mehrzad, L., Rahul, N. G., Thomas, L., & Xiaolin, J. (2021). Future industrial networks in process automation: Goals, challenges, and future directions. *Appl. Sci.*, 11, 3345. <https://doi.org/10.3390/app11083345>
2. Eghbal, N., & Lu, P. A parallel data stream layer for large data workloads on WANs.(2020). *IEEE 22nd International Conference on High Performance Computing and Communications; IEEE 18th International Conference on Smart City; IEEE 6th International Conference on Data Science and Systems (HPCC/SmartCity/DSS)*, pp. 897–902. <https://doi.org/10.1109/HPCC-SmartCity-DSS50907.2020.00119>
3. Pan, M., Wen, X., Chen, Y., Lu, Z., Wang, Z., & Wang, L. (2020). A cloud radio access network simulation platform for networked automatic driving. *2020 IEEE 6th International Conference on Computer and Communications (ICCC)*, pp. 839–845. <https://doi.org/10.1109/ICCC51575.2020.9345210>
4. Xie, Q., & Jin, L. (2019). Resilience of dynamic routing in the face of recurrent and random sensing faults. *CoRR abs/1909.11040*
5. Xu, Y., Wang, Y., He, J., Su, M., & Ni, P. (2019). Resilience-oriented distribution system restoration considering mobile emergency resource dispatch in transportation system. *IEEE Access*, 7, 73899–73912. <https://doi.org/10.1109/ACCESS.2019.2921017>
6. Rohbani, N., Shirmohammadi, Z., Zare, M., & Miremadi, S. (2017). LAXY: A location-based aging-resilient Xy-Yx routing algorithm for network on chip. *IEEE Transactions on Computer-Aided Design of Integrated Circuits and Systems*, 36(10), 1725–1738. <https://doi.org/10.1109/TCAD.2017.2648817>
7. Al-Sharidah, A. H., & Al-Essa, H. A. (2017). Toward cost effective and optimal selection of IT disaster recovery cloud solution. *Computer Science and Electronic Engineering (CEEC)*, pp. 43–48.
8. Como, G., Savla, K., Acemoglu, D., Dahleh, M. A., & Frazzoli, E. (2013). Robust distributed routing in dynamical networks–Part II: Strong resilience, equilibrium selection and cascaded failures. *IEEE Transactions on Automatic Control*, 58(2), 333–348. <https://doi.org/10.1109/TAC.2012.2209975>
9. Benslimane, Y., Plaisent, M., Bernard, P., & Bahli, B. (2014). Key challenges and opportunities in cloud computing and implications on service requirements: Evidence from a systematic literature review. *2014 IEEE 6th International Conference on Cloud Computing Technology and Science (CloudCom)*, pp. 114–121.
10. Gamalel-Din, S., Salama, R., & Al-Sowaiel, M. (2014). An expert consultant for cloudifying e-learning environments. *2014 International Conference on Future Internet of Things and Cloud (FiCloud)*, pp. 308–315.
11. Linthicum, D. S. (2017). Connecting fog and cloud computing. *IEEE Cloud Computing*, 4(2), 18–20. <https://doi.org/10.1109/MCC.2017.37>
12. Michalák, P., & Watson, P. (2017). PATH2iot: A holistic distributed stream processing system. *2017 IEEE International Conference on Cloud Computing Technology and Science (CloudCom)*, pp. 25–32.
13. Arthurs, P., Gillam, L., Krause, P., Wang, N., Halder, K., & Mouzakitis, A. (2021). Ataxonomy and survey of edge cloud computing for intelligent transportation systems and connected vehicles. *IEEE Transactions on Intelligent Transportation Systems*. <https://doi.org/10.1109/TITS.2021.3084396>
14. Pahl, C. (2015). Containerization and the PaaS Cloud. *IEEE Cloud Computing*, 2(3), 24–31. <https://doi.org/10.1109/MCC.2015.51>
15. Chung, M. T., Le, A., Nguyen, Q.-H., Nguyen, D.-D., & Thoai, N. (2016). Provision of Docker and InfiniBand in high performance computing. *2016 International Conference on Advanced Computing and Applications (ACOMP)*, pp. 127–134.
16. Chung, M. T., Nguyen, Q.-H., Nguyen, M.-T., & Thoai, N. (2016). Using Docker in high performance computing applications. *2016 IEEE Sixth International Conference on Communications and Electronics (ICCE)*, pp. 52–57.





Nilayam Kumar Kamila et al.,

17. Nilayam, K. K., Sunil, D., & Bhagirathi, N. (2016). Neural network enabled WSN management for energy efficient routing mechanism. *Indian Journal of Science and Technology*, 9(26), ISSN: 0974-6846
18. Fan, C., Wang, Y., & Wen, Z. (2016). Research on improved 2D-BPSO-based VM-container hybrid hierarchical cloud resource scheduling mechanism. *2016 IEEE International Conference on Computer and Information Technology (CIT)*, pp. 754–759.

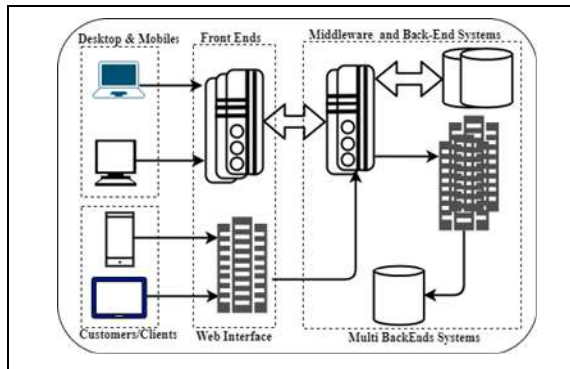


Figure 1: System Architecture with Middleware and Back-End System

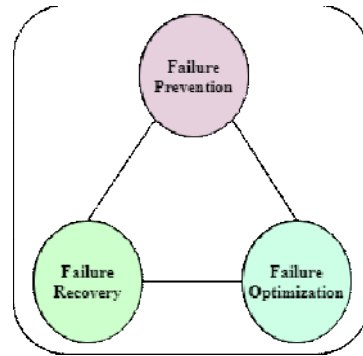


Figure 2: Enterprise System Failures and their Associativity

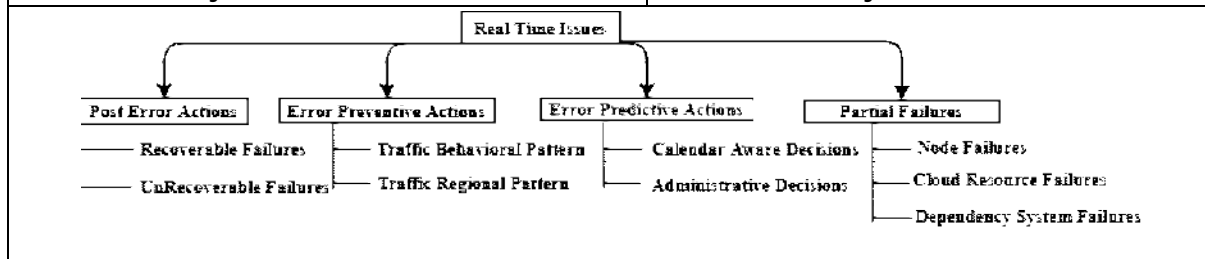


Figure 3: Enterprise System Real-Time Issues and Action Types

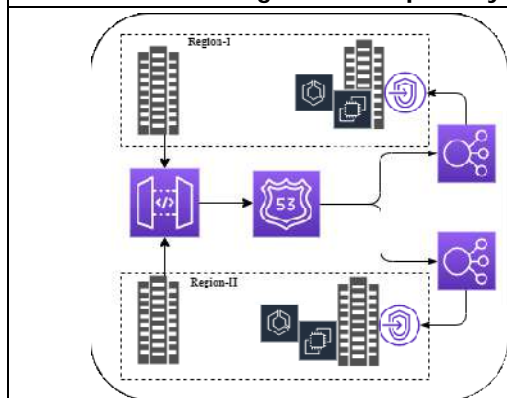


Figure 4: Cloud System with Multi-Region Application Availability

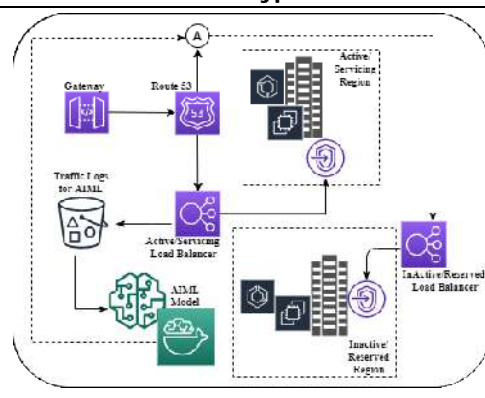


Figure 5: Machine Learning-Based Cloud Traffic Switch





Nilayam Kumar Kamila et al.,

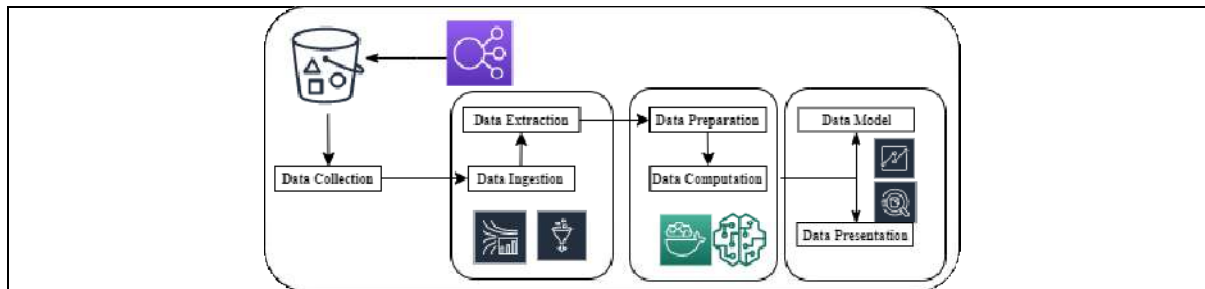


Figure 6: Machine Learning Design with Load Balancer Traffic Flow

Amazon Web Services Sign-In

URL	Status	Domain	Size	Response Time
/	302	console.aws.amazon...	155B	239ms
home	200	console.aws.amazon...	830B	108ms
oauth?client_id=arn%3Aaws%3A...	302	signin.aws.amazon.c...	0	202ms
signin?redirect_uri=https%3A%2...	200	signin.aws.amazon.c...	14.6KB	78ms
4/28 Requests		15.6KB/348KB (83.9KB/1.14MB Uncompressed)		Fully Loaded 2.5s (Onload 1.1s)

Figure 7: Load Validation Response Time for Cloud Environment Interaction

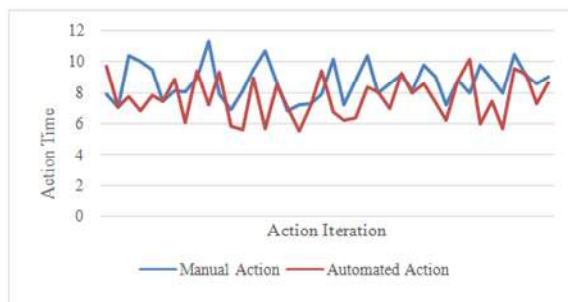


Figure 8: Action Time Comparison for Each Iteration for Manual vs Automated Actions

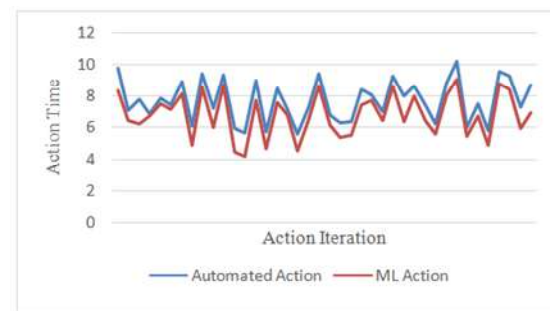


Figure 9: Action Time Comparison for Each Iteration for Automated vs ML Actions



Figure 10: Average Response Time vs Action Samples for Automated and ML Action

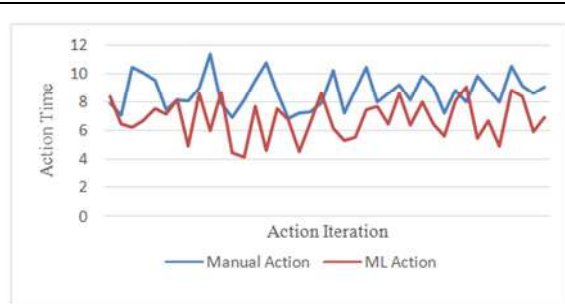


Figure 11: Action Time Comparison for Each Iteration for Manual vs ML Actions





Nilayam Kumar Kamila et al.,

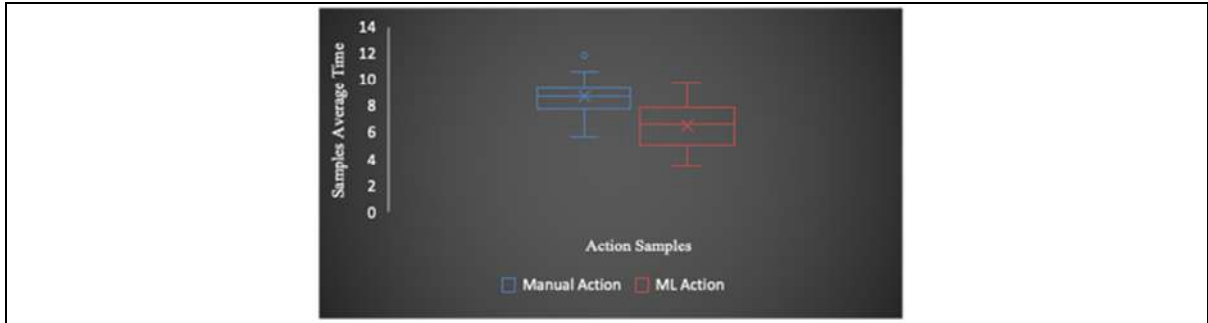


Figure 12: Average Response Time vs Action Samples for Manual and ML Action





Development and Standardization of Naturally Fortified Litti –Chokha

Pramod K. Raghav^{1*}, Uma Kizhuveetil², Kirti Joshi² and Sweta Kumari³

¹Prof., JVWU University, Jaipur, Rajasthan, India.

²Assistant Professor, JVWU University, Jaipur, Rajasthan, India.

³B.tech + M.tech (FBT) Student, JVWU University, Jaipur, Rajasthan, India.

Received: 17 Aug 2021

Revised: 19 Sep 2021

Accepted: 21 Oct 2021

*Address for Correspondence

Pramod K. Raghav*

Prof., JVWU University,
Jaipur, Rajasthan, India.



This is an Open Access Journal / article distributed under the terms of the **Creative Commons Attribution License** (CC BY-NC-ND 3.0) which permits unrestricted use, distribution, and reproduction in any medium, provided the original work is properly cited. All rights reserved.

ABSTRACT

In addition to being popular today in India, Litti Chokha, a traditional dish that comes from Bihar state, is now a dish of people globally. Litti appears to be baati with similar durability and shelter that makes food easy to store and carry on long journeys. The nutritional value of the different filled spices and herbs adds to the potential value of the food in nutraceuticals. In addition, chickpea is an excellent source of minerals (calcium, phosphorus, magnesium, zinc, and iron), fatty acids unsaturated, and β -carotene. Due to these properties and compatibility with wheat flour and chickpeas, Litti is suitable as an amplification agent. In this research, Remove these words development and standardization of the preparation of chickpea flour fortified Litti was studied. Nutritionally enhanced litti were prepared using wheat flour and chickpea flour incorporated in various ratios (20%–60%). Litti prepared from 40% incorporation (C2) had a higher acceptance compared to others. The variant C2 contained protein 8.20g, fat 3.22g, carbohydrate 26.83g, energy 523.0 kcal, and fiber 7.06g.

Keyword: Litti - Chokha, Chickpea, Fortified Food, Product Development, and Sensory Evaluations.

INTRODUCTION

Food fortification is defined as the practice of adding vitamins and minerals to commonly used foods during processing to increase their nutritional value. The 2008 and 2012 Copenhagen Agreement included the enhancement of food in one of the most profitable development priorities. Although mandatory food fortification has been used as a strategy to prevent micronutrient deficiencies in High-Income Countries (HIC), dating to the first ionization of salt in Europe and North America in the 1920s (Hill, 2002).

Litti

Litti-chokha is a conventional Bihari meal that's famous and cherished through each Bihari household. Litti is just like Rajasthani Baati in appearance, however, it has a stuffing made up of sattu mixed with spices and condiments. Littis are spherical highly spiced fried balls of wheat flour or sattu with a crisp outer texture. It is regularly served





Pramod k. Raghav et al.,

with chokha that's a vegetable dish made with boiled/ roasted mashed highly spiced aggregate of potatoes and brinjals. Sattu is ready through dry roasting particularly barley or Bengal gram. They are made into flour after roasting. In Bihar, sattu is served as a savory drink or maybe crammed in a litti/paratha (Sharma 2019).

Wheat

Wheat, any of numerous species of cereal grasses of the genus *Triticum* (own circle of relatives Poaceae) and their fit for human consumption grains. The dietary composition of the wheat grain varies fairly with variations in weather and soil. On average, grains are composed of 12% water, 70% carbohydrates, 12% protein, 2% fat, 1.8% minerals, and 2.2 % crude fibers. Thiamin, riboflavin, niacin, present, however, the milling methods eliminate the maximum of these vitamins with the bran and germ (Shewry, 2007).

Chickpea

Chickpea (*Cicer arietinum*) is a member of the legume, pea, or pulse own circle of relatives, "*Fabaceae*". This mild brown-colored pulse is taken into consideration to be a very good supply of protein. Thought to had been first grown in Mesopotamia as much as 7,500 years ago, chickpeas are taken into consideration as one of the earliest cultivated greens on Earth. Chickpeas are divided into kinds: Desi and Kabuli (Frimpong, 2009).

Sattu

Sattu (*Roasted Bengal Gram*) is made from grains. Due to its high protein content, long shelf life, and excellent taste, sattu is a popular food supplement, especially in rural areas of India. Bengal gram is the legume of the first choice for sattu, especially in Bihar and eastern Uttar Pradesh, but legumes or cereals alone cannot provide balanced nutrition. However, mixing legumes with cereals can improve overall nutrition (Mridula, 2004).

Kalonji

The kalonji (*Nigella Sativa*) he became relating to is *Nigella sativa*. The species is hermaphrodite (has each male and lady organs) and is pollinated with the aid of using Bees. "This *Nigella sativa* is recuperation for all illnesses besides death." Medicinal flowers had been used for treating illnesses numerous long times in numerous indigenous and conventional structures of medicine (Darakhshan, 2015).

Black pepper

Black pepper (*Piper nigrum*), an Indian local spice, has been broadly utilized in human food plans for numerous heaps of years. Piperine has additionally been observed to own anti-mutagenic and anti-tumor influences. Clinical research is limited, however numerous have said the useful healing results of black pepper with inside the remedy of smoking cessation and dysphasia (Ames, 1993).

Garlic

Garlic (*Allium sativum*) is commonly used for conditions related to the heart and blood system. Garlic produces a chemical called allicin. People usually use garlic to treat high blood pressure, high blood cholesterol or other fat content, and arteriosclerosis. It is also used for the common cold, osteoarthritis, and many other conditions (Onyeagba, 2004).

Ginger

Ginger, (*Zingiber officinal*), herbaceous perennial plant of the family *Zingiberaceae*, probably native to southeastern Asia, or its aromatic, pungent rhizome (underground stem) used as a spice, flavoring, food, and medicine. Ginger contains about 2% essential oil; the principal component is zingiberene and the pungent principle of the spice is zingerone. The oil is distilled from rhizomes for use in the food and perfume industries (Altman, 2001).

Asafoetida

Asafoetida (*Ferula assa-foetida*) has been fed on as a spice and a people's medication for centuries. Asafoetida is used as a flavor enhancer in foods and as a traditional medicine for many diseases in many parts of the world. Asafoetida is an oleogumresin obtained from the stem of the *Ferula* plant in the *camellia* family. Asafoetida acts as memory





Pramod k. Raghav et al.,

enhancer, antioxidants, antispasmodic, antibacterial, anticancer, antitoxic, improve digestion, lower blood pressure, prevent liver damage, deworming and reverse effects (Mahendra, 2012).

MATERIAL AND METHODS

In this study, wheat flour and chickpeas were used as the main ingredients to prepare litti. All the ingredients were purchased from Jaipur's local market.

Ingredients

Chickpea, Wheat Flour, Sattu, Brinjals, Potato, Tomato, Green Chilli, Onion, Salt, Kalonji, Black Pepper, Ginger Powder, Garlic Powder, Asafoetida Powder, Carom Seed, Cumin Powder, Dry Mango Powder, Coriander Leaves, Mustard Oil, Refined Oil.

Procedure

Take the bowl; pour chickpea flour and wheat flour in different ratios (1:4, 2:3, and 3:2). Mix refined oil (as moion). Add carom seed, kalonji, and salt. Thoroughly mix all the ingredients. Add a sufficient amount of water for making the soft dough. For Stuffing : In a bowl mix, all the ingredients such as roasted gram flour (Sattu) carom seed powder, asafoetida powder, ginger powder, black pepper, kalonji powder, dry mango powder, garlic powder, cumin powder, salt, and mustard oil. The formulation for Litti: Take the prepared dough and cut it into small pieces. Each Dough should be a 5-6 inch ball. Make a round cover and fill the stuffing in it. Fold the edges and press the joined edges together. Roll the stuffed dough balls to make a round shape litti. Fry the litti in hot oil on a low flame until become golden brown in color.

Sensory Evolution

A 9-point hedonic scale was used to perform the sensory evaluation. A panel of 5 semi-trained panel members was chosen for the process (Larmond, 1977).

Nutrient Content

Moisture content is done using the hot air oven (AOCA, 2012). Nutrient content (Protein, Carbohydrate, Energy, Fiber) of litti were calculated using IFCT (Indian Food Composition Table, 2017)

pH Content

pH was calculated using a pH meter (Ranganna, 1986).

RESULTS AND DISCUSSION

Sensory Analysis

The litti is prepared by the incorporation of chickpea flour in different concentrations. That is 20 %, 40%, 60% (C1, C2, C3,) which is compare with control. The mean score obtained for color varied from 7.33±0.82 to 8.16±0.41. The data indicated that the mean score obtained for the taste was between 7.16±0.75 to 8.00±0.63. The mean scores for fresh control & dry control were all most similar (7.16±0.75). The mean score secured for the appearance was ranging from 7.33±0.82 to 7.66±0.82 the variant with 20%, and 60% levels of incorporation showed almost similar score as the dry control (7.66±0.52). However, the fresh control secured a minimum score (7.33±0.82). The mean score secured for the texture of litti were ranging from 7.00±0.89 to 7.50±0.55 the C2 with a 40% level of incorporation show a higher score. However, both the control obtained min. score (7.00±0.89). The mean score registered for the overall acceptability varied from 7.33±0.82 to 7.66±0.52 the C2 and C3 with 40 & 60% incorporation and fresh control & dry control obtained a similar score i.e., 7.33±0.82 & 7.33±0.82 respectively. Compared with other variants, Litti prepared with 40% incorporation (C2) has higher acceptability.





Pramod k. Raghav *et al.*,

Nutrient content

The moisture content of Litti

The moisture content of prepared variants of Litti was observed is given in Table No. 3 highest moisture content in C1 is 4.12 ± 0.06 and the lowest moisture content in dry control is 2.55 ± 1.09 . The Moisture content Observed of litti fresh control 4.01 ± 0.27 g, dry control 2.55 ± 1.09 g, C1 4.12 ± 0.06 g, C2 3.12 ± 0.84 , C3 2.96 ± 0.85 g, respectively.

Nutrient content of Litti

The nutrient content of litti was calculated using IFCT (Indian Food Composition Table, 2018) were added to obtain the nutrient content for 70g of each variant of litti. The result is presented in Table No. 4 shows an analysis of proximate composition for protein, fat, carbohydrate, energy, crude fiber. The protein content of litti was lower in dry control (7.24g) and highest in C3 (8.68g). The fat content of litti was lower in fresh and dry control (2.80g), and C3 is highest (3.43g). Carbohydrate of litti was lower in C3 (25.39g) and highest in dry control (29.72g). The energy of litti was lower in C3 (514.8kcal) and higher in dry control (539.3kcal). The fiber of litti was lower in fresh control (3.98g) and higher in dry control (11.34g). Observed the Nutrient content of litti protein content 8.68g, fat content 3.43g, carbohydrates 29.72g, energy 539.3kcal, and fiber 11.34g, respectively.

pH Analysis

pH: pH was calculated using a pH meter. Table No. 5 shows analysis pH in litti. The pH content of litti was 6.62 ± 0.01 (dry control) to 6.71 ± 0.01 (C3) which shows that the pH of litti was slightly towards the acidic side. Observed the pH content of litti fresh control 6.70, dry control 6.62, C1 6.65, C2 6.69, C3 6.71, respectively.

CONCLUSION

This study has demonstrated that addition of increasing levels (20%- 60 %) of chickpea flour in the litti affected the quality of sensory attributes. Litti with 40 % chickpea flour has highest acceptability. The findings of the present study may help in developing commercial processing technology for effective utilization of chickpea flour especially for preparation of litti. So it can be inferred from the present study that the litti developed by using chickpea flour was highly acceptable. Therefore, results suggest that there is a great scope for use and marketing of value added litti using chickpea and it can be concluded that chickpea can be utilized for achieving food and nutritional security for nation.

REFERENCES

1. Altman RD, Marcussen KC. (2001) Effects of a ginger extract on knee pain in patients with osteoarthritis. *Arthritis Rheum.* 44(11):2531–2538.
2. Ames BN, Shigenaga MK, Hagen TM. (1993) Oxidants, antioxidants, and the degenerative diseases of aging. *Proc Natl Acad Sci U S A*;90: 7915 - 22.
3. AOAC, (2012) Association of Official Agricultural Chemists (AOAC). International 19th Edition, *Association of Official Analytical Chemists International*: Gaithersburg, MD, USA.
4. Garg B. (2020) Litti Chokha: 7 Benefits of eating Litti Chokha for Health *Digital Marketing Deal*.
5. Darakhshan S, Bidmeshki Pour A, Hosseinzadeh Colagar A, Sisakhtnezhad S. (2015) Thymoquinone and its therapeutic potentials. *Pharmacol Res*; 95–96:138–58. DOI: 10.1016/j.phrs.2015.03.011.
6. Darnton-Hill A, Nalubola F. (2002) Fortification strategies to meet micronutrient needs: successes and failures. *Proceedings of the Nutrition Society*; 61: 231-341.
7. Frimpong A, Sinha A, Tañan B (2009) Genotype and growing environment influence chickpea (*Cicer Argentina L.*) seed composition. *J Sci Food Agric* 89: 2052–2063.
8. Ranganna S. (1986) Handbook of Analysis and Quality Control for Fruit and Vegetable Products, *Tata McGraw-Hill Education*.





Pramod k. Raghav et al.,

9. IFCT (Indian Food Composition Table) (2017), National Institute of Nutrition (Indian council of medical research) department of health research ministry of health & family welfare, the government of India Hyderabad-500 007, Telangana.
10. Larmond E (1977) laboratory methods for sensory evaluation of food. *Research Branch Canada Department of Agriculture*, Publication No. 1637: 19-63).
11. Mridula D, Wanjari OD, Ilyas SM, Goyal RK, Manikantan MR, Bharti DK (2004) Techno-economic facets of sattu processing units. *Technical Bull CIPHET/Pub/9/2003*
12. Onyeagba R, Ugbogu OC, Okeke CU, Iroakasi O (2004). Studies on the antimicrobial effects of garlic (*Allium sativum* L.), ginger (*Zingiber officinale* Roscoe), and lime (*Citrus aurantifolia* L.). *Afr. J. Biotechnol.* 3:552-554
13. Sharma S. K., (2019) A signature dish of Bihar: Litti and Chokha *MOJ Food Process Technol.*;7(1):1–2. DOI: 10.15406/mojfpt.2019.07.00210
14. Shewry, P. R. (2007). Improving the protein content and composition of cereal grain. *Journal of cereal science*, 46(3), 239-250.
15. Mahendra P., Bisht S. (2012) Ferula asafoetida: Traditional uses and pharmacological activity; *Pharmacogn Rev.*; 6(12): 141–146. doi: 10.4103/0973-7847.99948

Table No. 1 Fortification of Chickpea Flour Litti

Ingredients	20% incorporation	40% incorporation	60% incorporation	Dry control	Fresh control
Wheat flour	400	300	200	500	500
Chickpea	100	200	300	-	-
Sattu	300	300	300	300	300
Carom Seed	18	18	18	18	18
Asafoetida Powder	4	4	4	4	4
Ginger Powder	10	10	10	10	-
Garlic Powder	5	5	5	5	-
Cumin Powder	10	10	10	10	10
Black Pepper	10	10	10	10	-
Kalonji	13	13	13	13	13
Dry Mango Powder	5	5	5	5	5
Salt	24	24	24	24	24

Table No. 2 Acceptability Evaluation of Food Product (Litti) In Terms of Sensory Attributes

Parameter	Fresh Control	Dry Control	C1	C2	C3
Colour	7.50±0.55	7.33±0.82	7.50±0.55	8.16±0.41	7.66±0.52
Taste	7.16±0.75	7.16±0.75	8.00±0.63	7.83±0.75	7.66±1.03
Appearance	7.33±0.82	7.66±0.52	7.66±0.82	7.50±0.84	7.66±0.82
Texture	7.00±0.89	7.00±0.89	7.33±0.52	7.50±0.55	7.16±0.75
Odor	7.33±0.82	7.00±1.09	7.66±0.52	7.83±0.41	7.50±0.84
Overall acceptability	7.33±0.82	7.33±0.82	7.50±0.55	7.66±0.52	7.66±0.52





Pramod k. Raghav et al.,

Table No. 3 Mean Moisture Content of Litti

Variants of Litti	Moisture (g)
Fresh control	4.01±0.27
Dry control	2.55±1.09
C1	4.12±0.06
C2	3.12±0.84
C3	2.96±0.85

Table No. 4 Mean Nutrient Content of Litti

Variants of Litti	Protein (g)	Fat (g)	Carbohydrate(g)	Energy (kcal)	Fiber (g)
Fresh control	8.04	2.80	28.45	526.2	3.98
Dry control	7.24	2.80	29.72	539.3	11.34
C1	7.72	3.01	28.28	532.4	9.22
C2	8.20	3.22	26.83	523.0	7.06
C3	8.68	3.43	25.39	514.8	4.90

Table No. 5 - Mean pH content of Litti

Variant of Litti	Fresh control	Dry control	C1	C 2	C3
pH	6.70±0.01	6.62±0.01	6.65±0.01	6.69±0.01	6.71±0.01

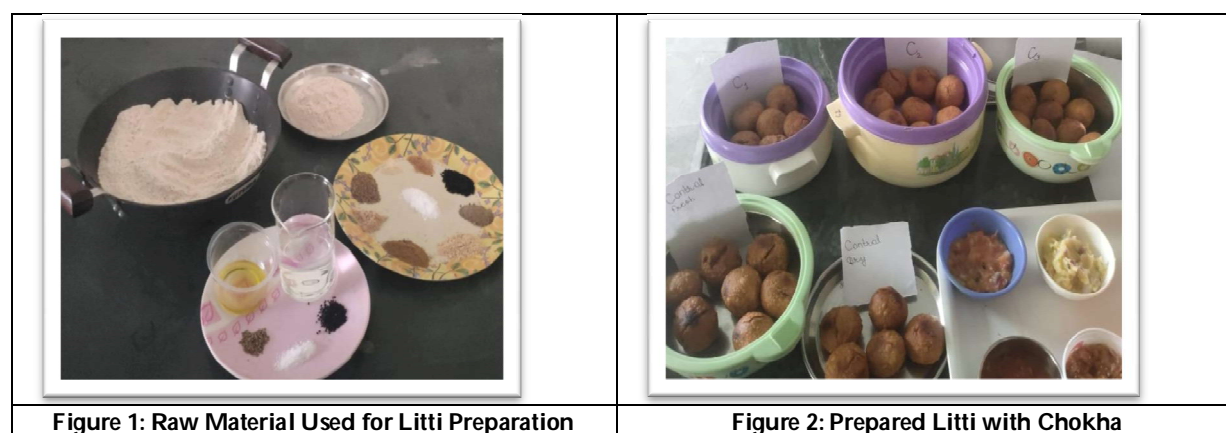


Figure 1: Raw Material Used for Litti Preparation

Figure 2: Prepared Litti with Chokha

